U.S. GEOLOGICAL SURVEY PROFESSIONAL PAPER

Digitized by Google

Digitized by Google

Digitized by Google

THE
UNIVERSITY
OF CHICAGO
LIBRARY

ed by Google

QE75
F.A26
no.352-A
cop 2
(GL)
305
AUG 22 1966
UNIVERSITY OF CHICAGO LIBRARY
Rosenw
SERIAL RECORD

Recent Sedimentation and Erosional History of Fivemile Creek Fremont County, Wyoming

---

U.S. GEOLOGICAL SURVEY PROFESSIONAL PAPER 352-A

Prepared as part of a program of the
Department of the Interior for development
of the Missouri River basin and part of
the soil and moisture program

March 3, 1849

Digitized by Google

Digitized by Google

Recent Sedimentation and Erosional History of Fivemile Creek Fremont County, Wyoming

By RICHARD F. HADLEY

EROSION AND SEDIMENTATION IN A SEMIARID ENVIRONMENT

GEOLOGICAL SURVEY PROFESSIONAL PAPER 352-A

Prepared as part of a program of the Department of the Interior for development of the Missouri River basin and part of the soil and moisture program

UNITED STATES GOVERNMENT PRINTING OFFICE, WASHINGTON : 1960

Digitized by Google

QE 75
f. A26
no. 352

UNITED STATES DEPARTMENT OF THE INTERIOR

FRED A. SEATON, *Secretary*

GEOLOGICAL SURVEY

Thomas B. Nolan, *Director*

The UNIVERSITY OF CHICAGO LIBRARY

77-500 507/s

For sale by the Superintendent of Documents, U.S. Government Printing Office
Washington 25, D.C.

Digitized by Google

CONTENTS

	Page
Abstract	1
Introduction	1
Physiographic features	1
Fieldwork	3
Acknowledgments	3
Terraces and alluvial deposits	4
Terrace 1	4
Terrace 2	4
Terrace 3	5
Modern flood plain	5
Physical properties of alluvial deposits	5
Size-frequency analyses	6
Roundness and sphericity of terrace 3 gravels	8
Heavy-mineral data	9
Causes of terrace development	10
Problems of terrace correlation	12
History of terrace development	13
References	15

ILLUSTRATIONS

[Plates 1-2 in pocket]

	Page
PLATE 1. Geologic map of Fivemile Creek, Wind River basin, Wyoming, showing relation of erosional and depositional features.	
2. Index map of Fivemile Creek showing location of sampling sections.	
3. Views of upper part of Fivemile Creek valley showing terraces, and a vertical exposure of alluvium underlying terrace 1 showing torrential crossbedding and coarse gravel lenses	Facing 4
4. Pebbles in the 16–32 mm class from terrace 3 gravels showing change in degree of roundness in 55-mile length of terrace	Facing 5
FIGURE 1. Index map of Wyoming showing location of areas mentioned in this report. Shaded area studied in detail	2
2. Longitudinal profile of Fivemile Creek showing heights of terrace remnants at location of sampling sections	3
3. Generalized valley cross section of Fivemile Creek showing relation of terraces and alluvial fills	4
4. Distribution of particle sizes in alluvial deposits underlying terrace 1	6
5. Distribution of particle sizes in alluvial deposits underlying terrace 2	7
6. Distribution of particle sizes in alluvial deposits underlying the modern flood plain	8
7. Relation of roundness and sphericity to distance from head of terrace for pebbles in 16–32 mm class from terrace 3	9

TABLES

	Page
TABLE 1. Terrace heights above present stream level on Fivemile Creek, Fremont County, Wyo	4
2. Summary of textural relationships	8
3. Average roundness for samples of terrace 3 gravels	9
4. Effect of composition on abrasion of terrace 3 gravels	9
5. Heavy-mineral data for alluvial deposits of terraces 1 and 2	10

Digitized by Google

RECENT SEDIMENTATION AND EROSIONAL HISTORY OF FIVEMILE CREEK, FREMONT COUNTY, WYOMING

By Richard F. Hadley

ABSTRACT

A study of the terrace sequence was made along Fivemile Creek, Fremont County, Wyo. Three terraces and the modern flood plain border the present stream; the highest (terrace 3) is a gravel-capped, rock-cut surface and the lower two (terraces 1 and 2) are composed of alluvium. The three terraces and flood plain stand about 28, 18, 9, and 3 feet above the present stream.

The alluvium underlying the flood plain and terraces 1 and 2 and the gravels of terrace 3 were sampled for laboratory study. Textural analysis of terrace 1 alluvium showed a normal decrease in median diameter in a downstream direction, ranging from 0.185 to 0.123 mm near the mouth of the stream. Terrace 2 alluvium showed very little change of median gram size in the 55-mile length of the terrace; the median diameter ranging from 0.017 to 0.023 mm. Samples of flood-plain alluvium were highly variable in texture. Studies of roundness and sphericity of terrace 3 gravels in the 16–32 mm size range show that values of both indexes increase markedly from the head to the mouth of the valley. Roundness is also affected by mineral composition. The heavy-mineral suites from terraces 1 and 2 alluvium showed some marked differences in mineral content.

Terraces on Wind River which are correlative of terrace 3 have been traced to glacial moraines in the Wind River Mountains. Therefore, development of the terrace sequence on Fivemile Creek began in late Wisconsin time. No satisfactory evidence such as archeological sites or vertebrate remains were found by which terraces 1 and 2 could be dated. Historical evidence shows, however, that the latest trenching of the valley and formation of the modern flood plain has occurred since 1920. Measurements of aggradation on flood plains in historical time and other evidence indicate a probable rapid rate of accumulation of alluvial deposits.

INTRODUCTION

The erosional history of many stream valleys in the arid or semiarid regions of Western United States is recorded in alluvial terraces that were formed during periods of alternating erosion and deposition. Terrace sequences similar to the one in the valley of Fivemile Creek are common to many other stream valleys in the Rocky Mountain and Great Plains regions. The stratigraphy of alluvial fills has been studied in Colorado (Bryan and Ray, 1940); in Wyoming (Leopold and Miller, 1954); in the Hopi Country, Ariz. (Hack, 1942); near Gallup, N. Mex. (Leopold and Snyder, 1951); Texas (Albritton and Bryan, 1939); and in several other localities scattered through the Western States. All of these studies concern a sequence of alluvial fills that were deposited in late Pleistocene or Recent time. A chronology of events based on cultural evidence or fossil remains has been developed as a result of the many studies, although details of depositional morphology often vary from place to place. This report describes the postglacial history of Fivemile Creek, Fremont County, Wyo., and the sedimentary characteristics of the alluvial valley fills.

In the Wind River basin of central Wyoming the streams that drain the Wind River and Owl Creek Mountains are similar. Fivemile Creek was chosen for this study because its erosional and depositional features are common to the stream valleys of the region. The stream heads near the base of the Owl Creek Mountains and joins the Wind River near Shoshoni, Wyo., (fig. 1) draining an area of about 400 square miles. Fivemile Creek is an ephemeral stream, but it has been subjected to large floods several times in the last 35 years. On July 24, 1923, when heavy rains produced large floods in most tributaries of the Wind River the maximum discharge near the mouth of Fivemile Creek was estimated to be 3,500 cfs (Follansbee and Hodges, 1925, p. 111). The records for the Geological Survey gaging station Fivemile Creek near Shoshoni, Wyo., cover the period 1941–42 and 1948–54 and the maximum discharge observed is 3,200 cfs which is slightly less than the estimate for the 1923 flood (U.S. Geol. Survey, 1954, p. 152).

PHYSIOGRAPHIC FEATURES

The most prominent physiographic features of the Wind River basin are the gravel-capped, gently sloping surfaces standing at different levels above the major streams and their tributaries. Blackwelder (1915, p. 309) describes these surfaces as vestiges of Tertiary and Quaternary erosion cycles in central western Wyoming. These high erosion surfaces are not discussed in this report, but it is necessary to mention them briefly

Digitized by Google

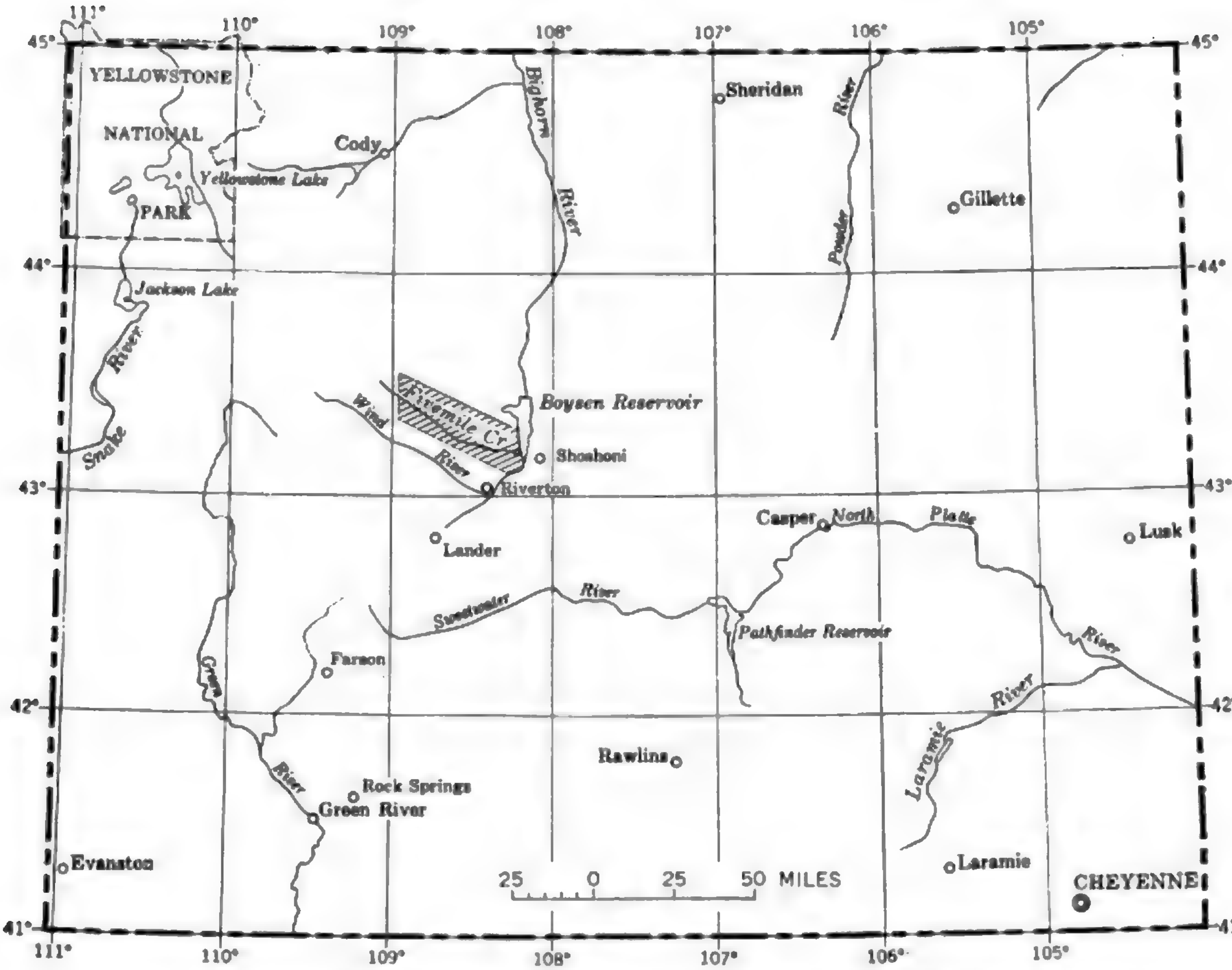

FIGURE 1.—Index map of Wyoming showing location of areas mentioned in this report. Shaded area studied in detail.

in relation to the terraces being considered in this investigation.

Blackwelder (1915, p. 310) describes four erosion surfaces which he believes to be younger than the elevated "Wind River peneplain," which is Pliocene in age. Blackwelder's youngest erosion surface (Lenore) is directly associated with the features described in this report. The Lenore cycle is represented by gravel-covered terraces, standing 10 to 30 feet above Wind River and Owl Creek, which have been traced to moraines of the Pinedale stage of glaciation (Blackwelder, 1915, p. 321). This terrace is the highest surface considered in this report. Throughout the length of Fivemile Creek it stands 25 to 30 feet above the present stream and joins a corresponding terrace along Wind River at the junction of the two streams.

The valley of Fivemile Creek may be divided into three reaches, each having distinct geologic and topographic characteristics. The longitudinal profile (fig. 2) indicates a fairly uniform gradient for the upper 20 miles where the channel traverses a shale valley alined between upturned Mesozoic sandstone units. Downstream from this reach the channel is confined in a canyon 1½ miles long cut into the Mesaverde formation. From below the point where the channel is cut into the Mesaverde formation, about mile 30 from the source, to the junction with Wind River, the stream traverses nearby horizontal sandstone and shale beds of the Eocene Wind River formation and maintains a generally uniform though lesser gradient.

Differential erosion of the alluvium and bedrock is reflected in the alternating wide and narrow sections of the channel throughout its sinuous course. Where bedrock crops out near the stream, the channel is confined and very narrow. Other places it has been widened until it reaches bedrock underlying the valley

Digitized by Google

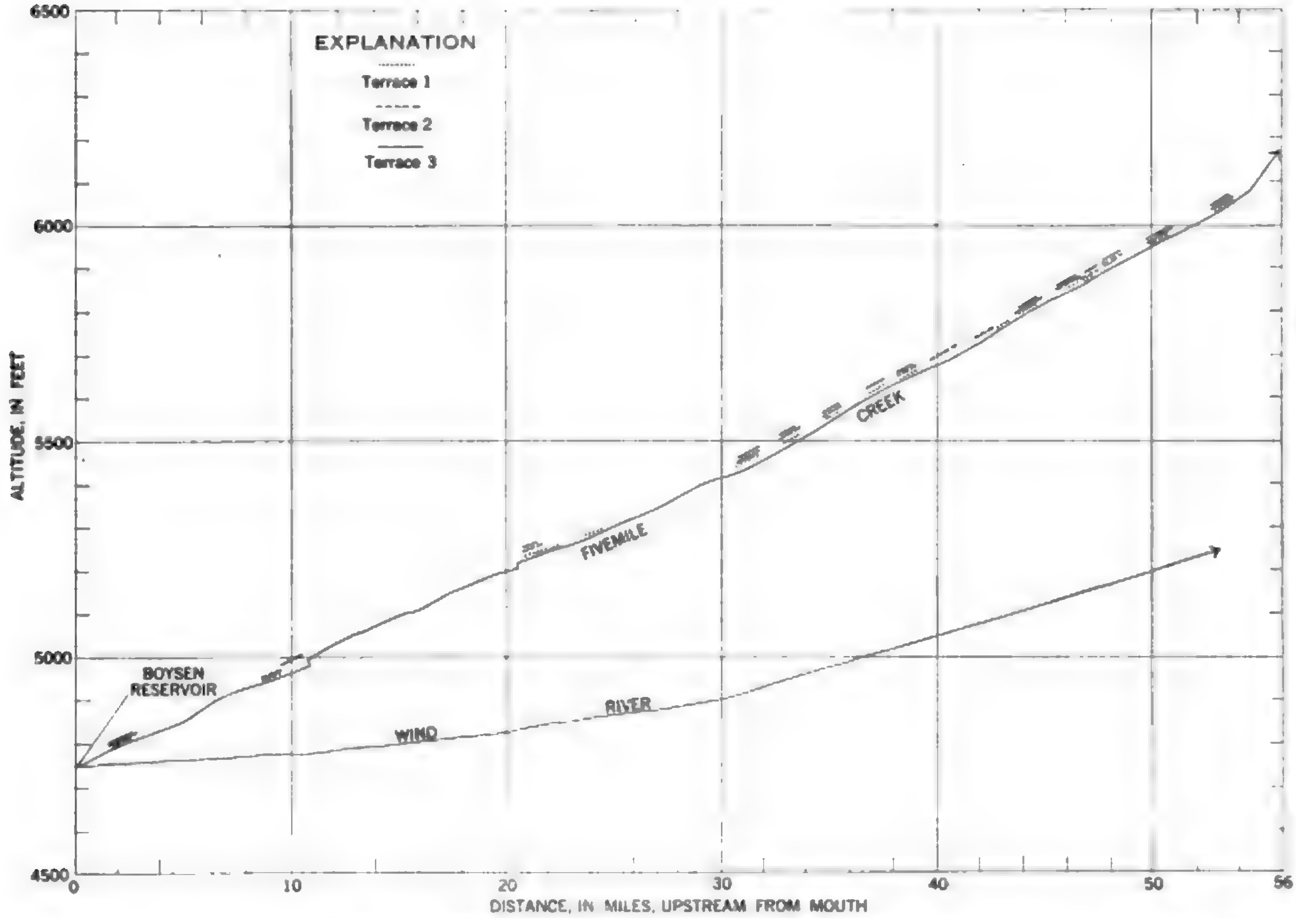

FIGURE 2.—Longitudinal profile of Fivemile Creek showing heights of terrace remnants at location of sampling sections.

side slopes. The valley floor is mantled with alluvium to a depth of about 20 feet, and these alluvial deposits underlie and form the terraces discussed in this report.

FIELDWORK

The fieldwork for this study was carried our during the summers of 1948 and 1949 as a part of the soil and moisture program of the Department of the Interior under the general supervision of R. W. Davenport. Field activities were supervised by H. V. Peterson. Laboratory studies and analysis of the samples were made at the University of Minnesota in partial fulfillment of a master of science degree.

The terraces and other prominent features of Recent erosion and deposition were mapped by planetable in 1948 along the part of the valley within the boundaries of the Wind River Indian Reservation from sec. 17, T. 5 N., R. 1 W. to sec. 25, T. 4 N., R. 1 E. (See pl. 1.) The height of the individual terraces above the present stream level was measured and the gradient of the stream bed was determined. Random elevations were taken on the terraces to determine their gradient. It was found that the gradients of the present stream and of the terraces are nearly the same.

Although the lower 35 miles of the valley was not mapped in detail, reconnaissance showed that the terraces in the upper part of the valley extend to the junction of Fivemile Creek and Wind River. The lower terraces, however, exist only as small remnants at many places in the lower part of the valley.

During the field season of 1949 the alluvial terraces were sampled throughout the length of the stream. This sampling was done primarily to determine if variations in the sediments could be used as a means of identifying the deposits. The location of the sampling sections appears in plate 2.

ACKNOWLEDGMENTS

The author is indebted to Profs. George A. Thiel and Herbert E. Wright of the Geology Department at the University of Minnesota, who made many helpful suggestions during the preparation of this report.

Digitized by Google

TERRACES AND ALLUVIAL DEPOSITS

River terraces have two essential components: (a) The top, or tread, which may or may not be the original surface of deposition; (b) the scarp, or riser, which is formed by subsequent downcutting by the stream. These two components may be formed by lateral stream corrasion on a rock surface or by cut and fill in deposits of stream alluvium.

Three terraces and the irregular modern flood plain are alined along the axis of the valley of Fivemile Creek (fig. 3). The modern flood plain rises 2 to 4

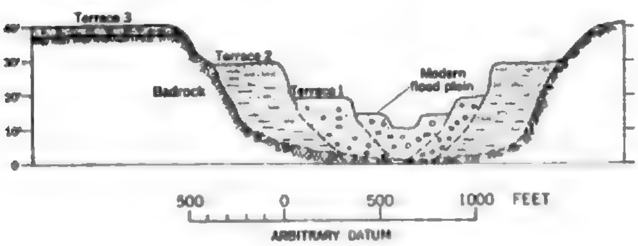

FIGURE 3.—Generalized valley cross section of Fivemile Creek showing relationship of terraces and alluvial fills.

feet above the present stream. Terrace 1 stands 8 to 10 feet above the channel and terrace 2 stands 18 to 20 feet above the channel. Terrace 3 stands 25 to 30 feet above the present stream and is a gravel-capped, rock-cut surface.

The three terraces and flood plain are conspicuous throughout the valley and can be traced with assurance. (See pl. 3*A*, *B*.) Although in some places the terraces are represented by disconnected remnants, their relative elevations are remarkably consistent along the valley (see table 1). The terraces can be identified by the alluvial materials of which they are composed. Heights of terraces 1, 2 and 3 above the present stream levels at different cross sections are given in table 1.

TABLE 1.—*Terrace heights, in feet, above present stream level, on Fivemile Creek, Fremont County, Wyo.*

Location (pl. 1)	Terrace 1	Terrace 2	Terrace 3
NW¼ sec. 16, T. 5 N., R. 1 W.	8.4	18.5	29
SE¼ sec. 13, T. 5 N., R. 1 W.	9.6	22	30
NE¼ sec. 22, T. 5 N., R. 1 W.	12.2	20	30
NE¼ sec. 23, T. 5 N., R. 1 W.	9.6	16.5	25
NE¼ sec. 24, T. 5 N., R. 1 W.	7	20	28
NW¼ sec. 29, T. 5 N., R. 1 E.	8	18.5	27
SW¼ sec. 29, T. 5 N., R. 1 E.	10	...	...
NW¼ sec. 33, T. 5 N., R. 1 E.	...	15.2	...
NW¼ sec. 4, T. 4 N., R. 1 E.	...	18.8	...
SW¼ sec. 3, T. 4 N., R. 1 E.	9.3	19	30
NE¼ sec. 10, T. 4 N., R. 1 E.	9.2	24.4	27
SE¼ sec. 14, T. 4 N., R. 1 E.	11.1	20	25
SE¼ sec. 24, T. 4 N., R. 1 E.	9.5	24.3	30
SE¼ sec. 30, T. 4 N., R. 2 E.	11.8	20	28
SE¼ sec. 8, T. 3 N., R. 3 E.	9	...	...
SW¼ sec. 24, T. 3 N., R. 3 E.	8.2	22.8	28
NW¼ sec. 35, T. 3 N., R. 4 E.	7.0	20.4	29
SE¼ sec. 18, T. 3 N., R. 6 E.	...	16.2	...
SW¼ sec. 19, T. 3 N., R. 6 E.	10	20	26

TERRACE 1

A prominent surface standing 8 to 10 feet above the present stream is designated as terrace 1. This surface is almost continuous in the upper part of the stream valley but has been eroded extensively in the lower part so that only small, isolated remnants are found. In the reach immediately above the mouth of the stream where the channel has been widened to nearly 1,000 feet, terrace 1 is entirely absent.

The alluvial material underlying terrace 1 is coarser than that beneath the next higher surface. Terrace 1 alluvium has not undergone as much weathering and erosion as the older deposits, and there is no evidence of leaching or soil development.

Terrace 1 is distinguished nearly everywhere along the valley by a dense growth of rabbitbrush (*Chrysothamnus* sp.) which in places reaches a height of 3 to 4 feet. This dense cover of vegetation is in marked contrast to the barren aspect of terrace 2.

The longitudinal profile of terrace 1 is nearly parallel to the profile of the present streambed (fig. 2). The surface has slight local relief caused by rivulet washing and does not slope toward the channel perceptibly. It has the characteristics of a depositional surface, and the effects of subaerial erosion subsequent to deposition are slight. Throughout the valley, wind-blown sand is prominent on terrace 1.

The underlying alluvial deposit is predominantly sand containing many gravel stringers. Many exposures show torrential crossbedding in gravelly material, indicating that most of the material was deposited by a stream capable of moving coarse gravel. (See pl. 3*C*.)

In most places terrace 1 rests unconformably against the older deposits of terrace 2 and in a few places it is in contact with the bedrock. In the places where the deposits underlying terraces 1 and 2 are in contact and the vertical exposure is free of slumped material, the abrupt textural change from one to the other is apparent.

TERRACE 2

Throughout the valley a distinct surface stands 18 to 20 feet above the present stream level. This surface, designated terrace 2, is indicated on the geologic map and the accompanying cross sections (pl. 1).

This terrace can be traced almost continuously throughout the valley. In places where it has been dissected by gullies disconnected remnants can be correlated readily. Terrace 2 is extensive and, unlike terrace 3, is found on both the north and south sides of the channel in most places. In the lower part of the valley it is a broad, flat area which has been con-

Digitized by Google

A. View of upper part of Fivemile Creek valley showing terraces

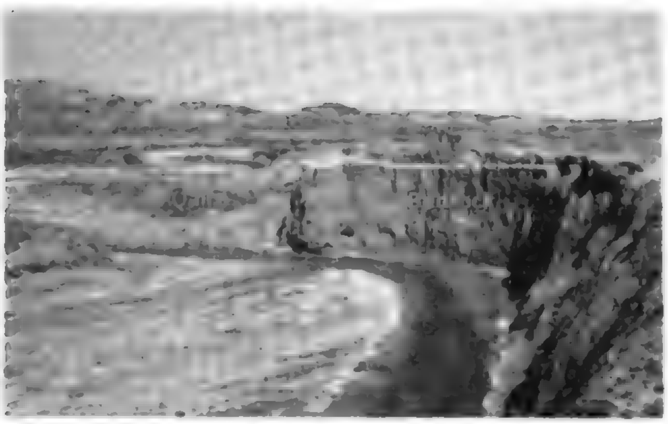

B. View of upper part of Fivemile Creek valley showing terraces and bedrock

C. Vertical exposure of alluvium underlying terrace 1 showing torrential crossbedding and coarse gravel lenses

Digitized by Google

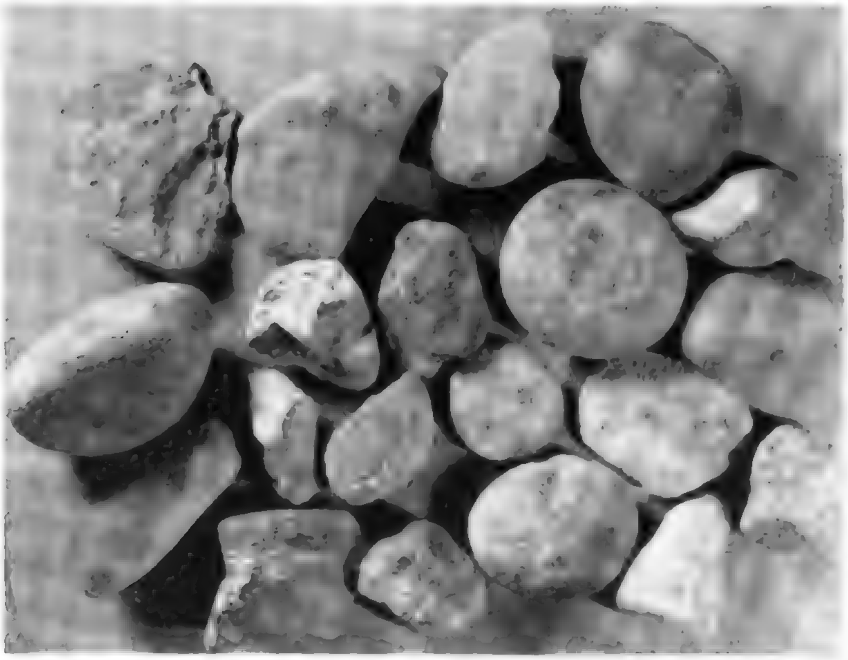

Pebbles in the 16-32 mm class from terrace 3 gravels showing change in degree of roundness in 55-mile length of terrace

Digitized by Google

verted to farmland on the Riverton Reclamation withdrawal area. The gradient of terrace 2 is generally the same as that of the present streambed and, like terrace 3, it does not slope perceptibly toward the stream channel.

The alluvial material which underlies terrace 2 is predominantly very fine sand and silt. The source of the material was probably the Mesozoic sedimentary formations cropping out at the head of the valley. Salt sage (*Atriplex* sp.), the typical vegetation on this surface, grows above the general level on small hummocks that are the result of rivulet washing.

The surface is covered with a thin mantle of windblown sand in scattered parts of the lower valley. This sand occurs locally in dunes, but it makes up only a small fraction of the total material underlying terrace 2 in the lower valley.

The deposits of alluvium underlying terrace 2 are in unconformable contact with the bedrock units in which the channel is confined. Sharp contacts, however, are not extensively exposed because of slumping subsequent to deposition of the alluvial material. In some reaches bedrock is exposed below the gravels of terrace 3, and the alluvium of terrace 2 abuts against the bedrock of the channel wall at a lower elevation. It is obvious that the deposits underlying terraces 3 and 2 are not of the same age. There is slight leaching of calcium carbonate to a depth of 4 to 6 inches in terrace 2 and some evidence of profile development.

Particle-size analyses of the deposits are given in another section of this report.

TERRACE 3

The surface, standing generally 25 to 30 feet above the present stream, was designated terrace 3 (pl. 3*A*, *B*). It is shown on the geologic map and the cross sections (pl. 1). This surface, which corresponds to the Lenore surface of Blackwelder (1915, p. 321), is consistently present on the south side from the head of Fivemile Creek near the base of the Owl Creek Mountains to its junction with the Wind River, about 55 miles. Throughout its length this surface overlies Cretaceous and Tertiary sedimentary rocks and is capped by gravel which ranges in thickness from 5 to 15 feet. Random samples taken of the gravel at intervals along the surface show a predominance of igneous rock pebbles and limestone and quartzite pebbles, indicating that the principal source of the material was upstream in the foothills of the Owl Creek and Absaroka Mountains where rocks of these types crop out. Some of the pebbles may have been contributed by slope wash from higher gravel-capped surfaces along the valley. Most pebbles have a thin coating of calcium carbonate and the deposit is deeply weathered.

Terrace 3 is absent on most of the north side of the present channel. Erosion probably removed this part of the terrace by undercutting after the stream had entrenched itself in the gravel deposits. South of the channel, however, terrace 3 is in places a quarter of a mile wide. The underlying formations, although consisting of beds of nonresistant shale and poorly cemented sandstone, constitute a barrier against erosion of the terrace riser which, in many places forms the channel wall. (See pl. 3*B*.)

Terrace 3 is a nearly plane surface with a maximum relief of 2 or 3 feet. The minor irregularities in relief have been caused by dissection after the deposition of the gravel. The gradient of the surface is nearly equal to that of the present streambed, averaging about 26 feet to the mile, and the surface does not slope perceptibly toward the axis of the valley.

MODERN FLOOD PLAIN

The flood plain of the stream is a poorly defined surface 2 to 4 feet above the present streambed (pl. 1). Spring and summer floods overflow this surface resulting in aggradation in some reaches of the stream and degradation in others. Throughout the valley the surface is being constantly changed by the stream.

The alluvial material underlying the modern flood plain is composed mainly of sand, although gravel lenses and stringers occur along the slip-off slopes of meanders. Much of the material has probably been derived from sloughing banks and headward-cutting gullies in the older terraces, but undoubtedly some material has been transported from the mountain regions by waters from summer rainstorms and spring snowmelt.

The significance of these terraces in reconstructing the postglacial erosional history of the valley of Fivemile Creek is apparent. The terraces represent cycles of aggradation and degradation within the valley as the stream regimen varied with internal and external conditions.

PHYSICAL PROPERTIES OF ALLUVIAL DEPOSITS

Samples of the alluvium underlying terraces 1 and 2 and the modern flood plain and gravels on terrace 3 were collected at different sections throughout the valley of Fivemile Creek. Size-frequency analyses of the samples of alluvial terrace deposits and a study of the effect of transportation on the roundness and sphericity of pebbles of different lithology in terrace 3 gravels were made. The location of sampling sections was

Digitized by Google

determined by the nature of the deposits and the exposures which showed best the contrasts between the alluvial fills. Samples were collected both from the surface (channel samples) and from pits.

The channel samples were taken in the vertical exposures of the terraces along the creek. The sampled sections were chosen so that a section near maximum thickness would be obtained. It was noted in the field that the alluvial fills underlying terraces 1 and 2 were uniform in texture throughout the length of the valley, and this observation was substantiated by mechanical analyses.

In the upper part of the valley, terrace 3 is exposed in scarp faces or in the terrace lip adjacent to the channel; but in the lower part of the valley where terrace 2 is extensive the scarps of terrace 3 stand at a distance from the channel and have been modified by slumping. In such locations it was necessary to dig a pit in order to obtain representative gravel samples.

SIZE-FREQUENCY ANALYSES

Mechanical analysis of the individual samples of terrace 1 alluvium showed a normal decrease in grain sizes in a downstream direction (fig. 4). The variability at a given sampling location was not large enough to mask this decrease. The 18 samples were, therefore, grouped into 4 composite samples (1–A, 1–B, 1–C, 1–D) so that the overall changes in texture of the deposit were obtained.

The alluvium of terrace 1 is much coarser than that of terrace 2. The median diameter for the 4 composite samples ranges from 0.185 mm at the head of the valley to 0.123 mm at the downstream end. The weight of particles with a diameter greater than 2 mm ranged from 1 percent in sample 1–D to 21 percent in sample 1–A. This distribution indicates that the competence of the stream which deposited the alluvium of terrace 1 was not extremely high even during floodflow. The absence of a concentration of fine material in terrace 1 deposits may be interpreted to mean that the velocity was too high for deposition of silt and clay when they were part of the suspended load.

The sorting coefficients for terrace 1 samples are markedly different from those calculated for samples of terrace 2. Coefficients range from 1.79 to 3.14 (see table 2) which means, according to the classification of Trask, that all of the samples are well sorted except 1–A, which has a coefficient of 3.14. This coefficient, however, is only slightly more than the normal sorting coefficient of 3.00.

The skewness coefficients calculated for samples of terrace 1 range from 1.06 to 2.66 (see table 2). These results indicate that the maximum sorting of samples 1–A and 1–C lies on the fine side of the median diameter, whereas the maximum sorting of 1–B is on the coarse side. It should be noted that the mechanical analyses of samples from terraces 1 and 2 disclose marked differences in texture and other physical properties.

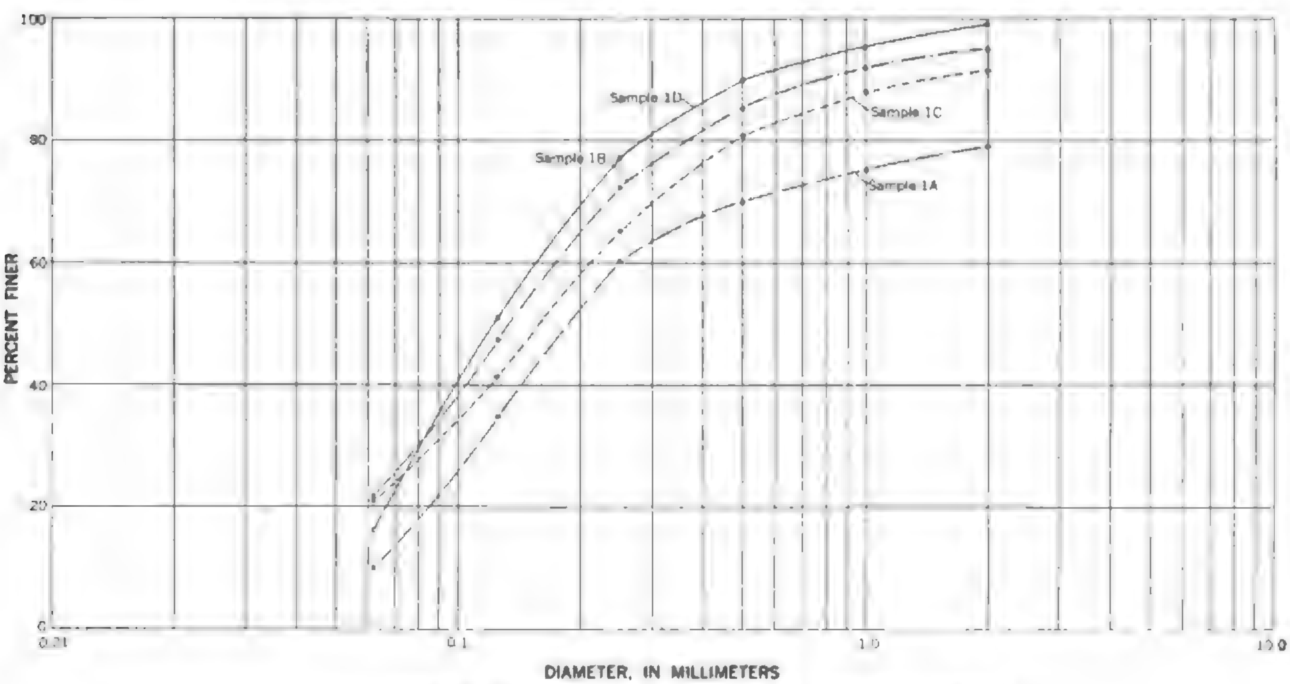

FIGURE 4.—Distribution of particle sizes in alluvial deposits underlying terrace 1.

Digitized by Google

Preliminary mechanical analysis of terrace 2 alluvium showed that the percentage of any grade size did not vary for samples from the head and mouth of the valley. After noting the slight variations in grain size, composite samples were made from the individual samples of terrace 2 alluvium. The 17 samples collected were consolidated into 4 composite samples for analysis (2–A, 2–B, 2–C, 2–D) representing sections of the terrace in downstream order. The size-distribution curves of particle size from the mechanical analysis data of terrace 2 composite samples are shown in figure 5.

Mechanical analysis of the four composite samples of terrace 2 alluvium showed little change in median grain size from the head of the valley to its mouth (table 2). The median diameter ranges from 0.017 to 0.023 mm in the 55-mile length of the terrace, with the upstream and downstream samples having nearly the same median diameter. Samples of this alluvium were examined by P. D. Trask (written communication, 1947). He noted that the samples show no consistent change in average diameter downstream. This lack of change is rare in an alluvial deposit which has been identified as a sedimentary unit. The velocity of the stream depositing terrace 2 alluvium must have been below the critical velocity for the transportation by suspension of particles of this size (Plumley, 1948, p. 544). The stream, therefore, probably had a low mean velocity with a marked absence of high flows. This conclusion is supported by the paucity of particles coarser than sand in the deposits.

The sorting coefficient was determined for the samples of terrace 2 according to Trask's classification (Twenhofel and Tyler, 1941, p. 111). The coefficients ranged from 4.33 to 5.18 (see table 2). According to Trask, if the coefficient is more than 4.50, the material is poorly sorted. Therefore, by Trask's standards, the samples of terrace 2 are poorly sorted.

The coefficient of geometrical quartile skewness indicates the degree of symmetry of the size distribution with respect to the median (Twenhofel and Tyler, 1941, p. 111). This coefficient of skewness was calculated for the terrace 2 samples (see table 2) and ranged from 0.73 to 1.33. When the skewness is unity, the mode coincides with the median diameter. When the skewness is greater than unity, the maximum sorting of the material lies on the fine side of the median diameter; if it is less than unity, on the coarse side (Twenhofel and Tyler, 1941, p. 112). Therefore, samples 2–A, 2–C, and 2–D with coefficients of 1.26, 1.09 and 1.33 have maximum sorting on the fine side of the median diameter. Sample 2–B has its maximum sorting on the coarse side of the median.

Samples of the flood-plain alluvium were analyzed individually because of their highly variable texture. Five samples were collected at scattered points along the valley. (See pl. 2.) They are lettered in the same sequence as the samples of terraces 1 and 2; sample

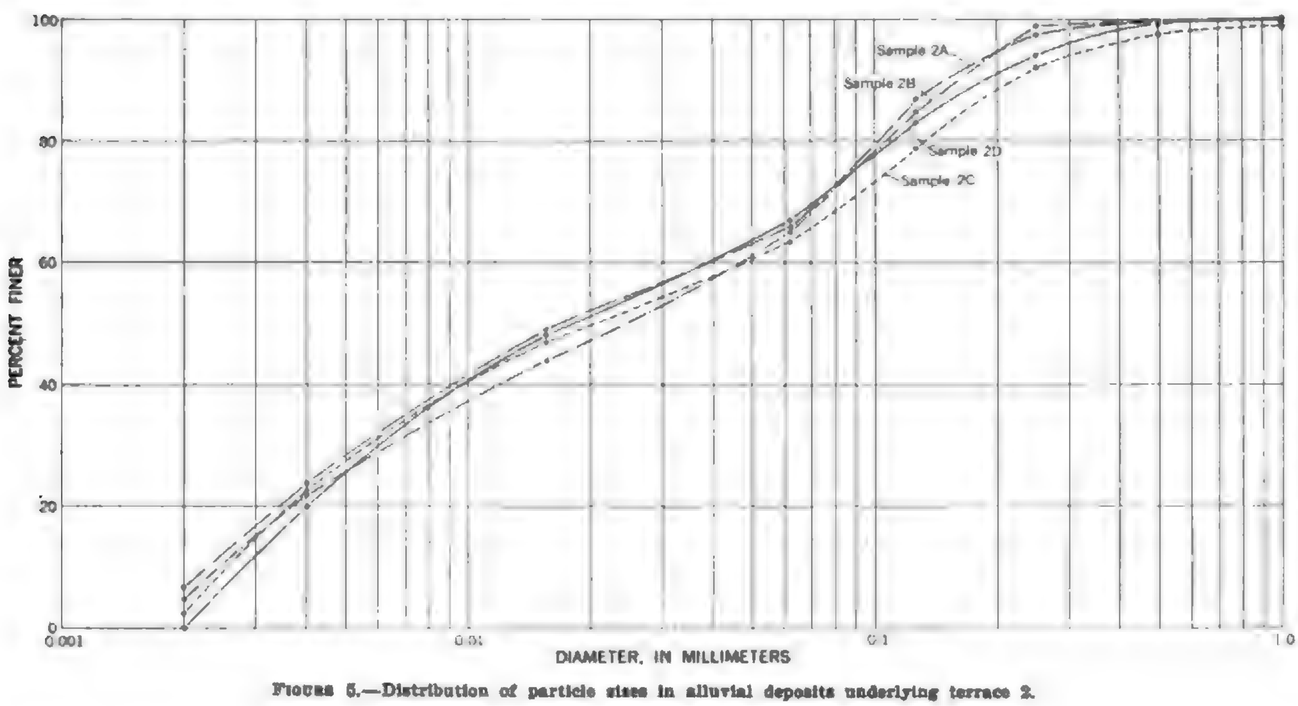

FIGURE 5.—Distribution of particle sizes in alluvial deposits underlying terrace 2.

Digitized by Google

4–A was taken from the upper end of the valley and sample 4–E from the downstream end.

The size-distribution curves show that the fraction with grains greater than 2 mm in diameter ranges from 16 to 32 percent (fig. 6). By comparing these percentages with the curves for terraces 1 and 2, it is evident that the present stream is depositing coarser material in either of the older terraces. Trask (written communication, 1947) states:

> It is not surprising that the sand in the present stream is coarser than the sand in the alluvium, because hand-lens inspections of the sand from the streambeds and from the alluvium in walls of the gullies from some 30 or more areas through Wyoming, Utah, Colorado, New Mexico, and Arizona indicated clearly that the sand in the present streams is coarse, on the average about twice as coarse, as the sections above.

Because the present stream gradient and the gradient of the alluvial terraces above it are nearly the same, conditions of deposition today must differ greatly from former ones. Evidently the velocity and thereby the competence of the modern stream is higher during floodflow.

The coefficients of sorting for the flood-plain samples range from 1.70 to 4.00 (see table 2). Samples 4–A and 4–E are well sorted, being below 2.5 in Trask's classification. Samples 4–B, 4–C, and 4–D fall between the limits of normal and poor sorting. This relationship shows clearly the erratic texture of flood-plain alluvium.

The skewness coefficients range from 1.08 to 2.79 (see table 2). Therefore, for all flood-plain samples the maximum sorting lies on the fine side of the median diameter.

TABLE 2.—*Summary of textural relationships*

Sample	Median diameter (mm)	Third quartile	First quartile	Coefficient of sorting	Coefficient of skewness
1–A	0.185	0.930	0.096	3.14	2.66
1–B	.136	.285	.068	2.05	1.06
1–C	.100	.385	.071	2.33	1.06
1–D	.123	.233	.073	1.79	1.12
2–A	.017	.067	.0042	4.55	1.26
2–B	.024	.089	.0047	4.36	.73
2–C	.021	.110	.0044	5.18	1.09
2–D	.018	.090	.0048	4.33	1.33
4–A	.550	1.20	.29	2.00	1.15
4–B	.730	2.50	.23	3.30	1.08
4–C	.800	3.20	.20	[illegible]	2.55
4–D	.320	2.20	.13	4.00	2.79
4–E	.560	1.10	.37	1.70	1.29

ROUNDNESS AND SPHERICITY OF TERRACE 3 GRAVELS

Six samples of terrace 3 gravels were collected at different points throughout its 55-mile length. The pebbles in the 16–32 mm range were used in a study of the changes in degree of roundness and sphericity with distance of transportation and the effect of the mineral composition of the pebbles on these two values.

The roundness of the pebbles in the 16–32 mm range collected from the terrace 3 gravels was determined by use of visual comparison charts. The sphericity of the same suites of pebbles was determined by the Wadell method which is expressed by the formula $d_n/D_s=\psi$ where d_n is the true nominal diameter of the pebble or the volume of a sphere of the same volume and D_s is

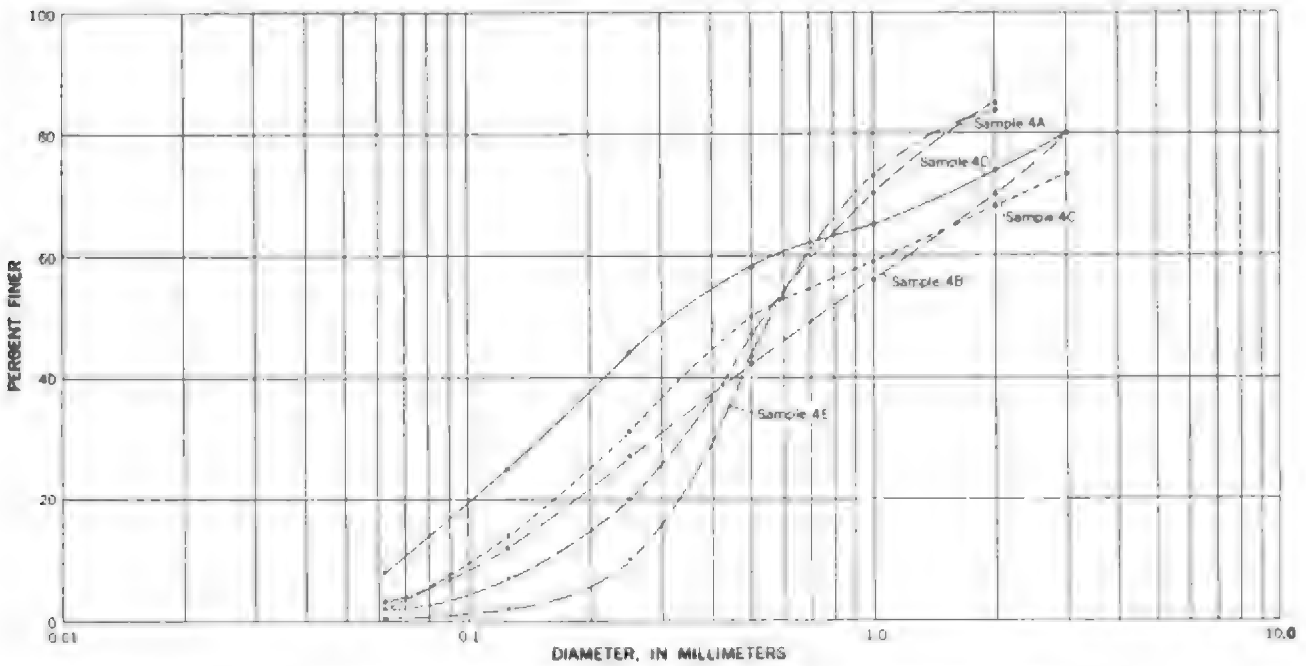

FIGURE 6.—Distribution of particle sizes in alluvial deposits underlying the modern flood plain.

Digitized by Google

the diameter of the circumscribing sphere (Krumbein and Pettijohn, 1938, p. 284).

Suites of 20 pebbles each were selected at random from the 16–32 mm fraction of terrace 3 gravels. Roundness and sphericity were determined for the individual pebbles and the averages were plotted for the single samples (fig. 7). The mineral composition of each pebble was determined and the effect of erosion during transportation noted.

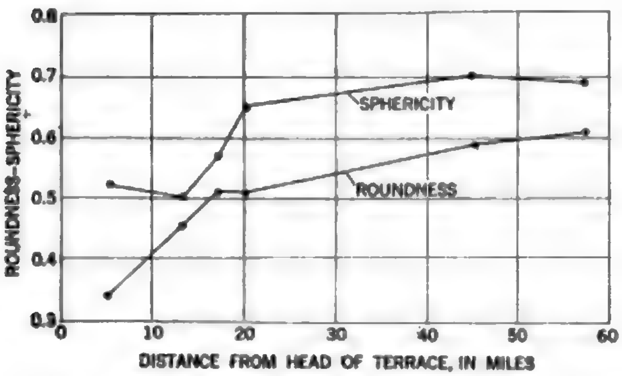

FIGURE 7.—Relation of roundness and sphericity to distance from head of terrace for pebbles in 16–32 mm size class from terrace 3.

Shape and roundness in gravels have been interpreted by geologists in many ways. Pettijohn (1949, p. 53) states that available data are insufficient to determine the geologic significance of these characteristics. He does say, however, that roundness is a good index to the maturity of a sediment. Pettijohn states further that both experimental and field studies show that gravel sizes are readily rounded through short transport, whereas prolonged abrasion is necessary for the rounding of sand. This may account for the similarity observed under the microscope in the roundness of the finer material of terraces 1 and 2 as compared with the coarse gravels of terrace 3.

The effects of distance of transportation on the roundness and sphericity of terrace 3 gravels are given in plate 4.

It will be noted that the roundness increases rapidly in the first stages of transportation and levels off after a certain roundness has been reached. (See table 3.) Perfect roundness, which is a value of 1.0, is never reached because of the nonhomogeneity of the material and the rigor of the abrasive processes (Pettijohn, 1949, p. 410). The sphericity of the pebbles is variable in the first few miles and then increases fairly constantly to the mouth of the stream except for sample 3–6, which shows a decrease in sphericity, perhaps because of breakage. In general, in the samples of terrace 3 gravels for which roundness and sphericity were determined there is a trend toward greater roundness with increasing sphericity. In studies of Black Hills terraces gravels, Plumley (1948, p. 558) found the same condition.

The pebbles are rounded to varying degrees because of their mineral composition (see table 4). The limestone pebbles in sample 3–1 have an initial roundness of 0.42; this value increased to 0.62 in the 55 mile-length of terrace. Plumley (1948, p. 558) suggests that limestone pebbles 16–32 mm in size reach a limit of rounding of about 0.73–0.74 when transported about 200 miles. Quartz pebbles in sample 3–1 have a roundness value of 0.30. This value increased to 0.70 at the mouth of the stream, which seems high and may be due to an influx of well-worn gravel from higher terraces that previously underwent more intensive abrasion. The absence of sandstone pebbles in sample 3–6 is to be expected because the sandstone cropping out in the area would probably disintegrate rapidly when subjected to stream abrasion.

TABLE 3.—*Average roundness for samples of terrace 3 gravels*

Sample	Approximate miles from head of stream	Average roundness	Average sphericity
3-1	5	0.34	0.52
3-2	13	.45	.50
3-3	16	[1] .51	.57
3-4	20	.51	.65
3-5	45	.59	.70
3-6	56	.61	.69

[1] Contribution of material from Teapot Draw may account for the sharp rise in short distance.

TABLE 4.—*Effect of composition on abrasion of terrace 3 gravels*

Composition	Sample 3-1		Sample 3-6	
	Number of pebbles	Average roundness	Number of pebbles	Average roundness
Limestone	5	0.42	4	0.62
Quartz	6	.30	7	.70
Chert	4	.17	4	.52
Granite	1	.30	1	.30
Siltstone	2	.45	3	.63
Sandstone	2	.50		
Quartzite			1	.60

HEAVY-MINERAL DATA

Heavy-mineral counts were made of samples from terraces 1 and 2 to determine whether the alluvial deposits could be identified on the basis of heavy-mineral suites. Samples 1–3 and 1–17 were chosen as representative of terrace 1 and samples 2–2 and 2–16 of terrace 2. Locations of sections from which samples were taken are shown on plate 2. Sample numbers increase downstream. The samples were sieved and a 10-gram part of the alluvium remaining on the 115-mesh screen (0.125-mm openings) was used for the bromoform separations. The results of the heavy-mineral counts appear in table 5.

Digitized by Google

No attempt was made to correlate the results of the heavy-mineral counts of the samples studied. There are, however, some significant differences: (a) The high percentage of zircon grains in samples 2–2 and 2–16 is in direct contrast to the rareness of zircon in samples 1–3 and 1–17. (b) Magnetite was not present in samples of terrace 2 and its occurrence was common in samples of terrace 1. (c) The contributions of tributaries between the upstream samples, 2–2 and 1–3, and the downstream samples, 2–16 and 1–17, probably are responsible for the high percentage of garnet grains in the downstream samples.

These data are not sufficient for correlation of these alluvial deposits on the basis of heavy-mineral content. A more detailed statistical analysis of the samples throughout the valley might show some definite trends that could be used for correlation.

TABLE 5.—*Heavy-mineral data for alluvial deposits of terraces 1 and 2*

Minerals	Percent of total grains present			
	Sample 1–3	Sample 1–17	Sample 2–2	Sample 2–16
Apatite	53.0	20.7	39.2	32.0
Biotite	3.0	8.4	2.3	5.0
Carbonate	1.7	2.3	2.9	2.3
Chlorite	(1)	(1)	.3	(1)
Epidote	(1)	12.2	(1)	4.7
Garnet	8.6	27.5	1.1	8.4
Hematite	(1)	(1)	.3	(1)
Hornblende	2.3	(1)	5.2	9.1
Muscovite	(1)	.8	.3	(1)
Staurolite	(1)	(1)	1.1	.3
Sphene	(1)	(1)	.3	(1)
Tourmaline	(1)	1.0	2.6	(1)
Zircon	2.7	1.3	40.8	27.5
Leucoxene	(1)	(1)	(1)	.7
Rutile	(1)	(1)	(1)	.3
Magnetite	16.9	4.9	(1)	(1)
Amphiboles	9.9	19.8	1.6	7.4
Unknown	1.7	.3	1.1	1.7

[1] Mineral not present in sample.

In summary, the alluvium underlying terraces 1 and 2 show marked differences in texture and other physical properties. Terrace 2 alluvial grains show no consistent change in median diameter, ranging from 0.017 to 0.023 mm, throughout the 55-mile length of the valley. Terrace 1 alluvium shows a normal increase in finer grade sizes in a downstream direction. The median diameter of alluvial grains decreases from 0.180 to 0.120 mm from the sampling section farthest upstream to the mouth of Fivemile Creek.

Frequency studies of flood-plain alluvium show that the present stream is depositing much coarser material than that found in older alluvium.

Studies of roundness and sphericity of terrace 3 gravels in the 16–32 mm range show that both indexes increase markedly from the head of the valley to the mouth. Roundness is also affected by mineral composition. Granite pebbles were the least abraded by transport, and quartz pebbles reached the highest index of roundness at the mouth of the stream.

The heavy-mineral suites in terraces 1 and 2 alluvium showed marked differences in some minerals. Zircon grains were common in terrace 2 alluvium whereas they were rare in the other. Magnetite was not found in terrace 2 samples but was abundant in terrace 1.

Differences in characteristics of the alluvium of the four fills suggest striking differences in runoff and erosional features during their deposition, and as a corollary, differences in climate during those periods.

CAUSES OF TERRACE DEVELOPMENT

It is generally agreed (Blackwelder, 1915, p. 307; Jahns, 1947, p. 42) that the formation of alluvial terraces in the erosional history of a stream that is progressively aggrading or degrading in an attempt to maintain equilibrium conditions can be attributed to one or several of the following causes:

1. Readjustment of stream grades by removal of channel obstructions or piracy in the lower reaches of the valley.
2. A series of general crustal uplifts.
3. Broad climatic variations, causing variation in the discharge of the stream, as well as in vegetational cover of the drainage basin.

We may now ask which of the above processes were responsible for conditions that now exist along Fivemile Creek. It should be remembered that the conditions observed in this valley apply in a broad sense to many other stream valleys in the Rocky Mountain and Great Plains regions.

Removal of obstructions in the channel could account for terraces within the drainage basin, but it can hardly explain the counterparts of these terraces in other stream valleys of the region, especially those of different master stream systems. Terrace 3, the highest terrace, exists along the Wind River and also along Muddy Creek a few miles to the north. The gradient of the surfaces and the texture of the alluvium would not be so uniform if they had resulted from the smoothing out of a rapids or from the elimination of a falls. A terrace system with marked similarities over a large area must be explained by some other means.

Before a detailed study was made on Fivemile Creek, the author felt that the terraces might have been preserved partly by buried bedrock spurs in the valley. If, however, the alluvial material had accumulated on the upstream side of such an obstacle and remained as a terrace facet, the gradient probably would not have been uniform. Also, the height of the terraces above the streambed would probably vary between these bedrock spurs. Such a spur cuts across the valley in SE¼

Digitized by Google

sec. 13, T. 5 N., R. 1 W. Some change in the texture of alluvium underlying terrace 1 occurs immediately upstream, but the bedrock was evidently eroded at a rate nearly equal to the downcutting of the streambed and has not caused a nick point on the profile of the stream. It seems evident, therefore, that the terrace system in this valley is the result of a more wide-spread phenomenon.

A series of crustal uplifts could cause trenching of the stream flood plains simultaneously throughout the region affected by the uplift. But, as Blackwelder (1915, p. 307) points out, the uplifts, if equal everywhere, would cause rejuvenation first in the lower courses of the streams. The terrace features developed during any given erosion cycle would be distinctly older in the lower part of the valley than farther upstream. The weathering of alluvium underlying terraces in this valley does not differ greatly from place to place, thus indicating that the terraces are the result of a process acting equally throughout the region at the same time and probably at a rapid rate. Although the terrace systems of valleys far from the mountains could be the result of uplift accompanying the mountain-building, the marked similarities from valley to valley suggest a more general cause.

In recent years the importance of climatic changes in terrace formation has been recognized increasingly. In the 19th century Gilbert stated (1877, p. 132) that, "river terraces as a rule are carved out, and not built up. They are always the vestiges of flood plains, and flood plains are usually produced by lateral corrasion." At the present time, however, many terrace systems are attributed to climatic fluctuations of glacial and postglacial time. Cotton believes (1948, p. 206) that a similarity in terrace patterns from one valley to another indicates that climatic change probably causes terracing.

The hypothesis of climatic terraces was developed by Huntington (1914, p. 23) and is often referred to as Huntington's principle. Huntington studied terrace systems in both Asia and America, and his studies in the Southwestern United States are closely related to this problem. Huntington (1914, p. 28) states that all terraces form in a similar manner as follows: The first cycle begins when the streams are deepening and widening their channels and are cutting into bedrock. Deposition is then brought about by a climatic change which encourages erosion. The process is reversed later and results in trenching of the alluvium. The vestiges of these alternating processes are terrace remnants.

The manner in which changes in climate affect stream regimen seems to be a moot question in the literature. Huntington (1914, p. 23) contends that degradation is caused by increased precipitation. Dutton (1882), Barrell (1908), and Gregory (1915, 1917) agree that downcutting is associated with a change to more humid climate. Bryan (1925, 1941) attributes valley trenching to periods of aridity. In a more recent study Leopold (1951) cites a change in rainfall intensities in New Mexico as a possible cause for arroyo cutting in the Southwest since 1880. All agree, however, that changes in climate have a marked effect on stream regimen. An increase in rainfall may increase the extent of a protective vegetative cover. This cover on the slopes reduces the ratio of runoff to infiltration. On the valley floor the vegetation may induce deposition. However, it may be that aggradation of channels proceeds more rapidly during droughts as a result of dissipation of flow in parched streambeds (Schumm and Hadley, 1957).

Some investigators have noted sand dunes as evidence for associating aridity with periods of erosion (Hack, 1942; Albritton and Bryan, 1939). There is some question whether dunes always indicate aridity. Cooper (1935) believes that dune building may be promoted by dry climate and absence of vegetation, but lowering of the water table by entrenchment can also be responsible. The dunes on terrace 1 may have been formed as Cooper suggests rather than by a change to a drier climate.

The general climatic fluctuations in Western United States in the past 9,000 years are fairly well documented by findings in the fields of botany, geology, and climatology. There is no need here to elaborate on the findings of several investigators of postglacial climatology but the following paragraph briefly summarizes the situation:

Beginning with the retreat of the last ice sheet, the climate became increasingly warmer from about 5000 B.C. to about 1000 B.C. (Willett, 1949, p. 47–50). This peak of warmth has been called the Climatic Optimum or Altithermal (Antevs, 1948). The period was characterized by widespread aridity, and most of the pluvial lakes in Western United States were lowered considerably or completely dried up (Flint, 1947, p. 494). In the next 2,350 years (2000 B.C. to A.D. 350) the climate changed to become generally wetter, and colder. This period is part of Matthes' (1939, p. 520) "Little Ice Age" which ended about A.D. 1850. Willett, however (1949, p. 49), cites historical evidence for a second warm period lasting from A.D. 400 to A.D. 1000 and he indicates that in the Western United States both lake levels and tree-ring records tend to confirm that this period was very dry. From about the year A.D. 1000 to the present, oscillations of the

Digitized by Google

climate have been small but the climate has been generally colder and wetter than the milder postglacial periods (Willett, 1949, p. 49).

PROBLEMS OF TERRACE CORRELATION

Correlation of alluvial terrace sequences from valley to valley on a regional scale has been attempted by many writers (Bryan, 1940, 1941, 1954; Hack, 1942; Albritton and Bryan, 1939; Leopold and Snyder, 1951; Leopold and Miller, 1954; Judson, 1953). Correlation and dating of terraces by these investigators generally have been based on archeological finds, differences in terrace morphology, degree of weathering, or height of terrace remnants above present stream grade. Correlating remnants of Fivemile Creek terraces within the valley presents no problem because of the distinct lithologic and topographic characteristics of the individual alluvial fills. Terraces 1, 2 and 3 are probably remnants of three distinct valley fills throughout the length of the valley. However, it is difficult to date these terraces and correlate them with similar sequences in stream valleys throughout the Great Plains from Montana to New Mexico. No archeological sites were discovered in Fivemile Creek valley that could be used to date the alluvium. Two hearths associated with bones *Bison bison* were found in the terrace 2 fill, but no artifacts were present and the bones are not diagnostic. Therefore, dating of events which may have changed stream regimen and produced the terraces is hazardous.

Blackwelder (1915, p. 307–340) describes the sequence of glaciation in the Wind River Mountains and traces several terrace deposits to glacial moraines. This sequence has been studied further by Moss (1951) and Holmes and Moss (1955) and modified by Richmond (1948, 1957). This report is not concerned primarily with the late Pleistocene terraces of outwash gravels described by these investigators, but the youngest terrace in Blackwelder's sequence (Lenore) is terrace 3 along Fivemile Creek.

Blackwelder (1915, p. 324) traced the Lenore surface to moraines of the Pinedale glacial stage of Wisconsin age, and Richmond (1948, p. 1,400) traced the seven terraces related to the morainal sequence in the Wind River Mountains down the Wind River to Wind River Canyon which is about 10 miles below the mouth of Fivemile Creek. Richmond also tentatively correlates the Wind River sequence with the work of Bryan and Ray (1940) on the Cache la Poudre River in the Front Range of Colorado. In his correlation, the Lenore terrace of Blackwelder is comparable to terrace 3 of Bryan and Ray which is traceable to the Long Draw moraine. From the evidence it seems certain that terrace 3 on Fivemile Creek (Lenore of Blackwelder, 1915) was formed during the Pinedale glacial stage of Wisconsin time. The maximum age of the Fivemile Creek terrace sequence therefore is tentatively fixed. The possible correlation of the alluvial fills underlying terraces 1 and 2 with similar sequences throughout Western United States will now be considered.

Bryan (1941, p. 228–229) established an alluvial chronology for postglacial erosional events or periods of alternate deposition and erosion in Southwestern United States, and several writers since then have correlated alluvial sequences with Bryan's original chronology. In a recent reconnaissance study of postglacial terrace sequences in eastern Wyoming, Leopold and Miller (1954, p. 38) tentatively correlate Fivemile Creek terraces with Bryan's alluvial chronology and several other studies (Leopold and Miller, 1954, p. 58–59).

Alluvial deposits underlying terrace 1 have been correlated with Moorcroft period of deposition or stability (Leopold and Miller, 1954, p. 38) in eastern Wyoming. In that correlation the Moorcroft is contemporaneous with San Pedro cultural stage in Whitewater Draw, Ariz. (Sayles and Antevs, 1941), which has been given a radiocarbon age of about 2,500 years (550 B.C. ± 310 years) (Flint and Deevey, 1951, p. 280). Leopold and Miller (1954) also correlate Moorcroft deposition with the "main fill" at Chaco Canyon, N. Mex., which Bryan (1941, p. 230; 1954, p. 37) dates as beginning before A.D. 500–700 and continuing to A.D. 1250; and the upper part of the Nakaibito formation (Leopold and Snyder, 1951, p. 11) which is tentatively dated between A.D. 900 and 1100 on the basis of Pueblo II potsherds.

The author believes that alluvium underlying terrace 1 along Fivemile Creek is younger than the alluvial fills just described. Although no datable evidence such as artifacts or vertebrate remains were uncovered, a general argument for more recent deposition of terrace 1 alluvium will be presented based on physical characteristics of the deposits. At the 18 sampling sections located throughout the valley there is no evidence of soil profile development or leaching of calcium carbonate. At two sampling sections well-preserved sandburs with sharp spines were found buried about 3 feet below the surface. This would seem to indicate that terrace 1 alluvium was deposited in the past few hundred years and is probably not contemporaneous with fills that have been reliably dated as being deposited 1,500–2,000 years ago (San Pedro stage, Ariz.).

Terrace 2 is correlated with Kaycee deposition. The Kaycee deposition has been dated and correlated by Leopold and Miller with the Chiricahua cultural

Digitized by Google

stage on Whitewater Draw, Ariz. (Sayles and Antevs, 1941) which has been given a radiocarbon age of about 4,000 years (2150 B.C., ±270 years) (Flint and Deevey, 1951, p. 280). Kaycee deposition is also correlated with the lower part of the Nakaibito formation near Gallup, N. Mex. (Leopold and Snyder, 1951), where potsherds of Pueblo I and II culture indicate the date of deposition to be approximately between A.D. 700 and 1100.

The alluvial deposits underlying terrace 2 may fit into a postglacial alluvial chronology as Leopold and Miller have suggested (1954, p. 38), but a lack of datable evidence restrains the author from making any correlation. The Kaycee formation as described by Leopold and Miller (1954, p. 10–11) and its correlatives in the Southwest generally have a well-developed soil profile to a depth of 1–2 feet. At the 17 sampling sections located on terrace 2 there was little evidence of soil profile development and surface leaching of calcium carbonate seldom exceeded 4–6 inches. Data available on rates of weathering and soil profile development (Jenny, 1941, p. 31–50) indicate that leaching of calcium carbonate from eluvial horizons and profile development undoubtedly would be present more prominently in terrace 2 alluvium if it were deposited 2,500–4,000 years ago, as suggested by the correlation chart of Leopold and Miller (1954, p. 58–59).

The modern flood plain of Fivemile Creek, in many reaches, has been formed since about 1920 according to residents of the area and personnel connected with irrigation works on the Riverton project. The present channel presumably was started by unusual floods of July and September 1923 (Follansbee and Hodges, 1925, p. 111) and the return of waste water from irrigation along the channel since 1920. Before these events the valley floor of Fivemile Creek reportedly was aggraded and without a well-defined channel and flood plain in many reaches. Although the alluvial deposit underlying the modern flood plain may be contemporaneous in part with Lightning deposition (Leopold and Miller, 1954, p. 38) the author prefers to associate it with comparable fills in eastern Wyoming that are known to be less than 100 years old (Schumm and Hadley, 1957, p. 170).

Using radiocarbon dates associated with early cultures, such as the Cochise in southern Arizona (Flint and Deevey, 1951) and dating fills with similar physical characteristics by other cultural evidence, a great disparity in age is apparent from valley to valley even within one physiographic province. For example, the San Pedro cultural stage discovered in Arizona on Whitewater Draw (Sayles and Antevs, 1941) has been assigned an age of about 2,500 years based on radiocarbon dating of charcoal found in the valley fill (Flint and Deevey, 1951). Correlation of San Pedro deposition with the upper part of the Nakaibito formation near Gallup, N. Mex., where potsherds of Pueblo I and II age (A.D. 700–1100) were found (Leopold and Snyder, 1951, p. 15) indicates a spread in dates covering about 1,700 years. When dealing with a postglacial chronology of perhaps 8,000–10,000 years in length, an age difference in deposits of 1,000–2,000 years based on datable evidence certainly precludes placing them in the same depositional phase of an alluvial sequence.

Alternating epicycles of erosion and deposition in the alluvial valleys of the semiarid West are undoubtedly related to postglacial climatic changes, but it does not seem necessary to expect the resulting alluvial fills and terraces to be contemporaneous from valley to valley. As Flint points out (1947, p. 483) it is difficult to draw climatic inferences from evidence in one stream or to infer that a climatic change will affect all streams in the same way.

In summary, even though Fivemile Creek terraces can be correlated in a general way with similar sequences in other parts of Wyoming, New Mexico, and Arizona, the author does not believe that the terraces can now be accurately dated. Definite physical similarities between Fivemile Creek terraces and other terrace sequences have been described in the literature and dated reliably on the basis of archeological evidence. However, certain incongruities in ages that have been assigned to various alluvial fills make correlation difficult.

The unweathered character of terrace 1 alluvium and the discovery of well-preserved sandburs in the fill at two localities substantiate the premise that this deposit is very recent.

The poorly developed soil profile and minor leaching of terrace 2 alluvium indicate to the author that correlation with deposits having well-developed soils and deeper leaching (Kaycee of Leopold and Miller 1954) is not warranted.

HISTORY OF TERRACE DEVELOPMENT

The question of what hydrologic conditions may have existed at the time Fivemile Creek terraces were being formed now will be considered. Factors of stream mechanics cannot always be determined for the ancient stream. Mackin (1948, p. 503) points out that, even after the type of deposit is distinguished, we cannot proceed to work directly from the grade sizes represented in the deposits to the characteristics of the

Digitized by Google

depositing stream. We may, however, draw analogies from conditions observed in modern streams.

During the formation of terrace 3 the stream was probably deepening and widening its channel and had begun cutting into bedrock. This downcutting and widening could have been relatively rapid because the shale, sandstone, and siltstone formations cropping out in the valley are generally nonresistant to erosion. Although the valley of Fivemile Creek was never glaciated, terraces which are probably the correlatives of terrace 3 have been traced to glacial moraines at the heads of many valleys in this region (Blackwelder, 1915, p. 320; Moss, 1951; Holmes and Moss, 1955; Richmond, 1948). From his work on Pacific Creek, Sweetwater County, Wyo., Moss found evidence to support the hypothesis that streams, aided by severe periglacial climate, developed terraces at the same time as the glacial streams. Thus, it is inferred that glacial climate continued long enough to allow terrace 3 to be cut to a gradient of about 26 feet to the mile. The thin veneer of gravel found on terrace 3 is probably the residual of a thicker deposit laid down at the same time that the terrace tread was formed.

After the deposition of the upper terrace gravels, some climatic change took place which caused the stream to entrench a new channel in the gravel deposit. Bryan (1941, p. 235) attributes such downcutting to periods of aridity while Huntington (1914, p. 23) contends that increased precipitation is the cause of degradation. Regardless of the climatic conditions, the stream evidently cut vertically through the gravels of the upper terrace and entrenched itself deeply in the bedrock, widening the channel and removing the gravels at many places.

A reversal of conditions started aggradation of the widened trench, filling the inner channel to a level below the upper terrace. Dark bands visible in the vertical exposure of the deposit may represent interruptions in deposition. If that interpretation is correct, the deposition of this alluvium must have taken place in several stages. The textural analysis reveals a paucity of particles coarser than sand in the sampled sections, which implies a uniform streamflow to satisfactorily explain such a deposit. Consideration must be given to the effect of climate on the stream regimen as well as the vegetative cover, which may or may not have affected the character of the deposit. A hypothetical set of stream conditions may be assumed. After the stream had entrenched itself in the bedrock to a depth below the present streambed, the regimen shifted to aggradation. The terrace 2 deposit, about 20 feet of which is exposed in the vertical section, is consistently very fine sand and silt throughout the length of the valley. A deposit of this thickness could hardly be attributed entirely to overbank silting during flood periods. To deposit 20 feet of silt over a flood plain throughout a valley 55 miles long would require an extreme change in stream level as the deposit became thicker. Also, there is not enough evidence to support the hypothesis that the deposit is eolian in origin. The alternative which seems most applicable is a stream of lower velocity than the stream that flows in the present channel. The silt was deposited from suspension possibly aided by vegetation.

Could such streamflow conditions prevail long enough to allow the accumulation of such a volume of sediment? The study of modern valley sedimentation by Happ, Rittenhouse, and Dobson (1940, p. 20–22) lists some figures for known rates of silt accumulation in stream valleys of the Southern United States. They show that between 2 known dates 25 years apart 3 feet of sediment accumulated in a valley on a gradient of about 18 feet to the mile, and that deposits in the last 100 years in some valleys may reach 8–10 feet. These figures can only be used as an example of what streams can accomplish. The author is not prepared to say whether the conditions in Fivemile Creek at the time of deposition of terrace 2 were analogous to those described by Happ, Rittenhouse, and Dobson.

The extent of flood-plain aggradation in the last 30 years has been measured by the author in several valleys in the Cheyenne River basin of eastern Wyoming and western Nebraska. The many fence lines that cross flood plains, perpendicular to the direction of flow, provide excellent measuring sections when the age of the fences can be accurately determined. On the Joss Ranch, sec. 31, T. 36 N., R. 64 W., Niobrara County, Wyo., a cross section of the flood plain along a fence line showed aggradation of 3 feet at posts that had been in place 31 years. Partly buried trees and multiple node development on grass stems also indicate that aggradation in the valley is active at the present time. On Whitehead and Prairie Dog Creeks in Sioux County, Nebr., rapid aggradation in the past 20 to 30 years can be measured with considerable accuracy on fence lines and cottonwood trees. On Whitehead Creek the flood plain has been built up as much as 4 feet in 30 years. Therefore, the accumulation of a deposit about 20 feet thick such as terrace 2 on Fivemile Creek could have been accomplished in a short time.

After the alluvium of terrace 2 had reached a depth of about 18 to 20 feet the stream regimen shifted to degradation. As the stream entrenched itself in the alluvium, downcutting apparently proceeded without much lateral corrasion. This supposition is substan-

Digitized by Google

tiated by the extensive remnants of terrace 2 standing on both sides of the stream throughout the greater part of the valley. The depth of trenching as determined by test borings in the valley show that the thickness of alluvium below the streambed is relatively thin.[1] After the stream had reached a position substantially the same as the present stream the stream regimen shifted to aggradation. The channel fill deposits that are represented by this period of aggradation reveal many sedimentary structures which give rise to speculation concerning the climatic conditions during deposition. In contrast to the older alluvium in the valley, this deposit is sandy with many stringers of coarse gravel. Torrential crossbedding is evident in many places and the over-all texture of the material indicates that it may have been deposited by a stream of seasonal high velocity and high competence. The climate during deposition might well have been semiarid with frequent storms of high intensity.

The deposit forming the lower terrace accumulated in the channel trench to a thickness of 8–10 feet. It unconformably overlies the older deposits in many places and abuts against scarps cut in the older alluvium in vertical contacts where slumping has not obscured the relationship.

After the deposit reached its present thickness, the stream regimen once again shifted to degradation. The downcutting progressed until the stream reached the position in the channel bottom very near to that of the present stream. The development of the present streambed followed the abandonment of the modern flood plain. The overbank silt deposits and channel gravels transported by stormflow which are being contributed to the flood plain at the present time make it a rather poorly defined surface in the process of formation.

REFERENCES

Albritton, C. C., and Bryan, Kirk, 1939, Quaternary stratigraphy in the Davis Mountains, trans-Pecos, Tex.: Geol. Soc. America Bull., v. 50, p. 1423–1474.

Antevs, Ernst, 1948, The Great Basin, with emphasis on glacial and postglacial times, part 3: Utah Univ. Bull., v. 38, no. 20, p. 168–191.

Barrell, Joseph, 1908, Relations between climate and terrestrial deposits, part 3: Jour. Geol., v. 16, p. 363–384.

Blackwelder, Eliot, 1915, Post Cretaceous history of the mountains of central western Wyoming: Jour. Geol., v. 23, p. 307–340.

Bryan, Kirk, 1925, Date of channel trenching (arroyo cutting) in the arid Southwest: Science, v. 42, no. 1607, p. 338–344.

——— 1940, Erosion in the valleys of the Southwest: New Mexico Quart. (November), p. 227–232.

[1] U.S. Bureau of Reclamation, 1951, Fivemile Creek bedrock profile: U.S. Bur. Reclamation, Billings, Mont., unpublished records.

Bryan, Kirk, 1941, Pre-Columbian agriculture in the Southwest, as conditioned by periods of alluviation: Assoc. Am. Geog. Annals, v. 31, no. 4, p. 219–242.

——— 1954, The geology of Chaco Canyon, N. Mex.: Smithsonian Misc. Colln., v. 122, no. 7, p. 30–38.

Bryan, Kirk, and Ray, L. L., 1940, Geologic antiquity of the Lindenmeier site in Colorado: Smithsonian Misc. Colln., v. 99, no. 2, p. 48–69.

Cooper, W. S., 1935, The history of the upper Mississippi River in late Wisconsin and postglacial time: Minnesota Geol. Survey Bull. 26, 116 p.

Cotton, C. C., 1948, Landscape: New Zealand, Whitcombe and Tombs, Publishers, p. 201–206.

Dutton, C. E., 1882, Tertiary history of the Grand Canyon district: U.S. Geol. Survey Mon. 2, 264 p.

Flint, R. F., 1947, Glacial geology and the Pleistocene epoch: New York, John Wiley and Sons, p. 487–488.

Flint, R. F. and Deevey, E. S., 1951, Radiocarbon dating of late-Pleistocene events: Am. Jour. Sci., v. 249, no. 4, p. 280–281.

Follansbee, Robert and Hodges, P. V., 1925, Floods in the Rocky Mountain region: U.S. Geol. Survey Water-Supply Paper 520–G, p. 105–129.

Gilbert, G. K., 1877, Report on the geology of the Henry Mountains: U.S. Geog. and Geol. Survey of the Rocky Mountain region, p. 132.

Gregory, H. E., 1915, The formation and distribution of fluviatile and marine gravels: Am. Jour. Sci., ser. 4, v. 39, p. 487–508.

——— 1917, Geology of the Navajo country: U.S. Geol. Survey Prof. Paper 93, 161 p.

Hack, J. T., 1942, The changing physical environment of the Hopi Indians: Peabody Mus. Nat. History Papers, v. 35, no. 1, 85 p.

Happ, S. C., Rittenhouse, Gordon, and Dobson, G. C., 1940, Some principles of accelerated stream and valley sedimentation: U.S. Dept. Agr. Tech. Bull. 695, p. 20–22.

Holmes, G. W. and Moss, J. H., 1955, Pleistocene geology of the southwestern Wind River Mountains, Wyoming: Geol. Bull. Soc. America, v. 66, p. 629–654.

Huntington, Ellsworth, 1914, The climatic factor as illustrated in arid America: Carnegie Inst. Washington Pub. 192, p. 22–28.

Jahns, R. H., 1947, Geologic features of the Connecticut Valley, Mass., as related to recent floods: U.S. Geol. Survey Water-Supply Paper 996, p. 42–43.

Jenny, Hans, 1941, Factors of soil formation: New York, McGraw-Hill Book Co., Inc., p. 31–50.

Judson, S., 1953, Geologic antiquity of the San Jon site eastern N. Mex.: Smithsonian Misc. Colln., v. 121, no. 1, 70 p.

Krumbein, W.C., and Pettijohn, F. J., 1938, Manual of sedimentary petrography: Appleton, Century, Crofts, Publishers, p. 187–220.

Leopold, L. B., 1951, Rainfall frequency, an aspect of climatic variation: Am. Geophys. Union, Trans., v. 32, no. 3, p. 347–357.

Leopold, L. B., and Miller, J. P., 1954, A postglacial chronology for some alluvial valleys in Wyoming: U.S. Geol. Survey Water-Supply Paper 1261, p. 36–38, 58–59.

Leopold, L. B., and Snyder, C. T., 1951, Alluvial fills near Gallup, N. Mex.: U.S. Geol. Survey Water-Supply Paper 1110–A, p. 11–15.

Mackin, J. H., 1948, Concept of the graded stream: Geol. Soc. America Bull., v. 59, p. 463–512.

Digitized by Google

Matthes, Francois, 1939, Report of the committee on glaciers: Am. Geophys. Union Trans., part 4, p. 520.

Moss, J. H., 1951, Early man in the Eden Valley: Pennsylvania Univ. Mus. Mon., 124 p.

Pettijohn, F. J., 1949, Sedimentary Rocks: New York, Harper and Bros., p. 53, 410.

Plumley, W. J., 1948, Black Hills terrace gravels: a study in sediment transport: Jour. Geol., v. 58, p. 554–558.

Richmond, G. M., 1948, Modification of Blackwelder's sequence of Pleistocene glaciation in the Wind River Mountains, Wyoming [abs.]: Geol. Soc. America Bull., v. 59, p. 1,400–1,401.

Richmond, G. M., 1957, Three pre-Wisconsin glacial stages in the Rocky Mountain region: Geol. Soc. America Bull., v. 68, p. 239–262.

Sayles, E. B., and Antevs, Ernst, 1941, The Cochise culture: Medallion Papers no. 29, Gila Pubelo, Globe, Ariz., 81 p.

Schumm, S. A., and Hadley, R. F., 1957, Arroyos and the semiarid cycle of erosion: Am. Jour. Sci., v. 255, p. 161–174.

Twenhofel, W. H., and Tyler, S. A., 1941, Methods of study of sediments: New York, McGraw-Hill Book Co., p. 47–136.

Willett, H. C., 1949, Long period fluctuations of the general circulation of the atmosphere: Jour. Meteorology, v. 6, no. 1, p. 34–50.

Digitized by Google

QE75
.A26
no. 352-B
(&)

AUG 16 1960

The Shape of Alluvial Channels in Relation To Sediment Type

UNIVERSITY OF CHICAGO
LIBRARY
Rosenau
SERIAL RECORD

GEOLOGICAL SURVEY /PROFESSIONAL PAPER/ 352-B

U.S. Geological Survey,

March 3, 1849

Schumm—SHAPE OF ALLUVIAL CHANNELS IN RELATION TO SEDIMENT TYPE—Geological Survey Professional Paper 352-B

QE75
F.H26
No 352-B

USGS Prof. Paper

The Shape of Alluvial Channels in Relation To Sediment Type

By S. A. SCHUMM

EROSION AND SEDIMENTATION IN A SEMIARID ENVIRONMENT

GEOLOGICAL SURVEY PROFESSIONAL PAPER 352-B

UNITED STATES GOVERNMENT PRINTING OFFICE, WASHINGTON : 1960

Digitized by Google

UNITED STATES DEPARTMENT OF THE INTERIOR

FRED A. SEATON, *Secretary*

GEOLOGICAL SURVEY

Thomas B. Nolan, *Director*

For sale by the Superintendent of Documents, U.S. Government Printing Office
Washington 25, D.C.

... GOVERNMENT
DEPOSITORY COLLECTION

Digitized by Google

CONTENTS

	Page
Abstract	17
Introduction	17
Selection of a parameter representative of sediment type	17
Methods of investigation	18
Channel shape and sediment type	20
Effect of sediment type on downstream variations in channel shape	25
Conclusions and possible applications	28
References	30

ILLUSTRATIONS

		Page
Plate 5.	Stream channels illustrating range of channel characteristics at measured cross sections . . . Facing	22
Figure 8.	Relation between width-depth ratio and weighted mean percent silt-clay (M)	21
9.	Relation between channel width and weighted mean percent silt-clay (M)	22
10.	Relation of width-depth ratio to weighted mean percent silt-clay (M) for unstable cross sections	23
11.	Relation between width-depth ratio and weighted mean percent silt-clay (M) for cross sections with channel floor covered by more than 40 percent gravel, cobbles and boulders	24
12.	Relation of width-depth ratio to M along the Smoky Hill-Kansas River	25
13.	Relation between width and depth for streams with not greatly different values of M in a downstream direction	26
14.	Relation of channel width to depth for the Smoky Hill-Kansas River	27
15.	Relation of channel width to mean annual discharge for the Smoky Hill, Republican and Kansas Rivers	28
16.	Relation of channel maximum depth to mean annual discharge for the Smoky Hill, Republican and Kansas Rivers	29

TABLE

Table 1.	Channel and sediment data	19

Digitized by Google

EROSION AND SEDIMENTATION IN A SEMIARID ENVIRONMENT

THE SHAPE OF ALLUVIAL CHANNELS IN RELATION TO SEDIMENT TYPE

By S. A. Schumm

ABSTRACT

The weighted mean percent silt-clay in the channel and banks of stable alluvial stream channels is used as a parameter (M) descriptive of the physical characteristics of sediment. Silt-clay is defined as alluvial material smaller than 0.074 mm. As the percentage of silt and clay in banks and channel increases, the shape of stream channels expressed as a width-depth ratio (F) varies according to the equation, $F=255\ M^{-1.08}$ Neither mean annual discharge nor the mean annual flood significantly affects this relation in spite of the importance of discharge to the absolute width and depth of a channel.

Downstream changes in width and depth of a stream channel are greatly influenced by sediment type. As M increases downstream along a given river, the depth increases more rapidly and the width less rapidly with discharge than if M was constant, and width-depth ratio decreases. Conversely, as M decreases downstream the depth increases less rapidly and the width more rapidly with discharge than if M was constant, and width-depth ratio increases. The downstream changes in width, depth and width-depth ratio along the Smoky Hill–Kansas River system is presented as an example of the importance of sediment type to stream regimen.

Unstable channels may be recognized by changes in width-depth ratio. In general, aggrading channels have a higher width-depth ratio than indicated by M; whereas degrading channels have a lower width-depth ratio than indicated by M.

INTRODUCTION

Lack of a simple quantitative expression of the physical properties of alluvium has hindered study of hydraulics and morphology of streams. In most studies of rivers and canals the median grain size (D_{50}) has been used as the one parameter most descriptive of sediment type. However, even although of the same median grain size, sediment samples can vary widely in composition, depending on the sorting of the sample. If well sorted, the sample may consist of one type of material, such as sand; but if poorly sorted, a sample may be composed of several types, such as silt, sand, and gravel.

Studies of the behavior of sediment grains under different physical environments reveal that there is a great change in sediment character within the range 0.05 to 1.0 mm. For example, Hjulstrom's (1935) compilation of data, concerning the critical velocity of water required to initiate movement of sediment grains of uniform material, shows that the critical velocity increases as grain size decreases below 0.1 mm and increases also with grain size above 0.5 mm. According to Hjulstrom (1935, fig. 18), the velocity required to move a particle 0.02 mm in diameter is about the same as that required to move a grain 2.0 mm in diameter. Bagnold (1954, p. 88, fig. 28) indicates that a similar relation exists between the threshold velocity of wind and grain size for windblown sand, although the zone of minimum velocity exists only for a range of about 0.07 to 0.1 mm. In addition, Rubey's (1933, p. 339, fig. 1) study of settling velocities of sediment shows that between 0.06 and 1.0 mm there is a transition zone between the viscous resistance formula (Stokes Law) and the impact-of-water formula. His analysis suggests that in being transported by water there is a fundamental difference in the behavior of sediment grains smaller than 0.05 mm from those larger than 1.0 mm.

It is the purpose of the present study to discuss the effect of one variable, sediment character, on the shape of alluvial stream channels. It is a simplification to relate any one aspect of stream morphology to one other variable, but this may be proper as long as both the writer and reader are aware that other factors may be important and that their importance may be identified as additional information becomes available.

Valuable information on the hydrology of rivers in Kansas was provided by E. R. Leeson. F. F. Zdenek made grain-size analyses for the many sediment samples and calculated the values for mean annual flood and mean annual discharge for rivers other than those in Kansas. The writer also wishes to acknowledge the suggestions for improvement of the manuscript made by the following: W. M. Borland, Elliott Flaxman, C. R. Miller, and M. G. Wolman.

SELECTION OF A PARAMETER REPRESENTATIVE OF SEDIMENT TYPE

To obtain a valid expression of sediment type perhaps some grain-size parameter within the critical range 0.05 to 1.0 mm might be selected which would be more descriptive of sediment properties than median grain size alone. For example, Burmister (1952) has

Digitized by Google

prepared tables from which one may estimate the permeability and drainage characteristics of a soil from the grain size below which 10 percent of the sample is finer (Hazen's effective size, D_{10}). Other investigators have shown that the susceptibility of soils to erosion (Bouyoucos, 1935) and the strength of cohesive soils (Trask, 1959) are related to a sand-clay ratio.

In this study the percentage of silt and clay (taken as that part of each sample passing a 200-mesh sieve, and equivalent to sediment grains smaller than 0.074 mm) was selected for comparison with stream-channel characteristics. This selection avoids the use of an absolute value for grain size, the importance of which can be masked by sorting of the sample. In addition, the value can be readily obtained from the cumulative grain-size curve.

Burmister (1952, p. 20) gives some physical reasons for the selection of the 200-mesh sieve as the boundary between silt-clay and sand. He states that the soil becomes less well drained and that capillarity increases with increase in material passing the 200-mesh sieve; in addition, the 200-mesh sieve is the practical lower limit of sieving for grain-size analyses. Any grain size between 0.05 mm and perhaps 0.1 mm could be used as the boundary between silt-clay and sand; however, it is convenient to use either the 200-mesh (0.074 mm) or 230-mesh (0.0625 mm) sieves, and the 200-mesh sieve was selected for use here.

If, as suggested above, sediment less than 0.074 mm greatly influences the physical properties of sediment, then this fine fraction of the sample may be considered as the matrix in which the remainder of the sediment is fixed. The data available show that, in general, D_{10} decreases as percentage of silt and clay increases. Burmister's work (1952) indicates that a smaller value of D_{10} is associated with lower permeability and higher cohesion, supporting the suggestion that this fraction of the sediment is most effective in increasing the resistance of alluvium to erosion.

METHODS OF INVESTIGATION

Assuming that the shape of a stream channel depends on the resistance of sediment composing the perimeter of the channel and the erosion potential of stream discharge, then sampling of bank and channel sediment at stable channel cross sections is necessary. Data were assembled for 90 cross sections, most of which were at or near Geological Survey gaging stations. Generally the gaging stations are located at stable reaches of the river. However, they often are located at bridges which might be assumed to affect the shape of the cross section. In such situations, wherever practical, the samples were collected some distance upstream or downstream from the bridge. Sometimes, however, the depth of water necessitated obtaining samples and water depth from the bridge by using a small clam-shell type dredge.

At most sections only the width and depth of the channel were measured. At others a survey was made of the channel cross section. The measurement of width and depth was to some extent subjective. Depth was measured to the lowest part of the channel from the edge of the first surface or bank above the channel floor. It is, therefore, a maximum depth. Width was measured from the edge of this bank to the corresponding elevation on the opposite side of the channel. In general, the upper limit of the measured depth could be selected not only as the edge of a terrace or bank but also as the lower edge of permanent vegetation and the upper limit of fairly recent deposition or erosion along the sides of the channel.

The gradient of the channel at the cross sections was measured with a hand level for many locations. For others, the gradient was measured on large scale topographic maps.

Composite sediment samples were taken from the channel floor and both banks. In general, the surface inch of the channel and banks was sampled along the selected cross sections; however, when the clam-shell dredge was used the samples often included a depth as much as 4 inches of channel material. Depending on channel width, samples of channel sediment were taken from 10 to 20 points across the stream.

In the laboratory the samples were subjected to a standard grain-size analysis. The samples were first sieved and if they contained more than 20 percent silt-clay were then prepared for hydrometer analysis. One important deviation from the usual procedure was made to aid in the dispersion of the samples (I. S. McQueen and R. F. Miller, oral communication). Fifty grams of the sediment was placed in 700 to 800 ml of distilled water and allowed to stand overnight. The liquid was then decanted, removing most of the salts that might prevent total dispersion of the sample by sodium hexametaphosphate. The percentages of silt and clay in bank and channel samples, as well as the median-grain size, were taken from the plotted cumulative grain-size curves of each sample.

The sediment composing the perimeter of each channel is expressed as a weighted mean percent silt-clay, designated M, which is calculated as follows:

$$M=\frac{Sc\times W+Sb\times 2D}{W+2D}$$

in which Sc is percentage of silt and clay in channel alluvium, Sb is percentage of silt and clay in bank alluvium, D is channel depth, W is channel width.

Digitized by Google

Calculations of the width-depth ratio and M were made by slide rule and are presented in table 1 with other data on the cross sections and sediment. Data were collected at 90 cross sections, but it was later discovered that the channels were unstable at some of these cross sections. Data from 10 unstable channels were segregated from those for the stable channels because of: (a) channel aggradation (4 sections), (b) scour below a dam or a concrete ford (2), (c) bedrock exposed in the channel (2), (d) bridge construction upstream (1), and (e) backwater effects (1 section; see table 1, cross sections 81–90).

In addition, 11 other cross sections are segregated from the 69 stable sections listed in table 1, for these channels contain a high percentage of gravel, cobbles, and even boulders (table 1, cross sections 70–80). Therefore, unless otherwise stated this study is concerned primarily with channels formed in alluvium containing only small amounts of gravel and cobbles. The 11 cross sections containing the coarser sediment and the 10 unstable sections will be discussed separately.

Mean annual flood (recurrence interval 2.33 years) and mean annual discharge were obtained from data published in Geological Survey water-supply papers and unpublished reports for those sections at or near gaging stations.

TABLE 1.—*Channel and sediment data*

[Location numbers in parentheses for cross sections 1–14 are author's original cross-section numbers]

Cross section	Location	Median grain size, D_{50} (mm)	Silt-clay in bank (percent)	Silt-clay in channel (percent)	Weighted mean silt-clay, M (percent)	Width (feet)	Depth (feet)	Width-depth ratio (F)	Gradient (S)	Mean annual flood (cfs)	Mean annual discharge (cfs)	Drainage area (sq mi)
	Sage Creek, S. Dak.:											
1	(2)	0.06	98	55	73	16	7	2.3	0.0055	—	—	1.7
2	(3)	.06	93	66	79	20	7	2.9	.0045	—	—	3.4
3	(4)	.12	96	40	64	31	5	6.2	.0045	—	—	9.5
	Sand Creek, Nebr.:											
4	(4)	.72	70	14	23	75	7	10.7	.0015	—	—	17.9
5	(5)	.73	60	15	22	65	7	9.3	.003	—	—	22.2
6	(6)	.35	65	10	20	36	4	9.0	.001	—	—	22.5
	Arroyo Calabasas, N. Mex.:											
7	(A)	.84	18	3	4.1	79	3	26.3	.013	—	—	2.8
8	(6)	.60	26	3	4.8	92	4	23.0	.009	—	—	24.2
9	(7)	.75	16	5	5.8	100	4	25.0	.011	—	—	26.8
	Bayou Gulch, Colo.:											
10	(3)	.68	13	4	4.4	130	3	43	.010	—	—	19.7
11	(6)	.55	6	4	4.1	126	1.5	85	.016	—	—	22.9
	Medano Creek, Colo.:											
12	(1)	.24	.5	1	1	340	2	170	.017	—	—	25.8
13	(2)	.24	.5	1	1	800	3	267	.019	—	—	26.1
14	(3)	.24	.5	.5	.5	570	2.5	228	.016	—	—	28.8
15	Saline River at Russell, Kans.	3.57	98	5.7	11	93	3	31	—	4,300	88.2	1,502
16	Paradise Creek near Paradise, Kans.	.50	74	5	20	32	7.8	4.1	.001	1,300	11.1	212
17	North Fork Solomon River near Downs Kans.	.60	89	1.2	16	57	8.6	9.6	.0006	3,000	151	2,390
18	Solomon River at Bennington (Niles), Kans.	.41	90	4	11	112	5	22	—	7,000	558	6,770
19	Prairie Dog Creek at Norton, Kans.	.60	82	1.5	19	45	6.2	7.2	.0005	2,600	35.2	721
20	Sappa Creek at Stamford, Nebr.	.60	97	2	28	43	6.0	7.2	.0013	1,800	111	3,840
21	Sappa Creek at Beaver City, Nebr.	.70	96	17	43	26	6.3	4.1	[illegible]	1,350	[illegible]	1,500
22	Beaver Creek at Beaver City, Nebr.	.70	95	3	19	40	4.5	8.9	.001	1,000	28.8	2,080
23	Beaver Creek at Ludell, Kans.	1.10	95	2.5	26	28	8.0	3.5	.001	450	12.5	1,460
24	Frenchman Creek at Hamlet, Nebr.	.27	92	8.7	31	36	6.5	5.5	.0013	860	[illegible]	1,480
25	Blackwood Creek at Culbertson, Nebr.	.02	91	75	81	27	8.4	3.2	[illegible]	690	5.8	290
26	Red Willow Creek near Red Willow, Nebr.	.11	91	30	45	45	7.1	6.3	.001	2,220	43.1	400
27	South Loup River near Cumro, Nebr.	.25	80	9.4	16	143	7.3	19.6	.003	2,080	165	1,340
28	Niobrara River near Colclesser, Nebr.	[illegible]	47	2	2.2	224	3.4	65.9	.008	—	—	2,000
29	White River at Chadron, Nebr.	.15	86	22.5	56	25	[illegible]	2.5	—	880	20.4	676
30	White River at Interior, S. Dak.	.50	80	3	5.3	393	5.5	80.6	[illegible]	10,900	302	—
31	Cheyenne River at Edgemont, S. Dak.	.75	56	.6	3	221	5.0	44.2	.0025	3,660	113	7,143
	Smoky Hill-Kansas Rivers system											
32	Willow Creek near Cheyenne Wells, Colo.	1.10	72	3	16	15	1.7	8.8	—	—	—	—
33	Smoky Hill River near Arapahoe, Colo.	.85	49	3	6.1	65	2.3	28	0.008	—	30 (est)	—
34	Smoky Hill River near Sharon Springs, Kans.	.41	25	4	4.5	300	2.3	80	—	—	—	—
35	Smoky Hill River at Russell Springs, Kans.	1.30	21	2	2.4	263	3.0	88	—	—	—	—
36	Smoky Hill River at Gove, Kans.	.60	63	3	4.3	236	2.6	90	—	—	—	—
37	Smoky Hill River near Arnold, Kans.	.98	30	2	2.4	345	2.5	138	—	5,800	86.2	5,220
38	Smoky Hill River near Russell, Kans.	.61	76	1	5.3	115	3.5	33	.00066	8,000	215	6,965
39	Smoky Hill River at Dorrence, Kans.	1.20	69	.5	4.4	130	4.0	33	.0007	—	—	—
40	Smoky Hill River near Kanopolis (Longley), Kans.	.63	96	4	14	92	5.5	17	.0005	9,200	314	7,857
41	Smoky Hill River near Bridgeport (Lindsborg), Kans.	.40	85	3	13	60	5.0	14	—	6,750	240	8,110
42	Smoky Hill River at Abilene, Kans.	.038	97	87	89	125	18	7	—	11,800	1,254	18,830
43	Smoky Hill River near Junction City, Kans.	1.20	90	.5	6	152	5.0	31	.0004	13,000	1,454	19,900
44	Kansas River at Wamego, Kans.	.70	93	1	2.6	636	10	64	.0006	39,000	4,398	55,240
45	Kansas River near Topeka, Kans.	.75	87	.5	3	800	15	44	.0005	48,000	5,155	56,710

Digitized by Google

TABLE 1.—*Channel and sediment data*—Continued

[Location numbers in parentheses for cross sections 1-14 are author's original cross-section numbers]

Cross section	Location	Median grain size, D_{50} (mm)	Silt-clay in bank (percent)	Silt-clay in channel (percent)	Weighted mean silt-clay, M (percent)	Width (feet)	Depth (feet)	Width-depth ratio (F)	Gradient (S)	Mean annual flood (cfs)	Mean annual discharge (cfs)	Drainage area (sq mi)
	Republican River system											
46	Arikaree River near Arikaree, Colo	1.10	82	3	4.7	206	2.2	94	...	...	...	...
47	Arikaree River at Haigler, Nebr	.25	66	3	8	68	3.0	23	0.002	3,500	19.5	1,460
48	Republican River near Stratton, Nebr	.38	31	3	3.4	400	3.0	133	...	...	...	...
49	South Fork Republican River near Benkleman, Nebr.	.48	44	1.5	3.4	100	2.3	43	.002	1,300	86.8	2,880
50	Republican River near Benkleman, Nebr	.26	23	6	6.7	123	2.5	49	.008	2,175	105	4,770
51	Republican River near McCook, Nebr	.52	88	.5	4.4	115	2.7	43	.009	...	...	5,760
52	Republican River near Bostwick (Hardy), Nebr.	.63	39	1	2.8	154	5.0	31	.0008	12,000	848	22,400
53	Republican River at Concordia, Kans	.70	31	.3	1.4	280	5.0	80	.0007	13,000	...	23,540
54	Republican River at Junction City, Kans	.60	49	1	3.4	300	6.5	46	.0007	15,000	1,000	24,900
	Powder River system											
55	South Fork Powder River near Kaycee, Wyo	[illegible]	71	9	11.3	119	2.3	52	0.004	3,900	35	1,150
56	Middle Fork Powder River above Kaycee, Wyo.	22.0	60	14	20	35	2.5	14	.005	574	58	450
57	Middle Fork Powder River near Kaycee, Wyo.	.40	69	15	23	47	4.4	11	.0015	1,650	128	980
58	Powder River below Arvada, Wyo	.21	70	4	6.5	175	3.5	50	.0011	...	...	...
59	Powder River near Locate, Mont	.42	58	13	16	234	4.5	52	...	9,400	639	...
60	Crazy Woman Creek near Arvada, Wyo	.50	75	2	17	33	4.4	7.5	...	1,150	40	956
61	Little Powder River at Broadus, Mont	4.10	82	5.5	22	40	5.5	7.3	...	1,280	89	...
62	Bighorn River near Kane, Wyo	.16	35	20	21	220	8.5	26	...	16,100	2,588	15,900
63	Badwater Creek near Lysite, Wyo	.43	47	3	5.7	50	2.3	22	.0037	...	...	...
64	Badwater Creek at Lysite, Wyo	.34	56	5	7.3	100	2.5	44	.0037	...	...	...
65	Owl Creek near Thermopolis, Wyo	.21	69	2	14	35	3.9	[illegible]	.0015	585	34	484
66	Cottonwood Creek at Winchester, Wyo	1.0	15	8	3.4	133	3.5	38	...	...	...	...
67	Gooseberry Creek at Pulliam, Wyo	8.0	45	2.5	5.7	59	2.4	25	.006	311	10	371
68	Greybull River near Basin, Wyo	.50	72	7	9.9	134	3.1	43	.0015	2,140	178	1,130
69	Bates Creek near Alcova, Wyo	.90	63	11	15	69	2.8	25	.0035	600	16	377
	Gravel streams eliminated [1]											
70	Powder River at Moorhead, Mont	...	65	7	9.2	212	4.0	53	0.0016	7,450	466	...
71	Powder River at Broadus, Mont	...	38	11	12	380	5.0	76	.0014	...	...	...
72	Red Fork at Barnum, Wyo	...	77	1.5	9.6	35	2.5	14	.003	640	30	142
73	Clear Creek at Buffalo, Wyo	...	35	.06	2.1	60	1.9	31.5	.004	...	...	120
74	Tongue River near Acme, Wyo	...	38	.8	3.7	100	4.3	23.3	.001	3,450	401	894
75	Little Bighorn River at Hardin, Mont	...	59	1.0	6.3	91	4.5	20	...	1,820	260	...
76	Little Bighorn River at Lodgegrass, Mont	...	49	.5	5.2	60	3.5	17	.0023	...	...	...
77	Popo Agie River near Riverton, Wyo	...	37	.9	4.6	100	5.5	18	...	4,910	602	2,010
78	Little Popo Agie River near Lander, Wyo	...	9	.5	1.3	34	2.1	16.2	.001	...	...	106
79	Horseshoe Creek near Glendo, Wyo	...	85	1.0	7.5	64	2.7	23.7	.0025	525	22	203
80	North Fork Powder River near Kaycee, Wyo	...	56	.3	16	21	4.0	5.2	...	...	...	...
	Miscellaneous sections eliminated [1]											
81	Saline River near Salina, Kans	0.013	92	91	91	56	10	5.6	...	...	...	...
82	White River near Rocky Ford, S. Dak	1.10	88	1.2	5.1	170	4	42.5	...	...	...	...
83	Smoky Hill River near Weskan, Kans	.78	14	3	[illegible]	36	3	12	...	...	...	...
84	Smoky Hill River near Elkader, Kans	1.20	55	4	[illegible]	500	4	125	0.006	3,000	32.1	3,560
85	Smoky Hill River near Ellis, Kans	.72	18	.5	1.9	72	3	[illegible]	...	6,300	97.7	5,630
86	Republican River near Naponee, Kans	.62	47	.5	3.6	127	4.5	28	.0007	11,350	726	...
87	Powder River near Sussex, Wyo	.07	64	51	52	177	3.7	[illegible]	.0008	5,850	[illegible]	3,090
88	Powder River near Arvada, Wyo	.15	78	32	34	170	4.5	38	[illegible]	8,600	382	6,050
89	Badwater Creek at Bonneville, Wyo	.17	22	7	7.5	291	3	97	...	1,280	8.37	700
90	Badwater Creek near Bonneville, Wyo	.37	21	7	7.3	224	2.5	89.5	...	...	...	...

[1] Sections not plotted on figure 8.

CHANNEL SHAPE AND SEDIMENT TYPE

The shape of each cross section expressed as a dimensionless width-depth ratio is plotted against M in figure 8 for 69 cross sections (table 1). The correlation between channel shape and sediment is such that

$$F=255\ M^{-1.08}$$

where F is the channel shape expressed as a width-depth ratio and M is the weighted mean percent silt-clay. Neither the percentage of silt and clay in the banks nor in the channel alone show a correlation with width-depth ratio.

The wide range of channel shapes represented on figure 8 suggests that for alluvial channels in which pebbles and gravel cover only negligible parts of the channel, the shape of the channel is dependent on sediment type expressed as M. It is interesting to note that for those sections near gaging stations, the mean annual discharge ranged from 20 to 5,150 cfs (cubic feet per second). In addition, many of the streams are ephemeral, in contrast to the perennial flow of the Smoky Hill, Kansas, and Republican Rivers. Drainage area ranges from about 1.7 square miles for the smallest ephemeral stream to 56,710 square miles for the Kansas River at Topeka. In spite of the wide range in stream

Digitized by Google

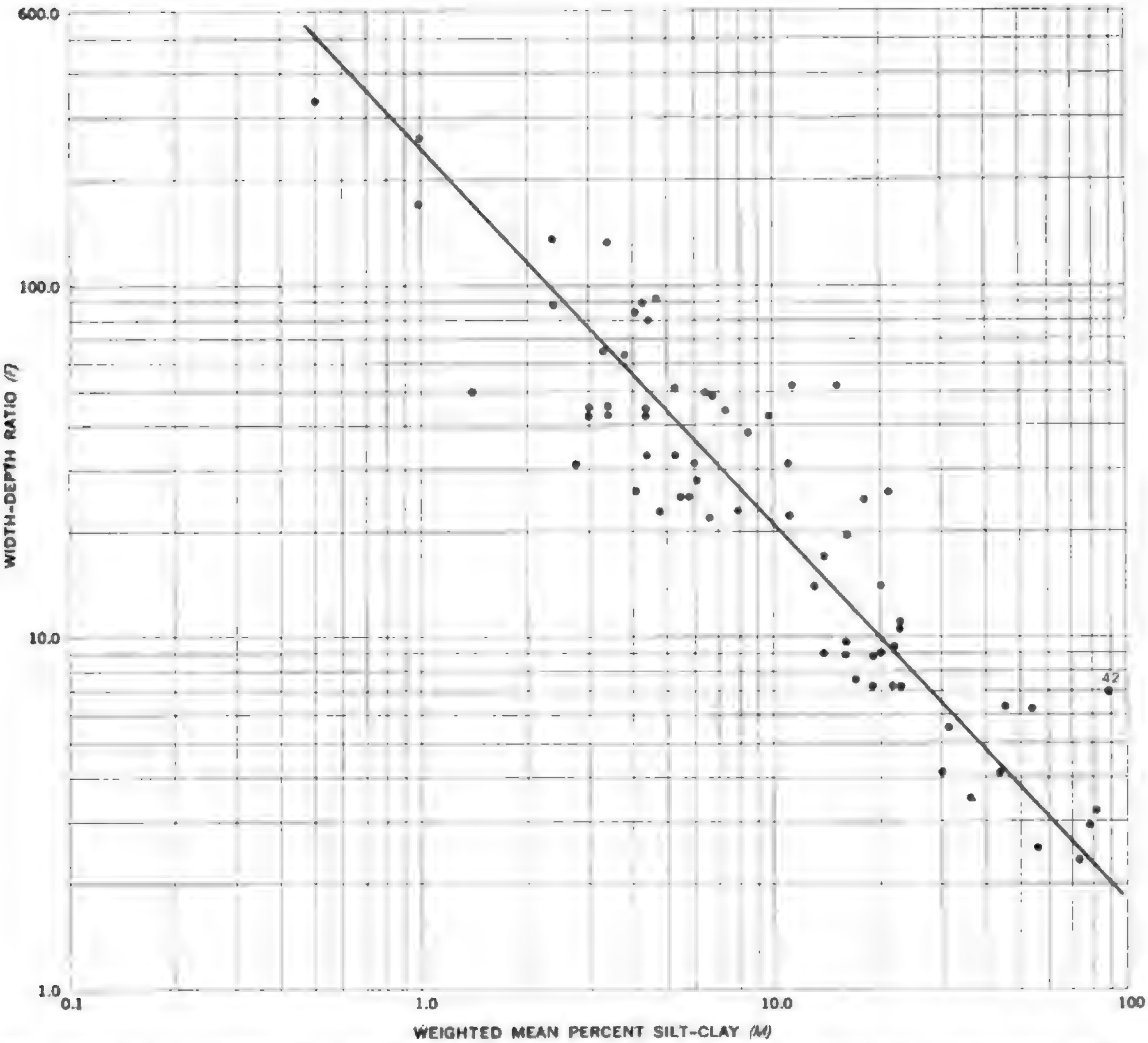

FIGURE 8.—Relation between width-depth ratio and weighted mean percent silt-clay at different cross sections. The regression line was determined graphically. Standard error is 0.202 log units, and correlation coefficient is 0.91. Point 42 is for Smoky Hill River at Abilene, Kans.

regimen and sediment type, the correlation coefficient for the regression line is 0.91. The variety of stream types represented are illustrated in plate 5 *A–F*.

The correlation of figure 8 shows that channels containing little silt-clay are relatively wide and shallow; whereas those composed predominantly of silt-clay are relatively narrow and deep. The correlation seems to justify the selection of M as a parameter descriptive of sediment characteristics. A plot of the median grain size against percentage of silt and clay in the channel samples shows no correlation, indicating that median grain size has no relation to channel shape for the range of channels investigated.

545323—60——2

The scatter of points on figure 8, although not excessive, may be partly explained on the basis of normal stream variability. Note that the scatter of points appears greater where M is less than 25, if point 42 is disregarded. Sandy streams are generally unstable in that they may scour or deepen their channels during floods. In any event, changes in channel elevation of 1 foot are common after a flood. Where the channels are hundreds of feet wide such a small change in depth causes a relatively large change in the width-depth ratio and thus greater scatter of the points representative of sandy channels. Point 42 on figure 8 is for the Smoky Hill River at Abilene. The introduction of

Digitized by Google

large amounts of silt-clay into this reach of the river markedly alters its appearance (pl. 5*E*). This may cause point 42 to lie well above the curve, but the gaging-station records suggest little change in gage height in this reach, and it was not eliminated as were sections 81 to 90.

Also more refined techniques might further reduce the scatter. For example, channel maximum depth might be replaced by a mean depth, obtained by dividing the area of cross section by width. Mean depth was calculated for 20 sections at which the cross-sectional area was known. Where mean depth was used to calculate width-depth ratio, the ratio increased on the average by 1.5. However, neither the slope of the regression line nor the scatter about the regression line were changed.

It is hazardous to attempt to extrapolate the relationship of figure 8 as a general law for alluvial channel shape, but it is interesting to note that Rubey's (1952) comparison of the Illinois and Mississippi Rivers reveals differences similar to those noted between the sections characterized by high M and low M in this study. Fisk (1944, p. 50) concluded from studies of the alluvial valley of the Mississippi River that the channel is wide and shallow where the river flows through sandy deposits and conversely is deep and narrow in the fine-grained materials of the deltaic plain. Most investigators have recognized from experience that sandy channels are wide compared with those cut in silty or clayey materials (Leopold and Maddock, 1953, p. 46).

The reason for the relation between channel shape and percentage of silt and clay (fig. 8) is found in studies made by hydraulic engineers. Lane (1937, p. 124) states, "* * * the greater the width-depth ratio the greater will be the ratio of the velocity acting on the bottom to that acting on the sides of a channel." Where a narrow trench is cut in an alluvial valley, the tractive forces acting on the channel sides will be great, causing widening of the channel. Widening will continue until the resistance of the banks to scour prevents it. If the material in which the channel is cut is highly cohesive (has a high percent of silt-clay) the channel will be narrow, but if the alluvium lacks cohesion (has a small percent of silt-clay) the channel will widen to a greater extent. Canals that carry a high bedload in friable or easily eroded material require high velocities on the bed to move the load and low

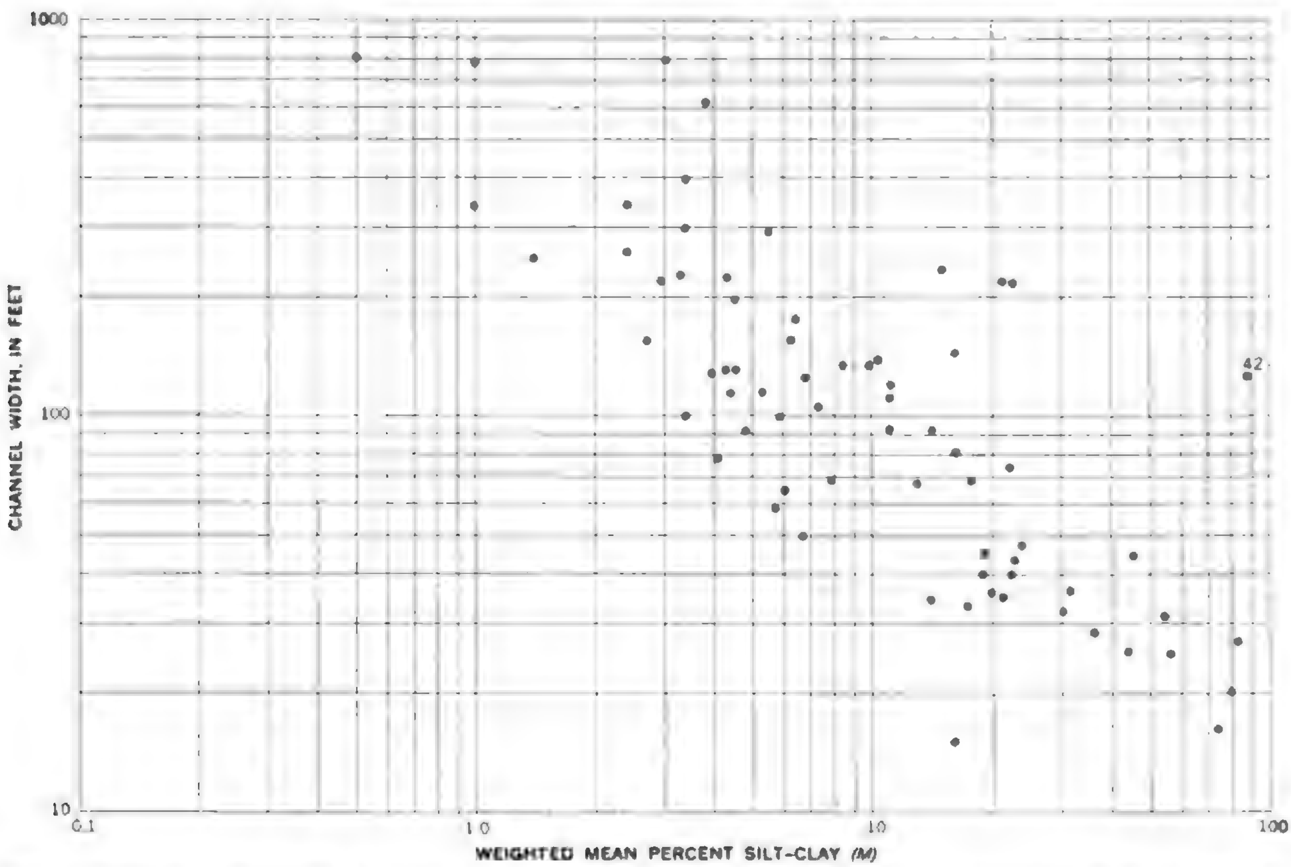

FIGURE 9.—Relation between channel width and weighted mean percent silt-clay at different cross sections (M). Point 42 is for the Smoky Hill River at Abilene, Kans.

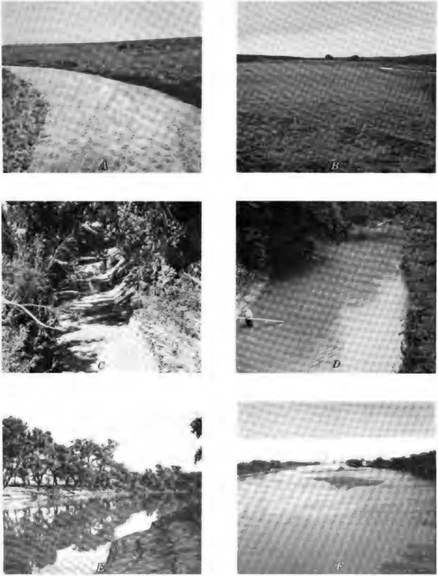

STREAM CHANNELS ILLUSTRATING RANGE OF CHANNEL CHARACTERISTICS AT MEASURED CROSS SECTIONS

A, Smoky Hill River near Arapahoe, Colo. (cross section 33); *B*, Smoky Hill River above Cedar Bluff Reservoir, Kans. (cross section 37); *C*, White River near Chadron, Nebr. (cross section 29); *D*, Sappa Creek at Stamford, Nebr. (cross section 20); *E*, Smoky Hill River near Abilene, Kans. (cross section 42); *F*, Kansas River near Topeka, Kans. (cross section 45).

Digitized by Google

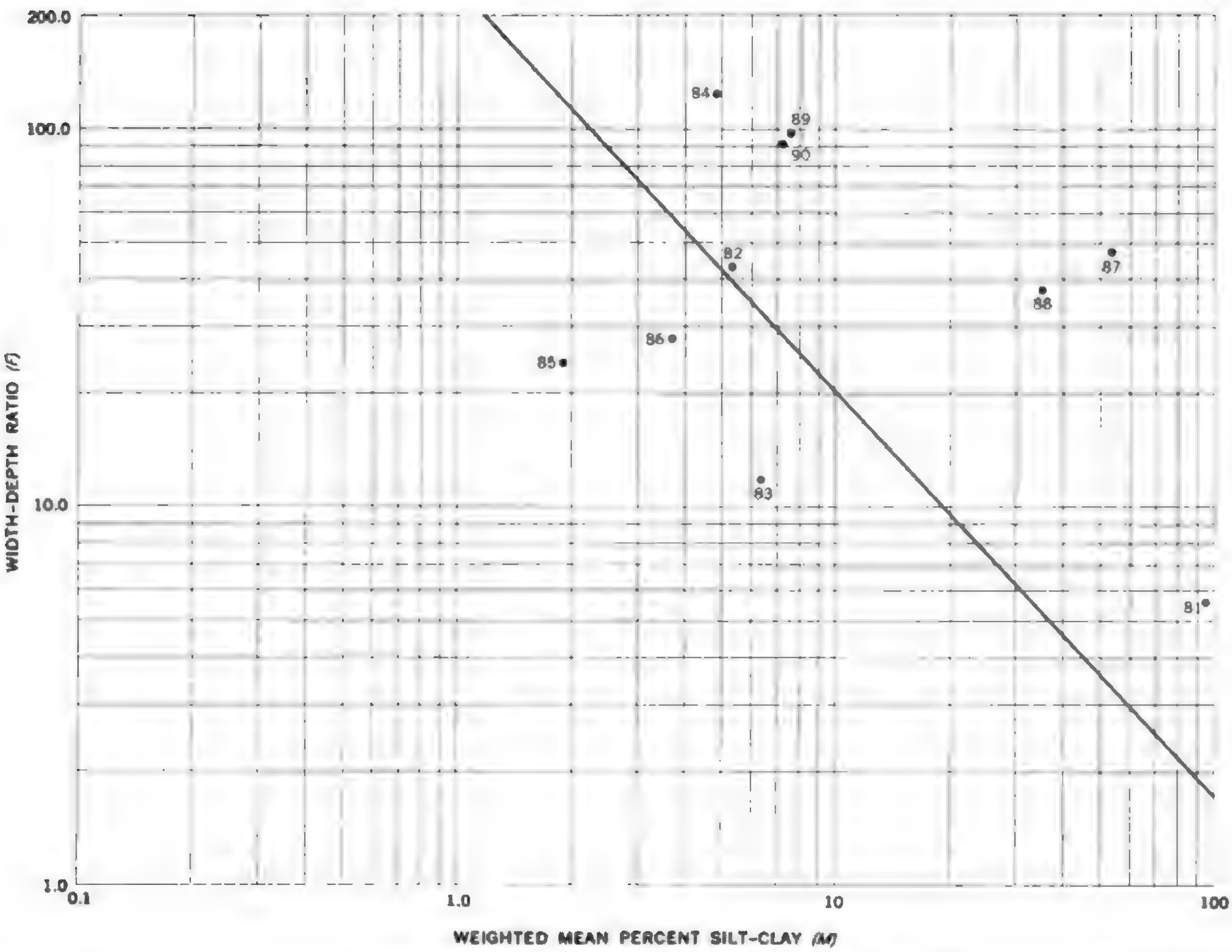

FIGURE 10.—Relation of width-depth ratio to weighted mean percent silt-clay (*M*) for unstable cross sections. Numbers refer to cross sections listed in table 1. Regression line is that determined from data on figure 8.

velocities along the banks to prevent cutting them, thus a high width-depth ratio is required for a stable channel in friable material (Lane, 1937, p. 124).

It is also noteworthy that the shape of the channels seems to be independent of discharge. Plots of mean annual flood and mean discharge against width-depth ratio showed no recognizable correlation. The absolute size of the channel, the width and depth in feet, is related to mean discharge (Leopold and Maddock, 1953), but the ratio of width to depth is apparently determined by sediment type (*M*) for the channels sampled. The data show a correlation between channel width and *M* (fig. 9), but the scatter of points is such that the width may vary as much as 10 times for any one value of *M*. Nevertheless, the lack of correlation between channel depth and *M*, suggests that perhaps channel width is more sensitive to changes in *M* than depth.

A discussion follows on the 21 cross sections eliminated because of instability or the presence of excess coarse sediment on the channel floor.

In figure 10 the width-depth ratio is plotted against *M* for the 10 cross sections eliminated from prior discussion. The regression line of figure 8 has been drawn on figure 10 to show where the 10 points lie in relation to the regression line for stable channels. The two cross sections which show scour either downstream from a dam (85) or downstream from a concrete ford (83) lie far below the regression line. The two cross sections in which bedrock was exposed (82, 86) lie close to the regression line; whereas, those in which the rating curves of gage height to discharge show a progressive increase in gage height with constant discharge, suggesting aggradation, (84, 88, 89, 90) lie above the curve. The location of point 81 is probably the result of recorded backwater effects due to floods on the Smoky Hill River,

Digitized by Google

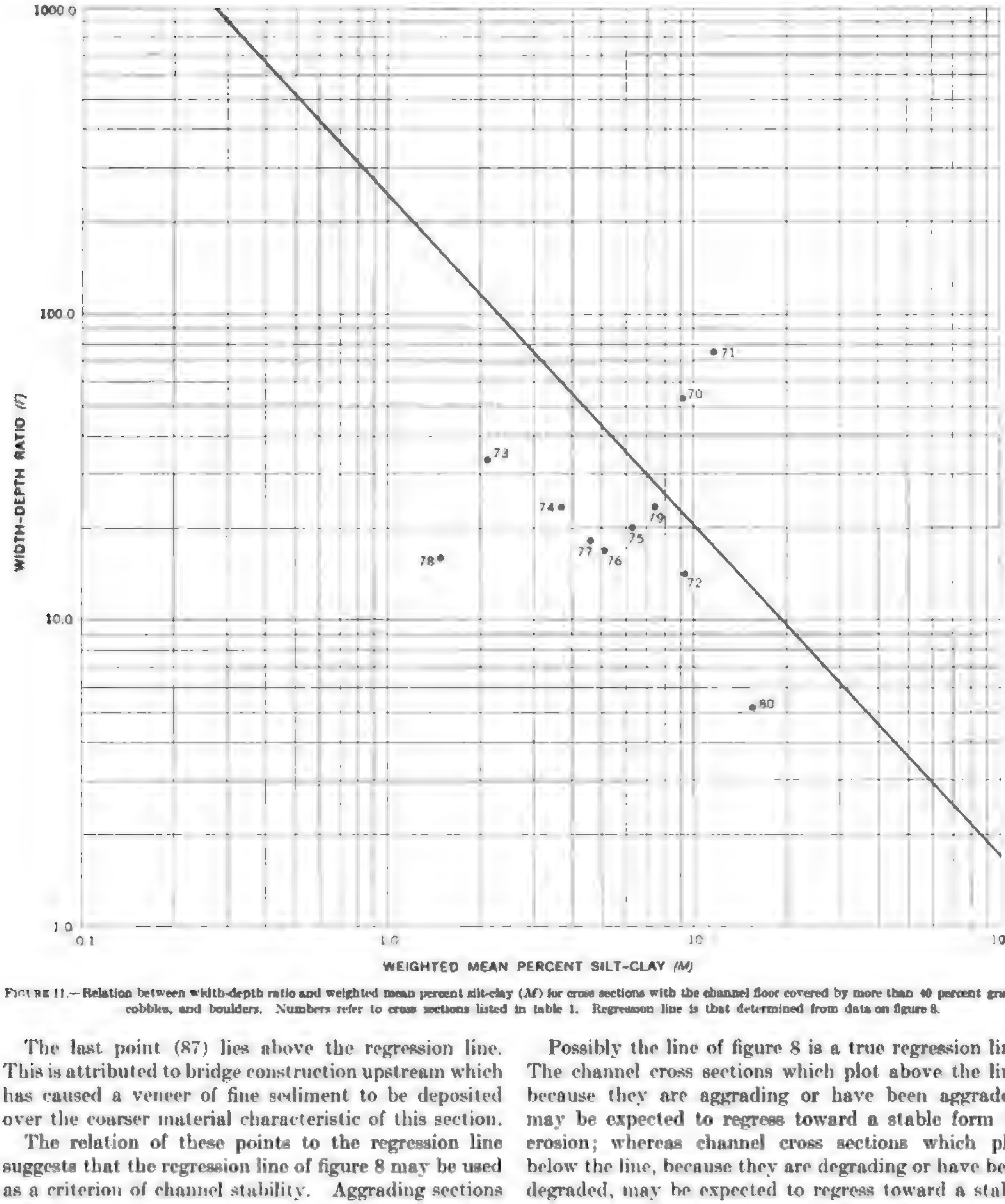

FIGURE 11.—Relation between width-depth ratio and weighted mean percent silt-clay (M) for cross sections with the channel floor covered by more than 40 percent gravel, cobbles, and boulders. Numbers refer to cross sections listed in table 1. Regression line is that determined from data on figure 8.

The last point (87) lies above the regression line. This is attributed to bridge construction upstream which has caused a veneer of fine sediment to be deposited over the coarser material characteristic of this section.

The relation of these points to the regression line suggests that the regression line of figure 8 may be used as a criterion of channel stability. Aggrading sections will have a larger width-depth ratio than expected on the basis of M; whereas degrading channels will have smaller width-depth ratios than expected on the basis of M alone.

Possibly the line of figure 8 is a true regression line. The channel cross sections which plot above the line, because they are aggrading or have been aggraded, may be expected to regress toward a stable form by erosion; whereas channel cross sections which plot below the line, because they are degrading or have been degraded, may be expected to regress toward a stable form by a combination of bank erosion and aggradation.

The other cross sections not plotted in figure 8 are those with appreciable gravel along the perimeter of the channel cross section. All of these sections have

Digitized by Google

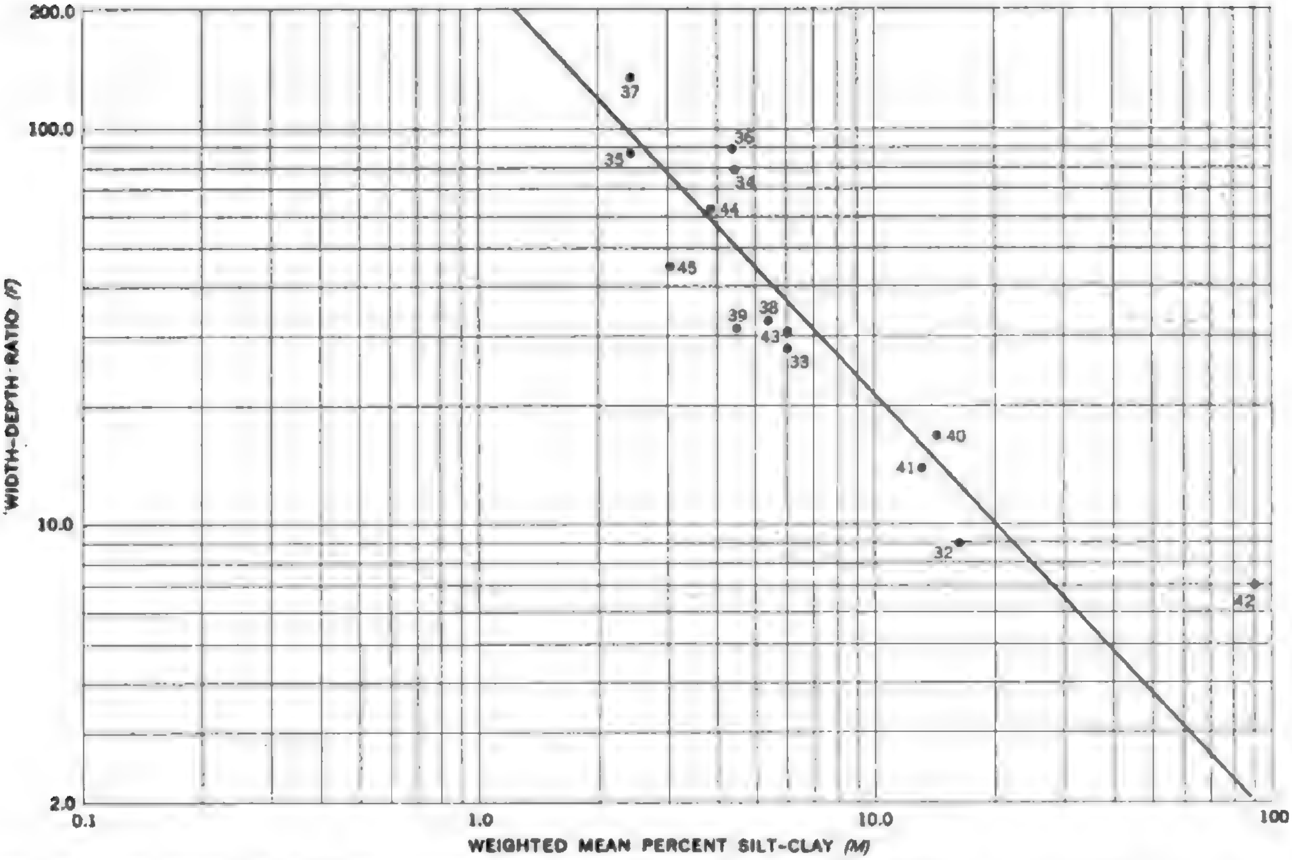

FIGURE 12.—Relation of width-depth ratio to M along the Smoky Hill-Kansas River. Regression line is that determined by data on figure 8. Numbers refer to cross sections listed in table 1.

greater than 40 percent of the channel floor covered by coarse sediment. Data from these cross sections are plotted on figure 11. Only three points lie far from the regression line. The remaining eight points fall reasonably close to but below the regression line. The reason for this is not clear for it was expected that a gravel or cobble veneer would prevent bottom scour and result in a higher width-depth ratio.

However, data compiled on the width and depth of irrigation canals [1] show that channels and banks containing coarse noncohesive materials are protected by the larger sizes of alluvium. Therefore, the width-depth ratio of channels containing gravel and cobbles should be relatively low as seen on figure 11.

EFFECT OF SEDIMENT TYPE ON DOWNSTREAM VARIATIONS IN CHANNEL SHAPE

This discussion has been concerned solely with data from a great variety of streams. Most studies of fluvial morphology and regime canals deal with the relations between discharge and channel dimensions along a single river or canal. The relation shown in figure 8 suggests that the effect of M on downstream changes in channel dimensions is important.

The Smoky Hill-Kansas River system is of particular interest with regard to the effect of downstream variations of M to channel shape, width, and depth. To illustrate this M and width-depth ratio for 14 cross sections are plotted on figure 12.

In eastern Colorado and western Kansas the Smoky Hill River is wide, shallow, ephemeral (pl. 5*A*, *B*; fig. 12, points 33 to 37), and M is generally less than 10. M increases in central Kansas to about 12 (fig. 12, points 40 and 41); between Salina and Abilene the Saline and Solomon Rivers introduce large amounts of silt-clay into the river, and M increases sharply to more than 80 (pl. 5*E*; fig. 12, point 42). Downstream from Abilene the river becomes progressively more sandy (fig. 12, point 43) to the confluence with the Republican River, the beginning of Kansas River. The Republican River introduces large amounts of sand into the Kansas River, and M decreases to about 3 (pl. 5*F*; fig. 12, points 44, 45).

[1] Simons, D. B., 1957, Theory and design of stable channels in alluvial materials: Unpub. thesis, Colorado State Univ., 394 p.

Digitized by Google

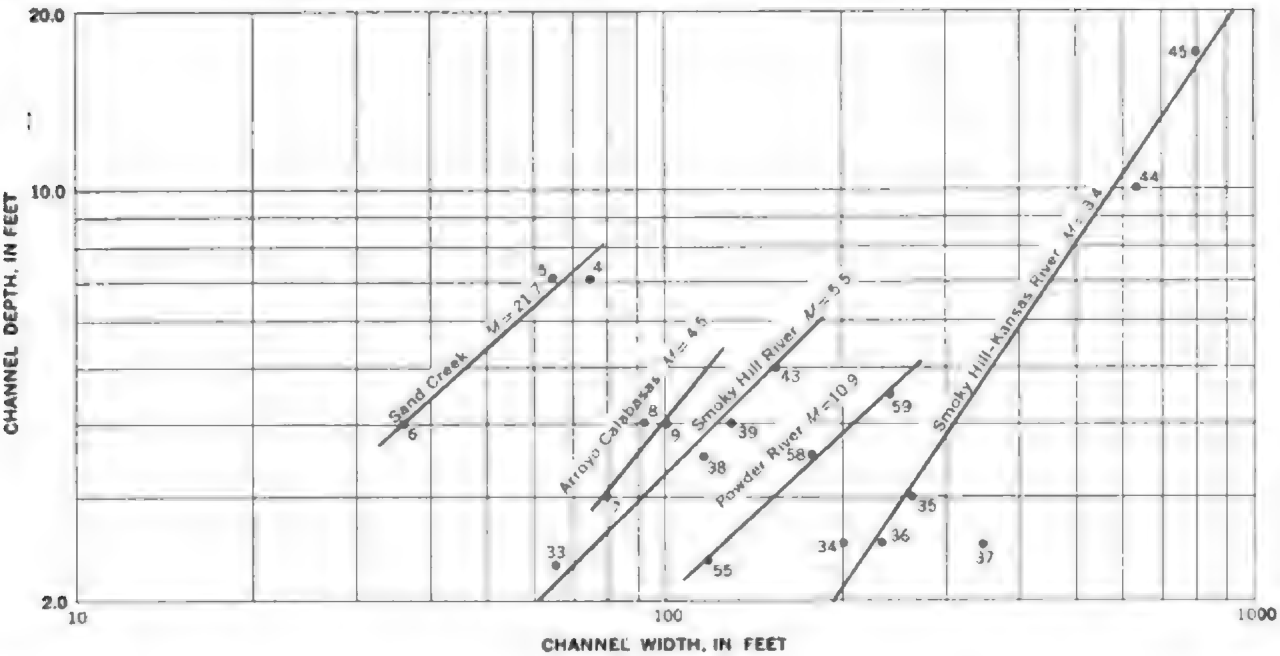

FIGURE 13.—Relation between width and depth for streams with not greatly different values of M in a downstream direction. Number following name of stream is mean value of M for points forming each line, and numbers beside points refer to cross sections listed in table 1.

Lacey (1930) showed that the depth and width of regime canals increase in an orderly manner with discharge and suggested that the intercept or position of the regression line of width to depth for each canal is determined by grain size. Plotting width against maximum depth for all the 69 cross sections results in an undecipherable pattern; however, when data for individual streams are plotted a group of curves results (fig. 13).

In figure 13 each regression line is drawn in relation to points representing cross sections having not greatly different values of M. The positions of the lines representative of ephemeral streams are apparently determined by M. The Sand Creek line, with a high value of M, lies high and to the left. The Arroyo Calabasas regression line lies lower to the right as M decreases. However, mean annual discharge is also important in determining the position of the curves, for both the Smoky Hill River and Powder River curves, with a higher value of M, lie to the right of Arroyo Calabasas regression line. Nevertheless, the regression lines for rivers with approximately equal discharge would probably have intercepts determined by M.

In contrast to the straight regression lines which may be drawn through points representative of cross sections with nearly similar values of M, the width-depth data for the Smoky Hill-Kansas River system reveals that the variability of M in a downstream direction has a marked effect on the relation of channel width to depth (fig. 14).

In a downstream direction along the Smoky Hill River, M decreases from 16 to 2.4 between cross sections 32 and 37. This change is accompanied by a relatively large increase in channel width in relation to depth. However, between cross sections 37 and 41 M increases from 2.4 to 13 and depth increases as channel width decreases to about one-fourth of its former value. The introduction of large quantities of silt and clay into the channel between cross sections 41 and 42 causes an abrupt increase in channel depth with a proportionally smaller increase in width. Downstream from cross section 42, M decreases from 89 to 6 and channel depth decreases sharply. Between cross sections 43 and 45, M decreases and width again increases more than depth.

Two large dams on the Smoky Hill River are another probable cause of some variation in the plot of figure 14. The Cedar Bluffs Dam, completed in 1951, is located between cross sections 37 and 38. The Kanopolis Dam, completed in 1948, is located between cross sections 40 and 41.

It has been shown that the construction of a dam may cause upstream and downstream changes in channel character. For example, cross section 85, located a short distance downstream from the Cedar Bluffs Dam, was classed as an unstable channel because of recent degradation. However, in spite of the possible effects of these structures on streamflow and channel character,

Digitized by Google

the relation between gage height and discharge for each cross section showed no progressive change which would indicate channel instability. In addition, cross sections 37 through 41 show no unusual scatter on figure 12.

However, if it is assumed that the dams have an effect on channel width and depth, then the major portion of this effect can be eliminated by discarding cross sections 37 through 41 from figure 14. This will cause some alteration of the figure, for the second and third segments of the graph will be replaced by a line between cross sections 36 and 42; however, the greater part of the variability of the figure will remain to be explained by downstream variations of M.

Annual discharge increases progressively in a downstream direction (table 1) so the variations in channel shape are not the result of water losses. Therefore, figure 14 suggests that as M changes in a downstream direction neither channel width nor depth will show a consistent relation with mean annual discharge. Depending on the change in alluvial character either width or depth may decrease in a downstream direction.

This effect of sediment type on the relation between width and mean annual discharge can be demonstrated by plotting the two variables in the manner of Leopold and Maddock (1953) for cross sections for which discharge data are available (fig. 15) along the Smoky Hill, Republican, and Kansas Rivers. It is important to remember here that width and depth as used in this study are not the same as the width and depth for mean annual discharge as used by Leopold and Maddock (1953).

The relation between mean annual discharge and channel width is almost a straight line for the Republican-Kansas River cross sections, in which M ranges from 1.4 to 8; however, the same variables show great irregularity for the Smoky Hill-Kansas River cross sections in which M ranges from 2.4 to 89.

Maximum depth and mean annual discharge at the same cross sections (fig. 16) have a somewhat similar relation, for the river with the greatest variation in M has the greatest variation of maximum depth with mean annual discharge.

Again the presence of dams on the rivers may be important. In addition to the Cedar Bluffs and Kanopolis Dams on the Smoky Hill River, there are two dams on the Republican River. The Trenton Dam, completed in 1955, is located between cross sections 50 and 51, and the Harlan County dam, completed in 1952, is lo-

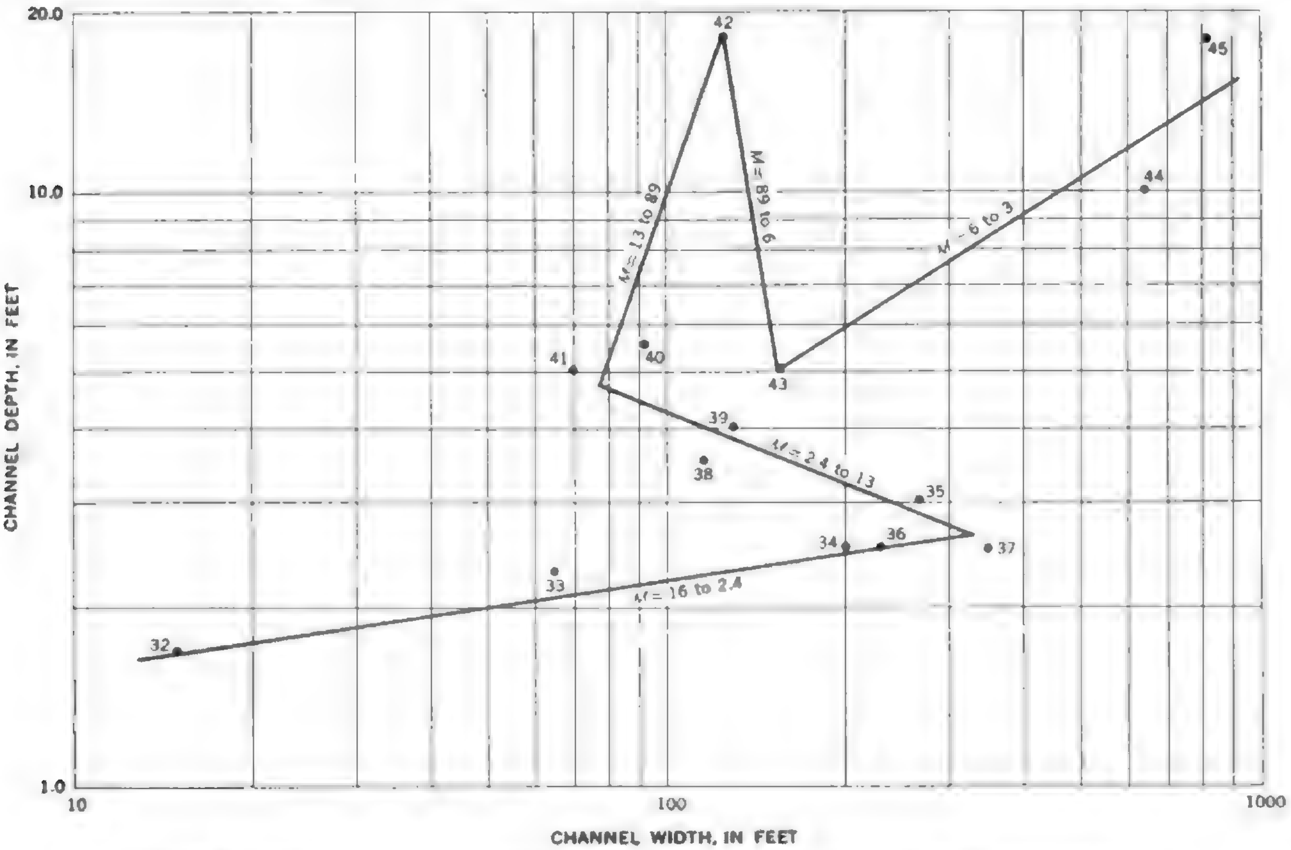

FIGURE 14.—Relation of channel width to depth for the Smoky Hill-Kansas River. Numbers refer to cross sections listed in table 1.

Digitized by Google

cated between cross sections 51 and 52. Any effects of these structures on the stream channels could have been expected before the cross sections were studied in 1958, and as mentioned above scour occurred at cross section 85 below the Cedar Bluffs Dam. In addition, channel degradation may also have occurred at cross section 86, a short distance below the Harlan County dam, for bedrock is exposed in the channel at that cross section.

In spite of the existence of the dams, if cross sections 37 through 41 were eliminated from the Smoky Hill River data and cross sections 50 through 52 were eliminated from the Republican River data the Smoky Hill River plots on figures 15 and 16 would still show great variation in contrast to the slight variation of the Republican River data. Therefore, although the effects of the dams should not be minimized, the writer believes that the cross-section data collected in 1958 and plotted on figures 15 and 16 were not significantly influenced by the structures, for the upstream cross sections were located several miles above the water level of the reservoir and none of the downstream sections were closer than 20 miles to the dams.

To summarize (see figs. 12–16) if M remains constant downstream then the width and depth of the channel will increase at a uniform rate with discharge, excluding the influence of other variables, and width-depth ratio will remain constant. If M increases, downstream channel depth will increase more rapidly than width, which may even decrease, and the width-depth ratio will decrease. If M decreases, downstream channel width will increase more rapidly than depth, which may even decrease, and width-depth ratio will increase.

CONCLUSIONS AND POSSIBLE APPLICATIONS

This study suggests that M represents the resistance to erosion or general behavior of sediment in a stream channel containing only small amounts of gravel. A study of this aspect of the physical properties of sediment is needed before it will be possible to suggest other than that the silt-clay acts as a binding agent in which

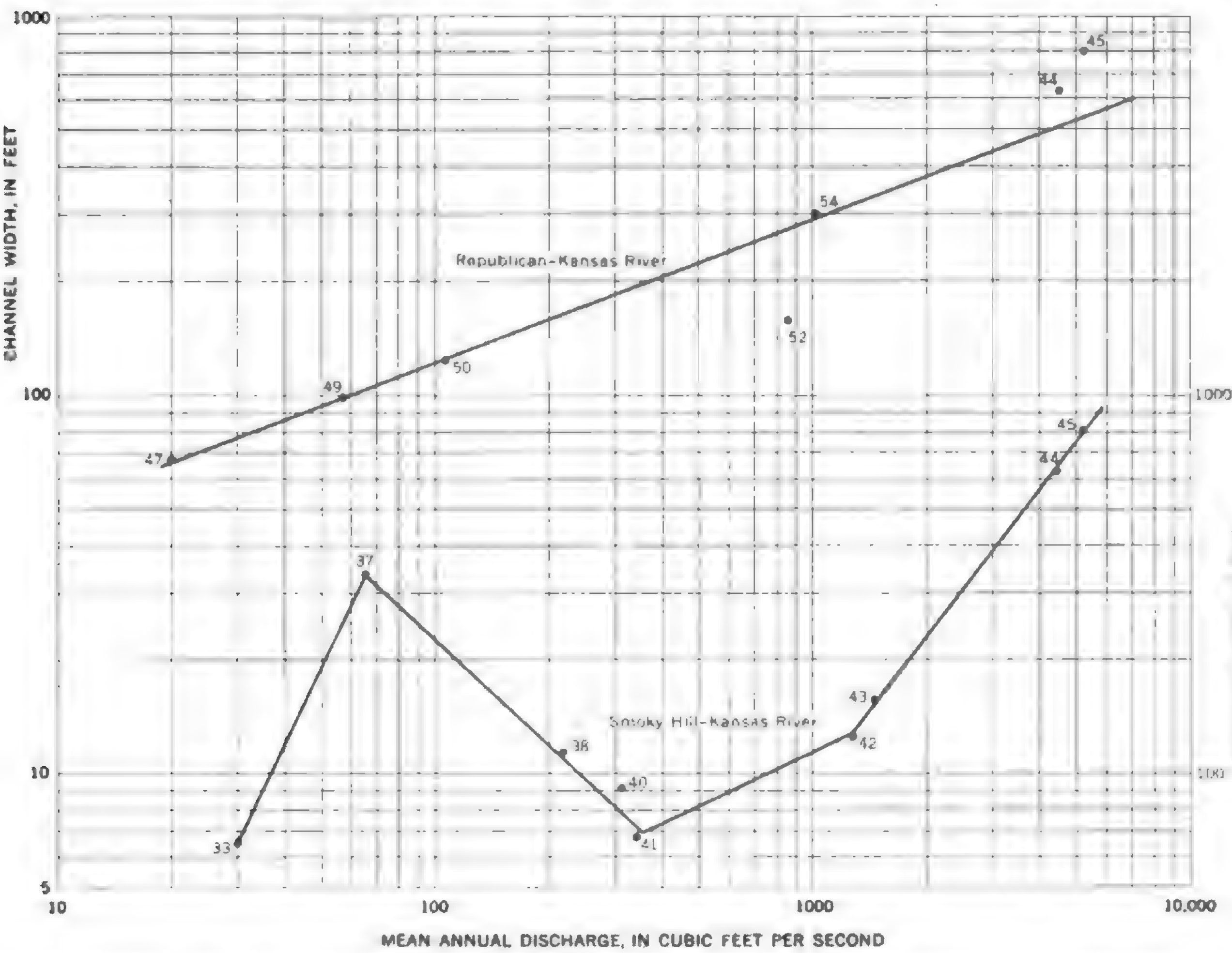

FIGURE 15.—Relation of channel width to mean annual discharge for the Smoky Hill, Republican and Kansas Rivers. Numbers refer to cross sections listed in table 1.

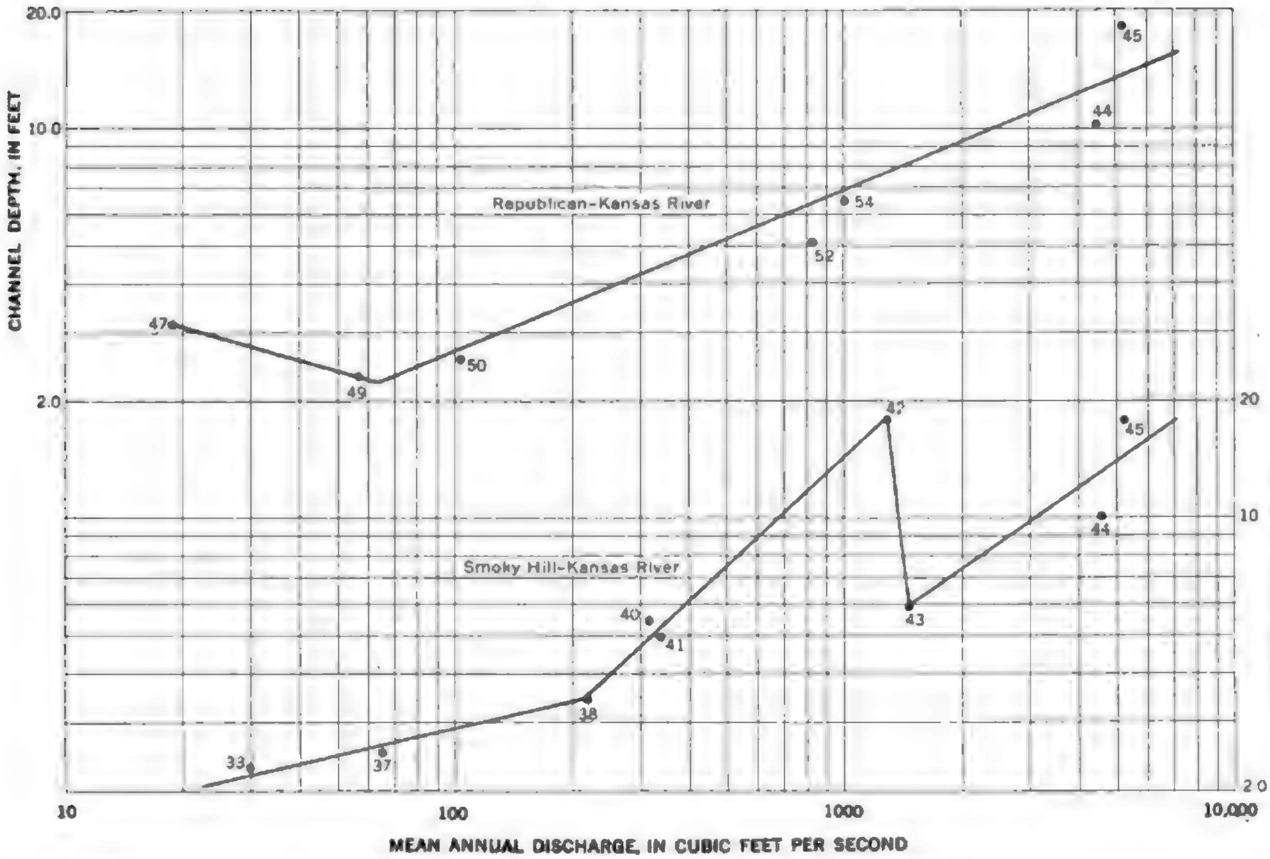

FIGURE 16.—Relation of channel maximum depth to mean annual discharge for the Smoky Hill, Republican, and Kansas Rivers. Numbers refer to cross sections listed in table 1.

the larger sediment grains are fixed. Undoubtedly, the type of clay present and the ratio of silt to clay are also important.

The importance of the percentage of silt and clay in the perimeter of a stream channel to channel shape has been demonstrated. As M increases the width-depth ratio decreases according to the following equation:

$$F=255\ M^{-1.08}$$

Neither mean annual discharge nor mean annual flood affect this relation significantly, at least for the channels sampled in this study.

The relation of the unstable channels (fig. 10) suggests that the position of a point in relation to the regression line of figure 8 may indicate that aggradation or degradation is occurring within a channel. Aggrading channels will have a higher width-depth ratio than indicated by M; whereas degrading channels will have a lower width-depth ratio than indicated by M.

As M increases downstream along a given river, the depth increases more rapidly and the width less rapidly with discharge than if M were constant downstream, and width-depth ratio decreases. Conversely as M decreases downstream along a given river the depth increases less rapidly and the width more rapidly with discharge than if M were constant, and width-depth ratio increases. Changes in M downstream along the Smoky Hill-Kansas River system support the conclusion that width-depth ratio varies with M regardless of discharge, and whereas both width and depth of a channel may increase with discharge, a change in M along the river will change the rate of their increase downstream and may even cause either width or depth to decrease downstream.

The use of percentage of silt and clay in sediment or some similar parameter, as an indication of the physical properties of alluvium, seems to open several profitable lines of research into fluvial morphology. For example, perhaps M may be of more value in studies of longitudinal stream profiles than median grain size. The adjustment of the cross sections of a stream to changed hydrologic conditions by widening or deepening of the channel may be related to M. In

Digitized by Google

addition, it may be possible to use the regression line of figure 8 and the equation derived therefrom to aid in the prediction of the stable form of canals or rivers subjected to different types of modification or increased discharge.

REFERENCES

Bagnold, R. A., 1954, The physics of blown sand and desert dunes: London, Methuen & Co., 265 p.

Boyoucos, G. J., 1935, The clay ratio as a criterion of susceptibility of soils to erosion: Am. Soc. Agronomy Jour., v. 27, p. 738–741.

Burmister, D. M., 1952, Soil mechanics: New York, Columbia Univ. Press, 155 p.

Fisk, A. N., 1944, Geological investigation of the alluvial valley of the Lower Mississippi River: U.S. War Dept., Corps of Engineers, Vicksburg, Miss., 78 p.

Hjulstrom, Filip, 1935, Studies of the morphological activity of rivers as illustrated by the River Fyris: Geol. Institution, Univ. Upsala Bull. [Sweden], v. 25, p. 221–527.

Lacey, Gerald, 1930, Stable channels in alluvium: Inst. Civil Engineers Proc., v. 229, p. 259–285.

Lane, E. W., 1937, Stable channels in erodible material: Am. Soc. Civ. Eng. Trans., v. 102, p. 123–142.

Leopold, L. B., and Maddock, Thomas, Jr., 1953, The hydraulic geometry of stream channels and some physiographic applications: U.S. Geol. Survey Prof. Paper 252, 57 p.

Rubey, W. W., 1933, Settling velocities of gravel, sand, and silt particles: Am. Jour. Sci., 5th series, v. 25, p. 325–338.

——— 1952, Geology and mineral resources of the Hardin and Brussels quadrangles (in Illinois): U.S. Geol. Survey Prof. Paper 218, 179 p.

Trask, P. D., 1959, Effect of grain size on strength of mixtures of clay, sand, and water: Geol. Soc. Am. Bull., v. 70, p. 569–580.

Digitized by Google

UNIVERSITY OF CHICAGO
LIBRARY
SERIAL RECORD

Effect of Sediment Characteristics on Erosion and Deposition in Ephemeral-Stream Channels

U.S. GEOLOGICAL SURVEY PROFESSIONAL PAPER 352-C

QE75
.A26
no. 352-C
(C1)

Effect of Sediment Characteristics on Erosion and Deposition in Ephemeral-Stream Channels

By S. A. SCHUMM

EROSION AND SEDIMENTATION IN A SEMIARID ENVIRONMENT

GEOLOGICAL SURVEY PROFESSIONAL PAPER 352-C

UNITED STATES GOVERNMENT PRINTING OFFICE, WASHINGTON : 1961

UNITED STATES DEPARTMENT OF THE INTERIOR

STEWART L. UDALL, *Secretary*

GEOLOGICAL SURVEY

Thomas B. Nolan, *Director*

For sale by the Superintendent of Documents, U.S. Government Printing Office
Washington 25, D.C.

Exchange Univ. Pa.

Digitized by Google

CONTENTS

	Page
Abstract	31
Introduction	31
Acknowledgments	32
Methods of investigation	32
Areas of study	33
Sage Creek, S. Dak	33
Sand Creek, Nebr	41
Arroyo Calabasas, N. Mex	49
Bayou Gulch, Colo	53
Medano Creek, Colo	57
Comparison of sediment and channel characteristics between areas	61
Relation between sediment and channel characteristics	61
Summary of comparisons	62
Deposition in ephemeral streams	63
Cross sections	63
Slope	65
Vegetation	67
Causes of deposition	67
Erosion in ephemeral streams	68
Channel incision	68
Bank caving	69
Practical considerations	69
References	70

ILLUSTRATIONS

	Page
Figure 17. Index map showing location of study areas	33
18. Index map of Sage Creek, S. Dak	34
19. Longitudinal profile and cross sections, Sage Creek, S. Dak	36
20. Sage Creek, S. Dak., above section 8	38
21. Sage Creek, S. Dak., below section 8	40
22. Variations in channel and sediment characteristics, Sage Creek, S. Dak	42
23. Index map of Sand Creek, Nebr	43
24. Longitudinal profile and cross sections, Sand Creek, Nebr	45
25. Sand Creek, Nebr	46
26. Aerial photographs of Sand Creek, Nebr	48
27. Variations in channel and sediment characteristics, Sand Creek, Nebr	49
28. Index map of Arroyo Calabasas, N. Mex	50
29. Longitudinal profile and cross sections, Arroyo Calabasas, N. Mex	52
30. Arroyo Calabasas, N. Mex	54
31. Variations in channel and sediment characteristics, Arroyo Calabasas, N. Mex	56
32. Index map of Bayou Gulch, Colo	56
33. Longitudinal profile and cross sections, Bayou Gulch, Colo	57
34. Bayou Gulch and Medano Creek, Colo	58
35. Variations in channel and sediment characteristics, Bayou Gulch, Colo	60
36. Index map of Medano Creek, Colo	60
37. Cross sections, Medano Creek, Colo	61
38. Relation between width-depth ratio and weighted mean percent silt-clay	63
39. Relation between stream gradient and weighted mean percent silt-clay	64
40. Relation between width-depth ratio and weighted mean percent silt-clay	65
41. Comparison of the longitudinal profile of Newlin Creek, Colo	68

TABLES

	Page
Table 1. Precipitation at stations near the study areas	35
2. Channel and sediment data, Sage Creek, S. Dak	35
3. Channel and sediment data, Sand Creek, Nebr	44
4. Channel and sediment data, Arroyo Calabasas and Arroyo de los Frijoles, N. Mex	51
5. Channel and sediment data, Bayou Gulch, Colo	55
6. Channel and sediment data, Medano Creek, Colo	59
7. Mean values of channel and sediment data	62
8. Ratio of drainage area to channel length	68

Digitized by Google

THE EFFECT OF SEDIMENT CHARACTERISTICS ON EROSION AND DEPOSITION IN EPHEMERAL STREAM CHANNELS

By S. A. Schumm

ABSTRACT

This study of five semiarid valleys emphasizes the importance of physical properties of sediment in determining stream-channel shape and differences in the mechanics of erosion and deposition between areas. Prerequisites for selection of the five areas were a progressive decrease in the percent silt-clay in stream channels and banks, active aggradation or erosion within a reach of the stream channel, and nearly uniform lithology within each drainage basin.

A comparison of the data obtained from each area demonstrates that in a drainage channel composed of fine-grained, highly cohesive sediment, deposition occurs on the sides of the channel as well as on the channel floor. The result is a reduction in the channel width-depth ratio across an aggrading reach. Vegetation seems to aid deposition by its rapid growth on recently deposited fine alluvium, but it is not the initial cause of aggradation. Bank caving yields only small amounts of sediment and, caved blocks are often nuclei for deposition along channel sides because of their resistance to disintegration. Degradation in the finer sediments is generally by upstream headcut migration.

In contrast, those channels containing only small amounts of silt-clay are aggraded from bottom to top. No plastering of fine sediments on the banks occurs. Less vegetation grows on these poorly cohesive, highly mobile sediments. Headcutting occurs only where the coarser sediments are capped by a layer of fine material. In general, a break in the longitudinal profile of this type channel is quickly removed by channel degradation. Bank caving seems to supply more sediment to the stream load, for the blocks of poorly cohesive alluvium disintegrate upon impact.

Deposition causes marked changes in the ephemeral-stream channels. As the reach of maximum aggradation is approached channel gradient decreases, and depending on the amount of silt-clay in channel and banks, the width-depth ratio may increase or even decrease. In all channels studied percent silt-clay increases and median grain size decreases with aggradation. At the lower end of an aggrading reach, the gradient steepens, but sediment is still fine and vegetation generally covers the entire valley floor. The reach of maximum deposition may migrate upstream with time, but renewed degradation on the downstream reach of steep gradient may cause a trench to cut through the valley plug, renewing through transport of sediment and runoff.

The aggradation in the study areas is apparently a result of high sediment yields in the headwater parts of the drainage basins. Deposition in the channel occurs; however, where the rate of increase of drainage area per mile of channel length is low. In these reaches of small tributary contribution, water loss into the alluvium and the subsequent increase in sediment concentration causes deposition.

The shape of stable cross sections, expressed as a width-depth ratio, is dependent on the weighted mean percent silt-clay in banks and channels such that width-depth ratio increases with decreased silt-clay in the alluvium. Gradient also shows an inverse relation to weighted mean percent silt-clay for these small streams of low annual discharge.

It is suggested that the relation between channel shape and silt-clay can be used as a criterion of channel stability, for aggrading channels generally plot well above the width-depth, silt-clay regression line; whereas, degrading channels plot below the line.

The study suggests that preventive conservation may be the most practical solution to some erosion problems, such as arroyo cutting. Deposition, if it is desired to fill a trenched channel, should be induced in reaches where conditions are most favorable for natural aggradation. Conservation measures should be modified depending on the character of the valley and its alluvium. Only certain critical reaches of a channel need be controlled to prevent erosion over larger areas.

INTRODUCTION

Recently there has been an increase in studies of stream morphology. Leopold and Maddock (1953) have discussed downstream changes in width and depth of a stream channel with increased discharge. Additional studies by Wolman (1955), Leopold and Miller (1956), and Wolman and Leopold (1957) have tended to confirm Leopold and Maddock's conclusions under diverse conditions and have revealed much about stream-channel development. The writer in another investigation introduced a parameter for sediment type and stressed the importance of the effect of sediment type on channel shape (Schumm, 1960b). All the above investigations were restricted to stable channels, or at least channels that were not rapidly aggrading or degrading. The present study concerns some small ephemeral-stream channels that are being actively aggraded or eroded.

Digitized by Google

A knowledge of the mechanics of deposition and erosion in semiarid valleys would not only be academically valuable, but could also provide the basis for conservation measures aimed at restoring gullied valleys to their prior condition. Much has been written on the need for careful use of the semiarid valley floor, for it may be the only productive land within a drainage basin. For example, Peterson (1950), as a result of interviews with several early settlers, states that at the time of white settlement in the valley of San Simon Creek, Ariz., the valley floor was flat and unbroken. Large areas were covered with grass, luxuriant enough to be harvested for hay. The creek itself was perennial throughout most of its length and lined with trees. During the 1880's, 50,000 head of cattle are said to have grazed the valley. At present the valley floor is trenched from its confluence with the Gila River for nearly 70 miles upstream, although a reach of about 2 miles is uncut about 40 miles above the mouth. The stream is now ephemeral, and barren flats and miniature badlands border the gully. Other valleys in the West have a similar history.

Much thought has been devoted to the development of conservation measures; nevertheless, until the mechanics of sediment deposition and removal are better understood, truly effective conservation measures will not be realized. This report is a contribution toward the development of that necessary understanding of semiarid erosional and depositional processes.

Many students of stream activity have recognized that the type of sediment transported by a stream greatly influences the characteristics of that stream. Therefore, in order to form general conclusions, areas of diverse sediment types must be studied.

A study of the relation between sediment type and stream-channel shape (Schumm, 1960a) has shown that for stable stream channels containing less than 40 percent gravel and cobbles, the channel shape expressed as a width-depth ratio (F) bears the following relation to a weighted mean value for the percent silt-clay in bank and channel samples (M) : $F=255\ M^{-1.08}$. Silt-clay is defined as the sediment passing through the 200-mesh sieve, smaller than 0.074 mm.

Areas which had a wide range in the percent silt-clay in channel and banks were selected for study because it was believed that such differences might be fundamental with regard to the mechanics of sediment deposition and erosion.

This report is composed of two main parts. The first contains a geographic description of each study area as well as a discussion of the changes in sediment and channel characteristics along each channel. In the second part the data collected in the five study areas are combined to show the relations between sediment type and channel character, and the causes of, and the differences in, erosional and deposition processes in the study areas. In addition, conclusions and their practical application are discussed.

ACKNOWLEDGMENTS

During the summer of 1957 the following assisted the writer in the field: William Krummel, C. T. Sumsion, and R. H. Taylor. Irene Lapke performed the hydrometer analysis of the finer sediment samples. The writer wishes to acknowledge the constructive criticism offered by J. H. Mackin, M. G. Wolman, and J. T. Hack.

John Rutter, superintendent, Badlands National Monument, and Philip Ward, ranger, Great Sand Dunes National Monument, aided the fieldwork, and their courtesy and assistance are greatly appreciated.

METHODS OF INVESTIGATION

Five drainage basins were selected for study. Both a range in alluvial characteristics from area to area and active deposition or erosion within the channel were basic prerequisites. To eliminate as many variables as possible, areas were selected in which differences in lithology within a drainage basin did not affect the stream in any recognizable manner. This necessitated the selection of small drainage basins; the largest basin chosen had a drainage area of about 90 square miles.

The reaches of each channel in which deposition was important generally could be readily identified, perhaps most easily by the recognition of recently deposited alluvium by its fresh appearance and lack of vegetative cover. Downstream changes in channel shape and gradient and sediment character, also confirmed the location of aggrading reaches. These deposition criteria will be discussed in more detail under "Deposition in ephemeral streams." Unfortunately discharge data were not available for each channel studied.

The five areas selected, although scattered from southern South Dakota to northern New Mexico (fig. 17), fulfilled all the basic requirements and were similar in annual precipitation and land use. Similar observations were made in each area. Where topographic maps of good quality, large scale, and small contour interval were available, the fieldwork was limited to the collection of data at many locations along the channel. Cross sections were chosen primarily to illustrate the changes occurring in the channel and on the flood plain as deposition or erosion became increasingly important in the downstream direction. Photo-

Digitized by Google

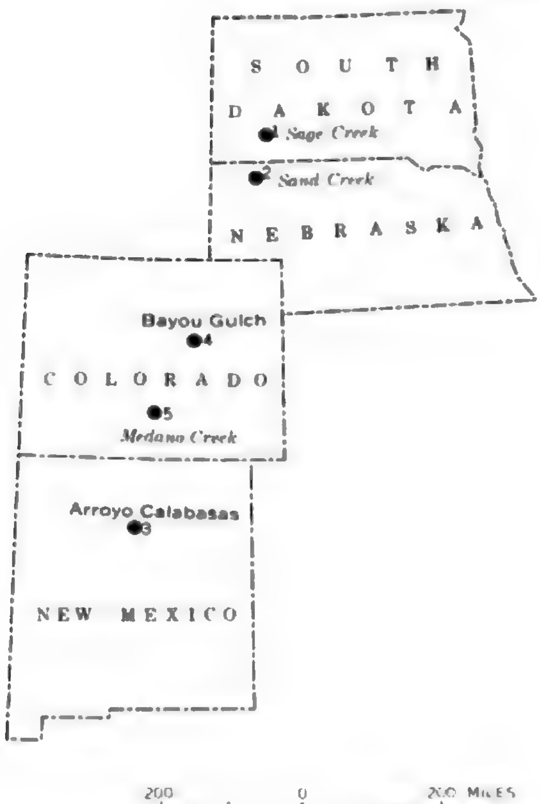

Figure 17.—Index map showing location of five study areas.

graphs and sediment samples of channel, bank, and overbank deposits were taken, and the gradient of the stream was measured at each section. The locations of the sections were marked on maps or aerial photographs. The longitudinal profile of the stream was surveyed along the aggrading reach when topographic maps were not available. In brief, the downstream changes in channel character accompanying deposition were documented by many surveyed cross sections of the channels, spaced closely enough to reveal the manner of channel filling. In addition, observations were made on the influence of vegetation on deposition.

The width and depth of the drainage channels were especially difficult to determine: (a) where recent incision formed a steep-sided trench, in which all the runoff was contained; or (b) where a filled channel held only the smaller flows. In the first type, depth of water during the recent floods was estimated from observations of the height of scour or deposition on the banks. In the second type, depth was measured to the lowest elevation on the profile from the edge of the first permanent surface or bank above the channel floor. On figures 19, 24, 29, 33, and 37 the dashed line on each cross section shows the width measured at that section. Width was measured from one edge of a bank to the opposite, at a distance above the channel floor determined by channel depth.

Samples of sediment were taken from the stream channel, its banks, and the flood plain. Samples of the surface inch of channel sediment were taken from 10 to 15 points along the cross sections, depending on channel width. These samples were combined to give a composite sample of the channel alluvium.

In the laboratory, a size analysis of each sediment sample was made. Since the author had found previously (Schumm, 1960), that the median grain size of the sample alone is not the most important characteristic of the sediment, the cumulative grain-size curve was used to select other parameters of possible value, such as those used to determine the engineering properties of granular materials. Burmister (1952) has prepared tables which allow estimation of permeability, cohesion, and frost-heaving characteristics of a soil from the grain size below which 10 percent of the sample is finer (Hazen's effective size, D_{10}). Burmister's tables were used to describe in general terms the physical properties of each sample.

The percent silt-clay in the sample, taken as that part of each sample passing the 200-mesh sieve, was also selected for comparison between areas. Burmister gives physical reasons for selecting the 200-mesh sieve or 0.074 mm as the boundary between silt-clay and sand, for the soil becomes less well drained and capillarity increases as the percentage of material passing the 200-mesh sieve increases; in addition, the 200-mesh sieve is the practical lower limit of sieving. In a recent paper Dunn (1959) demonstrates that the resistance of alluvium to tractive force is, related directly to the silt-clay content of the sediment. Dunn, however, defines silt-clay as sediment finer than 0.06 mm.

AREAS OF STUDY

For each of the five study areas a geographic description will be presented. This will be followed by a general description and a quantitative description of sediment and channel variations downstream. Comparisons of the five areas will be made in a later section.

SAGE CREEK, SOUTH DAKOTA

DESCRIPTION

Location.—Sage Creek, a tributary to the White River, (figs. 17, 18) drains an area of about 92 square miles in the southeastern corner of Pennington County, S. Dak. The northern drainage divide is about 11 miles south of the town of Wall, and the eastern divide is about 7 miles west of the town of Interior. The headwaters lie within the boundary of Badlands National Monument. That part of Sage Creek studied in detail

gitized by Google

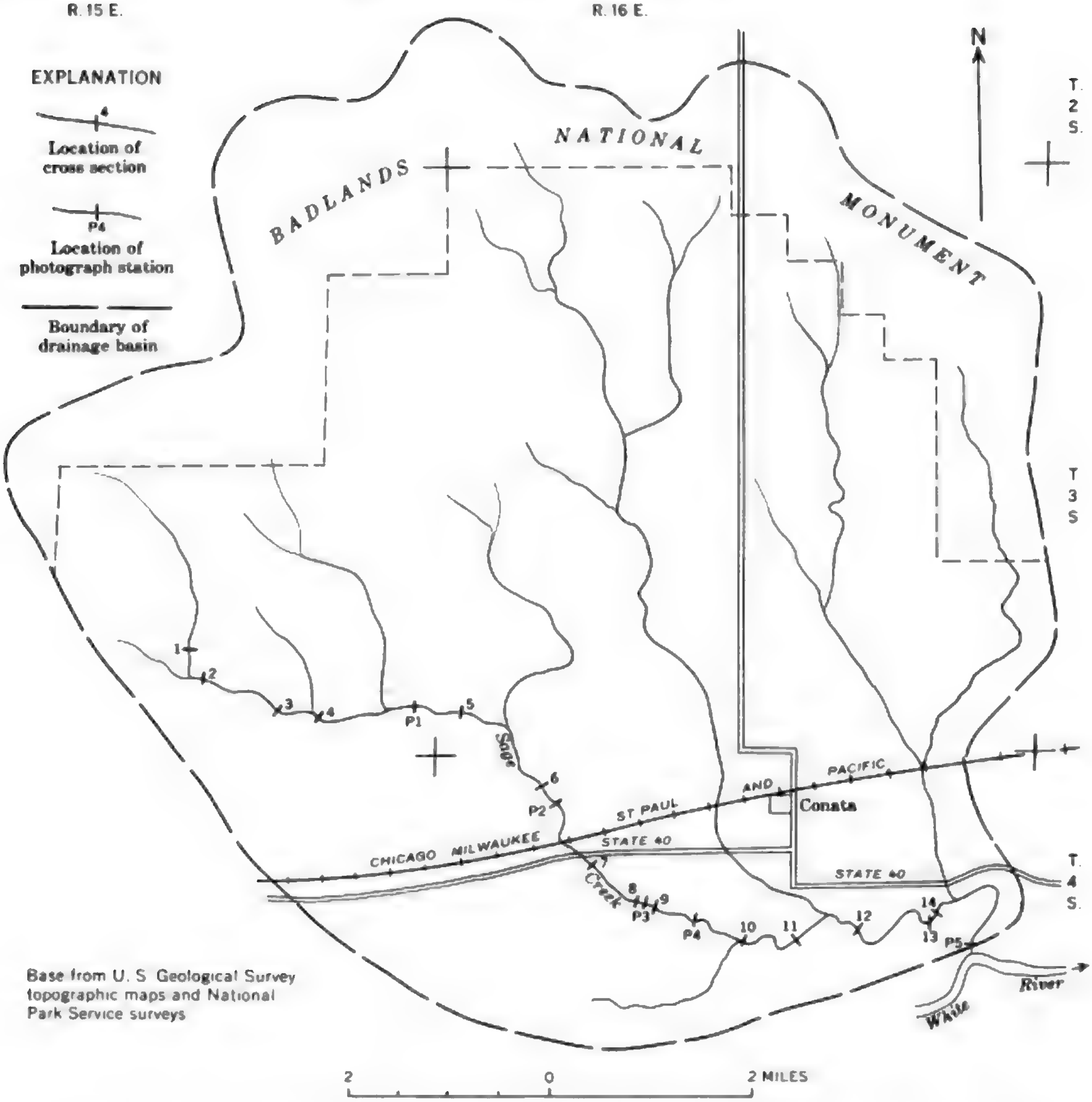

FIGURE 18.—Index map of Sage Creek, S. Dak., drainage basin showing location of cross sections and photograph stations.

is shown on two Geological Survey topographic maps, the Conata and Bouquet Table quadrangles.

Annual precipitation.—The mean annual precipitation at Interior, based on a 10-year record, is 16.53 inches (table 1). The greatest part of this mean annual precipitation, 13.97 inches, occurred during the period April through October. According to Thornthwaite's climate classification (1941), the Sage Creek area is semiarid.

Vegetation and land use.—Most of the drainage basin is used as grazing land, although some alfalfa is grown on that part of the basin that lies on the flood plain of the White River. Vegetation is of the short grass prairie type, although in the badlands vegetation is generally absent.

Physiography and geology.—The headwaters of Sage Creek drain the precipitous badland escarpment known locally as the Wall. This escarpment, composed of

Digitized by Google

TABLE 1.—*Precipitation at stations near the study areas*

[U.S. Weather Bureau data]

Station	Length of record (years)	Mean precipitation (inches)												
		Annual	January	February	March	April	May	June	July	August	September	October	November	December
Interior, S. Dak.	10	16.53	0.45	0.34	0.78	1.75	2.97	2.64	2.62	1.74	1.05	1.20	0.52	0.47
Fort Robinson, Nebr.	40	17.19	.47	.63	1.00	2.19	2.79	2.49	2.07	1.64	1.51	1.29	.48	.63
Santa Fe, N. Mex.	40	14.19	.66	.74	.81	1.07	1.46	1.19	2.28	1.90	1.68	1.11	.71	.58
Santa Fe (AP), N. Mex.	15	10.80	.32	.42	.54	.67	.71	.93	1.80	2.42	1.29	.99	.23	.48
Parker (9E), Colo.	23	13.42	.34	.36	.69	1.91	2.21	1.60	1.83	1.83	1.05	.75	.56	.29
Blanca, Colo.	11	9.20	.10	.25	.17	1.09	.87	.56	2.20	2.05	.73	.82	.19	.17
La Veta Pass, Colo.	30	20.98	1.13	1.73	2.54	2.39	1.78	1.09	2.19	2.13	1.27	1.44	1.69	1.60

TABLE 2.—*Channel and sediment characteristics, Sage Creek, S. Dak.*

[Class: A=aggrading; D=degrading; S=stable; U=unclassified]

Cross section	Class	Drainage area (square miles)	Distance between cross sections (miles)	Median grain size D_{50} (mm)	Hazen's effective size D_{10} (mm)	Trask sorting index	Silt-clay (percent)	Gradient	Channel width (feet)	Channel depth (feet)	Width-depth ratio (F)	Weighted mean silt-clay, M (percent)
Channel sediment												
1	U	1.65		0.04	0.00055	3.63	74	0.0055	33	3.0	11.0	
2	S	1.71	0.076	.06	.00036	11.20	55	.0055	16	7.0	2.3	73
3	S	3.42	1.36	.06	.001	1.42	68	.0045	20	7.0	2.9	79
4	S	9.48	.94	.12	.009	4.61	40	.0045	31	5.0	6.2	54
5	U	13.08	2.12	3.00	.005	11.80	29	.0007	34	6.5	5.4	44
6	A	14.33	1.21	.10	.007	5.96	45	.002	32	6.2	4.9	53
7	A	14.59	1.06	.09	.0001	13.80	47	.002	12	4.0	3.0	61
8	U	18.11	1.32	.034	.0001	4.45	86	.002	22	8.0	2.8	87
9	D	18.12	.30					.0022	18	10.0	1.8	
10	A	45.12	1.36	.067	.0012	2.14	60	.002	21	3.0	7.0	67
11	A	45.40	.91	.032	.0002	1.63	92	.002	15	3.0	5.0	91
12	A	80.25	1.44	.047	.016	1.29	78	.0022	22	4.0	5.5	78
13	U	80.65	.99						12	2.5	4.8	
14	U	82.84	.38	.044	.004	1.54	93	.0017	32	6.5	4.9	89
Mean				0.31	0.0037	5.29	64					
Bank sediment												
2				0.028	0.0005	2.20	93					
3				.030	.0003	2.24	93					
4				.028	.0005	2.00	96					
5				.035	.001	1.83	90					
6				.032	.00032	1.68	84					
7				.038	.0013	2.00	83					
8				.031	.0007	2.68	88					
10				.033	.0006	1.91	96					
11				.027	.0013	2.13	89					
12				.015	.0045	2.00	79					
13				.007	.0002	5.10	97					
14				.060	.015	1.19	81					
Mean				0.030	0.0022	2.25	89					
Overbank sediment												
1				0.040	0.0006	3.63	74					
7				.035	.0002	1.89	90					
13				.007	.0002	5.10	97					
14				.044	.0007	1.78	85					
Mean				0.032	0.0004	3.10	87					

Digitized by Google

the sandstones, siltstones, and claystones of the White River group of Oligocene age, is being eroded rapidly. On many of the slopes a depth of 0.5 inch of material is eroded during 1 year (Schumm, 1956). Sediment eroded from the scarp must be transported at least 10 miles across a gently sloping surface formed by the northward retreat of the badland scarp, to reach the White River. In spite of the gentle slope of this surface, about 20 feet to the mile, it is trenched by ephemeral streams. A few residuals or outliers of the main badland mass rise above it.

Over almost the entire drainage area the White River group is exposed at the surface, although a geologic map of the area (Ward, 1922), which unfortunately fails to cover the entire drainage basin, suggests that the Pierre shale of Cretaceous age crops out in the lower part of the Sage Creek valley. However, since the creek flows on an alluvial fill derived predominantly from the White River group, no change in valley character was recognized due to change of rock type.

Alluvium.—The sediment derived from the erosion of the White River Badlands is fine grained (table 2). Median grain size of channel sediment for all sections is 0.31 mm, Trask's sorting coefficient is 5.29, and Hazen's effective size is 0.0037 mm. Using Burmister's tables (1952), it is found that a soil having D_{10} of 0.0037 mm is nearly impermeable. Potential capillarity of the soil is high, and it is very susceptible to frost heaving. This indicates that the alluvium in general is highly cohesive, and much energy is required to detach a particle from the mass of alluvium. The mean percent silt-clay in the channel samples is 64, confirming the highly cohesive nature of this material.

Samples taken of overbank deposits and deposits on the sides of the channel contain an even greater percent silt-clay and smaller value for D_{10} (table 2), indicating even higher cohesion.

Samples were taken from the recently trenched valley sides. These contained 89 percent silt-clay and D_{10} was 0.0022 mm, indicating that the fill is impermeable. The potential capillarity is high, and the banks are susceptible to frost heaving.

GENERAL CHANNEL VARIATIONS

Considering the nature of the alluvium, a general discussion will now be presented of the changes in channel characteristics at the 14 sections surveyed.

On figure 18 the location of the 14 surveyed sections and 5 photograph stations are shown. Photographs of some sections, shown on figures 20 and 21, pertain to the following discussion. Cross sections are shown at their respective positions on the longitudinal profile in figure 19 which is based on topographic maps.

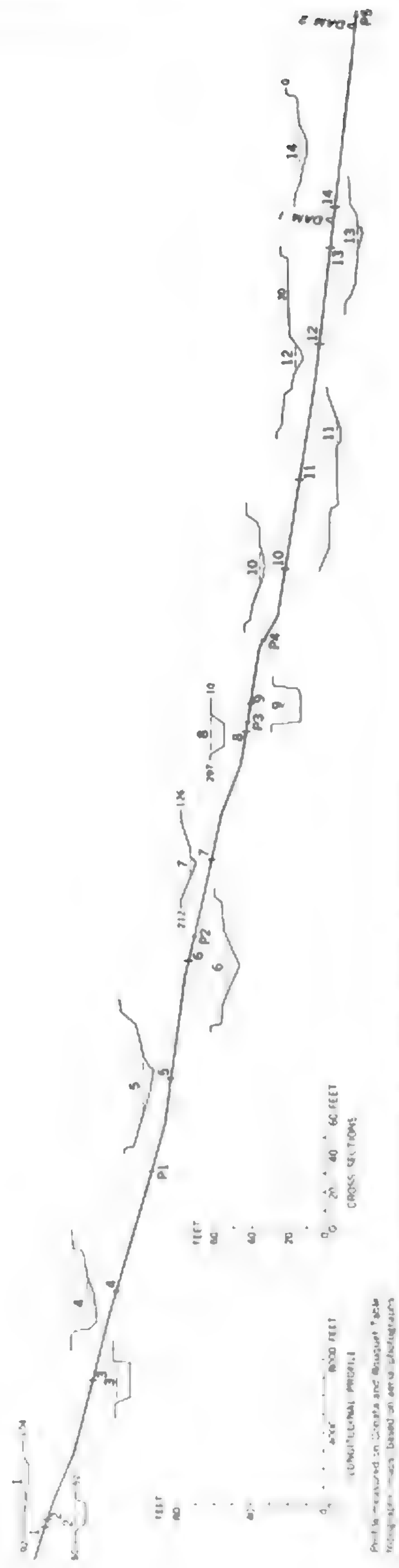

FIGURE 19.—Longitudinal profile in 1948 and cross sections measured in 1957 on Sage Creek, S. Dak. Numbers at ends of some cross sections give distance in feet to edge of flood plain.

Digitized by Google

The uppermost section (No. 1) has only a poorly defined channel. Past deposition has smoothed the valley floor until now flood waters cover a width of about 240 feet (fig. 20*A*). A short distance below section 1 is a headcut below which the valley floor is trenched. The headcut is not shown on figure 19, for its height is much less than the contour interval of the topographic maps on which figure 19 is based.

Bank caving has widened the newly incised channel between sections 2 and 3 (figs. 19, 20*B*), but the cohesiveness of the bank material prevents rapid disintegration of the slump blocks. Some of the larger fragments on which vegetation still grows are nuclei for deposition in the channel (fig. 20*C*).

At section 3 this process has become more pronounced, and locally what seem to be incipient point bars are forming about slump blocks. The channel widens and deepens rapidly downstream as tributaries join the main channel. At section 4 an inner channel has formed; that is, deposition has built terraces along both banks (fig. 20*D*). The characteristic mode of deposition in this area seems to be a plastering of sediment along the sides of the channel. The recently deposited, fine-grained highly cohesive sediment aids plant growth, and all recent sediment deposits are covered with grass and weeds, which in turn further increase deposition.

Midway between photograph station 1 and section 5 there is a noticeable decrease in stream gradient (fig. 19), suggesting that deposition probably increases below section 5. Downstream the inner terraces encroach on the channel proper and mount higher on the original banks of the channel until at section 6 only about 3 feet of these banks are exposed, and a short distance downstream only 1 foot (fig. 20*E*), and finally at section 7 (fig. 20*F*), the banks are completely covered. Owing to this deposition along the sides of the channel, bank caving has stopped. Overbank deposition is important at section 7, and the vegetation on the surface adjacent to the channel is partly buried. Downstream from section 7 the channel becomes shallower and narrower, approaching complete filling by building from the sides as well as from the bottom of the original channel. Thus in about 5 miles the channel of Sage Creek has been transformed from a raw trench to one almost completely aggraded. The complete filling of the channel, however, is interrupted by renewed trenching below section 8. At section 8 the channel is deeper and wider than at section 7; however, at section 8 much recently deposited alluvium is found in the channel, suggesting that aggradation may be occurring or has occurred after channel erosion.

Figure 21*A* shows a reach of intense erosion accompanied by channel widening below section 8. At section 9 the channel is at maximum depth but about 1 mile downstream at photograph station 4 (fig. 21*B*) deposition has begun again, especially along the sides of the channel and on slump blocks in the bottom. A short distance below this point a remnant of the old channel floor is preserved on the west wall of the new trench. It lies 6 feet below the prairie surface, suggesting that complete filling had not occurred before the renewed trenching. This may explain the absence of a headcut above section 8. Between photograph station 4 and section 10 (fig. 21*C*), more than 1 mile downstream, channel deposition becomes increasingly important, until at section 10 the cross section most nearly resembles that of section 7 (fig. 19).

Deposition at section 10 (fig. 21*C*) was heavy during the floods before the survey, and at this section the manner of deposition is most clearly illustrated. Just above section 10 the stream bends sharply to the north. With rapid deposition, the point bar deposit on the inside of the bend is expected, but of greater interest is the deposition on the outside of the bend where bank cutting should logically occur. Figure 21*D* is a view of the deposit on the outside bank. The fieldbook is at the contact between what may be deposition by floods in the spring of 1957 and earlier floods. The sediment is laid in against the bank, effectively narrowing the channel at this section with little or no decrease in channel depth.

A trench dug across the deposit reveals that stratification is not horizontal; rather it curves downward from the bank toward the channel. Therefore, these lateral deposits are built upward as well as outward from the bank. The deposit shown on figure 21*D* has been scoured by recent floods, but on the inside of the bend (figs. 21*C*, *E*) the building of the deposit outward into the channel has not been hindered by erosion. Complete filling of the channel by a union of the lateral deposits and deposition on the channel floor will result in a channel-fill deposit containing concave-up stratification (Schumm, 1960a). This type of lateral deposition could only occur in areas of fine-grained cohesive sediments containing a high percentage of silt-clay. Figure 21*E* shows the growth of weeds on the recent deposits. The cohesiveness, ability to hold water, and the fertility of the fine sediment aids rapid and luxurious vegetative growth.

Proceeding downstream from section 10, the water table apparently approaches the surface, for willow and cottonwood saplings appear which further promote deposition. At section 12 the growth of willows is dense and at section 13 (fig. 21*F*) the channel is almost completely filled. A dam built in the fall of 1956 may be the cause of ponded water in the channel

Digitized by Google

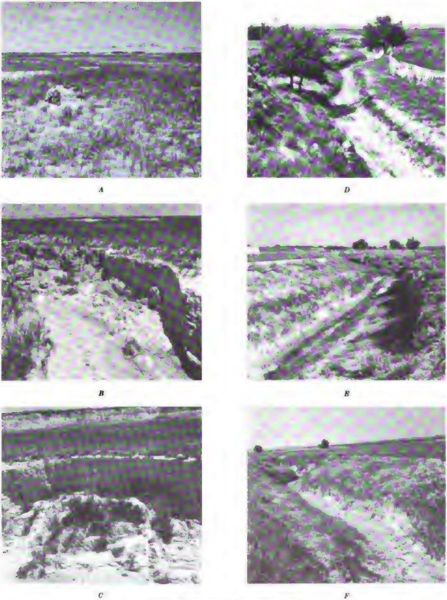

A D

B E

C F

FIGURE 20.—Sage Creek, S. Dak., above section 8

Digitized by Google

at section 13, but the heavy deposition alone might have caused it. The 8 months since construction of the dam probably has been insufficient for that structure to cause accumulation of any measurable alluvial deposit at section 13. At section 14 just below the new dam, overbank deposition ranges in depth from 1 to 1½ feet. A second dam was constructed at the mouth of Sage Creek in the fall of 1956.

Probably little runoff enters the White River from the mouth of Sage Creek. The upper dam diverts much of the flow across the flood plain and into the river upstream. The remaining runoff is held by the lower dam. As a result high flows in the White River enter the lower end of Sage Creek and deposit sediment in that channel, thus plugging the mouth of the creek. This type of deposit has been termed a "reverse delta" by Leighly (1934).

QUANTITATIVE CHANNEL VARIATIONS

As shown in the general discussion of variations, there are marked changes in channel character along Sage Creek. A comparison now will be made of the channel and sediment characteristics at each cross section. The parameters of most importance to this discussion are channel gradient, the shape of the channel expressed as a width-depth ratio, median-grain size, sorting index of sediment, and the percent silt-clay in each channel sample. As noted above, the percent silt-clay is taken as that part of the sample smaller than the 200-mesh sieve or 0.074 mm.

To illustrate graphically the changes, the value for each of the above indices is plotted against section number on figure 22.

On figure 22 the width-depth ratio is much lower at section 2 than at section 1. This change occurs abruptly as one passes the headcut between sections 1 and 2 because channel degradation commonly causes a narrow and deep channel. Where the trench at sections 3 and 4 has been widened by bank caving, the width-depth ratio is higher. Gradient is less at sections 3 and 4 than at sections 1 and 2, and it shows a large decrease between sections 4 and 5. Percent silt-clay also decreases to a minimum for the sections at section 5; however, the largest median grain size was found at section 5 (3 mm). To keep within the limits of the diagram, median grain size for section 5 is not plotted on figure 22.

A question arises at this point as to the reason for increased median grain size at section 5. Perhaps the low graident at section 5 (fig. 19) causes deposition of the coarser fraction of the sediment in the channel; whereas, the finer fraction continues downstream and is deposited where the channel becomes smaller because of aggradation (section 7). Deposition becomes important below section 5, and this is accompanied by a decrease in width-depth ratio and sediment size and an increase in percent silt-clay and gradient.

To understand the above changes in channel and sediment character as measured at the cross sections, the manner of channel filling by aggradation should be summarized. In general, the beginning of aggradation decreases channel gradient and relatively coarse sediment is deposited in this reach of the channel. The finer sediments continue to move down the channel across the reach of reduced gradient. At some point down stream, however, aggradation has almost completely filled the channel, and it is here that overbank flooding and deposition become important. With each flow of water much fine sediment is deposited in the remaining vestiges of the channel and on the flood plain. Continued deposition on the flood plain causes steepening of the gradient of the valley. The finer fraction of the alluvium is therefore found on the steeper reaches of the channel and valley floor. The above is discussed in more detail later in the report.

To return to a discussion of the cross sections on Sage Creek, the renewed degradation beginning below section 8 and continuing below section 9 causes a decrease in the width-depth ratio at section 9. Percent silt-clay decreases and median grain size increases at section 10,

EXPLANATION OF FIGURE 20

A, Cross section 1, view upstream. Channel has been filled by aggradation and is now grass covered. Badlands are visible in background.

B, Cross section 2, view upstream. Remnants of blocks of alluvium in channel are the result of bank caving, and indicate active widening of channel.

C, Recent deposition around blocks of bank material which have caved into the channel near cross section 3. The block has not rotated, and flood-plain vegetation is flourishing on the surface of the block several feet below its original position.

D, Station 1, view upstream. The inner terrace formed by lateral deposition along both banks is best displayed in this reach, between sections 4 and 5.

E, View upstream from station 2 a short distance downstream from section 6. Lateral deposition of fine sediment has almost covered banks of gully.

F, Cross section 7, view downstream. Banks are completely covered by recent deposits. The small raw channel at the bottom of the gully may be the result of renewed degradation.

Digitized by Google

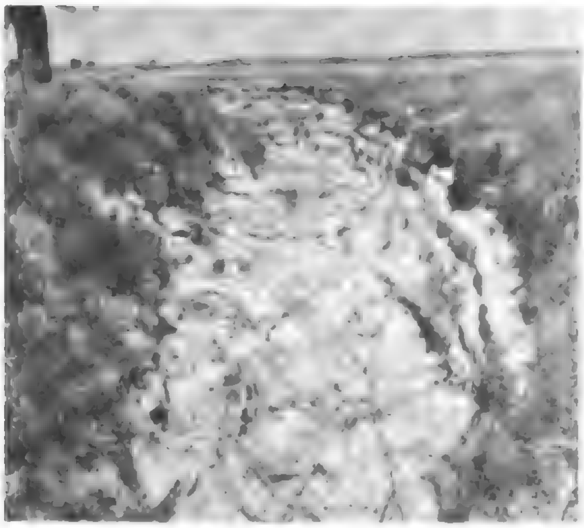

A

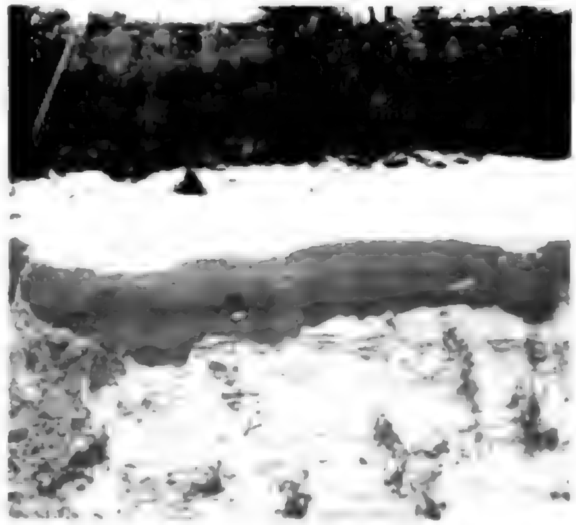

D

B

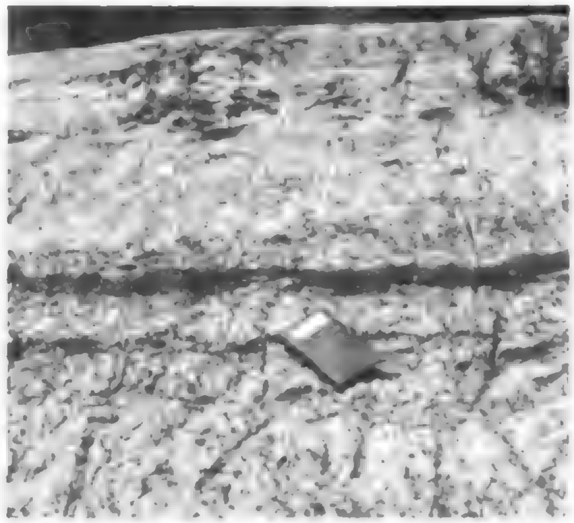

E

C

F

FIGURE 21.—Sage Creek, S. Dak., below section 8.

but the general trend of the channel sediment is toward increasing fineness below section 7. Gradient also decreases slightly as does width-depth ratio below section 10. The plot of sorting index indicates little except that the sediment is less well sorted on the aggrading reach between sections 5 to 7.

The percent silt-clay in samples of the inner terrace (table 2) changes little in a downstream direction, suggesting that sediments with more than 70 percent silt-clay are very susceptible to the type of deposition in the Sage Creek channel.

SUMMARY OF SAGE CREEK AREA

In a drainage channel carrying large sediment loads of fine-grained highly cohesive sediment, deposition occurs on the sides of the channel and deposition can occur on the outside of bends as well as on the streambed itself. The result is a reduction in the width-depth ratio across the aggrading reach. Median grain size increases and percent silt-clay and gradient decreases as deposition begins. This is followed by a decrease in median grain size and an increase in silt-clay and gradient as deposition increases. The final result will be a broad convex stream profile, the downstream part covered by the finer sediment.

Rapid growth of vegetation on recently deposited alluvium seems to aid deposition. Bank caving yields only minor amounts of sediment except in the recently cut reach, and caved blocks become nuclei for deposition along the sides of the channel.

SAND CREEK, NEBRASKA

DESCRIPTION

Location.—Sand Creek (fig. 17) drains an area of about 26 square miles in western Dawes County and northeastern Sioux County. The southern drainage divide is 6 miles north of the town of Crawford, Nebr., and the headwaters drain a part of the Pine Ridge escarpment, which here forms the major drainage divide between the White and Cheyenne River basins. Sand Creek flows to the east from the escarpment and enters the White River northeast of Crawford (fig. 23). No topographic maps were available for this area.

Annual precipitation.—Mean annual precipitation is 17.19 inches (table 1) based on a 40-year record at Fort Robinson, 3 miles southwest of Crawford. Most of this precipitation occurred during the months of April through October. According to Thornthwaite's (1941) climate classification, the Sand Creek area lies near the east limit of semiaridity.

Vegetation and land use.—The short grass prairie vegetation, covering all the drainage basin except the badland areas near the western divide, affords good grazing land. Only a small part of the basin shows evidence of former attempts at agriculture; however, farming is important to the south and along the White River. A large part of the headwater area of the drainage basin is badlands.

Physiography and geology.—The upper reaches of Sand Creek are supplied with large amounts of sediment derived from erosion along the western drainage divide. A photograph taken near the divide (fig. 25*A*) shows the removal of the protective grass cover from slopes by gullying and the formation of badlands. Badland development is characteristic of the White River group of Oligocene age.

The westward migration of the White River drainage divide leaves a pediment at the base of the Pine Ridge escarpment. The area near the scarp resembles that near Sage Creek, S. Dak., but farther to the east this surface has been dissected to form an area of gently

EXPLANATION OF FIGURE 21

A, View downstream from station 3. Recent trenching has exposed cottonwood tree roots on floor of channel. View typical of conditions at section 9 except for exposed roots.

B, View upstream, station 4. This reach is about 1 mile downstream from section 9. Deposition of sediment has begun here on floor of channel and along banks. Depth of gully is 16 feet.

C, Cross section 10, view upstream. Progressive deposition in the channel between station 4 and this section has almost filled the channel. The maximum depth of the gully was probably only 10 feet in contrast to the upstream sections.

D, Lateral bank deposit on outside of bend at cross section 10. Fieldbook is at contact of what is assumed to be the deposits from the 1956 and 1957 floods. A trench dug into these deposits reveals stratification planes curving downward (convex) toward the channel floor.

E, Weeds growing on recently deposited alluvium at cross section 10. Older plants (cockleburrs) are partly buried. Establishment of vegetation is rapid on the fine alluvium.

F, Cross section 13, view downstream. A more advanced stage of aggradation and vegetative growth is shown at this section about 3.3 miles downstream from cross section 10.

Digitized by Google

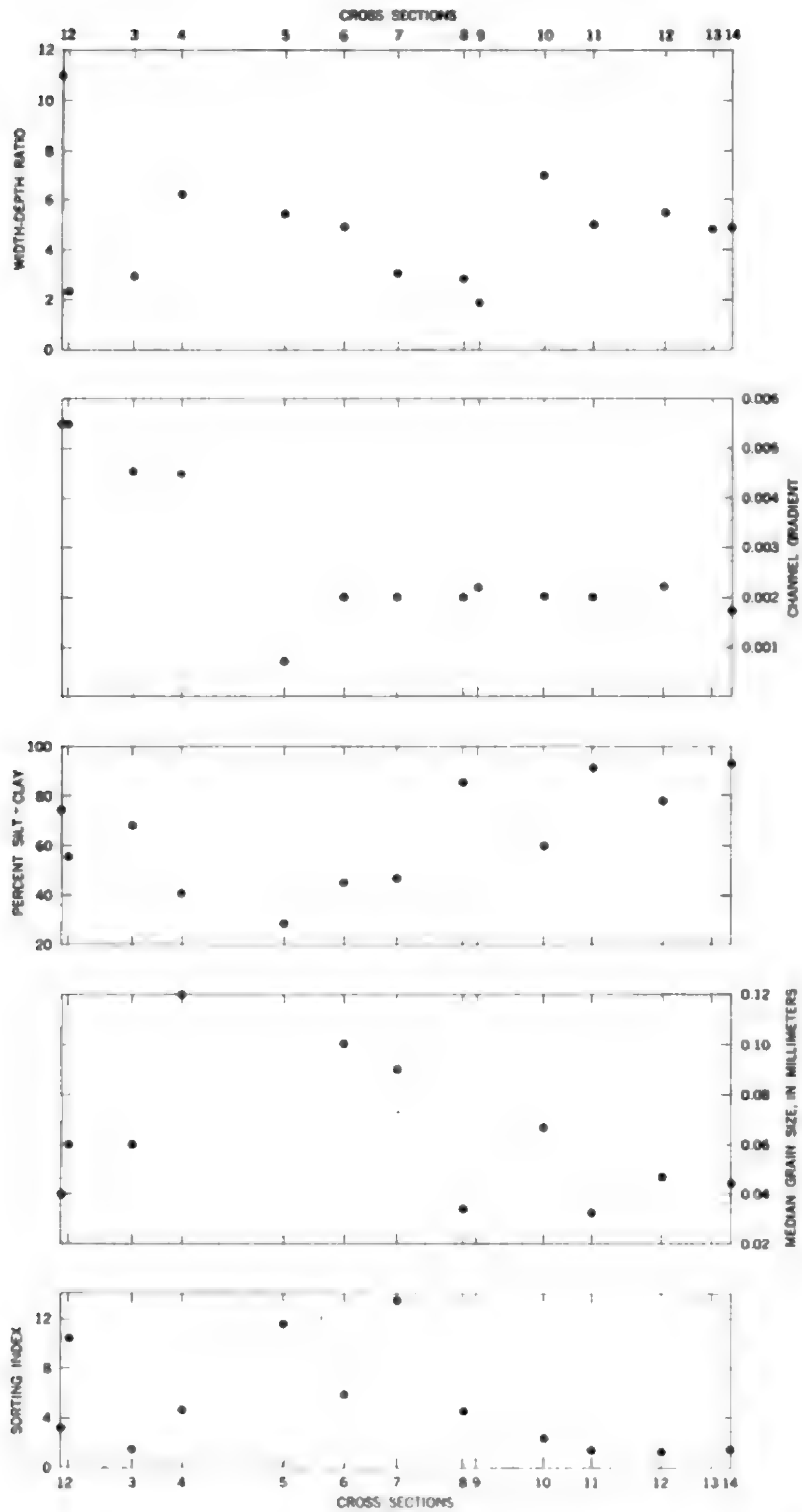

FIGURE 22.—Variations in channel and sediment characteristics, Sage Creek, S. Dak. The spacing of the cross sections along the abscissa is proportional to the distances between sections in the field.

Digitized by Google

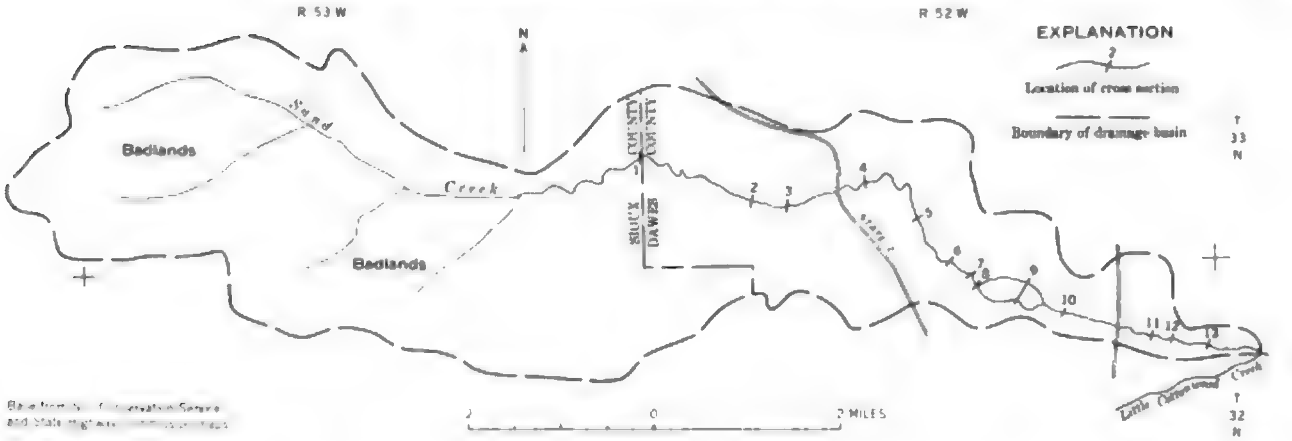

FIGURE 23.—Index map of Sand Creek basin showing locations of cross sections.

rolling hills that contributes relatively little sediment to the channel.

Again, as in the South Dakota area, almost the entire drainage basin of Sand Creek is underlain by formations of the White River group. A negligible part, as regards influence on the stream, is underlain by the Pierre shale of Cretaceous age.

Alluvium.—Although derived from erosion of rocks of the White River group, the alluvium sampled in the Sand Creek valley is somewhat different from that derived from the South Dakota badlands (table 3). As suggested by the name of the creek, it is coarser. Median grain size for all channel samples is 0.37 mm; Trask's sorting index is 2.81 and Hazen's effective size 0.040 mm. Burmister's tables indicate that a soil with D_{10} of 0.040 is not impermeable, but it is drained with difficulty and is near the approximate lower limit of effective use of well points for lowering ground water (0.02 mm). The mean values for all sections show that potential capillarity is high and that the soil is very susceptible to frost heaving.

The above data suggest that the sediment would be cohesive and difficult to detach from adjacent particles, but the individual samples differ from the South Dakota area in that the channel samples taken above the aggrading reach are proportionally more sandy (compare figs. 22 and 27), having as little as 10 percent silt-clay at section 6.

Samples of the bank material contain 69 percent silt-clay, and D_{10} is 0.0044. Effective size (D_{10}) is larger than that for the Sage Creek sediment, but it still indicates a nondrainable system with high capillarity and high susceptibility to frost heaving.

GENERAL CHANNEL VARIATIONS

The high sediment yields from badlands in the headwaters of Sand Creek cause deposition in the downstream reaches of the channel. No topographic maps were available so the profile was surveyed from above section 6 to the mouth of Little Cottonwood Creek (fig. 23). At sections 4 and 5 the altitude of the channel floor was obtained by altimeter. Above State Highway 2 the gradient was measured at each section. On figure 24 are shown the longitudinal profile of the stream, the cross sections across the aggrading reach, and the profile of the flood plain above the channel.

Starting upstream in the area of badlands (fig. 25*A*), a continuous channel exists to the area of major aggradation at section 9. The channel is relatively deep at sections 1 and 2, but it becomes shallower and wider until at sections 3 and 4 (fig. 25*B*) it is a fairly wide sandy channel. The gradient at section 4 is about one-half of that of section 1, and as the aggrading reach is approached, the gradient decreases and the channel becomes shallower. Bank caving occurs in many places. At section 6 (fig. 25*C*) a recent slump has occurred. The large block, although cohesive (D_{10} is 0.005), has broken into many smaller fragments. The lack of other blocks in reaches of bank cutting strongly suggests that, unlike the Sage Creek area (D_{10} is 0.00035) slump blocks will not remain in the channel and form nuclei for channel deposition but will be swept away.

564835 O—61——3

Digitized by Google

TABLE 3.—*Channel and sediment data, Sand Creek, Nebr.*

[Class: A = aggrading; D = degrading; S = stable; U = unclassified]

Cross section	Class	Drainage area (square miles)	Distance between cross sections (miles)	Median grain size D_{50} (mm)	Hazen's effective size D_{10} (mm)	Trask sorting index	Silt-clay (percent)	Gradient	Channel width (feet)	Channel depth (feet)	Width-depth ratio (F)	Weighted mean silt-clay, M (percent)
Channel sediment												
1	U	10.6		0.30	0.045	2.95	16	0.003	20	4	5	
2	U	16.1	2.0	.70	.074	2.17	7	.0018	10	6	2.7	42
3	S	16.5	.6	.30	.020	2.28	17	.0035	36	3	12	23
4	S	17.9	1.25	.72	.0013	2.77	14	.0015	75	7	10.7	23
5	S	22.2	1.00	.73	.030	2.93	15	.003	65	7	9.3	22
6	S	22.5	.75	.35	.075	1.82	10	.001	36	4	9	20
7	A	22.7	.30	.024	.0013	2.62	87	.0015	44	4	11	87
8	A	23.1	.15	.020	.0013	2.25	91	.0005	40	1.5	26.6	89
9	A	23.9	.60	.019	.0013	2.48	100	.003				
10	D	24.2	.50	.027	.0010	2.39	85	.0065	15	10	1.5	90
11	D		1.20	1.10	.14	1.98	5	.0017	21	10	2.1	27
12	U		.30	.49	.13	1.53	5	.0017	16	7	2.3	21
13	U	25.7	.45	.055	.0013	8.35	56	.001	6	4	1.5	
Mean				0.37	0.040	2.81	39					
Bank sediment												
2				0.040	0.011	1.47	90					
3				.049	.0014	1.30	70					
4				.053	.0016	1.29	70					
5				.050	.002	1.64	60					
6				.045	.006	2.74	65					
7				.030	.002	2.17	88					
8				.043	.0013	3.27	63					
10				.014	.00065	3.59	93					
11				.080	.008	2.12	48					
12				.095	.010	1.82	39					
Mean				0.050	0.0044	2.14	69					
Overbank sediment												
2				0.040	0.011	1.47	90					
9				.019	.0002	4.06	92					
12				.026	.001	2.32	100					
13				.017	.0011	2.93	93					
Mean				0.026	0.0033	2.69	94					

Point bars and sandbanks are forming on the major bends of the channel, and in many places coarse gravel is introduced into the channel at the cut banks. Below section 6, pronounced changes occur, which are due to deposition. Between sections 6 and 7 the gradient decreases. There is a change in the nature of channel sediment and some tendency for deposition along the banks (fig. 25*D*). Changes in channel depth are much greater than those in channel width. Vegetation grows on both sides of the channel, and it in turn aids further deposition. Deposition increases downstream until at section 8 (fig. 25*E*) the channel is almost completely filled and can be recognized only by its bare appearance. Vegetation, however, is encroaching on this bare channel from both sides. Flood waters at section 8 cover a width of 190 feet of the valley floor. A short distance below section 8 the vegetation has covered the entire channel, and the gradient of the valley floor increases sharply in this area of maximum deposition. The deposition, no longer confined to filling the channel, has built up the center of the valley until it has a convex cross section at sections 9 and 10 (fig. 24). There is ponded water on the south side of the valley between sections 8 and 9 where deposition in the valley center has exceeded that near the south margin forming an undrained depression or natural lake.

The aerial photographs (fig. 26 *A*, *B*,) show the area of greatest deposition along Sand Creek. The light color of the recently deposited alluvium delimits the aggrading areas. Downstream from the area of major deposition vegetation becomes dense on the flood plain and trees are more abundant.

At section 9 there is a channel at the south side of the valley. Cross section 9 (fig. 24) reveals that the edge of this channel is higher than the rest of the valley floor. Field investigation shows that this channel carries only minor amounts of water. It has not been aggraded completely because the flood waters are diverted to the low north side of the valley, where renewed trenching has occurred at section 10. The headcut and longitudinal profile of the floor of the recent trench are shown on figure 24. Thus, although the locus of points of maximum deposition is migrating up channel, following it is a trench, which unless controlled will probably unite with the upper channel to form a continuous channel throughout Sand Creek valley. Figure 25*F* shows the new channel dissecting the valley fill. Much bank caving is in progress, widening the channel. Downstream at the confluence of Sand and Little Cottonwood Creeks the channel has filled again and overbank deposition is important.

QUANTITATIVE CHANNEL VARIATIONS

It has been suggested under the general discussion that marked changes occur in channel and sediment characteristics as the aggrading area is approached and crossed and that these changes differ somewhat from the changes in the Sage Creek area. The values for sediment and channel characteristics are plotted for each cross section on figure 27.

Above section 6 width-depth ratio is a maximum at section 3 but shows a general increase from section 1 to section 6. Gradient decreases at downstream sections in the manner to be expected. Percent silt-clay remains nearly constant. Median grain size varies but not in relation to any known control. Thus above section 6 the parameters vary in a downstream direction, probably much as they would in any channel. Between sections 6 and 7 deposition becomes noticeable, and at section 7 a pronounced change in channel and sediment character occurs. Width-depth ratio increases, suggesting a widening and shallowing of the channel or a greater decrease in depth than in width. This increase continues to section 8 beyond which the channel is completely filled. Accompanying the increase in width-depth ratio is a slight decrease in gradient, a great increase in percent silt-clay, and a decrease in median grain size.

Continuing downstream toward the headcut, at section 10, little change occurs except for an increase in gradient and a sharp decrease in width-depth ratio. Stream gradient is initially decreased by deposition and then steepened as deposition becomes excessive. With renewed trenching gradient decreases, but it still is steeper than above the aggrading reach. Percent silt-

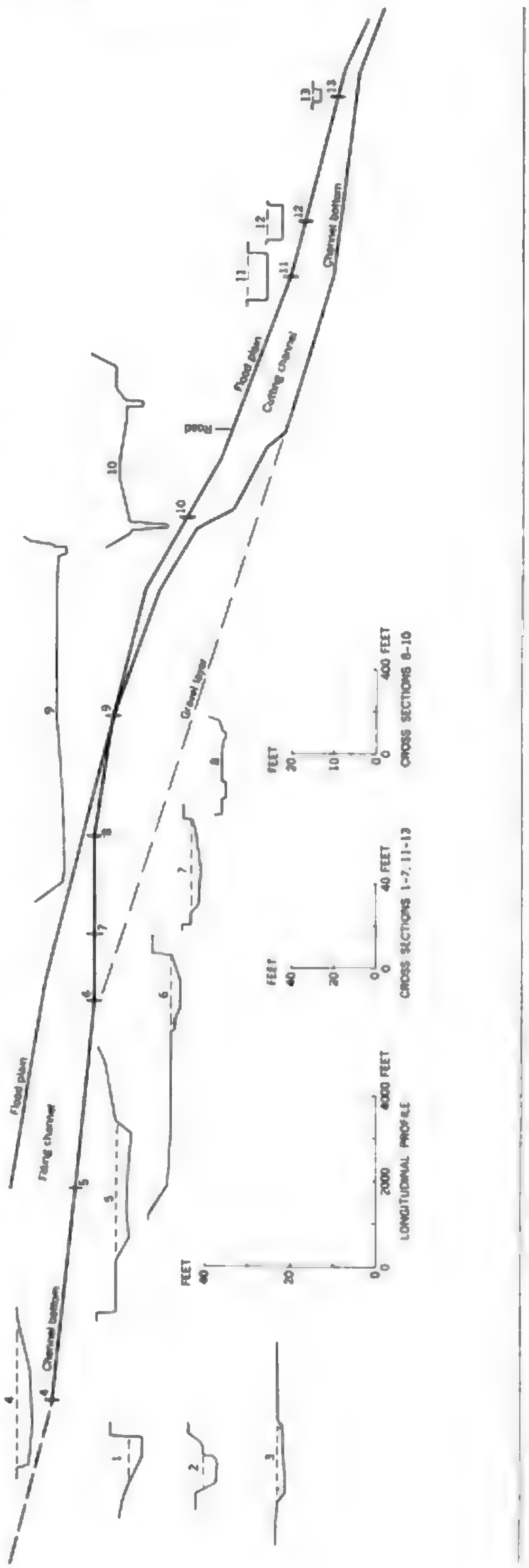

FIGURE 24.—Longitudinal profile and cross sections surveyed between section 4 and the mouth of Sand Creek, Nebr. Note that the scale of cross sections 8, 9 and 10 is smaller than for the remaining cross sections.

Digitized by Google

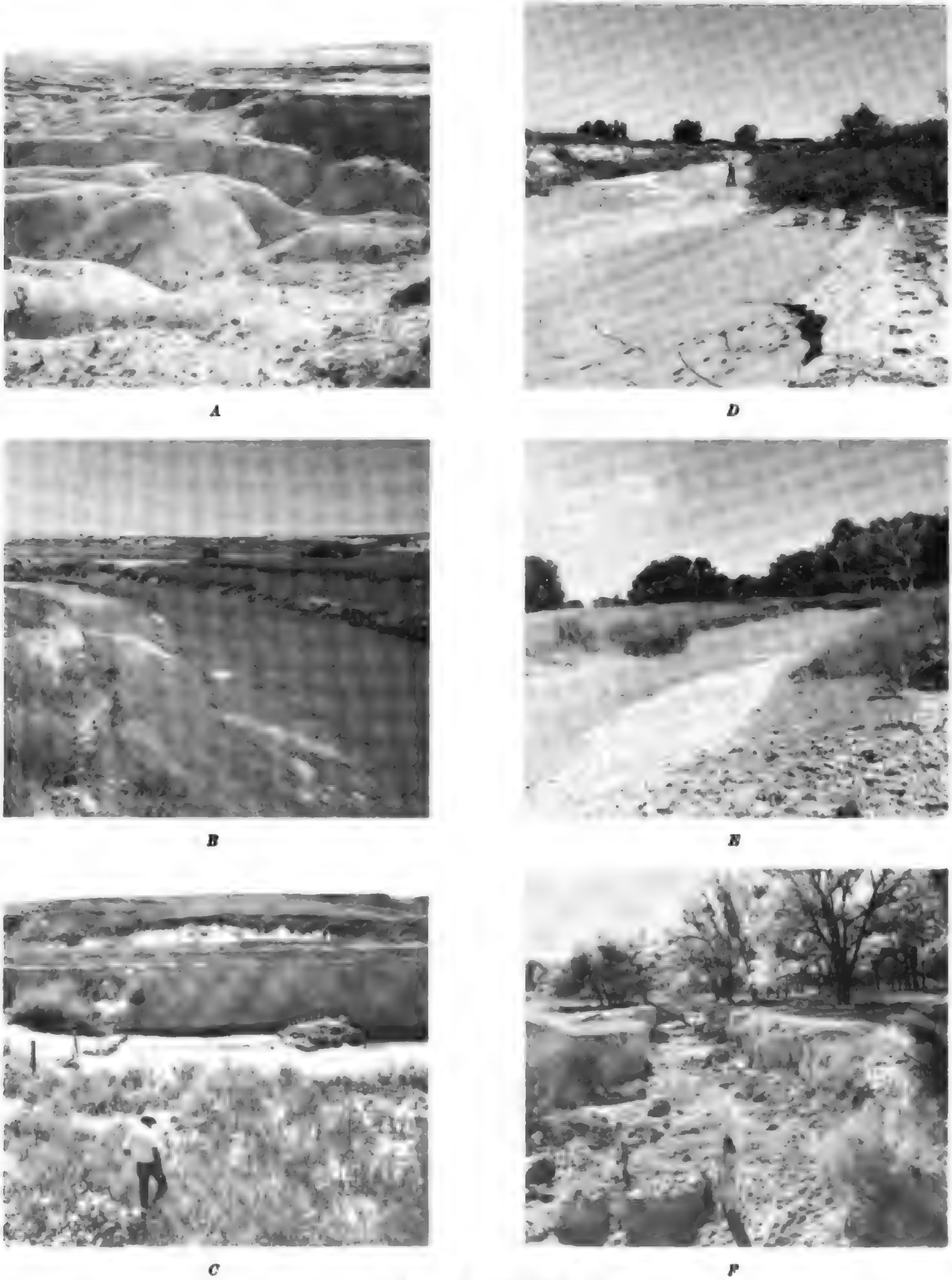

FIGURE 25.—Sand Creek, Nebr.

Digitized by Google

clay decreases and median grain size increases. Downstream from section 11 recent cutting probably has not occurred, and the channel and sediment characteristics vary accordingly.

Between sections 8 and 13 the samples of overbank material show a slight increase in the percent of silt-clay (table 3). The sorting index does not change greatly between sections 1 and 12.

HISTORIC CHANGES

Conversations with local ranchers reveal that the zone of maximum deposition, now located above and below section 9 (fig. 24), was about a mile downstream, near the county road, in 1917, 40 years ago. The filling of the valley has been a type of backfilling, that is, a migration upstream of the zone of maximum deposition rather than a general raising of the lower part of the valley.

A fence at section 9 has been replaced 5 times in 40 years as each installation was partly buried by alluvium. Total deposition at section 9 was estimated by the owner to be about 15 feet.

The headcut, now near section 10, started about 1950 between ½ to 1 mile below the county road. It has then advanced at least 1 mile in 7 years. This information suggests that incision did not begin at the confluence of Sand and Little Cottonwood Creeks but on the section of steepest gradient below the road. This indicates further that the shallowing of the channel below the road may not be due predominantly to deposition but may result from lack of recent trenching in lower reaches of the valley. Segments of the old shallow channel are preserved near the new trench below the road. The old channel was about 5 feet deep and 13 feet wide; whereas, the new channel is now 13 feet deep and 20 feet wide.

The two aerial photographs in figure 26 show the changes that have occurred at and near the reach of maximum deposition between 1939 and 1954, a period of 15 years. Upon comparing the photographs, the channel between sections 7 and 8 seems to have filled. Above section 7 the photographs suggest no more than minor channel changes. Overbank deposition is present farther to the west (upstream) in 1954 as indicated by the upstream and lateral expansion of the light-colored areas of recent deposition, and the cutoff channel has been filled. The lake between sections 8 and 9 was formed by 1954, and the darker patches of flood plain to the north of the lake are gray probably due to flooding and recent deposition on these surfaces. Also, the aggradation in the center of the valley has forced the channel to the south side of the valley in 1954. Another noticeable difference between the two photographs is the growth of vegetation on the light-colored surfaces of recent deposition, shown on the 1939 photograph near the county road, giving them a darker appearance on the 1954 photograph.

In addition, a trenched channel exists below the county road in the 1954 photograph in contrast to the smaller 1939 channel. Perhaps the darker color of the valley below the road in the 1954 photograph is the result of this trenching, for the channel now carries all the flood water, preventing overbank deposition. Marked changes have occurred, suggesting progressive aggradation in the upper area and trenching downstream. The upper limit of both deposition and new vegetation seem to have moved up channel.

SUMMARY OF SAND CREEK AREA

In a drainage channel in which the sediment is composed of silt-clay and sand in the proportion 2 to 3, deposition occurs on the channel floor. Plastering of fine sediments on the channel banks occurs only in those aggrading reaches in which sand has become a minor part of the sediment. The width-depth ratio therefore increases along the aggrading reach until the channel has been completely filled.

Vegetation is of little importance except in the reaches of channel where fine sediments cover the banks and channel floor. Sediment from bank caving is moved downstream almost immediately and rarely aids in the beginning of channel deposition. A noticeable contrast with Sage Creek is the short distance in which deposition appears and channel-filling is completed, between sections 6 and 9 (6,000 feet).

EXPLANATION OF FIGURE 25

A, Badlands in headwaters of Sand Creek. Removal of the protective sod cover allows development of badlands in soft rocks of the White River group.

B, Cross section 3, view downstream. Relatively wide sandy channel typical of Sand Creek above aggrading reaches.

C, Cross section 6. Note recent slump block at base of bank. Fence to left shows signs of recent partial burial.

D, Cross section 7, view downstream. Note development of berms along sides of channel. Vegetative growth is promoted by deposition of fine sediments.

E, Cross section 8, view downstream. Channel is almost completely filled by recent deposition. Vegetation is encroaching on the parts of the channel that are bare.

F, Recently formed gully at county road between cross sections 10 and 11.

Digitized by Google

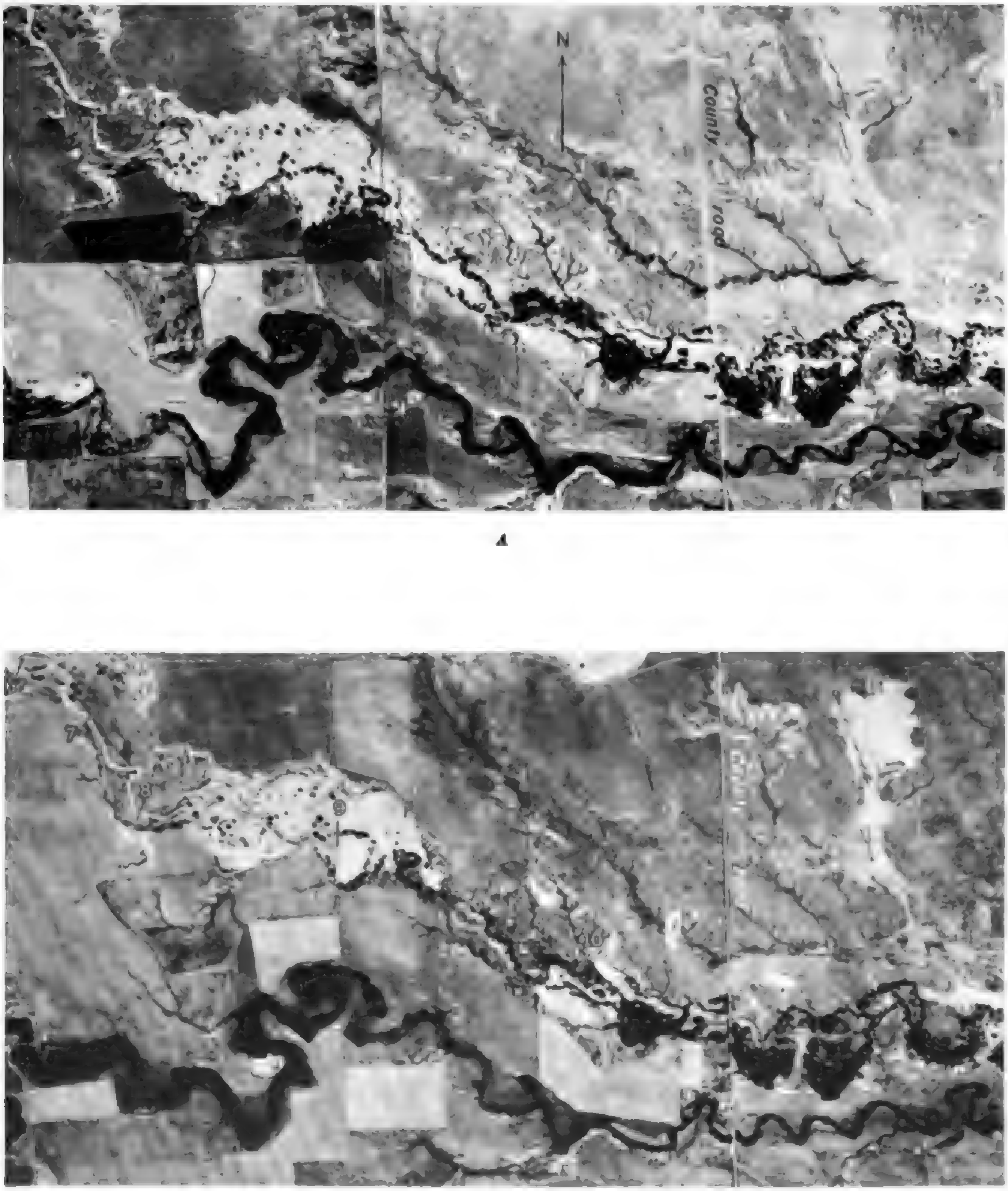

FIGURE 26.—Aerial photographs of part of the Sand Creek drainage basin, Nebr. A, taken in 1939; B, taken in 1954. Light-colored area at upper left of both photographs is area of maximum deposition. Locations of cross sections 6 to 10 are given on photograph B.

Digitized by Google

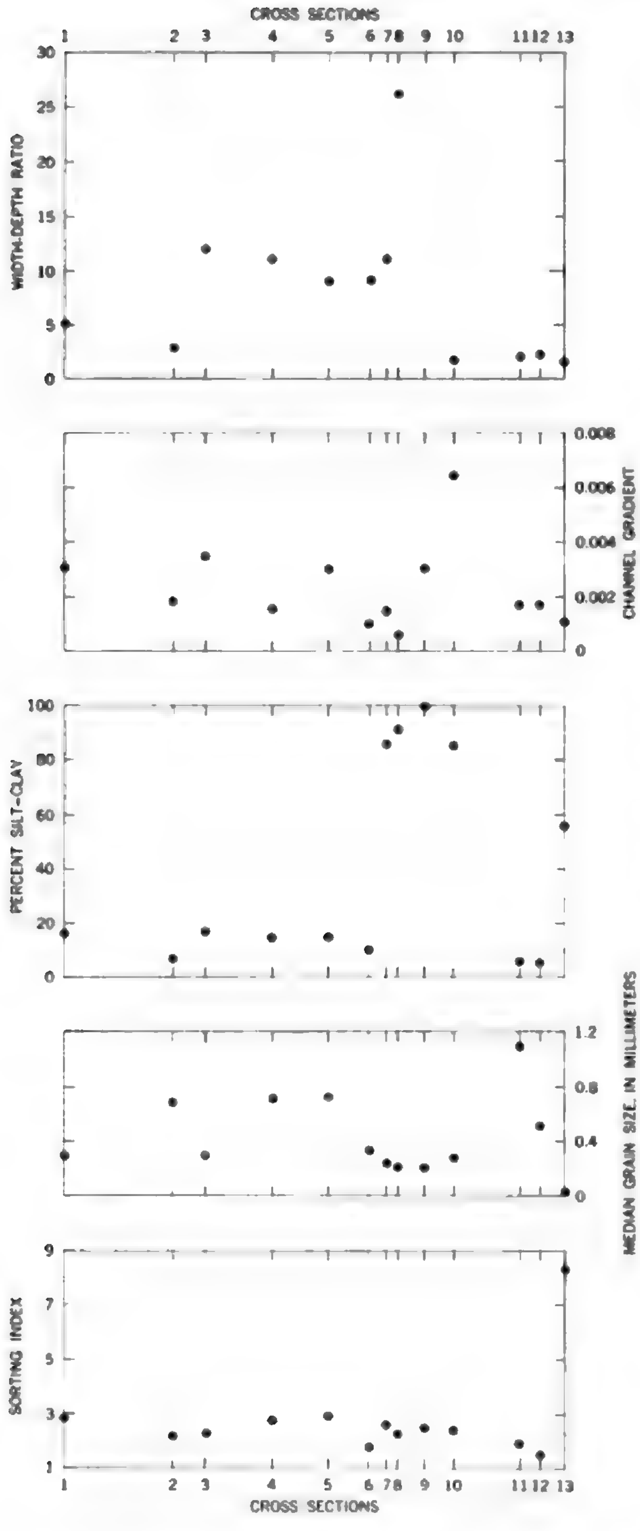

FIGURE 27.—Variations in channel and sediment characteristics, Sand Creek, Nebr. (The spacing of the cross sections along the abscissa is proportional to the distances between cross sections in the field.

In summary, the Sand Creek channel had few similarities in the manner of aggradation with Sage Creek. These differences are attributed mainly to the smaller percentage of silt-clay in the alluvium of Sand Creek.

ARROYO CALABASAS, NEW MEXICO

DESCRIPTION

Location.—Arroyo Calabasas (fig. 17) drains an area of about 48 square miles in central Santa Fe County, N. Mex. The drainage basin lies parallel to and about 1 mile northwest of U.S. Highway 85 between Santa Fe and the Santa Fe Airport (fig. 28), and a part of its headwaters lies within the Santa Fe city limits. Arroyo Calabasas is a tributary to the Santa Fe River. The Arroyo Calabasas drainage basin is shown on the following Geological Survey topographic maps: Santa Fe, Agua Fria, Turquoise Hill, Tetilla Peak, and Montoso Peak.

Annual precipitation.—A 40-year record of precipitation for Santa Fe (table 1) gives a mean annual precipitation of 14.19 inches. Of this total, 10.69 inches fell during the months of April through October. At the Santa Fe Airport a 15-year record gives a mean annual precipitation of only 10.80 inches. A comparison of the same 11 years of record from the 2 stations shows an average of 3.1 inches less rainfall at the airport. The Sangre de Cristo Mountains to the east probably produce a sufficient orographic effect to cause this difference in rainfall between mouth and headwaters of Arroyo Calabasas. The drainage basin apparently lies within a narrow zone of semiarid climate between the more humid mountains and the arid zone to the west.

Vegetation and land use.—Vegetational cover is poor except on the untrenched valley bottoms. Piñon and juniper grow on the hills. Grass is nearly absent except in the valleys, but slopes have a scant cover of Russian-thistle. Cattle and horses graze the undissected valley bottoms. The few dwellings within the drainage basin apparently are owned by people who work in the city of Santa Fe. No land cultivation has been attempted within the drainage basin.

Physiography and geology.—Unlike the two areas described previously, no prominent escarpment forms the drainage divide and no pediment development has taken place. Instead, a dendritic drainage pattern has developed, dissecting the poorly consolidated sediments into a network of valleys and divides. Hilltops are convex, bordered by valley-side slopes of varying steepness depending on the activity of the adjacent ephemeral stream.

The Arroyo de los Frijoles is a major tributary to Arroyo Calabasas. Their drainage areas are about

Digitized by Google

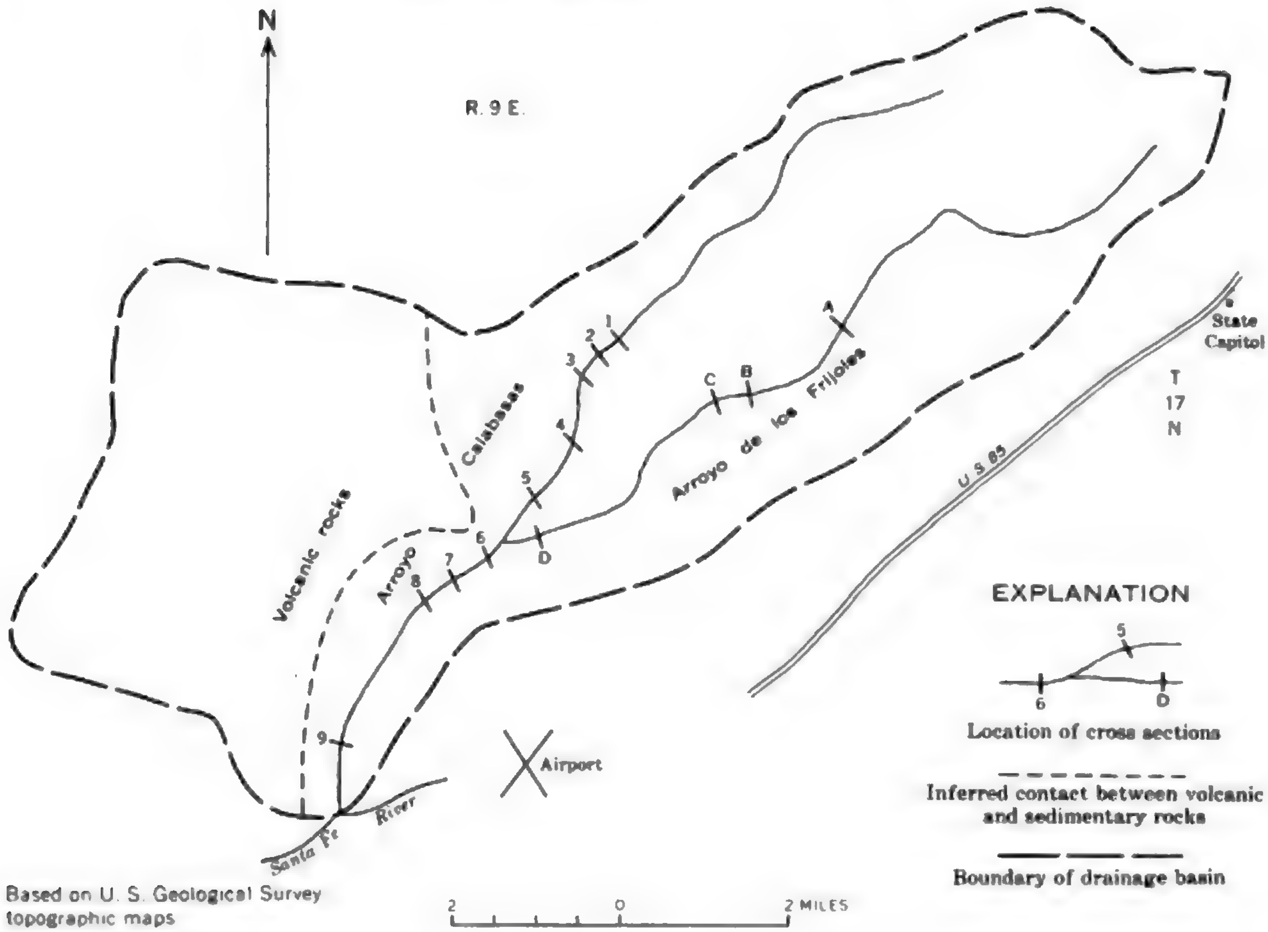

FIGURE 28.—Index map of Arroyo Calabasas, N. Mex., drainage basin showing location of cross sections.

equal at the junction of the two (fig. 28). In the field, Arroyo de los Frijoles seems to be the main stream, for at the junction it is a well-defined trench; whereas, the Arroyo Calabasas channel is completely aggraded and grassed a short distance above the junction.

The drainage basins are underlain by the unconsolidated or partly consolidated silts and sands (marls) of the Santa Fe group of middle (?) Miocene to Pleistocene (?) age. The irregular shape of the drainage basin is due to volcanic rocks in the western part of the basin. The extent of the volcanic rocks, as inferred from the topographic maps, is indicated on figure 28. The streams draining this area enter Arroyo Calabasas near its mouth, but the resistance and permeability of the volcanic rocks result in little sediment and runoff from this part of the basin.

Alluvium.—The stream channels transporting sediment eroded from the Santa Fe formation seem to be filled entirely with sand, and the percent silt-clay in the channel of Arroyo Calabasas is only 17 (table 4). Median grain size is 0.59 mm; Trask's sorting index is 2.01, and Hazen's effective size, 0.17 mm. Burmister's tables suggest that soil with D_{10} of 0.17 mm is permeable with free flow. Potential capillarity is slight and frost heaving is negligible. The above factors suggests that none of the particles in the channels are bound together but act independently. The bank material, however, where sampled, has a mean of 20 percent silt-clay and D_{10} of 0.040 mm. Thus, although the material in the channel bottoms is not cohesive the material in the banks is, forming stable sides to the channel.

The samples taken in the channel are not truly representative, for in some sections gravel, cobbles, and even a boulder in some places cover about 5 percent of the streambed. However, this small fraction of larger grain sizes did not seem to influence the general channel and sediment character in any noticeable manner, and for convenience only the finer material was sampled.

Digitized by Google

TABLE 4.—*Channel and sediment data, Arroyo Calabasas and Arroyo de los Frijoles, N. Mex.*

[Class: A=aggrading; S=stable; U=unclassified]

Cross section	Class	Drainage area (square miles)	Distance between cross sections (miles)	Median grain size D_{50} (mm)	Hazen's effective size D_{10} (mm)	Trask sorting index	Silt-clay (percent)	Gradient	Channel width (feet)	Channel depth (feet)	Width-depth ratio (F)	Weighted mean silt-clay, M (percent)
Channel sediment												
A	S	3.83		0.84	0.28	1.68	3.	0.013	79	3.	26	4.1
B	A	4.68	1.17	.58	.18	1.91	4	.013	257	2	129	4.1
C	U	4.81	.27					.013	88	2.5	35	
D	S	12.85	2.90	1.00	.20	2.10	5	.014	67	4.5	15	8.5
1	S	8.47		.85	.16	2.34	6	.010	84	5	17	9.0
2	S	8.91	.30	.90	.26	2.33	2.	.010	63	1	63	2.4
3	A	9.30	.43	.51	.24	1.53	.5	.013				
4	A	9.85	.61	.56	.27	1.52	2	.014				
5	A		.76	.035	.0012	3.37	80	.018				
6	S	24.2	.64	.50	.18	1.47	3	.009	92	4	23	4.8
7	S	25.8	.49	.75	.16	2.01	5	.011	100	4	25	5.8
8	A	26.4	.34	.48	.14	1.92	5	.009	90	1.5	60	5.1
9	A	42.3	1.89	.031	.0015	1.94	89					
Mean				0.59	0.17	2.01	17					
Bank sediment												
A				0.28	0.034	2.00	18					
B				.30	.060	1.83	12					
D				.13	.001	3.16	35					
1				.15	.005	4.13	34					
2				.20	.045	2.14	14					
6				.16	.040	2.30	26					
7				.30	.035	2.00	16					
8				.32	.090	1.42	8					
Mean				0.23	0.040	2.37	20					
Overbank sediment												
3				0.034	0.0049	2.16	80					
4				.33	.044	2.07	16					
9				.033	.0015	1.94	89					
Mean				0.13	0.003	2.39	62					

GENERAL CHANNEL VARIATIONS

Five cross sections were surveyed on Arroyo Calabasas above the confluence with Arroyo de los Frijoles; 3 were surveyed on Arroyo de los Frijoles, and 4 below the junction of both streams.

Above the junction, Arroyo Calabasas has a broadly convex longitudinal profile (fig. 29). At section 1 the stream channel is 8 feet deep and seems recently cut (fig. 29). Downstream the channel is progressively filled with sand until at section 3 recent floods have covered the entire valley floor (fig. 30*A*). The valley floor in turn becomes better covered with vegetation until at section 5 there is no indication that a channel exists upstream (fig. 30*B*). This part of the valley is used for grazing.

A short distance below section 5 is the junction of Arroyo Calabasas and Arroyo de los Frijoles. Section 6, located just below the junction, was surveyed across the deep channel, which is continuous in the Frijoles drainage basin (fig. 30*C*). A headcut has started to migrate up the Arroyo Calabasas valley, but the valley floor is hanging 8 feet above the trenched channel near the junction.

The longitudinal profile of Arroyo de los Frijoles is flatter than that of Arroyo Calabasas near their junction (fig. 29), but 3 miles upstream it steepens and at section *B* the channel is 30 feet higher than the corresponding point in the Calabasas channel. At section *A* the channel is shallow and sandy (fig. 29). Downstream at section *B* (fig. 29) the channel has widened considerably and aggraded. The photograph of the channel below section *B* (fig. 30*D*) shows that sand has been deposited out of the channel and among the trees near the channel. Several channels have formed; these cut around the partly buried brush and trees forming islands and a braided channel. No headcut is present, but the channel

Digitized by Google

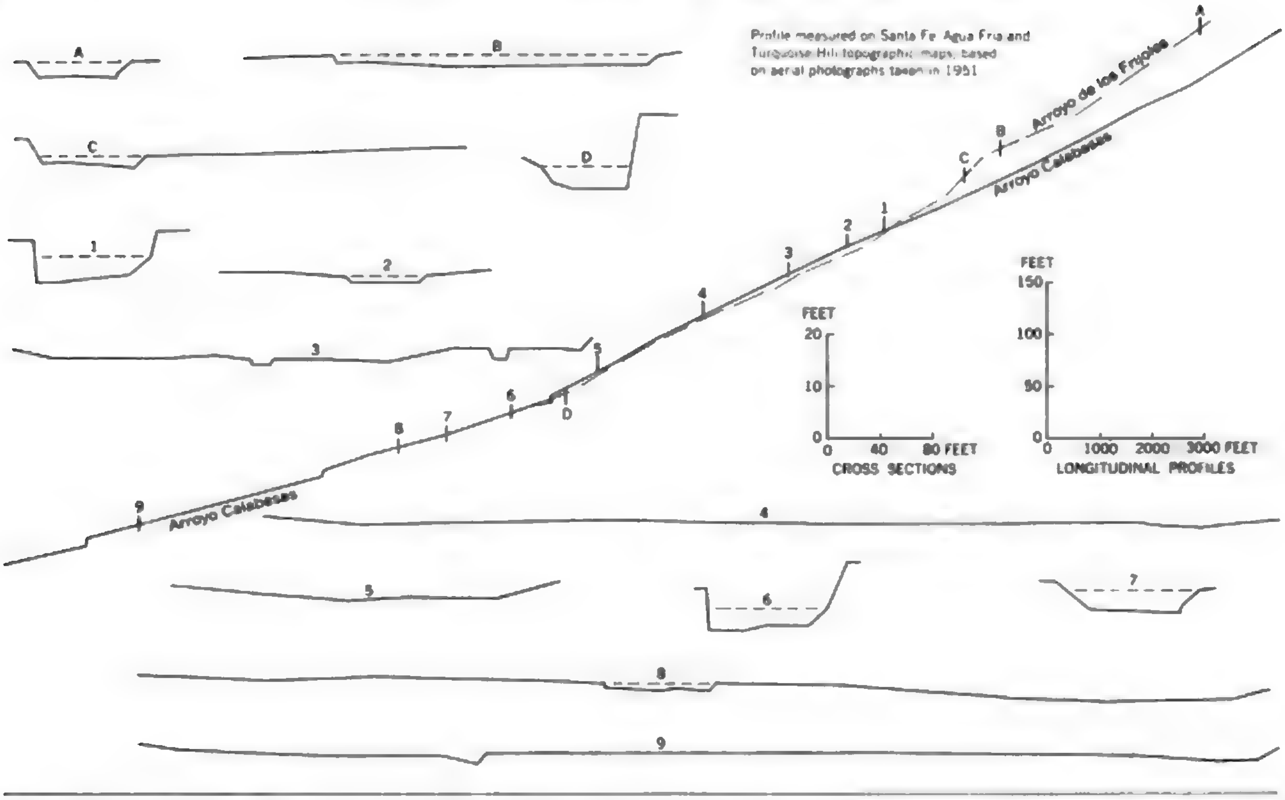

FIGURE 29.—Longitudinal profile and cross sections surveyed along Arroyo Calabasas and Arroyo de los Frijoles, N. Mex. Cross sections on Arroyo de los Frijoles are given a letter designation.

is nevertheless being lowered downstream from the aggraded cross section *B*, as indicated by plant roots that are exposed in the banks and by the rough appearance of the channel floor (fig. 30*E*) as contrasted with the smooth, flat floor characteristic of reaches of deposition. At section *C* the channel is narrower and bordered by well-defined banks. Continuing downstream the channel becomes deeper until at section *D* it is 5 feet deep. This, then, is the first example of channel rejuvenation in which headcutting is not important. A definite nick in the longitudinal profile is noted (fig. 29), but the noncohesive material in the channel prevents the development of a headcut, so typical of rejuvenation in the finer, more cohesive alluvium (Sage Creek between sections 1 and 2; Sand Creek near section 10). Below the junction of the two streams the channel, perhaps due to the decrease in gradient (fig. 29), is filled within a short distance.

At section 7 the channel is only 4 feet deep and at section 8 it is only 1.5 feet deep (fig. 30*F*). The width changes little, for the lack of large amounts of silt-clay prevent any deposition along the sides. Even at section 8 the remnants of the once high banks seem unchanged. Channels are filled solely from the bottom up. Deposition is complete below section 8 and vegetation covers the fill. A small discontinuous gully has formed between sections 8 and 9, but as its headcut moves upstream the lower end of the channel is filled. Here a headcut has formed. Samples of the alluvium taken across the valley show that, where the channel has been filled, the alluvium contains 66 percent silt-clay, which forms a tough, cohesive layer over the underlying predominantly sandy channel fill. This cohesive layer plus the vegetation cover is a protective cap, and headcut erosion again is the means of gully lengthening.

At section 9 the channel is completely filled, and the valley floor resembles that of section 5 (fig. 30*B*). The grass cover is good and cattle graze the valley floor. Below section 9 is another headcut that has worked headward from the junction of Arroyo Calabasas with the Santa Fe River (fig. 29).

Vegetation apparently does not aid the filling of channels here. The sandy nature of the alluvium prevents deposition along the banks, and no vegetation was noted in the channel bottom. The lack of vegetation in the channel is attributed to the lack of cohesion of the channel sediment. Any plant that takes root in the channel bottom would be washed out during the first

Digitized by Google

flood as the sandy sediment is set in motion. The growth of weeds in a sandy channel downstream from a stock-water reservoir demonstrates that the channel sediments will support vegetation if undisturbed. The reservoir has retained all flow, and the seeds and plants were not washed out of the sediment by floods.

Blocks of bank-caved material were not common in the channel, probably because the low cohesion of the bank material allows crumbling and removal of fallen material by the next flood.

QUANTITATIVE CHANNEL VARIATIONS

To simplify this discussion the data obtained at the cross sections on Arroyo de los Frijoles have been plotted as if they were sections measured upstream from section 1 on Arroyo Calabasas (sections A–D, fig 31).

Moving downstream from section A (fig. 31), three areas of deposition are crossed at sections B; 3, 4, 5; and 8, 9. These sections are characterized by a high width-depth ratio. Deposition causes filling of the channels from bottom to top without changing the width, thereby greatly increasing this ratio. Even in the trenched areas, this ratio is nearly 20, which greatly exceeds that in the areas of finer grained sediment.

Gradient is steep between sections B and C owing to recent incision. It is steep also at section 5 and where measured below section 9 near the Santa Fe River (X on fig. 29). These last two increases in gradient are due to the steepening of the valley floor by deposition. Each of the steeper reaches of deposition is associated with sediments of smaller grain size, although percent silt-clay is high only at sections 5 and 9. Perhaps this is because aggradation at section B is not so far advanced as at sections 5 and 9. This relation seems anomolous—finer sediment on the steepest parts of the longitudinal profile—but it is simply the result of channel and flood-plain deposition as discussed previously.

The samples at sections 3, 4, and 8 are not so fine as those at sections 5 and 9 even though in areas of heavy aggradation, because they were taken in the last vestiges of the channels, which were generally little more than sand-filled swales. However, the valley floor as a whole is characterized by finer sediments. For example, sediments adjacent to these inadequate channels contained up to 80 percent silt-clay (table 4). As mentioned above, D_{50} and percent silt-clay show the greatest changes on the aggraded reaches. If the samples taken at sections 5 and 9 were not plotted on figure 31, percent silt-clay would show hardly any change; whereas, D_{50} would decrease, but only slightly in a downstream direction.

The sorting index is highest at section 5 in the aggraded Arroyo Calabasas valley above the junction with Arroyo de los Frijoles.

SUMMARY OF ARROYO CALABASAS AREA

In a drainage area in which silt-clay occurs in small amounts the channels are filled from bottom to top. No plastering of fine sediments on the banks occurs, and vegetation is not an important cause of deposition. Vegetation, however, becomes important in stabilizing the deposit when flooding occurs over the entire valley floor.

Headcutting occurs only where channel-filling has been completed, and the coarser sediments are capped by a layer of fine material which supports a heavy grass cover. The suggestion here is that a channel in coarse sediment, when filled, may acquire the characteristics of an area of finer sediment.

The gradient of the valley increases on the reaches of deposition due to piling up of sediment on the valley floor. These steep gradient sections are covered with the finest sediments.

BAYOU GULCH, COLORADO

DESCRIPTION

Location.—Bayou Gulch (figs. 17, 32) drains an area of about 23 square miles in northeastern Douglas and northwestern Elbert Counties, Colo. It is a tributary of Cherry Creek, entering that stream at a point about 3 miles north of Franktown and about 5.5 miles south of Parker. State Highway 83 crosses Bayou Gulch about 0.4 mile above the mouth. The drainage basin is shown on the Castle Rock and Elizabeth quadrangles.

Annual precipitation.—Based on a 23-year record of precipitation at Parker (9E) (table 1) the mean annual precipitation is 13.42 inches. Of the total, 11.81 inches fell during the months of April through October. According to Thornthwaite's climate classification (1941) the area is semiarid.

Vegetation and land use.—Vegetational cover is heavy. Pine trees grow on the divides and cottonwood trees are plentiful along the upper reaches of the creek. Alfalfa is raised on a terrace above the present flood plain. The rest of the drainage basin is used for grazing except for a few fields of wheat and corn on the divide.

Physiography and geology.—This drainage basin, except for the heavier vegetational cover and a general appearance of coarser sediment, resembles that of the Santa Fe area. A dendritic drainage pattern has incised the poorly consolidated sediments into a network

Digitized by Google

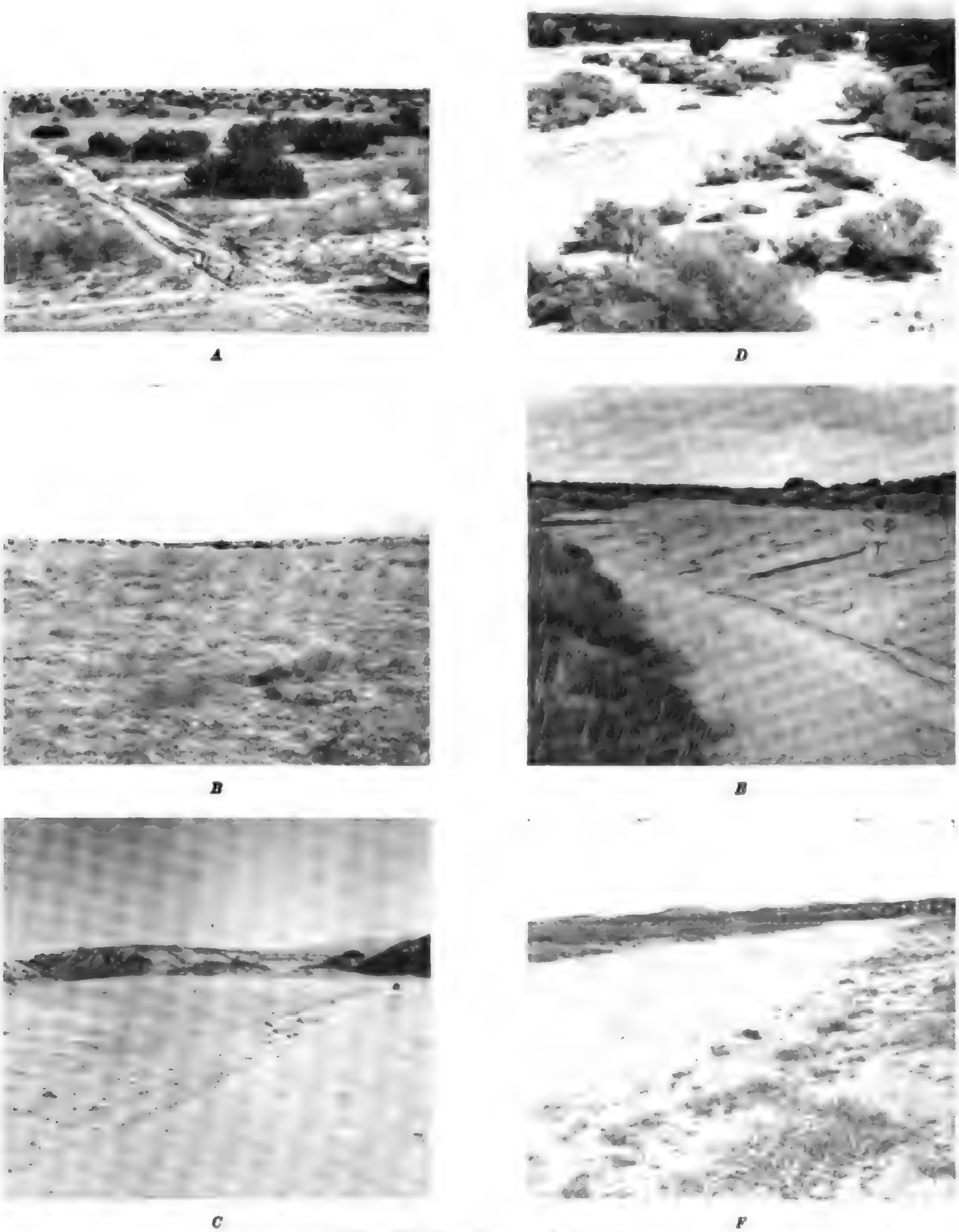

FIGURE 30.--Arroyo Calabasas, N. Mex.

Google

of valleys and rounded divides in marked contrast to the South Dakota area.

The entire drainage basin is underlain by poorly consolidated sandstones and shales of the Denver formation of Late Cretaceous and Paleocene age.

Alluvium.—The channel sediment contains 5 percent silt-clay (table 5). The median grain size is 0.57 mm, Trask's sorting index is 1.84, and Hazen's effective size is 0.17 mm. The characteristics of the channel sediment here and its behavior are little different than that in the Santa Fe area (table 4) for effective size is the same for both areas; however, the mechanics of aggradation seem to be somewhat different, and, indeed, the width-depth ratios are greater in this area. The bank material in Bayou Gulch differs from that in the Santa Fe area, for silt-clay is only 8 percent where sampled. Median size is 0.49 mm and D_{10} is 0.12, indicating that cohesion is low and that the banks would not have any great resistance to erosion in contrast to the more cohesive banks of the Santa Fe area.

GENERAL CHANNEL VARIATIONS

Above section 1 (figs. 32, 33) the channel narrows as the divide is approached. In the reaches of permanent flow above section 1, vegetation is encroaching on the channel but with difficulty because of the mobility of the channel material.

Below section 1 (fig. 34*A*) a wide sandy channel is characteristic of Bayou Gulch to its mouth. At sections 4 and 5 (fig. 34*B*) channel deposition may be occurring, for sand has been deposited over the flood plain, and the channel has been filled and widened. The observer has difficulty in determining what process is operative in each section of this channel. Where deposition is assumed to occur, widening of the sand-covered areas

TABLE 5.—*Channel and sediment data, Bayou Gulch, Colorado*

[Class: A=aggrading; S=stable; U=unclassified]

Cross section	Class	Drainage area (square miles)	Distance between cross sections (miles)	Median grain size D_{50} (mm)	Hazen's effective size D_{10} (mm)	Trask sorting index	Silt-clay (percent)	Gradient	Channel width (feet)	Channel depth (feet)	Width-depth ratio (*F*)	Weighted mean silt-clay, *M* (percent)
Channel sediment												
1	S	13.00		0.74	0.27	1.63	2	0.013	207	2.5	83	
2	S	18.95	0.43	.50	.13	1.85	6	.009	122	2	61	5.9
3	S	19.66	.24	.58	.17	1.69	4	.010	130	3	43	4.4
4	A	21.95	.47	.55	.17	1.84	2	.011	330	2	165	2.0
5	A	22.44	.16	.47	.06	2.50	12	.010	250	1.5	167	12.2
6	U	22.90	.95	.55	.21	1.51	4	.016	128	1.5	85	4.1
Mean				0.57	0.17	1.84	5					
Bank sediment												
2				0.82	0.26		2					
3				.40	.055		13					
4				.48	.075	2.13	10					
5				.27	.070		11					
6				.46	.15	1.60	6					
Mean				0.49	0.12		8.4					

EXPLANATION OF FIGURE 30

A, Cross section 2. Channel has been filled and flood waters cover area between truck and hill in background. Three small sandy swales convey low flows through this reach.

B, Cross section 5, view upstream. The valley floor is grass covered and is utilized for grazing. No channel is present at this cross section.

C, Near cross section 6, view upstream toward confluence of Arroyo de los Frijoles on right. Headcut on Arroyo Calabasas is less than 200 feet upstream from confluence.

D, Channel of Arroyo de los Frijoles near cross section *B*. Several channels appear to be degrading between sagebrush and juniper trees, thereby forming a braided channel.

E, Irregular channel surface suggests incipient degradation in Arroyo de los Frijoles downstream from cross section *C*.

F, Near cross section 8, view downstream. Channel is being progressively filled. Compare with photograph of section 6 (fig. 30 *C*).

Digitized by Google

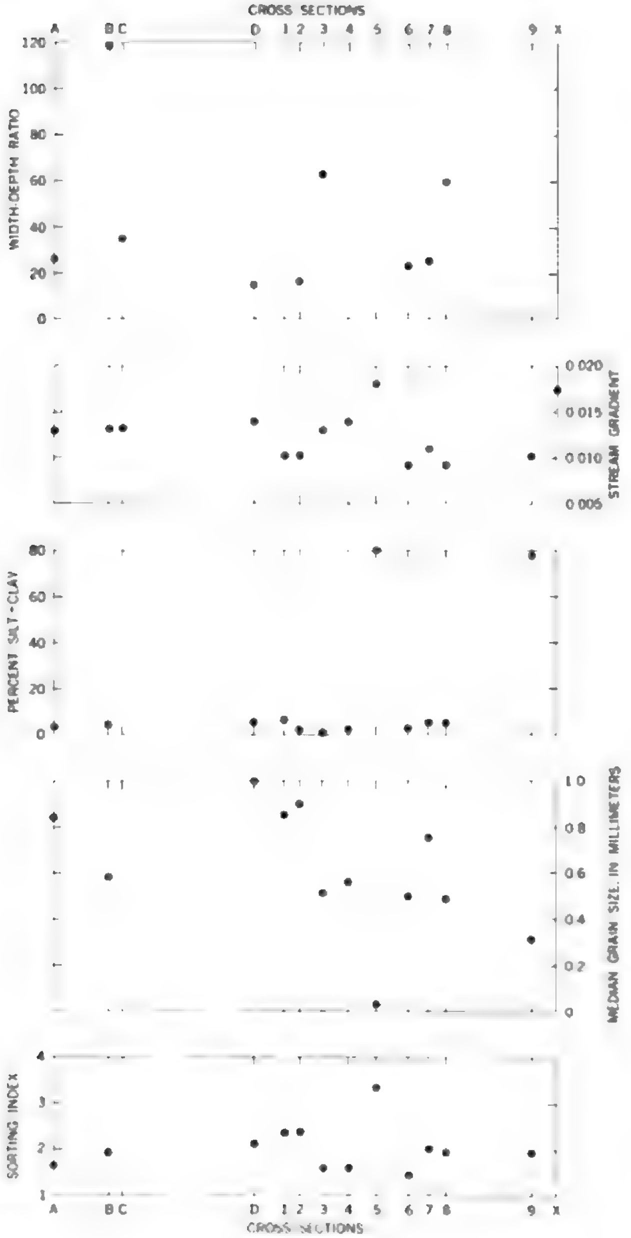

FIGURE 31.—Variations in channel and sediment characteristics, Arroyo Calabasas and Arroyo de los Frijoles, N. Mex. The spacing of the cross sections along the abscissa is proportional to the distances between cross sections in the field.

can be noted, but in contrast to the other areas investigated, there is no veneer of fine sediments over the coarser material and no encroachment of vegetation into the channel.

Below section 5, in order to confine the channel and thereby to prevent deposition of sand on the adjacent field and possible cutting around the bridge abutments, a dike has been built. The dike is sand piled in a ridge

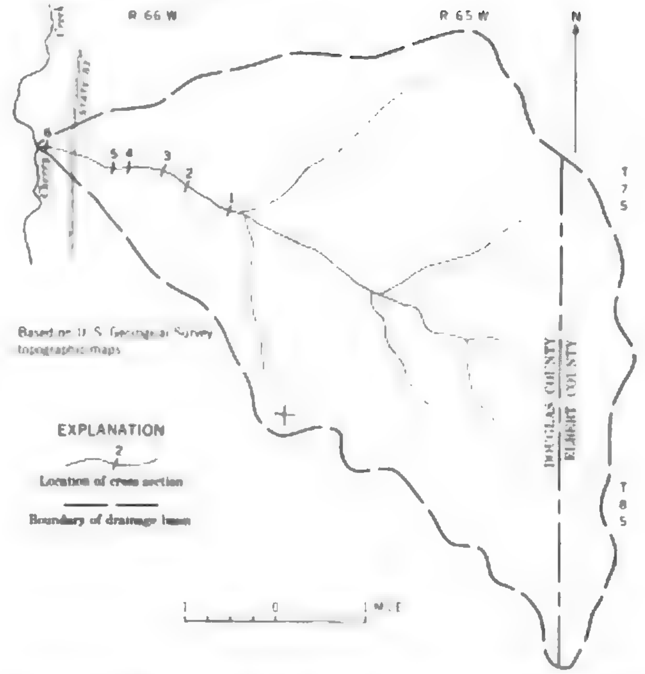

FIGURE 32.—Index map of Bayou Gulch, Colo., drainage basin showing location of cross sections.

along the channel, and although it looks unstable it seems to be effective at least for the low floodflows.

At the bridge over Bayou Creek, the gradient steepens in response to erosion (fig. 33). In contrast, the 1939 stream profile, obtained from the topographic maps, shows no such steepening. This steepening and the narrowing of the channel at section 6 (fig. 34*C*) suggest strongly that erosion is occurring or has occurred in the past in the lower reaches of Bayou Gulch. Owing to the lack of cohesion in the sediment, no headcut is present, and as will be shown later, the only indication that erosion is occurring other than the profile change is the increase in gradient at section 6 and a decrease in the width-depth ratio. Above section 6, 2 feet of sand has been deposited on the surface adjacent to the channel, indicating recent deposition before incision.

Very little vegetation grows on what are assumed to be reaches of major deposition, sections 4 and 5. Although bank caving has contributed to channel widening, the caved material is removed by the next flood.

QUANTITATIVE CHANNEL VARIATIONS

The downstream changes are summarized in figure 35. The major change in channel width-depth ratio is at the aggrading reach where the channel becomes very wide and shallow, sections 4 and 5. Gradient varies little but it increases at section 6 where the steepening is attributed to incision of the channel. The percent

Digitized by Google

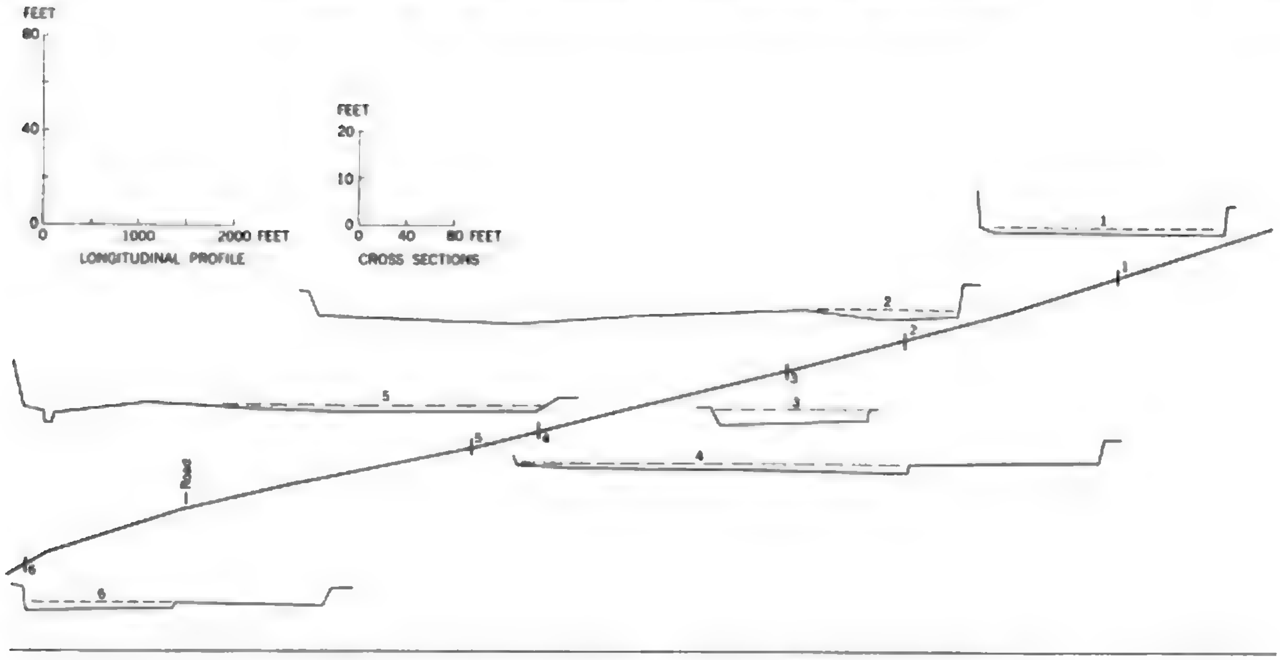

FIGURE 33.—Longitudinal profile and cross sections surveyed along Bayou Gulch, Colo.

of silt-clay in the samples is a maximum at section 5 where deposition is most noticeable.

Median grain size decreases downstream but increases slightly at section 6 due perhaps to channel incision. Sorting index varies slightly but increases at section 5, suggesting that sorting is poorer on reaches of deposition.

SUMMARY OF BAYOU GULCH AREA

The conclusions reached are little different from those of the Santa Fe area. The sediment is deposited on the channel floor, resulting in an increase in width-depth ratio. Vegetation apparently does not aid initial deposition.

In spite of the similarity of the Santa Fe and Bayou Gulch areas the width-depth ratio is much greater in Bayou Gulch. This is probably due to the decreased silt-clay content of bank material (see tables 4, 5).

MEDANO CREEK, COLORADO

DESCRIPTION

To complete the series of silt-clay to sand sediment types, Medano Creek was selected because both channel and bank material are composed almost entirely of sand.

Location.—Medano Creek (figs. 17 and 36) drains an area of about 29 square miles along the west flank of the Sangre de Cristo Mountains in the southeastern part of Saguache County and the northeast corner of Alamosa County. The part of the stream investigated lies within the boundary of the Great Sand Dunes National Monument in San Luis Valley. The drainage basin is shown on the Huerfano Park and Great Sand Dunes National Monument quadrangles.

Annual precipitation.—Precipitation records at the Great Sand Dunes National Monument headquarters are of short duration, but an 11-year record at Blanca, about 20 miles to the south, shows the mean annual precipitation to be 9.20 inches (table 1). However, rainfall in the mountains is much higher than in the San Luis Valley. A 30-year record at La Veta Pass about 16 miles to the east shows mean annual precipitation to be 20.98 inches. Thus the climate ranges from subhumid to arid from divide to the lower parts of the valley.

Vegetation and land use.—Vegetation ranges from typical alpine types in the high mountains to none on the sand dunes adjacent to the part of the creek studied. The basin is not used for agriculture.

Physiography and geology.—The mountains are composed of Permian sedimentary rocks and Precambrian metamorphic and igneous rocks. Sediments derived from erosion in the mountains are not found in large amounts in the channel sediment a short distance below the mountain front, for as the stream flows between the mountains and the main sand dune mass to the west (fig. 34*D*), windblown sand becomes the predominant sediment found in the channel. What might be a perennial flow from the mountains is, within a few miles, completely absorbed by the sand. In 1957 the channel

Digitized by Google

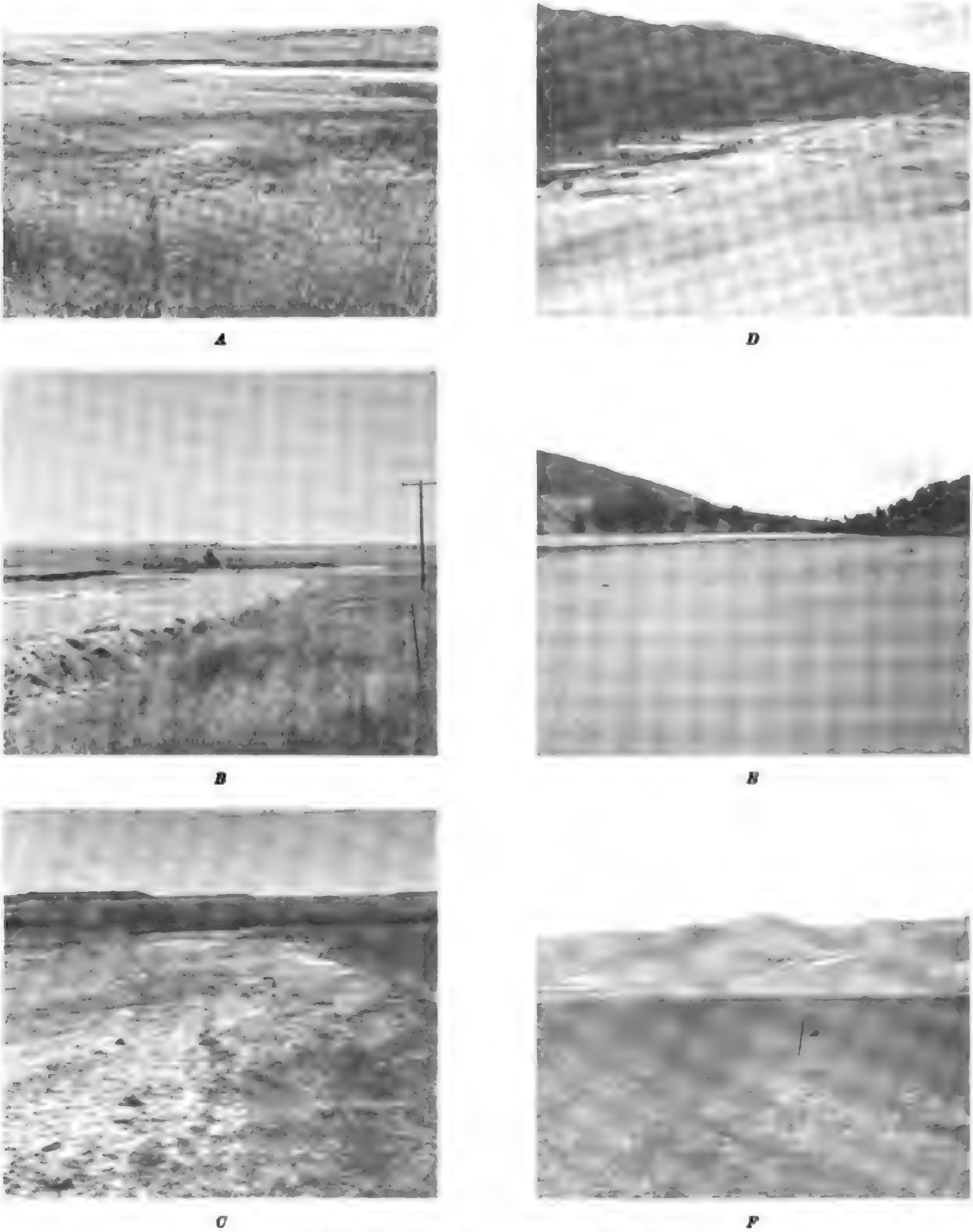

FIGURE 34. Bayou Gulch and Medano Creek, Colo.

Digitized by Google

TABLE 6. *Channel and sediment data*

[Class S=stable]

Cross section	Class	Drainage area (square miles)	Distance between cross sections (miles)	Median grain size D_{50} (mm)	Hazen's effective size D_{10} (mm)	Trask sorting index	Silt-clay (percent)	Gradient	Channel width (feet)	Channel depth (feet)	Width-depth ratio (F)	Weighted mean silt-clay, M (percent)
Channel sediment												
1	S	25.85		0.24	0.15	1.23	1	0.017	340	2	170	1
2	S	26.10	0.36	.24	.15	1.23	1	.019	800	3	267	1
3	S	28.84	.65	.24	.15	1.23	.5	.016	820	2.5	328	.5
Mean				.24	.15	1.23	.8					
Bank sediment												
1				0.24	0.014	1.23	0.5					
3				.31	.019	1.19	.5					
Mean				.28	.017	1.21	.5					

contained migrating sand dunes 2 miles below the campgrounds of the national monument.

The eolian sand aparently accumulates here due to a re-entrant in the mountain front. Sand blown along the mountain front is trapped in this pocket, and over the years has accumulated into a tremendous mass of sand in places more than 500 feet high (fig. 34*F*).

Alluvium.—Both the banks and channel of Medano Creek, in the reaches studied, are composed of sand derived from the main dune mass to the west (table 6). In the channel at the 3 cross sections surveyed, median grain size is identical, 0.24 mm, as is D_{10}, 0.15 mm. Mean percent silt-clay is 0.8. Sorting index is 1.23. The bank material has even less silt-clay, 0.5 percent, but median size is 0.28 mm and D_{10} is 0.17 mm.

The almost complete absence of silt-clay indicates (Burmister, 1952) that the material in banks and channel is freely drained and has no cohesion. The banks, in fact, are at the angle of repose of dune sand, about 26°.

Although by inspection this area would seem to have the coarsest sediment, the average median size for all cross sections is finer than for any of the other areas. This is due to the excellent sorting of the windblown sand; no appreciable sediment larger than 0.5 mm or smaller than 0.15 mm was found in the samples.

QUANTITATIVE CHANNEL VARIATIONS

Neglecting changes in channel character near and in the mountains, the several miles of channel readily accessible showed only slight changes. At section 1 the channel is confined between the dunes to the west and sand piled against the mountain front (fig. 34*E*). Downstream, however, the channel widens and width-depth ratio increases (fig. 37; table 6). Gradient decreases but the character of the alluvium remains almost constant.

Water was flowing in the channel during the study, and discharge was estimated as 10 cubic feet per second. A remarkable feature is that the water was flowing on a part of the channel well above the lowest point on the cross section. The water covered only a small part of the total channel width, about 80 to 100 feet, and ranged in depth from a thin film to 0.3 foot. During a flood, however, water would cover 800 feet of channel at the campground (fig. 34*F*).

EXPLANATION OF FIGURE 34

A, Bayou Gulch, view upstream between cross sections 2 and 3. Channel is relatively wide and sandy. Bank cutting is common in this reach.

B, Bayou Gulch, view downstream toward cross section 5. Small levee on right side of channel prevents flooding of field to right of photograph.

C, Bayou Gulch, view downstream from highway bridge toward cross section 6. Tree line indicates location of Cherry Creek.

D, View from crest of sand dunes in Great Sand Dunes National Monument across Medano Creek toward the Sangre de Cristo Mountains.

E, Medano Creek, cross section 1, view upstream. Note that water is flowing on only a small part of the cross section. The cross section plotted on figure 37 shows that the water is not flowing on the lowest part of the channel floor.

F, Medano Creek, cross section 3, view to west toward main sand-dune mass. Point in channel from which photograph was taken is about 2 feet lower than part of channel on which water is flowing.

504885 O—61——5

Digitized by Google

Possibly between floods the water shifts laterally across the channel, building up by deposition that part of the channel on which it flows. This would and does result in the peculiar situation of water flowing at an altitude higher than much of the channel bottom. The channel surface on which water flows is braided. Possibly, this is because there are no banks confining the small flows and also because water loss into the sand is high.

Although only a shallow layer of water was moving downstream, large amounts of sand were in movement. Sand grains and even a few half-submerged pebbles were being rolled along the channel bottom. The water was clear, owing to the low percent silt-clay, and this enabled the author to see antidunes form on the channel bottom and move upstream. The upstream movement of the antidune itself could be observed rather than just its effect on the water surface.

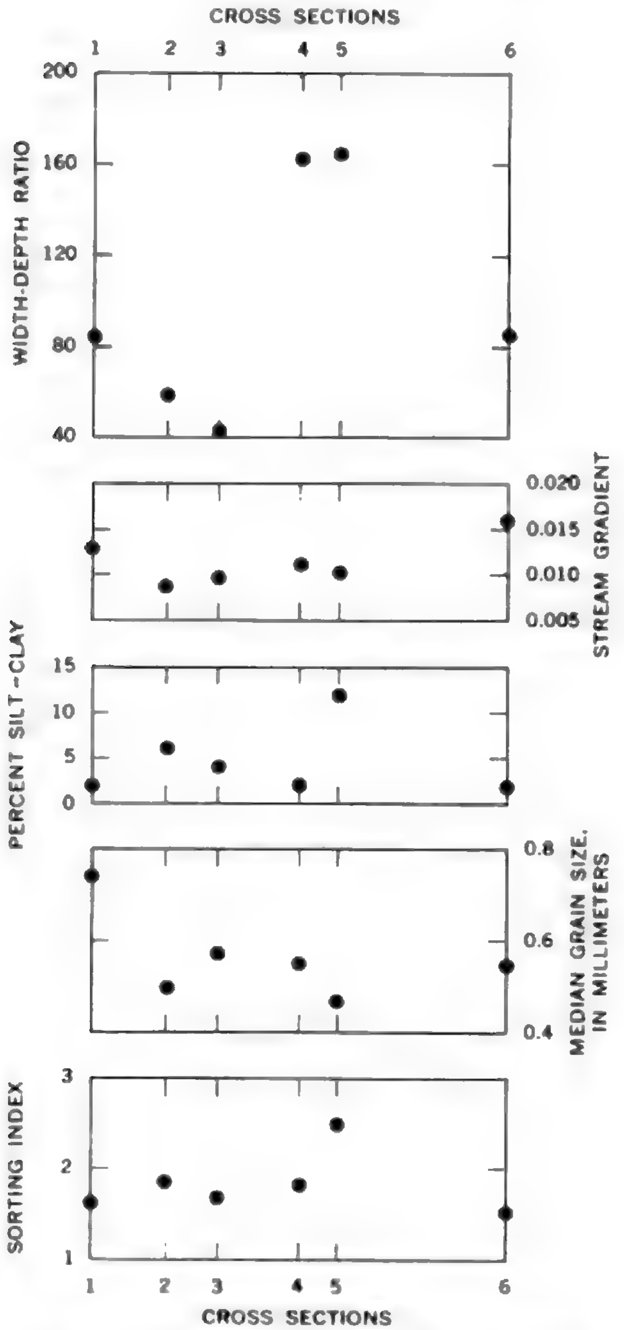

FIGURE 35. Variations in channel and sediment characteristics, Bayou Gulch, Colo. The spacing of the cross sections along the abscissa is proportional to the distances between cross sections in field.

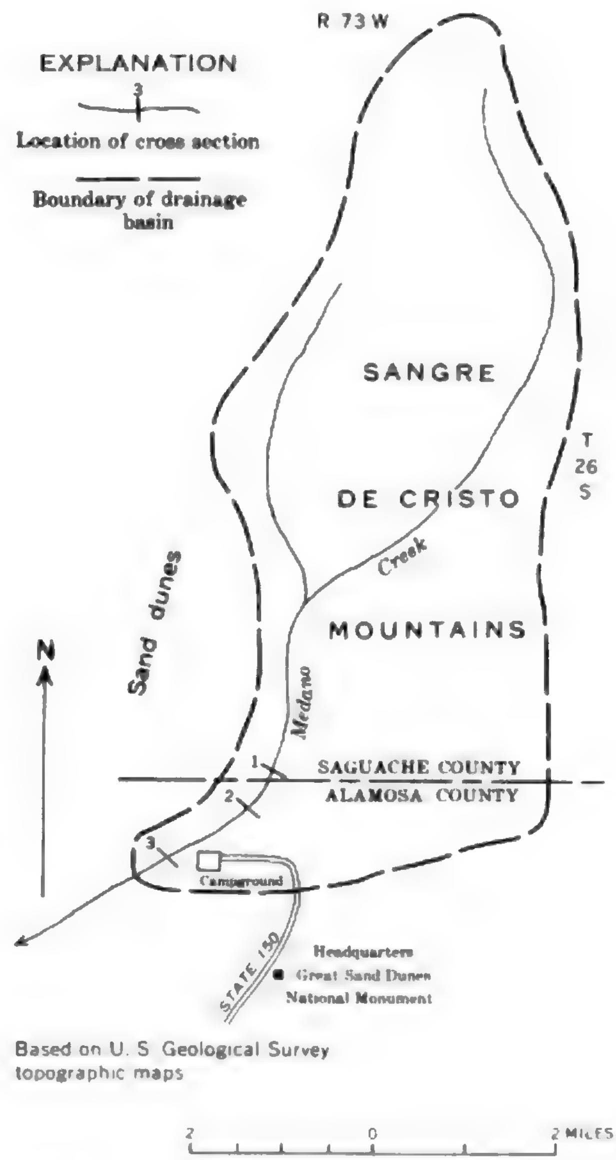

FIGURE 36. Index map of Medano Creek, Colo., showing location of cross sections.

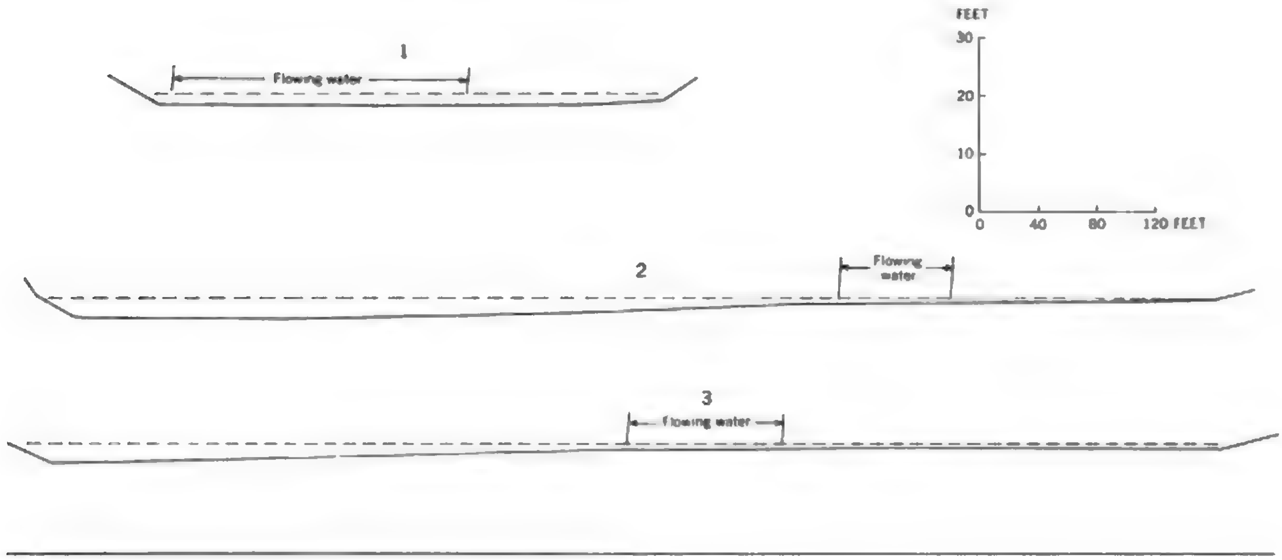

FIGURE 37.—Cross sections surveyed along Medano Creek, Colo.

Water flowing at and above the campground was completely absorbed by the sandy channel within one-half mile downstream. It was not possible to study the aggrading reach below the campground because sand dunes had migrated into that part of the channel. In addition, a veneer of windblown sand covered the channel making the distinction between aeolian and fluvial deposition difficult.

SUMMARY OF MEDANO CREEK AREA

This channel, composed of dune sand with banks of the same material, is the widest and shallowest of the channels studied. The channel and sediment character changes little downstream. Even though average median sediment size is the smallest sampled, this channel is typical of those carrying the less cohesive sediments.

COMPARISON OF SEDIMENT AND CHANNEL CHARACTERISTICS BETWEEN AREAS

In the preceding section the changes in sediment type and channel character along a stream are discussed for five areas differing in alluvial characteristics. In this part of the report, the differences and comparisons among the five areas will be reviewed, additional data will be presented, and practical applications of the conclusions will be discussed.

During this investigation, which was aimed mainly at revealing the mechanics of erosion and deposition in small ephemeral-stream channels, data were collected at some cross sections that were ultimately determined to be stable rather than aggrading or degrading. This was unavoidable, for during the early stages of the study, the stable cross sections could not be readily identified. However, the availability of the stable cross section data allows comparison of the stable channel characteristics among the five study areas. In addition, if the stable sections are discussed first, then the characteristics and variability of the unstable sections can be compared with the characteristics of stable cross sections.

RELATION BETWEEN SEDIMENT AND CHANNEL CHARACTERISTICS

The stable channel cross sections were selected from all those studied. The separation was made partly for comparative purposes, for it is assumed that those sections approaching or having reached stability will afford a better basis for comparison of channel and sediment characteristics among the five areas than a mean value for all sections studied in each area.

The mean values for channel and sediment characteristics for the stable cross sections as well as similar data for those sections which are being actively aggraded are shown in table 7. It was more difficult to determine if a particular section was being actively degraded although three cross sections are so classed (tables 2, 3). Those sections not listed in table 7 were either doubtfully stable or not being aggraded and are the unclassified channels of tables 2–5. All cross sections classed as aggrading, however, are not listed on table 7, for at many such sections the channel was completely filled.

The study areas are listed on this table in the order in which they were discussed in the preceding sections, namely, in the order of apparent coarsening of the channel alluvium and increasing width-depth ratio.

Digitized by Google

TABLE 7.—*Mean values of channel and sediment data*

Study area	Type of cross section	Cross section	Median grain size D_{50} (mm)	Hazen's effective size D_{10} (mm)	Trask sorting index	Silt-clay (percent)	Gradient	Channel width (feet)	Channel depth (feet)	Width-depth ratio (F)	Weighted mean silt-clay, M (percent)
Sage Creek	Stable	2, 3, 4	0.080	0.0035	5.74	[illegible]	0.0048	22	6.3	3.8	69
	Aggrading	6, 7, 10, 11, 12.	.067	.0049	4.96	65	.002	20	4.0	5.1	70
Do	Stable	3, 4, 5, 6	.53	.032	2.45	14	.0023	[illegible]	5.3	10.3	22
	Aggrading	7, 8	.022	.0013	2.43	89	.001	42	2.7	18.8	88
Arroyo Calabasas	Stable	A, D, 1, 2, 6, 7.	.81	.21	1.99	4	.011	81	3.6	28.1	5.7
	Aggrading	B, 3, 8	.52	.19	1.79	3.2	.012	[1] 173	[1] 1.8	[1] 94.5	[1] 4.6
Bayou Gulch	Stable	1, 2, 3	.61	.19	1.72	4	.011	153	2.5	62	5.1
	Aggrading	4, 5	.51	.12	2.17	7	.010	290	1.8	166	7.1
Medano Creek	Stable	1, 2, 3	.24	.15	1.23	0.8	.017	653	2.5	255	.8
	Aggrading										

[1] Based on sections B and 8 only.

A glance at table 7, however, immediately suggests the order to be incorrect, for there is no progressive increase in median grain size (D_{50}) or D_{10} from area 1 to 5 in spite of appearances in the field. The percent silt-clay in the channel samples, however, progressively decreases from a high value for the Sage Creek area to a negligible amount for the Medano Creek area, although the values for Arroyo Calabasas and Bayou Gulch are the same.

The character of the sediment forming the perimeter of the channel can be expressed as a weighted mean percent silt-clay, designated M (Schumm, 1960b). M is calculated as follows

$$M=\frac{Sc\times W+Sb\times 2D}{W+2D}$$

in which Sc=percent silt-clay in channel alluvium,
Sb=percent silt-clay in bank alluvium,
D=channel depth,
W=channel width.

The weighted mean percent silt-clay, hereafter referred to as M in the text, is given for all cross sections at which bank and channel samples were collected (see tables 2–6), and the mean values for stable and aggrading sections are presented in table 7. M for the stable cross sections decreases in a manner similar to that for channel silt-clay.

It is interesting to note that the mean sorting index decreases progressively from area 1 to 5; the samples become better sorted as the percent silt-clay decreases. This may be explained by the fact that none of the streams contained appreciable amounts of gravel, so as the finer components of the sediment were eliminated the sorting naturally improved.

The mean width and depth of the channels bear an inverse relation to each other, but both show a progressive change as percent silt-clay decreases. The mean width-depth ratio shows a progressive increase as channel percent silt-clay and M decreases. In figure 38 the values of width-depth ratio for 18 stable cross sections are plotted against weighted mean percent silt-clay (M) of the channel and bank samples taken at each of the cross sections.

The relation is such that a narrow and deep channel is associated with sediments high in silt-clay; whereas, those channels containing little silt-clay are wide and shallow. The regression line for figure 38, although not the best fit for the data shown, is based on data for 69 cross sections including those plotted on figure 38 (Schumm, 1960b).

The gradients of the streams show a general steepening with decreasing silt-clay, but this is not progressive, for the Sand Creek area has a somewhat gentler gradient than Sage Creek. A plot of M against gradient (fig. 39) reveals that stream gradient increases as M decreases. Thus for those small ephemeral streams where the annual rainfall is in the range 10 to 20 inches both channel shape and gradient are related to M. It is probable that a different relation exists between gradient and M for larger streams and those in more humid regions. The relation between M and width-depth ratio is valid for a large range of streams in different climatic regions (Schumm, 1960b).

SUMMARY OF COMPARISONS

Differences in sediment type among the study areas are related to variations in channel characteristics. As progressively wider and shallower sections of the stable channels were considered an accompanying decrease in the percent silt-clay composing the perimeter of the channel was noted. In addition, a decrease in channel gradient occurred as M increased.

It is assumed that these relations may be only the most obvious. Further work may reveal that other aspects of fluvial hydraulics and morphology are related to a parameter, such as M, expressive of the physical properties of the alluvium forming stream channels.

Digitized by Google

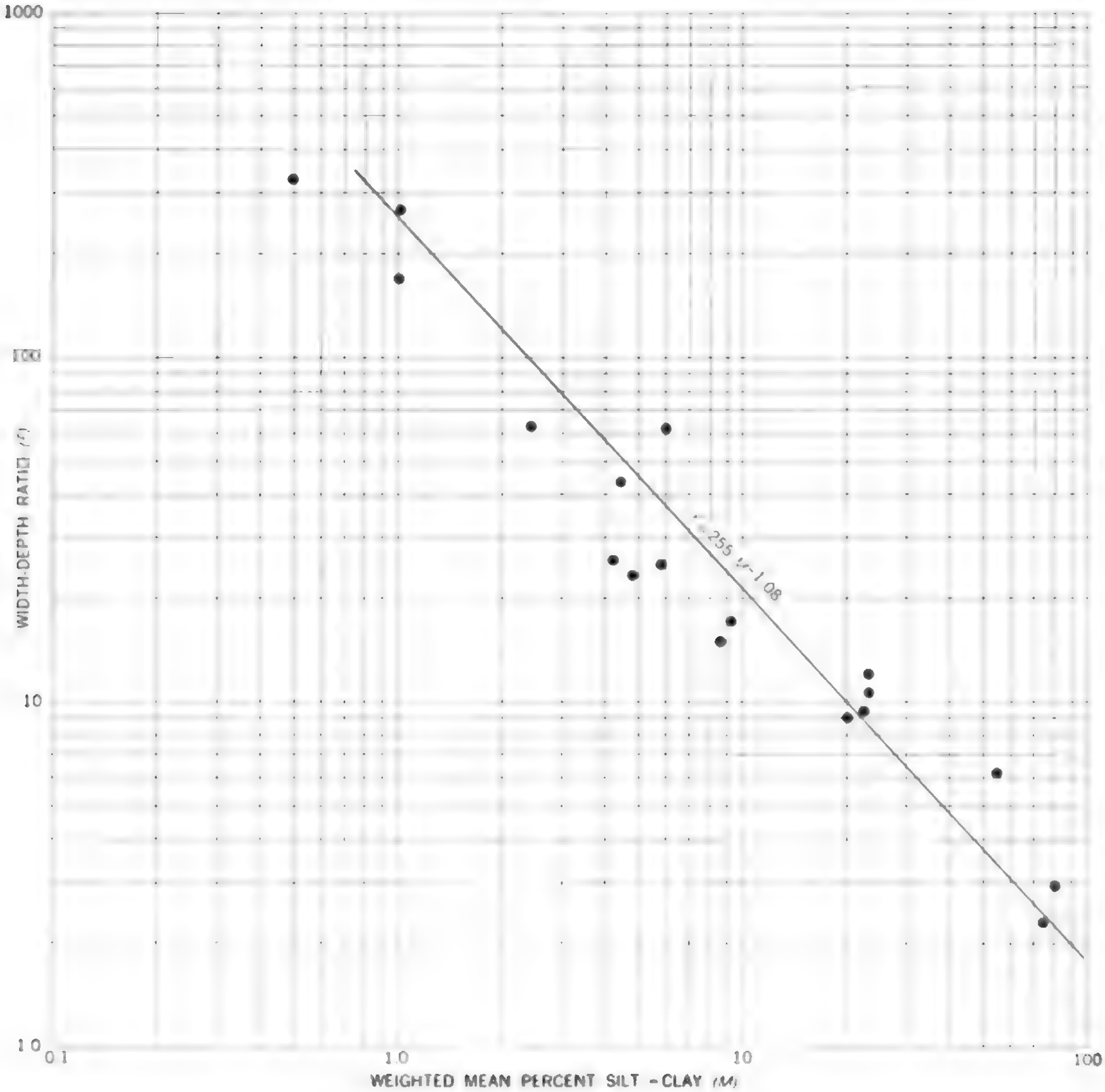

FIGURE 38.—Relation between width-depth ratio (F) and weighted mean percent silt-clay (M) in bank and channel sediments for stable cross sections.

DEPOSITION IN EPHEMERAL STREAMS

CROSS SECTIONS

During the discussion of the study areas, some comparisons between the manner of aggradation in each area were made. The changes in width-depth ratio as an aggrading reach was approached and crossed indicates that as deposition increased the channels containing highly cohesive sediments with a high percent silt-clay became progressively narrower; whereas, channels containing low-cohesion sediments became shallower with little change in width. The modification of the shape of a stream channel by aggradation seems to be determined by the mechanics of sediment deposition in the channel.

Blench (1957, p. 13) describes lateral deposition of silt along the sides of Indian regime canals and explains how this phenomenon is used in the repair of breached canals and in design. According to Blench, the typical Indian canal has a sand bed and berms of silty-clay

Digitized by Google

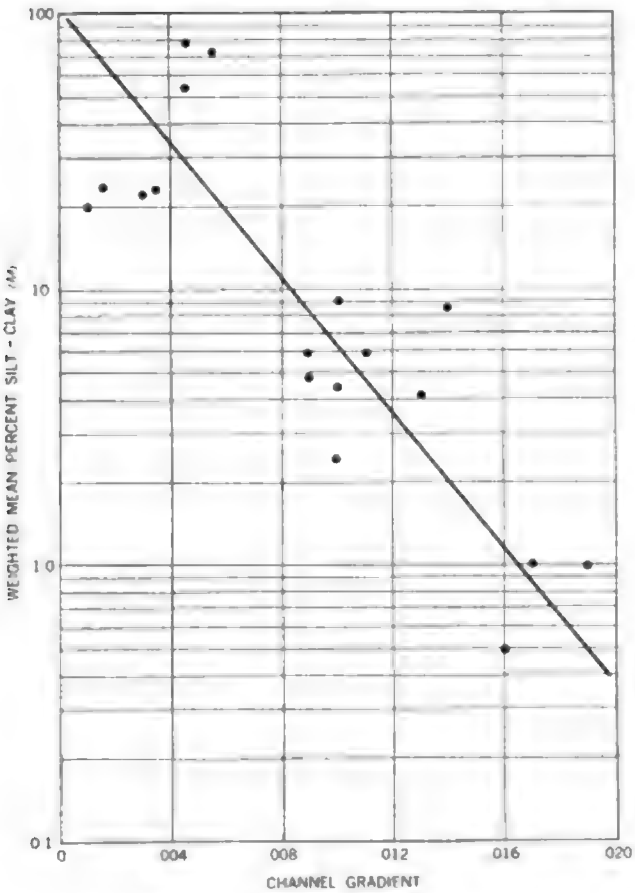

FIGURE 39. Relation between stream gradient and weighted mean percent silt-clay (M) for stable cross sections.

loam. The berms are deposited from suspended load. Two study areas of this investigation, Sage Creek and even Sand Creek at section 7, show berm development. The channels with low percent silt-clay in banks and channel, Bayou Gulch, Arroyo Calabasas, and Medano Creek, show only deposition on the channel bottom.

Lateral deposition is due both to the cohesiveness of the finer sediment and to its high concentration throughout the mass of flowing water. Hjulstrom's (1935, p. 274) calculations demonstrate that a mixture of silt and clay with an average grain size of 0.001 mm will have a concentration 5 meters above the channel floor only slightly less than that measured just above the channel floor; whereas, the concentration of sediment with an average size of 0.10 mm rapidly decreases to 10 percent of that just above the channel at a height of only 25 cm. Thus, under similar conditions of turbulence the finest sediment is available for deposition along the banks; whereas, the coarse material will only be deposited on the channel floor.

It has been suggested that the correlation between width-depth ratio and M might be used as a criterion of aggradation or degradation (Schumm, 1960b). That is, since stable channels fall about the line described by the equation $F=255\ M^{-1.08}$, then points that plot well above this line might be assumed to be aggrading; whereas, those plotting below the line would be degrading. To test this hypothesis the data for stable degrading, and aggrading cross sections were plotted on figure 40 about this regression line.

The 11 aggrading sections plotted all fall above the regression line; however, only 7 would be recognized as aggrading from their position on the graph. The unstable condition of the remainder would be obscured by the natural scatter about the regression line. However, since the Sage Creek cross sections have a decrease in width-depth ratio with aggradation, these points would not be expected to fall above the regression line. In any event, it seems that those cross sections which plot well above the regression line may be considered aggrading.

Of 3 cross sections originally classed as degrading, there are adequate data for plotting of 2 (Sand Creek sections 10 and 11; table 3). These two sections plot below the regression line of figure 40. Perhaps on the basis of the location on figure 40 of sections known to be aggrading or degrading, it may be possible to classify the remaining cross sections, that is, those listed as unclassified on tables 2 through 6.

Twelve of the 49 cross sections studied are unclassified. Insufficient data are available to allow computation of width-depth ratio or M for six of these. The remaining 6 cross sections (Sand Creek 2 and 12; Sage Creek 5, 8, and 14; Bayou Gulch 6) are plotted on figure 40. Four of these are located close to the regression line (Sage Creek 2 and 8, Sand Creek 5, Bayou Gulch 6), and these sections may be stable.

If the field information on the nature of these cross sections is considered, each is located on a reach of channel either affected in the past by channel changes or to be affected by channel changes in the future. For example, the channels of Sage Creek at section 2 and Bayou Gulch at section 6 have been degraded in the past but have apparently reverted to a stable form. Sand Creek section 5, on the other hand, has not yet been affected by the aggradation occurring downstream at section 6. Sage Creek section 8, although believed to have been eroded and then subjected to recent deposition, also has a form characteristic of a stable channel. The erosion occurring a short distance downstream, however, will undoubtedly cause marked changes at this section in the near future.

Digitized by Google

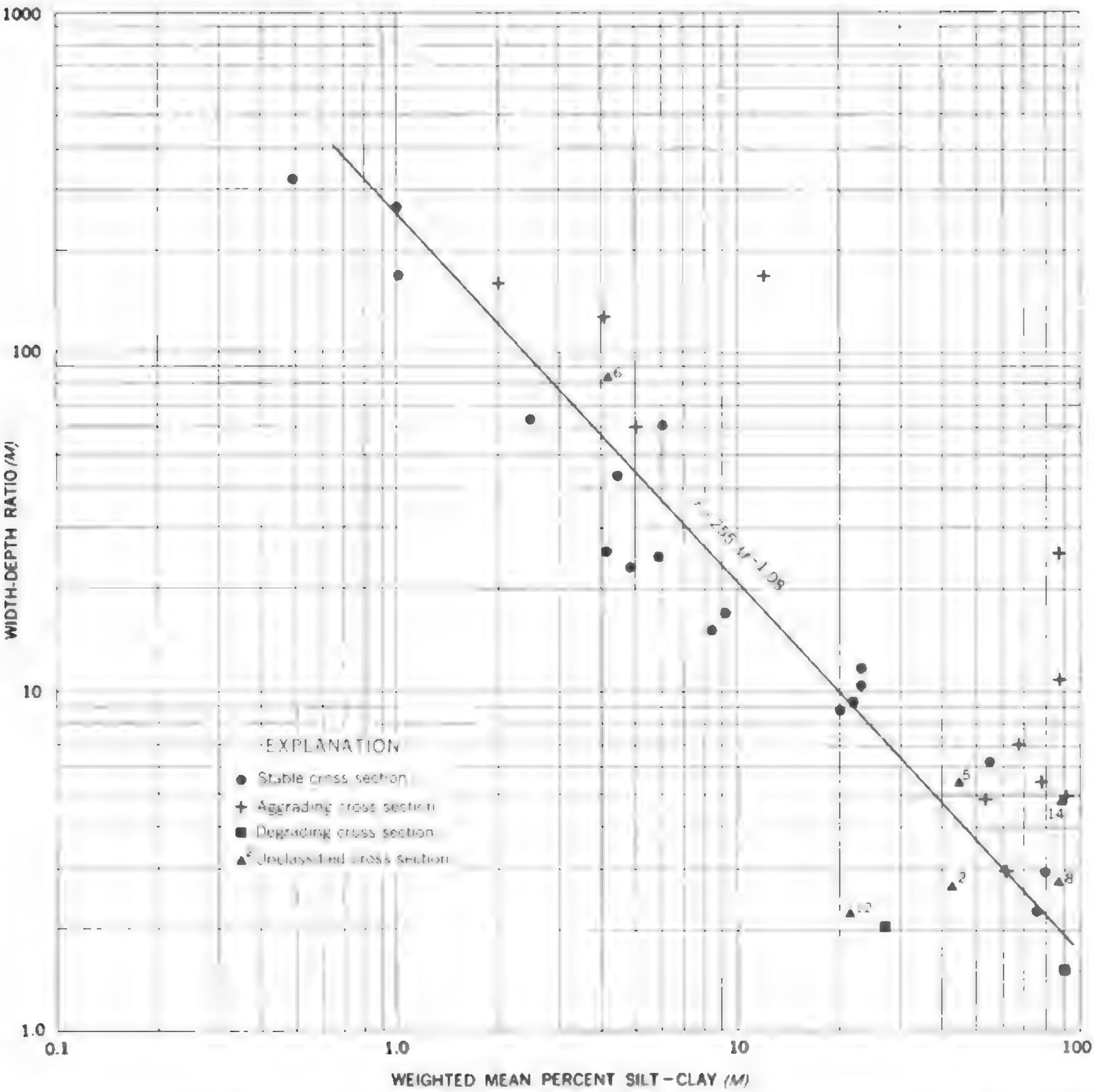

FIGURE 40.—Relation between width-depth ratio and weighted mean percent silt-clay for stable and unstable cross sections. Numbers refer to cross sections, tables 2, 3, and 5.

The remaining two sections plot far from the regression line. Sage Creek section 14 plots well above the line, and it was noted in the field that water diverted onto the flood plain by a small dam enters the channel and causes deposition at this section. Sand Creek section 12 plots well below the line indicating channel erosion. Section 12 is located only 0.3 mile below section 11 which was previously classified as degrading. Either degradation is still occurring at section 12 or the section has not been able to adjust its form as yet to stable conditions. The above suggests that the location of the unclassified sections with regard to the regression line of figure 40 makes it possible to classify the sections as to their stability or lack of it.

SLOPE

In addition to changes in channel shape accompanying aggradation, there are concomitant changes in the

Digitized by Google

longitudinal profile of the stream. As is well known and was noted in each of the study areas, stream gradient is decreased on the upstream part of the aggrading reach. The slopes measured at the cross sections in the field do not show this in all cases (figs. 22, 27, 31, 35) but the longitudinal profiles do (figs. 19, 24, 29, 33).

All the graphs and longitudinal profiles show an increase in gradient downstream on the aggarding reach. In all aggrading channels this steepening enables the stream to increase its capacity for sediment load. Generally, incision occurs on the steepened reach (Schumm and Hadley, 1957). Where the channel is completely filled by deposition on the steeper reach, the anomalous situation arises that the finer alluvium is found on the steeper aggrading reaches. See section 10 on figure 27 and sections *B*, 5, and *X* on figure 31.

The data collected at cross sections located on the aggrading reaches of the study areas give a fairly complete picture of what might occur at one cross section during the complete filling of the channel. During the discussion of the historic changes on Sand Creek it was concluded that the upstream limit of aggradation shifted upchannel as aggradation progressed. Channel aggradation, therefore, may be somewhat analagous to backfilling of the channel, rather than to a general filling of the channel simultaneously over a long distance.

Assuming that aggradation begins at one particular point in the channel and then progresses upstream, it is possible to outline the steps in the complete cycle of aggradation and retrenching of that channel. Gradient is decreased by the initial channel deposit, and if it is not swept away by the next flood, this alluvial deposit induces further deposition in the channel. As the channel fills, the zone where major deposition of the coarser fraction of the alluvium occurs, migrates upchannel, and progressively finer sediment is deposited over the originally coarser grained sediment at the site of initial aggradation.

In several reaches of the Sand Creek and Arroyo Calabasas channels the sediments in the banks, where exposed by trenching, show a progressive coarsening of the alluvium from top to bottom of the deposit. Thus, at any one point in an aggrading channel, sediment size generally decreases as deposition progresses, and accompanying this is a decrease in channel size. When the channel is almost filled overbank deposition becomes very important. Continued overbank deposition of fine sediment causes a steepening of the valley floor. In a short time the channel is completely filled, and floodwaters cover almost the entire valley floor. Nevertheless, a short distance upstream the channel still exists, but it is being filled. The progressive shallowing of the channel downstream is best shown between cross sections 6 and 9 on figure 24 as is the decrease in gradient as deposition in the channel begins (fig. 24, sections 6–8). The steepening of the gradient after complete filling of the channel (fig. 24, sections 9, 10) is also clearly shown (see also Schumm and Hadley, 1957, figs. 3*B*, 6*A*). Accompanying the change in gradient, percent silt-clay increases from section 6 to a maximum for all sections at 9, and median grain size decreases from cross section 6 to 9.

In the trench above the aggrading reach on Sand Creek the sediments exposed in the bank between sections 5 and 6 from bottom to top are: 2 feet coarse gravel and cobbles; 6 feet coarse-to-fine sand and silt; 6 feet of silt and clay with some fine sand. In the trench below the aggrading reach the same type of sequence occurs. From auger holes bored in the recent sediments, the gravel layer was found at the level of the channel floor between sections 5 and 6, at a depth of 2.5 feet at section 6; at 4.0 feet at section 7; and at 9.3 feet at section 8. The gravel reappears in the channel floor just above the country road, and its inferred relation to the longitudinal profile is shown by the dashed line below the profile on figure 24. This gravel layer may be the level of the channel floor before aggradation. If this is so, the convexity on the longitudinal profile shown between sections 6 and 10 above the gravel layer (fig. 24) is probably the recent channel and valley fill. Renewed trenching has occurred on the lower end of the deposit between sections 10 and 11. This cycle of channel filling, aggradation and steepening of the valley floor, and retrenching of the alluvium has been previously discussed as the common pattern in semiarid valleys (Schumm and Hadley, 1957).

To summarize, the decrease in grain size and increase in silt-clay across an aggrading reach, as shown on figures 22, 27, 31, and 35, indicates that as one moves downstream along an aggrading ephemeral stream relatively coarse sediment will be found upstream and the finer sediments will be found on the downstream edge of the deposit. In addition, there should also be an upward decrease in grain size from bottom to top of the deposit at any one location. The change in gradient is from a decrease in the filling channel to an increase where the channel has been filled and flood-plain deposition is dominant.

In the studying of aggrading channels, it is important to recognize and to anticipate marked variations in channel character and sediment type downstream due to aggradation. In other words, the orderly relation shown in many streams will be disrupted by aggradation, and anomalies are to be expected. This is especially true of channels which do not have permanent

Digitized by Google

flow between floods. The generally assumed ability of a stream to adjust to changed conditions does not apply to ephemeral streams in channels that are being rapidly aggraded. The ephemeral streams, when attempts to adjust fail, follow a pattern of alternate deposition and erosion (Schumm and Hadley, 1957).

VEGETATION

Observations have shown that the influence of vegetation differed between the silty and sandy study areas. In silty sediments, typified by the Sage Creek area, growth of vegetation was rapid on the modern sediments. The photographs of the Sage Creek channel (figs. 20*C–F*; 21*C*, *E*, *F*) show vegetation on the banks, berm, and channel bottom. Figure 21*E* shows that vegetation quickly establishes itself after the spring floods. In a channel the vegetation grows only on areas where deposition has occurred since channel incision. Vegetation, therefore, may aid deposition once it has begun, but fresh alluvium in the channel seems necessary for growth of vegetation.

The establishment of vegetation on the noncohesive, highly mobile sediments is much more difficult. These channels were remarkably free of vegetation even when aggrading (figs. 25*B*, *C*; 30*C*, *E*, *F*), but as soon as a veneer of finer sediment was deposited on the sand, vegetation began to encroach on the channel and (figs. 25*D*, *E*; 30*A*, *B*) eventually completely covered it.

As discussed in the description of Arroyo Calabasas, vegetation does grow in the sandy channels when undisturbed—such as below dams that have not spilled recently—but flow in the streams of high bed movement will cause washing out of seeds and plants and prevent the development of permanent vegetation. Vegetation, therefore, will accelerate deposition but in the areas studied is not the cause of it.

CAUSES OF DEPOSITION

One of the primary purposes of this investigation is to determine, if possible, the reason for aggradation in the study areas. The major part of the sediment load is derived from different sources in the different areas. In the Bayou Gulch and Arroyo Calabasas drainage basins the sediment is produced by slope erosion and by channel erosion along the dendritic patterned tributaries and main channel. The sediment is not derived from any restricted zone within the basin, but each tributary conveys sediment to the main channel. In the Sage and Sand Creek basins, most of the sediment is derived from an escarpment forming the headwater divide.

In any event, each of the study areas is one of high sediment production. No matter what its source, high sediment yields are probably the cause of aggradation in these stream channels. The increase in sediment yields and retrenching of the Sage, Sand, and Arroyo Calabasas channels cannot be attributed to any special cause, such as climate change or overgrazing. In the absence of such evidence the channel cutting can be related only to the presence of reaches of steeper gradient in each valley, which have been built up by deposition to be inevitably trenched. This sequence of events has been proposed as the normal cycle of development of ephemeral streams (Schumm and Hadley, 1957).

Although causes for aggradation may not be completely understood, the reason for its occurrence in a particular segment of a stream channel should be considered. It seems that aggradation in these channels is associated with segments of the stream that receive only small contributions from tributaries. The loss of water into the channels of ephemeral streams (Babcock and Cushing, 1941) and its function in promoting aggradation (Schumm and Hadley, 1957) have been studied and found important. It is logical to assume that in those reaches of the channel where contributions of runoff from tributaries is minor, the concentration of sediment will increase and aggradation might occur. Other factors would undoubtedly complicate this relation, and it is know that the entrance of a steep-gradient tributary often results in deposition at and below its junction with the main channel.

Listed in the tables giving the basic data for each study area are the drainage area above each section and the stream channel length between each section (tables 2–5). The increase in drainage area per mile of channel length above and on the aggrading reaches are presented in table 8. A comparison of the ratios shows a marked difference. In each area, except that of the Arroyo de los Frijoles and Arroyo Calabasas, deposition is occurring in reaches where the increase of drainage area is much less per unit length of channel than on the stable reaches. As previously noted, most of the Arroyo Calabasas drainage basin to the west of the channel, below the junction with Arroyo de los Frijoles, is composed of volcanic rocks from which little runoff and sediment reaches the stream. If most of this area is omitted from the calculation, then the ratio on the aggrading reach drops to about one-half of its value upstream, and the ratios are comparable to those for the other study areas. This relation suggests that aggradation occurs in these small ephemeral streams on reaches of small tributary contribution, a result, perhaps, of increased sediment concentration due to water loss into the alluvium of the valley floor.

An additional important point must be the difference in general appearance between the same valley where

Digitized by Google

TABLE 8.—*Ratio of drainage area to channel length*

Study area	Non-aggrading reach	Aggrading reach	Drainage area (square miles)	Channel length (miles)	Area-length ratio
Sage Creek	1-6	....	12.7	5.7	2.2
		6-7	26	1.1	2
Sand Creek	2-6	....	6.4	3.6	1.8
		6-10	1.7	1.6	1.1
Arroyo de los Frijoles and Arroyo Calabasas.	0-6	....	19.4	3.2	6.0
		6-9	18.1	2.7	6.7
		[1] 6-9	[1] 7.2	2.7	2.7
Bayou Gulch	1-4	....	9.0	1.1	8.1
		4-5	.5	2	2.5

[1] Adjusted for noncontributing area

the channel is completely filled and grassed and where trenched. In the flat-floored valley the alluvium may contain much water, thereby supporting heavy vegetation. In addition a veneer of fine sediment generally overlies the coarser sediment. In areas of predominant sand and gravel, therefore, the valley floor will be an area of much finer sediment. Upon renewed trenching, however, the coarser sediment will be exposed and a wide shallow channel will form, which will appear inconsistent with the fine surface sediment. Thus, the sampled surface of an untrenched valley floor may give an erroneous picture of the composition of the major part of the valley alluvium and its behavior during erosion.

EROSION IN EPHEMERAL STREAMS

The phase of the semiarid cycle of valley erosion that has received the most attention is channel incision or arroyo cutting. In this section, the differences between erosion and channel development in the different study areas will be discussed.

CHANNEL INCISION

Comparisons of channel erosion in the study areas and elsewhere show that after initial cutting of a grassed valley floor, the channel extends headward by headcut migration. The perpetuation of a headcut seems to require some resistant material capping the alluvium. This resistant cap may be formed by the binding action of plant roots, or a veneer of silt and clay overlying the coarser materials. If this resistant zone were lacking, the headcut would be rounded and lowered as it retreated upchannel, and it would lose its identity in a short distance. Where trenching was renewed and a headcut was not formed, Arroyo Calabasas, Bayou Gulch, and Sage Creek below the aggrading reach, a well-defined channel was already present, typified by a generally uniform resistance in vertical section. In the broad sandy channels without fine sediments and vegetation no headcut will form.

An interesting example of the removal of a nick or break in the profile of a sandy channel was found in Newlin Creek, a tributary to Cherry Creek located to the west Bayou Gulch in Douglas County, Colo. The profile of Newlin Creek, when plotted from a topographic map (Parker, Colo.) prepared in 1939, showed a prominent nick in the channel (fig. 41). The part of the Newlin Creek profile showing the nick, between the two secondary roads, in sections 17 and 20, was resurveyed in 1957. The altitude of the channel at the

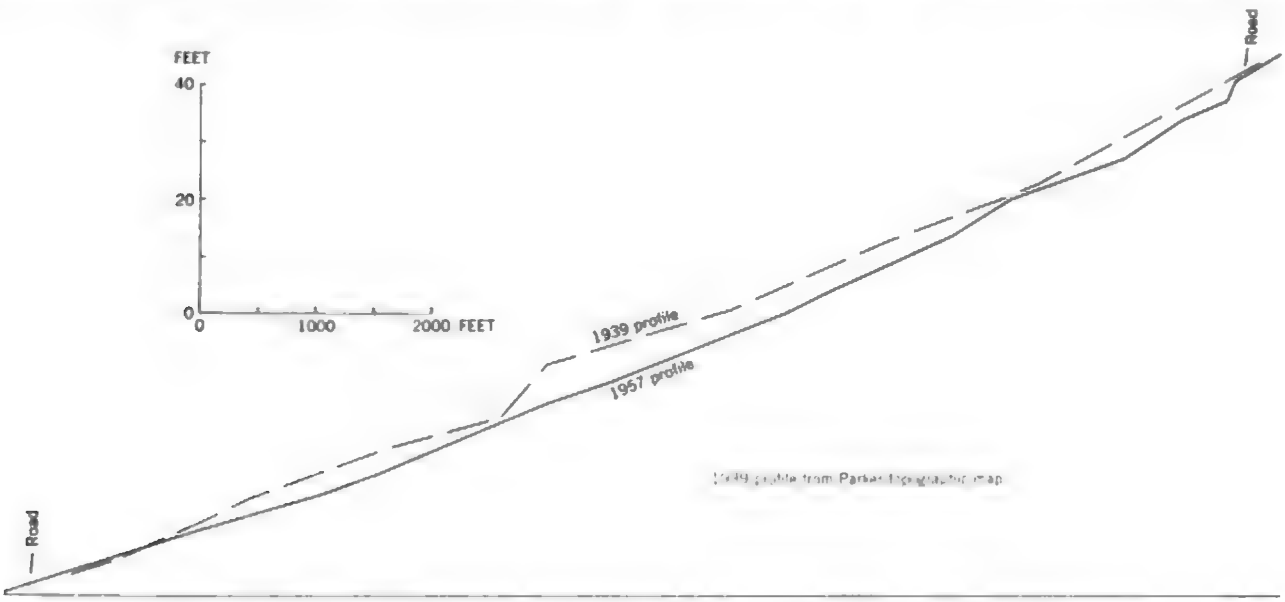

FIGURE 41.—Comparison of the longitudinal profile of Newlin Creek, Colo., in 1939 and 1957.

Digitized by Google

lower road had not changed measurably during the 18-year period, but the profile between the roads had been smoothed by removal of the nick. The small break in the 1957 longitudinal profile at its upper end is due to the road crossing at that point, which may have retarded further degradation, for the road acts as a small dam.

The changes occurring on Newlin Creek agree with those observed by Brush (1957) during flume experiments and suggest that in poorly cohesive material, not capped by a more resistant layer, the headward migration of the nick will be accompanied by a decrease in its height.

The change in channel characteristics along Newlin Creek from above the upper road to below the original position of the nick in 1939 illustrates the changes occurring during degradation of a sandy channel. Above the upper road, the channel is 130 feet wide, and sand is being deposited over another 100 feet of the valley floor. Width-depth ratio approaches 90. Below the road degradation begins; the channel narrows to 40 or 50 feet, and width-depth ratio decreases to 17. The degradation causes erosion along many interconnected water courses, forming vegetation-covered islands separated by degrading sandy channels. One channel probably will become dominant after continued erosion.

Downstream, evidence of greater erosion appears; roots of trees are exposed and cobbles and boulders appear in the channel bottom. At the site of the former nick; the gully is 10 feet deep and is 20 to 40 feet wide; width-depth ratio is about 3. Below the lower road the channel seems aggraded, shallowing and widening to its junction with Cherry Creek. Sediment samples taken in the eroding channel show only minor variation in grain size ($D_{50}=0.60$) and percent silt-clay (2.0).

BANK CAVING

Another important phenomenon that occurs during the development of a stable channel is bank caving. The relative amount of bank caving along the streams studied and its effect is markedly different in areas of cohesive and noncohesive sediment.

In poorly cohesive alluvium, or that with a small percent silt-clay, the channel widens rapidly by bank caving after initial dissection; whereas, in cohesive sediment, predominantly silt-clay, the blocks of sediment that fall into the channel are resistant and do not move or disintegrate readily, although this will depend on velocity of water movement. They may even form the nucleus for deposition along the banks and prevent further channel widening (fig. 20*C*). Vegetation, growing on banks before the caving, often continues to grow on the fallen block if rotation of the block was not great. The vegetation in turn promotes further aggradation in the channel.

Blocks of poorly cohesive alluvium, on the other hand, disintegrate upon impact or later under the eroding action of flood waters, and the sediment adds to the bed and suspended load of the stream. Slumping or caving of bank material into the stream channel and the function of slump blocks in sediment supply and aggradation, therefore, differ with type of bank material.

PRACTICAL CONSIDERATIONS

Because of a critical need for effective control of erosion and deposition in ephemeral streams, an attempt will be made to suggest how some of the information and conclusions stated previously might have a practical application. The differences in erosion and deposition in the study areas suggest that different types of conservation techniques may be necessary for different types of alluvium filling the valley.

Generally, in valleys where the streams are ephemeral conservation measures are not begun until improvement will require large expenditures of time and money. For example, once a gully has formed the only solution is to build either a dam or diversion structure above the headcut, to prevent its headward migration, or to plug the gully and fill it by inducing deposition in the trench (Peterson, 1950). However, if it were possible to determine at what point in the valley trenching would begin, then it might be more economical and certainly more practical to prevent the initial erosion.

Some studies in semiarid valleys suggest that a discontinuous gully will form on the steeper parts of an alluvial valley (Schumm and Hadley, 1957). If good topographic maps are available for the areas concerned, it would be possible to plot the longitudinal profile of the stream and discover the steeper reaches where trenching might begin. If maps are not available, the valley profile could be surveyed, or perhaps, the critical gradient changes could be revealed by photogrammetric methods. Once the steeper reaches have been discovered, the valley floor could be protected by restricting grazing. However, since in many areas the valley floor affords the best grazing and because the critical reach would need to be fenced, this solution may not be acceptable to the local rancher. Another possibility would be the construction of small earth diversion dikes to slow and spread the flow of water across the steeper reach. This, however, might cause deposition and further steepening on this already critical reach. This discussion of preventive conservation measures on the steeper parts of the alluvial fill empha-

Digitized by Google

sizes that only certain parts of a valley need be protected to conserve the entire valley.

In three of the study areas selected for this investigation, problems of erosion and deposition are acute. Conservation measures should be directed at not maintaining but restoring the valley floor to its ungullied state. This may be possible only by inducing deposition in the gully proper, thereby filling and healing the trench. Such a project can succeed best where the method used is designed to take advantage of a natural tendency to deposition. In each valley studied deposition was shown to occur naturally where tributary contribution is small, where gain of drainage area per mile of channel is less than normal (table 8). Therefore, if these limited observations are confirmed elsewhere, a structure placed in a valley to promote deposition should be located where the ratio of increase of drainage area to channel length is small.

Deposition also may be induced by using reverse delta deposition near the confluence of the channel with a trunk stream. If a dam is built on the tributary a short distance above its mouth, the retention of water will allow flood waters to enter the channel from the main stream, causing deposition below the dam and plugging of the valley. Deposition in the reservoir above the dam will also be important. The lower end of Sage Creek has been filled in this manner. Once deposition has started, care should be exercised that renewed trenching on the toe of the alluvial deposit does not occur.

If incipient aggradation could be recognized in a channel, it might be accelerated by conservation measures. As indicated by a reexamination of changes in sediment and channel character across the aggrading reaches (figs. 22, 27, 31, 35) deposition may be detected, where it is not obvious, by a decrease in gradient and an increase in percent silt-clay in the channel sediment. Perhaps width-depth ratio can be used, for width-depth ratio is increased by aggradation except for those areas of high silt-clay where initial deposition is along the channel banks for example, Sage Creek. Perhaps in similar channels if the width-depth ratio in any reach is much higher than that upstream or downstream, deposition may be expected (fig. 40).

Vegetation aids deposition only after deposition has begun. Vegetation is readily established on the fine alluvium but not in predominantly sandy material. It appears therefore if vegetation does not occur naturally in a channel, it probably cannot be induced to grow there without great expense. Planting grass and trees in a semiarid valley would be practical only as a means of stabilizing an alluvial deposit. But care should be exercised that the conservation measure may not have an eventual adverse effect on valley stability. More work is required on this and other problems related to deposition, but it becomes increasingly apparent that a careful study of each valley should be made before conservation measures of any type are initiated.

REFERENCES

Babcock, H. M. and Cushing, E. M., 1941, Recharge to ground water from floods in a typical desert wash, Pinal County, Arizona: Am. Geophys. Union Trans., v. 22, pt. 1, p. 49–56.

Blench, T., 1957, Regime behavior of canals and rivers: London, Butterworth's Publications, 138 p.

Brush, L. M., Jr., 1957, Laboratory study of knickpoint behavior in noncohesive materials [abs.]: Geol. Soc. American Bull., v. 68, p. 1704.

Burmister, D. M., 1952, Soil mechanics: New York, Columbia Univ. Press, 155 p.

Dunn, I. S., 1959, Tractive resistance of cohesive channels: Jour. Soil Mechanics and Foundations Div., Am. Soc. Civil Engineers Proc., SM 3, p. 1–24.

Hjulstrom, Filip, 1935, Studies of the morphological activity of rivers as illustrated by the River Fyris: Univ. Upsala Geol. Inst. Bull., v. 25, p. 221–527.

Leighly, J. B., 1934, Turbulence and the transportation of rock debris by streams: Geog. Rev., v. 24, p. 543–464.

Leopold, L. B. and Maddock, Thomas, Jr., 1953, The hydraulic geometry of stream channels and some physiographic implications: U.S. Geol. Survey Prof. Paper 252, 57 p.

Leopold, L. B. and Miller, J. P., 1956, Ephemeral streams—hydraulic factors and their relation to the drainage net: U.S. Geol. Survey Prof. Paper 282–A, p. 1–37.

Peterson, H. V., 1950, The problem of gullying in western valleys: *in* Trask, P. D., Applied sedimentation: New York, John Wiley & Sons, 707 p.

Schumm, S. A., 1956, The role of creep and rainwash on the retreat of badland slopes: Am. Jour. Sci., v. 254, p. 693–706.

——— 1960a, The effect of sediment type on the shape and stratification of some modern fluvial deposits: Am. Jour. Sci., v. 258, p. 177–184.

———1960b, The shape of alluvial channels in relation to sediment type: U.S. Geol. Survey Prof. Paper 352–B, p. 17–31.

Schumm, S. A. and Hadley, R. F., 1957, Arroyos and the semiarid cycle of erosion: Am. Jour. Sci., v. 255, p. 161–174.

Thornthwaite, C. W., 1941, Atlas of climatic types in the United States, 1900–1939: U.S. Dept. Agr. Misc. Pub. 421, 7 p.

Ward, Freeman, 1922, Geology of a portion of the badlands: South Dakota Geol. Survey Bull. 11, p. 1–59.

Wolman, M. G., 1955, The natural channel of Brandywine Creek, Pennsylvania: U.S. Geol. Survey Prof. Paper 271, 56 p.

Wolman, M. G. and Leopold, L. B., 1957, River flood plains—Some observations on their formation: U.S. Geol. Survey Prof. Paper 282–C, p. 87–109.

Digitized by Google

QE 75
.A26
no. 352-D

Geol

1963

Channel Widening and Flood-Plain Construction Along Cimarron River in Southwestern Kansas

U.S. GEOLOGICAL SURVEY/PROFESSIONAL PAPER/352-D

THE UNIVERSITY OF CHICAGO LIBRARY
OCT 23 1963

March 3, 1849

Schumm and Lichty—CHANNEL WIDENING AND FLOOD-PLAIN CONSTRUCTION, CIMARRON RIVER, KANSAS—Geological Survey Professional Paper 352-D

QF75
A26
352-D

Digitized by Google

Channel Widening and Flood-Plain Construction Along Cimarron River in Southwestern Kansas

By S. A. SCHUMM *and* R. W. LICHTY

EROSION AND SEDIMENTATION IN A SEMIARID ENVIRONMENT

GEOLOGICAL SURVEY PROFESSIONAL PAPER 352-D

Major channel changes along the Cimarron River are related to the frequency and magnitude of floods and the departure of annual precipitation from normal

UNITED STATES GOVERNMENT PRINTING OFFICE, WASHINGTON : 1963

Digitized by Google

UNITED STATES DEPARTMENT OF THE INTERIOR

STEWART L. UDALL, *Secretary*

GEOLOGICAL SURVEY

Thomas B. Nolan, *Director*

For sale by the Superintendent of Documents, U.S. Government Printing Office
Washington, D.C. 20402

U. S. GOVERNMENT
DEPOSITORY COLLECTION

Digitized by Google

CONTENTS

	Page
Abstract	71
Introduction	71
Cimarron River, southwestern Kansas, 1874–1960	71
Cimarron River, 1874–1913	71
Cimarron River, 1914–42	74
Cimarron River, 1943–54	76
Cimarron River, 1955–60	76
Summary	76
Factors influencing Cimarron River channel changes	76
Land use	76
Floods	77
Precipitation	78
Vegetation	79
Summary	79
Mechanics of channel widening and flood-plain construction	79
Channel widening	80
Effect of channel widening on gradient	81
Flood-plain construction	81
Island formation	81
Direct flood-plain construction	84
Flood-plain stratigraphy	84
Summary	85
Comparison of Cimarron River channel changes with those of other rivers	86
Summary	87
Conclusions	87
References	88

ILLUSTRATIONS

	Page
FIGURE 42. Index map of Cimarron River area	72
43–44. Photographs showing:	
43. Channels of Cimarron River in southwestern Kansas	75
44. Channel changes of Cimarron River in southwestern Kansas and pre-1914 alluvium	77
45–46. Graphs showing:	
45. Acres of plowed land and number of head of livestock	78
46. Average annual precipitation in southwestern Kansas	80
47. Transverse profiles of Cimarron River valley	82
48. Photographs of Cimarron River flood plain in southwestern Kansas	83
49–50. Sketches showing:	
49. Parts of Cimarron valley covered by low, moderate, and high flows	84
50. Channel areas favorable for flood-plain formation	84
51. Section showing flood-plain stratification	85
52. Index map of Red River area near Burkburnett, Tex	87

TABLES

	Page
TABLE 1. Channel width of the Cimarron River, Kans	73
2. Peak discharge of the Cimarron River, southwestern Kansas	79
3. Changes in channel depth between date of bridge construction and 1960	81

Digitized by Google

CHANNEL WIDENING AND FLOOD-PLAIN CONSTRUCTION ALONG CIMARRON RIVER IN SOUTHWESTERN KANSAS

By S. A. Schumm and R. W. Lichty

ABSTRACT

The channel of the Cimarron River in southwestern Kansas has changed significantly during historic times. The average width of the river was 50 feet in 1874. During and after the major floor of 1914, the river widened until an average width of 1,200 feet was reached in 1942. During the period 1943–54 flood-plain construction occurred, and the river narrowed to an average width of 550 feet in 1954. During the period 1954–60 both channel widening and narrowing occurred.

The period of channel widening was initiated by the maximum flood of record, which was followed by a long period of deficient precipitation, and was terminated by the major flood of 1942. The period of flood-plain construction was characterized by above-average annual precipitation and floods of low to moderate peak discharge. The influence of the changed climatic conditions on vegetational growth is the key to Cimarron River behavior. During the years of above-average annual precipitation, which are associated with floods of low to moderate peak discharge, vegetation became established in the wide sandy channel. The presence of vegetation in the channel in turn aided deposition and flood plain formation.

The new flood plain was constructed in a period of 12 years, predominantly by vertical accretion. It is composed of a mosaic of islands, abandoned channels, and areas of flood plain constructed adjacent to the low-water channel. Although initially a flood plain may be formed by overbank flooding and vertical accretion, lateral migration of the stream may rework the alluvium and destroy all evidence of vertical accretion.

The channel changes which have occurred along Cimarron River seem typical of sandy rivers in semiarid regions. Channel widening instead of degradation and channel narrowing instead of aggradation are characteristic.

INTRODUCTION

Flood plains are of historic interest to man. They offered fertile land, abundant water, and game to the primitive hunter and agriculturalist and became sites of early civilizations. The flood-plain dweller of today faces many of the same problems as did his ancestors. For this reason a better understanding of river and flood-plain changes may be helpful in preventing a repetition of past disasters.

Geomorphic processes proceed at rates that generally are difficult to assess, and the opportunity seldom arises to obtain data on the rates. Nevertheless, a record of modern flood-plain destruction and rebuilding is available for the Cimarron River in southwestern Kansas. This record of stream-channel and flood-plain changes, the reasons for the changes, and a description of the mechanics of the changes are presented in this report as a contribution toward a better understanding of fluvial erosion and deposition in a semiarid region.

The Cimarron River enters western Kansas about 5 miles north of the Oklahoma boundary (fig. 42) and flows northeastward through Morton, Stevens, and Grant Counties and then southeastward through Haskell, Seward, and Meade Counties before reentering Oklahoma. The Cimarron Valley in southwestern Kansas is underlain almost completely by rocks of Tertiary and Quaternary age, although small outcrops of Triassic and Cretaceous rocks occur in Morton County. The geology and ground-water resources of this area have been discussed by McLaughlin (1942, 1946), Bryne and McLaughlin (1948), and Frye (1942).

The initial widening of the Cimarron River, after the major flood of 1914, was discussed by McLaughlin (1947); his paper directed the writers' attention to the interesting series of events that have occurred along this river during the last half century.

The writers wish to acknowledge particularly the suggestions and encouragement of T. G. McLaughlin, as well as the use of his photographs (figs. 43*B*, 44*A*). Messrs. Robert Evans and Rice Davies of Liberal, Kans., very kindly gave us the benefit of their knowledge of river changes since the 1914 flood. Richard Aro instructed the writers in the techniques of tree-ring counts and made valuable suggestions with respect to the interpretation of these data.

CIMARRON RIVER, SOUTHWESTERN KANSAS, 1874–1960

CIMARRON RIVER, 1874–1913

The Cimarron River in Kansas appeared to be typical of streams in a more humid environment at the turn

Digitized by Google

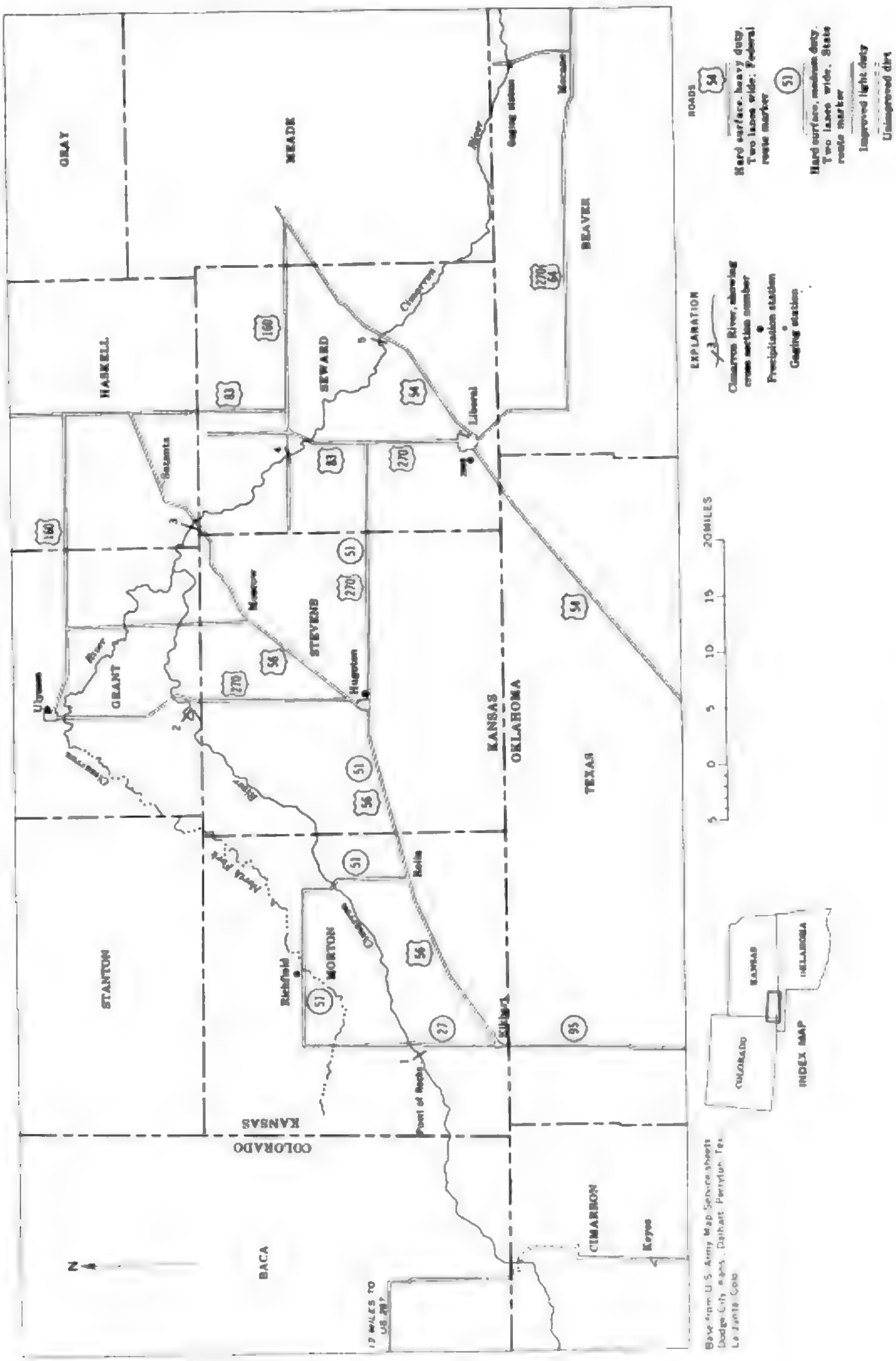

FIGURE 42.—Index map of Cimarron River area.

of the century. Haworth (1897, p. 22) stated that "The Cimarron seems to have reached base-level and to have begun meandering across its flood plain. Beautiful ox-bow curves are frequent, and a sluggish nature is everywhere manifest during times of low water." (See fig. 43A.)

According to Johnson (1902, p. 664),

> Wherever within the High Plains belt the Cimarron Valley shows a living stream, it is always a meandering looping stream of uniform width, narrow, clear and deep * * *. The bottom land upon which it wanders supports a coarser and longer-stemmed grass than the uplands, the grass roots reaching to the ground water, which lies at a depth here, as a rule, of only 2 or 3 feet * * *.

The Cimarron River elsewhere, upstream to the southwest in the Oklahoma Panhandle and downstream to the southeast in Oklahoma, during historic times has always been typically a wide, shallow, sandy river. As suggested by Johnson, the great difference between the Cimarron River in Kansas and the river elsewhere may be that, in Kansas, a perennial flow was maintained by ground water. Additional testimony, confirming that the Cimarron River was a narrow, meandering perennial stream at the turn of the century, was presented by McLaughlin (1947).

Information on the width of the Cimarron River is available as a result of the survey of 1874. The data were compiled by McLaughlin (1947), and data for 120 cross sections are presented in table 1. Thirty-five of the 155 sections originally listed by McLaughlin were not remeasured; therefore, the mean values for channel widths by counties as presented in table 1 will differ slightly from those presented by McLaughlin (1947).

TABLE 1.—*Channel width, in feet, of the Cimarron River, Kans.*

[Channel width: 1874 and 1939, data from McLaughlin (1947); 1954, data from aerial photographs, scale 1:27,250; 1960, data from photomosaic sheets, scale 1:63,360; *n* equals number of sections measured]

Section	Location	Channel width			
		1874	1939	1954	1960
	Morton County				
	T. 34 S., R. 43 W.				
1	West line sec. 19	53	2,900	1,080	1,280
2	West line sec. 20	53	3,000	1,050	1,350
3	West line sec. 21	46	3,200	1,500	1,500
4	West line sec. 22	40	2,500	700	900
5	North line sec. 22	33	2,100	1,500	1,650
6	West line sec. 14	79	1,600	1,000	1,400
7	East line sec. 14	66	2,300	1,200	1,400
	T. 34 S., R. 42 W.				
8	West line sec. 7	139	1,300	900	900
9	East line sec. 7	66	2,150	1,000	1,100
10	East line sec. 5	59	1,400	650	650
11	East line sec. 4	46	2,600	400	400
12	North line sec. 3	73	1,800	1,100	1,200
	Morton County—Continued				
	T. 33 S., R. 42 W.				
13	West line sec. 35	46	3,200	950	800
14	North line sec. 35	46	800	850	850
15	East line sec. 26	[illegible]	800	650	650
	T. 33 S., R. 41 W.				
16	West line sec. 29	66	2,200	350	360
17	West line sec. 28	66	2,600	500	1,100
18	East line sec. 28	46	1,100	1,000	1,200
19	South line sec. 22	66	1,500	[illegible]	500
20	West line sec. 23	66	2,000	550	1,050
21	West line sec. 24	66	2,400	1,000	1,100
22	NE corner sec. 24	46	2,500	1,660	1,650
	T. 33 S., R. 40 W.				
23	East line sec. 18	33	300	250	250
24	South line sec. 8	33	2,100	1,000	1,000
25	West line sec. 9	66	2,900	800	900
26	SW corner sec. 3	56	2,400	450	[illegible]
27	NE corner sec. 3	[illegible]	2,600	1,000	800
	T. 32 S., R. 40 W.				
28	NE corner sec. 35	33	1,100	180	180
	T. 32 S., R. 39 W.				
29	West line sec. 30	46	2,600	550	800
30	East line sec. 30	53	1,300	400	650
31	East line sec. 29	53	1,400	250	300
	Average for Morton County (*n*=31)	56	2,030	800	900
	Stevens County				
	T. 32 S., R. 39 W.				
32	West line sec. 27	53	2,200	700	1,300
33	West line sec. 26	46	2,500	400	600
34	North line sec. 26	46	2,100	1,500	800
35	NE corner sec. 23	36	2,200	650	900
36	North line sec. 13	33	1,800	700	1,000
37	North line sec. 12	40	700	500	500
	T. 31 S., R. 38 W.				
38	SW corner sec. 29	46	1,300	850	600
39	SW corner sec. 21	40	1,700	300	400
40	North line sec. 21	46	1,000	500	800
41	West line sec. 15	[illegible]	1,100	550	800
42	NE corner sec. 15	46	800	300	[illegible]
	Average for Stevens County (*n*=11)	43	1,500	680	770
	Grant County				
	T. 30 S., R. 37 W.				
43	West line sec. 32	26	600	280	280
44	West line sec. 33	40	500	150	150
45	West line sec. 34	40	600	280	280
46	South line sec. 28	40	500	150	150
47	West line sec. 27	50	800	150	150
48	North line sec. 34	66	800	150	150
49	West line sec. 35	132	300	100	100
50	South line sec. 26	99	[illegible]	100	100
51	South line sec. 23	66	[illegible]	100	100
52	West line sec. 24	66	300	200	200
53	North line sec. 25	66	700	150	150
	T. 30 S., R. 36 W.				
54	West line sec. 21	66	200	200	200
55	West line sec. 22	66	300	400	400
56	West line sec. 23	66	800	150	150
	T. 30 S., R. 35 W.				
57	West line sec. 34	26	1,300	150	150
58	South line sec. 27	26	1,300	650	650
59	SW corner sec. 23	17	1,100	100	100
60	North line sec. 26	33	700	100	100
61	West line sec. 25	43	500	100	100
	Average for Grant County (*n*=19)	54	630	190	190

Digitized by Google

TABLE 1.—*Channel width, in feet, of the Cimarron River, Kans.*—Continued

Section	Location	Channel width			
		1874	1939	1954	1960
	Haskell County				
	T. 30 S., R. 34 W.				
62	North line sec. 20	33	800	100	100
63	East line sec. 30	33	500	[illegible]	200
64	South line sec. 29	33	600	200	200
65	East line sec. 32	26	[illegible]	450	600
66	South line sec. 33	33	300	300	[illegible]
	Average for Haskell County (n=5)	32	480	250	260
	Seward County				
	T. 31 S., R. 34 W.				
67	North line sec. 8	66	300	200	1,200
68	North line sec. 21	33	600	1,000	1,400
69	North line sec. 28	20	1,400	600	800
70	West line sec. 27	66	1,000	[illegible]	[illegible]
71	North line sec. 34	122	1,000	[illegible]	700
72	West line sec. 35	43	1,500	500	500
73	West line sec. 36	33	1,600	1,000	1,000
74	South line sec. 36	13	1,000	400	400
	T. 32 S., R. 33 W.				
75	West line sec. 6	16	1,100	260	550
76	North line sec. 7	15	1,200	800	900
77	North line sec. 18	16	300	150	150
78	West line sec. 17	16	1,000	700	700
79	North line sec. 20	18	1,000	400	400
80	West line sec. 21	18	600	300	300
81	North line sec. 28	16	1,100	150	150
82	West line sec. 27	16	900	400	400
83	North line sec. 34	13	500	400	500
84	West line sec. 35	10	1,000	500	500
85	West line sec. 36	13	1,300	500	500
86	South line sec. 36	20	500	100	100
	T. 33 S., R. 33 W.				
87	West line sec. 6	40	500	200	200
88	North line sec. 7	13	700	550	300
89	North line sec. 18	33	1,800	1,300	1,200
90	South line sec. 18	13	440	300	300
91	East line sec. 20	20	1,410	300	400
92	South line sec. 21	26	[illegible]	300	300
93	West line sec. 27	26	790	500	400
94	West line sec. 26	20	1,100	700	800
95	West line sec. 25	33	350	100	100
96	North line sec. 36	33	1,320	150	150
97	East line sec. 36	33	1,180	800	800
	T. 33 S., R. 31 W.				
98	South line sec. 31	33	880	300	900
	T. 34 S., R. 31 W.				
99	West line sec. 8	20	1,320	400	600
100	West line sec. 9	20	270	200	800
101	North line sec. 16	20	1,140	250	400
102	West line sec. 15	26	260	250	230
103	North line sec. 22	26	1,230	300	650
104	SE corner sec. 15	33	970	300	400
105	SE corner sec. 23	30	620	200	300
106	East line sec. 26	33	570	500	500
	Average for Seward County (n=40)	26	900	440	530
	Meade County				
	T. 34 S., R. 30 W.				
107	South line sec. 30	33	1,050	300	500
108	South line sec. 31	79	570	400	200
	T. 35 S., R. 30 W.				
109	East line sec. 6	40	1,320	300	300
110	South line sec. 5	48	1,410	300	300
111	South line sec. 9	53	530	350	350
112	East line sec. 16	33	1,250	300	300
113	East line sec. 15	33	800	700	700
114	East line sec. 14	66	1,000	1,400	1,400
115	East line sec. 13	132	1,000	2,000	2,000
	Meade County—Continued				
	T. 35 S., R. 29 W.				
116	East line sec. 18	100	1,100	1,300	1,300
117	East line sec. 9	93	1,600	1,200	900
118	East line sec. 10	145	1,000	950	600
119	East line sec. 11	304	1,300	750	750
120	East line sec. 13	132	800	1,650	1,650
	Average for Meade County (n=14)	92	1,080	830	800
	Average width for 120 sections	50	1,200	550	600

In 1874 the river averaged 50 feet in width through the 6 counties of southwestern Kansas; however the channel ranged in width from 10 to 304 feet (table 1). Some of the variation in width is due to the fact that measurement of channel width was made along section lines which were not normal to the channel. Nevertheless, the channel of the river in Kansas between 1874 and 1914 was narrow and probably relatively stable. The flood plain was grassed and afforded excellent grazing. Wild hay and alfalfa were cut and stacked on the flood plain during these early days (fig. 43*A*). The contrast between the river at that time and during the following 46 years is remarkable.

CIMARRON RIVER, 1914–42

Beginning in 1914 and continuing intermittently until 1942, the channel of the Cimarron River widened, until almost all the flood plain was destroyed. The channel widening began, according to the testimony of residents of the Cimarron valley, during the major flood of May 1914. This flood is the greatest of record, having an estimated gage height of 13 feet near Mocane, Okla. (fig. 42); peak discharge is estimated to have been 120,000 cfs (cubic feet per second). (See table 2.)

During the 1874 survey, the channel north of Elkhart was 66 feet wide (fig. 42). Only minor changes in width occurred between 1874 and 1914; however, in 1916 a bridge 644 feet long was required to span the channel, and in 1939 the channel at the bridge was about 1,400 feet wide (McLaughlin, 1947, p. 82). The data presented on table 1 show that the average channel widening during the period 1914–39 was 1,150 feet.

Although no aerial photographs are available to document channel changes between 1939 and 1954, other data indicate that the channel continued to widen through 1942. For example, a major flood near Liberal, Kans., occurred in 1942 with a peak discharge of 69,000 cfs. This flood originated in the headwaters

Digitized by Google

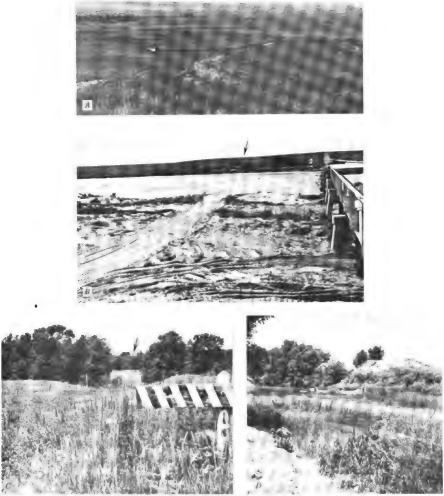

FIGURE 43.—Cimarron River in southwestern Kansas. *A*, Valley of Cimarron River in southeastern Meade County, Kans., prior to the flood of 1914. Photograph taken by W. D. Johnson in the 1890's. *B*, Cimarron River at old Highway 270 bridge north of Hugoton, Kans. (cross section 2, fig. 42), in 1943. Channel was about 700 feet wide. Arrow indicates position of windmill. Photograph taken by T. G. McLaughlin. *C*, Valley of Cimarron River at old Highway 270 bridge in 1960. Arrow indicates position of windmill shown in *B*. Trees in foreground are growing in abandoned channel shown at right end of profile *B B'* (fig. 47). Present channel is beyond trees in background. *D*, Channel of Cimarron River at old Highway 270 bridge in 1960. Channel is 110 feet wide. Compare channel shown in this view with channel in 1943 shown in *B*.

690-450 O—63——2

Digitized by Google

area (peak discharge 80,000 cfs near Boise City, Okla.) and destroyed many bridges as it moved through the Cimarron River valley in Kansas. At the close of 1942 the river was at its maximum width, for the flood plain was completely destroyed at some locations. Good evidence for complete destruction of the flood plain north of Hugoton, Kans. (fig. 42), is provided by a photograph taken of the channel in 1943 (fig. 43*B*). At that time the entire valley floor was river channel. The present channel is only 110 feet wide and is located at the north edge of what was the 1942 channel (fig. 43*C*). The trees in the foreground of figure 43*C* began their growth at the south edge of the channel in 1943, as indicated by tree-ring counts. The survival of these trees is proof that the channel was never again as wide as it was after the 1942 flood.

CIMARRON RIVER, 1943–54

After the flood of 1942, a reversal of river activity occurred. Cross sections, when remeasured on aerial photographs taken in 1954, showed that the channel had become narrower (table 1). The narrowing was accomplished by flood-plain construction and, to a minor extent, by island formation. The channel width, as measured on the 1954 photographs, had decreased to an average of 550 feet (fig. 43*C*, 43*D*, 44*A*, *B*).

In 12 years the river had repaired about half the damage caused by widening during the period 1914–42. Great variability occurs among the data. At some cross sections the river narrowed to one-fifth or less of its former maximum width (table 1, sections 11, 16, 17, 31, 33, 47, 48, 51, 57, 59, 60, 61, 62, and 81), whereas at other cross sections the river width did not change (table 1, sections 54 and 66) or continued to widen (table 1, sections 14, 55, 65, 68, 114, 115, 116, and 120).

CIMARRON RIVER, 1955–60

New aerial photographs, which became available during preparation of this report, allowed measurements to be made of 1960 channel widths. The measurements were made on photoindex sheets and are less accurate than those made from contact prints of the 1954 photographs. The measurements show, however, that the period 1954–60 was not a continuation of the period 1943–54. Of 120 sections remeasured, only 10 showed continued narrowing of more than 50 feet (Table 1, sections 13, 27, 34, 38, 66, 88, 93, 108, 117, and 118); 70 sections were at about the same width; and of the remaining 40 sections, 38 showed renewed widening of more than 50 feet, whereas sections 65 and 68 have continued to widen since the first survey in 1874. The period may be characterized as one of relative stability with some tendency toward widening of the channel.

SUMMARY

The major changes in width of the Cimarron River during the 46-year period 1914–60 can be grouped into 3 distinct periods: the period 1914–42 of channel widening and flood-plain destruction (figs. 43 and 44); the period 1943–54 of channel narrowing and flood-plain construction; and the period 1955–60 of relatively minor changes (figs. 43 and 44).

The channel widening along the Cimarron River may be related to arroyo cutting, which has been prevalent throughout the Southwest since the latter part of the 19th century. However, there are two major differences between arroyo cutting and the channel changes along the Cimarron River. One is the nature of the change, widening instead of predominant deepening. The other is a trend toward rapid natural restoration of the valley to its former condition.

FACTORS INFLUENCING CIMARRON RIVER CHANNEL CHANGES

The causes of natural phenomena of the type discussed in this paper are generally complex and varied. Nevertheless, all available information will be considered in an attempt to explain the cause of destruction and rebuilding of the Cimarron River flood plain.

LAND USE

McLaughlin (1947), after an analysis of information on number of head of livestock and acres of cultivated land in southwestern Kansas, suggested that "accelerated erosion in the Cimarron valley is believed to be the result of overcultivation of land and the subsequent abandonment of thousands of farms, leaving large areas with lessened resistance to run-off." Unfortunately, there is little information on runoff for the period of channel widening. McLaughlin's data, when brought up to date (fig. 45), indicated that the period of flood-plain construction occurred during a period of major agricultural activity, 1941–50. This peak of agricultural activity probably began with the demand for more agricultural products during the war. The period 1941–50 was also a time of above average annual precipitation (fig. 46), a further stimulus to agricultural activity during these years. This coincidence of flood-plain construction and agricultural activity would seem to support McLaughlin's hypothesis; however, a shorter period of major agricultural activity also occurred between the years 1929–33 (fig. 45) during the period of channel widening. On the basis of these conflicting data, it is difficult to evaluate the effects of agricultural activity on the Cimarron River.

McLaughlin (1947) also concluded that, because there was no major change in number of head of livestock,

Digitized by Google

grazing was not an important factor determining channel changes. Data on number of livestock in southwestern Kansas are presented on figure 45. Livestock density was greatest during the period of channel narrowing 1942–48. The activities of man and animals in the Cimarron River basin undoubtedly had their effects on the regime of the river, but any relation between cultivation, grazing, and channel change is obscure.

FLOODS

The period of greatest channel widening began in 1914 and ceased in 1942. Unfortunately, adequate streamflow data are not available during the period of channel widening to establish a definite trend, but the record presented in table 2 shows that large floods occurred in 1936, 1938, 1941, and 1942. Furthermore, according to C. O. Bryant (written communication),

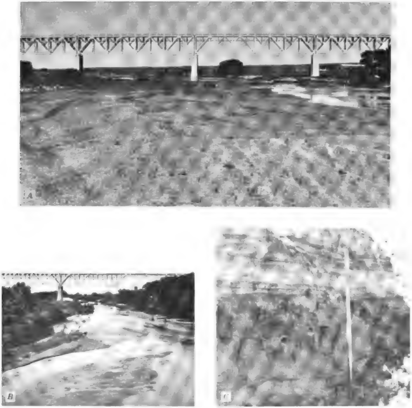

FIGURE 44.—Cimarron River in southwestern Kansas. *A*, Rock Island Railroad bridge near Arkalon in 1942. Channel was about 450 feet wide at point from which photograph was taken. Photograph taken by T. G. McLaughlin. *B*, Rock Island Railroad bridge near Arkalon in 1960. Channel is about 150 feet wide. Concrete bridge support on left of this photograph corresponds to center support shown in *A*. *C*, Pre-1914 alluvium exposed in cutbank near Highway 56 crossing. At base of cut is coarse crossbedded sand. Above sand is 2.5 feet of dark-colored homogeneous cohesive pre-1914 alluvium. Overlying the pre-1914 alluvium is 3 feet of alternate layers of sand and mud deposited from overbank floods.

Digitized by Google

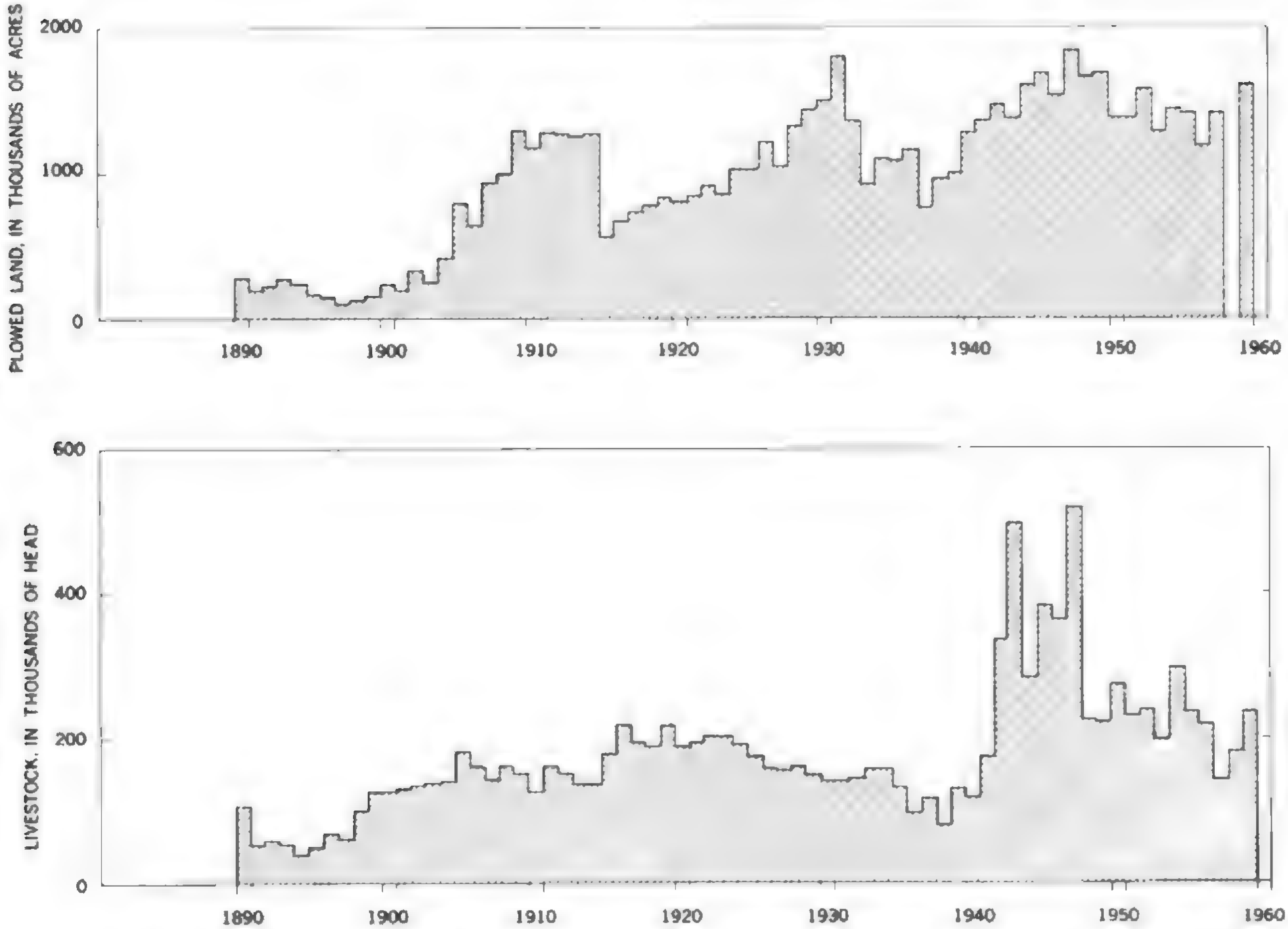

FIGURE 45.—Acres of plowed land and number of head of livestock in southwestern Kansas (Stanton, Morton, Grant, Stevens, Haskell, Meade, and Clark Counties) from 1890 to 1959. Data from annual reports of Kansas State Board of Agriculture. Information on plowed land for 1958 not available.

the Chicago, Rock Island and Pacific Railroad bridge near section 5 (fig. 42) had undergone extensive flood damage in June 1923, October 1930, and June 1937. This period, therefore, was one of destructive floods.

The period of flood-plain construction, 1943–54, was characterized by floods of low to moderate discharge. Only two large floods occurred after 1942—in May 1951 and July 1958 (table 2). The May 1951 flood approached the 1942 flood in peak discharge, but according to McLaughlin (oral communication), most of the flood waters entered the Cimarron River from North Fork Cimarron River in southeastern Grant County (fig. 42). This flood did not widen the channel appreciably because extensive channel narrowing occurred during the period 1943–54 along the Cimarron River below its confluence with the North Fork Cimarron River. The 1958 flood may have caused minor channel widening, but it obviously did not have the effect of pre-1942 floods, for the period 1955–60 was characterized by stability or only minor channel widening. Therefore, although major floods caused serious flood-plain destruction between 1914 and 1942, the post-1942 floods were not important in this respect.

PRECIPITATION

Although discharge records are incomplete, data on precipitation have been collected for long periods at several weather stations in the Cimarron River drainage basin. Precipitation data were compiled for four stations (Richfield, Hugoton, Ulysses, and Liberal, Kans.) since 1910. The records at each station show virtually the same trends during the period 1910–59, and they were combined to give an average for precipitation in the Cimarron River basin in Kansas (fig. 46).

Digitized by Google

TABLE 2.—*Peak discharge of the Cimarron River, southwestern Kansas*

[Data from U.S. Geol. Survey Water-Supply Papers. Water-year is from Oct. 1 to Sept. 30]

Water-year	Date	Momentary maximum		Station
		Gage height (feet)	Discharge (cfs)	
1896	Apr. 12		90	Cimarron River near Liberal, Kans.
1914	May 2	13.0	[1] (120,000)	Cimarron River near Mocane, Okla.
1935			[2] (67,000)	
1938	Sept. 5	11.0	[illegible]	Cimarron River near Liberal, Kans.
1939	July 2	8.70	5,350	Do.
1940	May 8	7.08	2,800	Do.
1941	Sept. 24	10.5	47,000	Do.
1942	Apr. 21	12.1	69,000	Do.
1943	Oct. 20	3.70	625	Cimarron River near Satanta, Kans.
1944	May 30	3.69	2,400	Do.
1945	Aug. 22	5.12	2,560	Do.
1946	May 29	3.96	6,360	Do.
1947	Oct. 7	5.03	2,950	Do.
1948	Sept. 11	[illegible]	5,330	Cimarron River near Mocane, Okla.
1949	June 7	5.50	10,500	Do.
1950	Aug. 3	4.53	6,220	Do.
1951	May 7	9.94	53,400	Do.
1952	Aug. 23	2.18	1,080	Do.
1953	Aug. 20	3.60	4,650	Do.
1954	Aug. 15	3.81	[illegible]	Do.
1955	May 22	5.45	11,200	Do.
1956	Aug. 21	3.40	2,460	Do.
1957	May 16	5.06	9,300	Do.
1958	July 8	6.75	21,800	Do.
1959	May 4	3.43	3,860	Do.
1960	June 8	3.70	[illegible]	Do.

[1] Maximum stage known. Estimated on basis of extension of average-stage-discharge relation (L. W. Furness, U.S. Geol. Survey, Topeka, Kans., written communication.

[2] Estimated on basis of highwater-mark elevation and subsequently defined stage-discharge relation at U.S. Highway 283, 4.3 miles south of Englewood, Kans. (L. W. Furness, U.S. Geol. Survey, Topeka, Kans., written communication).

The data show four periods of significance: (1) 1915–30, a period of great annual variability—years of precipitation in excess of the normal separated by years of drought; (2) 1931–40, a period of great precipitation deficiency; (3) 1941–51, a period of above-average precipitation; and (4) 1952–59, a period of below average precipitation. It is significant that channel widening occurred during periods 1 and 2 of variable or deficient rainfall, whereas channel narrowing occurred during period 3 of excess precipitation.

VEGETATION

The flood plain and banks of the river were vegetated prior to 1914 (fig. 43*A*). The grassed flood plain was relatively stable; however, if bank vegetation was destroyed by the 1914 flood, subsequent floods of lower peak discharge could have continued the destruction of the flood plain. Except for the 5-year period 1917–21, the great variability of precipitation during the period 1914–30 probably was unfavorable for the establishment of new vegetation in the channel or on the banks, and the period of prolonged drought 1930–40 certainly checked the growth of any new vegetation, which might have hindered the further widening of the channel. During the 9-year period of above-average precipitation after 1942, only floods of low peak discharge occurred. After 9 years of above-average precipitation, the major flood of 1951 had only minor effects on the channel, for much of the 1942 channel had been stabilized by perennial vegetation and converted to flood plain (fig. 43*C*). The establishment of perennial vegetation was a great aid to flood-plain formation. The growth of new vegetation and the resulting flood-plain construction were clearly dependent on the climatic and runoff characteristics for the period after 1942.

The period 1954–60 affords an opportunity to check the above theory of flood-plain formation, for it was a period of overall rainfall deficiency during which a large flood occurred. These conditions, according to the previous conclusions, should promote channel widening or at least prevent continued narrowing. The records (table 1) reveal that some widening did occur. The widening was not great, apparently because of the change in flood-plain vegetation since 1914—from grass to trees, grass, and weeds. The trees that border the channel offer considerable protection to the banks, and channel widening may be less easily accomplished under these conditions.

SUMMARY

The period of channel widening was characterized by below-average precipitation and by floods of high peak discharge, whereas the period of flood-plain construction was characterized by above-average precipitation and floods of low peak discharge. The influence of these conditions on vegetational growth is the key to the behavior of Cimarron River. Wet years and low water allow a vigorous growth of perennial vegetation, which stablized the existing deposits and promoted additional deposition. The stabilization of the new flood plain by vegetation was so effective that the floods of 1951 and 1958 did not cause great changes in the valley.

MECHANICS OF CHANNEL WIDENING AND FLOOD-PLAIN CONSTRUCTION

The Cimarron River affords an exceptional example of recent channel and flood-plain modification. The almost complete destruction of the flood plain makes a discussion of the manner of widening hypothetical; however, information from other sources and comparison of Cimarron River characteristics with those of other streams permit some conclusions to be drawn with regard to the manner of channel widening. A comparison of the aerial photographs taken in 1939, 1954 and 1960, information obtained by surveying five cross sections (fig. 42), and examination of flood-plain stratigraphy put a discussion of the flood-plain construction on a firmer basis.

Digitized by Google

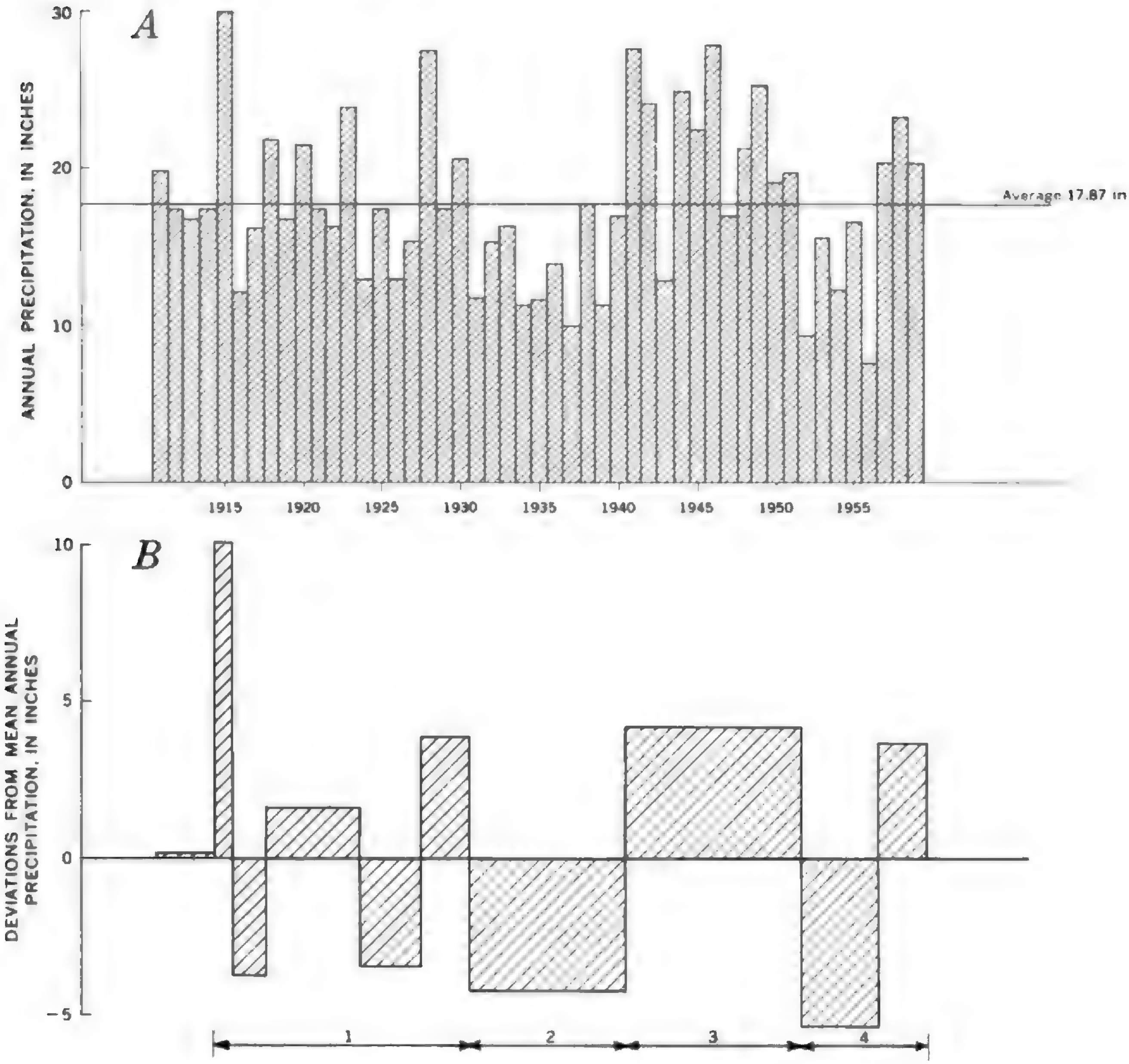

FIGURE 46.—Average annual precipitation in southwestern Kansas, 1910–59. *A*, Average annual precipitation for Liberal, Ulysses, Hugoton, and Richfield, Kans. *B*, Cycles of excess and deficient rainfall. The length of each cycle was determined by inspection of *A*, and the average departure during each cycle was then computed.

CHANNEL WIDENING

The pre-1914 Cimarron River meandered across a grassed flood plain. On the basis of old photographs, the channel was determined in some localities to be as much as 7 feet deep. After the 1914 flood, the channel widened 450 to 600 feet (McLaughlin, 1947). The major flood apparently first destroyed the meander pattern; the point bars were eroded, and the valley was in effect gutted. When the meander belt was destroyed, the protective bank vegetation and finer sediments were removed; the flood-plain sediments beneath the grassed surface were then exposed. The pre-1914 flood-plain sediments are exposed at several localities along the river (fig. 44C). In a sand pit on the north bank of the river at the Highway 56 crossing (fig. 42), 40 feet of alluvium is exposed. Thirty-five feet of the exposure is composed of cross-bedded gravel and coarse sand. Over this lies a dark-colored fine-grained (medium

Digitized by Google

grain size is 0.025 mm) zone that shows the columnar structure of a soil. The structure and dark color of this material suggest that it formed the surface of the pre-1914 flood plain. Overlying this alluvium is from 1 to 2 feet of fine sand and silt on which the present flood-plain vegetation grows. Where exposed the pre-1914 alluvium shows no stratification and appears homogeneous except for the presence of scattered pebbles. The alluvium is dense and cohesive, at least when dry, and may have offered considerable resistance to flood-plain destruction.

At present a part of the pre-1914 flood plain, which escaped destruction, is being eroded at the county road crossing north of Keyes, Okla. The bank on the north side of the river here averages 7 feet in height. The upper 1 to 1½ feet of the bank is composed of sand, which overlies 3 feet of pre-1914 alluvium. Beneath the pre-1914 alluvium, the cross-bedded channel sands are exposed at the base of the bank. The channel sands are being eroded from beneath the cohesive pre-1914 alluvium, causing slumping of the bank into the channel. Widening of the channel is occurring now, and it probably occurred in the past by bank caving that was caused by the removal of sand from beneath the cohesive pre-1914 flood-plain sediment.

EFFECT OF CHANNEL WIDENING ON GRADIENT

The gradient of the channel, as it was converted from a meandering to a straight channel, must have steepened appreciably. The gradient steepened from somewhat less than the gradient of the valley to a value probably closely approaching that of the valley itself. McLaughlin (1947) concluded that some degradation occurred during and after the 1914 flood. This conclusion is based on the formation of tributary gullies along the widened channel and on the reappearance of streamflow near the Highway 56 crossing, about 1 mile farther upstream in 1943 than prior to 1914. Gully formation, however, can be explained by the shortening of tributary stream courses by channel widening, which would induce erosion in the tributary valleys. In addition, part of the upstream migration of the head of the perennial reach near Satanta in 1943 may be explained by a rise in the water table after the floods of 1941 and 1942. Observation wells in the valley alluvium show a rise of water on the order of 3 feet after 1940. Initial channel widening and meander pattern destruction probably were associated with some degradation; but with continued bank erosion, the large amounts of bank sediments added to the channel for transport must have prevented further deepening and probably caused some aggradation of the channel.

Evidence is available to show that during the latter part of the period of channel widening and during the period of flood-plain construction the altitude of the channel floor has not changed appreciably. Data of maximum channel depth, measured from the crown of the roadbed at the time of bridge construction and again in 1960, are presented in table 3. The data show that changes in altitude of the channel are small. A change greater than 1 foot occurred at only one of the six bridges. These data support the hypothesis that degradation and aggradation may have occurred only locally after the 1914 flood; for during the period of flood-plain construction and channel narrowing there has been no consistent change in level along the Cimarron River. Similarly, Coldwell's (1957) observations on the Washita River showed that the river has widened its channel from 100 to 150 feet in 1939 to 200 to 350 feet in 1954 with no change in the altitude of the channel at the Pauls Valley gaging station.

TABLE 3.—*Changes in channel depth between date of bridge construction and 1960*

[Data for date of bridge construction and distance from crown of road to deepest part of channel at date of construction from State Highway Commission of Kansas]

Location of bridge crossing (highway)	Date of bridge construction	Distance from crown of road to deepest part of channel (feet)	
		At date of bridge construction	1960
U.S. 54	1935	20	18
U.S. 83	1948	18	18
U.S. 56	1930	23	24
U.S. 270	1949	22	[illegible]
Kansas 51	1938	18	17
Kansas 27	1935	12	12.5

FLOOD-PLAIN CONSTRUCTION

Favorable conditions—namely, above-average precipitation and floods of low to moderate peak discharge—permitted the Cimarron flood plain to begin to re-form after the 1942 flood. Undoubtedly, the fact that the channel was wide enough to occupy almost the entire area of the former flood plain was important.

The new flood plain was built almost entirely by a vertical accretion of sediments, which occurred in two ways as follows: (1) By island formation in the channel and subsequent attachment of the island to one bank by channel abandonment and (2) by deposition on and building up of areas not occupied by the low-water channel. Each process will be discussed in some detail.

ISLAND FORMATION

In the widening channel, sand bars and dunes formed. Bars that formed during the drought years had little

Digitized by Google

chance of becoming permanent features; however, during years of average or excess precipitation, the growth of vegetation on the higher parts of the channel and on bars was the first phase of flood-plain construction. Vegetation converted the bars to permanent features of the channel.

When the channel was wide and dry, the movement of sand by wind was common. The migrating sand collected in vegetation along the perimeter of islands and built natural levees of wind-blown sand. One of these levee dunes occurs at section 1 and is shown on cross section A–A′ (fig. 47) at 950 feet. Once an island be-

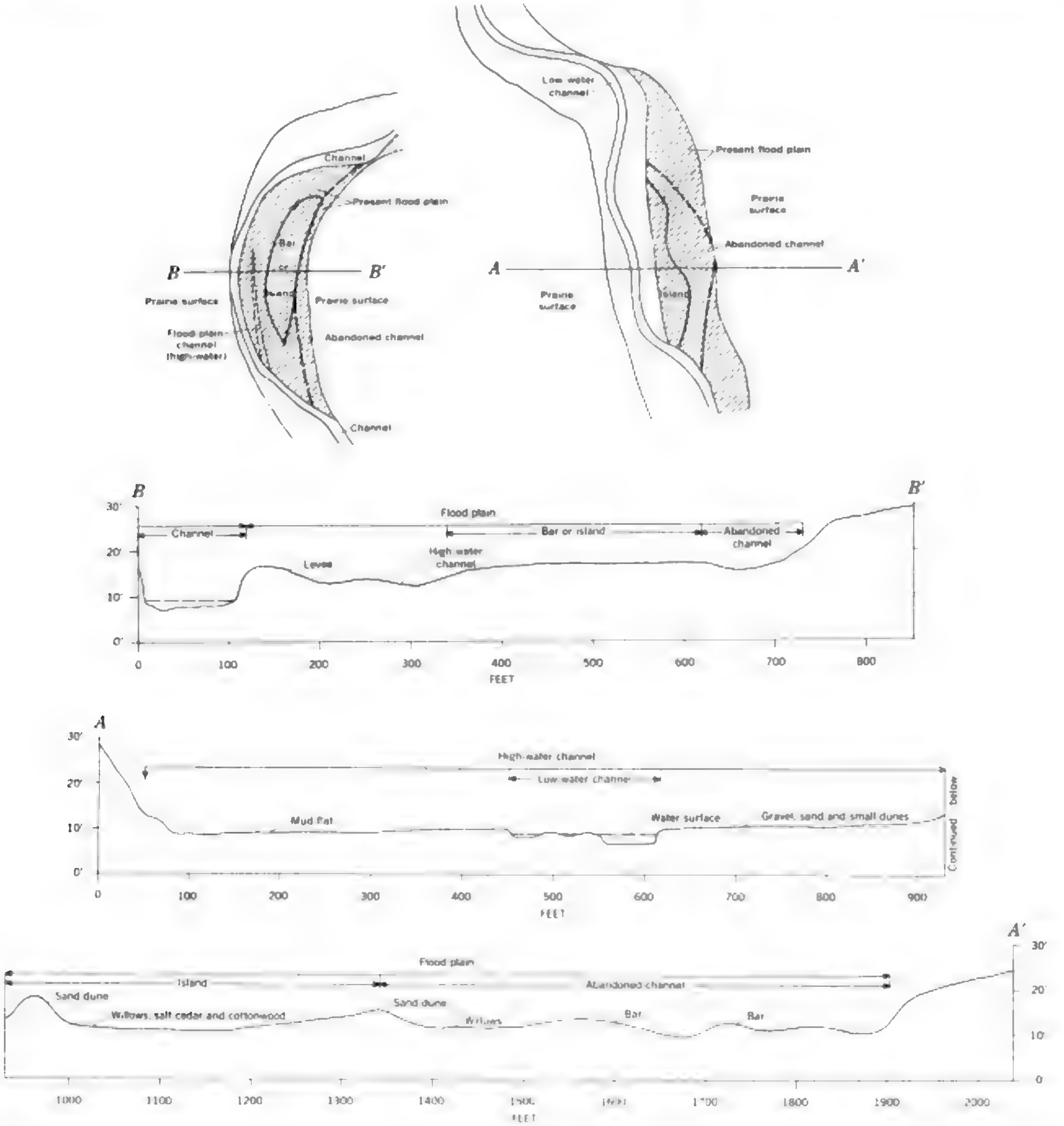

FIGURE 47. Transverse profiles of the Cimarron River valley. B–B′, Cimarron valley near old Highway 270 crossing, cross section 2 (fig. 42). A–A′, Cimarron valley at cross-section 1 (fig. 42).

Digitized by Google

came established in the channel, it would be perpetuated by deposition from subsequent floods and by the accumulation of aeolian sand deposits.

The formation of an island narrows the channel, but the presence of the island itself causes further narrowing. Depending on the orientation of the island in the channel, one or the other of the channels surrounding the island will be aggraded and abandoned (fig. 48*A*). For example, an island will rarely be situated so as to divide the water flow equally around the island. Generally, one channel will carry a larger discharge than the other. When this situation occurs, the channel carrying the lesser discharge is a branch channel. Laboratory experiments reveal that at a stream fork the channel which carries the smaller discharge has the highest concentration of bedload (Linder, 1952). In

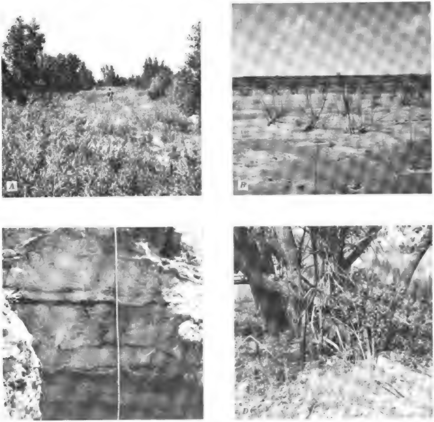

FIGURE 48.—Cimarron River in southwestern Kansas. *A*, Abandoned branch channel near State Highway 51 crossing north of Rolla, Kans., in 1960. On 1954 aerial photographs this channel contained no vegetation. *B*, One-year-old salt cedar saplings growing on mud-veneered part of channel shown at north side of profile *A*–*A'*, (fig. 47). Light-colored sediment is aeolian sand. *C*, Mud layers in flood-plain alluvium near bridge north of Moscow, Kans. Thin discontinuous mud layer just above thicker continuous layer in upper part of photograph is uppermost mud layer shown on figure 51. *D*, Partly buried automobile frame near country-road bridge north of Moscow, Kans. This frame is one of a group installed to aid bank stabilization. Trees growing to rear of frame are about 15 years old.

perennial streams this relationship may not be important, but in ephemeral streams deposition is important as the flood waters wane. The branch channel would thus be aggraded until it could carry only a minor percentage of the total discharge, and it would soon be abandoned. The cross sections in figure 47 show abandoned branch channels and islands.

The island formation and attachment method of flood-plain formation is less important than it appeared initially, for many islands that occupy the channel of Cimarron River at present were not formed in the channel but were fashioned by the detachment of portions of flood plain by channel changes. The island theory was first proposed to explain flood-plain formation and channel changes along the Red River during the Texas-Oklahoma boundary controversy (Glenn, 1925).

DIRECT FLOOD-PLAIN CONSTRUCTION

If, when the river was at its greatest width in 1943, a low-water channel meandered across the greatly widened sandy high-water channel, then a flood plain may have been already partially formed. Cross section *A–A′* of figure 47 shows the low-water channel occupying the center of a much wider sandy channel. During the survey, water filled the low-water channel. The surface to the left (north) of the low-water channel had been flooded recently and a veneer of mud had been deposited on this surface to a depth of one-half inch. This locality was revisited in the spring of 1961, and the surface was found to be supporting a new growth of salt cedar (fig. 48*B*). The presence of these plants will aid further deposition at this site. Apparently, during years of above average precipitation and low flow, the surface adjacent to a low-water channel becomes vegetated. It is then raised by deposition from flows that overtopped the low-water channel.

Figure 49 illustrates how the flows of different height affect the channel. Low flows are confined to the low-water channel and play no part in flood-plain formation, except as they afford a source of moisture for bank vegetation. Moderate flows escape the low-water channel and deposit sediment on the incipient flood plain, as on the north side of profile *A–A′* (fig. 47). High flows tend either to destroy or to build up the incipient flood plain, depending on vegetational cover.

Because the high flows tend to be destructive during the initial phase of flood-plain construction, the first patches of permanent flood-plain appear on those parts of the valley floor protected from the full force of floods. For example, aerial photographs show that initial flood-plain formation occurred in sheltered parts of the valley, at the mouth of tributaries, and in the lee of islands (fig. 50). The formation of the initial areas of flood plain naturally shielded other parts of the valley floor, which in turn became vegetated and aggraded. The coalescence of these newly formed flood-plain patches formed the existing flood plain. Each succeding flood deposited sediment on these areas, which were gradually built up to a level several feet above the present channel.

FLOOD-PLAIN STRATIGRAPHY

If the foregoing outline of flood-plain formation along the Cimarron River is correct, stratigraphic evidence in the banks of the channel should confirm it. Cross section *A–A′* of figure 47 shows the present low-water channel. The banks of the low-water channel are composed of channel sand. If these banks were built higher by overbank deposition, then each flood should have left a deposit of sand and silt as the flood waters receded from the higher surface. Depending on the sediment load carried by the water and the ability of

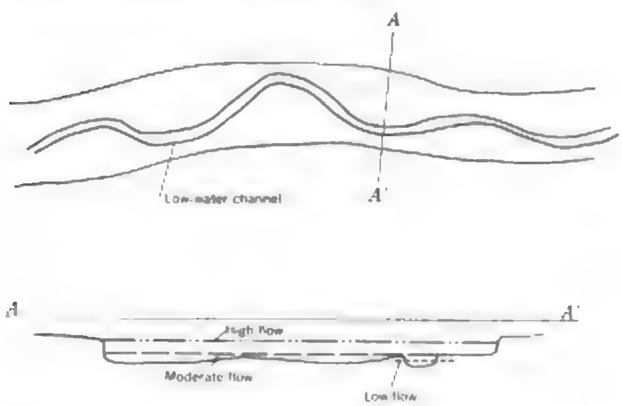

FIGURE 49.—Sketch illustrating parts of the Cimarron valley covered by low, moderate, and high flows. Enlargement of profile, ×4.

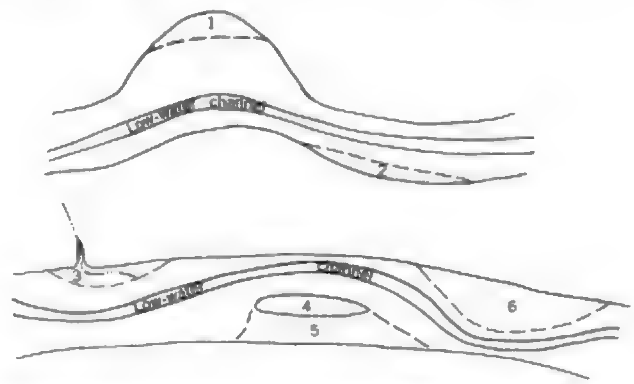

FIGURE 50.—Channel areas favorable for flood-plain formation. 1, Crest of valley meander; 2, Lee of valley bend; 3, Mouth of tributary; 4, Island; 5, Lee of island (abandoned channel); 6, Surface above low-water channel.

the higher surface to trap and hold the sediment, the rise of the flood-plain surface might be rapid or slow. Specific evidence of flood deposition would be a layer of mud left by the receding waters, as observed in 1960 on the left side of the channel. (See section A–A′ fig. 47, and fig. 48B.)

At each reach of the channel visited in Kansas the recent flood-plain deposits, where exposed by excavation, show alternating thin layers of mud and sand (fig 48C). The mud layers are horizontal and in some places could be traced back from the channel across the flood plain to the edge of the valley. Individual mud layers were traced in existing sand pits and in holes augered or dug into the flood plain.

To examine these deposits in more detail, a vertical cut, which exposed 5 feet of the flood-plain alluvium, was made near the county road crossing north of Moscow. The base of the cut was at the level of the present channel. A diagrammatic sketch of this section is shown in figure 51. Six mud layers appear in this section (fig 48C).

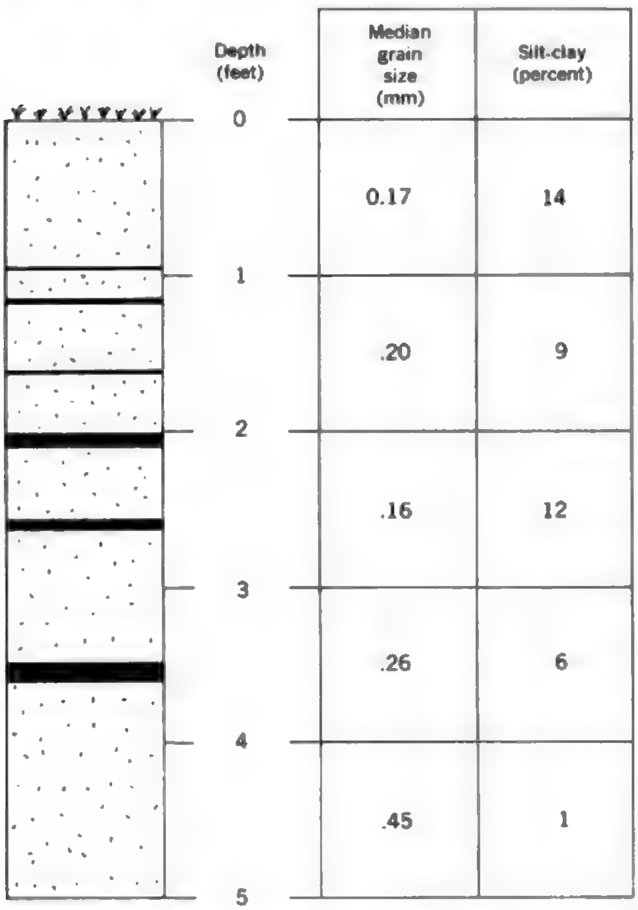

FIGURE 51.—Flood-plain stratification near county-road bridge north of Moscow, Kans. The six mud layers are shown by black lines. (See also fig. 48C.)

The flood plain is composed of sedimentary units deposited by overbank floods. A deposit of sand is overlain by a thin layer of fine sediment (the mud layer), which is deposited during the recession of the flood waters. A part of the sand above the uppermost mud layer (fig. 51) is composed of wind-blown sand trapped by vegetation on the flood-plain surface; undoubtedly, a part of the sand found between mud layers is aeolian, for the mud deposited in the channel in 1960 is now covered by a thin veneer of wind-blown sand (fig. 48B).

Other evidence of overbank deposition might be a graded deposit; that is, the alluvium exposed in the banks should show a decrease in grain size upward. In figure 51 the grading would be well defined if it were not for the occurrence of two thick mud layers between 2 and 3 feet. Except for the sample containing the mud layers, the percent silt clay also increases upward as expected. The stratigraphic evidence supports the concept of flood-plain formation by vertical accretion.

Cores were taken from several cottonwood trees growing on the newly constructed flood plain in 1961 to afford more precise information on the age of the flood plain. Trees at the south edge of the flood plain near the old Highway 270 crossing were 17 years old. Two trees were cored at the north edge of the flood plain near the bridge north of Moscow. These trees had grown around an automobile frame (fig. 48D), one of a group installed to aid in stabilizing the bank. The frame is now located about 250 feet from the present bank of the Cimarron River. The cored trees were found to be 14 and 15 years old. These ages support the conclusion that flood-plain construction began after the 1942 flood.

Trees on the flood plain have been partly buried by alluvium. Pits were dug at the base of three cored trees to determine the depth of burial. One small tree, located on the flood plain near Satanta, was 13 years old in 1961 and has been buried by 2 feet of alluvium. Two trees on the flood plain near the county road crossing north of Moscow and closer to the channel than those shown in figure 48D were excavated to the main root system at depths of 1.8 and 2.0 feet. These trees were both 11 years old. This evidence indicates that about 2 feet of flood-plain deposition has occured during the last 11 to 13 years.

SUMMARY

Once started by a major flood, the widening of the Cimarron River channel did not cease because of the ease of bank erosion and the occurrence of large floods. The widening of the channel apparently occurred by bank caving as the coarse sand was washed from be-

Digitized by Google

neath the relatively resistant pre-1914 flood-plain sediments.

During channel widening, degradation was probably not important. Channel gradient steepened, however, as the course of the river was shortened by destruction of the meander pattern.

The channel narrowing or flood-plain construction along the Cimarron River was the result of three factors as follows: The river had widened excessively; precipitation was above average; and the large floods were infrequent and did not erode the newly formed flood plain. The new flood plain is composed of a complex of coalesced islands, abandoned branch channels, and areas of flood plain built adjacent to the low-water channel. Large parts of the wide channel were not occupied by low-water flows, and these areas were sites of vegetational growth. The increased plant cover reduced flow velocities over these areas and promoted sediment deposition.

An examination of flood-plain stratigraphy indicates that the flood plain is composed predominantly of overbank sediment deposited during floods. An individual flood deposit consists of a layer of sand covered by a veneer of mud.

COMPARISON OF CIMARRON RIVER CHANNEL CHANGES WITH THOSE OF OTHER RIVERS

Too often in the consideration of unstable channels one is prone to think only of degradation or aggradation of the channel. Observations along Cimarron River clearly show, however, that both channel widening and narrowing may occur without a major change in the altitude of the channel floor (table 3). The rate and method of flood-plain formation noted along the Cimarron River is not unique, for similar changes have been noted along other rivers. For example, the widening of the channel of Washita River, as described by Coldwell (1957), occurred without significant changes in the altitude of the bed of the stream.

Hefley (1935) stated that the Canadian River in eastern Oklahoma has widened since the major flood of 1906 from less than half a mile to more than 2 miles in some places.

Bryan (1927) reported that the Rio Salado, a tributary to the Rio Grande near San Acacia, N. Mex., ranged from 12 to 49 feet in width in 1882, but in 1918 its width ranged from 330 to 550 feet. Bryan (1927, p. 19) stated that "Unlike many similar streams in New Mexico, which have not only widened their channels but deepended them in the same period, the Rio Salado, at least in the vicinity of Santa Rita, has even yet banks that are only 3 to 10 feet high and average 5 feet high." Leopold and Wolman (1957) reported that the channels of the Verde and Gila Rivers in Arizona were widened by large floods, but that narrowing of the channel followed establishment of vegetation. These changes may be similar to those which occurred along Cimarron River.

Smith (1940) reported on recent channel changes of several rivers in western Kansas, indicating that they have undergone Cimarron-type changes. The Smoky Hill River originally "had alternating sandy stretches and grassy stretches with series of pools. Later the former were widened, and the latter were sanded up * * *." Smith further stated that the Republican River was greatly affected by the flood of 1935.

> Formerly a narrow stream with a practically perennial flow of clear water and with well-wooded banks, the Republican now has a broad, shallow sandy channel with intermittent flow. The trees were practically all washed out and destroyed, much valuable farmland * * * was sanded over, and the channel has been filled up by several feet.

The Republican and Smoky Hill Rivers are typical of streams having sandy channels, as they have only from 2 to 5 percent silt and clay, in the sediment forming the perimeter of their channels (Schumm, 1961).

The Red River flood plain near Burkburnett, Tex. (fig. 52) was the object of intensive study as a result of the boundary dispute between Oklahoma and Texas (Glenn, 1925; Sellards, 1923). The Red River was never a narrow, meandering stream in historic times: a survey in 1874 showed the river to be about 4,000 feet wide. The channel, however, has undergone some important changes. For example, comparison of a special map prepared in 1920 (Sellards, 1923) with aerial photographs taken in 1953 showed enlargement of the flood plain. Over a 10 mile reach of the river 5.5 square miles of flood plain were added. The width of the Red River was measured at 20 sections between the confluence of the Pease and Red Rivers to the west and the confluence of Whiskey Creek and Red River to the east on aerial photographs taken in 1937, 1953, and 1957. In 1937 the river averaged three-quarters of a mile in width, close to the average for the 1874 survey. In 1953 the average width had decreased to half a mile. This channel narrowing may have been contemporaneous with that along Cimarron River. In 1957 the river averaged two-thirds of a mile wide, indicating a significant widening between 1953 and 1957. The photographs show all the types of flood-plain formation noted along the Cimarron River (fig. 50), and as suggested by Glenn (1925), the attachment of islands to the flood plain was important in the formation process.

The Red River transports large amounts of sand, red silt, and clay. The flood-plain sediments, where observed near the main highway bridges (Highways 81,

Digitized by Google

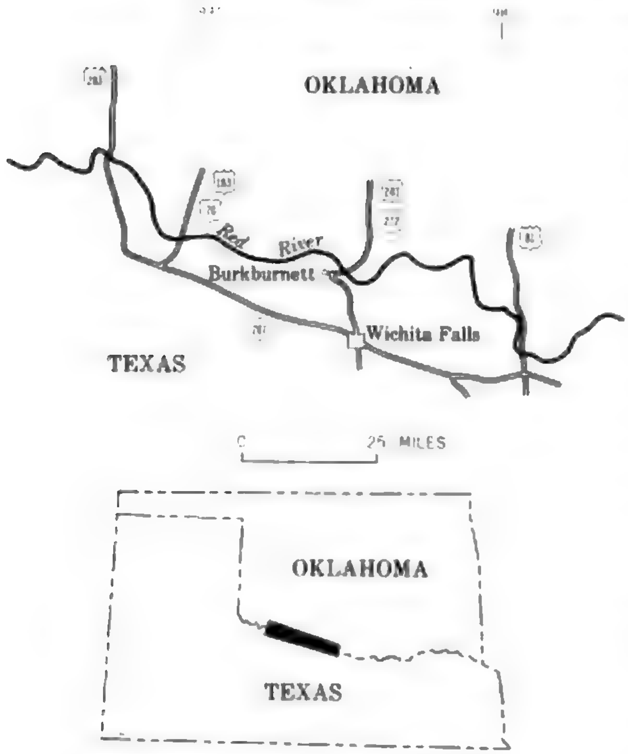

FIGURE 52.—Index map of Red River area.

281, and 183, fig. 52) show stratification characteristic of vertical accretion deposits. One section was sampled in detail near Burkburnett, Tex., where it was possible to obtain a sample of one thick mud layer not mixed with sand. The median grain size (0.002 mm) and silt and clay content (89 percent) of this layer are very similar to the median grain size (0.001 mm) and silt and clay content (85 percent) of mud recently deposited over sand at the margin of the channel. The similarity between the mud layers of the bank and the mud being deposited in the channel and the occurrence of mud layers in the banks at this location and elsewhere indicate that the Red River flood plain and islands, where observed, are built by the vertical accretion of sediment.

SUMMARY

The channel changes along the Cimarron River appear to be similar to changes which have occurred along the Washita, Canadian, Smoky Hill, Republican, and Red Rivers and Rio Salado. The changes differ from the degradation and aggradation characteristic of other unstable streams, for these rivers widen and narrow their channels as an alternative to aggradation and degradation

CONCLUSIONS

Flood-plain destruction along the Cimarron River occurred as a result of channel widening, which was initiated by the maximum flood on record. Large floods and below-average precipitation hindered a return to stability, and, in fact, were the means by which flood-plain destruction was perpetuated.

In contrast to floods observed in humid regions (Wolman and Eiler, 1958), floods in semiarid and arid environments may be tremendously destructive to the channel and flood plain. This destruction by floods may be a characteristic of erosion in a semiarid region where climatic fluctuations are common, and the streams are ephemeral or carry very low flows during long periods. Often these streams cannot adjust as readily as perennial streams to a change in stream regimen or a climatic fluctuation. Large floods may trigger an adjustment by initiating periods of severe erosion or deposition (Schumm and Hadley, 1958), and the events along Cimarron River may be of this type.

Most of the Cimarron River flood plain was constructed in only 12 years. Although rapid rates of erosion and deposition are commonly observed on other rivers, we are not aware of rates of flood-plain formation elsewhere as rapid as on the Cimarron River.

Observations in the valleys of the Cimarron and Red Rivers show that the flood plains were formed predominantly by overbank flooding and the vertical accretion of sediment. Generally, patches of flood plain in the most sheltered parts of the channel formed first. These patches coalesced and joined the islands and abandoned channels to form a composite flood plain. The flood plain, however, can be built simultaneously over large areas when an area of channel between the low-water channel and the edge of the valley is transformed as a unit to flood plain (fig. 50).

After the flood plain has been formed by vertical accretion, the stream may begin to meander. This reworking of the flood-plain alluvium by lateral migration of the stream would form a flood plain composed predominantly of lateral accretion deposits, as described by Wolman and Leopold (1957) and Adler and Lattman (1961). A flood plain may be formed by different processes, but a meandering stream migrating from one side of the valley to the other would leave a flood plain showing stratigraphic evidence only of lateral accretion. Therefore, the presence of lateral-accretion deposits forming the major part of a flood plain may not mean that the flood plain was initially formed by point-bar construction.

The type of changes occurring along the Red and Cimarron Rivers can be attributed to a large extent to the sandy alluvium forming the flood plain and channel. Channel widening instead of degradation and flood-plain construction instead of aggradation may occur commonly along sandy rivers in semiarid regions.

Digitized by Google

REFERENCES

Adler, A. A., and Lattman, L. H., 1961, Flood plain sediments of Halfmoon Creek, Pennsylvania: Mineral Industries Expt. Sta. (Pennsylvania State Univ.) Bull. 77, p. 1–11.

Bryan, Kirk, 1927, Channel erosion of the Rio Salado, Socorro County, New Mexico: U.S. Geol. Survey Bull. 790, p. 17–19.

Bryne, F. E., and McLaughlin, T. G., 1948, Geology and ground-water resources of Seward County, Kansas: Kansas Geol. Survey Bull. 69, 140 p.

Coldwell, A. E., 1957, Importance of channel erosion as a source of sediment: Am. Geophys. Union Trans., v. 38, p. 908–912.

Frye, J. C., 1942, Geology and ground-water resources of Meade County, Kansas: Kansas Geol. Survey Bull. 45, 152 p.

Glenn, L. C., 1925, Geology and physiography of Red River boundary between Texas and Oklahoma: Pan American Geologist, v. 43, no. 5, p. 365.

Haworth, Erasmus, 1897, Underground waters of southwestern Kansas: U.S. Geol. Survey Water-Supply Paper 6, 65 p.

Hefley, H. M., 1935, Ecological studies on the Canadian River flood plain in Cleveland County, Oklahoma: Ecological Mon., v. 7, p. 345–402.

Johnson, W. D., 1902, The High Plains and their utilization: U.S. Geol. Survey 22d Ann. Report, pt. 4, p. 631–669.

Leopold, L. B., and Wolman, M. G., 1957, River channel patterns: braided, meandering and straight: U.S. Geol. Survey Prof. Paper 282–B, p. 39–84.

Lindner, C. P., 1952, Diversions from alluvial streams: Am. Soc. Civil Engineers Proc., v. 78, no. 112, 25 p.

McLaughlin, T. G., 1942, Geology and ground-water resources of Morton County, Kansas: Kansas Geol. Survey Bull. 40, 126 p.

——— 1946, Geology and ground-water resources of Grant, Haskell, and Stevens Counties, Kansas: Kansas Geol. Survey Bull. 61, 221 p.

——— 1947, Accelerated channel erosion in the Cimarron Valley in southwestern Kansas: Jour. Geology, v. 55, p. 76–93.

Schumm, S. A., 1960, The shape of alluvial channels in relation to sediment type: U.S. Geol. Survey Prof. Paper 352–B, p. 17–30.

——— 1961, Effect of sediment characteristics on erosion and deposition in ephemeral stream channels: U.S. Geol. Survey Prof. Paper 352–C, p. 31–70.

Schumm, S. A., and Hadley, R. F., 1958, Arroyos and the semiarid cycle of erosion: Am. Jour. Sci., v. 255, p. 161–174.

Sellards, E. H., 1923, Geologic and soil studies on the alluvial lands of the Red River valley: Texas Univ. Bull. 2327, p. 27–87.

Smith, H. T. U., 1940, Notes on historic changes in stream courses of western Kansas, with a plea for additional data: Kansas Acad. Sci. Trans., v. 43, p. 299–300.

Wolman, M. G., and Leopold, L. B., 1957, River flood plains: Some observations on their formation: U.S. Geol. Survey Prof. Paper 282–C, p. 87–107.

Wolman, M. G., and Eiler, J. P., 1958, Reconnaissance study of erosion and deposition produced by the flood of August 1955 in Connecticut: Am. Geophys. Union Trans., v. 39, p. 1–14.

Digitized by Google

QE 75
f. A26
no. 352-E

Geol

1964

UNIVERSITY OF CHICAGO LIBRARY
JUN 18 1964

Geomorphology of Segmented Alluvial Fans in Western Fresno County, California

U.S GEOLOGICAL SURVEY/PROFESSIONAL PAPER/352-E

Prepared in cooperation with the California Department of Water Resources

U.S. DEPARTMENT OF THE INTERIOR
March 3, 1849

Bull—GEOMORPHOLOGY OF ALLUVIAL FANS IN FRESNO COUNTY, CALIFORNIA—Geological Survey Professional Paper 352-E

Geomorphology of Segmented Alluvial Fans in Western Fresno County, California

By WILLIAM B. BULL

EROSION AND SEDIMENTATION IN SEMIARID ENVIRONMENT

GEOLOGICAL SURVEY PROFESSIONAL PAPER 352-E

Prepared in cooperation with the California Department of Water Resources
A study of the interrelations of alluvial-fan morphology, drainage-basin characteristics and tectonic and climatic events

---

UNITED STATES GOVERNMENT PRINTING OFFICE, WASHINGTON · 1964

Digitized by Google

UNITED STATES DEPARTMENT OF THE INTERIOR

STEWART L. UDALL, *Secretary*

GEOLOGICAL SURVEY

Thomas B. Nolan, *Director*

For sale by the Superintendent of Documents, U.S. Government Printing Office
Washington, D.C. 20402

U. S. GOVERNMENT
DEPOSITORY COLLECTION

Digitized by Google

CONTENTS

	Page
Glossary	v
Abstract	89
Introduction	89
Purpose and scope	89
Acknowledgments	90
Geographic setting	90
Location and topographic features	90
Drainage	90
Climate and vegetation	91
General geology	92
Regional setting	92
The Coast Range orogeny	93
Geomorphology of the alluvial fans	93
Definitions and general features	93
Fan size and slope	94
Radial profiles of alluvial fans	94
Relation of stream and fan-segment gradients	100
Geomorphology of the alluvial fans—Continued	
Possible causes of fan segmentation	103
Tectonic hypothesis	105
Fans associated with progressively gentler stream gradients	106
Fans associated with progressively steeper stream gradients	110
Cross-fan profiles	114
Change in shape downslope	114
Stream channels	114
Fanhead trenches	117
Causes of the fanhead trenching	120
Summary and conclusions	126
References cited	127
Index	129

ILLUSTRATIONS

[Plates are in pocket]

PLATE 6. Topographic map of parts of Fresno, Merced, and San Benito Counties, Calif.
7. Drainage basins and alluvial fans studied in Fresno, Merced, and San Benito Counties, Calif.

		Page
FIGURE 53.	Map of parts of Fresno, Merced, and San Benito Counties, Calif., showing area discussed in this paper	91
54.	Relations of fan area and slope to drainage-basin area and lithology	95
55.	Types of radial profiles of alluvial fans in California	96
56.	Radial profiles of the Tumey Gulch fan	97
57.	Segments of the Tumey Gulch fan	98
58.	Radial profiles of six fans whose streams head in the foothill belt	99
59.	Radial profiles of fans whose streams head in the Diablo Range	100
60.	Longitudinal profiles of two streams and two low terraces and the surface of the upper part of their alluvial fans	101
61.	Relation of the gradients of fanhead trenches to the gradients of their adjacent lower fan segments	102
62.	Terraces in the foothill belt of western Fresno County	103
63.	Moisture content for core holes on the unirrigated parts of the Arroyo Hondo and Arroyo Ciervo fans	104
64.	Diagrammatic sketches showing the steepening of stream gradients due to a hypothetical climatic change	105
65.	Diagrammatic sketches showing two types of alluvial-fan and stream-gradient history	106
66.	Relation of stream terraces to fan segments for Little Panoche Creek	107
67.	Soils and fan-segment boundaries of the Little Panoche Creek fan	109
68.	Diagrammatic sketch showing stages of fan-segment development	111
69.	Radial profiles of the San Emigdio Creek and Santiago Creek fans, Kern County, Calif	112
70.	Diagrammatic sketches showing stages of alluvial-fan development	113
71.	Channel deviation from medial position on fanheads of alluvial fans in parts of Fresno and Merced Counties	114
72.	Topographic map of the alluvial fans of Capita Canyon, Chaney Ranch Canyon, and Marca Canyon	115
73.	Cross-fan profiles of Capita Canyon, Chaney Ranch Canyon, and Marca Canyon fans	116
74.	Position of stream channels on the fanheads of the piedmont plain east of the Panoche Hills	116
75.	Mudflow deposits on the natural levees of Arroyo Hondo	117
76.	The fanhead trench of Tumey Gulch	117

Digitized by

		Page
Figure 77–80.	Changes in the—	
	77. Depth of the Tumey Gulch fanhead trench, 1921–55	118
	78. Depth of the Arroyo Ciervo fanhead trench, 1921–56	119
	79. Width and length of the Panoche Creek fanhead trench, 1854–1959	119
	80. Channel configuration of Arroyo Hondo, 1855–1954	121
81.	Index map of central California showing the location and altitude of weather stations referred to in this report	122
82.	Trends of annual rainfall for five stations in California, 1853–1958	123
83.	Trends of daily rainfall size classes, 1881–1958, Sacramento, Calif	124
84.	Trends of daily rainfall size classes, 1901–58, Mendota Dam, Calif	125

TABLE

	Page
Table 1. Basic data on drainage basins and alluvial fans of selected streams in western Fresno County, Calif	92

GLOSSARY

Alluvial fan, a stream deposit whose surface forms a segment of a cone that radiates downslope from the point where the stream channel emerges from a mountainous area.

Apex, the highest point on an alluvial fan, generally where the stream emerges from the mountain front (Drew, 1873, p. 447).

Braided distributary channels, secondary channels that extend downslope from the end of the main stream channel or fanhead trench and are characterized by repeated division and rejoining.

Cross-fan profile, a topographic profile of alluvial fan(s) roughly parallel to the mountain front.

Drainage basin, the area drained by a stream upstream from the fan apex.

Ephemeral stream, a stream, or part of a stream, that flows only briefly in direct response to precipitation.

Fanhead trench, a stream channel entrenched into the upper, and possibly the middle, part of the fan.

Fan segment, a part of an alluvial fan that is bounded by changes in slope.

Intermittent stream, a stream, or part of a stream, that flows only part of the time because it receives water from seasonal sources such as springs and bank storage, as well as from precipitation.

Piedmont plain, a broad sloping plain formed by the coalescence of many alluvial fans.

Radial line, a straight line on the fan surface extending from the apex to the toe.

Radial profile, a topographic profile along a radial line.

Thalweg, the line along the deepest part of the stream channel.

Digitized by Google

GEOMORPHOLOGY OF SEGMENTED ALLUVIAL FANS IN WESTERN FRESNO COUNTY, CALIFORNIA

By William B. Bull

ABSTRACT

The alluvial fans fringing the western border of the San Joaquin Valley in Fresno County, Calif., are derived from drainage basins that are generally similar with respect to topography, climate, and tectonic environment but that range in size from 0.2 to 296 square miles and in lithology from predominantly sandstone to predominantly mudstone or shale. Fans derived from mudstone or shale-rich basins are generally 35–75 percent steeper than fans of similar area derived from sandstone-rich basins and roughly twice as large as fans derived from sandstone basins of comparable size.

The radial profiles of the fans are not smooth curves, but, instead, comprise three or four straight-line segments. The surfaces represented by these segments form bands of approximately uniform slope that are, mainly, concentric about the fan apexes. Longitudinal profiles of terraces show that intermittent uplift has changed the stream-channel slope upstream from the fan apexes. The slope of the area of deposition and the slope of the stream channel upstream from it tend to be the same. The segmentation is a result of intermittent uplift that has changed the stream-channel slopes and the succeeding depositional slopes.

Most of the fans are associated with stream channels that have become progressively steeper. Each time the channel was steepened, the succeeding fan deposits formed a new fan-shaped segment of steeper slope that was deposited on the upper part of the pre-existing fan.

The Little Panoche Creek fan, however, has a history that is associated with progressively gentler stream-channel gradients, because the rate of downcutting by the stream has exceeded the average rate of uplift of the reach immediately upstream from the apex. The intermittent character of the uplift resulted in the cutting of a series of paired terraces which preserve a record of the deformation of the mountain front and fan-head areas. With each uplift, the end of the deepened stream channel moved farther down the fan. After each episode of trenching, the lower part of the stream channel and its adjacent area of fan deposition ultimately attained a more gentle gradient than previously.

Fan segmentation is useful for deciphering part of the tectonic history of the area because the fan profiles and the relative ages of the fan segments reflect part of the erosional and tectonic history of the drainage basins.

Two periods of fanhead trenching, apparently unrelated to tectonic activity, have been recorded since 1854 when many fans were receiving deposits near their apexes. One was from about 1875 to 1895 and the other from about 1935 to 1945. Many channels have been deepened 25–40 feet.

Rainfall data from five stations in central California show two periods of much greater than average annual rainfall, which were also periods of high frequency of large daily rainfall. They coincide with the two periods of maximum channel trenching.

INTRODUCTION

PURPOSE AND SCOPE

Alluvial fans are common in the arid and semiarid areas of the world. Ground water in many parts of the Western States is pumped from alluvial-fan deposits and recharge of many ground-water basins is through the alluvial-fan deposits that fringe the basins. Despite the importance of alluvial fans, little detailed work has been done on their sedimentary and geomorphic characteristics until recently.

This report presents data on the geomorphology of alluvial fans collected as part of an investigation of the geology of alluvial fans and their drainage basins in western Fresno County, Calif. The primary purpose of the investigation was to obtain a better understanding of the alluvial fans and their drainage basins so that the causes, magnitude, rate, and duration of near-surface subsidence could be understood better. The sedimentary features of the alluvial-fan deposits and the geomorphic and lithologic characteristics of their drainage basins are described in detail elsewhere (Bull, 1964).

The geomorphology study provided information concerning deposition and erosion of the fans. This information is reported separately in this paper because it did not reveal many criteria that could be used in appraisal of subsidence.

The relations of fan size and slope to drainage-basin area and lithology were studied. The overall shape of the alluvial fans was studied by means of radial and cross-fan profiles, and the different types of stream channels are described. Reasons for the characteristc fan shapes and the history and causes of channel trenching that occurred during the last century are discussed.

Digitized by Google

The maps used in the study include the following: General Land Office plats and survey notes of 1853–58 and 1879–81; U.S. Geological Survey 7½ minute quadrangles, 1922–31, scale 1:31,680, contour intervals 5 and 25 feet; and U.S. Geological Survey 7½ minute quadrangles, 1955–56, scale 1:24,000, contour intervals 5, 10, 20, and 40 feet.

The investigation was made under the supervision of J. F. Poland, research geologist of the Ground Water Branch, U.S. Geological Survey, in charge of land-subsidence investigations in California, and in co-Resources.

ACKNOWLEDGMENTS

operation with the California Department of Water

S. N. Davis and G. A. Thompson of Stanford University gave advice on certain aspects of the study. Ranchers, sheepherders, farmers, and other people living in the area gave firsthand accounts of the history of channel trenching. The author also thanks his colleagues in the Geological Survey, C. S. Denny, L. A. Heindl, R. H. Meade, J. F. Poland, F. S. Riley, and W. E. Wilson, for their critical review of the manuscript.

GEOGRAPHIC SETTING

LOCATION AND TOPOGRAPHIC FEATURES

The area discussed in this paper includes about 1,400 square miles of the west side of the San Joaquin Valley and the adjacent Diablo Range in central California (fig. 53). The northern edge of the area is 10 miles south of Los Banos, and the southern boundary is the south side of the drainage basin of Domengine Creek, 12 miles north of Coalinga. The alluvial fans are in western Fresno County and in a small part of Merced County, and the drainage basins of some of the fans extend into San Benito County.

Between the flood plains of the San Joaquin River and Fresno Slough and the foothills to the southwest is a belt of coalescing alluvial fans 12–19 miles wide. The altitude at the base of this piedmont plain ranges from 130 to 175 feet, and the alluvial fans rise to altitudes of about 340–900 feet at their apexes. The slopes of the fans range from about 10 feet per mile near the base of the larger fans to about 150 feet per mile on the upper slopes of some of the smaller fans. The local relief on the fans is generally less than 5 feet, except on the upper parts where the main stream channels are incised as much as 40 feet. Erosional stream channels are not present on the fans except for minor dendritic channels on parts of some older fan surfaces bordering the Panoche Hills.

The Diablo Range in the southwestern part of the area consists of several groups of foothills fringing the San Joaquin Valley and the main range, which is generally about 10–15 miles from the western margin of the valley (pl. 6). The foothills include the Ciervo Hills, whose highest point is about 3,400 feet, and the Panoche Hills, which rise to an altitude of about 2,700 feet. The main Diablo Range has several peaks higher than 5,000 feet. Both the foothill belt and the main Diablo Range are rugged and have many steep canyons. (See pl. 6.)

Most of the geographical features mentioned in this report can be found on plate 6, and the specific drainage basins and their associated alluvial fans are outlined and identified on plate 7. The approximate boundaries of the alluvial fans were determined from aerial photographs and contour maps and by 400 gypsum content determinations. The average gypsum content of fans whose streams head in the foothill belt is five times the gypsum content of fans whose streams head in the main Diablo Range (Bull, 1964, table 12). Plate 7 also shows the section-line grid for all section references.

DRAINAGE

The drainage basins in the foothill belt are generally less than 10 miles long. The lengths of the drainage basins that head in the main Diablo Range and cross the foothill belt—Little Panoche, Panoche, and Cantua Creeks—range from 14 miles for Cantua Creek to 22 miles for Panoche Creek. Plate 7 shows how the larger basins extend around the smaller basins to drain the west side of the foothill belt. In general the streams flow toward the northeast at right angles to the trough of the San Joaquin Valley.

The streams are intermittent or ephemeral. Precipitation is too low and drainage basins are too small to support perennial streams. Little Panoche, Panoche, and Cantua Creeks are intermittent streams that receive enough ground water to flow along the entire length of their drainage basins for a few weeks after most winter rainy seasons. The channels of the ephemeral streams are always above the water table and these streams flow briefly and only in direct response to rainfall.

During the summer and autumn, reaches with flow generally alternate with dry stretches on the intermittent streams, and as the streams approach the San Joaquin Valley, they disappear. During winter floods, several hundred cubic feet per second of water may flow in these streams. Flash floods are not common on the larger streams.

The intermittent streams were described in the 1850's by the surveyors who mapped the area for the General

Digitized by Google

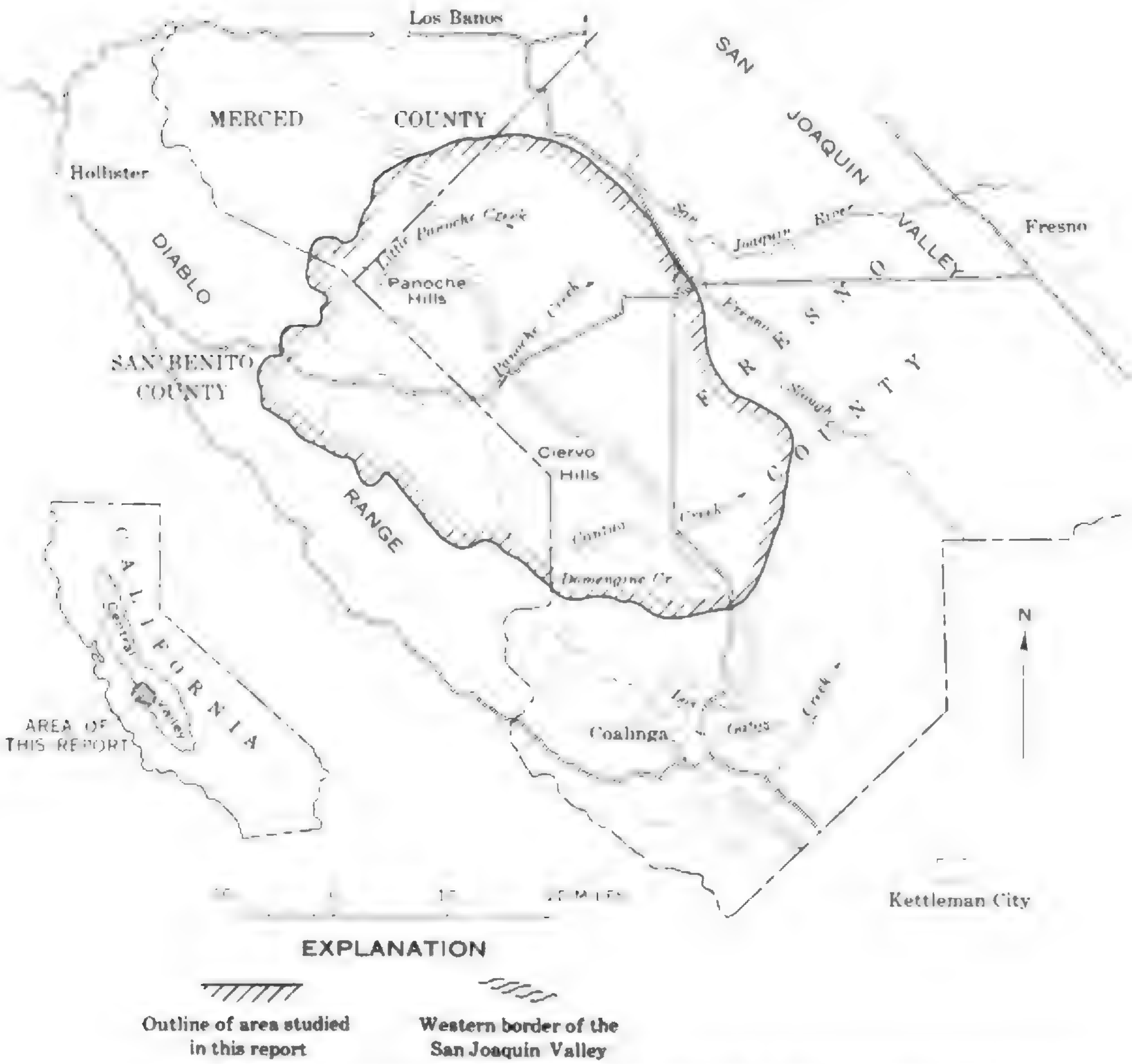

FIGURE 53.—Map of parts of Fresno, Merced, and San Benito Counties, Calif., showing area discussed in this paper.

Land Office. Panoche and Little Panoche Creeks were described in October 1854 by A. McNeill, who noted "* * * the large creek [Panoche Creek] being at this time perfectly dry and never affording any water except in the rainy season." For Little Panoche Creek he remarked that "There is however no timber or water, the creek being dry, and consequently there is little inducement for settlement." J. F. Minturn made the following notes about Cantua Creek in May 1855. "The water in this stream sinks after running about ¾ of a mile into the plains. At the edge of the hills the water runs throughout the year." These descriptions show that the streams were nearly the same 100 years ago as they are today, except that Cantua Creek rarely flows throughout the year now, and Little Panoche Creek has more water than was suggested by McNeill. These descriptions were based partly on conditions at the time of year at which the observations were recorded.

The ephemeral streams have a "flashy type" of flow which ranges from clear water to viscous mud.

CLIMATE AND VEGETATION

Nearly all the precipitation in the area occurs as rain. The average annual rainfall is 15–20 inches for most of the main Diablo Range. The main range creates a rain shadow across the foothill belt and the west side

of the San Joaquin Valley. Consequently, the average annual rainfall is about 8–15 inches in the foothills and 6½–8 inches in the valley; it also decreases slightly from north to south. Most of the rainfall comes during the winter. The winter rains are carried by cyclonic storms that move inland across the Pacific coast. The spring and infrequent summer rains result generally from cyclonic storms but also occur as scattered thunderstorms.

This semiarid region is hot in the summer and mild in the winter. The daily temperature range is often 30°–40°F particularly during the summer. The prevailing winds are from the northwest. The lower slopes of the main Diablo Range are brush covered, but oak, pine, and cedar grow at the higher altitudes. The foothills and alluvial fans support shrubs such as shadscale and short grasses such as downy chess and redstem filaree.

The vegetation on the foothills and in the San Joaquin Valley is sparse, particularly during dry years. A more luxuriant growth mantles the flooded parts of alluvial fans and may continue to grow in a dry year following a wet year, if sufficient moisture is left in the ground to support the dense growth. The dryness and hot temperatures discourage the growth of many plants at the low altitudes during the summer.

GENERAL GEOLOGY

REGIONAL SETTING

The Diablo Range is mainly a broad anticline that has smaller folds trending obliquely to the course of the main range. Joaquin Ridge is one of the smaller anticlines, and Cerro Bonito and the Griswold Hills mark the trend of part of the Ciervo anticline. The Vallecitos is a conspicuous syncline to the southwest of the Ciervo anticline. Monoclinal folds are the dominant structures in much of the foothill area.

The core of the Diablo Range consists of deformed and slightly metamorphosed shale and graywacke of the Franciscan Formation of Jurassic to Late Cretaceous Age and of ultrabasic intrusive rocks. The Franciscan Formation is overlain unconformably by predominantly Cretaceous marine rocks, which dip toward the San Joaquin Valley and form the east flank of the Diablo Range. The Cretaceous marine rocks consist mainly of mudstone, sandstone, and shale which are more than 20,000 feet thick. Easily eroded Tertiary marine and unconsolidated continental sediments are exposed mainly along the foothill belt and in basins such as the Vallecitos.

Some of the basic data on selected drainage basins and alluvial fans are in table 1. The total relief of a drainage basin is the difference in altitude between the highest point of the basin and the point where the stream enters the San Joaquin Valley. The mean slope of a drainage basin is the average slope of all the land within the basin and is computed with data from contour maps. Mean slope partly controls the amount and rate of erosion in a drainage basin. The slope values in table 1 are the tangents of average slopes. The lithology and geomorphology of these drainage basins are described in detail elsewhere (Bull, 1964).

TABLE 1.—*Basic data on drainage basins and alluvial fans of selected streams in western Fresno County, Calif.*

Stream	Code letter on plate 7	Drainage basin total relief (feet)	Percentage of mudstone and shale in drainage basin	Approximate mean drainage-basin slope	Drainage-basin area (square miles)	Alluvial-fan area (square miles)	Overall alluvial-fan slope
Laguna Seca Creek	A	1,270	48	0.20	11.1	11.3	0.015
Wildcat Canyon	B	1,140	42	.16	11.4	8.3	.015
Little Panoche Creek	C	3,150	35	.24	104	53.6	.0070
Moreno Gulch	D	1,830	67	.45	11.7	20.6	.017
Gres Canyon	E	620	57	.33	.18	.36	.029
Marca Canyon	F	1,500	60	.48	1.9	4.6	.025
Chaney Ranch Canyon	G	620	40	.29	.53	.51	.026
Capita Canyon	H	1,760	67	.50	2.6	5.9	.022
Dosados Canyon	I	1,520	63	.41	.93	2.1	.023
Escarpado Canyon	J	1,130	60	.39	.56	1.4	.029
Panoche Creek	K	4,550	32	.27	296	260	.0035
Unnnamed	L	770	86	.37	.49	[1] .20	.022
Tumey Gulch	M	2,590	67	.30	29.1	49.6	.012
Arroyo Ciervo	N	2,740	68	.34	8.0	10.3	.018
Unamed	O	1,600	51	.30	1.7	3.6	.022
Arroyo Hondo	P	2,550	52	.29	25.7	54.6	.0094
Cantua Creek	Q	4,610	32	.35	49.4	75.6	.0047
Salt Creek	R	3,480	41	.39	25.2	28.2	.0074
Martinez Creek	S	3,230	34	.26	8.9	7.1	.013
Domengine Creek	T	3,500	38	.33	11.2	11.4	.011

[1] Small fan area owing to removal of lower part of fan by Panoche Creek.

Digitized by Google

THE COAST RANGE OROGENY

Alluvial fans are characteristic of structurally disturbed regions (Blackwelder, 1931, p. 136–138). The area discussed in this paper has been subject to intermittent uplift that culminated in the Coast Range orogeny. This orogeny and subsequent periods of uplift determined most of the geomorphic and sedimentary characteristics of the alluvial fans in western Fresno County.

The Coast Range orogeny was preceded by several periods of uplift (Taliaferro, 1943, p. 151–158) one of which resulted in the deposition of the Tulare Formation of Pliocene and Pleistocene(?) age. In western Fresno County, parts of the Tulare consist of coarse fluvial sediments that were eroded from the ancestral Diablo Range to the west. The Tulare to the east of the Panoche Hills contains cobbles of glaucophane schist and other Franciscan rock types such as slaty shale and graywacke. The source area for these rock types was the main Diablo Range and part of Glaucophane Ridge. East of the Ciervo Hills the Tulare Formation includes red chert and serpentine detritus, rock types that are common in the main Diablo Range. Some parts of the Tulare appear similar lithologically to the present-day alluvial fans. For example, the Tulare south of the apex of the Panoche Creek fan may be part of the fan of an ancestral Panoche Creek.

> The deposition of these late Pliocene and early Pleistocene(?) beds [the Tulare Formation] was brought to a close by an even more important and widespread diastropic event [the Coast Range orogeny] than that through which they originated (Taliaferro, 1943, p. 148).

Although the age of the Coast Range orogeny is generally considered to be middle or late Pleistocene (Eaton, 1928; Reed and Hollister, 1936; Stille, 1936; Putnam, 1942; Bailey, 1943; Taliaferro, 1943), within the area studied it can be dated only as post Tulare. The Tulare generally is accepted as being of Pliocene and Pleistocene(?) age, and if this is the age of the Tulare in western Fresno County, then the foothill belt and probably the main Diablo Range were elevated during Pleistocene time.

Middle to late Pleistocene fossils have been found in tilted and folded strata in southern California, and some of these beds have been tilted by minor earth movements since the Coast Range orogeny (Bailey, 1943). Movements younger than the Coast Range orogeny also affected the Diablo Range causing changes in the development of alluvial fans as will be shown later.

Flat-lying beds of the Tulare Formation on the highest parts of the Panoche Hills suggest that during Pliocene and early Pleistocene time these beds probably covered the site of the present foothill belt, which has since been uplifted. Subsequent erosion has separated the remnants of the Tulare from their source areas in the Diablo Range.

The streams that now head in the main Diablo Range either maintained their original courses through the rising foothill belt, or took new courses around the areas of maximum uplift. Deposition of alluvial fans then took place east of the foothill belt on the older fan deposits of the Tulare Formation.

The streams that now head in the foothill belt did not exist before the Coast Range orogeny. The orogeny formed the foothills and started the deposition of new alluvial fans that are now several hundred feet thick.

The western part of the San Joaquin Valley was uplifted also. A map of the top of a widespread lacustrine clay, the Corcoran Clay Member of the Tulare Formation, shows that the western edge of the Corcoran was uplifted several hundred feet relative to its eastern edge since the end of the pluvial period associated with the clay (R. E. Miller, written communication, 1962). Alluvial-fan deposition has obscured any topographic expression of this folding in the San Joaquin Valley.

GEOMORPHOLOGY OF THE ALLUVIAL FANS

DEFINITIONS AND GENERAL FEATURES

An alluvial fan is a stream deposit whose surface forms a segment of a cone that radiates downslope from the point where the stream channel emerges from a mountainous area. The deposit may consist of water-laid sediments or mudflow deposits; the alluvial fans in western Fresno County are made up of both. A radiating surface gives a fan the distinctive shape of a segment of a cone. The channel may contain either a perennial, intermittent, or ephemeral stream. In western Fresno County the source areas range from low, rolling hills to steep, rugged mountains.

Stream channels are commonly entrenched into the fanheads, the area close to the apex, and Eckis' (1928, p. 240) term "fanhead trench" gives a good description of this feature. Downslope from the end of the fanhead trench most of the stream channels divide into several braided distributary channels which are about 1–3 feet deep and commonly change position during floods.

A piedmont plain is a broad sloping plain formed by the coalescence of many alluvial fans. The terms "compound alluvial fan" and "bajada" (Tolman, 1909, p. 142; Blackwelder, 1931, p. 136) have the same meaning. Blackwelder noted that "parallel to the mountain front the convexities of the component fans impart to the bajada an undulating surface."

Digitized by Google

FAN SIZE AND SLOPE

Alluvial fans and their drainage basins or source areas act as open systems because changes in drainage-basin conditions cause changes in fan characteristics. The area and slope of a fan are related to the size and lithology of its drainage basin. The fan slope used in computing quantitative relations is the average overall slope from the fan apex to the outer margin where the fan coalesces with another fan or with the river deposits in the trough of the San Joaquin Valley. Radial profiles drawn near the middle of a fan from apex to toe were used to help locate the lower end of the slope to be measured. The boundaries shown on plate 7 were used to determine most of the fan areas.

In general, "* * * large deep canyons have broad fans of low gradient; short ravines have small steeply sloping fans" (Blackwelder, 1931, p. 136). This general relation is true for fans in western Fresno County, as is shown by figure 54.

Statistical-fitting procedures were not used in drawing the lines, but the set of equations for each lithologic group was checked by inserting terms from the equations of figures 54*A* and 54*B* in the equations of figure 54*C*.

Overall fan size is controlled mainly by drainage-basin features, such as size, slope, rainfall, and erodibility of the exposed rocks. The fans studied range in size from 0.4 to 260 square miles. Figure 54*A* shows that all the fans derived from basins underlain mainly by mudstone and shale, and half the fans derived from basins underlain mainly by sandstone, are larger than their basins. The plotted points scatter moderately about straight lines described by the equations shown on the figure. On the logarithmic graph the slopes of the lines (0.88) are equal and show that fan area increases in about the same exponential manner as drainage-basin area increases, despite appreciable differences in lithology. The coefficients of the equations (1.3 and 2.4) show that, on the average, fans derived from drainage basins characterized mainly by mudstone and shale are roughly twice as large as the fans derived from drainage basins of comparable size characterized mainly by sandstone.

The fans studied range in overall slope from 0.0035 (0°12′) to 0.029 (1°40′). Figure 54*B* shows that the overall fan slope decreases with an increase in drainage-basin size. In drainage basins of comparable size, all but the smallest fans of mudstone and shale basins slope more steeply than fans of sandstone basins.

The relation of fan area to fan slope is shown in figure 54*C*. In general, fan slope decreases with increasing fan area. Fans derived from mudstone and shale drainage basins are larger than fans of similar slope that are derived from sandstone basins; and fans (in the size range 1–100 square miles) that are derived from mudstone and shale basins are 35–75 percent steeper than fans of similar area that are derived from sandstone basins.

The apexes of fans of mudstone and shale drainage basins are, on the average, 520 feet above the trough of the San Joaquin Valley, whereas the apexes of fans of sandstone drainage basins have an average height of 400 feet above the valley trough. The relative heights of the fan apexes, and the relations shown by figure 54, show that for drainage areas of comparable size fans derived from mudstone and shale are not only larger, but also are thicker than fans derived from sandstone. Presumably, these differences in fan volume can be attributed largely to the greater erodibility of the mudstone and shale.

In the area studied, downcutting of the stream channels in the mountains has not kept pace with uplift. The effect of uplift on stream gradients is described in the section "Tectonic hypothesis." The relations between fan slope, fan area, and drainage-basin area and lithology may be different in areas where downcutting by streams has exceeded uplift of the mountains, and erosion of part of the fan has occurred.

RADIAL PROFILES OF ALLUVIAL FANS

The radial profiles of an alluvial fan reflect its depositional history, which is controlled partly by erosional and tectonic changes in the drainage basin upstream from the fan. The radii of a fan are restricted by adjacent fans, and by stream deposits at the toe of the fan if the fan is built into a narrow valley.

The overall radial profiles of most alluvial fans are gently concave upward. Most investigators have reported that the slopes of alluvial fans decrease gradually away from the mountain front. Blissenbach (1954, p. 176) said that "from the apex of the fan the surface dips towards the base in which direction the angles of dip gradually become flatter." Trowbridge (1911, p. 714) stated that "The slope of the piedmont plain away from the mountains varies rather uniformly with distance away from the mountains." Krumbein (1937, p. 588–590), in his studies of the San Antonio Canyon fan in southern California, concluded that the slope of the profile decreases at such a constant rate that the slope can be expressed as a negative exponential function.

The slopes of the fans in western Fresno County do not decrease gradually away from the mountain front. All the fans have distinct breaks in slope, which give their radial profiles a segmented appearance. The fan segments generally have a constant slope and appear

Digitized by Google

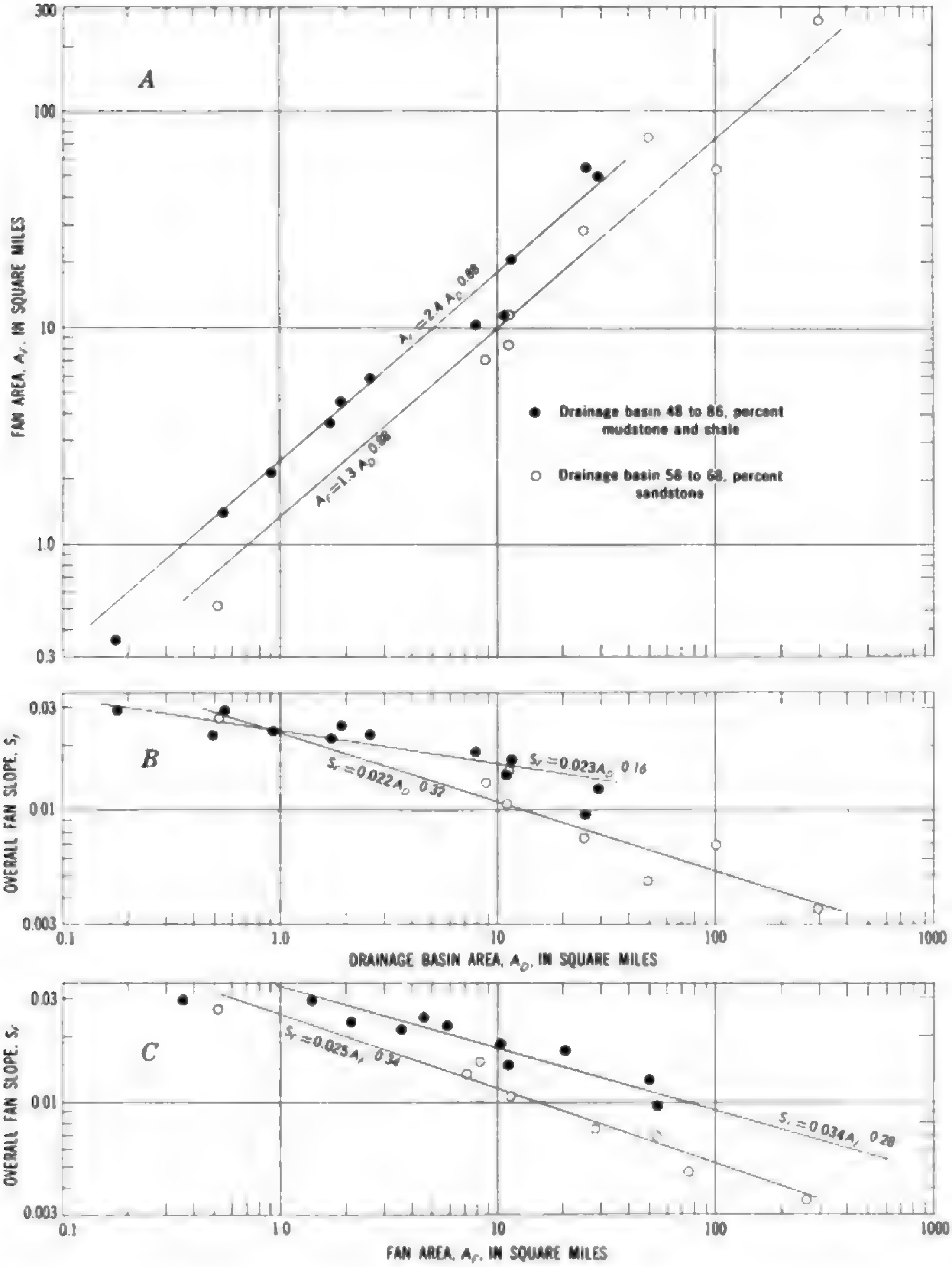

FIGURE 54.—Relations of fan area and slope to drainage-basin area and lithology. *A*, Relation of fan area to drainage basin area. *B*, Relation of fan slope to drainage-basin area. *C*, Relation of fan slope to fan area.

Digitized by Google

as straight lines on a radial profile. The fans of Little Panoche Creek and Cantua Creek, however, each have a segment that is concave in addition to their straight-line segments (fig. 59).

The uniform slopes of straight-line segments of the radial profiles are not merely the result of interpolation between widely spaced survey control points. Maps made 30 years apart by somewhat different techniques, show consistent fan shapes, except in areas that have been affected by intense land subsidence. For example, the fan segmentation of the upper part of the Tumey Gulch fan (figs. 56, 57) was studied by using data from the Monocline Ridge quadrangle which was mapped by planetable methods in 1923 (1:31,680, 5-ft contour interval) and 1955 (1:24,000, 10-ft contour interval). According to authorities at the Pacific Area Office of the Topographic Division of the U.S. Geological Survey (oral communication), some interpolation was necessary for the 1923 map, which was based partly on surveyed profile lines spaced 1,000 feet apart. No interpolation was used on the 1955 map because the individual contour lines were surveyed in this part of the quadrangle. The radial profiles obtained from both maps are the same, and show that the fan segments have constant slopes for several miles.

A survey of topographic maps of other areas in California and in Nevada has also shown that segmented alluvial fans in western Fresno County are by no means unique. Slopes of many other California fans are segmented also as is illustrated in figure 55 which shows some common types of radial profiles. The dots represent altitudes from topographic maps. The profile of the San Antonio Canyon fan was drawn on the same radial line used by Krumbein (1937, fig. 5). Most of the profile of the fan was prepared from a topographic map with a 5-foot contour interval whereas Krumbein used a map with a 50-foot contour interval. The upper and lower segments are straight, but the middle segment is concave as is shown by the chord and the extended lines of the straight segments. The upper seg-

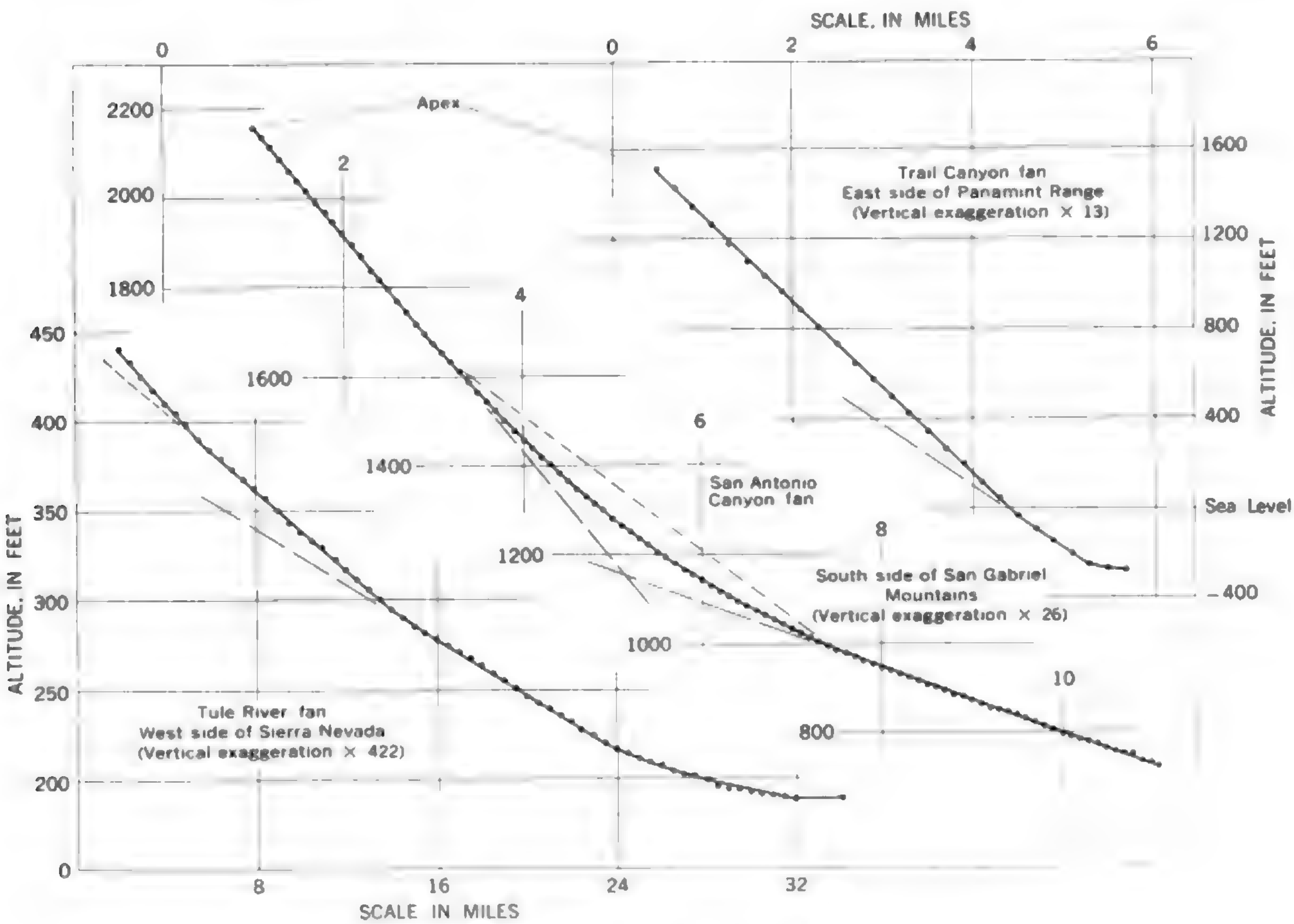

FIGURE 55.—Types of radial profiles of alluvial fans in California.

Digitized by Google

ment of the San Antonio Canyon fan has a gradient that is constant through a decrease in altitude of 500 feet in 2 miles. The base of the fan merges with other alluvial deposits near the Puente Hills. The Trail Canyon fan has a radial profile that is virtually a straight line except for a small straight-line segment of lesser slope near the toe of the fan, which merges with the old lakebed of Death Valley. The radial profile of the Tule River fan consists mainly of straight-line segments also, but the lowest part of the fan, where it merges with the deposits of Tulare Lake, has a concave profile. The angular relation between any two adjacent straight segments is indicated by extending the trace of the lower segment upslope; the curvature of the curving segment is indicated by a chord.

The profiles are subjective to the extent that different people will draw slightly different lines through the same set of control points. The author has tried to keep the profiles simple by not breaking curves into a large number of short straight segments and by averaging gently undulating slopes with straight lines rather than depicting them in detail as a series of convex and concave curves.

Vertical exaggeration is necessary to show clearly the segmented shape of the radial profiles. Steep fans such as the Trail Canyon fan require little exaggeration (13 times), but gentle fans such as the Tule River fan require much exaggeration (422 times).

A detailed study of the Tumey Gulch fan in western Fresno County shows that the angular relations and the length of the segments vary from one side of the fan to the other but that the overall profiles are very similar. Eight radial profiles of this fan are shown in figure 56 and the locations of the profiles are shown in figure 57. Each profile has three straight-line segments, and the angle between the upper and middle segments is larger than the angle between the middle and lower segments.

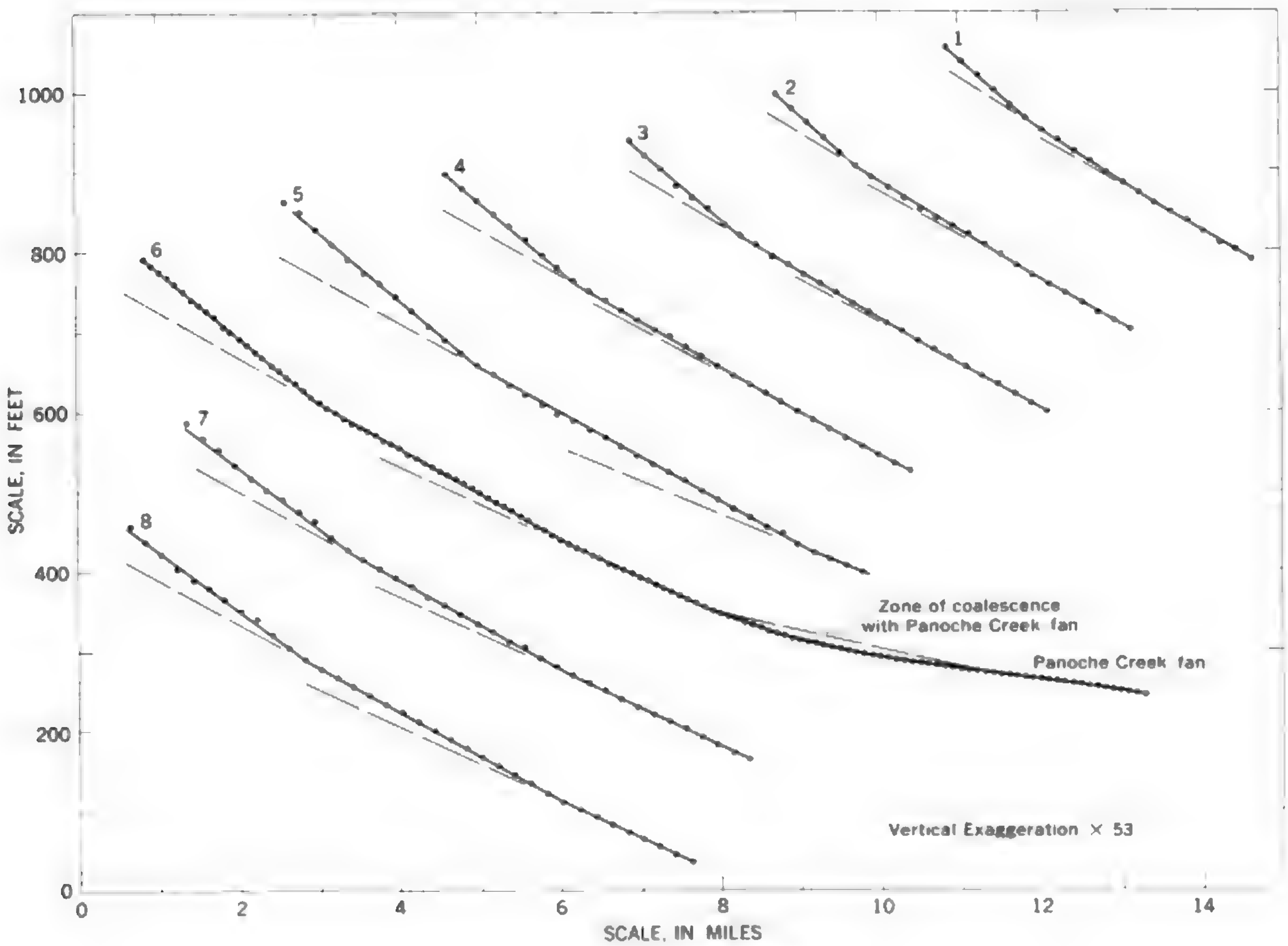

FIGURE 56.—Radial profiles of the Tumey Gulch fan.

Digitized by Google

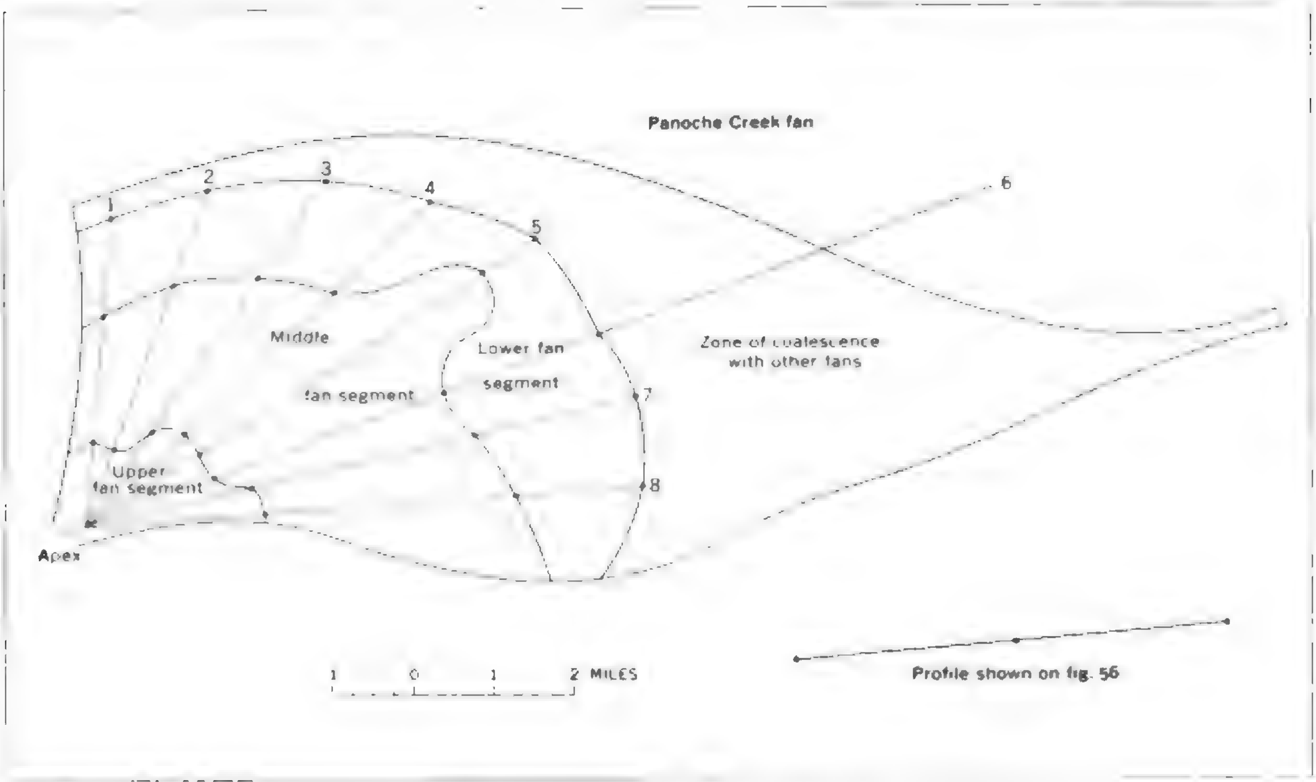

FIGURE 57.—Segments of the Tumey Gulch fan.

Profile 6 has been extended onto the Panoche Creek fan. The zone of coalescence between the Tumey Gulch and Panoche Creek fans for profile 6 is concave, but the profiles of the coalescence zone for half of the radial profiles (not shown in fig. 56) are straight. Most of the radial profiles in this paper show the topographic profile of a specific alluvial fan but not the profiles of zones of coalescence of two alluvial fans.

The radial profiles of figure 56 show two dimensions of the fan segments and the map of the Tumey Gulch fan in figure 57 shows the third dimension of the three fan segments. The general shape of the boundaries between the fan segments is concave toward the apex, and the upper segments have lobate tongues extending downslope.

The boundaries between the fan segments of the Capita Canyon fan (fig. 72) show that the same general features exist for this small fan. The boundaries between the fan segments cross the contour lines at a large angle, and the lobate tongue of the upper fan segment centers about the present-day stream channel.

If the upper fan segment of the Capita Canyon fan continues to spread downslope, the adjacent lower fan segment may be overlapped. Part of the lower fan segment of the Tumey Gulch fan was almost overlapped by the middle segment in the vicinity of profile 5 (figs. 56, 57).

Radial profiles near medial radial lines were drawn for 12 fans whose streams head in the foothill belt, all were found to have three straight-line segments. Radial profiles for six of these fans are shown in figure 58. (See pl. 7 for location.) Only a half or one-third of the control points are shown for most of the profiles. The average slope of the upper segments is 1°14′ (range 0°55′–1°46′); the average slope of the middle segments is 0°48′ (range 0°32′–1°14′); and the average slope of the lower segments is 0°37′ (range 0°22′–0°51′). The average angular difference between the upper and middle segments is 0°26′ (range 0°14′–0°44′); the average angular difference between the middle and lower segments is 0°11′ (range 0°4′–0°24′). The drainage-basin areas of the fans shown in figure 58 range from 2.6 square miles for Capita Canyon to 29 square miles for Tumey Gulch. Lengths of segments vary, but the lower segment of most fans is short.

The radial profile of each fan is distinct, but the fans whose drainage basins are adjacent to each other generally have roughly similar radial profiles. An example shown in figure 58 is the profiles of the Arroyo Ciervo and Arroyo Hondo fans. Other adjacent fans

Digitized by Google

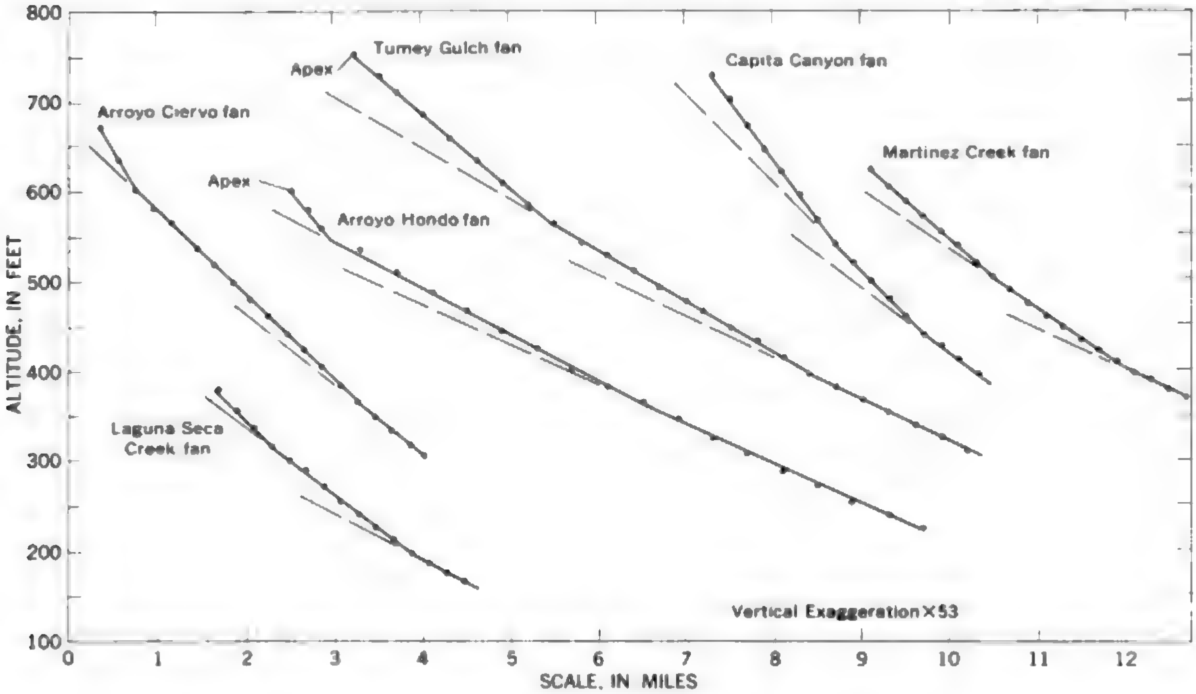

FIGURE 58.—Radial profiles of six fans whose streams head in the foothill belt.

with similar profiles, not shown in the figure, are the Martinez Creek and Domengine Creek fans, and the Capita Canyon fan and the adjacent fans to the north and south of it.

The upper segments of most of the fans are the youngest. Maps made a century ago by the General Land Office show that the stream channels were not entrenched into the upper segments of some fans. Aerial photographs show a fresh pattern of braided distributary channels on the upper fan segments as well as on the middle and lower segments, which indicates that deposition has occurred recently on most upper fan segments. The degree of soil-profile development is about the same on the upper and middle parts of most fans and cannot be used to differentiate the ages of these fan surfaces. Patches of older soils occur on the lower parts of some fans, and locally at the mountain front, where fan deposits have been warped by uplift. Charcoal from 10.5 feet below the surface of the upper fan segment of the Arroyo Hondo fan (pl. 7) gave a radiocarbon age determination of 1,040±200 years before the present time (Rubin and Alexander, 1960, p. 156). The total thickness of deposits of the fan segment at this locality is estimated, by extending the slope of the adjacent fan segment, to be 24 feet. If the rate of deposition for the 24 feet is assumed to be constant, the segment has been growing for only 2,000–3,000 years.

Radial profiles of fans whose streams head in the main part of the Diablo Range have a different number of fan segments. (Compare figs. 58 and 59.) Each of the three fans has four distinct segments. The segments of the Panoche Creek fan are straight, but the uppermost segments of the Cantua Creek and Little Panoche Creek fans are slightly concave.

The Little Panoche Creek fan has two anomalous features. First, it has a steeper slope than the Cantua Creek fan, although its drainage area is twice that of Cantua Creek. Second, unlike other fans, the surface of the uppermost fan segment of the Little Panoche Creek fan is underlain by old soils that indicate that deposition has not occurred on the upper fan segment during Recent time. The history of the Little Panoche Creek fan is discussed in detail on pages 106–109.

The Panoche Creek fan, whose basin drains 296 square miles of the Coast Ranges, is the most gently sloping fan in the area studied. The slope ranges from 0°17′24″ on the uppermost fan segment to 0°8′14″ on the lowest fan segment.

Drainage-basin characteristics such as lithology and mean slope (table 1) do not seem to be related to the segmentation of a radial profile. For example, the Capita Canyon basin (67 percent mudstone, mean slope 0.50) is the source area of a fan whose radial profile (fig. 58) is similar in shape to the radial profiles (fig. 58) of the fans of the Martinez Creek basin (34 per-

Digitized by Google

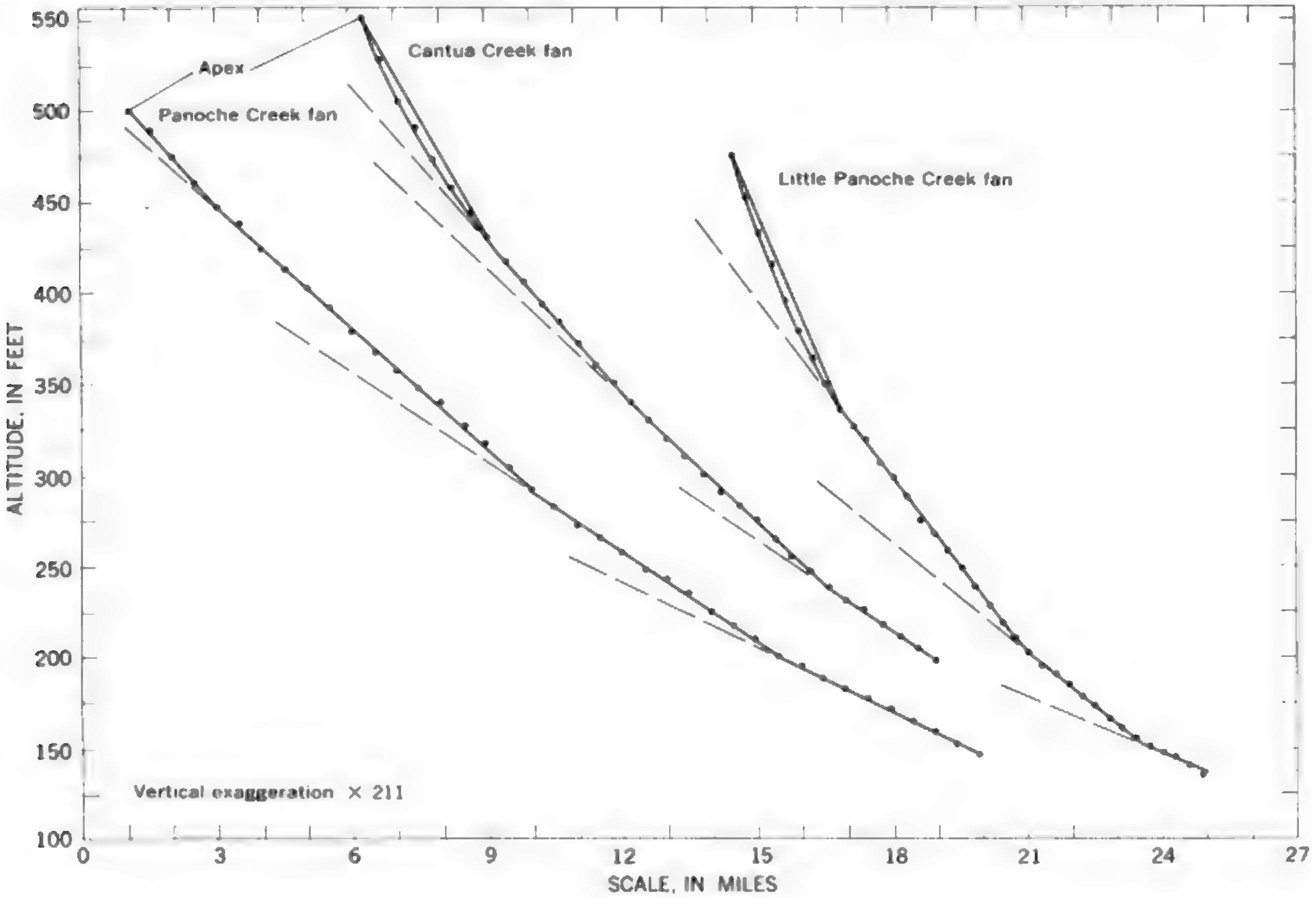

FIGURE 59.—Radial profiles of fans whose streams head in the Diablo Range.

cent mudstone and shale) and the Laguna Seca Creek basin (mean slope 0.20).

No consistent relation between the grain-size distribution of the fan deposits and fan segmentation has been found. Grain-size analyses of 200 surface and subsurface samples show a general decrease in maximum and median grain sizes and an increase in clay content in the downslope direction (Bull, 1964). The grain-size distribution of a particular area of a fan is influenced greatly by the periods of fanhead trenching that allow deposition to start from various points on the upper and middle parts of the fan.

RELATION OF STREAM AND FAN-SEGMENT GRADIENTS

Alluvial fans and their drainage basins are hydrologic units that function as open systems, and climatic or tectonic changes in the drainage basins affect the rate, mode, and locus of deposition on the fans. The gradient of a stream and of its fan tend to attain a steady state or equilibrium, and are sensitive to changes in the drainage basin. This tendency is important in considering the possible causes of fan segmentation.

In the area studied, steep fans form at the mouths of canyons having steep longitudinal profiles, and the gently sloping fans form at the mouths of valleys having gentle longitudinal profiles. This general relation also occurs in the White Mountains of California and Nevada where Kesseli and Beaty (1959, p. 10) have noted that "* * * the steepness of the alluvial fans is in direct relation to the steepness of the mountain canyons providing the debris out of which they are constructed."

In western Fresno County, the slope of the valley floor upstream from the apex of a fan and the upper fan segment are virtually the same. In fact, the upper fan segments and the valleys for a distance of ½–1 mile upstream from the apex have the same general slope. Of 10 valleys, 5 of them have slightly lower gradients above their apexes than their upper fan segments and 5 have slightly higher gradients than the upper fan segments. The average difference in slope is 0°10′ (range in difference, 0°3′–0°17′), which is only half the average difference in slope between the uppermost and the adjoining downslope segments of the same fans.

Digitized by Google

On most fans the slope of the upper fan segment and of the valley upstream from it are similar even where the underlying rock type is not the same (fig. 60). The stream channel of Capita Canyon is in Cretaceous and Tertiary marine rocks and slopes slightly more than the adjacent fan segment. The stream channel of Laguna Seca Creek is in Recent alluvium and slopes slightly less than the adjacent fan segment. These two stream channels were formed after the deposition of the upper fan segments. On the other hand, the terrace deposits of an unnamed stream and Arroyo Ciervo probably were deposited during the same interval as the surficial deposits of their upper fan segments, because the fans and low terraces have the same gradients. Maps made by the General Land Office show that the terrace cutting of both these streams occurred since 1858.

The previously discussed evidence shows that near the apex of most fans, deposits have accumulated that have the same general slope as the valleys upstream from the fans. Erosion predominates in the valleys before the fans have attained the same gradients as the valleys.

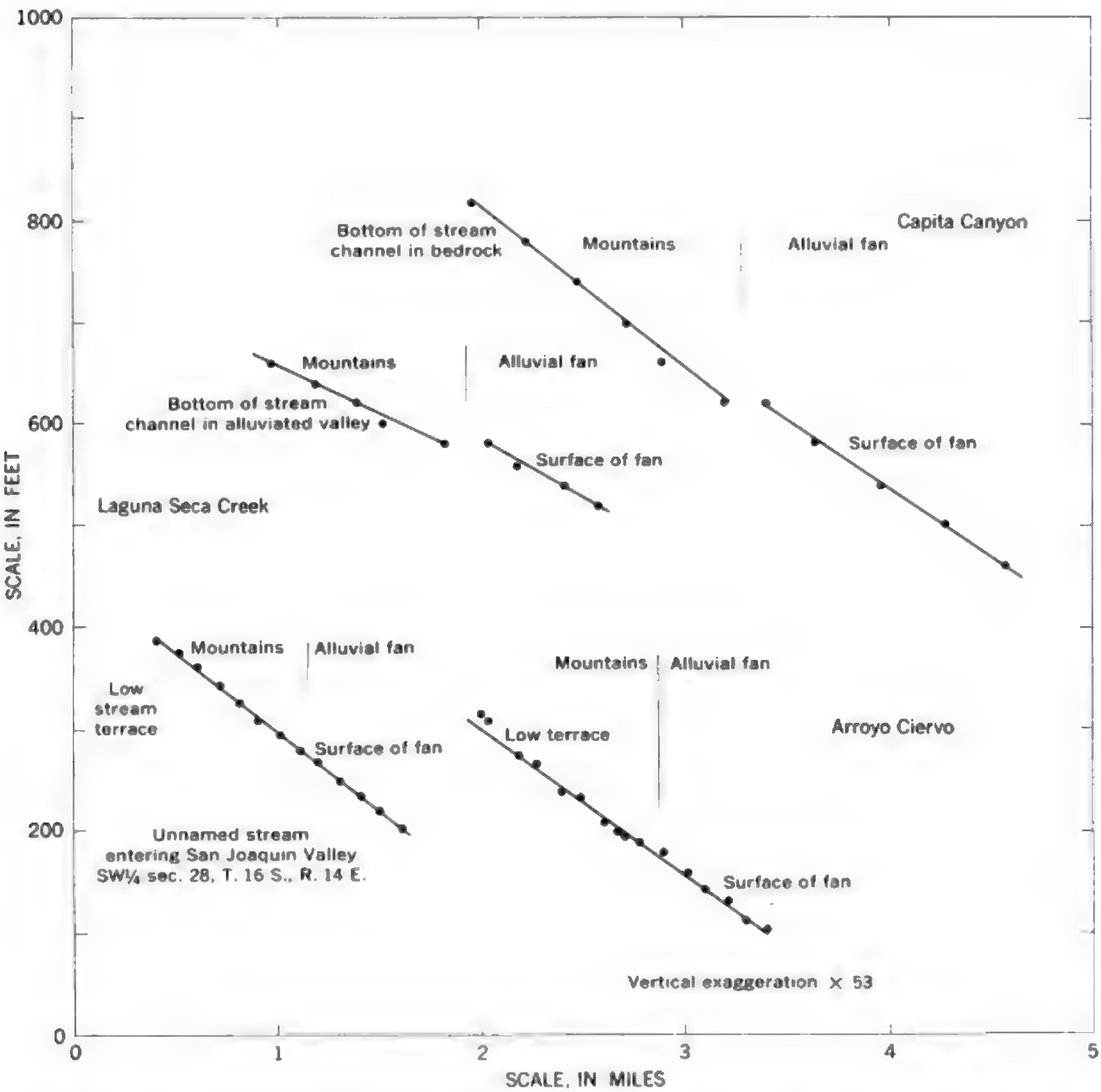

FIGURE 60.—Longitudinal profiles of two streams and two low terraces and the surface of the upper part of their alluvial fans.

Digitized by Google

After the same gradient has been attained, aggradation of the upper fan surface and stream valley maintains this common gradient—examples are the unnamed stream and Arroyo Ciervo of figure 60.

The fanhead trenches also tend to be cut down to the same gradients as adjacent lower fan segments. This adjustment of stream gradients to depositional gradients is illustrated by the gradient relations of some fanhead trenches shown in figure 61, and the same relation probably existed for the streams when the main channel ended at the top of the upper fan segment. Part of the fanhead trenches of the streams shown in figure 61 have been cut down to the same gradient as that of the adjacent lower fan segment. About a mile of the Tumey Gulch and Moreno Gulch fanhead trenches now have the same gradients as their adjacent lower fan segments, and about 5 miles of the Panoche Creek fanhead trench now has the same gradient as its adjacent lower fan segment. Most of this adjustment has occurred in the last century (fig. 77). Streams probably tend to backfill if cut to a gradient less than their adjacent lower fan segment.

The relation of the stream and fan-segment gradients is significant because it shows that the area of deposition and the stream channel upslope from it tend to maintain a uniform and common gradient. Therefore, the fan segments probably are the result of changes in stream-channel gradient that cause deposition on steeper or gentler slopes.

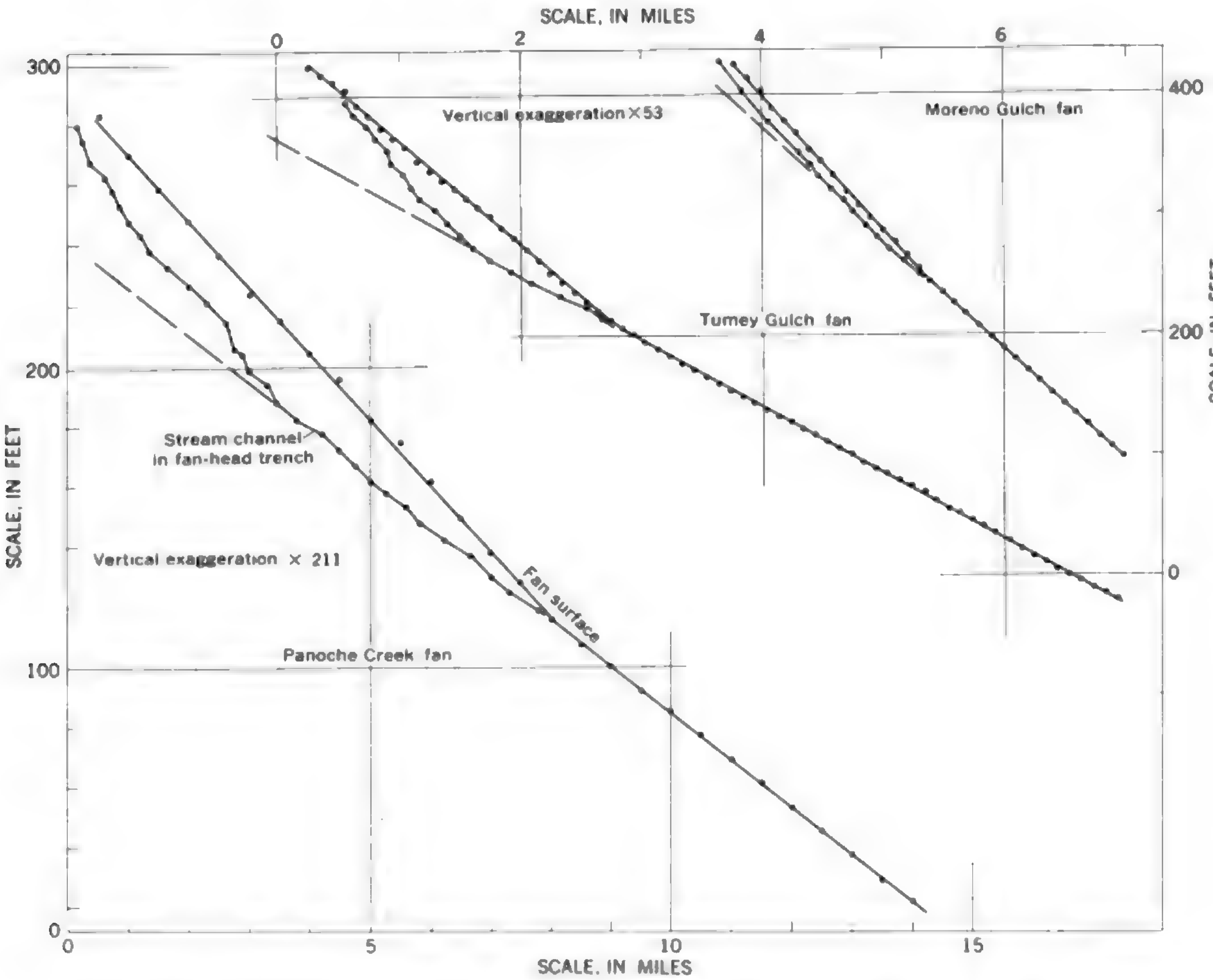

FIGURE 61.—Relation of the gradients of fanhead trenches to the gradients of their adjacent lower fan segments.

Digitized by Google

POSSIBLE CAUSES OF FAN SEGMENTATION

An explanation for the formation of segmented fans is essential to the understanding of their depositional history. Alluvial fans in western Fresno County have three to four segments which appear as straight, or rarely as slightly curving, lines on the radial profiles of the fans. The fan deposits accumulate on surfaces that have about the same gradient as the stream channel upstream from the area of deposition. Therefore, changes in the gradient of the stream channel probably have caused changes in the slope of succeeding fan segments. First, the evidence for changes in the environment of deposition will be presented, and then the possible causes of fan segmentation will be discussed.

The prominent paired, or matched, terraces of western Fresno County (Arnold and Anderson, 1910, p. 155, pl. IV–A; Anderson and Pack, 1915, p. 104–106) reflect changes in the erosional history of the drainage basins. The terraces are classified in this paper as high and low terraces. High terraces generally are more and low terraces generally less than 30 feet above the present-day stream channels. Two high terraces and one low terrace are shown in figure 62*A*. Figure 62*B* shows one pair of terraces about 100 feet above Arroyo Ciervo and a second pair of terraces, less distinct than the first, about 300 feet above the valley floor. The lower pair of terraces and the present valley floor diverge downstream. The area pictured is upstream from a zone of pronounced monoclinal folding. Paired, or matching, terraces, have a two-phase origin: first, the surface is formed by beveling or deposition; and second, the surface is entrenched by accelerated erosion. The several levels of paired terraces along the valleys indicate that the area has been rejuvenated repeatedly.

The terraces show that erosional and depositional rates have varied from time to time in western Fresno County. Changes in erosional conditions probably changed the stream gradients and the slopes of the adjacent fan deposits. The accelerated erosion that causes terracing may be due to either uplift or climatic fluctuations, or both (Bryan, 1923, p. 21–25), or to changes in base level. The entrenchment that caused the formation of many of the low terraces was caused mainly by climatic changes during the last century. (See section on "Causes of the Fanhead Trenching.") The high terraces, on the other hand, reflect tectonic changes. This is discussed on pages 106, 107.

The number of fan segments seems to be related to the number of terraces. For example, the Arroyo Ciervo fan has three segments separated by two changes in fan slope, and the drainage basin has two paired high terraces. Little Panoche Creek has four segments separated by three changes in fan slope, and the drainage basin has three paired terraces. In the following discussion, climatic, base-level, and tectonic changes will be examined as possible causes of the terracing and fan segmentation.

The alluvial fans in western Fresno County are of Quaternary age. Therefore climatic changes that affected the erosional and depositional conditions probably occurred during the formation of the fans. Extensive glaciation occurred in the Sierra Nevada during Pleistocene time, but this part of the Coast Ranges was not glaciated.

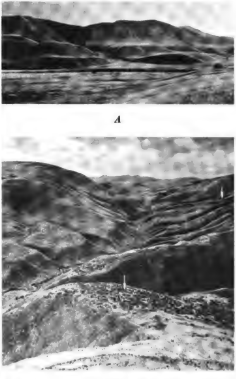

FIGURE 62.—Terraces in the foothill belt of western Fresno County. *A*, Terraces along Cantua Creek. Looking southeast from NE¼SE¼ sec. 35, T. 17 S., R. 14 E. The fence is on a low terrace and two high terraces occur between it and the skyline. *B*, Paired high terraces along Arroyo Ciervo. Looking southwest from NW¼NE¼ sec. 36, T. 16 S., R. 13 E. Arrows mark location of upper terrace.

Digitized by Google

The moisture content of some of the fan deposits, as shown by tests of core samples, provides evidence concerning possible precipitation changes in the area during fan deposition. Irrigation has produced extensive near-surface subsidence on certain fans in western Fresno County; about 125 square miles have subsided or probably would subside if irrigated. This settling of the land surface is caused by the compaction of deposits by the overburden load as the clay bond supporting the voids is weakened by water percolating through the deposits for the first time (Bull, 1964). Prior to irrigation the moisture content of these compactible deposits while in the root zone is below field capacity because plants and air remove much of the soil moisture during the hot, dry summers, reducing the moisture content to the wilting coefficient. Moisture tests (fig. 63) and the presence of near-surface subsidence indicate that these deposits continue to be moisture deficient after burial below the root zone, thus proving that water from succeeding winter rains and floods does not percolate below the root zone. The native moisture contents of these deposits represent moisture conditions that have not changed appreciably since burial below the root zone.

For example, moisture content for two 300-foot core holes in the Arroyo Hondo and Arroyo Ciervo fans are shown in figure 63. Grain-size analyses indicate that there are no major changes in lithology in the 300-foot sections. The moisture content fluctuates with depth partly because of variations in the clay content of the samples. Moisture-equivalent tests of samples from the same core holes indicate that the moisture condition of the upper 120 feet of deposits is roughly 50 percent of field capacity—about at wilting-coefficient conditions. A sharp increase in the moisture content of the Arroyo Ciervo fan deposits at about 130 feet indicates deposition under slightly wetter conditions than at present, but the deposits are still much drier than field-capacity conditions. The deficient moisture condition of these fan deposits indicates that major changes in the amount of precipitation and stream flow have not occurred during the deposition of the upper 100–200 feet of deposits, which span the time of formation of the fan segments.

An explanation of fan segmentation based on climatic change would require thick valley fills upstream from fans on which the upper segment is the youngest. In figure 64, the initial fan profile is shown (for simplicity) as a single straight line. Diagram *A* shows a fan and a stream channel upstream that have developed a common gradient. As the result of a hypothetical climatic change the stream deposits material on its bed and on the fan steepening the gradient of both surfaces (diagram *B*). In order to maintain similar fan and stream gradients, a large amount of valley filling would have to occur in conjunction with the steepened fan surface. Such a process would require more than 100 feet of valley fill less than a mile upstream from the apexes of fans such as those of Arroyo Ciervo and Tumey Gulch. The valley fill along Arroyo Ciervo is less than 20 feet thick and, along other streams that head in the foothill belt, the fill does not appear thick.

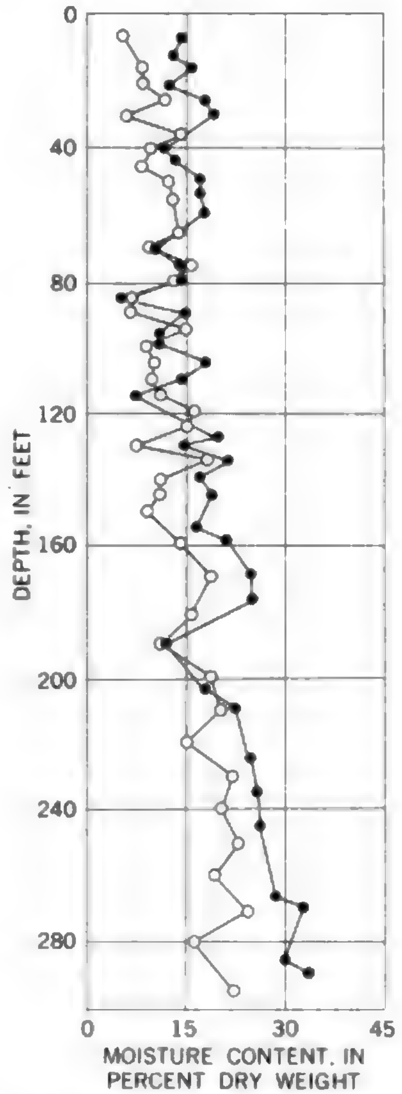

FIGURE 63.—Moisture content for core holes on the unirrigated parts of the Arroyo Hondo (○) and Arroyo Ciervo (●) fans.

Digitized by Google

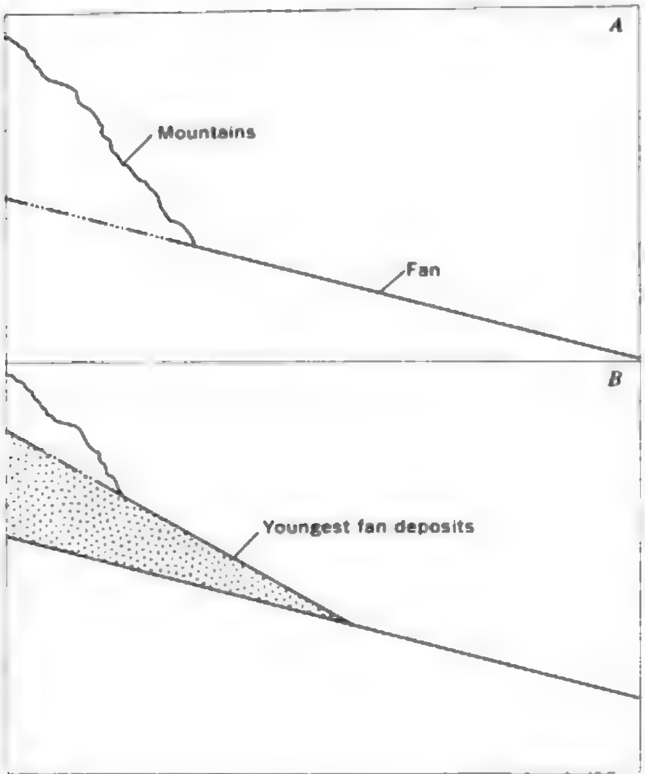

FIGURE 64.—Diagrammatic sketches showing the steepening of stream gradients due to a hypothetical climatic change.

If segmentation is caused by climatic changes, then fans with similar and adjacent drainage basins should have similar shapes. However, this is not true of fans in the area studied. The upper segment of the Tumey Gulch fan is much larger than the upper segment of the Arroyo Hondo fan. The drainage basins of the two fans have a similar size, lithology, mean slope, vegetation, and rainfall distribution. These facts indicate a similar rate of deposition and suggest that the upper segment of the Tumey Gulch fan started to form much sooner than the upper fan segment of the Arroyo Hondo fan. This, in turn, suggests that the causes of the fan segmentation did not necessarily occur over large regions at the same time.

Both regional and local base-level changes should be considered as possible causes of fan segmentation. Pleistocene lowering of sea level probably caused entrenchment of the San Joaquin River. This regional change in base level should have caused entrenchment of the streams into the fans along the west side of the San Joaquin Valley if the streams were perennial at that time. Entrenchment would steepen the stream gradients, but entrenchment also would prevent deposition on the fan. Thus, regional base-level changes apparently did not affect the development of fan segmentation.

Evidences of intermittent local base-level changes are common and are described in the next section.

TECTONIC HYPOTHESIS

The third possibility is that fan segmentation is caused mainly by tectonic changes. Parts of the mountains probably were uplifted more than 2,000 feet during and since the Coast Range orogeny. The abrupt breaks in slope between the fan segments cannot represent tectonic hinge points, however, because the segment boundaries are strongly concave toward the apexes of the fans (figs. 57, 72). This concentric distribution shows that the fan segments are depositional features instead of purely tectonic forms.

The following explanation is in accordance with the facts available from western Fresno County at the present time. In brief, terrace cutting caused by uplift of the mountains formed a steeper stream gradient, and subsequent deposition on the fan built a new fan segment at a new gradient. Repeated periods of uplift produced additional terraces and fan segments.

This explanation applies to two types of fan-segment history in western Fresno County. All the drainage basins have been uplifted, but the location of the area of maximum differential uplift (generally the mountain front) with respect to the fan apex partly determines the locus of successive stages of fan deposition. Most of the fan apexes are immediately downstream from the area of maximum differential uplift, and the stream-channel gradient upstream from the apex has become progressively steeper because downcutting has not kept pace with the uplift. Intermittent uplift associated with progressively steeper stream gradients causes fan segmentation in which the uppermost segment is the youngest, as in figure 65*A*. The second type of fan segmentation occurs where the fan apex is several miles downstream from the area of maximum differential uplift, and the stream-channel gradient upstream from the area of deposition has become progressively gentler, because the downcutting by the stream has exceeded the minor uplift in the reach immediately upstream from the apex. Intermittent uplift, or possibly climatic change, associated with progressively gentler stream gradients, causes fan segmentation in which the lowest segment is the youngest, as in figure 65*B*.

Digitized by Google

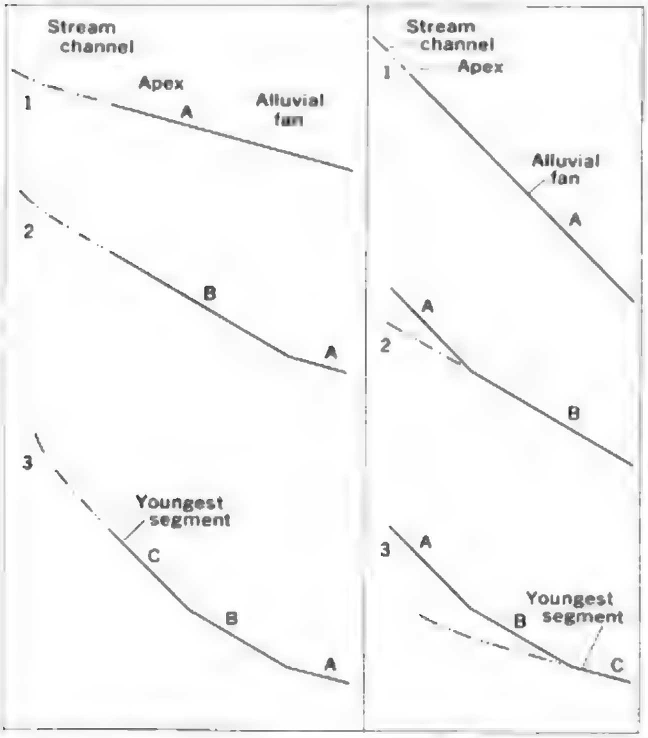

FIGURE 65.—Diagrammatic sketches showing two types of alluvial-fan and stream-gradient history. Fan associated with (*A*) has progressively steeper stream gradients and (*B*) progressively gentler stream gradients. Successive alluvial-fan surfaces A–C are shown in alphabetical order.

FANS ASSOCIATED WITH PROGRESSIVELY GENTLER STREAM GRADIENTS

Little Panoche Creek and Wildcat Canyon have fans whose uppermost segment is the oldest and whose younger segments are associated with progressively gentler stream gradients. For purposes of discussion, the Little Panoche Creek fan includes a small area near the mountain front on which some erosion has occurred. These two fans do not represent the usual occurrence in western Fresno County, because on most fans the upper segment is the youngest and because most of the fans have a history of progressively steeper gradients upstream from their apexes. Little Panoche Creek is the only stream in the area, however, that had broad terraces for which topographic maps of sufficient detail are available to allow accurate plotting of longitudinal terrace profiles. These profiles are shown in figure 66 to illustrate the relations between tectonic environment and stages of alluvial-fan deposition. A direct relation between terraces and fan segments can be shown for this type of fan.

Three prominent paired terraces occur near the mouth of Little Panoche Creek. All three are underlain by a 2- to 20-foot veneer of sand and gravel that was deposited on truncated deformed Tulare sediments. The upper terrace is dissected and much of the soil that formed in the surficial deposits has been removed by erosion. Two to four feet of caliche-cemented gravel, representing the Cca horizon (U.S. Dept. Agriculture, 1960) of a well-developed soil, commonly is found at or near the surface. The middle terrace is not extensively dissected and a moderately well developed soil has formed on the surficial deposits. The soil profile consists of 2 feet of red clayey sand and gravel that is underlain by weakly cemented calcareous material. The lower terrace is not dissected, and visible soil-profile development has not occurred. Examination of fossils[1] collected by the author from a ledge several feet beneath the Tulare dip slope (fig. 66) suggests that this part of the Tulare Formation is of Pleistocene Age. The distribution and stage of development of the terrace soils suggest that the upper and middle terraces are of late Pleistocene age and that the lower terrace is of Recent age.

Part of the tectonic history of the Little Panoche Creek drainage basin is revealed by the various surfaces shown in figure 66. Deposition of the Tulare Formation ceased in this area when the Coast Range orogeny uplifted this part of the Panoche Hills. The dip slope of the upper, or possibly the uppermost, Tulare shows a pronounced decrease in gradient near the mountain front, where gently folded Tulare beds can be seen in roadcuts.

Little Panoche Creek cut a wide valley through the hills. A period of uplift caused the stream to cut down leaving parts of the former valley floor as the upper terrace. The upper part of the fan was upwarped slightly causing it to be abandoned by Little Panoche Creek. The profile of the upper terrace (fig. 66) shows that minor anticlinal folds were superimposed on the warped surface near the mountain front where the differential uplift was greatest. Little Panoche Creek continued to cut down and then laterally during a period of little or no tectonic activity. A second period of uplift during which a narrow band of monoclinal folding occurred along the mountain front caused another stream rejuvenation, which resulted in the formation of the middle terrace. The relations of the folded and unfolded parts of the terraces indicate a differential uplift at the mountain front of 20–30 feet during each of these periods of folding.

A period of regional uplift, or possibly a climatic change, then caused the formation of the lower terrace whose smooth profile indicates that differential uplift at the mountain front did not occur. The lower terrace

[1] Examination made by D. W. Taylor. U.S. Geol. Survey Cenozoic fossil loc. 22692.

Digitized by Google

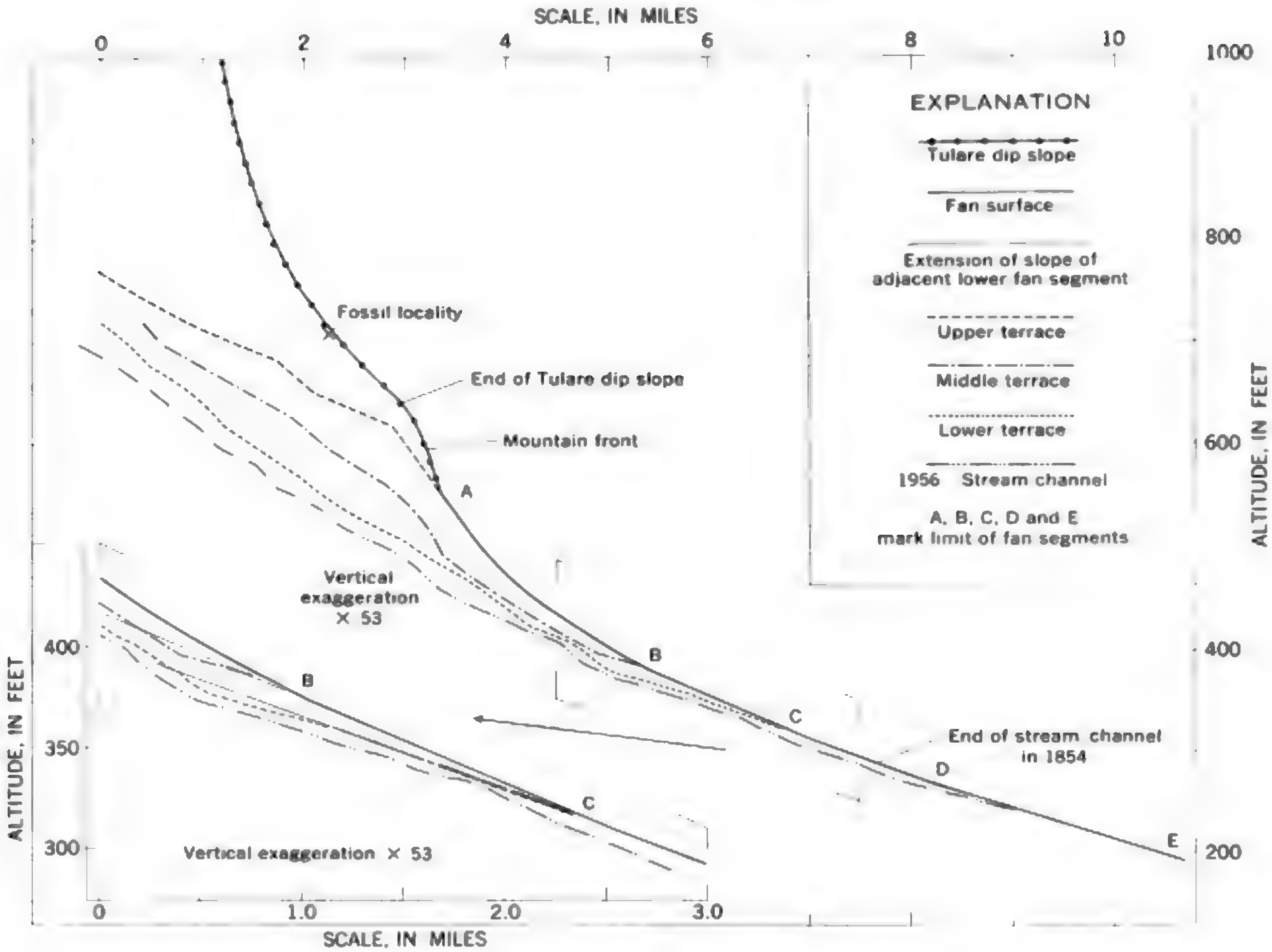

FIGURE 66.—Relation of stream terraces to fan segments for Little Panoche Creek.

converges with the stream channel downstream. Most of the convergence may be due to channel trenching caused by fluctuations in rainfall during the past century.

The longitudinal profiles in figure 66 show both divergent and convergent patterns in the downstream direction. The upper and lower terraces diverge downstream 50 feet in the first 3 miles. The divergence indicates steepening of the stream gradient by headward erosion, as the mountain front was uplifted intermittently by anticlinal and monoclinal folding.

Terrace divergence occurs upstream from the zone of maximum differential uplift, and terrace convergence occurs downstream from the zone of maximum differential uplift. Most of the terrace convergence occurs within 2 miles of the folded zone at the mountain front.

The uplifts accelerated the deepening of the stream channel, but the channel downstream from the mountain front was not uplifted appreciably. The net effect in this reach was trenching of the stream channel and extension of the end of the channel farther out on the fan. Each time this happened the area of deposition and the stream channel upstream from it developed a more gentle gradient than previously.

The slopes of the terraces are continuous with the slopes of the fan segments. The slope of the upper terrace continues onto segment A–B (fig. 66). The old mouth of Little Panoche Creek has been preserved because of an overall lateral migration to the south of this part of Little Panoche Creek. The middle terrace ends at the upslope end of fan segment B–C, and the lower terrace ends at the upslope end of the fan segment C–D. The gradient of the lower part of each terrace approximates the gradient of the adjacent lower fan segment. (See insert, fig. 66.) The soil-profile development on the fan segments and the terrace

Digitized by Google

profiles both confirm that the segment nearest the mountains was formed first and that the two adjacent lower segments are younger.

The present-day stream channel ends on the upper part of the lowest fan segment (D–E), and maps made by the General Land Office show that the end of the channel in 1854 was just upslope from the upper end of this lowest segment. Thus most deposition is occurring on the lowest segment on the south side of the fan, but the stream channel is shallow and narrow enough to permit major floods to flow over the banks and deposit material on parts of the three lower segments.

Fan-segment boundaries, soil types, and selected contour lines reveal part of the history of the Little Panoche Creek fan (fig. 67). The positions of the concentric contour lines indicate that the present fan apex is 2–3 miles downslope from the mountain front (see pl. 7 for complete outline of fan) and that the old alluvial slope upstream from the apex was mainly an erosional surface. The soils data indicate a general decrease in grain size in the downslope direction. The fan-segment boundaries and the distribution of the younger alluvium (particularly the conspicuous lobes of sandy deposits) both show that most of the deposition of the younger alluvium has occurred on the north and east sides of the fan and that little deposition has occurred in the central part of the fan, where older soils and clayey younger soils predominate. The fan-segment boundaries and the areal distribution of the older and younger alluvium also indicate that the overall amount of deposition of the younger alluvium was small compared to the other fans in western Fresno County. The small amount of deposition may be due partly to the fact that the Little Panoche Creek drainage basin is the only source area studied that is underlain by a large amount of resistant Franciscan rocks.

The information shown in figures 66 and 67 can be used to reconstruct the history of the Little Panoche Creek fan. A fan-shaped alluvial slope was formed after the initial deformation of the Tulare Formation. The upper part of the slope was a small narrow erosional area, and the lower part of the slope was a large broad depositional area. The slope of the valley floor represented by the upper terrace was continuous with the upper part of the alluvial slope. Remnants of the alluvial slope are represented in figure 67 by the areas of older alluvium. The uppermost (A–B) and lowest (D–E) segments (fig. 66) were formed at this time. The uplift that caused the cutting of the upper terrace warped the uppermost segment (A–B) and determined the location of the present fan apex. The uplift also caused accelerated erosion that ultimately decreased the stream gradients in the reach upstream from the area of deposition. The fan segment B–C was deposited. Erosion that accompanied the cutting of the middle terrace caused another decrease in stream gradient in the reach upstream from the area of deposition, and the fan segment C–D was deposited at a lower gradient than that of the fan segment B–C. The segment C–D occurs on both sides of the fan which means that the stream changed position on the fan and cut through the segment B–C. Change in the position of the entrenched stream is plausible because the present-day stream channel is shallow and narrow enough at the apex to allow floods to top its banks, as it did during a flood in September, 1958, and to form natural levees such as those indicated by the 350-foot contour line of figure 67. During the deposition of the fan segments B–C and C–D, slight amounts of deposition partly covered the older alluvium on the fan segment D–E. Areas of older alluvium, however, are not exposed on the downslope part of the east side of the fan, which has been the area of principal deposition for more than a century. A new fan segment whose slope is gentler than the segment C–D and whose slope is partly controlled by the gradient of the present stream, probably is forming on this part of the fan.

The segment B–C probably had a larger areal extent formerly. Before deposition of the segment C–D, B–C would have intersected the surface of the old alluvial slope (D–E) at a point between C and D. Subsequent deposition of the fan segment C–D made an area of active deposition that probably encroached both upslope and downslope from the area where the former slopes intersected. The D fan-segment boundary line has a lobate shape that indicates downslope expansion of the fan segment. The C fan-segment boundary line, however, does not have a shape that suggests progressive overlapping by the adjacent lower fan segment.

The Little Panoche Creek fan is representative of fans whose segmentation is associated with progressively gentler stream gradients during their history. Although intermittent uplift steepened the stream gradient upstream from the mountain front, the fan apex was 2–3 miles downslope from the mountain front, and the successive areas of deposition were downstream from reaches of progressively gentler stream gradients. Each new stage of fan deposition was farther downslope and on a more gentle gradient than the previous stage.

Digitized by Google

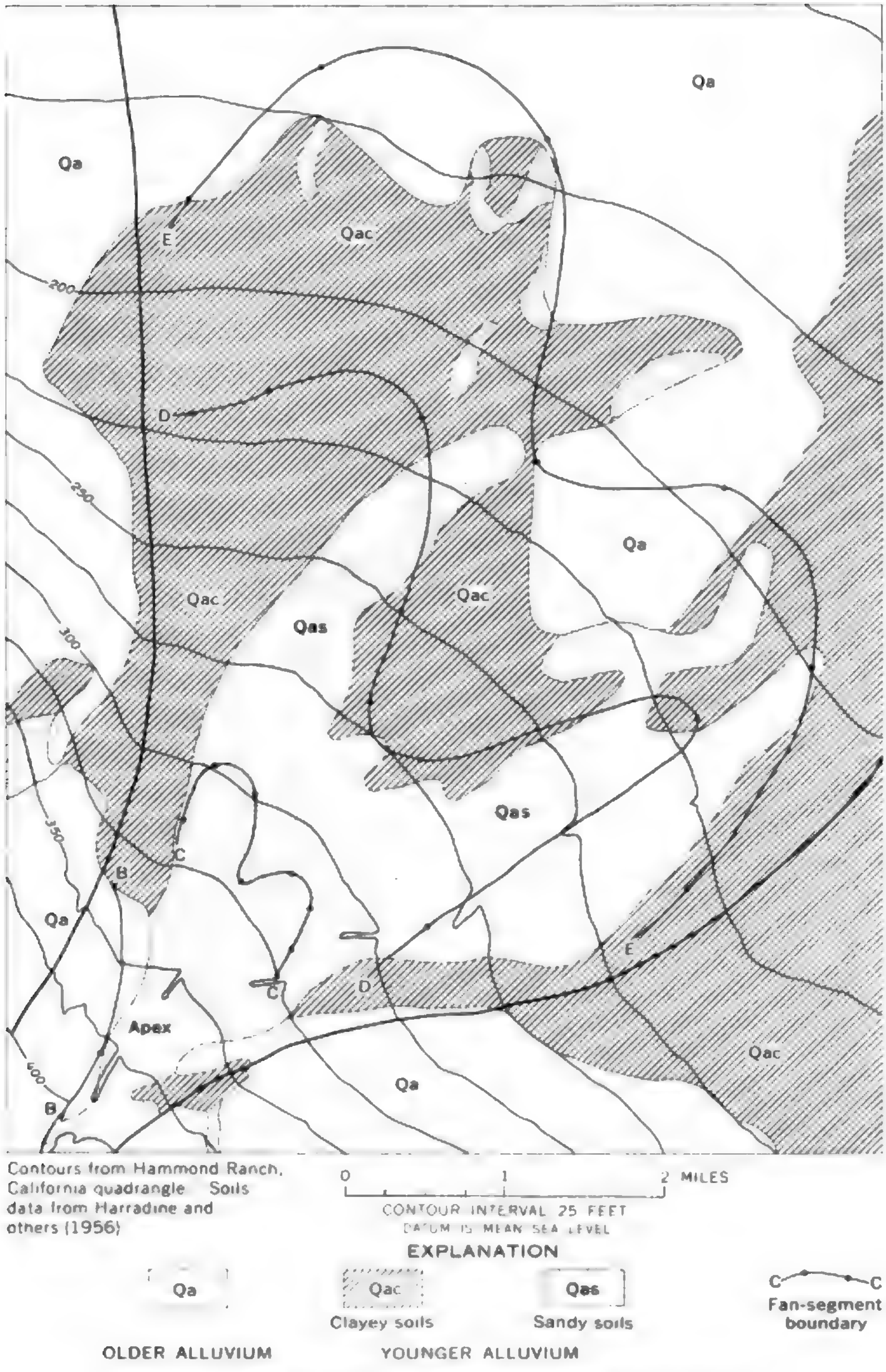

FIGURE 67.—Soils and fan-segment boundaries of the Little Panoche Creek fan.

Digitized by Google

FANS ASSOCIATED WITH PROGRESSIVELY STEEPER STREAM GRADIENTS

Most of the fans studied show a sequence of fan-segment development that is reversed from the Little Panoche Creek fan—their uppermost segments are the youngest and their lowest segments are the oldest. The youngest terrace (or stream channel of a century ago) has a slope that is continuous with the upper fan segment (fig. 60). Before the current period of fan-head trenching, the areas of most active deposition were just downstream from the mountain front. The tectonic history of most of the drainage basins is similar to that of the Little Panoche Creek basin, except that the upper parts of the fans have not been warped appreciably. The gradients of the streams above the apexes have become progressively steeper, as is shown by the downstream terrace-gradient divergence upstream from the mountain front in figure 66. In contrast, the apex of the Little Panoche Creek fan is 2–3 miles downslope from the mountain front, and the reach upstream from the area of deposition has been intermittently decreased in gradient.

Figure 68 shows diagrammatically four successive stages in the development of a single fan segment, for a fan whose upper segment is the youngest. In profile A the fan and stream channel for a short distance upstream from the apex have developed a common gradient. This equilibrium then is destroyed by rapid monoclinal folding along the mountain front, which raises the valley bottom about 40 feet, steepening the stream gradient (profile A′). The deformation induces trenching headward from the mountain front (profile B) leaving parts of the uplifted stream channel as paired terraces. The terraces probably were continuous with prior fan surfaces which have since been buried by the deposits of younger fan segments. A substantial increase in the rates of erosion and deposition results in the rapid accumulation of sediments on the fan, particularly on its upper part, where the emergent stream enters a reach characterized by a reduction in gradient. In profile C, erosion has deepened the valley and deposition raised the fan surface until a common gradient has again been attained. The fan surface now has two segments which appear as straight lines on the radial profile. Deposition continues on the fan, and the valley upstream from the apex is aggraded in order to maintain a common gradient (profile D). The upper fan segment is extended farther onto the fan, and the change in slope moves from Y to Z. Most of the deposition has occurred on the upper fan segment, but enough deposition occurs on the rest of the fan to prevent the formation of well developed soil profiles.

The above discussion postulates that a fan segment that appears as a straight line on a radial profile may be the result of rapid uplift of the drainage basin followed by a time of little or no uplift, during which the stream channel and fan attain a common slope. A fan segment that appears concave may represent the case in which a fan surface has not had sufficient time to develop a constant slope after a period of rapid uplift. (See profile B, fig. 68). A concave surface also could be the result of a period of gradual continuing uplift. During a period of continuous uplift the stream gradient would gradually steepen and the depositional slope of the fan also would become progressively steeper.

The segmented fans of western Fresno County indicate at least three or four episodes of uplift of the different parts of the Diablo Range rather than continuous uplift of the entire range. The profiles differ a little from fan to fan, indicating differences in the times and amounts of uplift and rates of erosion in their respective structural areas and drainage basins. Part of the uplift probably occurred in the last 3,000 years, as is indicated by the Arroyo Hondo radiocarbon date.

Alluvial fans whose drainage basins are in a different tectonic setting than that of western Fresno County are those along the southern border of the San Joaquin Valley, about 100 miles to the southeast of the area studied. Figure 69 shows the strikingly similar radial profiles of two large alluvial fans whose drainage basins head in the San Emigdio Mountains. These two profiles are markedly different from the radial profiles of western Fresno County fans because they have pronounced concave middle segments. The geologic environment of the two areas is similar in many respects. Both have similar climate and drainage-basin characteristics.[2] The Santiago Creek drainage basin has a total relief of 5,080 feet, and the rocks exposed in the drainage basin consist of 90 percent sedimentary rocks and 10 percent metamorphic and plutonic rocks. The San Emigdio Creek basin has a total relief of 7,330 feet, and the rocks exposed in the drainage basin consist of 40 percent sedimentary rocks and 60 percent metamorphic and plutonic rocks. Terraces that diverge downstream are common upstream from the mountain front (McGill, 1951, pl. 2).

The major difference between the San Emigdio Mountains and the Diablo Range is in their structural history and tectonic setting. The Diablo Range has been formed by anticlinal and monoclinal folding, and by minor faulting. The main part of the San Emigdio

[2] Drainage basin information for the fans heading in the San Emigdio Mountains from J. M. Parsons, Calif. Dept. Water Resources (oral communication, July 1961).

Digitized by Google

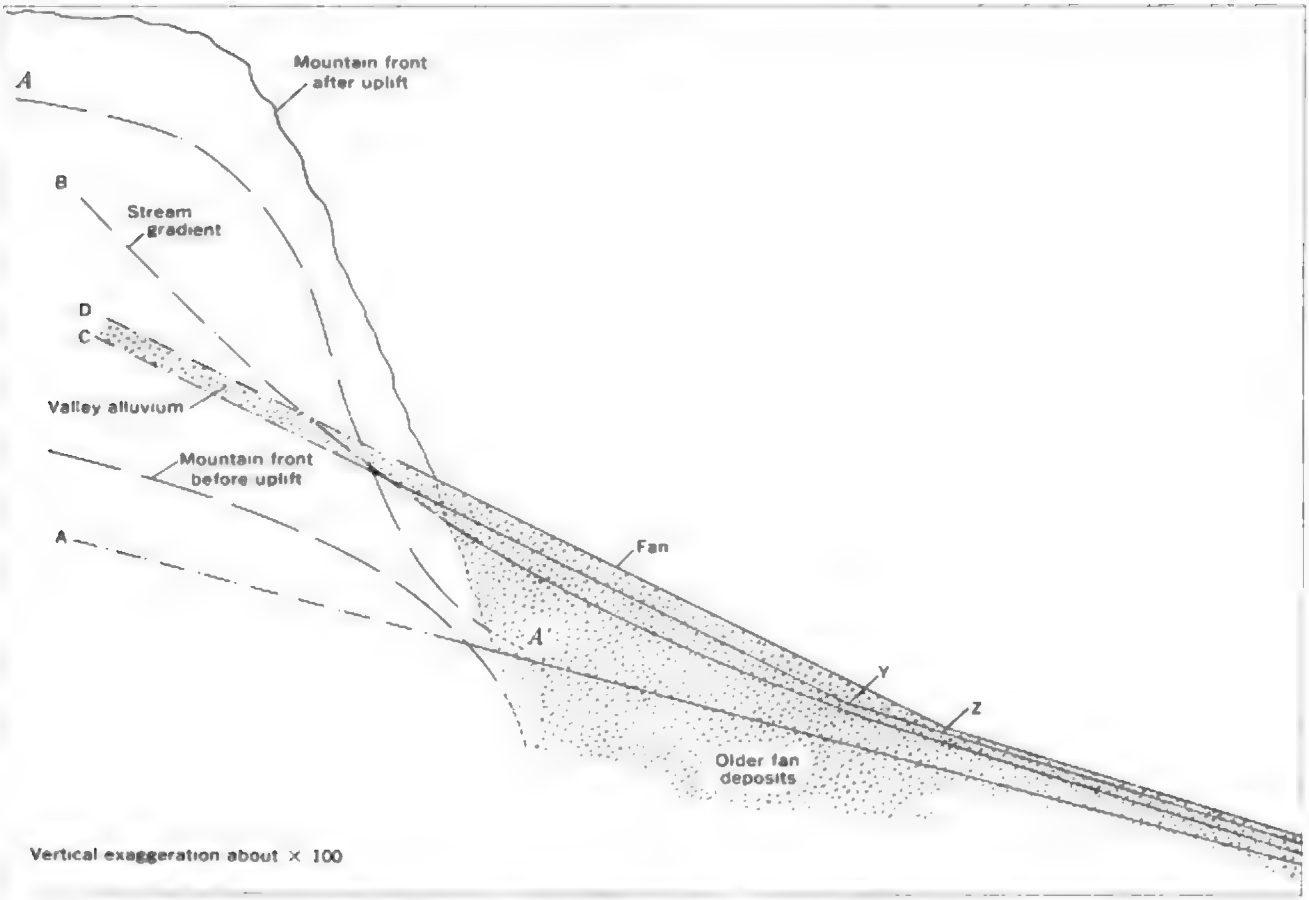

FIGURE 68.—Diagrammatic sketch showing stages of fan-segment development.

Mountains is characterized by thrust faulting and tight asymmetric folds that lean toward the San Joaquin Valley. The marked difference in radial profiles of the two fans on the northern side of the San Emigdio Mountains as compared to those for fans in western Fresno County is ascribed by the author to the different tectonic history of the two source areas.

Large changes in slope between fan segments presumably indicate greater uplift and steepening of the valley upstream from the apex than do small changes in fan slope. Uplift in western Fresno County has been mainly as monoclinal and anticlinal folding. The valley slopes could not have been made much steeper than the fan slopes if there had been a similar fault-block tilting of the mountains and fans; such fans there would have little or no segmentation. An example is the Trail Canyon fan (fig. 55) on the east side of the Panamint Range. Eastward tilting of this part of the Panamint Range and Death Valley has been described by Greene and Hunt (1960). On the west side of the Panamint Range, by contrast, some of the valley slopes have been steepened more than the fan slopes, and the segmentation of these fans is more pronounced.

Some stages of alluvial-fan development for fans whose upper segment is the youngest are summarized in figure 70. A stream channel and fan have developed a common gradient as shown in diagram 1, figure 70. Uplift steepens the stream gradient and the new fan deposits are laid down with a steeper gradient. The stream channel gradient may have been steeper after the uplift, but the slopes in diagram 2 represent equilibrium conditions near the end of the stage. Another period of uplift makes the third segment, completing a three-segment fan. Deposition continues on the fan and the stream channel upstream from the fan apex maintains the same slope as the fan by aggrading slightly (diagram 4). A temporary period of channel trenching occurs (diagram 5) and the low terrace and upper fan segment have a common slope. The downstream end of the fanhead trench has the same gradient as the adjacent lower fan segment. Valley alluviation and stream entrenchment (diagrams 4 and 5) may occur several times during the development of a fan as is

Digitized by Google

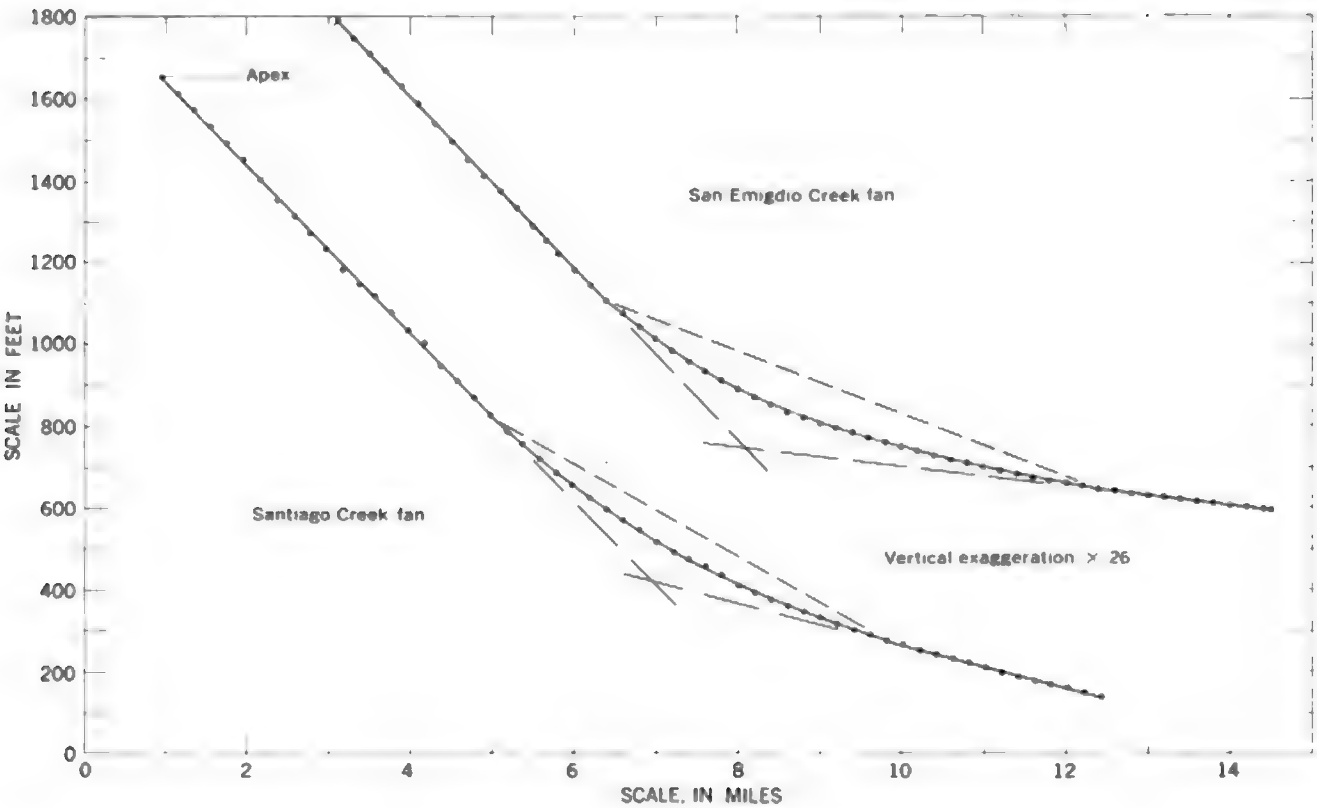

FIGURE 69.—Radial profiles of the San Emigdio Creek and Santiago Creek fans.

shown by old terrace and channel patterns on aerial photographs. Deposition probably was occurring mainly on the upper segment a century ago, but channel trenching then caused deposition to occur mainly on the middle segment as the end of the channel moved downslope (diagram 5). Present-day deposition is restricted to the area downslope from the first or second fan segment of most fans.

When an area becomes tectonically stable, permanent trenching of the fans occurs as the mountains are eroded and the streams cut below the fan apexes. Erosion gradually removes the deposits that are higher than the main channels, and the fans become alluviated slopes that are characterized by large areas of erosion as well as areas of deposition. Such slopes are common in the Basin and Range Province of California and Nevada.

Fan segmentation should be helpful in deciphering part of the tectonic and erosional history of the drainage basins of other mountain ranges. Fans are formed adjacent to a mountain front after uplift, and renewed uplift that causes progressive steepening of the stream gradients will keep the principal loci of deposition close to the mountain front. Segmentation on such fans can be attributed chiefly to tectonic causes and the youngest fan segment will be adjacent to the mountain front. If renewed uplift does not occur the stream will cut downward establishing progressively gentler gradients, and the locus of principal deposition will be progressively farther downslope from the fan apex. If it is not segmented the fan may have a smooth concave profile. Fan segmentation associated with progressively gentler stream gradients is common, however, and can be attributed to climatic as well as tectonic causes. In western Fresno County this type of fan history (Little Panoche Creek fan) can be shown to have been caused chiefly by uplift of the mountains several miles upstream from the present fan apex. However, many segmented fans in the Basin and Range Province of California and Nevada also have surficial deposits that are older near the mountains and younger near the base of the fan. Climatic changes during fan deposition should be considered as a possible dominant cause of the progressive decrease in stream gradient and associated segmentation of many of the basin and range fans.

Digitized by Google

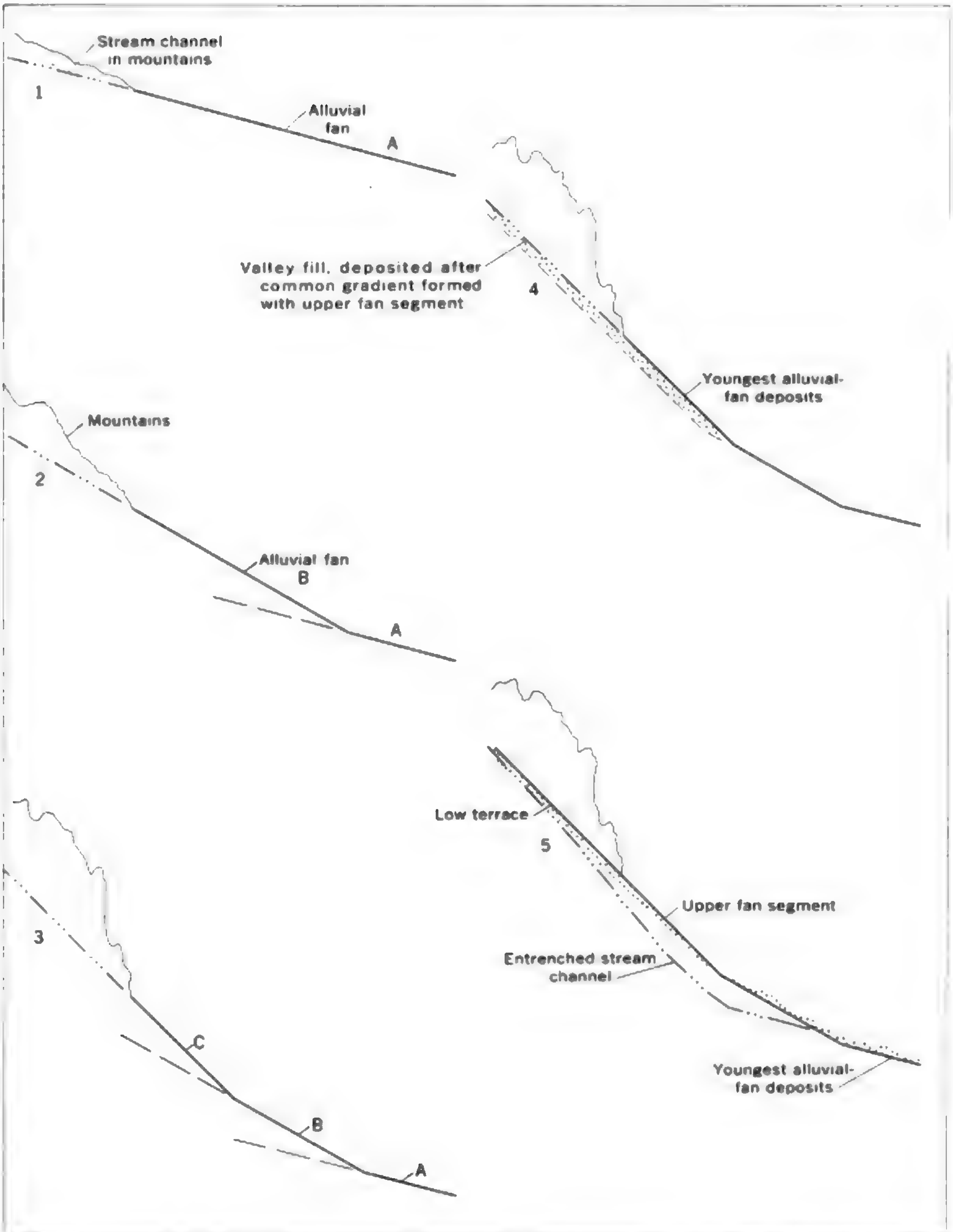

FIGURE 70.—Diagrammatic sketches showing stages of alluvial-fan development. Successive alluvial-fan surfaces A–C are shown in alphabetical order.

CROSS-FAN PROFILES

Cross-fan profiles parallel to the mountain front show the convexities of the alluvial fans (figs. 73, 74). The amount of convexity depends on where the profile is drawn and on the coalescing of adjacent fans. The convex shape of a series of cross-fan profiles shows that an alluvial fan is part of a gently sloping cone. The central part of the fan generally is higher than the sides because of greater deposition on the central part.

Stream channels control the place of deposition, and the present-day channel deviation from the medial position on the fanheads of 75 fans is shown in figure 71. The distribution of channel deviation is fairly uniform from the medial position to a deviation of about 50°, but two-thirds of the channels are within 30° of the medial position. Only three channels have a deviation of more than 50°. Thirty-nine streams have an average deviation toward the northwest of 26°, and 35 streams have an average deviation toward the southeast of 23° The predominance of stream channels within 30° of the medial position implies that more deposition occurs there than in areas farther from the medial position which are not frequented as often by streams.

CHANGE IN SHAPE DOWNSLOPE

The progressive downslope decrease in the convexity of cross-fan profiles is well illustrated in the area. The fans of Capita, Chaney Ranch, and Marca Canyons are described as examples (figs. 72 and 73). The respective drainage areas for these fans are 2.6, 0.53, and 1.9 square miles. The fan of Chaney Ranch Canyon is small and coalesces with the other fans within 2 miles of the mountain front.

The Capita Canyon fan excellently displays features characteristic of many fans whose streams head in the foothill belt. The convexity of the upper part of the fan (downslope to profile *D–D'*) stands out clearly, as shown by the conspicuous curvature of the contour lines. The downslope decrease in convexity is well shown by the progressive straightening of the contour lines toward the base of the fan. The depth of the fanhead trench decreases markedly downslope from the upper fan segment and the stream channel becomes a distributary channel that is about 2 feet deep.

The six cross-fan profile lines *A–A'* through *G–G'* are spaced at half-mile intervals except for the quarter-mile spacing between *A–A'* and *B–B'* (figs. 72 and 73). The profiles across the lower parts of the fans are flat compared to the profiles across the upper parts of the fans. The decrease in the convexity of the cross-fan profiles progressively farther from the mountain front occurs much as would be expected in a series of profiles drawn progressively farther from the apex of part of a true cone.

STREAM CHANNELS

Leopold and Wolman (1957) described three characteristic channel patterns of rivers: braided, meandering and straight. A braided channel is characterized by the repeated division of the channel around islands of alluvium; a meandering stream has a series of regular looplike bends; a straight channel has little or no curvature.

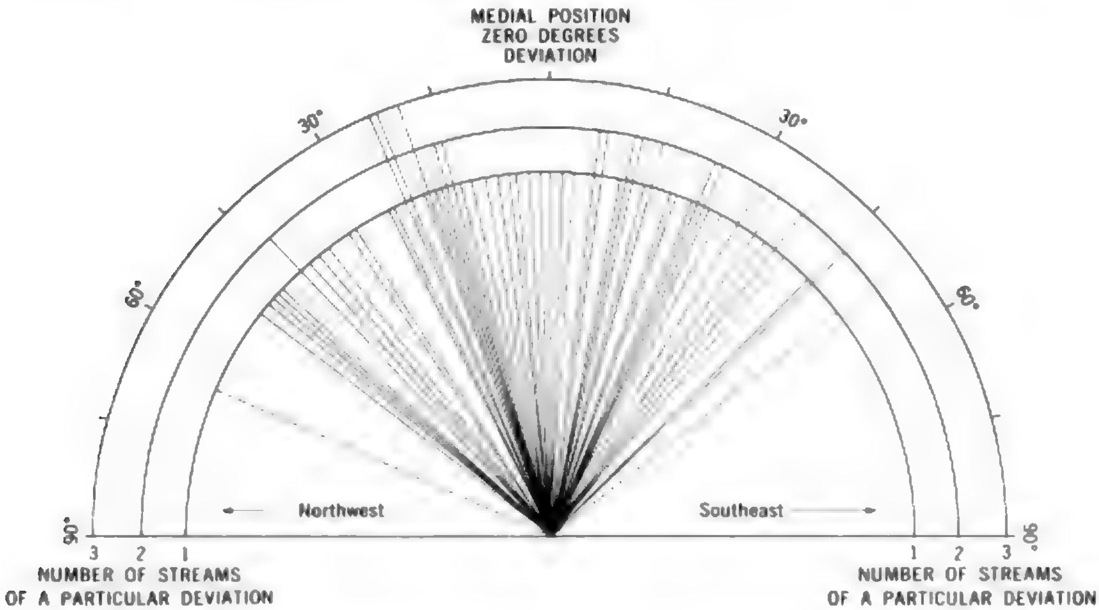

FIGURE 71.—Channel deviation from medial position on fanheads of alluvial fans in parts of Fresno and Merced Counties

Digitized by Google

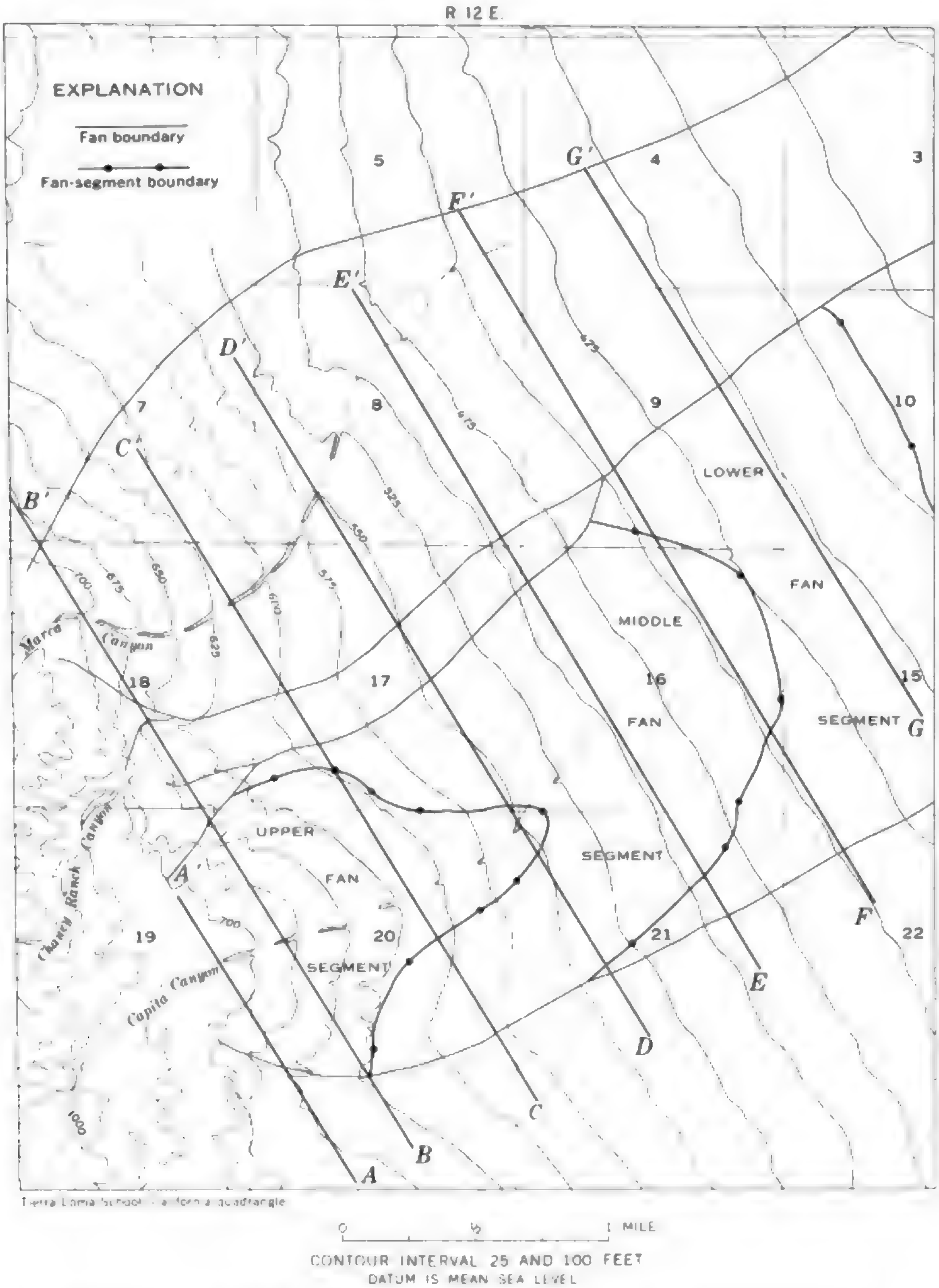

FIGURE 72.—Topographic map of the alluvial fans of Capita Canyon, Chaney Ranch Canyon, and Marca Canyon. Profiles A–A' to F–F' are shown in figure 73.

Digitized by Google

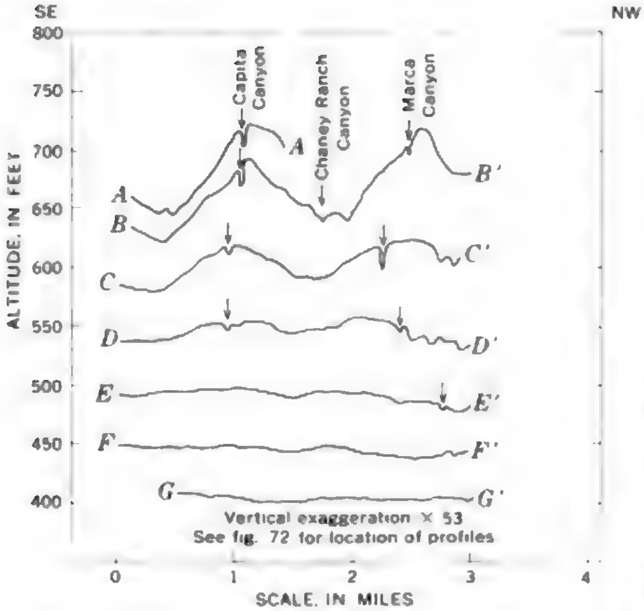

FIGURE 73.—Cross-fan profiles of Capita Canyon, Chaney Ranch Canyon, and Marca Canyon fans. Vertical exaggeration × 53. See figure 72 for location of profiles.

All three of these channel patterns are common on the fans in western Fresno County. The most common channel pattern of the fanhead trenches is the meandering type, as illustrated by Panoche Creek. (See fig. 79.) Panoche Creek also has some relatively straight sections of channel, and straight channels are common on the alluvial fans of ephemeral streams. (See Capita Canyon, fig. 72). In the straight sections, the thalweg, or the deepest part of the channel, generally weaves back and forth between the channel banks. This also occurs on straight stretches of perennial streams (Leopold and Wolman, 1957, p. 53–55). The braided channel pattern is characteristic of the distributary channels downslope from the end of the fanhead trenches but is not present in the fanhead trenches themselves.

A cross-fan profile drawn about parallel to the east edge of the Panoche Hills, and less than a mile from the hills, is show in figure 74. The stream channels are commonly on the highest parts of the fans, but they may be on any other part of a fan, as shown by the arrows in figure 74. Streams, such as the one occupying Gres Canyon, deposit so little material that they remain at the bottom of the trough formed by two adjacent large fans. The fans have a variety of cross-sectional shapes, many of which reflect the influence of the size and shape of adjacent fans. The profile between mileage markers 1–4 on the line of the section is representative of an area where several fans have coalesced.

The main channels of some of the streams do not flow at right angles to the contours of the fan. The stream channels of Marca Canyon (fig. 72, secs. 17, 18) and part of the channel of Arroyo Hondo are examples of these streams. Arroyo Hondo apparently is migrating sideways toward the downslope side of the channel; at the present time the downslope bank is 7–12 feet high in contrast to the 2- to 4-foot bank on the upslope side from which the channel has moved. These anomalous positions of stream channels may have been started by the entrenchment of a minor channel. Once such an entrenchment is started, natural levees tend to be concentrated on the lower side of the channel. The entrenchment of the channel and the formation of natural levees temporarily prevent the stream from breaking out of its channel and flowing directly down the slope. Natural levees of this type are shown by the contour lines along parts of the stream of the Marca Canyon fan (fig. 72, secs. 8, 17).

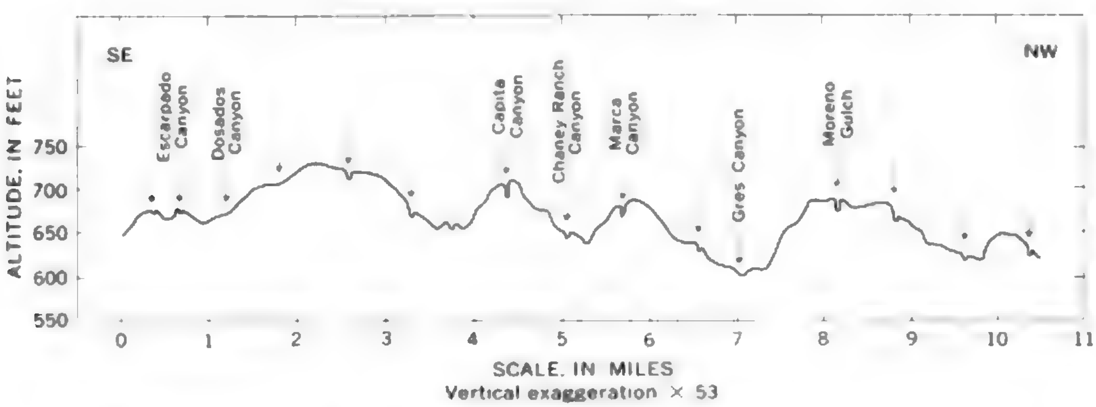

FIGURE 74.—Position of stream channels on the fanheads of the piedmont plain east of the Panoche Hills.

Digitized by Google

Natural levees are a common feature on most fans in the area. Many natural levees were formed before the recent entrenchment of the streams, and natural levees are being made along the shallow reaches of the channels at the present time. Figure 75 shows mudflow deposits on the natural levees of Arroyo Hondo. The channel was shallow enough for the mudflow to flow over the banks and spread out to add another increment to the natural levees. Bushes helped to keep the deposition within 100 feet of the channel in most places. Natural levees along the intermittent streams are made of water-laid sediments that probably were deposited as the velocity of flow decreased after the stream left the main channel. Natural levees about 3–5 feet high are shown in figure 79 along the downslope part of Panoche Creek in the NW¼ sec. 10 and the NE¼ sec. 20, T. 14 S., R. 13 E.

FANHEAD TRENCHES

The stream channel of almost every fan in the area is entrenched into the upper part of the fan. The fanhead trenches of the ephemeral streams are narrow and the fanhead trenches of the intermittent streams are wide. The sides of these incised channels in many places are nearly vertical walls. The depth of the fanhead trenches decreases away from the mountains, and eventually the channel splits into several distributary channels.

Fanhead trenches are a natural feature of alluvial fans, and traces of abandoned trenches can be found on several fans. The present cycle of arroyo cutting already had started on some fans when the first land survey was made in the early 1850's. Later surveys and the accounts of some of the first settlers show that channel trenching started on other fans in the period between 1875 and 1885. This date is about the same as the time of the channel trenching in parts of Arizona, Utah, Colorado, and New Mexico (Bryan, 1925). Cattlemen and sheepherders who have lived 30–40 years in the area agree that much of the deepening of these channels has occurred since about 1935, although the channels on most of the fans had their present areal extent by 1930.

Many of the fanhead trenches are terraced. Tumey Gulch has scattered remnants of paired terraces 7–20 feet above the present channel, and Arroyo Hondo has 3- to 5-foot terraces, which are paired in some places. Paired terraces are excellently preserved in the fanhead trench of Arroyo Ciervo, where a narrow slot about 8–15 feet wide has been cut 5–9 feet deep into the bottom of the first-stage fanhead trench to form the terrace. The channels of the large intermittent streams are flanked by broad terraces 3–10 feet above present stream grade. Most fanhead terraces have been formed since about 1935.

The fanhead trench of Tumey Gulch a mile from the edge of the foothills is shown in figure 76. At this point the channel is 37 feet below the surface of the fan. The bushes along one side of the channel indicate the location of a narrow terrace remnant. The original land surveys show that Tumey Gulch had the same extent and position in 1854 as it does today, but in 1854 the channel was shallow enough for the surveyors to walk across as they chained the section lines.

FIGURE 75.—Mudflow deposits on the natural levees of Arroyo Hondo. Arrow marks outer edge of mudflow. View northwest from the SW¼SE¼ sec. 2, T. 17 S., R. 14 E.

FIGURE 76.—The fanhead trench of Tumey Gulch looking upstream from SW¼SW¼ sec. 29, T. 15 S., R. 13 E.

Digitized by Google

The changes in the depth of Tumey Gulch between 1921 and 1955, based on data from topographic maps, are shown in figure 77. The fanhead trench terminates at the downslope end of the upper fan segment. The shallow channel shown in the middle fan segment is one of several distributary channels. In 1921 the fanhead trench was as much as 20 feet deep. By 1955 the upslope part of the trench was partly filled, but in places the trench was deeper than 30 feet and the deepest part was moving upstream. More than a mile of the downslope end of the 1955 trench is a continuation of the slope of the middle fan segment. Similar fanhead-trench and fan-gradient relations exist for other fans (fig. 61).

Figure 78 shows the changes in the depth of the fanhead trench of Arroyo Ciervo between 1921 and 1956. The 1858 maps do not show a gully, but the 1880 mapping reveals that a gully extended to the downslope end of the upper fan segment. Topographic maps show the 1921 channel to be 4–6 feet deep and the 1955 channel to be as much as 26 feet deep. Most of the channel deepening between 1921 and 1956 occurred within the upper fan segment and, like the channeling in Tumey Gulch, the deepening increases upstream. The channel entrenched in the Arroyo Ciervo fan differs from that in the Tumey Gulch fan because it extends downslope past the upper segment.

Unlike the channel widths of ephemeral streams, which apparently have not changed much since first reported, the channel widths of the intermittent streams have increased from about 20 to several hundred feet during the past 100 years. The pairs of numbers in figure 79 show changes in the width of Panoche Creek between 1854 and 1959. Many sections of the channel are from two to six times wider than they were in 1854. The lines of measurement along which the width was measured generally are not perpendicular to the stream channel because the surveyors in 1854 noted the channel widths between section corners; therefore the 1959 measurements also were made along section lines.

The length and depth of the channel of Panoche Creek also have changed since 1854. The fanhead trench was 5 miles long in 1854 and 10 miles long in 1959, and the channel has been deepened by erosion in some places as much as 25 feet.

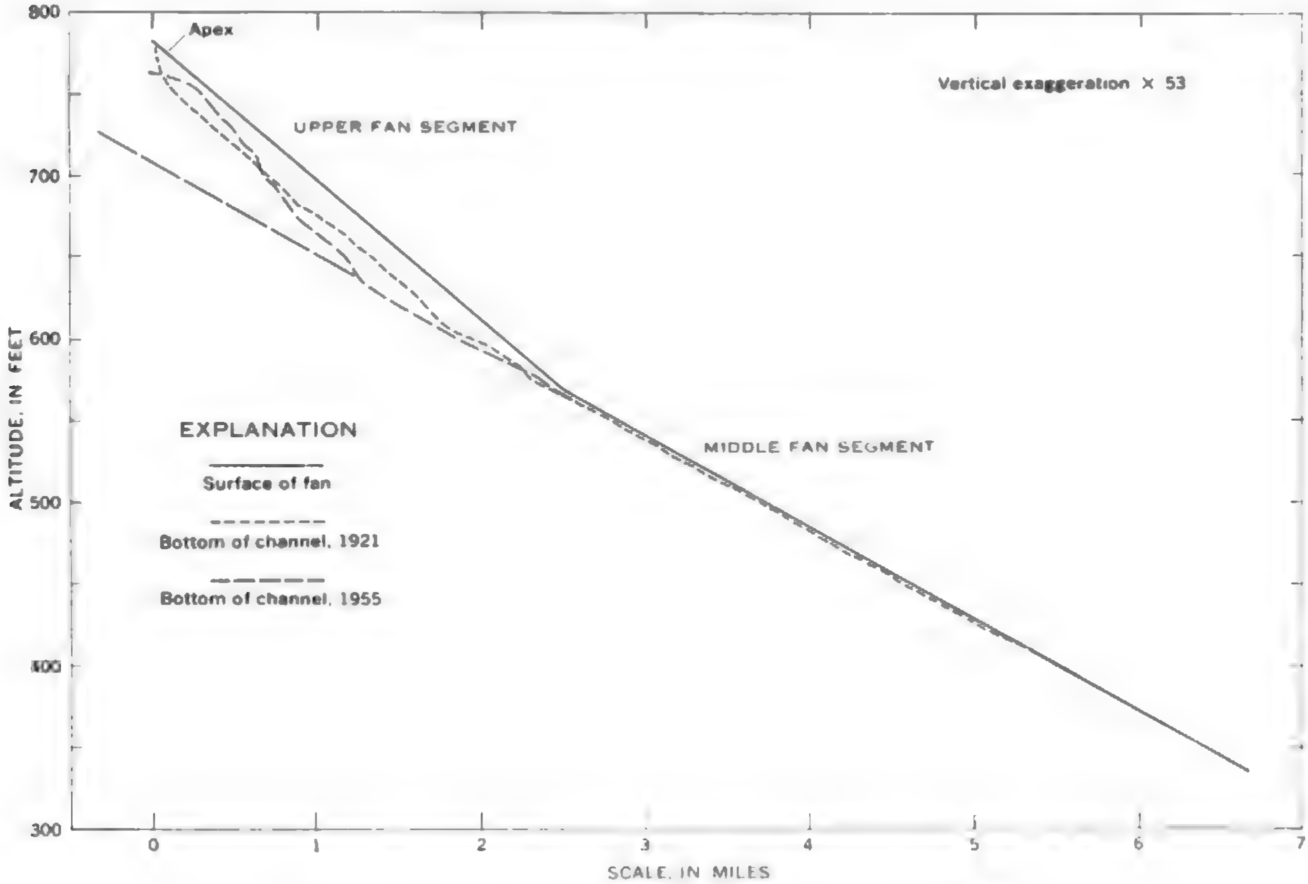

FIGURE 77.—Changes in the depth of the Tumey Gulch fanhead trench, 1921–55

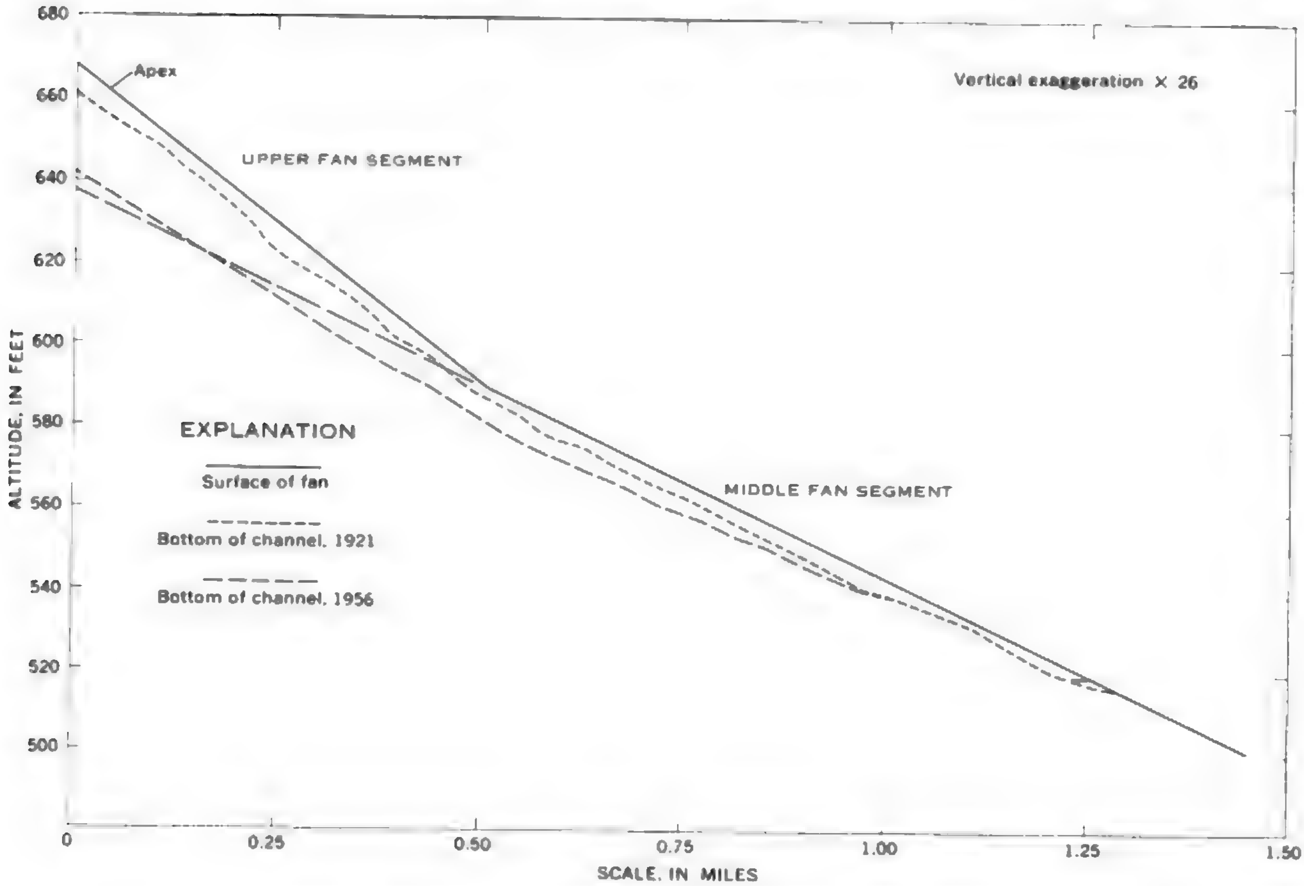

FIGURE 78.—Changes in the depth of the Arroyo Ciervo fanhead trench, 1921–56.

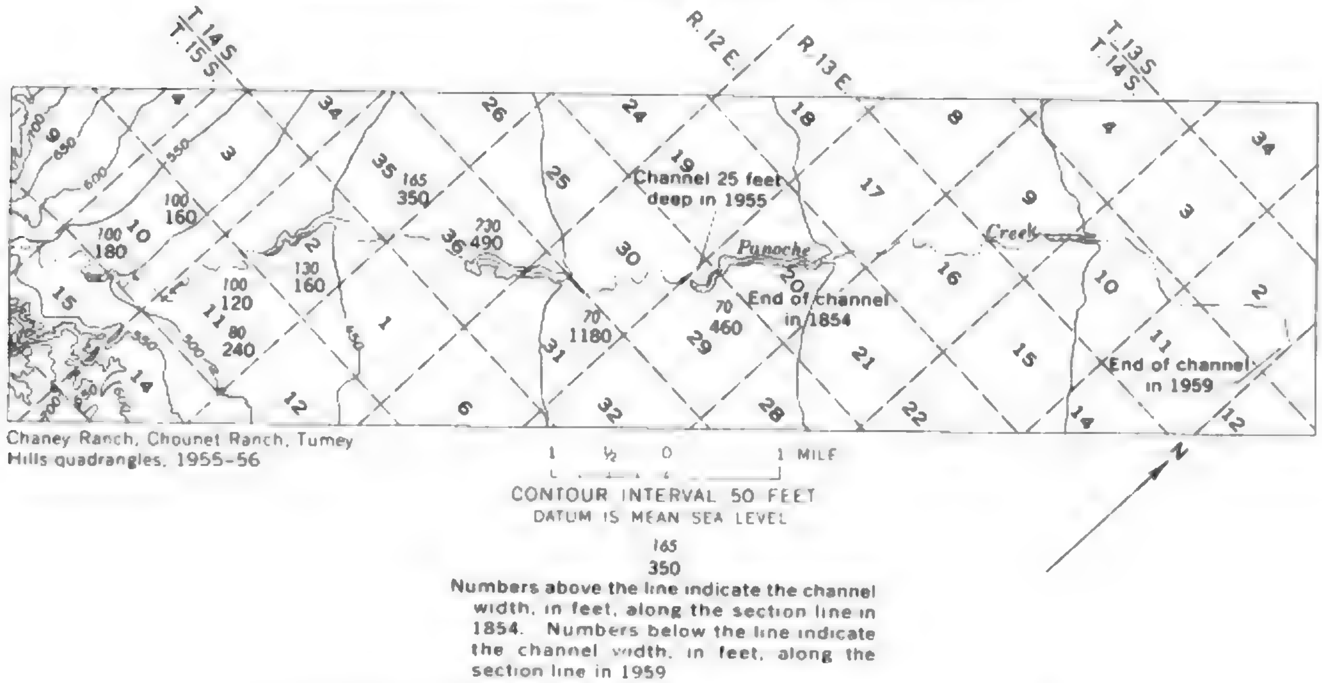

FIGURE 79.—Changes in the width and length of the Panoche Creek fanhead trench, 1854–1959.

Digitized by Google

The changes in the channel of Panoche Creek are less noticeable on the uppermost fan segment than on the second fan segment away from the hills. The average depth of the channel on the uppermost segment is less than on the second segment, and the width of the channel on the uppermost segment has increased

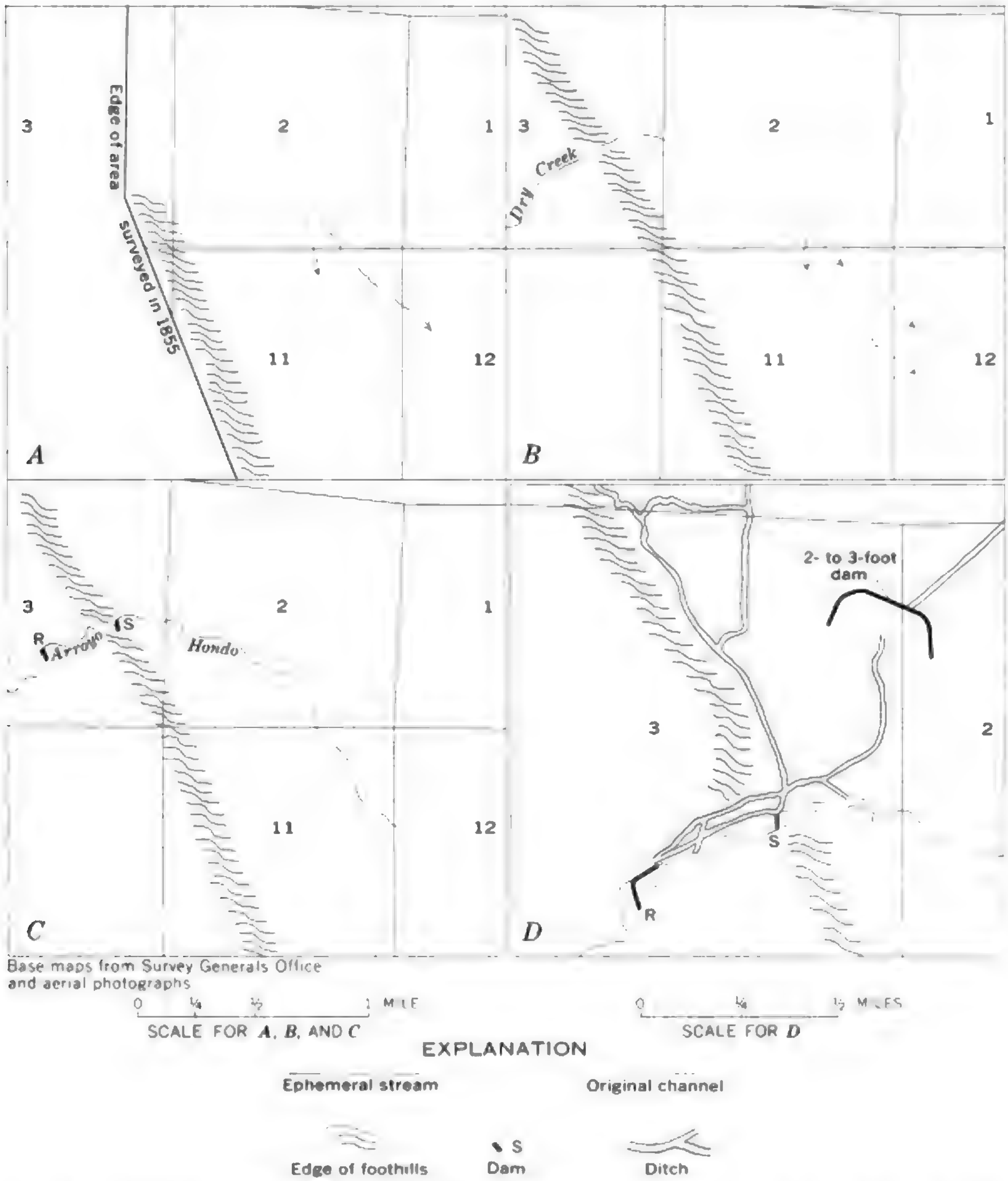

Figure 80.—Changes in the channel configuration of Arroyo Hondo, 1855–1954. *A*, 1855; *B*, 1881; *C*, 1924 and 1954; *D*, 1954.

Digitized by Google

from about one to three times the 1854 width, but the channel width on the second segment has increased from about 2.0 to 17 times the 1854 width.

Some of the changes in Arroyo Hondo (Dry Creek on the 1881 map) since 1855, based on maps made in 1855, 1881, 1924, and 1954, are shown in figure 80. Sometime between 1890 and 1924 the name "Dry Creek" was changed to Arroyo Hondo, which is Spanish for "deep stream," possibly because the channel had been deepened, not only on the alluvial fan but also along the valley in the foothills. In 1855 the entrenched stream either did not exist or it did not extend more than one-quarter of a mile into the valley. Figure 80*A* shows two channels on the Arroyo Hondo fan. These may have been deep parts of some braided distributary channels on the fanhead rather than principal channels. By 1881 a more noticeable channel had formed along the valley of Arroyo Hondo and this channel extended about 0.4 mile onto the fanhead. The distributary channels are still present, but now one is shown to be discontinuous and the other apparently has a new downstream extension. The stream channel had its present position in 1924 and appears to be an extension of the channel near the foothills to the distributary channels farther downslope.

The letters R and S in figure 80*C* and 80*D* mark the location of dams built in 1890 and 1907 respectively. The dams diverted the flow of the stream into ditches which were used by the early settlers to carry water out to the valley. The original channel downstream from these dams is preserved; immediately downstream from dam R it is about 9 feet deep and downstream from dam S about 16 feet deep. In 1959 the channel was 27 feet deep adjacent to dam R and 25 feet deep adjacent to dam S showing that the stream channel had deepened 18 feet adjacent to dam R since 1890 and deepened 9 feet adjacent to dam S since 1907.

Aerial photographs of the fan of Moreno Gulch taken in 1940 showed three deep discontinuous gullies, apparently similar to those on the Arroyo Hondo fan in 1881. Small fans were at the downslope end of the three gullies and at the end of the main channel of Moreno Gulch. Farming of the land prevented the discontinuous gullies from becoming a continuous channel. Entrenched streams apparently have formed from discontinuous gullies in other semiarid regions (Bryan, 1928, p. 279–281; Leopold and Miller, 1956, p. 29–33; Schumm and Hadley, 1957).

CAUSES OF THE FANHEAD TRENCHING

Channel trenching has been ascribed by most authors to periods of increased runoff during which floods deepened stream channels. The increased runoff has been attributed to the removal of vegetation by overgrazing and to climatic fluctuations.

Accelerated erosion in the southwestern States was ascribed to overgrazing by Rich (1911), Bailey (1935), and Thornthwaite, Sharpe, and Dosch (1942). On the other hand, Gregory (1917, p. 132) said that some parts of Arizona not used for grazing present the same features as the areas that were overgrazed. Leopold (1951a) studied the vegetation of several areas in the southwest that had been photographed between 1895 and 1903 and again between 1937 and 1946. He concluded that better quality forage might have been available in some spots at the turn of the century, but his general impression was that there has been little change in the volume of growth during the 50-year interval and therefore that grazing was not a primary cause of arroyo cutting.

It is unlikely that overgrazing was the dominant factor in starting the channel trenching in western Fresno County, because traces of older gullies on some fans indicate that fanhead trenches existed before sheep were brought into California in 1853 and before large-scale cattle ranching was introduced in western Fresno County. Adolph Domengine (oral communication, August 1959), a rancher, said that there are more stock now than in the 19th century because feed and water can be brought in now to support the herds during dry years.

Severe reduction in vegetation might increase the runoff to the streams and perhaps Bryan (1928, p. 281) was close to the truth when he said that "* * * the introduction of livestock and the ensuing overgrazing should be regarded as a mere trigger pull which timed a change about to take place."

Variation in the intensity and amount of rainfall is the most likely regional cause for the fanhead trenches. Richardson (1945, p. 17) and Antevs (1952, p. 382) stated that vegetation is the immediate factor controlling erosion which in turn is controlled by precipitation.

The precipitation records of five U.S. Weather Bureau stations were examined to determine if trends in the amount of rainfall coincided with the times of fanhead trenching. These weather stations are: New Idria in the Diablo Range; Coalinga in a sheltered valley adjacent to the San Joaquin Valley; Mendota Dam station in the trough of the San Joaquin Valley; Fresno on the east side of the San Joaquin Valley; and Sacramento in the southern Sacramento Valley. Their locations and altitudes are shown in figure 81.

Digitized by Google

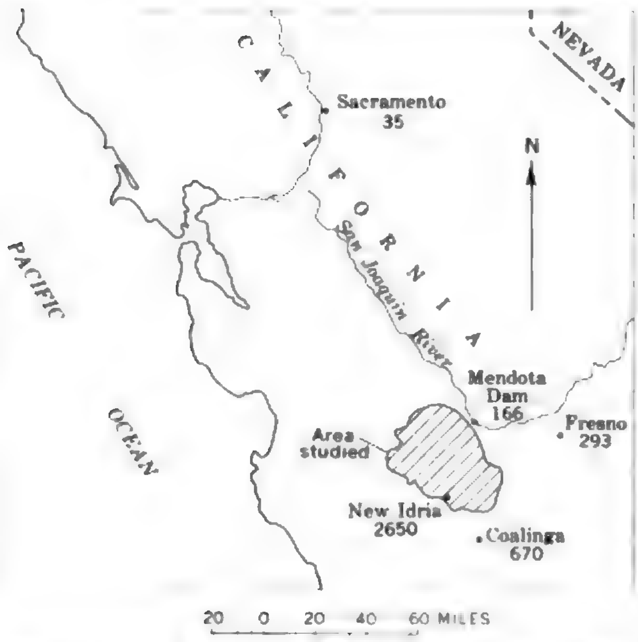

FIGURE 81.—Index map of central California showing location and altitude, in feet, of weather stations referred to in this report.

The trends of the annual rainfall (Weather Bureau climatic year July 1–June 30) at the five stations are shown in figure 82; second order moving averages were used to remove minor irregularities in the curves. The patterns of rainfall at the stations are similar despite the variety of physiographic settings and the distances between stations. This similarity suggests that cyclonic storms that move southeastward across the Pacific coast are a common source of rainfall for all the stations. Annual rainfall decreases generally from north to south and increases with an increase in altitude. The New Idria station, at an altitude of 2,650 feet, receives only slightly less rain than the Sacramento station 150 miles to the north at an altitude of 35 feet.

The period of highest rainfall, well defined at all the stations, was between 1935 and 1945. Although several peaks of excessive rainfall between 1850 and 1910 are shown on the Sacramento record, the broadest highest peak occurred in the general period 1875–95. The Fresno record shows highs during the same time interval. The 1875–95 and 1935–45 intervals coincide with the two periods of fanhead trenching reported since 1854. This conclusion contrasts with the work of Thornthwaite, Sharpe, and Dosch (1942) and Leopold (1951b) who, in their discussions of accelerated erosion in the southwest, suggested that there is no significant relation between annual precipitation and periods of arroyo cutting.

Leopold (1951b) pointed out that the New Mexico records show significant trends in the number of rains of a given size group. He showed that between 1850 and 1870 there was a decrease in the annual number of rains of 0.01–0.49 inch in a day, and he pointed out that this decrease would weaken protective vegetation such as summer grasses. This, combined with a high frequency of large rains at some stations, apparently contributed to the accelerated erosion. The trends of the daily rainfall size classes of California stations were analyzed in about the same way as Leopold treated the New Mexico data.

Figure 83 shows the trends of some daily rainfall size classes at Sacramento. Rainfall of 0.01–0.24 inch per day would promote the growth of grasses but would provide little runoff. The number of rains in this size class was at its lowest level for the years between 1881 and 1900 and about average between 1935 and 1945. Between 1875–95 and 1935–45 the number of days of rainfall of more than 0.50 inch were among the highest on record. These heavy rains would produce above-normal runoff to erode the stream channels. Again, the years that had a high frequency of large daily rainfall coincide with the times of known arroyo cutting in western Fresno County. A comparison of figures 82 and 83 shows that periods of large annual rainfall were also periods of more than the usual number of large daily rainfalls. This suggests that in this region years of high annual rainfall coincide with years of abnormally large numbers of large daily rainfalls.

Mendota Dam is the only station in western Fresno County for which daily rainfall records are available as far back as 1900. The trend in the amounts of daily rainfall are shown in figure 84. Daily rainfalls greater than 0.50 inch are not as common at Mendota Dam as at Sacramento. The period between 1930 and 1945 shows the same general characteristics as the Sacramento record except that there was a high frequency of daily rainfalls in the 0.01–0.24-inch-size class as well as a marked increase in the 0.50–0.99-size class. The pronounced peak in the 0.50–0.99-size class coincides with the period of high annual rainfall and with the time at which channel deepening was known to have occurred.

The rainfall analyses offer a reason for the arroyo cutting that began on some streams about 1880. The periods of most of the arroyo cutting (1875–95, 1935–45) also were periods of above-normal daily and annual rainfall. A combination of a high frequency of the large rainfalls and a low frequency of the small rainfalls coincided to produce above-normal runoff and less vegetation, thus allowing the above-normal runoff to erode the stream channels. Once started, channels probably became semipermanent although they may

Digitized by Google

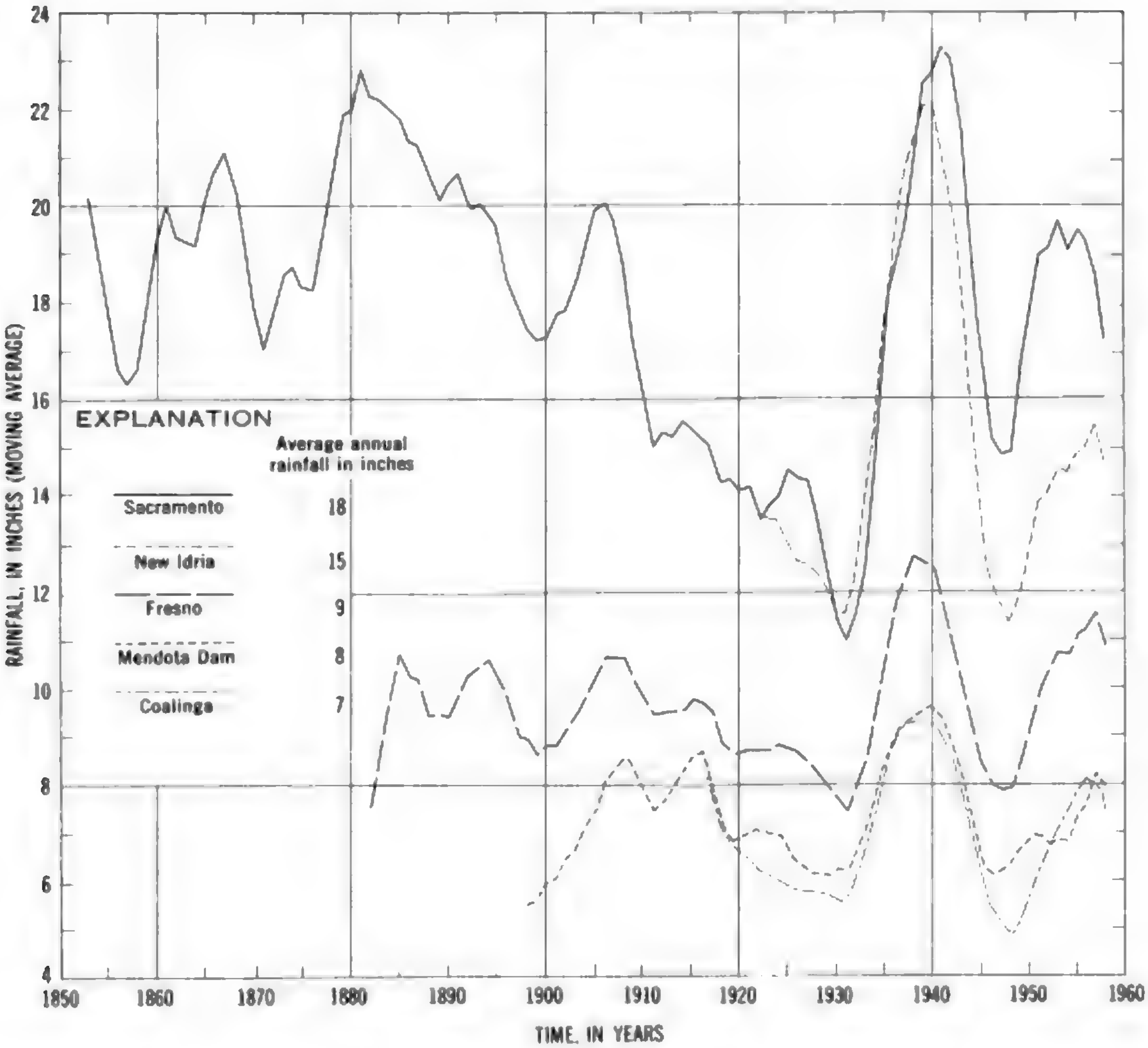

FIGURE 82.—Trends of annual rainfall for five stations in California, 1853–1958.

have been partly filled with deposits during dry periods such as 1920–35 and 1945–52. Figures 83 and 84 show a low frequency of large rainfalls during dry-year periods and therefore few large runoffs to keep the channels scoured of the material deposited in them by small amounts of runoff. About 1935 the channels began to be deepened again, coincident with another period of high frequency of large daily rainfalls. Renewal of channel entrenchment resulted in the terraces within the fanhead trenches.

Digitized by Google

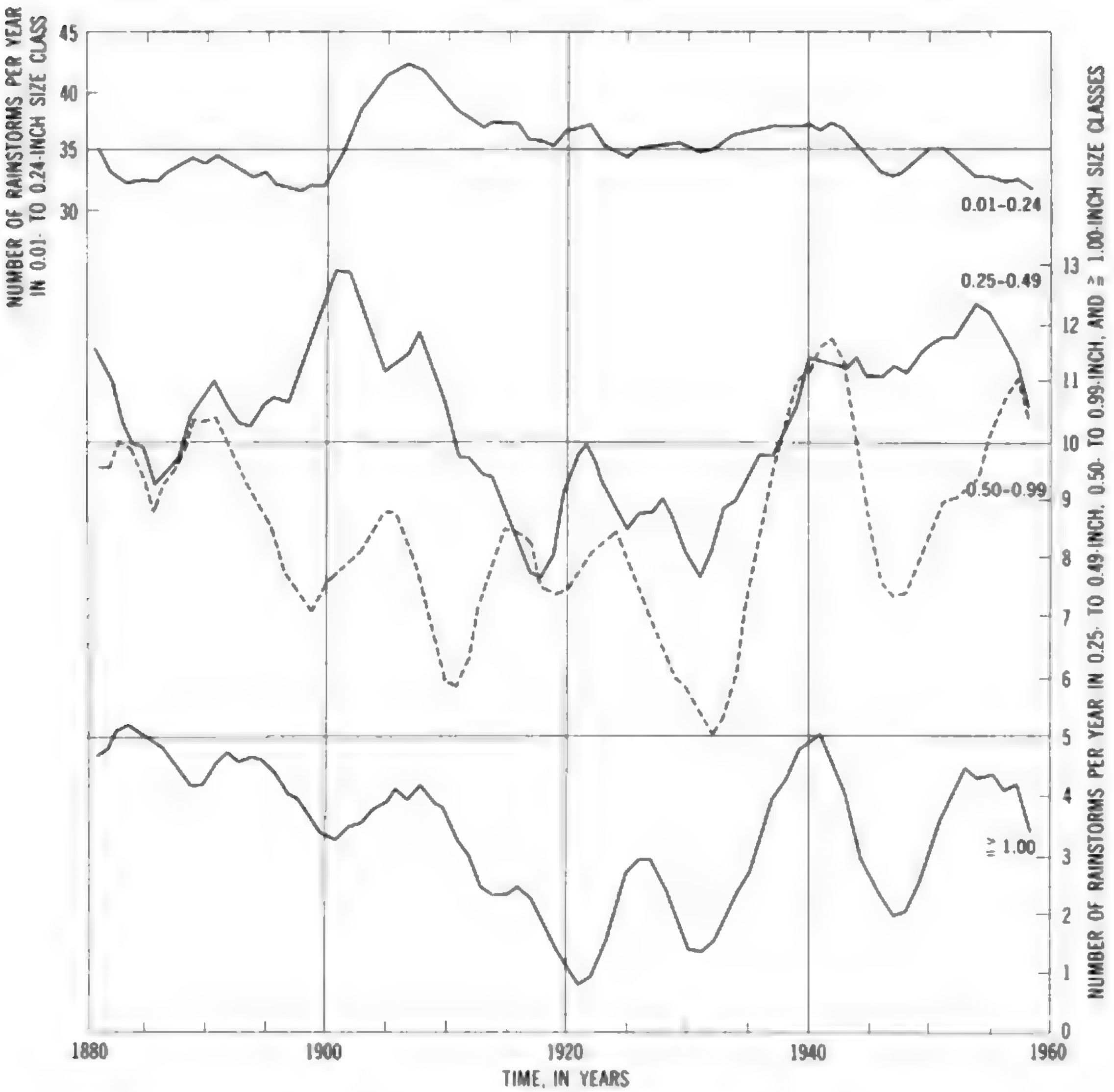

FIGURE 83.—Trends of daily rainfall size classes, 1881–1958, Sacramento, Calif.

Digitized by Google

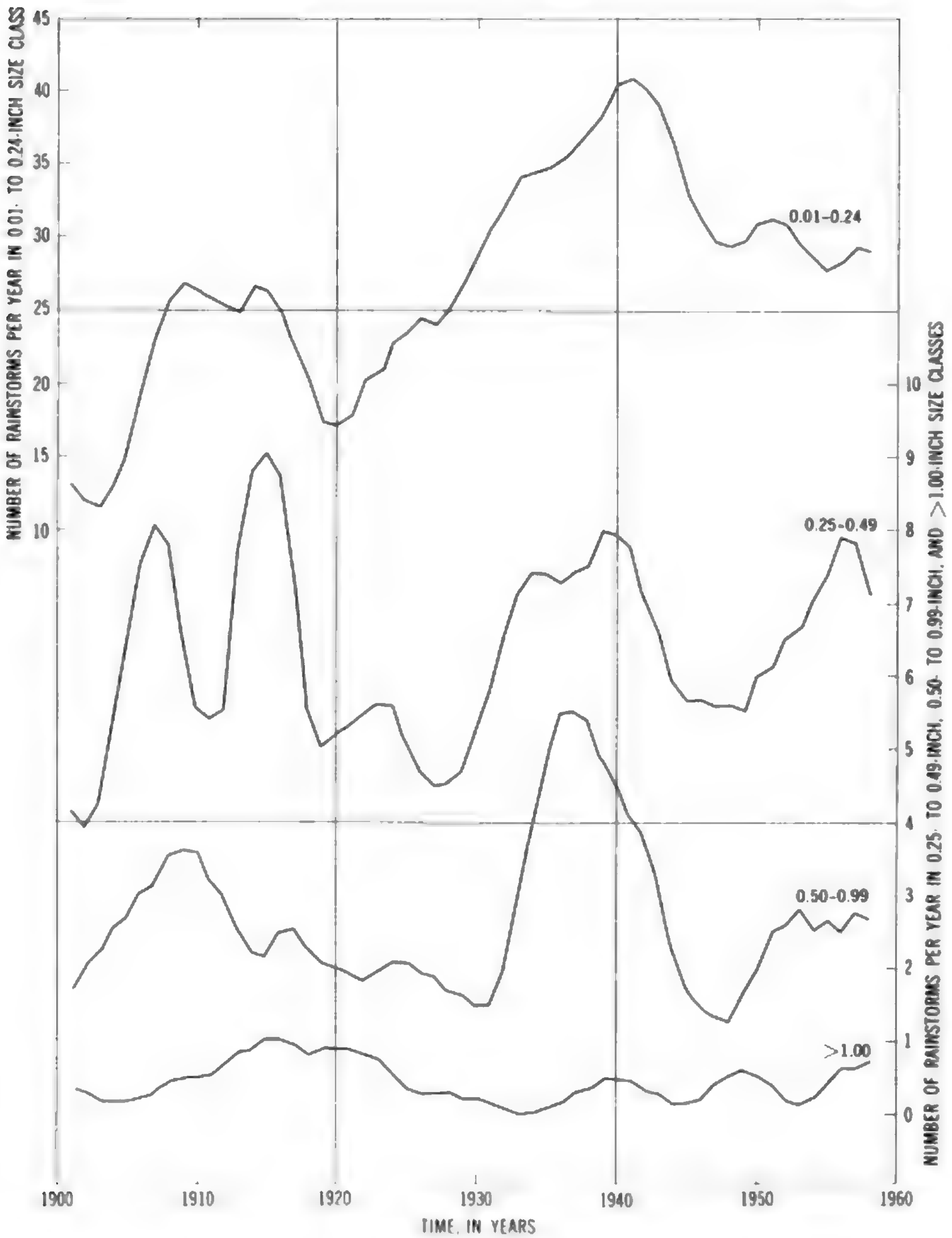

FIGURE 84.—Trends of daily rainfall size classes, 1901–58, Mendota Dam, Calif.

Digitized by Google

SUMMARY AND CONCLUSIONS

Between the trough of the San Joaquin Valley and the Diablo Range in western Fresno County is a belt of coalescing alluvial fans 12–19 miles wide. The shapes, areas, slopes, and histories of deposition of the individual fans reflect a tendency toward a state of equilibrium, or balance, among a complex set of controlling factors, which include the area, lithology, mean slope, and vegetative cover of the drainage basin; slope of the stream channel; climatic and tectonic environment; and the geometry of the adjacent fans and the depositional basin itself. Changes in one or more of these factors will tend to cause a readjustment of the fan morphology.

The fans are derived from drainage basins that are generally similar with respect to topography, climate, and tectonic environment but that range in size from 0.2 to 296 square miles and in lithology from predominantly sandstone to predominantly mudstone or shale. The fan slopes range from 10 feet per mile near the base of the larger fans to 150 feet per mile near the apexes of some small fans. Fans derived from mudstone or shale-rich basins are generally 35–75 percent steeper than fans of similar area derived from sandstone-rich basins, and roughly twice as large as fans derived from sandstone basins of comparable size. These facts indicate that the volume of fan deposits derived from the two rock types differs; presumably the difference can be attributed mainly to the greater erodibility of the mudstone and shale.

The equations expressing these relations between fan area, A_f, drainage-basin area, A_d, and fan slope, S_f, are as follows. Drainage basins underlain by 48–86 percent mudstone and shale:

$$A_f = 2.4A_d^{0.88}$$
$$S_f = 0.023A_d^{-0.16}$$
$$S_f = 0.034A_f^{-0.23}$$

Drainage basins underlain by 58–68 percent sandstone:

$$A_f = 1.3A_d^{0.88}$$
$$S_f = 0.022A_d^{-0.32}$$
$$S_f = 0.025A_f^{-0.34}$$

The overall radial profiles of the alluvial fans are gently concave, but the slopes do not decrease at a uniform rate downslope from the apexes. Instead, the radial profiles of most of the fans consist of several straight-line segments. The surfaces represented by these segments form bands of approximately uniform slope that are, in most cases, concentric about the fan apexes. The fans whose streams head in the foothill belt have three segments, each of which has a constant slope. The fans of streams that head in the main Diablo Range have four segments. The three lower segments have constant slopes, but two fans have uppermost segments that are concave.

The changes in fan slope are associated with changes that have occurred in the slope of the stream channel upstream from the fan apex. Longitudinal profiles of terraces show that intermittent uplift has changed the slope of the stream channels upstream for most fan apexes. The slope of the area of deposition and the slope of the stream channel upstream from it tend to be the same. Therefore, changes in the stream-channel slope caused by intermittent uplift have caused changes in the slope of the succeeding depositional surfaces and thus have produced the fan segmentation.

Most of the fans are associated with stream channels that have become steeper as a result of the intermittent uplift. Each time the channel was steepened the succeeding fan deposits formed a new fan segment of steeper slope that was deposited on the upper part of the preexisting fan.

The Little Panoche Creek fan, however, has a history that is associated with progressively gentler stream-channel gradients, because the rate of downcutting by the stream has exceeded the average rate of uplift of the reach immediately upstream from the apex. The intermittent character of the uplift resulted in the cutting of a series of paired terraces which preserve a record of the deformation of the mountain front and fanhead areas. With each uplift, the end of the deepened stream channel moved farther down the fan. After each episode of trenching, the lower part of the stream channel and its adjacent area of fan deposition ultimately attained a more gentle gradient than previously.

Progressive trenching and extension of the downslope end of stream channels would occur also in tectonically stable areas. In such cases the overall fan profile—including upper reaches long since abandoned as areas of deposition—might be expected to show a smooth curvature, as the result of a gradual and continuous flattening of gradients and downslope migration of the locus of deposition. Under these circumstances all but the uppermost edge of any given constant-slope fan segment would be covered and obliterated by subsequent downslope deposition at progressively flatter gradients. In the case of the Little Panoche Creek fan, however, intermittent uplift and accompanying channel trenching repeatedly caused rapid downstream displacement of the locus of deposition. In this manner the intervening part of the preexisting fan slope was preserved, together with a set of paired terraces which terminates at the upslope end of the fan segment that was receiving deposits when the terrace cutting started.

Digitized by Google

Fan segmentation is useful for deciphering part of the tectonic history of some mountain ranges, and in certain cases, segmentation may be an indicator of climatic change, because the fan profile and the relative age of the fan segments reflect part of the erosional and tectonic history of the drainage basin.

The stream channels of the alluvial fans may be braided, straight, or meandering. Some of the channels are not perpendicular to the contours of the fan. Natural levees are a typical feature along intermittent and ephemeral stream channels, where streams have flowed over their banks occasionally to deposit sediment as the flows spread out and decreased in velocity.

Reports of early settlers, old maps, and field evidence indicate that two periods of fanhead trenching, apparently unrelated to tectonic activity, have occurred since 1854, when many fans were receiving deposits near their apexes.

The trenches generally have a maximum depth of 20–40 feet, and commonly terminate at the downslope ends of fan segments. The downslope part of many of the trenches tends to be eroded down to the same slope as the adjacent lower fan segment.

The fanhead trenching occurred principally during two periods of exceptionally high annual rainfall; one from about 1875 to 1895 and the other from about 1935 to 1945. These periods of high annual rainfall were also periods of high frequency of large daily rainfalls and about average frequency of the small daily rainfalls. Most of the small daily rainfalls would be absorbed by the soil to support vegetation that would tend to check erosion, but the larger rains would furnish the large runoff required to erode the stream channels.

Relict fanhead trenches, nearly obliterated by filling and bank slumping, may be seen on several fans, indicating that relatively short-term cycles of trenching and backfilling of the main stream channel may be a typical morphogenetic response to short-term climatic oscillations.

REFERENCES CITED

Anderson, Robert, and Pack, R. W., 1915, Geology and oil resources of the west border of the San Joaquin Valley north of Coalinga, California: U.S. Geol. Survey Bull. 603, 220 p.

Antevs, E., 1952, Arroyo-cutting and filling: Jour. Geol., v. 60, p. 375–386.

Arnold, Ralph, and Anderson, Robert, 1910, Geology and oil resources of the Coalinga district, California: U.S. Geol. Survey Bull. 398, 354 p.

Bailey, R. W., 1935, Epicycles of erosion in the valleys of the Colorado Plateau Province: Jour. Geol. v. 43, p. 337–355.

Bailey, T. L., 1943, Late Pleistocene Coast Range orogenesis in southern California: Geol. Soc. America Bull., v. 54, p. 1549–1568.

Blackwelder, Eliot, 1931, Desert plains: Jour. Geology, v. 39, p. 133–140.

Blissenbach, Erich, 1954, Geology of alluvial fans in semiarid regions: Geol. Soc. America Bull., v. 65, p. 175–189.

Bryan, Kirk, 1923, Geology and ground-water resources of the Sacramento Valley, California: U.S. Geol. Survey Water-Supply Paper 495, 285 p.

——— 1925, Date of channel trenching in the arid Southwest: Science, v. 62, p. 338–344.

——— 1928, Historic evidence on changes in the channel of Rio Puerco, a tributary of the Rio Grande in New Mexico: Jour. Geology, v. 36, p. 265–282.

Bull, W. B., 1964, Alluvial fans and near-surface subsidence in western Fresno County, California: U.S. Geol. Survey Prof. Paper 437–A (in press).

Drew, Frederick, 1873, Alluvial and lacustrine deposits and glacial records of the upper Indus basin: Geol. Soc. London Quart. Jour., v. 29, p. 441–471.

Eaton, J. E., 1928, Divisions and duration of the Pleistocene in southern California: Am. Assoc. Petroleum Geologists Bull., v. 12, p. 111–141.

Eckis, Rollin, 1928, Alluvial fans in the Cucamonga district, southern California: Jour. Geology, v. 36, p. 224–247.

Greene, G. W., and Hunt, C. B., Observations of current tilting of the earth's surface in the Death Valley, California, area: Art. 124 *in* U.S. Geol. Survey Prof. Paper 400–B, p. B275–B276.

Gregory, H. E., 1917, Geology of the Navajo country, Arizona: U.S. Geol. Survey Prof. Paper 93.

Harradine, F. F., and others, 1956, Soil Survey of the Mendota Area, California: U.S. Dept. Agriculture, ser. 1940, no. 18, 96 p., soil map 1 : 63, 360.

Kesseli, J. E., and Beaty, C. B., 1959, Desert flood conditions in the White Mountains of California and Nevada: U.S. Army Quartermaster Research and Engineering Command, Tech. Rept. EP–108, 107 p.

Krumbein, W. C., 1937, Sediments and exponential curves: Jour. Geology, v. 45, p. 577–601.

Leopold, L. B., 1951a, Vegetation of the southwestern watersheds in the nineteenth century: Geol. Rev., v. 41, p. 295–316.

Leopold, L. B., 1951b, Rainfall frequency: An aspect of climatic variation: Am. Geophys. Union Trans., v. 32, p. 347–357.

Leopold, L. B., and Miller, J. P., 1956, Ephemeral streams—hydraulic factors and their relation to the drainage net: U.S. Geol. Survey Prof. Paper 282–A, 37 p.

Leopold, L. B., and Wolman, M. G., 1957, River channel patterns: braided, meandering and straight: U.S. Geol. Survey Prof. Paper 282–B, p. 39–84.

McGill, J. T., 1951, Quaternary geology of the north-central San Emigdio Mountains, California: California Univ. at Los Angeles, unpub. thesis.

Putnam, W. C., 1942, Geomorphology of the Ventura region, California: Geol. Soc. America Bull., v. 53, p. 691–754.

Reed, R. D., and Hollister, J. S., 1936, Structural evolution of southern California: Tulsa, Oklahoma, Am. Assoc. Petroleum Geologists, 157 p.

Rich, J. L., 1911, Recent stream trenching in the semiarid portion of southwestern New Mexico, a result of removal of vegetation cover: Am. Jour. Sci., v. 32, p. 237–245.

Richardson, H. L., 1945, The significance of terraces due to climatic oscillation: Discussion: Geol. Mag., v. 82, p. 16–18.

Rubin, Meyer, and Alexander, Corrinne, 1960, U.S. Geol. Survey radiocarbon dates V: Am. Jour. Sci. Radiocarbon Supp., v. 2, p. 129–185.

Schumm, S. A., and Hadley, R. F., 1957, Arroyos and the semiarid cycle of erosion: Am. Jour. Sci., v. 255, p. 161–174.

Digitized by Google

Stille, Hans, 1936, Present tectonic state of the earth: Am. Assoc. Petroleum Geologists Bull., v. 20, p. 849–880.

Taliaferro, N. L., 1943, Geologic history and structure of the central Coast Ranges of California: California Div. Mines Bull. 118, p. 119–163.

Thornthwaite, C. W., Sharpe, C. F. S., and Dosch, E. F., 1942, Climate and accelerated erosion in the arid and semiarid southwest, with special reference to the Polacca Wash drainage basin, Arizona: U.S. Dept. Agr. Tech. Bull. 808, 134 p.

Tolman, C. F., 1909, Erosion and deposition in the southern Arizona bolson region: Jour. Geology, v. 17, p. 136–163.

Trowbridge, A. C., 1911, The terrestrial deposits of Owens Valley, California: Jour. Geology, v. 19, p. 706–747.

U.S. Dept. Agriculture, 1960, Soil classification, a comprehensive system, 7th approximation: Soil Survey Staff, Soil Conserv. Service, 265 p., 44 figs., 6 tables.

Digitized by Google

INDEX

[Italic page numbers indicate major references]

Page

- Alluvial fans ... 89, 93
  - area ... 92
    - relation to drainage-basin area, lithology ... *94*
  - boundaries ... 90, 94
  - cross-fan profiles ... *114*
  - definition ... v
  - deposits ... 89
    - lithology ... 100, 104
    - moisture content ... 104
  - radial profiles ... *91*
    - definition ... v
    - of streams heading in foothill belt ... *97*
  - segmentation. *See* fan segments.
  - slope ... 92
    - concepts of previous investigators ... 94
    - relation to drainage-basin area, lithology ... *94*
  - zone of coalescence ... 98, 110
- Alluvial slopes ... 108, 112
- Apex, definition ... v
- Arroyo Ciervo, drainage basin and fan characteristics ... 92, 99
  - fanhead trenching ... *118*
  - moisture content of deposits ... 101
  - terraces ... 101, 103
  - valley fill, amount of ... 104
- Arroyo Hondo, drainage basin and fan characteristics ... 92, 99, 105
  - fanhead trenching ... *120*
  - moisture content of fan deposits ... 101
  - natural levees ... 117
- Braided distributary channels, definition ... v
- Cantua Creek ... 90
  - drainage basin and fan characteristics ... 92, 100
  - terraces ... 103
- Capita Canyon, cross-fan profiles ... *114*
  - drainage basin and fan characteristics ... 92, 99
  - terraces ... 103
- Capita Canyon, cross-fan profiles ... *114*
  - drainage basin and fan characteristics ... 92, 99
  - fan segmentation ... 98
- Chaney Ranch Canyon, drainage basin and fan characteristics ... 92
- Ciervo Hills ... 90
- Climatic changes ... 91, 122
  - effect on erosion of stream channels ... *122*
  - effect on fan segmentation ... *108*
- Coast Range orogeny ... 93
- Cross-fan profiles ... *114*
  - change in shape downslope ... 114
  - definition ... v
- Death Valley region fans ... 95, 111
- Diablo Range ... 90, 110
- Domengine Creek, drainage basin and fan characteristics ... 92, 99
- Dosados Canyon, drainage basin and fan characteristics ... 92
- Drainage basin ... 90
  - area ... 92
    - relation to fan area, slope ... *94*
  - definition ... v
  - mean slope ... 92, 99
  - percentage mudstone and shale ... 92
    - relation to fan area, slope ... 94, 99
  - total relief ... 92
  - vegetation ... 92
- Ephemeral stream ... 90
  - definition ... v
- Escarpado Canyon, drainage basin and fan characteristics ... 92
- Fan segments, as indicators of tectonic history ... 104
  - causes of fan segmentation ... *103*
  - concentric distribution ... 98, 105
  - decreasing slope ... 94, 99, 110
  - definition ... v
  - relation of stream and fan-segment gradients ... *100*
  - relative age ... 99, *105*
  - uniform slope ... 94, 110
- Fanhead trenches ... *117*
  - causes of trenching ... *120*
  - definition ... v
  - history of trenching ... *118*
- General Land Office surveys ... 90, *117*
- Glossary ... v
- Gres Canyon, drainage basin and fan characteristics ... 92
- Intermittent stream ... 90
  - definition ... v
- Laguna Seca Creek, drainage basin and fan characteristics ... 92, 99
- Little Panoche Creek ... 91
  - alluvial-fan history ... *108*
  - drainage basin and fan characteristics ... 92, 100
  - fan segmentation ... 99
  - lithology of fan ... *108*
  - terraces ... *106*
    - relation to fan segments ... *107*
- Moreа Canyon, cross-fan profiles ... *114*
  - drainage basin and fan characteristics ... 92
- Martinez Creek, drainage basin and fan characteristics ... 92, 99
- Moreno Gulch, drainage basin and fan characteristics ... 92
- Natural levees ... *116*
- Near-surface subsidence ... 104
- Panoche Creek ... 90
  - drainage basin and fan characteristics ... 92, 100
  - fanhead trenching ... *118*
- Panoche Hills ... 90, 93
- Piedmont plain, definition ... v
- Radial line, definition ... v
- Radiocarbon date of fan deposits ... 99
- Rainfall ... *91*
  - annual trends ... *120*
  - daily trends ... *122*
- Salt Creek, drainage basin and fan characteristics ... 92
- San Antonio Canyon fan ... 95
- San Emigdio Creek fan ... *110*
- Santiago Creek fan ... *110*
- Soils, profile development ... 99, 106
  - relative ages ... 99, *108*
- Stratigraphy ... 92
- Stream channels ... 116
  - deviation from medial position ... 114
  - gradients, relation to fan segments ... *100*, *105*
    - relation to tectonic activity ... *106*
  - patterns ... 114, 116
- Tectonic activity ... 93
  - amount of ... 93, *104*
  - effect on stream gradients and fan morphology ... *105*
  - variation of ... *110*
- Terraces, Arroyo Ciervo ... 103
  - Cantua Creek ... 103
  - high, mode of formation ... 103, 106
  - Little Panoche Creek ... 106
  - longitudinal profiles, diverging and converging ... *107*
  - low ... 101, 117
    - mode of formation ... *122*
  - relation of terraces to fan segments ... *108*
- Thalweg, definition ... v
- Trail Canyon fan ... 96, 111
- Tulare Formation ... 93
  - deformation of ... 93, 104
  - fossil locality ... 108
- Tule River fan ... 96
- Tumey Gulch, drainage basin and fan characteristics ... 92, 104
  - fan segmentation ... *97*
  - fanhead trenching ... *117*
- Wildcat Canyon, drainage basin and fan characteristics ... 92

Clastic Sedimentation in Deep Springs Valley California

GEOLOGICAL SURVEY PROFESSIONAL PAPER 352-F

Clastic Sedimentation in Deep Springs Valley California

By LAWRENCE K. LUSTIG

EROSION AND SEDIMENTATION IN A SEMIARID ENVIRONMENT

GEOLOGICAL SURVEY PROFESSIONAL PAPER 352-F

A study of the bolson environment and the formation of alluvial fans

Digitized by Google

UNITED STATES DEPARTMENT OF THE INTERIOR

STEWART L. UDALL, *Secretary*

GEOLOGICAL SURVEY

Thomas B. Nolan, *Director*

U. S. GOVERNMENT
DEPOSITORY

For sale by the Superintendent of Documents, U.S. Government Printing Office
Washington, D.C. 20402

Digitized by Google

CONTENTS

	Page
Abstract	131
Introduction	132
Acknowledgments	133
Physical Setting	133
Geography	133
Location and topography	133
Drainage	133
Alluvial fans	134
Vegetation	134
Climate	135
Precipitation	135
Temperature	137
Winds	137
Summary of Geology	137
Aspects of Pleistocene Geology	140
Basic Data	141
Clastic sediments	145
Largest particles	145
The pebble fraction	145
The granule-to-clay fraction	149
Granules	149
Silt and clay	154
Parameters of the size distribution	156
Mean size	156
Standard deviation	158
Basic Data—Continued	
The granule-to-clay fraction—Continued	
Parameters of the size distribution—Continued	
Skewness	158
Kurtosis	160
Summary of size-distribution parameters	162
Clay mineralogy	162
Sediment Transport	165
Competence considerations	165
Distribution of estimated tractive force	167
Directions of sediment transport	167
Channels on alluvial fans	170
Cause of trenching	174
Tectonic explanation	175
Tractive-force explanation	175
Contrast between the modern and former processes	176
Mudflows	176
The former process	177
Frequency of precipitation	179
Process rates	180
Formation of the alluvial fans	182
The evolutionary hypothesis	182
The equilibrium hypothesis	182
The climatic hypothesis	183
References	190

ILLUSTRATIONS

PLATE 8. Generalized geologic map of Deep Springs Valley, Calif. .... In pocket
9. Map and profile of the active channel on the Antelope Springs fan .... In pocket

		Page
FIGURE 85-89.	Aerial photographs:	
	85. Antelope Springs fan	135
	86. Southeastern part of Deep Springs Valley	136
	87. Wyman-Crooked Creeks fan	137
	88. Paiute Chute	138
	89. Crystal Peak reentrant	139
90.	Map showing sampling stations in the north end of Deep Springs Valley	142
91.	Map showing sampling stations on the Antelope Springs fan	143
92.	Graph showing the relation of maximum particle size to slope at stations in the north end of Deep Springs Valley	146
93.	Graph showing the relation of maximum particle size to slope at stations on the Antelope Springs fan	147
94.	Map showing mean pebble size in the north end of Deep Springs Valley	148
95.	View of a shallow wash in the Crystal Peak area	149
96.	Map showing mean pebble roundness in the north end of Deep Springs Valley	150
97.	Map showing pebble lithology in the north end of Deep Springs Valley	151
98.	View of the basalt mass and small fan at the base of Piper Mountain	152
99.	Map showing the distribution of granules in the north end of Deep Springs Valley	153
100.	Map showing silt:clay ratios and the inferred wind track in the north end of Deep Springs Valley	155
101.	Map showing the mean size of the granule-to-clay fraction in the north end of Deep Springs Valley	157
102.	Graph showing the relation of the mean size of the granule-to-clay fraction to distance from the fan apex in the Antelope Springs channel	158

Digitized by Google

Page

Figure 103. Map showing the standard deviation of the granule-to-clay size fraction in the north end of Deep Springs Valley ... 159
104. Graph showing the relation of the standard deviation of the granule-to-clay size fraction to distance from the fan apex in the Antelope Springs channel ... 160
105. Map showing the skewness of the granule-to-clay size fraction in the north end of Deep Springs Valley ... 161
106. Graph showing the relation of the skewness of the granule-to-clay size fraction to distance from the fan apex in the Antelope Springs channel ... 162
107. Map showing the kurtosis of the granule-to-clay size fraction in the north end of Deep Springs Valley ... 163
108. Graph showing the relation of the kurtosis of the granule-to-clay size fraction to distance from the fan apex in the Antelope Springs channel ... 164
109. Three-component diagram showing montmorillonite : illite : kaolinite and (or) chlorite ratios for 43 clay samples ... 164
110. Lateral view of the upper reach of the Owens Valley mudflow ... 166
111. View downstream in the upper reach of the Owens Valley mudflow ... 166
112. Map showing estimated tractive force and inferred sediment transport paths in the north end of Deep Springs Valley ... 168
113. Map showing estimated tractive force and inferred sediment transport paths on the Antelope Springs fan ... 169
114. Map showing the distribution of estimated tractive force on Paiute Chute ... 170
115. Map showing the distribution of estimated tractive force in the channel of a miniature fan in Westgard Pass ... 170
116. Map showing the distribution of estimated tractive force in a second miniature fan in Westgard Pass ... 171
117–127. Photographs:
117. Antelope Springs channel, 1.5 miles above the mountain front ... 171
118. Low terrace in the Antelope Springs channel, 1 mile above the mountain front ... 171
119. Apex region of the Antelope Springs fan ... 172
120. Hanging fan above the Antelope Springs channel ... 173
121. Low Terrace at station 9 in the Antelope Springs channel ... 173
122. Wyman-Crooked Creeks fan ... 173
123. Downfan at the bankfull deposition zone above station 126 on the Antelope Springs fan ... 173
124. Channel heading in the bankfull deposition zone at station 126 ... 174
125. Gravels, winnowed of fine sediment, on the Antelope Springs fan ... 174
126. Small plunge pool at the contact between a dissecting channel and the bankfull deposition zone above the highway ... 174
127. Bankfull deposition zone near station 318 in the Antelope Springs channel. 174
128. View of a channel cut by a mudflow in the Guil Basin, France ... 177
129. View of the aftermath of a mudflow in the Grand Tetons, Wyo ... 178
130–136. Photographs:
130. Lower reach of the Owens Valley mudflow showing clear-water dissection. 179
131. Lower reach of the Owens Valley mudflow showing floating debris on the thin deposit ... 179
132. Apex region of the active channel in Paiute Chute ... 179
133. Fine matrix in the levee wall along the active channel of Paiute Chute ... 179
134. Antelope Springs channel at station 400 ... 180
135. Fire-hearth site in the Antelope Springs channel ... 181
136. Painted gravel bar at section $A-A'$ in the Antelope Springs channel ... 181
137. Diagram showing the formation of alluvial fans during one cycle, according to the climatic hypothesis ... 185

TABLES

Page

Table 1. Slope and maximum particle-size measurements in Deep Springs Valley ... 186
2. Mean size, mean roundness, and lithology of pebbles in Deep Springs Valley ... 187
3. Basic data on the tails of the granule-to-clay size distribution ... 189
4. Sedimentary parameters of the granule-to-clay size fraction ... 189
5. Sample modes and their weight percentage of the granule-to-clay size fraction ... 190
6. Clay-mineral ratios of selected samples ... 190

Digitized by Google

CLASTIC SEDIMENTATION IN DEEP SPRINGS VALLEY, CALIFORNIA

By Lawrence K. Lustig

ABSTRACT

This report treats the size distribution of sedimentary deposits in Deep Spring Valley, Calif., and the formation of alluvial fans.

The distribution of clastic sediments and the parameters of the size distribution have been mapped when possible. Maps of the mean size, mean roundness, and lithology of pebbles, and the weight percentage of granules and silt: clay ratios of the granule-to-clay size fraction are presented. Maps of the mean size, standard deviation, skewness, and kurtosis of the granule-to-clay size fraction are also included. The largest particles exhibit fluctuation in size in a downfan direction and cannot be mapped on a reasonable contour interval; the relation of maximum particle size to local slope is shown on scatter diagrams. These data indicate that size fluctuation and poor sorting of sediments are characteristic of the environment.

Granules range in abundance from about 3 to 5 percent in the basin center to about 15 to 20 percent near bedrock outcrops. Because the abundance of granules is greatest in coarse polymodal sediments—whereas their abundance decreases with decreasing grain size and the tendency toward unimodality—it is suggested that granules consist of aggregates of sand-sized particles that are rapidly reduced to these components by mechanical weathering rather than by the action of water. The general absence of granules in ancient sediments is thought to be related to the scarcity of discrete constituents in source rocks in the 2- to 4-mm size range.

Clay is scarce in both the surface sediments and modern mudflows. The weight percentage of clay in the granule-to-clay fraction ranges from about 0 to 6 percent and averages about 2 percent in the 90 samples studied. Silt is much more abundant than clay and is the primary mode in most of the polymodal samples. The mapped distribution of silt-clay ratios shows that these ratios are probably governed in part by wind transport and deposition. The path of infinite silt: clay ratios is interpreted as a reflection of the present wind track in the basin.

The maps of mean size, standard deviation, skewness, and kurtosis of the granule-to-clay size fraction are interrelated, and proper interpretation of both the distribution and mixing of sediments within the basin is greatly aided by considering this interrelation. The tails of the distribution, namely granules and silt-clay, are shown to be of primary importance because they exert a marked effect upon the several parameters. Skewness and kurtosis are shown to be mappable and useful parameters in such studies. The field zero skewness, for example, defines a zone of sediment mixing in the basin because it reflects a balance between the tails of the size distribution. Kurtosis isopleths, however, show a high that trends across the zero skewness field, indicating that, although balance of the tails is attained, the magnitude of the spread of the tails increases. It is thought that skewness and kurtosis, which are commonly neglected in basin studies, provide information of a nature not attainable by other means. Moreover, absolute values of kurtosis may be of importance in sediment transport problems because these values probably reflect the competence of flow to some extent.

A semiquantitative method, based upon measurement of the integrated intensity of the (001) reflection, was used to determine clay-mineral ratios. The data show that a considerable range of montmorillonite: illite values occurs despite the rather uniform climatic conditions that prevail, thus suggesting a relation between clay minerals and source-rock composition. Kaolinite and (or) chlorite comprise about 20 percent of the average sample and are relatively constant in abundance.

The competence of transport is approximated by using field data to estimate tractive force in the expression $\tau = \gamma\, dS$. Maximum particle size and local slope values are substituted for d, the depth of flow, and S, the slope of the energy gradient, respectively; the specific weight γ is omitted. The dS products, which are directly proportional to tractive force, are given for about 500 sampling stations, and the distribution of values is shown by maps.

A set of orthogonals, drawn through isopleth trends, is thought to represent paths of sediment transport. The predictive possibilities of the method are tested, and the results show that this particular set of orthogonals does represent sediment transport paths because the orthogonals coincide with active channels on alluvial fans. The results also show that tractive force within the channels is generally greater than that associated with surface sediments. It is suggested that this implies a change in process and that the greater tractive force associated with the modern process results from an increase in the average density of flow.

The data and observations of alluvial fans acquired during this investigation suggest that the following characteristics of fans are common to those in the western part of the Great Basin and perhaps to other fans as well; any hypothesis of the formation of the fans must therefore account for these features:

1. The loci of deposition on alluvial fans have shifted from areas well within their catchment areas to the middle reaches of fans, far below the mountain front.

Digitized by Google

2. Trenches in the apex regions of fans are misfit relative to present flow conditions by reason of their excessive depth, which ranges to about 200 feet.
3. Paired terraces that are continuous with fan surfaces occur within catchment areas and may extend to the divide.
4. Abandoned braided channels occur on fan surfaces at higher elevations than the floors of the modern active channels.
5. Fan surfaces and abandoned channels exhibit desert varnish and (or) weathering stain, whereas in the active channels and on modern deposits these are absent.
6. Hanging fans occur in tributary canyons within the catchment areas, and their surfaces are continuous with both terraces and fan surfaces below the mountain front.
7. The estimated tractive force is greater within the active channels than on fan surfaces.
8. The percentages of clay and organic material in both surface sediments and modern mudflows are extremely small.

The applicability of three general hypotheses of the formation of alluvial fans, namely the evolutionary or Davisian, dynamic equilibrium, and climatic, is discussed. It is concluded that although certain elements of truth are contained within each of these three hypotheses, the climatic explanation can best account for the characteristics cited above. It is thought that the conditions and consequences of one climatic cycle, of the several that have occurred during the formation of the fans, are as follows.

During a period of fan building, aggradation occurred within catchment areas and on fan surfaces, below the mountain front, at correlative levels. Precipitation was more frequent and more widespread than today. In response to this climatic regime, the abundance of both clay and vegetation was greater, and the fan surfaces were more resistant to erosion. Water: sediment ratios were higher, and the medium of transport had a lesser tractive force. Floods of more frequent occurrence spilled over numerous shallow channels onto the fan surfaces, spreading laterally as they emerged from the mountain front. Sediment was deposited over wide areas of the fans as a consequence of these conditions.

Climatic change was manifested by a change from widespread to local precipitation and by a lesser frequency of precipitation. This resulted in a reduction of vegetation and a decrease in the abundance of clay. Both catchment slopes and previous deposits became more easily erodible, thus contributing toward a reduction in the water: sediment ratio of a given flood and the more frequent occurrence of mudflows. These flows of greater density, viscosity, and tractive force deepened the trunk channels in catchment areas and trenched the upper reaches of the fans. Terraces in catchment areas and hanging fans in tributary canyons were thus produced, and the sediment removed in the process was deposited far downfan.

The shift of the loci of deposition downfan, in response to climatic conditions, produces growth of fans at their lower boundaries and a general decrease of slope in the upper reaches. The sediment added in these lower reaches is redistributed and incorporated into the basin fill during the subsequent climatic episode. At this time, lake levels will rise, the trenches will gradually fill with sediment, and aggradation in catchment areas and on fan surfaces will again occur.

The morphology of fans thus tends toward equilibrium with successive climatic fluctuations. The attainment of such equilibrium, however, is a function of the duration and intensity of each climatic episode, and it may or may not occur during these periods. Fan growth is both upward and outward, during alternate intervals, and will continue for some finite period, at the end of which time a given basin will be completely filled with sediment.

INTRODUCTION

Two of the most common generalizations that emerge from the literature on alluvial fans are (1) local floods in arid regions transport sediment to the mountain front and deposit it in a fanlike form as a consequence of a decrease in gradient and the absence of lateral restriction, and (2) alluvial fans are the product of a balance between erosion of the mountains and deposition in adjacent basins.

Although each of the foregoing statements appears to be quite logical, their widespread acceptance tends to obscure the fact that the formation of alluvial fans is poorly understood. The problem can best be considered in terms of its component parts, namely: (1) What is the distribution of sediments on alluvial fans? (2) What is the competence of the transporting medium? (3) What is the dominant mechanism of sediment transport today? (4) Has this or another transport mechanism been dominant in the past? (5) What is the nature and significance of channels on alluvial fans? (6) Is the modern process one of fan building or of degradation? (7) Does this process differ from that of the past? and (8) What is the rate of the modern process?

This study was undertaken to answer these questions and thereby enlarge our understanding of the formation of alluvial fans. A considerable part of the paper is devoted to question (1) above, the distribution of sediments, and to such component questions as: (1) What is the size distribution of sediments on alluvial fans and on the valley floor? (2) Are all the sedimentary parameters mappable? and (3) Which parameters would best serve to characterize the clastic sediments of a bolson environment?

The field investigation covered by this report comprised 8 months during the summers of 1960 and 1961 in eastern California and western Nevada. Quantitative data were obtained in Deep Springs Valley, Calif., and observations of a qualitative nature, particularly of channels on alluvial fans, were made in Fish Lake, Eureka, Saline, Panamint, Death and Owens Valleys. All are in the general vicinity of Deep Springs Valley.

In considering the question of the distribution of sediments within the environment, the first four moments of the size-frequency distribution were studied. If conclusions are based upon study of but a single

Digitized by Google

parameter, such as the mean size or median size, then it must be assumed that this parameter is the most significant. The writer would hesitate to make this assumption, because the significance of other variables, such as kurtosis, is not well understood. For this reason the mean size, standard deviation, skewness, and kurtosis of the size distribution were mapped, thus providing a sound basis for a discussion of sediment mixing and the geologic significance of these parameters.

It was thought that the best approach to the question of possible differences between the modern and former processes lay in consideration of the competence of the transporting medium. Accordingly, a field approximation for this variable was sought and the results mapped. The conclusions that are presented, regarding differences between past and present processes, stem largely from a consideration of these maps and their implications and are supported by other data and field observations.

ACKNOWLEDGMENTS

The project reported on in this paper served as the basis for a doctoral thesis submitted to Harvard University in 1962. The project was conducted largely under the guidance of the late John P. Miller. The many stimulating discussions of the problems involved and the technical assistance which he provided, in both Cambridge and the field, more than satisfied the requirements of an adviser. Of still greater importance, however, was his interest in the study and evident enthusiasm; these provided a source of encouragement that cannot be too strongly emphasized.

The writer is indebted to Raymond Siever for several valuable suggestions during discussions of many aspects of the problem and to Alan V. Jopling, who read an initial draft of this manuscript. This paper has benefited from the constructive criticism of both Gordon M. Wolman and Lucien M. Brush, Jr., to whom the writer is grateful for their fine reviews.

Field assistance was capably provided by Donald Newberg in 1960 and Stephen Eittreim in 1961.

Blair Jones, of the U.S. Geological Survey, and Clem Nelson, of the University of California, provided valuable insight into the problems of their respective work on the basin hydrology and geology during discussions in the field.

Lorenzo Aristarain simplified the task of clay-mineral determinations for the writer by supplying several key references as well as valuable discussions of techniques.

F. M. Fryxell, of Augustana College, Rock Island, Ill., and J. Tricart, of the Institut de Geographie, Strasbourg, France, kindly granted permission for the reproduction of their previously published photographs in this report.

Meyer Rubin, of the U.S. Geological Survey laboratory, furnished the radiocarbon-age determination of the fire hearth (sample W–185).

These acknowledgments would be incomplete without mention of the information, hospitality, and assistance generously given by several residents of the Deep Springs area. Among these are Mr. Rudehouse, former manager of the Deep Springs Junior College; Alma Rossi, of Big Pine; and Bill Jenkins, former foreman of the Deep Springs highway maintenance station.

PHYSICAL SETTING

GEOGRAPHY

LOCATION AND TOPOGRAPHY

Deep Springs Valley is located in the western part of the Great Basin, one mountain range east of Owens Valley, Calif., and approximately midway between Mono Lake to the northwest and Death Valley to the southeast. Considering the Great Basin in its entirety, Deep Springs Valley is an atypical basin only by reason of its small size and perfect closure (pl. 8).

The White Mountains border the valley on the west, as far south as Westgard Pass. South of the pass, as well as on the east side of the valley, the name Inyo Mountains is applied. The maximum relief is about 3,100 feet in the vicinity of Deep Springs playa and about 5,600 feet in the north end of the valley. From the northwest corner of the drainage basin (pl. 8) to a point about 10 miles south along the divide, elevations generally range from 10,000 to 11,000 feet. Elevations decrease gradually to 7,300 feet at Westgard Pass, then rise again and average about 8,500 feet around the south rim of the basin. Elevations elsewhere are generally 6,000–7,000 feet at the divide, excepting breaks at Soldier Pass and Piper Mountain which are at 5,400 and 7,700 feet, respectively.

DRAINAGE

The interior drainage of Deep Springs Valley is typical of closed basins. About 40 ephemeral streams enter the valley proper, an area of about 47 square miles. Total drainage area of the basin (pl. 8) is about 144 square miles, exclusive of the valley proper.

The relation between fan area and catchment area noted by Denny (1965) in Death Valley does not hold in Deep Springs Valley. The Wyman-Crooked Creeks drainage area, for example, is nearly equal to the entire area of the valley (pl. 8) and is about three times as large as the Westgard Pass catchment area. Planimetric measurement of the respective fans from either topographic sheets or aerial photographs, however,

Digitized by Google

would show that they are roughly equal in area.

Several reasons exist for this discrepancy between fan area and catchment area. A relation between the drainage area of a watershed and discharge has been demonstrated by many workers, but correlation of fan area with drainage area implies that the planimetric measurements reflect volumes. Clearly, the basic relation involved is that the volume of sediment removed from a given drainage basin should equal that which is deposited below the mountain front. Because differences in relief can occur despite equality of watershed areas, the planimetric measurement of drainage areas may not accurately reflect the volumes of sediment that have been removed. Likewise, such measurements may also fail to reflect the volumes of sediment in alluvial fans, because planimetric areas are a function of the surface slopes, which will vary.

A second consideration involves basin tectonics. It is not reasonable to assume that the downfaulted basin floors are horizontal in the light of much seismic evidence to the contrary. The volumes of sediment in alluvial fans may therefore differ because of basement tilting and subsequent burial of sediment, despite present equivalent surface expression.

ALLUVIAL FANS

Each of the ephemeral streams in Deep Springs Valley traverses an alluvial fan. The fans are larger on the west and northwest sides of the basin than on the southeast. The larger fans generally extend 2–3 miles from their apexes into the valley, whereas fans in the vicinity of Paiute Chute (pl. 8) can be as small as a few hundred feet in extent. The depth of alluvium is unknown, but it exceeds 700 feet in the vicinity of the bench mark in the north end of the valley (pl. 8), where a waterwell of this depth did not reach bedrock.

The general aspect of alluvial fans in Deep Springs Valley is similar to that of fans elsewhere in the Basin and Range province and need not be considered in detail. The most important features of fans, the active and abandoned channels, will be treated below. The approximate limits of the two fans discussed extensively in this report, Antelope Springs and Wyman-Crooked, are shown on plate 8.

Although some fans are clearly defined, merging of adjacent fans is not uncommon. These produce a continuous apron of alluvium and render difficult the task of drawing individual fan boundaries on maps. The merger of the Antelope Springs fan (pl. 8) with those adjacent to it can be seen in figure 85, and the apron of debris that occurs southeast of the playa is shown in figure 86. The darker areas visible owe their color partly to a preponderance of dark quartzite, in contrast to much white marble on the Antelope Springs fan, and partly to the presence of varnish and desert pavement.

An occurrence of color contrast on a single fan that does not result from the presence of a desert pavement is found on the Wyman-Crooked Creeks fan (fig. 87) in the north end of the valley. Although the dark area seen in the background contains a greater abundance of basalt than other parts of the fan surface, much of the color contrast results from the presence of weathering stain or varnish. No closely packed mosaic of stones occurs, however. Both the spacing of particles and range in size is comparable to that which occurs elsewhere on the fan. The presence of varnish in Deep Springs Valley is therefore independent of desert pavements, although both may occur together.

The alluvial fans considered in detail in this report are too few in number to provide valid correlations among such variables as slope, drainage area, and lithology. The data obtained suggest, however, that fans containing coarse debris are generally of steeper slope than, for example, the Antelope Springs fan. The slope of the latter ranges from 3 to 8 percent over much of its surface, and the largest particles present do not exceed 4 feet in intermediate diameter. Slopes on the Wyman-Crooked Creeks fan (fig. 87) range from about 2 to 11 percent and boulders 6–8 feet in diameter are not uncommon. Still greater slopes and larger particles occur on the fans rimming the south end of the basin (fig. 86) and on Paiute Chute (fig. 88), just north of the playa. On the other hand, the reentrant (fig. 89) just north of Crystal Peak (pl. 8) is as much as 16 percent in slope and consists mainly of granitic sand with few large particles. Particle size is, of course, largely a function of the lithology of the source area and the presence or absence of joints, cleavage, and other structural features. Given a source rock that produces no particles larger than cobbles, for example, neither discharge, slope, nor any other factor can enlarge the resulting particle size. Fans consisting of the finer debris contributed by such a source rock, however, are usually of gentle slope.

VEGETATION

The vegetation in the Deep Springs Valley drainage basin reflects orographic control. Sage and other shrubs floor the valley, attaining a maximum height of about 3–4 feet. The active channels on alluvial fans are generally bare of vegetation, but scattered-to-dense sage occurs on the bordering low terraces. In the active channel of the Wyman-Crooked Creeks fan (fig. 87), however, phreatophytes are abundant. This may reflect subsurface seepage beneath the channel, which is derived from the perennial flow in Wyman Canyon.

Digitized by Google

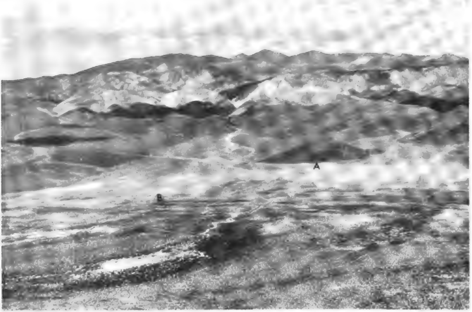

FIGURE 85.—Aerial view of the Antelope Springs fan showing its merger with adjacent fans. Note the contrast between the color of the sediments within the channels and that of the fan surface, which is darker. The transition from a relatively straight to a braided channel pattern on the fan coincides with the first depositional zone below the mountain front. The former lake level at about 5,200 feet and the linear ridges that mark the most recent expansion of Deep Springs Lake are designated as *A* and *B*, respectively.

Piñon and juniper occur between elevations of about 6,000 and 9,000 feet, together with sage that becomes less abundant with increasing altitude. Above 9,000 feet, the famous bristlecone pine is dominant in the White Mountains. These trees are restricted to some extent by lithology as well as altitude. They are most prevalent in areas where the white Reed Dolomite of Precambrian(?) age crops out; this can readily be seen either in the field or on aerial photographs. The writer noticed that the rather gnarled bristlecones all appeared to twist in the same direction along their axes. This was true whether they occurred on north- or south-facing slopes. From a chance encounter with a botanist in the mountains, who was engaged in a study of the trees, the writer learned that "as everyone knows, the twisting is in response to the Coriolis Force."

CLIMATE

PRECIPITATION

Climate is also a function of elevation, as attested to by records from the two weather stations in the area. One of these stations is in the White Mountains at an elevation of 10,150 feet, in the northwest corner of the drainage basin (pl. 8). The other station is in the valley at an elevation of 5,225 feet. The average annual precipitation in the mountains is about 13 inches, whereas it ranges from 3 to 5 inches in the valley. The maximum 24-hour precipitation for these two stations was 3.10 and 1.50 inches, respectively. It should be pointeed out, however, that one cannot state with certainty that the latter values were maxima in the area; they are maxima only for their respective locations and for the period of record.

Digitized by Google

FIGURE 86.—Aerial view of the southeastern part of Deep Springs Valley. Note the apron of alluvium, produced by the merger of fans, beyond the playa and to the right. The channel at *A* is entrenched, and lighter colored sediment, indicative of modern transport, can be seen along its course and at the lower boundary of the fan.

During the winter months precipitation in the White Mountains is derived mainly from the residue of cyclonic storms that migrate across the Sierra Nevada and Owens Valley from west to east. The sporadic occurrence and distribution of thunderstorms and cloudbursts in desert areas in summer, however, is well known and Deep Springs Valley is no exception. Although the period of observation in the area was short, comprising only two summers, the writer gained the impression that certain tracks of thunderstorms across the valley were followed with greater frequency than others. The track of six thunderstorms in 1961 was from the southeast, over the playa, and directly across the Antelope Springs fan to the mountains (pl. 8). A second group of storms also arrived from the southeast, but these entered the valley between Paiute Chute and the general vicinity of Soldier Pass. These storms produced some minor precipitation at the valley weather station and proceeded to the Wyman-Crooked Creeks canyon area.

Storms arriving from the north or northeast produced rainfall on Piper Mountain (7,700 ft) and continued in a southerly direction, again passing over the valley weather station.

The remaining storms entered the valley from the southwest, west, or northwest. In these instances, precipitation usually ceased somewhere within the drainage area of the White Mountains and little, if any, rain fell in the valley proper.

Despite the paucity of data on the frequency of track of these storms, two facts are indicated. First, the frequency of precipitation is not everywhere equal within the basin. It will later be shown that this accords with the occurrence of certain hanging fans in tributary valleys. Second, frequency of precipitation in the valley proper is also not everywhere the same, and the total amount of precipitation on basin floors is not great. This may account for the preservation of scattered lake terraces in desert basins; in

Digitized by Google

FIGURE 87.—Aerial view of the Wyman-Crooked Creeks fan. The darker color of the fan surface, above the dashed line, results from numerous basalt boulders and varnished or stained boulders. The basalt boulders are derived from basalt outcrops within the catchment area and from the dark mass in the background. Note the vegetation in the active channel, which is entrenched to a depth of about 40 feet, and the abandoned distributary channels at higher elevations than the active channel.

addition, it suggests that local runoff on alluvial fans is small compared with that in the mountains.

TEMPERATURE

The difference between the average annual temperature at the White Mountain weather station (pl. 8) and that in the valley is 18°F. Maximum temperatures greater than 105° have not been officially recorded in the valley, but in the absence of an official shade tree, temperatures from 115° to 120° were common. During two rather warm periods sun temperatures of 130° were recorded; ground temperatures are probably even greater.

WINDS

Information on wind intensities and dominant tracks in the valley is not available. The usual diurnal fluctuation of track, up and down canyons, was observed. It is unknown, however, whether any net transport of fine sediment results from this process.

Only three major duststorms occurred during the period of observation. The direction of sediment transport during each storm was from south to north, again prompting the question of frequency of track. Data on silt: clay ratios, to be discussed below in the section entitled "Silt and clay," suggest that the observed track may in fact be preferred in the valley.

SUMMARY OF GEOLOGY

The geology in the Deep Springs Valley area has been treated by Knopf (1918), Miller (1928), Nelson (1962, 1963), and others. Nelson conducted a detailed stratigraphic study and mapped the geology of the area. Much of the information to follow stems from his work complemented by personal observations. An outline of the geology, pertinent to this report, is shown on plate 8.

In the White Mountains the stratigraphic section consists of 21,000 feet of Precambrian(?) and Lower

Digitized by Google

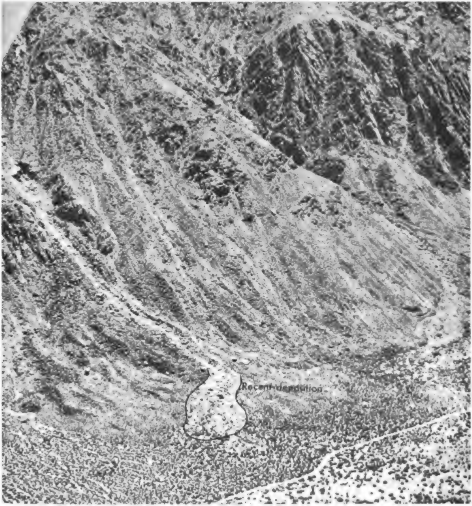

FIGURE 88.—Aerial view of Paiute Chute. Note the prominent active channel and the bordering levee walls. Several similar chutes occur in this general area, on the east side of the valley. The area of recent deposition on this young fan is below the termination of the active channel and at the lower margin of the fan, bounded as shown in the photograph.

Digitized by Google

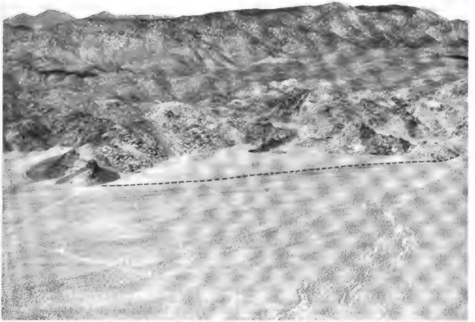

FIGURE 89.—Aerial view of the Crystal Peak reentrant. Crystal Peak is the small ping to the left of the dashed line that delineates the steeply sloping reentrant. Surface slopes are as much as 16 percent.

Cambrian strata and about 1,600 feet of Middle Cambrian sedimentary rocks; the latter are relatively restricted in outcrop area. Of the 10 formations described by Nelson (1962), only those pertinent to a discussion of the distribution of clastic sediments in the valley are mentioned here.

The sedimentary sequence has been folded, intruded by a granitic batholith and one or more stocks, and faulted. Structurally, the White Mountains are a southerly plunging anticline within the drainage basin considered. Because the fold axis trends nearly due south, whereas the topographic trend is southeast, the adjacent syncline to the east is exposed farther south in the Inyo Mountains. Erosion of the fold in the White Mountains has therefore revealed the oldest rocks in the section. The structural relationships become apparent in Wyman Canyon (pl. 8) where, despite considerable local complexity, repetition of strata to either side of the Precambrian(?) heart of the fold can be seen.

The formations of Precambrian(?) age encountered in Wyman Canyon, which cuts across the fold axis, are the Wyman, Reed, and Deep Spring. The Wyman Formation is greater than 9,000 feet thick (base unexposed), and the Reed Dolomite and Deep Spring Formation are 2,000 and 1,500 feet thick, respectively. These units crop out over a distance of about 6 miles along the canyon. The Wyman Formation consists of crumpled and contorted schists, phyllites, shales, and quartzites which are mottled gray, brown, or black and are generally banded. The overlying Reed Dolomite is a white to light-bluish-gray dolomite, and the younger Deep Spring Formation consists mainly of reddish-brown or yellowish-brown sandstones. South of Wyman Canyon the Wyman Formation gradually pinches out because the fold plunges in this direction. It comprises only a minor percentage of the rock types within the Antelope Springs catchment area, whereas the Reed Dolomite and Deep Spring Formation crop out in abundance.

Digitized by Google

A Cretaceous(?) granitic intrusive, of roughly 5 square miles in outcrop area, has pierced the sedimentary rocks between Antelope Springs and Wyman canyons and a contact metamorphic sequence occurs. South of the Antelope Springs drainage area the younger, Lower Cambrian sedimentary rocks, crop out. Dark sandstones and shales with varying amounts of limestone predominate; this assemblage, in varying proportions, continues around the south end of the basin. The contact between the sedimentary rocks and the granite occurs east of the playa, and the Inyo Range on the east side of the valley is granitic from this point northward.

Scattered remnants of Tertiary basalt and an underlying white friable tuff crop out along Crooked Creek, to the north of the Wyman-Crooked Creeks fan (fig. 87), and in the northeast corner of the basin.

The foregoing summary of the geology of the area indicates that certain rock types are sufficiently distinctive and restricted in area to serve as indices of probable source area at sampling stations in the valley. An abundance of sedimentary rocks derived from the Wyman Formation, for example, unquestionably indicates transport from the Wyman-Crooked Creeks system (pl. 8) in the northwestern part of the basin even if it occurs near the playa. Knowledge of the distribution of basalt remnants and color and other distinctions among specific basalt sources also proved useful during this study, particularly in treating the problem of sediment mixing within the basin and attendant effects upon the sedimentary parameters. Although several fine distinctions were drawn during the study, for convenience the lithologic data on the valley sediments have been summarized under the gross headings of granitic rocks, sedimentary rocks and basalt (table 2).

ASPECTS OF PLEISTOCENE GEOLOGY

No evidence of extensive glaciation in the White Mountains, within the drainage basin considered, was noted by the writer. This may not be true for the part of the range farther north, however. During the Pleistocene the snowline was undoubtedly much lower than it is today, but even at the headwaters of Wyman and Crooked Creeks (pl. 8) at elevations of 10,000–11,000 feet, evidence of cirques or moraines is lacking. A buried soil occurs in the headwaters of Crooked Creek, and signs of frost action were noted at several localities; these features represent the only evidence of Pleistocene climates in the mountains. An extensive snow cover and local ice caps probably existed in the higher parts of the range, however. If so, then combined with greater precipitation and lower temperatures, these local caps and the snow cover must have contributed to a much greater runoff and discharge than obtain today.

Miller (1928) was the first to discuss the Pleistocene lake in the valley and its probable extent. He estimated that its maximum depth was on the order of 400–500 feet. Given present elevations, a lake 500 feet deep would nearly cover the entire valley floor. The highest known stand of the lake was at about 5,200 feet, which accords with gravel deposits around the south end of the valley. The 5,200-foot contour follows the base of the low bedrock hill to the right of the Antelope Springs fan (fig. 85). Color contrasts also suggest a former high stand at this level. If the lake did not rise above this level, however, then according to present elevations, it could not have reached the northern end of the valley. The bench mark at 5,220 feet (pl. 8) would represent the northern limit of the former lake. A 5,200 foot-level would appear to insure that the lake did not overflow the basin; but present topography is not sufficient proof of this, and a former connection should be sought.

The former connection of many lakes in the Mohave region with the Pleistocene Owens Lake, as a result of overflow from one basin to another, is well known; the subject has been reviewed by Blackwelder (1954), among others. Westgard Pass, however, is at an elevation of 7,300 feet (pl. 8), sufficient to ensure that Deep Springs Lake was not part of this chain by way of Owens Lake. If a former connection in some other direction is sought, then the "new map" showing the distribution of pluvial lakes by Feth (1961) is of no greater assistance than the original compilation by Flint (1957, p. 227). It is probable that every basin in this region contained a lake, although not all overflowed their basin. A field reconnaissance of the Great Basin could provide much of the missing data.

Deep Springs Valley is adjacent to Eureka Valley, to the east, and Fish Lake Valley, to the northeast. A direct connection between Fish Lake Valley and Deep Springs Valley is possible, but field evidence suggests that the two may also have been connected by way of Eureka Valley. Horse Thief Canyon, which connects Fish Lake and Eureka Valleys, was traversed, and many solution pockets were noted by the writer along the base of the canyon walls. The divide between these two valleys is within Fish Lake Valley at an elevation of about 5,280 feet, and Horse Thief Canyon runs downgrade over its entire length into Eureka Valley.

Soldier Pass (pl. 8), which joins Deep Springs and Eureka Valleys, was also traversed. A carbonate-cemented pebble conglomerate probably formed in Pleistocene time and now largely stripped away, crops

Digitized by Google

out along the floor and walls of the pass. The gravel fraction consists entirely of angular granitic fragments. The beds dip to the west, suggesting postlake uplift and tilting. Other evidence of uplift during Recent time can be seen at several localities on the east side of Deep Springs Valley. In the vicinity of the present playa another carbonate-cemented conglomerate crops out above the valley floor; scarps trend abruptly across alluvial deposits, and springs and bogs occur in this zone. Nelson (oral commun., 1961) has suggested that a major fault follows the zone east of the playa to the north and then turns east through Soldier Pass. Differences in elevation within the Inyo Mountains on either side of the pass are in accord with this suggestion.

Uplift of about 200 feet in the vicinity of Soldier Pass appears reasonable. If this is true, then the pluvial Deep Springs Lake overflowed through the pass into Eureka Valley. A small isolated playa occurs in a reentrant of the Inyo Mountains, on the Eureka Valley side of the divide, at the same latitude as the Deep Springs playa. Overflow from the pluvial Deep Springs Lake may have spilled into this sink, which has subsequently been uplifted.

Another conglomerate locality in the north end of Deep Springs Valley also indicates postlake uplift and tilting. These carbonate-cemented conglomerates occur near the most southern of the group of small drainage systems just southwest of Piper Mountain (pl. 8). The beds dip to the west, and in a few places they are as much as 200 feet above the present valley floor. They represent an absolute criterion for uplift, because the gravels are of lithologic types derived solely from the Wyman-Crooked Creeks drainage area across the valley. The gravels are well rounded and range in size from pebbles to large cobbles. This occurrence suggests that sediment from the Wyman-Crooked Creeks system must formerly have been transported directly across the valley floor in a more easterly direction than today. Former channels on the Wyman-Crooked Creeks fan also trend in this direction. Uplift and tilting, following withdrawal of the lake, produced the present southerly trend leading to the playa.

In summary, it is considered probably that Deep Springs Lake did extend over the entire valley floor, but the absolute depth or extent of this lake cannot be judged from present topography. This example of postlake uplift probably holds true for many of the western basins. Traverses of likely interbasin canyons provide a better field test of possible former connections between lakes than does examination of present elevations of accordant levels.

BASIC DATA

The quantitative data obtained in Deep Springs Valley are listed in tables 1 through 6 and were used to construct the various maps presented in this report. Sampling stations in the north end of the valley and on the Antelope Springs fan are shown in figures 90 and 91, respectively. The data include (1) measurements of local slope and maximum particle size at 496 stations; (2) 12,400 determinations of pebble size, roundness, and lithology; (3) sedimentary parameters of 90 samples of the granule-to-clay size fraction; and (4) approximate clay-mineral ratios for 43 samples. A planetable map of the active channel on the Antelope Springs fan (pl. 9) was constructed from data from about 600 stations on a scale of 1 inch = 100 feet.

Sampling stations in the north end of the valley are 1,000 feet apart, based upon an arbitrary grid system. The bench mark at 5,220 feet (pl. 8) was used as point 0.0 (fig. 90). Stations were located by means of pace and compass, or by odometer and compass if the point could be reached by jeep. Although the odometer was checked over measured miles for accuracy and tire pressures were not overlooked, some lack of precision must inevitably result because of the roughness of terrain. The same is true of paced distances in the area. The resultant inaccuracies of the maps, however, do not detract from the general trends shown.

Sampling stations on the Antelope Springs fan are located along contours that differ in elevation by 50 feet, determined by altimeter, and are 200 feet apart on each contour line.

Stations on Paiute Chute (fig. 88) and on the miniature fans in Westgard Pass, treated below, are 100 and 5 feet apart, respectively. Bearings taken from each station to the fan apex permitted the plotting of sampling points. This procedure was also followed at each station on the Antelope Springs fan (fig. 91).

The largest particle within a 50-foot radius of the sampling stations was located by observation, and the length of the intermediate axis was measured to the nearest tenth of a foot. Both the search for the largest particle and its measurement required some digging in many places. Slopes were measured to the nearest one-half percent with an Abney level over a 100-foot reach between the particle and the apex region of the fan. Because paths of sediment transport do not necessarily coincide with a straight line from the fan apex to a given particle, the 100-foot reach chosen was that which appeared to be the most probable transport path from field observation. If a particle occurred within a channel or boulder train, for example, then slope was measured along these trends regardless of deviation in direction from the apex. The rock types of the largest

Digitized by Google

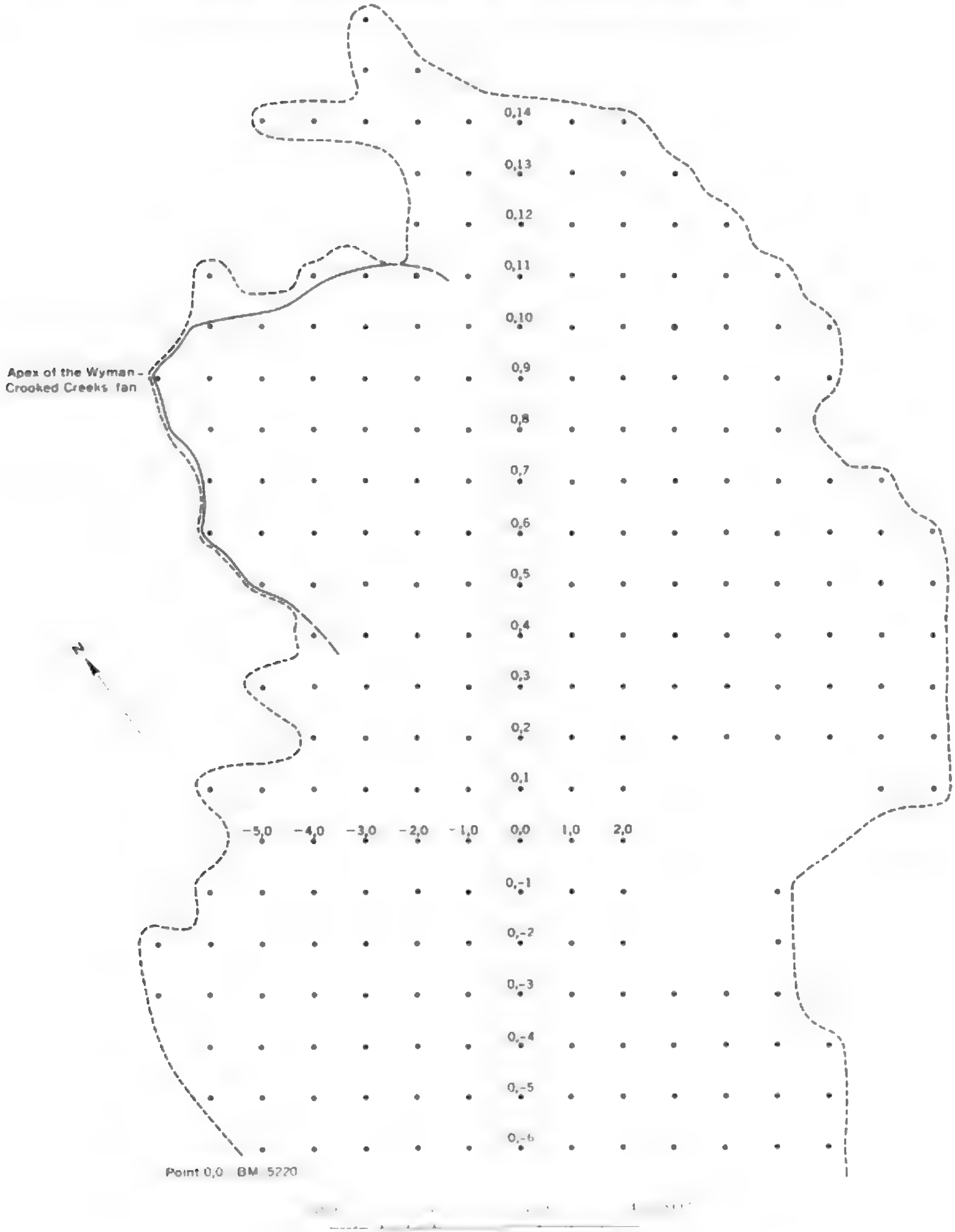

FIGURE 90.—Map showing sampling stations in the north end of Deep Springs Valley

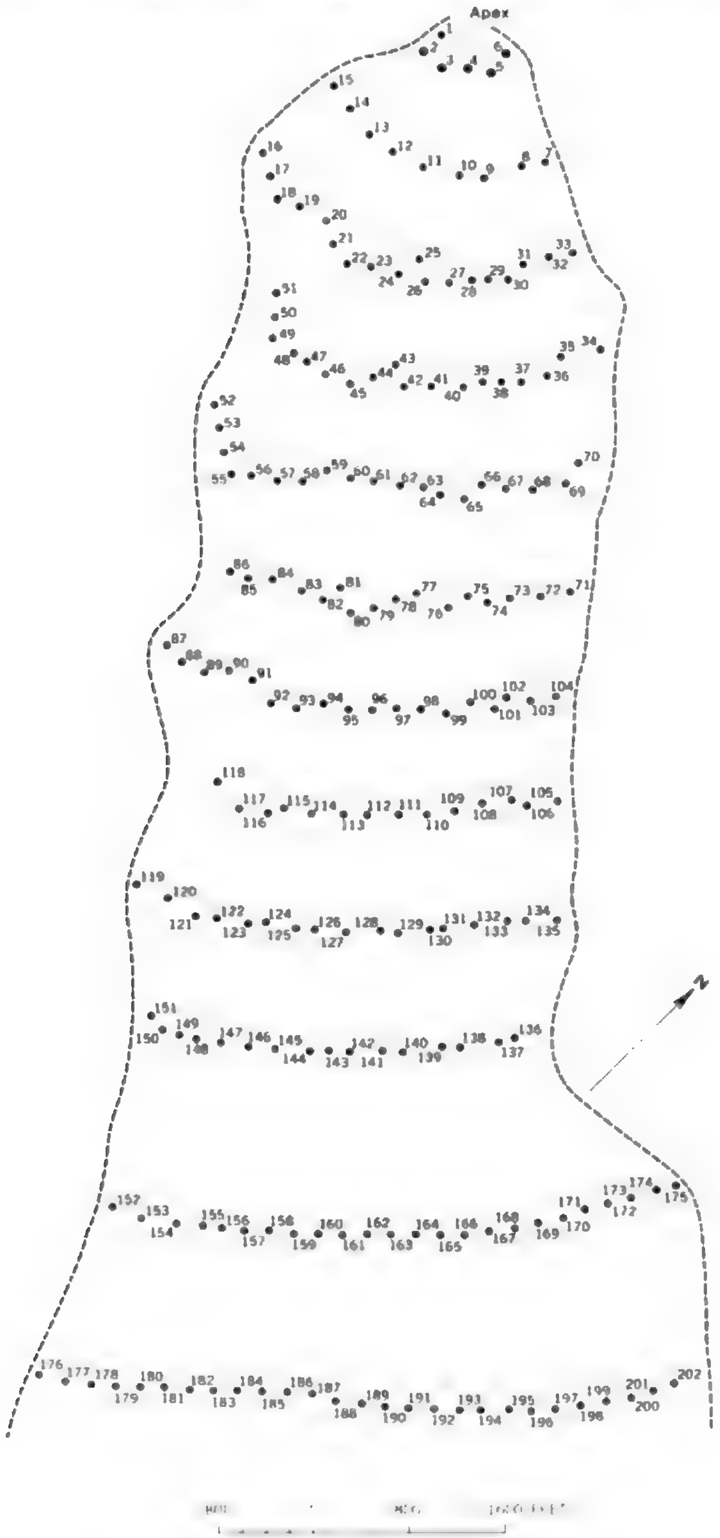

FIGURE 91.—Map showing sampling stations on the Antelope Springs fan.

766-976 O—65——3

Digitized by Google

particles were also obtained, but they are not included in the tables.

Data on pebbles were obtained only in the north end of the valley. At each sampling station (fig. 90) 50 pebbles were selected. These were obtained by pacing off a rough square, of about 12 paces to a side, and picking up the pebble nearest to the toe of the boot with each pace. Unlike the method described by Miller (1958) for sampling the Sangre de Cristo streams, the pebbles were not selected with eyes averted because of possible objection to the entire procedure by reptiles and other desert denizens.

For each pebble, the smallest, intermediate, and largest axis was measured with a vernier caliper to the nearest tenth of a millimeter, and the lithology was determined with a hand lens. The roundness of each pebble was determined by visual means and recorded as angular, subangular, subrounded, rounded, or well rounded. These categories were later assigned values of 0, 1, 2, 3, and 4, respectively, and the mean roundness for each rock type and for the entire sample was calculated.

In order that these procedures not appear to be open to the influence of preconceptions, it might be well to point out that the time requirements and other factors insured objectivity. The number of stations sampled per day was understandably small, because of the amount of data gathered. This prevented consecutive sampling from the valley floor to the mountain front along sampling lines. Also, as a matter of convenience, sampling lines were often left uncompleted and were returned to several days later when sampling along perpendicular lines. These factors alone would be sufficient to insure that one would not select larger or smaller particles of a given degree of roundness according to some concept of what the data "should be" at a given point. In addition, no mean value was computed until all stations in the north end had been sampled. The maps of the several variables presented indicate that the arbitrary sampling grid cuts across most trends at odd angles; this would not result from subjective sampling.

Samples of the granule-to-clay fraction were obtained from a total of 290 stations. Excepting grab samples from two mudflows, the upper 4 inches of sediment within a 5-foot radius of each point was obtained with a can or small shovel and successively quartered until the remainder would fill a 4- by 6-inch sample bag. Much care was expended to insure that the finer fraction not be lost during this procedure. Ultimately, 90 samples were chosen for analysis. These include 66 from the north end of the valley, 19 from the active channel on the Antelope Springs fan (fig. 9), 2 from Paiute Chute, 2 from a mudflow in Owens Valley, and 1 from a thin mudflow in Wyman Canyon.

These samples were split in order to obtain about 50 grams of each and then wet sieved through a 62-micron mesh. After oven drying, the granules were separated from the sands, and the latter were sieved with U.S. Standard Sieves; this provided a separation at half phi intervals. The less than 62-micron fraction was washed into settling tubes, and any additional sediment of this size that was obtained as a pan fraction during sieving of the sands was added. Silt and clay were separated at the 4-micron boundary by successive decantations. Time intervals for decantation were determined by settling velocities at the temperatures that prevailed. Because of the height of fall, which was 25 cm, the average time interval was about 4.25 hours. Most samples required about 10 decantations, but this varied, of course, with the amount and proportions of the sediment. The <4-micron fraction was drawn off, and after a few days were allowed for settling, a concentrated slurry was obtained and clay-mineral mounts were made by sedimentation on glass slides. The silt fraction was oven dried and weighed, and the weight of clay was determined by difference.

The mudflow samples were boiled in chlorox several times before separation of the size fractions, and the weight of organic matter was later determined by difference.

The weight percent of each class interval, from granules to clay, was calculated and the results cumulated. The cumulative percents were then plotted on arithmetic probability paper against phi diameter, and the values necessary for determination of the statistics used were read from each curve. The statistical measures used in this report to characterize the size distribution of the granule-to-clay fraction are those suggested by Folk and Ward (1957). They are as follows:

$$\text{Mean size } (Mz)=\frac{\phi_{16}+\phi_{50}+\phi_{84}}{3},$$

$$\text{Inclusive graphic standard deviation } (\sigma_I)=\frac{\phi_{84}-\phi_{16}}{4}+\frac{\phi_{95}-\phi_5}{6.6},$$

$$\text{Inclusive graphic skewness } (Sk_I)=\frac{\phi_{16}+\phi_{84}-2(\phi_{50})}{2(\phi_{84}-\phi_{16})}$$

$$\text{and} \qquad +\frac{\phi_5+\phi_{95}-2(\phi_{50})}{2(\phi_{95}-\phi_5)},$$

$$\text{Graphic kurtosis } (Kg)=\frac{\phi_{95}-\phi_5}{2.44(\phi_{75}-\phi_{25})}.$$

These measures represent a reasonable compromise between including a sufficiently large percentage of the size distribution to obtain the information desired and attempting to minimize the effort expended in attaining it. McCammon (1962) has recently reviewed the efficiency of various statistics of mean size and sorting. He shows that the measure of mean size (Mz) used in

Digitized by Google

this report has an efficiency of 88 percent, whereas $\frac{\phi_{16}+\phi_{84}}{2}$, for example, has an efficiency of 74 percent. The respective efficiencies of inclusive graphic standard deviation (σ_I) and $\frac{(\phi_{75}-\phi_{25})}{1.35}$ are 79 and 37 percent. To further increase the efficiencies of the statistics chosen, it would be necessary either to include additional percentiles within the range considered or to increase the range, or both.

CLASTIC SEDIMENTS

The clastic sediments of Deep Springs Valley range in size from boulders to clay. At a given point, therefore, a volume sufficient to fill a small truck might be required in order to investigate the size distribution of a single sample. For this reason, and also because the implications of the size distribution are the primary concern, it was thought best to treat three discrete fractions of the total sediment. These are the largest particles, the pebble fraction, and the granule-to-clay fraction. Although this treatment is not entirely satisfactory, several considerations show it to be useful. First, separate treatment of the largest particles permits a discussion of competence; second, the weight percentages determined for such significant size classes as silt and clay are maxima; finally, the alternatives are in some respects still less satisfactory. If particles that occur at a given tape interval are measured, for example, there is an inherent tendency to skew the distribution toward the larger particles because pebbles will invariably be selected in preference to granules when both are present.

LARGEST PARTICLES

The 496 particles that represent the maximum size present at each station are listed in table 1 together with the slopes on which they occurred. Although large particles occur more frequently near apex regions of fans, they are not restricted to these areas. Figure 92 shows the relation between maximum size and slope for stations in the north end of the valley (fig. 90). The only station omitted from figure 90 is −7, 9 where a 16.5-foot particle occurred on a slope of 11 percent. The next largest size present at these stations was slightly <8 feet in intermediate diameter, and for reasons of convenience the ordinate was not extended beyond 10 feet.

The scatter of points on figure 92 is apparent. This can partly be explained by considering that several fans are represented and that variations of lithology, and especially joint spacings, will produce blocks of unequal size at the source. A plot of slope and maximum particle size for 202 stations on the Antelope Springs fan (fig. 93) shows a rather good trend, except for the particles on gentle slopes.

Blissenbach (1952, 1954) claimed that the relation between maximum particle size and slope was arithmetic for fans in Arizona and that the decrease in size downfan was uniform. His data were scanty, however; even the data for Antelope Springs (fig. 93), consisting of a limited size range, would not plot well on an arithmetic scale. In this report, the scatter of points is thought to be of greater significance than the general trend because understanding of process is the goal.

Particles larger than 1 foot in diameter occur in areas of zero slope, and particles larger than 5 feet in diameter occur on slopes of 2 percent in the north end of the valley (fig. 92). On the other hand, particles as small as 0.2 foot in diameter are the maximum size present on slopes as steep as 14 percent. For the Antelope Springs fan, where the range of both size and slope is more restricted (fig. 93), particles half the size of the largest present occur on slopes as gentle as 2 percent. Conversely, particles as small as 0.1 foot in diameter can represent the maximum size on slopes as great as 5 percent, although this fan exhibits maximum slopes of only 8 percent. It might be argued that the examples cited are the extremes of the distribution and therefore of little consequence. Regardless of the trend of the means, however, the extreme values require explanation.

The fact that boulders have been reported on playas (McAllister and Agnew, 1948; Kirk, 1952; Clements, 1952; and others) clearly indicates that the phenomenon of large particles in areas of zero slope is not restricted to Deep Springs Valley. Guilcher and Cailleux (1950) observed pebbles moving along an icy road in Denmark under the impetus of the wind. This observation led to a wind tunnel experiment by Grove and Sparks (1952) who duplicated the phenomenon. Extrapolation of their data by Schumm (1956) indicated that a velocity of 122 miles per hour would be required to move a rock weighing 1 pound across ice. Although the movement of boulders on playas is usually considered apart from any question of transport on fans, it is obvious that any boulder must first have been moved down a fan if it occurs on a playa. An explanation for the fluctuation of maximum particle size in a downfan direction will be offered below (p. 167).

THE PEBBLE FRACTION

The distribution of the mean pebble size in the north end of Deep Springs Valley is shown on figure 94. Although several trends are apparent, the most striking feature of the map is fluctuation in size, which is represented by closures around high and low values.

Digitized by Google

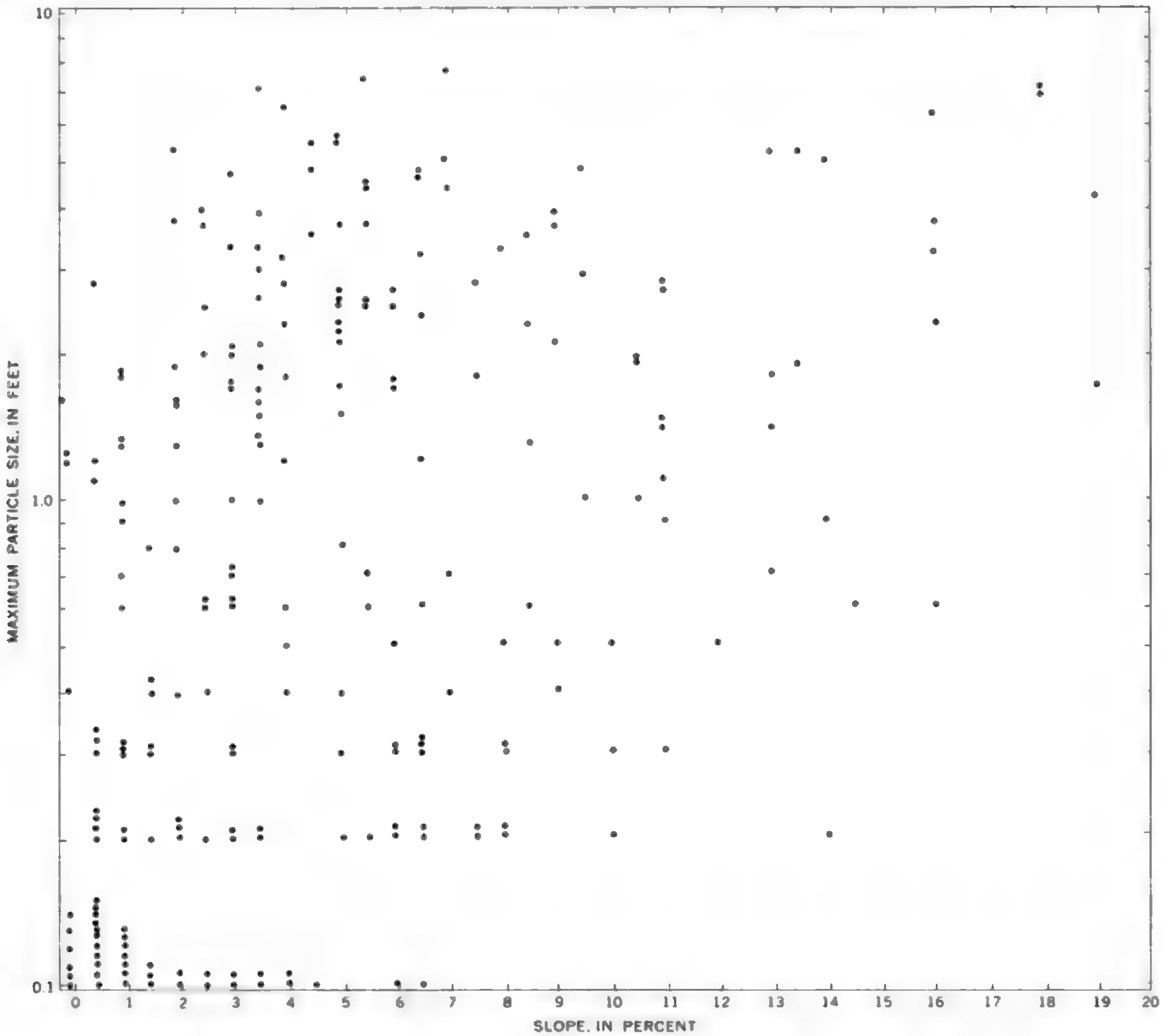

FIGURE 92.—Graph showing the relation of maximum particle size to slope at stations in the north end of Deep Springs Valley.

Some closures around high values are the result of sampling in a wash. This is true, for example, of the 34-mm high in the southwest corner of the map and the 28-mm high farther north. This 28-mm high defines the shallow wash shown in figure 95. Other high and low values result from extremes at only one or two points; this deserves further consideration.

First, it should be acknowledged that two individuals will seldom, if ever, produce identical isopleth maps from the same data. Nevertheless, there are limits that will restrict the possible differences. If the pebble data (table 2) were in accord with a uniform decrease in size downfan, then isopleths would be forced to conform with the basin boundary to some extent, or trends on individual fans would at least emerge more clearly. Neither is true of the map under consideration. Second, the question can be raised whether the mean or the extremes of the distribution is to be emphasized. If stress is to be placed upon average or mean trends, then the variations can be reduced by constructing a moving average map. Choice of a larger isopleth interval would also achieve this end. As with the largest particles, however, the fluctuations in size probably are significant and for this reason no attempt should be made to obscure the fact that they occur by smoothing the data. Each point on the map represents the average of 50 measurements; the map is therefore thought to depict accurately the distribution of pebble size.

Digitized by Google

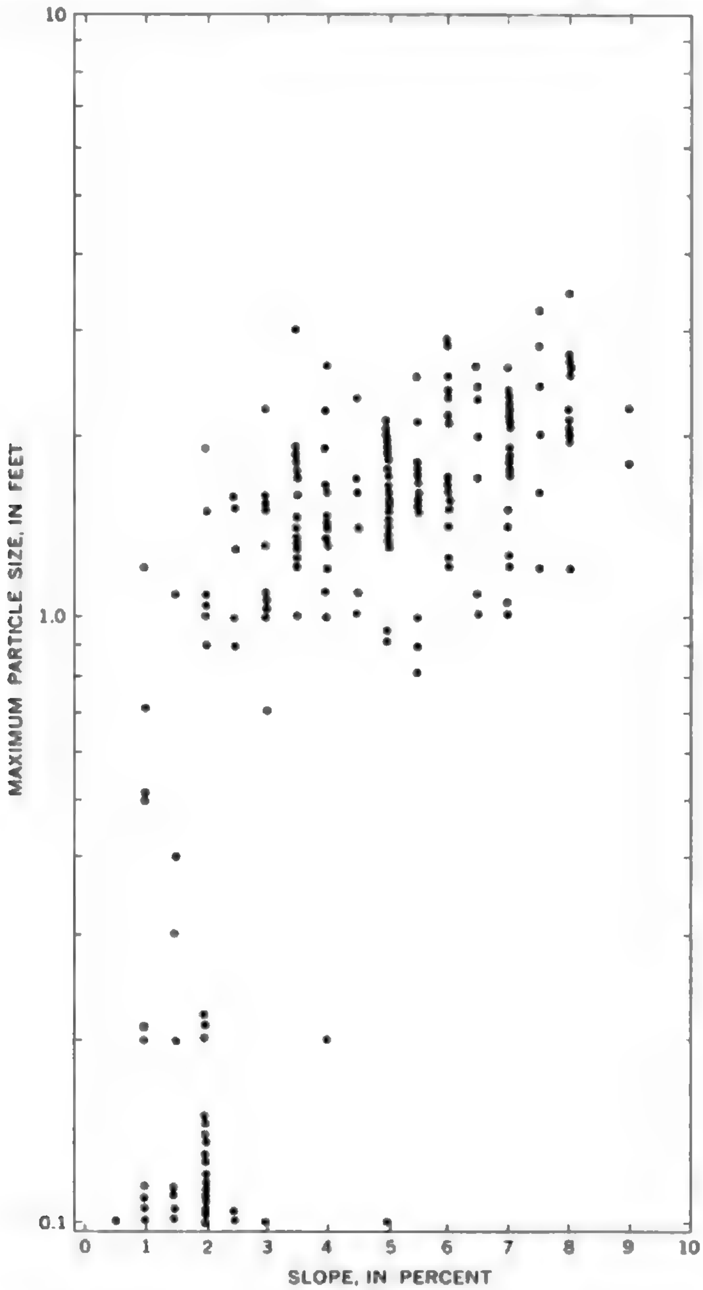

FIGURE 93.—Graph showing the relation of maximum particle size to slope at stations on the Antelope Springs fan.

Digitized by Google

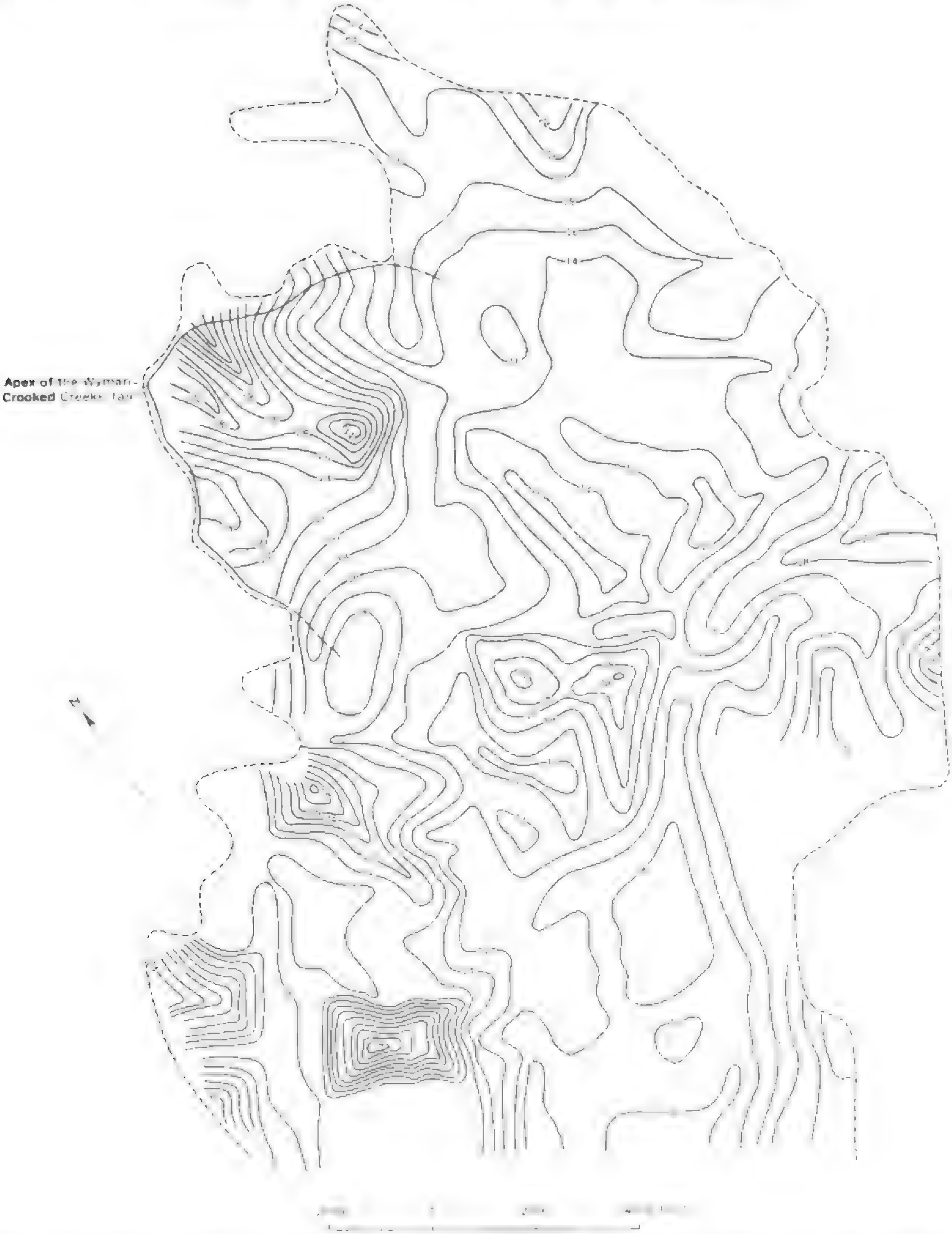

FIGURE 94.—Map showing mean pebble size (in millimeters) in the north end of Deep Springs Valley. Dashed line represents approximate bedrock basin boundary.

Digitized by Google

FIGURE 95.—View of a shallow wash in the Crystal Peak area. The wash at this point is approximately 193 feet wide and 2 feet deep. The sediments are predominantly of sand size, consisting of granitic weathering products. The boulder in the foreground (arrow), however, is about 4 feet in diameter.

The roundness (fig. 96) and the lithology (fig. 97) of pebbles in the north end of Deep Springs Valley are correlative. Fields of high mean roundness outline two main lithologic groups. These are the metamorphic and sedimentary types that issue from the Wyman-Crooked Creeks canyons (pl. 8) and the basalts derived from the cap on Piper Mountain and the low tilted masses at its base. The latter can be seen in figure 98. The color contrast at the base of the slope roughly coincides with the 50-percent contour in this area on figure 97 and with the roundness field of 1 on figure 96. Quartz and feldspar pebbles, derived from coarse grained granites and a few pegmatites, and scattered pebbles from aplite dikes are included in the plutonic rock percentage. These pebbles, in addition to the angular granite pebbles that occur close to their source areas, are more angular than the sedimentary, metamorphic, and volcanic rock types. For this reason the mean roundness reflects the lithologic distribution. The occurrence of closures on both the roundness and lithology maps is worthy of note. These reflect fluctuations in the distribution similiar to those found for mean size (fig. 94).

It is apparent from the roundness and lithology maps that a zone of mixing of sediments occurs along the central and east-central parts of the basin. Sediments from the Wyman-Crooked Creeks system, the northern and northeastern parts of the basin, and from the granitic Inyo Mountains on the east all merge in this area. The sedimentary parameters of the granule-to-clay fraction, to be discussed below, also reflect this mixing of sediments.

THE GRANULE-TO-CLAY FRACTION

GRANULES

In a review of the various size grades, Pettijohn (1957, p. 47) notes that the results of many studies indicate that granules (2–4 mm) are less abundant in nature than are other size groups. He also states that there appears to be a deficiency of very coarse sand as well. The basis for these statements is the fact that a sedimentary deposit consisting of both gravel and sand generally exhibits a distinct mode for each of these two fractions. The break in the frequency curve, between these 2 modes, falls within the 1- to 4-mm size range.

Several attempts have been made to explain the frequency minimum. Sundborg (1956, p. 191–194), for example, argues on hydraulic grounds that particles between 1 and 6 mm are those most readily moved when bed transport commences and are the last to come to rest when it ceases. According to this argument, granules are scarce in nature because they are in nearly constant motion, relative to other size classes, and therefore simply wear out. Kagani (1961) also advances a hydraulic explanation and, in addition, advocates placing size-class boundaries at all conspicuous frequency minima. This would, in effect, tend to remove granules entirely from consideration as a distinct size class.

An investigation of the clastic sediments in Deep Springs Valley, Calif., provided a good opportunity to consider the problem of the scarcity of granules. Because sediment transport is typically both brief and intermittent in a bolson environment, the conditions postulated by Sundborg (1956) do not pertain. A simple test of the hydraulic theory can therefore be applied; granules should occur in no lesser abundance than other size classes if the theory is correct. The basic data for the following discussion are listed in table 5; the weight percentages of granules are listed in table 3.

The weight percentage of granules in the granule-to-clay size fraction was determined for 90 samples. In addition to 19 samples from the Antelope Springs active channel (pl. 9), 71 samples were studied. These include 66 from the north end of the valley, 2 from Paiute Chute, and 3 from mudflows. Of these samples, 24 were unimodal and 47 were bimodal. In the unimodal group no mode coincided with the granule, very coarse sand, fine-sand, and clay sizes. Granules, however, occurred as the primary mode of 4 and the secondary mode of 5 of the bimodal samples. Among the

Digitized by Google

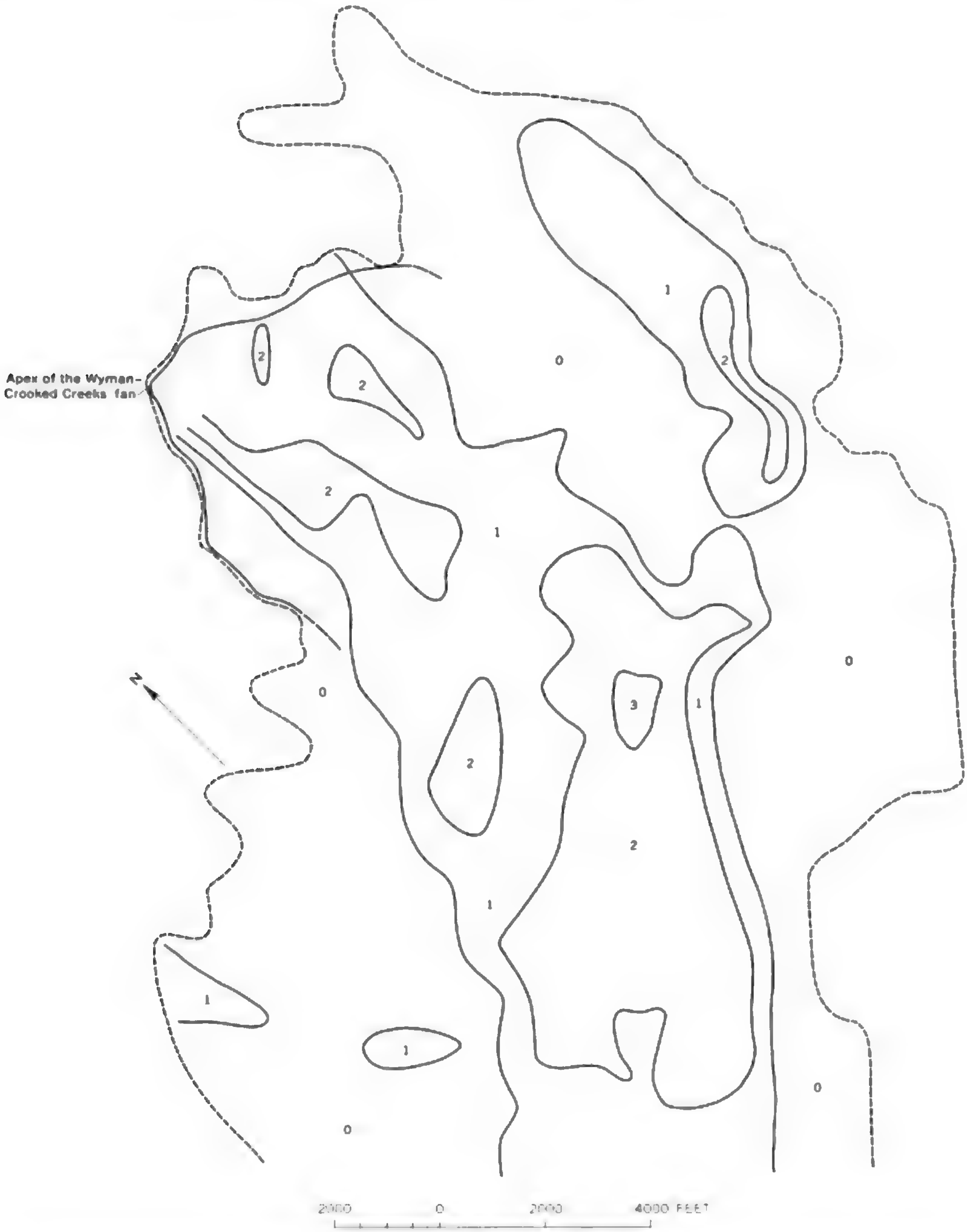

FIGURE 96.—Map showing mean pebble roundness in the north end of Deep Springs Valley. Dashed line represents approximate bedrock basin boundary. Isopleth values: 0=angular; 1=subangular; 2=subrounded; 3=rounded; 4=well rounded.

Digitized by Google

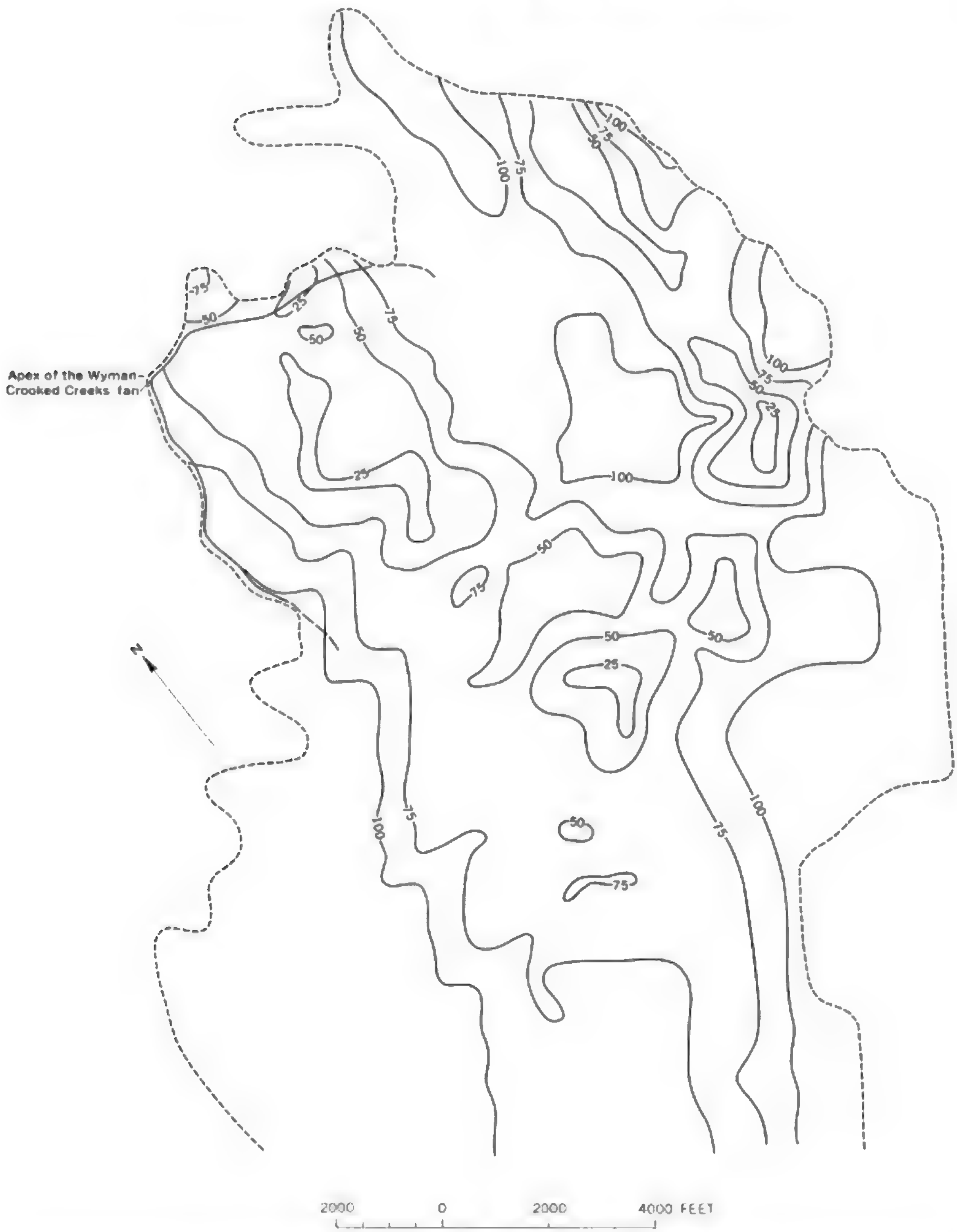

FIGURE 97.—Map showing pebble lithology in the north end of Deep Springs Valley. Dashed line represents approximate bedrock basin boundary. Values represent the percentage of plutonic rocks, including quartz and feldspar. Isopleth interval 25 percent.

766-976 O—65——4

Digitized by Google

FIGURE 98.—View of the basalt mass and small fan at the base of Piper Mountain. The roundness and lithology of pebbles in the north end of the valley are greatly affected by the basalt particles derived from this area. The lighter colored debris in the foreground is mainly granitic and is derived from the northernmost point in the basin, to the left of the photograph.

19 Antelope Springs channel samples, 13 were unimodal and 6 were bimodal. Granules again failed to occur as the modal class in the unimodal sediments. The secondary mode of 5 of the 6 bimodal samples, however, did coincide with the granule size class. If the frequency of occurrence of the 8 size classes as both primary and secondary modes is calculated, then one finds that granules occur more frequently than 3 and less frequently than 4 of the size classes. On this basis, therefore, granules are very nearly the median mode of the bolson sediments.

The basis for this calculation is arbitrary and results in an exaggeration of the frequency of modal occurrence of granules. Although the fact is frequently overlooked, modality is also arbitrary, however. Only a single sample among the 90 studied was unimodal when class intervals were chosen at half phi units; the remaining 89 samples were polymodal. Upon grouping weights to produce intervals in accord with the full phi units of the Wentworth size classification, however, the 37 unimodal samples discussed previously were produced. Because any classification of size must be considered arbitrary rather than natural, the obvious conclusion to be drawn is that the unimodal samples result from averaging of the data. Many of the bimodal samples could be transformed into unimodal distributions by setting the class intervals equal to 2 phi units. In the limit, of course, any sediment could be shown to be not only unimodal but of the same size class as any other.

A more pertinent factor than frequency of occurrence as a modal class, however, is the absolute abundance of granules. Their abundance in the granule-to-clay size fraction (fig. 99) ranges from 15 to 20 percent near the basin margin to the north and east and is slightly less on the western side, in the Wyman-Crooked Creeks fan area. This fact may reflect greater absolute transport distances for these sediments. At least 3–5 percent of this fraction consists of granules at any point in the center of the basin. Although this percentage is a maximum for the total sediment, because gravel has been omitted, it is pertinent to the observations of Yatsu (1959), who argued that the break in slope along the intersection of an alluvial fan with the valley floor coincides with the modal frequency break in the gravel-to-sand distribution referred to above. Granules should, therefore, be absent below this break in slope or in the central part of the basin. The evidence from Deep Springs Valley, however, suggests a decrease in abundance of granules toward the basin center but not their disappearance.

The granule high in the southwestern part of the area shown is difficult to account for, except as an actual "island" of granules. It will be shown below that the area between this high and the 25-percent granule high to the east is, in effect, a crossroad of sediment mixing in the basin. The seemingly anomalous high may therefore represent the sum of granule contributions from the northeast and eastern trends which has subsequently been isolated by a flood of finer sediments from the Wyman-Crooked Creeks system.

The decrease in abundance of granules within relatively short distances from source areas not only requires explanation but serves to refute the hydraulic answer provided by Sundborg (1956). Because transport of the surface sediments considered here is relatively infrequent, constant motion of the granule size class cannot be appealed to in the search for the cause. Selective sorting in a downfan direction might appear to be a likely alternative. The studies referred to by Pettijohn (1957, p. 47), however, treated ancient as well as recent sediments. If selective sorting of sediment is the general explanation for the reported scarcity of granules, then it is difficult to understand why granule concentrations are absent in ancient sediments; lag deposits would necessarily have to accumulate in some areas but, to the writer's knowledge, none have been reported in the literature. A mechanical theory, suggested by the data from Deep Springs Valley, is thought to be the most reasonable explanation.

About 80 percent of the granules examined was found to consist of polymineralic rock fragments; quartz and feldspar grains constituted the remainder.

Digitized by Google

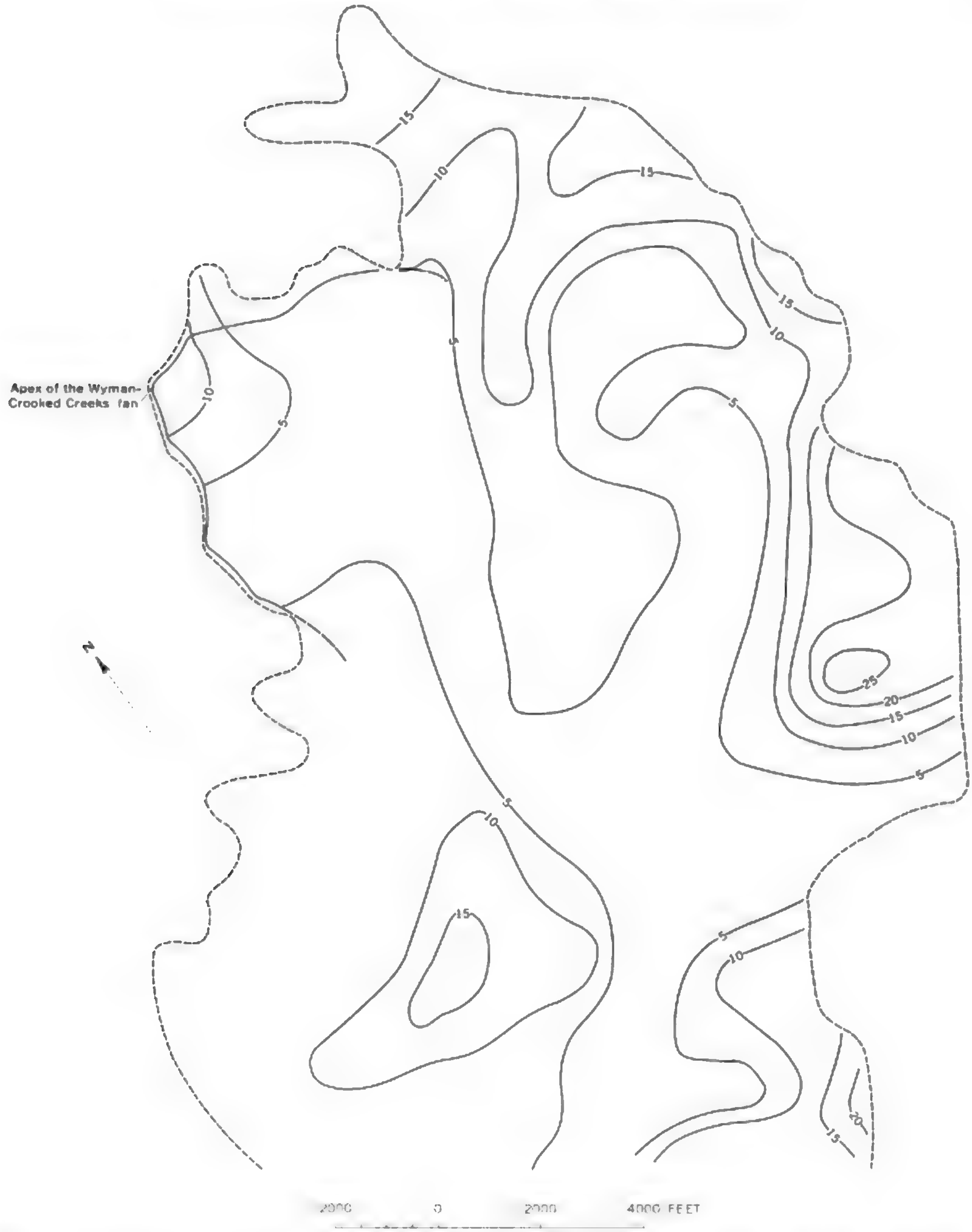

FIGURE 90.—Map showing the distribution of granules in the north end of Deep Springs Valley. Isopleth interval 5 percent by weight of the granule-to-clay size fraction

Digitized by Google

This implies that the plutonic rocks, which are the primary source of the clastic sediments considered, must consist of mineral grains that are predominantly less than 2 mm in size. The results of Dake (1921), who found that less than 10 percent of the quartz grains in plutonic rocks exceeded 1 mm in size, tend to confirm this implication. The fact that medium or coarse sand is the dominant size class in all of the unimodal samples studied, whereas granules are more abundant in the bimodal samples, suggests that the polymineralic granules are unstable aggregates of sand-size grains. These aggregates tend to disappear in nature by reason of rapid reduction to their components. The reduction is achieved by mechanical disintegration through weathering and is aided by periods of transport, however brief. The transition from polymineralic granules to sand-size components is accompanied by a consequent change from predominantly bimodal to unimodal frequency distributions. The deficiency of discrete mineral grains in the 2- to 4-mm size range in plutonic source rocks should be regarded as the fundamental cause of the relative scarcity of granules in nature.

SILT AND CLAY

The most striking single feature shared by all but 2 of the 90 samples studied is the scarcity of clay. The 2 exceptions will be explained below. The weight percentage of clay (table 3) in samples from the north end of the valley ranged from 0 to 6.37 and averaged about 2.0 percent. Samples from the Antelope Springs channel (pl. 9) range from 0 to 2.76 percent. Samples from Paiute Chute and the Owens Valley mudflow averaged about 2.5 and 3.0 percent, respectively. Although much care was taken in both collection and analysis of the samples, it is probable that some clay was lost. Because these weight percentages apply to the granule-to-clay fraction alone, however, the percentage of clay would be still lower if the total sediment provided the basis for calculation.

In contrast to the scarcity of clay, silt is very abundant. Silt occurred as either the primary or secondary mode in 31 of the 47 bimodal samples, referred to previously, and had the greatest modal frequency on this basis. The relative abundance of silt to clay is given in table 3. Noteworthy is the fact that even the thin atypical Wyman mudflow, which contained 17.38 percent clay, had a silt: clay ratio of more than 4 to 1. This ratio is in accord with those of the more typical samples from the Owens Valley mudflow (BP-1, BP-2) and Paiute Chute.

Because silt: clay ratios appeared to be consistent in the mudflow samples despite dissimilarity of the flows, it was thought that this variable might prove to be significant. Accordingly, the ratios for samples in the north end of the valley were plotted (fig. 100). Isopleths were not drawn for two reasons. First, it was apparent that four general areas occurred in which silt: clay ratios were markedly low in comparison to a relatively uniform and higher value elsewhere in the basin. Second, samples that contained no clay had, of course, infinite ratios. The path along which these infinite values occurred was recognized as that of the most frequent wind track observed in the field (p. 137). For these reasons the four areas of low ratio were outlined, and an average value was obtained for the samples that occur within each area. The same procedure was used to separate the remainder of the basin area into fields of average silt: clay values, as shown, and the inferred wind track was drawn along the path of 0 clay percent.

Several features of figure 100 are worthy of discussion. If the inferred wind track is followed as drawn, from the southeast corner northward, then the field of lowest silt: clay values in the basin (1.37) can be seen to lie in a reentrant to the right that is a natural depositional area. One of the samples within this field is 5, —1 which is one of the two exceptional samples noted above. The high clay content (26.58 percent) of this sample can best be explained by recourse to the wind deposition postulated.

The loop drawn in the inferred wind track to the northeast of the 1.37 field could not have been constructed exactly as shown from the data alone; the latter indicate only that the path must turn sharply to the left. A small incipient playa occurs precisely in this area, however. On several occasions, while in the field, gusts of wind approached this playa and circled it for a considerable length of time. The resulting windblown cloud of dust could be readily observed. The silt: clay ratios reflect this fact; high values encircle the playa and attest to the winnowing of clay, whereas much clay is present on the playa proper. The great bulk of Piper Mountain (pl. 8) apparently deflects the wind track to the west of the playa as shown (fig. 100); the remainder of the track is problematical. The field with average ratios of 4.44 may reflect both deposition of windblown clay along the elongate tongue pointing west and some contribution of clay from the northeast corner of the basin by runoff. The clays derived from the basalts in the northeast corner are well delineated by the 6.50 field.

The infinite value that occurs in the extreme north end of the basin is also interpreted as part of the wind track. Wind directions in this area were not noted in the field, however, and the track is arbitrarily shown leaving rather than entering the basin. Upon

Digitized by Google

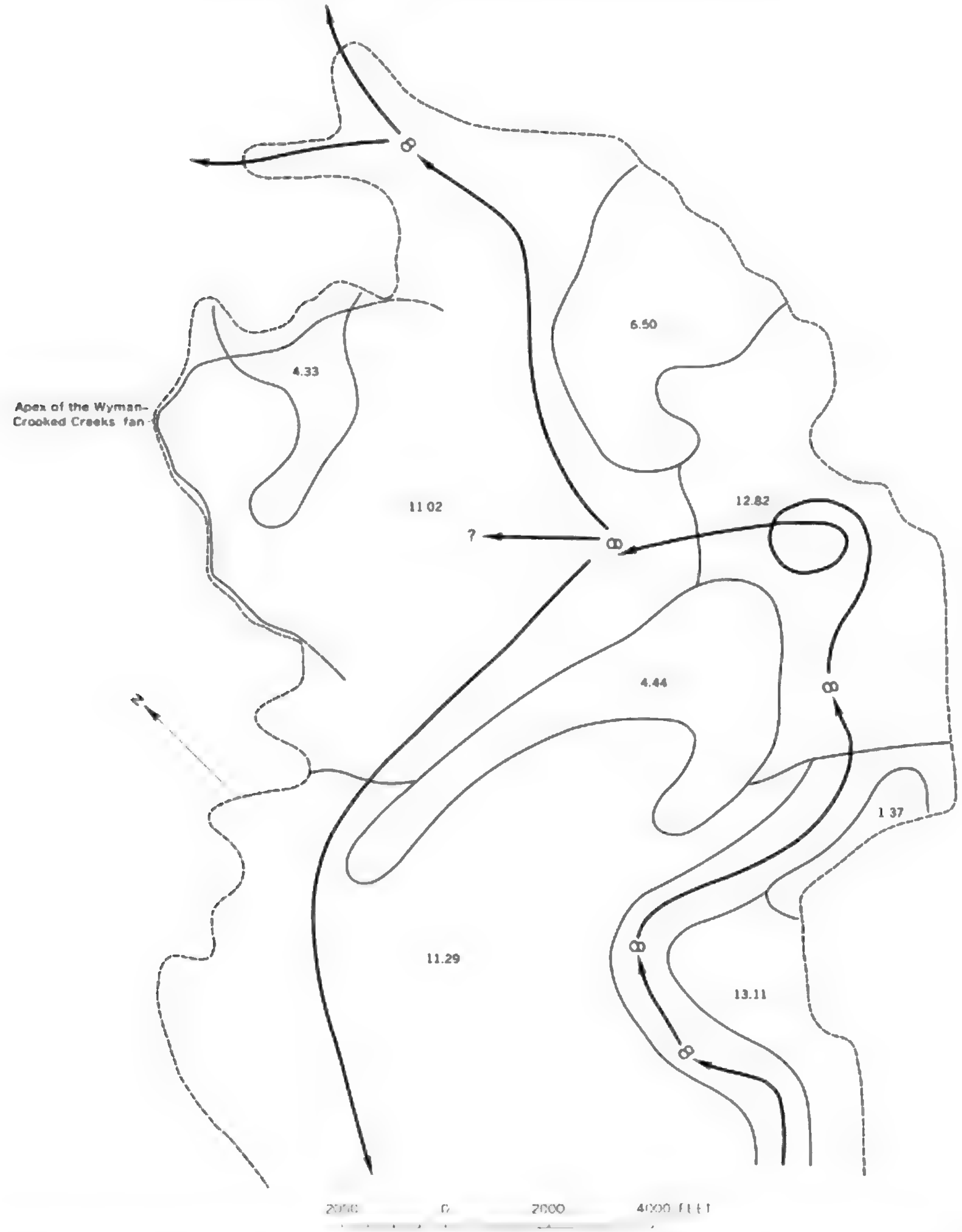

FIGURE 100.—Map showing silt : clay ratios and the inferred wind track in the north end of Deep Springs Valley. Values are means of sample ratios within areas shown. Infinite values occur along track.

Digitized by Google

occasion, the winds might equally well enter the basin along this route.

The remaining field of low silt: clay ratios (4.33) in the northwestern part of the basin is not thought to result from wind action. The basalt mass in this area (fig. 87) has probably contributed to the relatively high clay content represented by the field.

Samples from the Antelope Springs channel contain less clay, on the average, than do those from the north end of the valley or elsewhere (table 3). This may be attributed to the fact that much runoff occurs within the channel or that the rock types present do not weather as readily as basalt and granite. No consistent downchannel changes in clay abundance or in silt: clay ratios occur. This probably results from the fact that each zone of bankful deposition (pl. 9), to be discussed below, acts as a separate source area at various points in the channel system.

In summary, the study of silt and clay indicate that (1) clay is relatively scarce, whereas silt is abundant today; this is true not only for fan surface and channel samples but for mudflows as well; (2) silt: clay ratios reflect, in part, the effect of wind action, and in Deep Springs Valley the dominant wind track can be inferred from these ratios; and (3) wind action can affect the size distribution of basin sediments by reapportionment of the finer fractions.

PARAMETERS OF THE SIZE DISTRIBUTION

It should be apparent from the foregoing discussion of granules and silt: clay ratios that any attempt to characterize the granule-to-clay fraction in a bolson environment that ignores the tails of the frequency distribution is apt to be useless. The statistical measures used in this report were chosen, as noted above, because they encompass a reasonably large percentage of the total distribution of any given fraction and therefore reflect the variations in abundance of granules and silt and clay in the basin sediments.

Previous studies of the size distribution of sediments have treated beach, dune, and river sands in various combinations (Mason and Folk, 1958; Friedman, 1961). These studies have mainly sought to establish criteria for distinction between the environments cited, and they have met with varying degrees of success. The approach consisted of the determination of mean size, standard deviation, skewness, and kurtosis, followed by plotting of these variables against each other in one or more of the six possible combinations. In the present report the approach employed was to contour the areal distribution of each of the parameters. Certain of these maps have no parallel in the literature, to the writer's knowledge, and therefore cannot be compared with previous work. In addition, the granule-to-clay fraction has been treated as a distinct sedimentary unit, whereas the usual practice is to consider only the <2-mm fraction or else to treat the entire sediment if gravel and sand occur together. For this reason the absolute values (table 4) of the size-distribution parameters also cannot be compared with previous results. The treatment in this report, however, lends itself particularly well to both visual interpretation of the distribution of sediments and the geologic interpretation of skewness and kurtosis.

MEAN SIZE

The distribution of mean size of the granule-to-clay fraction in the north end of Deep Springs Valley is shown on figure 101. Because the contour interval is in phi units, the values are inversely proportional to mean size in terms of millimeters. It is instructive to compare this map with those of mean pebble size (fig. 94) and others and to note the approximate correspondence of closures or fluctuations. In figure 101, the large 2.0-phi closure on the Wyman-Crooked Creeks fan, the contour gap near the apex, and the size reversal along the northern edge of the fan all have their equivalents on the pebble map. This distribution probably reflects the fine sediment that is contributed from the basalt mass (fig. 87) at the basin margin. The silt: clay field of 4.33 (fig. 100) in this region and the location of the 5-percent granule contour (fig. 99) around the fan apex indicate that this is true.

Size fluctuation in the center of the pebble map (fig. 94), which bears resemblance to a pair of "sunny-side" eggs, is represented on figure 101 by the 1.5-phi reversal belt in the same location.

The flood of fine sediments contributed from the weathering of basalts in the northeast corner of the basin is roughly outlined by the linear 2.0-phi field on the right side of figure 101. This contribution was noted in discussion of silt: clay ratios and is shown on figure 100. There is also a general deficiency of granules within the area (fig. 99).

The zones of sediment mixing in the north end of the valley apparently result not only from the intersection of sediment transport paths, but they also reflect additional complications produced by wind action and the differing size contributions of individual rock types. The mean-size distribution (fig. 101) suggests that mixing occurs, but the map cannot reveal how or why without recourse to the additional data discussed.

Fluctuation of mean size in the Antelope Springs channel (pl. 9) is shown on figure 102. As noted above, each zone of bankfull deposition probably represents

Digitized by Google

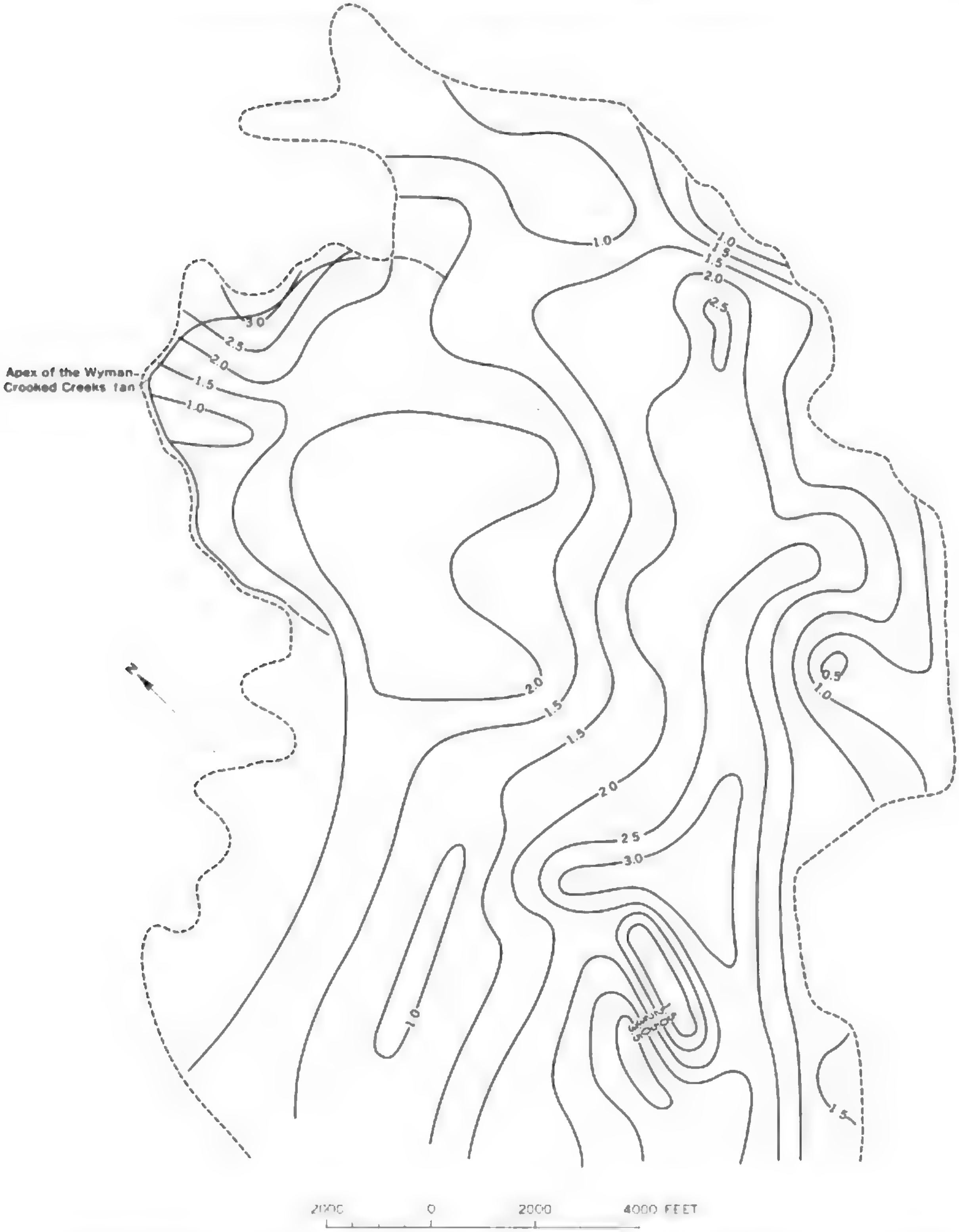

FIGURE 101.—Map showing the mean size of the granule-to-clay fraction in the north end of Deep Springs Valley. Isopleth interval 0.5 ϕ. $\phi = -\log_2 D$ (mm).

Digitized by Google

an individual source area for the respective reach below, and variation in mean size in a down-channel direction can be expected.

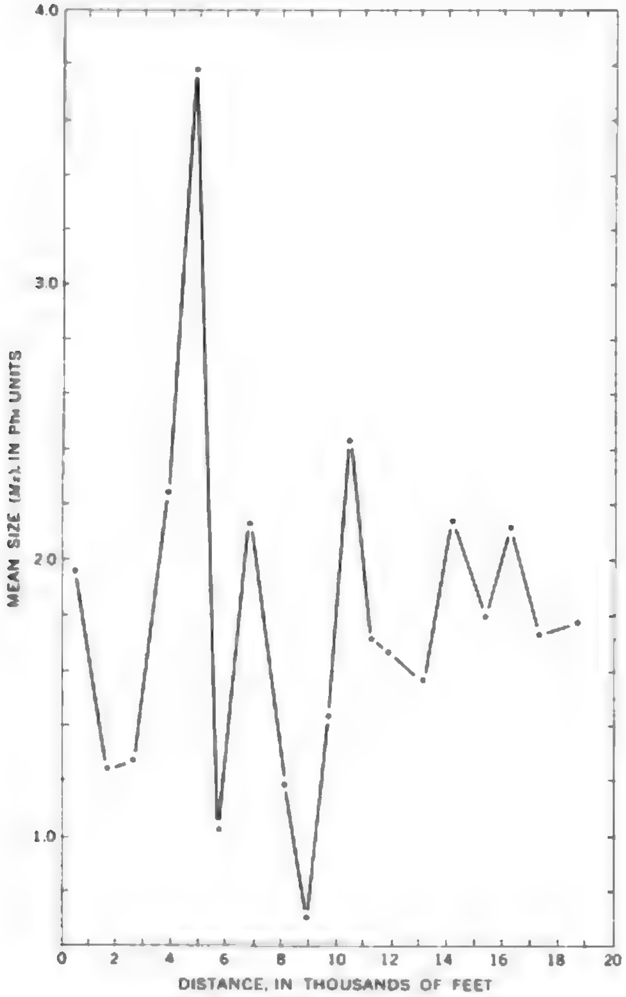

FIGURE 102.—Graph showing the relation of the mean size of the granule-to-clay fraction to distance from the fan apex in the Antelope Springs channel.

STANDARD DEVIATION

The inclusive graphic standard deviation (σ_I) of the granule-to-clay fraction in the north end of Deep Springs Valley is shown on figure 103. The degree of sorting increases down the Wyman-Crooked Creeks fan toward the basin center, from the northeastern rim of the basin. The map suggests that the more highly sorted material in the lower right corner, enclosed by the 1.9$\sigma\phi$ isopleth, may be derived from the Wyman-Crooked Creeks fan because of the accordance of trends. This was not implied by the mean-size map (fig. 101); the origin of the sediments in this area was indeterminate.

Sorting decreases to either side of the best sorted sediments, culminating in 2 belts of 2.7$\sigma\phi$, labeled A and B, but the reason is not evident from the map. If silt : clay ratios and the inferred wind track (fig. 100) are considered, however, then one explanation can be offered. The area of windblown clay deposition in the basin reentrant (1.37 field) is adjacent to one of these isopleths (A_1) on figure 103. The surface samples in the 1.37 field contain abundant fine material and are well sorted (1.5$\sigma\phi$). The belt of 2.7$\sigma\phi$ values to the left at A_2, however, lies just to the north of the inferred wind track, and the poorly sorted material in this zone might be expected because of the 3.1$\sigma\phi$ high that heads into this area from the northeast.

The other 2.7$\sigma\phi$ belt to the west (B) and the large adjacent 2.3$\sigma\phi$ field probably result from influx of clay (fig. 100) combined with the granule concentration (fig. 99) in this area. The distribution of mean size of both pebbles (fig. 94) and the granule-to-clay fraction (fig. 101) also shows high values in this part of the basin.

The data on granules and silt: clay ratios, which represent the tails of the granule-to-clay-size frequency distribution, show that standard deviation also reflects the complex mixing of sediments in the north end of the valley. Standard deviation, like mean size, cannot alone describe the distribution of sediment.

Standard deviation is plotted against distance from the fan apex in the Antelope Springs channel on figure 104. The data suggest a general downstream trend; standard deviation decreases from about 2.0 to 1.0$\sigma\phi$. This decrease accords with a disappearance of granules, the low abundance of clay, and the fact that most of the channel samples are unimodal. These factors may indicate that the sediments have been subjected to more frequent runoff than have those in the north end of the valley and therefore tend to become better sorted.

SKEWNESS

Inclusive graphic skewness (Sk_I) of the granule-to-clay fraction in the north end of Deep Springs Valley is shown in figure 105. The general appearance of this map, in contrast to those showing mean size (fig. 101) and standard deviation (fig. 103), is striking. The writer must confess that if he were confronted with such a map in the literature, the urge to test the validity of the contouring would be irresistible. The reader is provided with the opportunity to satisfy his own urge through access to the basic data in table 4.

The most important single feature of the distribution is the field of zero skewness. This defines more clearly than before the zone of sediment mixing in the basin because it reflects a balance between the tails of the frequency distribution. With recourse again to the granule (fig. 99) and silt : clay ratio (fig. 100) distribu-

Digitized by Google

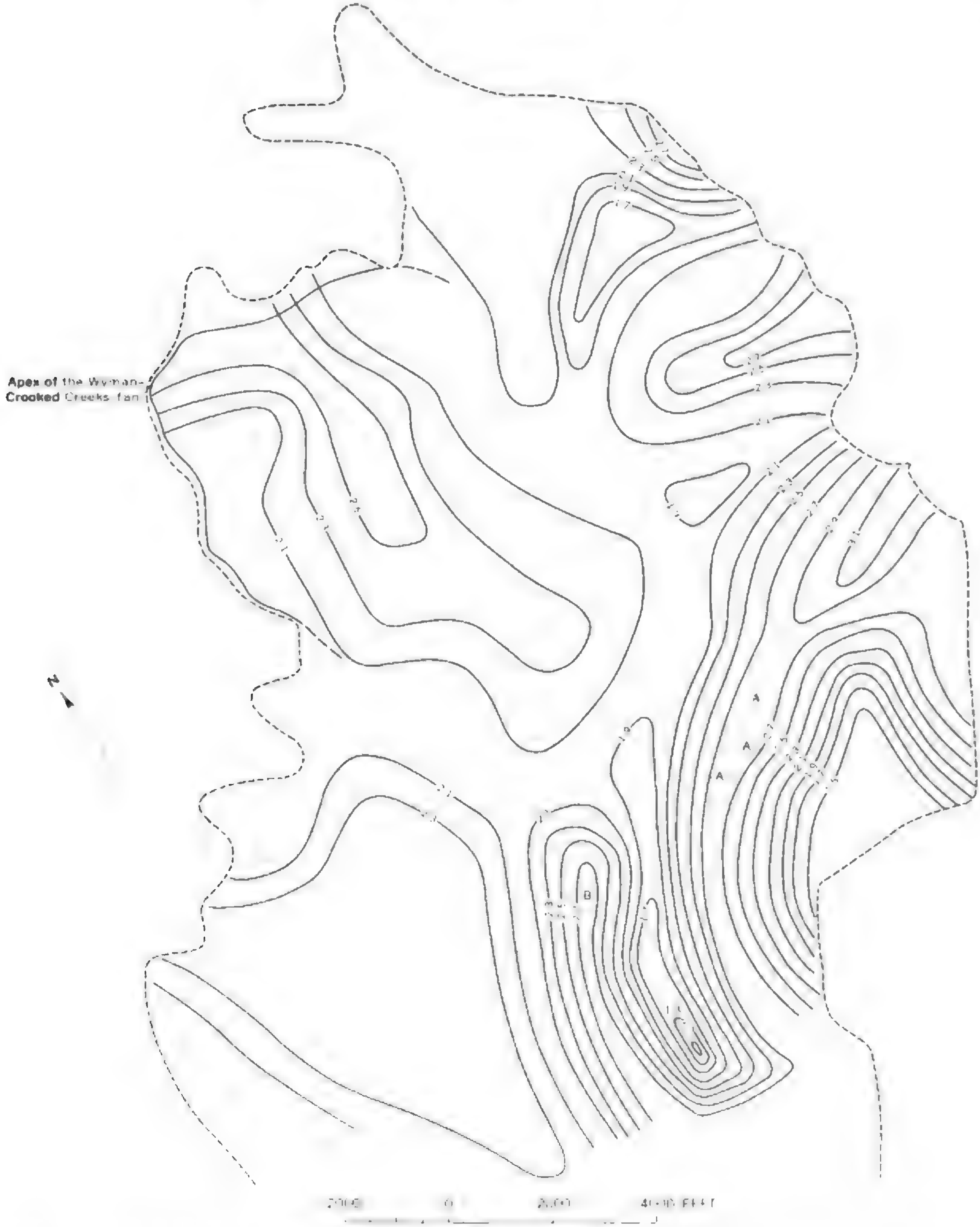

FIGURE 103.—Map showing the standard deviation of the granule-to-clay size fraction in the north end of Deep Springs Valley. The sorting of sediments in the regions labeled *A* and *B* is discussed in the text. Isopleth interval 0.2 $\sigma\phi$.

766-976 O—65——5

Digitized by Google

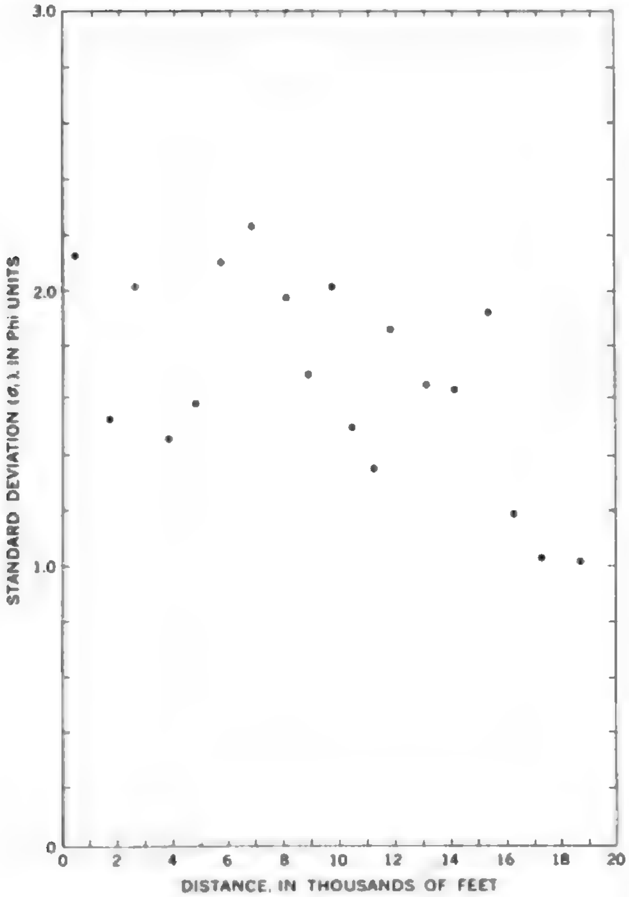

FIGURE 104.—Graph showing the relation of the standard deviation of the granule-to-clay size fraction to distance from the fan apex in the Antelope Spring channel.

tions, the skewness map can be seen to depict accurately the effects of mixing of sediments within the basin. High skewness values occur in areas where granules are abundant and decrease to zero where this size class either disappears or is balanced by an influx of fine-grained sediment.

Skewness of the granule-to-clay fraction in the samples from the Antelope Springs channel is shown on figure 106. Skewness ranges from +0.62 to −0.30. The channel samples are, on the average, only slightly positively skewed, and values fluctuate around +0.15, approximately. This might be expected in light of data previously provided; two-thirds of the samples are unimodal, and all have a high concentration of sediment in the medium-sand size class.

KURTOSIS

As defined in the discussion of basic data (p. 144), graphic kurtosis is the ratio of the spread of the tails of the distribution to that of the central portion. It is a measure of considerable sensitivity, and it was anticipated that kurtosis might prove useful in a treatment of bolson sediments, because the tails of the distribution are of primary concern. One would expect that the kurtosis distribution would complement that of skewness, because the latter reflects the relative balance of the tails whereas kurtosis reflects their relative abundance. This expectation has largely been satisfied; it will be shown by comparison of skewness (fig. 105) with kurtosis (fig. 107) distributions in the north end of Deep Springs Valley.

Kurtosis values are shown (fig. 107) in terms of departure from normality ($Kg = 1.00$) times 100. This means that the largest map value (85), for example, represents samples for which the spread from ϕ_5 to ϕ_{95} is 1.85 times as large as it would be for samples with normal kurtosis. It is evident that the belt of greatest departures on figure 107 cuts across the upper portion of the zero skewness field (fig. 105) in an east-west direction. This shows that although the tails of the distribution become balanced, the magnitude of the spread of the tails remains high and actually increases to the west. Consideration of the granule distribution (fig. 99) and silt: clay ratios (fig. 100) provides good reason for the location of the high kurtosis closure in the basin center; an abundance of both clay and granules occurs there.

The adjacent high kurtosis closure to the south, with a map value of 30, reflects the complexities of sediment mixing referred to above. These complexities include windblown clay deposition, the occurrence of granules and coarse sands contributed by the eastern reentrant, products of the weathered basalt from the northeast, and sediments derived from the Wyman-Crooked Creeks system. Kurtosis is sufficiently sensitive to the presence or absence of fine sediment in the basin samples to suggest that the inferred wind track (fig. 100) may be slightly mislocated as drawn. If the track were shifted slightly to the north along its reach between the 1.37 and 4.44 silt: clay ratio fields, then it would better coincide with the break between the two adjacent kurtosis highs of 85 and 30 (fig. 107).

The remainder of the inferred wind track need not be altered. It is interesting to note the support that each variable lends to the other. This would, of course, be predicted from theoretical considerations. The kurtosis low (−20) to the east of the two highs discussed above, roughly accords with the loop in the wind track (fig. 100) at the incipient playa. As the wind track is followed from the playa to the west and then south it coincides with a well-defined area of nearly normal kurtosis values that border the dominant (85) high. Another belt of high kurtosis values that extends from the northeast corner of the basin to its center is prob-

Digitized by Google

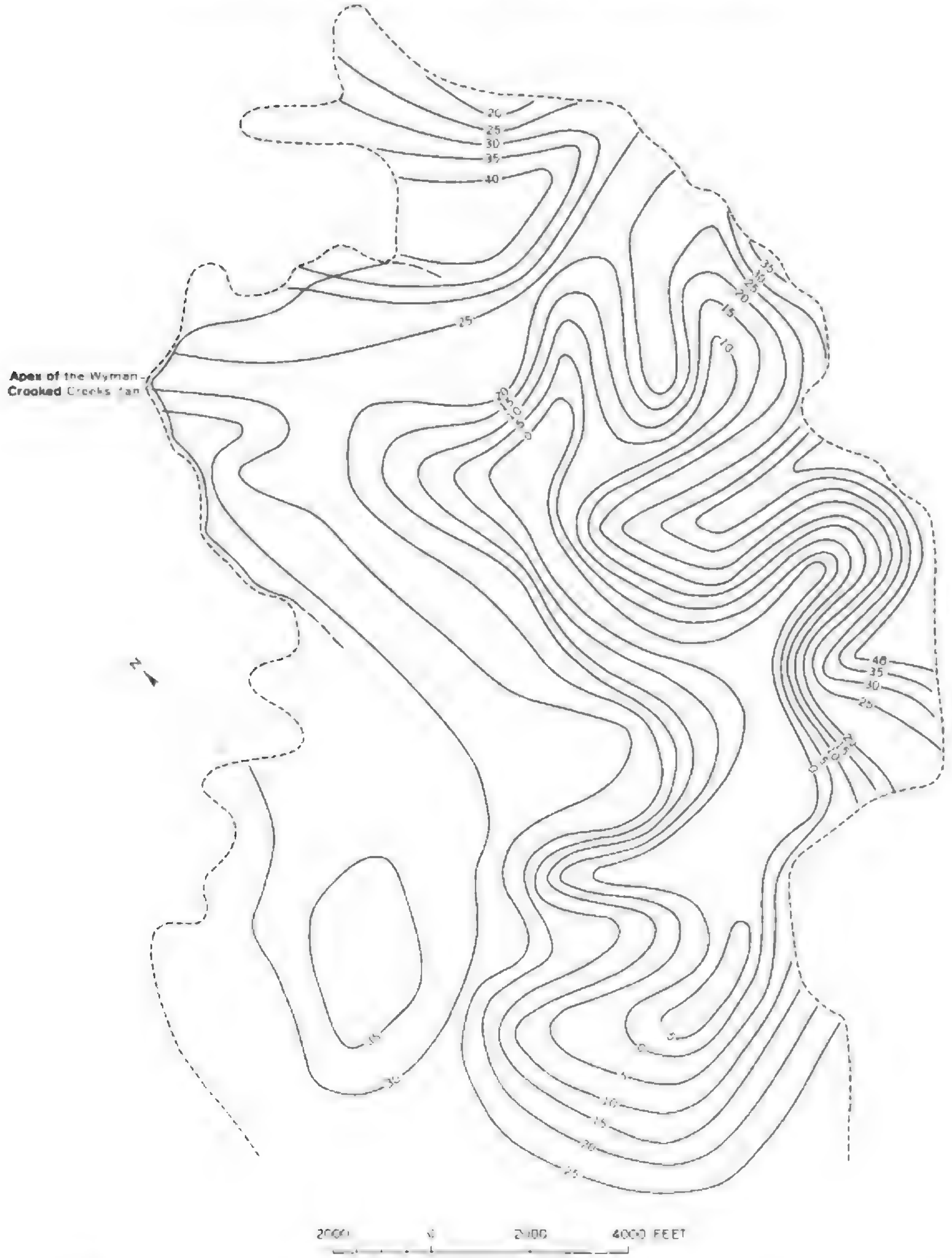

FIGURE 106.—Map showing the skewness of the granule-to-clay size fraction in the north end of Deep Springs Valley. Isopleth values=100×departure from Sk_I=0.0.

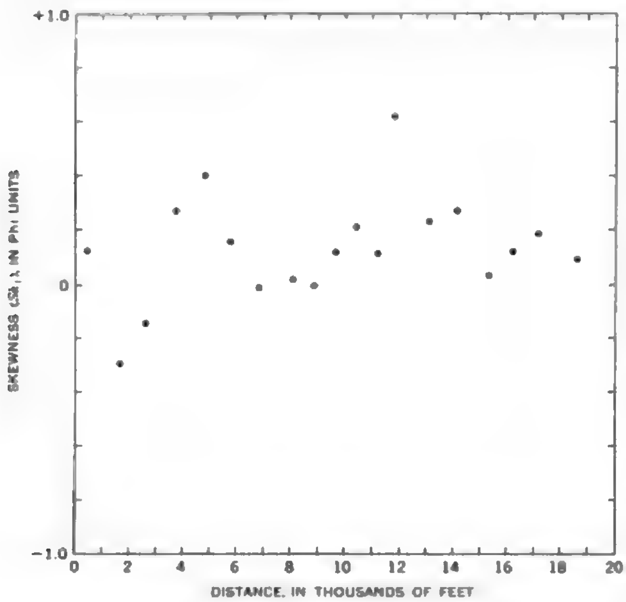

FIGURE 106.—Graph showing the relation of the skewness of the granule-to-clay size fraction to distance from the fan apex in the Antelope Springs channel.

ably a reflection of the merger between the granule tongue (fig. 99) in the upper part of the basin and the 6.50 silt: clay ratio field (fig. 100).

Finally, kurtosis values on the Wyman-Crooked Creeks fan are worthy of note. Despite the fact that the basalt on the north side of the fan (fig. 87) contributes fine sediment, as shown by both the mean size (fig. 101) and silt: clay (fig. 100) distributions, granules are relatively scarce (fig. 99) and this has produced low kurtosis values. The zero field ($Kg = 1.00$) accords with the fan limits in this region (fig. 107). In addition, kurtosis is the only parameter discussed thus far to suggest that the sedimentary trend of the fan is toward the east as well as toward the south. The probability that sediments from the Wyman-Crooked Creeks area were formerly transported to the east was mentioned earlier in connection with Pleistocene history. Sediment transport paths inferred from the tractive force data, to be discussed below, also support this contention. These facts also attest to the usefulness and sensitivity of kurtosis in the interpretation of clastic sediments in such an environment.

A scatter plot of kurtosis against distance downfan in the Antelope Springs channel (fig. 108) shows that within a wide scatter kurtosis decreases slightly, approaching normality near the end of the channel.

SUMMARY OF SIZE-DISTRIBUTION PARAMETERS

It has been shown that each of the parameters of the granule-to-clay fraction is a mappable variable and that useful information can be derived from such maps. The tails of the size distribution are of fundamental importance in the interpretation of bolson sediments because they have a marked effect upon the parameters. It is probable that significant quantities of granules and deposition or winnowing of fine sediment are common to all bolsons. The parameter maps and their implications should, therefore, have application to basins other than Deep Springs Valley and possibly to ancient sedimentary deposits as well.

The map of each of the four parameters of the size distribution required some knowledge of the distribution of the tails for satisfactory interpretation and, of course, all the maps are indeed interrelated. For this reason it is not possible to claim that certain of the parameter maps are of greater significance than others, but the reader of this report will probably agree at this point that the two orphans of basin studies, namely skewness and kurtosis, have been much neglected in the past. In addition to the merits of these two variables in investigations of sediment mixing, their absolute values may someday prove to be of significance. If competence is affected by the range of size of the sediment present (Fahnestock, 1961), then absolute kurtosis values are the best means of comparing range of size. Hence, the kurtosis of sediments should be considered in sediment-transport problems.

CLAY MINERALOGY

To determine the kinds of clay minerals present in the basin sediments and their relative abundance, 43 samples were studied. These include 18 from the Antelope Springs channel, 20 from the northern end of Deep Springs Valley, 2 from Paiute Chute, and 3 samples from mudflows. Two of the last were obtained from a mudflow that occurred in Owens Valley, west of Big Pine, Calif., on August 22, 1961. These samples are listed in table 6 together with their respective clay-mineral ratios that are discussed below.

Oriented clay aggregates were prepared on glass slides by sedimentation, and diffraction data were obtained from a Norelco X-ray diffractometer with automatic recording unit. The samples were initially run untreated; after saturation with distilled water a second pattern was obtained for each. All untreated samples exhibited one peak intensity corresponding to an interlayer spacing ranging from 14.21 A to 15.80 A. Saturation with water shifted this peak to smaller 2 θ values, indicating expansion. The expanded interlayer spacings ranged from 17 A to 20 A.

Because this paper is not devoted to an intensive quantitative study of clay mineralogy and because of the marked expansion with water noted above, glycolation was not deemed necessary. The mineral

Digitized by Google

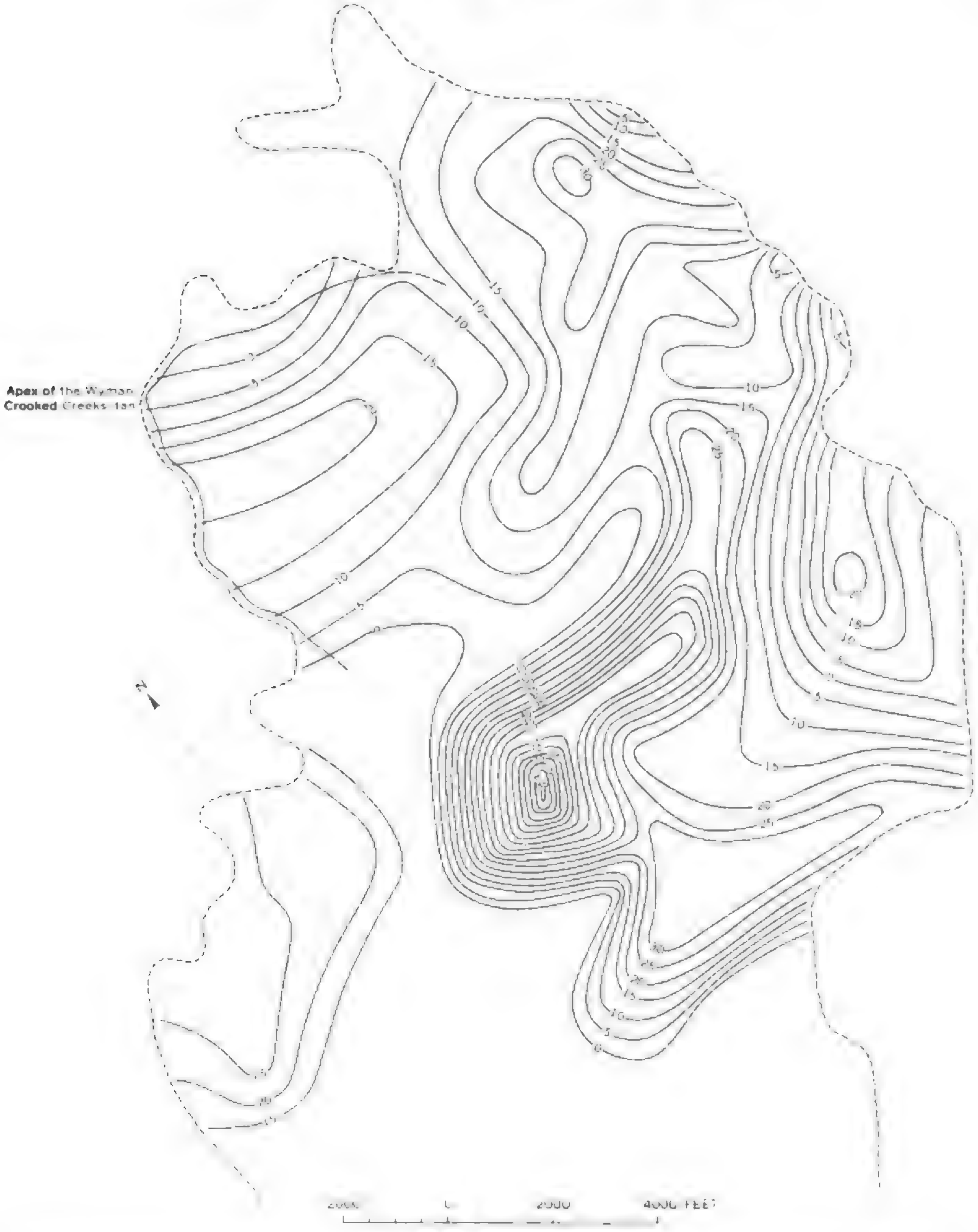

FIGURE 107.—Map showing the kurtosis of the granule-to-clay size fraction in the north end of Deep Springs Valley. Isopleth values=100×departure from K_G=1.00.

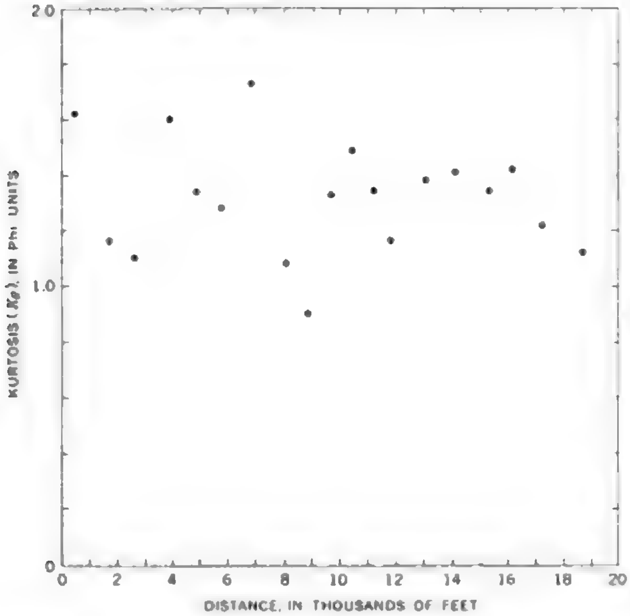

FIGURE 108.—Graph showing the relation of the kurtosis of the granule-to-clay size fraction to distance from the fan apex in the Antelope Springs channel.

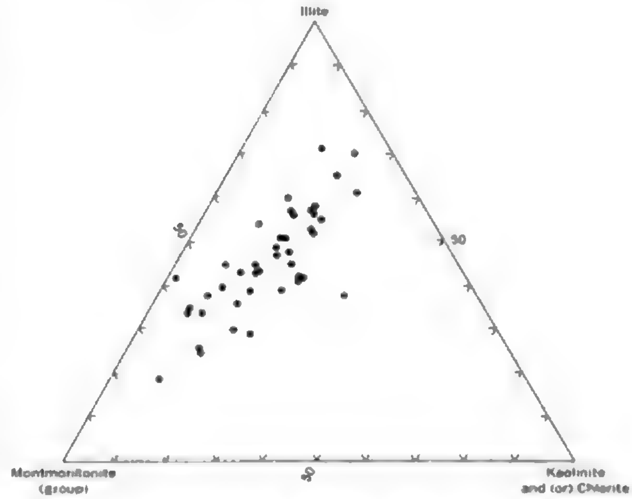

FIGURE 109.—Three-component diagram showing montmorillonite : illite : kaolinite and (or) chlorite ratios for 43 clay samples.

group that expands from 2 A to 4 A in the presence of water is designated as montmorillonite in the ratios presented. It should be stressed, however, that this designation undoubtedly includes various mixed-layer clay minerals. This is attested to by the lack of sharpness of many of the peaks and not uncommon base distance of about 4° 2 θ.

A nonexpanding clay mineral with an interlayer spacing of 10 A has been designated as illite and a second mineral, with a peak corresponding to a spacing of 7 A, as kaolinite and (or) chlorite. The separation of the (002) reflection of chlorite from the (001) reflection of kaolinite by heating or other methods was not attempted. It was noted, however, that no recognizable peak corresponding to 14 A was present after water saturation of the samples. This would suggest that chlorite is not very abundant in the samples studied; the fact that chlorite and (or) kaolinite is not abundant can be seen from the data (fig. 109).

To determine the ratio of montmorillonite: illite: kaolinite and (or) chlorite, as they are defined above, the integrated areas of the (001) reflections were determined by planimeter. These areas are linear functions of the weight percent of each mineral (Talvenheimo and White, 1952). Many factors will, of course, affect the reflection intensities. Among these are the polarization, Lorentz, and temperature factors, the degree of crystallinity, chemical composition, and others (Cullity, 1956). Because these factors have been ignored and because montmorillonite is defined on the sole criterion of expandability, the results presented must be regarded as approximations.

Weaver (1958) stated that a sample with equal amounts of montmorillonite and illite will yield an integrated intensity ratio of 3:1 in favor of montmorillonite. This result holds for 14 A montmorillonite; other ratios, varying with the montmorillonite interlayer spacing, have been published. As previously indicated, a montmorillonite group rather than pure 14 A montmorillonite is treated in this report. Because some value must be chosen, however, a factor of 3.0 was assigned for montmorillonite group spacings as wide as 14.9 A and 3.5 for spacings of 15.0 A and greater. Accordingly, planimeter measurements of the integrated intensity values for the (001) reflection of illite have been multiplied by 3.0, as appropriate, in order to arrive at the montmorillonite: illite ratios given.

Johns, Grim, and Bradley (1954) state that equal amounts of kaolinite, sedimentary chlorite, and illite will yield equal integrated intensities. The illite: kaolinite and (or) chlorite ratios can therefore be determined directly from planimeter measurements of the integrated intensities of the respective (001) reflections.

The montmorillonite (group): illite: kaolinite and (or) chlorite ratios, determined as described above, were recalculated to a base of 10 and used to plot the three-component diagram shown on figure 109. Despite the qualitative to semiquantitative approach employed, which renders the data valid only as a first approximation, two conclusions may be drawn from the diagram. First, a considerable range of montmorillonite: illite values exist despite the fact that all samples occur in

Digitized by Google

a relatively uniform climatic environment. This suggests a relationship between clay-mineral type and source-rock composition, which is to some extent borne out by the data. Samples exhibiting high montmorillonite: illite values occurred mainly in basalt-rich areas, whereas all samples but one from the Antelope Springs channel contained more illite than montmorillonite. The source rocks of the Antelope Springs sediments are complex, but they include no basalt. The suggestion that a correlation exists is supported by previous work.

Droste (1961) studied the clay-mineral assemblages in several California basins that are in the neighborhood of Deep Springs Valley. He found that the clay suites strongly reflect parent rock types; samples rich in montmorillonite often contained volcanic glass. Eardley and Gvosdetsky (1960) also reported the occurrence of abundant montmorillonite in association with an ash layer in their study of a core from the Great Salt Lake.

The approximate constancy and relative scarcity of kaolinite and (or) chlorite suggested by the data on figure 109 also agrees with Droste's (1961) results. In Deep Springs Valley the sum of illite plus montmorillonite in the average sample is about 80 percent.

Because of these facts, the writer was tempted to treat clay mineralogy in the same manner as other variables already discussed and map the distribution in the basin. The data obtained, however, are both too few and too approximate. In addition, recourse to mixing of clays by means of wind action in order to explain exceptions proved necessary in an initial attempt. For these reasons it was considered best not to proceed beyond the presentation on figure 109. Clay mineralogy might well prove to be a mappable parameter in many western basins, however, if detailed studies were undertaken.

SEDIMENT TRANSPORT

An important aspect of the transport of sediments on alluvial fans is the competence of the transporting medium. Although the occurrence of large particles on alluvial fans implies a high degree of competence, it should be borne in mind during the discussion that follows that the nature of the source rock is a factor of importance. The competence of the transporting medium may have been sufficient to move still larger particles than those seen on fans, had they been available at the source. It cannot be assumed, therefore, that the competence of transport was necessarily greater on fans that exhibit the largest particles.

COMPETENCE CONSIDERATIONS

Competence is usually equated with the velocity of flow, and the relationship is stated in terms of particle diameter. Leliavsky (1955, p. 24) states that the earliest formula was provided in 1753 by Brahms who employed particle weight rather than diameter; but the report of Suchier (1883), listing velocities required to transport particles of "pea," "hazelnut," and "pigeon egg" dimensions, is typical of several early treatments. Gilbert (1914) considered the transport of particles as large as 6 mm in diameter, as did Nevin (1946) who reviewed the competence problem. The basic competence curves of Hjulström (1935, p. 298) have been extended and modified to include the transport of cobbles (Menard, 1950) and boulders (Fahnestock, 1961). Menard's work provides some information on the velocities necessary to keep a moving cobble in motion, but these are not comparable to the velocities required to initiate movement. The study by Fahnestock has produced the most pertinent data; the particles considered were as large as 1.8 feet in diameter. It was found that these particles moved more readily than would have been predicted; this was attributed to the presence of a mixture of sediment sizes. Even the data of Fahnestock (1961), however, cannot be safely extrapolated to include particles from several to many times as large, that occur on alluvial fans. The use of any velocity power law is, therefore, best avoided.

As an alternative measure of competence, tractive force can be employed. This is expressed as $\tau = \gamma d S$, where γ is the specific weight of the transporting medium, d is the depth of flow, and S is the slope of the energy gradient. The tractive force thus defined pertains to the shear exerted on the upper layer of the bed material. The formula, or some variant thereof, is widely used in engineering studies and provides one of the few available means of obtaining an approximation of the competence of transport. It is used in this report because S and d can more readily be estimated than the velocity of flow.

It should be emphasized that, at best, only an approximation to the true competence of transport can be sought in the field. For this reason several slightly more sophisticated formulae have not been considered. The shear exerted upon a boulder in a channel bed, for example, might be determined from the relationship $\frac{F/A}{\rho r^2/2} = C_D$ (Rouse, 1950, p. 122), where A is the area of the projecting surface, normal to the direction of flow, ρ is the density and r the velocity of flow, C_D is a drag coefficient, and F is the force or shear exerted. Any attempt to substitute values for the density, velocity, and drag coefficient required, however, would

Digitized by Google

be a guess at best; such variables cannot be derived from field data.

Having chosen the simple expression $\tau = \gamma dS$, the main problem lies in equating field data with the required variables so that tractive force, or competence, can be determined. The key to a field approximation of tractive force is thought to lie in consideration of the largest particles. Several boulders contained pockets of pebbles, sand, silt, and clay on their uppermost side, several feet above fan surfaces. Because the finer sediment in these pockets is diverse in both lithology and size, it may represent a part of the sediment load that was transported together with the boulder and trapped upon cessation of the flow. Although later floods might have emplaced some of this sediment, this possibility seems more remote. The fan surfaces show no sign of subsequent floods; weathering stain or varnish extend down the sides of boulders to precisely the level of the fan surface on which they rest.

These observations suggest that either the depth of flow exceeded the diameter of the largest particle during transport or the finer sediment was acquired by the rolling of boulders through a shallower flow. Leopold and Miller (1956) state that cobbles moved in flash floods in arroyos even when the water was no deeper than half the diameter of the rolling object. On the other hand, the upper reaches of the Owens Valley mudflow (figs. 110, 111) clearly exceeded in depth the diameter of the largest particle. Depth of flow can therefore range from a lower limit of half the diameter of the largest particle to several times this value. Because a relationship exists, maximum particle size has been substituted for *d*, the depth of flow, in the tractive force expression. This value may be too low for the upper reaches of fans and too high for the lower reaches. It should be noted that this substitution cannot be made in areas that contain desert pavements, because in such areas the largest particles break down to smaller fragments and the original dimensions are therefore unknown.

The required slope in the tractive-force expression is that of the energy gradient, whereas the slopes measured in the field, by methods previously described (p. 141), are equivalent to bed gradients. Many measurements indicate that the bed slope is often a good approximation of the energy gradient, however. Moreover, efforts were made to measure a reach that corresponded with the most probable paths of sediment transport. Although local runoff may produce modification of slopes on fan surfaces, this modification might well consist of uniform lowering over a given reach. For these reasons the local slopes at each sampling point have been substituted for *S*, the slope of the energy gradient, in the tractive force expression.

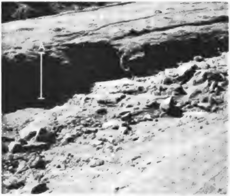

FIGURE 110.—Lateral view of the upper reach of the Owens Valley mudflow. The depth of flow at *A* was about 12 feet and exceeded the diameter of the largest particle that was transported. The mudflow has been dissected by a subsequent high-water stage; flowing water is visible below *A* and to the left of center. Note the dark color and viscous character of the mudflow deposit.

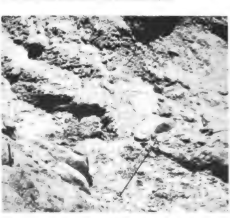

FIGURE 111.—View downstream in the upper reach of the Owens Valley mudflow. Much of the mudflow has been flushed from the channel by the turbulent water; the width of flow at *A* is about 5 feet. Openwork gravels may result from this process when subsequent high-water stages flush material in bankfull deposition zones.

Field values are believed to be better approximations of the slopes that prevailed during true flow conditions than values obtained from topographic maps.

The remaining variable is specific weight, or density times the acceleration of gravity. Because no single value for the density of a flow down an alluvial fan can reasonably be substituted in the tractive-force expression, this variable has been omitted. The tractive-

Digitized by Google

force approximation in this report consists, therefore, of computing dS products, which are directly proportional to tractive force. These products were computed for each sampling station, their distribution mapped, and the maps interpreted as reflections of the competence of the transporting medium. The actual tractive-force values can only be determined if one assumes an arbitrary value for the specific weight of the transporting medium.

DISTRIBUTION OF ESTIMATED TRACTIVE FORCE

The distribution of slope-maximum particle-size products, or estimated tractive force, in the north end of Deep Springs Valley is shown on figure 112, and the distribution on the Antelope Springs fan is shown on figure 113. The basic data are listed in table 1, and the location of sampling stations is shown on figures 90 and 91.

The spacing of isopleths of estimated tractive force on the Antelope Springs fan (fig. 113) is rather uniform and is only slightly less so in the north end of the valley (fig. 112). The size distribution of pebbles (fig. 94) does not accord with a uniform decrease toward the basin center, however, and the relation of maximum particle size to slope (figs. 92, 93) exhibits considerable scatter. Large particles occur more frequently in apex regions (p. 145), but they are by no means restricted to these areas, as attested to by the occurrence of boulders on playas. Unless an exceedingly gross contour interval is chosen, the distribution of the largest particles cannot be mapped. If the isopleths shown on figures 112 and 113 reflect the distribution of competence, then one is confronted with the fact that, although the decrease in competence downfan is fairly uniform, maximum particle size exhibits considerable fluctuation.

This anomaly requires explanation. If one stresses the fact that a decrease in the average maximum particle size occurs on fans in order to obviate the problem, then the question of why the average size should decrease, will arise. This could be answered by recourse to selective sorting, but the bolson environment is notorious for the poor sorting that occurs therein. The floods described by Krumbein (1940) and Sharp and Nobles (1953), for example, both produced poor sorting and an irregular decrease of size. Moreover, floods of sufficient competence to transport the largest particles present probably lie in the mass transport region of the sediment transport spectrum, for which a high degree of selective sorting is not characteristic.

It is possible that floods of variable discharge could transport sediment over correspondingly varied distances downfan, but this would still fail to explain the transport of large particles across regions of gentle or zero slope. It is thought that transport by density flows, attended by buoyancy and momentum effects, provides the most reasonable answer to the observed anomaly.

DIRECTIONS OF SEDIMENT TRANSPORT

If slope-maximum particle-size isopleths are accepted as an approximation of competence isopleths, then orthogonals to these contours should represent directions of sediment transport. This assumes only that competence should decrease in the direction of flow. Although an infinite set of orthogonals can be drawn through any isopleths, those orthogonals shown (figs. 112, 113) represent a logical choice because they were drawn through contour trends. After drawing these orthogonals, it became apparent that their paths correspond closely to the location of channels on the fans. Field notes confirmed this correspondence, but to test the predictability of the method, two additional areas were studied. Paiute Chute (fig. 88) is a small fan that contains a very obvious active channel. Traverses were made up the active channel to the fan apex and down the fan surface, following boulder trains and other features suggestive of a former flow path, north of the channel. Slope and maximum particle size were determined as before at 100-foot intervals along these 2 routes. Slope-maximum particle-size products and sample locations are shown on figure 114 and the basic data are listed in table 1.

Figure 114 shows that competence, approximated as before, decreases in a relatively uniform manner downfan. The data (table 1) show that the largest particle in the active channel occurred approximately at midfan in this instance. Estimated tractive force isopleths drawn for Paiute Chute would show a trend in the contours along the path of the active channel, because the values within the channel are greater than on the fan surface.

Two miniature deposits in Westgard Pass (pl. 8) were treated in a similar manner. Despite their small size, each contains a pronounced active channel, and estimated tractive-force data were obtained. Values along the active channels of these small fans are shown on figures 115 and 116, respectively, and the basic data are listed in table 1. Sampling stations were 5 feet apart, and slopes were measured by placing a Brunton compass on a board 1 foot long on the channel floors. One of the fans (fig. 116) was too small to allow a surface traverse, and the opportunity to chase a possible flood in another area interfered with completion of a surface traverse on the other (fig. 115).

Digitized by Google

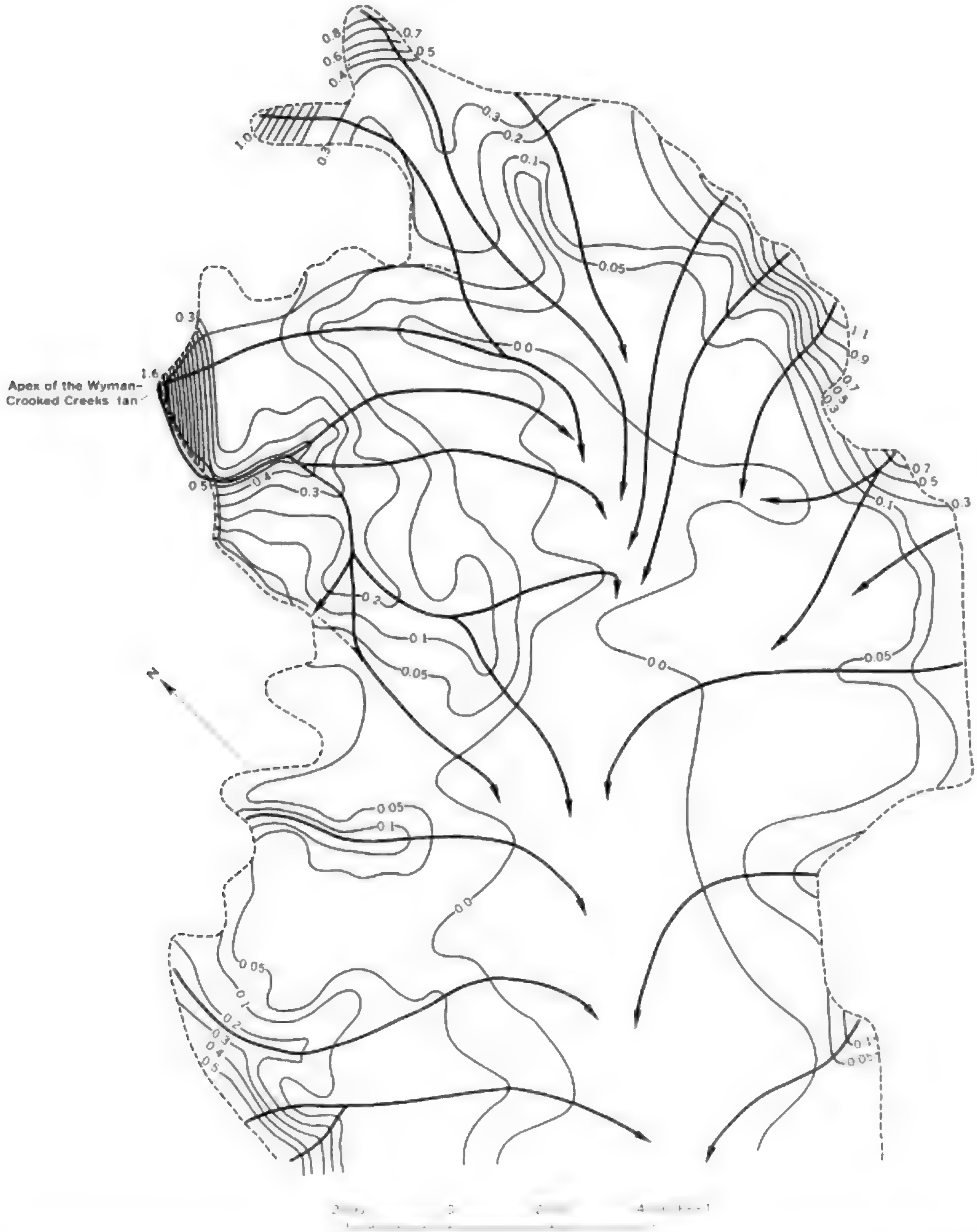

FIGURE 112.—Map showing estimated tractive force and inferred sediment transport paths in the north end of Deep Springs Valley. Isopleth values are slope-maximum particle-size products. Arrows indicate inferred paths of sediment transport. Dashed line represents approximate bedrock basin boundary.

Digitized by Google

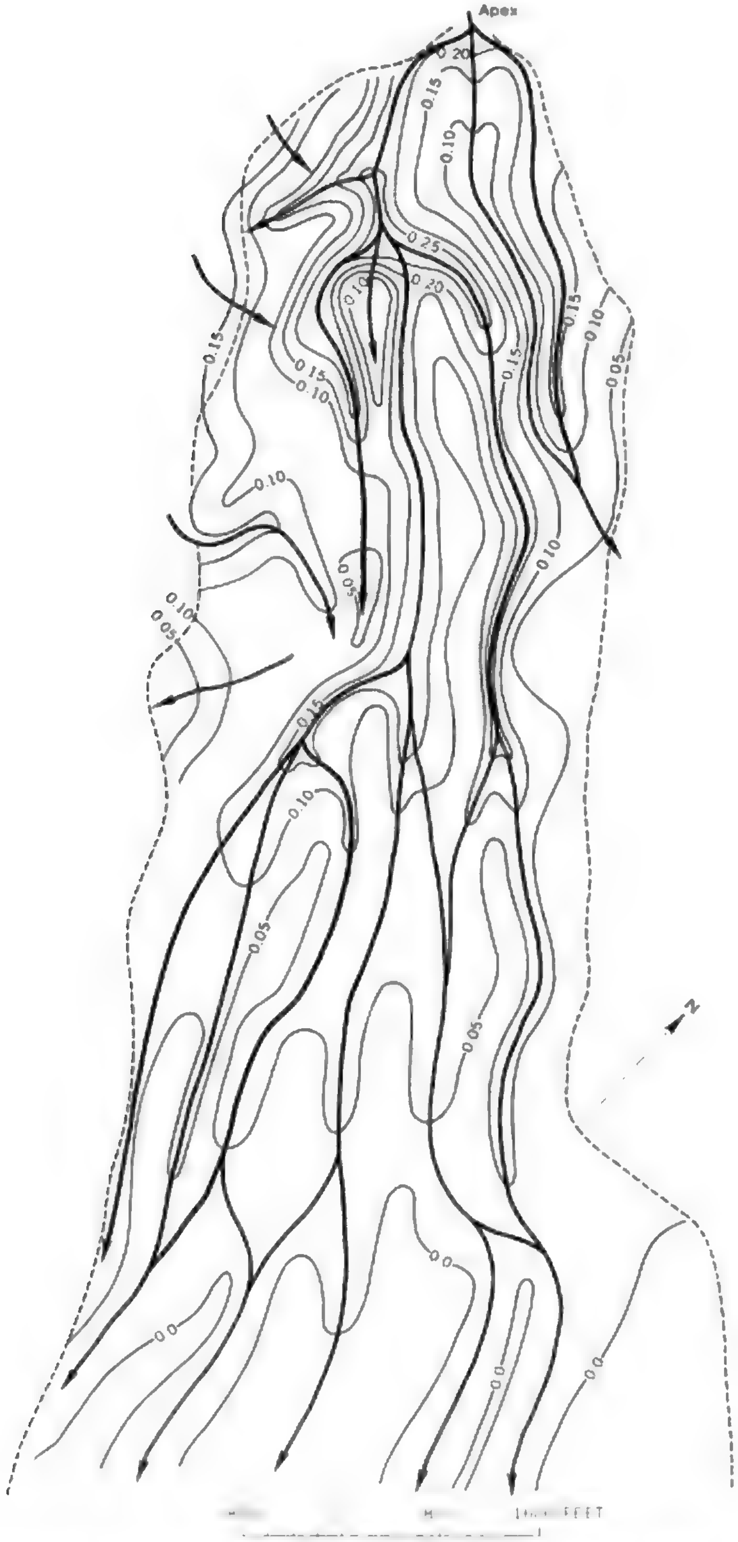

FIGURE 113.—Map showing estimated tractive force and inferred sediment transport paths on the Antelope Springs fan. Isopleth values are slope-maximum particle-size products. Arrows indicate inferred paths of sediment transport. Dashed line represents approximate fan boundary.

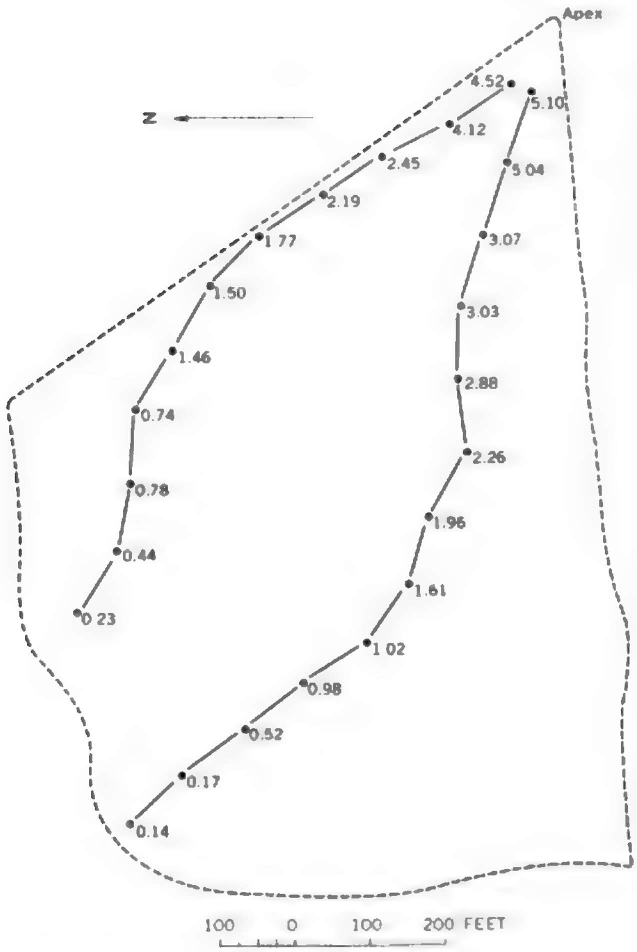

FIGURE 114.—Map showing the distribution of estimated tractive force on Paiute Chute. Values at the left were obtained from the fan surface at the indicated sampling stations; values at the right were obtained within the active channel. It is apparent that values in the channel are greater than on the surface. If estimated tractive-force isopleths were drawn, they would be convex downfan over the active channel.

The results show, however, that the values approximating competence again decrease downfan with greater regularity than does maximum particle size.

The evidence cited suggests that orthogonals drawn through estimated tractive-force isopleths delineate paths of sediment transport. Those orthogonals drawn through dominant trends in the contours coincide with active channels on alluvial fans, which are the most recent paths of sediment transport.

CHANNELS ON ALLUVIAL FANS

All the fans observed, both in Deep Springs Valley and in the neighboring basins noted above, contain channels that extend from trunk canyons far above their apex region to the middle or lower reaches of the fans. Channels are invariably entrenched and depths in the apex regions of the fans range from 20 to 200 feet below the surface. The sediment transported by modern floods is confined within these channels and can be readily distinguished in the field because of the color contrast with surface material. Regardless of actual color, the recent sediment is of lighter hue because weathering stain is absent; not only the more obvious channel on the Antelope Springs fan but parts of channels on adjacent fans can be distinguished by color contrast. (See fig. 85.)

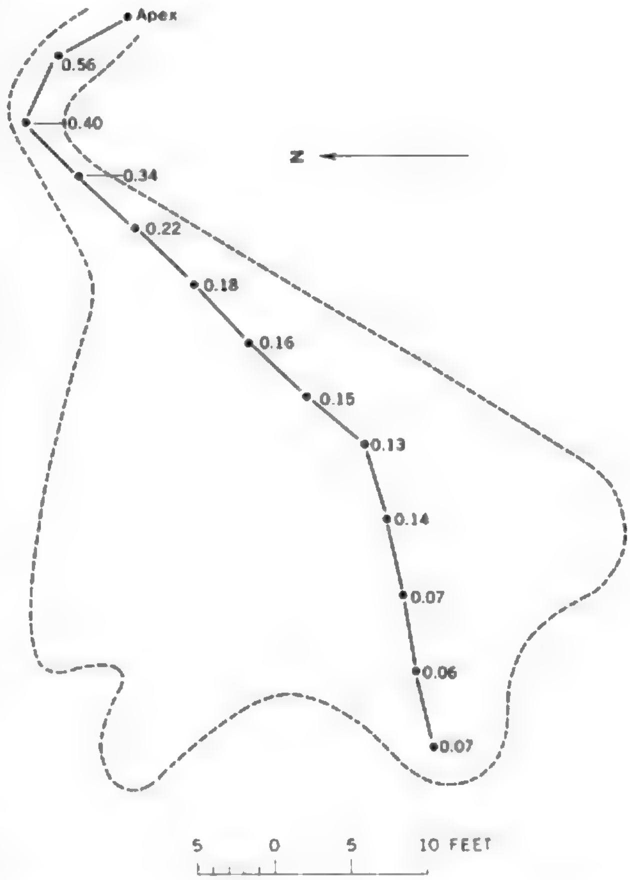

FIGURE 115.—Map showing the distribution of estimated tractive force in the channel of a miniature fan in Westgard Pass. Although the values fluctuate slightly, they decrease downfan far more consistently than maximum particle size.

Because recent sediment transport has occurred along entrenched channels, no material has been added to the fan surfaces "at the mountain front" on any fan. From a purely qualitative viewpoint it is impossible to observe this and conceive that this state of affairs has always obtained; the modern process must differ in

Digitized by Google

kind from that of the past. Further visual evidence is provided by the terraces that occur within the trunk canyons above fan apexes. These extend back into the mountains over distances on the order of miles and in some instances to the divide areas. The low terraces shown on figures 117 and 118 are about 1 mile above the apex region of the Antelope Springs fan. In the general vicinity of the mountain front, the highest terrace level present is continuous with the fan surface below; this is true for all fans. The aerial view of the Antelope Springs apex region (fig. 119) illustrates this continuity. The higher of the two terrace levels that occur on the right side of the channel in the photograph is clearly identical with the level of the fan surface. The hanging fan seen at this point will be discussed below. The two levels on the right side of the channel are more evident in a ground view (fig. 120). The terrace relationships within the Antelope Springs drainage system are similar to those observed elsewhere in the Basin and Range province by the writer, and these relations suggest that at some former time aggradation took place within catchment areas as well as on the fan surfaces. Degradation has occurred since that time, however, and the loci of deposition have shifted far downfan.

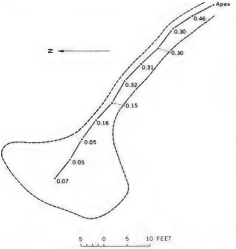

FIGURE 116.—Distribution of estimated tractive force in the channel of a second miniature fan in Westgard Pass. Although the values fluctuate slightly, they decrease downfan far more consistently than maximum particle size.

FIGURE 117.—View of the Antelope Springs channel, 1.5 miles above the mountain front. Note the terrace at *A*, about 8 feet above the bed along the right bank of the channel. This represents the former level of aggradation within the catchment area; it is continuous with the fan surface, below the mountain front. The heterogeneous character of the channel sediments and the occurrence of uprooted trees and shrubs are typical of the active channel.

FIGURE 118.—View of a low terrace in the Antelope Springs channel, 1 mile above the mountain front. Note that bedrock has been exhumed by channel cutting and that the part of the dipping strata below the terrace level is lighter in color than that above, which is weathered. The height of the low terrace is about 2.5 feet.

The active channel on the Antelope Springs fan (pl. 9) was mapped in its entirety and may be used as an example to substantiate this conclusion. The areas designated as zones of bankfull deposition represent the only parts of the fan where recent sediment has actually attained the level of the fan surface. At all points above the first bankfull zone, sediment has clearly been removed and not added. The low terrace

Digitized by Google

FIGURE 119.—Aerial view of the apex region of the Antelope Springs fan. Note the hanging fan (outlined) that is formed by the fill in the small tributary canyon to the right. Its surface is continuous with that of the Antelope Springs fan and with terraces farther upstream. The abandoned braided channels, visible on the fan surface in the foreground, are at a higher elevation than the floor of the active channel.

near the fan apex has a cover of sage and other vegetation, and the surface sediment exhibits a weathering stain. A view of this terrace in section near station 9 is shown in figure 121. A few hundred feet below station 9 and on the opposite side of the channel, this low terrace has been removed by erosion within the active channel. The fact that the active channel has indeed been deepened in the apex region is suggested by the abandoned channels (pl. 9) with floors at the level of the low terrace. Other abandoned channels, farther downfan, are visible in the aerial view of figure 119. It is apparent that the floors of all the abandoned channels, although below the fan surface, are at a higher elevation than is the floor of the active channel. This can also be seen on the Wyman-Crooked Creeks fan. The aerial view (fig. 87) shows several meandering and braided channels that are abandoned; the active channel is incised to a depth of about 40 feet below their floors. The ground view (fig. 122) indicates that the area occupied by the abandoned channels may again represent the level of a low terrace, as on the Antelope Springs fan, because there is a higher accordant level that was not apparent from the air.

The deposition that occurs today on the Antelope Springs fan is restricted predominantly to those areas at and below the first zone of bankfull deposition (pl. 9). It does not occur in widespread sheets over this entire area, but in various transitory locations that depend upon the migration of braided channels. The aerial view of the fan (fig. 85) clearly shows the point at which extensive braiding begins; this point corresponds to the location of station 126 on plate 9. The various channels that head in the bankfull depositional zones may result from the high-water stages that follow

Digitized by Google

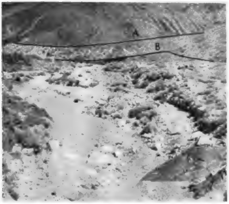

FIGURE 120.—View of the hanging fan above the Antelope Springs channel. The surface level of the hanging fan (*A*) is continuous with the higher of the 2 terraces that are present and is about 25 feet above the floor of the active channel, which terminates the fan. The low terrace is labeled *B*. The bedrock in the lower right corner of the photograph has been exhumed.

FIGURE 121.—View of the low terrace at station 9 in the Antelope Springs channel. Note the alternation of beds of coarse and fine sediment in the terrace, which is about 5 feet high. The largest particles on the floor of the active channel generally exceed the size of those present in the banks and on the fan surface in this area.

FIGURE 122.—Ground view of the Wyman-Crooked Creeks fan. The accordance of the surface of the ridge at *A* and the top of the low hill at *B* suggests that these may be remnants of a former continuous level. The active channel follows the base of the ridge at *A* and is incised to a depth of about 40 feet, below the general level seen in the foreground.

FIGURE 123.—View downfan at the bankfull deposition zone above station 126 on the Antelope Springs fan. There is a tendency toward convexity of profile in this region. The dissecting channel in the center of the photograph heads abruptly in the gravels, which are at, or slightly above, the elevation of the fan surface.

on the heels of mudflows (figs. 110, 111) and may be enlarged by seasonal runoff. Valley precipitation, as previously discussed, is probably insufficient to produce these features. The view downfan at station 126 (figs. 123, 124) shows the abrupt occurrence and rapid enlargement of one such channel. Two other channels, heading in the bankfull deposition zone just above the highway (pl. 9), are shown at the point of contact with the gravels in figures 125 and 126. The gravels are commonly openwork to considerable depth. Relatively clear water, flowing across and through these depositional sites, can account for both the winnowing of finer sediment and the fluctuation in mean size of the granule-to-clay fraction (fig. 102) noted above.

The last zone of bankfull deposition (fig. 127) is opposite station 318 (pl. 9) and clearly indicates that coarse debris has been transported far downfan in recent time. It is probable that deposition in the mid-

Digitized by Google

FIGURE 124.—Closeup view of the channel beading in the bankfull deposition zone at station 136. Note the rapid enlargement of the channel over a short distance and the convexity of profile.

FIGURE 125.—View of gravels, winnowed of fine sediment, on the Antelope Springs fan. The largest particle visible is about 4 feet in intermediate diameter. Note the poor sorting of the gravels and the abundance of finer sediment in the foreground, suggesting winnowing.

FIGURE 126.—View of a small plunge pool at the contact between a dissecting channel and the bankfull deposition zone above the highway. An abrupt break in profile at the contact is typical; here the plunge pool is about 2 feet deep. The fresh light-colored debris in the right background is slightly above the level of the fan surface.

FIGURE 127.—View of the bankfull deposition zone near station 318 in the Antelope Springs channel. This fresh deposit is slightly above the general surface level. It represents sedimentation at the lower limits of the fan that tends to build it outward, into the valley proper.

dle and lower reaches of the Antelope Springs fan and degradation elsewhere is typical of most fans in the region today. This fan is entrenched only to a small extent in comparison with larger fans that contain channels as deep as 200 feet; and yet, abandoned channels and terrace levels occur as described. If the catchment and apex region has been subjected to degradation and if deposition occurs predominantly below midfan today then this fan is not being built up by modern processes in a manner suggested by the usual view of fan building. The question to be answered is "Why has trenching of fans occurred between the divide areas and midfan?"

CAUSE OF TRENCHING

The occurrence of trenches in alluvial fans is a fact noted by many authors, certain of whom have discussed

Digitized by Google

the results produced by trenching rather than its cause. Eckis (1928), for example, thought that a geomorphic cycle was involved and that the onset of trenching signaled the beginning of the end for the fans. Buwalda (1951) considered the more effective transport of sediment to be expected, arguing that the trenches would act like flumes and funnel material downfan. Many authors have offered the view that deposition will occur where the trenches end and the width : depth ratio increases. This truth has little bearing upon the cause of trenching of alluvial fans, however. Two possible causes will be considered here, tectonic movements and variation in tractive force.

TECTONIC EXPLANATION

Tectonic explanations for a variety of phenomena have been invoked in local studies within the Basin and Range province and elsewhere. The trenching of fans referred to in this report, however, is extremely widespread and requires a regional rather than local explanation. If uplift induces downcutting, then approximately synchronous movements of most of the ranges in the Basin and Range province must be invoked to explain the trenching of fans. Even where uplift can be demonstrated for an individual range, however, several difficulties emerge from direct cause-and-effect correlation of uplift and the trenching of fans.

The tectonic hypothesis is predicated on the concept that uplift will increase channel slopes and the velocity of flow, thereby inducing erosion or degradation. The actual increase in slope that can occur from a given uplift is seldom cited, however. If the White Mountains (pl 8.) are used as an example, the calculation is instructive.

The range is about 20 miles wide, and the relief is roughly 5,000 feet. An approximation to the overall slope, from the divide to a fan apex, is therefore 0.094 foot per foot. The actual channel slope will exceed this value near the divide but will be less than this value near the mountain front. If an absolute uplift of 1,000 feet occurred instantaneously, this value would become 0.113, an increase of 0.019 foot per foot. This is a rather small increase in view of the extreme uplift conditions postulated. Epply (1961) has shown that even the most severe earthquakes with high Mercalli intensities are usually associated with throws along faults of no more than about 30 feet. The effect of the average uplift upon slope will therefore be extremely small.

Moreover, velocity and slope are related by the Manning equation, namely, $v=\frac{1.49}{n}R^{2/3}S^{1/2}$, where v is velocity, R is the hydraulic radius, and S is the slope. The exponents in this equation show that changes in the hydraulic radius, which is a function of discharge, have a greater effect upon velocity than changes in slope. In addition, it has been pointed out by many authors that velocities are not necessarily high in the mountains, where steep slopes occur. The mean velocity of rivers, in fact, tends to either increase or remain constant in a downstream direction (Leopold, 1962). This would be expected because drainage area and, consequently, discharge, both increase downstream.

It is true that local fault scarps can produce a nickpoint that will retreat through time, but aside from other considerations, this explanation for trenching would again require simultaneity of tectonic activity on a regional scale. It is probable, therefore, that the main role to be ascribed to tectonism in regard to trenching is the change induced in the pattern of precipitation and vegetation, both of which vary orographically and can affect the processes under discussion. Magnitudes of uplift cannot be directly equated with sedimentation or erosion. The cause of trenching will be further pursued by considering the implications of the tractive-force distribution.

TRACTIVE-FORCE EXPLANATION

The sediment transport orthogonals (figs. 112, 113), which coincide with fan channels, generally intersect estimated tractive-force isopleths where they are convex downfan. Because the estimated tractive-force values decrease downfan, this means that tractive force within the channels is greater than at adjacent points on the fan surfaces. This was shown to be true for Paiute Chute (fig. 114), for example. Because modern floods are confined within the channels, the tractive force associated with the modern process must be greater than that which accompanied transport in the past. If this is true, then one or more of the three component variables that comprise tractive force must be greater today than in the past.

Of the three component variables, it might appear that deviation of past and present slope would be simplest to ascertain. If an active channel is traced downfan, then a point will eventually be reached at which the slope of the channel intersects the fan surface; this is a zone of bankfull deposition (pl. 9). It would not, however, be correct to conclude that the slope today must be less than in the past, because the slope in question is that which obtained before deposition in these zones. The deposit is itself an indication of change in process. The information desired is whether change in slope altered tractive force and therefore initiated the trenching indirectly. In this

Digitized by Google

sense the answer is indeterminate but field observations suggest that the slopes of the channels do not markedly differ from those of fan surfaces, except in the vicinity of zones of bankfull deposition.

The depth of flow may be greater today than in the past, if the depth of the confining channels or trenches is accepted as a criterion. This would imply greater discharge and a correspondingly greater tractive force in the channels. The fact that former lakes throughout the region are today playas, however, suggests that the discharge of modern floods is probably less than floods of the past. The modern floods, in fact, may be misfit (Dury, 1958) in relation to their confining trenches in the upper reaches of fans; evidence of overbank flooding in the vicinity of the mountain fronts is generally lacking. Moreover, if an increase in tractive force initiated trenching, then selection of depth of flow as the responsible variable would be equivalent to attributing both cause and effect to this factor.

The remaining component, specific weight of the medium, can be considered in terms of density. If the density of the average flow is greater today than in the past, then mudflows should be a more frequent mechanism of transport. Observations suggest that this may be true. It remains to be proved that sound reasons exist for postulating that a contrast in density characterizes the difference between the modern and former processes. The tractive-force hypothesis, however, can be summarized at this point. The implication of the maps of estimated tractive force is that the modern process is attended by a greater tractive force than that of the past. Greater tractive force provides a logical explanation for the cause of trenching; simply stated, the explanation is that the shearing stress on fan surfaces increased at some time in the past. The stress was produced during sediment transport, and each effective flood deepened the channels until the designation "trench" could more fittingly be applied; this is still true today. Although a combination of factors may have brought about the increase in tractive force, an increase in the density of flow, including buoyancy effects, is thought to be an important cause. The evidence for this suggestion will be considered in the following discussion.

CONTRAST BETWEEN THE MODERN AND FORMER PROCESSES

MUDFLOWS

Descriptions of mudflows, the magnitudes of the particles transported, and descriptions of attendant features such as levees, have been provided by Rickmers (1913), Pack (1923), Blackwelder (1928), Sharp (1942), Wooley (1946), Kesseli and Beaty (1959), and several others cited in this report. Such information is common knowledge today, but the important question is whether mudflows actually cut channels by reason of their high density and consequent high tractive force. Most reports convey the impression that mudflows serve only to build fans, but some information to the contrary does exist in the literature. This is worthy of stress because it is germane to any discussion of past and present processes.

A statement by Wooley (1946, p. 78) is revealing:

> The mudflow of 1938 scarred the surface of the fan in a course 60 to 125 feet wide from the apex down the crest of the slope. The courses of a number of earlier mudflows are marked by windrows or small ridges of alluvium, which remain along the edge of the flow as the channel is cut deeper.

And on page 80 of the same report he states:

> Although degradation by mudflows is not an uncommon natural process in the deserts and semiarid areas of the west, there is little information available as to the mechanics of mudflow operation.

In a recent paper treating erosion of the Wasatch Mountain front, Croft (1962) provides numerous examples and much pertinent data attesting to the fact that mudflows in recent time have caused much channel erosion. Two photographs taken from the literature and reproduced here serve to illustrate the point. Figure 128 shows one of the many trenches produced by the catastrophic flood of June 1957 in the basin of the Guil River, France; figure 129 shows the results of 1 of 100 mudflows that occurred in Grand Teton National Park, Wyo., in August 1941. These particular examples were chosen because neither area is semiarid. They therefore illustrate the fact that degradation in the upper reaches of the path of flow is a characteristic feature of mudflows. When they occur, erosion results whether the climate is humid or arid. If these two examples are compared with the view of Paiute Chute (fig. 88), it can be seen that the features of all three are identical.

The views suggest that debris is stripped from the upper reaches of each area and is transported to and deposited on the lower slopes. This is precisely the relationship observed on most alluvial fans in the Basin and Range province today. The catchment areas up to the divides, and the apex regions of the fans, are source areas for mudflows; deposition occurs below midfan.

The actual mechanics of mudflows is poorly understood, and the hypothesis set forth in this report, namely, that mudflows produce degradation primarily by reason of their greater tractive force, is based largely upon inference and deduction. As pointed out in the American Society of Civil Engineers, Task Force

Digitized by Google

FIGURE 128.—View of a channel cut by a mudflow in the Guil Basin, France (after Tricart, 1961, fig. 2). The region is fairly humid, but the results of the mudflow are comparable with the features of Paiute Chute (fig. 88); addition of sediment largely occurs in the lower reaches of the path of flow.

Committee on Hydromechanics report (1963), however, there can be no question that the effect of dispersions of sediment is to increase viscosity, which in turn, alters the bed form because of a reduction in fall velocity of the bed material. The report cites Le Conte (1896) on page 125 as follows:

> The results show conclusively the powerful influence of viscosity due to sediment in suspension. A channel lined with cobblestones will stand a clear water velocity of 6 to 8 feet per second, but when it is followed by a more viscous stream heavily charged with material in suspension, although at a reduced velocity of only 4 to 6 feet per second, the cobblestones will be at once picked up and transported with the flow.

Although the flows discussed by Le Conte are not the equivalent of modern mudflows, it is suggested that density flows can erode the floors of channels by the removal of bed material that is too large to be transported by clear water. The fact that there is no evidence to the contrary, coupled with the several observations previously cited, implies that greater tractive force is associated with the modern process as a result of an increase in the average density of flow.

THE FORMER PROCESS

If the onset of trenching was initiated by density flows of higher tractive force, such as the relatively infrequent modern mudflows, then the inference to be drawn from the tractive-force hypothesis is that sediment transport was formerly achieved by a medium of lesser density. Given flows of lesser density than a mudflow but of necessarily greater density than clear water, and the absence of the deep confining channels of today, it appears probable that the flows of the former process must have spread laterally below the mountain front and aggraded the apex regions that are being eroded today. It is suggested, therefore, that the former process was more nearly akin to sheet floods than to the channelized density flows of today. Discharge was probably greater in the past; but because of lesser density and shallow depth of flow, the resultant tractive force was less.

If the former flows were of lesser density, then the water: sediment ratios must have been greater. This accords with the concept that greater precipitation prevailed in the area during several former time intervals. From this point of view the relative scarcity of clay and abundance of silt in nearly all the samples studied is worthy of note.

One might argue that the surface samples have been winnowed of clays by local runoff, but clearly, the basin surface today represents a time plane. If these samples have been winnowed, then samples obtained from fan cross sections should also contain little clay. Bull (1960) has examined such sections in the attempt to find criteria that will aid in distinguishing among mudflow deposits, water-laid deposits, and intermediate types. Although clay content is probably not a diagnostic feature of deposits in other areas, it is instructive to note that the main criterion used by Bull to distinguish ancient mudflow deposits in Fresno County, Calif., is a high clay content. He gives a value of about 30 percent for the samples studied. The Owens Valley mudflow, however, is by no means an atypical example of mudflows of today. The nature of the flow can be seen from the photographs of the upper reach (figs. 110, 111) as well as of the lower reach (figs. 130, 131). Samples from this mudflow contained 2.41 and 4.22 percent clay; these values pertain to the granule-to-clay fraction alone and therefore are maxima for the flow.

Sample locations in the active channel of Paiute Chute are shown in figures 132 and 133. The matrix of a recent flow is still present in the channel banks or levees; data on clay content are therefore pertinent. The percentage of clay, again in the granule to clay fraction, is 2.10 at the apex and 3.00 at midfan.

Digitized by Google

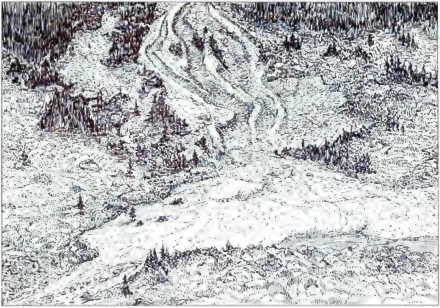

FIGURE 129.—View of the aftermath of a mudflow in the Grand Tetons, Wyo. (after Fryxell and Horberg, 1943, pl. 2, fig. 1). Note the similarity of the chutes that occur here and those shown in figures 88 and 128. The large deposit in the foreground is derived from preexisting talus deposits that were trenched by the mudflow.

Similar low values were obtained from the mudflow of Wrightwood, Calif. (Sharp and Nobles, 1953); little clay was present.

These data suggest that former transport conditions may have differed from those of today by reason of greater clay content. One might argue that a greater clay content in former flows implies still greater density of flow, but it should be recognized that the rate of production of clays is, in good part, a function of precipitation. Little clay will be produced if precipitation is deficient; from this point of view, if more clay was associated with the former process, then this supports the inference that water: sediment ratios were formerly greater. It should also be noted that given a greater abundance of clay in the surface sediments of fans, cohesion and resistance to trenching will be increased.

A second factor suggesting that fluctuation in regime may have occurred is the contrast between the organic content of mudflows today and that of older deposits. Despite the typical dark-brown to deep black color of the Owens Valley mudflow (figs. 110, 111, 130, 131), the organic content was quite low. Weight percentages are 1.89 and 2.80 in the granule to clay fraction for the 2 samples obtained. Wyman Canyon is choked with vegetation and contains a perennial stream. Predictably, the thin atypical Wyman mudflow contained a much higher percentage (14.05) of organic matter. Eardley and Gvosdetsky (1960) reported evidence of about six thin mudflow deposits in core samples from the Great Salt Lake. They state that a high humus content is present in these old flows but do not give percentages; such data are extremely rare. Croft (1962) reported the organic content of soils developed on old and recent mudflow deposits, but these values are not comparable to the content of mudflows. The paucity of data permits only the conclusion that the organic content of modern flows is not great. This results, of course, from the fact that vegetation is not abundant today. It is probable that both clay and vegetation were formerly more abundant, because both require the same type of climatic regime. Higher precipitation is not the only characteristic of the former regime, however; the frequency of precipitation must also be considered.

Digitized by Google

FIGURE 130.—View of the lower reach of the Owens Valley mudflow showing clear-water dissection. Although the deposit is undergoing dissection, it is apparent that sedimentation has occurred across a wide flat area at the lower boundary of the fan. The fenceposts shown parallel the main highway through the valley, which is about 8 miles below the mountain front of the Sierra Nevada at this point. Note the dark color of the deposit.

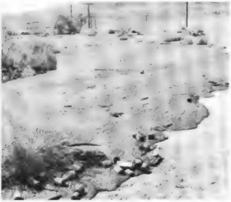

FIGURE 131.—View of the lower reach of the Owens Valley mudflow showing floating debris on the thin deposit. The flow was quite dense and viscous in this area (approx. 0.25 mile south of the clear-water flow shown in fig. 130), and in addition to the cans seen in the foreground, many cobble-size particles were also rolled and carried across a wide area of low slope.

FREQUENCY OF PRECIPITATION

In semiarid or arid regions much of the annual precipitation today falls in few and infrequent storms. The slopes are largely bare of vegetation, little clay is present, and resistance to erosion is low. This combination of conditions favors the occurrence of mudflows. Given a more equitable distribution, as well as an absolute increase of annual precipitation, this situation will be reversed, and mudflows will become less frequent. The precipitation that accompanied the mudflows in the Grand Tetons (Fryxell and Horberg, 1943) represented a great departure from the norm for that area. Rainfall throughout the summer of 1941 was above average and was higher in each succeeding

FIGURE 132.—View of the apex region of the active channel in Paiute Chute. The intermediate axis of the large boulder to the right of center is 10.4 feet in length. The divide of the small catchment area extends along the ridge summit shown. Fine sediment is rather scarce.

FIGURE 133.—View of the fine matrix in the levee wall along the active channel of Paiute Chute. The occurrence of the fine matrix surrounding the tightly wedged granitic boulders indicates that a mudflow produced the deposit and that Paiute Chute is not of rockslide or similar origin. The sample bag in the center of the photograph is 4 by 6 inches.

Digitized by Google

month; it was five times the average during the month of August, when the flows occurred. During June, July, and August no more than 3 successive days passed without recorded precipitation. The mudflows in the Guil Basin (Tricart, 1961) were also brought on by uncommonly high precipitation. Heavy rainfall over a period of 48 hours, entirely without precedent in the region, produced the flows. It cannot be claimed, therefore, that mudflows can only occur where the frequency of precipitation is low, but observations suggest that they are much more common in such areas. Variations in the frequency of precipitation are known to have occurred in semiarid areas (Leopold, 1951) and, by implication, in arid areas as well. It is thought that such changes in the frequency of precipitation can account for the prevalence of a former flow regime that was characterized by higher clay content, organic content, and water: sediment ratios.

Although the requirement of greater frequency of precipitation is often stated during discussions of former processes, it is difficult to prove on the basis of field evidence. One can, of course, easily argue in the case at hand that if the frequency of precipitation remained at its present value in the Great Basin while annual precipitation increased, then the only result would be more intense cloudbursts and still greater degradation by mudflows. It is thought, however, that the hanging fan shown in figures 119 and 120 does constitute field evidence that a greater frequency of precipitation must formerly have prevailed.

The fill in the small tributary canyon to the right of the main channel represents the level of aggradation that was attained throughout the Antelope Springs catchment area and by the fan proper. This is the high terrace level. The fill has been truncated by erosion within the main channel, and it may best be designated a hanging fan. This same phenomenon was observed in several small canyons that are tributary to the lower reaches of Wyman Canyon and in basins other than Deep Springs Valley. The occurrence of these hanging fans suggests that precipitation and sediment transport no longer occur in every canyon within the catchment areas. The infrequent cloudbursts of today may follow preferred tracks, as noted previously, and most of the precipitation will occur in the divide areas. The mudflows and the resultant trenches occur primarily in the trunk canyons and in the larger tributary canyons that head near divide areas. The precipitation pattern that accompanied uniform aggradation in the catchment areas must have differed from that which pertains today. Precipitation was certainly widespread rather than localized and, hence, was probably more frequent in occurrence.

The relationship discussed above may well be relevant to the problem posed by many hanging valleys that have been interpreted in terms of tectonism. Uplift of a range may result in more frequent precipitation in the divide areas and a decreased probability of precipitation in certain tributary valleys. A contrast in both discharge and frequency of floods could account for greater erosion within the main valleys and the bypassing of tributary valleys. For reasons cited previously, this explanation for hanging valleys would appear much more reasonable than any assumed linear relationship between uplift and downcutting.

PROCESS RATES

A charcoal pod was found at station 400 in the Antelope Springs channel (pl. 9). A general view of the channel in this area is shown in figure 134. The pod occurred 6 feet above the channel floor in the right bank, which is 12 feet high at this point (fig. 135). The presence of fire-blackened stones directly above the charcoal indicated that the pod was a fire hearth. A radiocarbon date of 1,380 ±250 years B.P. was obtained for a sample from this hearth. The field relationship therefore indicates that 6 feet of deposition and 12 feet of erosion have occurred since this date.

FIGURE 134.—View of the Antelope Springs channel at station 400. The view is downchannel from the fire-hearth site. Note the fresh character of the cobbles to the left of the meandering channel, indicating that modern transport has extended far out into the valley. The sage ranges from about 1 to 3 feet in height.

Any estimate of the process rates involved will depend upon the establishment of some arbitrary ratio between the rate of deposition and the rate of erosion. If it is assumed that the rate of erosion is equal to the rate of deposition, then 18 feet of either process has oc-

Digitized by Google

curred in the last 1,130–1,630 years. This yields respective rates of 0.016 and 0.011 foot per year. If it is assumed that the rate of deposition was only half as great as the rate of erosion, which may be more reasonable at this location, then the equivalent of 24 feet of process has occurred during the same period. The respective rates in this case would be 0.021 and 0.015 foot per year.

FIGURE 135.—View of the fire-hearth site in the Antelope Springs channel. The channel bank is 12 feet high at this point, and the bottom of the hearth is 6 feet below the top of the bank. Note the fire-blackened stone resting directly upon the charcoal pod, thus indicating that it is in fact a fire hearth.

These rates, ranging from about 1 to 2 feet per hundred years, should properly be applied only to events in the vicinity of the sample. Some estimate of the time of the last expansion of Deep Springs Lake can therefore be made, because the linear ridges that indicate this expansion (fig. 85) are in this general area. If it is assumed that the 6 feet of deposition in this area coincided with the expansion of the lake, then the linear ridges on the basin surface are 300–600 years younger than the fire hearth, depending upon the rate of deposition chosen. The high stand represented by the ridges occurred, therefore, between 700 and 1000 B.P., if the radiocarbon date is correct. Langbein (1961) has estimated the date of the last expansion of several lakes based upon the time represented by the total dissolved salt content. The value obtained for Owens Lake was 1,700 years, and a few other lakes expanded still more recently. The estimated date of the last expansion of Deep Springs Lake is therefore not unreasonable.

If the relatively minor climatic changes of Recent time could bring about the expansion and contraction of lakes and trenching to a depth of 12 feet at the fire-hearth location discussed above, then the much greater changes that marked the Pleistocene Epoch in this area may have coincided with the initiation of trenching in catchment and upper fan areas. It is worthy of note that an erosion rate of about 3 feet per hundred years would suffice to produce even the deepest trenches that occur in the region.

To obtain some future data on process rates in Deep Springs Valley, chains were installed in the channel bed at five locations in the Antelope Springs channel (pl. 9). At each section, particles in the channel were painted in order that some information on sediment transport might also be obtained in the course of the monitoring program. At sections *A–A′*, *B–B′*, and *C–C′*, entire gravel bars were painted; the first mentioned is shown in figure 136. Section *C–C′* is in the vicinity of the fire hearth. At sections *D–D′* and *E–E′* no gravel bars were present, and particles that occurred on the channel floor were alined perpendicular to the

FIGURE 136.—View of the painted gravel bar at section *A–A′* in the Antelope Springs channel. The bar is about 70 feet long and consists mainly of particles as large as cobbles; few larger particles occur.

Digitized by Google

direction of flow. The information gained from this program over a period of years will not only provide data on modern process rates, but it should also serve to confirm the contention that trenching is the dominant long-term process in the upper fan reaches today.

FORMATION OF THE ALLUVIAL FANS

The formation of alluvial fans has been discussed ever since these striking sedimentary deposits were first noted during the early western exploratory surveys. The opinions expressed to explain the formation of fans may be conveniently grouped into three general categories, namely (1) evolutionary, (2) equilibrium, and (3) climatic hypotheses. Although the writer favors the climatic hypothesis, each holds some measure of truth, and because the truth often occupies middle ground in such problems, each hypothesis is treated here.

THE EVOLUTIONARY HYPOTHESIS

The concept that all landforms result from a geographic cycle that proceeds through the successive stages of youth, maturity, and old age is today commonly termed "Davisian philosophy." The specific choice of anthropomorphic stage names was probably influenced by the publication of the doctrine of evolution in the 19th century; the concept can therefore be appropriately designated an evolutionary hypothesis. Davis (1905) applied this concept to alluvial fans by emphasizing the importance of stage and thereby denigrating process. He suggested that alluvial fans would form in basins adjacent to uplifted mountain ranges in desert regions. The stage of youth was thought to be indicated by V-shaped canyons in the mountains and by small but rapidly growing fans. As the mountains wore down, Davis reasoned, the fans would continue to enlarge, and thus would fill the basin with sediment, and in the final stage—old age—the mountain remnants would be buried beneath a continuous cover of alluvium.

The inevitable reaction to one of the several failings of the concept of cycles, namely to treat processes and thereby gain some insight into the mode of formation of any given landform, set in with the advent of quantitative geomorphology. The modern view of the geographic cycle has, to a large degree, been summarized by Chorley (1962), who equates Davisian philosophy to closed-system thinking or the single-cause school of thought. Davis was quite correct in two important particulars, however.

First, despite the writer's disenchantment with tectonic explanations for magnitudes of sedimentation and erosion, as previously explained, it cannot be denied that slope and discharge are both intimately related to the production of sediment. An infinite discharge over a zero slope will have little more effect than zero discharge down a vertical rock wall. From this point of view, there can be no question that some uplift must first occur to provide the requisite differential relief for the formation of an alluvial fan at some initial time t_o.

Second, unless an infinite duration of uplift is postulated, then a given basin must completely fill with sediment at some finite time t_f. It is therefore reasonable to assume that at time t_f some mountain remnants will indeed be buried beneath an alluvial cover. The extent of this cover will depend upon coincidence, or its absence, of time t_f in each of many basins. The peneplain conceived by Davis (1889) will probably not result, but it is undeniable that old age, as Davis defined it, must ultimately be attained by any given basin.

The evolutionary hypothesis, admittedly based upon deduction, provides a reasonable description of alluvial fans in their formative and ultimate stages of development or morphology. Largely omitted, however, is consideration of the time between t_o and t_f and of the processes involved in fan formation.

THE EQUILIBRIUM HYPOTHESIS

The equilibrium hypothesis relates the morphology of a landform, or Davisian stage, with the processes acting upon it in terms of dynamic systems in which mass and energy are considered as functions of time. The two general systems defined by Von Bertalanffy (1950) are closed systems, in which materials and energy cannot be exchanged beyond the confines of a well-defined boundary, and open systems, in which materials, energy, or both can be exchanged with outside environments. As pointed out by Strahler (1952), most landforms represent open dynamic systems that tend toward equilibrium or a steady state. This view is widely accepted today (Leopold and Langbein, 1962; Chorley, 1962).

Although the equilibrium hypothesis is basically valid, certain difficulties of both application and interpretation arise when considering alluvial fans. An assumption must be made that a balance exists between erosion of the mountains and deposition in an adjacent basin. This is obviously reasonable, but if alluvial fans are in dynamic equilibrium, then a second, more particular assumption must be made, namely that the rates of sedimentation and erosion on a given fan are equal. Unless these rates are equal, then a fan will either grow or diminish in size as a function of the difference between the two rates. Denny (1965) contends that these rates are equal, or nearly so, and that alluvial fans are therefore in dynamic equilibrium with the

Digitized by Google

processes acting upon them. Aside from correlations between planimetric measurements of source areas and their respective fans, which are somewhat suspect for reasons cited above (p. 133), little evidence exists to substantiate this contention. Rates of sedimentation and erosion on alluvial fans are not known. The amount of local runoff required to remove sediment from fans in order to balance the sediment added is also not known. Local runoff, however, can only be produced by either flows from the mountains or precipitation in the valley proper. It is not obvious that either of these sources will suffice to achieve the required balance; mountain floods must overcome seepage into the permeable alluvium, and local precipitation is not great. Because of orographic effects, the precipitation on most basin floors, and presumably on the fans as well, is very low, ranging from less than 2 inches per year in Death Valley to about 5 inches per year in basins at higher elevations. Moreover, the fact that highly erodible sediments, which represent former lake levels, have existed for thousands of years on the lower reaches of many fans does not support the view that a balance has been achieved or dynamic equilibrium attained.

The primary problem involved in the application of the equilibrium hypothesis, therefore, is to demonstrate conclusively that dynamic equilibrium has indeed been attained, rather than to merely assume that this is true. Even if one grants that alluvial fans have attained a steady state, however, a second problem will arise, namely the proper interpretation of this information.

Possible misinterpretation can be illustrated by consideration of the formation of playas. If their widespread occurrence, time contemporaneity, and the existence of strand lines at higher elevations are ignored, then it may be erroneously concluded that climatic change or other cyclic phenomena are not pertinent and that the interrelationship of their morphology with present processes is sufficient for an understanding of their formation.

Morphology and processes may be clearly interrelated, but the demonstration of dynamic equilibrium at any instant in time, even if conclusively proven, does not preclude the possibility that changes in both the intensities and types of processes may have occurred through time. Moreover, unlike water bodies, many landforms adjust to such changes very slowly, and although they tend toward equilibrium with modern processes, they may in fact be far removed from a steady state today. Leopold and Langbein (1962) state that it is improbable that time periods as long as geologic epochs could elapse before the attainment of equilibrium by fluvial processes in adjustable channels. Although the absolute duration of an epoch depends upon the geologic period considered, their meaning is clarified by a declaration of agreement with Hack (1960), who thought that no important time period is necessary. These statements do not, however, refute the fact that Pleistocene relicts that are thousands of years old exist today in all parts of the world. Hanging valleys, raised beaches, river terraces, dry waterfalls, the strand lines cited previously, and many other features attest to a lack of equilibrium with modern processes; in the absence of proof to the contrary, it is not unreasonable to suppose that some trenches in alluvial fans may be akin to the misfit river channels discussed by Dury (1958). Why, then, in the absence of any substantial proof should alluvial fans be thought to have attained dynamic equilibrium?

The concept of dynamic equilibrium of landforms represents a major advance beyond the application of Davisian principles. As previously stated, however, this does not mean that certain truths should be ignored merely because they are founded upon deduction. The equilibrium hypothesis requires blending with caution, lest a new generation of workers seek everywhere to demonstrate equilibrium as those before them sought cycles and peneplains. Dynamic equilibrium for any given landform must be conclusively proved, rather than simply claimed because the concept is in vogue, and if demonstrated to exist, then equilibrium conditions should not be cited as proof that the modern processes are necessarily identical with those of the past.

THE CLIMATIC HYPOTHESIS

The evidence suggesting that present climatic conditions are not identical with those of the past is legion. In response to changes in temperature, precipitation, evaporation rates, and the location of cyclonic storm tracks, changes in the regimen of rivers and lakes and in the distribution of plants and animals occurred. Jamieson (1863) recognized more than a century ago that climatic change regulated the expansion and contraction of saline lakes in arid regions. In the Great Basin, the existing lakes are largely confined to the area north of the 39th parallel. Hubbs and Miller (1948) have suggested that this comparatively wet region is representative of the former pluvial conditions that prevailed in those parts of the province that are driest today. Studies of pluvial lakes in New Mexico, such as Lake Estancia (Leopold, 1951), for example, indicate that this is true.

The occurrence of alternating climatic episodes, based upon various kinds of evidence, has been suggested by Bryan (1941), Judson (1953), and Miller and Wendorf (1958) in New Mexico, by Hack (1942)

Digitized by Google

in Arizona, by Richmond (1962) in Utah, by Hunt (1954) in Death Valley, and by many others. Morrison (1961) is one of several workers that has suggested that climatic changes have been virtually synchronous throughout the Great Basin. Most of the reports cited treat climatic fluctuation within Recent time. Although less drastic than the Pleistocene fluctuations, changes during Recent time have been sufficient to produce recognizable imprints upon the sedimentary record, and four or five distinct climatic episodes are thought to have occurred within this time interval.

Data on the age of the alluvial fans in the Basin and Range province are generally unavailable. Although all the fans are not necessarily of equal age, it seems most probable that climatic changes have occurred during their formation. Because climatic change induces changes in the regimen of streams and alters the abundance of vegetation and edaphic characteristics, the climatic hypothesis requires that features thought to attest to such changes be widespread and common to most fans in the region. The features and characteristics of the fan environment that are thought to be indicative of climatic change have been previously discussed in this report. They include the following:

1. The loci of deposition on alluvial fans have shifted from areas well within catchment basins to the middle or lower reaches of the fans, far below the mountain front.
2. Trenches in the apex regions of the fans are misfit relative to present flow conditions by reason of their excessive depth, which is as much as 200 feet.
3. Paired terraces that are continuous with fan surfaces occur within catchment areas and in some places extend to the divide.
4. Abandoned channels occur on fan surfaces at higher elevations than the floors of the active channels.
5. The fan surfaces and the abandoned channels exhibit weathering stain and (or) desert varnish, whereas in the active channels and on modern deposits these are absent.
6. Hanging fans occur in tributary canyons within the catchment areas, and their surfaces are continuous with terraces and fan surfaces below the mountain front.
7. The estimated tractive force is greater within the active channels than on the fan surfaces.
8. The percentages of clay and organic material in both surface sediments and modern mudflows are extremely low.

The formation of the type of alluvial fan discussed in this report according to the climatic hypothesis is shown on figure 137. The observations and data that have been presented suggest the occurrence of the following events during one climatic cycle.

During a period of fan building (fig. 137*A*) aggradation occurred within catchment areas and on fan surfaces at continuous levels. Precipitation was both more abundant and more frequent than it is today. In response to this climatic regime, the abundance of both clay and vegetation was greater, and the fan surfaces were more resistant to erosion. Although discharge was greater, water: sediment ratios were higher, and the medium of transport had a lesser tractive force. Frequent floods spilled over numerous shallow channels onto the fan surfaces, spreading laterally below the mountain front. Sediment was deposited over wide areas of the fans as a consequence of these conditions.

Climatic change, manifested by a change from widespread to local or concentrated precipitation and by a lesser frequency of precipitation, produced a reduction of vegetation and a decrease in the abundance of clay. Catchment slopes and surface deposits became more easily erodible, thus contributing toward a reduction in water: sediment ratios and a greater frequency of mudflows. These flows of greater density, and correspondingly greater tractive force, deepened the trunk channels in catchment areas and trenched the upper reaches of the fans (fig. 137*B*). Terraces and hanging fans in the catchment areas were produced by these processes, and the sediment removed was deposited farther downfan, far below the mountain front.

The trenching of fans does not signal their demise within a geographic cycle, as suggested by Eckis (1928). During an episode of trenching, in response to the climatic conditions outlined above, the shift in the loci of deposition results in the addition of material at the lower limits of the fans. During any part of a climatic cycle, the fans are therefore constantly growing; they grow upward during intervals of general aggradation within the catchment areas and below the mountain front, and are built outward into the basin during periods of trenching in the upper reaches.

The sediment added at the lower margins of the fans may be redistributed and obscured by a subsequent rise in lake level within a given basin. This will produce an alternating alluvial fan-lacustrine facies, such as those commonly reported from core studies. At this time the conditions postulated in figure 137*A* will again occur; the trenches will fill with sediment, and deposition on fan surfaces will again build them upward, provided that the magnitude of the climatic shift is sufficient to accomplish this result before conditions change once again.

Digitized by Google

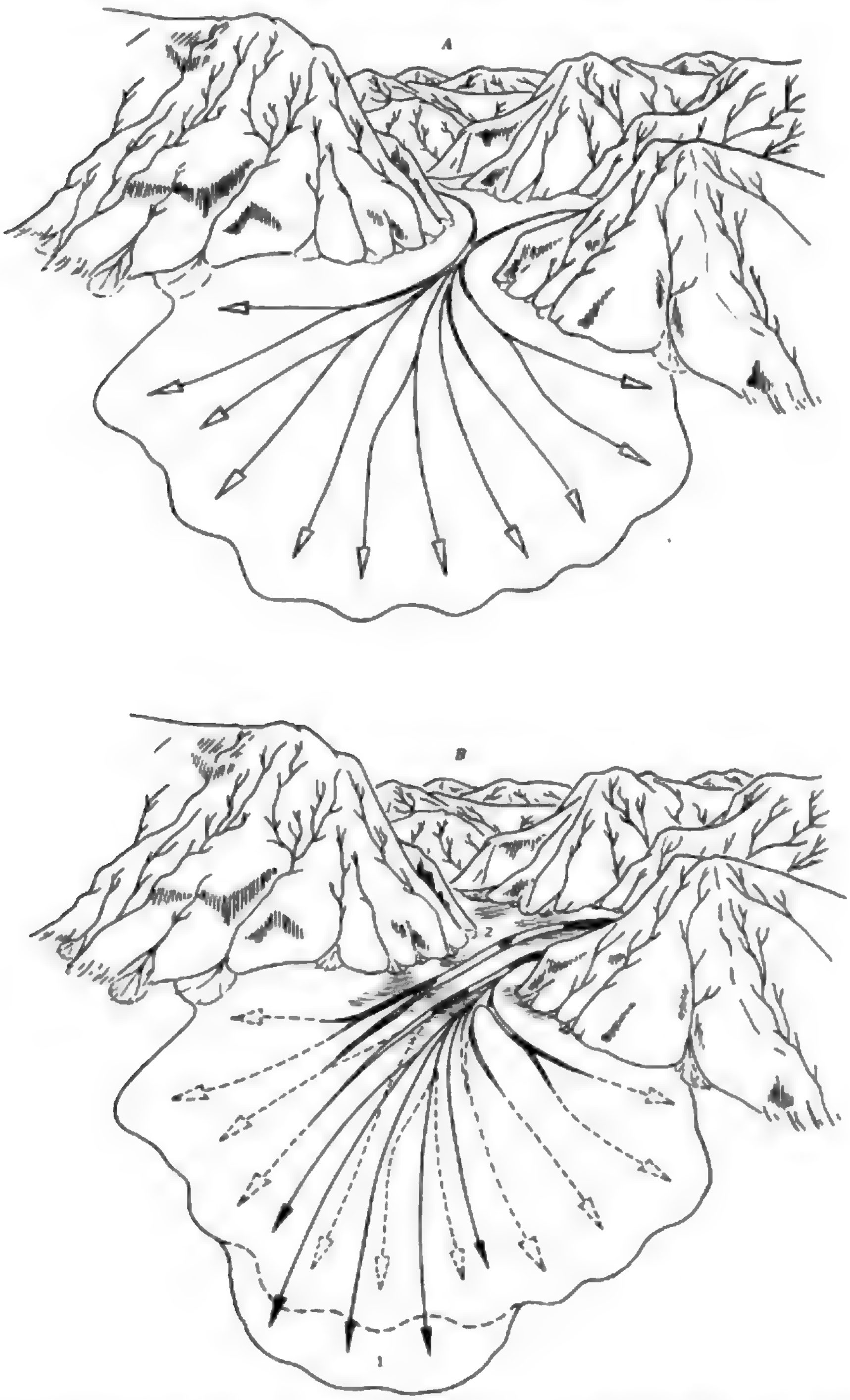

FIGURE 137.—Diagram showing the formation of alluvial fans during one cycle, according to the climatic hypothesis. *A*. During more humid or pluvial periods aggradation occurs within the catchment area and below the mountain front at continuous levels. Frequent floods with high water: sediment ratios spill over the shallow braided channels below the mountain front and deposit sediment over wide areas, building the fans upward. *B*. During a subsequent drier climatic period trenching occurs along main channels within the catchment area and on the upper reaches of the fan. Mudflows and other infrequent density flows transport the sediment they erode to the lower reaches of the fan, building it outward, into the valley (1). The terraces within the catchment area and the abandoned channels on the fan surface are produced as a consequence of this change in process. The small tributary canyon (2) receives little of the infrequent and localized precipitation. Because of trenching in the main channel, the previously deposited sediment is left as a hanging fan at the level of the high terrace as shown.

Digitized by Google

Both the Davisian and equilibrium theories therefore contain elements of truth. An understanding of the formation of alluvial fans, however, requires recognition of changes of processes through time that are accompanied by consequent changes in fan morphology. Because the most likely cause of such changes is climatic fluctuation, known to have occurred throughout the region, the climatic hypothesis is thought to provide the most reasonable explanation of the formation of fans. It should not be concluded that the equilibrium and climatic hypotheses are mutually exclusive from the foregoing treatment. As summarized so well by Braithwaite (1955, p. 339)—

> The world is not made up of empirical facts with the addition of the laws of nature: what we call the laws of nature are conceptual devices by which we organize our empirical knowledge and predict the future. From this point of view any general hypothesis whose consequences are confirmed by experience is a valuable intellectual device; and the profitable use of such a hypothesis does not presuppose that it will not at some future time be subsumed under some more general hypothesis in a more widely applicable deductive system, nor that the facts that it explains will not some time be explicable by a quite different hypothesis in another deductive system.

TABLE 1.—*Slope and maximum particle-size measurements in Deep Springs Valley, Calif.*

Sample	Slope (feet per foot)	Maximum particle size (feet)	Sample	Slope (feet per foot)	Maximum particle size (feet)
North end of Deep Springs Valley (fig. 90)					
−5, −6	0.160	2.2	−2, 1	0.010	0.3
−4, −6	[illegible]	.2	−1, 1	.020	.1
−3, −6	.035	2.0	−4, 2	.130	.7
−2, −6	.086	2.1	−3, 2	.060	.3
−1, −6	.010	.2	−2, 2	.020	1.6
−6, −5	.160	3.7	−1, 2	.020	.1
−5, −5	.100	.2	−5, 3	.105	1.0
−4, −5	.085	1.6	−4, 3	.145	.6
−3, −5	.040	2.3	−3, 3	.030	.6
−2, −5	.085	1.3	−2, 3	.020	1.9
−1, −5	.090	2.0	−1, 3	[illegible]	3.8
−6, −4	.110	2.7	−4, 4	.030	.2
−5, −4	.065	3.2	−3, 4	.020	[illegible]
−4, −4	.060	1.8	−2, 4	.025	4.0
−3, −4	.025	3.7	−1, 4	.030	4.7
−2, −4	.030	1.7	−5, 5	.075	.2
−1, −4	.025	.6	−4, 5	.065	2.3
−7, −3	.086	7.0	−3, 5	.065	3.7
−6, −3	.060	1.7	−2, 5	.035	1.7
−5, −3	[illegible]	.1	−1, 5	.035	3.9
−4, −3	.050	2.1	−6, 6	.080	.5
−3, −3	.030	1.7	−5, 6	.040	3.2
−2, −3	.085	1.5	−4, 6	.060	[illegible]
−1, −3	.015	.1	−3, 6	.065	2.5
−7, −2	.105	1.9	−2, 6	.035	1.9
−6, −2	.070	.4	−1, 6	.025	2.5
−5, −2	.060	.3	−6, 7	.070	7.7
−4, −2	.080	.2	−5, 7	.040	6.4
−3, −2	.035	.2	−4, 7	.045	4.6
−2, −2	.030	.2	−3, 7	.045	5.4
−1, −2	.005	.1	−2, 7	.040	2.5
−6, −1	.120	.5	−1, 7	.030	.3
−5, −1	.060	.1	−6, 8	.090	3.5
−4, −1	.065	.1	−5, 8	.070	5.1
−3, −1	.035	.2	−4, 8	.095	4.8
−2, −1	.030	.6	−3, 8	.035	3.3
−1, −1	.000	.1	−2, 8	.025	2.0
−5, 0	.060	.2	−1, 8	.025	.6
−4, 0	.080	1.7	−7, 9	.110	16.5
−3, 0	.110	1.4	−6, 9	.080	2.2
−2, 0	.036	2.8	−5, 9	.095	2.9
−1, 0	[illegible]	.9	−4, 9	.075	2.8
−6, 1	.100	.5	−3, 9	.040	.6
−5, 1	.090	.4	−2, 9	.030	3.3
−4, 1	.080	.3	−1, 9	.030	.7
−3, 1	.065	.2	−6, 10	.060	2.7

TABLE 1.—*Slope and maximum particle-size measurements in Deep Springs Valley, Calif.*—Continued

Sample	Slope (feet per foot)	Maximum particle size (feet)	Sample	Slope (feet per foot)	Maximum particle size (feet)
North end of Deep Springs Valley (fig. 90)—Continued					
−5, 10	0.085	3.3	4, 3	0.025	0.3
−4, 10	.060	.8	5, 3	.060	.5
−3, 10	.060	.4	6, 3	.085	.6
−2, 10	.040	.1	7, 3	.090	.5
−1, 10	.020	.4	8, 3	[illegible]	1.8
−6, 11	.080	.3	0, 4	.010	.3
−4, 11	.130	1.4	1, 4	[illegible]	.3
−3, 11	.080	1.5	2, 4	.015	.4
−2, 11	.060	1.7	3, 4	.010	1.3
−1, 11	.045	3.5	4, 4	.010	1.0
−2, 12	.055	[illegible]	5, 4	.065	.3
−1, 12	[illegible]	5.5	6, 4	.065	.2
−2, 13	[illegible]	4.8	7, 4	.080	.3
−1, 13	.055	4.5	8, 4	.140	.9
−5, 14	[illegible]	6.2	0, 5	.015	.4
−4, 14	.065	7.4	1, 5	[illegible]	.8
−3, 14	[illegible]	3.7	2, 5	.015	.3
−2, 14	.100	2.5	3, 5	.020	.2
−1, 14	.080	3.3	4, 5	.010	.7
−3, 15	.070	4.4	5, 5	[illegible]	.7
−2, 15	.065	4.7	6, 5	[illegible]	.4
−3, 16	.190	4.2	7, 5	.085	.3
0, −6	.005	.1	8, 5	.110	1.4
1, −6	[illegible]	.1	0, 6	.000	1.2
2, −6	.010	.0	1, 6	.015	.3
3, −6	[illegible]	.1	2, 6	.015	.1
4, −6	[illegible]	.3	3, 6	.010	.1
5, −6	.020	.2	4, 6	[illegible]	1.2
6, −6	.055	.2	5, 6	.085	.1
0, −5	.005	.2	6, 6	.065	.6
1, −5	.010	.1	7, 6	.070	.7
2, −5	.010	.2	8, 6	.125	1.9
3, −5	.005	.0	0, 7	.020	1.3
4, −5	[illegible]	.0	1, 7	.020	.1
5, −5	.030	.1	2, 7	[illegible]	.1
6, −5	.060	.2	3, 7	.010	.1
0, −4	.000	.1	4, 7	.000	1.6
1, −4	.000	.0	5, 7	.030	.1
2, −4	.005	.1	6, 7	[illegible]	1.0
3, −4	.010	.1	7, 7	.140	5.0
4, −4	[illegible]	.0	0, 8	.010	.1
5, −4	.045	.1	1, 8	.025	.1
6, −4	.060	3.0	2, 8	.025	.1
0, −3	.005	.1	3, 8	[illegible]	1.3
1, −3	.005	.1	4, 8	.010	1.8
2, −3	.000	.1	5, 8	.010	.9
3, −3	.005	.1	0, 9	.020	.2
4, −3	.005	.0	1, 9	.035	.1
5, −3	.065	.3	2, 9	[illegible]	1.0
0, −2	.005	.3	3, 9	.015	.8
1, −2	[illegible]	.1	4, 9	.010	.6
2, −2	.010	.1	5, 9	.065	.7
5, −2	.065	.6	6, 9	.125	5.2
0, −1	[illegible]	.3	0, 10	.080	1.0
1, −1	[illegible]	.1	1, 10	.040	.5
2, −1	[illegible]	.0	2, 10	.025	.4
5, −1	.110	1.1	3, 10	.030	.3
0, 0	.000	1.2	4, 10	.015	.4
1, 0	[illegible]	.1	5, 10	[illegible]	1.3
2, 0	[illegible]	.1	6, 10	.180	7.0
0, 1	.005	1.1	0, 11	.050	2.5
1, 1	.005	.2	1, 11	.035	1.3
2, 1	.000	.4	2, 11	.080	2.0
7, 1	.110	.3	3, 11	.035	1.0
8, 1	.160	.6	4, 11	[illegible]	1.2
0, 2	.010	1.8	5, 11	[illegible]	6.7
1, 2	[illegible]	.2	0, 12	.035	2.6
2, 2	.005	.1	1, 12	[illegible]	2.5
3, 2	[illegible]	.3	2, 12	.080	2.7
4, 2	.050	.3	3, 12	.110	2.8
5, 2	.060	.3	4, 12	[illegible]	5.2
6, 2	.140	.2	0, 13	.040	1.2
7, 2	.100	.3	1, 13	[illegible]	1.5
8, 2	.110	.9	2, 13	.065	2.4
0, 3	.015	.1	3, 13	[illegible]	1.7
1, 3	[illegible]	.1	0, 14	.160	2.3
2, 3	.005	.2	1, 14	.090	3.9
3, 3	.005	.1	2, 14	.105	1.9
Paiute Chute; on fan surface (fig. 110)					
1 [1]	0.080	2.9	7	0.200	6.1
2	.120	3.4	8	.455	4.7
3	.135	5.8	9	.690	3.6
4	.245	3.0	10	.490	8.4
5	.235	6.2	11 [1]	.425	10.4
6	.230	6.5			

See footnotes at end of table.

Digitized by Google

TABLE 1.—*Slope and maximum particle-size measurements in Deep Springs Valley, Calif.*—Continued

Sample	Slope (feet per foot)	Maximum particle size (feet)	Sample	Slope (feet per foot)	Maximum particle size (feet)
Paiute Chute; in recent channel (fig. 114)					
1 [1]	0.085	4.1	8	0.370	6.1
2	.065	3.0	9	.400	7.2
3	.300	5.2	10	.505	6.0
4	.140	7.0	11	[illegible]	5.8
5	.175	5.8	12	.630	8.0
6	.215	7.5	13 [2]	.680	7.2
7	.300	9.8			
Westgard Pass (fig. 115)					
1 [1]	0.170	0.4	7	0.270	0.6
2	.160	.4	8	.230	.8
3	.230	.3	9	.430	.5
4	.250	.5	10	.380	.9
5	.320	.4	11	.500	.8
6	.200	.6	12 [2]	.600	.7
Westgard Pass (fig. 116)					
1 [1]	0.230	0.3	6	0.400	0.8
2	.260	.3	7	.440	.7
3	[illegible]	.2	8	.500	.6
4	.400	.4	9	.580	.5
5	.300	.4	10	.660	.7
Antelope Springs fan (fig. 91)					
1	0.075	2.8	36	0.060	2.5
2	.060	2.2	37	.060	1.5
3	.070	1.7	38	.070	1.9
4	.070	2.1	39	.080	2.0
5	.080	2.0	40	.060	1.4
6	.080	[illegible]	41	.060	1.6
7	.065	2.4	42	.070	2.3
8	.060	2.7	43	.080	2.1
9	.060	2.6	44	.050	1.3
10	.065	1.5	45	.060	2.7
11	.070	1.8	46	.065	2.0
12	.060	2.2	47	.075	1.6
13	.080	2.7	48	.070	1.7
14	.065	1.7	49	.050	1.7
15	.075	1.2	50	.070	2.1
16	.070	2.6	51	.060	1.9
17	.070	[illegible]	52	.060	2.1
18	.060	1.8	53	.075	2.0
19	.070	1.4	54	.060	[illegible]
20	.070	1.7	55	.065	1.7
21	.075	3.2	56	.065	2.1
22	.070	1.8	57	.060	[illegible]
23	.065	1.1	58	.060	1.6
24	.060	2.0	59	.065	1.0
25	.090	2.5	60	.080	1.3
26	.050	2.6	61	.050	1.3
27	.075	2.4	62	.060	2.4
28	.080	2.4	63	.065	2.3
29	.080	2.6	64	.060	2.8
30	.070	1.5	65	.050	2.5
31	.065	1.6	66	.070	1.2
32	.065	2.6	67	.050	3.0
33	.070	2.3	68	.065	[illegible]
34	.070	1.0	69	.065	1.5
35	.080	2.1	70	.050	1.8

TABLE 1.—*Slope and maximum particle-size measurements in Deep Springs Valley, Calif.*—Continued

Sample	Slope (feet per foot)	Maximum particle size (feet)	Sample	Slope (feet per foot)	Maximum particle size (feet)
Antelope Springs fan (fig. 91)—Continued					
71	0.065	0.8	137	0.035	1.6
72	.045	1.0	138	.030	1.3
73	.055	.9	139	.025	1.3
74	.070	[illegible]	140	.030	1.5
75	.060	1.2	141	.040	.3
76	.070	1.2	142	.035	1.3
77	.080	2.9	143	.040	1.4
78	.070	2.3	144	.030	1.0
79	.080	1.5	[illegible]	.035	1.2
80	.040	1.0	146	.030	2.2
81	.060	1.7	147	.035	1.3
82	.060	1.8	148	.040	1.4
83	.060	1.7	149	.020	1.9
84	.035	1.7	150	.030	1.0
85	.080	[illegible]	151	.035	1.7
86	.050	1.3	152	.035	1.5
87	.080	[illegible]	153	.035	.9
88	.065	1.0	[illegible]	.025	1.5
89	.040	1.3	155	.030	.9
90	.080	2.0	156	.020	.1
91	.065	1.5	157	.020	1.1
92	.045	1.7	158	.025	.1
93	.070	2.1	159	.030	.1
94	.085	2.0	160	.020	.1
95	.080	1.9	161	.010	.5
96	.080	.9	162	.020	.1
97	.060	2.5	163	.020	.1
98	.060	2.6	164	.020	.1
99	.065	2.3	165	.030	.1
100	.065	1.7	166	.015	.1
101	.060	3.2	167	.030	1.0
102	.040	2.2	168	.030	.1
103	.060	1.2	169	.025	1.6
104	.085	1.4	170	.030	1.5
105	.040	1.1	171	.025	1.3
106	.035	[illegible]	172	.030	1.1
107	.060	1.7	173	.020	.1
108	.060	.9	174	.025	.1
109	.065	1.6	175	.020	.3
110	.060	1.5	176	.030	.7
111	.060	1.5	177	.015	.5
112	.060	1.4	178	.030	.1
113	.060	[illegible]	179	.015	.1
114	.045	1.1	180	.010	1.2
115	.060	1.6	181	.015	1.1
116	.060	[illegible]	182	.010	.2
117	.065	3.0	183	.015	.2
118	.065	1.8	184	.030	.1
119	.080	1.5	185	.020	.1
120	.080	[illegible]	186	.020	.1
121	.035	1.7	187	.010	.1
122	.040	[illegible]	188	.015	.1
123	.040	1.2	189	.020	.2
124	.020	1.0	190	.010	.1
125	.035	1.8	191	.010	.5
126	.045	1.4	192	[illegible]	.4
127	[illegible]	1.4	193	.020	.1
128	.040	[illegible]	194	.010	.7
129	.040	1.6	195	.005	.1
130	.030	1.5	196	.015	.1
131	.050	1.3	197	.010	.1
132	.040	1.4	198	.010	.1
133	.035	1.2	199	.020	.2
134	.045	1.6	200	.030	.1
135	.025	1.0	201	.005	.1
136	.030	1.0	202	.010	.1

[1] At toe of fan. [2] At fan apex.

TABLE 2.—*Mean size, mean roundness, and lithology of pebbles in Deep Springs Valley, Calif.*

Sample	Mean size (mm)	Mean roundness	Lithology (per 50 pebbles)			Sample	Mean size (mm)	Mean roundness	Lithology (per 50 pebbles)		
			Granitic rocks	Sedimentary rocks	Basalt				Granitic rocks	Sedimentary rocks	Basalt
−5, −6	21.9	0.3	50	0	0	−3, −4	[illegible]	1.4	50	0	0
−4, −6	17.4	.2	50	0	0	−2, −4	28.3	1.3	49	1	0
−3, −6	15.1	.4	50	0	0	−1, −4	12.0	.7	50	0	0
−2, −6	13.6	.4	50	0	0	−7, −3	26.0	1.6	50	0	0
−1, −6	16.9	.2	50	0	0	−6, −3	21.0	1.5	49	1	0
−6, −5	31.5	.0	50	0	0	−5, −3	18.6	.5	50	0	0
−5, −5	19.3	.4	49	1	0	−4, −3	18.7	.5	50	0	0
−4, −5	17.9	.1	50	0	0	−3, −3	18.9	.1	50	0	0
−3, −5	14.2	.2	50	0	0	−2, −3	17.8	.2	50	0	0
−2, −5	13.1	.2	50	0	0	−1, −3	18.8	.5	49	1	0
−1, −5	15.9	.4	50	0	0	−7, −2	31.6	1.0	50	0	0
−6, −4	18.4	.1	50	0	0	−6, −2	18.1	.1	50	0	0
−5, −4	17.3	.4	50	0	0	−5, −2	18.7	.1	50	0	0
−4, −4	17.3	.2	50	0	0	−4, −2	14.2	.1	50	0	0

Digitized by Google

TABLE 2.—*Mean size, mean roundness, and lithology of pebbles in Deep Springs Valley, Calif.*—Continued

Sample	Mean size (mm)	Mean round-ness	Lithology (per 50 pebbles)			Sample	Mean size (mm)	Mean round-ness	Lithology (per 50 pebbles)		
			Granitic rocks	Sedimentary rocks	Basalt				Granitic rocks	Sedimentary rocks	Basalt
-3, -2	17.4	0.4	50	0	0	5, -5	12.6	0.3	50	0	0
-2, -2	15.2	.3	50	0	0	6, -5	17.6	.0	50	0	0
-1, -2	10.9	1.9	33	16	1	0, -4	8.9	2.2	41	6	3
-6, -1	17.6	.0	50	0	0	1, -4	10.9	2.2	38	12	0
-5, -1	18.5	.1	50	0	0	2, -4	9.1	1.8	47	1	2
-4, -1	15.9	.1	50	0	0	3, -4	11.1	2.4	38	7	5
-3, -1	15.6	.1	50	0	0	4, -4	8.3	2.0	32	9	9
-2, -1	19.3	.3	50	0	0	5, -4	12.9	.1	50	0	0
-1, -1	11.8	1.8	34	13	3	6, -4	21.2	.0	50	0	0
-6, 0	16.6	.0	50	0	0	0, -3	10.5	2.4	36	12	2
-4, 0	17.6	.1	50	0	0	1, -3	11.7	2.0	41	9	0
-3, 0	22.4	.1	50	0	0	2, -3	7.7	2.2	40	2	8
-2, 0	12.4	1.5	32	16	2	3, -3	7.4	2.1	39	8	3
-1, 0	9.5	2.0	38	7	5	4, -3	6.3	2.4	29	10	11
-6, 1	16.2	.1	50	0	0	5, -3	13.8	.0	50	0	0
-5, 1	16.0	.1	50	0	0	0, -2	10.2	2.3	37	12	1
-4, 1	30.4	.2	50	0	0	1, -2	10.9	2.5	33	10	7
-3, 1	20.6	.2	50	0	0	2, -2	7.7	2.3	42	5	3
-2, 1	19.6	2.1	28	15	7	5, -2	22.8	.0	50	0	0
-1, 1	13.3	2.2	29	17	4	0, -1	11.3	2.0	35	12	3
-4, 2	16.2	.0	50	0	0	1, -1	9.0	2.3	38	11	1
-3, 2	15.5	.1	50	0	0	2, -1	9.9	2.1	39	11	0
-2, 2	12.4	1.8	34	12	4	5, -1	21.3	.0	50	0	0
-1, 2	10.3	2.3	35	12	3	0, 0	15.3	1.8	27	21	2
-5, 3	23.9	.0	50	0	0	1, 0	11.8	2.2	25	23	2
-4, 3	17.3	.0	50	0	0	2, 0	11.9	2.2	29	17	4
-3, 3	20.6	1.4	39	11	0	0, 1	11.9	1.8	34	12	4
-2, 3	13.0	1.6	32	15	3	1, 1	10.0	2.1	34	12	4
-1, 3	11.6	2.0	24	19	7	2, 1	10.8	2.2	29	16	5
-4, 4	15.1	.0	50	0	0	7, 1	15.9	.0	50	0	0
-3, 4	19.9	1.9	33	14	3	8, 1	22.4	.1	50	0	0
-2, 4	14.6	1.8	34	9	7	0, 2	14.1	1.7	35	14	1
-1, 4	14.6	1.6	31	18	1	1, 2	11.9	1.9	30	13	7
-5, 5	24.1	.1	50	0	0	2, 2	18.2	3.3	9	40	1
-4, 5	18.7	.3	50	0	0	3, 2	9.2	2.4	37	10	3
-3, 5	15.9	1.5	34	13	3	4, 2	14.0	.1	50	0	0
-2, 5	15.4	2.0	31	16	3	5, 2	14.3	.2	50	0	0
-1, 5	17.3	.8	38	10	2	6, 2	31.2	.0	50	0	0
-6, 6	19.2	.0	50	0	0	7, 2	17.8	.0	50	0	0
-5, 6	19.2	.2	47	2	1	8, 2	18.2	.0	50	0	0
-4, 6	21.8	2.0	29	19	2	0, 3	21.1	1.8	25	21	4
-3, 6	10.1	1.7	32	14	4	1, 3	17.3	2.7	8	42	0
-2, 6	17.5	2.4	9	40	1	2, 3	20.5	3.1	7	42	1
-1, 6	17.3	1.9	19	27	4	3, 3	11.9	2.1	27	18	5
-6, 7	16.1	.3	47	3	0	4, 3	12.1	.2	46	4	0
-5, 7	20.7	2.3	27	17	6	5, 3	12.4	.2	50	0	0
-4, 7	23.7	2.3	10	37	3	6, 3	20.1	.1	50	0	0
-3, 7	23.9	2.1	11	34	5	7, 3	16.4	.0	50	0	0
-2, 7	18.5	1.5	9	40	1	8, 3	35.6	.0	50	0	0
-1, 7	13.9	1.6	21	26	3	0, 4	14.6	1.5	21	25	4
-6, 8	26.9	2.1	28	17	5	1, 4	13.1	2.1	32	18	0
-5, 8	29.6	1.8	20	25	5	2, 4	10.6	2.2	29	16	5
-4, 8	26.0	1.9	11	29	10	3, 4	12.2	2.2	29	19	2
-3, 8	35.6	1.2	24	17	9	4, 4	17.3	2.1	13	2	35
-2, 8	18.2	2.1	15	35	0	5, 4	11.6	.6	43	6	1
-1, 8	13.7	.7	45	1	4	6, 4	14.4	.9	41	9	0
-7, 9	43.3	3.0	31	15	4	7, 4	15.5	.0	50	0	0
-6, 9	32.1	1.1	19	27	4	8, 4	18.6	.0	50	0	0
-5, 9	24.3	2.0	15	32	3	0, 5	15.5	1.8	22	26	2
-4, 9	25.8	1.8	11	34	5	1, 5	13.4	2.4	14	32	4
-3, 9	20.3	2.3	14	34	2	2, 5	17.3	2.4	9	39	2
-2, 9	10.6	1.4	26	24	0	3, 5	11.1	.7	40	4	1
-1, 9	15.7	.7	48	1	1	4, 5	14.4	1.8	20	1	29
-6, 10	10.6	1.3	18	24	8	5, 5	17.9	.2	50	0	0
-5, 10	28.0	2.1	14	30	6	6, 5	16.2	.1	49	1	0
-4, 10	19.2	1.3	27	20	3	7, 5	17.6	.1	49	1	0
-3, 10	14.8	1.1	23	25	2	8, 5	17.9	.2	48	2	0
-2, 10	10.4	.9	43	4	3	0, 6	14.3	1.7	34	14	2
-1, 10	15.2	.7	47	1	2	1, 6	16.2	1.7	28	21	1
-6, 11	17.0	.6	39	7	4	2, 6	13.8	1.0	42	7	1
-4, 11	23.1	1.8	8	16	26	3, 6	13.1	.9	45	2	3
-3, 11	16.4	.9	31	13	6	4, 6	8.2	.9	46	1	3
-2, 11	18.2	.5	49	1	0	5, 6	14.6	.4	49	0	1
-1, 11	14.9	.3	43	9	[illegible]	6, 6	15.7	.1	50	0	0
-2, 12	18.8	.7	[illegible]	2	[illegible]	7, 6	21.6	.0	50	0	0
-1, 12	18.1	.2	48	1	1	8, 6	21.0	.0	50	0	0
-2, 13	17.2	[illegible]	[illegible]	3	[illegible]	0, 7	16.4	1.7	29	20	1
-1, 13	18.0	[illegible]	[illegible]	[illegible]	[illegible]	1, 7	15.6	.7	[illegible]	[illegible]	0
-6, 14	20.2	.1	44	[illegible]	[illegible]	2, 7	[illegible]	[illegible]	[illegible]	[illegible]	0
-5, 14	17.9	[illegible]	[illegible]	[illegible]	[illegible]	3, 7	11.0	.4	[illegible]	[illegible]	0
-3, 14	17.3	.5	[illegible]	[illegible]	[illegible]	4, 7	11.3	1.7	19	[illegible]	31
-2, 14	[illegible]	[illegible]	[illegible]	[illegible]	[illegible]	5, 7	14.7	2.1	[illegible]	[illegible]	42
-1, 14	[illegible]	[illegible]	[illegible]	[illegible]	[illegible]	[illegible]	[illegible]	[illegible]	[illegible]	[illegible]	0
-3, 15	[illegible]	[illegible]	[illegible]	[illegible]	[illegible]	[illegible]	[illegible]	[illegible]	[illegible]	[illegible]	0
-2, 15	[illegible]	.0	[illegible]	[illegible]	[illegible]	[illegible]	[illegible]	[illegible]	[illegible]	2	1
[illegible]	24.5	[illegible]	[illegible]	[illegible]	[illegible]	[illegible]	[illegible]	1.0	[illegible]	1	1
0, -6	[illegible]	[illegible]	[illegible]	4	[illegible]	[illegible]	[illegible]	[illegible]	[illegible]	[illegible]	[illegible]
1, -6	[illegible]	[illegible]	[illegible]	[illegible]	[illegible]	[illegible]	[illegible]	[illegible]	[illegible]	[illegible]	[illegible]
[illegible]	[illegible]	[illegible]	[illegible]	[illegible]	[illegible]	[illegible]	[illegible]	.7	[illegible]	[illegible]	[illegible]
[illegible]	[illegible]	[illegible]	[illegible]	[illegible]	[illegible]	[illegible]	[illegible]	2.3	[illegible]	[illegible]	42
[illegible]	[illegible]	[illegible]	[illegible]	[illegible]	[illegible]	[illegible]	[illegible]	[illegible]	[illegible]	[illegible]	1
5, -6	[illegible]	[illegible]	[illegible]	[illegible]	[illegible]	[illegible]	[illegible]	.8	[illegible]	[illegible]	[illegible]
6, -6	[illegible]	[illegible]	[illegible]	[illegible]	[illegible]	[illegible]	[illegible]	[illegible]	[illegible]	[illegible]	[illegible]
[illegible]	[illegible]	[illegible]	[illegible]	[illegible]	[illegible]	[illegible]	[illegible]	[illegible]	50	[illegible]	[illegible]
[illegible]	[illegible]	[illegible]	[illegible]	[illegible]	[illegible]	[illegible]	[illegible]	[illegible]	[illegible]	[illegible]	35
[illegible]	[illegible]	[illegible]	[illegible]	9	[illegible]	[illegible]	[illegible]	[illegible]	50	[illegible]	[illegible]
[illegible]	[illegible]	[illegible]	[illegible]	[illegible]	[illegible]	[illegible]	[illegible]	[illegible]	[illegible]	[illegible]	[illegible]
[illegible]	[illegible]	[illegible]	39	6	4	[illegible]	[illegible]	[illegible]	[illegible]	2	1

Digitized by Google

TABLE 2.—*Mean size, mean roundness, and lithology of pebbles in Deep Springs Valley, Calif.*—Continued

Sample	Mean size (mm)	Mean roundness	Lithology (per 50 pebbles)			Sample	Mean size (mm)	Mean roundness	Lithology (per 50 pebbles)		
			Granitic rocks	Sedimentary rocks	Basalt				Granitic rocks	Sedimentary rocks	Basalt
1, 10	12.7	0.6	50	0	0	0, 12	[illegible]	0.4	50	0	0
2, 10	12.7	.7	49	0	1	1, 12	16.9	1.6	36	1	13
3, 10	16.6	1.5	33	0	17	2, 12	[illegible]	[illegible]	23	[illegible]	27
4, 10	18.5	2.2	16	1	33	3, 12	18.6	1.2	50	0	0
5, 10	15.3	.2	50	0	0	4, 12	27.1	1.7	33	[illegible]	13
6, 10	15.9	.6	50	0	0	0, 13	19.0	.7	[illegible]	0	0
0, 11	14.4	.4	46	4	0	1, 13	21.6	2.3	28	0	22
1, 11	13.3	.9	46	1	3	2, 13	19.6	1.2	24	0	26
2, 11	13.3	1.3	39	0	11	3, 13	[illegible]	.0	50	0	0
3, 11	15.0	1.9	25	0	25	0, 14	20.4	.8	40	0	10
4, 11	16.1	1.6	32	9	9	1, 14	25.3	1.0	13	0	37
5, 11	17.0	.1	50	0	0	2, 14	[illegible]	.2	50	0	0

TABLE 3. *Basic data on the tails of the granule-to-clay size distribution*

Sample	Granules (weight percentage)	Clay (weight percentage)	Silt/Clay	Sample	Granules (weight percentage)	Clay (weight percentage)	Silt/Clay
Antelope Springs active channel (pl. 9)							
9	4.21	1.55	6.44:1	291	[illegible]	2.76	2.26:1
62	9.39	.57	5.61:1	301	2.88	[illegible]	∞
85	15.69	.83	6.44:1	318	2.92	1.24	3.67:1
126	.25	[illegible]	5.21:1	353	3.92	2.12	3.11:1
149	.14	1.17	21.89:1	400	[illegible]	1.41	4.94:1
190	14.21	1.42	4.97:1	427	1.28	.91	10.84:1
214	8.28	1.72	5.64:1	463	7.29	1.51	3.62:1
241	15.35	.84	9.75:1	480	[illegible]	1.80	2.94:1
279	17.71	.20	[illegible]	512	.18	.77	4.80:1
				558	.99	1.74	1.65:1
Paiute Chute							
P-1 [1]	10.60	2.10	4.32:1	P-2 [1]	12.90	3.00	4.99:1
Mudflows							
BP-1 [3]	17.12	2.41	4.89:1	Wy-1 [5]	0.00	[illegible]	4.29:1
BP-2 [4]	8.42	4.22	3.67:1				
North end of Deep Springs Valley (fig. 90)							
−5, −4	6.06	1.43	5.36:1	0, 1	2.81	0.99	11.82:1
−4, −4	10.29	.49	26.58:1	7, 1	4.94	2.17	1.69:1
−7, −3	9.04	.98	7.23:1	2, 2	2.00	.75	11.47:1
−2, −3	16.76	1.71	6.20:1	4, 2	6.01	3.62	6.11:1
−5, 0	7.51	1.10	7.48:1	0, 3	5.27	3.79	3.05:1
−3, 0	8.40	4.12	2.96:1	6, 3	28.50	.00	∞
−1, 0	13.31	.84	32.96:1	8, 3	30.00	2.01	6.80:1
−1, 3	2.16	1.34	11.82:1	3, 4	3.14	2.46	4.92:1
−3, 5	6.86	.98	17.60:1	0, 5	3.30	.97	13.30:1
−6, 6	1.85	1.16	8.46:1	4, 5	3.27	3.11	5.06:1
−5, 7	4.76	2.15	4.76:1	6, 5	17.82	1.61	16.64:1
−4, 7	4.02	2.70	5.76:1	8, 5	21.19	1.72	8.00:1
−6, 8	5.69	.92	5.63:1	2, 6	7.95	.00	∞
−7, 9	13.32	1.67	8.90:1	0, 7	5.34	1.11	11.60:1
−5, 9	6.08	2.14	7.10:1	4, 7	.34	1.48	10.15:1
−5, 10	1.79	6.37	3.91:1	6, 7	23.60	.64	27.28:1
−3, 10	2.04	1.83	5.76:1	2, 8	5.75	1.45	7.67:1
−1, 12	8.76	1.31	8.46:1	3, 8	2.84	2.34	6.48:1
−2, 14	14.99	.00	∞	0, 9	10.91	.78	15.30:1
0, −6	5.02	2.35	7.04:1	3, 9	8.60	1.38	11.19:1
3, −6	1.90	2.59	11.05:1	5, 9	8.02	1.37	10.78:1
4, −5	2.62	3.93	5.81:1	1, 10	3.52	1.07	8.95:1
6, −5	20.40	.70	12.00:1	4, 10	3.94	2.18	7.91:1
0, −4	5.70	1.66	8.00:1	6, 10	15.19	1.74	10.06:1
2, −4	1.74	3.91	11.12:1	0, 11	11.39	.84	11.23:1
3, −4	5.61	.00	∞	3, 11	4.15	1.68	7.16:1
5, −4	11.88	1.04	19.18:1	5, 11	22.65	1.68	6.25:1
4, −3	12.58	3.53	8.16:1	2, 12	9.99	.67	7.30:1
1, −2	11.19	2.48	6.78:1	4, 12	9.99	1.28	4.16:1
2, −2	3.68	.00	∞	1, 13	16.58	.88	10.44:1
1, −1	5.59	3.23	10.87:1	3, 13	15.04	2.60	6.70:1
3, −1	3.79	26.58	1.06:1	0, 14	10.21	.89	9.95:1
2, 0	2.28	1.29	7.81:1	2, 14	16.06	1.26	9.44:1

[1] At fan apex.
[2] At midfan.
[3] 2 miles below mountain front.
[4] 8 miles below mountain front.
[5] At BM 5220.

TABLE 4.—*Sedimentary parameters of the granule-to-clay size fraction, in phi units*

Sample	Median	Mz	σ_I	Sk_I	K_G	Sample	Median	Mz	σ_I	Sk_I	K_G
Antelope Springs active channel (pl. 9)											
9	1.96	1.96	2.12	0.12	1.62	301	[illegible]	2.43	1.55	0.21	1.49
62	1.28	1.22	1.53	−.30	1.16	318	1.67	1.71	1.35	.11	1.84
85	1.65	1.27	2.01	−.15	1.10	353	[illegible]	1.66	1.86	.03	1.16
126	2.14	2.24	1.46	.27	1.60	400	1.73	1.56	1.66	.28	1.38
149	3.32	3.78	1.89	.40	1.34	[illegible]	1.90	[illegible]	1.63	.27	1.41
190	1.02	[illegible]	2.10	.15	1.28	463	1.71	1.69	1.92	.03	1.34
214	2.26	2.13	2.23	−.02	1.73	[illegible]	2.07	2.11	1.19	.12	1.42
241	1.30	1.18	1.97	.03	1.06	512	1.66	1.72	1.03	.19	1.22
279	[illegible]	.70	1.69	−.01	.90	558	1.73	1.77	[illegible]	[illegible]	1.13
291	[illegible]	1.49	2.01	.12	1.33						
Paiute Chute											
P-1 [1]	1.64	1.53	2.17	0.07	1.89	P-2 [2]	1.30	1.67	2.67	0.27	1.06
Mudflows											
BP-1 [3]	0.96	1.13	2.47	0.25	1.15	Wy-1 [5]	6.30	6.29	1.67	0.03	0.83
BP-2 [4]	1.83	2.01	2.73	.31	1.19						
North end of Deep Springs Valley (fig. 90)											
−5, −4	1.70	1.80	[illegible]	0.18	1.24	7, 1	1.12	1.27	1.56	.19	[illegible]
−4, −4	.74	1.25	[illegible]	.29	1.13	2, 2	1.51	1.71	[illegible]	[illegible]	1.17
−7, −3	1.01	1.20	2.08	.27	1.22	4, 2	2.90	2.89	2.77	[illegible]	1.14
−2, −3	.49	1.08	[illegible]	.41	1.11	0, 3	1.93	2.03	[illegible]	[illegible]	1.31
−5, 0	[illegible]	1.37	2.03	.29	1.24	6, 3	−.18	[illegible]	1.71	[illegible]	1.01
−3, 0	1.49	1.72	2.30	.37	1.20	8, 3	.55	1.11	2.65	.40	[illegible]
−1, 0	.70	1.07	[illegible]	.34	1.19	3, 4	2.51	2.38	[illegible]	.04	1.40
−1, 3	1.78	2.02	[illegible]	[illegible]	1.17	0, 5	1.61	1.70	[illegible]	.17	1.08
−3, 5	1.70	2.35	[illegible]	[illegible]	1.06	4, 5	2.00	[illegible]	2.46	.25	1.15
−6, 6	1.56	1.73	1.98	.25	1.17	6, 5	2.73	2.49	3.13	−.08	.77
−5, 7	1.60	1.61	2.12	.24	1.20	8, 5	[illegible]	1.06	2.62	.41	.97
−4, 7	[illegible]	2.28	2.36	.24	1.19	2, 6	1.22	1.44	2.09	.22	1.44
−5, 8	.81	1.34	1.64	.29	1.22	0, 7	[illegible]	2.14	2.09	.00	1.22
−7, 9	[illegible]	1.64	[illegible]	.22	[illegible]	4, 7	2.37	2.44	[illegible]	.22	1.22
−5, 9	1.68	1.97	2.42	[illegible]	1.08	6, 7	.60	1.25	3.77	.40	[illegible]
−5, 10	2.89	3.39	2.60	.28	.97	2, 8	1.72	1.78	2.15	.16	1.14
−3, 10	1.65	1.83	2.06	.25	1.12	3, 8	2.21	[illegible]	2.18	.20	[illegible]
−1, 12	1.51	1.61	2.24	.15	1.18	0, 9	1.30	1.49	2.27	.22	1.11
−2, 14	.71	[illegible]	2.22	.30	1.09	3, 9	1.40	1.73	2.67	[illegible]	1.08
0, −6	2.10	2.30	2.38	.24	1.18	5, 9	1.92	[illegible]	2.25	.15	[illegible]
3, −6	3.13	3.85	2.65	.12	.87	1, 10	[illegible]	1.82	1.71	.10	[illegible]
4, −5	3.10	3.23	2.91	.10	1.20	4, 10	2.46	2.51	2.39	.11	1.17
6, −5	.57	.79	2.23	.27	1.24	6, 10	[illegible]	[illegible]	2.78	[illegible]	.96
0, −4	2.11	2.01	2.21	.07	1.14	0, 11	.71	1.12	2.23	[illegible]	1.18
2, −4	3.80	[illegible]	2.74	.00	1.01	3, 11	1.66	[illegible]	2.14	.27	1.16
3, −4	1.31	1.27	1.28	−.06	[illegible]	5, 11	.42	[illegible]	2.48	[illegible]	1.04
5, −4	1.95	2.11	2.72	.15	.98	2, 12	.61	.67	1.61	.34	1.26
4, −3	3.20	2.98	3.13	−.06	[illegible]	4, 12	.70	.87	1.85	.25	1.25
1, −2	1.89	2.04	2.67	.16	1.04	1, 13	[illegible]	.81	2.22	.41	1.89
2, −2	1.52	1.61	1.59	.15	1.28	3, 13	1.52	1.81	2.80	[illegible]	1.14
1, −1	3.30	3.38	2.93	.08	.82	0, 14	1.20	[illegible]	2.13	.20	1.19
2, 0	1.99	2.10	1.83	.21	1.33	2, 14	.94	1.30	2.46	.28	1.02
0, 1	1.82	1.84	1.97	.28	1.85						

[1] At fan apex.
[2] At midfan.
[3] 2 miles below mountain front.
[4] 8 miles below mountain front.
[5] BM 5220.

Digitized by Google

TABLE 5.—*Sample modes and their weight percentage of the granule-to-clay size fraction*

Sample	Primary mode	Weight percent	Secondary mode	Weight percent
Antelope Springs active channel (pl. 9)				
9	Medium sand	26.31	None	
62	do	29.38	do	
85	do	25.55	Granules	15.60
126	do	31.84	None	
149	Very fine sand	33.79	do	
199	Medium sand	22.75	Silt	[illegible]
214	Fine sand	26.36	Granules	6.25
241	Medium sand	22.49	do	15.35
279	do	23.88	do	17.71
291	do	24.92	None	
301	Fine sand	30.21	Granules	2.88
318	Medium sand	30.36	None	
353	do	21.95	do	
400	do	31.49	do	
437	do	33.06	do	
463	do	26.50	do	
480	do	33.52	do	
512	do	45.95	do	
563	do	43.43	do	
Paiute Chute				
P-1 [1]	Medium sand	25.41	Granules	10.60
P-2 [2]	Coarse sand	16.91	Silt	14.70
Mudflows				
BP-1 [3]	Medium sand	17.46	Granules	17.12
BP-2 [4]	do	18.80	Silt	15.07
Wy-1 [5]	Silt	77.25	None	
North end of Deep Springs Valley (fig. 90)				
−5, −4	Medium sand	21.55	None	
−4, −4	Coarse sand	22.90	Silt	12.00
−7, −3	do	22.24	None	
−2, −3	Very coarse sand	23.07	Silt	10.78
−5, 0	Coarse sand	35.15	None	
−3, 0	Very coarse sand	19.81	Silt	12.20
−1, 0	do	22.71	do	[illegible]
−1, 3	Medium sand	24.15	do	14.31
−3, 5	Coarse sand	19.12	do	17.39
−5, 5	do	26.40	None	
−6, 7	do	22.09	do	
−4, 7	Medium sand	21.28	Very fine sand	16.17
−5, 8	Coarse sand	29.63	None	
−7, 9	Very coarse sand	17.34	Silt	[illegible]
−5, 9	Coarse sand	19.86	do	15.21
−5, 10	Silt	24.81	Medium sand	[illegible]
−3, 10	Coarse sand	23.27	Very fine sand	15.44
−1, 12	Medium sand	20.04	None	
−2, 14	Coarse sand	30.64	Silt	9.65
0, −6	Medium sand	18.67	Very fine sand	17.39
2, −6	Silt	31.95	Medium sand	14.25
4, −5	Very fine sand	[illegible]	None	
6, −5	Coarse sand	22.80	Granules	20.40
0, −4	Very fine sand	18.96	None	
2, −4	Silt	40.35	Very coarse sand	7.46
3, −4	Medium sand	32.30	None	
5, −4	Silt	19.96	Medium sand	13.47
4, −3	do	28.80	Granules	12.55
1, −2	Very fine sand	17.17	[illegible]	15.06
2, −2	Medium sand	31.97	None	
1, −1	Silt	35.10	Medium sand	12.37
5, −1	do	28.05	Coarse sand	15.39
2, 0	Medium sand	36.60	None	
0, 1	do	35.04	do	
7, 1	Coarse sand	[illegible]	do	
2, 2	do	35.16	do	
4, 2	Very fine sand	22.33	Medium sand	12.94
0, 3	Medium sand	20.71	Very fine sand	16.99
6, 3	Granules	36.50	Silt	4.62
8, 3	Very coarse sand	20.49	do	13.72
3, 4	Very fine sand	22.90	None	
0, 5	Coarse sand	18.24	Very fine sand	15.84
4, 5	Medium sand	18.76	do	17.09
6, 5	Silt	26.80	Granules	17.82
8, 5	Granules	21.19	Silt	13.75
2, 6	Coarse sand	21.08	Very fine sand	13.79
0, 7	Very fine sand	21.69	None	
4, 7	Medium sand	24.30	Very fine sand	21.00
6, 7	Granules	23.60	Silt	13.46
2, 8	Medium sand	19.71	None	
3, 8	do	21.15	do	
0, 9	Coarse sand	20.15	Silt	11.91
3, 9	do	30.60	do	15.29
5, 9	Very fine sand	17.37	Medium sand	16.68
1, 10	Medium sand	28.28	None	
4, 10	Very fine sand	21.12	Medium sand	17.14

TABLE 5.—*Sample modes and their weight percentage of the granule-to-clay size fraction*—Continued

Sample	Primary mode	Weight percent	Secondary mode	Weight percent
North end of Deep Springs Valley (fig. 90)				
6, 10	Silt	17.48	Very coarse sand	17.26
0, 11	Coarse sand	22.90	Silt	[illegible]
3, 11	do	[illegible]	Very fine sand	15.21
5, 11	Granules	22.65	Silt	10.45
2, 12	Coarse sand	30.39	None	
4, 12	do	24.99	do	
1, 13	Very coarse sand	24.92	Silt	[illegible]
3, 13	Silt	16.60	Very coarse sand	15.75
0, 14	Medium sand	[illegible]	None	
2, 14	Coarse sand	18.02	Silt	11.89

[1] At fan apex.
[2] At midfan.
[3] 2 miles below mountain front.
[4] 8 miles below mountain front.
[5] BM 5220

TABLE 6.—*Clay-mineral ratios of related samples, in parts per ten*

Sample	Mont-morillo-nite group	Illite	Kaolinite and (or) chlorite	Sample	Mont-morillo-nite group	Illite	Kaolinite and (or) chlorite
Antelope Springs active channel (pl. 9)							
9	6.2	2.8	1.0	300	2.1	[illegible]	2.1
85	1.3	6.5	2.2	318	2.2	5.7	2.1
126	2.6	5.6	1.8	353	[illegible]	[illegible]	1.8
149	3.1	4.8	2.1	400	2.1	5.5	2.4
199	.7	7.0	2.3	437	3.1	4.2	2.7
214	2.4	5.3	2.3	463	3.2	4.2	2.6
241	4.0	4.3	1.7	480	[illegible]	4.7	1.9
279	2.5	6.0	1.5	512	1.8	7.1	1.0
291	3.7	3.9	2.4	563	2.2	5.6	2.2
Paiute Chute							
P-1	7.1	1.9	1.0	P-2	5.5	3.4	1.1
Mudflows							
BP-1 [1]	2.4	5.2	2.4	Wy-1 [2]	5.7	3.5	0.8
BP-2 [1]	4.8	2.9	2.3				
North end of Deep Springs Valley (fig. 90)							
2, 14	3.3	4.1	[illegible]	−5, 8	1.1	[illegible]	2.1
3, 13	5.8	[illegible]	.8	3, 8	[illegible]	4.5	1.3
4, 12	[illegible]	2.5	1.5	−6, 7	4.3	3.9	1.8
5, 11	5.1	3.0	1.9	−4, 7	3.4	5.4	1.2
6, 10	6.0	2.6	1.4	−5, 6	3.9	[illegible]	1.6
−5, 10	5.6	4.2	.2	−3, 5	4.3	[illegible]	1.4
4, 10	4.8	4.0	1.2	−1, 3	2.6	5.7	1.7
−5, 9	3.1	5.1	1.8	1, −1	[illegible]	4.3	1.7
6, 9	4.7	3.6	1.7	0, 1	4.5	[illegible]	1.0
3, 9	3.0	5.1	1.9	4, 7	3.4	5.2	1.4

[1] At Big Pine.
[2] BM 5220

REFERENCES

American Society of Civil Engineers, Task Force Committee on Hydromechanics, 1963, Friction factors in open channels: Am. Soc. Civil Engineers Proc., Jour. Hydraulics Div., v. 89, no. HY 2, p. 97–143.

Antevs, E. V., 1948, The Great Basin, with emphasis on glacial and post-glacial times. 3, Climatic changes and pre-white man: Univ. Utah Bull., v. 38, no. 20, p. 168–191.

———1952, Cenozoic climates of the Great Basin: Geol. Rundschau, v. 40, p. 94–108.

Blackwelder, Elliot, 1928, Mudflows as a geologic agent in semi-arid mountains: Geol. Soc. America Bull., v. 39, p. 465–484.

Digitized by Google

Blackwelder, Elliot, 1954, Pleistocene lakes and drainage in the Mohave region, southern California: California Div. Mines Bull. 170, Chap. 5, p. 35–40.

Blissenbach, Erich, 1952, Surface angle and particle size distribution on alluvial fans: Jour. Sed. Petrology, v. 22, p. 25–28.

———1954, Geology of alluvial fans in semi-arid regions: Geol. Soc. America Bull., v. 65, p. 175–190.

Braithwaite, R. B., 1955, Scientific explanation: A study of the function of theory, probability, and law in science: London, Cambridge Univ. Press, 376 p.

Bryan, Kirk, 1941, Correlation of the deposits of Sandia Cave, New Mexico, with the glacial chronology: Smithsonian Misc. Colln., v. 99, no. 23, p. 45–64.

Bull, W. B., 1960, Type of deposition on alluvial fans in western Fresno Co., California [abs.]: Geol. Soc. America Bull., v. 71, p. 2052.

Buwalda, J. P., 1951, Transportation of coarse material on alluvial fans [abs.]: Geol. Soc. America Bull., v. 62, p. 1497.

Chorley, R. J., 1962, Geomorphology and general systems theory: U.S. Geol. Survey Prof. Paper 500–B, p. B1–B10.

Clements, T., 1952, Wind-blown rocks and trails on Little Bonnie Claire Playa, Nye Co., Nevada: Jour. Sed. Petrology, v. 22, p. 182–186.

Croft, A. R., 1962, Some sedimentation phenomena along the Wasatch mountain front: Jour. Geophys. Research, v. 67, p. 1511–1524.

Cullity, B. D., 1956, Elements of X-ray diffraction: Reading, Mass., Addison-Wesley, 514 p.

Dake, C. L., 1921, The problem of the St. Peter sandstone: Missouri School Mines and Metall. Bull., v. 6, p. 158–163.

Davis, W. M., 1889, The rivers and valleys of Pennsylvania: Natl. Geog. Mag., v. 1, p. 183–253.

———1905, The geographical cycle in an arid climate: Jour. Geology, v. 13, p. 381–407.

Denny, C. S., 1965, Alluvial fans in the Death Valley region, California and Nevada: U.S. Geol. Survey Prof. Paper 466, 62 p.

Droste, J. B., 1961, Clay minerals in sediments of Owens, China, Searles, Panamint, Bristol, Cadiz, and Danby Lake basins, California: Geol. Soc. America Bull., v. 72, p. 1713–1722.

Dury, G. H., 1958, Tests of a general theory of misfit streams: British Geog. Inst. Trans. and Papers Pub. 25, p. 105–118.

Eardley, A. J., and Gvosdetsky, V., 1960, Analysis of a Pleistocene core from Great Salt Lake, Utah: Geol. Soc. America Bull., v. 71, p. 1323–1344.

Eckis, Rollin, 1928, Alluvial fans of the Cucamonga district, southern California: Jour. Geology, v. 36, p. 224–247.

Eppley, R. A., 1961, Earthquake history of the United States; Part II, Stronger earthquakes of California and western Nevada: U.S. Dept. Commerce Pub. 41-1, rev. ed. (1960), 55 p.

Fahnestock, R. K., 1961, Competence of a glacial stream: U.S. Geol. Survey Prof. Paper 424–B, p. 211–213.

Feth, J. H., 1961, A new map of the western coterminous United States showing the maximum known or inferred extent of Pleistocene lakes: U.S. Geol. Survey Prof. Paper 424–B, p. 110–112.

Flint, R. F., 1957, Glacial and Pleistocene geology: New York, John Wiley & Sons, 553 p.

Folk, R. L., and Ward, W. C., 1957, Brazos River bar; a study in the significance of grain size parameters: Jour. Sed. Petrology, v. 27, p. 3–26.

Freidman, G. M., 1961, Distinction between dune, beach, and river sands from their textural characteristics: Jour. Sed. Petrology, v. 31, p. 514–529.

Fryxell, F. M., and Horberg, C. L., 1943, Alpine mud flows in Grand Teton National Park, Wyoming: Geol. Soc. America Bull., v. 54, p. 457–472.

Gilbert, G. K., 1914, Transportation of debris by running water: U.S. Geol. Survey Prof. Paper 86, 263 p.

Grove, A., and Sparks, P. W., 1952, Le deplacement des galets par le vent sur la glace: Rev. Géomorphologie Dynamique, v. 3, p. 37–39.

Guilcher, A., and Cailleux, A., 1950, Relief et formations quarternaires du centre-est des Pays-Bas: Rev. Géomorphologie Dynamique, v. 1, p. 128–143.

Hack, J. T., 1942, The changing environment of the Hopi Indians of Arizona: Harvard Univ., Peabody Mus. Archeol. and Ethnol. Papers, v. 35, no. 1, 85 p.

———1960, Interpretation of erosional topography in humid temperate regions: Am. Jour. Sci., Bradley Volume, v. 258A, p. 80–97.

Hjulström, Filip, 1935, Studies of the morphological activity of rivers as illustrated by the River Fyris: Upsala, Univ., Geol. Inst. Bull., v. 25, p. 221–527.

Hubbs, C. L., and Miller, R. R., 1948, The zoological evidence: correlation between fish distribution and hydrographic history of western United States. Part II, The Great Basin: Univ. Utah Bull., v. 38, no. 20, 166 p.

Hunt, Alice, 1960, Archeology of the Death Valley salt pan, California: Univ. Utah Anthropol. Papers, 47, 313 p.

Hunt, C. B., 1954, Pleistocene and recent deposits of the Denver area, Colorado: U.S. Geol. Survey Bull. 996–C, p. 91–139.

Jamieson, T. F., 1863, On the parallel roads of Glen Roy, and their place in the history of the glacial period: Geol. Soc. London Quart. Jour., v. 19, p. 235–259.

Johns, W. D., Grim, R. E., and Bradley, W. F., 1954, Quantitative estimates of clay minerals by diffraction methods: Jour. Sed. Petrology, v. 24, p. 242–251.

Judson, Sheldon, 1953, Geology of the San Jon site, eastern New Mexico: Smithsonian Misc. Colln., v. 21, 70 p.

Kagani, H., 1961, Modal analysis of marine sediments in the southern part of Tokyo Bay: Japanese Jour. Geology and Geography, v. 32, p. 523–532.

Kessell, J. E., and Beaty, C. B., 1959, Desert flood conditions in the White Mountains of California and Nevada: U.S. Army Quartermaster Research and Eng. Tech. Rept. EP–108, 107 p.

Kirk, L., 1952, Trails and rocks observed on a playa in Death Valley National Monument: Jour. Sed. Petrology, v. 22, p. 173–181.

Knopf, Adolph, 1918, A geologic reconnaissance of the Inyo Range and the eastern slope of the Sierra Nevada, California: U.S. Geol. Survey Prof. Paper 110, 130 p.

Krumbein, W. C., 1940, Flood gravel of San Gabriel Canyon, California: Geol. Soc. America Bull., v. 51, p. 639–676.

Langbein, W. B., 1961, Salinity and hydrology of closed lakes: U.S. Geol. Survey Prof. Paper 412, 20 p.

Le Conte, L. J., 1896, Discussion of "The Suspension of Solids in Flowing Water," by E. H. Hooker: Am. Soc. Civil Engineers Trans., v. 36, p. 338–340.

Digitized by Google

Leliavsky, Serge, 1955, An intrdouction to fluvial hydraulics: London, Constable & Son, 257 p.

Leopold, L. B., 1951, Pleistocene climates in New Mexico: Am. Jour. Sci., v. 249, p. 152–167.

———1951, Rainfall frequency—an aspect of climatic variation: Am. Geophys. Union Trans., v. 32, p. 347–357.

———1962, Rivers: Am. Scientist, v. 50, p. 511–537.

Leopold, L. B., and Langbein, W. B., 1962, The concept of entropy in landscape evolution: U.S. Geol. Survey Prof. Paper 500–A, 20 p.

Leopold, L. B., and Miller, J. P., 1956, Ephemeral streams—Hydraulic factors and their relation to the drainage net: U.S. Geol. Survey Prof. Paper 282–A, 37 p.

McAllister, J. F., and Agnew, A. F., 1948, Playa scrapers and furrows on Racetrack Playa, Inyo Co., California [abs.]: Geol. Soc. America Bull., v. 59, p. 1377.

McCammon, R. B., 1962, Efficiencies of percentile measures for describing mean size and sorting of sedimentary particles: Jour. Geology, v. 70, p. 453–465.

Mason, C. C., and Folk, R. L., 1958, Differentiation of beach, dune, and aeolian flat environments by size analysis, Mustang Island, Texas: Jour. Sed. Petrology, v. 28, p. 211–226.

Menard, H. W., 1950, Sediment movement in relation to current velocity: Jour. Sed. Petrology, v. 20, p. 148–160.

Miller, J. P., 1958, High mountain streams—effects of geology on channel characteristics and bed material: New Mexico Inst. Mining and Technology Mem. 4, 53 p.

Miller, J. P., and Wendorf, Fred, 1958, Alluvial chronology of the Tesuque Valley, New Mexico: Jour. Geology, v. 66, p. 177–194.

Miller, W. J., 1928, Geology of Deep Springs Valley, California: Jour. Geology, v. 36, p. 510–525.

Morrison, R. B., 1961, Correlation of the deposits of Lakes Lahonton and Bonneville and the glacial sequences of the Sierra Nevada and Wasatch Mountains, California, Nevada, and Utah: U.S. Geol. Survey Prof. Paper 424–D, p. D122–D124.

Nelson, C. A., 1962, Lower Cambrian-Precambrian succession, White-Inyo Mountains, California: Geol. Soc. America Bull., v. 73, p. 139–144.

———1963, Preliminary geologic map of the Blanco Mountain quadrangle, Inyo and Mono Counties, California: U.S. Geol. Survey Mineral Inv. Map MF–256.

Nevin, C., 1946, Competency of moving water to transport debris: Geol. Soc. America Bull., v. 57, p. 651–674.

Pack, J. F., 1923, Torrential potential of desert waters: Pan Am. Geol., v. 40, p. 349–356.

Pettijohn, F. J., 1957, Sedimentary rocks: 2d ed., New York, Harper & Bros., 718 p.

Richmond, G. M., 1962, Quaternary stratigraphy of the La Sal Mountains, Utah: U.S. Geol. Survey Prof. Paper 324, 135 p.

Rickmers, W. R., 1913, The Duab of Turkestan; a physiographic sketch and an account of some travels: London, Cambridge Univ. Press, 564 p.

Rouse, Hunter, 1950, Engineering hydraulics: New York, John Wiley & Sons, 1039 p.

Schumm, S. A., 1956, The movement of rocks by wind: Jour. Sed. Petrology, v. 26, p. 284–286.

Sharp, R. P., 1942, Mudflow levees: Jour. Geomorphology, v. 5, p. 222–227.

Sharp, R. P., and Nobles, L. H., 1953, Mudflows of 1941 at Wrightwood, southern California: Geol. Soc. America Bull., v. 64, p. 547–560.

Strahler, A. N., 1952, Dynamic basis of geomorphology: Geol. Soc. America Bull., v. 63, p. 923–938.

Suchier, A., 1883, Die Bewegung der Geschiebe des Oberrhein: Deutsche Bauzeitung, no. 56, p. 331.

Sundborg, Åke, 1956, The River Klaralven; a study of fluvial process: Geografiska Annaler, v. 38, p. 127–316.

Talvenheimo, G., and White, J. L., 1952, Quantitative analysis of clay minerals with the X-ray spectrometer: Analytical Chemistry, v. 24, p. 1784–1789.

Tricart, J., and others, 1961, Mécanismes normaux et phénomènes catastrophiques dans l'évolution des versants du bassin du Guil (Hautes-Alpes, France): Zeitschr. Geomorphologie, v. 5, p. 277–301.

Von Bertalanffy, Ludwig, 1950, The theory of open systems in physics and biology: Science, v. 111, p. 23–29.

Weaver, C. E., 1958, Geological interpretation of argillaceous sediments: Am. Assoc. Petroleum Geologists Bull., v. 42, p. 254–271.

Wooley, R. R., 1946, Cloudburst floods in Utah, 1850–1938: U.S. Geol. Survey Water-Supply Paper 994, 127 p.

Yatsu, E., 1959, On the discontinuity of grainsize frequency distributions of fluvial deposits and its geomorphological significance: Internat. Geog. Union, Regional Conf. Japan, Toyko 1957, Proc., p. 224–242.

U.S. GOVERNMENT PRINTING OFFICE 1965 O—766-076

Digitized by Google

QE75
.A26
no. 352-G

Geol
1966

THE UNIVERSITY OF CHICAGO LIBRARY
JUL 11 1966

Channel and Hillslope Processes in a Semiarid Area New Mexico

45
4

GEOLOGICAL SURVEY/PROFESSIONAL PAPER/352-G

Leopold and others—CHANNEL AND HILLSLOPE PROCESSES, SEMIARID AREA, NEW MEXICO—Geological Survey Professional Paper 352-G

Channel and Hillslope Processes in a Semiarid Area New Mexico

By LUNA B. LEOPOLD, WILLIAM W. EMMETT, and ROBERT M. MYRICK

EROSION AND SEDIMENTATION IN A SEMIARID ENVIRONMENT

GEOLOGICAL SURVEY PROFESSIONAL PAPER 352-G

UNITED STATES GOVERNMENT PRINTING OFFICE, WASHINGTON : 1966

Digitized by Google

UNITED STATES DEPARTMENT OF THE INTERIOR

STEWART L. UDALL, *Secretary*

GEOLOGICAL SURVEY

William T. Pecora, *Director*

DEPOSITORY COLLECTION

For sale by the Superintendent of Documents, U.S. Government Printing Office
Washington, D.C. 20402 - Price 50 cents (paper cover)

CONTENTS

	Page
Abstract	193
Acknowledgments	193
Alluvial fills in western valleys	193
Geographic setting	195
Valley alluvium	195
The local bedrock	198
Relation of valley alluvium and colluvium to headwater areas	199
Study areas	201
Methods of study	201
Magnitude and frequency of rainfall and streamflow, 1958-64	202
Channel form and bed materials	203
Spacing of gravel bars	207
Movement of coarse particles	209
Scour and fill	215
Hillslope erosion	220
Erosion plot on Slopewash Tributary	220
Slope-retreat pins on Slopewash Tributary	222
Other measurements of slope erosion on Slopewash Tributary	227
Erosion nails on Coyote C. Arroyo	227
Tracing of fluorescent sand	227
Channel enlargement on Slopewash Tributary	228
Soil creep or mass movement	228
Slopewash Tributary	228
Coyote C. Arroyo	229
Headcut enlargement	229
Fence Line Headcut	229
Coyote C. Arroyo Headcut	230
Movement of large particles in headwater rills	232
Slopewash Tributary	232
Gunshot Arroyo	232
Morning Walk Wash	234
Sedimentation in channels and reservoirs	235
Analysis of sediment budget	236
Climatological observations during aggradation	240
References	243
Summary of data:	
A, Nonrecorded rain-gage data, Arroyo de los Frijoles, 159-63	247
B, Recorded rain-gage data at Main Project Reach, 1959-62	247
C, Erosion-pin plot in Slopewash Tributary, 1959-64	248
D, Slope-retreat pins in Slopewash Tributary, 1959-64	249
E, Iron-pin lines in Slopewash Tributary, 1958-64	250
F, Erosion nail lines in Coyote C. Arroyo, 1961-64	250
G, Nail sections A-J in Slopewash Tributary, 1959-64	251
H, Mass-movement line in Slopewash Tributary, 1959-64	251
I, Mass-movement line in Coyote C. Arroyo, 1961-64	251
J, Movement of coarse particles in Morning Walk Wash, 1961-64	252

ILLUSTRATIONS

	Page
FIGURE 138. Location map	195
139. Detailed area map	196
140. Photographs showing typical aspects of valleys and terraces	197
141. Diagrammatic cross section of alluvial valley	198
142. Stratigraphic cross sections of minor tributaries	200
143. Topographic map of Arroyo de los Frijoles	202
144. Topographic map of Slopewash Tributary	204
145. Sketch map of Coyote C. Arroyo	205
146. Photographs of several study areas	207
147-150. Graphs showing:	
147. Magnitude and frequency of streamflows, Arroyo de los Frijoles	208
148. Relation of channel width and drainage area to channel length	209
149. Bed-material grain-size analyses	210
150. Distribution of coarsest particles along length of channel	211
151. Sections showing spacing and composition of gravel bars	212
152. Photographs of painted rock experiments	214
153-156. Graphs showing:	
153. Effect of spacing and particle size on ability of flows to move rocks	215
154. Summary of data relating discharge, size, and spacing for painted rock experiments	216
155. Transport distance of rocks as function of particle weight	217
156. Transport distance of rocks as function of discharge	219

Digitized by Google

		Page
FIGURE 157.	Photograph of scour chain	220
158–161.	Graphs showing:	
	158. Downstream pattern of scour and fill for different time periods	221
	159. Depth of scour as function of discharge	222
	160. Scour and fill, Main Project Reach	223
	161. Accumulative net changes in bed elevation, Arroyo de los Frijoles	224
162.	Photographs of erosion pins	225
163.	Sketch map showing slope-retreat pins, Slopewash Tributary	226
164.	Graph showing 6-year net erosion, Slopewash Tributary	227
165.	Photograph of Fence Line Headcut	229
166.	Photographs of headcuts and valley alluvium	230
167.	Topographic map and profile, Coyote C. Arroyo headcut	231
168.	Photograph of Green Rock Gulch	232
169.	Profile of Gunshot Arroyo showing movement of coarse particles	233
170.	Topographic map of dam and reservoir, Coyote C. Arroyo	235
171–174.	Graphs of:	
	171. Precipitation parameters, 1853–1962, for station at Santa Fe, N. Mex	241
	172. Individual summer rains	241
	173. Individual nonsummer rains	242
	174. Average annual intensity of rainfall	243

TABLES

		Page
TABLE 1.	Characteristics of locations studied	201
2.	Summary of flows at three locations along Arroyo de los Frijoles, 1958–63	203
3.	Relation of transport distance to flow discharge	218
4.	Mean depth of scour as a function of discharge	220
5.	Summary of particle movement, Morning Walk Wash, 1961–62	234
6.	Observed sedimentation in reservoir behind dam on Coyote C. Arroyo, 1961–64	232
7.	Observed rates of channel changes in Coyote C. Arroyo, 1961–64	236
8.	Data on measured rates of erosion and deposition	237
9.	Average rates of erosion and deposition	238

CHANNEL AND HILLSLOPE PROCESSES IN A SEMIARID AREA, NEW MEXICO

By Luna B. Leopold, William W. Emmett, and Robert M. Myrick

ABSTRACT

Ephemeral washes having drainage areas from a few acres to 5 square miles are shown by actual measurement to be accumulating sediment on the streambed. This aggradation is not apparent to the eye but is clearly shown in 7 years of annual remeasurement.

A similar aggradation was in progress in the same area some 3000 years ago as evidenced by an alluvial terrace later dissected by the present channel system. At that time as well as at present, aggradation occurred even in tributary areas draining a few acres. Colluvial accumulations merge with channel deposits and blanket the valleys and tributary basins even up to a few hundred feet of the drainage divides.

The present study concerned the amounts of sediment produced by different erosion processes in various physiographic positions in the drainage basins. Measurements show that by far the largest sediment source is sheet erosion operating on the small percentage of basin area near the basin divides.

Mass movement, gully head extension, and channel enlargement are presently small contributors of sediment compared with sheet erosion on unrilled slopes. As in previous studies, not all of the erosion products could be accounted for by accumulations on colluvial slopes and on beds of channels. The discrepancies are attributed primarily to sediment carried completely out of the basins studied and presumably deposited somewhere downstream.

Aggradation of alluvial valleys of 5 square miles area and smaller both in the present epicycle, and in prehistorical but post-glacial times in this locality, cannot be attributed to gullying or rill extension in the headwater tributaries but to sheet erosion of the most upstream margins of the basins.

Studies of rainfall characteristics of the 7 years of measurement compared with previous years in the 100-year record do not provide a clear-cut difference which would account for the presently observed aggradation of channels. Longer period of measurement of erosion and sedimentation will be necessary to identify what precipitation parameters govern whether the channels aggrade or degrade.

ACKNOWLEDGMENTS

This study was conceived and initiated by Dr. John P. Miller and the senior author in the summer of 1958, and fieldwork was continued during each succesive summer for periods of 1–3 weeks. Immediately following the field season of 1961 Dr. Miller died from bubonic plague contracted during that fieldwork. We resolved to prosecute the work thereafter with especial diligence.

An important part of the observations made during the first 5 years consisted of the data on the movement of the hundreds of individual cobbles which had been painted for identification. Emphasis was gradually shifted to the observations on rates of erosion and sediment movement which had been begun as only an auxiliary part of the original investigation. It is with these observations that the present paper is primarily concerned.

For permission to work on the property known as Las Dos and for many other courtesies we are grateful to the late Mrs. Adelina Otero-Warren. Dr. Bergere Kenney has kindly encouraged the work to continue on that property.

The slope-area measurements of discharge and many other observations when we were not in the area were made under the direction of Wilbur L. Heckler, district engineer for the U.S. Geological Survey in Santa Fe. Louis J. Reiland, Leo G. Stearns, Charlie R. Sieber, Leon A. Wiard, and others of the Santa Fe office contributed materially to these observations.

Field assistants and technical associates during various seasons included Brandis Marsh, Peter Sparks, Macklin Smith, Olav Slaymaker, Thomas Detwyler, Garnett Williams, and Lehn Franke.

The C^{14} analysis of the charcoal sample was run by Dr. Meyer Rubin in the laboratory of the Geological Survey in Washington, D.C.

For their review, comments, and suggestions, we are indebted to Stafford C. Happ, Asher P. Schick, George H. Dury, S. A. Schumm, R. F. Hadley, M. R. Collings, W. L. Heckler, and L. J. Reiland.

ALLUVIAL FILLS IN WESTERN VALLEYS

To cross any valley in the foothills of a large part of the western conterminous United States is to traverse a flat floor of stream-deposited alluvium. Many such floors, once smooth and undissected, are now trenched by arroyos or troughlike gullies. Abandoned flood plains or alluvial terraces can be seen in many such valleys, representing the surfaces of previous valley fills.

Digitized by Google

A large literature describes the local sequences of alluviation and erosion in such valleys, and there appears to be considerable contemporaneity in the timing of these alterations in post-Pleistocene time over an area that stretches from Wyoming to Texas. When grazing by cattle reached peak intensity about 1880, the most recent epicycle of valley trenching began in what is now believed to be a coincidence of climatic conditions conducive to erosion and degradation of the vegetative cover by overuse.

The alluvium which now fills these valleys and which is being trenched is usually similar in texture to that representing the fills of previous epicycles, though in some places the recent fill material is somewhat coarser. This alluvium is predominantly silt, often fine sandy silt, sometimes silty fine sand. The amount of clay is generally not great. The fills may be only a few feet deep in ephemeral tributaries draining several acres, and can be at least 50-feet thick through long distances. The latter figure applies to the alluvial valley, 150 miles in length, of the Rio Puerco, a tributary to the Rio Grande.

Three periods of late Pleistocene and recent alluviation are recognized in many places in Western States. The most recent fills now being eroded are less deep than those of previous periods of aggradation represented by the terraces which stand above the present valley floors, so even larger amounts of alluvium were stored in valleys in the past than are now observed.

Thus an immense amount of silty and fine-sandy alluvium has been produced by ephemeral drainage basins in the five states—Arizona, New Mexico, Utah, Colorado, and Wyoming—and has been deposited in valleys. When a period of valley trenching occurred, much was eroded out, carried downstream, and the process repeated.

It is logical to suppose that the source of sediment which would contribute to such aggradation during the periods of alluviation would be rill and gully erosion in the headwater tributaries. Deposits in the valley must have been derived from the basin upstream. But alluviation, when it occurred in the main valleys or master streams, also affected minor tributaries as well. The ground surface seems to sweep from valley floor up to the adjacent hills and up tributary valleys in concave-to-the-sky profiles. The topography of the adjacent hills seems to have been drowned in a sea of alluvium, softening and smoothing the surface configuration of the whole landscape. This phenomenon occurs widely and is the general rule in Nebraska, Kansas, Missouri, and the driftless area as well as in New Mexico, Wyoming and other parts of the Rocky Mountain area.

So widespread has been the phenomenon of valley aggradation with silty alluvium and so large are the volumes of sediment involved that the geomorphologist may wish to see examples of present-day streams currently undergoing such alluviation, and to discern the areal sources of the material being deposited. But, interestingly, it is difficult to designate channels undergoing such a process—at least any that are identifiable by visual or qualitative criteria. The processes which were so important even in the historic past cannot easily be observed at present.

Furthermore, if Leopold and Miller (1954) were correct in their assertion that the source of the valley alluvim was not in channel and gully erosion of the headwaters, then the processes of such sediment production must have been mass wasting and sheet erosion. The first of these is a process little studied and the second is a process studied far more on agricultural than on grazing or uncultivated areas. Little is known about rates of such processes on nonagricultural land, nor have the effects of relief, land slope, vegetation density, or other relevant factors been observed.

The present investigation was initiated to study both process and rate of aggradation and degradation in the channels, rills, and on the hillslopes of a drainage basin typical of many parts of the semiarid West. This paper is a progress report on that study.

Investigations of the kind described here involve the operation of field stations and specific experiments over a period of several years. Results can be obtained only at infrequent intervals because of the sporadic character of the precipitation. The general method, then, was to establish observation stations which could be visited for resurvey during a period of a few weeks in summer each year, and to maintain a more restricted number of observations after each important storm. The area chosen, Arroyo de los Frijoles near Santa Fe, N. Mex., was one in which previous work had been done by Leopold and Miller (1956), and for this reason it provided a familiar geographic and geologic background on which to base further investigations.

Our objective was to integrate several aspects of fluvial processes operating in the area: specifically, to study sheet erosion on the divide and interstream areas, slope retreat adjacent to steep-walled gullies that prevail in the uplands, and in particular, the movement of coarse and fine sediment down the arroyos of various dimensions. To this end, various kinds of measuring devices were gradually developed and installed. The results reported here represent information collected during 7 years of observation, but some measurements have been made for only a part of the 7-year period.

Digitized by Google

GEOGRAPHIC SETTING

Arroyo de los Frijoles and the other ephemeral channels discussed here are a few miles west-northwest of Santa Fe, N. Mex. (figs. 138 and 139). They are typical of many small arroyos or dry channels in the lowlands of the Rio Grande Depression at the base of the Sangre de Cristo Range. As one approaches Santa Fe from the west, the Sangre de Cristo Mountains appear to be abutted by a broad sloping surface underlain by poorly consolidated sand and gravel. There are actually several surfaces differing but slightly in elevation. However, the local relief is considerable, with rolling hills dissected by gullies, rills, and broad sandy-floored washes. As is typical of arid regions everywhere, these channels present almost endless variety. They range from tiny rills near the drainage divide to deep, wide arroyos incised in flat alluvial valleys. Vegetation is sparse, both adjacent to the channels and on the interfluves between them. In general the area is a woodland association, including juniper, piñon, sage, and a low-density understory of grasses.

Because of its geological character and climate, the area studied is characterized by huge amounts of both fine and coarse sediment readily available for transportation. During runoff sediment may be derived from the unconsolidated country rock or from recent alluvium adjacent to the channels.

An arroyo discharges water only when a moderately heavy rain falls on the drainage basin. This is a summer phenomenon because heavy rains fall only from thunderstorms. No flow occurs during the winter. Ordinarily during a summer there are about three rainstorms of sufficient magnitude to produce runoff. However, only exceptional rains affect an entire drainage basin the size of the Arroyo de los Frijoles at Sand Plug Reach (drainage area = 3.75 sq mi).

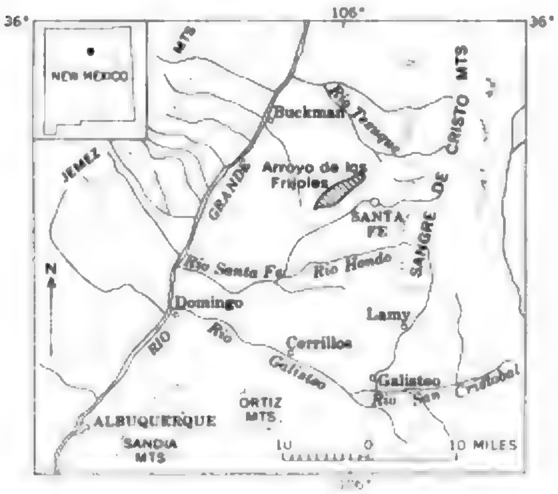

FIGURE 138.—Area in New Mexico where detailed studies were made.

VALLEY ALLUVIUM

Many widely separated areas in southwestern United States have undergone three periods of alluviation followed by erosion, and there is evidence of approximate simultaneity of the respective events from one area to another. That some or all of these events should have occurred in the study area would be a logical supposition.

Arroyo de los Frijoles through most of its length is incised into an alluvial fill of silty sand which at present has a surface configuration characterized by two terraces, and paired remnants of each are common along the principal drainage ways. The higher terrace stands about 5 feet above the channel bed in upper tributaries and tends to remain about the same height downstream along the 7-mile reach which we have studied in detail. The terrace tread is uniform and flat, and vegetated, as are the hills, with piñon and juniper and an understory of grass. Along much of the stream length the terrace is bounded by a vertical wall, at least on one side of the channel, but elsewhere it slopes down to the lower terrace in a subdued S-shaped profile which may have a maximum slope of 1 : 5. Such a rounded scrap is generally vegetated with bunch grasses of low density. The terrace tread grades in a smooth curve to the adjacent hills, and its whole width seldom is more than 300 feet.

The low terrace averages about 1–2 feet above the present streambed and is seldom bounded by vertical banks. Its surface tends also to be somewhat irregular and can usually be recognized by the occurrence of rabbit brush, locally called chamiso [*Chrysothamnus nauseosus* (Pall.) Britt.], which occurs neither on the higher terrace nor on the presently active point bars.

Typical aspects of the valleys and the terraces are shown in figure 140.

The stratigraphic relation of the alluvium of the high terrace to the bedrock underlying the adjacent hills is commonly seen in the vertical banks. The valley fill was laid in a shallow U-shaped trough cut into the friable and poorly consolidated bedrock, and the bed of the present channel lies very near the bottom of this trough in the smaller valleys and probably close to it even in the main stream. That is to say, the present stream has cut nearly through the valley alluvium and most of the depth of alluvium can be seen in the cut banks or vertical walls.

The relation of the alluvium underlying the tread of the lower terrace to that of the upper terrace is difficult to decipher. So nearly the same is the alluvium under the two terrace treads that even when a vertical bank

cuts through both, no stratigraphic contact is obvious, though an inset relation is suggested by the contacts seen. The same difficulty is often observed in alluvial fills of western valleys. We have concluded after inspection of many sections, that the lower terrace represents the top of an inset fill and that Arroyo de los Frijoles is an example of a two-fill, two-terrace alluvial valley (see Leopold and Miller, 1954, p. 5, for a discussion of the classification of terraces and fills). A diagrammatic cross section is presented of this valley in figure 141. We here apply the name Coyote terrace deposits to the alluvial deposit under the higher terrace so prominent along streams in the vicinity which will be referred to as the Coyote terrace.

The type locality for the Coyote terrace deposits will be along the Arroyo de los Frijoles at what we will

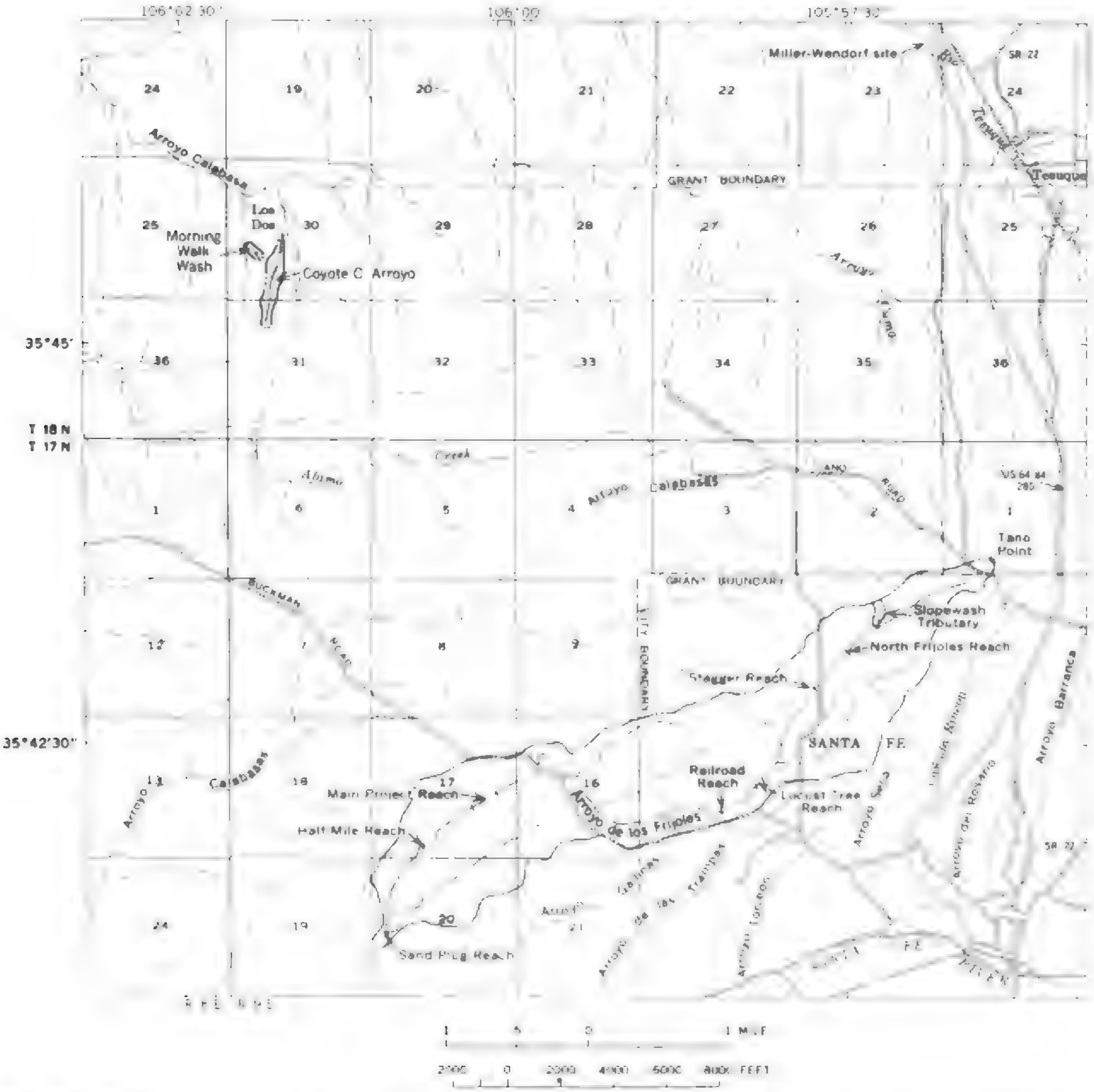

FIGURE 139.—Drainage basins of Arroyo de Los Frijoles, Coyote C Arroyo and Morning Walk Wash. Named reaches are locations where detailed studies were made. Also included are principal stream channels and roadways within the area.

Digitized by Google

A

B

C

Figure 140.—Typical aspects of the valleys and the terraces. *A*, Drainage basin of Coyote C. Arroyo; the man is standing on a flat surface of alluvium or colluvium. *B*, Two terrace levels along Arroyo de los Frijoles; the lower terrace, about 18 inches above the channel bed, is in the foreground; at the tree near the channel edge, the upper terrace stands 5 feet above the present bed and grades smoothly to adjacent hills. *C*, Arroyo de los Frijoles; the channel is cutting into the upper terrace material that here stands 8 feet above the present bed elevation; the view is on the left bank just downstream from Fence Line Headcut; bedrock crops out in the channel bed at this place, dipping downstream.

describe here as our main-project reach, in the NW¼ SE¼ sec. 17, T. 17N., R. 9E., 4.2 miles from Santa Fe. The name is derived from Coyote C. Arroyo at Las Dos (see p. 205), where a sample of charcoal buried in this deposit gave a date of 2800±250 years B.P. (USGS sample W1328).

Coyote terrace deposit is alluvium consisting of red-brown, slightly indurated silty sand or fine sand, sometimes fine sandy silt, with occasional discontinuous lenses of fine gravel. When dry, the cut banks stand vertically and are hard to dig with a shovel. The alluvium is 5–10 feet thick and rests on bedrock, which here is unconsolidated sand and gravel. The top several inches may contain more fine sand or silt than at greater depths. No soil zonation is apparent though the upper 6 inches are slightly darker from the admixture of humus and incipient soil development.

The Coyote terrace forms a curving surface as it rises away from the valley floor and joins the hillslopes underlain by the Santa Fe Group. The alluvium interfingers with colluvium at the valley sides and extends upstream in minor tributary valleys, where the distinction between valley alluvium and colluvium at the base of the slope often cannot be made.

In the Tesuque Valley just 4 miles to the north, similar alluvial terraces have been studied by Miller and Wendorf (1958) at a location shown on figure 139. There, two terraces occur at 18–20 feet and 8–10 feet above the present channel; the alluvium underlying the higher one contains dateable artifacts and charcoal. A C^{14} date of charcoal lying 130 inches below the surface of the upper terrace was 2230±250 years. Between the

795-885 O—66——2

Digitized by Google

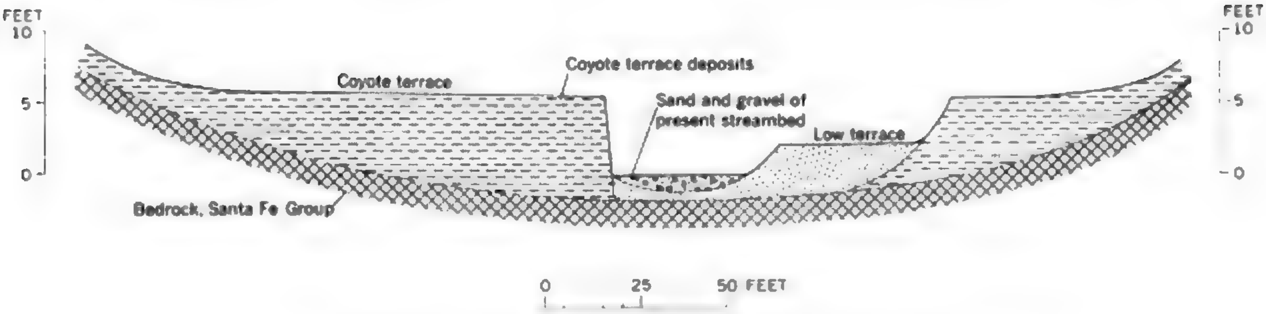

FIGURE 141.—Diagrammatic cross section, Coyote terrace deposits.

Tesuque area and Arroyo de los Frijoles, the agreement of dates, the similarity in form, the comparable character of the alluvial materials, and the geographic proximity of the areas suggest that the respective periods of deposition and erosion in the valleys of the whole area are correlative and may be considered Coyote terrace deposits.

Though the terrace heights and the depth of alluvium of the Coyote terrace deposits differ somewhat from valley to valley as indicated by the comparison between Arroyo de los Frijoles and Tesuque Creek, such a valley fill is ubiquitous in all the ephemeral valleys in the area. It typifies all the drainages rising in the foothills which lie west of the Sangre de Cristo Range and east of the escarpment of La Bajada, a distance of 11 miles or more in most places, and extending north-south at least from Cuyamungue, 12 miles north of Santa Fe, to San Cristobal, 25 miles south of the city. This area of more than 100 square miles has been seen, at least in reconnaissance, during this study, and our impression is that similar relations would be observed over a much larger area in central New Mexico. The Coyote terrace deposits correspond to Deposition 2 in the regional alluvial chronology of Kirk Bryan. (See Leopold and Miller, 1954, p. 58.)

THE LOCAL BEDROCK

The hills being drained by the network of ephemeral channels are composed of the upper beds of Santa Fe Group. The whole group is at least several thousands of feet thick, but that part with which we are concerned includes the upper zones only, principally the Tesuque and Ancha Formations (Miller, and others, 1963, especially p. 50–51 and pl. 1). The geologic map by these authors includes similar landscape 3 miles north of our study area which they mapped as Tesuque Formation described as follows (p. 50):

> The Tesuque Formation of the Santa Fe Group, as defined here, consists of poorly consolidated, water-laid silt, sand, and gravel, mostly tan in color. . . . Abrupt changes in texture, both vertically and horizontally, are the rule. Bedding is locally distinct, but few beds can be traced more than a mile or two. Some of the sandstone beds are fairly well sorted and locally crossbedded. Their coherence is due to cementation by calcium carbonate. At most places, even in unconsolidated materials, the sediments are highly calcareous.
>
> The Tesuque Formation was derived from Paleozoic and Precambrian rocks of the mountains. The presence of a considerable quantity of quartzite pebbles, for example near Tesuque, indicates drainage southward from Rio Santa Cruz or Rio de Truchas, which requires a radical difference from the present drainage pattern.

Miller, Montgomery, and Sutherland (1963) consider the Tesuque Formation to be Tertiary. They identify a Pleistocene or upper Pliocene Ancha Formation consisting of remnants of a once-continuous sheet of unconsolidated gravel which extended originally from the western part of the Sangre de Cristo range to the Rio Grande. The gravels were considered to be laid down as fan deposits derived from glacial action and carried out to cover the older Tesuque beds as glacial outwash deposits.

Those workers did not map as Ancha Formation any of the deposits in the area just to the north; the bedrock materials with which we deal are probably entirely Tesuque Formation. Because, as Miller, Montgomery, and Sutherland stated (1963, p. 51), 100–300 feet of dissection has occurred since deposition of the fan gravel comprising the Ancha Formation, the concentration of gravel on many hilltops which we observe in our study area may represent a lag concentrate of gravel derived from Ancha beds which now have been removed.

Other than the gravel concentrate on hilltops, the decription given by Miller and his associates fits the bedrock materials. Those authors, as well as we, observed many places where the upper surface of the Santa Fe beds is weathered. A zone of caliche, 2–3 feet thick locally, permeates the sandy, or elsewhere the gravelly, bedrock materials. This caliche where it crops out does not affect the alluvium or colluvium and indicates processes of soil formation and weathering related to events prior to the deposition of the Coyote alluvium.

Digitized by Google

RELATION OF VALLEY ALLUVIUM AND COLLUVIUM TO HEADWATER AREAS

The surface of the Coyote terrace can be followed as remnants along the main valley of Arroyo de los Frijoles and other washes upstream to where the present channel is only a few feet wide. Similarly, the surface can be followed up lateral tributaries where it grades to the adjacent hills. Colluvium deposited by rills and unconcentrated wash merges and interfingers with alluvial deposits of the main valleys and tributaries. Excavation by shovel in the bed of any small, even any steep, tributary reveals alluvial-colluvial material within a few hundred feet of the watershed divide. The same relation of alluvium to headwater slopes was found in eastern Wyoming by Leopold and Miller (1954) who summarized their findings in these words (p. 83):

> The terraces of master streams can be traced directly into many tributaries of moderate size, indicating that erosion of alluvium in the master streams was accompanied by gully erosion in tributaries, even the ephemeral ones.
>
> * * * likewise, aggradation in the main stream valleys was accompanied by deposition in tributary valleys and draws. Probably these deposits were derived by mass movement and sheet erosion on upland slopes.
>
> It seems logical that the shift in relations between runoff and vegetation which caused erosion of all major streams would also affect the smallest tributary valleys in a similar way at the same time. . . . As the deposit in the main valley gradually increased . . ., the wash slopes that were graded to the main river accumulated material which blanketed all except the most prominent hills and uplands. The area of upland from which alluvial materials were being derived by erosion shrank, while the area of deposition increased.

The percentage of area of a small basin blanketed with alluvium-colluvium is exemplified in Coyote C. Arroyo. (See fig. 139 for location.) This typical drainage basin has an area of 0.064 sq mi (40.8 acres) of which 0.022 sq mi (14.4 acres) is covered by alluvium-colluvium, the remainder being hillslope and hilltop area of Tesuque Formation. In this example, then, 34 percent of the surface area was alluviated, and the average distance from the head of deposition in small swales to the watershed divide was 190 feet. The alluviation extends headward astonishingly close to the drainage divides. The proximity of the colluvial-alluvial deposits to drainage divide can be seen in figure 140*A*.

The relation of the small tributary draws to the headwater slopes may be typified by the two examples in figure 142. Profiles of the surface of the alluvium-colluvium merge smoothly into the unrilled hillslope underlain by bedrock. Cross profiles drawn nearly parallel to the contours of the side hills demonstrate, in conjunction with the stratigraphic evidence seen in the channel walls and in pits dug in the plane of the profile, that alluvial and colluvial material fill a former channel system cut into the bedrock and that subsequently the present channels have reevacuated parts of the earlier system. The present channel network incised into the alluvium makes a present topography similar to that existing before the Coyote terrace deposition.

This conclusion is supported by observations of the extent of gravel which more or less covers many of the rounded hilltops of the area. In the Slopewash Tributary example in figure 142, section *B–B′* crosses from west to east a gravel-covered hilltop, a gravel-free area, and again a gravel-covered hilltop. At the base of the channel on the right bank the bedrock is permeated with a white cement, presumably $CaCO_3$.

Exposures elsewhere also indicate that hilltops covered with lag gravel are usually underlain by bedrock. Thus the deep layers of silt exposed in present channel walls were deposited in channels which dissected the bedrock. The alluvium lapped up against the gravel-covered slopes and in places covered the gravel.

Investigations of the relation of the alluvium to the bedrock topography showed that the underlying Tesuque Formation generally appears no more weathered at the contact than elsewhere. In some places, however, alluvium was deposited over a surface heavily cemented with caliche. The caliche appears as a hard cement where the Tesuque was gravel, and where the Tesuque was silty, as a whitish calcification of a zone extending 3–4 feet below the contact, and especially concentrated on fracture planes. Hard nodules of caliche in the silt are seldom seem, but amorphous soft masses without sharp boundaries are common.

These facts support the conclusion reached by Miller, Montgomery, and Sutherland (1963), that a long period of weathering under subhumid conditions was followed by a semiarid climate during which caliche permeated an undulating topographic surface. Our observations add the additional postulation that, subsequently, this topography was first alluviated and later erosion developed a drainage network similar to and about the same depth as the present one; the erosion removed part but not all of the materials which had undergone calichefication.

To summarize, alluviation during Coyote terrace time aggraded not only the main valleys but small tributary draws as well. Post-Coyote terrace erosion reexcavated much of the earlier topography. The problem posed by this sequence of events is the following:

If alluviation took place in all the headwater draws at the time the main valleys were being aggraded, where did all the debris come from, and by what processes?

Digitized by Google

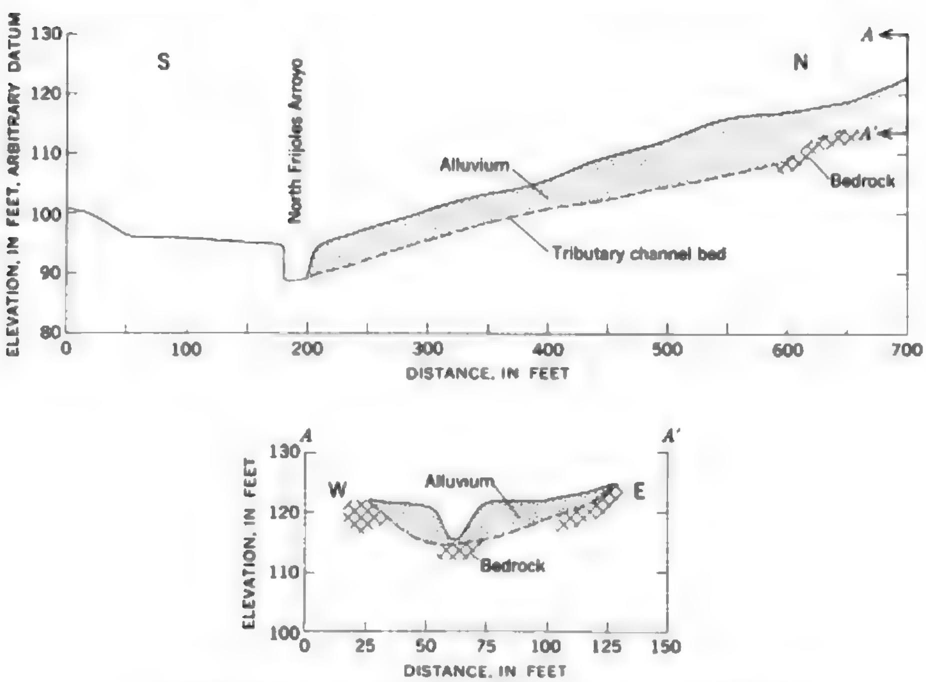

A.—UNNAMED TRIBUTARY TO NORTH FRIJOLES ARROYO AT STAGGER REACH

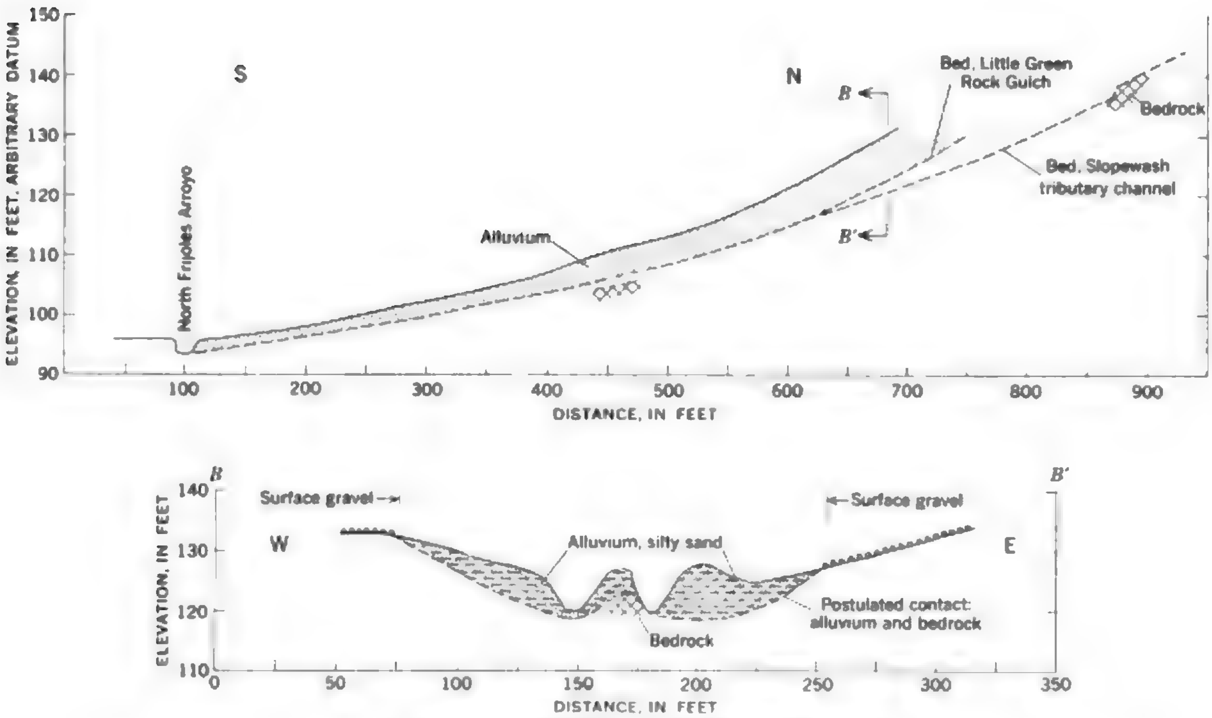

B.—SLOPEWASH TRIBUTARY TO NORTH FRIJOLES ARROYO

FIGURE 142. Two examples of small tributaries showing stratigraphic and topographic relation of alluvium to bedrock.

Digitized by Google

Clearly, the sediment was derived from the hills above the areas of alluviation but not from rills or gullies on these hills, as evidenced by the absence of gullies or rills of any depth or importance outside of those which were being alluviated. Thus the sediment must have been derived from processes other than rill and gully erosion, specifically, sheet erosion or mass movement. This hypothesis attributes to the latter processes greater efficacy than we at least would have supposed. We were led, then, to devise methods of measurement which would allow the construction of a sediment budget, however approximate, to ascertain whether relative importance of present processes would shed light on these events of the past.

Another problem is highlighted by the postulates stated. It is usual to suppose that alluviation of a master stream would provide a rising base level for the tributaries which enter into it. Then the aggradation in the tributary would similarly provide a rising base level for its own subtributaries. Though this scheme is a simple one and would lead to field relations here observed, it also implies that the alluviation of the headwater tributaries would lag in time that of the main stem. But these inferences do not agree with field observations in the Arroyo Frijoles area.

It seems much more likely that in our study area the relation of runoff to vegetation which would lead a main stream to aggrade would similarly have the same result on the tributaries. We believe that control by base level is a relatively minor factor in alluviation of the valleys studied.

The remainder of this paper is organized around the measurement program instituted to investigate these questions. The sample areas studied will be described, the measurement methods outlined, and the results summarized. These measurements will then be discussed in terms of the problems outlined (see p. 236). We begin with a discussion of the study areas.

STUDY AREAS

The areas of special study shown in figure 139 include Arroyo de los Frijoles through its uppermost 7 miles and some smaller basins of several acres in an area 4 miles distant, near Las Dos. The principal basin, Arroyo de los Frijoles, has a channel width which ranges from the smallest recognizable rills a few inches wide to an arroyo 100–200 feet wide. All channels more than a foot wide have a flat predominantly sandy surface dotted in places with scattered gravel.

Larger scale maps, figures 143–45, show details of the areas of intensive study and will be referred to in later discussions.

Figure 146 illustrates the character of the country and the aspect presented by main and tributary channels. Figure 146, *A* and *B*, shows a small tributary within a few hundred feet of the headwater divide, a subbasin we called Slopewash Tributary.

At a point 1.1 miles from the furthest divide the North Frijoles Reach is typical, figure 146. One mile farther downstream the channel is larger, as shown at Locust Tree Reach (fig. 146*D*). Main Project Reach, 4.9 miles from the headwater divide and at a place where the drainage area is 2.87 sq mi, is illustrated in figures 146*E* and *F*.

Some characteristics of each of the study areas are indicated in table 1.

TABLE 1.—*Characteristics of locations studied*

Location	Drainage area (sq mi)	Elevation (ft above msl)		Relief (ft)	Length (ft)
		At headwater	At downstream point		
Arroyo de los Frijoles:					
Slopewash Tributary	0.05	7,280	7,200	80	1,200
North Frijoles Arroyo:		7,388			
At gaging station	.66		7,168	220	5,800
At Stagger Reach	.70		7,111	277	8,300
At mouth	1.36		7,048	340	11,750
At Locust Tree Reach	1.49		7,037	351	12,400
At Railroad Reach	1.61		6,987	401	15,400
At Main Project Reach	2.87		6,790	598	28,000
Sand Plug Reach:					
At Stump section	3.18		6,696	692	32,600
At Rocky Nose section	3.75		6,672	716	34,800
Gunshot Tributary, at mouth		6,798	6,723	75	1,150
Arroyo Falta	.12	6,800	6,620	180	5,000
Coyote C. Arroyo, at dam	[illegible]	6,735	6,550	185	3,600
Morning Walk Wash:					
South gully		6,633	6,540	93	700
North gully		6,615	6,540	75	870

METHODS OF STUDY

Observations of nearly all the types described here began in the period 1958–61 and are continuing as this paper is written. Water stages of flow are measured by recorders at gaging stations installed on North Frijoles Arroyo and at Main Project. The duration of individual flows is generally two hours or less and current-meter measurements for the construction of stage-discharge rating curves are impracticable without a full-time resident hydrographer. Stage-time hydrographs are obtained from the stage recorders, but maximum discharge for each flow is computed using a survey profile of high-water marks. This, combined with cross-sectional areas of flow determined by scour chains (described below), permits the computation of discharge using an estimated value of flow resistance.

A network of 12 nonrecording rain gages is observed after each significant summer rain.

Depths of scour and fill in channels are measured by chains set vertically in a dug hole in the streambed. At maximum depth of scour the chain is bent over by the flow and is usually covered by fill on the receding stage (Emmett and Leopold, 1964).

Digitized by Google

FIGURE 143.—*Arroyo de los Frijoles.*

Erosion pins, consisting of a 10-inch nail put through a washer, driven flush with the ground surface, are used to record increments of surface erosion. Some of these pins are arranged in a grid over certain plots, but generally the nails are in a line as a transect from hilltop to base or across a channel as a cross-section.

Mass-movement pins are set on a line between immovable bench marks, and are surveyed for alignment by transit.

Many rocks have been painted for identification and observed for movement after each flow.

The individual plants on some 3×3-ft quadrats have been mapped and are to be remapped periodically to observe changes with time.

Although the methods are simple, the labor after each storm (about 3 per summer) and during the annual resurvey of all observation points is rather great.

MAGNITUDE AND FREQUENCY OF RAINFALL AND STREAMFLOW, 1958–64

Rainfall has been measured since 1959 at 12 locations within the drainage basin, as shown in figure 143. Summary of data A (p. 247) contains a partial summary of the data collected from these sites.

The gages were not read after each shower, but efforts were made to read them at least after every flow-producing storm. The sporadic nature of storms is indicated by the unequal distribution of rainfall among stations.

At the Main Project Reach a recording rain gage has been installed at the location of the water-stage recorder. Precipitation data (summary of data B) collected here allow a better indication of the rainfall characteristics. The record is too incomplete to show the mean annual precipitation which at that location must be about 12 inches per year.

The 1,300 cfs (cubic feet per second) flow of July 25, 1962, the second highest flow recorded at the Main Project Reach, was caused by a storm which registered 1.5 inches in 25 minutes at the Main Project gage.

Channel discharge is measured or estimated at three places in Arroyo de los Frijoles: Main Project, Locust Tree, and North Frijoles. Gaging stations are installed at the Main Project and at North Frijoles reaches. During the period 1958–63, runoff occurred at the three

Digitized by Google

measuring stations on the dates indicated in table 2, in which are presented values of peak discharge. Spaces in the table usually refer to no flow; however, in a few instances some flow may have occurred but was of negligible magnitude. Flow data discussed in this report are all peak values.

TABLE 2.—*Summary of peak discharges, in cubic feet per second, at three locations along Arroyo de los Frijoles, 1958–63*

[(a) and (b) refer to separate flows or different peak flows occurring on the same day]

Date	North Frijoles	Locust Tree	Main Project
1958			
August 18			20
September 6	15–20		10–15
September 13	194	1,220	3,060
1959			
May 23	140	50–75	3–5
June 15			2–4
July 23			10–15
August 17		20–25	20–25
August 24	50	15	
October 29	.5		1
1960			
July 14	67	360	35
August 4			152
September 15(a)	1		10–20
(b)			10–15
October 9	3–5		
October 16(a)	5–7		
(b)	9–10		10–15
October 17			10–15
1961			
June 26			1
July 8	58	495	98
August 12	85	300–400	80–90
August 23	3–5	3–5	.3
September 18 (a)	10		40
(b)			60
September 19	230	650	250
1962			
June 30	.3	30	
July 5	6–8	150	40
July 6	.3		10
July 18			3
July 22	.5		
July 25	85	450	1300
July 30	90	450	300
September 19	1		
1963			
July 20	10	5	15
September 21	5	301	316

Most storms are intense and so local that only a part of the drainage basin is affected by each. Only twice (September 13, 1958, and July 25, 1962) was there increasing discharge in the downstream direction due to heavy rainfall over the entire basin, and these two storms caused the greatest flows during the period of record.

For each of the three measurement locations, the peak flows experienced were arranged according to rank and recurrence intervals were computed. These are plotted against their corresponding discharge and are shown as dashed lines in figure 147. Recurrence intervals are determined by the U.S. Geological Survey method, $T=\frac{n+1}{m}$, where T=recurrence interval in years, n= number of years of record, and m=magnitude or rank of flood, the highest being number one.

Excepting the two storms just mentioned, the spotty distribution of precipitation implies that data collected at each of the three reaches may be considered as independent flows. If this were in fact true, a type of station-year analysis might be attempted by combining 5-years of record for each of three locations into a synthetic 15-year record. The solid line on figure 147 gives this average frequency of the three reaches. The solid circles on this graph represent all flows at the three stations, arranged in order of magnitude.

For small flows all moderate-size drainage areas are capable of receiving sufficient rainfall to produce a similarity in flow frequency. For drainage areas larger than some given size, further increases in area would not increase the size of flood of a given frequency. This feature is indicated by the fact that a flow of 2-year recurrence interval is about the same at Locust Tree and Main Project Reaches despite the fact that the drainage area of the latter is about twice that of the former.

The present data exceed by fivefold the values presented by Leopold and Miller (1956, fig. 21, p. 24). The latter values should not be considered applicable to the foothill area of ephemeral streams though they were so considered in that report. It is now obvious that flow frequencies of the gaged streams emanating from the high mountains are not comparable with and are smaller than values for ephemeral washes in the foothills, despite the lower mean annual precipitation of the latter areas.

The problem of flow frequency is of paramount importance to evaluation of erosion and sediment transport processes. Though the method of determining frequency is still open to further study in ephemeral basins, figure 147 expresses the occurrence of events in the studied basin during the period of observation.

CHANNEL FORM AND BED MATERIALS

A salient aspect of the change in channel characteristics downstream is the increase in width, shown in figure 148. As defined here, channel width refers only to the active channel which is swept free of vegetation except for annual plants. In some places the actual width between the steep banks is greater than indicated on figure 148. Such reaches usually include remnants of the lower terrace, which not only supports some vegetation but also stands 1–2 feet above the presently active bed.

The variability of channel width quite evident in figure 148 seems large, but one does not realize how large the variance is in the usual channel until he begins to make quantitative measurements. On a perennial eastern stream not much larger in drainage area than Arroyo de los Frijoles, the ratio of the standard deviation to mean channel width averages about 0.25 (data from Wolman, 1955, fig. 37), whereas for a reach of Arroyo

Digitized by Google

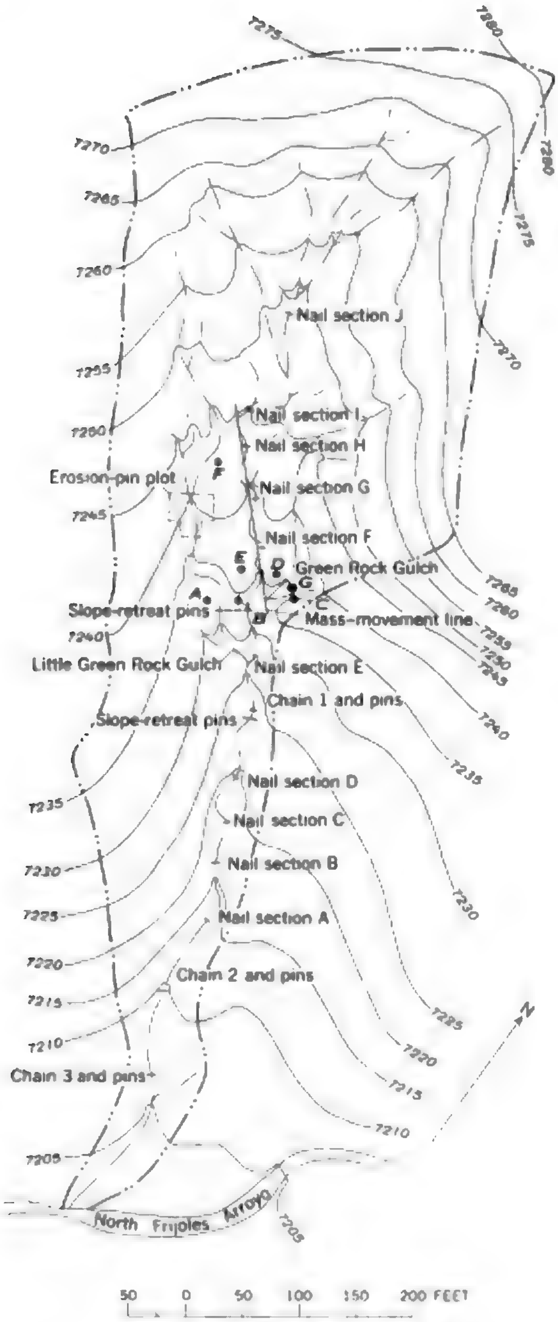

FIGURE 144.—Slopewash Tributary

de los Frijoles below the junction of North and South Frijoles it is about 0.39. Also, the variability of width is not so great above that junction where the drainage area is less than 1 sq mi. In an ephemeral basin, it appears that when the drainage area exceeds the size of the usual summer thunderstorm, only parts of the basin contribute runoff. Thus different reaches of channel experience different sequences of flows, and this probably tends to increase the variance of channel width.

The increase in drainage area with channel length is shown in the top part of figure 148. At three places, sudden increases in drainage area occur where relatively large tributaries enter the main channel. However, as mentioned above, it appears that these increases in drainage area affect channel width only incidentally, as the size of a given storm may or may not extend over the whole contributing area.

The bed of Arroyo de los Frijoles is predominantly sandy with scattered fine gravel and cobbles, but there are local concentrations of rocks. Considering first the nongravelly areas which predominate, sieve analyses are shown in figure 149*A*. The median diameter for all surface samples are within the limits of medium to coarse sands.

Three samples from Arroyo de los Frijoles provide comparison of median grain diameter at points downstream in the same basin.

Location sampled	Drainage area (sq mi)	Median grain size (mm)
Slopewash Tributary	0.05	0.56
North Frijoles Reach	.56	.78
Main Project Reach	2.87	.72

Though a larger number of samples may have yielded a more uniform set of values, at least it can be said that there is no progressive decrease of the size of sand downstream.

Figure 149*B* illustrates the composition within the area of a gravel concentration or bar. Clearly, the majority of the larger particles are in the top 2 inches (discussed in more detail on p. 212) and the composition over the full depth of the concentration is more coarse than in a nonbar area. Downstream tips of gravel bars are characterized by material a little finer than in nonbar areas. This is an expected pattern and is observed in other depositional phenomena such as mudflows.

The largest particle occurring in each 100-foot segment of the channel of Arroyo de los Frijoles was measured, and the results are plotted in figure 150. The size of the material in the Slopewash Tributary is as large as that in North Frijoles and, indeed, almost as large as that anywhere in the whole length of the stream. Maximum particle size actually increases somewhat downstream, and local variations from section to section are commonly two to threefold.

In gravelly perennial streams the occurrence of pools and riffles is characterized by considerable bed relief.

Digitized by Google

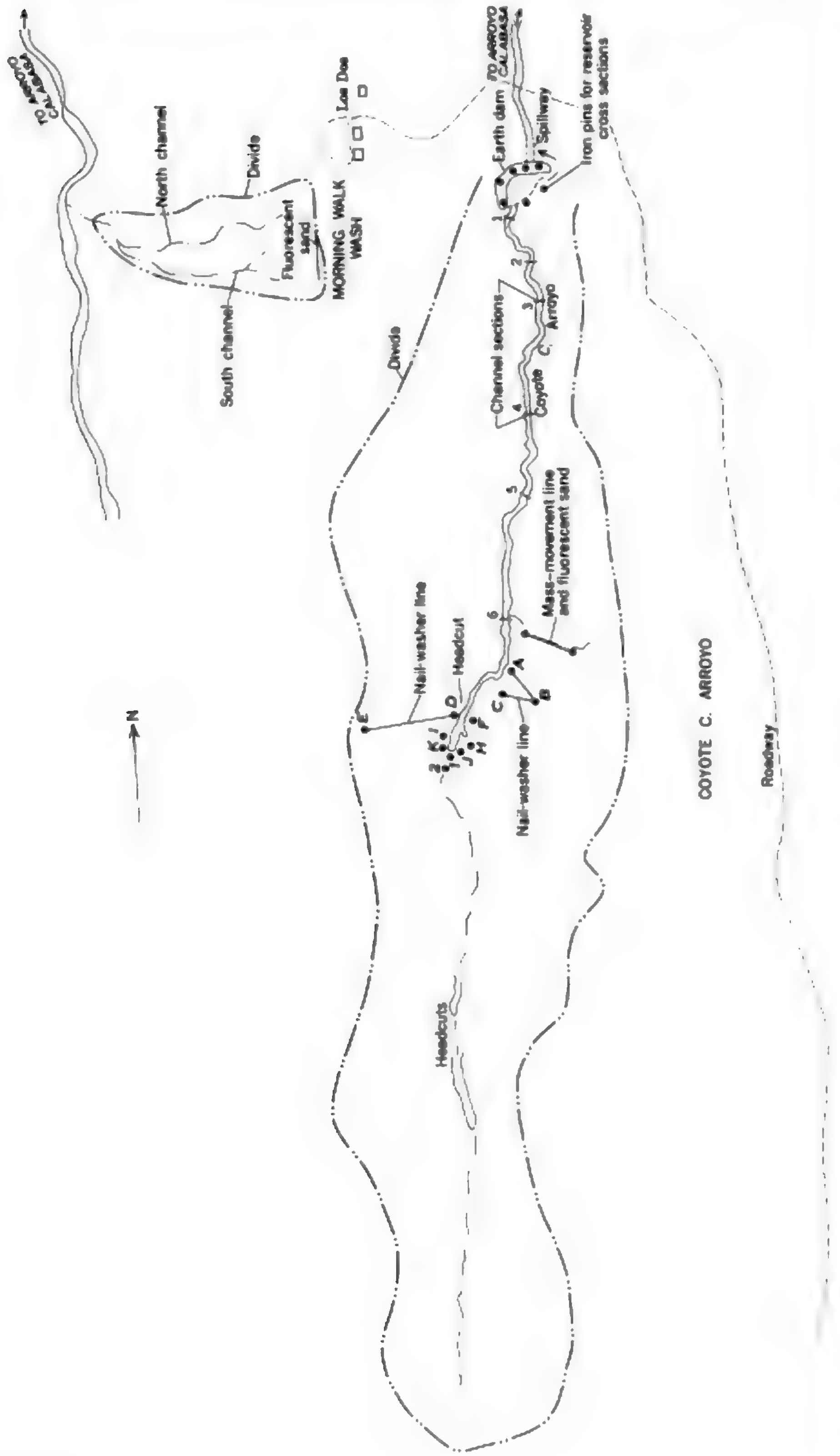

FIGURE 145.—Drainage basins of Coyote C. Arroyo and Morning Walk Wash; solid circles labelled in bold type are nail-and-washer observation points or iron pins for resurvey; channel cross-section locations are labeled 1–6.

A

B

C

D

Digitized by Google

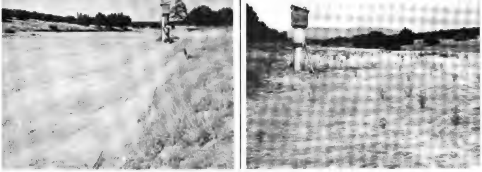

E

F

FIGURE 146 (Above and left).—Photographs illustrating several of the individual study areas. *A*, Slopewash Tributary; the area shown is along the mass-movement line (see fig. 144 for location). *B*, Slopewash Tributary; the area shown is within the erosion plot. *C*, North Frijoles Reach, Arroyo de los Frijoles; the view is downstream from above the gaging station. *D*, Locust Tree Reach, Arroyo de los Frijoles; view upstream; visible in the foreground are rock groups from the painted rock experiments. *E*, Main Project Reach, Arroyo de los Frijoles; the view is downstream from above the gaging station. *F*, Main Project Reach, Arroyo de los Frijoles, looking upstream.

The riffle is a gravel bar or accumulation which is a topographic high, a feature which rises well above the mean bed elevation. The pool is a trough below mean bed elevation.

In the larger ephemeral streams of the area here studied, there is no such relief on the dry streambed. In fact the bed is remarkably flat across its width and closely resembles a gently inclined plane, for the longitudinal profile is quite straight.

Only in detailed mapping did we become aware of the fact that local concentrations of gravel on the sand bed correspond in principle to the riffle of the perennial river. These bars, as we call them, are so slightly elevated above mean channel bed elevation that they would not be recognizable as a topographic high. Rather, we have mapped them merely by inspection of surface texture. Because some gravel particles occur everywhere, designation of a bar is rather subjective, but generally it implies individual cobbles spaced within several diameters; whereas in areas not called bars the spacing of cobbles would be 20–50 diameters or more. Typical gravel concentrations are illustrated in figure 152*D*.

SPACING OF GRAVEL BARS

The position of gravel bars in the vicinity of the Main Project Reach as mapped each summer during the period 1958–63 is shown in figure 151. It seems apparent that the position of a gravel bar remains remarkably stable. This is true despite the fact that two or three flows of sufficient magnitude to move the material on the bars occurred between the successive mappings. For example, the largest flow measured during the entire period of study occurred between mappings in 1958 and 1959, and at that time scour to depths of 0.4–1.4 feet occurred. Thus all the material of the surface of the channel bed moved downstream, yet the bars were rebuilt in approximately the same places as before. However, with each annual mapping, a few bars are missing in the new map that were present in the old map, and also a few new bars appear.

Beginning in 1961, a more intensive effort was made to map gravel accumulations. It is this effort, rather than an actual increase, which, in figure 151, shows more extensive areas of gravel beginning in 1961.

In accordance with observations elsewhere the gravel bars are spaced on the average at a distance equal to five to seven times the channel width, and this ratio persists through all the years of record.

Measurements of gravel size and density on the surface of gravel bars were made at two different times separated by major flows. It was found that both the size distribution and density of particles greater than 1 inch in diameter remained almost the same.

Digitized by Google

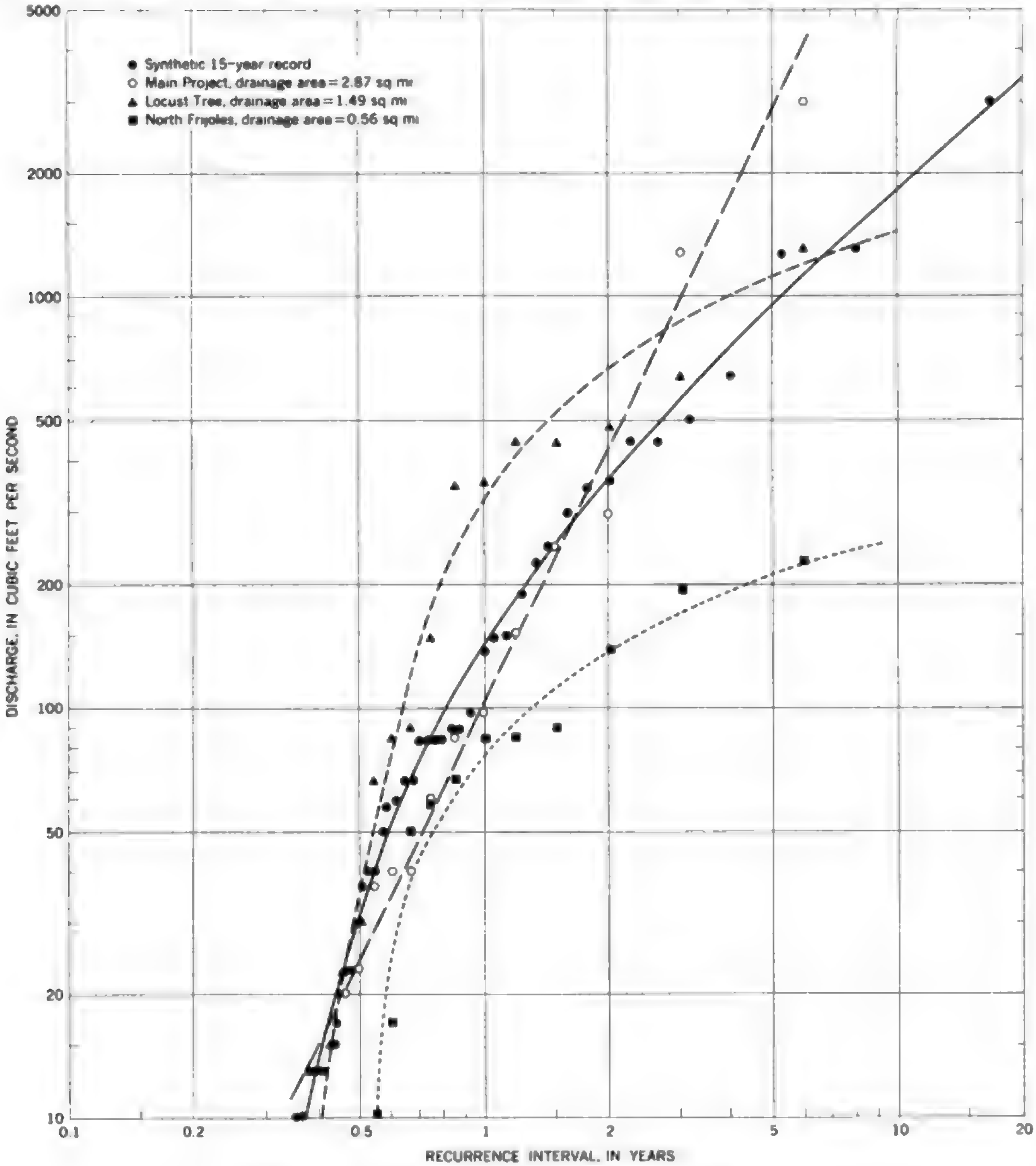

FIGURE 147.—Magnitude and frequency of flows, Arroyo de los Frijoles, 1958–62.

Digitized by Google

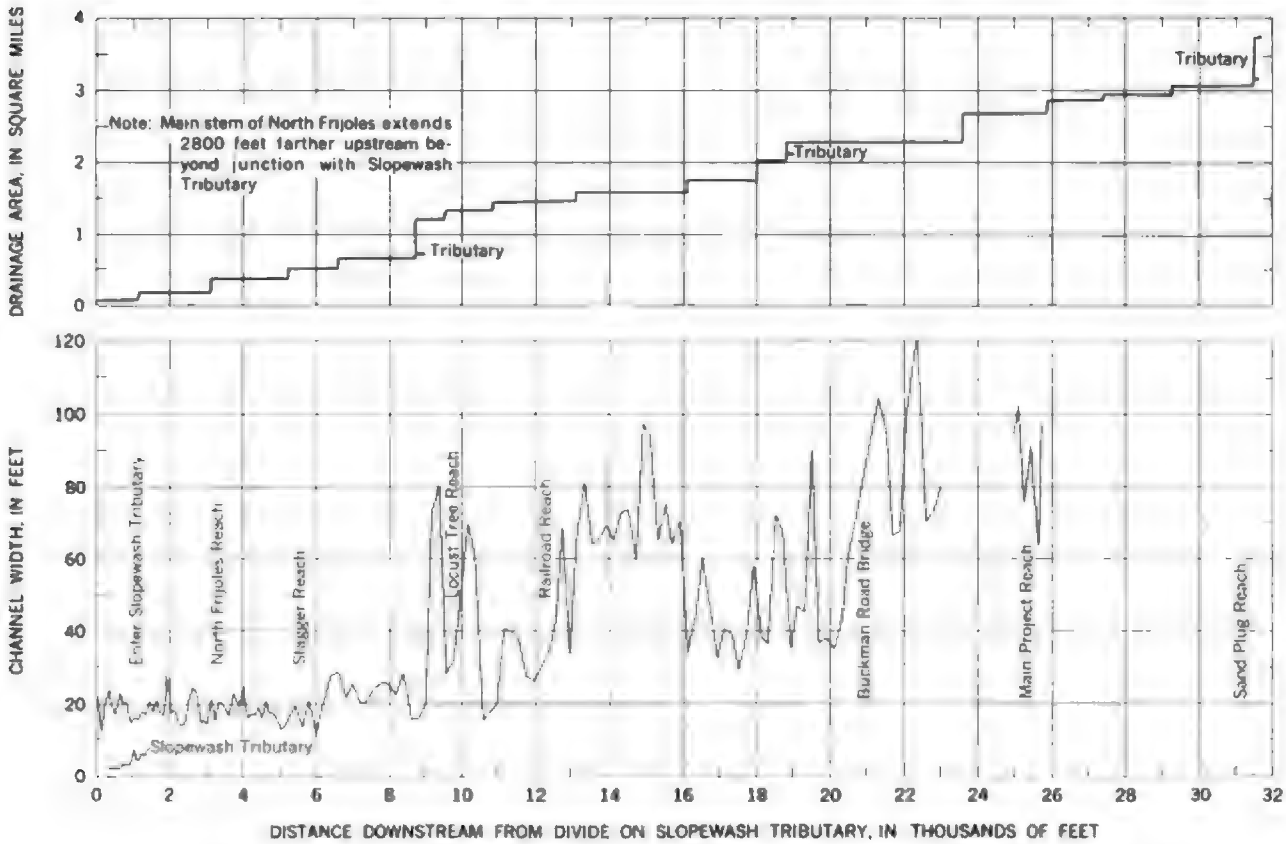

FIGURE 148.—Relation of channel width and drainage area to channel length, Arroyo de los Frijoles.

MOVEMENT OF COARSE PARTICLES

We had hypothesized that gravel bars owe their existence to the fact that particles in juxtaposition are less easily moved by flowing water than when widely separated. Marked cobbles arranged in groups of various spacings and collected after individual flows would provide a means of testing under field conditions whether this hypothesis would be sustained.

The following procedure was developed: Cobbles taken from the channel were completely painted. Each was given an indentification number equal to its weight in grams, and this number was painted on the cobble. The rocks were placed in the channel in groups, each group contained a chosen particle-size distribution and comparable groups differed in spacing of the rocks. After each flow the entire length of the channel was searched for painted rocks. Those found were recorded, collected, and replaced to await the next flow. This procedure was carried out after each significant stormflow during the summers of 1958–63, inclusive, and discontinued thereafter.

In these studies a group of particles consisted of 24 individual rocks arranged in a parallelogram. The distance or spacing between particles was one of three values, 2 feet, 1 foot, or 0.5 foot.

Except for the initial summer (1958) the individual groups included four particles in each of the following size (weight) classes:

Weight class (grams)	*Intermediate axis, approximate mean diameter (mm)*
300–500	65
500–900	85
900–1,700	105
1,700–3,300	125
3,300–6,500	160
6,500–13,000	230

Individual particles in the grid were arranged in a Latin Square pattern, in which each line of six particles includes one and only one of each of the size classes, and in each cross-tier, no rocks of the same size are in juxtaposition.

Digitized by Google

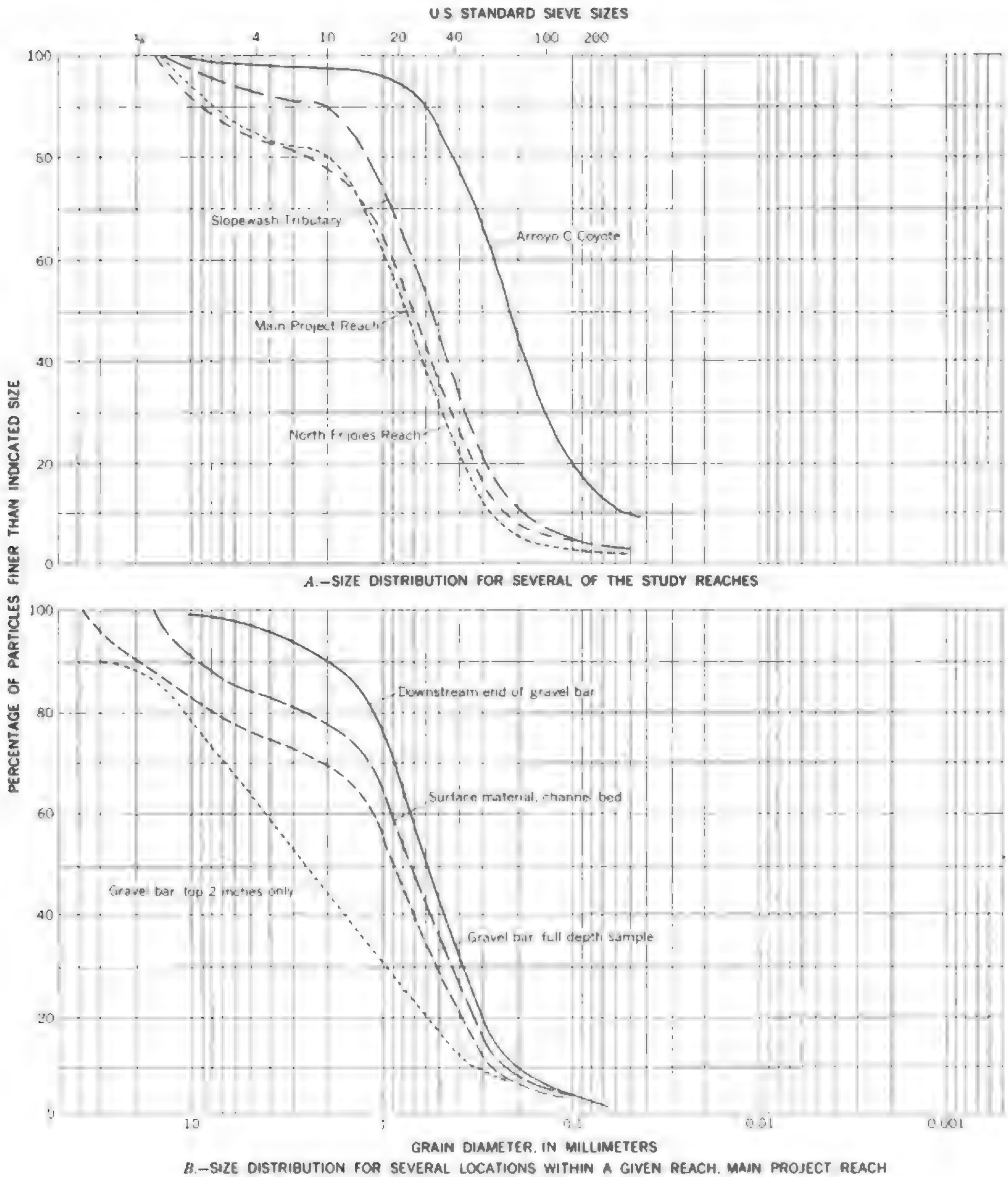

FIGURE 149.—Bed-material grain-size distribution, sieve analyses.

Digitized by Google

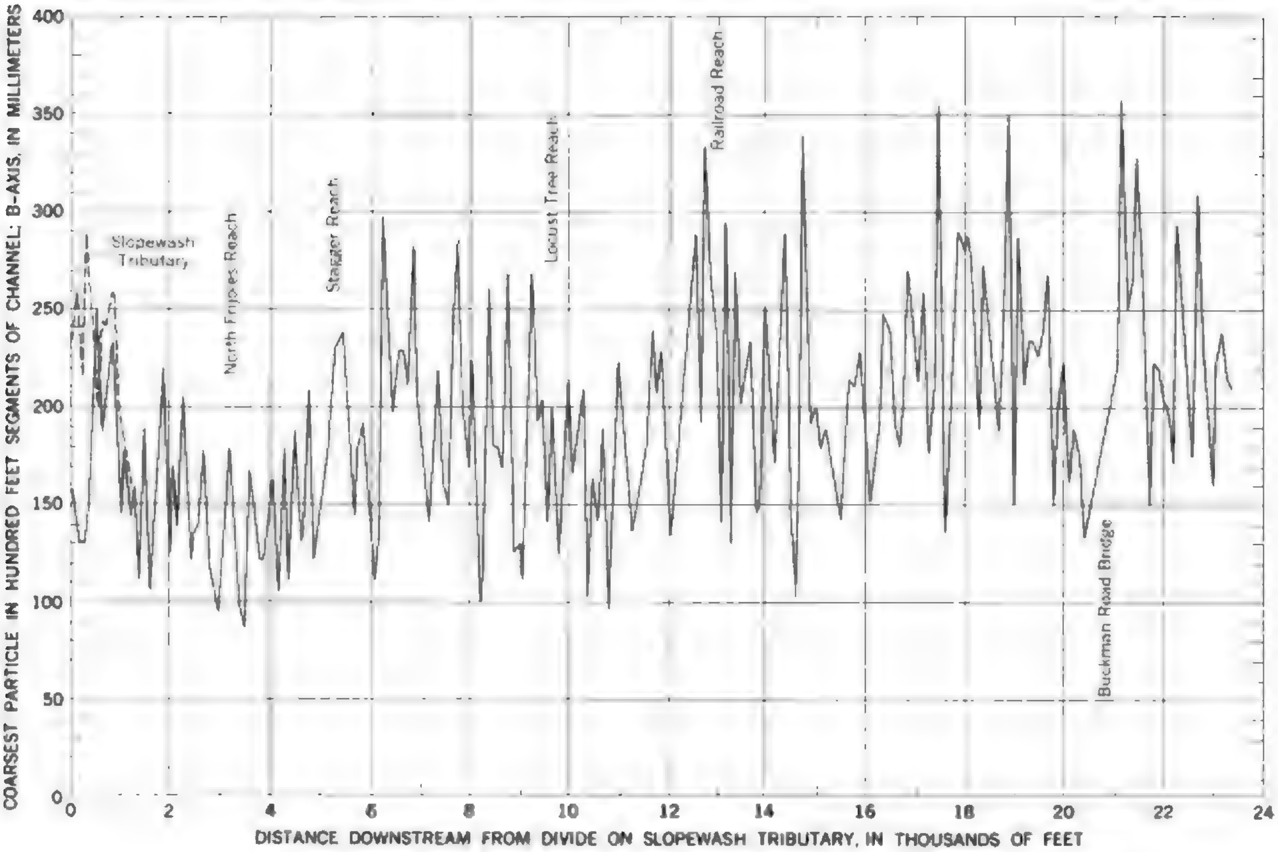

FIGURE 150.—Downstream distribution of coarsest particle in each 100-foot segment of channel.

Also, for several flows, the experiment included some rock groups composed of only one weight class. In this arrangement, rocks were spaced on 1, 2, or 3 diameters rather than by the absolute distances of 0.5, 1.0, or 2.0 feet.

At the Main Project where the channel is straight, there were initially eight ranges of rock groups about 110 feet apart. The groups having 1-foot spacing lay along the centerline of the channel and the groups having ½-foot and 2-feet spacing on either side, alternating from one range to another. Arrangement of the four upstream ranges was the obverse of that for the four downstream ranges so as to eliminate bias in across-the-channel variation. The position of each particle was individually recorded together with its weight and dimensions of the long, intermediate, and short axes. In addition there were two lines of boulders (as much as 97,500 g) spaced 9 feet apart across the channel in this reach. At various times additional temporary ranges of particle groups have been installed at the Main Project Reach, but the eight ranges and two lines of large particles described above were maintained during the entire investigation. After each flow we measured the distance that individual particles moved, and in preparation for the next flow, reconstructed each particle group in accordance with the specifications described.

Procedure at other reaches was basically the same as for the Main Project Reach. At the Locust Tree Reach there were originally two ranges, three since 1960, each including groups having two different spacings, and also a line of large rocks spaced 6 feet apart. The channel is so narrow at the North Frijoles Reach that the groups having different spacings were located along the length of the channel rather than along a line perpendicular to it.

At the Railroad Reach there was a single line of angular basalt boulders weighing as much as 111,000 grams and spaced 4 feet apart. The Stagger Reach had two lines of basalt boulders weighing as much as 47,500 grams, and spaced 3 feet apart. Basalt is a lithology foreign to the drainage basin and was derived from highway and railroad fills.

Tracing the downstream movement of painted gravel particles during a flow involved certain difficulties. An

Digitized by Google

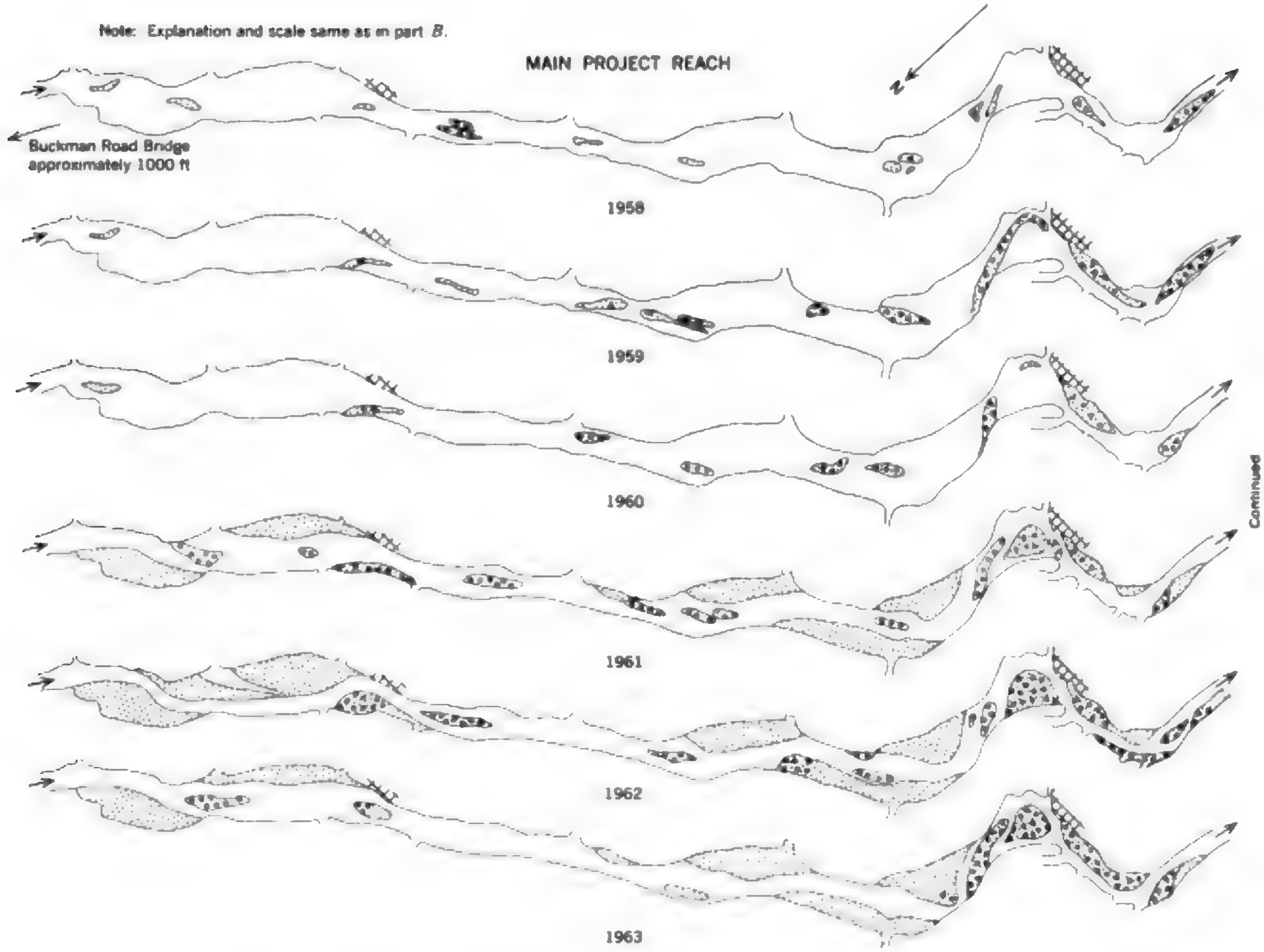

A.—SAND AND GRAVEL BARS FROM BELOW BUCKMAN ROAD BRIDGE TO HALF-MILE SECTION

FIGURE 151.—Spacing and composition of

initial problem was to find a paint that is weather resistant during long periods of immobility and is abrasion-resistant during transport. Oil-base paints proved unsatisfactory because they peeled excessively. Except for the first year, water-base masonry paint was used with satisfactory results.

Even if the paint remains intact and every particle found is identifiable, there are still losses due to burial of particles in the sand, entrapment in brushy areas, or transport outside the search area. The rocks from a given group may move downstream distances ranging from a few feet to 3 miles, depending on the magnitude of the flow. Because of their bright color, painted rocks are plainly visible in the sandy channel unless completely buried. Many particles are found partly buried (fig. 152) and the data on losses indicate that others become completely buried. Recoveries range from more than 90 percent in small flows to 2 percent for one exceptionally large flow. Apparently the losses have decreased since adoption of a water-base masonry paint, but even under optimum conditions losses of 10–30 percent during small flows and 30–50 percent during large flows are to be expected. The greatest losses occur in the smaller size classes.

Deep burial in the sandy channel seldom occurs in the area studied. Many holes 4 feet deep were drilled in the channel bed for installation of scour chains, and no coarse gravel was encountered. The composition of

Digitized by Google

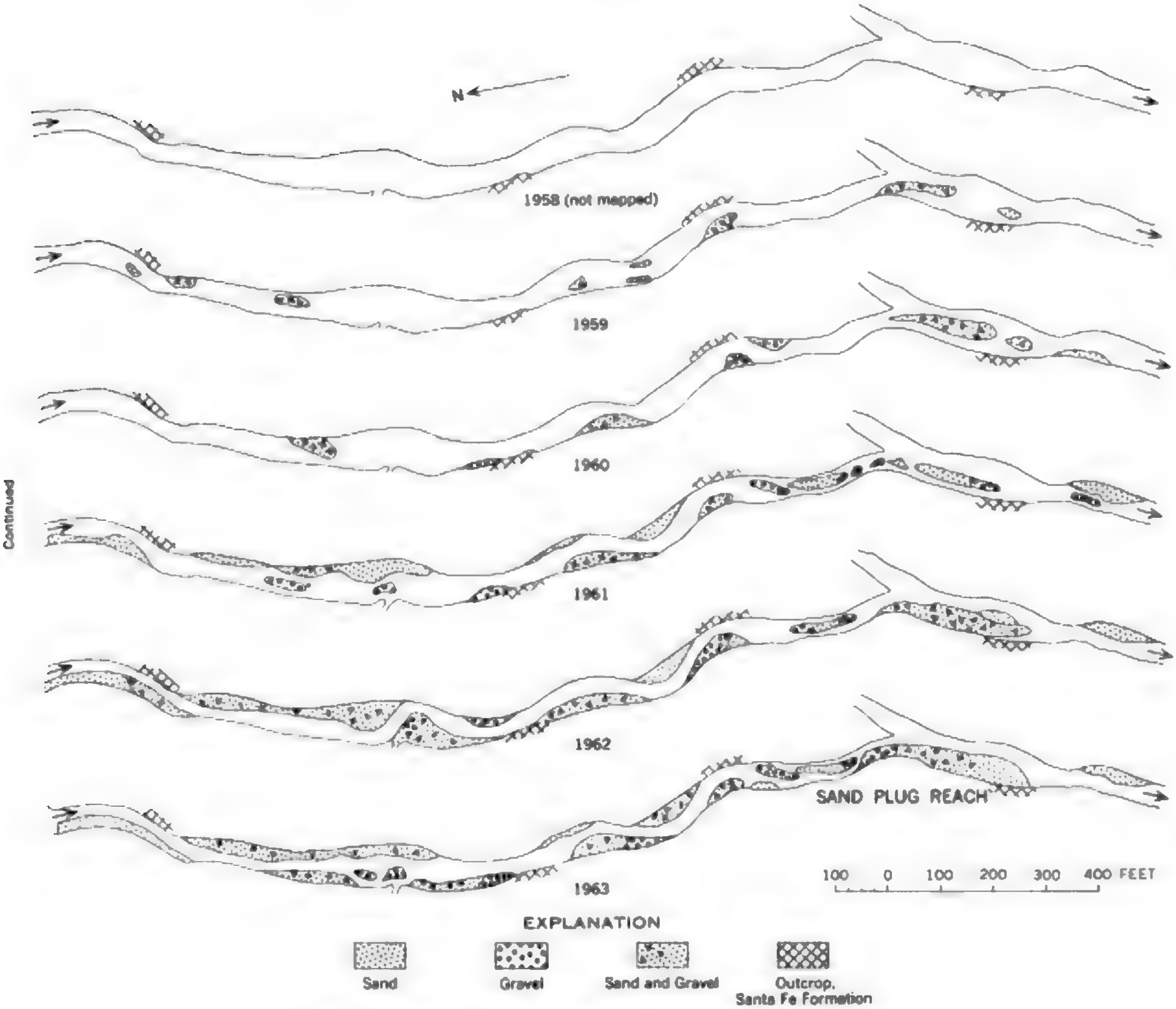

B.—SAND AND GRAVEL BARS FROM HALF-MILE SECTION TO SAND PLUG REACH

gravel bars, Arroyo de los Frijoles, 1958–63.

gravel bars lends support to the conclusion that coarse particles occur only at or near the channel surface. A typical bar (fig. 152*D*) is strewn with coarse gravel, and in a typical cross section it is apparent that this is only a surface veneer extending at most a few grain-diameters deep.

Even when the bed scoured more than a foot in a high flow and subsequently filled to the original elevation, large gravel particles did not become deeply buried and, for the most part, projected slightly above the refilled surface.

The explanation of this phenomenon appears to be the Bagnold-dispersive-stress (1956) caused by grain-to-grain impact during motion. The stress increases as the diameter squared and the large particles, subjected to highest stress, are forced to the bed surface where the dispersive stress is zero.

Subsequent to these observations, some streambeds in Maryland (annual precipitation 44 inches) were sampled to determine whether similar phenomena occur. It was found that gravel-bed streams in a subhumid region also tend to have a concentration of the largest particles at the surface of the channel bed (Leopold and others, 1964, p. 211).

For the purpose of segregating the influence of size and spacing on particle movement it is not necessary to consider the distance a given rock moved during a flow; that is, whether it was actually found downstream or

795-885 O—66——4

Digitized by Google

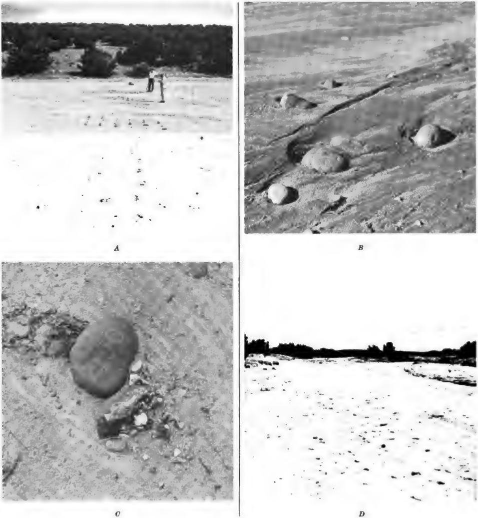

FIGURE 152.—The painted rock experiments and a naturally occurring accumulation of large particles. *A*, Main Project Reach, showing Latin Square position of painted rock groups in the sandy channel. *B*, Rocks moved from Main Project Reach during flood of August 4, 1960; note scour pits around each boulder. *C*, Detail of rock weighing 7,100 grams at Main Project Reach, partially buried by sand and organic debris during flow of August 4, 1960. *D*, Gravel bar at Sand Plug Reach, Arroyo de los Frijoles, looking upstream.

Digitized by Google

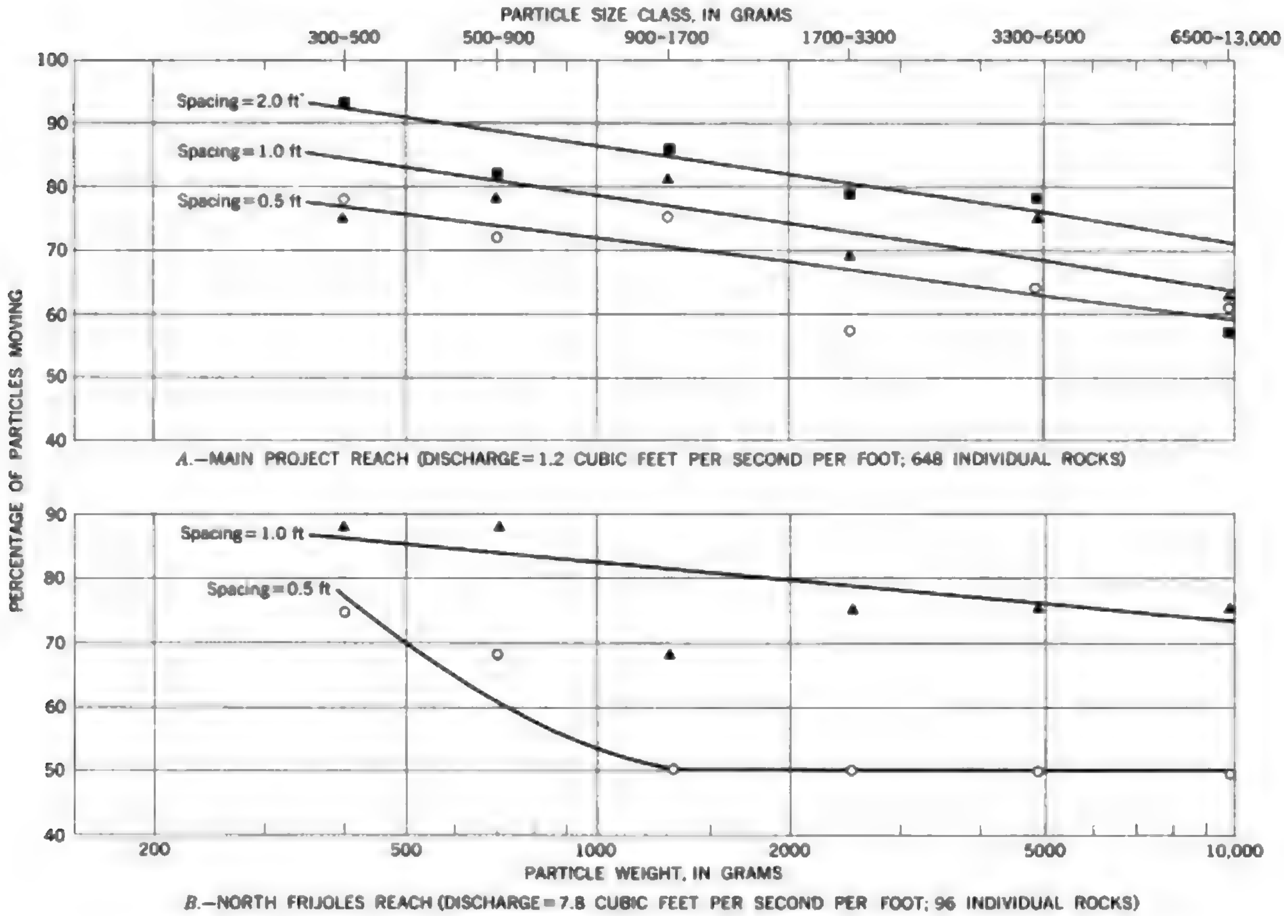

FIGURE 153.—The effect of spacing on percentage of rocks moving for a given discharge and particle size.

was simply missing. The particle had moved and how far it had moved was of no consequence. For each flow the percentage moved by size class and spacing was studied. In all, 14,000 observations were available for rock movements. The consistency of the data ranged from excellent to poor. A typical set of data are plotted on figure 153 to illustrate. From the set of graphs exemplified in this figure, further analysis was made in a manner explained in a separate paper by Langbein and Leopold. The pertinent results are presented in figure 154.

In summary, the results show that a larger flow is required to move particles which are close to one another than if they are spaced far apart. The influence of spacing decreases with increasing spacing and becomes negligible for spacings greater than about eight diameters. For example, a discharge of 11 cfs per ft would not move 500-gram particles if spaced at one diameter, but the same discharge would move 5,000-gram particles if spaced more than five diameters apart.

The effect of spacing on particle movement leads to the concept that a gravel bar is a kinematic wave caused by particle interaction, and is comparable in theory to concentrations of cars on a highway.

Owing in part to the phenomenon just described, the distance a coarse particle moves during a given flow is only slightly related to its size (fig. 155 and table 3). Particles lost are assumed to have moved distances comparable to those found. For some flows, all the particles recovered, regardless of size, were transported distances roughly equal. This is probably related to downstream decrease in discharge due to percolation into the channel. The relation of distance moved to maximum discharge during the flow is shown in figure 156. In general, the small particles do not travel materially farther than the large ones, and nearly half the flows include examples of larger particles moving farther than small ones. There is thus no neat progression of transport distances inverse to particle size.

SCOUR AND FILL

Scour and fill data from the Arroyo de los Frijoles are being collected by means of scour chains buried ver-

Digitized by Google

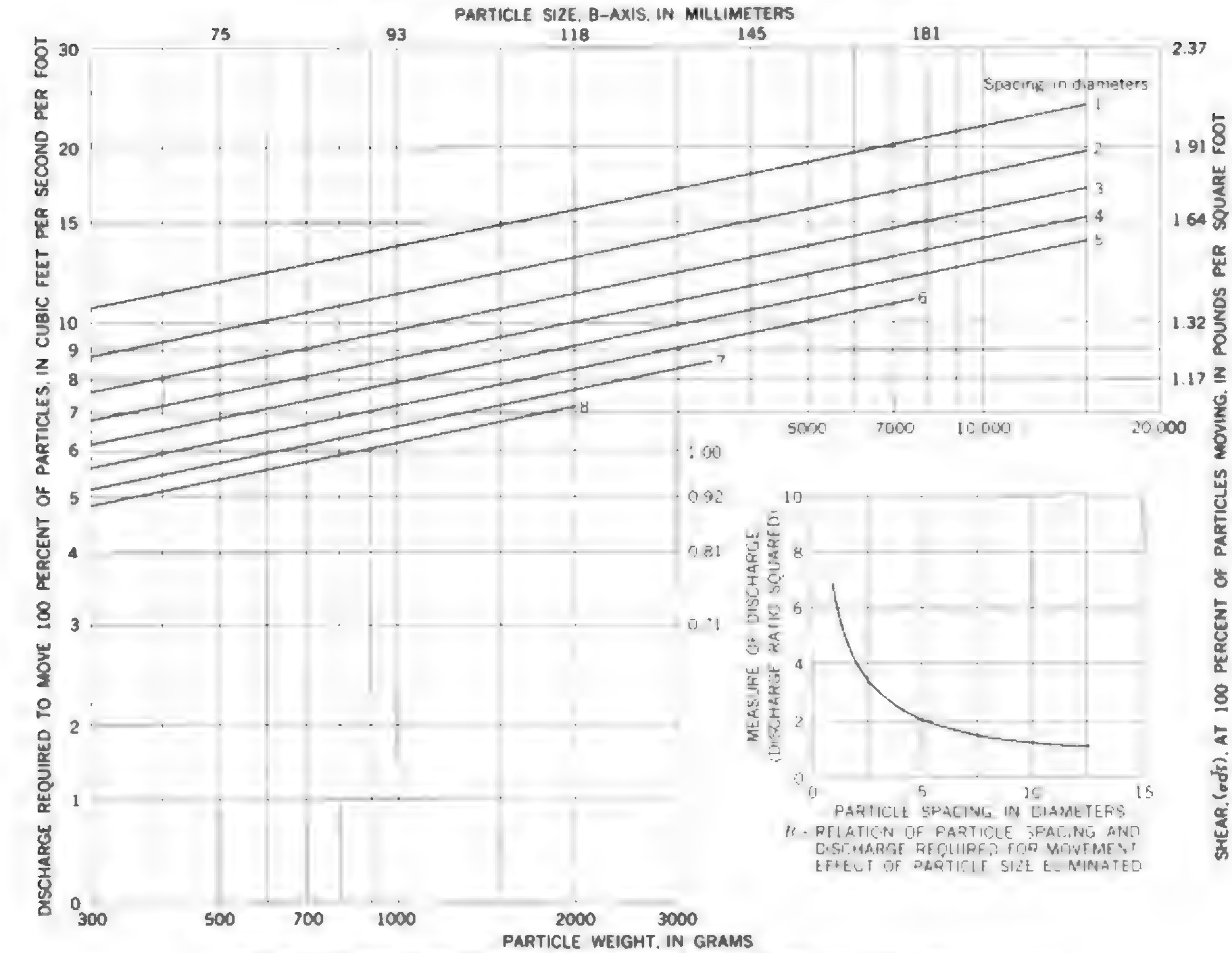

A.—RELATION BETWEEN DISCHARGE, SIZE, AND SPACING FOR 100 PERCENT OF PARTICLES MOVING

FIGURE 154.—Summary of data relating discharge, size, and spacing for painted rock experiments.

tically in the streambed with the top link at or slightly above the bed surface. After a flow the elevation of the streambed is resurveyed and the bed is dug until the chain is exposed. If scour has occurred, a part of the chain will be lying horizontally at some depth below the channel bed (fig. 157). The difference between the previous streambed elevation and the elevation of the horizontal chain is the depth of scour. The difference between the existing bed elevation and the elevation of the horizontal chain is the depth of fill. If no scour has occurred the depth of fill is the increase in bed elevation.

Scour chains, each 4 feet in length, were installed along a reach of nearly 6 miles, beginning in Slopewash Tributary and ending at Sand Plug Reach. The location of the chains usually followed the low-water channel. Over most of the study reach chains were placed at 1,000-foot intervals. In the Main Project Reach of 2,000 feet, chains were placed at 100-foot intervals. This spacing was believed sufficient to determine any downstream trend in the scour pattern in this arroyo. At seven of the chain sections, additional chains were installed across the width of the channel and provide an indication of any lateral variation in scour.

Scour-and-fill data are available for most of the 22 significant flows in the 7-year period, 1958–64. All data obtained during the scour-chain record are on file with the U.S. Geological Survey, Washington, D.C., 20242. However, since some chains were installed before others, an equal length of record does not exist for each chain location. In addition some chains, usually those in the uppermost or lowermost reaches, were not surveyed after each flow. These missing segments of data disallow a complete picture of scour and fill for individual storms,

Digitized by Google

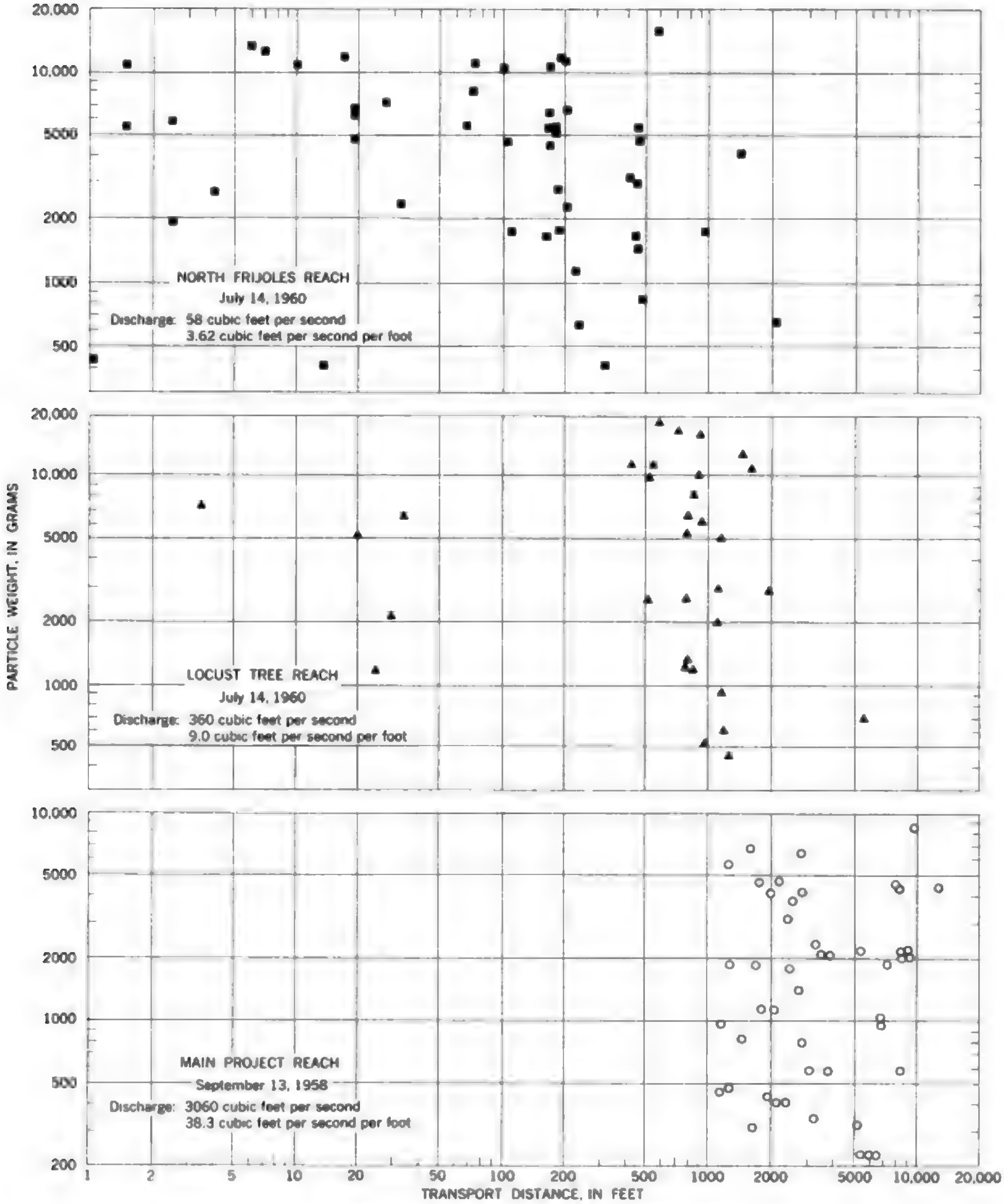

FIGURE 155.—Transport distance of coarse particles as a function of particle weight.

TABLE 3.—*Relation of transport distance to flow discharge*

[Leaders indicate that data are insufficient for an average or that category is inapplicable. Distance measurements centered in two columns represent data from adjacent size classes averaged together]

Location	Date	Discharge: Cfs	Discharge: Cfs per ft	200–300	300–500	500–900	900–1,700	1,700–3,300	3,300–6,500	6,500–13,000	13,000–26,000	26,000–52,000	52,000–104,000	Average for all sizes
				Average transport distance, in feet, by size class of particle, in grams										
Main Project	9-13-58	2,080	26.3	3,980	2,326	3,862	3,809	4,537	4,815	...	...	...	...	4,026
	7-25-62	1,300	16.3	...	1,771		1,702		1,793		1,811	1,067	363	1,775
	7-30-62	300	2.75											
	9-18-61	60	.75	...	1,272		748		680		280	...	...	784
	9-19-61	280	3.13											
	8-04-60	152	1.90	...	496	630	605	172	126	99	...	...	...	486
	7-08-61	98	1.22	...	776	673	378	449	194	462	13	...	...	446
	8-12-61	80–90	1.06	...	489	260	130	81	85	141	2	...	...	196
	7-06-62	40	.80	...	277		126		200		...	...	...	165
	7-14-60	35	.44	...	126	103	76	121	38	24	0	0	0	98
	8-07-59	20–25	.26	...	3	11	...	...	...	0	0	0	0	7
	7-23-59	10–15	.16	...	15	8	7	0	0	0	0	0	0	11
Locust Tree	9-19-61	650	16.2	...	1,694		1,905		1,808		...	...	...	1,818
	7-08-61	495	12.5	...	926	1,982	471	941	1,302	496	...	...	...	1,123
	7-25-62	450	11.2	...	...	...	1,285		1,120		...	...	...	1,198
	7-30-62	450	11.2											
	7-14-60	360	9.0	...	...	2,198	796	1,116	720	806	757	...	...	1,061
	8-12-61	300–400	8.8	...	938		692		317		...	...	...	863
	7-08-62	150	3.75	...	...	...	266		84		...	...	...	234
	8-23-59	60–75	1.56	...	225	347	276	280	107	...	...	...	...	228
	8-17-59	20–25	.56	...	397	290	126	29	34	...	...	...	...	161
	9-06-58	10	.26	...	...	73	...	29	8	...	...	...	...	84
North Frijoles	9-19-61	220	14.4	...	789		674		847		972	...	...	870
	8-23-59	140	8.7	...	...	644	...	443	124	78	...	...	...	254
	8-12-61	85	5.32	...	560		316		142		170	...	...	322
	7-26-62	85	5.32	...	498		243		119		...	...	...	279
	7-14-60	67	4.18	...	108	659	336	242	289	78	...	...	...	216
	7-08-61	58	3.62	...	540	291	330	325	217	159	118	...	...	294
	8-24-59	50	3.12	...	117	229	218	110	79	48	71	...	...	126
	9-06-58	15–20	1.09	268	98	...	57	...	...	...	...	...	...	158
Stagger Reach	9-19-61	...	...	...	...	...	...	...	...	...	1,313	2,140	...	1,727
	7-14-60	...	...	...	...	...	...	...	...	...	456	304	...	400
	7-30-62	...	...	...	...	...	...	...	...	...	647	191	...	373
	8-12-61	...	...	...	...	...	...	...	...	...	49	199	...	109
	7-06-62	...	...	...	...	...	...	...	...	...	39	61	...	53
	7-26-62	...	...	...	...	...	...	...	...	...	45	35	...	38
	7-08-61	...	...	...	...	...	...	...	...	...	...	14	...	14
Railroad Reach	7-08-61	...	...	...	...	...	...	...	...	...	1,665	43	148	879
	7-14-60	...	...	...	...	...	...	...	...	...	381	280	...	340

but the net change in bed elevation since the time of the initial survey may still be obtained.

By 1959 the majority of the chains had been installed along the arroyo. Scour-and-fill data for a sample flow, for the year 1962, and for the period 1958–62 are shown in figure 158. The upper part of the figure shows the drainage area of Arroyo de los Frijoles and the general location of the chains by chain number. For the two individual flows, the lower dashed line represents the depth of scour. The upper dashed line represents the depth of fill. The heavy solid line represents the net change in bed elevation after scour and fill.

The nature of the flash flow is such that the entire length of the arroyo may not be flooded with each storm. The flow-producing rain may be so located that only lower reaches received runoff, or, for a smaller storm near the headwaters, a part or possibly the entire flow may be absorbed into the ground by percolation before is reaches a downstream section. A third possibility remains that a particular chain section may be left dry or has very little scour because it was not in the low-water path of flow. For a single storm, then there is a considerable variation in the recorded depth of scour from section to section. This variation is further exemplified in the Main Project Reach where the chains are placed at 100-foot intervals. In spite of individual variations a general consistency prevails among the data, that is, at most sections along the channel there is a scour and subsequent fill. All flows produce this same pattern; the magnitude of scour is primarily dependent upon hydraulic factors of individual flows, and these factors are related to the intensity and total amount of rainfall.

North Frijoles, Locust Tree, and Main Project reaches of the channel are the objects of special study and are also the reaches where flow rates are measured. It is within these reaches that the chain sections are located to determine cross-channel patterns of scour. The mean depth of scour at a section may be determined by averaging the values from the several chains at each of the sections. Mean values of scour for each recorded flow are tabulated in table 4. The data are plotted in figure 159. Despite considerable scatter among the data, the mean scour depth appears to be proportional to the square root of discharge per unit width of channel.

An increasing depth of scour downstream is not observed in any single profile (fig. 158).

Probably for similar reasons, the depth of scour is apparently independent of channel width. Channel widths have been illustrated on figure 148. No sys-

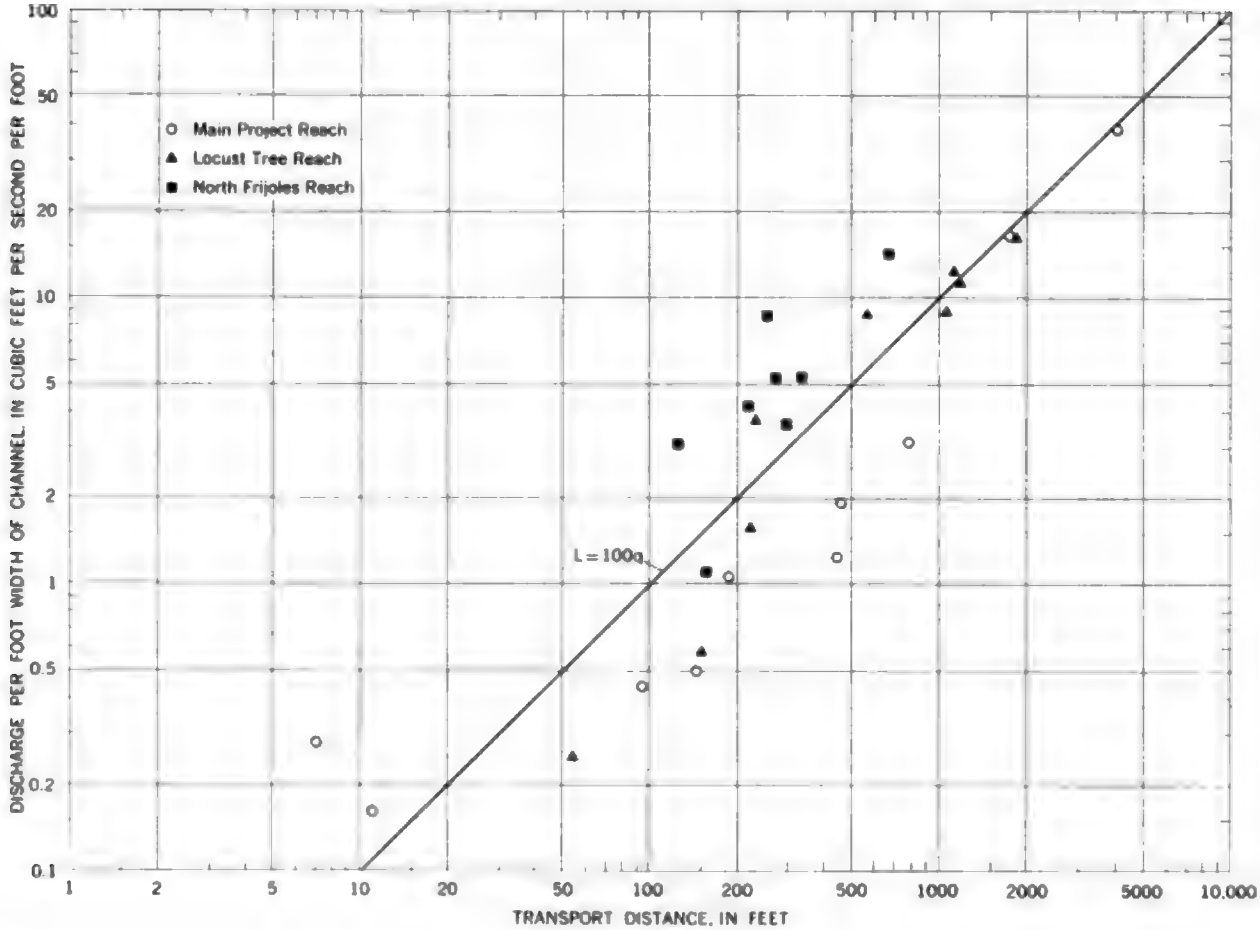

FIGURE 158.—Average transport distance of coarse particles as a function of discharge (sizes approximately 200–13,000 g).

tematic relation of local depth of scour to the corresponding channel width could be established.

The seven chain sections provided data to study lateral variations in scour across the width of the channel. One of these sections, chosen as representative of a typical reach, is illustrated on figure 160. This figure, illustrating a Main Project section near station 25,000 feet, indicates a net aggradation for the 6-year period. The whole width of the channel scours during nearly every flow, but the amount of scour and fill varies across the width.

The progressive effect of scour and fill over the length of the channel is illustrated in figure 161. Except for several isolated reaches, aggradation is occurring over the entire length of the channel. For the period of record, this aggradation amounts to an average of 0.04 ft per yr including those reaches which show a net scour.

Net scour in individual reaches can be partially explained either by natural or man-caused events. For examples, at a stationing of 32,000 feet (fig. 161) the large flow of 1958 cut through a fan-type deposit (literally a sandplug and hence the name for this reach) at the chain location and indicated a large net scour. This fan had earlier been deposited at the mouth of an entering tributary. At this sand fan most of the channel width was accumulating a net fill and now, 1964, an islandlike deposit over a foot high occupies a large part of the channel width. Channel-wide, a net aggradation does exist at that location, but because of the placement of the chain a net scour shows on the graph of figure 161.

Also, in some of the upstream reaches of the channel, excavation of sand by local contractors is responsible, at least in part, for the apparent net degradation at these sections.

The downstream profiles of the channel bed showing progressive accretions of sediment during aggradation probably represent as detailed an historical record of this process as has been compiled.

Digitized by Google

FIGURE 157.—Horizontal part of chain lying at depth of maximum scour, here about half a foot. Vertical part of chain disappears below man's band.

The record demonstrates some nonuniformity along a channel 6 miles long, some short reaches not following the general trend. The reaches not participating in the aggradation do so consistently, but as in the Sand Plug Reach at the lower end of the studied length, the reason for its deviation relates to special and understandable local circumstances. Interestingly, the random pattern of storm occurrence does not lead to a random location of reaches of sediment accretion, for the increment of deposition is rather uniform from year to year.

The exaggeration of scale in figure 161 must be kept in mind, and the variations in yearly increments are really very small considering the channel length involved. If one short reach aggraded a tenth of a foot more than another a thousand feet away, the channel slope in the reach would be changed by only 0.0001 foot per foot. The variability along the channel due to the irregularities of depositional increment are of this order. Thus, despite random character of storms and the local loss of flow to channel percolation the mean slope of the bed is maintained over long reaches.

A more complete discussion of the records of scour is given by Emmett and Leopold (1964). For the present purpose, suffice it to say that scour is associated with dilation of the grain bed through the scour depth, but that individual particles may move intermittently and at a speed much less than that of the water. The volume of material scoured and moved is large. Because of its low mean speed downstream, that whole volume does not move entirely out of a long reach but, in effect, is shifted downstream only a limited distance.

TABLE 4.—*Mean depth of scour as a function of discharge*

Date of flow	North Frijoles Reach				
	Discharge	Upper section		Lower section	
	(cfs)	Discharge (cfs per ft)	Scour (ft)	Discharge (cfs per ft)	Scour (ft)
9-6-58	17.5	0.87	0.018	1.46	0.080
9-13-58	194	9.7	.215	16.2	.977
5-23-59	140	7.0	.103	11.7	.460
8-24-59	50	2.30	.083	4.17	.000
7-14-60	67	3.50	.068	5.59	.135
11-16-60	9	.40	.023	.67	.315
7-08-61	58	2.90	.130	4.84	.268
9-19-61	230	11.50	.188	19.20	.598
7-05-62	7	......	......	.58	.040
7-30-62	90	4.50	.153	7.50	.175
7-20-63	10	.50	.180	.83	.128
9-21-63	5	.25	.293	.42	.448

Date of flow	Locust Tree Reach				
	Discharge		Scour (ft)		
	(cfs)	(cfs per ft)	Upper section	Middle section	Lower section
9-13-58	1320	34.0	0.820	......	......
5-23-59	62.5	1.69	.132	0.076	0.255
8-07-59	22.5	.56	.196	.060	.078
7-14-60	360	9.0	.260	.212	.265
7-08-61	498	12.47	.464	.406	......
8-12-61	350	8.75	.194	.368	.358
9-19-61	650	16.25	.280	.138	......
7-05-62	150	3.75	.274	......	......
7-30-62	450	11.2	.272	.334	.300
7-20-63	15	.88	.134	.076	.133
9-21-63	316	7.9	.314	.320	.305

Date of flow	Main Project Reach						
	Discharge (cfs)	Upper Reach		Lower Reach		Low-water chains	
		Discharge (cfs per ft)	Scour (ft)	Discharge (cfs per ft)	Scour (ft)	Discharge (cfs per ft)	Scour (ft)
8-18-58	20	0.235	0.053	0.286	0.023	......	......
9-13-58	3060	36.0	.830	43.6	.557	......	......
5-23-59	4	.047	.050	.057	.008	0.050	0.025
7-23-59	12.5	.147	.000	.178	.240	.156	.043
8-07-59	22.5	.265	.033	.321	.022	.282	.057
7-14-60	35	.412	.036	.500	.033	.439	.048
8-04-60	152	1.79	.088	2.17	.425	1.90	.128
7-08-61	98	1.15	.124	1.40	.118	1.23	.145
9-19-61	250	2.94	.125	......	......	3.13	.316
7-23-62	1300	15.3	.511	18.6	.810	16.3	.273
7-20-63	5	.059	.024	.072	.010	.062	.000
9-21-63	391	4.6	.236	5.59	.175	4.9	.234

HILLSLOPE EROSION

EROSION PLOT ON SLOPEWASH TRIBUTARY

To measure the rate of hillslope erosion a grid system of erosion pins was installed in 1959 on one of the slopes in the drainage area of Slopewash Tributary. The general location of this grid system, or erosion plot, is shown in figure 144, and the locality is illustrated in figure 143. The erosion plot consists of 61 nails with washers spaced on 5-foot centers on an area 50×50 feet having a relief of 5 feet and furrowed by two shallow and narrow rills. These rills join midway through the grid system into a single larger rill.

Digitized by Google

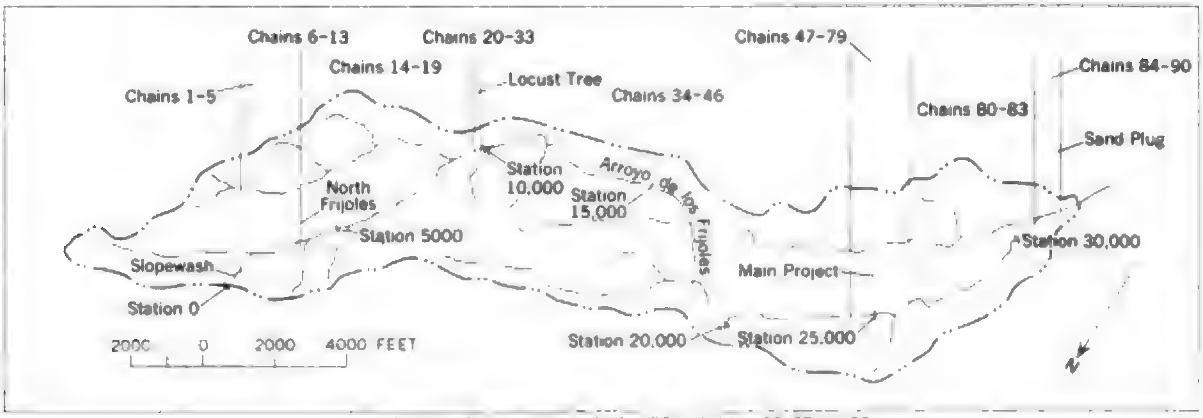

A.—LOCATION OF CHAINS ALONG ARROYO DE LOS FRIJOLES

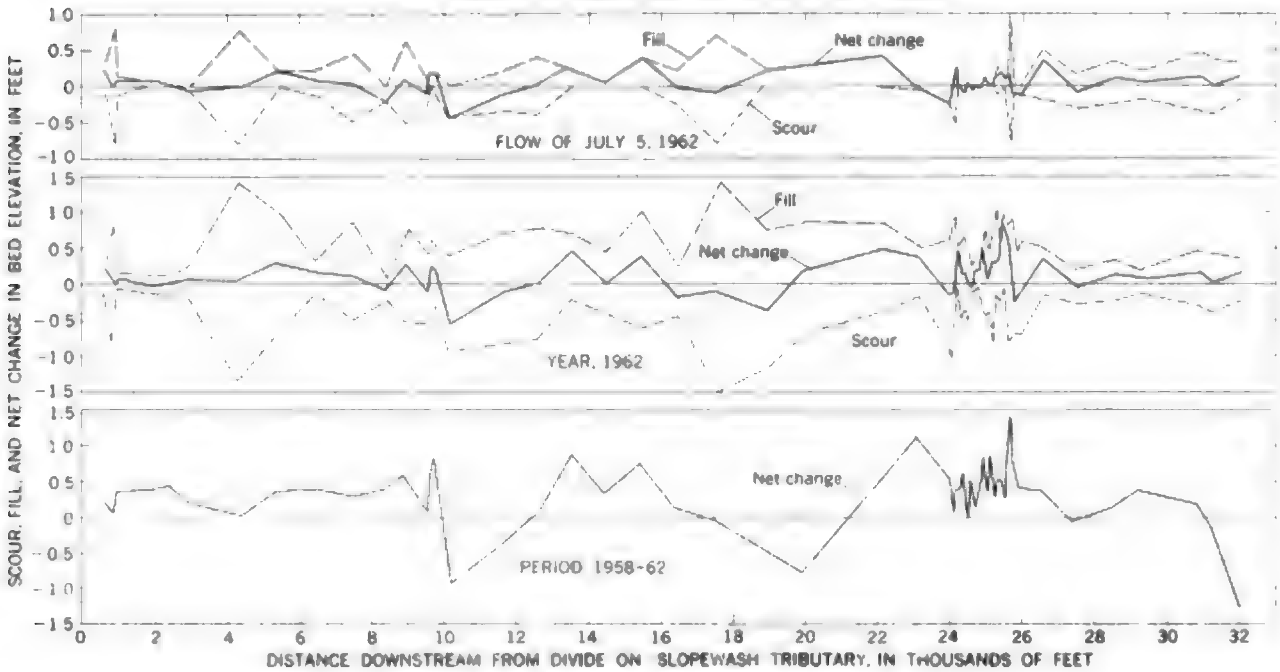

B.—SCOUR FILL AND NET CHANGE

FIGURE 158.—Downstream pattern of scour, fill, and net change in bed elevation for a single storm, a 1-year, and a 5-year period, 1958–62.

At the time of the installation, the nails (10-inch spikes) were slipped through a large washer and driven into the ground in a vertical position until the bottom of the washer was flush with the ground surface. Erosion undermines the washer, which then falls down a length of the pin. The pin protrudes above the washer at a distance equal to the erosion during the intervening period. While maximum erosion is marked by the washer, deposition may be recorded as the height of any material above the washer, a desirable feature in such places as a rill bottom where maximum and net erosion generally differ. Figure 162 shows typical erosion nails on the erosion plot and on transects. Elevations of all nail heads were measured and resurveys show that the nails remain stable and are not being heaved by frost action.

An attempt was made to map erosion values as topographic contours of erosion quantity, but because of the short length of record no systematic trend is apparent among individual values. At this time it appears that the pins on the steeper slopes adjacent to the rills show a slightly higher rate of erosion.

Pins in or near rills tend to show some deposition on the washer following scour. Depth of overland runoff

Digitized by Google

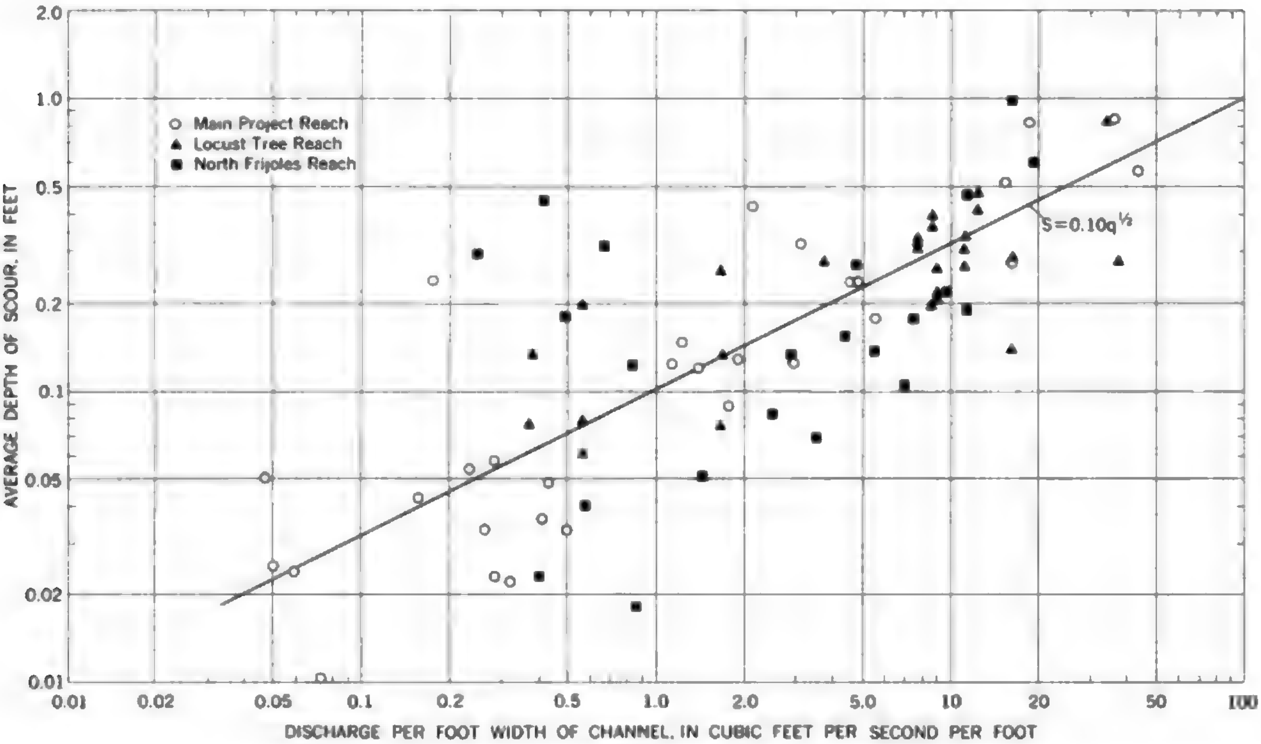

FIGURE 159.—Depth of scour as a function of discharge at chain sections; each point represents an average scour across the channel bed, based on 4–10 chains per cross-section.

is greater in such locations and it might be that erosion occurs during maximum overland flow depth and that deposition follows as the flow subsides. But deposition is the exception and not the general rule. The majority of the pins show very little or no filling on top of the washer.

Erosion data have been collected in the years 1961–64. Data in 1961 included only values of erosion and later, both erosion and deposition. The average erosion during the 5-year period, 1959–64, was 0.0117 ft per yr, and deposition on some of the pins averaged 0.0041 ft per yr—a net average rate of erosion of 0.0076 ft per yr.

Summary of data C contains data from the erosion-pin plot in Slopewash Tributary.

SLOPE-RETREAT PINS ON SLOPEWASH TRIBUTARY

Fifty-seven erosion pins are arranged on four lines transverse to the steep sides of Slopewash Tributary. These pins are the nail-with-washer just described, and are designated as "slope-retreat pins" on the location map of figure 144. An enlarged sketch elaborating details of these pins is shown in figure 163.

The pins are arranged in three groups, each group consisting of two lines spaced 2 feet apart. Each line, with pins spaced at 2-foot intervals, extends down the steep slopes to the channel bed and, for one pair of lines, cuts across the channel and up the steep slopes on the opposite side of the tributary. The slopes range in steepness from 21 to 38 degrees, and these generalized slope angles are marked on figure 163 for identification.

The pins were installed in 1959 and erosion measurements were made once a year in the period 1961–64. Net values of erosion for the period are shown below the pin numbers on figure 163.

For the 57 pins, the average rate of net erosion is 0.0142 ft per yr. This figure consists of an average rate of maximum erosion of 0.0281 ft per yr and an average deposition of 0.0139 ft per yr. Individual measurements varied from a net deposition to an erosion of more than 0.08 ft per yr. A summary of all data from the slope-retreat lines is included in summary of data D.

Perhaps more meaningful rates of erosion could be obtained by dividing the 57 pins into 3 categories. Category 1 includes pins 1–29 of the upper line, category 2 includes pins 30–45 of the upper line, and category 3 includes the 12 pins, 46–57, in the lower line. Categories 1 and 3 are similar in their physiographic locations, but the pins in category 2 differ in that here apparent erosion is being disguised by channel deposits on some of the pins near the channel edge and by an accumulation of sloughed material on some of the lower

Digitized by Google

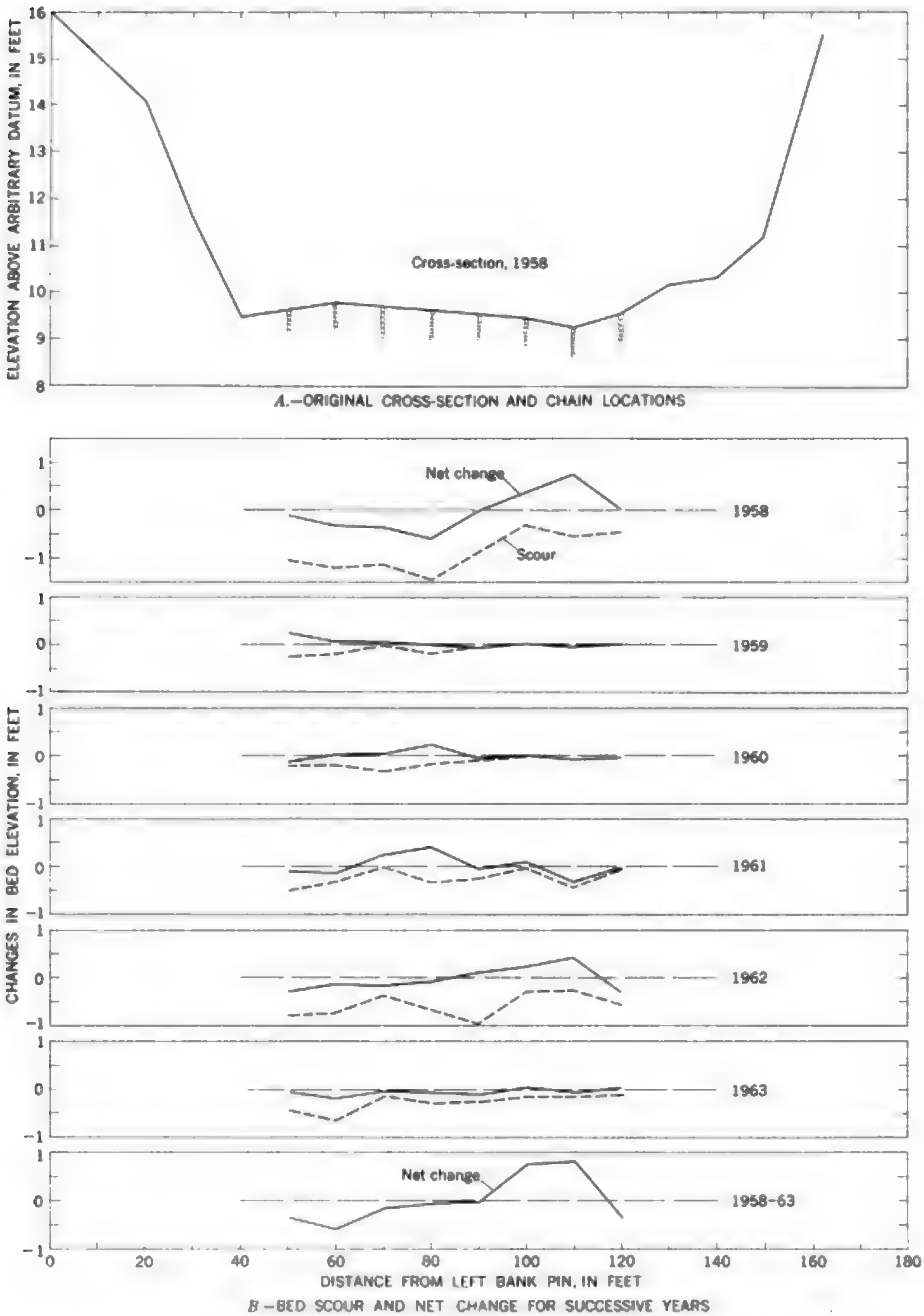

FIGURE 160.—Scour and net change in bed elevation, upper chain section, Main Project Reach.

Digitized by Google

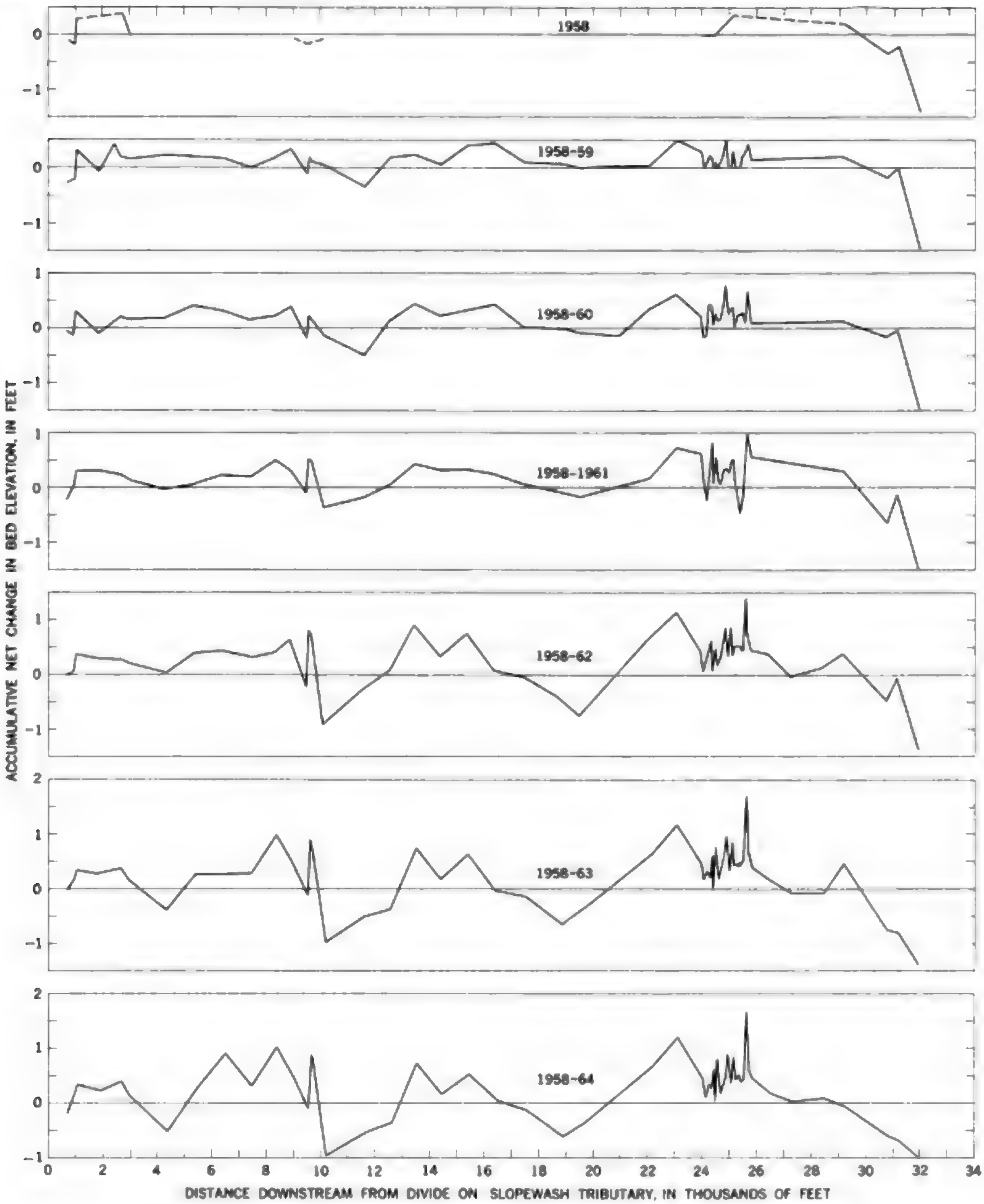

FIGURE 161.—Downstream pattern of accumulative net changes in bed elevation, Arroyo de los Frijoles.

Digitized by Google

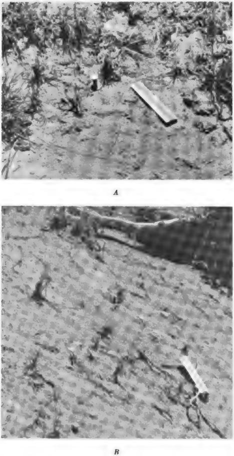

FIGURE 162.—Erosion pins consisting of 10-inch spike and washer. *A*, Erosion pins in grid system, Slopewash Tributary (scale is a 6-inch ruler). *B*, Erosion pins on slope-retreat line, Slopewash Tributary.

pins on the sloping bank. Thus the 16 pins in this category actually show an average of a net deposition. Most likely this apparent deposition is only temporary, as a scour of the channel deposit will not only expose the lower nails again but will also allow the sloughed material to continue its downslope journey to the channel.

Rates of net erosion for pins in each of the three categories are: category 1, 0.0210 ft per yr; category 2, −0.0034 ft per yr (the minus represents net deposition); and category 3, 0.0183 ft per yr. More complete computations are included at the end of summary of data D.

Excepting those pins just mentioned in category 2, generally only those pins on the channel bed showed consistent deposition above the washer, and the fact that in most places these pins were completely buried indicates an aggrading channel. Undoubtedly much of the aggraded material is derived from the erosion of the steep slopes adjacent to the channel. However, the erosion rate on these slopes more than compensates for the volume accumulation of sediment on the channel bed. Implicit, then, is that much of the eroded fine-grained sediment is being carried further downstream.

Oddly, in the pin lines here discussed, the greatest rates of erosion were on the less steep slopes (upper left group on fig. 163), but in considering all observations, steep slopes generally show a greater rate of erosion than less steep slopes. No attempt is made at this time to ascribe to either of these two sets of measurements the percentage of total sediment which each produces. While the gentler slopes have a smaller erosion rate, their land area within the watershed is greater. Consequently, in terms of total volume of sediment, the gentler slopes may yield the greater amount.

Location and elevation of pins along lines CB and BA as well as the net 6-year erosion at each are indicated on the profiles of figure 164. The profiles provide an insight to the occasional contradictory data among pins. It appears that the greater steepness in local surface slope (that slope within 1–2 ft of the pin) is accompanied by the greater erosion. The greatest erosion is indicated by those pins on the very steep slopes just adjacent to, but not in, the channel bed. The pins on a locally flat slope, especially those just downhill of a steeper slope (see pins 2CB and 3CB, fig. 164) actually show a deposition occurring. This deposited material was undoubtedly derived in part from the greater erosion on the steeper slopes just uphill, for example, from pin 1CB. Pins on relatively unbroken slopes are in general agreement with each other and usually indicate about the average rate of erosion. Thirteen of the 17 pins showed a net erosion and 4 a deposition. If only those pins showing a net erosion were considered, the average rate of erosion would increase from the reported 0.0072 ft per yr to 0.017 ft per yr. The former value is in agreement with the value from the erosion plot and the latter with the value from the slope-retreat lines. Generally, the topography along the iron-pin lines is intermediate between that of the erosion plot and that of the slope-retreat lines.

Digitized by Google

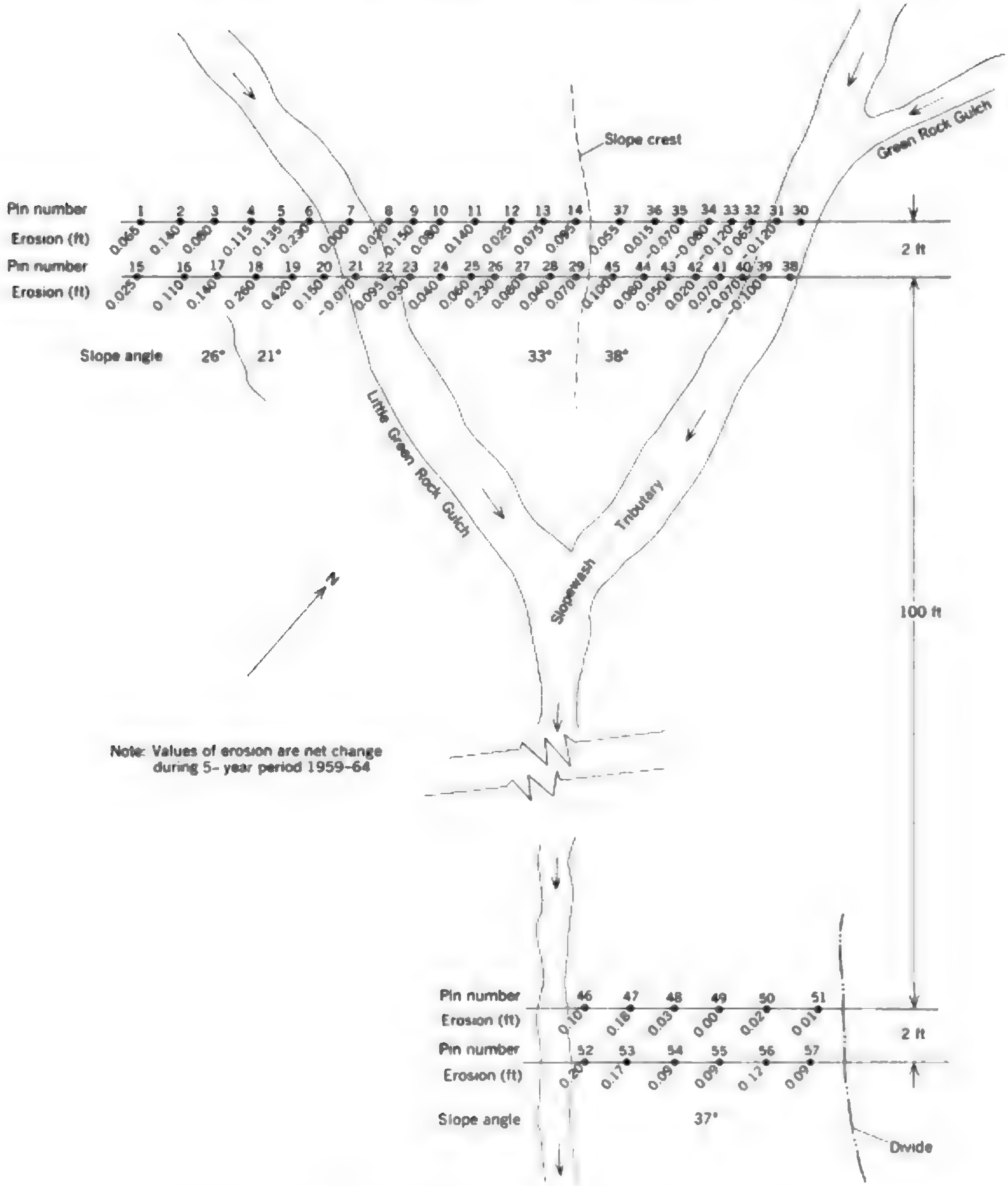

FIGURE 163.—Sketch map showing details of the slope-retreat pins, Slopewash Tributary.

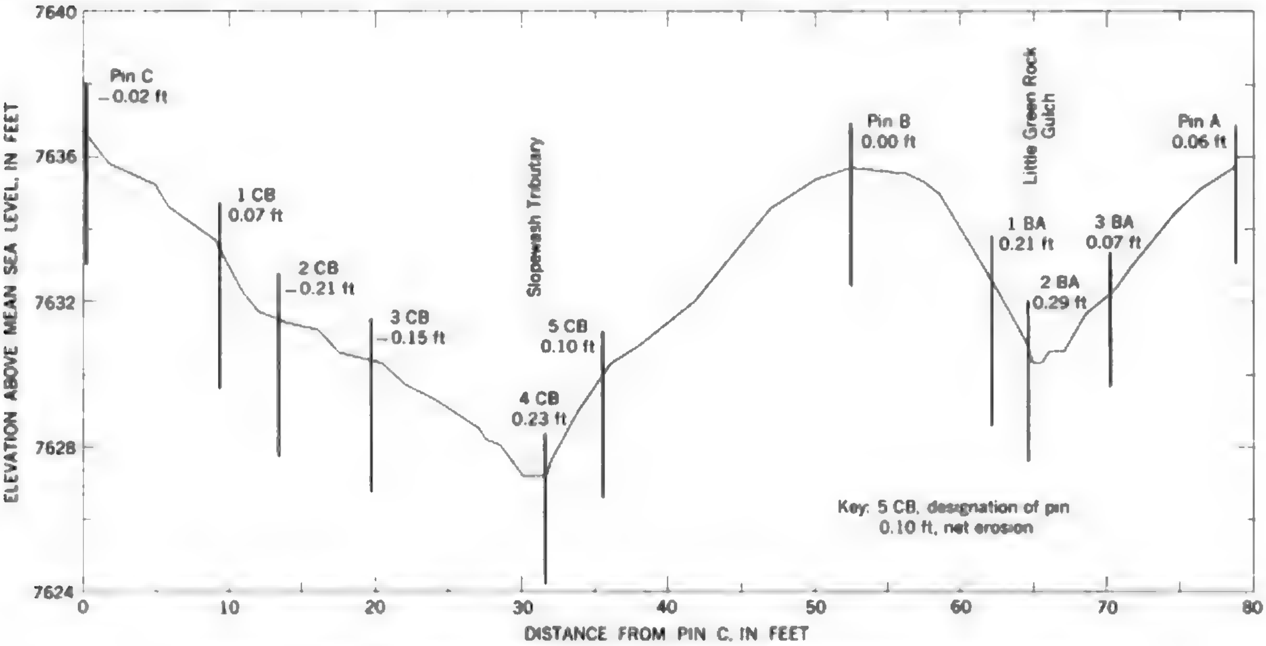

FIGURE 164.—Six-year (1958–64) net erosion on iron-pin line CBA, Slopewash Tributary drainage area.

OTHER MEASUREMENTS OF SLOPE EROSION ON SLOPEWASH TRIBUTARY

The second additional set of measurements for rates of erosion consists of eight iron pins located at the chain-sections below the junction on Slopewash Tributary (see fig. 144 for chain-section locations). These are 4-foot lengths of iron reinforcing rod, installed and observed as previously described. For each chain-section, a pin was located on each sloping bank and, for two of the sections, a pin was situated in the channel bed.

Installation was made in 1958 and data were collected in 1958–64, excepting 1961. The average rate of erosion for the bank pins is 0.0108 ft per yr and the bed pins indicate an average deposition of 0.0033 ft per yr. These rates are in agreement with the other observed rates for slope erosion and channel aggradation.

EROSION NAILS ON COYOTE C. ARROYO

On slopes leading into the headcut of Coyote C. Arroyo, a total of 65 erosion pins with washers are located on 3 lines, as shown in figure 145. The pins were installed in 1961 and have been remeasured yearly to 1964. Profiles were run on the pins to determine the slope, and also a resurvey of the pin elevations indicates no heaving due to either freeze-thaw or wet-dry actions. The average of the 65 pins indicates a yearly net erosion of 0.0237 foot. All the data for the pins are tabulated in summary of data F.

Rates of erosion for each of the three lines were consistent, ranging from 0.021 to 0.027 ft per yr. These values approximate the higher values for the slope-retreat pins in Slopewash Tributary, and it is believed that they exceed somewhat the average rate of erosion for the entire drainage of Coyote C. Arroyo, as is evidenced by a lower value for the grid system than for the slope-retreat lines in Slopewash Tributary.

Attempts to correlate individual rates of erosion with individual local ground slopes did not result in a neat regression of erosion rates with lessening slopes. To the observer on the ground, it appears rather instinctive that greater erosion is occurring on the steeper slopes; however, the disparity in the data is sufficient to mask attempts to illustrate graphically the relation of slope to rate of erosion.

TRACING OF FLUORESCENT SAND

A fluorescent sand (ASTM mesh size 40) was placed along three lines in two of the study areas to trace the movement of individual fine-grained sediment. One line was along the hillcrest of Morning Walk Wash (see fig. 139). The other two lines were in Coyote C. Arroyo, one along the nail line ED and the other along the mass-movement line (see fig. 145).

The sand was placed in 1961 and the initial position was marked. In 1962 the movement of this sand was determined by searching for grains at night with a black light. Despite a relatively large amount of erosion indicated by the erosion nails, the individual sand

Digitized by Google

grains appeared remarkably stable. For the short distance of 5–10 feet individual grains moved in quantity. However, for distances greater than this very few grains could be found. Maximum distance at which we found a grain was about 50 feet.

The original concentration of the grains was not recorded and it is not known how many of the grains had actually moved but could not be found. The concentration of grains in the initial position was still large in 1962. However, it is believed that many grains, either by moving completely out of the searched area or by being covered, were not found.

In 1964 a second attempt was made to trace the movements of the fluorescent sand. The concentration at the original placement area had considerably lessened over that observed in 1962. Many grains were found within 50 feet of the original line and a few were found between 50 and 100 feet. Below 100 feet, but within several hundred feet, a few grains were found which fluoresced with the same characteristics as the placed grains, but comparison of these with grains from other observations indicated that they probably were native fluorescent minerals.

If any conclusion may be drawn from these experiments it would be that grains on the flat of a watershed divide are moved very slowly but that, once they are on the steeper slopes and within an area capable of overland flow, they are moved much more rapidly. This conclusion is supported by a 1-year set of data for erosion pins on a transect across a divide near the houses of Las Dos. These pins are referred in the project files as Corral Flat nail and washer line, but because of the short period of record are not elsewhere presented in this report. The 1-year of data show no erosion or deposition exceeding 0.005 foot, and the average for the line indicates little or no systematic movement of individual grains.

CHANNEL ENLARGEMENT IN SLOPEWASH TRIBUTARY

Although the slope retreat pins give an indication for the rate of channel enlargement, another set of measurements was designed specifically to provide rates of bank recession and channel aggradation-degradation. This set of measurements, designated as nail sections A–J (location shown on fig. 144, consists of 10 observation sections spaced approximately at 50-foot intervals along Slopewash Tributary. At each section a nail with washer was located on each sloping bank and one at the center of the channel bed. Rates of erosion and deposition were observed as previously described.

The sections were installed in 1959. Data have been collected yearly to 1964, excepting 1960. These data show that the average rate of bank erosion for the side pins is 0.0248 ft per yr. Deposition occurring at some of these pins averages 0.0058 ft per yr. The net bank recession is then equal to 0.0190 ft per yr. The channel bed pins indicate an eroded depth of 0.0694 ft per yr. This depth probably occurs as scour while surface runoff is flowing in the channel. Subsequent fill amounts to 0.1024 ft per yr. This leaves a net deposition of 0.0330 ft per yr, indicating an aggrading channel. This observation is consistent with other measurements indicating a channel aggradation. The channel aggradation is not confined to lower reaches of the channel but also extends upstream into the uppermost headwater rills. All nails in the channel on sections A–H show net deposition, and these vary in distance to watershed divide from 400 to 800 feet. Still, the amount of deposition in the small channels does not account for the volume eroded from upslope surfaces.

This excess of sediment is being supplied to the main streams and accounts for the aggradation observed there and reported in the section on scour and fill.

A summary of data for the nail sections are included in summary of data G.

SOIL CREEP OR MASS MOVEMENT

SLOPEWASH TRIBUTARY

To measure the magnitude of downslope soil movement occurring as soil creep, lines of mass-movement pins were installed in Slopewash Tributary and in Coyote C. basin (see figs. 144 and 145 for locations). The line in Slopewash Tributary is along the east fork some 100 feet above the junction of the tributaries. The line chosen crosses the meandering channel several times, and thus the pins are on the steep slopes (about 1:1) of the channel banks, alternately on one side and the other of the tributary. In figure 146 the photograph was taken with the camera at the north end of the line and the man is standing at the south end.

The two ends of the line are monumented and located in such a place that the monuments themselves are subject to no downhill movement. Iron rods, 4-feet long, were used to monument these end points. Generally at 5-foot spacings along the length of the line, ¼-inch galvanized iron pipes, 10 inches long, were driven vertically into the ground. At the time of installation they generally protruded about 0.1 foot above the ground surface. A transit was set up over the center of the monument on the north end of the line, oriented to the center of the monument at the south end of the line, and the distance of each pin away from the line of sight was recorded. Similar measurements are made on a resurvey except that the angle of the pin from the ver-

Digitized by Google

tical and any increase in protrusion above the ground surface are also recorded.

Resurveys were made annually from 1961 to 1964. The average rate of downslope creep of the pin tops is 0.225 in. per yr. Considerable variations exist among individual measurements. However, all pins show net downhill movement for the 5-year period. Individual variations probably reflect local influences of the particular pin location; for examples, a twig, rock, local slope, or proximity to the channel.

All of the soil profile to the full depth of the pin is not moving as fast as the average rate reported. Most pins are rotating downhill, indicating that the top layers of soil creep at a faster rate than the lower layers. The average rotation of the pins is 1.4° per year. For seven of the pins the pin angles themselves explain all the observed downslope creep, the point of rotation being very nearly at, or slightly above, the bottom of the pin. For the other eight pins the center of rotation is a short distance below the bottom of the pin. For this latter set of pins it follows then that the entire soil profile, at least to the depth of these pins, must move downslope some distance. An average value of the downhill movement for the bottom of all pins is 0.003 in. per yr (a computed, not an observed value). This value, being so nearly equal to zero, indicates that only about the top 8 inches of soil are involved in mass-movement and that the soil nearest the surface has the greatest movement.

Since the pins are leaning downhill and some of the pin length protrudes above the ground surface, a more meaningful value of downhill creep would be that computed for the pin at the ground surface rather than at the pin top. These computations show the average rate of soil creep at the ground surface as 0.205 in. per yr, slightly less than the 0.225 in. per yr attributed to the tops.

Movement at the ground surface and at the pin base, along with the depth of inserted pin, allows computation of the volume of material moving. This value is 0.87 cu in. per in. of slope base per year, or 32 cu ft per mile of slope base per year.

The increasing protrusion above the ground surface observed at the mass-movement pins was also used to study erosion rates. The average rate of erosion for these pins is 0.025 ft per yr. Generally, these are the steepest slopes (approximately 45°) for which erosion values were obtained and they show the largest rate of erosion.

A summary of the downhill movement of the pin tops, rotation of the pins, and erosion at the pins are included in summary of data H.

COYOTE C. ARROYO

A mass-movement line of pins as just described was also installed along a tributary to Coyote C. Arroyo (location shown on fig. 145). The average downhill movement of the pin tops for the period 1961–64 was 0.267 in. per yr. During the period one pin showed an unexplained uphill movement.

The average downhill pin rotation during the period of observation was 1.7° per year. The relation of downhill movement to pin rotation is the same for these pins as for the pins in Slopewash Tributary.

The pins on this line showed greater erosion than those in Slopewash Tributary. Thus, computations for the rate of downhill movement at the ground surface used a value for the length of pin exposed equal to the original protrusion plus one-half of the erosion. Computations show the average rate of movement at the surface as 0.202 in. per yr, a figure remarkably close to that obtained in Slopewash Tributary. The volume rate is somewhat less than that in Slopewash owing to a smaller depth of soil movement, here 7.5 inches. The computed volume rate of mass-movement is 25.5 cu ft per mile of slope base per year.

A summary of data for the mass-movement line in Coyote C. Arroyo is included in summary of data I.

HEADCUT ENLARGEMENT

FENCE LINE HEADCUT

Fence Line Headcut is a tributary to the Arroyo de los Frijoles, entering on the left bank about 1,500 feet below the Main Project Reach. Figure 165 is a photograph of this headcut in 1964. In 1960 the headcut was staked with six iron pins, each 4 feet in length. The rate of enlargement of the headcut is determined by

FIGURE 165.—Fence Line Headcut.

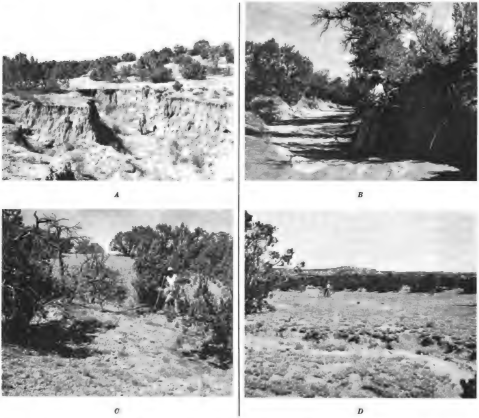

FIGURE 166.—Aspects of the drainage area of Coyote C. Arroyo. *A*, The largest headcut, cut in valley alluvium of Coyote C. Arroyo (also see map of fig. 167). *B*, Channel of Coyote C. Arroyo about 800 feet downstream from headcut pictured in *A*; man points with shovel to position where C^{14} sample was obtained to date the Coyote terrace deposits. *C*, View near the watershed divide of Coyote C. Arroyo; note the lag gravel typical of headwater areas not covered by colluvium. *D*, Typical view of the valley alluvium; coarse particles are found here only in watercourses, as in that in foreground.

measuring the distance from the iron pins to the vertical walls of the cut. Resurveys indicate that the headcut is slowly enlarging at all points of measurements, but that the greatest rate of enlargement is at the upstream end where the headcut is advancing nearly 1.5 ft per yr. Height of the vertical walls of the cut averages 6 feet.

The average volume of sediment discharged by this one gully is estimated at over 500 cu ft per yr, mostly from headward advancing.

COYOTE C. ARROYO HEADCUT

Coyote C. Arroyo is a discontinuous gully involving four headcuts. About 2,000 feet below the headwater divide is the largest of the headcuts, below which the gully is continuous to the master stream. The area around this largest headcut has been studied in detail and figure 166 includes photographs of the vicinity. Rate of headcut enlargement is being recorded by yearly planetable mapping and by measurements from iron pins driven at known distances from the vertical walls.

Digitized by Google

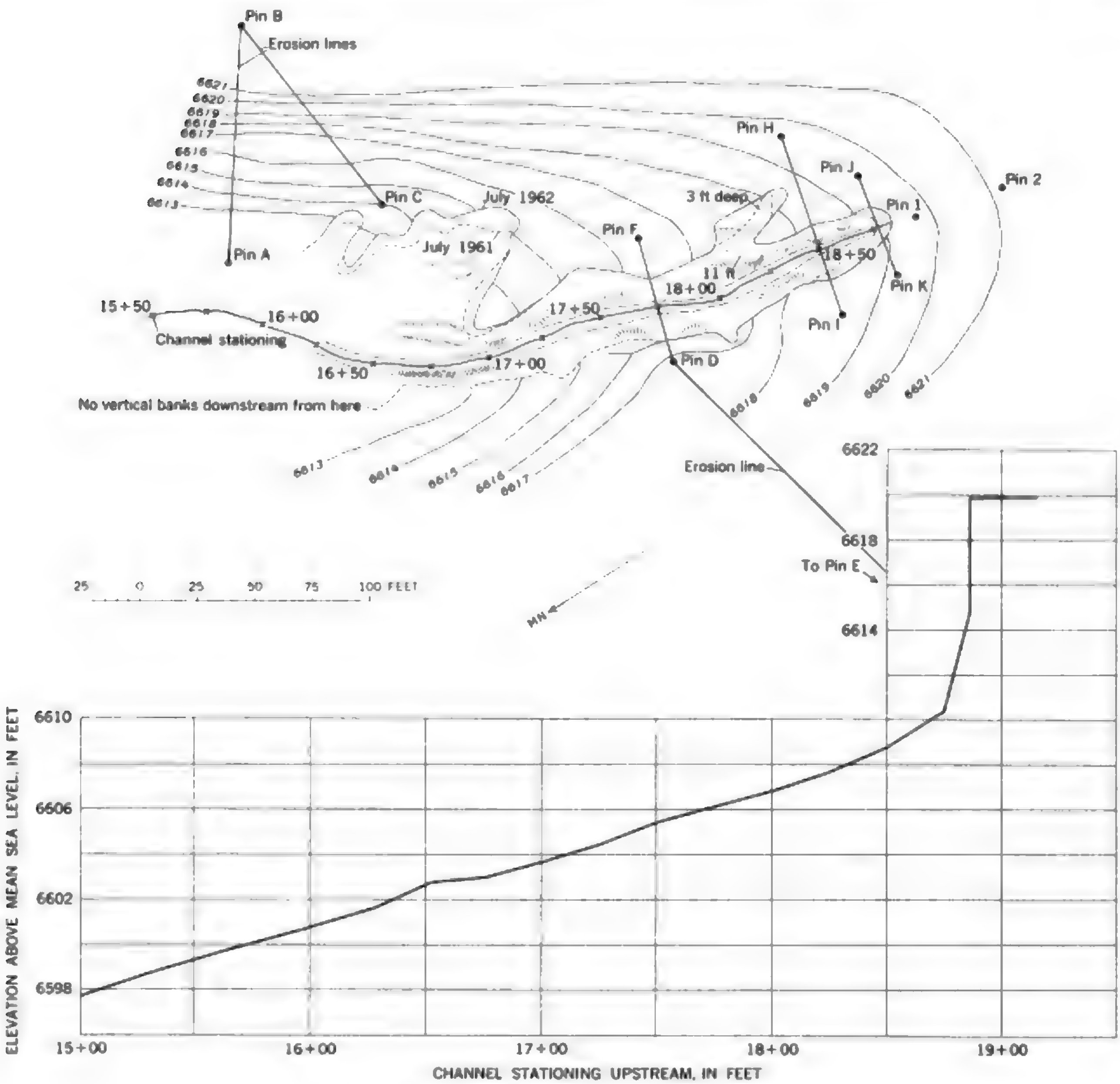

FIGURE 167.—Topographic map and profile of Coyote C. Arroyo headcut.

The planetable map of 1962 is shown in figure 167 and, as a dashed line, the outline of the headcut as it appeared the previous year. Most of the headcut has retreated some and the greatest amount of retreat is recorded in extremities which extend either up the primary direction of the channel or in the direction of tributary swales. Measurements from the pins to the cut bank indicate a lateral retreat of 0.4 ft per yr and a retreat at the most headward extreme of 2.6 ft per yr. Thus, while the map of figure 167 provides some insights about headcut retreat, mapping is not sufficiently accurate to delineate the relatively minute retreats which are occurring.

The initial 400 feet of channel profile is shown below the headcut map to provide an indication of channel slope and the sloughed material associated with the headcut. The average slope of the channel here is 0.03 ft per ft compared to 0.02 ft per ft in the channel 1,000 feet downstream. The volume of material contributed to the stream by the enlargement of this headcut has

Digitized by Google

been computed to be 1,650 cu ft per yr for the period 1961–64.

MOVEMENT OF LARGE PARTICLES IN HEADWATER RILLS

SLOPEWASH TRIBUTARY

Two of the channels that have been studied in detail with respect to movement of individual rocks, Green Rock Gulch and Little Green Rock Gulch, are shown in figure 144. The former is also illustrated in figure 168. Starting at or near the mouth of these two channels individual rocks, each 3–6 inches in diameter, were completely painted. They were then replaced in the rills at measured distances from the mouth. This distance, in feet, was painted on each rock for identification and the total number of rocks at each distance was recorded. A total of 250 rocks was painted in Green Rock Gulch and placed at distances of 1–47 feet upstream of the mouth. Forty rocks were painted in Little Green Rock Gulch and placed from 21 to 36 feet upstream of the mouth.

The initial placement was in 1959 and resurveys were made annually. At the time of the resurveys the movements of the individual rocks were easily discernible because identification numbers on the painted rocks were no longer in consecutive order nor at the distance corresponding to their number.

Although the number of rocks moving has not been large, the recovery percentage is high. In 1964, 5 years after placement, 88 and 78 percent respectively of the rocks in the two gulches are still accounted for. Missing rocks are usually those that moved but later were obscured by either vegetation or a sand covering, that is, they were not buried in place. This is suggested by some of the rocks in the main study which were reported as missing in a given flow but were found after a subsequent flow.

FIGURE 168.—Green Rock Gulch, a tributary to Slopewash Tributary. Rocks wash into this minor rill from the lag gravel covering some of the hillslopes seen in the background.

The data have not been sufficient to describe a trend in movement. Both the upper and the lower halves of the reach on Green Rock Gulch show about 25 percent of their rocks moving or missing. Because of the large number of rocks not moving and the large variability in distance of those moving, the data are perhaps not yet meaningful. However, the longest distances recorded to date are of rocks originally placed in the lower 10 feet of channel and these have moved as much as 540 feet.

GUNSHOT ARROYO

Gunshot Arroyo is the first tributary entering Arroyo de los Frijoles below the sweeping S-curve half-mile downstream of the Main Project Reach. Measurements in Gunshot Arroyo include the tracing of large particle movements in the channel bed and on a steep sloping bank of the channel, the retreat of a knickpoint formed in the channel by an outcropping of semiresistant Santa Fe formation, channel enlargement, and degradation-aggradation studies.

In 1960 the initial survey and installations included the selection, painting, and replacing of rocks in the channel. The rocks, ranging in diameter from about 3 to 10 inches, were completely painted and numbered with the distance in feet corresponding to the initial position upstream of the junction with Arroyo de los Frijoles. The largest number is 880 and the watershed divide is located at station 1,150 feet. The rocks were placed at 10-foot intervals.

In 1962 a complete resurvey was made of the existing measurements and a longitudinal-profile survey was run from 150 feet below the mouth of the arroyo to and over the watershed divide. This profile is shown on figure 169. No vertical or cut banks were observed above station 620 feet and the channel disappeared above station 1,050 feet.

Superposed on the profile of figure 169 is a schematic illustration of the rock movements as recorded in 1962. Each rock position is identified as to moving, missing, or stationary. For those rocks which were found, the distance moved in feet is indicated by the number above the original position of the rock.

Most rocks below station 750 feet moved. Downstream from station 750 feet to station 450 feet, most of the moving rocks were found. Below station 450 feet a large percentage of the rocks were reported missing. The upper of the two mentioned subreaches has a gravel bed and the lower a sand bed. In the lower reaches of the channel most rocks that had moved were found partly buried in sand and, with few exceptions, those which had traversed the length of the tributary

Digitized by Google

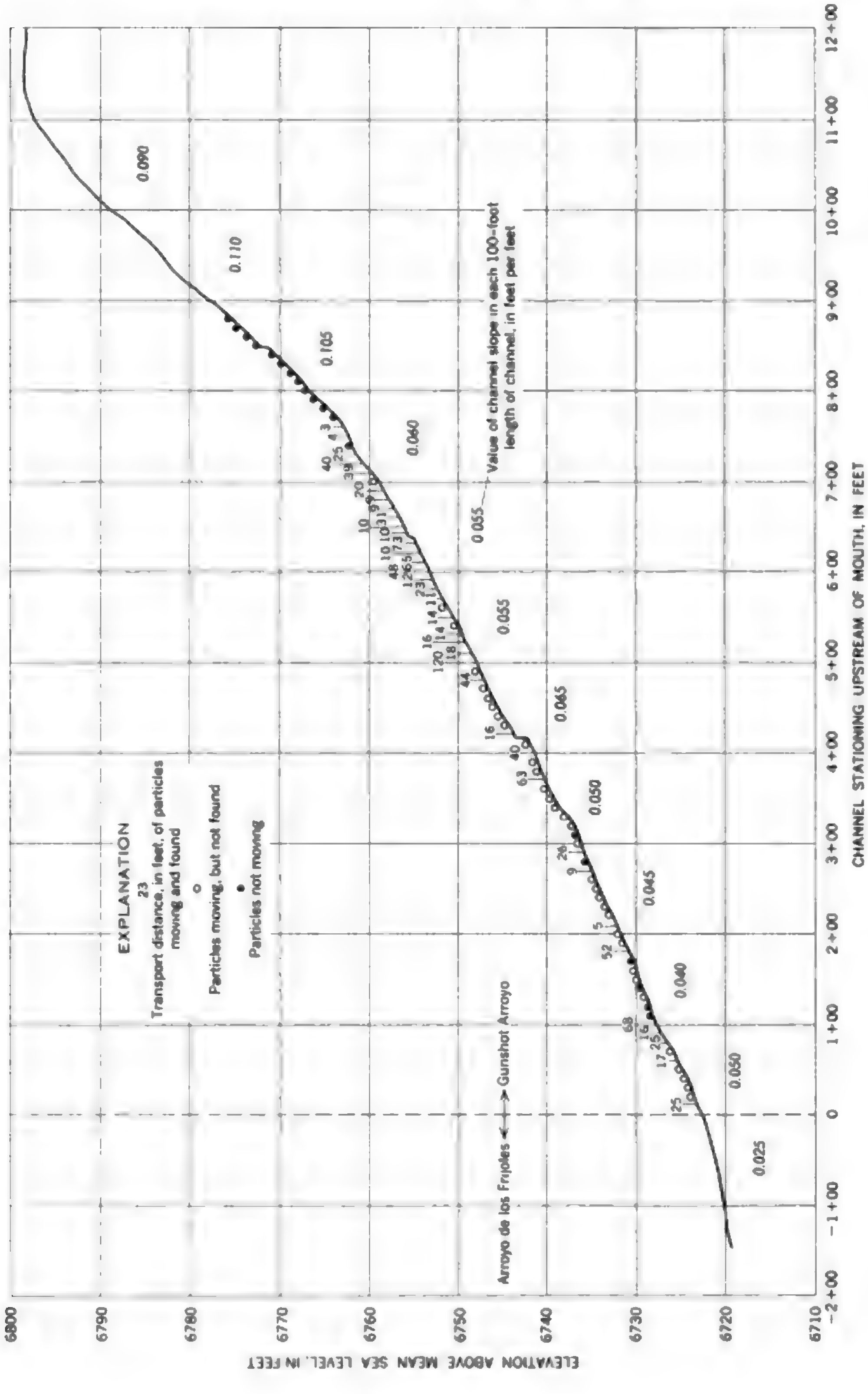

FIGURE 169.—Profile of Gunshot Arroyo illustrating movement of coarse particles, 1960–62. Average B- or intermediate-axis diameter of particles is 130 mm.

and into the channel of Arroyo de los Frijoles were not found. The rocks above station 750 feet were consistent in that none had moved despite the fact that these were on the steepest slopes.

At the time of the 1962 survey the rocks moving and found averaged a transport distance of 39 feet; the maximum distance recorded was 120 feet. If consideration were given to the missing rocks, which probably were transported entirely out of the tributary, these distances would be considerably increased. Of the rocks originally placed, 37 percent were missing and 22 percent had not moved.

After the 1962 survey the rocks found were returned to their original position, but the missing positions were not filled. Resurveys in 1963 and 1964 of these remaining rocks recovered only one rock reported missing in 1962. This adds credence to the probability that missing rocks were transported entirely out of the tributary.

In 1963 the number of total missing rocks increased to 82 per cent, and all but 2 of the 55 rocks remaining after the 1962 survey had moved. Of these 14 were found and averaged a transport distance of 218 feet and a maximum distance of 930 feet. The large increase in percentage of missing rocks is probably attributable to the storm which caused a 1,300 cfs flow at Main Project and which occurred between the surveys of 1962 and 1963. Most rocks remaining for the latter survey were from upstream positions and had longer distances to travel before being exposed to the greater chance of loss in the main channel. By 1964 the number of missing rocks had increased to 85 per cent.

Painted rocks on a typical steep slope (approximately 45°) at station 190 feet were resurveyed in 1962, 1963, and 1964. The rocks painted were native to the slope and generally ranged in intermediate-axis diameter from 1 to 3 inches. On an uncounted number of rocks painted in 1960, 175 remained in 1962 and 164 remained in 1964. Thus, in the last 2 years only 6 per cent have moved off the slope and have become lost in the channel. Between annual surveys an average of only 3 per cent of the rocks (excluding those missing) moved over one foot, but a gradual slumping was noticeable. In 1964, 118 rocks (72 per cent) had slumped downhill a measurable amount, and this slumping averaged 0.6 foot for the 4-year period. It appears that the effects of gravity, aided by such processes as freeze-thaw and wet-dry, have an appreciable influence on coarse particles on steep slopes.

The monumented knickpoint in the Santa Fe formation at station 417 feet averages about 1.3 feet in height, and between 1960 and 1964 no measurable amount of upstream retreat was recorded.

Scour chains placed in the arroyo bed at station 25 feet, 230 feet, and 468 feet indicate the channel is aggrading at a rate of 0.06 ft per yr for the 2-year period 1962–64. Although this is a short-term record, the value is in agreement with that of the main arroyo, 0.04 ft per yr.

MORNING WALK WASH

In 1961, painted rocks were placed at 10-foot intervals in the channel of Morning Walk Wash near Las Dos (fig. 139). The painted rocks ranged in diameter from 3 to 5 inches, the average rock size native to the gullies. A total of 166 such rocks were placed along the thalwegs of the two main channels and a smaller rill draining the hillslope.

A resurvey in 1962 indicated a very large percentage of the rocks had moved. Table 5 is a condensed presentation of the rock movements between 1961 and 1962. For example, in the north gully three times as many rocks had moved in the lower reaches than in the upper reaches and the rocks in the lower reaches tended to move greater distances. Many of the rocks were found in a fan deposit at the mouth of the channel.

As in Gunshot Arroyo the rocks found during the

TABLE 5.—*Summary of particle movement Morning Walk Wash, 1961–62*
[L, lower reach; U, upper reach]

Particles	South gully			South rill	North gully		
	L	U	Total or average		L	U	Total or average
Total originally placed	44	43	87	12	34	33	67
Percent moving, on basis of:							
Total found	41	40	40	25	77	12	45
Total found plus total missing	93	63	78	25	91	30	61
Percent not moving or not found	48	77	62	100			
Distance moved, in feet, on basis of total found:							
Average	177	339	258	211			
Maximum	473	723		[1] 613			

[1] Lower reach.

survey were returned to their original position to await movement during subsequent flows, but the missing positions were not filled with new rocks. Thus data after 1962 became less meaningful except to determine the depletion rate of the originally placed rocks. Data for one of the painted rock experiments in headwater channels are included in summary of data J for 1961–64.

The condition of the paint on the rocks found indicates that the rocks are transported with only little abrasive action, that is, they are not broken up in place and removed as smaller particles, this despite the rolling and tumbling over other rocks in their trip downstream.

Two monumented cross sections of the channels were installed in 1961 and resurveyed yearly to 1964. During this period the upper section, 170 feet above channel mouth, showed no significant changes, while the lower section at the mouth showed about 0.2 foot of deposition in each channel bed. This value is consistent with other observations for channel aggradation.

SEDIMENTATION IN CHANNELS AND RESERVOIRS

About 1937, at the lower end of Coyote C. Arroyo some 1,900 feet downstream of the present position of the largest headcut, an earth dam was constructed across the arroyo. In 1961 the reservoir behind the dam was topographically mapped by planetable, and it was planned that resurveys would allow the determination of the amount of fill accumulating within the reservoir. Contours of equal deposition occurring during 1961–62, as well as original topography, are shown in figure 170.

Computations determining the volume amount of sediment collected in the reservoir during the period 1961–64 are shown in table 6. This amount totals 6,245 cu ft or 2,082 cu ft per yr. If the average rate of erosion shown by the erosion nails is assumed as a basin-wide average, the reservoir is shown to collect only about 5 percent of the total eroded sediment. However, the computation of this percentage may be of only academic interest because, as was remarked previously, values of the erosion rate computed from the pins installed in this basin are believed to be too large for the basin as a whole. Most of the sedimentation was in the year 1961–62.

The field-sketch map of figure 145 shows six channel cross sections at various distances up the arroyo. These cross sections were first surveyed in 1961; they have

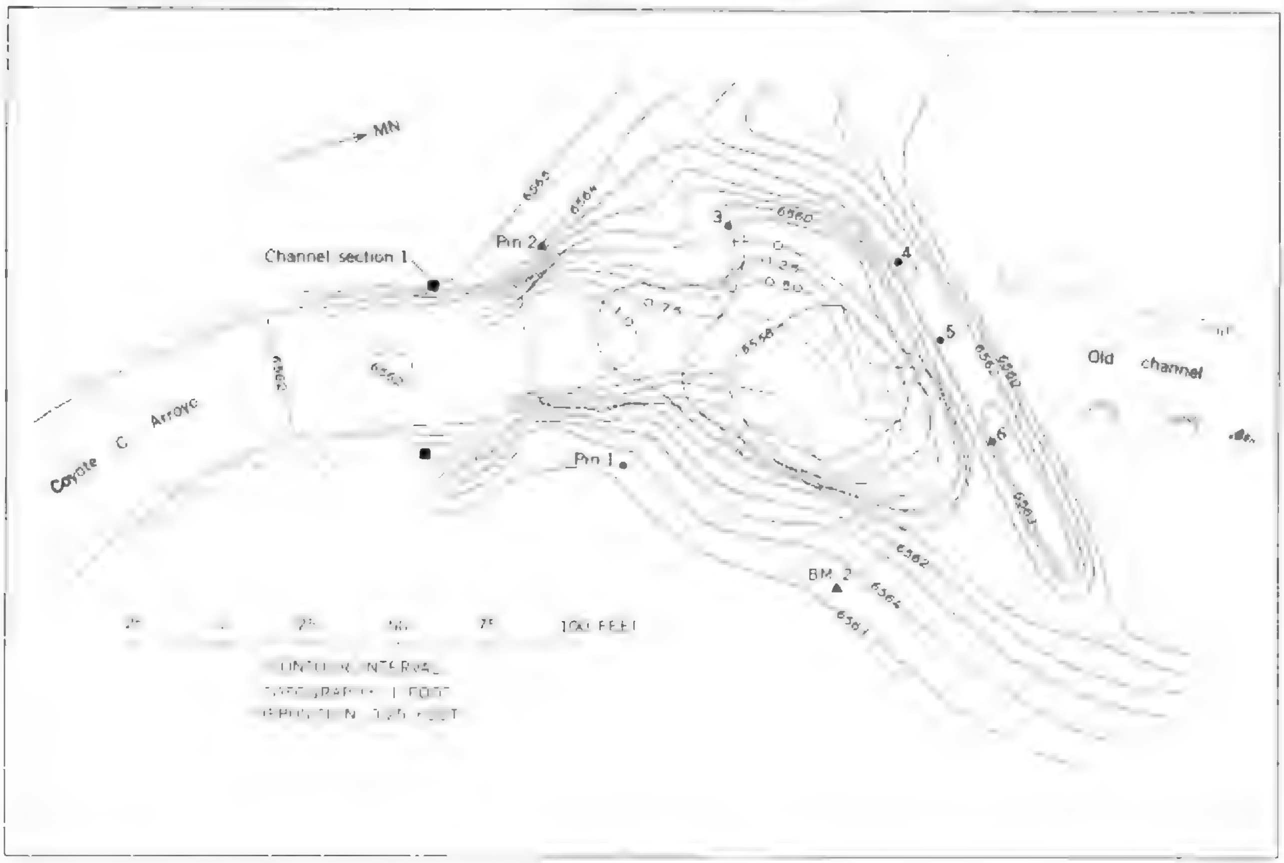

FIGURE 170.—Topography of dam and reservoir on Coyote C. Arroyo and contours of deposition, 1961–62.

Digitized by Google

TABLE 6.—*Observed sedimentation in reservoir behind dam on Coyote C. Arroyo, 1961–64*

Cross section	End pins	Decrease in area of cross section due to deposition (sq ft)			Effective width of section (ft)	Average depth of deposition (ft)			Effective area of reservoir (sq ft)	Amount of sedimentation [1] (cu ft)		
		1961–62	1961–63	1961–64		1961–62	1961–63	1961–64		1961–62	1961–63	1961–64
1	BM 2-6	10.0	10.0	10.4	30	0.33	0.33	0.35	1,000	330	330	350
2	BM 2-5	28.3	20.2	24.3	43	.54	.61	.56	825	445	505	460
3	BM 2-4	29.0	35.0	39.0	53	.55	.72	.74	900	500	650	665
4	1-5	30.5	50.5	55.5	55	.55	.92	1.01	913	505	840	920
5	1-4	34.0	68.0	73.0	60	.57	1.13	1.22	1,436	820	1,620	1,750
6	1-3	15.5	8.5	14.5	35	.44	.24	.42	1,850	815	445	775
7	1-2	51.5	44.5	39.5	40	1.29	1.11	.99	1,336	1,725	1,485	1,325
	Total									5,140	5,875	6,245
	Rate—cu ft per yr									5,140	2,938	2,082

[1] Amount of sediment contributed from basin (40.8 acres):

$$\frac{2082}{40.8 \times 43{,}560} = 0.0012 \text{ ft per yr}$$

been resurveyed yearly to 1964 and allow computation of deposition in the channel. Stationing and channel changes are summarized in table 7. The volume accumulations of sediment in the 1,435-foot reach included by the sections are also shown in the table. These data indicate that 3,192 cu ft per yr of sediment is deposited in this reach, which corresponds to channel aggradation of about 0.10 ft per yr. This value represents about 8 percent of the total eroded sediment indicated by the erosion pins.

The percentages of total eroded sediment accounted for by the surveys in the reservoir and in the lower reach of channel are not total reservoir and channel storage of sediment for the entire basin. Our studies have indicated that even headwater rills are aggrading, thus there is much more channel length in the basin available for sedimentation processes. Although the surveyed reservoir is the only man-built barrier, other natural reservoirs are also available. The discontinuous nature of the channels provides many alluvial fans and flats which may be considered as natural reservoirs; at least, sedimentation rather than erosion is occurring in these areas.

ANALYSIS OF SEDIMENT BUDGET

To account for sediment volumes contributed by erosion and to compile a balance sheet is not easy, because of the variance within the measurement data. With regard to what appears to be the main process contributing debris (sheet or surface erosion), the problem is how to average the rates observed by the nail and washer data at various localities and derive a figure applicable to the whole contributing area. To use the data on volumes contributed by headcuts presents little problem because there are only a few headcuts per square mile in the study area. Bank cutting and consequent channel enlargement is not an important source of sediment, as indicated by measured cross sections of channels. The data on mass-movement pins present a special problem because, lacking knowledge of certain details of the

TABLE 7.—*Observed rates of channel changes in Coyote C. Arroyo*

Section	Channel stationing (ft)	Change in channel shape (+, deposition; −, scour; (sq ft)			Length of reach (ft)	Volume of sediment [1] (cu ft)		
		1961–62	1961–63	1961–64		1961–62	1961–63	1961–64
1	30	+30.75	+29.00	+28.25	120	3,690	3,480	3,390
2	210	+8.75	+10.00	+11.00	165	1,445	2,100	2,310
3	365	+16.75	+14.10	+14.75	225	3,770	3,180	3,320
4	650	−2.70	−.50	.00	290	−785	−145	0
5	955	+.70	+.80	+1.10	395	265	315	435
6	1,435	−1.30	−.25	+.50	240	−310	−60	120
Total						8,075	8,870	9,575
Rate—cu ft per yr						8,075	4,435	3,192

[1] Amount of sediment contributed from basin (40.8 acres):

$$\frac{3192}{40.8 \times 43{,}560} = 0.0018 \text{ ft per yr}$$

Digitized by Google

process, the total area subject to effective sediment contribution from this source is difficult to estimate.

No great problem is presented by channel aggradation, for these measurements are far more complete than for other processes. Two important sources of possible error remain—the unmeasured volume of debris passing out of the basin as bedload or suspended load, and the trap efficiency of the reservoirs.

These difficulties face any investigator who is constructing a sediment budget. No perfect solution is available, but at least the assumptions made in the computations can be stated and the implications of the assumptions can be analysed. Although the quantities are only roughly approximate, a summary of debris inflow, outflow, and storage is attempted. Table 8 summarizes the average values of the measurement quantities. These values are arithmetic averages of individual readings taken over the period of measurement at the respective measurement points. Because comparison of mean and median values shows no great disparity, we used mean values exclusively in this report.

The main assumptions enter the computations in progressing from average-measurement data, table 8, to computations of average rates of erosion and deposition summarized in table 9.

The main source of data on sheet erosion is the pin-and-washer installations. More variance is noted between successive years than among the respective pins in the same year. Within a given group of nails the mean rate of erosion for the 3-year period was plotted by individual pins against the local ground surface slope at the pin, but no correlation was found. This lack of correlation is attributed to the fact that each group of nails applied to only a small range of slope values. Some influence of slope probably can be seen in the comparison of values of surface erosion in table 8. For example, the average land slope on the erosion plot of Slopewash Tributary is less than on the nail lines of Coyote C., and the corresponding net erosion rates are 0.008 and 0.024 ft per yr respectively.

But it appeared unjustifiable to correlate these net erosion values for different localities merely with slope because many other factors probably are also operative. The significance could not be tested statistically with only seven localities.

The average value of surface erosion for the whole basin (0.015 ft per yr; see table 9) represents our best judgment of the order of magnitude. This value is in agreement with the result obtained by equal weighting of number of pins and number of years of data, 0.0145.

Two values of volume eroded by headcut retreat are available. Approximately the average of these two was

TABLE 8.—*Data on measured rates of erosion and deposition*

[SWT, Slopewash Tributary]

Erosion	
Surface erosion:	
Erosion plot, SWT:	
Pins	61
Years	5
Net erosion—ft per yr	0.008
Slope-retreat pins, SWT:	
Pins	57
Years	5
Net erosion—ft per yr	0.014
Nail lines, Coyote C. Arroyo:	
Pins	65
Years	3
Net erosion—ft per yr	0.024
Nail sections, bank, SWT:	
Pins	20
Years	5
Net erosion—ft per yr	0.019
Mass-movement pins, SWT:	
Pins	15
Years	5
Net erosion—ft per yr	0.025
Iron pins, SWT:	
Pins	19
Years	6
Net erosion—ft per yr	0.007
Chain section pins, on banks, SWT:	
Pins	8
Years	6
Net erosion—ft per yr	0.011
Gully erosion:	
Coyote headcut:	
Years	3
Retreat (ft per yr):	
Laterally	0.4
Headward	2.6
Volume of material eroded—cu ft per yr	1,650
Fence line headcut:	
Years	4
Retreat (ft per yr):	
Laterally	0.15
Headward	1.5
Volume of material eroded—cu ft per yr	500
Mass movement (soil creep):	
Slopewash Tributary:	
Pins	15
Years	5
Downhill movement at ground surface—in. per yr	0.205
Volume of material moved—cu ft per mile of slope base per yr	32
Coyote C. Basin:	
Pins	12
Years	3
Downhill movement at ground surface—in. per yr	0.202
Volume of material moved—cu ft per mile of slope base per yr	25
Movement of individual rocks:	
Morning Walk Tributary:	
South gully and rill:	
Rocks	99
Years	3
Rocks moved—percent	75
Average distance moved—ft per yr	190

Digitized by Google

TABLE 8.—*Data on measured rates of erosion and deposition*—Continued

Erosion—Continued

Movement of individual rocks—Continued	
Morning Walk Tributary—Continued	
North Gully:	
Rocks	67
Years	3
Rocks moved—percent	67
Average distance moved—ft per yr	96
Gunshot Arroyo:	
Rocks	88
Years	4
Rocks moved—percent	100
Average distance moved—ft per yr	93
Green Rock Gulch:	
Rocks	250
Years	5
Rocks moved—percent	23
Average distance moved—ft per yr	59
Little Green Rock Gulch:	
Rocks	40
Years	5
Rocks moved—percent	32
Average distance moved—ft per yr	1

Deposition

Aggradation of channels:	
Slopewash Tributary:	
Nail section:	
Number of chains, pins or sections	10
Years	5
Average net aggradation—ft per yr	0.033
Pins at chain section:	
Number of chains, pins, or sections	2
Years	6
Average net aggradation—ft per yr	0.003
Arroyo Frijoles, mainstem: including North Branch:	
Number of chains, pins, or sections	90
Years	6
Average net aggradation—ft per yr	0.040
Coyote C. Arroyo:	
Number of chains, pins, or sections	6
Years	3
Average net aggradation—ft per yr	0.100
Gunshot Arroyo:	
Number of chains, pins, or sections	3
Years	2
Average net aggradation—ft per yr	0.060
Filling of small reservoirs:	
Coyote C. Arroyo Dam:	
Drainage area—sq mile	0.064
Years	3
Volume deposition—cu ft	6,245
Sediment collected—ton per sq mile per yr	1,633
Big Sweat Dam:	
Drainage area—sq mile	0.0060
Years	1.2
Volume deposition—cu ft	95.3
Sediment collected—ton per sq mile per yr	660

applied to the number of headcuts per square mile estimated from detailed knowledge of the area.

Mass-movement pins are installed on sloping gully walls which are steeper than the hillslopes in general. Though when the measurements were begun we had not expected downhill creep to be of significance in a semiarid climate, our observations and those of others (for summary see Leopold and others, 1964, p. 349–353) indicate that it is a process which cannot be disregarded. Mass wasting should deliver debris to the rills and channels in proportion to the rate of downhill creep and to the total length of channel in a given area. A drainage density was computed by using a Horton analysis of the number and lengths of channels. In a square mile the order of the largest channel including rills is seven. The number and lengths of various orders are as follows:

Order	Number	Length (miles)	Adjustment to channel segments		
			Length (mile)	Number	Number × length (miles)
7	1	1.2	0.80	1	0.8
6	2.5	.70	.48	4.5	2.2
5	11	.22	.11	14.5	1.6
4	45	.11	.05	56	2.8
3	140	.05	.027	185	5.0
2	400	.025	.013	540	7.0
1	1,200	.01	.01	1,600	16.0
Total					35.6

By this estimate there are about 35 miles of channel and rill in a square mile area, and because there are two banks of a channel, the length of channel boundary possibly subject to debris production by creep is some 70 miles. Using an average of 28 cu ft per mile of slope-base per year,

$$28 \times 70 = 1{,}960 \text{ cu ft per yr per sq mi},$$

which at 100 lbs per cu ft is 98 tons per sq mi per yr.

Movement of individual rocks was not included as a separate item of contribution to sediment production.

TABLE 9.—*Average rates of erosion and deposition*

Erosion

Surface erosion:	
Average rate—ft. per yr	0.015
Percentage of total basin contributing	65
Erosion rate—tons per sq mi per yr	13,600
Gully erosion:	
Average volume per headcut—cu ft per yr	1,000
Headcuts per sq mi	4
Erosion rate—tons per sq mi per yr	200
Mass movement:	
Average downhill rate at ground surface—in. per yr	0.20
Length of channel affected—mi per sq mi	35.6
Average volume eroded—cu ft per sq mi per yr	1,960
Total volume—tons per sq mi per yr	98
Total erosion—tons per sq mi per yr	13,900

Deposition

Aggradation of channels:	
Channel area—sq ft per sq mi	579×10^3
Average rate of deposition—ft per yr	0.05
Deposition—tons per sq mi per yr	1,440
Collected in dams—tons per sq mi per yr	1,633
Total deposition—tons per sq mi per yr	3,073

Digitized by Google

Depositional data consisted of channel aggradation which was computed into tons per square mile as follows:

Order	Segment length (miles)	Width (ft)	Channel area (sq ft)
7	0.5	28	75,000
6	2.2	16	186,000
5	1.6	8	67,000
4	3.3	3.5	61,000
3	5.0	2.5	66,000
2	7.0	1.3	48,000
1	16.0	.9	76,000
Total			579,000

Then 579×10^3 sq ft of channel area aggrading at 0.05 ft per yr is 28,900 cu ft; at 100 pounds it equals 1,440 tons per sq mi per yr.

The collection of sediment behind the dam in Coyote C. Arroyo gave a figure of 1,633 tons per sq mi per yr. The production and trapping of sediment may be summarized as follows:

	Total sediment (tons per sq mi per yr)	*Sediment production (percent)*
Surface erosion	13,600	97.8
Gully erosion	200	1.4
Mass movement	98	.7
Total	13,900	100±
Deposition in channels	1,440	10
Trapped in reservoir	1,633	12
Total	3,073	22±

By far the largest contribution of sediment is by sheet erosion. Channel deposition is only about half of the total sediment trapped, the latter being only about one-quarter of that produced. It is recognized that if the budget were correct and the reservoir trap efficiency were 100 percent, the total of deposition in channels and trapped in the reservoir would equal sediment production. It is our opinion that the sediment moved as sheet erosion does not all get into the channel, but is temporarily stored in thin deposits widely dispersed over the colluvial area, and that furthermore, there is a very low trap efficiency to the reservoir.

Other measurements of sediment accumulation in western United States give values of 1,200 to 2,400 tons per sq mi per yr (Brown, 1945).

To our knowledge, of the published reports on sediment yield from semiarid drainage basins, by far the most excellent is that of Hadley and Schumm (1961), who measured, among other things, sediment accumulation in a large number of stock ponds and small reservoirs. These data were studied in relation to geologic formation, runoff, and various geomorphic characteristics of basins. Their data are far more comprehensive than ours insofar as sediment accumulation in reservoirs is concerned. The only unique feature of the present data is that we attempt to assess the relative importance of different processes of sediment production.

Despite their deficiencies, our data bear comparison with the more extensive values published by Hadley and Schumm, as in the following:

Sediment accumulation:	*Acre ft per sq mi per yr*	*Tons per sq mi per yr*[1]
Coyote C. Arroyo (0.064 sq mi) accumulation in reservoir and channel	1.41	3,073
Average curve for all lithologies, for 0.06 sq mi area (Hadley and Schumm)	1.8	3,930

[1] Based on 100 lbs per cu ft.

For small basins the sediment accumulation observed by us in New Mexico is of the same order of magnitude as in basins of similar size in Wyoming underlain by shale or other lithologies high in silt content. Hadley and Schumm (fig. 30, p. 173) showed that for the Cheyenne Basin sediment accumulation was related to relief ratio (basin relief divided by basin length). The average relief ratio for our Coyote C. and Slopewash tributaries is 0.59. Entering this value in the Hadley-Schumm curve for all lithologies, the estimated value of sediment accumulation is 2.4 acre ft per sq mi per yr, and in the curve of those authors applicable to Fort Union formation only, the value is about 2.5. These values are slightly higher than the 1.41 observed in Coyote C. Arroyo but still of the right order of magnitude.

The finding of Hadley and Schumm (fig. 26, p. 163) that sediment accumulation per unit area of basin decreases rapidly with increasing drainage area is in keeping with our result that sheet erosion basin-wide estimated from erosion pins gives a value of sediment production about 4.5 times larger than can be accounted for in channel aggradation and reservoir accumulation. This feature is probably related in part to the same cause postulated by those authors: absorption of water in the dry channel beds below areas affected by local storms. But the fact remains that even in our detailed study of deposition, sediment spread thinly over colluvial areas does not show up in measurement data.

Another interesting comparison is with data on sediment production by dry sliding of debris on the steep

Digitized by Google

slopes of southern California. Krammes (1960) measured debris in metal troughs laid on contour in burned and unburned areas in San Dimas Experimental Forest near Glendora. He found a sediment yield of 24.7 tons per acre per year (15,800 tons per sq mi per yr) after a brush fire, which compared with 2.69 (1,720 tons per sq mi per yr) before the fire had denuded the slopes. Of the total annual yield 89 percent of the debris was contributed during nonrain periods by dry sliding. The figure for prefire condition is about half the sediment yield observed by us in New Mexico, but the postfire figure is five times larger than our value.

Returning to the question posed earlier in this report, it appears that in semiarid areas of the type studied sheet erosion not only predominates as a sediment source but also seems quite capable of providing the sediment making up the bulk of alluvial fills during periods of aggradation. Indeed, the present channels are aggrading, and at 0.05 ft per yr the observed rate would eventuate in a fill as deep as the Coyote alluvium under the high terrace in 100–200 years. No doubt such a rate would not be sustained as an average for so long a period because in a century there would be some years, no doubt, during which net degradation would occur.

Nonetheless, the present processes and their rates appear quite capable of resulting in deposition of alluvial fills comparable to those of past periods which filled major valleys. The present is, then, a reasonable picture of conditions during which valley aggradation occurred in post-Pleistocene time.

The importance of sheet erosion makes it quite possible that aggradation can occur in tributaries, even in small channels only a few hundred feet from the watershed divide. Gully or rill erosion was probably insignificant or absent during the deposition of the principal alluvial fills in these valleys. Gully erosion assumes its important role during periods of valley trenching or arroyo cutting as was observed in the post-1880 period.

CLIMATOLOGICAL OBSERVATIONS DURING AGGRADATION

From the archeologic materials and a C^{14} date, it is computed that the upper part of the Tesuque formation accumulated in the Tesuque Valley, a few miles from our study area, at an average rate of 104–156 yr per ft (Miller and Wendorf, 1958, p. 190). During the period 1958–64 we observed an average rate of channel bed change that would result in aggradation at the rate of about 25 yr per ft. The present landscape is similar to that under conditions which probably prevailed in the same area, let us say, in the first centuries of the Christian era. But the land at present has hardly begun to recover from widespread devastation of the overgrazing in the late 19th century. The combination of a grazed range and the present climatic swing provides comparable rainfall-runoff conditions to those caused by a somewhat more unfavorable climate but uncomplicated by the effects of grazing animals.

What are the salient aspects of climate in relation to vegetation which create the difference between a period of aggradation and one of degradation in valleys? This question has merited the attention of many geomorphologists and has been answered tentatively in a variety of ways. Considerable evidence points to a coincidence of increasing aridity with degradation and increasing humidity with aggradation, but there are opposite views. Reaching a firm conclusion will have to await continuation of just the kinds of observations being here reported. Because we cannot hope to obtain a definitive answer to the question with 7 years of measurement, we are publishing our results principally to encourage others to join us in similar programs of simple measurement over a period of time in order that there will gradually become available concurrent data on rate of channel change, precipitation, and runoff.

The precipitation record for Santa Fe, N. Mex., is the longest in the United States. This record has been analysed in detail for its relation to the erosion problem (Leopold, 1951) and even then, 14 years ago, the difficulty of analysis lay not in the length of the precipitation record but in the lack of quantitative data on land erosion and channel changes. Our measurement data are not yet enough, but the nature of the problem can be more clearly seen than was possible without them, as will now be explained.

Leopold (1951) showed that the mean annual precipitation at Santa Fe did not significantly change between the first and second half of the century of record, but the frequency of daily rainfall amounts did change. In the present discussion we will review briefly that argument and bring the analysis up to date of the present writing, 1964.

Three graphs are presented in figure 171. Graph *A*, the annual march of yearly precipitation totals, is plotted without any averaging. Graphs *B* and *C* show that part of the annual amounts contributed in summer (July–Sept. incl.) months. The mean summer total of 6.06 inches consists mostly of thunderstorm rainfall which each season begins about July 15 after a relatively dry late spring and early summer. Thunderstorms are nearly daily occurrences in the nearby mountains from mid-July to early September. Graph *C* shows that part of the summer rainfall made up by rains totalling one inch or more in a day.

In the three parts of figure 171, trends in the 114 years are not easily discernible without the use of mov-

Digitized by Google

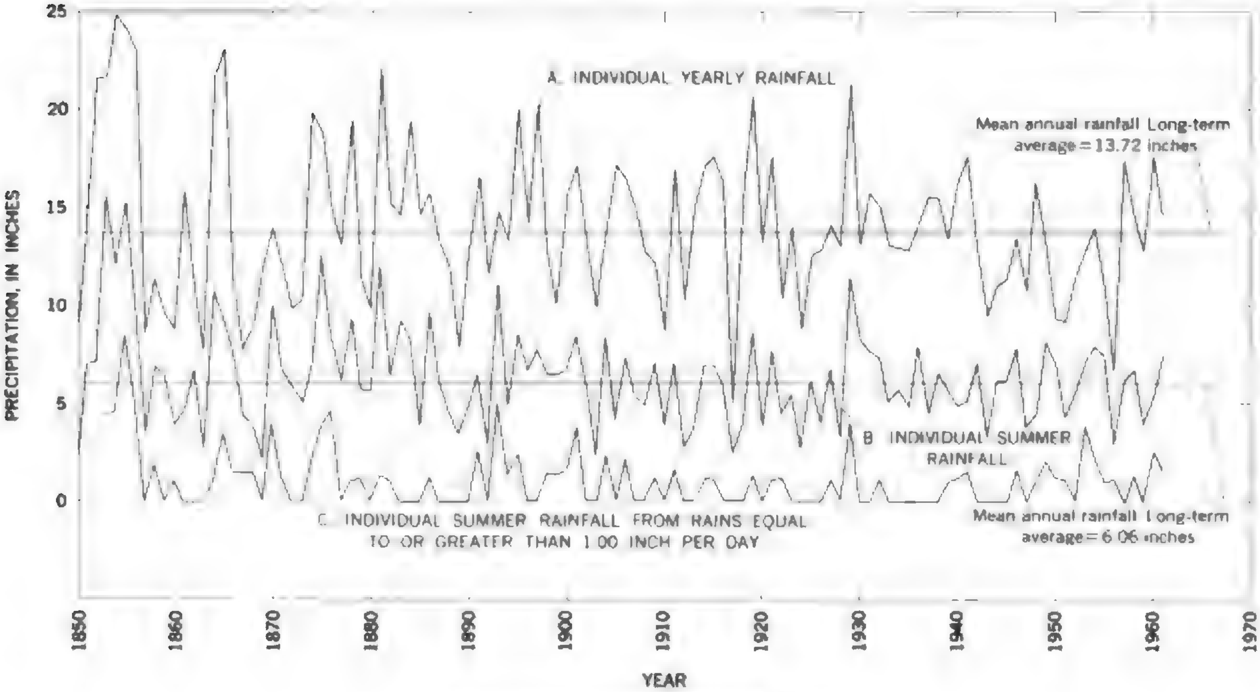

FIGURE 171.—Precipitation, Santa Fe, N. Mex.

ing averages. Inspection of the graphs reveals the dry period of the 1940's and early 1950's and the heavy summer rainfalls of the early 1850's.

Figures 172 and 173 break the precipitation record into its summer and nonsummer components, and then again into the number of rains of different categories of size of daily rainfalls. The secular change in number of nonsummer rains of less than 0.5 inch in a day so prominent in Leopold's analysis is obvious here, figure 173*B*. A more subdued but parallel trend is seen also

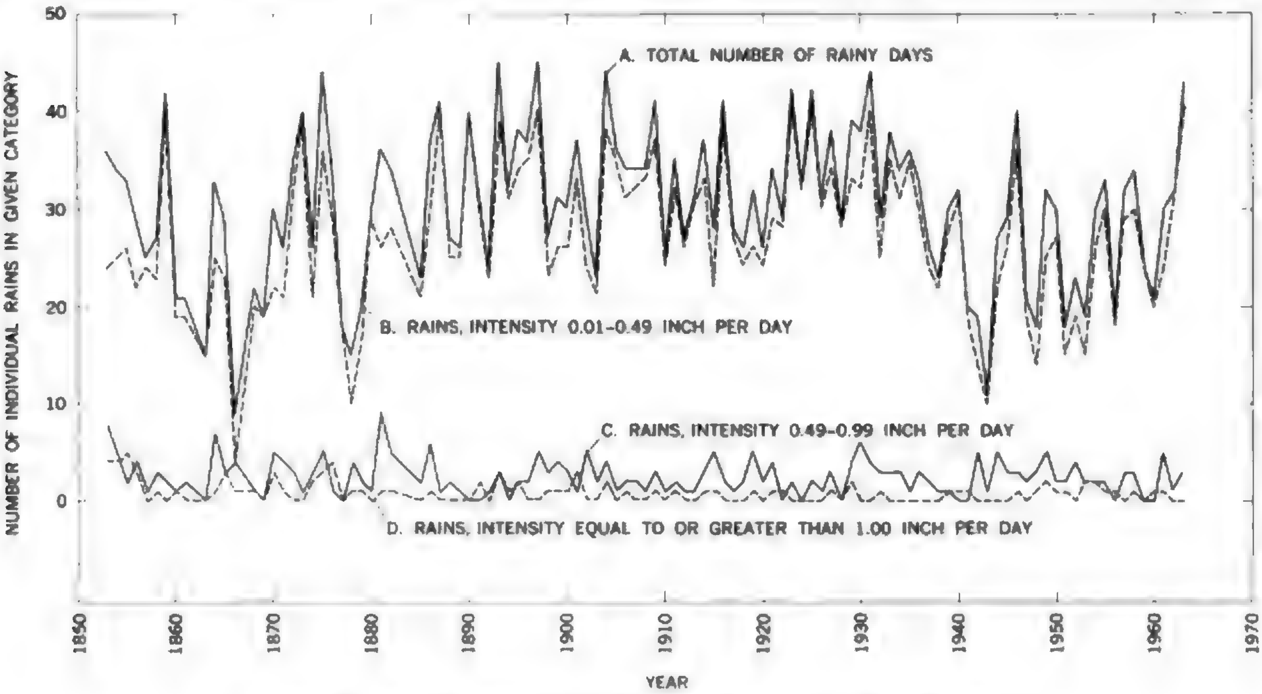

FIGURE 172.—Number of individual summer rains (July–Sept. incl.), Santa Fe, N. Mex.

Digitized by Google

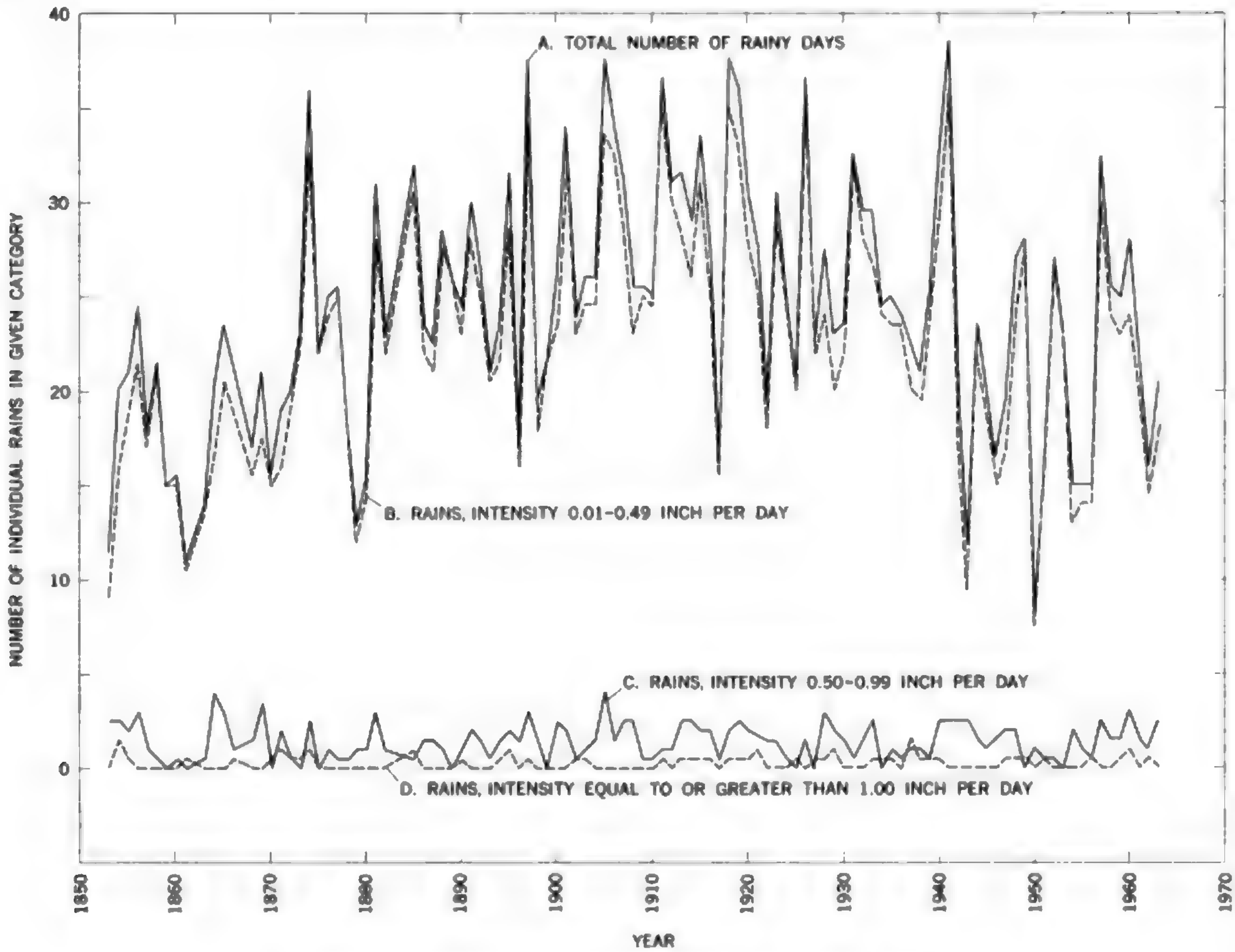

FIGURE 173.—Number of individual nonsummer rains, Santa Fe, N. Mex.

in the number of summer rains less than 0.5 inch per day. These secular changes leave the general impression that the last 25 years were more similar to the first 25 years of record than to the middle of the record period; that is, 1942–57 seems to resemble 1853–72.

This impression is strengthened by examination of figure 174 which shows the annual march of the average intensity of rain expressed as inches per day per rainy day, that is, the number of inches of rain in a year divided by the number of rainy days that year. The rains of the early and final part of the record were more intense than during the middle of the record.

Similar analysis led Leopold (1951) to argue that the period coincident with the advent of heaviest grazing, 1850–80, was characterized by a deficiency of the low-intensity rains which succor vegetation and by more than the average number of heavy rains which could act upon a weakened vegetal cover and promote erosion. This argument is a reasonable one, but to demonstrate its validity one needs concurrent and detailed data on erosion rates. Such concurrent data are now available for the 7-year period 1958–64, but this period includes years of both high and low intensity rainfall. The precipitation data are not clearly of the character that one could say unequivocally that erosion should be large or should be small. In short, the 7-year record is not long enough.

But the nature of the question ought to be clear from the data presented. Geomorphologists must make quantitative observations of erosion rates and channel changes over a long enough period to be clearly related to the concurrent precipitation record.

It is our hope that the presentation even of the short record now available will spur our colleagues to establish similar areas and continue simple measurements over a period of time so that those who follow us will have more to work with in analysis of this hydrologic and geomorphic problem.

Digitized by Google

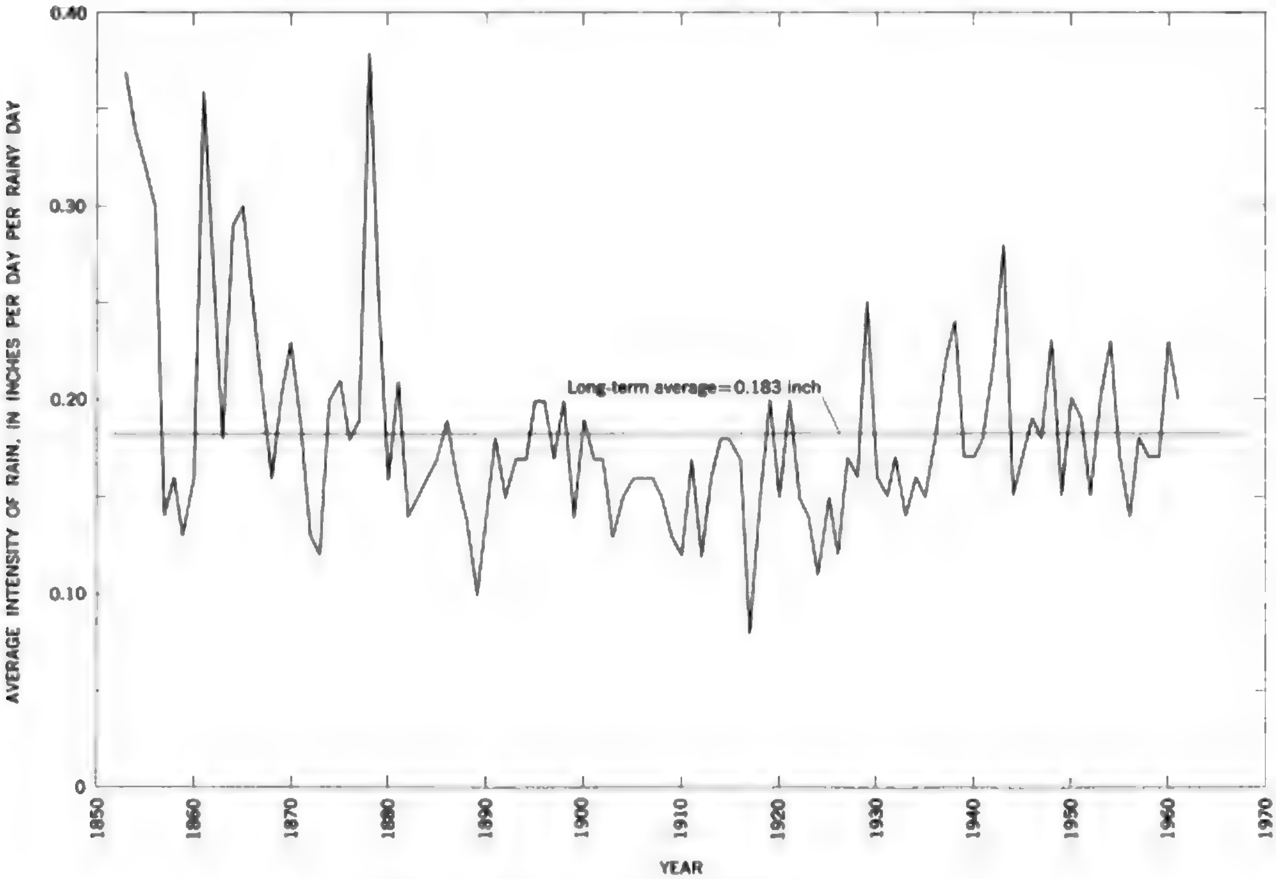

FIGURE 174.—Average annual intensity of rainfall, Santa Fe, N. Mex.

REFERENCES

Bagnold, R. A., 1956, The flow of cohesionless grains in fluids: Royal Soc. [London] Philos. Trans., ser., A no. 964, v. 249, p. 235–297.

Brown, C. B., 1945, Rates of sediment production in Southwestern United States: U.S. Soil Conserv. Service, SCS–TP–65, 40 p.

Emmett, W. W., and Leopold, L. B., 1964, Downstream Pattern of River-Bed Scour and Fill: Proc., Federal Inter-Agency Conf. on Sedimentation, Jackson, Miss.

Hadley, R. F., and Schumm, S. A., 1961, Hydrology of the upper Cheyenne River Basin: U.S. Geol. Survey Water-Supply Paper 1531–B, 198 p.

Krammes, J. S., 1960, Erosion from mountain side slopes after fire in southern California: U.S. Forest Service, Pacific S. W. Forest and Range Expt. Sta., Research Note 171.

Leopold, L. B., 1951, Rainfall frequency, an aspect of climatic variation: Am. Geophys. Union Trans., v. 32, no. 3, p. 347–357.

Leopold, L. B., and Miller, J. P., 1954, A post-glacial chronology for some alluvial valleys in Wyoming: U.S. Geol. Survey Water-Supply Paper 1261 89 p.

——— 1956 Ephemeral streams—hydraulic factors and their relation to the drainage net: U.S. Geol. Survey Prof. Paper 282–A, 37 p.

Leopold, L. B., Wolman, M. G., and Miller, J. P. 1964, Fluvial processes in geomorphology: San Francisco, W. H. Freeman Co., 522 p.

Miller, J. P., and Wendorf, F., 1958, Alluvial chronology of the Tesuque Valley, New Mexico: Jour. Geol., v. 66, no. 2, p. 177–194.

Miller, J. P., Montgomery A., and Sutherland, P. K., 1963, Geology of part of the Southern Sangre de Cristo Mountains, New Mexico: New Mex. Inst. of Mining and Tech. Mem. 11, 106 p.

Wolman, M. G., 1955, The natural channel of Brandywine Creek, Pennsylvania: U.S. Geol. Survey Prof. Paper 271, 56 p.

Digitized by Google

SUMMARY OF DATA

Digitized by Google

A.—*Summary of nonrecorded rain-gage data, Arroyo de los Frijoles, 1959–63*

[Date of observation may be several days after storm date. Record should not be considered as annual precipitation. Tr., trace amount. Gage locations shown on fig. 143]

Date of observation	Precipitation, in inches, at rain-gage—											
	1	2	3	4	5	6	7	8	9	10	11	12
8-07-59	0.80	1.13	0.80	0.80	0.88	1.06	0.80	1.20	1.20	0.80	1.00	[illegible]
8-19-59	[illegible]	.25	....	....	....	....	....	....	.20	....	....	[illegible]
8-24-59	.50	.28	.50	.35	.22	.36	....	....	.30	....	[illegible]	.65
10-[illegible]-59	1.00	....	1.46	1.40	....	[illegible]	[illegible]	....	....	1.32	[illegible]	1.26
6-10-60	.76	.70	.85	.80	.85	[illegible]	[illegible]	.90	1.06	.94	1.10	1.10
7-15-60	.50	.00	.80	.65	.35	Tr.	Tr.	Tr.	.00	.00	.00	1.02
8-05-60	.20	[illegible]	.80	....	.75	[illegible]	.65	[illegible]	.25	1.10	.35	.61
10-17-60	1.30	2.70	2.40	1.90	2.20	2.30	2.20	2.30	2.40	2.50	2.50	[illegible]
5-23-61	.00	[illegible]	[illegible]	.00	.00	.00	Tr.	.10	.30	.10	.20	....
6-16-61	[illegible]	[illegible]	.40	.30	[illegible]	.20	.20	.20	.20	.30	.20	....
6-19-61	[illegible]	.40	.00	.00	.00	[illegible]	Tr.	[illegible]	.10	.20	Tr.	.51
6-29-61	.10	.20	[illegible]	.30	[illegible]	[illegible]	[illegible]	.60	.30	.10	Tr.	.16
7-10-61	[illegible]	.10	.80	[illegible]	.40	.60	[illegible]	[illegible]	[illegible]	[illegible]	[illegible]	.87
8-14-61	[illegible]	1.30	1.30	1.00	1.10	1.00	[illegible]	1.20	1.30	1.40	[illegible]	1.23
8-23-61	1.10	1.10	1.15	1.10	.90	[illegible]	[illegible]	.90	.98	1.10	.55	1.13
9-19-61	[illegible]	.88	[illegible]	[illegible]	.87	1.00	.62	1.00	.79	.80	.75	1.35
7-02-62	....	.20	.70	....	....	....	....	....	....	....	....	.90
7-09-62	.20	.50	.35	1.30	[illegible]	.20	.20	.30	.20	....	.40	1.09
7-27-62	....	2.00	[illegible]	[illegible]	.30	[illegible]	.60	.70	1.00	1.10	.90	1.50
8-01-62	.40	[illegible]	1.10	....	.60	.00	.50	[illegible]	.20	.00	.00	.00
6-12-63	.79	....	1.20	.90	[illegible]	.75	.80	.72	.71	[illegible]	.50	[illegible]
6-17-63	.20	.35	....	[illegible]	[illegible]	.60	.75	.75	.60	.55	.55	.35
7-10-63	Tr.	....	.02	Tr.	Tr.	.00	Tr.	Tr.	Tr.	Tr.	Tr.	[illegible]
7-22-63	1.00	.00	.75	.50	.30	.25	.20	.10	.00	.00	.00	[illegible]
8-27-63	.15	.20	.20	.40	.30	.30	.35	.40	.20	.25	[illegible]	.40
9-23-63	1.30	1.30	1.40	1.10	1.00	[illegible]	1.30	1.30	1.20	1.30	1.10	1.07

B.—*Summary of recording rain-gage data, Arroyo de los Frijoles, 1959–62*

[Date of observation is within several days of major precipitation, but total precipitation includes also that between observations. Records should not be considered complete for use as annual precipitation. Gage located at Main Project Reach; see fig. 143]

Date of observation	*Precipitation (inches)*	*Date of observation*	*Precipitation (inches)*
8-07-59	1.06	7-08-61	.60
8-20-59	.26	7-28-61	.31
8-24-59	.80	8-13-61	1.33
8-26-59	.23	8-15-61	.10
10-02-59	.08	8-23-61	1.13
10-30-59	1.50	9-12-61	.70
11-13-59	.50	9-19-61	.80
12-17-59	.01	9-20-61	.10
		10-27-61	.70
1-21-60	.50	12-06-61	.10
2-29-60	.50		
5-18-60	.00	1-16-62	.30
6-10-60	1.10	3-09-62	.20
7-15-60	1.20	3-26-62	.20
8-05-60	.81	5-01-62	.10
8-23-60	.25	6-11-62	.10
10-07-60	.70	6-30-62	1.10
10-17-60	1.89	7-02-62	.00
12-12-60	.60	7-09-62	1.09
		7-23-62	.70
1-12-61	.10	7-26-62	1.50
4-03-61	1.30	7-30-62	.00
4-18-61	.38	8-02-62	.00
6-16-61	.20	8-28-62	.20
6-19-61	.60	9-17-62	.50
6-29-61	.30	11-26-62	.30

Digitized by Google

C.—Summary of data, erosion-pin plot in Slopewash Tributary, 1959–64

[Minus values in the net change columns represent deposition rather than erosion]

Pin	1959-61	1959-62		1960-63		1960-64		Net change 1959-64	
	Erosion (ft)	Erosion (ft)	Deposition (ft)	Erosion (ft)	Deposition (ft)	Erosion (ft)	Deposition (ft)	Total (ft)	Yearly average (ft per yr)
1	0.02	0.00	0.01	0.04	0.04	0.015	0.020	−0.005	−0.001
2	.01	.03	.00	.03	.03	.025	.005	.020	.004
3	.01	.00	.01	.02	.02	.010	.005	.005	.001
4	.04	.06	.01	.05	.00	.040	.000	.040	.008
5	.03	.06	.00	.05	.00	.045	.000	.045	.009
6	.02	.04	.03	.04	.01	.040	.005	.035	.007
7	.02	.04	.00	.04	.04	.010	.025	−.015	−.003
8	.02	.03	.00	.04	.01	.030	.000	.030	.006
9	.02	.03	.03	.035	.04	[illegible]	.040	.030	.006
10	.03	.08	.00	.025	.00	.045	.000	.045	.009
11	.04	.13	.11	.11	.11	.020	.025	−.005	−.001
12	.01	.00	.00	.015	.00	.020	.000	.020	.004
13	.03	.05	.02	.045	.03	.020	.005	.015	.003
14	.02	.03	.00	.03	.02	.025	.000	.025	.005
15	.03	.05	.00	.05	.00	.125	.000	.125	.025
16	.01	.04	.00	.02	.01	.035	.000	.035	.007
17	.01	.02	.00	.02	.00	.020	.005	.015	.003
18	.02	.02	.00	.02	.01	.015	.000	.015	.003
19	.02	.03	.00	.03	.00	.030	.005	.025	.005
20	.02	.04	.02	.03	.01	.025	.005	[illegible]	.004
21	.03	.05	.00	.05	.00	[illegible]	.005	.045	.009
22	.03	.06	.00	.05	.01	.055	.000	.055	.011
23	.02	.06	.00	.075	.00	.115	.000	.115	.023
24	.02	.03	.04	.03	.03	.020	.000	[illegible]	.004
25	.03	.04	.03	.04	.00	[illegible]	.000	.145	.029
26	.06	.06	.00	.09	.00	.130	.000	.130	.026
27	.01	.02	.00	.02	.00	.025	.005	.020	.004
28	.01	.02	.00	.02	.00	.030	.005	.025	.005
29	.01	.03	.00	.03	.00	.045	.005	.040	.008
30	.02	.03	.00	.08	.00	.050	.000	.050	.010
31	.01	.03	.01	.04	.01	.035	.000	.035	.007
32	.03	.00	.01	.02	.02	.035	.000	.035	.007
33	.01	.00	.04	.00	.07				
34	.02	.04	.02	.035	.035	.025	.000	.025	.005
35	.02	.03	.00	.02	.01	.015	.000	.015	.003
36	.01	.01	.00	.02	.00	.025	.000	.025	.005
37	.01	.02	.00	.02	.00	.035	.000	.035	.007
38	.01	.02	.00	.02	.00	.040	.000	.040	.008
39	.02	.04	.00	.04	.00	.065	.000	.065	.013
40	.03	.05	.05	.05	.03	.040	.005	.035	.007
41	.02	.00	.02	.03	.03	.030	.035	−.005	−.001
42	.02	.04	.00	.06	.01	.075	.005	.070	.014
43	.03	.02	.00	.05	.00	.050	.000	.050	.010
44	.04	.07	.00	.08	.00	.090	.000	.090	.018
45	.01	.02	.02	.02	.02	.015	.020	−.005	−.001
46	.01	.03	.00	.02	.00	.025	.000	[illegible]	.005
47	.01	.03	.00	.03	.00	.030	.000	.030	.006
48	.07	.10	.07	.11	.07	.065	.005	.060	.012
49	.04	.05	.00	.05	.01	.055	.005	.050	.010
50	.03	.05	.00	.05	.00	.055	[illegible]	.050	.010
51	.03	.04	.00	.035	.00	.035	.005	.030	.006
52	.03	.03	.03	.04	.01	.030	.000	.030	.006
53	.02	.07	.00	.10	.00	.175	.000	.175	.035
54	.01	.02	.00	.02	.00	.025	.005	.020	.004
55	.01	.02	.00	.02	.00	.025	.000	.025	.005
56	.02	.03	.00	.05	.01	.040	.000	.040	.008
57	.04	.07	.07	.06	.03	.065	.005	.060	.010
58	.02	.04	.00	.03	.01	.020	.005	.015	.003
59	.01	.04	.00	.03	.00	.035	.005	.030	.006
60	.01	.00	.00	.02	.06	.010	.035	−.025	−.005
61	.02	.03	.02	.035	.00	.035	.000	.035	.007

Summary

Average erosion, 0.0117 ft per yr.
Average deposition, 0.0041 ft per yr.
Net average erosion, 0.0076 ft per yr.

Digitized by Google

D.—*Summary of data, slope-retreat pins in Slopewash Tributary, 1959–64*

[Minus values in the net change columns represent deposition rather than erosion]

Pin	1959–61		1961–62		1962–63		1963–64		1959–64		Net change 1959–64	
	Erosion (ft)	Deposition (ft)	Erosion (ft)	Deposition (ft)	Erosion (ft)	Deposition (ft)	Erosion (ft)	Deposition (ft)	Erosion (ft)	Deposition (ft)	Total (ft)	Yearly average (ft per yr)
1	0.01	0.00	0.03	[illegible]	0.01	0.01	0.025	0.000	0.075	0.010	0.065	0.013
2	.06	.00	.04	[illegible]	.02	.01	[illegible]	.000	.150	.010	.140	.028
3	.05	.00	.03	.00	.01	.03	.035	.015	.125	.045	.080	.016
4	.04	.00	.05	.00	.01	.01	.015	.000	.125	.010	.115	.023
5	.07	.00	.04	.00	.02	.01	.015	[illegible]	.145	.010	.135	.027
6	.17	.00	.03	.00	.02	.02	.030	.000	.250	.020	.230	.046
7	.01	.16	.21	.17	.05		.060	.000	[illegible]	.330	[illegible]	.000
8	.01	.00	.05	.00	.00	.06	.070	.030	.110	.090	.020	.004
9	.02	.00	.02	.00	.09	.01	.030	.000	.160	.010	.150	.030
10	.03	.00	.01	.00	.04	[illegible]	.015	.000	.095	.010	.080	.016
11	.03	.00	.01	.00	.06		.040	.000	.140	.000	.140	.028
12	.02	.03	.05	.07	.03	.02	.015	.000	.145	.120	.025	.005
13	.01	.00	.02	.00	.06	.02	.005	.000	.095	.020	.075	.015
14	.04	.00	.02	.00	.03		.005	.000	.095	[illegible]	.095	.019
15	.00	.00	.02	.00	.025	.025	.030	.015	.065	[illegible]	.035	.006
16	.04	.00	.02	.00	.015		.035	.030	.110	.000	.110	.022
17	.04	.00	.08	.00	.025		[illegible]	.000	.140	[illegible]	.140	.028
18	.15	.00	.11	.00	.03	.03	.040	[illegible]	.330	.070	.260	.052
19	.29	.00	.13	.00	.02	.02	.030	.020	.460	.040	.420	.084
20	.08	.00	.07	.00	.04	.04	.025	.025	.215	.065	.150	.030
21	.00	.16	.22	.10	.03	.03	.030	[illegible]	.280	.350	−.070	−.014
22	.03	.01	.03	.00	.03	.04	[illegible]	.005	.140	.045	[illegible]	.019
23	.02	.04	.05	.02	.04	.04	.030	.020	.150	.120	.030	.006
24	.01	.03			.04	.05	.070	.000	.120	.080	.040	.008
25	.02	.00	.02	.00	.06	.05	.030	.000	.110	.060	.050	.012
26	.04	.00	.01	.03	.175		.035	.000	.260	.030	.230	.046
27	.03	.00	.02	.00	.05	.05	.035	.005	.135	.055	.080	.016
28	.02	.00	.02	.00	.04		.000	.040	.080	.040	[illegible]	.008
29	.03	.00	.01	.01	.02		.020	.000	.080	.010	.070	.014
30												
31	.02	.00			.01	.07	.065	.125	.085	.205	−.120	−.024
32	.02	.00			.01	.09	.090	.085	.110	.175	−.065	−.013
33	.03	.00	.04	.04	.02	.07	.075	.145	.135	.255	−.120	−.024
34	.04	.00	.00	.09	.01	.02	.025	.045	.075	.155	−.080	−.016
35	.01	.00	.00	.01	.00	.02	.030	.080	.040	.110	−.070	−.014
36	.02	.00	.00	.02	.02	.03	.030	.005	.070	.055	.015	.003
37	.02	.00	.01	.00	.03	.02	.015	[illegible]	.075	.020	.055	.011
38												
39	.03	.00			.02	.13	.090	.110	.140	.240	−.100	−.020
40	.03	.00			.04	.11	.060	.080	.120	.190	−.070	−.014
41	.02	.00	.00	.01	.05	.00	.030	.000	.080	.010	.070	.014
42	.01	.00	.02	.05	.02	.03	.050	.000	.100	.080	.020	.004
43	.00	.00	.03	.06	.01	.01	.080	.000	.120	.070	.050	.010
44	.01	.00	.06	.04	.01	.00	.040	.000	.120	.040	.080	.016
45	.01	.00	.05	.00	.02	.01	.030	.000	.110	.010	.100	.020
46					.19	.04	.060	.000	.140	.040	.100	.020
47			.11	.00	.00	.04	.110	.000	.220	.040	.180	.036
48			.05	.00	.00	.03	.010	.000	.060	.030	.030	.006
49			.03	.00	.01	.00	.000	.040	.040	.040	.000	.000
50			.04	.00	.00	.02	.020	.020	.060	.040	.020	.004
51			.02	.00	.02	.02	.000	.010	.040	.030	.010	.002
52			.03	.00	.08	.00	.090	.000	.200	.000	.200	.040
53			.03	.00	.07	.00	.070	.000	.170	.000	.170	.034
54			.10	.06	.01	.00	.030	.000	.150	.060	.090	.018
55			.02	.01	.01	.00	.070	.000	.100	.010	.090	.018
56			.10	.04	.00	.15	.210	.000	.310	.190	.120	.024
57			.09	.04	.00	.02	.060	.000	.150	.060	.090	.018

Summary of erosion rates, in foot per year

Pins	*Erosion*	*Deposition*	*Net erosion*	*Pins*	*Erosion*	*Deposition*	*Net erosion*
1–29	0.0326	0.0116	0.0210	46–57	0.0272	0.0089	0.0183
30–45	.0197	.0231	.0034	1–57	.0261	.0139	.0142

E.—Summary of data, iron-pin lines in Slopewash Tributary, 1958–64

[Minus values in net-change column represent deposition rather than erosion]

Pin	Protrusion, in feet						Net change, 1958–64
	1958	1959	1960	1962	1963	1964	
C	0.12	0.09	0.10	0.12	0.10	0.10	−0.02
1-cb	.12	.10	.16	.20	.21	.19	.07
2-cb	.11	.04	.00	.00	.00	−.10	−.21
3-cb	.26	.12	.12	.08	.07	.11	−.15
4-cb	.30	.22	.28	.50	.35	.53	.23
5-cb	.06	.12	.13	.15	.16	.16	.10
B	.12	.13	.11	.12	.12	.12	.00
1-ba	.09	.15	.12	.21	.32	.30	.21
2-ba	.21	.27	.35	.35	.38	.50	.29
3-ba	.11	.11	.12	.18	.17	.18	.07
A	.14	.16	.19	.15	.20	.20	.06
C							
1-cd	.15	.15	.16	.21	.21	.22	.07
2-cd	.04	.02	−.05	−.10	−.20	−.17	−.21
3-cd	.11	.12	.15	.15	.15	.13	.02
D	.11	.12	.11	.16	.20	.17	.06
1-db	.24	.10	.20	.15	.15	.36	.12
B							
E	.11	.11	.12	.13	.16	.13	.02
Average net erosion							0.0072

F.—Summary of data, erosion-nail lines in Coyote C. Arroyo, 1961–64

[Minus values in rate column represent deposition rather than erosion. Values in erosion columns do not include that erosion necessary to remove any deposition reported in previous years. Values in deposition columns represent data only for year of observation]

Pin	1961–62		1961–63		1961–64		Rate
	Erosion (ft)	Deposition (ft)	Erosion (ft)	Deposition (ft)	Erosion (ft)	Deposition (ft)	Erosion (ft per yr)
Line BA							
1	0.085	0.000	0.090	0.000	0.095	0.000	0.032
2	.055	[illegible]	.070	.010	.070	.000	[illegible]
3	.070	.000	.070	.000	.070	.000	.023
4	.065	.000	.080	.000	.095	.000	.032
5	.050	.000	.050	.000	[illegible]	.000	.030
6	.050	.015	.050	.020	[illegible]	.000	.015
7	.060	.000	.085	.000	.105	.000	.035
8	.030	.000	.050	.030	.020	[illegible]	.007
9	.055	.000	.070	.000	.090	.000	.030
10	.060	.000	.055	.000	.070	.000	.023
11	.050	.000	.060	.000	.055	.000	.018
12	.035	.015	.045	[illegible]	.090	.000	.030
13	.140	.000	.175	.000	.170	[illegible]	.057
14	.050	.000	.060	.000	.070	.000	[illegible]
15	.060	.010	.090	.010	.100	.000	.033
16	.080	.000	.085	.000	.110	.000	.037
17	.060	.000	.045	.015	.050	.000	.017
18	.055	.025	.060	.015	.050	.000	.017
19	.080	.000	.065	.000	.090	.000	.030

F.—Summary of data, erosion-nail lines in Coyote C. Arroyo, 1961–64—Continued

Pin	1961–62		1961–63		1961–64		Rate
	Erosion (ft)	Deposition (ft)	Erosion (ft)	Deposition (ft)	Erosion (ft)	Deposition (ft)	Erosion (ft per yr)
20	0.070	0.000	0.075	0.000	0.100	0.000	0.033
21	.060	.000	[illegible]	.000	.070	.000	.023
Average net erosion							0.027
Line BC							
1	0.085	0.000	0.100	0.000	0.120	[illegible]	0.040
2	.060	.000	.080	.000	.085	[illegible]	.028
3	.055	.000	[illegible]	[illegible]	.115	[illegible]	.038
4	.065	.000	.075	.000	[illegible]	[illegible]	.030
5	.050	.000	.060	.020	.070	.000	.023
6	.065	.000	.100	[illegible]	.100	.000	.033
7	.050	.060	.055	.055	−.010	.025	−.011
8	.110	.000	.090	.000	.070	.005	.021
9	.040	.000	.055	.010	[illegible]	.000	[illegible]
10	.020	.000	.030	.010	.030	.000	.010
11	[illegible]	.000	.060	.000	.060	.000	.020
12	.040	.000	.070	.000	.065	.000	[illegible]
13	.045	[illegible]	.055	.000	.070	.000	[illegible]
14	.080	.000	.070	.000	[illegible]	[illegible]	.027
15	.050	.000	[illegible]	.000	.065	.000	.022
16	.040	[illegible]	.055	.000	.060	.000	.020
17	[illegible]	.000	.080	.000	.080	.000	.027
18	.045	.000	.070	.000	.070	.000	.023
19	.045	.000	[illegible]	.000	.075	.000	.025
Average net erosion							0.023
1	0.055	0.000	0.065	0.000	0.070	0.000	0.023
2	.070	.000	.070	.000	.080	.000	.027
3	.060	.000	.060	.000	.060	[illegible]	.020
4	.045	[illegible]	.040	.000	.070	.000	.023
5	.040	.000	.050	.000	.050	[illegible]	.017
6	.030	.000	.050	.000	.080	[illegible]	.027
7	.050	.000	[illegible]	[illegible]	.070	.000	.023
8	.070	.015	.080	.000	.020	.075	−.018
9	.075	.035	.105	.010	.105	.000	.035
10	.065	.000	.075	.000	.130	.000	.043
11	.070	.050	.075	.030	.060	.000	.020
12	.090	.000	.135	[illegible]	[illegible]	.000	.040
13	.070	.020	.070	.010	[illegible]	.000	.020
14	.040	.050	.065	[illegible]	.075	.000	.025
15	.060	.000	.075	.000	.075	.000	.025
16	.075	.000	[illegible]	.000	.110	.000	.037
17	.045	[illegible]	.065	.000	.075	.000	.025
18	.045	.000	.035	.000	.050	[illegible]	.017
19	.060	[illegible]	.065	.000	.075	.015	[illegible]
20	.070	.100	.075	.060	.035	.000	.012
21	.110	.050	.100	.000	.060	.050	.003
22	.080	.030	.065	.060	.070	[illegible]	.023
23	.070	.130	.055	.110	.015	.060	−.015
24	.070	.030	.085	.015	.060	.000	.020
25	.080	.000	.070	.000	.115	.000	.038
Average net erosion							0.021
Average net erosion for all 65 pins							.0237

G.—Summary of data, nail sections A–J in Slopewash Tributary, 1959–64

[Pin: LB, left bank; CL, centerline; RB, right bank]

Section	Pin	1959–61		1961–62		1962–63		1963–64		1959–64		Rate		
		Erosion (ft)	Deposition (ft)	Erosion (ft)	Deposition (ft)	Erosion (ft)	Deposition (ft)	Erosion (ft)	Deposition (ft)	Erosion (ft)	Deposition (ft)	Erosion (ft per yr)	Deposition (ft per yr)	Net change (ft per yr)
A	LB	0.040	0.000	0.020	0.000	0.000	0.000	0.050	0.000	0.065	0.000	0.013	0.000	0.013
	CL	.120	.010	.060	.270	.000	.190	.185	.283	.365	.755	.073	.151	−.078
	RB	.040	.000	.000	.000	.030	.000	.035	.000	.105	.000	.021	.000	.021
B	LB	[illegible]	.000	.030	.000	.000	.000	.070	.000	.120	.000	.024	.000	.024
	CL	.000	.020	.020	.000	.040	.100	.000	.060	.060	.180	.012	.036	−.024
	RB	.030	.000	.010	.000	.000	.000	.150	.000	.190	.000	.038	.000	[illegible]
C	LB	.100	.030	.030	.060	.140	.060	.085	.075	.355	.215	.071	[illegible]	.028
	CL	.040	.030	.000	.300	.040	.200	.030	.100	.140	.630	.028	.126	−.098
	RB	.010	.000	.030	.000	.000	.000	.150	.000	.190	.000	.038	.000	.038
D	LB	.050	.000	.010	.000	.000	.000	.000	.000	.060	.000	.012	.000	.012
	CL	.100	.020	.000	.000	.020	.120	.050	.050	.170	.190	.034	.038	−.004
	RB	.010	.000	.000	.000	.030	.000	.060	.000	.100	.000	.020	.000	.020

G.—*Summary of data, nail sections A–J in Slopewash Tributary, 1959–64*—Continued

Section	Pin	1959–61		1961–62		1962–63		1963–64		1959–64		Rate		
		Erosion (ft)	Deposition (ft)	Erosion (ft)	Deposition (ft)	Erosion (ft)	Deposition (ft)	Erosion (ft)	Deposition (ft)	Erosion (ft)	Deposition (ft)	Erosion (ft per yr)	Deposition (ft) per yr)	Net change (ft per yr)
E	LB	0.020	0.000	0.010	0.040	0.050	[illegible]	0.100	0.000	0.180	0.040	0.036	0.008	0.028
	CL	.040	.030	.010	.210	.000	.120	.230	.170	.280	.540	.056	.108	−.052
	RB	.000	[illegible]	.050	.060	.060	.060	.020	[illegible]	.130	.110	.026	.022	[illegible]
F	LB	....	....	.010	[illegible]	.000	.000	.010	.000	[illegible]	[illegible]	[illegible]	[illegible]	[illegible]
	CL	....	....	.060	.230	.000	.140	.100	.100	[illegible]	.470	.032	[illegible]	−.062
	RB	....	....	.040	.050	.040	.080	[illegible]	.000	.100	[illegible]	[illegible]	.016	.004
G	LB	.060	[illegible]	.030	.000	[illegible]	.000	.070	.000	.160	[illegible]	.032	[illegible]	.032
	CL	.030	.060	.180	.160	.140	.140	.155	[illegible]	.505	.540	.101	[illegible]	−.007
	RB	.020	[illegible]	.030	.000	[illegible]	[illegible]	[illegible]	.000	.050	[illegible]	.010	[illegible]	.010
H	LB	.000	[illegible]	.050	[illegible]	[illegible]	[illegible]	[illegible]	.020	.110	.140	[illegible]	[illegible]	−.006
	CL	[illegible]	.210	.230	.350	.350	.140	[illegible]	.030	.610	.730	.122	.146	−.024
	RB	.040	.000	[illegible]	.000	.010	[illegible]	.010	.000	.050	[illegible]	.018	[illegible]	.018
I	LB	[illegible]	.000	.090	[illegible]	[illegible]	.000	[illegible]	[illegible]	.140	[illegible]	.028	[illegible]	[illegible]
	CL	.010	[illegible]	.230	.230	.150	.120	.140	.135	.530	.455	.106	.090	[illegible]
	RB	.030	.000	.020	.000	.020	.000	.120	.000	.190	[illegible]	.038	[illegible]	.038
J	LB	.010	[illegible]	.030	.000	[illegible]	.000	[illegible]	[illegible]	.040	[illegible]	.008	.000	.008
	CL	.120	[illegible]	[illegible]	.230	.110	.120	.190	.160	.650	.590	.130	.118	.012
	RB	.010	.000	.020	.000	.000	.000	.080	.000	.090	.000	.018	.000	.018

Summary of average eroison rates, in foot per year

Pins	*Erosion*	*Deposition*	*Net erosion*
Bank	0.0248	0.0058	0.0190
Channel	[illegible]	.1024	[illegible]

H.—*Summary of data, mass-movement line in Slopewash Tributary, 1959–64*

[Erosion for 1959–61 not measured]

Pin	1959–61		1959–62			1959–63			1959–64			1959–64		
	Downhill movement (in.)	Pin rotation (degrees)	Downhill movement (in.)	Pin rotation (degrees)	Erosion at pin (ft)	Downhill movement (in.)	Pin rotation (degrees)	Erosion at pin (ft)	Downhill movement (in.)	Pin rotation (degrees)	Erosion at pin (ft)	Downhill movement (in. per yr)	Pin rotation (degrees per yr)	Erosion at pin (ft per yr)
1	[illegible]	0	0.83	3	0.01	1.24	4	0.10	1.80	7	[illegible]	[illegible]	1.4	[illegible]
2	.02	0	.07	0	−.05	.13	4	−.02	.27	0	.01	.054	0	.002
3	1.06	5	.90	10	.21	1.20	7	.17	1.50	10	.17	[illegible]	2.0	[illegible]
4	1.01	5	1.27	5	[illegible]	1.69	8	.11	2.09	11	.18	.418	2.2	.032
5	.82	0	1.03	3	.09	1.42	7	.10	1.48	5	.13	.296	1.0	.026
6	1.08	0	1.48	3	.10	1.91	6	.12	2.07	9	.14	.414	1.8	.028
7	.67	0	.77	3	.07	1.20	6	.08	1.15	7	.11	.230	1.4	[illegible]
8	1.02	4	1.31	5	[illegible]	2.01	11	.13	2.60	18	.18	.520	3.6	[illegible]
9	.30	0	.09	0	[illegible]	.12	0	.07	.24	1	.07	.048	.2	.014
10	.30	0	.01	1	.01	.09	1	.05	.18	3	.08	[illegible]	.6	.016
11	.66	0	.67	3	.15	1.65	7	.15	1.56	10	.17	.312	2.0	.034
12	−.20	0	[illegible]	0	.07	.21	3	.12	.01	6	.18	[illegible]	1.2	[illegible]
13	.11	0	.22	0	[illegible]	.50	6	.02	.42	8	.04	[illegible]	1.6	.008
14	[illegible]	4	1.78	5	.13	1.33	5	.08	[illegible]	6	.10	.276	1.2	.020
15	....	....	.63	0	.10	.33	2	.14	.44	4	.25	.088	.8	.050
Average	.62	1.3	.76	2.7	.08	1.03	5.1	.09	1.13	7.0	.13	.225	1.40	.025

I.—*Summary of data, mass-movement line in Coyote Arroyo, 1961–64*

Pin	Local ground slope (degrees)	1961–62		1961–63		1961–64			Yearly average 1961–64	
		Downhill movement (in.)	Pin rotation (degrees)	Downhill movement (in.)	Pin rotation (degrees)	Downhill movement (in.)	Pin rotation (degrees)	Protrusion (ft)	Downhill movement (in. per yr)	Pin rotation (degrees per yr)
1	31	−0.10	0	−0.01	0	0.07	1	0.22	[illegible]	0.3
2	30	−.15	1	−.19	0	−.19	10	.30	−.063	3.3
3	24	−.08	−1	.18	0	.28	2	.27	.093	.7
4	12	.16	−1	.23	0	[illegible]	1	.20	.067	.3
5	31	.44	1	.71	0	.75	3	.275	.250	1.0
6	30	.22	−2	.40	0	.45	0	.25	.150	0
7	30	.57	4	1.46	9	1.80	9	.53	[illegible]	3.0
8	[illegible]	.56	7	1.56	10	1.85	12	.36	.617	4.0
9	37	.26	−7	1.14	3	1.54	4	.46	.513	1.3
10	21	1.96	11	2.03	11	2.03	16	.27	.677	5.3
11	18	.00	0	.19	0	.28	0	.32	.093	0
12	22	.06	0	[illegible]	0	.49	3	.36	.163	1.0
Average	25	.33	1	.67	3	[illegible]	5	....	.267	1.7

Digitized by Google

J.—*Summary of data, movement of coarse particles in Morning Walk Wash, 1961–64*

[M, missing; N, not measured; 0, no movement. Rock number corresponds to distance upstream of alluvial fan at mouth of channel. Rocks were installed in 1961. Found rocks were returned to orignal positions after each survey. Missing positions were not refilled. Some rocks reported as missing were found in later surveys]

Rock	Distance moved (feet)		
	1962	1963	1964
South gully			
0	22	M	M
10	0	0	0
20	59	M	M
30	M	M	M
40	23	M	M
50	0	0	M
60	M	M	M
70	M	M	M
80	M	M	M
90	M	49	28
100	131	M	M
110	146	M	M
120	M	M	M
130	M	M	M
140	135	M	M
150	11	M	M
160	M	M	M
170	41	M	32
180	M	M	M
190	M	M	M
200	M	387	28
210	M	M	M
220	242	5	14
230	M	M	M
240	M	M	M
250	M	M	M
260	M	M	M
270	148	107	M
280	M	M	380
290	311	180	M
300	M	M	M
310	298	M	15
320	M	M	M
330	365	34	90
340	355	M	32
350	M	M	M
360	M	M	M
370	443	208	120
380	137	18	33
390	M	0	45
400	23	M	M
410	M	M	M
420	0	M	0
430	453	M	M
440	473	M	M
450	M	M	M
460	M	M	M
470	511	0	0
480	508	25	M
490	M	16	20
500	M	M	M
510	M	M	M
520	594	20	15
530	486	0	0
540	M	M	M
550	569	0	0
560	0	0	0
570	268	0	0
580	M	M	M
590	628	0	M
600	633	0	0
610	M	M	M
620	88	0	0

J.—*Summary of data, movement of coarse particles in Morning Walk Wash, 1961–64*—Continued

Rock	Distance moved (feet)		
	1962	1963	1964
South gully—Continued			
630	7	0	0
640	M	M	M
650	198	0	0
660	0	0	0
670	14	0	0
680	0	0	0
690	M	M	M
700	723	0	0
710	0	0	0
720	190	0	0
730	0	0	0
740	0	0	0
750	5	0	0
760	0	0	0
770	0	0	0
780	5	0	0
790	0	0	0
800	0	0	0
810	0	0	0
820	0	0	0
830	0	0	0
840	0	0	0
850	0	0	0
860	0	0	0
South rill			
570	0	0	N
580	613	3	N
590	0	0	N
600	10	0	N
610	2	0	N
620	0	0	N
630	0	0	N
640	0	0	N
650	0	0	N
660	0	0	N
670	0	0	N
680	0	0	N
North gully			
0	11	2	10
10	30	17	0
20	114	22	M
30	31	0	0
40	100	M	M
50	69	0	M
60	M	M	M
70	M	M	M
80	91	M	M
90	108	63	M
100	130	0	67
110	201	120	M
120	2	0	0
130	141	0	8
140	M	265	0
150	201	0	M
160	179	34	25
170	181	175	140
180	185	2	0
190	58	67	20
200	211	0	10
210	221	0	0

Digitized by Google

J.—*Summary of data, movement of coarse particles in Morning Walk Wash, 1961–64*—Continued

Rock	Distance moved (feet)		
	1962	1963	1964
North gully—Continued			
220	45	M	200
230	241	6	0
240	M	355	14
250	M	M	M
260	0	0	0
270	0	1	0
280	291	11	3
290	291	76	10
300	168	5	0
310	321	M	M
320	5	0	8
330	0	0	0
340	M	M	M
350	M	M	M
360	0	M	M
370	M	M	M
380	M	M	M
390	0	0	0
400	M	M	M
410	M	M	M
420	0	0	0
430	0	0	0
440	0	0	0
450	36	0	0
460	0	0	M
470	8	0	0
480	66	0	0
490	0	0	0
500	0	0	0
510	0	0	0
520	20	0	0
530	0	0	0
540	0	0	0
550	0	0	0
560	0	0	0
570	0	0	0
580	0	0	0
590	0	0	0
600	0	0	0
610	0	0	0
620	0	0	0
630	0	0	0
640	0	0	0
650	0	0	0
660	0	0	0

U.S. GOVERNMENT PRINTING OFFICE 1966 O—796-885

Digitized by Google

UNIVERSITY OF CHICAGO
17 011 713

UNIVERSITY OF CHICAGO
17 011 713

QE 75
f. A26
no. 352-H

Geol

UNIV. OF CHICAGO
MAY 18 1966

Erosion and Deposition in the Loess-Mantled Great Plains, Medicine Creek Drainage Basin, Nebraska

U.S.

GEOLOGICAL SURVEY/PROFESSIONAL PAPER/352-H

Prepared as part of a program of the Department of the Interior for development of the Missouri River basin and part of the soil and moisture program

March 3, 1849

BRICE—EROSION AND DEPOSITION, LOESS-MANTLED GREAT PLAINS, MEDICINE CREEK DRAINAGE BASIN, NEBRASKA—Geological Survey Professional Paper 352-H

Erosion and Deposition in the Loess-Mantled Great Plains, Medicine Creek Drainage Basin, Nebraska

By JAMES C. BRICE

EROSION AND SEDIMENTATION IN A SEMIARID ENVIRONMENT

GEOLOGICAL SURVEY PROFESSIONAL PAPER 352-H

Prepared as part of a program of the Department of the Interior for development of the Missouri River basin and part of the soil and moisture program

UNITED STATES GOVERNMENT PRINTING OFFICE, WASHINGTON : 1966

Digitized by Google

UNITED STATES DEPARTMENT OF THE INTERIOR
STEWART L. UDALL, *Secretary*

GEOLOGICAL SURVEY
William T. Pecora, *Director*

For sale by the Superintendent of Documents, U.S. Government Printing Office
Washington, D.C. 20402 — Price 55 cents (paper cover)

U. S. GOVERNMENT

REC'D NOV 14 1966

Digitized by Google

CONTENTS

	Page
Abstract	255
Introduction	255
Climate, by Cloyd H. Scott	258
Vegetation and paleoclimate	262
Climax plant communities	262
Characteristics of native grasses	262
Effects of drought	263
Effects of land use	263
Native trees and dendrochronology	264
Pre-Pleistocene rocks	264
Unexposed rocks	264
Exposed rocks	264
Niobrara Formation	264
Ogallala Formation	265
Pleistocene and Recent deposits	265
Terraces	265
General stratigraphy of the Pleistocene and Recent	268
Stratigraphy on Cedar Creek near Stockville	270
Stratigraphy on Cut Canyon near Curtis	271
Stratigraphy on Elkhorn Canyon near Maywood	272
Loveland Formation and Sangamon soil	274
Peorian Loess, Brady soil, Bignell Loess, and modern soil	275
Stockville terrace deposits	278
Mousel terrace deposits	278
Recent alluvium	278
Significance of carbonized fragments of grass	280
Sand dunes	280
Archeology and human occupation	280
Results of archeologic investigations	280
Settlement and land use	281
Drainage system	282
Evolution of the drainage system	282
Morphometry	284
Drainage transformation and variations in drainage texture	288
Gully erosion	290
Definition and classification of gullies	290
Age and activity of erosional scarps	291
Channel scarps and valley-bottom gullies	291
Development of valley-bottom gullies	295
History of late Recent gullying on Dry Creek	300
Valley-head and valley-side gullies	301
Measurement of valley-head and valley-side gullies on Dry Creek	304
Areal distribution of gullies	307
Formation of valley-head and valley-side gullies	309
Gullying and land use	313
Control of gullies	314
Suspended sediment and the hydraulic geometry of channels, by Cloyd H. Scott	315
Hydraulic relations at a section and in a downstream direction	315
Suspended-sediment discharge relations	321
Particle-size distributions of suspended sediment and bed material	322
Relative sediment contributions of the major tributaries	325
Geomorphic properties in relation to water and sediment discharge	328
Summary and conclusions	332
References	333
Index	337

ILLUSTRATIONS

		Page
FIGURE 175.	Regional physiographic map	256
176.	Location map	257
177.	Photograph of typical relief in southern part of basin	258
178.	Graph of average monthly temperature and maximum, average, and minimum monthly precipitation at Curtis, Nebr., 1931–55	259
179–180.	Graph of annual precipitation, 1895–1960—	
179.	Curtis, Nebr.	260
180.	McCook, Nebr.	261
181.	Graph of rainfall intensity-duration-frequency curves for Curtis, Nebr., 1951–58	262
182.	Photographs showing effect of land use on native vegetation	264
183.	Geologic section across lower tip of basin	266
184.	Geologic section across the basin	267
185.	Section showing general topographic and stratigraphic relations of Pleistocene and Recent deposits	268
186.	Channel profile, valley flat profile, and terrace profiles along the main course of Medicine Creek	270

Digitized by Google

Page

FIGURES
187–189. Profile and geologic section—
187. On Cedar Creek 271
188. Along road entering Cut Canyon 272
189. On Elkhorn Canyon 273
190–193. Photographs showing—
190. Terrace sequence and valley fills along Elkhorn Canyon 273
191. Valley fill of the Peorian Loess set unconformably against Sangamon soil and Peorian Loess 274
192. Peorian Loess overlying A horizon of Sangamon soil 276
193. Banding in Recent alluvium, Dry Creek 279
194. Block diagram showing evolution of the relief since deposition of the Peorian Loess 283
195. Photographs of remnants of the side slopes and valley flats of former drainage systems 284
196. Map showing area of capture of North Plum Creek by Deer Creek 285
197. Maps showing variations in drainage texture 287
198. Graph showing mean channel length in relation to channel order 289
199. Graph showing number of channels of each order in relation to channel order 290
200. Composite sketch showing varieties of valley-bottom gullies 292
201. Map of head scarps in major valley-bottom gullies 293
202. Profiles of valley and channel for some major tributaries 295
203. Graph showing local valley slope in relation to drainage area 296
204. Photographs of typical valley-bottom gullies 297
205. Profile showing changes in a large valley-bottom gully on Dry Creek 298
206. Profiles of a large valley-bottom gully in a tributary of Curtis Creek Canyon 299
207. Profile showing changes in a gullied tributary of Dry Creek 300
208. Profiles of channel, valley flat, and terraces on Dry Creek 301
209. Cross profiles of Dry Creek 302
210. Photographs showing downstream changes in channel of Dry Creek 303
211. Composite sketch showing varieties of valley-head and valley-side gullies 304
212. Photographs of valley-head and valley-side gullies 305
213. Graph of cumulative frequency distribution of enlargements of valley-head and valley-side gullies on Dry Creek 306
214. Aerial photograph of a severely gullied area on upper Dry Creek 308
215. Map showing areal frequency distribution of active valley-head and valley-side gullies 310
216. Graph showing frequency of active valley-head and valley-side gullies in relation to area of upland and adjusted frequency of first-order channels 311
217. Profiles and plan view of a large valley-head gully 312
218. Profile of a large valley-head gully 313
219. Photograph of the head scarp of a small valley-head gully on Dry Creek 314
220. Hydrographs of daily mean flows equaled or exceeded about 1 percent of time 316
221. Graph showing change of width, depth, and velocity with increasing discharge at a section, Dry Creek near Curtis 317
222–223. Graph showing change of width, depth, and velocity in a downstream direction for channels of—
222. Perennial streams 319
223. Ephemeral streams 320
224–225. Graph showing change of suspended-sediment load with increasing discharge at a section—
224. Perennial streams 323
225. Ephemeral streams 324
226–231. Graph showing—
226. Size distribution of suspended sediment 325
227. Size distribution of bed material 326
228. Cumulative water discharge and sediment discharge per square mile 327
229. Mean channel slope in relation to channel order 328
230. Adjusted frequency of first-order channels in relation to mean valley-side slope, mean slope of first-order channels, and mean length of first-order channels 329
231. Slope of first-order channels in lower Dry Creek subbasin in relation to length 330
232. Trial graph showing multiple linear regression of sediment discharge in relation to relief ratio, percentage of upland, and adjusted frequency of first-order channels 331

Digitized by Google

TABLES

Page

TABLE 1. Thickness and percentage of each rock type in seven exposed sections of the Ogallala Formation 265
2. Correlation of stratigraphic units and terraces of the Pleistocene and Recent in Nebraska and Wyoming 269
3. Measured and derived properties for the Medicine Creek basin and its major subbasins 288
4. Drainage system properties, listed according to channel order, for major subbasins of the Medicine Creek basin 294
5. Measurements relating to the size and topographic setting of major valley-bottom gullies 299
6. Number of gullies according to type and size in the Medicine Creek basin and in major subbasins 307
7. Gully frequencies and related data for subbasins of the Medicine Creek basin 309
8. Values of *b*, *f*, and *m* for streams in Medicine Creek basin 321
9. Areas in upland and valley flat in comparison with areas in two categories of land use 330

Digitized by Google

EROSION AND DEPOSITION IN THE LOESS-MANTLED GREAT PLAINS MEDICINE CREEK DRAINAGE BASIN, NEBRASKA

By James C. Brice

ABSTRACT

The Medicine Creek basin is representative of the loess-mantled Great Plains in climate, surface materials, and relief forms, but its relief, degree of dissection, and rate of erosion are higher than average. In operation, if not in rate, processes of erosion and deposition in the basin are considered to be representative of loess-mantled regions in a semiarid or subhumid climate.

About 12,000 years ago, the valley fill of the Peorian Loess was incised and the drainage system was ramified to approximately its present extent. During the subsequent episode of deposition (about 1,000–5,000 yr ago), the deposits of the Stockville terrace accumulated and the valley sides were graded. The formation of the Stockville terrace was followed by a minor episode of deposition, another of valley incision, and finally the accumulation of the late Recent alluvium, which has been intermittently incised during the past 500 years.

The property of the drainage system that is most useful in accounting for the areal distribution of gullies is called adjusted channel frequency, in the derivation of which the drainage basin area is adjusted by subtracting the area of upland. The slope of the exponential curves, relating mean channel length to channel order, changes at the lower channel orders because of drainage transformations, in late Recent time, that affected only channels of low order.

Gullies in the basin are widened, lengthened, and deepened mainly by scarp erosion. They are classified on the basis of topographic location as valley-bottom, valley-side, and valley-head gullies. Trenching of a valley reach to bedrock takes place not only by coalescence of discontinuous gullies but also by the successive upstream migration of several channel scarps. Many large valley-bottom gullies have evidently originated on locally steepened valley reaches, but the ratio of local slope to drainage area that is critical for the initiation of a gulley is not sharply defined. Valley-bottom gullies advance mainly because of plunge-pool action, but this mechanism is less important in the advance of valley-side and valley-head gullies. The areal frequency distribution of valley-head and valley-side gullies is correlated with two geomorphic properties: percentage of area in upland and adjusted frequency of first-order channels.

Hydraulic geometry of the channels is expressed by the slope of curves relating width, depth, and velocity to discharges equaled or exceeded 1, 2, and 25 percent of the time. At the gaging stations on Dry, Mitchell, and Brushy Creeks, the flow is categorized as ephemeral; at the others, as perennial. In a downstream direction, an increase in discharge of ephemeral streams is accommodated by relatively large changes in depth and velocity, but the increase in discharge of perennial streams is accommodated by a relatively large change in width. Curves relating suspended-sediment load to water discharge for the perennial streams are characterized by a break in slope at water discharges above normal but below the bankfull stage.

In general, the concentration of measured suspended sediment is higher in wet years than in dry, and the ephemeral streams have higher concentrations than the perennial streams. Differences in runoff and sediment discharge among five subbasins are attributed mainly to differences in relief ratio, adjusted frequency of first-order channels, and percentage of area in upland.

Active valley-head and valley-side gullies, and all but a few of the active valley-bottom gullies, are attributed to land use since settlement rather than to climatic change. Restoration of native vegetation to the heads of valleys, together with conservation measures on the upland, would be effective in the control and prevention of valley-head gullies, which are the most numerous in the basin.

INTRODUCTION

The purpose of this report is to give an integrated account of the geologic and hydrologic factors that are pertinent to erosion and deposition in a part of the loess-mantled Great Plains and to evaluate the major factors involved in gully erosion, channel deposition, and the discharge of water and sediment through channels. Climatic change as a cause of modern erosion is evaluated in the light of ecologic, stratigraphic, and archeologic evidence from terrace deposits of late Pleistocene and Recent age. Processes of scarp erosion are analyzed, gullies are classified, and the areal distribution of gullies is correlated with morphologic properties of the basin. Generalizations are made as to the hydraulic geometry of the channels and the relations between discharge and suspended-sediment load. Differences in runoff and sediment discharge among five subbasins are attributed mainly to differences in specific morphologic properties among the subbasins.

The Medicine Creek basin was selected by several cooperating agencies (U.S. Bur. of Reclamation, U.S. Agr. Research Service, and the Univ. of Nebraska) as a suitable area in which to investigate erosion and runoff. Collection of data, which was begun in 1951 and ended in 1958, was directed toward an

Digitized by Google

evaluation of soil and water conservation practices and also toward an understanding of the processes and causes of rapid erosion in this region, which is the major subject of the present report.

The regional setting of the Medicine Creek basin, which is in the loess-mantled part of the Great Plains, is shown in figure 175. The processes of erosion and deposition in the basin are characteristic of loess-mantled regions in a semiarid or subhumid climate, and they apply specifically to an area of about 115,000 square miles that is within the Missouri River basin and is mantled with 8 feet or more of loess. Most of this area is within the Great Plains, although part is in the Interior Plains. The Medicine Creek basin is dissected to a much greater degree than many parts of the Great Plains, and the local relief is greater than average. Nevertheless, nearly all the relief forms typical of the Great Plains occur within the basin, including areas of nearly flat upland and sharply dissected areas of narrow divides and flat-bottomed valleys. Gullies of all types and sizes occur, and the frequency of gullies ranges from high in some places to low in others.

Medicine Creek, which is a tributary to the Republican River, has a drainage area of about 690 square miles that lies between the Platte and the Republican Rivers. Major subbasins and general geographical features are shown in figure 176. Remnants of the upland surface reach a maximum altitude of about 3,150 feet in the northern part of the basin and descend gradually to an altitude of about 2,400 feet at the bluffs of the Republican River. The maximum local relief, about 200 feet, is in the northern part of the basin. In general, the upland is more sharply dissected in the northern part, and the divides tend to be flat but narrow; in the central and southern parts, the divides are broader and slope gently toward the valleys. The general aspect of the relief in the southern part of the basin is shown in figure 177, which is an oblique aerial view southwest from a point above Medicine

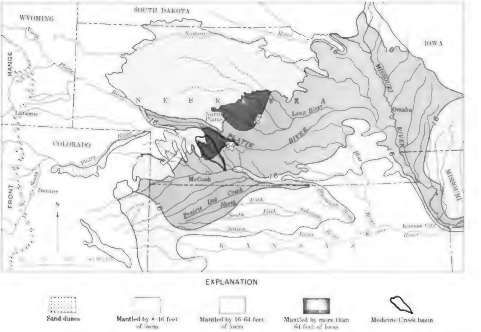

FIGURE 175.—Map showing the regional physiographic setting of Medicine Creek basin. Distribution and thickness of loess generalized from Thorpe and others (1952).

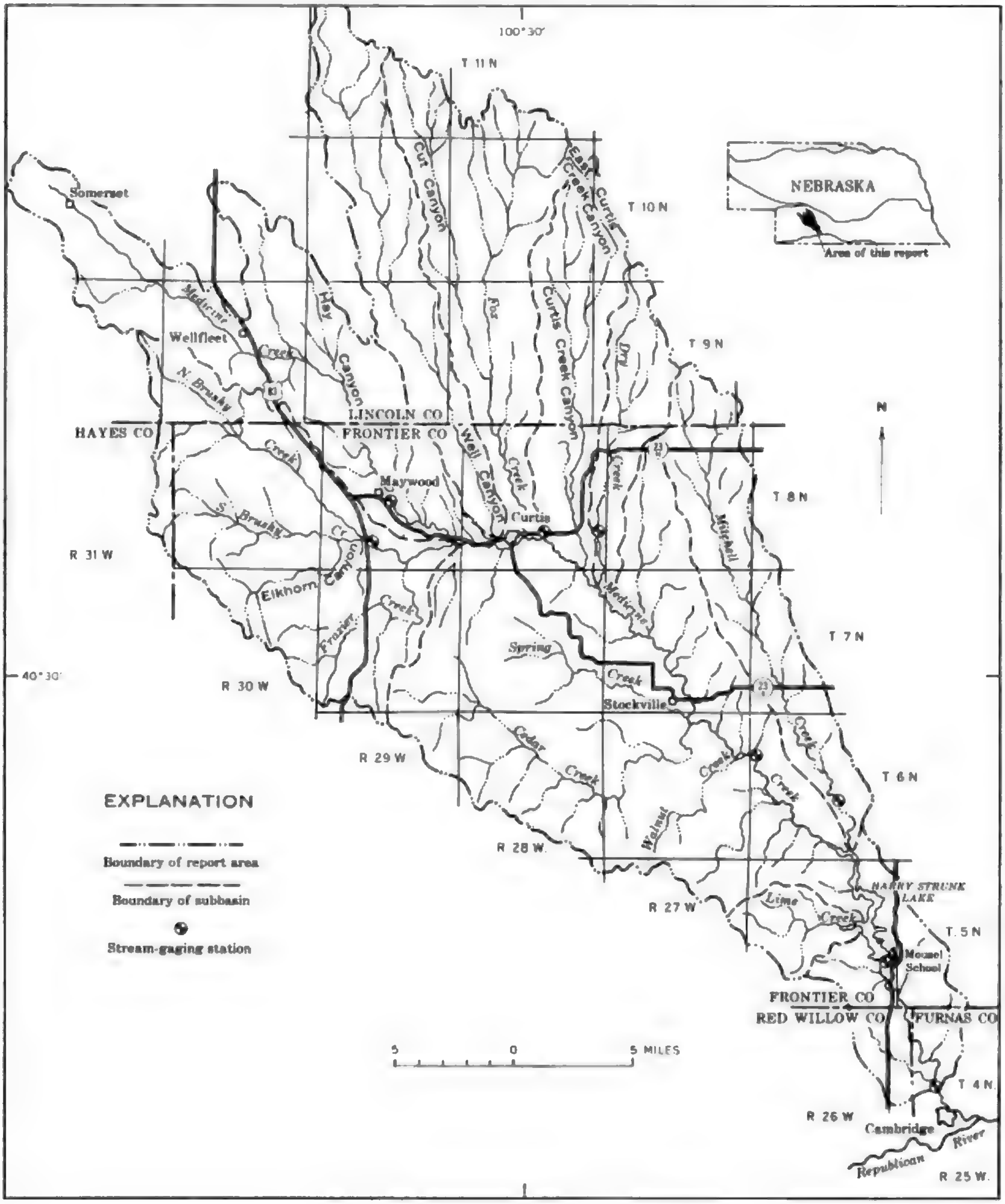

FIGURE 176.—Location map of Medicine Creek basin.

Digitized by Google

FIGURE 177.—Oblique aerial photograph of typical relief in southern part of Medicine Creek basin. Medicine Creek at lower left. Photograph by River Basin Surveys, Smithsonian Institution, 1948.

Creek and about 7 miles north of the town of Cambridge.

Fieldwork for geomorphic purposes was begun in the summer of 1953 and continued during the summers of 1954–56. Special hand-level and stadia-rod equipment was devised to permit the measurement of slopes without an assistant. Field studies, as well as office work, were facilitated by excellent topographic map and aerial photographic coverage of the entire basin. On the 1:24,000-scale topographic maps, prepared by photogrammetric methods and published by the Geological Survey in 1957–58, even minor topographic features are accurately represented. The Munsell color system was used for field description of loess and soil.

Data contributed by the cooperating agencies have been used in the preparation of this report. The detailed surveys necessary to measure rates of channel erosion on Dry Creek were made by the Bureau of Reclamation, who also contributed data on precipitation. Land use was tabulated by the Agricultural Research Service and the Soil Conservation Service. Runoff and suspended sediment were measured by the Geological Survey.

Many persons contributed to this report, which was prepared under the successive supervision of P. C. Benedict, regional engineer, and D. M. Culbertson, district engineer, U.S. Geological Survey. The section on native vegetation was read by E. J. Dyksterhuis, range conservationist for the Soil Conservation Service. Fossil snails were identified and information on snail ecology was given by W. J. Wayne of the Indiana Geological Survey. One carbon-14 age determination was made by Meyer Rubin, geochemist of the U.S. Geological Survey, and another by J. L. Kulp of Columbia University.

CLIMATE

By Cloyd H. Scott

The climate of the Medicine Creek basin is typical of the interior of continents of the middle latitudes with rather light rainfall, hot summers, cold winters, large variations in precipitation and temperature from year to year, and frequent changes in weather from day to day.

The mean annual temperature at Curtis, near the center of the basin, is about 52°F. Maximum and minimum temperatures above 100° and below 0°F occur occasionally. The coldest month is January when the average temperature is about 27°F, and the warmest month is July when the average temperature is about 78°. The monthly mean temperature at the U.S. Weather Bureau Station at Curtis for the years 1931–55 is shown in figure 178.

Much of the precipitation occurs during April through September, generally as thunderstorms. On the average, more than half the total annual precipitation occurs from May through August. Precipitation varies widely from the average (fig. 178); 7 months had no precipitation at least once during the period 1931–55, and some months had no precipitation several times during that period. Maximum amounts exceeded the averages by about two to seven times.

The annual precipitation also varies widely from year to year (fig. 179). The minimum annual amount of slightly less than 11 inches was recorded in 1934, and the maximum of about 38.2 inches was recorded in 1915. The 66-year average (1895–60) was about 21.5 inches, but the 25-year average (1931–55) was only 19.1 inches.

The 5-year moving averages (figs. 179 and 180) show the general trends of precipitation at Curtis and McCook from 1895 to 1960. The annual totals are highly variable from one year to another, but the 5-year moving averages show a somewhat cyclic trend. Even though the high- and low-precipitation years tend to be grouped somewhat, about half of the years have above-average precipitation amounts. However, during 1951–58 at Curtis, 5 years had precipitation below average; 4 of the years had more than 6 inches below average.

The 5-year moving average for Curtis indicates a long-term trend toward decreasing annual precipitation. The consistency of the precipitation data at Curtis was checked by plotting a double-mass curve of data at Curtis and at McCook. A pattern composed of data for McCook, Cambridge, and North Platte was first used; but the data for North Platte and Cambridge were inconsistent with the

Digitized by Google

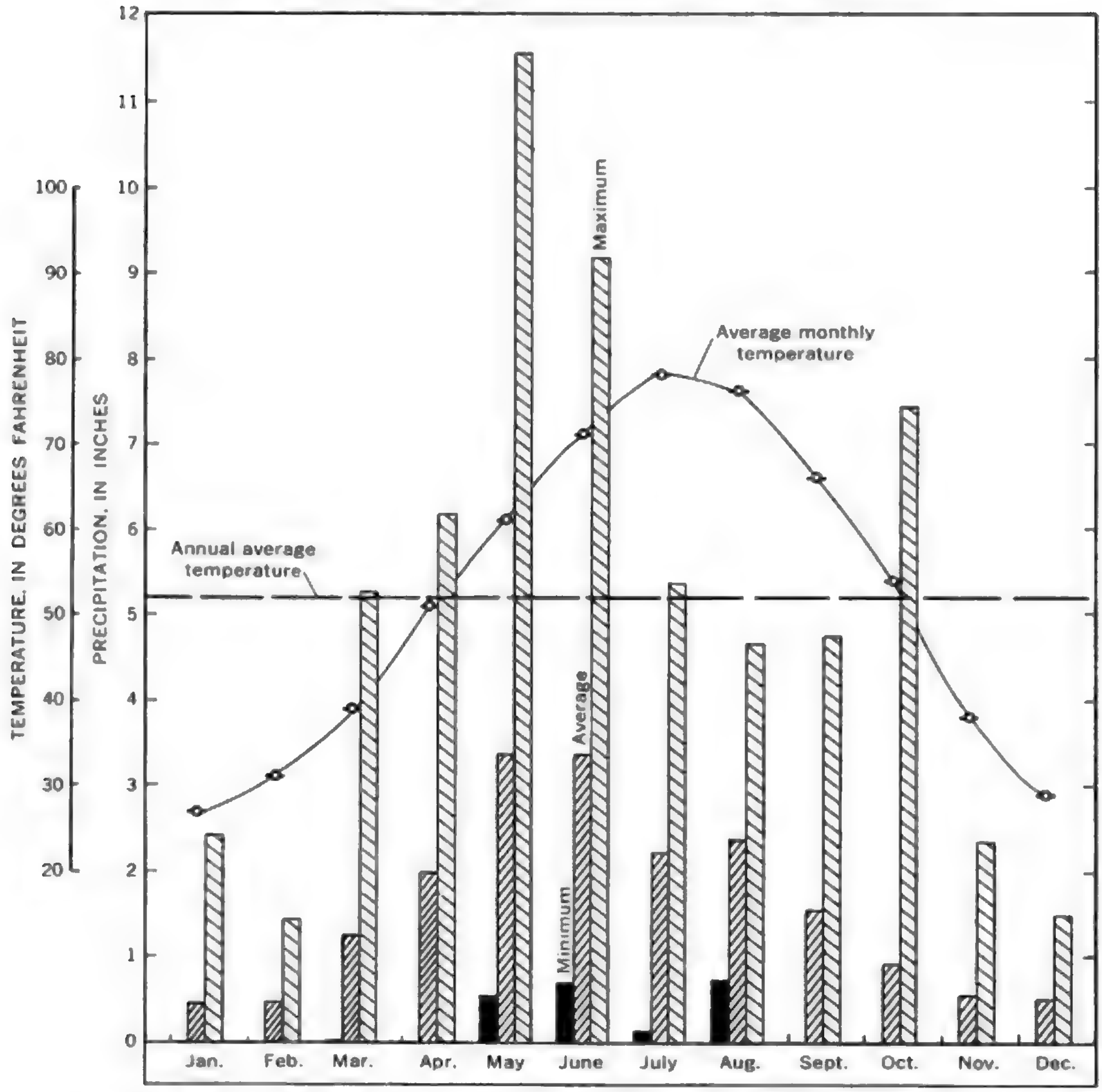

FIGURE 178.—Average monthly temperature and maximum, average, and minimum monthly precipitation at Curtis, Nebr., 1931–55

pattern, whereas the data for McCook seemed to be consistent. The double-mass curve showed a trend toward more precipitation at Curtis beginning about 1908 but returned to about the original slope in 1914. There is no record that the gage was moved in 1908, although the location was changed in 1914 (U.S. Weather Bureau, 1955a).

The pattern of the 5-year moving average for Curtis (fig. 179) is generally similar to the pattern for McCook (fig. 180) except that the precipitation for the period 1908–18 was higher at Curtis than at McCook and for the period 1940–52 was lower at Curtis than at McCook. The apparent secular decrease in annual precipitation at Curtis is probably a result of uneven areal distribution and is not considered to be representative of the region. As shown by the double-mass curve, the data at Curtis may have been somewhat biased for the years 1908–14.

Precipitation at Curtis averaged about 18.77 inches for the years 1951–58, or somewhat below the 66-year average of about 21.5 inches. Extremes of annual precipitation for this period ranged from 31.61 inches in 1951 to 12.36 inches in 1952. The occurrence of a high and a low in consecutive years is not unusual owing to the large variations in rain-

Digitized by Google

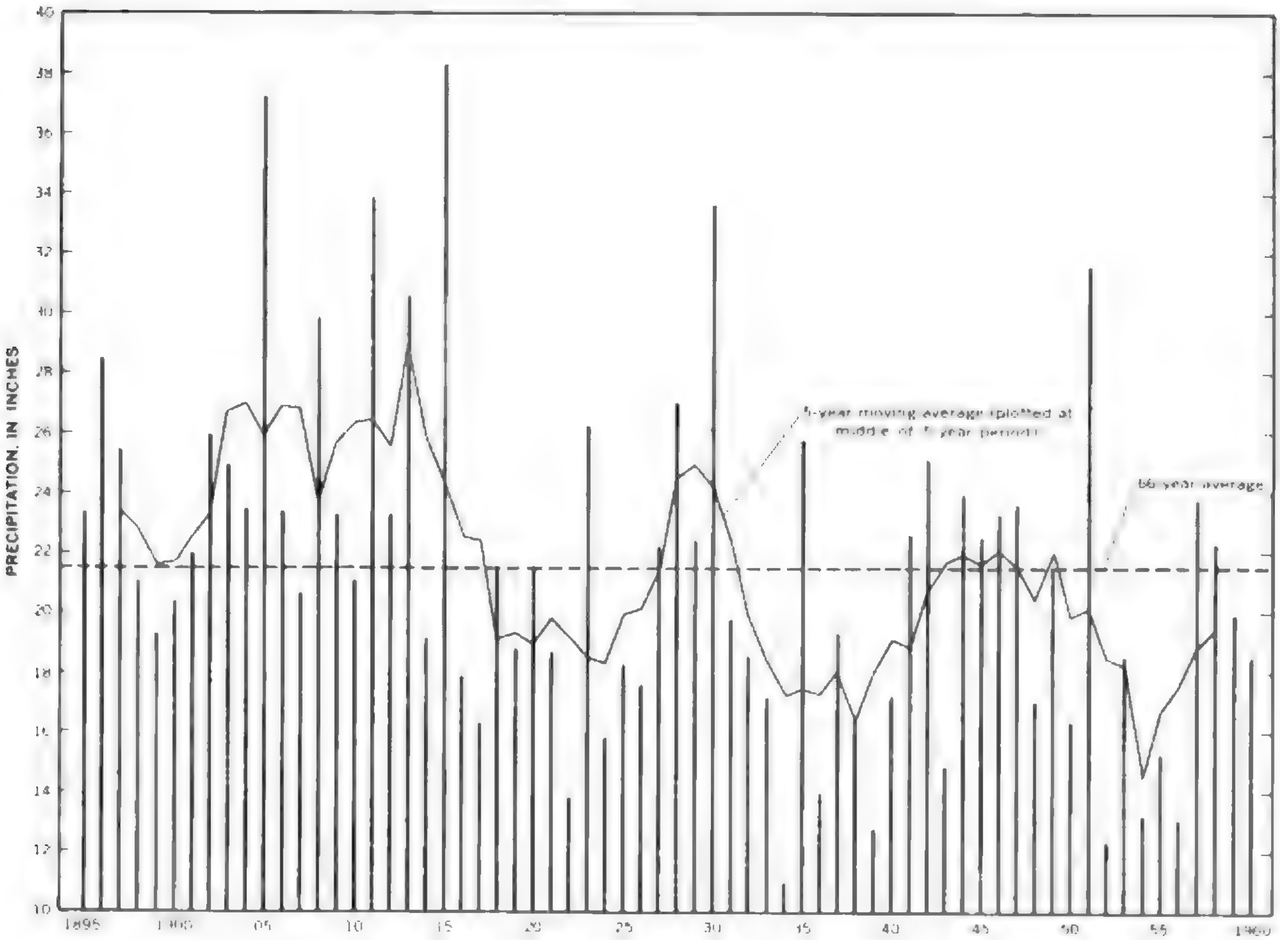

FIGURE 179.—Annual precipitation at Curtis, Nebr., 1895–1960.

fall over much of the central part of the continent. At Curtis, only 2 of 6 years since 1895 that had in excess of 30 inches of precipitation, were followed by years that had more than the long-term average amount. An extreme occurred in 1915–16 when the difference between precipitation amounts exceeded 20 inches.

Although averages and extremes give some indication of precipitation, a more meaningful description of rainfall can be obtained through the use of rainfall intensity-duration-frequency curves. Such curves (fig. 181) were developed for Curtis for return periods of 2 and 5 years based on the annual series of 1-, 6-, and 24-hour amounts. The California method of plotting positions, $T_r = n/m$, was used; a log normal distribution was assumed. T_r is the return period in years of item having order number m in a decreasing series, and n is the period of record in years.

An empirical factor of 1.13 (U.S. Weather Bureau, 1957) was used to convert the clock-hour amounts of rainfall to maximum 60-minute values. An inspection of the 6- and 24-hour amounts indicated that conversion for these periods was unnecessary.

The plot of rainfall intensity versus return period, which was used to define the curves of figure 181, showed little scatter from the average curve, which indicated that no extreme storms had occurred during the period.

The U.S. Weather Bureau (1955b) gives rainfall intensity-duration-frequency curves for about 200 stations, including North Platte, for the years 1906–51. Comparison of the curves for Curtis with those for North Platte shows that differences are minor between the two stations for both the 2- and 5-year return periods, even though only 8 years of record was used to define the curves for Curtis. The similarity between the short- and long-term curves and the fact that no extreme amounts of precipitation fell during the short period indicate that the rainfall regimen was well represented at Curtis during the years 1951–58, even though the

Digitized by Google

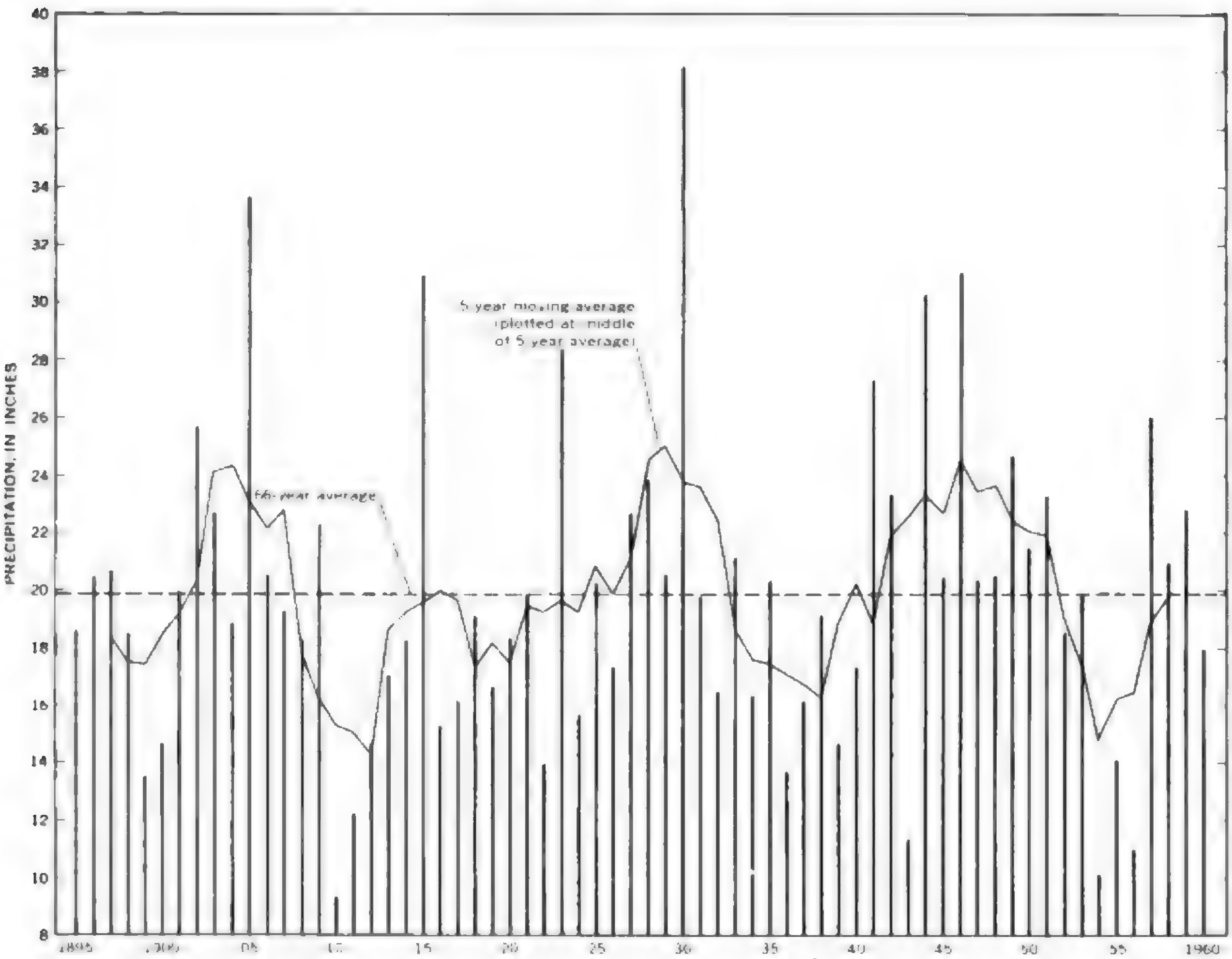

FIGURE 180.—Annual precipitation at McCook, Nebr., 1895–1960.

average precipitation for the period was somewhat lower than the long-term average.

Evaporation is also variable from year to year, although the variations probably are not as extreme as those of rainfall. The only evaporation data available are for a few years at Medicine Creek Dam, and these data were used to check evaporation maps in a technical paper by the U.S. Weather Bureau (1959a). According to the maps the average annual evaporation from a class A pan in Medicine Creek basin is about 75 inches, or about 3½ times the average annual precipitation; and lake evaporation is about 50 inches, or nearly 2½ times the average annual precipitation. Evaporation increases from north to south in the basin, but the average difference is only about 3 to 4 inches per year.

Data on wind speed and direction nearest Medicine Creek basin are those at North Platte. Because North Platte is in the valley of the Platte River, the wind speeds and directions may not be entirely representative of conditions in the Medicine Creek basin. The average wind speeds at North Platte range from about 12 to 13 miles per hour March through July and from a little less than 10 to slightly more than 11 miles per hour for the remainder of the year. December and January have the lowest average speeds with 9.8 and 9.7 miles per hour, respectively, and April has the highest average with 13.1 miles per hour. The prevailing direction is from the southeast April through August; south-southeast in September and January; northwest in February, October, and November; north in March; and west-northwest in December. The annual prevailing direction at North Platte is considered to be from the southeast (U.S. Weather Bureau, 1959b).

Digitized by Google

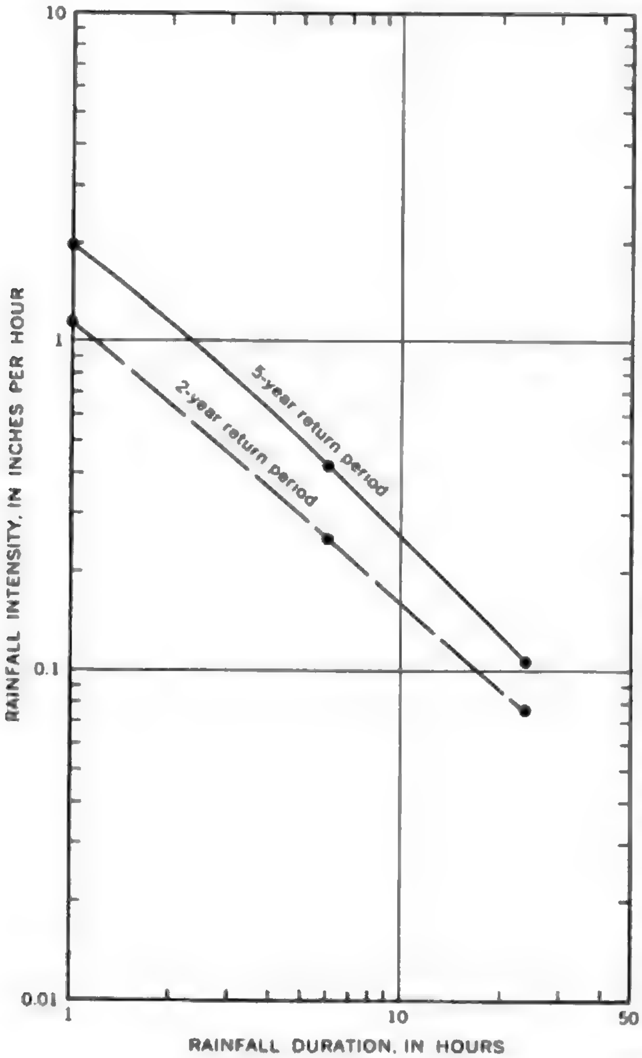

FIGURE 181.—Rainfall intensity-duration-frequency curves for Curtis, Nebr., 1951–58.

VEGETATION AND PALEOCLIMATE
CLIMAX PLANT COMMUNITIES

The Medicine Creek basin lies in a transitional zone between the tall-grass region to the east (prairie grassland) and the short-grass region to the west (plains grassland). Trees are restricted to valley bottoms, except where they have been artificially planted.

Some information regarding the history of plant communities appears in the notes of surveyors for the General Land Office who made brief reference to the grasses they saw while laying out the land-division grid in 1869–72.[1] Their comments also indicate the condition of the vegetal cover before white settlement. The following excerpts are from the notes of Deputy Surveyor D. V. Stephenson, made in the Medicine Creek basin during the summer of 1872: "land broken by steep ravines running in almost every direction, in bottoms of some of which there is some blue grass. The upland is about three-fourths covered with short buffalo grass. * * * grass almost entirely short buffalo, growing in bunches." Deputy Surveyor J. L. Slocum made the following notes, also in the summer of 1872: "Soil is dry and sandy, produces only short buffalo grass in scattering bunches—unfit for cultivation or grazing. * * * Considerable good grass in bottom of ravines, upland is sparsely covered with short buffalo grass." Deputy Surveyor Charles Wimpf wrote as follows, in August of 1869: "Bottoms of ravines filled with a thick very good grass which gives an excellent hay. The hills are covered with a short sweet grass." Although the term "buffalograss" may have been used loosely by the early surveyors, their comments do indicate that during 1869–72 the uplands and valley-side slopes were covered with a rather sparse growth of short grass, and the valley bottoms with a thicker growth of tall grass.

E. J. Dyksterhuis(writen commun. 1958), range conservationist for the Soil Conservation Service, considers that the climax community on the uplands in regions of climate and soils like those of the Medicine Creek basin contains a dominance of midgrasses with an understory of short grasses. He also says that the dominant midgrasses include western wheatgrass, needlegrasses, and little bluestem; little bluestem, side-oats grama, and blue grama dominate on the valley sides, and big bluestem and switchgrass on the valley bottoms.

CHARACTERISTICS OF NATIVE GRASSES

Characteristics of native grasses are summarized in this section from Weaver and Albertson (1943, 1944), U.S. Department of Agriculture (1948), and Phillips Petroleum Co. (1956).

Big bluestem is a coarse perennial native bunchgrass that reaches a height of 6 feet under favorable conditions. The root system is extensive; it may penetrate to a depth of about 8 feet and form a dense mat to a depth of 1 foot. Under favorable conditions it, together with other species of its community, will form a continuous sod; under less favorable conditions it forms separate, scattered bunches. Both rainfall and dust are largely intercepted by the foliage before reaching the ground. According to Clark (1937), a prairie covered by big bluestem may intercept as much as 53 tons of water per acre during a rainfall of 1 inch per hour, whereas a prairie covered by buffalograss will inter-

[1] Field notes of survey are on file at the Dept. of Educational Lands and Funds, State Capitol Bldg., Lincoln, Nebr.

Digitized by Google

cept about 28 tons per acre. Such intercepted rainfall commonly evaporates from the leaves of the plant without reaching the ground.

Buffalograss is native, sod forming, fine leaved, and perennial and typically grows to a height of 4 to 6 inches. The roots of well-developed buffalograss extend to a depth of 4 to 5 feet and form a very thick mat to a depth of 1 foot. Blue grama is a low native perennial grass whose flowering stems reach a height of about 18 inches. It is the most drought resistant of all the native prairie grasses, and it spreads, even during drought, mainly by means of seedlings. The root system is similar to that of buffalograss.

All these native grasses may form a dense thick, continuous sod, although the bluestems and blue grama are more likely to form separate bunches than buffalograss. The taller grasses intercept a greater amount of rainfall, which is usually lost to the soil; but a corresponding decrease in erosion by raindrop impact is effected. Windblown dust is retained more effectively by the taller grasses.

EFFECTS OF DROUGHT

Some insight into the influence of ancient arid climatic regimes on native grasses and on the ability of these grasses to prevent erosion may be gained by study of the effects of the drought of 1933–40 in Kansas and Nebraska. Such study was made by Weaver and Albertson (1943, 1944). These authors took for a base station Hays, Kans., which has an average annual precipitation of about 22.9 inches and which is located about 120 miles south of the Medicine Creek basin. Total precipitation at Hays for the 6 years preceding 1933 was below normal. Precipitation during each of the 4 driest years was about 16 inches.

According to Weaver and Alberston, decrease in grass cover as a result of drought varied with the intensity of grazing and of burial by dust and also with the type of grass cover, as grasses with shorter roots underwent greater destruction. The basal cover of short grasses in Kansas ranged between 80 and 95 percent in 1932, and this cover was commonly reduced to 20 percent or less during the worst years of the drought. In some localities, particularly those that had been overgrazed or covered by blown dust, the native plant population was reduced almost to zero. Where the effects of drought were moderate, the sod was interrupted by patches of bare ground, a square foot or less in area, that formed an irregular but continuous network. Where the effects of drought were more severe, the patches of bare ground were larger, up to several square yards in area; and in the most severely affected localities, the grass was so decimated that nearly all the ground was bare. These bare patches, described by Weaver and Albertson and noted by the writer (Brice, 1958) throughout the Medicine Creek basin in 1953–56, are important in slope erosion because erosion scarps commonly form at their edges.

The influence of ancient droughts and ancient episodes of aridity on the grasses of the Medicine Creek basin can be inferred from Weaver and Albertson's study. Short-term droughts would have reduced the cover of climax grasses, but erosion would not have been severe because these grasses are replaced by weeds during drought and recover rapidly after drought. Sheet-wash and raindrop impact would have removed soil from the irregular patches of bare ground between sod-covered areas, and low sod scarps would have formed on the slopes. During ancient episodes of aridity that lasted for hundreds or thousands of years, a climax community of grasses adapted to prevailing climate and rainfall distribution would have become established. Such a community would probably have consisted of an association of short grasses similar to the association now in eastern Colorado, where the average annual precipitation is about 15 inches. If this short-grass association were significantly different from that established before the arid episode, stream profiles and slopes would have been regarded by gullying and other erosional processes.

EFFECTS OF LAND USE

The pronounced effect of land use is strikingly shown by the contrast in vegetation on either side of a fence that follows the north-south section line between sections 15 and 16, T. 9 N., R. 27 W. (See fig. 182, *upper*.) The heads of two tributaries to East Fork of Dry Creek are isolated by this fence, and the aspect of the vegetation in these tributary heads is unlike that observed at any other place in the Medicine Creek basin. Although no information on the land-use history of the tributary heads was obtained, the contrast in vegetal cover at the fence is evident on both the 1937 and the 1952 aerial photographs. Therefore, the fence had divided areas of contrasting land use for at least 15 years, and the aspect of the vegetation in the tributary heads in 1953 suggested that it may have been disturbed in no important way since white settlement. Besides the much greater thickness of the sod and the dominance of tall grasses in the tributary heads, the thickness of brush such as wild plum, sumac, buckbrush, and wild rose is exceptional (fig. 182, *middle*). A few ash trees were observed on the

Digitized by Google

FIGURE 182.—Photographs showing effect of land use on native vegetation, East Fort Dry Creek, August 1953. *Upper*, Areas separated by a fence and contrasting sharply in vegetal cover. Denser vegetation is at right of fence. Although sparse, the vegetation at left of fence was better than average for the Medicine Creek basin in 1953. *Middle*, Dense cover of grass and brush in ungrazed valley head. View looking west. Vegetation more dense on south side of valley. *Lower*, Sparse cover of short grass, yucca, and weeds in heavily grazed valley head, 1.5 miles southeast of valley head shown in *middle*. Valley is oriented in north-south direction.

valley bottoms. The termination of the small valley-bottom gullies (fig. 182, *upper*) before reaching the fence may be fortuitous, but no gullies were observed in the tributary heads. By contrast, gullies are in most tributary heads in this part of Dry Creek (fig. 182, *lower*). Step scarps occur on the steep slopes of the heavily vegetated area, but they are much subdued and seem to be inactive. The upland drained by the tributary heads is planted in row crops or small grain, as elsewhere in the basin.

NATIVE TREES AND DENDROCHRONOLOGY

During the period 1869–72 General Land Office surveyors reported that trees in the Medicine Creek basin were confined to stream valleys, in which they identified cottonwood, ash, boxelder, elm, hackberry, and cedar. These same kinds of trees now grow from place to place in the valleys, but the wider valley flats have been mostly cleared of trees.

A tree-ring indication of precipitation during the past 400 years in western Nebraska, including the vicinity of North Platte, was reported by Weakly (1940, 1943). According to his interpretation, the climate has been characterized by frequent dry years and by less frequent droughts that lasted 5 years or more. The 13 droughts (period of five or more successive dry years) had an average duration of 13 years, and the average interval between droughts was about 20 years. The longest drought lasted from 1539 to 1564 (26 yr), but other lengthy droughts were from 1587 to 1605 (19 yr) and from 1688 to 1707 (20 yr).

PRE-PLEISTOCENE ROCKS

UNEXPOSED ROCKS

Neither the lithology nor the structure of unexposed rocks in the Medicine Creek basin has any apparent direct influence on the present relief. The Paleozoic and Mesozoic formations that overlie the Precambrian basement dip gently to the west and are overlain unconformably by Tertiary formations that dip gently to the east.

EXPOSED ROCKS

NIOBRARA FORMATION

The Niobrara Formation of Late Cretaceous age crops out along the banks of Harry Strunk Lake and from place to place along Medicine Creek downstream from the lake, but it is not exposed elsewhere in the basin. Where exposed, the Niobrara consists mainly of orange or white chalk interbedded with thin layers of altered volcanic ash.

Digitized by Google

OGALLALA FORMATION

Outcrops of the Ogallala Formation of Tertiary (Pliocene) age are mainly restricted to valley sides and channels of larger streams in the Medicine Creek basin, and the best exposures are along Medicine Creek and Cedar Creek in the vicinity of Stockville. No outcrops were observed in the northern parts of the basin where the loess cover is thickest. Available well logs indicate that the Ogallala underlies most of the basin and that its thickness increases from about 200 feet in the southern part to about 400 feet in the northern part. (See figs. 183 and 184.)

Exposed sections of Ogallala at seven localities were measured and described in detail. Thicknesses of described sections ranged from 6 feet at one locality on Cedar Creek to 73 feet at another locality downstream, and the total thickness of described sections was 290 feet. In general, the Ogallala consists of clay, silt, volcanic ash, sand, and gravel, poorly sorted into different beds that are cemented with (and partly replaced by) different amounts of carbonate. Five rock types were distinguished, and the total thickness of each type as represented in the seven measured sections is given in table 1.

TABLE 1.—*Thickness and percentage of each rock type in seven exposed sections of the Ogallala Formation*

	Thickness (ft)	Percent of total thickness
Gravel and sand	22	7.5
Sand, pebbly, and silt; loosely cemented, locally concretionary	156	54.0
Limestone, sandy, rather uniformly cemented	62	21.4
Ash, volcanic, and silt	26	9.0
Clay; alternating beds of fine-grained limestone	24	8.1

With regard to the origin of the Ogallala, Frye and others (1956) have presented convincing evidence that it was deposited by streams flowing eastward from the Rocky Mountain region. In the earlier part of their history these streams occupied broad, relatively shallow valleys eroded into Cretaceous bedrock. However, as alluviation proceeded, the deposits progressively overlapped the gentle valley sides, most divides were buried, and eventually a coalescent alluvial plain was formed.

PLEISTOCENE AND RECENT DEPOSITS

TERRACES

Three terraces were identified along Medicine Creek and its tributaries. The highest of these is named the Wellfleet terrace after the village of Wellfleet, Nebr., which is on Medicine Creek. Although Wellfleet is not built on the terrace surface, conspicuous flat-topped remnants of the terrace stand about 125 feet above the valley flat at intervals of a mile or more between Wellfleet and Maywood, Nebr. For example, the remnant in the SE¼ sec. 8, T. 8 N., R. 29 W., about 1 mile north of Maywood, is well defined both in the field and on the Curtis NW quadrangle sheet. There are similar flat-topped remnants along Well Canyon and other major tributaries, but the originally flat surface of the terrace has been dissected in most places.

The best preserved and most continuous terrace in the Medicine Creek basin is named the Stockville terrace after the town of Stockville, Nebr., which is built on a remnant of the terrace, along the west side of Medicine Creek. The Stockville terrace is represented along Medicine Creek by broad remnants that stand above the valley flat at a height of about 50 feet in the lower course of the creek and about 30 feet in its upper course. The Stockville terrace can be traced almost continuously along most tributary channels in the basin. Moreover, the sides and heads of valleys are broadly graded to the level of the Stockville terrace.

The lowest terrace of general importance in the Medicine Creek basin is named the Mousel terrace after the Mousel School, which is in sec. 25, T. 5 N., R. 26 W., on the east side of the valley of Medicine Creek. (See fig. 176.) The Mousel terrace is represented along Medicine Creek by widely scattered remnants that stand 15 to 20 feet above the valley flat. Similar remnants are along most major tributaries, such as Well Canyon, Cedar Creek, and Fox Creek; but the Mousel terrace cannot be traced along most minor tributaries because its surface has been buried by late Recent alluvium. Even where the terrace is well defined, there has been little grading of the valley sides to the level of the terrace; the slope that forms the riser of the Stockville terrace rises abruptly above the tread of the Mousel terrace.

A sequence of well-defined terraces appears along most streams in Nebraska, but general agreement has not been reached as to terrace nomenclature. Condra and others (1950) describe a sequence of six terraces in central Nebraska; and Schultz and others (1951) describe a sequence of five terraces that applies to Nebraska generally. Neither sequence would be expected to apply to all Nebraska streams because of complications, such as overlap of an older terrace deposit by a younger terrace deposit, that may be peculiar to a single stream.

Schultz and others (1948, 1951) have specifically applied their terrace sequence to alluvial terraces

Digitized by Google

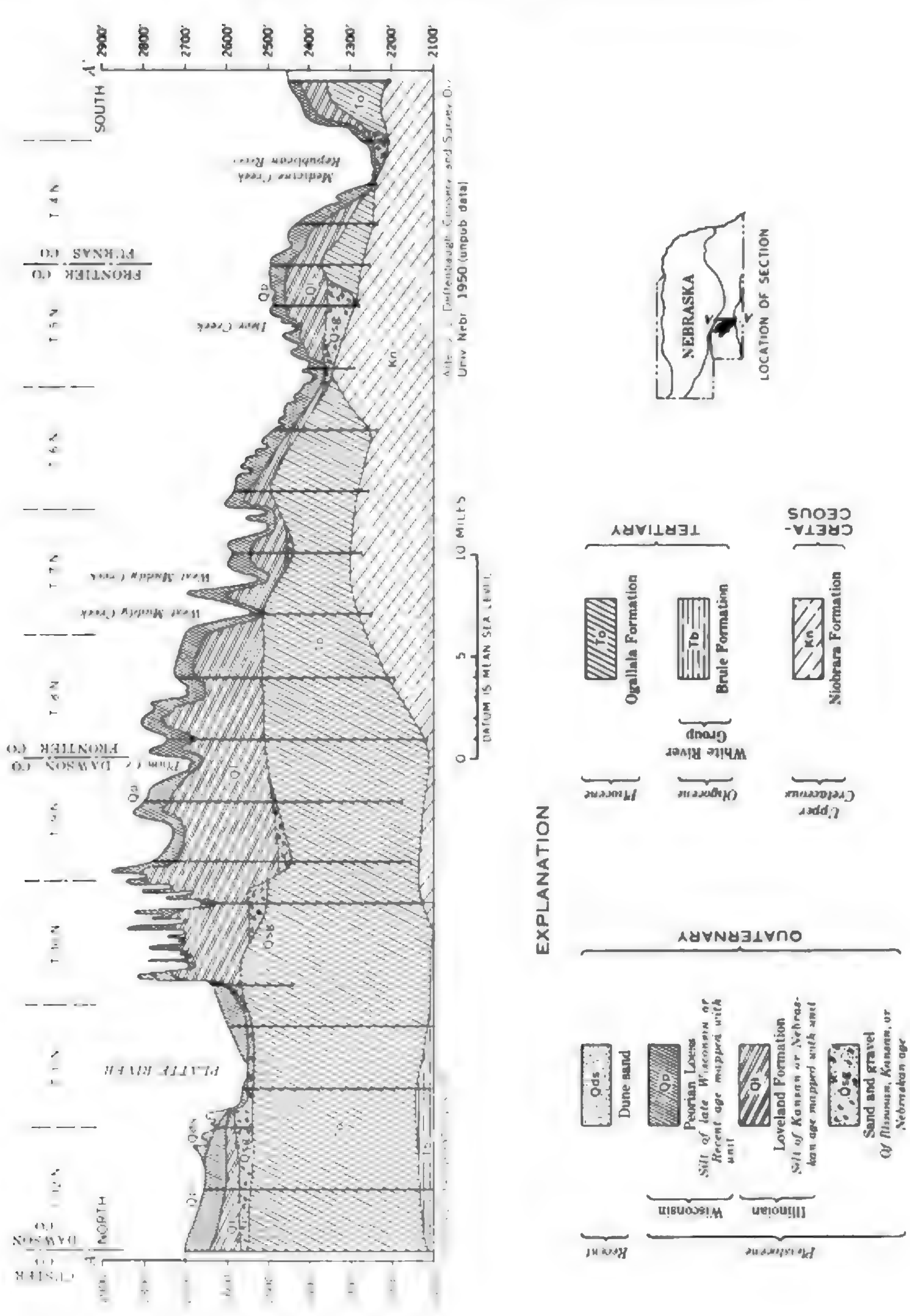

FIGURE 133.—Geologic section along a north-south line that crosses the lower tip of basin.

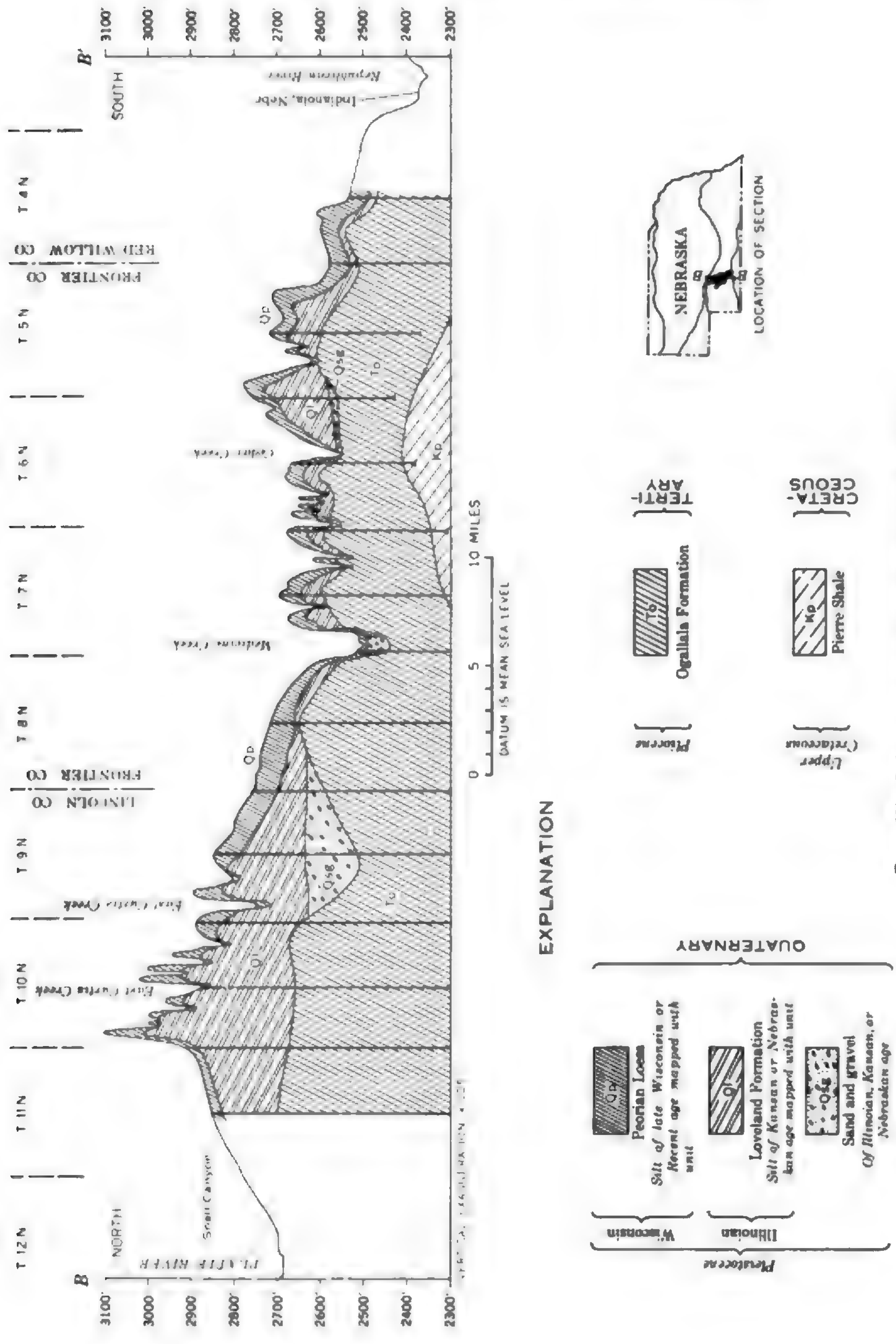

FIGURE 104.—Geologic section along a north-south line across the basin.

in the southern part of the Medicine Creek basin, in particular along Lime Creek. According to their nomenclature, alluvial terraces in Nebraska are numbered upward from the youngest and lowest, which is called Terrace-0, to the highest and oldest, which is called Terrace-5. Although their numerical system of terrace nomenclature is not used, the terrace sequence in this report is based on, and in general agreement with, the work of Schultz and others. Correlation of terrace deposits with Pleistocene time units is uncertain, particularly in view of the present controversy about the units. A tentative correlation of the Medicine Creek terrace sequence with other terrace sequences and with the Pleistocene time units is given in table 2.

The Stockville terrace of this report corresponds physiographically to Terrace-2 of Schultz and others (1948, 1951), and the Stockville terrace deposits correspond to fill A of Terrace-2. No terrace deposits corresponding to fill B of Terrace-2 were observed in the Medicine Creek basin by the writer.

The Wellfleet terrace, which is underlain by the upper part of the valley fill of the Peorian Loess, corresponds physiographically with the Terrace-3 of Schultz and others and with the Terrace no. 3 of Condra and others (1950, p. 35). No physiographic expression of the Terrace-4 of Schultz and others nor of the Terrace no. 4 of Condra and others was recognized in the Medicine Creek basin. At a locality on Medicine Creek (sec. 11, T. 5 N., R. 26 W.), Schultz and others (1948, p. 36) have identified a surface as the tread of Terrace-3. This surface is interpreted by the writer as a long valley-side slope graded to the level of the Stockville terrace. At this same locality the surface identified as Terrace-4 by Schultz and others is interpreted as the tread of Terrace-3, or the Wellfleet terrace. A terrace equivalent to Terrace-4 was doubtless once present in the Medicine Creek basin, but the physiographic expression has been obliterated by deposition of the upper part of the Peorian Loess and by grading of the valley sides during the time that the Stockville terrace deposits were accumulating.

GENERAL STRATIGRAPHY OF THE PLEISTOCENE AND RECENT

Stratigraphy of the Pleistocene deposits in Nebraska is well established, and satisfactory correlations have been made with the deposits of Kansas and other adjoining States, although nomenclature differs somewhat from State to State. For regional descriptions of the stratigraphic units the reader is referred to publications of the Nebraska Geological Survey (Condra and others, 1950; Lugn, 1935) and of the Kansas Geological Survey (Frye and Leonard, 1952). Leonard (1950, 1952) has established the ranges of land snails that are generally abundant in the Pleistocene deposits of Kansas.

The general relations of Pleistocene and Recent stratigraphic units in the Medicine Creek basin are shown in figure 185, and in table 2 correlation is tentatively made with formally named units in Nebraska and Wyoming. Long profiles of terrace deposits along the course of Medicine Creek are shown in figure 186. Correlation of the upper Wisconsin and Recent units is based on carbon-14 age determinations and on physiographic expression as terraces. Correlation of the older units is based on fossil evidence, on soil markers such as the Sangamon soil, and on lithology. Pleistocene and Recent deposits in the Medicine Creek basin consist of dune sand, loess, and alluvium, overlying a pre-Pleistocene (or lower Pleistocene) surface cut into the Ogallala Formation. The deposits of Nebraskan or Kansan age are mainly of alluvial silt and sand; gravel, in lesser amounts, is confined to the bottoms of former

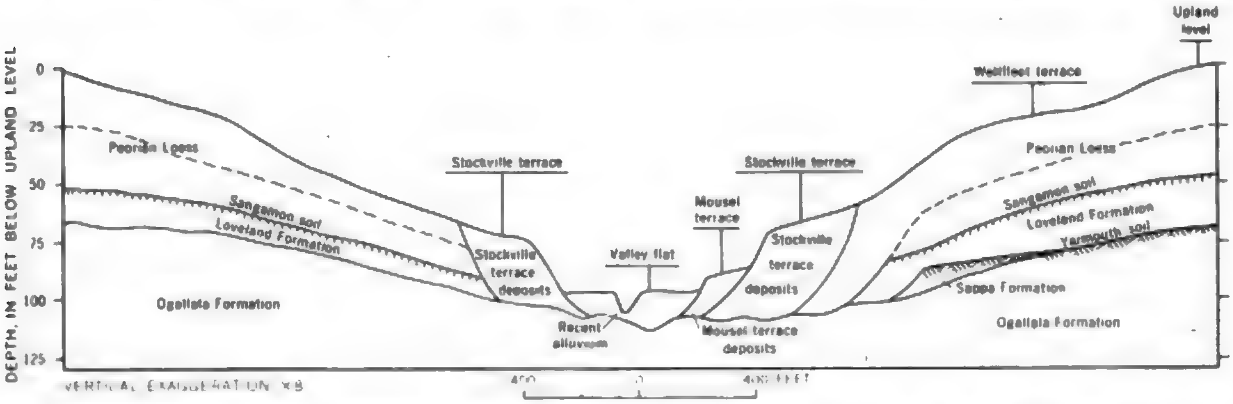

FIGURE 185.—General topographic and stratigraphic relations of Pleistocene and Recent deposits in the Medicine Creek basin. Differences in stratigraphy and relief on either side of the figure represent the range of differences among valleys in the basin.

Digitized by Google

TABLE 2.—*Correlation of stratigraphic units and terraces of the Pleistocene and Recent in Nebraska and Wyoming*

Age			Central Nebraska (Condra and others, 1950)	Central Nebraska terraces	Nebraska (Schultz and others, 1951)	Nebraska terraces	Wyoming (Leopold and Miller, 1954)	Wyoming terraces	Medicine Creek, Nebraska (This report)	Medicine Creek terraces	Generalized alluvial sequence western United States (Miller, 1958)
Recent					Wisconsin "VI" silt Soil Z Late Cochrane silt Early Cochrane silt (2,140 ± 150)[1] Soil Y	Terrace-0 Terrace-1	Lightning fm Moorcroft-deposition or stability Kaycee fm	Lightning terrace Moorcroft terrace	Recent alluvium (420 ± 160)[2] Mousel terrace deposits (1,343 ± 240)[2] (2,200 ± 200)[2]	Recent valley flats and terrace Mousel terrace	Deposition 3 Began A.D. 1200-1500[3] ended 1880 Deposition 2 Upper part—no younger than A.D. 1100-1200[3] Lower part—dates 2,200-2,400[4]
Recent		Altithermal					Paleosol	Kaycee terrace	Soil development	Stockville terrace	
?—?—?	Wisconsin	Mankato	Bignell silt	Terrace no. 2	Late Mankato silt Early Mankato silt		Ucross fm		Stockville terrace deposits		Deposition 1 (Probably correlates with a late Wisconsin glacial substage. Available dates suggest an age of 7,200-7,800[4])
Pleistocene	Wisconsin		Brady soil		Soil YY (9,880 ± 670)[5]	Terrace-2 fill A			Brady soil	Wellfleet terrace	
Pleistocene	Wisconsin	Cary	Upper Peorian silt Soil development	Terrace no. 3	Late Cary silt Early Cary silt Brady soil	Terrace-2 fill B			Peorian Loess		
Pleistocene	Wisconsin	Tazewell	Middle Peorian silt Soil development		Late Tazewell silt Early Tazewell silt Soil W	Terrace-3					
Pleistocene	Wisconsin	Iowan	Lower Peorian silt Todd Valley sand	Terrace no. 4	Todd Valley fm Early Iowan silt				Peorian Loess		
Pleistocene	Sangamon		Loveland soil		Sangamon soil	Terrace-4			Sangamon soil		
Pleistocene	Illinoian		Loveland fm Crete fm		Loveland fm Crete fm				Loveland Formation		
Pleistocene	Yarmouth		Sappa soil		Yarmouth soil Sappa fm				Yarmouth soil		
Pleistocene	Kansan		Upper Sappa fm Pearlette ash lenticle Lower Sappa fm Grand Island fm		Grand Island fm Red Cloud fm				Sappa Formation		
Pleistocene	Aftonian		Soil development		Fullerton fm						
Pleistocene	Nebraskan		Fullerton fm Holdrege fm		Holdrege fm						

1/ Years B.P., C[14] dates reported by Schultz and others (1951)
2/ Years B.P., C[14] dates given in this report
3/ Dates from pottery and dendrochronology
4/ Years B.P., C[14] dates from various localities
5/ Years B.P., C[14] date reported by Wedel and Kivett (1956)

WWWWW Denotes major periods of valley incision

Encloses the units underlying a physiographically expressed terrace. Wind-laid silt deposited subsequently on terrace surface is not shown

Digitized by Google

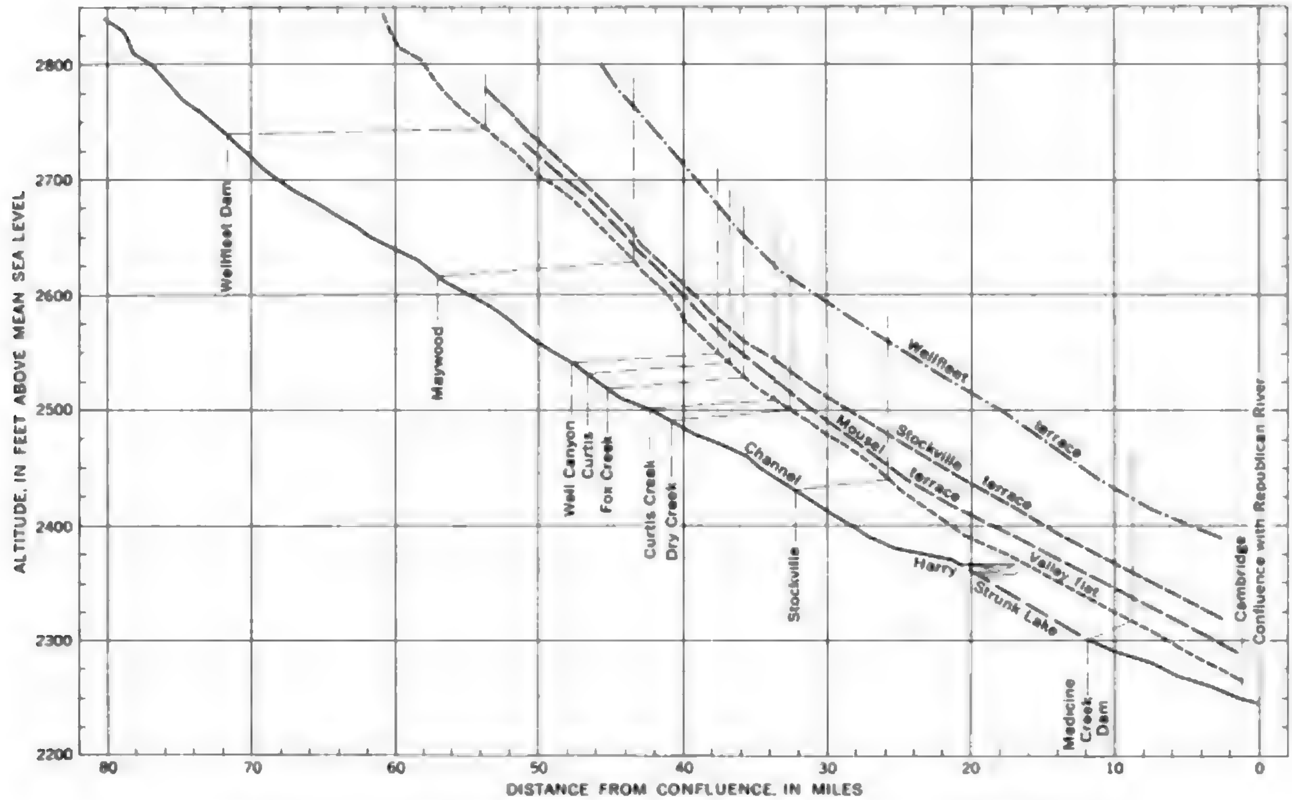

FIGURE 186.—Channel profile, valley flat profile, and terrace profiles along the main course of Medicine Creek.

valleys (figs. 183 and 184). Although loess may have been deposited during either Kansan or Nebraskan time, no loess of Kansan or Nebraskan age has been identified with certainty either on Medicine Creek or elsewhere in Nebraska. At two localities in the Medicine Creek basin, a paleosol was identified as the Yarmouth soil on the basis of snail fauna and high content of volcanic ash. Silts beneath the Yarmouth soil are correlated with the Sappa Formation. No deposits of ash of the Pearlette Ash Member of the Sappa Formation were seen in the Medicine Creek basin, but deposits up to 30 feet in thickness crop out in areas adjacent to the basin. No Pleistocene deposits older than the Sappa were recognized with certainty in the Medicine Creek basin.

The thickness and areal distribution of pre-Wisconsin stratigraphic units cannot be determined without data from drilling. Moreover, the logs must include full and accurate descriptions of the rocks that are penetrated, because the different Pleistocene stratigraphic units are similar in rock type to one another and to the Ogallala Formation. Two geologic sections (figs. 183 and 184) have been compiled from logs of test holes that were drilled by the Nebraska Conservation and Survey Division in cooperation with the U.S. Geological Survey. Figure 183 is simplified from an unpublished section by J. L. Deffenbaugh, based on his interpretation of logs of test holes drilled in 1948. On his original section, Deffenbaugh distinguishes the Loveland, Sappa, and Grand Island Formations. Figure 184 represents an interpretation, made by the writer, of logs of test holes drilled in 1960. Although the logs include full descriptions of the rocks penetrated, the writer was not able to distinguish with confidence any formational boundaries beneath the Sangamon soil and above the Ogallala Formation. To facilitate comparison of figures 183 and 184, some of the stratigraphic units distinguished by Deffenbaugh were combined in order that they correspond with the units shown on figure 184.

STRATIGRAPHY ON CEDAR CREEK NEAR STOCKVILLE

Along Cedar Creek, about 3 miles southwest of the village of Stockville (Bartley NW quad., NE¼ sec. 18, T. 6 N., R. 27 W.), several sections have been exposed by lateral cutting of the creek, and the terrace sequence is more complete and distinct than

Digitized by Google

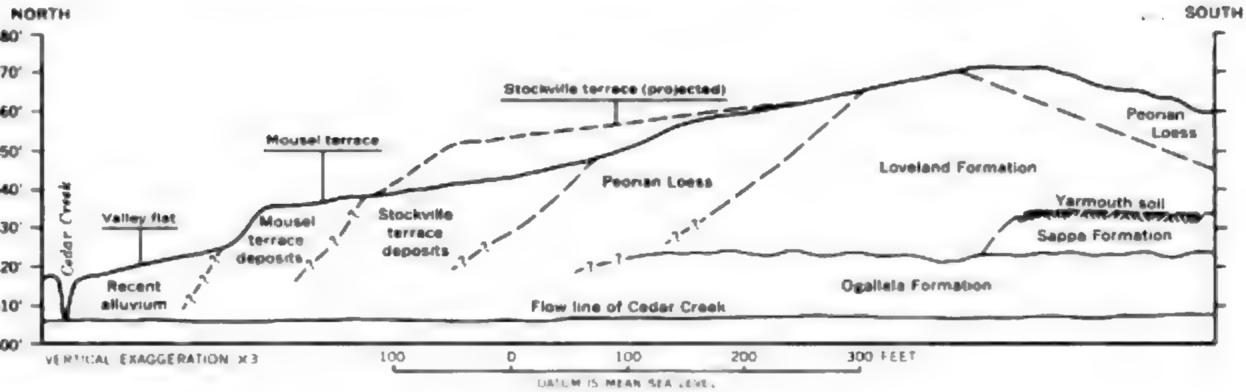

FIGURE 187.—Profile and geologic section on Cedar Creek.

usual for the Medicine Creek basin. The section described below applies to the right-hand (south) side of figure 187:

	Depth (ft)
Peorian Loess:	
Silt, pale-yellow (2.5*Y* 7/3 dry, 2.5*Y* 6/3 moist), calcareous. Surface soil not present	0–15
Loveland Formation:	
Silt, very pale brown (10*YR* 7/4 dry, 10*YR* 5/4 moist); a few streamers of fine sand near base	15–20
Gravel, sand, and silt, crossbedded, calcareous, locally cemented with carbonate	20–22
Silt, pale-brown (10*YR* 6/3 dry, 10*YR* 4/2 moist), noncalcareous; indistinct sedimentary lamination	22–26
Yarmouth soil:	
Silt, clayey, gray-brown (10*YR* 5/2 dry, 10*YR* 4/2 moist). Weak columnar structure, columns irregular, 2 to 5 in. wide; noncalcareous. Upper contact gradational	26–28.9
Sappa Formation:	
Sand, fine, and ashy light-gray (2.5*Y* 7/2 moist) silt; a few thin white irregular seams of volcanic ash. Upper 0.5 ft mottled with darker gray, gradational with unit above. Upper 2 ft is C_{ca} horizon of Yarmouth soil; contains meshwork of fine carbonate veinlets	28.9–32
Sand, fine, and ashy silt; a few streamers of sand and fine gravel near base; noncalcareous	32–35
Gravel and other debris from Ogallala Formation; crossbedded; a few streamers of fine sand	35–37
Ogallala Formation:	37–53

A snail fauna was collected from the lower part of the soil identified as Yarmouth and from the upper part of the unit identified as Sappa, and identification was made by Dr. W. J. Wayne of the Indiana Geological Survey. In the following table, the number of individuals of each species is given in the right-hand column.

Gastrocopta tappaniana (C. B. Adams)	2
proarmifera Leonard	3
Gyraulus circumstriatus (Tryon)	21
Helicodiscus parallelus (Say	3
Physa anatina Lea	2
Retinella electrina (Gould)	3
Lymnaea [Fossaria] parva	2
Vallonia gracilicosta Reinhardt	15
Valvata tricarinata (Say)	4

According to Leonard (1950), *G. proarmifera* is restricted to the Yarmouth, and none of the species in the collection is restricted to deposits younger than the Yarmouth. Correlation of the soil with the Yarmouth and of the underlying silt with the Sappa is, therefore, supported by the faunal evidence. *V. tricarinata* is aquatic, and the fauna as a whole indicates a moist environment such as would be afforded by a valley.

The stratigraphic and topographic relations shown in figure 187 indicate that the valley of Cedar Creek was cut not later than Kansan time and that at least five episodes of valley alluviation, each followed by cutting, have taken place since Yarmouth time.

STRATIGRAPHY ON CUT CANYON NEAR CURTIS

Near the confluence of Cut Canyon with Fox Creek, a significant section of Pleistocene deposits is exposed along the county road that descends eastward from the upland and crosses Cut Canyon in the NW¼ sec. 29, T. 9 N., R. 28 W. The presence of deposits of the Sappa indicates that the canyon was cut not later than Kansan time, and the Pleistocene sequence of pre-Wisconsin age seems to be complete. Both the Yarmouth and the Sangamon soils are well developed. Of the terrace deposits of late Wisconsin and Recent age, however, only the Stockville is exposed (fig. 188).

A stratigraphic section along the road, beginning 1,500 feet west of Cut Canyon bridge and ending 1,150 feet west of the bridge, is as follows:

	Depth (ft)
Peorian Loess:	
Silt, yellowish-gray, massive, homogeneous	0–30

Digitized by Google

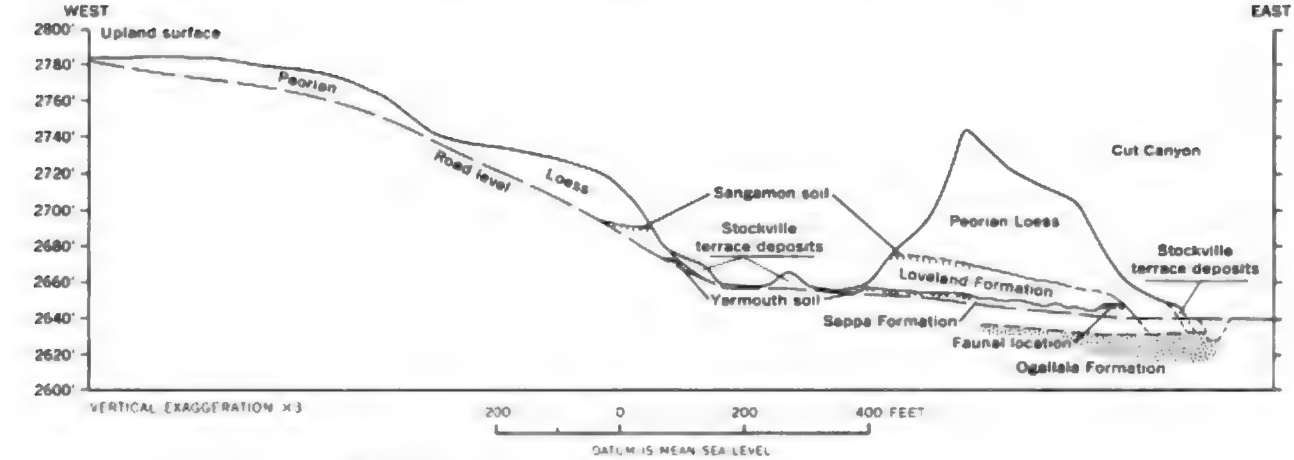

FIGURE 188.—Profile and geologic section along road entering Cut Canyon.

	Depth (ft)
Sangamon soil and Loveland Formation:	
Silt, yellowish-brown (10*YR* 5/4 when moist), friable; no distinct structure	30–32
Silt, light-yellowish-brown (10*YR* 6/4 when moist); weak prismatic structure, noncalcareous	32–38
Silt, clayey, approximately same color as unit above, but has pinkish cast	38–38.5
Silt, streaked and veined with abundant soft carbonate	38.5–43
Yarmouth soil:	
Silt, light-brownish-gray (5*Y* 7/2 when dry, 10*YR* 6/2 when moist), clayey; streaked with carbonate from unit above, but otherwise noncalcareous. Breaks into irregular small polyhedrons (5 to 10 mm in diameter) that fit together. Contact with unit above sharp but irregular	43–46.5
Silt, yellowish-brown (10*YR* 5/4 when moist); contains abundant small iron concretions	46.5–47

A stratigraphic section 800 feet west of the bridge is similar to that described above, except the Sappa Formation is exposed and the Yarmouth soil is somewhat different, as shown below:

	Depth (ft)
Yarmouth soil:	
Silt, olive-gray (5*YR* 4/2 when moist)	0–1
Silt, light-gray (10*YR* 7/2 when moist); crumb structure	1–2.5
Silt, light-gray, mottled with rust color; structure weakly prismatic, prisms have irregular sides, 1 to 3 cm wide	2.5–4.1
Silt, light-gray; no distinct structure	4.1–7.5
Sappa Formation:	
Sand, fine-grained, and silt; cross-laminated	7.5–9.5

No fossils were found at this section, but fossils were found in gray ashy silt, correlated with the Sappa, about 600 feet to the east. The faunas were identified by the writer, and the identification was checked and corrected by Dr. W. J. Wayne of the Indiana Geological Survey. The number of each species found is indicated in column at right in the following list:

Carychium exile canadense Clapp	2
perexiguum Baker	2
Gastrocopta pentodon (Say)	6
proarmifera Leonard	2
Gyraulus circumstriatus (Tryon)	19
Pupilla muscorum (Linné)	1
muscorum sinistra Franzen	1
Retinella electrina (Gould)	1
Vallonia gracilicosta Reinhardt	10
Valvata tricarinata (Say)	24
Vertigo nylanderi Sterki	3

According to Leonard (1950), *G. proarmifera* and *P. muscorum sinistra* are restricted to the Yarmouth and *C. perexiguum* is restricted to deposits of Nebraskan and Yarmouth age; none of the species found is restricted to deposits younger than Yarmouth age. Therefore, correlation of the ashy silt with the Sappa Formation is reasonable.

STRATIGRAPHY ON ELKHORN CANYON NEAR MAYWOOD

The Peorian Loess, Stockville terrace deposits, and late Recent alluvium are exposed along Elkhorn Canyon about 2 miles southwest of the village of Maywood, near a bridge where the county road crosses the canyon (Curtis SW quad., center of section line between secs. 31 and 32, T. 8 N., R. 29 W.). The exposure was studied after it had been thoroughly moistened by rainfall and runoff, because moistening greatly increases visibility of the sedimentary structures and textures. The relations between the different units are shown in figure 189, and a general view of the locality is shown in figure 190. Evidence was found in the late Recent alluvium for two episodes of cutting and filling, which took

Digitized by Google

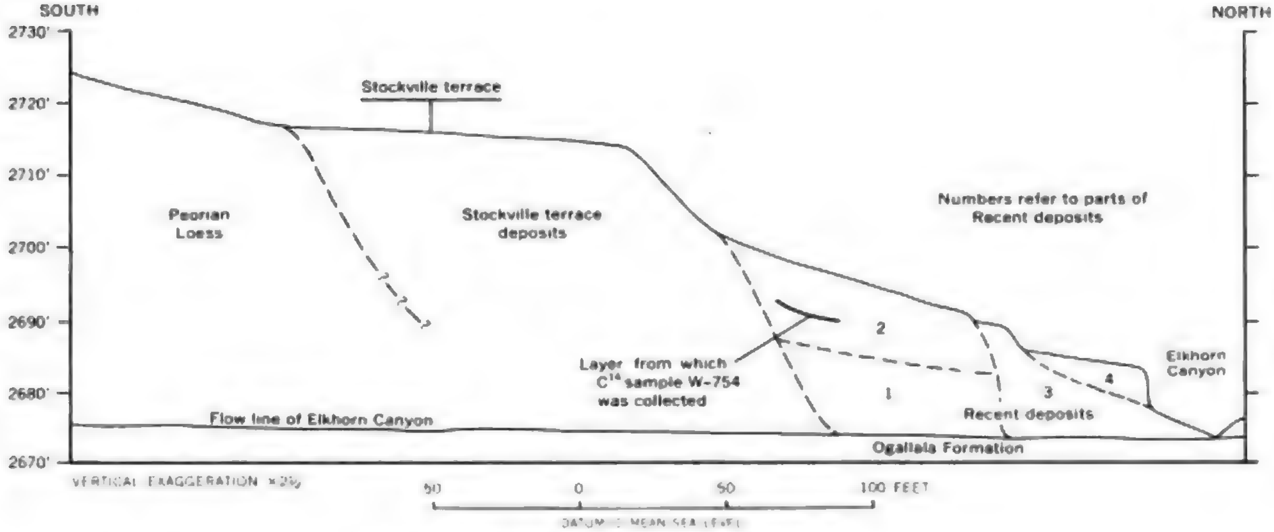

FIGURE 189.—Profile and geologic section on Elkhorn Canyon.

place (according to a carbon-14 age determination) within the past 300 to 400 years.

The late Recent alluvium consists of four parts, which are designated by the numbers 1 through 4 on figure 189. Part 1 is oldest, lightest in color, and most compacted, whereas the younger parts are successively darker in color and less compacted. The contact between part 1 and part 2, which lies at a depth of about 12 feet below the ground surface, is conformable and nearly horizontal. Beneath the contact, the deposits of part 1 show no evidence of erosion or of leaching. Part 2 is characterized by light brownish gray bands of fine sand and silt (2.5*Y* 6/2 moist) alternating with darker grayish brown bands of clayey silt (2.5*Y* 4/2 moist), whose darker colors result from a finer texture and a higher content of organic matter. Part 1 is also banded, but the banding is inconspicuous because of the relatively lighter color of the clay-rich layers. Part 2 is riddled with worm burrows, which are partly filled with castings and dark silt, and many of which terminate in a round cavity partly filled with castings. The darker clay-rich bands seem to have been preferred by the worms, for these bands contain castings in greatest abundance. Worm castings are much less apparent in part 1, although dark vertical streaks, which probably represent the filled burrows of worms, were seen from place to place, and the bedding is apparently riddled by worm burrows. A lens of charcoal and wood ashes, mixed with silt and containing a single large fragment of charred bone, was found interbedded in part 2 at a depth of about 7.5 feet below the ground surface and 3 to 4 feet above the contact with part 1. Charcoal (Geol. Survey sample W-754; analysis by Meyer Rubin) from the lens yielded a carbon-14 date of 420±160 years B.P. (before present).

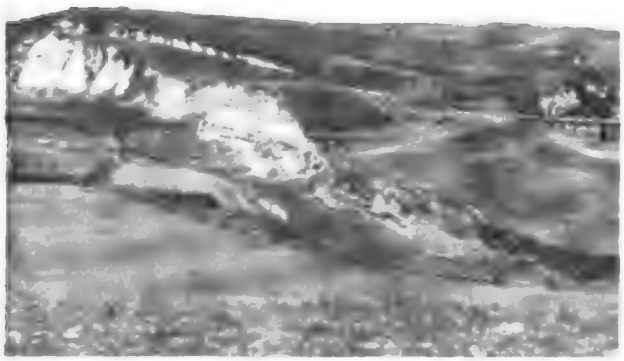

FIGURE 190.—View of terrace sequence and valley fills along Elkhorn Canyon. Prominent scarp marks front of Stockville terrace; lower scarp marks contact between parts 3 and 4 of late Recent alluvium.

Parts 1 and 2 of the late Recent alluvium are described here because the contact between these parts is considered to mark a distinct change in the rate of accumulation of the late Recent alluvium; the rate of accumulation of part 2 is considered to be much the more rapid. Furthermore, the more rapid accumulation of part 2 probably reflects an increase in rate of erosion on the uplands and valley sides. Part 1 is lighter in color because its slower rate of accumulation permitted a greater degree of oxidation of finely divided organic matter, which was originally intermixed with the silt and clay. A slower rate of accumulation of part 1 is also indi-

Digitized by Google

cated by the greater destruction of its sedimentary structures by earth worms. If the described changes from part 1 to part 2 do in fact reflect a change in rate of accumulation, this change took place about 500 years ago, as indicated by the position of the radiometrically dated charcoal. According to archeologic evidence, a period of drought may have begun about 500 years ago, when the region was apparently evacuated by people of the Upper Republican Culture.

Parts 3 and 4 of the late Recent alluvium are dark gray brown (10*YR* 5/2 moist) and show rather distinct banding. Carbonized fragments of grass stems, having an average length of about 0.5 mm, are scattered throughout, but they are more abundant in the darker, clay-rich bands. Dark laminae formed of ashes and charcoal, which probably represent the debris from grass fires, were seen from place to place. Much of the alluvium seems to have passed through the digestive tracts of earth worms, whose castings dominate the texture and account for the loose consolidation.

The steeply dipping erosional contact that separates parts 1 and 2 from part 3 is attributed to the passage of a major gully head scarp along the valley of Elkhorn Canyon. Part 3 of the late Recent alluvium, which was deposited in the gully left by this head scarp, was in turn trenched by a second head scarp following consecutively behind the first. The former sides of the trench made by the second head scarp are represented by a pair of low terraces that were traced (on aerial photographs) to their terminus about 3 miles upvalley. Deposits formed behind the second head scarp (part 4) were in turn trenched by a third head scarp following consecutively behind the second. In 1952 the third head scarp was 13,300 feet upvalley from this locality, and it advanced about 500 feet during the period 1937–52.

Relatively little time is required for the formation of a series of low terraces by the passage of consecutive gullies, because deposition is rapid on the floor of a gully and the head scarps travel rapidly as a result of concentration of flow on the gully bottom. The average rate of advance of the third head scarp during the period 1937–52 is probably conservative, partly because the head scarp has reached bedrock. An average advance of about 200 feet a year, attained by some head scarps in the Medicine Creek basin during the period 1937–52, would be adequate to account for passage of the events described during a period of about 350 years. On the other hand, these events would not likely be compressed into a period of much less than 350 years.

LOVELAND FORMATION AND SANGAMON SOIL

The most useful and distinctive soil marker within the Pleistocene deposits is the Sangamon soil, which is developed on the Loveland Formation. No other soil in the region, including the modern soil, approaches the Sangamon in depth of profile or in degree of development of the C_{ca} horizon. On the uplands the Loveland consists of loess, which mantles the valley sides and merges into contemporaneous valley-fill deposits of silt and sand. The maximum observed thickness of Loveland in the Medicine Creek basin is 35 feet (along Cedar Creek), and the average thickness is about 20 feet. At some exposures in valleys, the Loveland is missing and the Sangamon soil is developed on the Ogallala Formation.

Moist loess of the Loveland is typically light yellowish brown (10*YR* 6/4), but darker colors (10*YR* 5/3 and 10*YR* 5/4) were observed at some localities. The Sangamon soil, as observed from a distance, is a distinct dark-brown humus-rich band that separates loess of the Loveland from the distinctly lighter colored loess of the Peorian. (See fig. 191.) This band ranges from about 4.5 to about 2 feet in thickness and from yellowish brown (10*YR* 5/4) where the soil is weakly developed to very dark gray brown (10*YR* 4/3) where it is strongly developed. A C_{ca} horizon is nearly everywhere present in the soil, but its depth below the dark band ranges from about 2 feet in some localities to about 25 feet in others, and its thickness is also variable. The variations indicate that development of the Sangamon in some localities was nearly continuous, whereas in other localities the developing soil was intermittently buried by fresh accumulations of silt.

In spite of the conspicuous development of the humus-rich part of the Sangamon soil profile, it contains an abundance of fresh ferromagnesian min-

FIGURE 191.—Valley fill of the Peorian Loess set unconformably against Sangamon soil and Peorian Loess. Steeply dipping unconformity, indicated by arrows, is exposed on either side of the small valley, and the valley fill of the Peorian is between the arrows.

Digitized by Google

erals and hence has undergone little chemical weathering. About 20 species of heavy minerals were identified under the petrographic microscope; of these, clinozoisite, green hornblende, apatite, and brown hornblende are by far the most abundant. In addition, calcic feldspar (labradorite) was identified among the light minerals.

PEORIAN LOESS, BRADY SOIL, BIGNELL LOESS, AND MODERN SOIL

An account of the involved history of the terms "Peoria" and Peorian has been given by Leonard (1951, p. 323). In this report, the term Peorian Loess is applied to deposits that are stratigraphically above the Sangamon soil and terminate in the Brady soil. The absolute time at which the Sangamon Interglaciation ended has not been determined, but a reasonable estimate can be made by extrapolating from existing carbon-14 dates; the estimate of Frye and Willman (1960, p. 2) is between 50 and 70 thousand years B.P., as measured by carbon-14. The Brady soil has been dated, by means of a carbon-14 age determination on organic carbon from the A horizon of the soil, at 9,160±250 years B.P. (Rubin and Suess, 1956, p. 443). This date is probably too young because of root hairs in the sample.

In general, the Peorian Loess mantles the whole of the Medicine Creek basin except the modern valley flats and the Stockville and Mousel terraces. On the uplands the Peorian consists of massive silt, which grades laterally (at least at the surface) to fine sand in the vicinity of dune areas. This massive silt is called loess because its topographic position indicates that it is eolian and because the snails that it contains are not aquatic. In valley locations also, the greater part of the thickness of the Peorian consists of massive silt, except in the valleys in the vicinity of dune areas, where it consists of silt and fine sand. The lowermost 10 to 20 feet of the Peorian in the valleys commonly consists of silt interbedded with fine gravel, silty clay, or sand; and this lowermost part contains, in some localities, aquatic snails or pelecypods. The massive silt of the valleys is not called loess because its agent of deposition is not apparent. Where a vertical face cut in this silt is exposed to wind and rainwash, it commonly shows well-defined lamination that could be attributed either to wind or to water. Eolian deposition of silt on the uplands was probably accompanied by an equal or greater amount of eolian deposition in the valleys, but the silt in the valleys was probably reworked by water before final deposition. Deposits of the Peorian in valley locations, whether of massive silt or of some other sediment type, are called the valley-fill deposits of the Peorian.

Leonard (1951) recognizes three biostratigraphic zones in the Peorian Loess of Kansas, but these zones are not marked by any physical discontinuities in the loess. The basal zone, which is devoid of molluscan fossils, is overlain by a lower molluscan faunal zone and an upper molluscan faunal zone. Between the upper and lower faunal zones is a transitional faunal zone, which bears elements of both the lower and upper faunal assemblages.

A snail fauna was collected about 25 feet stratigraphically above the Sangamon soil at a locality on Dry Creek to ascertain the approximate position of these faunal zones relative to the total thickness of the loess of the Peorian in the Medicine Creek basin. The locality is in the NW¼ sec. 16, T. 9 N., R. 27 W. The stratigraphic position of the fauna is about midway of the total thickness of the loess on Dry Creek. A sample of loess weighing about 25 pounds was collected, and the contained snails were obtained by washing the loess through a sieve. Identification of the snails was made by Dr. W. J. Wayne of the Indiana Geological Survey, and the faunal list is as follows (the number of individuals of each species is given in right-hand column):

Columella alticola (Ingersoll)	2
Discus cronkhitei (Newcomb)	2
shimeki (Pilsbry)	24
Euconulus fulvus (Müller)	2
Pupilla muscorum (Linné)	4
Succinea grosvenori Lea	16
Vallonia gracilicosta Reinhardt	2
Vertigo modesta (Say)	3
tridentata Wolf	10

Of the nine species listed, five belong to the upper and transitional zones of Leonard, and four occur in all three zones. Because of the absence of *S. avara* and the numerical dominance of *D. shimeki* and *S. grosvenori*, which are upper zone species, the assemblage is assigned by the writer to the upper zone. The fauna in this single locality indicates that at least half of the total thickness of the Peorian in the Medicine Creek basin was deposited during the time represented by the upper faunal zone of Leonard. Leonard correlated his upper zone with the Tazewell Stade of the Wisconsin Glaciation.

During accumulation of the Peorian on the uplands, a period of incision to bedrock took place in the valleys. Valley fill of the Peorian that accumulated after this incision is set unconformably against the Loveland Formation, the Sangamon soil, and the lower part of the Peorian. (See figs. 185 and 191, both of which show valley fill of the Peorian set unconformably against the Sangamon soil and

Digitized by Google

the lower part of the Peorian.) From a distance the valley fill of the Peorian looks almost white, whereas the loess of the Peorian that overlies the Sangamon soil has a yellowish cast. On the uplands no physical discontinuity within the Peorian was discerned.

Molluscan fauna collected from the base of the valley fill of the Peorian at two localities indicates that deposition of the valley fill began in Tazewell time. The first locality is on the bank of Dry Creek, about 700 feet upstream from the gaging station, in the SE¼ sec. 24, T. 8 N., R. 28 W. Here the valley fill rests unconformably on the Ogallala Formation. Identification of the fauna was made by the writer, with the assistance of Dr. W. J. Wayne. The faunal list is as follows:

Columella alticola (Ingersoll)
Discus cronkhitei (Newcomb)
shimeki (Pilsbry)
Gyraulus circumstriatus (Tryon)
Physa anatina Lea
Pupilla muscorum (Linné)
Retinella electrina (Gould)
Succinea grosvenori Lea
Vallonia gracilicosta Reinhardt
Vertigo gouldi coloradensis Cockerell
modesta (Say)
Zonitoides arboreus (Say)

According to Leonard (1952, p. 19), *D. shimeki* and *D. cronkhitei* are reliable indexes to the upper (Tazewell) faunal zone of the Peorian. None of the other species in the assemblage is restricted to deposits either older or younger than this upper faunal zone.

A second fauna from the valley fill of the Peorian was collected at the side of Mitchell Creek, near a county road in the NW¼ sec. 9, T. 6 N., R. 26 W. Identification was made by the writer, with the assistance of Dr. W. J. Wayne. The faunal list is as follows:

Discus cronkhitei (Newcomb)
Euconulus fulvus (Müller)
Gastrocopta armifera (Say)
Lymnaea (Stagnicola) palustris (Müller)
Retinella electrina (Gould)
Succinea grosvenori Lea
Vallonia gracilicosta Reinhardt
Vertigo tridentata Wolf

Although this assemblage is different from the assemblage collected from the valley fill of the Peorian on Dry Creek, a correlation with the upper molluscan faunal zone of Leonard (1951, 1952) is indicated by the presence of *D. cronkhitei* and *S. grosvenori*.

The average thickness of the loess of the Peorian in the Medicine Creek basin is about 50 feet, and the maximum thickness is about 80 feet. Thicknesses were measured at exposures in upland localities and from the logs of test wells drilled by the Nebraska Conservation and Survey Division. (See figs. 183 and 184.) The thickness of the loess reaches a maximum in the vicinity of the Platte River, gradually decreases southward to a minimum in a belt which is about 30 miles south of the Platte River and 10 miles north of the Republican River, then again increases in thickness in the direction of the Republican. A well near the north side of the Republican River valley penetrated a thickness of 60 feet of loess, whereas a well near the south side of the valley penetrated a thickness of only 30 feet. About 50 feet of loess of the Peorian is exposed in the vertical wall of a deep pit, 1.5 miles west of Eustice, Nebr. (fig. 192).

The valley fill of the Peorian is thicker than the loess. The exposed thickness of valley fill of the Peorian on the main stem of Medicine Creek, as measured from the surface of the Wellfleet terrace to the modern valley flat, is about 125 feet. On the assumption that the valley fill extends to bedrock, as it does on Dry Creek, the total thickness on Medicine Creek is about 200 feet. On the same assumption, the total thickness on Well Canyon, at a locality about 7 miles north of Curtis, is 180 feet. The exposed thickness in the upper reaches of Dry Creek is 42 feet, and the total thickness is about 65 feet.

Loess of the Peorian in the Medicine Creek basin is a massive friable light-colored silt, similar to loess that has been described in other regions. The loess when dry is typically light gray (10*YR* 7/2) and when moist is light brownish gray or pale

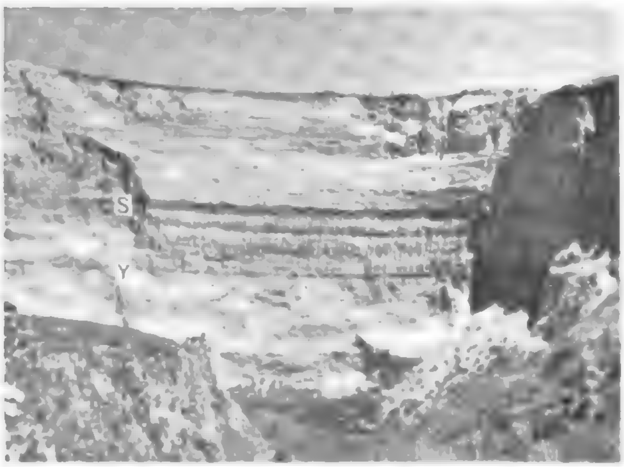

FIGURE 192.—Peorian Loess (50 ft thick) overlying a horizon of Sangamon soil (upper dark band, marked S). Units beneath Peorian Loess are Loveland Formation (20 ft), Yarmouth soil (lowermost dark band, marked Y), Sappa Formation (33 ft), and Pearlette Ash Member of Sappa Formation (20 ft). Excavation, made for removal of Pearlette, is 1.5 miles west of Eustice, Nebr. Photographed by C. H. Hembree, 1956.

Digitized by Google

brown (10*YR* 6/2 or 6/3). Although the loess appears to be homogeneous when viewed from a distance, closer inspection reveals abundant hollow tubules made by rootlets, worm burrows, and small botryoidal structures which are worm castings. Within 5 feet of the ground surface, the loess may show such an abundance of these botryoidal structures as to indicate that all of it has passed through the digestive tracts of earth worms. Snail shells are generally present and are locally abundant. Lamination, although not usually observable, may appear where erosion by wind and raindrops has been sufficiently delicate to etch the laminae into relief.

Thin sections of seven samples of loess of the Peorian, collected at different localities in the Medicine Creek basin, were studied under the petrographic microscope. The most distinctive textural features of loess, when viewed at high magnification, are the rather close packing arrangement and the presence of birefringent clay coatings around detrital silicate grains. Grains larger than 125 microns in maximum diameter constitute less than 1 percent by volume of the samples, and grains larger than 31 microns constitute 55 to 75 percent by volume. Particles larger than 31 microns may be regarded as the framework or skeleton of the loess, and particles smaller than 31 microns may be regarded as the matrix. The clay grain coatings, which are evidently authigenic, may be regarded as cement. The framework grains are mainly separated by their clay coatings and by the matrix. Contacts between framework grains are mainly tangential or long, and an average of about two contacts per grain was observed.

The birefringent clay coatings around detrital silicate grains consist of crystalline flakes oriented parallel with the surface of the coated grain. These coatings merge with the matrix and probably account in considerable part for the coherence of the loess and for the ability of loess to maintain a vertical face. Clay coatings on flat grains, such as mica flakes and glass shards, are in general thicker than coatings on equant grains. Clay coatings on grains are not characteristic of siltstones deposited under water. In loess the coatings are probably formed by wetting and drying of the surface layer during deposition. Kubiena (1938, p. 134) has attributed the formation of grain coatings in soils to such wetting and drying. After rainfall, the soil solution may fill all pore spaces in the soil, but evaporation at the ground surface causes the soil solution to retreat to the angles of the intergranular spaces and to the surfaces of grains. As the soil dries, substances that were peptized or dissolved in the soil solution are left as coatings on grains. Although the grain coatings described by Kubiena were of humus, coatings of clay also probably form by wetting and drying.

In this region loess of the Peorian is generally calcareous, but the calcium carbonate is not uniformly disseminated. Calcium carbonate in the loess occurs in the form of silt-sized grains, which are doubtless primary; as powdery streaks and vein fillings; as fine-grained aggregates that line or fill rootlet tubules, worm burrows, or other openings; and as concretions. Many loess outcrops show zones up to several feet thick that are noncalcareous. Frankel (1957) has reported vertical variations in the distribution and concentration of secondary calcareous concretions and in the abundance and state of preservation of fossil mollusks in the loess in Nebraska. He attributes these variations to an intermittent rate of loess deposition. Slow deposition of loess is accompanied by solution of snail shells and by accumulation of secondary carbonate at depth. Rapid accumulation of loess is indicated by unaltered snail shells. Frankel suggests that many phantom soils are present. The writer has observed that massive silt, accumulated as valley fill and indistinguishable from upland wind-laid loess, is more commonly noncalcareous than upland loess.

The Brady soil was named and described by Schultz and Stout (1948) from a locality on the steep south side of the Platte Valley near Bignell, Nebr. This locality is also the type section for the overlying Bignell Loess (Schultz and Stout, 1945). According to the writer's observations, the humic zone of the type Brady soil is about 1.3 feet thick, and the soil is weakly calcareous throughout; soft streaks and films of carbonate appear to a depth of 2.2 feet from the top of the soil, and these are conspicuous from 1.3 to 2.2 feet. Overlying the Brady soil is a thickness of 8 to 10 feet of Bignell Loess, on which the modern soil is developed. This modern soil is noncalcareous to a depth of 3.2 feet and shows a distinctly columnar structure to a depth of 1.3 feet. Above the modern soil is about 1 foot of lighter silt, evidently colluvial and related to cultivation of fields upslope from this locality. The modern soil appears to be more strongly developed than the Brady soil.

In spite of the fact that Medicine Creek basin is adjacent to the type locality of both the Brady soil and the overlying Bignell Loess, the Brady soil, as separately developed from the modern soil, was observed at only three exposures, all in the northern part of the basin.

Digitized by Google

General deposition of a thin layer of Bignell Loess over the uplands of the Medicine Creek basin is indicated by abnormally thick A horizons that commonly appear in the modern soil. The modern soils of Lincoln County, Nebr., have been mapped and described by Goke and others (1926); and the soils of Frontier County, Nebr., by Bacon and others (1939). The Medicine Creek basin lies within these two counties. Principal soils of the loess-mantled areas are the Holdredge very fine sandy loam and the broken phase of the Colby very fine sandy loam. The Holdredge soil, which is developed mainly on areas of flat or rolling upland, is mature. The B horizon of the Holdredge lies between 10 and 24 inches in depth and shows an imperfectly developed columnar structure; and the C_{ca} horizon, which contains a concentration of carbonate in the form of streaks, splotches, or threads, lies between 3 and 4 feet in depth. A dark-brown zone, probably representing the Brady soil, lies between the B horizon and the C_{ca} horizon at many localities.

STOCKVILLE TERRACE DEPOSITS

Typical relations of the Stockville terrace deposits to other stratigraphic units are shown in figure 185. Along major valleys, the unconformity between the Stockville terrace deposits and older units is rarely marked by a scarp; if one were originally present, it has been obliterated by erosion on the valley-side slopes. Along minor valleys, the unconformity is usually marked by a distinct scarp.

The Stockville terrace deposits consist mainly of calcareous silt. In minor valleys the silt is less compact, the color is darker, and the bedding is less well defined than in major valleys. Dark humus-rich bands, beneath which the silt is leached to a depth of a foot or two, are observable at most exposures of the Stockville terrace deposits. The depth of burial of the uppermost band ranges, in different parts of the basin, from about 2 to 20 feet; and the number of bands varies from one exposure to the next. These bands, together with the underlying leached zone, probably represent immature soils that formed during periods of slow deposition. The Stockville terrace deposits occur in nearly all valleys of the present drainage system, including valleys of first order. The thickness, which depends on the size of the valley, is about 100 feet along Medicine Creek and Well Canyon, about 60 feet along Lime Creek, and about 30 feet along Dry Creek.

A fauna of snails and pelecypods was collected from the Stockville terrace deposits exposed along Medicine Creek in the NE cor. sec. 13, T. 6 N., R. 27 W. According to Dr. W. J. Wayne, who identified the fauna, none of the species is extinct, and all are fresh-water species that now inhabit parts of central United States. Leonard (1952, p. 16) concludes, from his study of Bignellian molluscan faunas in Kansas, that the environment of Bignell Loess deposition was very much like present conditions in the Great Plains. The Bignell Loess is considered by the writer to be the upland counterpart of the Stockville terrace deposits.

MOUSEL TERRACE DEPOSITS

The Mousel terrace deposits consist mainly of silt and differ from the Stockville terrace deposits only by being somewhat darker in color and more compact. In some localities the Mousel terrace deposits contain fragments of carbonized grass stems, which are rare in the Stockville terrace deposits. Along the main course of Medicine Creek, two buried humus-rich bands, which are interpreted to be immature soils, were observed in deposits of the Mousel terrace.

Charcoal suitable for carbon-14 age determination was collected from the Mousel terrace deposits on Dry Creek in the NW¼NE¼ sec. 1, T. 7 N., R. 28 W. The charcoal was in a lens of wood ashes and silt, buried at a depth of 14.5 feet below the ground surface. The age was reported as 2,200±200 years (J. L. Kulp, Lamont No. 239C).

RECENT ALLUVIUM

Where valley trenching has exposed the full thickness of the late Recent alluvium—as at localities on Dry Creek, Cedar Creek, Elkhorn Canyon, and Lime Creek—the alluvium rests on the bedrock floor of the valley. Therefore, at these localities the valleys were incised to bedrock during the episode of incision that followed accumulation of the Mousel terrace deposits. Incision to bedrock may have been confined to localities where the bedrock is high beneath the valley floor. In some valleys, such as Dry Creek and Elkhorn Canyon, accumulation of the late Recent alluvium has been interrupted by one or more episodes of incision during which the valley was trenched for part of its length by the upstream migration of intermittently spaced channel scarps. In other valleys, such as Well Canyon and Fox Creek, accumulation of the late Recent alluvium has evidently proceeded without the interruption of valley incision.

In the upper reaches of Dry Creek, where the previously untrenched valley flat is being trenched by headward migration of a major channel scarp, the silty late Recent alluvium consists of a banded

Digitized by Google

FIGURE 193.—Banding in late Recent alluvium, Dry Creek. (SW¼NE¼ Sec. 29, T. 9 N., R. 27 W.)

upper part, about 14 feet thick, and a lower part that is indistinctly banded and lighter in color. (See fig. 193.) The dark bands of the upper part are somewhat more clayey than the light bands, and the dark color is a result of a finer texture and a higher content of organic matter. Both light and dark bands are composed mostly of loosely consolidated silt, through which abundant fragments of carbonized grass stems are scattered. Earth-worm castings are a conspicuous feature of the upper banded part, but they are less apparent in the more compact silt of the lower part.

A similar division of the late Recent alluvium of Elkhorn Canyon into an upper part that is banded and a lower part that is indistinctly banded has already been described. The banded fill is attributed to a rate of accumulation so rapid that time has not been available for oxidation of finely divided organic matter in the clayey bands. If the accumulation of banded fill began at the same time on Dry Creek as on Elkhorn Canyon, the banded fill shown in figure 193 has accumulated during the past 500 years, approximately. This corresponds to an average rate of accumulation of about 0.34 inch per year, although the appearance of the banding indicates that the rate of accumulation was not uniform.

The banded alluvium seems to be characteristic of valleys that are being actively trenched, whereas the more compact unbanded alluvium is characteristic of more stable valleys. For example, the alluvium beneath the valley flats of Well Canyon and Fox Creek, which are not being actively trenched, is unbanded. On the other hand, distinctly banded alluvium is exposed in the walls of rapidly advancing trenches on Dry Creek and Curtis Creek Canyon.

The present rate of accumulation of alluvium on valley flats must be known in order to relate sediment discharge by streams from the drainage basin (sediment yield) to the amount of sediment that is eroded from uplands and valley-side slopes (gross erosion). In spite of a thorough search, exposures of the late Recent alluvium yielded no artifacts nor other materials that would give an accurate indication of the rate of accumulation. Valley flats in many localities were examined after runoff events, and the depth of accumulation of freshly deposited sediment was measured. The thickness of the freshly deposited silt layer ranges widely (from a fraction of an inch to about 6 in.) from one locality to another, and almost as great a range was observed from place to place at a single locality. Moreover, freshly deposited alluvium may either remain at its place of deposition or be removed during the next runoff event. Farmers were asked about the time required for fenceposts on the valley flat to become wholly or partly buried. In the upper part of Dry Creek, two farmers estimated independently that 5 or 6 feet of sediment had accumulated on the valley flat between 1920 and 1953. On Well Canyon one farmer estimated an accumulation of 2 feet on the valley flat in the past 40 years (1916–56) and another estimated an accumulation of 2 feet in the past 30 years (1926–56). On Medicine Creek, about 4.5 miles north of Cambridge, a farmer reported that the wire of a hogpen, last used before the 1935 flood on Medicine Creek, was buried to a depth of 6 feet by 1957. An average rate of accumulation of about 1 inch per year on the valley flats of the drainage basin is probably of the right order of magnitude. A range between ½ inch and 3 inches is estimated, and this range would be found not only from valley to valley but also from place to place within the same valley.

The rate of accumulation of alluvium within a trenched channel, downstream from an actively advancing channel scarp, must be considered separately from the rate of accumulation on an untrenched valley flat. Examination of freshly deposited alluvium on the floor of trenched channels, several hundred feet downstream from an actively advancing channel scarp, indicates that 0.5 foot or more of alluvium can be deposited during a single runoff event. At several localities on Dry Creek, tin cans and wire were found buried to a depth of several feet in alluvium that had accumulated on the floor of the trench. Evidently, alluvium accumulates rapidly

Digitized by Google

in trenched channels but is susceptible to removal by a second episode of trenching.

SIGNIFICANCE OF CARBONIZED FRAGMENTS OF GRASS

In this region the younger a fluvial deposit is, the darker is its color. The dark color is due in part to finely divided organic matter and in part to fragments of carbonized grass stems, which are more abundant in the younger deposits. The carbonized fragments are attributed to grass fires, inasmuch as uncarbonized plant fragments would decay in this environment. The scarcity of carbonized stems in the older deposits might mean that grass fires were uncommon during the deposition of these deposits, or it might mean that any fragments originally present have been destroyed by oxidation or by the activities of earth worms. In an effort to decide between these alternatives, five thin sections of the Stockville terrace deposits, one thin section of the Mousel terrace deposits, and two thin sections of the late Recent alluvium were examined. In mineralogy, degree of development of clay coatings around grains, and packing of particles, all these thin sections were similar to thin sections of loess. However, the upper Recent alluvium shows many open spaces, which are attributed mainly to the activity of earth worms. Although carbonized fragments in the Stockville terrace deposits are small, they show no signs of partial oxidation. The tentative conclusion is that grass fires were more common during deposition of the Mousel terrace deposits and the upper Recent alluvium than during deposition of the Stockville terrace deposits. A greater incidence of grass fires might reflect a drier climate, or it might reflect a greater use of fire drives as a method of hunting game. The extent to which fire drives were used by prehistoric man on the Great Plains is largely speculative (Wedel, 1961, p. 76).

SAND DUNES

The sand dunes within the Medicine Creek basin are part of a much larger dune area that is an outlier of the Sandhills of Nebraska. The geomorphology of the Sandhills has been briefly described by Smith (1955). In general, the dune relief in the Medicine Creek basin is irregular and hummocky, dominated by innumerable blowouts, most of which are stabilized by grass. However, an indistinct linear pattern was observed in aerial photographs of areas about 7 miles north and 10 miles northwest of Wellfleet. The pattern is made by low, discontinuous longitudinal dunes in subparallel arrangement. The dunes have a maximum length of about one-fourth of a mile, an average width of about 200 feet, and heights ranging from 10 to 30 feet; they show the furrowed crest that is typical of longitudinal dunes in the Sandhills. They are probably relicts of a more extensive dune system that has in most places been destroyed by blowouts but has in some places been modified into U-shaped dunes. Although the longitudinal dunes are oriented about N. 65° W., the ends of most of the U-shaped dunes are oriented more northerly. Elongated blowouts tend to be oriented at about N. 20°–30°W. Evidently, the prevailing wind direction has shifted since the formation of the longitudinal dunes. Most of the blowouts are clearly man induced, for they are associated with areas that formerly were or currently are cultivated.

The stream-dissected relief of the loess-mantled part of the basin is separated from the sand-dune relief by a transitional belt of ground that is intermediate both in relief and in particle size of underlying materials. The relief of this transitional belt is characterized by broad undrained depressions, generally elongated northward and separated by nearly level ground or by broad, rounded elevations. The underlying material, which is intermediate in particle size between dune sand and loess, is restricted to upland locations. The mixture of dune sand and loess, on which the Anselmo fine sandy loam and the Colby fine sandy loam are developed, is generally less than 3 feet thick and is underlain either by dune sand or by loess (Goke and others, 1926; Bacon and others, 1939). Because of seasonal shifts in wind direction, silt from the loess-mantled areas has become mixed with sand from the dune areas.

In general, the dune sand does not seem to have transgressed very much over the loess-mantled areas since the end of deposition of the Peorian—that is, within the past 12,000 years. In areas bordering the Sandhills, the surface of the Wellfleet terrace is generally free of windblown sand.

ARCHEOLOGY AND HUMAN OCCUPATION

RESULTS OF ARCHEOLOGIC INVESTIGATIONS

Archeologic investigations have been made in the Medicine Creek basin by the Nebraska State Historical Society, by the Nebraska State Museum, and by the River Basin Surveys of the Smithsonian Institution. Three cultural aspects have been distinguished. These are represented by the Early Lithic sites, which are buried about 35 feet beneath the surface of the Stockville terrace (Terrace-2); by Woodland sites on the Mousel terrace (Terrace-

1); and by Upper Republican sites on the Stockville terrace.

Personnel of the University of Nebraska State Museum have excavated two sites on Lime Creek, designated Ft–41 and Ft–42, and one site on Medicine Creek about a half a mile downstream from the mouth of Lime Creek (Ft–50). All these sites are in the lower part of the Stockville terrace (Terrace-2) at occupation levels marked by abundant artifacts and many hearths. No human remains were found. Schultz and others (1951), who investigated both the geologic and archeologic aspects of the sites, report dates of 9,167±600 years B.P. and 9,880±670 years B.P. from two charcoal samples taken from the bone-artifact zone of site Ft–41. A charcoal sample from the lower occupation zone of Ft–50 yielded a date of 10,493±1,500 years B.P.

Two Woodland sites in the Medicine Creek Dam area are described by Kivett (1949). Habitation areas (marked by shallow basins, post molds, shallow pits, flint tools, and scant pottery fragments) were on the Mousel terrace (Terrace-1) and were covered by about 18 inches of silt. The remains give Wedel (1949) the impression of a rather uncertain hold on the region by a culturally simple group. According to Kivett, calcite-tempered ware found at the site is a marker for the Keith focus, which is one of several western Woodland cultural complexes. Although no radiocarbon dates were obtained at the Woodland sites on Medicine Creek, a radiocarbon date of 1,343±240 years B.P. has been obtained from a Keith-focus site on Prairie Dog Creek in northern Kansas, about 60 miles southeast of the Medicine Creek sites (Wedel and Kivett, 1956).

The Upper Republican Aspect represents the latest wholly prehistoric culture on Medicine Creek and is the most abundantly represented by archeologic remains, which are on the Stockville terrace and are buried under a silt mantle 6 to 18 inches thick (Kivett, 1949). The date of the culture is estimated to be about 500 to 600 years B.P. (Kivett, oral commun., 1957).

The geologic significance of these archeologic researches may now be considered. Radiocarbon dates on charcoal from occupation levels in the lower part of the Stockville terrace indicate that deposition of the Stockville terrace deposits began about 10,000 years ago. If the Woodland sites on the Mousel terrace do indeed belong to the Keith focus and if this focus is correctly dated, then the terrace is older than 1,300 years. The silt mantle ranging in thickness from 6 to 18 inches covers Woodland sites on the Mousel terrace and Upper Republican sites on the Stockville terrace. Most of the sites are not adjacent to upland areas from which colluvium might be readily derived, and no fluvial sedimentary structures were observed. Probably most of the silt was deposited on both cultural sites by the wind after the passing of the Upper Republican Aspect—that is, during the past 500 years. Conditions under which the silt was deposited were of more than local magnitude, as the silt mantle appears on Upper Republican sites throughout the Republican River basin in southern Nebraska from Frontier County eastward to Webster County (Wedel, 1941). Probably the Upper Republican people inhabited the region during a wet period and emigrated about 500 years ago at the onset of a dry period. During the wet period a humic zone developed, which was buried by windblown silt accumulated during one or more later dry periods.

SETTLEMENT AND LAND USE

One of the first settlers of the basin came to the Stockville area in 1860. His dwelling was used for the formal organization of Frontier County in 1872, when the population of the county consisted of a few stockraisers and only two permanent settlers. Through the later 1870's, settlers gradually entered Frontier County, and a little village arose at Stockville. By 1880 farmers had begun to claim land and to settle on the divides. Until the Free Range Law was repealed in 1885, farming on the uplands was of little consequence. By 1900 most of the desirable land had been taken under the Homestead, Timber Claim, and Preemption Acts.

Bacon and others (1939) note that corn has been the main crop since farming began. The first settlers did not understand how to adjust their farming methods to the highly variable precipitation, and their practices were crude and wasteful. A series of dry years, accompanied by plagues of grasshoppers, culminated in the disastrous droughts of 1893 and 1894. Many of the early farmers were forced to leave the region, and agricultural development was delayed. The farmers who remained acquired larger holdings and gradually adjusted their farming methods to local conditions. Although corn remained the most important crop, increasing amounts of wheat, oats, rye, barley, and sorghums were grown.

Census figures have not been published for the basin as a unit, but satisfactory approximations of the population may be made from the precinct census. The total population was 7,750 in 1930, 6,400 in 1940, and 5,900 in 1950. The total population of the basin decreased by 23 percent between 1930 and 1950, and the proportion of persons living in the towns has increased from 42 percent in 1930

Digitized by Google

to 51 percent in 1950. Population density of the basin in 1950 was 8.7 persons per square mile.

The number of settlers and domestic animals in the basin before 1875 was too small to have any significant effect on erosion and deposition. The sparseness of the grass cover on the uplands during 1869–72 reported by surveyors cannot be attributed to grazing by livestock. According to the Federal census, cattle and horses in Frontier County increased from about 30,000 in 1890 to about 43,000 in 1935. Farming could have had little geologic importance before 1879, when, according to the Federal census, only about 600 acres in Frontier County had been plowed. Only about 104,000 acres of plowed land was reported in Frontier County in 1889, whereas about 425,000 acres was reported in 1929.

DRAINAGE SYSTEM

EVOLUTION OF THE DRAINAGE SYSTEM

According to the stratigraphic evidence presented in this report, major valleys of the Medicine Creek basin, such as Cut Canyon and Cedar Creek, were in existence during the Kansan Glaciation, and their bedrock floors were at about the same depth as at present. In the Republican River valley also, the bedrock floor has not been deepened since Kansan time according to a geologic section of the river valley near McCook, Nebr. (Bradley and Johnson, 1957 pl. 38). Drilling along two traverses between the Republican and the Platte Valleys (figs. 183 and 184) revealed buried valleys, cut into the Ogallala Formation and filled with pre-Wisconsin deposits. These valleys, which evidently had an eastward trend, were probably filled with alluvium and abandoned in Nebraskan or early Kansan time. Plum Creek, which flows eastward into the Platte River, is probably a relic of the early Pleistocene drainage. Deposits of Pearlette Ash Member of the Sappa Formation of Kansan age are distributed along the valley of Plum Creek and its former westward extension, which was captured by Deer Creek after deposition of the Peorian.

The valleys of most major tributaries (fifth and higher order) were established by incision and probably by extension of the drainage system during the episode of incision that followed deposition of the Sappa Formation. These incised valleys were subsequently filled with the Loveland Formation to levels that are generally 10 or 20 feet above the modern valley flats. Most valleys of lower order than fifth were probably not in existence in Sangamon time, for the Sangamon soil does not dip toward them.

There is no evidence of extension of the drainage system between the end of Sangamon time and the initial deposition of loess of the Peorian, although the valleys may have been incised. After about half of the total thickness of the Peorian had accumulated on the uplands, the valleys were incised to bedrock. The incision was followed by an episode of deposition during which the upper part of the Peorian accumulated in the valleys and on the uplands.

The landscape as it existed at the end of deposition of the Peorian can be reconstructed (fig. 194) from remnants such as those shown in figure 195 (*upper*). In a few places, as for example at the eastern tip of Dry Creek, the valley heads of Peorian time have been preserved. Deposition of the Peorian Loess and development of the Brady soil are tentatively assigned to the interval 60,000 to 12,000 years B.P.

The drainage system was developed to approximately its present pattern and extent during the episode of incision that followed deposition of the Peorian (fig. 194*B*). The incision is perhaps associated with a rapid retreat of late Wisconsin ice sheets and a rather abrupt climatic warming about 11,000 years B.P., the evidence of which is presented by Broecker and others (1960). Valleys were probably incised to about the same bedrock altitudes as during previous erosional episodes, but drainage was gradually increased. The extent of incision and increase in drainage density is strikingly shown in an area just outside the Medicine Creek basin, where the head of North Plum Creek was captured by Deer Creek. Although the Deer Creek drainage was incised about 100 feet below the surface of the Peorian, the North Plum Creek drainage just east of the point of capture was not incised, and the surface of the Peorian has been preserved almost intact. (See fig. 196.)

The lengthy duration of the episode during which the Stockville terrace deposits accumulated is indicated by extensive grading of valley-side slopes and valley heads to the level of the Stockville terrace. In profile, the valley-side slopes that join the Stockville terrace to the upland are straight for most of their length, gently convex upward at their intersection with the upland and gently concave upward at their intersection with the terrace. Most of the slopes are graded across the Peorian, but some are graded across older rock units, including the Ogallala. Accumulation of the Stockville terrace deposits and grading of slopes are assigned tentatively to the interval between the climatic warming of about 11,000 years B.P. and the middle of the Altithermal, about 5,000 B.P. The Stockville terrace and slopes graded to the terrace can be identified nearly every-

Digitized by Google

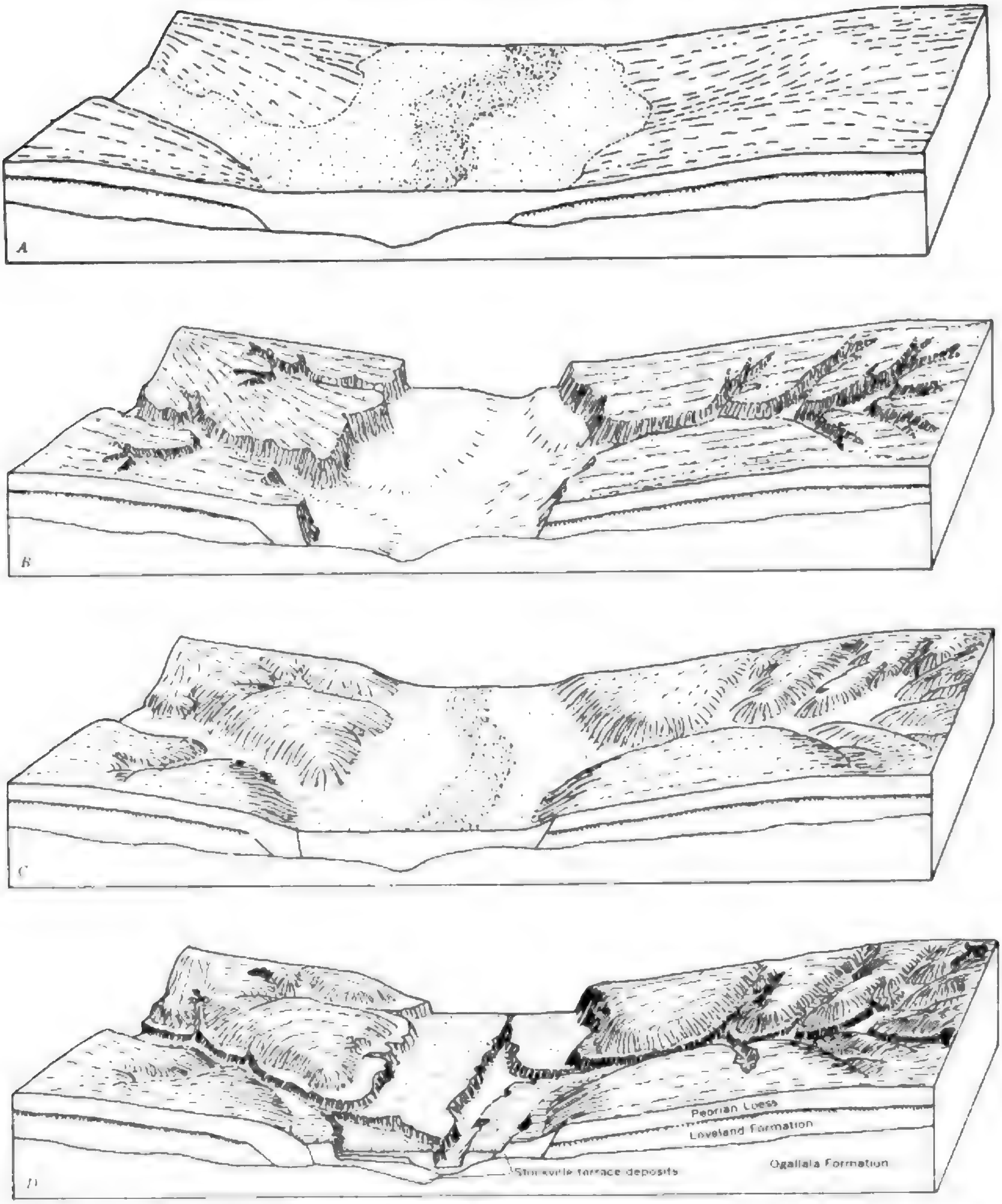

FIGURE 194.—Evolution of the relief since deposition of the Peorian Loess. *A*, Valleys were broad and valley sides gently sloping at end of deposition of the Peorian, about 12,000 years B.P. *B*, Drainage system was incised, extended, and branched during episode that lasted from about 12,000 to 11,000 years B.P. *C*, Valley sides and valley heads were graded during accumulation of Stockville terrace deposits, from about 11,000 to 5,000 years B.P. *D*, Relief was modified during the several episodes of incision and deposition that occurred during the past 5,000 years.

Digitized by Google

FIGURE 195.—Remnants of the side slopes and valley flats of former drainage systems. *Upper*, Looking south from the Platte-Republican drainage divide (in the NE¼ sec. 31, T. 11 N., R. 28 W.) along a fourth-order tributary to Fox Creek. Remnants of the valley sides of Peorian time are preserved on the divides between side tributaries, and these remnants show the general aspect of the former valley. *Middle*, Looking north along Well Canyon in the SW¼ sec. 27, T. 10 N., R. 29 W. Gentle slope on horizon (left) is slope of valley side of Peorian time. Steeper converging slopes on horizon (left center) are slopes of valley side of Stockville time. Remnant of the valley flat of Stockville time is in middle distance, and below this is a remnant of the valley flat of Mousel time. Narrow trench on modern valley flat showed little or no change from 1937 to 1952. *Lower*, Looking southeast from the upper end of a fifth-order tributary to Cut Canyon, in the NE¼ sec. 26, T. 10 N., R. 29 W. Crest of interstream divides between side tributaries in background indicate approximate level of valley flat of Peorian time. Valley head in foreground was graded in Stockville time, as were the steep side slopes leading to it.

where in the basin and constitute a reference surface to which the incision of later erosional episodes can be related.

The Stockville terrace was formed at some time before 2,200 years B.P., which is the carbon-14 date obtained from Mousel terrace deposits on Dry Creek. Tentatively, the Stockville terracing is placed at about 5,000 years B.P., and the cause is assigned to drought during the Altithermal, which was a well-established warm-dry climatic episode that lasted from about 6,000 to 4,000 B.P. In minor valleys (of fifth and lower order) the effects of this terracing cannot generally be distinguished from the effects of the Mousel terracing. During one or the other of these two episodes of erosion, trenching extended to the heads of many minor valleys. Other minor valleys were trenched for only part of their length, and still others escaped being trenched.

Deposition of the Mousel terrace deposits began at some time before 2,200 years B.P. and ended at some time before 420 years B.P. (carbon-14 date from late Recent alluvium on Elkhorn Canyon). Tentatively, this deposition is assigned to the interval 4,000 to 1,000 years B.P., which corresponds roughly with the dates of the "Deposition 2" described by Miller (1958, p. 38) in his generalized alluvial sequence in Western United States. (See table 2.) The terracing of the Mousel terrace must have been brief, inasmuch as the thickness and properties of the late Recent alluvium indicate that not much less than a thousand years would be required for its accumulation.

A tentative chronology of post-Sangamon depositional and erosional episodes in the Medicine Creek basin is summarized below:

	Years B.P.
Local incision of valley bottoms	Present to 500.
Accumulation of late Recent alluvium	Present to 900.
Terracing of Mousel terrace	900 to 1,000.
Accumulation of deposits of Mousel terrace	1,000 to 4,000.
Terracing of Stockville terrace	4,000 to 5,000.
Accumulation of deposits of Stockville terrace.	5,000 to 11,000.
Incision and extension of the drainage system to approximately its present pattern.	11,000 to 12,000.
Accumulation of Peorian Loess and development of Brady soil.	12,000 to 60,000.

MORPHOMETRY

Detailed measurements were made of the drainage basins of six major tributaries of the Medicine Creek basin, the locations of which are shown in figure 176. The purpose of the measurements was to determine the drainage-basin characteristics that correlate most closely with water and sediment yield and with the development of gullies. Where gaging

Digitized by Google

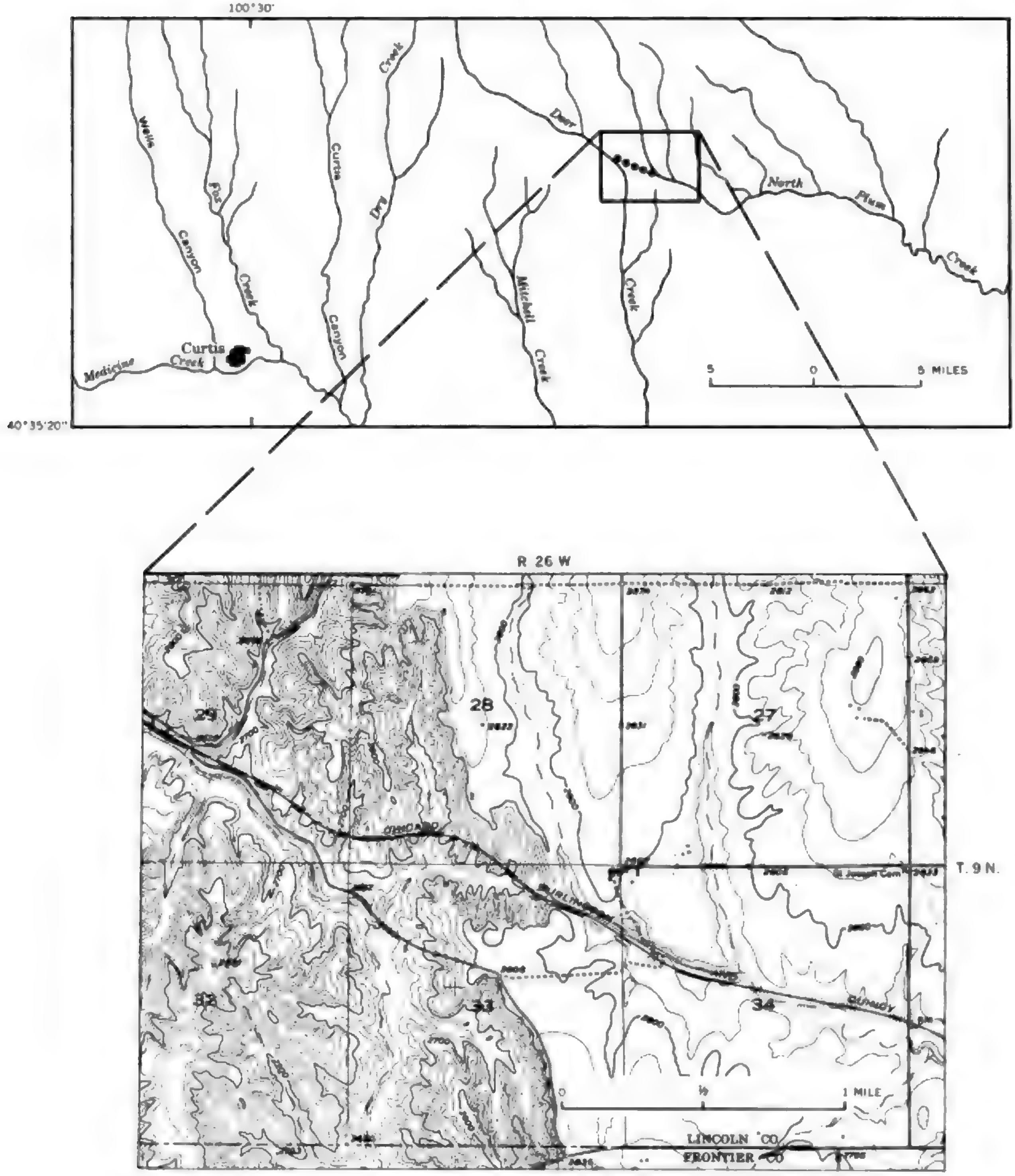

FIGURE 196.—Capture of head of North Plum Creek by Deer Creek. In inset, which is reproduced from the Stockville NE quadrangle, relict topography of the depositional surface of Peorian time is shown at right.

stations (also shown on fig. 176) are not at the mouth of a basin, only that part of the basin upstream from the station was measured.

Ordering of the drainage system was carried out according to the method of Strahler (1952, p. 1,120), which is a modification of the method of Horton (1945, p. 281). Strahler's method is not only more objective and convenient, but it is also more valuable for many hydrologic purposes. A channel segment of third or higher order obtained by Strahler's method is of approximately uniform cross-sectional area throughout its length, but this is not true of channels obtained by Horton's method. The word "channel" is used here in the same sense that the word "stream" is used by Horton and Strahler in connection with ordering. A channel is an established watercourse that may transmit water continuously, intermittently, or ephemerally. The flow of water in most channels of the Medicine Creek basin is ephemeral, and the term "stream" is inappropriate for them.

Properties of fluvially eroded landforms and recommended symbols for these properties are summarized by Strahler (1958, p. 282–283). The properties discussed in this report and the symbols used are listed below. Measured properties are those that can be directly measured or counted, and derived properties are those that cannot be directly measured but must be computed from measurements.

Measured properties:

- Total area of drainage basin, A
- Area of upland in drainage basin, Aa
- Area of valley system in drainage basin, A^* ($A^* = A - Aa$)
- Channel order, u (for examples: u_1, first order; u_2, second order)
- Number of channels of order u, N_u
- Channel length, L
- Channel length, mean length of segments of order u; L_u
- Basin relief, H
- Basin length, L_b

Derived properties:

- Channel slope, S_c
- Valley slope, S_v
- Bifurcation ratio, R_b

$$\left(R_b = \frac{N_u}{N_{u+1}} \right)$$

- Channel length ratio, R_L

$$\left(R_L = \frac{L_u}{L_{u-1}} \right)$$

- Channel frequency, F_u

$$\left(F_u = \frac{N_u}{A} \right)$$

- Adjusted channel frequency, F^*_u

$$\left(F^*_u = \frac{N_u}{A^*} \right)$$

- Drainage density, D

$$\left(D = \frac{\Sigma L}{A} \right)$$

- Relief ratio, R_h

$$\left(R_h = \frac{H}{L_b} \right)$$

- Elongation ratio, R_e

$$\left(R_e = \frac{\text{diameter of a circle}}{L_b} \right)$$

For practical purposes first-order channels in the Medicine Creek basin are defined as the lowest order of channels represented by V-shaped bends in contour lines on the available topographic maps. Fortunately, the accuracy of the topographic maps in representing small drainage channels is excellent, and the scale (1:24,000) and contour interval (10 ft) are also favorable for representation of small channels. Drainage patterns of several fifth-order basins were plotted both on aerial photographs and on topographic maps, and comparison showed that results obtained by the two methods were very similar.

Nearly all the first-order channels represented by V-shaped bends in contour lines are channels that formed immediately before or during accumulation of the Stockville terrace deposits, and the valley sides leading to these channels show some degree of grading. In only a few places has modern gullying proceeded far enough to form channels where no channels had existed previously.

Each of the six major subbasins was separately outlined on the topographic maps, and each subbasin area was measured with a polar planimeter. In addition, the area of upland in each subbasin was measured. Upland is defined as undissected remnants of the land surface that existed at the end of deposition of the Peorian. For practical purposes upland is distinguished on topographic maps by smooth contour lines—that is, by contour lines that do not have V-shaped indentations. Where areas of upland are continuous around the periphery of a drainage system—as in basins I–1′, A′, 0–4′, and C–2′ of figure 197—the area of upland was determined by measuring with a polar planimeter the area actually occupied by the drainage system and subtracting this area from total basin area.

For Dry Creek and Lime Creek, every channel of every order was drawn in color on topographic maps, counted, and measured individually. Sampling procedures, similar to those described by Leopold and Miller (1956, p. 16), were tested for the approximation of number, mean slope, and mean length of first- and second-order channels in the other subbasins. These procedures were used for Mitchell Creek, Well Canyon, Fox Creek, and Brushy Creek.

Digitized by Google

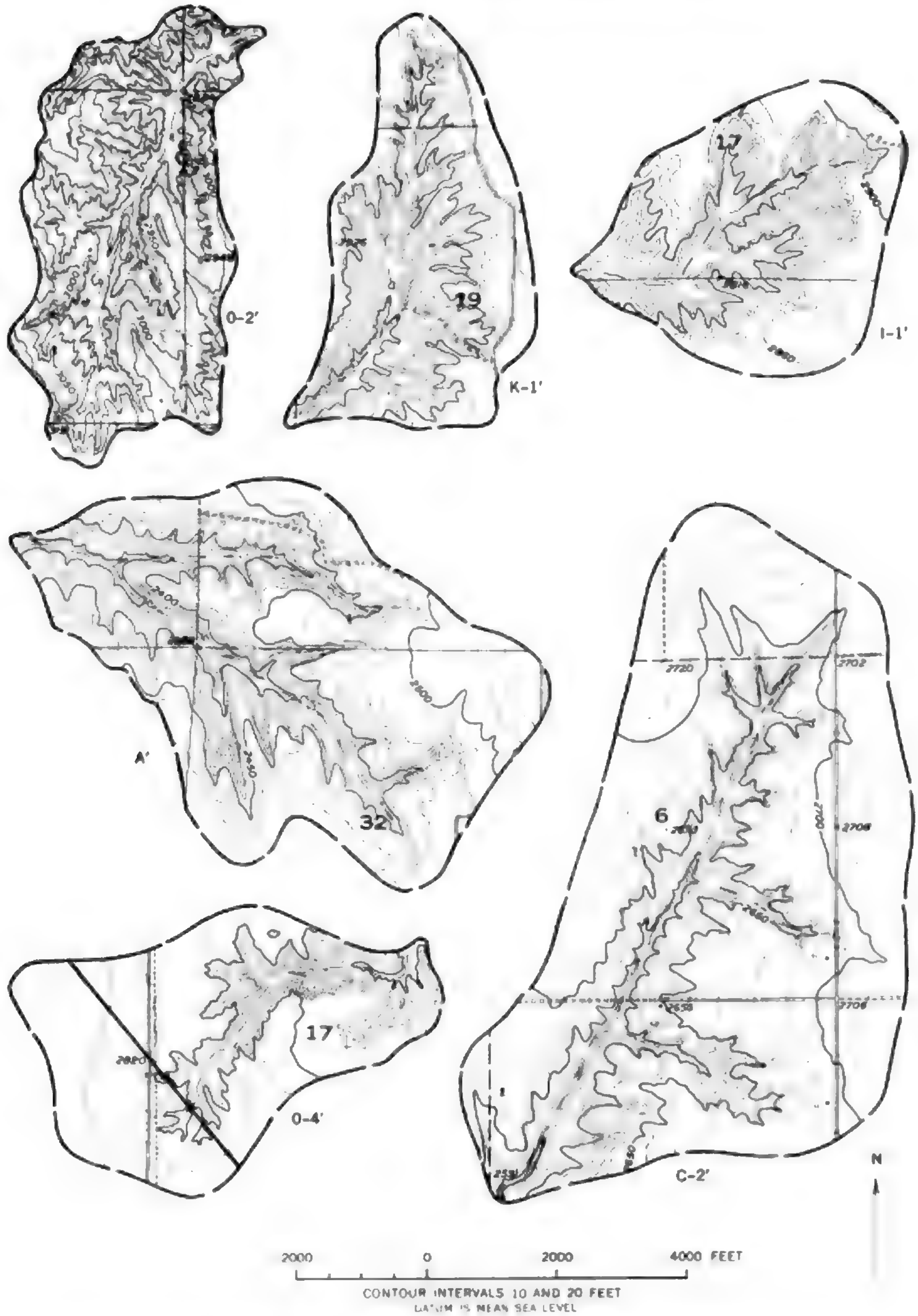

FIGURE 197.—Variations in drainage texture in the Medicine Creek basin. Basins shown are fourth or fifth order.

Two derived properties—drainage density and channel frequency—commonly are used but are ambiguous for so-called immature or youthful basins in which areas of undissected upland remain. For such basins a distinction must be made between the properties of the drainage system and the properties of the drainage basin. If a particular drainage system were transferred without any change in properties to a larger drainage basin, the values of drainage density and channel frequency would change regardless of the constancy of the drainage system. Drainage density is also ambiguous for another reason: a drainage system consisting of short channel segments may have the same total channel length as another drainage system that consists of fewer but longer segments. Melton (1958, p. 36) has proposed that the ratio of F/D^2 is constant for mature drainage basins, but this is not true of Medicine Creek, which for the most part is immature. To compare the channel frequency of two immature drainage systems whose drainage basins differ in percentage of upland, drainage basin area must be adjusted by subtracting the area of upland. Channel frequency, expressed as number of channels per square mile of area actually occupied by the valley system, is here called adjusted channel frequency.

Relief ratio was defined by Schumm (1956, p. 612) as the ratio between H, basin relief, and L_b, the longest dimension of the basin as measured parallel to the principal drainage channel. Basin relief is the difference in altitude between the highest and lowest points in the basin. A measure of basin shape, also devised by Schumm, is the elongation ratio, which is derived by dividing the diameter of a circle having area equal to that of the basin by the basin length, L_b.

A measure of mean valley-side slope is difficult to obtain because the side slopes leading to low-order channels are steeper than side slopes leading to high-order channels. For example, measurements on topographic maps indicate that slopes leading to first-order channels on the lower part of Dry Creek have a mean angle of about 25°, whereas slopes leading to the main channel (which is seventh order) have a mean value of about 12°. Slopes leading to the main channel of lower Dry Creek were measured in the field during the preparation of 12 transverse valley profiles. Of 23 slopes, 13 ranged from 8 to 11°, only 2 were greater than 15°, and none were less than 6°. The mean angle was 11.5°; the mean deviation, 3.3°; and the mode, 10°. Mean side slopes of third- and fourth-order channels probably represent the best approximation to mean values for the drainage system as a whole and are, therefore, quoted in table 3.

DRAINAGE TRANSFORMATION AND VARIATIONS IN DRAINAGE TEXTURE

Variations in drainage texture are accompanied by variations in most drainage-basin characteristics. The major variations in drainage texture within the Medicine Creek basin are illustrated by the representative fourth- and fifth-order drainage basins in figure 20. Basins 0–2′ and K–1′ are typical of the upper part of Medicine Creek; I–1′ and 0–4′, of the

TABLE 3.—*Measured and derived properties for the Medicine Creek basin and its major subbasins*

Drainage basin	Total area, A (sq mi)	Area of upland, A_u (percent)	Area of valley flat (percent)	Valley slope of main segment (ft per ft)	Mean valley side slope (ft per ft)	Mean upland slope (ft per ft)	Relief ratio, R_h	Elongation ratio, R_e	First-order channels: Mean length, L (ft)	First-order channels: Mean slope, S_c (ft per ft)	First-order channels: Adjusted frequency, F^*_u (channels per sq mi)
Lime Creek	11.6	37.0	14.0	----	0.179	0.026	0.0114	0.662	410	[illegible]	[illegible]
Mitchell Creek	52.1	51.8	11.5	0.00299	.200	[illegible]	.0050	.416	370	[illegible]	165
Brushy Creek (above gage)	73.3	25.9	16.0	[illegible]	.412	[illegible]	.0064	.724	192	.234	260
Dry Creek (above gage):											
Total	21.1	34.8	14.2	----	.260	.032	[illegible]	.475	267	.187	202
Upper only	[illegible]	25.0	----	.00550	----	----	----	----	260	[illegible]	214
Lower only	8.5	49.5	----	[illegible]	----	----	----	----	287	.160	186
Fox Creek:											
Total	72.5	[illegible]	27.2	.00360	.363	[illegible]	.0059	.446	250	.241	250
Upper only	[illegible]	12.6	----	.00336	----	----	----	----	----	----	----
Lower only	15.5	30.4	----	.00310	----	----	----	----	----	----	----
Well Canyon:											
Total	53.3	20.4	[illegible]	.00296	----	.036	[illegible]	.336	245	.251	[illegible]
Upper only	[illegible]	12.9	----	.00290	----	----	----	----	----	----	[illegible]
Lower only	30.6	26.5	----	.00284	----	----	----	----	----	----	220
Medicine Creek above gage above reservoir	549.0	[illegible]	----	----	----	----	.00436	----	----	----	200

Digitized by Google

central part; and A′ and C–2′, of the lower part. Major differences in these small basins, as in the larger subbasins of which they are representative, lie in the percentage of upland, the length and frequency of first-order channels, and relief ratio. These differences can be conveniently related to differences in geomorphic history.

In basins A′ and C–2′ valleys at the end of Peorian deposition were broad and shallow, and the gently sloping valley sides were graded all the way to the interstream divides. Divides were rounded, and no areas of flat upland remained. These valleys were deeply incised during the episode of erosion that preceded deposition of the Stockville terrace deposits, and channel frequency was increased. During accumulation of the Stockville terrace deposits, the transformed drainage system was smoothly graded, and the gently sloping tips of first-order tributaries were extended nearly to the former drainage divides. Basin C–2′ represents a less advanced stage of grading than Basin A′, which is nearer the mouth of Medicine Creek; it was incised first, and consequently underwent a longer period of grading during accumulation of the Stockville terrace deposits.

Basins I–1′ and 0–4′ are representative of the central part of the Medicine Creek basin, where the valleys at the end of deposition of the Peorian were more narrow than those in the lower part and were separated by broad, nearly flat uplands. Later, these valleys were deeply incised, and the drainage was extended into the upland; however, large areas were left undissected. The sides and heads of first- and second-order valleys were smoothed and somewhat reduced in angle during deposition of the Stockville terrace deposits, but they remained rather steep. The surface into which basin 0–4′ was incised is unusually flat, because it represents the valley flat and gently sloping valley side of Medicine Creek at the end of deposition of the Peorian.

In basin 0–2′, valleys at the end of deposition of the Peorian were narrow and steep sided (average slope angle about 14°). The channel frequency, already considerably higher than that in the lower part of Medicine Creek, was greatly increased during the episode of incision preceding deposition of the Stockville terrace deposits. Moreover, the newly incised valleys, although somewhat graded during Stockville time, retained their steep sides and heads. Later episodes of incision have further increased the frequency of first- and second-order channels. Basin K–1′ is similar in history, but it formed on a less steeply sloping surface and underwent a greater degree of grading during the deposition of the Stockville terrace deposits.

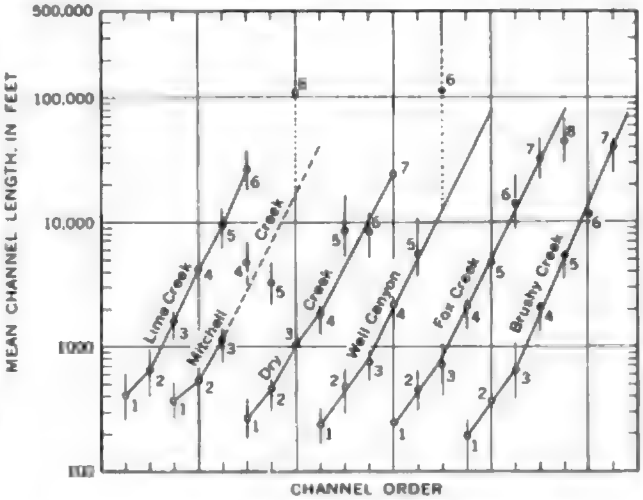

Figure 198.—Mean channel length in relation to channel order.

In summary, variations in the modern drainage pattern are related to two conditions that existed at the end of deposition of the Peorian—the extent of drainage transformation that preceded deposition of the Stockville terrace deposits and the amount of grading that took place during deposition of the Stockville terrace deposits. To a minor extent, the drainage pattern has been modified by episodes of incision that followed deposition of the Stockville terrace deposits. At the end of Peorian deposition, valleys were broad and shallow in the lower part of the basin, narrow and separated by flat divides in the central part, and narrow but separated by narrow divides in the upper part. Grading during deposition of the Stockville terrace deposits reached an advanced stage in the lower part of the basin, and in general the stage of grading decreases in an upstream direction.

The curves representing the relation of mean channel length to channel order (fig. 198) can be arranged in a sequence that illustrates some of the major variations in drainage texture. The length of channel segments (of orders one through five) shows a consistent decrease from Lime Creek, in the lower part of the basin, to Brushy Creek, in the central part. Also, R_L between orders one and two, as well as between orders two and three, is less than R_L between higher orders. The change in slope at the lower end of the curves applies only to orders one and two for Lime Creek, but it applies to orders one through four for Dry Creek and to orders one through three for Well Canyon, Fox Creek, and Brushy Creek.

An upward concavity of the curves representing the relation of mean channel length to channel order,

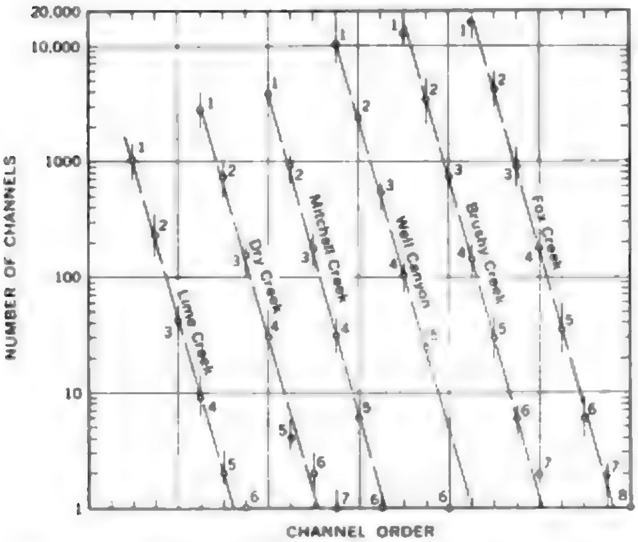

FIGURE 199.—Number of channels of each order in relation to channel order.

as plotted on semilogarithmic paper with channel order as independent variable, was noted by Strahler (1952) and Broscoe (1959, p. 5). Broscoe concluded that Horton's (1945) "law of stream lengths" may not apply when Strahler's method of ordering the drainage system is used. However, the basins analyzed by Strahler and Broscoe were of fourth or smaller order; basins of larger order must be analyzed for proper definition of the relation. In the Medicine Creek basin the relation is exponential, but the exponent changes at second or third order (fig. 21).

If a drainage system having low density of channels is transformed by the growth of new first- and second-order channels without extension of the higher order channels, a marked absolute shortening of lower order channels can take place without much shortening of higher order channels. The order of higher order channels may change, but the absolute length remains nearly constant. A transformation of this kind took place in the Medicine Creek drainage basin at the end of deposition of the Peorian. Furthermore, the transformation can take place without much change in the bifurcation ratio. The bifurcation ratios of the same subbasin, as well from one subbasin to another, are remarkably constant. (See fig. 199.) One result of a transformation of the kind described is a change in slope, at lower channel orders, of the curve relating mean channel length to channel order. The major subbasins that have undergone the greatest drainage transformation and, consequently, have the highest frequency of first-order channels are those that show the change in slope extending to third or even fourth order. In a sense the change in slope of the curve relating mean channel length to channel order is a measure of disequilibrium of the drainage system.

GULLY EROSION

DEFINITION AND CLASSIFICATION OF GULLIES

In a region such as the Medicine Creek basin, where many of the drainage channels have steep, unvegetated sides and are incised in massive silt, the distinction of a gully from other drainage channels is difficult. According to general usage, the essential features of a gully are its size (which is larger than a rill), recency of extension in length, steepness of sides and head, incision into unconsolidated materials, and ephemeral transmission of flow. Gullies in the Medicine Creek basin are incised into the sides, head, or bottom of previously established drainageways, which are deepened or extended by development of the gully. The lower limit of depth for a gully is placed at about 2 feet because channel head scarps that are less than 2 feet in height show a very slow rate of advancement. Most of the actively advancing head scarps in the Medicine Creek basin are greater than 6 feet in height. The lower limit of width is arbitrarily placed at about 1 foot. The criterion of recency of extension requires that some evidence be obtained for extension within a period of a few years. Extension can be established by comparison of aerial photographs, by comparison of field measurements made at intervals of a few years, or by indirect evidence observed in the field. If the sides and head of a drainage channel have a slope less than about 45°, the channel is probably not actively advancing and hence would not be considered a gully. In this report the following definition of a gully is followed: A gully is a recently extended drainage channel that transmits ephemeral flow, has steep sides, a steeply sloping or vertical head scarp, a width greater than about 1 foot, and a depth greater than about 2 feet.

The sides and heads of gullies in the Medicine Creek basin are steep slopes, straight in profile, that are here called erosional scarps or simply scarps.

In addition to the erosional scarps at the sides and heads of gullies, other erosional scarps are conspicuous elements of the landscape. These include step scarps on slopes (Brice, 1958), scarps that form the fronts of terraces, and scarps at the base of valley-side slopes. The inclination of a scarp ranges from about 45° to nearly 90°, and the height ranges from a foot to about 40 feet. Generally, the top of a scarp meets the surface into which it is cut at a sharp angle, but the base of the scarp decreases in

slope as it merges with the surface below. The term "channel scarp" is appropriate for a scarp that forms a break in the long profile of a well-defined channel. If a particular channel scarp is the headward terminus of a gully and attention is to be drawn to this fact, the channel scarp may be called a head scarp. Not all gully head scarps are channel scarps. The term "head cut," although commonly applied to the headward terminus of a gully, is unsatisfactory because it may refer either to the scarp at the head of a gully to to the whole gully head. Moreover, a channel may have many scarps along its length, and the designation of several of these as head cuts is confusing. The scarps that form the sides of a gully along its length are here called side scarps.

Study of gullies in the field and on aerial photographs of the Medicine Creek basin has shown that the depth of a gully, its areal pattern, and its rate of growth are more closely related to the topographic position of the gully head than to any other single factor. Of particular significance is the location of the gully head in relation to the previously established drainage system. On the basis of location, gullies are classified as valley-bottom gullies, valley-head gullies, and valley-side gullies. Inasmuch as valley bottoms grade smoothly into valley heads and valley sides, the distinction among the different classes of gullies is arbitrary. Moreover, a valley-bottom gully becomes a valley-head gully as its head scarp migrates into the valley head. The valley-head gullies are by far the most numerous kind, and nearly all of these are in steep valley heads that border areas of upland.

The size of a gully depends on its depth and areal dimensions; but because of the irregular shape of gullies, the areal dimensions cannot be expressed simply and consistently. For complexly branching gullies, it is not clear whether or not the unconsumed area between the branches should be considered part of the gully. The best approximation to an expression of gully size seems to be the maximum width of the gully head. Inasmuch as gully depth increases roughly in proportion to width of gully head, the width of the gully head is an indirect expression of gully depth. In an arbitrary ranking of gullies according to width of gully head, valley-side and valley-bottom gullies must be considered separately from valley-head gullies, which are relatively wider in proportion to depth.

AGE AND ACTIVITY OF EROSIONAL SCARPS

Obviously, a scarp is younger than the surface into which it is cut. All the scarps in the Medicine Creek basin are considered to be younger than the Stockville terrace deposits. Some of the slopes graded to the level of the Stockville terrace are steep, especially those in the upper parts of the drainage basin; but these slopes are not regarded as scarps because they have an inclination less than 45°. Also, the steepest part of these slopes (in a particular area of the basin) is graded to about the same angle, and the upper parts of the slopes decrease in angle as they merge with the older Peorian surfaces.

Regardless of the age of the surface it cuts, a scarp may be either active or inactive. A scarp is considered to be active if it has migrated a distance that can be measured by comparing of aerial photographs made in 1937 and in 1952 or if it shows field evidence of recent movement. In the field, inferences as to activity were made from the type of vegetation on the scarp, from the degree of inclination, or from evidence of recent or imminent slumping. A thick sod of native grass indicates an inactive scarp; a cover of brush (such as wild rose, buckbrush, or currant) indicates a moderately active scarp; and lack of vegetal cover, or a cover of weeds, indicates an active scarp. In general, the more nearly vertical a scarp, the more likely it is to be active. However, many scarps that were bare and nearly vertical showed little or no migration during the interval 1937–52. Even a bare and nearly vertical scarp was not regarded as active unless recently slumped silt was observed at the scarp base or unless fissures were observed on the ground surface beyond the scarp.

CHANNEL SCARPS AND VALLEY-BOTTOM GULLIES

Varieties of valley-bottom gullies are distinguished on the basis of position with respect to one another and to different topographic levels produced by trenching of the drainage system. The main varieties are indicated by numerals in figure 200. The two gullies at upper left (1), which are in the same valley bottom but are separated by a reach of undissected valley, are of the sort called discontinuous by Leopold and Miller (1956, p. 29). When the head scarp of a downvalley gully reaches the tail of an upvalley gully, a stage of coalescence is reached; and the two gullies are integrated into a single trench as the downvalley scarp advances. Similarly, the advance of a major scarp in a large valley is commonly preceded by the advance of a minor scarp (2). A scarp may be initiated on the floor of a trench, where it may advance either into freshly deposited sediment (3) or into previously undisturbed alluvium. Channel scarps on the floor of a

Digitized by Google

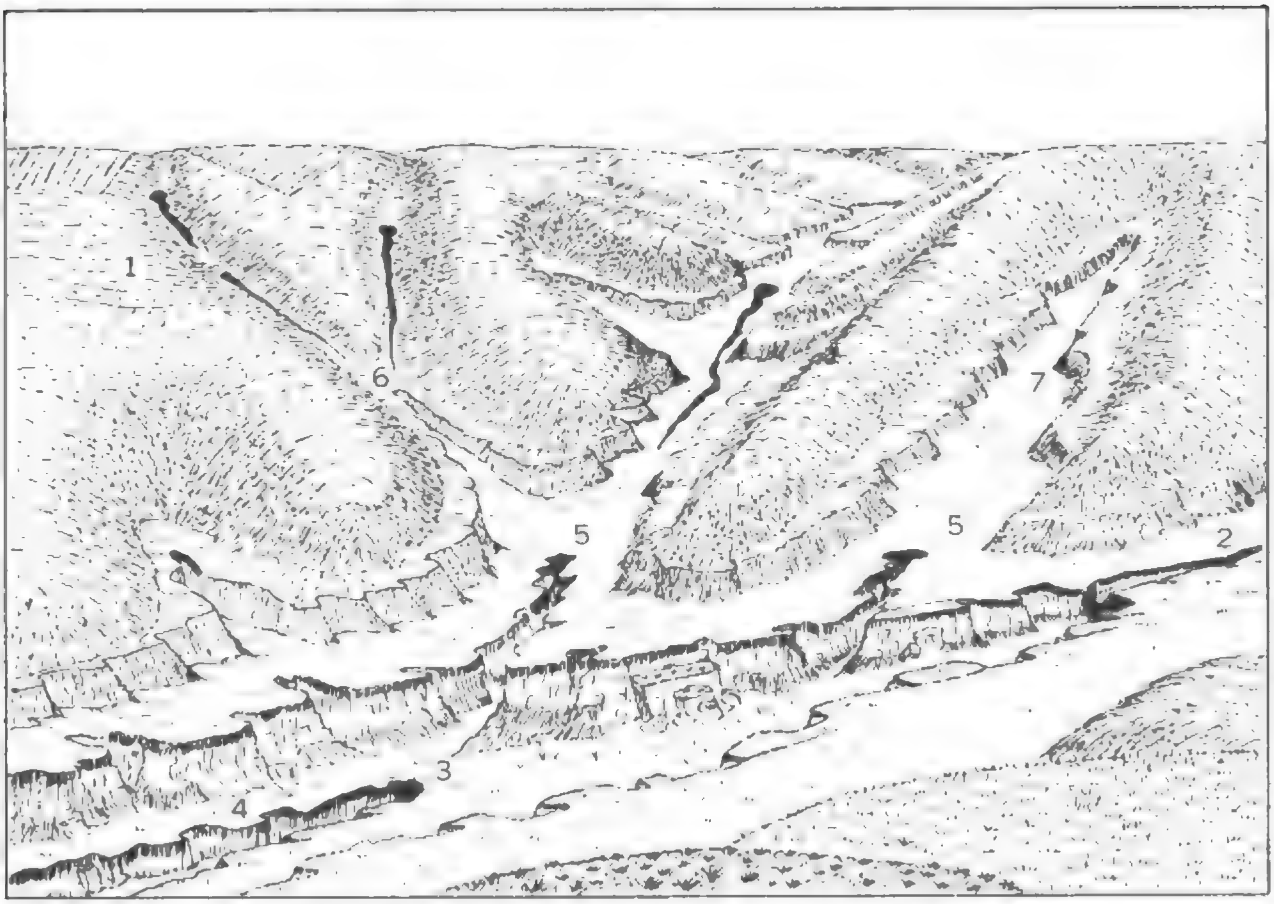

FIGURE 200.—Composite sketch, based on field sketches and photographs, showing the different varieties of valley-bottom gullies. Actively eroding scarps are indicated by darker shading. Numbered features are described in text.

trench are here described as inset. Remnants of the original gully floor, left along the gully sides after passage of an inset scarp, constitute an inset terrace (4). Another variety of valley-bottom gully is illustrated by the two gullies (5) in the middle ground of figure 200. Unlike the discontinuous gullies, which have no relation to the topographic level formed by trenching elsewhere in the drainage system, these gullies were initiated at the side scarps of the gully in the foreground and are accordant with its floor.

The location of the head scarps of major valley-bottom gullies in the Medicine Creek basin is shown in figure 201. Most of the gullies are in the size category of very large, but some are in the category of large. The scarps range in height from 10 to 25 feet and are in valleys of fourth or higher order. Advance of the scarps during the period 1937–52 ranges from a maximum of about 3,400 feet (for gully B4 on fig. 201) to a minimum of about 200 feet. Two significant facts relevant to the origin of the scarps are indicated by their areal distribution: Scarps are most numerous in the central and lower part of the basin, and scarps in large valleys are commonly upstream from the confluence of a large tributary.

The greater abundance of the scarps in the central and lower part of the basin is attributed to the relative narrowness of the valley bottoms there. (See table 4.) In general, the width of a valley bottom is much affected by the degree of trenching both before and after deposition of the Stockville terrace deposits. The branching valley at upper left (6) in figure 200 was represented by a relatively narrow and shallow trench before deposition of the Stockville terrace deposits. During deposition of the Stockville terrace deposits the valley sides were graded, and the valley has been little affected by post-Stockville trenching. By contrast, the valley at upper right (7) was represented by a relatively deep and wide trench before deposition of the Stockville terrace deposits. Post-Stockville trenching has extended to the valley head, and only narrow

Digitized by Google

FIGURE 201.—Head scarps of major valley-bottom gullies.

TABLE 4.—*Drainage system properties, listed according to channel order, for major subbasins of the Medicine Creek basin*

Subbasin	Channel order	Number of channels	Mean channel length (ft)	Mean channel slope (ft per ft)	Mean width of valley flat (ft)	Area of valley flat (sq mi)
Lime Creek	1	1,020	410	0.1100	25	0.37
	2	228	670	.0517	[illegible]	.28
	3	42	1,600	.0185	105	.25
	4	9	4,110	.0111	120	.16
	5	2	9,200	.00545	150	.10
	6	1	26,000	[illegible]	500	.47
Mitchell Creek	1	3,940	370	.100	35	1.83
	2	950	537	—	55	1.00
	3	172	1,170	—	90	[illegible]
	4	31	4,970	—	140	.77
	5	6	3,320	—	[illegible]	.11
	[illegible]	1	114,000	—	400	1.63
Dry Creek	1	2,824	267	.187	35	[illegible]
	2	725	458	.0673	60	.71
	3	153	1,023	.0343	96	.54
	4	30	1,816	.0155	125	.24
	5	4	8,830	.0088	160	.20
	6	2	8,600	.00576	200	.12
	7	1	25,500	.00296	260	.24
Well Canyon	1	10,310	245	.251	35	3.17
	2	2,460	480	—	[illegible]	2.85
	3	545	772	—	110	1.75
	4	104	2,195	—	140	1.23
	5	[illegible]	5,375	—	190	[illegible]
	6	1	126,000	—	545	2.18
Fox Creek	1	15,900	250	.241	35	4.98
	2	4,250	460	.100	70	4.90
	3	904	725	[illegible]	120	2.82
	4	177	2,040	.0215	[illegible]	1.94
	5	35	4,085	.0101	190	.97
	6	6	14,850	.0055	270	1.71
	7	2	32,000	.00406	440	1.01
	8	1	45,000	.00274	380	1.40
Brushy Creek	1	12,400	192	.234	35	[illegible]
	2	3,500	370	—	60	3.39
	3	729	674	—	95	1.67
	4	147	2,040	—	135	1.44
	5	29	5,450	—	165	.93
	6	6	12,832	—	240	.66
	7	2	40,500	—	360	.87

remnants of the Stockville terrace remain along the valley sides. The valley at right in figure 200 is typical of the upper part of the Medicine Creek basin; and the valley at left, of the central and lower part.

The association of major channel scarps with the confluence of a large tributary is notable on Fox Creek, Cut Canyon, Curtis Creek Canyon, and Well Canyon. Although the present scarps are upvalley from the tributary confluence, the possibility is good that the scarps were initiated at the confluence, where the slope of the main valley may be locally steepened. After a valley floor has been trenched, its long profile cannot be accurately reconstructed; however, long profiles drawn from contours at 10-foot intervals on the topographic maps indicate that the main valley profile is generally, but not everywhere, steepened upstream from the confluence of a large tributary. (See fig. 202.) On Curtis Creek Canyon a conspicuous steepening of the valley profile just upstream from the confluence of a large tributary is indicated on the topographic map. The steepening is probably due to deposition of a fan at the mouth of a tributary. This fan ponds the drainage in the main valley and leads to deposition upstream from the fan. Schumm and Hadley (1957) have shown that, in small drainage basins in eastern Wyoming and northern New Mexico, discontinuous gullies can form on locally steep valley reaches.

The proposal that gullies are initiated at a local steepening of the valley slope has as a corollary the proposal that local slope in an ungullied valley reach may be adjusted to water discharge. In the absence of discharge measurements for most valley reaches, the assumption may be made that the discharge in a reach is proportional to the upstream drainage area. The relation of local valley slope to drainage area for reaches along three valleys is shown in figure 203. Cut Canyon and Dry Creek are free of major channel scarps in their uppermost reaches, as shown in figure 202, but Coyote Creek has channel scarps throughout most of its length. In spite of the fact that the floors of all three valleys are well above bedrock, local slope is not constant in a given valley reach several hundred feet in length. The values of local slope plotted in figure 203 represent the best approximation obtainable from topographic maps for mean local slope in a reach bounded by contours and having a fall of 20 feet.

A general relation between local valley slope and drainage area is apparent from figure 203. Slope values applying to gullied reaches tend to plot above the average curve representing this relation, but some slope values applying to ungullied reaches also plot above it. Aside from chance, factors other than local slope and drainage area seem to be involved in the initiation of gullies, and the most important of these is probably valley width. The upstream reaches of Coyote Creek have a greater susceptibility to gullying than reaches of Cut Canyon because of the relative narrowness of the valley bottom of Coyote Creek.

The main valley of Well Canyon is relatively free of gullies, and the few gullies present have grown slowly. The channel scarps in the long profile of Well Canyon (fig. 202) did not advance during the interval 1937–52 by an amount measurable on aerial photographs nor did the intricate small-scale meanderings of the trenched channel reaches show any observable change. The aspect of a trenched channel on Well Canyon is shown in figure 195 (*middle*).

Digitized by Google

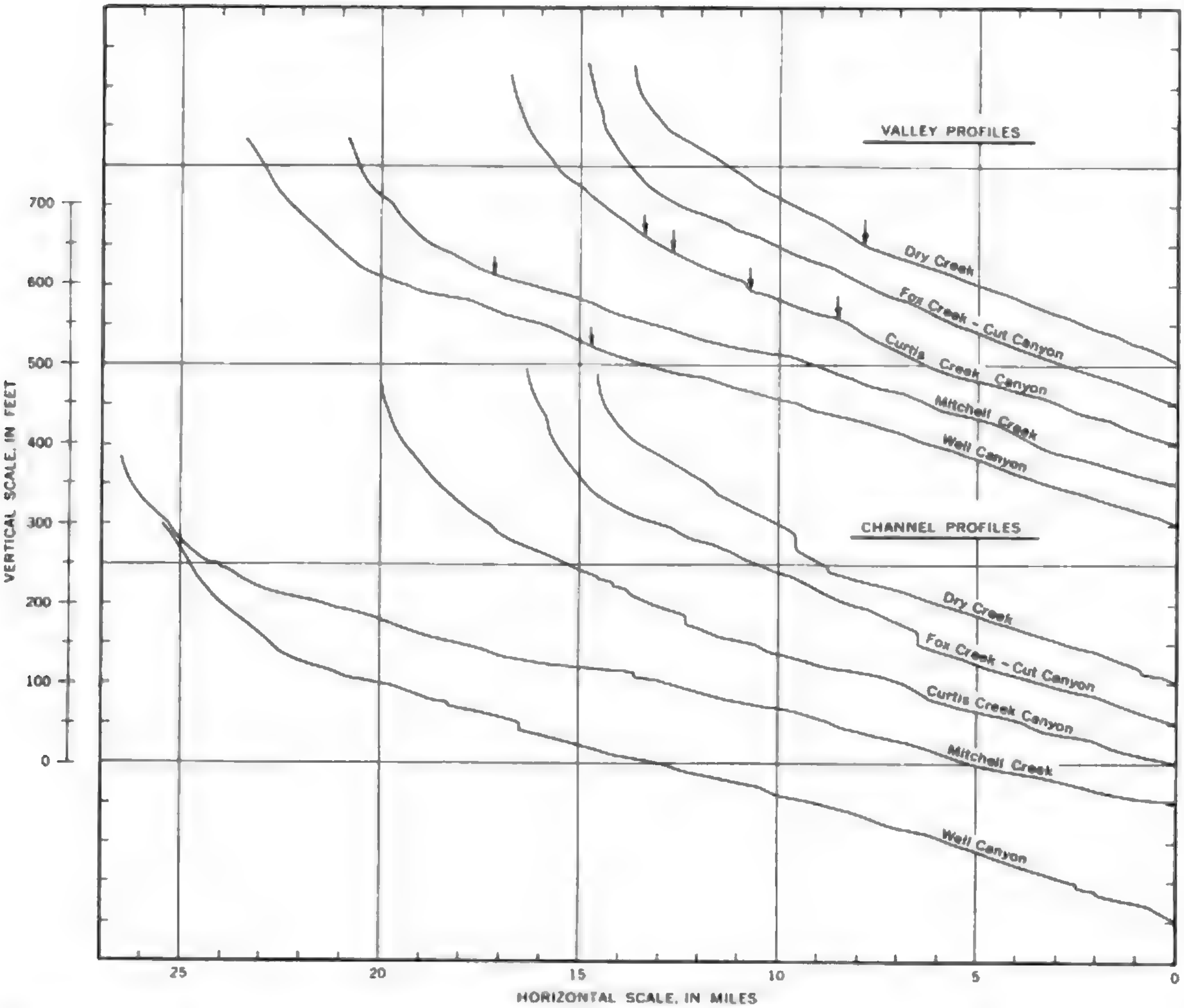

FIGURE 202.—Long profiles of valley and channel for some major tributaries to Medicine Creek. A break in the channel profile represents a channel scarp, and an arrow on the valley profile indicates the point of confluence of a large tributary. Profiles drawn from topographic maps.

The general slope of the valley profile, although somewhat less than that of Dry and Curtis Creeks, is not significantly different from that of Mitchell and Fox Creeks. The tributaries received by Well Canyon are relatively short, however, and the valley of Well Canyon is relatively wide at the point of confluence of the two largest tributaries. Upstream from the confluence of the northernmost of these tributaries, the valley profile of Well Canyon shows local steepening and the presence of a channel scarp. Neither local steepening nor a channel scarp occurs at the confluence of the other tributary. The inactivity of channel scarps in the main valley of Well Canyon is attributed to the lack of large tributaries, to relatively great valley width, and to the generally low valley slope.

DEVELOPMENT OF VALLEY-BOTTOM GULLIES

Photographs of typical valley-bottom gullies are reproduced in figure 204. After a gully has become large, neither the exact way in which it was initiated nor the point of initiation can be established. However, study of small gullies in various stages of development indicates that valley-bottom gullies may begin as small depressions scoured by flowing water on the valley bottom. Breaks in the sod cover—such as might result from an animal burrow, a trail, or an excavation by man—are likely spots at which scour can take place. The upstream side of a depression can evolve into a scarp and advance upvalley, meanwhile growing in height. Although most scarps in major valleys have apparently been ini-

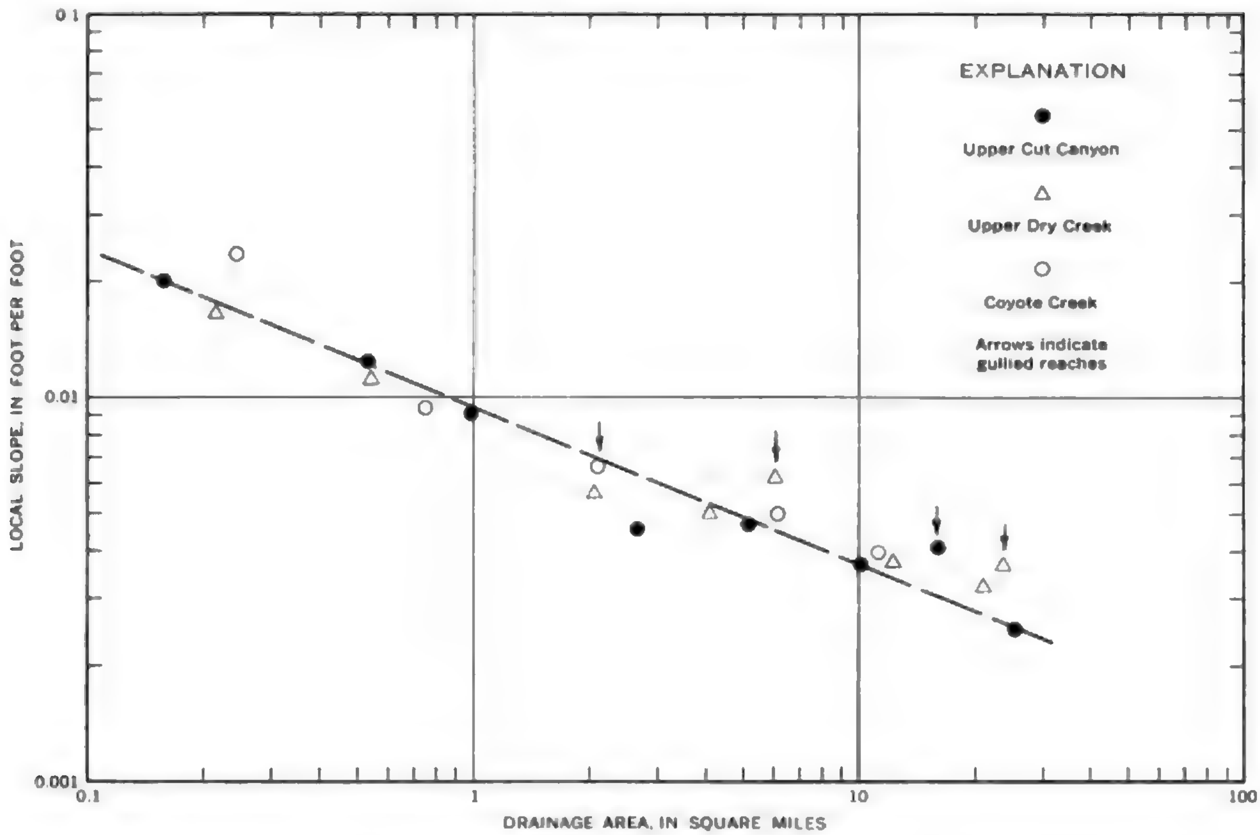

FIGURE 203.—Local valley slope in relation to drainage area for reaches along upper Cut Canyon, upper Dry Creek, and Coyote Creek.

tiated in a locally steepened valley reach, a scarp, once initiated, can continue to advance into reaches where the value of local slope is conservative in relation to drainage area (water discharge). Moreover, many gullies occur in valleys of fourth or smaller order in which no evidence of local steepening can be found. The value of the ratio of slope to drainage area that is associated with the initiation and rapid growth of a gully is not sharply defined.

Advance of a head scarp takes place as the massive silt at the base of the scarp becomes saturated and disintegrates. In this region the permeability of undisturbed dry loess in place is only about 0.8 foot per day (Holtz and Gibbs, 1952), but this value has no significance for a vertical face of loess that is immersed in water, as at the edges of a plunge pool. The loess in contact with the water continually sloughs along vertical joints and is removed by the turbulent water of the pool. In figure 204 (*upper left*) the recently collapsed base of a scarp may be seen at right of plunge pool. The cohesiveness of massive silt depends to a considerable extent on a cement formed by clay minerals that coat the silicate grains, and when wet the clay coatings have little or no cohesive effect. Gully side scarps regress by the same process. For a distance up to 12 feet from the edges of a gully, the ground is broken by cracks marking the boundaries of large blocks that have slumped because of saturation of the silt at their base. These blocks will eventually slump into the gully, as illustrated in figure 200. Head scarps can be maintained in massive silt whether or not they are capped by sod or some other resistant layer. Drainage is conveyed to many head scarps by a narrow channel, the bottom of which is bare of vegetation and is cut below the soil profile. A deep notch is formed by the intersection of this channel with the head scarp. The notch in the head scarp of gully B1 on Dry Creek changed very little between 1953 and 1957.

Downstream from a head scarp, long profiles of gullies change from year to year; the change depends on the amount of runoff. V. I. Dvorak (written commun., 1962) has compiled measurements of the long profiles of three major gullies on Dry Creek, which are designated gullies B1, B2, and B3 in figure 201. Changes in the long profile of gully B2 are typical and are represented in figure 205.

Digitized by Google

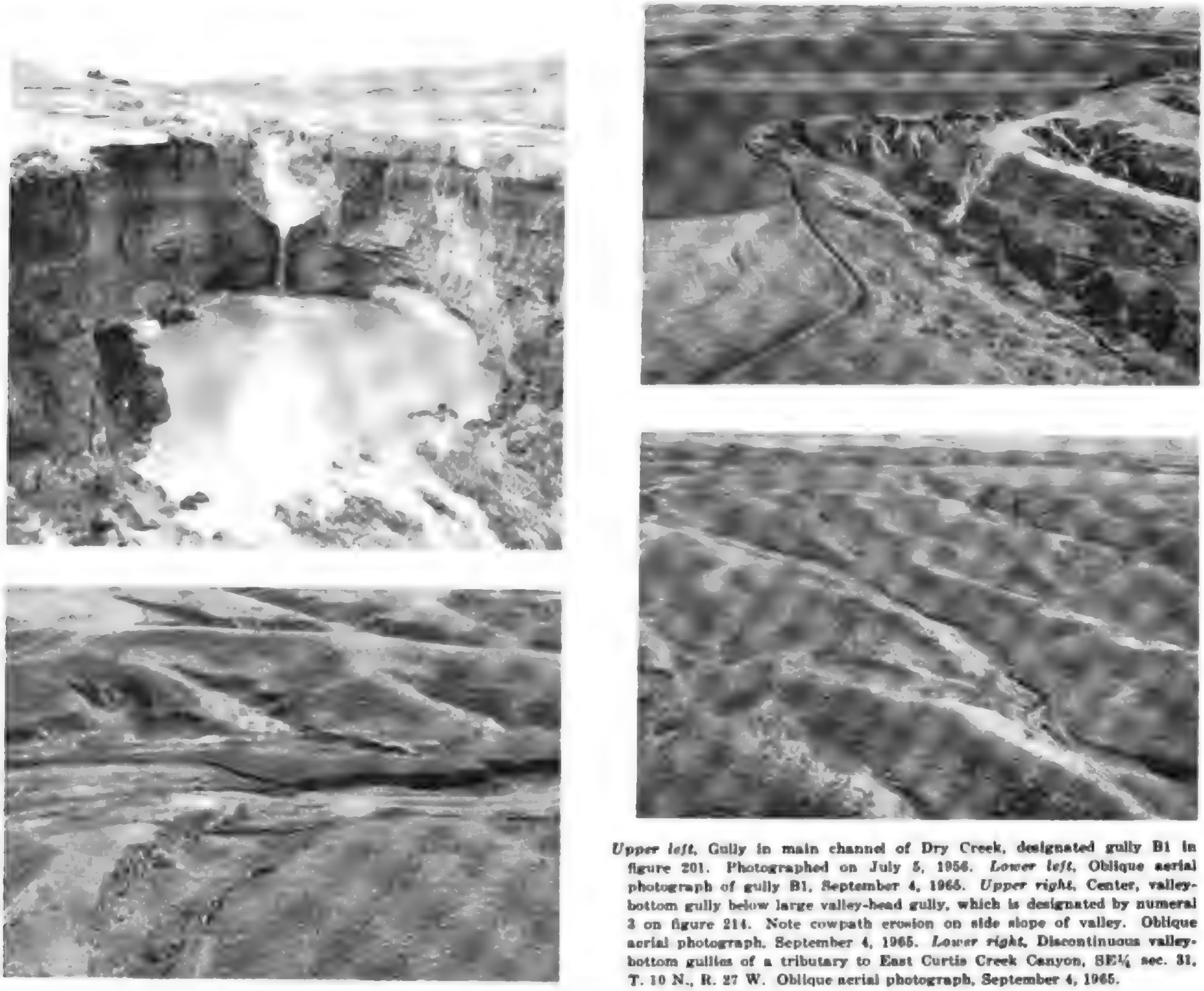

Upper left, Gully in main channel of Dry Creek, designated gully B1 in figure 201. Photographed on July 5, 1956. *Lower left*, Oblique aerial photograph of gully B1, September 4, 1965. *Upper right*, Center, valley-bottom gully below large valley-head gully, which is designated by numeral 3 on figure 214. Note cowpath erosion on side slope of valley. Oblique aerial photograph, September 4, 1965. *Lower right*, Discontinuous valley-bottom gullies of a tributary to East Curtis Creek Canyon, SE¼ sec. 31, T. 10 N., R. 27 W. Oblique aerial photograph, September 4, 1965.

FIGURE 204.—TYPICAL VALLEY-BOTTOM GULLIES

According to Dvorak, the relatively high runoff in 1951 was accompanied by gully slopes distinctly less than valley slopes, but during the succeeding drier years the gully slopes increased. Gully slope was steeper than valley slope for gully B2 in 1956 and for gullies B1 and B3 in 1960.

The maximum height attained by a head scarp is evidently controlled mainly by the steepness of the slope into which the head scarp is advancing. The highest head scarps in the basin, which reach a maximum of about 35 feet, are all in steep valley heads, whereas head scarps on the gently sloping valley bottoms all range from 10 to 25 feet in height. The height that a scarp can attain is also limited by the rate of deposition at, and downstream from, its base.

The cross profile of a valley-bottom gully changes in a direction downstream from the head scarp, but the nature of the change is not consistent from gully to gully. Typically, gully depth decreases very gradually in a downstream direction, whereas gully width reaches a maximum within a thousand feet of the head scarp and then decreases in a downstream direction. Downstream changes in the cross profile of a typical rapidly advancing valley-bottom gully (gully B4 in fig. 201) are shown in figure 206. The width of gully B4 remains nearly constant for about 5,000 feet downstream, but for other gullies the width decreases downstream at a much faster rate than depth. For example, in 1952 the width of a large valley-bottom gully on Curtis Canyon (gully B6) decreased from about 105 feet at a

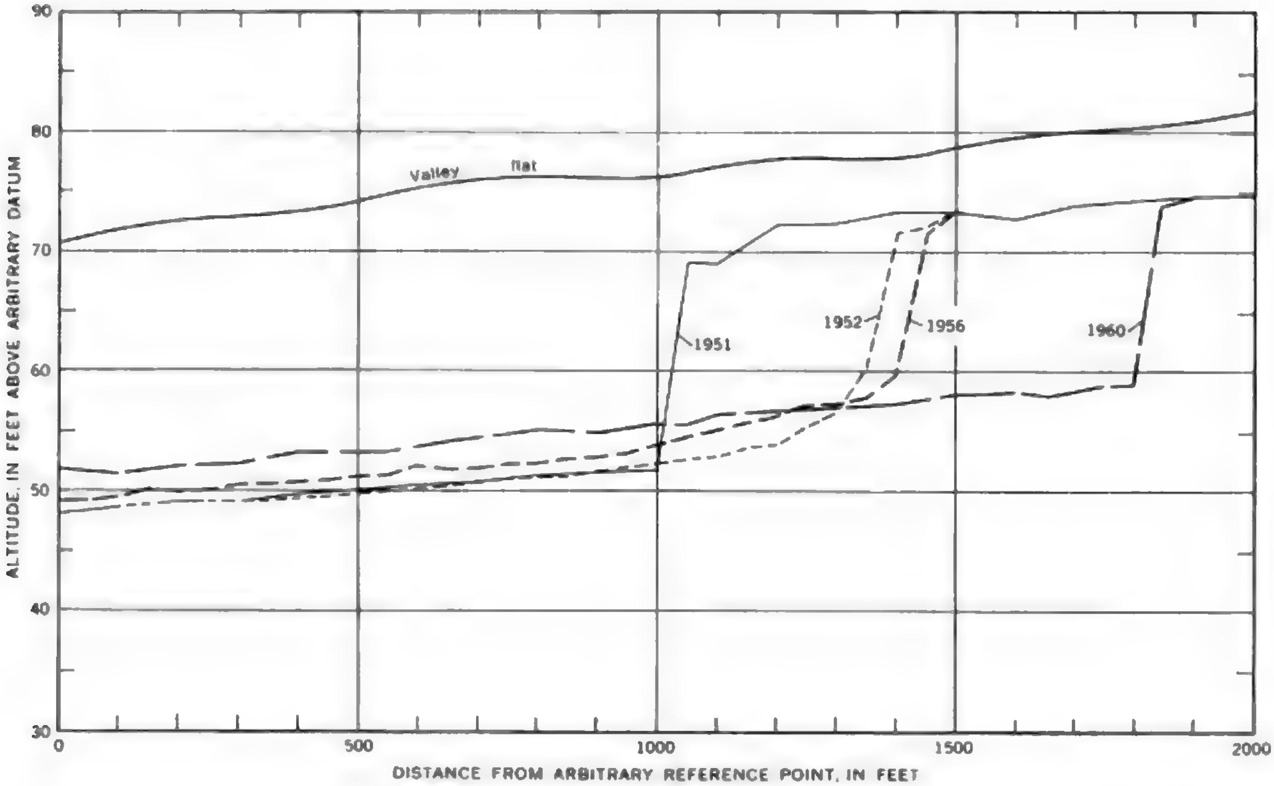

FIGURE 205.—Changes in long profile of a large valley-bottom gully on Dry Creek, 1951–60. Gully is designated B2 in figure 201. From V. I. Dvorak.

point 900 feet downstream from the head scarp to about 45 feet at a point 5,000 feet from the head scarp. Through this 5,000-foot distance, the depth of the gully changed little. Neither gully B4 nor B6 has a well-defined downstream terminus at which the gully floor merges with the valley floor; each merges downstream with a narrow but apparently stable channel that continues for miles along the valley bottom.

From his study of valley-bottom gullies on Dry Creek, Dvorak (written commun., 1962) concluded that widening downstream from the head scarp effectively ceased when the width-depth ratio was in the range of 3.5 to 5. At great width, the depth and velocity of flowing water would be insufficient to remove material that accumulated from bank slumping, and the channel bottom would assume a parabolic shape.

As is generally the case with channels in nature, the width-depth ratio that can be maintained for a gully probably depends on the magnitude of water discharge. Small gullies in the Medicine Creek basin have low values of the width-depth ratio, and large gullies have larger values. In 1956 none of the large valley-bottom gullies had attained a width-depth ratio greater than 6, which was the value measured for gully B5 at a point 390 feet downstream from its head scarp. However, none of these gullies had a drainage area greater than about 16 square miles. Gully B9, the drainage area of which was about 1.5 square miles, had in 1956 a width-depth ratio that did not exceed a value of 1 for a distance of 1,000 feet downstream from its head scarp.

The advance of major valley-bottom gullies during the period 1937–52 is given in table 5, together with pertinent information as to gully size and topographic setting. Gully advance and width of valley bottom were measured on aerial photographs; drainage area was measured on topographic maps; and height of head scarp was measured in the field. Slope of the valley bottom, which applies to the slope upvalley from the 1952 position of head scarps, was measured by field surveys for some of the gullies and on topographic maps for others. In general, the maximum depth of a gully is about equal to, or is greater than, the height of its head scarp. No correlation is apparent between the rate of advance and any of the other measurements. The estimate of the year at which active advance of the gully began is made by dividing gully length by average

Digitized by Google

TABLE 5.—*Measurements relating to the size and topographic setting of major valley-bottom gullies*

[Gully locations are indicated on fig. 201]

Gully	Drainage area in 1952 (sq mi)	Width of valley bottom (ft)	Slope of valley bottom (ft per ft)	Height of head scarp in 1956 (ft)	Advance of head scarp, 1937–52 (ft)	Estimated year of activation
B1	6.1	215	0.0056	24	900	1850
B2	5.6	[illegible]	.0055	22	750	?
[illegible]	.8	120	.0105	20	[illegible]	?
B4	3.4	140	.0082	16	3,400	1900
B5	9.7	200	.0058	[illegible]	2,400	1920
B6	9.3	160	.0062	18	1,750	1920
B7	15.9	180	.00415	18	2,800	[illegible]
B8	[illegible]	150	[illegible]	20	2,100	?
B9	1.4	120	[illegible]	23	2,100	1920

annual rate of advance during 1937–52. For Dry Creek, which has a continuous channel downstream from the head scarp, the point of origin is assumed to be at the confluence of East Fork.

Valley-bottom gullies advance only during periods of runoff. As a result of rainfall on July 4 and 5, 1956, which totaled about 1.9 inches, gully B5 advanced about 15 feet and gully B1 advanced 20 feet. The year 1937 was preceded by a period of relatively low rainfall (fig. 179) and, as observed on aerial photographs, most of the gullies were inactive in 1937 and were partly filled with sediment. A substantial part of the advance during the period 1937–52 took place in 1951 as a result of high runoff. For example, of the 750-foot advance made by gully B2 during the period 1937–52, about 350 feet was made during 1951. Differences in rate of gully advance (table 5) are probably in part due to unequal distribution of rainfall during 1951.

The development of a locally continuous channel by the coalescence of two discontinuous valley-bottom gullies, as described by Leopold and Miller (1956, p. 31), is illustrated in figure 207. Only the upper reach of the gullied valley bottom is shown in the illustration. The shallow channel shown at left continues downvalley for 1,300 feet and terminates at the head scarp of gully B3. No evidence of downvalley extension of gullies during the period 1937–56 was observed at this locality, and in general downvalley extension of a gully is uncommon. The long profile of a single discontinuous gully is rarely smooth, but it is ordinarily broken by one or more inset scarps.

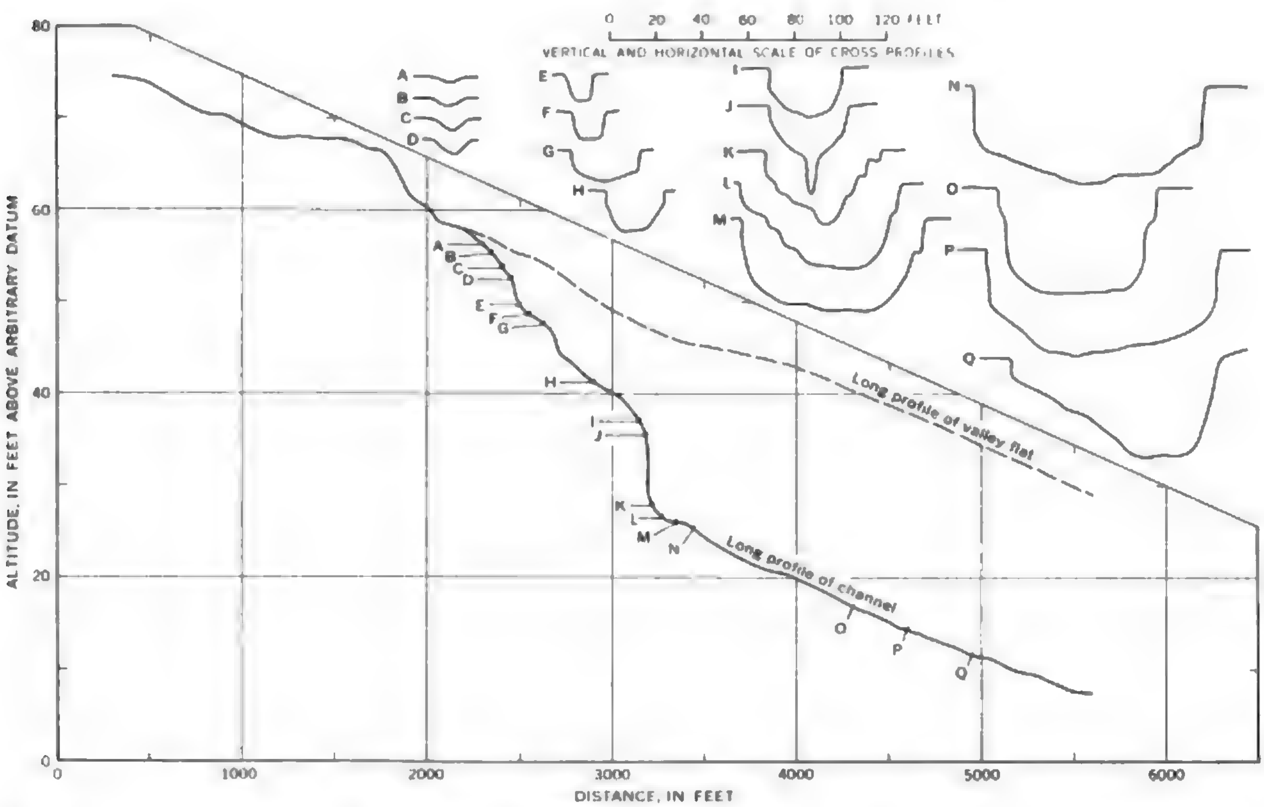

FIGURE 206.—Long profile and cross profiles of a large valley-bottom gully in a tributary to Curtis Creek Canyon. Gully is designated B4 in figure 201. Based on a field survey, 1956.

Digitized by Google

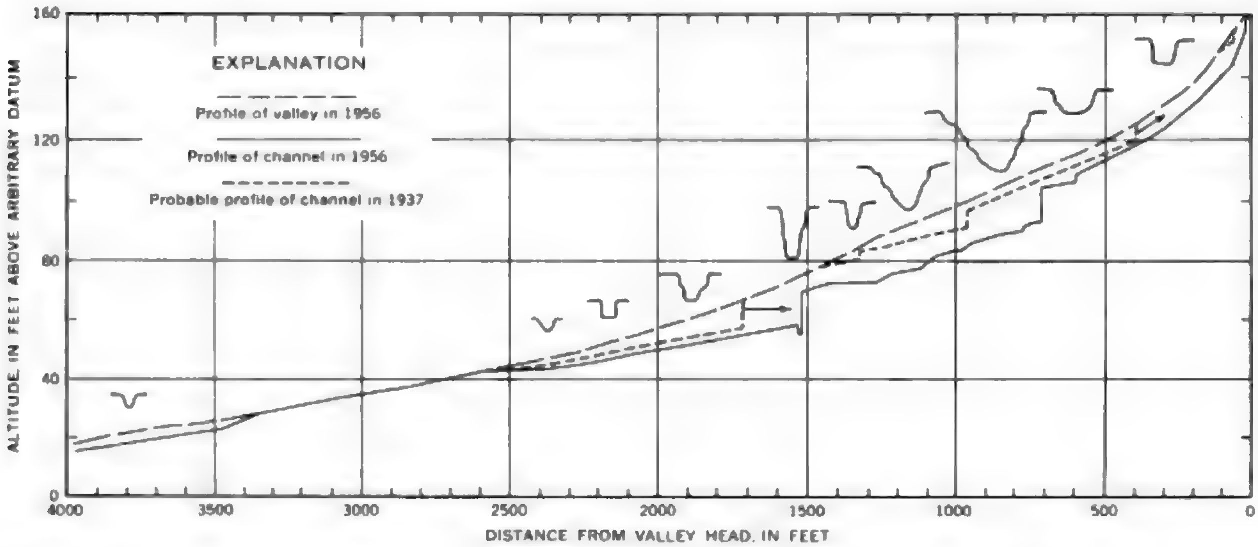

FIGURE 207.—Changes in long profile of a gullied tributary to Dry Creek, 1937–56. For the long profile in 1937, the position of head scarps was taken from aerial photographs, and other parts of the profile were estimated. Long and cross profiles in 1956 are based on a field survey.

The gradient of a discontinuous gully is less steep than the gradient of the valley floor into which it is advancing, and Leopold and Miller attribute this to the narrower width of the gully. As gullies coalesce and widen, a continuous channel is finally formed that has a gradient nearly parallel to the original valley floor. The gullies of the Medicine Creek basin, however, have not reached this final stage; channel scarps are advancing in succession along the valleys, and final regrading of a given reach will probably involve the passage of many channel scarps.

HISTORY OF LATE RECENT GULLYING ON DRY CREEK

Dry Creek was selected for detailed study of gully erosion by agencies involved in the Medicine Creek Watershed Investigations because the rate of erosion there seemed to be more severe than elsewhere in the basin. Periodic surveys were made of selected reaches of valley-bottom gullies to provide a basis for calculation of gross erosion by these gullies. A detailed geomorphic study of the Dry Creek channel and terraces was made by the writer, with the objective of deciphering the history of gullying in late Recent time and relating this history to white settlement and occupation.

A detailed long profile of Dry Creek, based on a field survey made by personnel of the Bureau of Reclamation in 1951, is shown in figure 208. The terrace profiles in figure 208 and the cross profiles in figure 209 are also based on this survey, supplemented with field surveys made by the writer. Station references used in the text and in figure 209 refer to distances in feet from the mouth of Dry Creek, are represented in figure 208.

In general, the upper reaches of Dry Creek are ungullied (fig. 210, *upper left*), the middle reaches (as represented in fig. 210, *lower left* and *upper right*) have been twice gullied in late Recent time, and the lower reaches (as represented in fig. 210, *lower right*) were ungullied until about 1937. The inset terrace (figs. 209 and 210, *lower left*) provides evidence for the two episodes of gullying. The inset terrace deposits accumulated in the wake of a major channel scarp, and the inset terrace was formed as these deposits were trenched by the advance of a second scarp. The first channel scarp probably began at about station 10,000 for the inset terrace becomes indistinct at this point. A reasonable date for the beginning of this first scarp is about 350 years ago, which is the date suggested (on the basis of a carbon-14 age determination) for gullying on Elkhorn Canyon.

The approximate age of the inset terrace deposits can be inferred from a cottonwood stump rooted on the terrace at station 43,300 (fig. 210, *lower left*) and from a tobacco tin buried to a depth of 5 feet in the deposits at station 43,700. The growth rings on the cottonwood stump indicate that it was about 40 years old at the time of cutting (1950); therefore, the inset terrace deposits had already accumulated in 1910. The tobacco tin, which is about 400 feet upvalley from the stump, was perhaps buried about this time or somewhat later. Because the inset terrace deposits accumulate in the wake of an advancing head scarp, their age decreases in an upvalley

Digitized by Google

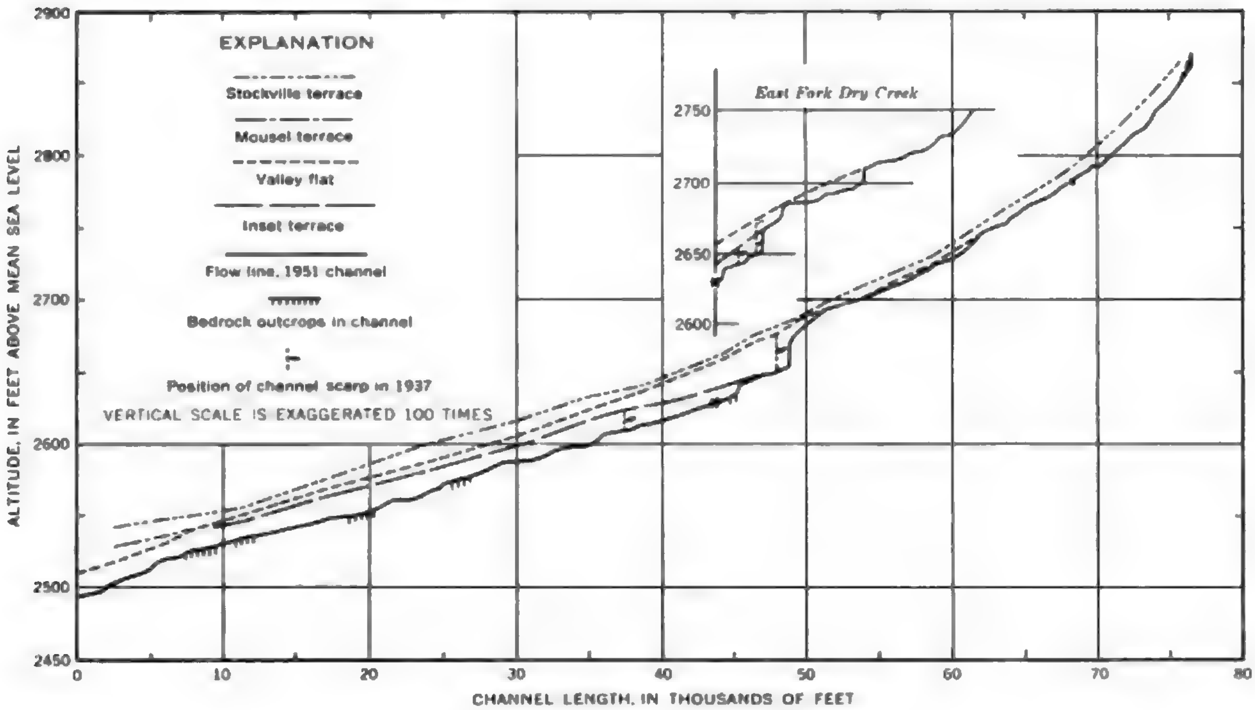

FIGURE 208.—Long profiles of channel, valley flat, and terraces on Dry Creek.

direction. The channel scarp that is trenching the deposits and thus forming the inset terrace was at station 37,400 in 1937 and had advanced 8,300 feet by 1951.

A new channel scarp began at or near the mouth of Dry Creek at a time not long before 1937, according to its position on the 1937 aerial photographs. This scarp had reached station 6,000 (fig. 210, *lower right*) by 1952, and it is moving rapidly upvalley at present.

VALLEY-HEAD AND VALLEY-SIDE GULLIES

Varieties of valley-head and valley-side gullies are distinguished mainly on the basis of shape of gully head in plan view. The main varieties in their characteristic topographic situations are illustrated in figure 211. A gully head that is on a relatively steep slope and receives a concentration of flow from a single direction, as from a narrow channel, tends to be narrow and pointed (gully 1, fig. 211). If the slope is less steep or the flow less concentrated, the gully head will be broadly lobed (2). If, on the other hand, the slope is gentle and the flow comes from diverse directions, the gully head will be complexly branching (3).

Situations favorable for the initiation of a gully are related to valley shape (as determined by past erosional history of the valley), to the presence of cultivated upland at the valley head, and to the activities of man and livestock. The valley at right has steep sides and head because it was deeply trenched both before and after deposition of the Stockville terrace deposits. The steep valley head, which receives heavy runoff from a field planted in row crops, is a favorable place for the formation of a gully. A large valley-head gully (gully 3, fig. 211), which began on the upper part of the valley head, has branched along the fence and into the field. The step scarps (4) on the steep valley sides began at animal trails along the slope contour and have grown in height as they slowly migrated upslope. The step scarp at extreme right has evolved into a valley-side gully (5). At the left side of the valley, two narrow valley-side gullies (1) are forming from cowpaths, and another valley-side gully (8) is advancing along a road ditch.

The valley at center is shallow and has a relatively gently sloping head because it was trenched to shallow depth before deposition of the Stockville terrace deposits, and post-Stockville trenching has not extended far upvalley. In addition, the valley head borders a divide rather than a tract of upland and, therefore, has a small drainage area. The three gullies in the valley head (6) are lobed and have grown slowly. In the background beyond the center valley, two gullies (7) in another valley head are

Digitized by Google

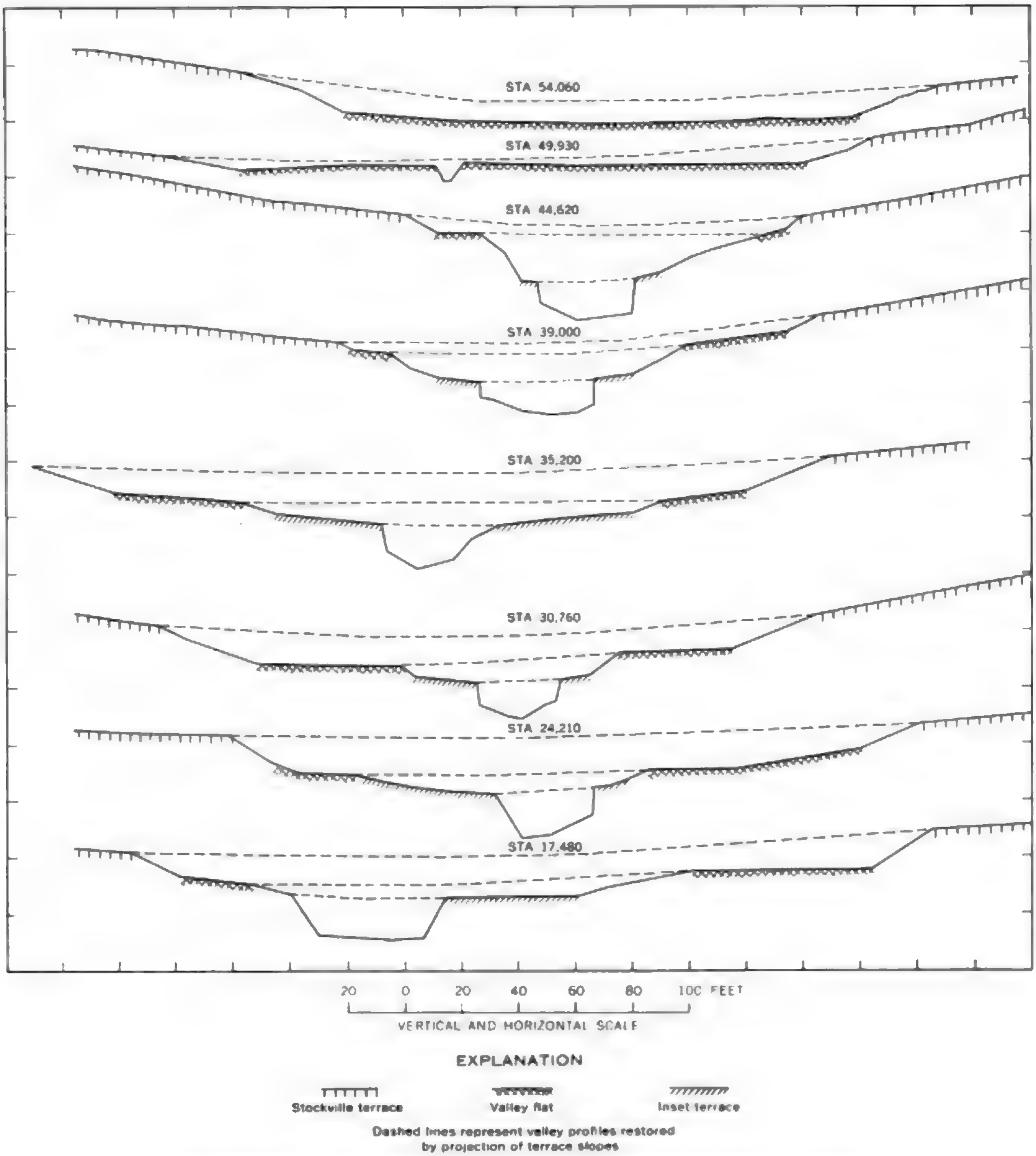

FIGURE 209.—Cross profiles of Dry Creek. Station numbers are distances in feet from mouth of creek.

Digitized by Google

Upper left, Upper reach of East Fork Dry Creek, 1953. Narrow incised channel is shown in middle ground. *Lower left*, Channel and inset terrace at station 43,300 in 1956. Cottonwood stump, near center, is rooted at outer edge of inset terrace. *Upper right*, at gaging station (sta. 17,660), August 17, 1953. Discharge about 300 cfs. *Lower right*, Channel at station 6,000 in 1953, looking downstream. On downstream side of cottonwood tree is a large channel scarp, advance of which has since felled the tree.

FIGUCE 210.—DOWNSTREAM CHANGES IN CHANNEL OF DRY CREEK

advancing rapidly—one in the direction of drainage from the road and the other in the direction of drainage from the barnyard.

The two valleys at extreme left are typical of many valleys in the upper part of the basin. Severe post-Stockville trenching has removed most of the deposits of Stockville age and left the valley sides raw and steep. The valley-side and valley-head gullies (2), which are lobed in plan view and have head scarps tens of feet in height, are advancing very slowly because their drainage area is small.

Photographs of valley-head and valley-side gullies are shown in figure 212. The valley-head gullies in figure 212 (*upper left* and *upper right*) are among the largest in the basin. As is typical, these gullies border areas of cultivated upland. The gully in figure 212 (*upper left*) extends for about 900 feet along a fence line. A narrow but deep valley-head gully, whose head scarp attains a height of 31 feet, is shown in figure 212 (*lower left*). Valley-side gullies typical of the sharply dissected upper part of the basin are shown along the sides of the three valleys in figure 212 (*upper right*). Some are moderately active and others are inactive. The growth rate of such gullies is slow because they border narrow divides and hence have small drainage areas. The valley-side gullies in figure 212 (*lower right*) originated from cowpaths and an old field road.

Digitized by Google

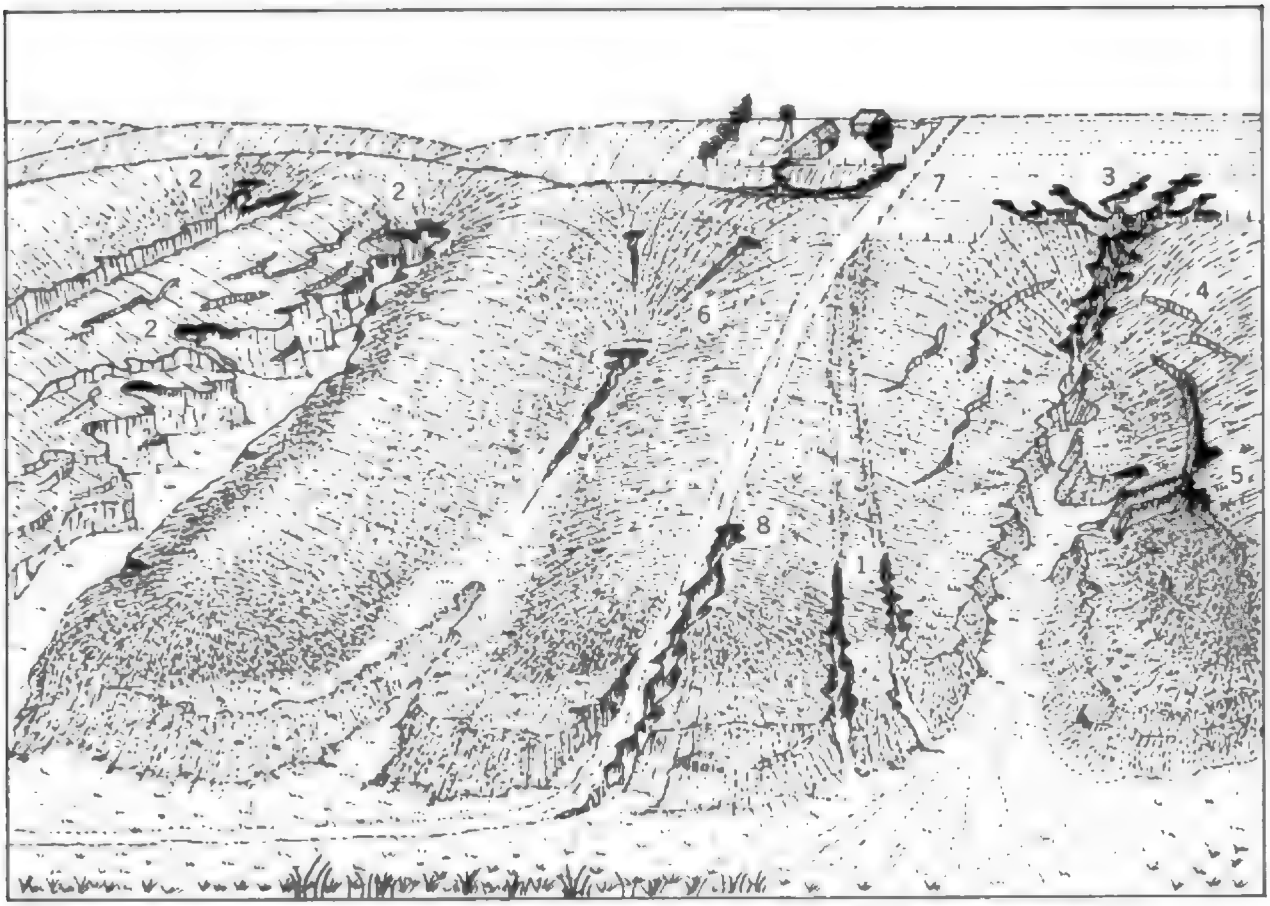

FIGURE 211.—Composite sketch, based on field sketches and photographs, showing different varieties of valley-head and valley-side gullies. Actively eroding scarps are indicated by dark shading. Numbered features are described in text.

MEASUREMENT OF VALLEY-HEAD AND VALLEY-SIDE GULLIES ON DRY CREEK

In the summer of 1953 measurement of the volume increase of valley-head and valley-side gullies during the period 1937–52 was made by field surveys and comparison of aerial photographs. On aerial photographs enlarged to a scale of 1 inch to 660 feet, reference lines across or near gully heads were drawn between fixed points, such as trees, fence corners, houses, or other landmarks. The position of gully head in 1937 was marked on a 1952 aerial photograph, which was then taken into the field to facilitate measurement of the volume increase. Changes in gully depth could not be determined from aerial photographs; but this is probably not a significant source of error, inasmuch as neither height of head scarp nor gully depth changes very much during a moderate advance. The horizontal dimensions of gullies were measured by pacing, and the depths were measured with a steel tape. Determination of volume was complicated by the irregular shape of most gullies. No volume increases less than about 30 cubic yards are reported because increases less than this amount are considered to be unrecognizable by comparison of aerial photographs. Volume increases, however, were measured for nearly all the gullies on Dry Creek that seem to be active, and erosion from gullies that seem to be inactive is probably not quantitatively important.

According to these measurements, the enlargement of all active valley-head and valley-side gullies on Dry Creek (216 gullies) for the period 1937–52 totaled 106,500 cubic yards. A plot of the frequency distribution of gully enlargements on logarithmic probability paper indicates a logarithmically normal distribution, and the skewness at the lower end of the curve is attributed to the omission of perhaps 10 gully enlargements less than 30 cubic yards. (See fig. 213.) The median enlargement is about

Digitized by Google

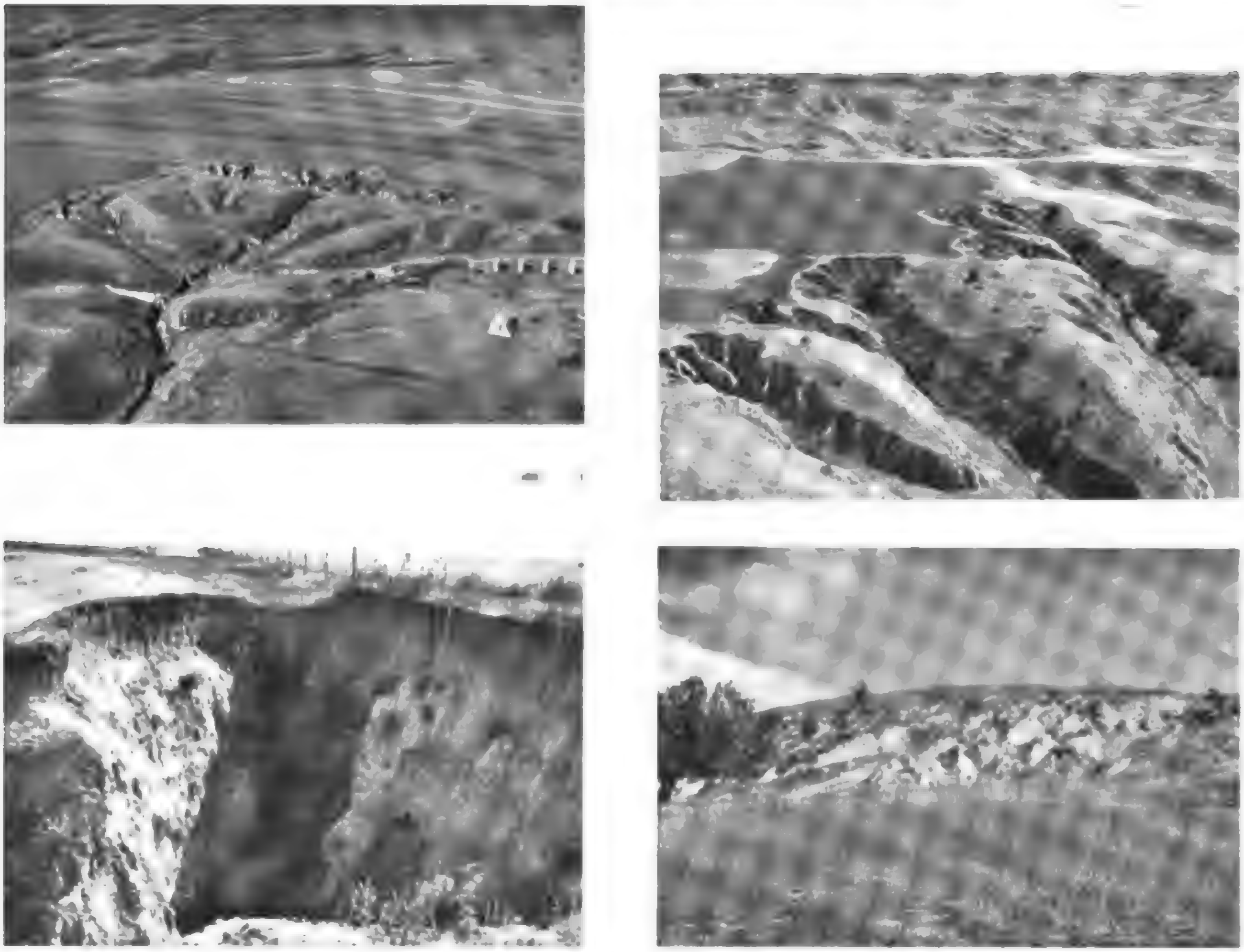

FIGURE 212.—Valley-head and valley-side gullies. *Upper left*, Center, large valley-head gully in Curtis Creek subbasin, NE¼ sec. 10, T. 8 N., R. 28 W. Oblique aerial view, September 4, 1965. *Lower left*, Valley-head gully in Dry Creek subbasin, center sec. 33, T. 9 N., R. 27 W., September, 1953. *Upper right*, Large valley-head gullies and smaller valley-side gullies in Curtis Creek subbasin, SW ¼ sec. 30, T. 10 N., R. 27 W. Oblique aerial view, September 4, 1965. *Lower right*, Valley-side gullies in Well Canyon subbasin, SW ¼ sec. 13, T. 9 N., R. 29 W.

200 cubic yards, and the range is from 28 to about 4,200 cubic yards.

A satisfactory approximation to the measured gully enlargement was reached by another method, which is based on the premise that active gullies can be recognized on aerial photographs and also on the premise that small gullies have small volume increases and large gullies have large volume increases. Several years after the gully measurements were made on Dry Creek, active gullies in the Medicine Creek basin were studied on aerial photographs and ranked into four categories according to size (not according to enlargement). On the basis of the measured gully enlargements on Dry Creek, each size category was assigned an enlargement range, according to the following scheme:

Gully size	*Enlargement range, 1937–52 (cu yd)*	*Geometric mean of enlargement range (cu yd)*
Small	50–100	63
Medium	100–600	245
Large	600–3,600	1,470
Very large	3,600–7,200	5,100

The number of gullies in each category on Dry Creek is shown in table 6. By multiplying the number of gullies in each category by the geometric mean of the enlargement, a total enlargement of 97,300 cubic yards was obtained, which is a reasonable approximation to the measured enlargement. Although this method is obviously subjective, no means of applying rigorously objective sampling methods to such irregular objects as gullies is

Digitized by Google

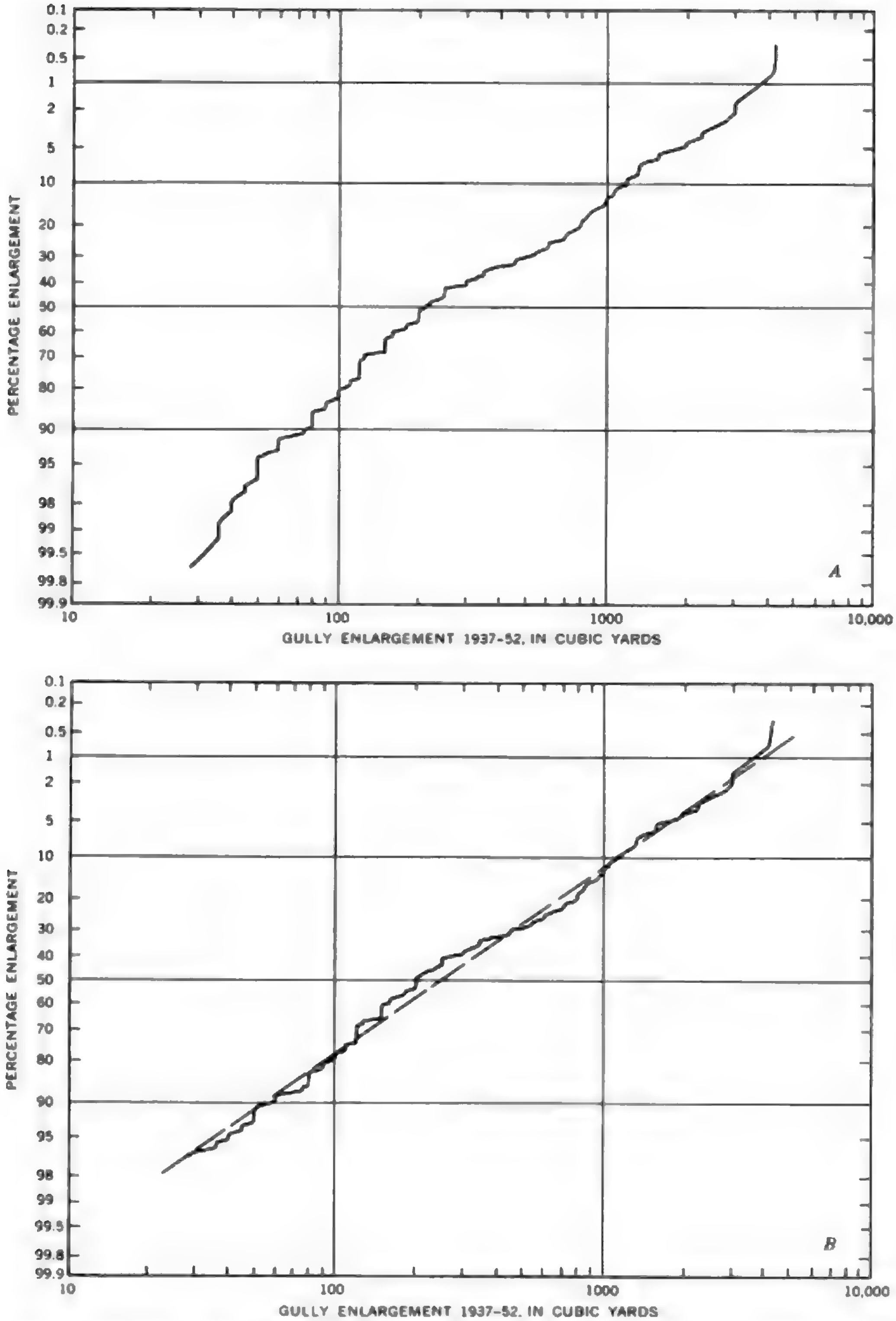

FIGURE 213.—Cumulative frequency distribution of 216 measured enlargements of valley-head and valley-side gullies on Dry Creek. *A*, Curve of 216 measured enlargements. *B*, Curve of 216 measured enlargements plus 7 hypothetical enlargements of less than 28 cubic yards.

Digitized by Google

TABLE 6.—*Number of gullies according to type and size in the Medicine Creek basin and in major subbasins*

Gully type	Size	Width of gully head (range in feet)	Number of gullies				
			Mitchell (subbasin C)	Dry (subbasin I)	Fox (subbasin K)	Brushy (subbasin N)	Medicine (subbasins A–O)
Valley head	Small	1–15	47	70	39	38	417
	Medium	16–60	99	110	90	302	1,357
	Large	61–180	28	35	16	90	360
	Very large	>180	1	2	...	3	20
Valley side	Small	1–10	22	8	7	10	112
	Medium	11–25	21	14	17	66	279
	Large	26–50	6	2	2	7	44
	Very large	>50	...	...	...	...	...
Valley bottom	Small	1–10	56	38	11	24	563
	Medium	11–25	33	27	23	82	477
	Large	26–50	10	10	9	19	152
	Very large	>50					

apparent. In the ranking of gullies into categories, a particularly difficult subjective decision lies in deciding whether the complex branches of a severely eroded valley head should be regarded as one gully or several. In the Dry Creek measurements, most of the branching valley heads were divided into several gullies, whereas in the later ranking of gullies according to size, the branching valley heads were regarded as one gully. For this reason the geometric mean of the largest size category (5,100 cu yd) is larger than the largest measurement reported (4,200 cu yd).

The topographic situations of gullies, as well as most of the topographic features characteristic of the Medicine Creek basin, are illustrated by the vertical aerial photograph reproduced as figure 214. Sec. 17, T. 9 N., R. 27 W., is approximately in the center of the area, and the valley of Dry Creek crosses it from left to right. Gullies numbered 3 and 5 on the photograph are in the very large category and have complexly branching heads. Total enlargement of all branches amounted to about 6,950 cubic yards for gully 3 during the period 1937–52 and about 5,610 cubic yards for gully 5. Figure 204 (*upper right*) is a view of gully 3 as seen from the air. Gullies 1 and 4 are in the large category, and the lobed shape of their heads indicates that they have not advanced beyond the steeper parts of the valley heads, although the head of gully 4 is beginning to branch. Enlargement during the period 1937–52 was 1,320 cubic yards for gully 1 and 2,250 cubic yards for gully 4. The group of four gullies indicated by the numeral 2 are in the medium category, and their enlargements ranged from 107 to 225 cubic yards.

Discontinuous valley-bottom gullies of small size are indicated by the two arrows at left of the numeral 4, and others of medium size are indicated by arrows in the lower left corner of the photograph. Small discontinuous valley-bottom gullies are also indicated by arrows on the valley flat of Dry Creek. The major valley-bottom gully on Dry Creek begins about 1 mile downstream (to the right) from this locality. A valley-side gully of medium size, which is advancing along a fence, is indicated by the numeral 6.

Among the notable relief features shown on the photograph are the differences among valleys in flatness of bottom and steepness of side. The valleys at right of numeral 4 have flat bottoms and steep sides because post-Stockville trenching extended to the valley heads; the valleys at left and below numeral 4 have narrow bottoms and gentle sides because their trenching was incomplete. Also notable, in the field at right center on the photograph, is a dark round spot that indicates a depression. Depressions of this sort, sometimes called buffalo wallows, are common on the Great Plains. Many hypotheses have been proposed as to their origin, but they probably originate in more than one way, and no hypothesis has been established as generally valid. In the Medicine Creek basin, many of the depressions probably mark the positions of sinkholes in the underlying Ogallala Formation.

AREAL DISTRIBUTION OF GULLIES

Experience in the recognition of Dry Creek gullies on aerial photographs and in the estimation of their size and activity was used in the collection of information on the distribution of gullies in the Medicine

Digitized by Google

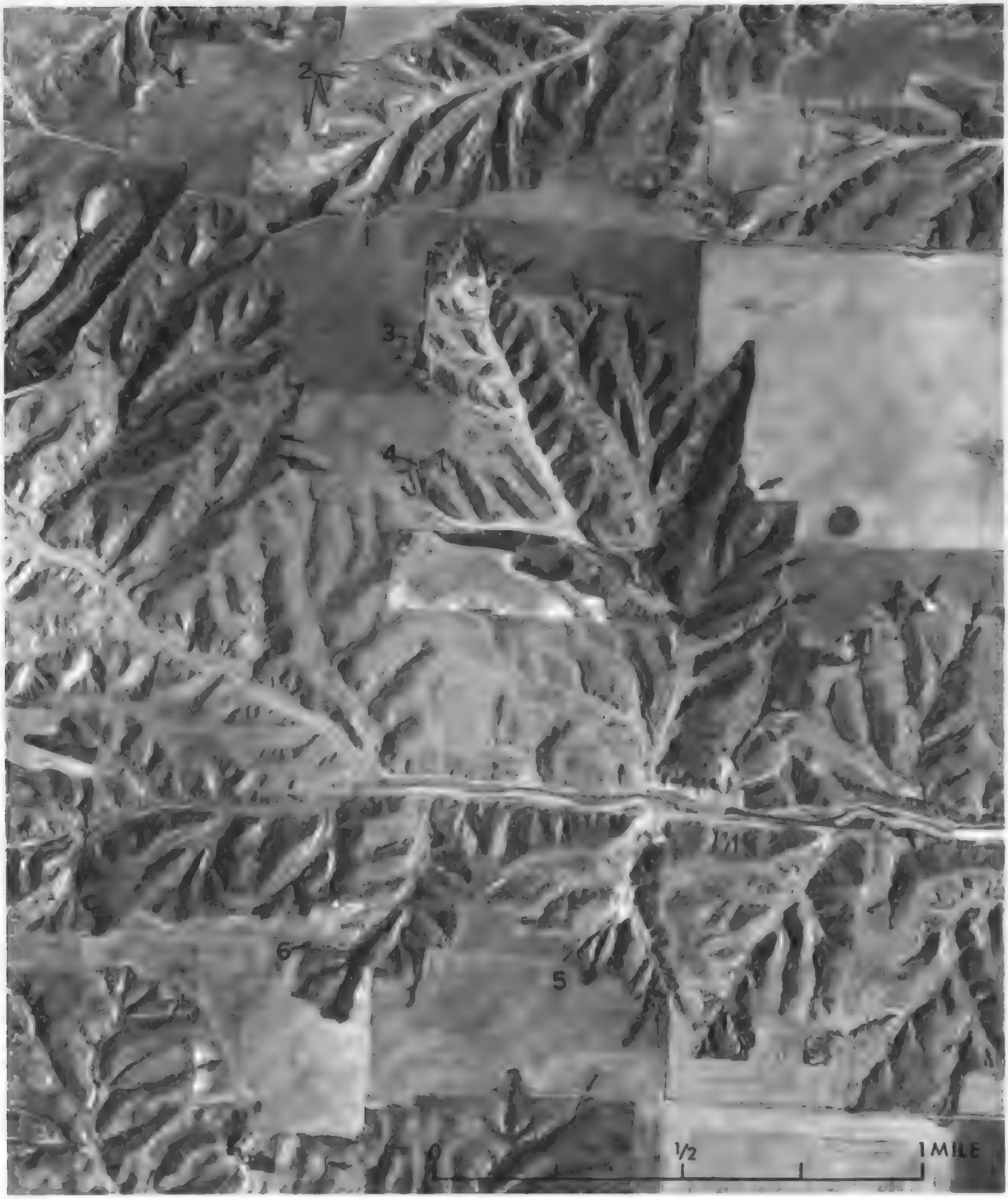

FIGURE 214.—Vertical aerial photograph of a severely gullied area on upper Dry Creek. Numbers indicate gullies described in text. Arrows indicate small- and medium-size discontinuous valley-bottom gullies described in text. Photograph by U.S. Commodity Stabilization Service.

Digitized by Google

Creek basin as a whole. Aerial photographs of the whole basin were studied stereoscopically, and all gullies in the basin that seemed to be active were plotted on topographic maps. Decisions as to the activity of a gully were checked by reference to 1937 aerial photographs. The gullies were grouped according to type (valley head, valley side, or valley bottom) and according to size (small, medium, large, very large). (See table 6.)

A map showing the frequency distribution of gullies according to subbasin was prepared (fig. 215). The basin was divided into 24 subbasins, corresponding generally to subbasins used by the Agricultural Research Service in their land-use tabulations, that are reasonably homogeneous in texture of relief. The frequencies of valley-head, valley-side, and valley-bottom gullies (excepting large and very large valley-bottom gullies) in each subbasin are given in table 7. Gully frequency refers to number of gullies per square mile of valley system rather than to number per square mile of drainage area. Gullies are directly related to the valley system and are not present in the upland except at its edges. Area of upland and characteristics of the valley system should be regarded as independent variables in their relation to gullying.

The frequency of active valley-head and valley-side gullies is low in the lower and upper part of the basin and ranges from moderate to high in the central part (fig. 215). The frequency ratio of valley-head and valley-side gullies to valley-bottom gullies ranges from about 0.6 in the lower part of the basin (subbasin A) to about 6 in the central part of the basin (subbasin 0–4). The distribution of gullies according to type and frequency is controlled mainly by the steepness of valley heads, the narrowness of valley bottoms, and the amount of upland drained by a valley head. In general, the steepness of valley heads is directly proportional, and the narrowness of valley bottoms is inversely proportional, to first-order-channel frequency.

TABLE 7.—*Gully frequencies and related data for subbasins of the Medicine Creek basin*

Subbasin	Drainage area (sq mi)	Area in upland (percent)	Area of valley system (sq mi)	Frequency of first-order channels	Frequency of valley-head and valley-side gullies	Frequency of valley-bottom gullies
A	27.2	46	15.0	113	3.2	5.3
B–1	43.4	38	26.4	150	2.9	4.2
B–2	11.6	37	7.3	140	3.7	5.5
C–1	[illegible]	50	10.8	190	16.0	4.3
C–2	29.8	52	14.4	150	3.5	3.4
D	74.4	45	[illegible]	160	5.7	2.6
E	10.9	42	6.3	165	5.2	6.1
F	58.9	34	35.3	170	6.9	4.1
G	23.2	42	13.4	[illegible]	12.4	5.0
H	16.5	48	7.4	185	11.7	4.2
I–1	12.6	[illegible]	9.5	214	18.5	5.1
I–2	8.5	[illegible]	4.3	186	14.2	5.3
J–1	17.6	12	15.5	275	[illegible]	3.0
J–2	22.6	45	12.6	200	16.4	4.6
K–1	57.0	12	49.8	260	1.5	4.2
K–2	15.5	30	10.8	200	9.1	1.6
L–1	[illegible]	12	19.9	260	.5	[illegible]
L–2	30.6	26	22.5	220	5.2	.9
M	27.5	30	19.3	180	6.8	1.6
N	73.8	28	52.4	260	10.0	2.3
O–1	14.6	...	...	...	...	...
O–2	16.0	10	18.5	450	.7	.4
O–3	35.4	12	31.1	350	2.1	.4
O–4	22.0	55	9.9	350	10.8	1.8

Gully frequency in relation to percentage of area in upland and to adjusted frequency of first-order channels is shown in a semiquantitative way in figure 216. Moderate to high frequencies of valley-head and valley-side gullies are associated with values of first-order-channel frequency and percentage of area in upland that plot to the right of the dashed line. On the other hand, values that plot to the left of the dashed line tend to have a higher frequency of small and medium valley-bottom gullies.

Points representing high gully frequency would probably be more widely separated from points representing low gully frequency were it not for the fact that the subbasins are not entirely homogeneous in topographic character. The severity of post-Stockville trenching not only varies from the upper to the lower part of the basin, but also from one minor side tributary to the next (fig. 214). The point indicated by a gully frequency of 10.8 and representing subbasin 0–4, at upper right in figure 216, is most anomalous. In spite of the relatively low gully frequency in this subbasin, it includes an area of exceptionally severe erosion that is about 3 miles northeast of Maywood. This area is also exceptional in that its drainage was greatly extended by post-Stockville erosion. Several large gullies there made advances ranging from 60 to 180 feet during the period 1937–52.

FORMATION OF VALLEY-HEAD AND VALLEY-SIDE GULLIES

The head scarps of many valley-head gullies originate on the steep upper part of the valley head and advance toward the upland. This is indicated by the position of short gullies and by the shape in plan view of long gullies. The width of many large valley-head gullies decreases sharply toward the lower part of the valley head, and the gullies are connected to the valley flat by a narrow trench. (See fig. 217 and gully 5 in fig. 214.) Gully 5 narrowed downvalley (in 1956) to a particularly deep trench about 25 feet deep, 15 feet wide at the top, and 5 feet wide

Digitized by Google

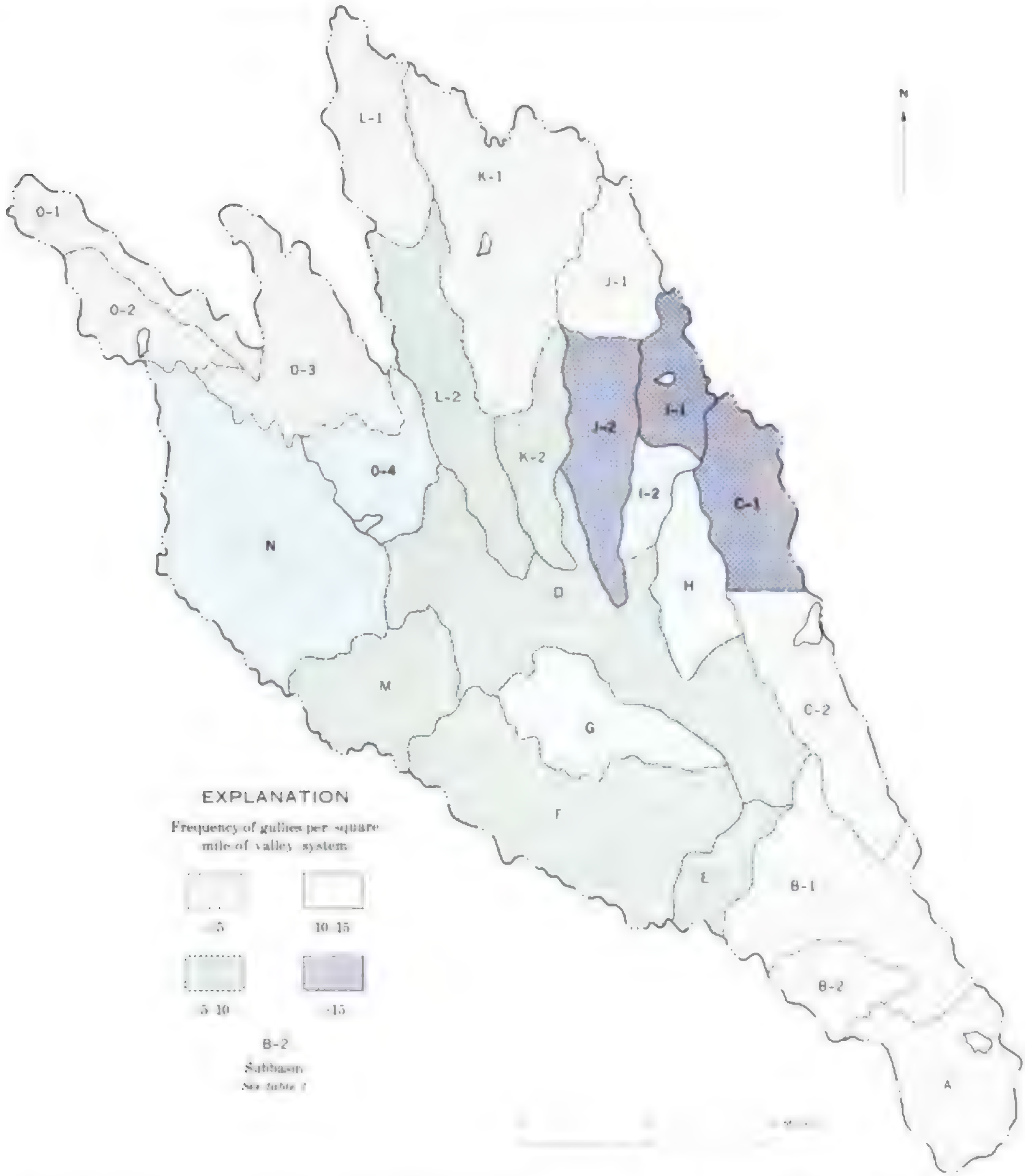

FIGURE 215.—Areal frequency distribution of active valley-head and valley-side gullies in the Medicine Creek basin. Subbasins illustrated in figure 197 are shown by heavy outlines. See table 7.

Digitized by Google

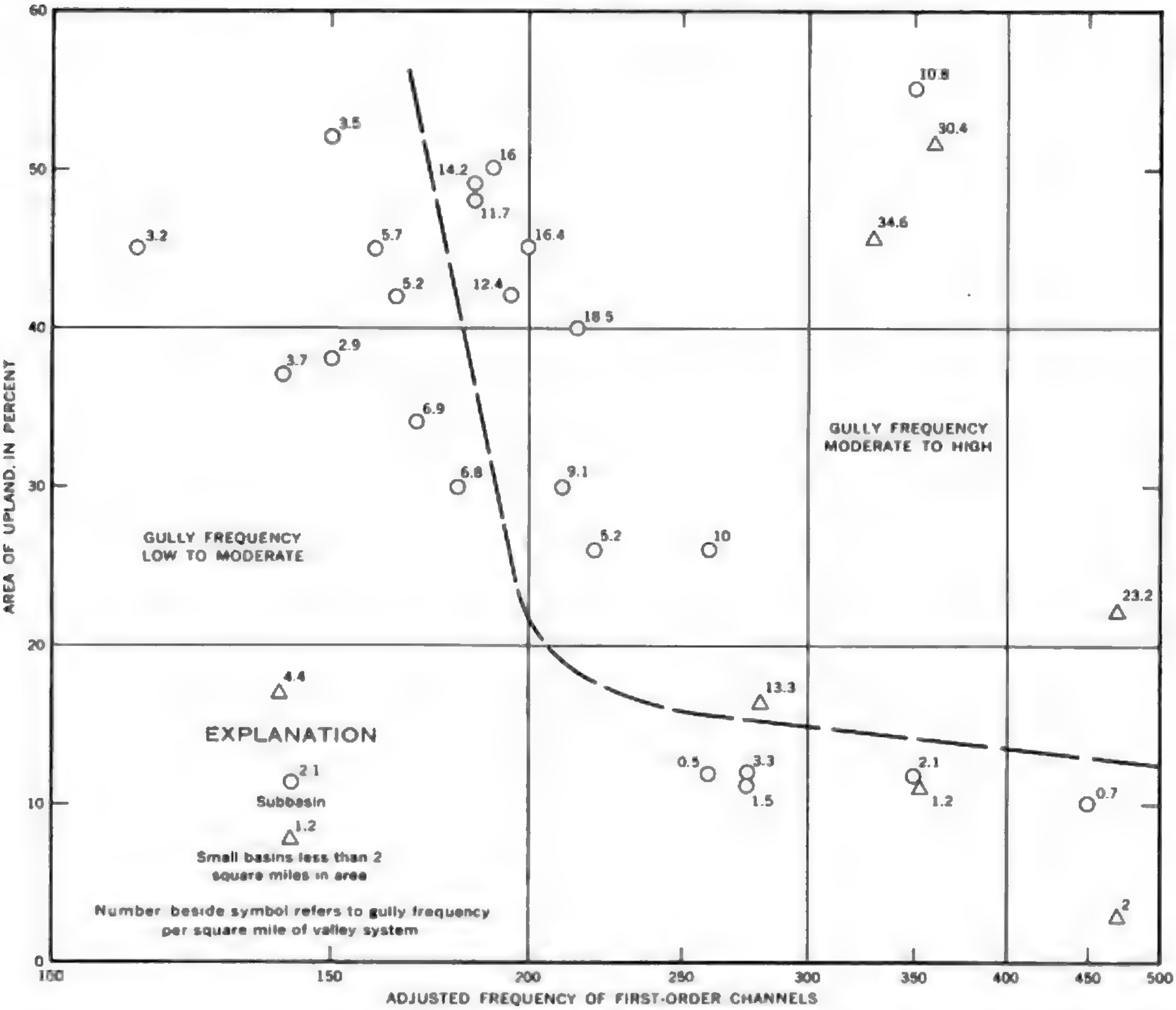

FIGURE 216.—Frequency of active valley-head and valley-side gullies in relation to area of upland and adjusted frequency of first-order channels.

at the bottom. Set in the bottom of this trench was a winding notch, sections of which passed underground.

Other valley-head gullies begin at an upvalley riser of the Stockville terrace, such as the one shown in the valley at center in figure 211, or as discontinuous valley-bottom gullies, such as the ones shown in the valley at upper left in figure 200. In the tabulation of all active gullies in the basin, valley-head gullies that are connected by a continuous, rather wide trench to the valley flat were given a separate designation because they probably began on the valley bottom rather than in the valley head. The percentages of valley-head gullies that fall in this category are as follows for several subbasins: Dry Creek, 7 percent; Brushy Creek, 22 percent; Mitchell Creek, 9 percent; Fox Creek, 6 percent; Lime Creek, 45 percent; and subbasin A, 65 percent. Thus, in the narrow valleys of the lower part of the basin, a greater percentage of valley-head gullies begins on the valley bottoms.

The head scarps of valley-head gullies reach a maximum height of about 35 feet, a value about 10 feet higher than the maximum height of head scarp measured for large valley-bottom gullies. This greater height is evidently related to the steeper slopes into which the valley-head and valley-side gullies are advancing and to the correspondingly steeper slopes at the base of their head scarps. (See figs. 217 and 218.) Material does not tend to accumulate at the base of the head scarp as it does in large valley-bottom gullies. In long profile, the head

Digitized by Google

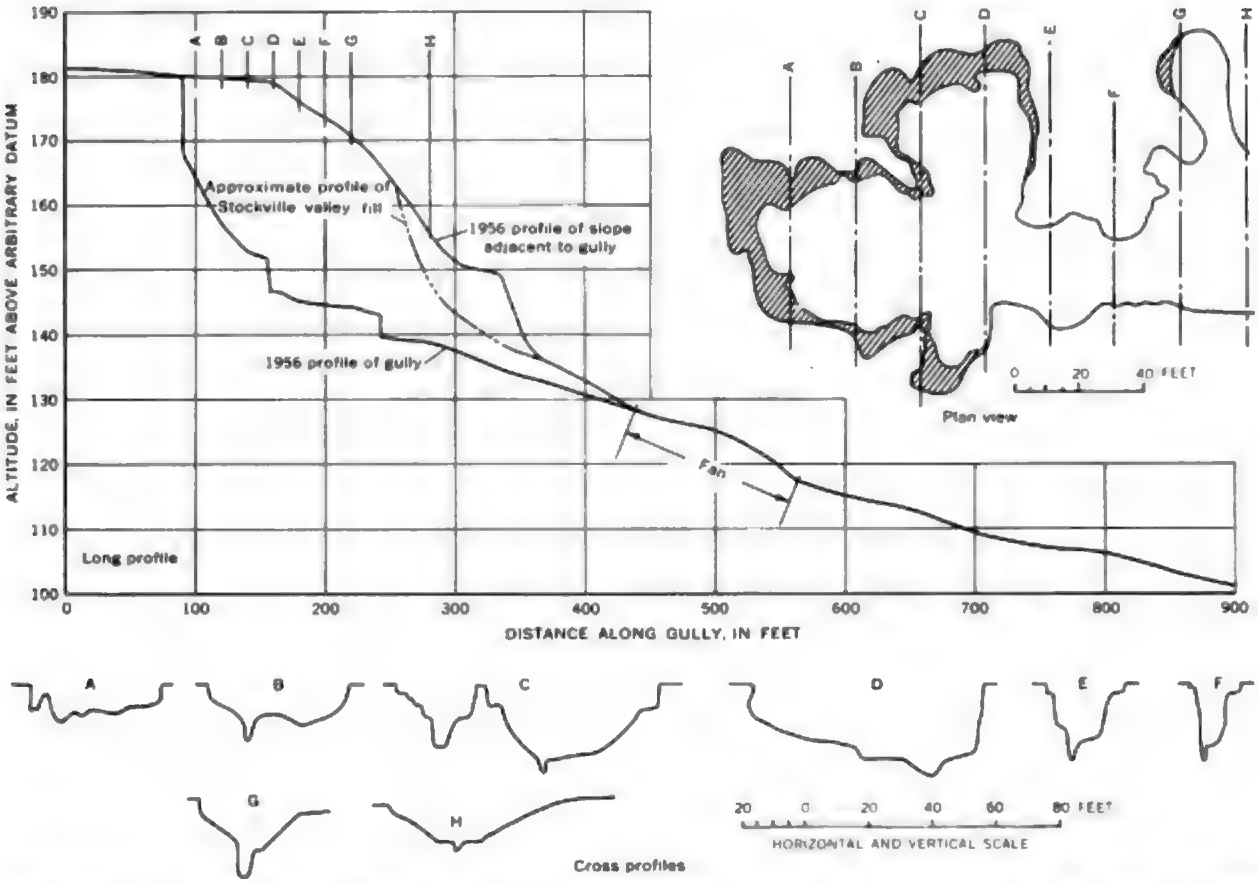

FIGURE 217.—Long profile, plan view, and cross profiles of a large valley-head gully, designated gully 4 in figure 214. Shaded area on plan view indicates enlargement during the period 1954–57. Based of field surveys. Location of cross profile H is beyond limit of area shown in plan view.

scarps are nearly vertical or even overhanging at the rim, and the channel profile downstream from the head scarp is typically broken by several channel scarps. The channel scarps deepen the gully as they advance and probably increase the height of the head scarp by merging with it. The modal value for height of head scarps of active valley-head and valley-side gullies on Dry Creek is about 10 feet.

The mechanism of head-scarp advance is not identical with that described for large valley-bottom gullies. Most valley-head gullies are advancing into surfaces underlain by a well-developed soil profile and, except for gullies advancing into cultivated upland, protected by a sod cover. The rills or trenches that lead to the gully head have not been incised through this profile; hence, the head scarp has a resistant rim. On the other hand, plunge pools are not conspicuous at the base of the head scarps, and saturation of the massive silt by plunge pool action is less important than that for large valley-bottom gullies. The water flowing over the rim of the head scarp has relatively small volume and velocity, and silt beneath the resistant rim is disintegrated by back trickle of water. Underground drainage, which probably enters the ground through rodent burrows upslope from the head scarp, is conveyed into the gully head at some point below the resistant rim. The abundance of rodent burrows intersected by some head scarps, as well as the overhanging of the resistant rim, is shown in figure 219. Head scarps less than 4 feet high do not advance rapidly because the resistance of the soil profile and the sod cover extend to about this depth.

Material that slumps from the head scarps and side scarps accumulates on the gully floor and is gradually removed by runoff. Deposition is uncommon in the trench that drains the gully head, but much deposition takes place where this trench enters the valley flat. The number of valley-head and valley-side gullies that discharge directly into the channels of major tributaries is insignificant, and

Digitized by Google

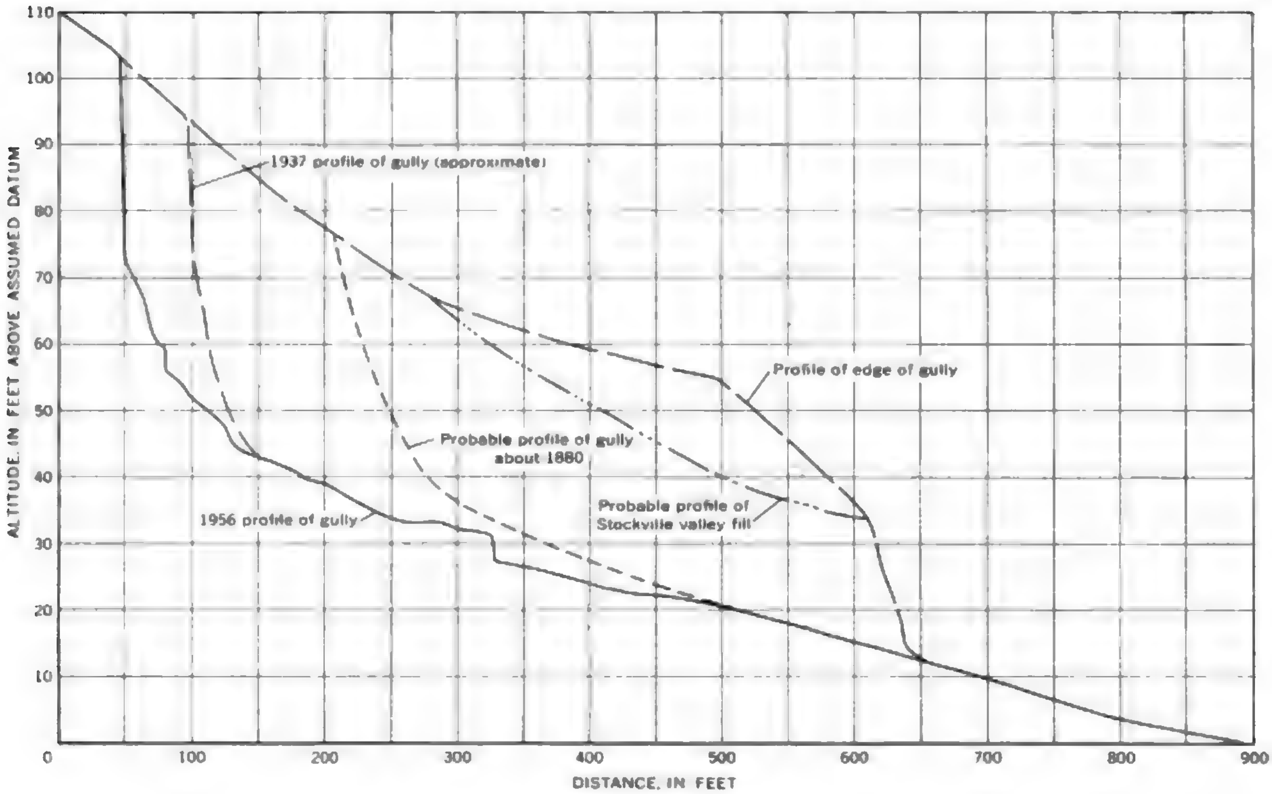

FIGURE 218.—Long profile of a large valley-head gully, designated gully 1 in figure 214.

most of the material eroded is probably deposited on valley flats.

Although the general conditions of topography and vegetation that are conducive to the formation of valley-head gullies can be stipulated, the localization of a gully in a particular valley head rather than in an adjoining valley head depends on events that cannot be reconstructed. Such events include the past methods of cultivation of the upland and the past land use of the valley head, as well as such fortuitous events as the digging of burrows by animals. Moreover, no correlation whatever is apparent between the size of a gully and its topographic situation. Study of the topography of seven of the largest valley-head gullies in the basin showed that the drainage areas ranged from 4 to 37 acres and that the slope of the upland draining into the valley head ranged from 0.02 to 0.06 foot per foot. The slope of the valley heads could not be accurately reconstructed, but all appeared to have been relatively steep. Other valley heads, similar in drainage area and steepness to the severely gullied valley heads, contain small gullies or none.

GULLYING AND LAND USE

That most of the active valley-head and valley-side gullies in the Medicine Creek basin are man induced is highly probable. Many of the valley-side gullies are directly associated with cultural features—such as roads, buildings, and fences—and nearly all the valley-head gullies have begun in valley heads that drain areas of cultivated upland. During past naturally induced episodes of erosion, gullying does not seem to have begun in valley heads. The two post-Stockville episodes of trenching stopped short of the valley heads or else progressed from downvalley to the valley heads. The drainage system is presently extending itself beyond the valley heads and into the upland, a process that last took place before accumulation of the Stockville terrace deposits. The lack of gullying in two tributary heads on Dry Creek, densely vegetated because of protection by fences, indicates that land use has caused gullying elsewhere. (See fig. 182.)

The role of land use in the initiation and growth of large valley-bottom gullies is uncertain. Geologic evidence indicates that valley-bottom gullying has taken place on Elkhorn Canyon and probably on

Digitized by Google

FIGURE 219.—Head scarp of a small valley-head gully on Dry Creek. Note animal burrows and overhanging rim of head scarp.

Dry Creek within the past 350 years and before the arrival of settlers. There is no evidence of late Recent valley-bottom gullying elsewhere in the basin, except that valley-bottom gullies, probably formed since settlement, are advancing rapidly at one or more localities in the valleys of major tributaries to Medicine Creek. The formation of these large valley-bottom gullies entirely from natural causes is improbable. The condition of the vegetal cover in relatively undisturbed areas indicates that the climate since settlement has not been particularly conducive to the formation of gullies.

Antevs (1952) concludes that arroyo cutting and filling in the semiarid southwest are controlled mainly by vegetation, which is in turn controlled naturally by climate. Channeling is a result of drought; filling takes place during climatic transitions; and soil development takes place during relatively moist periods. Arroyo cutting was caused mainly by drought in the past and by overgrazing since 1875. Bryan (1941) also concludes that a slight change in climate from the dry toward the less dry is adequate to convert ephemeral streams from a condition of erosion to alluviation.

These conclusions are reasonable, although the specific climatic conditions that prevailed during past episodes of cutting and filling cannot be reconstructed by any presently known method. During dry years in the Medicine Creek basin, gully advance has been negligible and alluviation has taken place in large valley-bottom gullies. Gullying does not literally take place during dry years, but rather during the wet years that occur from time to time during a general period of drought. A temporary effect of drought may be an increase in the rate of accumulation of valley fill, as is suggested by the character of the terrace deposits on Elkhorn Canyon; but valley fill accumulated during drought is subject to almost immediate incision. As to the climatic conditions that prevailed during episodes of filling, good faunal evidence indicates that the Stockville terrace deposits accumulated during a climatic regime very similar to the present climate. Past episodes of cutting are probably due to a series of droughts more rigorous than any recorded since white settlement.

CONTROL OF GULLIES

Valley-head gullies of moderate to large size have been stabilized in some parts of the basin. The most effective methods of stabilization have involved the construction of an arcuate ditch above the gully head and the diversion of drainage along grassed waterways on either side of the gully. As is true of gully control structures generally, these must be maintained; and lack of maintenance has resulted either in renewed activity of the gully head scarp or in trenching of the grassed waterways.

A heavy vegetal cover in a valley head inhibits formation of new gullies because gullies begin on the valley head rather than on the upland. The cultivation of upland to the very edges of valley heads has been unfortunate. Restoration of native vegetation in the valley heads and in the area of upland adjoining the valley head would probably be effective in preventing new gullies and in stabilizing gullies of small to moderate size.

No large valley-bottom gully in the Medicine Creek basin has been effectively controlled, and only one effort toward control was noted. Concrete blocks were placed in the head of the main gully on Dry Creek, but these had no apparent effect. The control problem is complicated by the fact that a given head

Digitized by Google

scarp may have in its wake a series of channel scarps, all of which must be controlled. A reduction of runoff on the valley bottom is the only apparent solution to the problem, and this can probably be achieved by construction of terraces on the upland, restoration of native vegetation of some parts of the valley bottoms, and more moderate grazing.

SUSPENDED SEDIMENT AND THE HYDRAULIC GEOMETRY OF CHANNELS

By Cloyd H. Scott

Medicine Creek has a well-sustained low flow. Fox Creek and Brushy Creek also receive groundwater inflow, although the volume is not so great as the volume received by Medicine Creek. Fox Creek has a well-sustained low flow, but Brushy Creek usually stops flowing for some time during the summer months. The other gaged tributaries, Dry Creek and Mitchell Creek, and most of the ungaged streams in the basin flow only after rainfall. Typical hydrographs of large flows are shown in figure 220. The magnitude of these flows was such that the daily mean discharge was equaled or exceeded about 1 percent of the time. Medicine Creek at Maywood rises and falls more slowly than the others because of reservoir regulation upstream.

Medicine Creek and its tributaries tend to be "flashy" streams; that is, the discharges increase rapidly in response to rainfall, and peaks are of short duration. This flashy condition is probably the result of several factors, the most important of which is the intensity of thunderstorms. One storm produced 1.70 inches of rain in 45 minutes at Tobiassen gage. Such intense storms do not occur often, but storms that produce as much as three-fourths of an inch of precipitation in an hour or less are common.

The thunderstorms result in runoff having moderately high suspended-sediment concentrations. The maximum observed concentration in the basin during the approximately 37 years of combined station record was 192,000 ppm (parts per million), and the maximum observed suspended-sediment concentration was more than 100,000 ppm in 5 of the 37 years of combined station record. All the annual maximum observed concentrations were in excess of 10,000 ppm for the period of record. Maximum concentrations in excess of those observed undoubtedly occurred during most years. Because concentrations do not remain high for very long, the maximum daily suspended-sediment concentrations are much less than the maximum observed concentrations. The maximum daily concentration during the period of record was 37,600 ppm at the Fox Creek station, but the maximum exceeded 20,000 ppm during only 3 years of combined station record. The maximum daily concentrations were larger than about 1,000 ppm for the combined record, and about one-third were between 10,000 and 20,000 ppm.

The material that makes up suspended sediment is relatively fine because of the general lack of sources of coarse material in the basin. The percentages of clay (finer than 0.004 mm) and silt (0.004 to 0.062 mm) are variable, but clay and silt together make up 90 percent or more of the suspended sediment. Ten percent or less of sand (0.062 to 2.00 mm) is generally finer than 0.125 mm except at the two stations on Medicine Creek, where a few samples contain 1 or 2 percent of sand ranging from 0.125 to 0.250 mm.

Stream-channel cross-sectional shapes are rather diverse within the basin, particularly the shapes of channels of ephemeral streams. In cross section, the channels of ephemeral streams range from shallow swales on the valley floor to deeply incised trenches, either wide or narrow. Figure 210 (*upper left*) illustrates a broad valley floor in which a narrow channel is forming. In figure 204 (*upper left*) a narrow trench is shown upstream from the head of a gully, and this trench is being widened and deepened by the advance of the gully head scarp. The broad trench formed by advance of the head scarp is only about twice as deep as the narrow trench, but a short distance downstream from the head scarp the width of the broad trench is several times that of the narrow trench. Head scarps are advancing in some valley floors where narrow channels are poorly defined or do not exist at all. As a result of the advance of these head scarps, the shape of the channel is changed from broad and shallow to broad and deep.

Dry Creek (fig. 210, *upper right*) and Brushy Creek both have broadly incised channels at the gaging stations, and Brushy Creek has a poorly defined low-flow channel in the broadly incised channel. Medicine Creek and Fox Creek, which are perennial streams, have well-defined low-flow channels at the gaging station.

HYDRAULIC RELATIONS AT A SECTION AND IN A DOWNSTREAM DIRECTION

As the discharge at a particular cross section (called "at a station" by Leopold and Maddock, 1953, p. 4) in a stream increases, the width, depth, and velocity increase. Previous investigators (Leopold and Maddock, 1953; Wolman, 1955; and Leopold and Miller, 1956) have shown that, within limits of

Digitized by Google

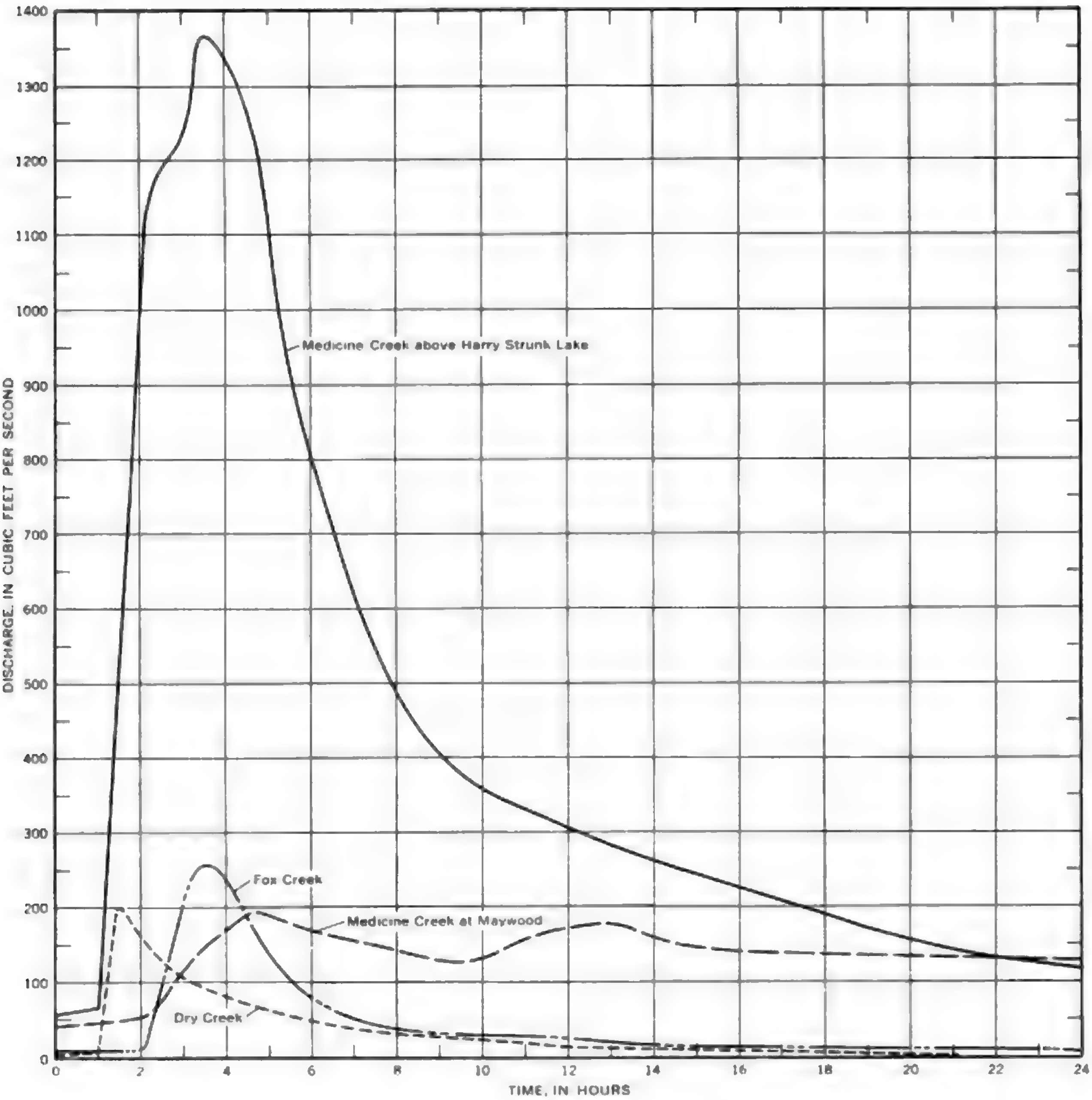

FIGURE 220.—Typical hydrographs of large flows.

bankfull discharge, these variables are simple power functions of the water discharge of the form

$$\bar{u} \alpha Q^{m}$$
$$d \alpha Q^{f}$$
$$w \alpha Q^{b}$$

where $\bar{u}$ is mean velocity (fps),
d is mean depth (ft),
w is width (ft), and
Q is water discharge (cfs).

The product of mean velocity, width, and mean depth must equal discharge; therefore, the sum of the exponents b, f, and m must equal 1.00.

Points on graphs of width, depth, and velocity versus discharge for the gaging stations in the Medicine Creek basin scatter rather widely from the mean, particularly for Brushy, Dry (fig. 221), and Mitchell Creeks. Scatter at the lower values of discharge is caused, in part, by natural variations

Digitized by Google

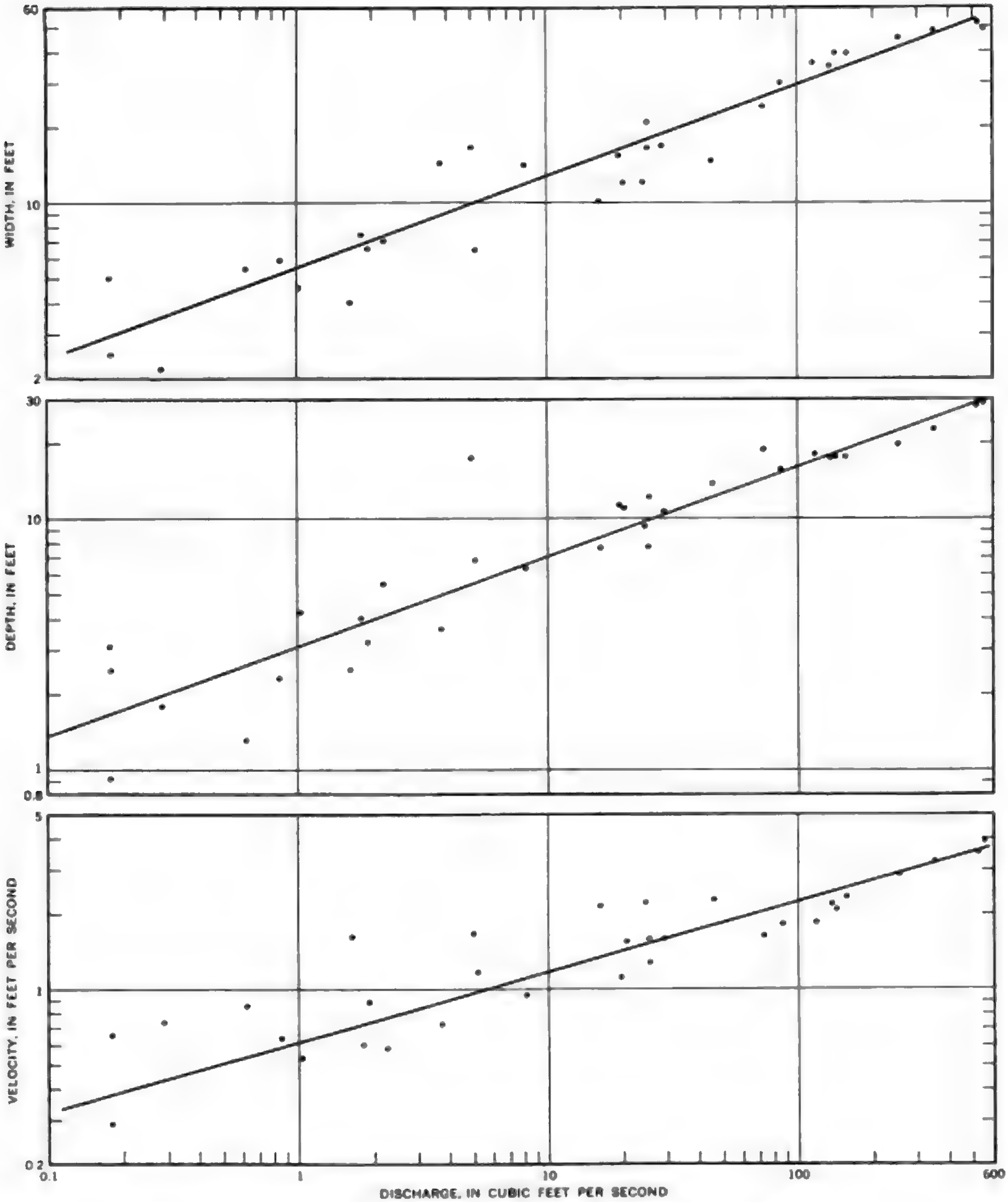

FIGURE 221.—Change of width, depth, and velocity with increasing discharge at a section, Dry Creek near Curtis.

Digitized by Google

in channel shape at the different sections used for making discharge measurements by wading. Flows too deep to be waded were measured at a single section at each of the stations, and the scatter on the plots is somewhat reduced at the higher discharges. There would be some scatter on the plots even if all measurements were made at a single cross section.

The slopes of curves relating width, depth, and velocity to discharge at each gaging station were fitted by eye and adjusted so that the values of b, f, and m summed to 1.00. The adjustments were small for all sections. The relations of width, depth, and velocity to water discharge at the individual sections have little meaning; therefore, the curves, without the defining points, were placed on one graph, and the discharges that were equaled or exceeded 1, 2, and 25 percent of the time were indicated on each of the curves. Discharges equaled or exceeded 1, 2, and 25 percent of the time were selected because the 1-percent discharge represents approximately bankfull flow at the Fox Creek station but less than bankfull flow for the other stations. The 25-percent discharge is approximately the modal discharge for the Fox Creek and both Medicine Creek stations, and the 2-percent discharge is about the lower limit for which reliable measurements of width, depth, and velocity are available for the Dry, Brushy, and Mitchell Creek stations.

The slopes of width-discharge relations for Dry and Brushy Creeks are greater than those for the other sections, and lines joining points of equal-discharge frequency indicate that the sections should be divided into two groups (figs. 222 and 223). The fact that Mitchell Creek does not fit with either group is attributed to the presence of a concrete control at the section and to a low-water road crossing a short distance downstream, which causes backwater at the section. Therefore, the Mitchell Creek section will not be considered further.

Lines that join points of equal frequency of discharge on the curves of the at-a-station relations represent the downstream relations of width, depth, and velocity to discharge, if the assumption is made that the relation at sections not on the same stream is representative of relations at different sections on the same stream. This assumption may be justified for two reasons. First, the discharges of equal frequency for the two Medicine Creek stations and the Fox Creek station plot about on a straight line even though the uppermost section on Medicine Creek, at Maywood, is somewhat affected by reservoir regulation. Second, the gaging sections are on reaches where flows are over loess, which covers much of the basin. The assumption implies that the channels of two streams are similar at the points along their lengths where the discharges are the same at equal frequencies of occurrence.

The values of b, f, and m for changes of width, depth, and velocity in a downstream direction obtained from figures 222 and 223 cannot be considered reliable because too few stations are available to establish averages. The values can be used to show general differences between the types of streams represented by the two groups.

The downstream relations of width, depth, and velocity to discharge could best be defined by measurements along a stream at several stations for which at-a-station relations of width, depth, and velocity to water discharge and flow-duration curves are available. However, gaging stations of the number required for such a study are found on few if any streams. When better data are lacking, discharge measurements might be made at several sections in a downstream direction at discharges of unknown frequency at each of the sections. Even though the frequency of the discharges were the same at all the sections measured, the plot of width, depth, and velocity against discharge would scatter from the average line because of variations in shape that exist from place to place in a natural channel. Of course, it would not be possible to obtain measurements of discharges of the same frequency at all sections, especially for channels of ephemeral streams.

Assume that a series of measurements are to be made in a downstream direction on Dry Creek at discharges that are equaled or exceeded about 2 percent of the time at each of the sections. Further assume that the downstream relation of width to discharge for Dry Creek is the same as that shown on figure 223 for discharges equaled or exceeded 2 percent of the time. If a measurement is made at the gaging station at a discharge assumed to be equaled or exceeded 2 percent of the time, but the discharge is actually the one equaled or exceeded 1 percent of the time, then the width will be greater than that indicated by the downstream relation at discharges equaled or exceeded 2 percent of the time by about 40 percent plus or minus the deviation from the at-a-station relation (fig. 221). About two-thirds of the points that defined the at-a-station relation for the Dry Creek station were within plus 35 and minus 35 percent of the mean line. As the difference between the slopes of the lines for the at-a-station relations and the downstream relations of width, depth, and velocity to discharge becomes less, the scatter from the average line attributable to differ-

Digitized by Google

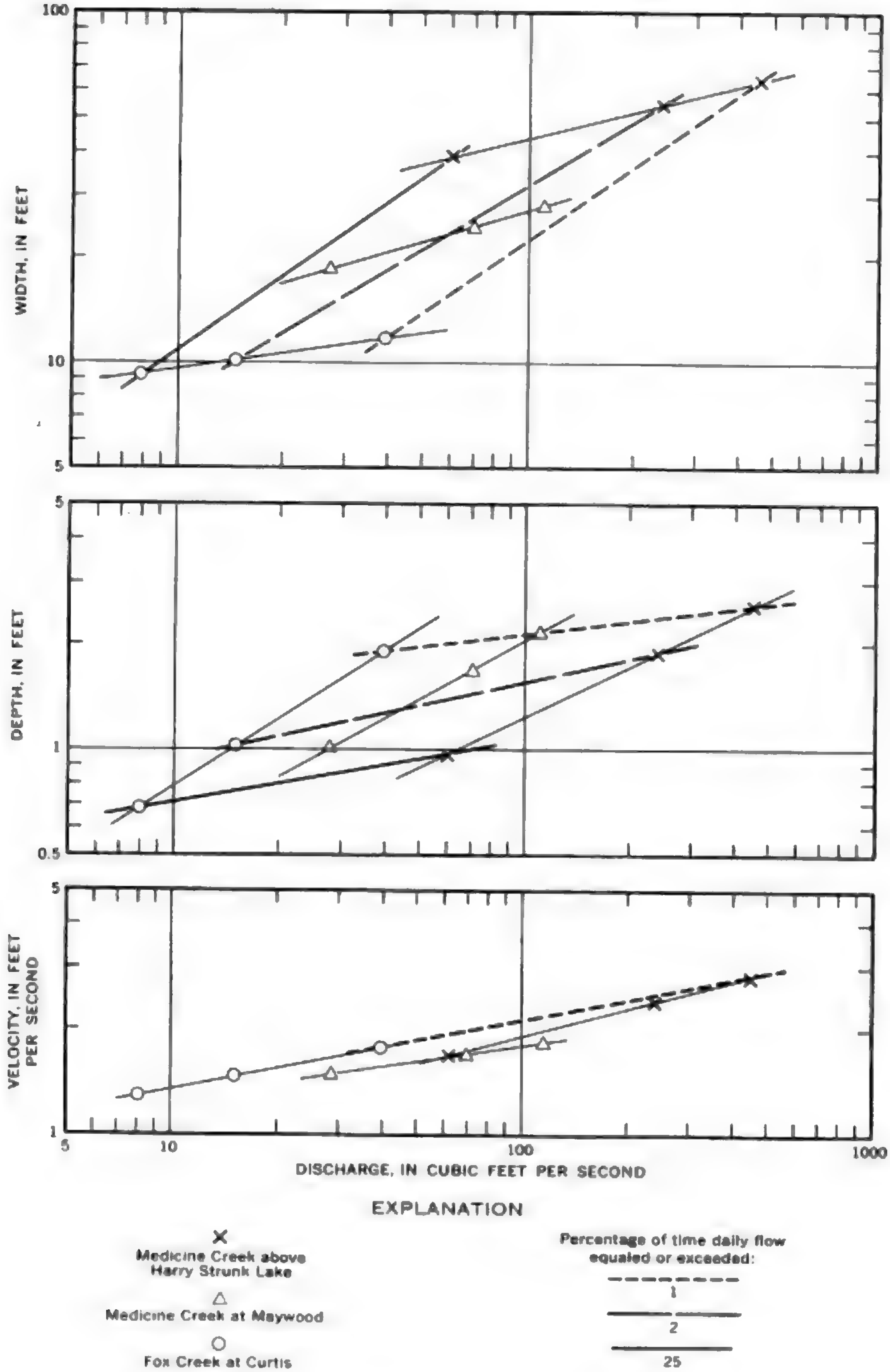

FIGURE 222.—Change, of width, depth, and velocity in a downstream direction for channels of perennial streams.

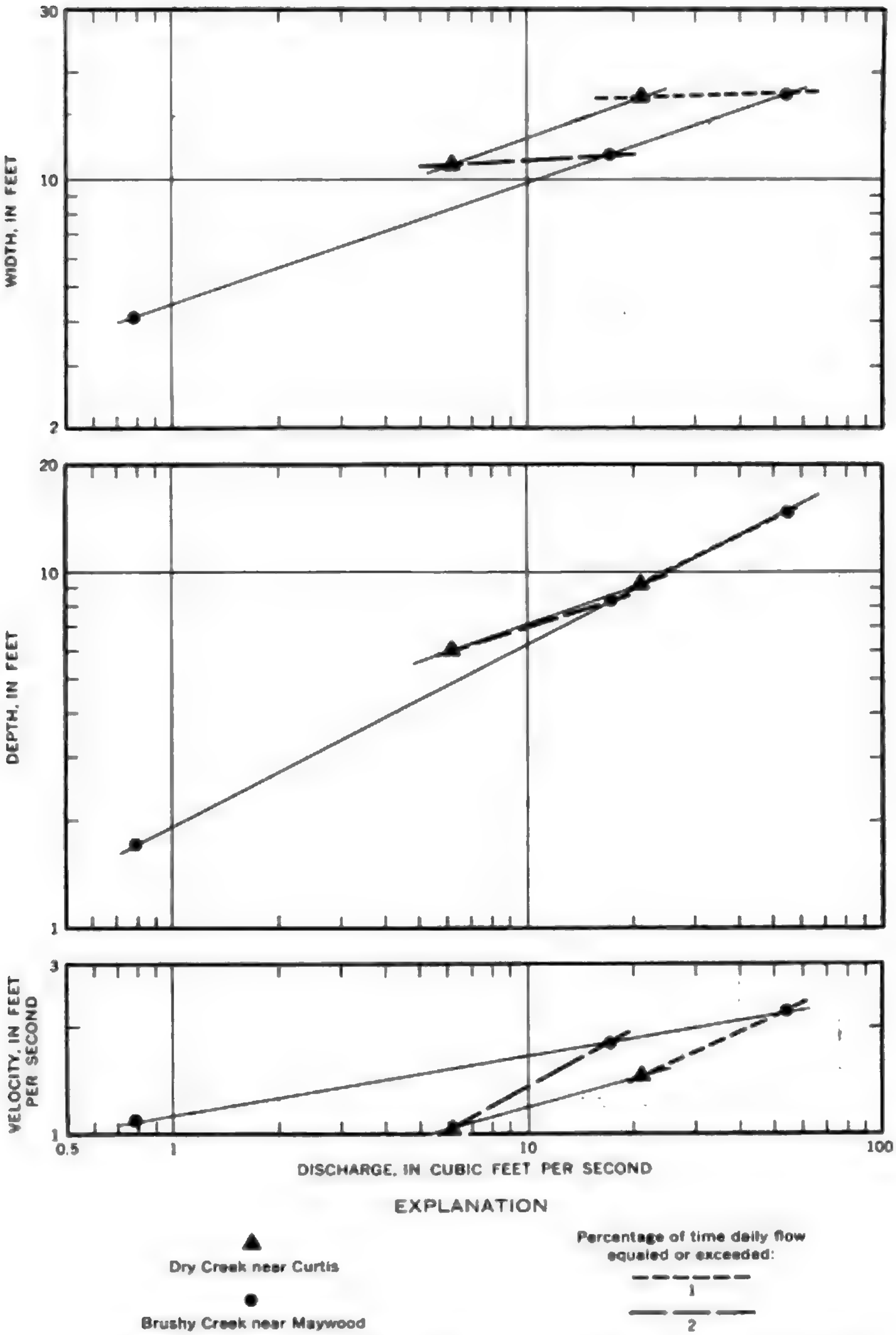

FIGURE 223.—Change of width, depth, and velocity in a downstream direction for channels of ephemeral streams.

Digitized by Google

ences in frequency of discharge at the various stations becomes less. Establishing fairly reliable downstream relations of width, depth, and velocity to discharge is possible if a sufficient number of sections are selected to provide a reliable average and if measurements of extremely high or low discharges are avoided.

The slopes of the relations of width, depth, and velocity to discharge (table 8) indicate differences between the perennial and ephemeral streams in the Medicine Creek basin. The at-a-station slope values may be considered reliable, but slopes for the downstream relations probably only indicate the correct order of magnitude. The differences between the at-a-station relations for the perennial and ephemeral streams reflect the differences in channel shapes. The channels of the perennial streams have fairly steep banks, and the width does not increase as rapidly as the depth. The channels of the ephemeral streams also have steep banks; but the bottoms of the channels are somewhat parabolic, and the width can increase rapidly as discharge increases until the limits of the steep confining banks is reached. However, a relatively large discharge is required for the width of water surface to reach the confining limits of the steep banks in the broadly incised channels of ephemeral streams. The changes of velocity with increasing discharge are about the same for perennial and ephemeral streams; therefore, the change of width is less and the change of depth is greater with increasing discharge for perennial streams than for the broadly incised ephemeral streams.

TABLE 8.—*Values of* b, f, *and* m *for streams in Medicine Creek basin*

	Perennial streams		Ephemeral streams	
	At a station [1]	Downstream [2]	At a station [1]	Downstream [2]
b	0.24	0.69	0.35	0.03
f	.56	.12	.43	.48
m	.20	.19	.22	[illegible]

[1] Unweighted average.
[2] At discharge equaled or exceeded 1 percent of time.

Depths of water in a channel normally do not increase very rapidly in a downstream direction. That is, it would not be expected that the depth at a cross section on a stream would be much greater than the depth at another section several tens of miles upstream. The downstream change in depth for perennial streams in Medicine Creek basin is relatively small, and the downstream change in velocity is about the same as the change in velocity at a station. Because the discharge at a constant frequency increases downstream, the width must increase rapidly. However, the width for the broadly incised ephemeral streams increases very little downstream. The increase in discharge is accommodated by relatively large changes in both depth and velocity in a downstream direction. The downstream change in width of the broadly incised ephemeral streams may be greater than that indicated on figure 223, but the change still would not be so large as the change of the perennial streams. Figure 204 (*upper left*) shows the main-stem channel of Dry Creek just below the gully scarp that forms the end of the broadly incised channel, and figure 210 (*upper right*) shows the main-stem channel at the gaging section. The top widths of the channel just below the gully scarp and in the vicinity of the gaging section are 40 to 50 feet. The distance is too short and the measurements are too rough to indicate the change in width along the Dry Creek channel; but if the width increased as rapidly as the indicated change of about 5 percent per mile on Medicine Creek between Maywood and the gage above Harry Strunk Lake, the width at the gage on Dry Creek should be more than 10 feet wider than the width in the vicinity of the head scarp.

SUSPENDED-SEDIMENT DISCHARGE RELATIONS

The curves relating suspended-sediment load to water discharge for the perennial streams (fig. 224) have breaks in slope at water discharges that are higher than normal but below bankfull stage. The curves applying to ephemeral streams show no corresponding breaks in slope (fig. 225), and in value of slope they are generally similar to the upper part of the curves applying to perennial streams. The breaks in the suspended-sediment rating curves result from a rather complex and uncertain set of conditions. The concentrations, peak and mean, for runoff periods are highly variable. Even two events, which may be very similar with respect to peak discharge and total discharge, may have very differpeak suspended-sediment concentrations and mean concentrations. The peak concentration generally occurs before the peak water discharge for stations in the Medicine Creek basin, but the length of lead is variable. The length of lead may be from 1 to 3 or or more for the perennial streams and is generally an hour or less for the ephemeral streams. The shorter lead time, in general, occurs with a small peak discharge. The variability in concentration of suspended sediment and in length of lead results because the suspended-sediment load is made up principally of fine material derived from sources

other than the streambed. The amount of fine material that is transported by the streams during a given storm depends on intensity and duration of rainfall, soil conditions at the time of the storm, and other factors. The leading concentration indicates that the sediment rating curve should describe a loop, but because of the variability of concentration from storm to storm and the variability of the lead time of concentration, the loop would not be defined by an average of many measurements for many storms. Instead, the points defined by the measurements would scatter with increasing discharge. (See fig. 224.) The measurements that define the points of figures 224 and 225 are somewhat biased, however, because only a few measurements were obtained before peak water discharge and practically none were obtained near peak sediment concentration. The generally rapid rises and mud roads prevented arrival of workers at the stations much before the occurrence of the peak water discharge, particularly on the ephemeral streams. Nearly all the measurements at those stations were obtained after the peak water discharge; therefore, the scatter of points is fairly uniform throughout the range of water discharge.

The lower part of the curves for the perennial streams is represented mostly by measurements made during small rises. A small increase in water discharge is accompanied by a relatively large increase in sediment concentration, and the lead time for smaller rises is generally short. As a result, the slope of the relation of water discharge to sediment discharge increases more rapidly for low water discharges than for the high water discharges.

The fact that the slope of the water-sediment discharge relation is slightly less than unity for the ephemeral streams indicates that the concentration remains about the same or decreases slightly in a downstream direction, but the fact that the slope of the water-sediment discharge relation is slightly greater than unity for perennial streams indicates that the concentration increases in a downstream direction. Because so few records are available to establish good average downstream relations, it is not possible to state that an actual difference exists between the slopes of the water-sediment discharge relations in a downstream direction for perennial and ephemeral streams.

PARTICLE-SIZE DISTRIBUTIONS OF SUSPENDED SEDIMENT AND BED MATERIAL

Average particle-size distributions of suspended sediment were obtained from unweighted averages of all size analyses at each of the stations. The size analyses were not weighted because a plot of water discharge against percentage of suspended sediment finer than 0.004 mm and coarser than 0.062 mm indicated no relation between instantaneous water discharge and particle-size distribution. The average size distributions for each year for each of the stations did show an inverse relation to annual water discharge; that is, the percentage finer than a given size decreased as water discharge increased. The relation was not very well defined, and the indicated change was not large; but the relation of annual water discharge to the average percentage finer than a given size does indicate the possibility of a relation between the percentage finer than a given size and instantaneous water discharge. The large variability of particle-size distributions for a given water discharge, however, prevent detection of a relation.

Average particle-size distributions of suspended sediment and bed material (figs. 226 and 227) indicate little difference between size distributions of suspended sediment and a large difference between size distributions of bed material for Medicine Creek at Maywood and Medicine Creek above Harry Strunk Lake. Medicine Creek above Harry Strunk Lake has a small percentage of material in the 0.125- to 0.250-mm range in suspension; such material is normally not in suspension at Maywood. Although the size distributions of suspended sediment are similar at the Medicine Creek stations, the distributions of bed material are very different. The bed material at Maywood has 36 percent of the material finer than 0.062 mm, 44 percent between 0.062 and 2.0 mm, and 20 percent coarser than 2.0 mm; at the station above Harry Strunk Lake only 8 percent is finer than 0.062 mm, 80 percent is between 0.062 and 2.0 mm, and only 12 percent is coarser than 2 mm. The increase of material in the 0.062- to 2.0-mm range is probably from the tributaries draining the area to the southwest of Medicine Creek. There are, however, no analyses of bed-material samples from any of these tributaries. The average distribution of only three samples, each of bed material from the low-flow channels of Brushy and Fox Creeks (fig. 50), indicates that the bed material at those stations is similar to bed material at Medicine Creek at Maywood, especially for the sizes finer than about 1.0 mm. Suspended-sediment size distributions for Brushy, Fox, Dry, and Mitchell Creeks (fig. 226) show that there is an apparent increase in fine material available for transport as suspended sediment from the west to the east side of the basin. Brushy Creek, on the west side of the basin, has a median suspended-sediment particle size of about 0.014 mm, whereas Mitchell Creek, on the east side

Digitized by Google

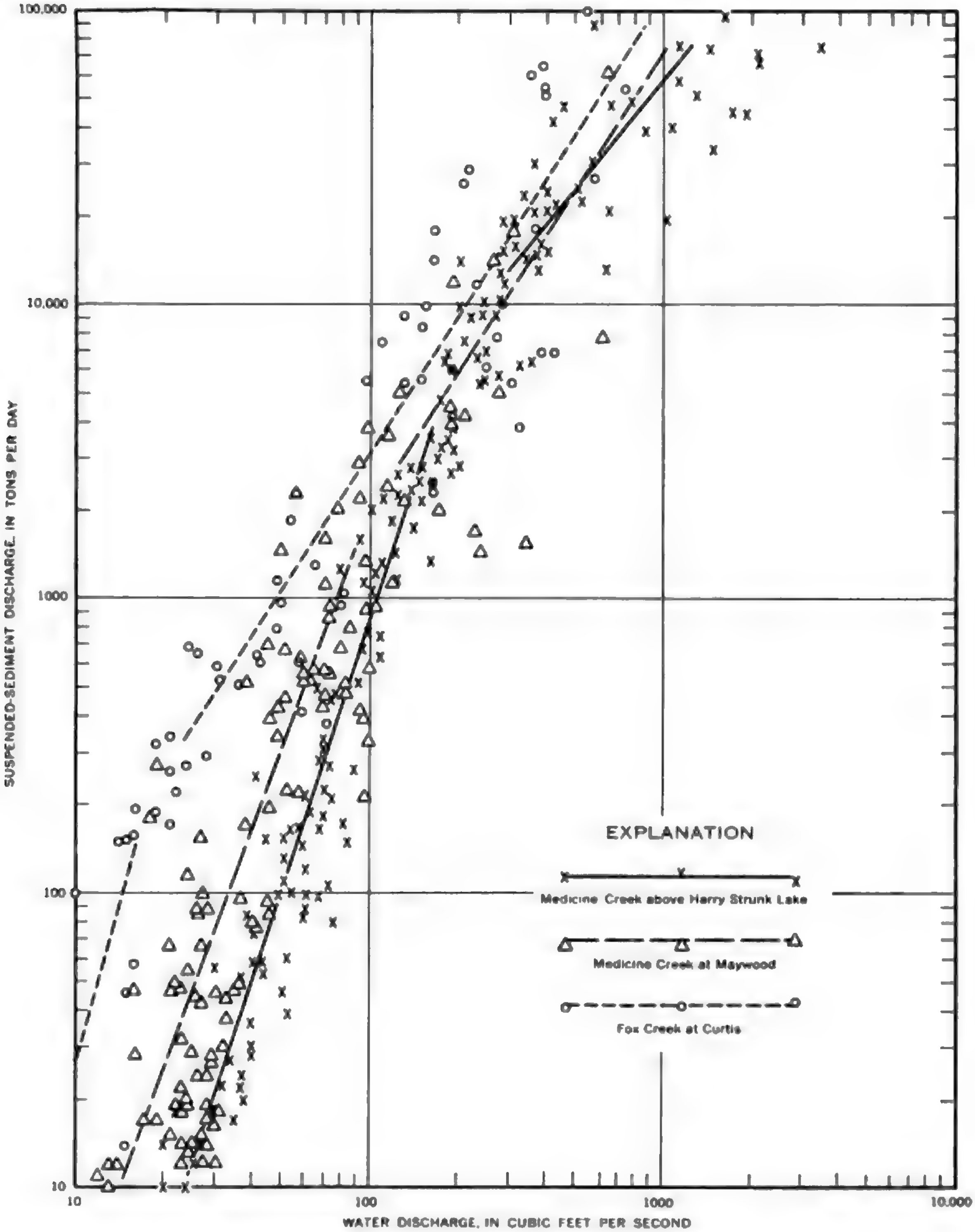

FIGURE 224.—Change of suspended-sediment load with increasing discharge at a section, perennial streams.

Digitized by Google

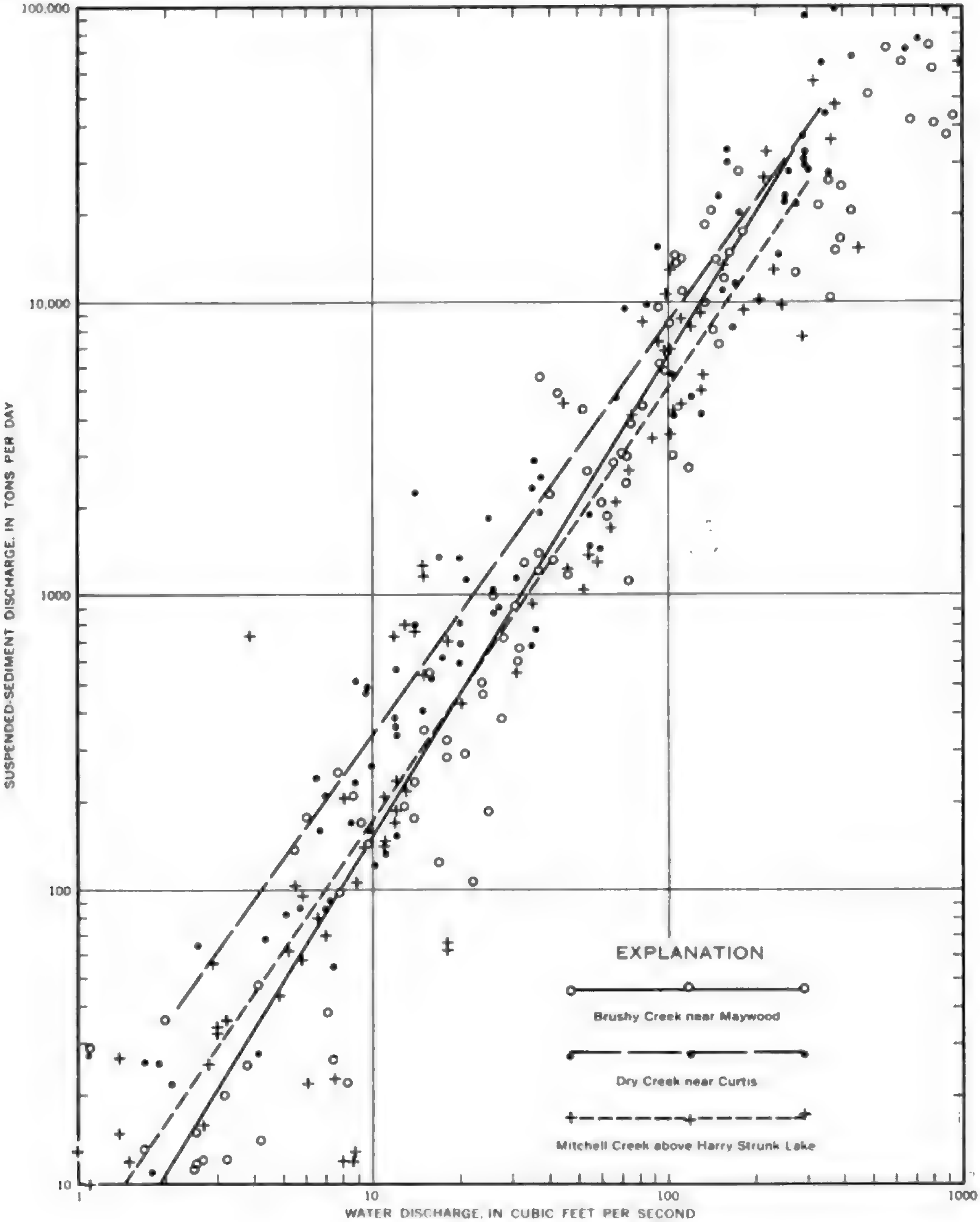

FIGURE 225.—Change of suspended-sediment load with increasing discharge at a section, ephemeral streams.

Digitized by Google

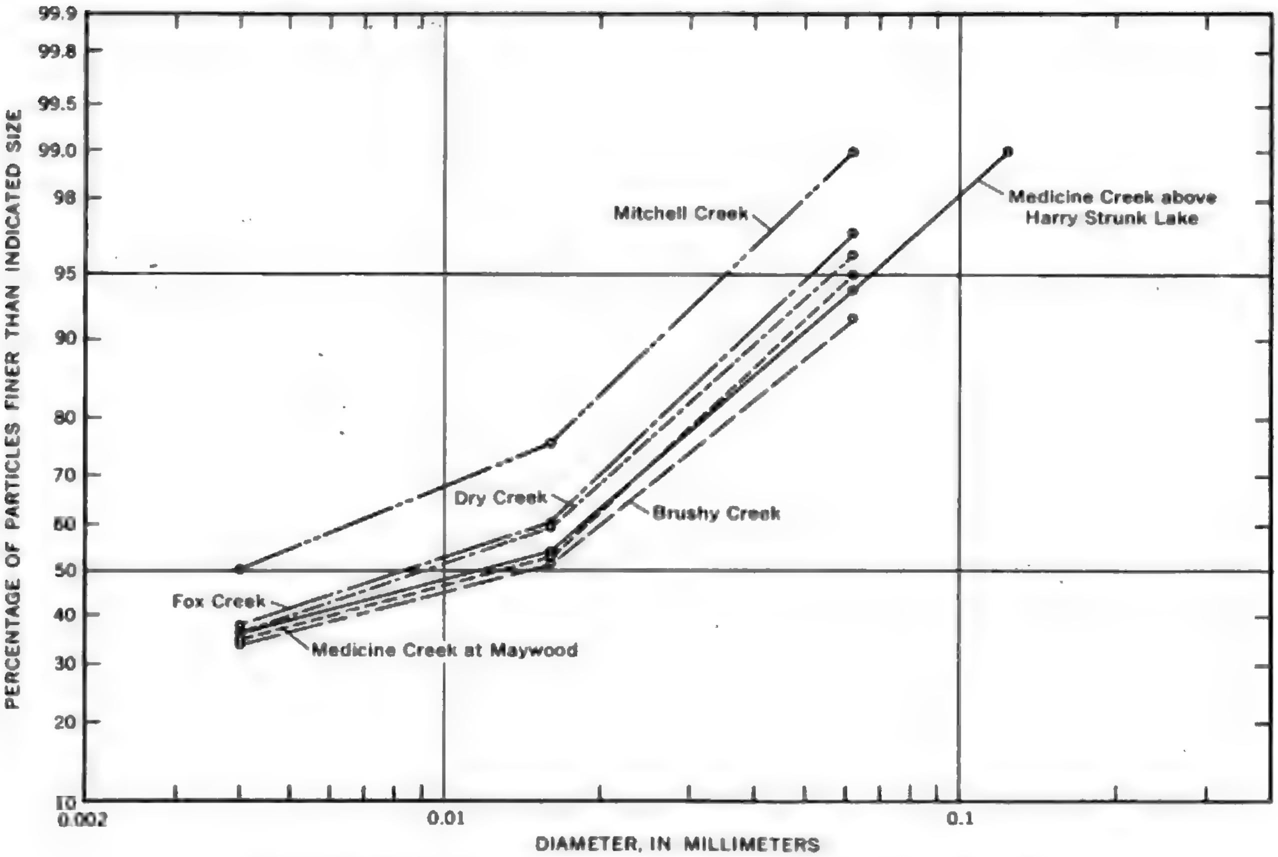

FIGURE 226.—Size distribution of suspended sediment at gaging stations in Medicine Creek basin.

of the basin, has a median particle size of about 0.004 mm. The decrease in median particle size from west to east reflects the increasing distance from the sand-dune area of the extreme western and northwestern parts of the basin.

The measured loads for all the stations are nearly the total loads because the suspended sediment contains little sand and the fine suspended sediment should have fairly uniform distribution in the vertical. Computations of total load were made by the Colby method (Colby, 1957) for the two stations on Medicine Creek, both of which have sand beds. Not many sets of data are available for computation of total loads, but the average percentage of measured load to total load is indicated. At low flow the measured load amounts to about 90 percent of the total load, but at high flow it amounts to more than 95 percent. Because all the suspended sediment at the Dry Creek gage results from storm runoff and a large part of the suspended sediment at the Brushy and Fox Creek gages results from storm runoff, the measured suspended sediment for those stations probably represents 95 percent or more of the total load for the period of record.

RELATIVE SEDIMENT CONTRIBUTIONS OF THE MAJOR TRIBUTARIES

In any basin or subbasin, erosion and deposition are taking place simultaneously, and sediment data collected at any point along a stream represent the net of erosion and deposition upstream from that point.

A measure of the net erosion and deposition in a basin is the discharge-weighted mean concentration of suspended sediment. This is the concentration that would result if all the water passing a point during some period of time were mixed with the suspended sediment passing during the same period. If the cumulative water volume is plotted against cumulative weight of sediment, the slope of a line that joins points of the graph defines the discharge-weighted mean concentration for the period of time for which the data are cumulated. The annual sediment loads and storm runoff for the station were reduced to a per-square-mile basis and are shown

Digitized by Google

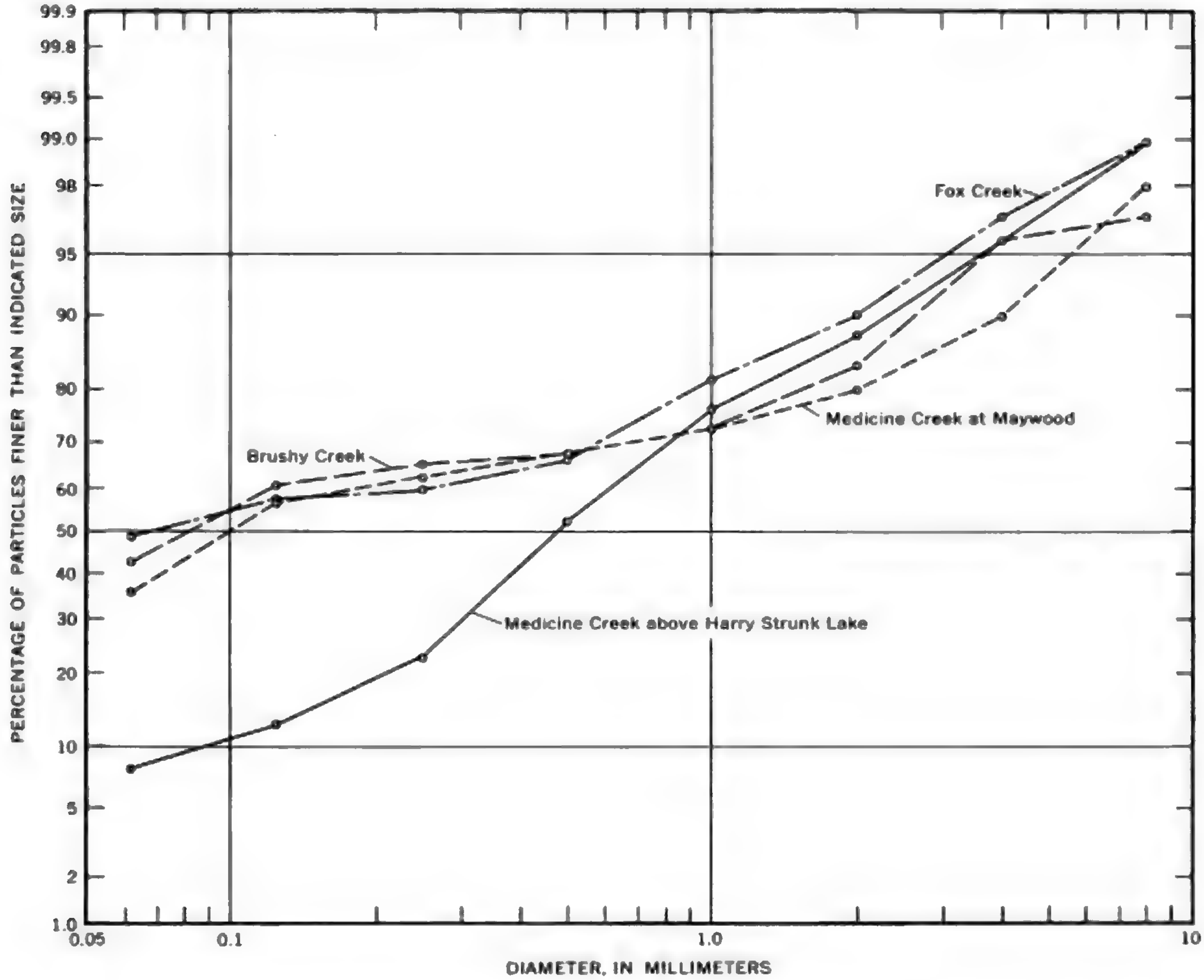

FIGURE 227.—Size distribution of bed material at gaging stations in Medicine Creek basin.

on figure 228. Reducing the values to a per-square-mile basis does not change the constant of proportionality and presents a comparison of storm runoff and sediment yields. Such a comparison is valid if precipitation over the entire basin is assumed to be uniform in amount. Because of the relatively small size of the basin and the low relief, the assumption of uniform precipitation probably is valid if several years record are considered. The differences in total precipitation for the years 1951–58 recorded at the Wellfleet, Curtis, and Stockville rain gages were less than 10 percent. As the time period is shortened, however, the probability of uniform precipitation becomes less.

Each of the stations shows a definite break in slope following the 1951 water year. The break in the curve probably occurs because the ratio between the variables is not constant at all rates of cumulation. If the ratio were constant at all rates of cumulation, the break would have to be explained by a physical change that would cause a greater reduction in sediment yield than in water yield (Searcy and Hardison, 1960). A break in the curve is drawn at the 1956 water year for the Dry Creek data; and breaks at the same year are indicative for Fox and Mitchell Creeks, but they are not drawn. For hydrologic data plotted in this manner, breaks that persist for less than about 5 years should be attributed to chance and ignored unless there is definite reason for believing that such a break should occur. The high rainfall and runoff during the 1951 water year explains the break at the end of that

Digitized by Google

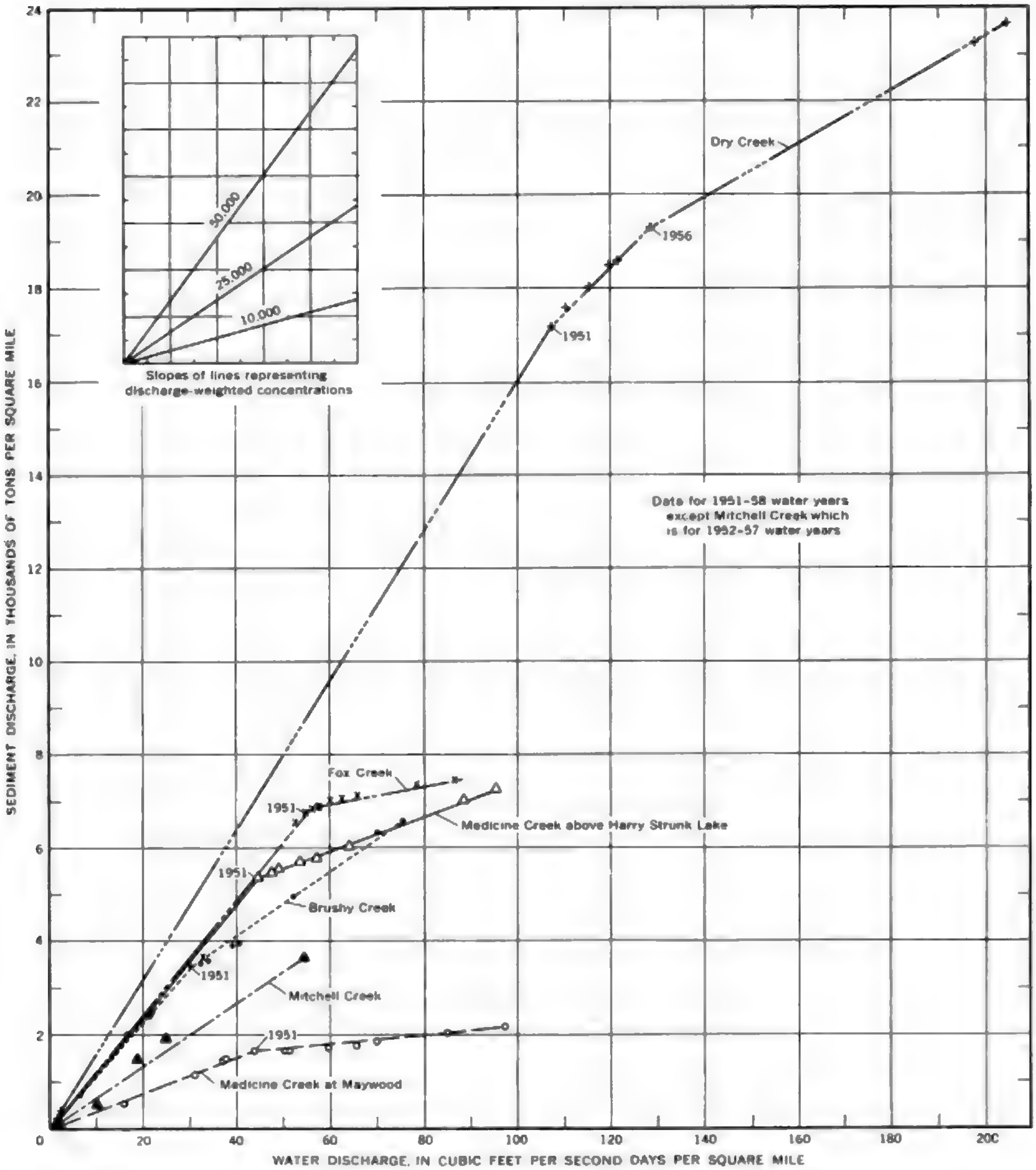

FIGURE 228.—Cumulative water discharge and sediment discharge per square mile at gaging stations in Medicine Creek basin. Year at which a curve changes in slope is indicated.

Digitized by Google

year. Data are available for only the part of the year when rainfall was extremely heavy. The reason for the break at the end of the 1956 water year is obscure. Runoff for the 1957 water year was generally greater than normal, but the break is in the wrong direction on the basis of the experience for the 1951 water year. Land-conservation work was being actively carried on during the period of the investigation, but there are too few data to evaluate the significance of the break.

The ephemeral streams—Brushy, Dry, and Mitchell Creeks—have higher discharge-weighted mean concentrations and generally yield larger amounts of sediment per square mile for storm runoff than the perennial streams.

GEOMORPHIC PROPERTIES IN RELATION TO WATER AND SEDIMENT DISCHARGE

One major objective of quantitative geomorphic measurements is to select drainage-basin properties that have the highest possible degree of correlation with runoff and sediment yield. If runoff and sediment yield are known for a large number of drainage basins in the same region, statistical methods can be used to evaluate the significance of different drainage-basin properties. If, as in the Medicine Creek basin, runoff and sediment yield are known for only five subbasins, evaluation of the properties cannot be made rigorously by statistical methods. Ideally, the properties selected should be independent of one another, unambiguous, and not unduly time consuming to obtain. For the Medicine Creek basin, properties that meet these qualifications and offer promise of good correlation with runoff and sediment yield are relief ratio, adjusted frequency of first-order streams, and percentage of area in upland.

Relief ratio was shown to correlate with mean annual sediment accumulation for small drainage basins in the upper Cheyenne River basin by Hadley and Schumm (1961, p. 173). Maner (1958) reports that relief ratio correlated more closely with sediment delivery rates than did size of sediment contributing area, drainage density, basin shape, or weighted-average land slopes. The drainage basins studied by Maner, which are in the Red Hills area of Oklahoma and Texas, range from 332 to 0.036 square miles. For these basins, relief ratio showed a correlation, as based on inspection of scatter diagrams, with basin size, basin shape, average land slopes, and drainage density. Maner concludes that sediment delivery rate in the Red Hills area is a function of several drainage-basin properties that evidently are expressed adequately by relief ratio.

For drainage basins that are incised in a level or gently sloping upland surface to approximately the same local relief, a correlation of relief ratio with size and shape properties is apparent. Basin relief increases at a much slower rate than basin length; therefore, relief ratio is reduced both by increase in basin size and by increase in basin length. Because of the decrease in valley-side slope with increasing channel order, the lower relief ratio of high-order basins is accompanied by a lower mean value of side slope. Similarly, because of the decrease in channel slope with channel order (fig. 229), the lower relief ratio of higher order basins is accompanied by a lower mean channel gradient. However, the relation of channel slope to channel order may not be consistent; therefore, relief ratio may not express adequately the slopes of low-order channels.

In a discussion of the interrelations of drainage-basin characteristics, Gray (1961) presents evidence to show that, for small basins, the properties of area, length of main stream, and length to center of area are highly correlated. In a region of homogeneous relief, a correlation also exists between these properties and the slope of the main stream. Although not discussed by Gray, relief ratio probably will express adequately all the above interrelated properties for some regions. In addition, relief ratio will express differences in relief between basins of about the same size. The effectiveness of relief ratio as a property probably depends on, among other things, the constancy in shape of long profile among the basins being compared. A basin whose main

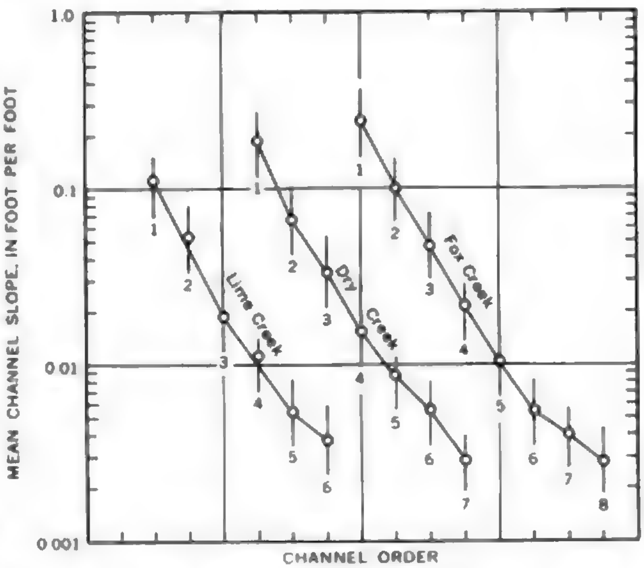

Figure 229.—Mean channel slope in relation to channel order for Lime, Dry, and Fox Creek subbasins.

Digitized by Google

stream is strongly concave upwards in long profile may have the same relief ratio as another basin, of equal size, whose main stream is nearly straight in long profile. However, such differences in long profile surely affect runoff and sediment yield.

Frequency of first-order streams was found by Morisawa (1959) to give a high correlation with peak intensity of runoff for drainage basins in the Appalachian Plateaus. The properties used by Morisawa in multiple regression analysis were relief ratio, basin circularity, and first-order channel frequency. She considers that these three properties express the shape, relief, and network composition of a drainage basin, that they vary independently of each other and of area, and that they do not duplicate any other geomorphic factor. For the Medicine Creek basin, relief ratio is considered to be an adequate expression of basin shape, but first-order channel frequency is an important property not only in relation to runoff and sediment yield but also in relation to gully erosion.

Frequency of first-order channels expresses the small-scale properties of a drainage basin and thereby complements relief ratio, which expresses the larger scale properties. Channel frequency must be adjusted for immature basins according to their differing percentages of upland area. In figure 230 scatter diagrams show the relation of adjusted frequency of first-order channels to mean valley-side slope, slope of first-order channels, and mean length of first-order channels. The number of points is too small to warrant the calculation of correlation coefficients, but the existence of a relation is apparent not only from the scatter diagrams but also from examination of the topographic maps. In addition, the reason for the correlation is apparent from geomorphic history. In subbasins where post-Peorian dissection was most intense, first-order channels are shorter, steeper, and more numerous. Much of the scatter of points in figure 230 is due to the fact that some of the subbasins are less homogeneous than others in texture of drainage.

The relation of length to channel slope for first-order channels in the lower part of Dry Creek is shown in figure 231. Each point represents the mean slope and mean length of 10 channels in a particular length group. Noteworthy is the fact that the shorter channels have relatively steeper slopes than the longer channels. In addition, the shorter channels have steeper valley heads and more concave profiles. This is of particular importance in gully erosion because steep valley heads promote the formation of new gullies.

In combination, relief ratio and frequency of first-order streams should give indirect expression to another important variable—the percentage of area in valley flat. An unusual geomorphic feature of the Great Plains generally is the flatness of valley

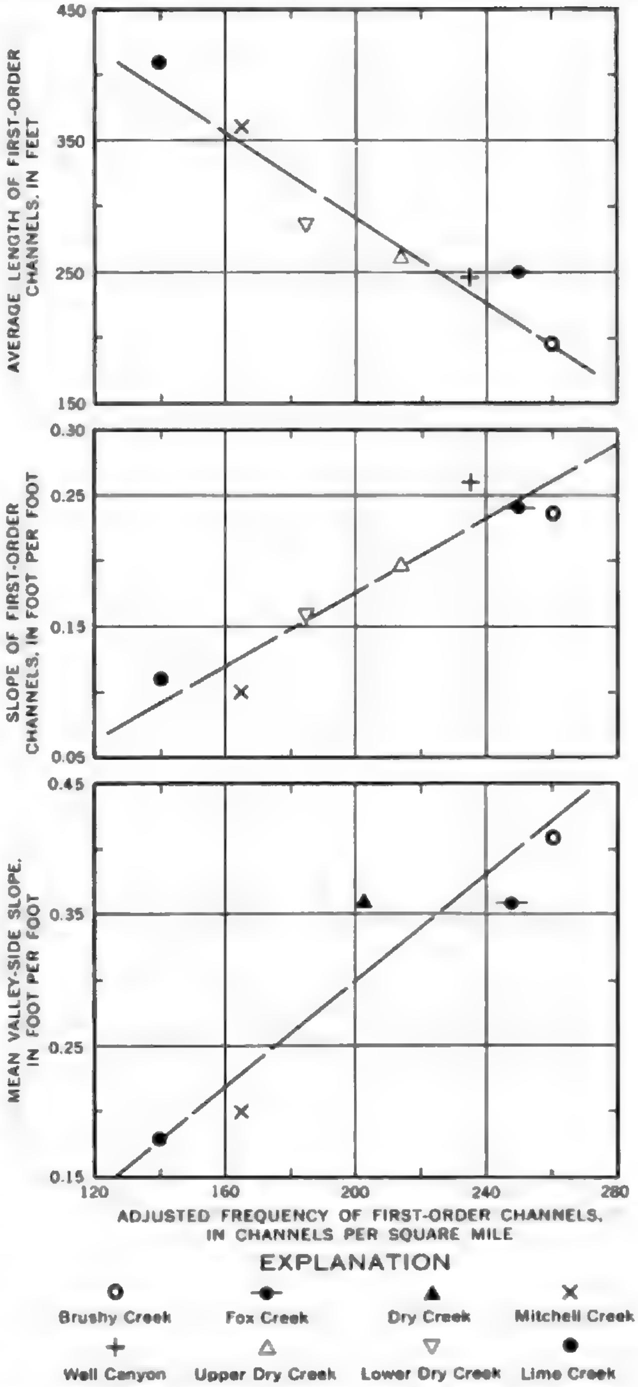

FIGURE 230.—Adjusted frequency of first-order channels in relation to mean valley-side slope, mean slope of first-order channels, and mean length of first-order channels.

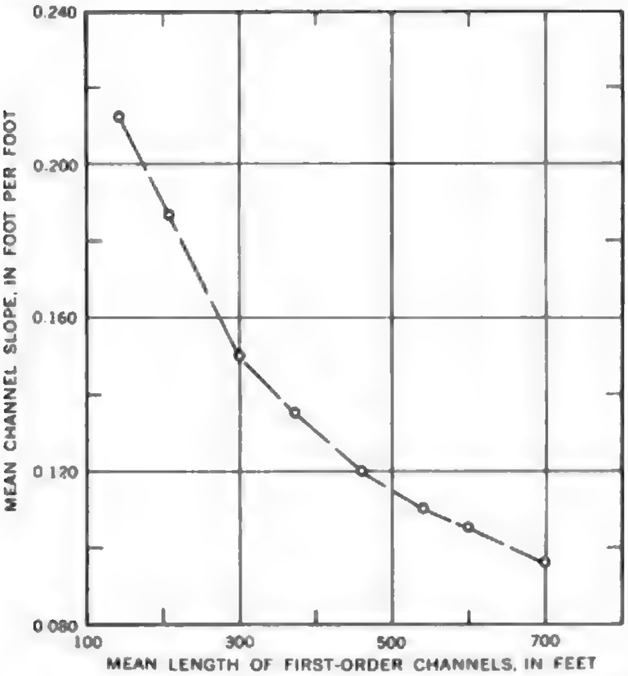

FIGURE 231.—Slope of first-order channels in lower Dry Creek subbasin in relation to length.

bottoms along channels of both low and high order. The percentage of area in valley flat for each channel order in each major subbasin has been calculated from the product of average width of valley flat and average length of channel. (See table 4.) The percentage distribution of valley flat according to channel order differs considerably from one subbasin to the next and depends mainly on the distribution of channel length according to order. In Well Canyon subbasin, for example, about 18 percent of the total area of valley flat is in the wide bottom along the main channel, whereas in Dry Creek subbasin only 8 percent is along the main channel. The probability of deposition of sediment on the main valley flat seems greater for Well Canyon than for Dry Creek, and the probability of rapid runoff is less because of the lower slope angle of the Well Canyon valley. The relief ratio gives an indication of the percentage of valley flat along channels of fourth and higher order, whereas the frequency of first-order channels gives an indication of the percentage along channels of first, second, and third orders. (See fig. 198, in which the slope of the curve relating channel length to channel order changes at about third order.)

Because of the immaturity of drainage in the Medicine Creek basin, a variable is needed to express the difference among subbasins in percentage of upland. The slope of the upland, which shows variation from one subbasin to the next, is related to the slope of channels. In general, the slope of the upland is less than the slope of first- and second-order channels, about equal to the slope of third-order channels, and greater than the slope of fourth-order and higher order channels. (See tables 3 and 4.) The percentage of upland gives a reasonably good indication of land use. (See table 9.) Similarly, the percentage of area in side slope and valley flat shows a correspondence with the percentage of area used for hay and pasture.

The probable effect of the selected properties (relief ratio, frequency of first-order streams, and percentage of area in upland) on runoff and sediment yield can be inferred. On the premise that lower slopes, wider valley flats, and larger (or longer) drainage basins all tend toward reduction of runoff and sediment yield because of greater opportunity for infiltration and for deposition of sediment, runoff and sediment yield should be positive functions of relief ratio. According to the graphs of Hadley and Schumm (1961), the function is exponential where mean annual sediment accumulation in reservoirs is the dependent variable. According to the graph of Maner (1958, fig. 3), the function is exponential where sediment delivery rate is the dependent variable. Sediment delivery rate is the ratio, expressed as a percentage, between annual rate of sediment yield and annual gross erosion rate.

An increase in frequency of first-order channels is associated with an increase in both valley slope and side slope for lower order channels; therefore, increase in water and sediment discharge should be a positive function of frequency of first-order channels. For drainage basins whose main channel is very long and bordered by wide valley flats, a high yield of water and sediment from lower order channels may be largely dissipated along the main channel.

TABLE 9.—*Areas in upland and valley flat in comparison with areas in two categories of land use*

[Land-use percentages are mean values from inventories taken in 1954, 1955, and 1957]

Subbasin	Area in side slope and valley flat (percent)	Area in hay and pasture (percent)	Area in upland (percent)	Area in row crops, small grain, and fallow (percent)	Ratio of row crops to small grain
Mitchell Creek	48.2	51.3	51.8	46.6	1.72
Dry Creek	65.2	69.7	34.8	28.7	1.48
Well Canyon	79.6	83.4	20.4	15.6	1.34
Fox Creek	83.5	86.2	16.5	12.7	1.87
Brushy Creek	74.1	77.7	25.9	21.7	.98

Digitized by Google

The effect of percentage of area in upland depends on the land use of the upland. If the upland is used mainly for row crops, runoff and sediment yield probably would be a positive function of percentage of area in upland. If, on the other hand, the upland were thickly sodded, the function probably would be negative. A positive function would be expected for the Medicine Creek basin.

The preceding inferences as to the geomorphic properties most highly correlated with runoff and sediment yield cannot, unfortunately, be rigorously tested for Medicine Creek because of the small number of subbasins for which data are available. Nevertheless, a trial multiple linear regression of sediment discharge in relation to the three selected variables (fig. 232) is given in order to illustrate the numerical effects of these variables. The trial regression is based on data in table 3 and figure 228. The uncertainties involved in correlation are apparent from the graphs in figure 232, and clearly no quantitative significance can be attached to the results.

In figure 232 the assumption is made that the sediment discharge of each subbasin for the period 1952–58 is correctly represented by the data. Data for 1951 were not used because no measurements for Mitchell Creek were made during that year. The 1958 suspended sediment for Mitchell Creek is estimated. Relief ratio is plotted against sediment discharge on semilogarithmic paper because previous work has indicated that this relation is exponential. Percentage of upland and adjusted frequency of first-order streams are plotted against sediment discharge on rectangular coordinate paper. When only relief ratio is considered (top graph, fig. 232), the sediment discharge of Fox Creek is very low and that of Mitchell Creek is high relative to the trial curve. This is perhaps accounted for by the fact that the percentage of upland on Fox Creek is lower than the average, and the percentage on Mitchell Creek is higher. When relief ratio and percentage of upland are held constant (bottom graph), a reasonably good correlation with adjusted frequency of first-order channels can be obtained for all the subbasins except Medicine Creek above Harry Strunk Lake, which shows a high sediment discharge not only for this trial regression curve but for the other two as well.

The relatively high sediment discharge of Medicine Creek above Harry Strunk Lake is attributed to yet another factor—the presence of raw vertical banks along a continuous incised channel for a distance of several miles upstream from the gaging station. In general, the banks along Mitchell, Fox,

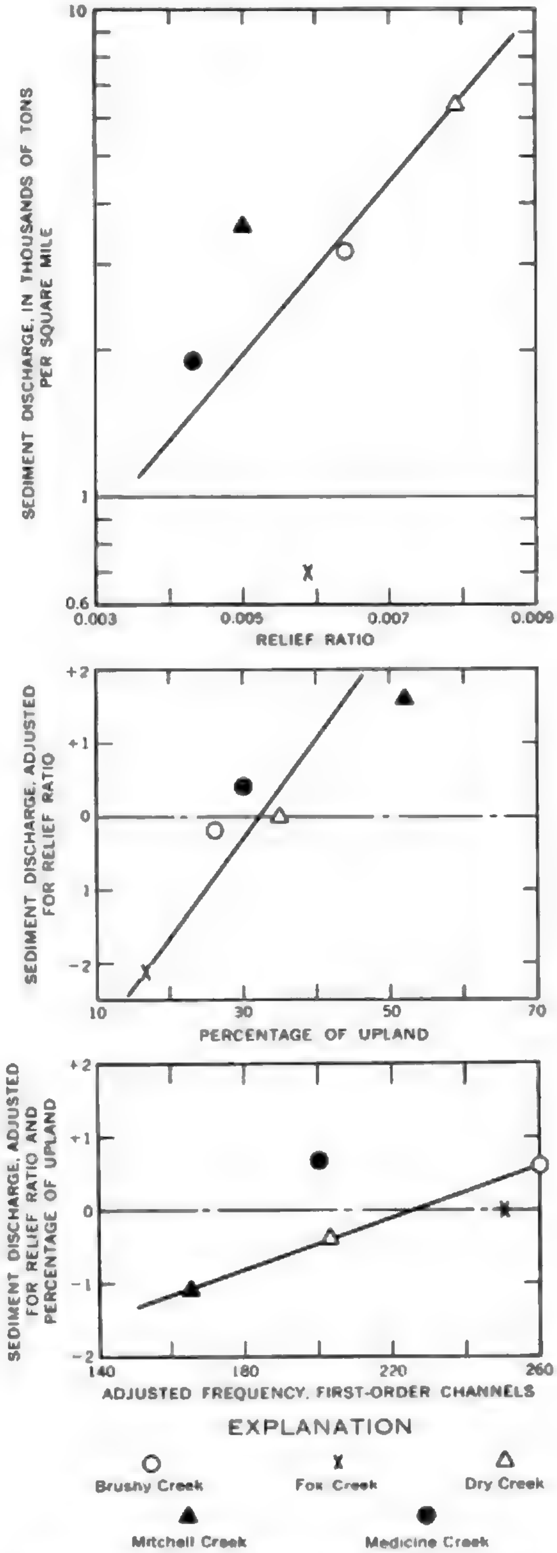

FIGURE 232. Trial graphic multiple linear regression of sediment discharge in relation to relief ratio, percentage of upland, and adjusted frequency of first-order channels.

Digitized by Google

and Brushy Creeks upstream from the gaging stations are more sloping and more protected by vegetation than the banks along Dry and Medicine Creeks. But Dry Creek is ephemeral, whereas the continuous flow along Medicine Creek obtains a continuous supply of sediment from bank erosion.

A trial graphical linear regression, in which water discharge was plotted as a dependent variable against the three geomorphic factors used in the sediment discharge regression, yielded results similar to those of the sediment yield regression. As with the sediment discharge, the water discharge of Medicine Creek above Harry Strunk Lake is much higher than expected. Probably, Medicine Creek receives a larger proportion of its water discharge from ground water than do Fox and Brushy Creeks. In addition, the assumption of uniform distribution of rainfall over the various subbasins during the period 1952–58 may be incorrect.

SUMMARY AND CONCLUSIONS

Annual precipitation at Curtis for the period 1895–1960 averaged 21.5 inches but ranged from 11 to 38.2 inches. More than half of the precipitation falls during 4 summer months, and much of this is thunderstorm rainfall. The 5-year moving average for Curtis indicates a long-term trend toward decreasing annual precipitation. Rainfall intensity-duration-frequency curves indicate that the rainfall regimen was satisfactorily represented at Curtis during the years 1951–58, although precipitation was lower than the long-term average. Potential evaporation is about three times average annual precipitation. The Medicine Creek basin lies in a transitional zone between prairie and plains grassland; the climax plant community consists of a dominance of midgrasses and an understory of short grasses.

The immediate effects of drought, as during the years 1933–40, are to reduce the grass cover in such a way as to leave bare patches of ground, but grasses are rapidly replaced by weeds. As a result of a secular climatic shift toward dryness, a climax community of short grasses would become established. Climatic change since the arrival of settlers has had little effect on the climax community, as indicated by the character and abundance of vegetation in areas that are neither grazed nor cultivated.

Geomorphic and stratigraphic evidence indicates that the drainage system grew to approximately its present pattern and extent during the episode of erosion (tentatively assigned to the interval 12,000 to 11,000 years B.P.) that followed deposition of the Peorian Loess. During the subsequent episode of deposition (about 11,000 to 5,000 years B.P.), deposits of the Stockville terrace accumulated in the valleys and the valley sides were graded. The deposits were incised (about 5,000 to 4,000 years B.P.) to form the Stockville terrace, and the deposits that subsequently accumulated in the valleys (4,000 to 1,000 years B.P.) were later incised (about 1,000 to 900 years B.P.) to form the Mousel terrace. Mousel terracing was followed by accumulation of the upper Recent alluvium that underlies the present valley flats. In some valleys the late Recent alluvium has been incised intermittently during the past 350 years. Thus, within the past 12,000 years, the valleys were trenched three times prior to the trenching that is taking place in some valleys at present. No clear evidence was obtained as to the causes of past episodes of erosion or of deposition. However, snails from the Stockville terrace deposits probably lived under climatic conditions similar to the present, and the terracing of the Stockville terrace corresponds approximately with the Altithermal, a well-established dry climatic period that lasted from about 6,000 to 4,000 years B.P.

Morphometric analysis of the drainage system shows that the slope of the exponential curves relating mean channel length to channel order changes at the lower channel orders, whereas the curves relating number of channels to channel order have a nearly uniform slope. This change in slope of the curve relating channel length to channel order is attributed to post-Peorian drainage transformation in which the lengths of first- and second-order channels were reduced relative to third-order channels. In order to compare the channel frequencies of immature drainage systems whose drainage basins differ in percentage of undissected upland, drainage basin area is adjusted by subtracting the area of upland. Channel frequency, expressed as number of channels per square mile of area actually occupied by the valley system, is called adjusted channel frequency.

Erosion by scarp retreat takes many forms in the basin, and gullies are regarded as a type of scarp erosion. Gullies are defined and are classified as valley-bottom, valley-side, and valley-head gullies. Many large valley-bottom gullies apparently originate on valley reaches that are locally steepened at the entrance of a major tributary. However, the ratio of local slope to drainage area that is critical for the initiation of a gully is not sharply defined because other factors (such as width of valley bottom) are important. In general, trenching of a valley reach to bedrock does not take place by the coalescence of two discontinuous gullies, but by the

Digitized by Google

passage of several channel scarps in succession. Saturation of massive silt at the edges of a plunge pool is the most important factor in the advance of channel scarps.

Steep-sided valleys that drain areas of cultivated upland are most susceptible to valley-head and valley-side gullying. The most significant geomorphic factors in the areal frequency distribution of valley-head and valley-side gullies are percentage of area in upland and adjusted frequency of first-order channels.

Generalizations regarding suspended sediment and the hydraulic geometry of channels are based on data from six gaging stations, two of which are on the main channel of Medicine Creek and four on tributaries. At the gaging stations on Dry, Mitchell, and Brushy Creeks the flow is categorized as ephemeral; at the others, as perennial. Water discharge tends to increase rapidly in response to rainfall, much of which falls during summer thunderstorms; and the discharge peaks are of short duration.

Hydraulic geometry of the channels is expressed by the slope of curves relating width, depth, and velocity to discharges equaled or exceeded 1, 2, and 25 percent of the time. At a station, the low-flow channels of perennial streams are well defined and have steep banks; with increasing discharge, width does not increase as rapidly as depth. By contrast, the low-flow channels of ephemeral streams are shallow and transient, and width increases rapidly with discharge until the steep sides of the incised trench are reached. In a downstream direction, the incised trenches of ephemeral streams do not widen appreciably, and increase in discharge is accommodated by relatively large changes in depth and velocity. The increase in discharge of perennial streams is accommodated by relatively rapid increase in width and by a slow increase in depth and velocity.

Curves relating suspended-sediment load to water discharge for the perennial streams are characterized by a break in slope at water discharges above normal but below the bankfull stage; curves for the ephemeral streams show no corresponding break. Peak sediment concentrations usually occur before peak water discharge, but the length of lead is variable and is generally shorter for smaller discharge events. In general, 90 percent or more of the suspended sediment is silt and clay, and the measured (suspended) load represents 90 to 95 percent of the total load. No relation was discerned between instantaneous water discharge and particle-size distribution. In general, the concentration of measured suspended sediment is higher in wet years than in dry, and the ephemeral streams have higher concentrations than the perennial streams.

An evaluation of geomorphic properties indicates that relief ratio, adjusted frequency of first-order channels, and the percentage of area in upland would be expected to have the highest correlation with runoff and sediment discharge. No rigorous statistical correlation can be made because of the small number of subbasins for which data are available, but a trial graphic multiple regression indicates that differences in runoff and sediment discharge can be accounted for reasonably well by differences in these three properties. They are not only important in themselves, but they also give indirect expression to other important properties. For example, the percentage of area in upland is related to area in row crops, small grain, and fallow.

Active valley-head and valley-side gullies, and all but a few of the active valley-bottom gullies, are attributed to land use since settlement. During the past two naturally induced episodes of erosion, gullying was mainly confined to valley bottoms. Although some valley incision has taken place within the past 500 years and before settlement, major episodes of the past are probably associated with droughts more severe than any since settlement. Restoration of native vegetation to the heads of valleys, together with conservation measures on the upland, would be effective in the control and prevention of valley-head gullies, which are the most numerous in the basin. These steps, if accompanied by more moderate grazing in the valleys, would probably prevent the initiation of new valley-bottom gullies; but no economically feasible means for arresting the present large valley-bottom gullies is apparent.

REFERENCES

Antevs, E. V., 1952, Arroyo-cutting and filling: Jour. Geology, v. 60, p. 375–385.

Bacon, S. R., and others, 1939, Soil survey of Frontier County, Nebraska: U.S. Dept. Agriculture, Bur. Chem. and Soils, ser. 1935, no. 9, 34 p.

Bradley, Edward, and Johnson, C. R., 1957, Geology and ground-water hydrology of the valleys of the Republican and Frenchman Rivers, Nebraska: U.S. Geol. Survey Water-Supply Paper 1360–H, p. 589–713.

Brice, J. C., 1958, Origin of steps on loess-mantled slopes: U.S. Geol. Survey Bull. 1071–C, 29 p.

Broecker, W. S., and others, 1960, Evidence for an abrupt change in climate close to 11,000 years ago: Am. Jour. Sci., v. 258, p. 429–448.

Broscoe, A. J., 1959, Quantitative analysis of longitudinal stream profiles of small watersheds: Columbia Univ., Dept. of Geology Tech. Rept. No. 18, Office of Naval Research Contract N6 ONR 271–30, 73p.

Bryan, Kirk, 1941, Pre-Columbian agriculture in the southwest, as conditioned by periods of alluviation: Assoc. Am. Geographers Annals, v. 31, p. 219–242.

Digitized by Google

Clark, O. R., 1937, Interception of rainfall by herbaceous vegetation: Science, v. 86, p. 591–592.

Colby, B. R., 1957, Relationship of unmeasured sediment discharge to mean velocity: Am. Geophys. Union Trans., v. 38, no. 5, p. 708–717.

Condra, G. E., and others, 1950, Correlation of the Pleistocene deposits of Nebraska: Nebraska Geol. Survey Bull. 15–A, 74 p.

Frankel, Larry, 1957, Relative rates of loess deposition in Nebraska: Jour. Geology, v. 65, p. 649–652.

Frye, J. C., and Leonard, A. B., 1952, Pleistocene geology of Kansas: Kansas Geol. Survey Bull. 99, 230 p.

Frye, J. C., and others, 1956, Stratigraphy of the Ogallala formation (Neogene) of northern Kansas: Kansas Geol. Survey Bull. 118, 92 p.

Frye, J. C., and Willman, H. B., 1960, Classification of the Wisconsinan Stage in the Lake Michigan glacial lobe: Illinois State Geol. Survey Circ. 285, 20 p.

Goke, A. W., and others, 1926, Soil survey of Lincoln County, Nebraska: U.S. Dept. Agriculture, Bur. Chemistry and Soils, no. 35, 31 p.

Gray, D. M., 1961, Interrelationships of watershed characteristics: Jour. Geophys. Research, v. 66, p. 1215–1223.

Hadley, R. F., and Schumm, S. A., 1961, Sediment sources and drainage basin characteristics in upper Cheyenne River basin: U.S. Geol. Survey Water-Supply Paper 1531–B, p. 137–198.

Holtz, W. G., and Gibbs, H. J., 1952, Consolidation and related properties of loessial soils: Am. Soc. Testing Materials, Symposium on consolidation testing of soils, Spec. Tech. Pub. 126, p. 9–33.

Horton, R. E., 1945, Erosional development of streams and their drainage basins, hydrophysical approach to quantitative morphology: Geol. Soc. America Bull. 56, p. 275–370.

Kivett, M. F., 1949, Archaeological investigations in Medicine Creek Reservoir, Nebraska: Am. Antiquarian, v. 14, p. 278–284.

Kubiena, W. L., 1938, Micropedology: Ames, Iowa, Collegiate Press, 243 p.

Leonard, A. B., 1950, A Yarmouthian molluscan fauna in the midcontinent region of the United States: Univ. Kansas Paleont. Contr., Mollusca, art. 3, 48 p.

——— 1951, Stratigraphic zonation of the Peoria Loess in Kansas: Jour. Geology, v. 59, p. 323–332.

——— 1952, Illinoian and Wisconsinan molluscan faunas in Kansas: Univ. Kansas Paleont. Contr., Mollusca, art. 4, 38 p.

Leopold, L. B., and Maddock, Thomas, 1953, The hydraulic geometry of stream channels and some physiographic implications: U.S. Geol. Survey Prof. Paper 252, 57 p.

Leopold, L. B., and Miller, J. P., 1954, A postglacial chronology for some alluvial valleys in Wyoming: U.S. Geol. Survey Water-Supply Paper 1261, 90 p.

——— 1956, Ephemeral streams—hydraulic factors and their relation to the drainage net: U.S. Geol. Survey Prof. Paper 282–A, 37 p.

Lugn, A. L., 1935, The Pleistocene geology of Nebraska: Nebraska Geol. Survey Bull. 10, 2d ser., 223 p.

Maner, S. B., 1958, Factors affecting sediment delivery rates in the Red Hills physiographic area: Am. Geophys. Union Trans., v. 39, p. 669–675.

Melton, M. A., 1958, Geometric properties of mature drainage systems and their representation in an E₄ phase space: Jour. Geology, v. 66, p. 35–54.

Miller, J. P., 1958, Problems of the Pleistocene in cordilleran North America, as related to reconstruction of environmental changes that affected early man, *in* Climate and man in the Southwest: Univ. Arizona Bull. 4, v. 28, p. 19–50.

Morisawa, M. E., 1959, Relation of quantitative geomorphology to streamflow in representative watersheds of the Appalachian Plateau province: Columbia Univ., Dept. of Geology Tech. Rept. No. 20, Office of Naval Research Contract N6 ONR 271, 94 p.

Phillips Petroleum Co., 1956, Series on pasture and range plants, booklet 2 on native grasses, 37 p., and booklet 3 on undesirable grasses and forbs, 45 p.

Rubin, Meyer, and Suess, H. E., 1956, U.S. Geological Survey radiocarbon dates III: Science, v. 123, no. 3194, p. 442–448.

Schultz, C. B., and others, 1948, Preliminary geomorphological studies of the Lime Creek area (Nebraska): Univ. Nebraska State Mus. Bull. 4, v. 3, p. 31–42.

——— 1951, A graphic résumé of the Pleistocene of Nebraska (with notes on the fossil mammalian remains): Univ. Nebraska State Mus. Bull. 6, v. 3, 41 p.

Schultz, C. B., and Stout, T. M., 1945, Pleistocene loess deposits of Nebraska, *in* Symposium on loess, 1944: Am. Jour. Sci., v. 243, p. 231–244.

——— 1948, Pleistocene mammals and terraces in the Great Plains: Geol. Soc. America Bull. 59, p. 553–588.

Schumm, S. A., 1956, Evolution of drainage systems and slopes in badlands at Perth Amboy, New Jersey: Geol. Soc. America Bull. 67, p. 597–646.

Schumm, S. A., and Hadley, R. F., 1957, Arroyos and the semiarid cycle of erosion: Am. Jour. Sci., v. 255, p. 161–174.

Searcy, J. K., and Hardison, C. H., 1960, Double-mass curves: U.S. Geol. Survey Water-Supply Paper 1541–B, 65 p.

Smith, H. T. U., 1955, Use of aerial photography for interpretation of dune history in Nebraska, U.S.A.: Internat. Cong., 4th, Rome-Pisa, 1953, Assoc. for study of the Quaternary, 7 p.

Strahler, A. N., 1952, Hypsometric (area-altitude) analysis of erosional topography: Geol. Soc. Am. Bull. 63, p. 1117–1142.

——— 1954, Statistical analysis in geomorphic research, Jour. Geology, v. 62, p. 1–25.

——— 1957, Quantitative analysis of watershed geomorphology: Am. Geophys. Union Trans., v. 38, no. 6, p. 913–920.

——— 1958, Dimensional analysis applied to fluvially eroded landforms: Geol. Soc. America Bull. 69, p. 279–300.

Thorp, James, and others, 1952, Map of Pleistocene eolian deposits of the United States, Alaska, and parts of Canada: Geol. Soc. America Bull.

U.S. Department of Agriculture, 1948, Grass, the yearbook of agriculture, 1948: Washington, U.S. Govt. Printing Office, 892 p.

U.S. Weather Bureau, 1955a, Substation history—Nebraska: U.S. Dept. Commerce, Key to meteorol. records documentation no. 1.1, 90 p.

——— 1955b, Rainfall intensity-duration-frequency curves: U.S. Dept. Commerce, Weather Bur. Tech. Paper 25, 53 p.

——— 1957, Rainfall intensity-frequency regime, Part 1,

Digitized by Google

the Ohio Valley: U.S. Dept. Commerce, Weather Bur. Tech. Paper 29, 44 p.

——— 1959a, Evaporation maps for the United States: U.S. Dept. Commerce, Weather Bur. Tech. Paper 37, 13 p.

——— 1959b, Climates of the States—Nebraska: U.S. Dept. Commerce, Climatography of the United States, no. 60–25.

Weakly, H. E., 1940, Tree-rings as a record of precipitation in western Nebraska: Tree-ring Bull. 6, p. 18–19.

——— 1943, A tree-ring record of precipitation in western Nebraska: Jour. Forestry, v. 41, p. 816–819.

Weaver, J. E., and Albertson, F. W., 1943, Resurvey of grasses, forbs, and underground plant parts at the end of the great drought: Ecol. Mon., v. 13, p. 63–117.

——— 1944, Nature and degree of recovery of grassland from the great drought of 1933–1940: Ecol. Mon., v. 14, p. 393–479.

Wedel, W. R., 1941, Environment and native subsistence economies in the central Great Plains: Smithsonian Misc. Colln., v. 101, no. 3, 29 p.

——— 1949, Some provisional correlations in Missouri Basin Archaeology: Am. Antiquarian, v. 14, p. 328–339.

——— 1961, Prehistoric man on the Great Plains: Univ. Oklahoma Press, Norman, Okla., 355 p.

Wedel, W. R., and Kivett, M. F., 1956, Additional data on the Woodruff Ossuary, Kansas: Am. Antiquarian, v. 21, p. 414–415.

Wolman, M. G., 1955, The natural channel of Brandywine Creek, Penn.: U.S. Geol. Survey Prof. Paper 271, 56 p.

Digitized by Google

INDEX

[Italic page numbers indicate major references]

A — Page

Acknowledgments *258*
Adjusted channel frequency .. 286, 288
Aerial photographs, use 274, 280, 286, 291, 298, 299, 304, 305, 309
Agricultural development of basin 281
Alluvial fan 294
Alluvium 268
  Rates of accumulation compared 273, 279
  See also Banded alluvium; Recent alluvium; Unbanded alluvium.
Altithermal, warm-dry climatic eposide 284, 332
Annual temperature 258
Anselmo loam 280
Archeology *280*
Arroyo cutting and filling 314
Artifacts 279, 281

B

Banded alluvium 279
Basin, circularity 329
  length 286
  measurement of areas 286
  properties 288
  relief 286, 288
  shape 288, 328
Bed material 322
Bibliography 333
Bifurcation ratio 286
Big bluestem 262
Bignell Loess 277, 278
Blowouts 280
Blue grama 262, 263
Blue grass 262
Brady soil 277, 282
Branched gully head 301, 307
Broscoe, A. J., cited 289
Brush, examples of thick 263
  indicator of scrap activity 291
Brushy Creek 286, 289, 315, 322, 331
Buckbrush 263
Buffalograss 262, 263
Bunchgrass 262
Buried valleys *282*

C

California method of plotting *T*. 260
Cambridge 279
Carbon 14 age determinations 268, 272, 273, 278, 281, 284, 300
Carbonates in loess, significance .. 277
Carbonized grass 274, 279, *280*
Castings, worm 273, 274
Cedar Creek 265, 278, 282
  Ogallala exposures in 265
  terrace sequence 270
Census 281
Channel, cross-sectional shapes .. 315
  definition 286
  frequency 286, 288, 289, 329, 332
  geometry 315
  hydraulics 315
  length 286, 329, 330, 332
  order 286, 289, 328, 330, 332
  scarp 278, 279, 290, *291*, 332
  shape 321
  slope 286, 328, 329, 330
  See also Trenched channel.
Charcoal samples 273, 281
Class A pan evaporation 261
Climate *258*, 260, 314, 332
  archeological evidence 281
  effect on by Wisconsin Ice retreat 282
Climax plant community *262*, 263, 332
Colby loam 278, 280
Colluvial soil 277
Conclusions *332*
Correlation of terraces 268
Cowpaths 301, 303
Coyote Creek 294
Cretaceous bedrock 265
Crops, area in 333
Curtis, climatic data 258
Curtis Canyon 279, 294, 297
Cut Canyon *272*, 282, 294

D

Deer Creek 282
Deffenbaugh, J. L., cited 270
Dendrochronology *264*, 300
Depth, relation to discharge 316
Discharge-weighted mean concentration of suspended sediment 325
Discontinuous gullies 291, 294, 299
Downstream hydraulic relations .. *315*
Drainage-basin characteristics, interrelations 328
Drainage-basin measurements 286
Drainage, density 286, 288, 328
  evolution *282*
  ordering 285
  properties 294
  texture variation *288*
  transformation *288*
Droughts 281, 314
  ancient 263, 264, 274
  effects *263*
Drought-resistant grass 262
Dry Creek 278, 279, 282, 286, 289, 294, 296, 298, *300*, 315, 330, 332
Dunes 268, *280*, 325
Dust interception 262, 263
Dyksterhuis, E. J., cited 258, 262

E

Earth worms 274, 277, 280
East Fort 263
Elkhorn Canyon 272, 278, 284
  head scarp 274
  Recent alluvium 279
  terrace sequence and valley fills 273
Elongation ratio 286, 288
Eolian silt, Peorian Loess 275
Ephemeral streams 321, 322, 328, 331
  channels 315, 318
Erosion rate 330
Erosional scarps 263, 290, *291*
Evaporation 261, 332
Exposed rocks *264*

F

Fence posts, rate of burial 279
Fire drives, use by prehistoric man 280
First-order channels 309, 331
Flashy streams 315
Flats 332
Formulas, landform 286
Fossils, list 271, 276
  See also Index fossils.
Fox Creek 265, 271, 278, 279, 286, 289, 294, 315, 322, 331
Frye, J. C., and others, cited 265

G

Gaging stations 315, 318, 333
Geologic section, Cut Canyon 272

Digitized by Google

Page

Geometric differences of ephemeral and perennial streams 321
Geomorphic properties in relation to water and sediment discharge 328
Grading 282, 289
Grand Island Formation 270
Grass 332
ability to prevent erosion 263
characteristics of native 262
indicator of scarp activity 291
Gray, D. M., cited 328
Gross erosion 279
Growth rings of trees 300
Gullies 264, 291, 300, 313
advance 315
areal distribution 307
coalescence 291, 299, 332
control of 314
Gully, definition and classification 290
erosion 290
formation 301
frequency distribution 309
man induced 313
measurement of advance 298
profile changes 296
size categories 305
slumping 296
See also Discontinuous gullies; Valley-bottom gullies; Valley-head gullies; Valley-side gullies.
Gully head, branched 301, 307
lobed 301, 307

H

Harry Strunk Lake 331, 332
Niobrara Formation 264
Head cut, use of term 291
Head scarps 274, 297, 298, 303, 309
advance 274, 290, 312
maximum height 311
Heavy minerals, Sangamon soil 274
Holdredge soil 278
Horton, R. E., cited 285, 289
Human occupation 280
Hydraulic geometry 333
Hydraulic relations at a section and in a downstream direction 315

I

Index fossils 268, 271, 272, 275, 276
Inset terrace 300

K

Kansan deposits 268
Kansan Glaciation 271, 282
Kulp, J. L., quoted 258, 278

L

Land use 281, 313, 330, 331
effects 263, 264, 301
Landform properties 286
Leonard, A.B., cited 268, 271, 275, 276, 278
Leopold, L. B., and Maddock, Thomas, quoted 316
Lime Creek 278, 281, 286, 289
Little bluestem 262
Load computations, B. R. Colby's method 325
Lobed gully head 301, 307
Loess 256, 268, 274
deposition rate 277
See also Bignell Loess.
Loveland Formation 271, 274, 275, 282

M

Maywood 265
McCook, climatic data 258
Mean channel length 289
Mean valley-side slope 288
Medicine Creek 256, 270, 278, 279, 315, 331, 332
Medicine Creek basin, climate 258
Niobrara Formation 264
Ogallala Formation 265
Melton, M. A., cited 288
Midgrass 262, 332
Mitchell Creek 286, 294, 315, 322, 331
Modern soil 277
Molluscan fauna, Peorian 275, 276
Morisawa, M. E., cited 329
Morphometric analysis 332
Morphometry 284
Mousel terrace 265, 278, 280, 284, 332
carbon-14 dating 284
Woodland sites 280
Multiple linear regression of sediment discharge 331
Multiple regression analysis, properties used by Morisawa 329, 333

N

Native grasses 262
Nebraskan deposits 268
correlation with 272
Needlegrass 262
Niobrara Formation 264
North Platte, ancient droughts at 264
climatic data 260
North Plum Creek 282

O

Ogallala Formation 265, 270, 271, 274
buried valleys in 282
Overgrazing 263
Oxidation 280

P

Paleoclimate 262
Paleosol 270
Parabolic channel shape 321
Particle-size distributions of suspended sediment and bed material 322, 333
Pearlette Ash Member of the Sappa Formation 270, 282
Pelecypod fauna 278
Peorian Loess 268, 271, 272, 275, 276, 277, 282, 332
Peorian postdepositional landscape reconstructed 282
Peorian valley heads 282
Percentage of area, in side slope 330
in upland 328, 331, 333
in valley flat 330
Perennial streams 315, 321, 333
Petrographic features, Peorian Loess 277
Platte Valley 282
Pleistocene and Recent deposits 265, 268
Pleistocene deposits 271
Pleistocene drainage, relic 282
Plum Creek 282
Plunge pools 296, 312, 333
Polar planimeter, use 286
Population 281
Post-Sangamon, chronology 284
Prairie 332
Precipitation 258, 263, 315, 326, 332
Pre-Pleistocene rocks 264, 268
Profile, Cut Canyon 272
main course of Medicine Creek 270
Purpose of report 255

R

Radiocarbon dating. *See* Carbon-14 age determination.
Raindrop impact 263
Rainfall, intensity-duration-frequency curves 260, 332
interception 262, 263
Ravines 262
Recent alluvium 265, 272, 273, 278, 279, 280, 284, 332
Recent deposits. *See* Pleistocene and Recent deposits.
Relief ratio 286, 288, 328, 329, 331, 333
Republican River valley 282

Page

Reservoir regulation ... 315, 318
Rodent burrows ... 312
Rubin, Meyer, cited ... 258, 273
Runoff ... 326, 328, 329, 330, 331
Runoff, reduction ... 314

S

Sand dunes ... 268, 280, 325
Sangamon soil ... 271, 274, 282
Sappa Formation ... 270, 271, 282
Saturation ... 296, 312
Scarps ... 290
See also Channel, scarp; Erosional scarps; Head scarps; Step scarps; Side scarps.
Schultz, C. B., and others, cited ... 265
Schumm, S. A., cited ... 288
Scour ... 295
Settlement ... 281
Short grass ... 262, 332
Side-oats grama ... 262
Side scarps ... 291
Silt ... 333
Slocum, J. L., quoted ... 262
Slumping ... 298, 312
Snails ... 268, 271, 275, 276, 278, 332
Sod ... 263
effects of breaks in ... 295
scarps ... 263
Soil marker ... 268, 274
Station hydraulic relations ... 315
Step scarps ... 264, 290
Stephenson, D. V., quoted ... 262
Stockville terrace ... 265, 268, 272, 278, 282, 286, 291, 292, 311, 313, 332
age ... 281
carbon-14 dating ... 284
Early Lithic sites ... 280
Strahler's, A. N., method of stream ordering ... 285, 286, 289
Stratigraphy, Cedar Creek near Stockville ... 270
Cut Canyon near Curtis ... 271
Pleistocene and Recent ... 268

Page

Stream, capture by Deer Creek ... 282
hydraulics ... 315
ordering method ... 285, 286, 289
Stream lengths, R. E. Horton's law of ... 289
Upland, definition ... 286
Summary ... 332
Sumac ... 263
Suspended sediment ... 279, 315,321, 325, 328, 329, 330, 331, 333
affect on hydraulic geometry of channels ... 315
contributions of major tributaries ... 325
particle-size distributions ... 322
Switchgrass ... 262

T

Tall grass ... 262
Tazewell Stade, Wisconsin Glaciation ... 275
Temperatures ... 258
Terraces, Cedar Creek ... 270
Elkhorn Canyon ... 273
rate of formation ... 274
sequence ... 265
See also Inset terrace; Mousel terrace; Stockville terrace; Wellfleet terrace.
Topographic maps, use ... 258, 286, 288, 294, 298
Trees ... 262, 264
Trenched channel ... 279

U

Unbanded alluvium ... 279
Unexposed rocks ... 264
Upland ... 286, 288, 330
slope ... 330
Upper Republican Culture ... 274, 281
U-shaped dunes ... 280

V

Valley-bottom gullies ... 264, 291, 295, 297, 298, 307, 309, 313, 314, 332, 333
Valley bottoms ... 264

Page

Valley fill, Elkhorn Canyon ... 273
Peorian ... 276
Valley flat ... 279, 329, 330
Valley-head gullies ... 291, 301, 303, 307, 313, 332, 333
formation ... 309
measurement ... 304, 309
Valley incision, Ogallala Formation ... 282
Valley-side gullies ... 291, 301, 303, 307, 313, 332, 333
formation ... 309
measurement ... 304
Valley, slope ... 286, 329
trenching ... 278
Vegetation ... 262, 314, 332, 333
role of, in gully control ... 314
Velocity, relation to discharge ... 316
V-shaped contour lines ... 286

W

Water-discharge functions ... 316
Water-sediment discharge relation ... 322
Wayne, W. J., cited ... 258, 271, 275, 276
Weakly, H. E., cited ... 264
Weaver, J. E., and Albertson, F. W. cited ... 263
Well Canyon ... 265, 278, 279, 286, 289, 294, 330
Wellfleet terrace ... 265, 268, 280
Wheatgrass ... 262
Width of stream, relation to discharge ... 316
Wild plum ... 263
Wild rose ... 263
Wimpf, Charles, quoted ... 262
Wind speed and direction ... 261
Windblown dust ... 263
Wisconsin deposits ... 268
Wisconsin ice, retreat ... 282
Worm burrows and casting ... 273, 277

Y

Yarmouth soil ... 270, 271

☆ U.S. GOVERNMENT PRINTING OFFICE: 1966—O 217-578

Digitized by Google

QE75
f A26
no 352-I

Geol
G

Rates of Slope Degradation as Determined from Botanical Evidence White Mountains California

1968

GEOLOGICAL SURVEY/PROFESSIONAL PAPER/352-I

Rates of Slope Degradation as Determined from Botanical Evidence White Mountains California

By VALMORE C. LAMARCHE, JR.

EROSION AND SEDIMENTATION IN A SEMIARID ENVIRONMENT

GEOLOGICAL SURVEY PROFESSIONAL PAPER 352-I

UNITED STATES GOVERNMENT PRINTING OFFICE, WASHINGTON : 1968

Digitized by

UNITED STATES DEPARTMENT OF THE INTERIOR

STEWART L. UDALL, *Secretary*

GEOLOGICAL SURVEY

William T. Pecora, *Director*

For sale by the Superintendent of Documents, U.S. Government Printing Office
Washington, D.C. 20402 - Price 75 cents (paper cover)

Digitized by Google

CONTENTS

	Page
Abstract	341
Introduction	341
Acknowledgments	342
Physical setting	342
General geology	342
Reed Dolomite	344
Topography and drainage	344
Climate and runoff	346
Soils and surficial materials	346
Surface features	346
Soil profile	348
Vegetation	349
Bristlecone pine	350
Tree-ring dating	350
Age estimate	353
Root exposure and slope degradation	353
Root systems	354
Effects of exposure	354
Buttress roots	354
Problems of measurement	354
Choice of datum	354
Asymmetrical exposure	355
Calculation of degradational rates	357
Degradational rates	358
Local rates	358
Slope transect	359
Selected areas	360
Area 1	361
Area 2	363
Area 3	367
Comparison	367
Relation to topography	369
Degradational processes and evidence of movement	372
Debris damming	372
Asymmetrical root exposure	373
Debris lobes and fans	373
Summary and conclusions	374
References	376

ILLUSTRATIONS

		Page
PLATE 10.	Topographic map of area 1, showing standing and fallen trees and exposed roots	In pocket
11.	Topographic map of area 2, showing standing and fallen trees and exposed roots	In pocket
FIGURE 233.	Map of study area, southern White Mountains	343
234.	Photograph of Reed Dolomite outcrop	344
235.	Map showing distribution of Reed Dolomite	345
236.	Graphical summary of climatic data from Crooked Creek Laboratory	347
237.	Photograph of miniature sorted stripes produced by frost action	348
238.	Photograph of rock stream	348
239.	Sketch illustrating cross dating and chronology	352
240.	Sketch of transverse section of eroded stem showing the geometrical basis for age estimation	353
241.	Photograph of stump of 350-year-old bristlecone pine that died about A.D. 1350	355
242.	Diagrams showing stages in development and exposure of a root system	355
243.	Sketch of cross section of exposed root near stem showing relation of root exposure to degradation	355
244.	Photograph of terrace and hollow due to damming effect of old tree	356
245.	Photograph of root system symmetrically exposed because roots extended directly upslope	356
246.	Photograph of root system exposed symmetrically because of location on ridge crest	356
247.	Sketch illustrating slope profile in the vicinity of a tree with asymmetrically exposed roots	357
248.	Graph of relation of root exposure to age and probable range of local degradational rates	358
249.	Graphs of slope profile, tree age, and depth of root exposure along slope transect	360
250.	Photograph of area 1, as viewed from the west; Blanco Mountain is in background	361
251.	Graph showing slope profiles and results of particle-size measurements	362
252.	Photograph of exposed root of specimen 110	362
253.	Graph of age and minimum slope degradation for area 1	364
254.	Outline map showing distribution of values of estimated local degradational rates in area 1	365
255.	Photograph of valley tributary to the South Fork of Birch Creek	365
256.	Photograph of upper part of area 2	365
257.	Photograph of surficial mantle in area 2	365
258.	Graph of age and minimum slope degradation for area 2	366

Digitized by Google

Page
FIGURE 259. Outline map showing distribution of values of estimated local degradational rates in areas 2 and 3, and slope profile of area 2 366
260. Photograph of part of area 3, viewed upslope 367
261. Topographic map showing location of trees studied in area 3, and profiles of area 3 368
262. Photograph of specimen 184 in area 3 369
263. Detailed maps of exposed roots of six trees in area 3, and profiles in vicinity of five of the trees 370
264. Graph of comparison of average and maximum depths of root exposure of trees in area 3 371
265. Graphs of comparison of degradational rates in areas 1 and 2, as indicated by frequency distributions of values of local degradational rates 371
266. Graph of comparison of degradational rates in areas 1 and 2 372
267. Photograph of log that forms debris dam on slope 372
268. Photograph of large debris pile in canyon tributary to Wyman Creek 374

TABLES

Page
TABLE 1. Grain-size distribution of samples of dolomitic soil in the White Mountains 349
2. Age, root exposure, and site data for trees in scattered localities in southern White Mountains 359
3. Age, root exposure, and site data for trees on slope transect, listed in order of increasing distance from base of slope 359
4. Data for trees in two selected areas 362
5. Age and root-exposure data for trees in area 3 367
6. Summary of degradational rates and topographic characteristics in three selected areas 369
7. Degradational rates for slope classes in crestal areas and on main slopes 369
8. Qualitative summary of major transport mechanisms 376

Digitized by Google

EROSION AND SEDIMENTATION IN A SEMIARID ENVIRONMENT

RATES OF SLOPE DEGRADATION AS DETERMINED FROM BOTANICAL EVIDENCE WHITE MOUNTAINS, CALIFORNIA

By Valmore C. LaMarche, Jr.

ABSTRACT

Methods of calculating long-term rates of slope degradation have been developed by studying exposed roots in relation to age of ancient bristlecone pines in dolomite areas in the semiarid White Mountains of east-central California. The Precambrian Reed Dolomite, a closely jointed but homogeneous and relatively resistant bedrock unit, underlies parts of a fluvially eroded terrane of high local relief where drainage channels and interchannel ridges are major topographic features.

A subalpine bristlecone-pine forest covers dolomite areas between altitudes of 9,500–11,500 feet. A few living trees are known to be more than 4,000 years old, but the average age of trees studied is about 1,000 years. Age determinations were made by counting annual growth rings. Uncertainties in assigned ages are due to incomplete growth records caused by weathering and decay of early formed wood and to the absence of certain growth increments in some samples.

Exposed tree roots are direct evidence of degradation. Developing roots of bristlecone pines are concentrated in the uppermost foot of soil and are uncovered and progressively exposed with time. Root exposure is due partly to the general lowering of the ground surface in the vicinity of a tree, but deep exposure of roots on the downslope side is also caused by the damming of surficial rock debris by the tree itself. The depth of root exposure, measured from the axis of an exposed root, must be corrected for local topographic changes related to the presence of the tree in order to estimate the minimum slope degradation.

Local degradational rates are estimated from tree or root age and depth of root exposure. Grouping of data from 76 bristlecone pines at scattered points within a 20-square-mile area suggests that degradational rates vary from place to place and reflect differences in the intensity of degradational processes that are closely related to existing topography. These rates range from less than 0.5 foot per 1,000 years on the gentle lower slopes of high ridges to perhaps 4 feet per 1,000 years along the adjacent steep banks of channels incised into alluvial fill. Degradational rates in crestal areas are high and apparently increase with ground-surface slope, whereas those of the main valley side slopes are lower and are not closely related to slope angle.

The best estimates of long-term rates of slope degradation are those based on study of samples containing a relatively large number of specimens from small topographically homogeneous areas. A comparative study of 72 dated trees in two selected areas showed that a rocky knoll has been degraded at about 1.2 feet per 1,000 years during the past 2,700 years, whereas the average degradational rate on a long valley side slope has been only about 0.8 foot per 1,000 years in the same period. These rates of degradation are similar to denudational rates that have been estimated for comparable areas in other regions.

Slope degradation indicated by widespread exposure of root systems of bristlecone pines involves production and removal of large volumes of rock debris. Frost action is a prime factor in the breakdown of bedrock, in the development of miniature patterned-ground features, and in soil creep. Accumulations of surficial material behind logs and standing trees are evidence of rapid downslope movement of weathered material. Cloudburst floods transport coarse sediment in the stream channels and produce mudflows that reach the alluvial fans flanking the range.

Transport rates of products of rock weathering on slopes and in stream channels are concluded to be great enough to account for the estimated degradational rates. The Reed Dolomite terrane seems to have been adjusted to the study production and removal of rock debris under conditions of the past 3,000 years, and local degradational rates do not appear to have changed measureably in this period.

INTRODUCTION

Elevated areas of the earth's surface are gradually being lowered as rock debris is removed by degradational agents. Despite their importance in comparing past with present rates of soil erosion, natural rates of slope degradation during the past several thousand years are little known (Leopold, 1956; Ruhe and Daniels, 1965). Direct observations of slope degradation and channel erosion are inadequate or lacking, however, so that sediment sources within a drainage basin must usually be inferred from indirect evidence (Anderson, 1957; Glymph, 1954).

This report describes the development and application of methods for obtaining long-term rates of slope degradation in areas where the exposed roots of old trees bear record of the prior levels of a progressively lowered land surface. The root systems of young trees of many species are concentrated at shallow depths. In time the roots will be uncovered and progressively exposed if the soil that overlies and encloses them is re-

Digitized by Google

moved by erosional agents. The depth of root exposure and the age of the tree can be used to estimate the local degradation rate. Although based on study of bristlecone pines (*Pinus aristata* Engelm.) in the White Mountains of California, the approach used in this report is valid wherever the landscape changes significantly within the lifetime of individual trees. Where combined with other geomorphic evidence, knowledge of local degradation rates can be applied to the study of landscape evolution and to problems of sediment production and transport.

No general agreement exists as to the usage of terms that refer to certain kinds of quantitative geomorphic changes. "Denudation" is widely used to describe the wearing down of a landscape. A denudation rate is often calculated from measurements of the sediment and dissolved load of streams (Corbel, 1959; Judson and Ritter, 1964). The rate expresses only the time required for the removal of a hypothetical layer of certain thickness uniformly ditributed over the entire drainage area upstream from the point of observation. Degradation and local aggradation on slopes, in stream channels, and on floodplains within the area may all contribute to the net result.

Degradation means "The gradual lowering of the surface of the land by erosive processes * * *" (Rice, 1940). In this report degradation refers to the actual decrease in altitude of the land surface, relative to a previous altitude, due to the production and removal of rock debris by weathering, mass-wasting, and erosion. The term "slope degradation," when applied to areas between permanent drainage lines and adjacent divides, is virtually synonymous with the term "hillslope erosion" as used by Schumm (1964), but its use does not necessarily imply that flowing water is a dominant transporting agent.

The investigation of root exposure in relation to slope degradation in the White Mountains was limited to about 20 square miles underlain by the Reed Dolomite (Nelson, 1962) because the bristlecone pines are virtually restricted to areas underlain by this formation. The study area lies at an altitude of about 10,000 feet and has an average relief of about 500 feet; however, within the area, Blanco Mountain reaches an altitude of 11,278 feet. The area is drained by streams flowing into Deep Spring Valley, a small desert basin 10 miles to the east. The Blanco Mountain 15-minute quadrangle map of the U.S. Geological Survey shows the area, which is in the Ancient Bristlecone Pine Forest of the White Mountain District, Inyo National Forest. The area is accessible by road from Big Pine, Calif.

The investigation was begun in the summer of 1962 with a reconnaissance study of about 100 trees. The work included the determination of ages of root wood and stem wood by tree-ring dating techniques. Study results showed that exposed roots are a common feature of older trees and that root exposure is the result of lowering of the ground surface and of differential downslope soil movement. The methods developed in the initial study were then applied to intensive study of 83 trees in 3 selected areas for comparision of rates and processes of degradation on contrasting types of slopes. These areas were mapped by planetable methods in 1963.

Rates of degradation were computed from the measurements of root exposure and the age determinations from tree-ring dating. The significance of various degradational processes has been inferred from indirect evidence, such as bedrock characteristics, dimensions and detailed features of the drainage network, dimensions and surface forms of slopes, textural and mineralogical features of the surficial mantle, microtopographic effects of vegetation, and climatic data.

ACKNOWLEDGMENTS

The work described in this report was the basis for a doctoral thesis submitted to Harvard University in 1964. Alan V. Jopling contributed his time and knowledge to many discussions. Elso S. Barghoorn and Martin H. Zimmerman were of great assistance in resolving some of the botanical questions which arose during this study. The Laboratory of Tree-Ring Research of the University of Arizona made available a partial chronology of the bristlecone pines in the study area. Special acknowledgment is given to C. W. Ferguson for his help and cooperation.

PHYSICAL SETTING

The study area consists of a fluvially eroded landscape where drainage channels and interchannel ridges are major topographic features. With its high local relief, sparsely vegetated slopes, and ephemeral stream channels, the area is similar to many other mountainous areas in semiarid regions. Mass-wasting processes and forms are ubiquitous but are restricted in scope to individual hillside slopes. Despite the rare occurrence of runoff, the area is being denuded through the removal of rock debris by water concentrated in stream channels.

GENERAL GEOLOGY

The White Mountains form the northern apex of a wedge-shaped complex of fault-block ranges and closed basins that lies east of Owens Valley in east-central California (fig. 233). The range, triangular in outline, is a tilted fault block 50 miles long and 20 miles wide that has been elevated relative to the adjacent basins since late Tertiary time (Knopf, 1918). Flanked by coalescing alluvial fans, the straight steep western

Digitized by Google

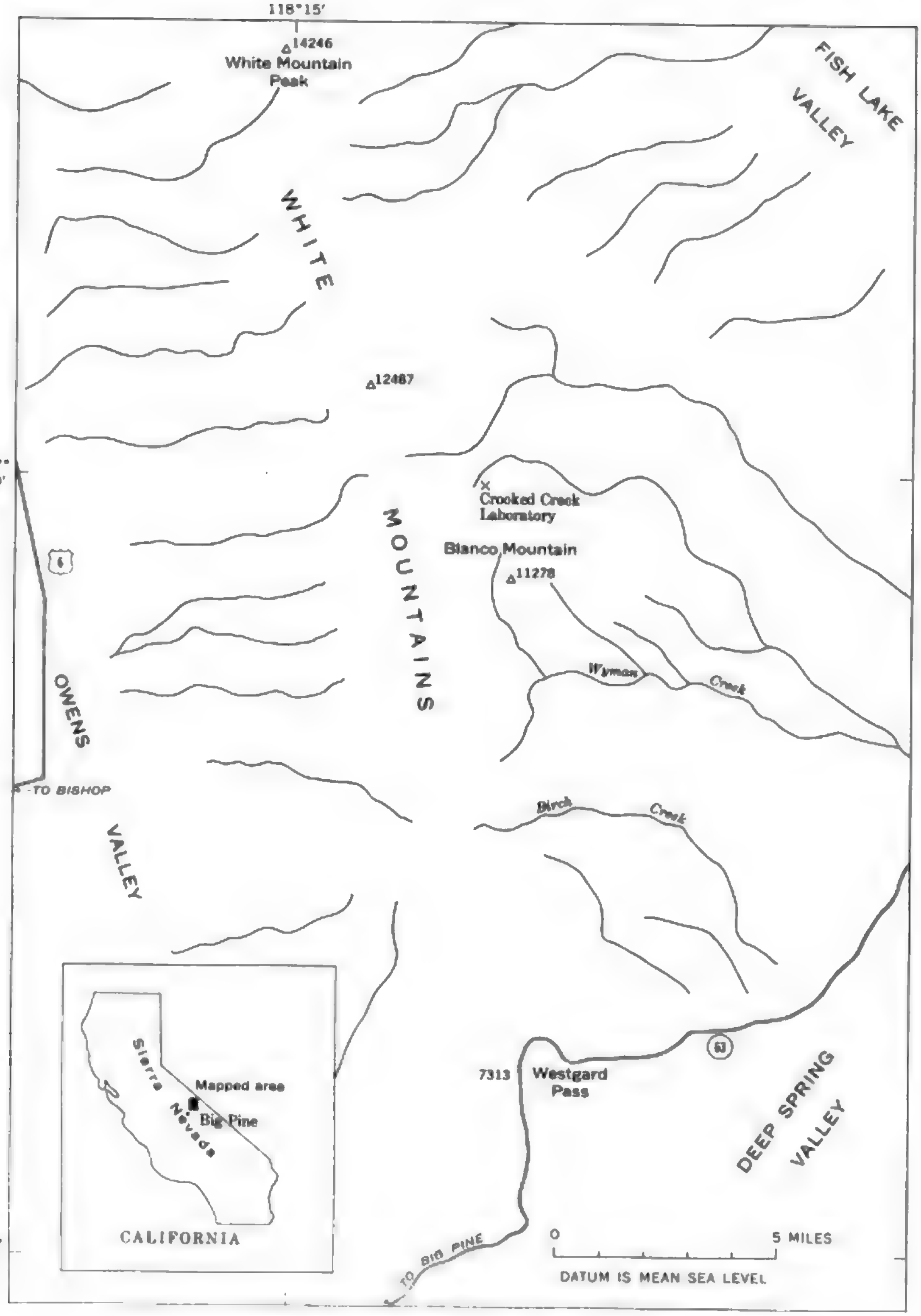

FIGURE 238.—Study area, southern White Mountains.

scarp faces the eastern scarp of the Sierra Nevada across Owens Valley, a deep structural depression. The range is bounded on the northeast by Fish Lake Valley and slopes gently to the southeast into Deep Spring Valley. The linear crest of the range, rising 2,000–10,000 feet above the basin floors, reaches its maximum altitude at White Mountain Peak (alt 14,246 ft).

The southern White Mountains are composed mainly of folded sedimentary and metamorphic rocks of Precambrian and Early Cambrian age (Nelson, 1962, Stewart, 1966) and of intrusive granitic rocks of probable Mesozoic age (Nelson, 1963). These are locally overlain by thin Tertiary basalt flows and associated alluvium and pyroclastic beds (Nelson, 1963). The major structural features are a broad south-plunging anticline and a granitic batholith that underlies much of the eastern and northern parts of the range. The structure is very complex. There are many faults, some of large displacement, and faults of several different ages, or periods of movement, can be distinguished locally.

REED DOLOMITE

Within the area studied the Reed Dolomite of Precambrian age (Stewart, 1966) is composed entirely of dolomite (Nelson, 1962). Bedding is seldom visible because the rock shows little compositional variation or textural change. Gentle to moderately steep dips (20°–45°) are indicated by the attitudes of the upper and lower contacts of the unit. To determine lithologic variations within the dolomite, hand specimens were collected at 100-foot intervals along a paced traverse across the width of the Reed outcrop east of Reed Flat (fig. 235.) The samples range from very fine grained white dolomite to medium-coarse-grained gray dolomite; some are oolitic. Thin sections were made of 5 of the 25 samples. A typical sample is composed of interlocking anhedral dolomite crystals and a few scattered silicate grains. Weathered surfaces of the rock are buff, cream-colored, or white. The light color of the weathered surfaces suggests that the dolomite has a fairly low iron content.

Intersecting joint sets, rather than bedding planes, determine the shape and appearance of bedrock outcrops (fig. 234), and the rock breaks along preferred directions controlled by joint orientation. Measurements of 23 joints at 8 localities on the knoll east of Reed Flat gave the following results when plotted on a stereographic projection: Two principal orientations at about N. 10° E., 40° W., and N. 30° E., 70° E., and a less frequent orientation at N. 80° W., vertical. The spaces between parallel joints or fractures range from 1–2 inches to several feet and seem to increase with slope of the bedrock surface.

FIGURE 234.—Reed Dolomite outcrop showing prominent jointing. Tape is extended 1 foot.

TOPOGRAPHY AND DRAINAGE

The southernmost stand of bristlecone pines in the White Mountains occupies an area 6 miles long and 3 miles wide that extends from Blanco Mountain on the north to Reed Flat on the south. Altitudes in the area generally range from 9,000 to more than 11,000 feet. Most of the Reed Dolomite terrane (fig. 235) is drained by two eastward-flowing streams—Wyman Creek on the north and Birch Creek on the south—with drainage areas of 29 and 15 square miles, respectively. The slopes bordering Reed Flat and Coldwater Flat drain into these adjacent closed basins, which have a combined drainage area of about 2 square miles.

The main divide separating this area from the Owens Valley drainage to the west is underlain by the Precambrian and Lower Cambrian Campito Formation. An undulating ridge marks the outcrop of this resistant sandstone and shale unit. Parallel to, and a mile east of, the divide is a discontinuous ridge of the equally resistant Reed Dolomite. Drainage from longitudinal valleys carved in the weak shale, thin-bedded dolomite, and limestone of the intervening Precambrian Deep Spring Formation is funneled into a few deep canyons that cut through the forested dolomite ridge. In the southern part of the area, folding and faulting of the Reed Dolomite and the underlying Wyman Formation is reflected in a series of northeast-trending dolomite spurs sepa-

Digitized by Google

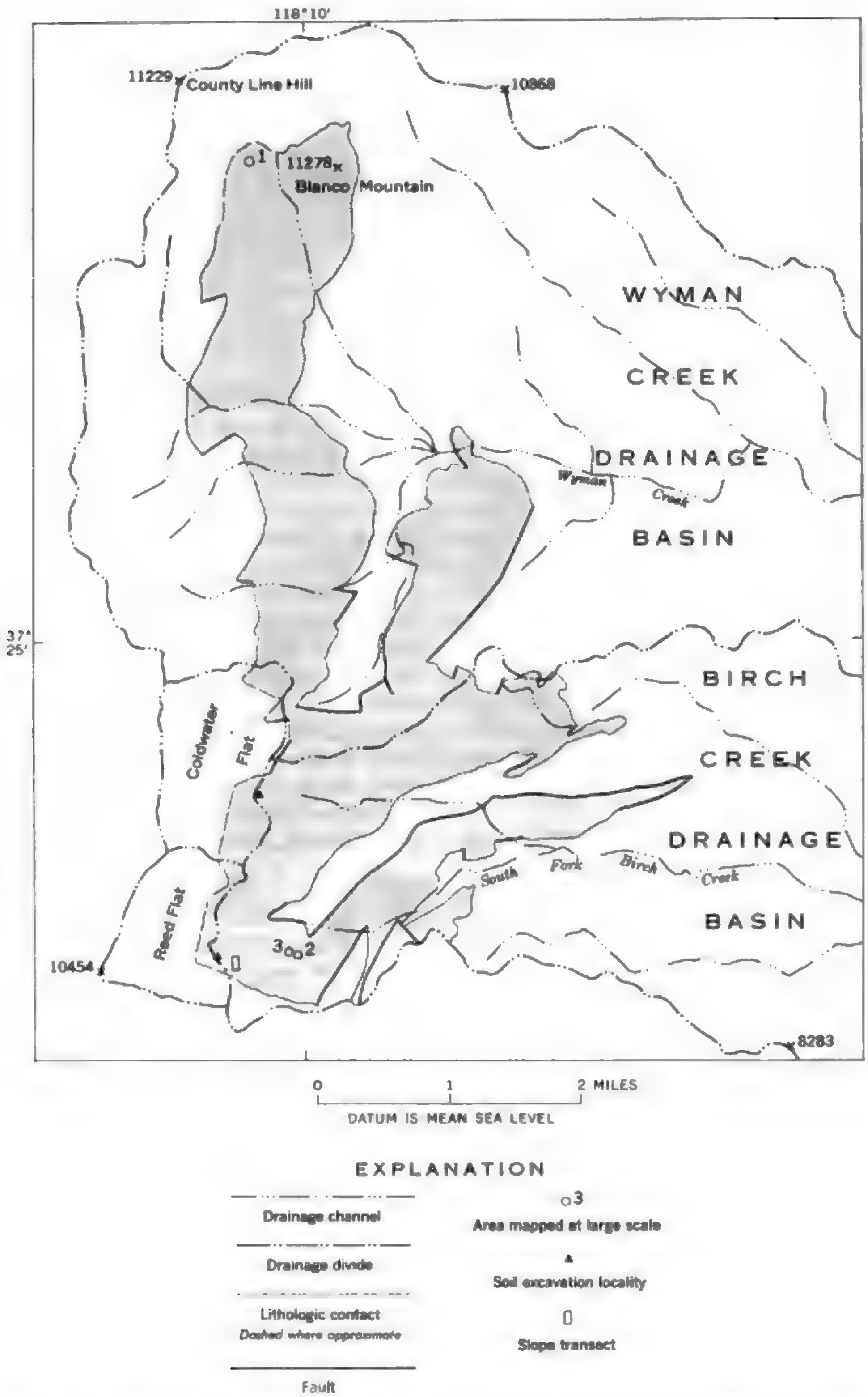

FIGURE 235.—Distribution of Reed Dolomite (shaded) in relation to drainage patterns in Blanco Mountain–Reed Flat area. Also shown is location of smaller areas mapped at large scale. Geology after Nelson (1963).

269-085 O-67-2

rated by valleys in the less resistant Wyman argilite and platy sandstone.

The slopes in the study area show a variety of forms and surface features; most are straight or smoothly curving, but a few are sharply faceted. Ridge crests are generally narrow and smoothly rounded, but some are surmounted by rocky pinnacles and are actually biconcave in cross profile. Outcrops, in the form of smooth surfaces and small cliffs, are typically limited to ridge crests and upper slopes. The lower slopes and valley bottoms are generally deeply mantled by colluvium and alluvium.

CLIMATE AND RUNOFF

The White Mountains are in the rain shadow of the Sierra Nevada. Eastward-moving winter storms, a major source of precipitation in the region, are depleted of moisture by the high mountain barrier to the west (D'Ooge, 1955). The higher parts of the White Mountains have a cold steppe climate, and the flanking valleys are classified as cold desserts (Kesseli and Beaty, 1959), having mean annual temperatures ranging from 56.0° F at Bishop)alt 4,108 ft) to 27.7° F at Barcroft Laboratory (alt 12,470 ft). Mean annual precipitation increases with altitude on the range, from 5.5 inches at Bishop to 15.5 inches at Barcroft, and may reach 18–20 inches near White Mountain Peak. At the higher altitudes, precipitation is mostly in the form of snow falling during October through May. Occasional intense rains are produced by summer thunderstorms.

The Crooked Creek Laboratory (alt 10,150 ft) of the University of California White Mountain Research Station is in the area, and daily weather observations have been recorded there since 1948. Shorter series of measurements, incidental observations, and estimates have also been made in the area (Kesseli and Beaty, 1959; Mooney and others, 1962). Meteorological data from Crooked Creek Laboratory are graphically summarized in figure 236.

Runoff from White Mountain watersheds is small owing to low precipitation and high potential water loss. Perennial streams are found only in those canyons that head in the highest parts of the range. Elsewhere, ground-water discharge maintains low summer flow only in some reaches of the major canyons. Most of the streams draining the White Mountains are ephermeral or intermittent; however, historical evidence discloses that occasionally heavy runoff occurs from many of these watersheds. Kesseli and Beaty (1959) summarized the records of flooding in and adjacent to the White Mountains during the period 1872–1957. Cloudbursts during the months of July and August were responsible for 40 of the 63 reported floods. Most of the other floods, distributed fairly uniformly throughout the rest of the year, apparently resulted from rapid snowmelt, often augmented by rainfall. Although the maximum 24-hour rainfall recorded at the U.S. Weather Bureau cooperative stations within the mountains during the 10-year period ending December 31, 1962, was only 1.45 inches (Crooked Creek, July 24, 1959), more than 8 inches of rain were caught in a portable rain gage during a 2-hour cloudburst in the northern White Mountains on July 19, 1959 (Kesseli and Beaty, 1959, p. 23). This downpour, concentrated in an area of 1–2 square miles, generated a debris flow that moved for more than 3 miles down a canyon to the edge of the range.

SOILS AND SURFICIAL MATERIALS

A mantle of surficial debris overlies bedrock of the Reed Dolomite throughout most of the area studied. The mantle consists of the products of the mechanical and chemical breakdown of bedrock and of a small amount of organic material. It ranges in thickness from a few inches to perhaps 30 feet and is apparently thickest on the lower slopes and the valley bottoms. Texture of the mantle ranges from pebbly loam to coarse rubble. Except locally, the mantle has not developed in place as a residual product of the disintegration of the immediately underlying rock. The thin veneer of debris on the upper slopes appears to be actively moving. The much thicker colluvial deposits on some of the lower slopes and the alluvial fill of the major canyons, derived from adjacent slopes and tributary drainage areas, are now being dissected by stream action.

SURFACE FEATURES

The debris mantle is characterized both by broad-scale textural differences associated with topographic site and by local surface irregularity and textural inhomogeneity. Areas of relatively fine soil on gentle slopes show well-developed patterned-ground features, including miniature sorted stripes, miniature sorted polygons and nets, and stone-banked terraces (terminology after Washburn, 1956). On the gentlest slopes, crude networks of pebbles surrounding elevated areas of fine soil form polygons or nets with individual cells from 3 to 6 inches in diameter. Sorted stripes consisting of 2- to 5-inch-wide bands of silt and fine sand alternating with narrower, depressed, pebble stripes occur on steeper slopes of as much as 25° (fig. 237). Stone-banked terraces, elongate parallel to the slope contours, and sorted steps, elongate downslope, are much larger features. These terraces average several feet in length and have borders, composed of pebbles and cobbles, as much as 1 foot high. The flat or gently sloping areas thus enclosed contain finer grained material sorted

Digitized by Google

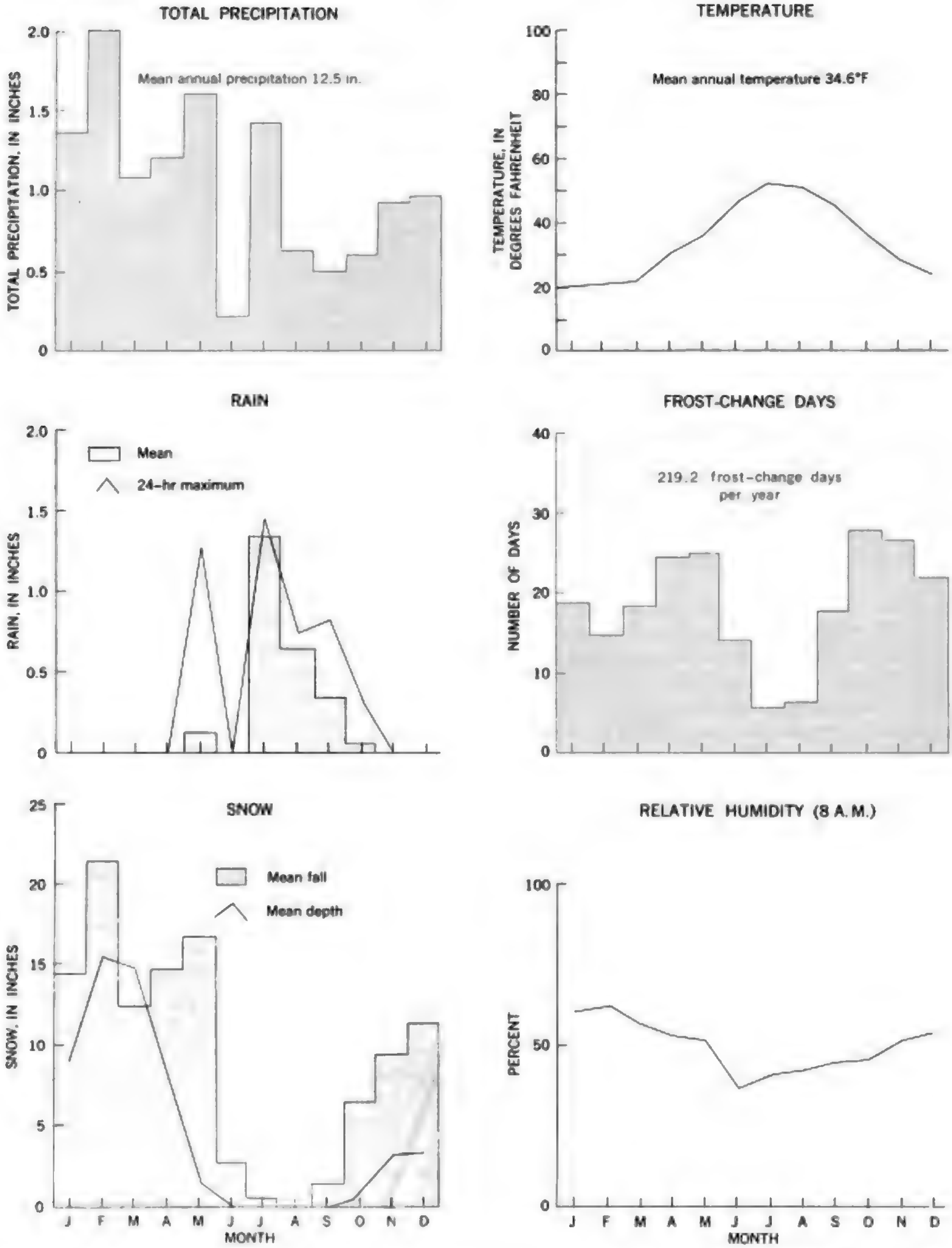

FIGURE 236.—Summary of climatic data from Crooked Creek Laboratory for 10-year period ending December 31, 1962. Frost-change days (days with maximum temperature greater than 32° F and minimum temperature of 32° F or less) calculated from original station records; all other data from Pace (1963).

FIGURE 237.—Miniature sorted stripes produced by frost action on gentle (12°) south-facing slope. Miniature polygons are found in flat areas and sorted steps, on steeper slopes.

into miniature stripes or nets. Even larger, but less regular, patterns of sorting of surface material characterize the steep sparsely vegetated slopes mantled by coarse debris. These are rock streams several feet wide and tens of feet long that have smaller fragments in the center and large pebbles and cobbles on the margins (fig. 238).

The patterned-ground features are actively developing. Tufts of grass and individual cushion plants have been overridden by small mud lobes and pebble streams. Grass, small plants, and even shrubs have been overturned and partly buried by downslope movement of the borders of terraces and steps. Rock streams have apparently been diverted by living trees and fallen logs. In a single winter, nonsorted miniature polygons formed in tire tracks that cross the silty sediment in Reed Flat.

Patterned-ground development in arctic and subalpine regions is generally attributed to frost action (Washburn, 1956). The miniature forms common in the White Mountains, more typical of tropical and subtropical mountains, are associated with shallow frost penetration, ephemaral snow cover, and numerous diurnal freeze-thaw cycles (Troll, 1958). With 219 frost-change days per year, an average snow depth of only 5 inches, and a mean minimum temperature of 22.3°F (Pace, 1963), the climate at an altitude of 10,000 feet in the White Mountains favors rapid development of patterned-ground and intense but shallow frost action.

SOIL PROFILE

Development of a soil profile in the dolomitic mantle is weak even in the most favorable locations. Soil texture and mineralogy were studied in excavations in areas of relatively deep soil, gentle surface slopes, and small surface-particle size. Litter 0–1 inch thick overlies a

FIGURE 238.—Rock stream, oblique upslope view. This elongate patch of fine-grained soil is moving downslope more rapidly than surrounding coarse rubble.

thin zone of reddish-brown soil containing numerous plant rootlets. This zone grades downward into a barren yellow to buff zone. At depths of 1–3 feet is a distinctive thin (1–4 in.) dark-brown zone filled with both dead and living plant rootlets. In contrast to the buff soil above and below, the dark-brown zone contains few pebbles and is uniform in texture.

Soil samples were collected from the walls of two excavations (fig. 235). Each composite sample represents from 6 inches to 1 foot of the profile, except in the dark-brown zone that was sampled separately. In addition, samples of the upper 6 inches of soil were collected at eight points along the slope transect described on page 359. The air-dry samples, which had no preliminary treatment, were dry-sieved through a set of screens with openings of 4.76, 2.00, 1.00, 0.25, and 0.065 mm; and the size fractions were weighed. The mineralogic compositions of selected size fractions of some samples were estimated. The content of silicate minerals was estimated from residues insoluble in hot hydrochloric acid. X-ray diffractometer methods were used for semiquantitative mineralogic analysis of the bulk samples and the insoluble residues.

The samples from all but the dark-brown zone have similar textural and mineralogic features. Nearly half the soil is composed of particles smaller than 0.25 mm, and most of the remainder, of fragments larger than 2 mm (table 1). The coarse fractions consist of dolomite

Digitized by Google

pebbles; the fine fractions, of dolomite grains and minor amounts of quartz and feldspar and accessory mica, chlorite, and goethite (pseudomorphic after pyrite). The intermediate-size fractions, which typically make up less than 10 percent of total original sample weight, are composed mainly of root casts and aggregates of fine sand and silt cemented by calcite.

The dolomite (which makes up most of the soil), the goethite, and some of the silicate grains are derived from the mechanical breakdown of the Reed Dolomite. Some of the silicate grains could have come from small outcrops of sandstone and shale of the Deep Spring Formation upslope from all the localities examined. Alternatively, windblown silt could have been added to the accumulating colluvial mantle.

TABLE 1.—*Grain-size distribution of samples of dolomitic soil in the White Mountains*

[Distribution of weight fractions (percent) by size (millimeters)]

Sample	Size range					
	<0.002	0.002–0.25	0.25–1.0	1.0–2.0	2.0–4.76	>4.76
SURFACE SAMPLES (TO 6-IN. DEPTH) FROM SLOPE TRANSECT						
14	10	28	5	2	5	50
15	6	20	3	1	6	64
16	6	20	6	2	6	60
17	10	23	8	2	6	51
18	9	26	9	6	12	37
19	9	33	6	5	10	37
20	5	26	6	5	12	47
21	5	29	8	6	15	39
SOIL HORIZONS SAMPLED IN EXCAVATIONS						
Upper						
4	10	22	10	2	2	54
5	9	16	6	3	5	60
8	15	18	6	3	3	49
9	7	43	10	4	10	26
10	12	19	9	6	13	41
11	3	32	7	4	10	44
Dark brown						
6	30	31	18	6	15	0
12	10	41	17	6	8	18
Lower						
7	21	22	8	3	5	41
18	2	33	6	5	11	43

The dark-brown zone is composed principally of aggregates of fine-grained calcite, but it contains a few dolomite pebbles and some fine-grained dolomite. Because this zone is parallel to the ground surface even in areas where the mantle is being incised by stream channels, and because it is locally connected to the upper dark zone by inclined layers of similar soil, it is thought to represent a true soil profile horizon that has developed in place, rather than a buried soil or accumulative layer.

The cement of the aggregates and casts and the coating on pebbles seen throughout the soil is interstitially precipitated calcite. Calcite precipitation probably takes place in the late spring and summer, when the moisture content of the soil is reduced by evaporation and plant transpiration. The original source of the calcium carbonate is apparently the clastic dolomite making up most of the soil. Dolomite ($CaMg\ (CO_3)_2$) dissolves congruently in water but rarely precipitates from dilute aqueous solutions under surface conditions (Garrels and others, 1960). Although seasonal precipitation of calcite alone from water originally containing dissolved dolomite would lead to progressively higher concentrations of magnesium in soil solutions, no evidence was found for the presence of secondary magnesian compounds in the soil. Perhaps periodic flushing by downward-moving water removes this dissolved magnesium.

A textural feature common to nearly all the soil samples is the bimodal distribution of particle sizes. If secondary aggregates in the intermediate size classes are disregarded, half of a typical sample is composed of dolomite pebbles and cobbles and half of very fine sand-size and silt-size dolomite and silicate grains. The two principal size classes reflect two distinct modes of rock breakdown—the large multigranular particles, separation along joint and fracture surfaces, and the small dolomite fragments, dislodgement from individual crystals along cleavage planes.

The relative proportions of the two kinds of clastic particles are related to the kind of process that produces them. Frost shattering—the result of the constrained expansion of freezing water—is capable of dislodging particles in both size classes. The abundance of course debris, the meteorological evidence of frequent freeze-thaw cycles, and the widespread development of patterned ground suggest that frost action is a primary mechanical weathering process in the White Mountains.

The growth of tree roots in fractures has clearly resulted in the dislodgement of large bedrock masses from cliffs. Similar wedging action by plant rootlets may contribute to the breakdown of soil particles. Interstitial crystal growth, colloid plucking, and other small-scale processes are probably active, especially within the soil. The processes of chemical alteration that are so active in the breakdown of silicate rocks are not operative except that of simple solution, the only such process that can affect the relatively pure dolomite.

VEGETATION

The broad pattern of plant distribution in the White Mountains is similar to that in other regions of high relief in the Southwest (Merriam, 1890). Four major

Digitized by Google

vegetational zones can be distinguished (Mooney, and others, 1962): desert scrub at altitudes below about 6,500 feet; pinyon-juniper woodlawn from 6,500 to 9,000 feet; subalpine coniferous forest from 9,000 feet to upper tree line, at about 11,500 feet; and alpine above tree line.

In detail, plant distribution is related in both kind and amount to topography, rock type, and soil and slope characteristics. The subalpine coniferous forest, which includes both bristlecone pine and limber pine (*Pinus flexilis* James), is neither continuous nor homogeneous within its broad altitudinal limits. Only scattered stands of conifers are found in topographically favorable locations underlain by limestone, shale, sandstone, or granite. These patches of forest, especially at lower altitudes, are composed mainly of limber pine. The dolomite areas support relatively dense continuous stands of bristlecone pine.

BRISTLECONE PINE

The bristlecone pine grows near upper tree line in many of the high mountain ranges of the Southwestern United States (Munns, 1938). Where geomorphic changes have been sufficiently rapid, the extreme longevity of many bristlecone pines makes possible the study of local degradational rates over the past several thousand years. The great age of some individual trees of this species was first discovered by Edmund Schulman in the White Mountains (Schulman, 1956), and by 1958, 17 specimens more than 4,000 years old were known in this area. Other bristlecone-pine stands in California, Nevada, and Utah are also known to contain very old trees. Currey (1965) recently described a 4,900-year-old bristlecone pine in eastern Nevada. The White Mountains support one of the largest known bristlecone pine stands containing a large number of old trees, but relatively few trees have attained extreme ages (in excess of 4,000 years), and some areas contain many acres of only young trees (< 500 years old). The oldest tree studied in this report is 3,100 years old, and the average age of those dated is only about 1,000 years. Most of the very old trees are found in restricted sites, near the lower forest border or on rocky exposed ridge crests. The great age attained by conifers apparently growing under the most severe local conditions has been discussed by Schulman (1954, 1956).

The mature bristlecone pines have a great variety of sizes and forms. The trees in areas of high stand density are tall and straight. Each has a single stem that is circular in cross section and bark covered around the entire circumference. In contrast, the very old trees are isolated or are in more open stands. They are typically squat and gnarled and have many dead branches and large areas of exposed deadwood. The bristlecone pines are not large because they grow slowly, adding only ½–2 inches of wood along a given radius in 100 years. The tallest specimen reported in the White Mountains (Billings and Thompson, 1957) is only 60 feet high. The Patriarch, a multiple-stemmed tree near upper tree line, is 37 feet in circumference, although it is only 1,500 years old (Schulman, 1958, p. 358).

Living bristlecone pines are rarely overturned. There are many standing dead trees, however, and dating of the outermost growth rings shows that some died more than 1,000 years ago. These trees apparently fall only after the supporting roots have decayed or been undermined by deep erosion. Some long-dead trees, firmly rooted in bedrock fractures, have weathered to mere stubs. The extent to which dead roots have been preserved depends on the length of time that they have been exposed—small branch rootlets are still present on roots that have been rapidly and recently uncovered. At the other extreme, the root systems of a few long-dead trees have been reduced to formless stubs projecting a few inches outward from the base of the stem.

The cool semiarid climate and the dense resinous nature of the wood seem to be responsible for the unusual persistence of the exposed deadwood. The stems and branches of standing trees and the roots lying above the ground surface are usually sound. Dead roots, fallen logs, and branches partly buried in the soil have rotted. Conditions seem to be most favorable for decay on the relatively moist north-facing slopes, which have denser vegetation and are littered with organic debris.

TREE-RING DATING

Precise ages can be asigned to individual growth increments in the secondary xylem of bristlecone pines in the White Mountains. The dating method involves the counting and correlation of annual rings exposed in cross sections or in cores taken with an increment borer. The method is based on the number of rings and on year to year variations in ring width that are correlative among most of the trees in the area.

During the summer growing season, new wood normally forms in a concentric sheath around a root or stem axis through activity of the cambial layer, which is immediately beneath the bark. Wood formed early in the season is light colored and possesses large thin-walled cells; wood formed toward the end of the growing season is much darker and has small thick-walled cells. A distinct annual layer is thereby defined, each layer appearing as a ring in transverse section. (See fig. 239.) The widths of rings formed in successive years differ. Certain years are characterized by narrow rings, not only at different points in the same tree, but also in most

Digitized by Google

nearby trees. Thus, a common response to some factor affecting the total seasonal growth is indicated. In semiarid regions the availability of soil moisture is thought to be a determining factor; relatively thin rings may represent dry years (Fritts, 1966; Schulman, 1956). The "sensitive" growth records of some bristlecone pines show large year to year fluctuations in ring width. Trees with more uniform growth have "complacent" records. Sensitivity is associated with a low average growth rate and is characteristic of trees growing on rocky exposed sites or near the lower forest border; it is also typical of old trees. The relation of site to ring-width variability in bristlecone pines in the White Mountains was illustrated by Fritts (1966).

Locally absent or "missing" rings are also associated with slow growth and high sensitivity. Such rings occur only locally, if at all, in many trees and may not be present in a particular sample. Rings which are absent in the growth records of sensitive trees are found to correspond to relatively narrow rings in more complacent records. False rings, representing more than one period of growth in a calendar year, can be distinguished from true annual rings (Glock, 1937, p. 10) and are rare in the White Mountains (Schulman and Ferguson, 1956, p. 137); they have been noted only in the wood of very young trees.

Cross dating (Douglass, 1914) is the correlation of distinctive sequences of wide and narrow rings (fig. 240). Simple ring counting yields precise dates only if no rings are missing from the sample, which must be from a living tree and must include the outermost ring as a dating control. However ring sequences in a sample can be cross dated with those in a dated sample from the same, or from a different, tree. This permits the dating of virtually any piece of wood from an area, provided that dated samples with overlapping or concurrent growth records exist. To utilize the cross-dating properties of sensitive growth records, and yet retain the precise dating possible with complete, but complacent, records, a chronology is made. This is a graph of the variation of average ring width with time and is constructed from the growth records of many trees in an area of homogenous ring-width variation.

A chronology for the period from A.D. 300 to A.D. 1954 was used in this study. It is based on the work (largely unpublished) of Edmund Schulman and C. W. Ferguson in the White Mountains. The chronology is similar to that published by Schulman (1956, p. 52), which is reproduced here in figure 239. Less precise control in the period prior to A.D. 300 is provided by samples from specimens with growth records extending back to about 2000 B.C. Distinctive sequences in these samples were dated by ring count and used to cross-date old samples that do not overlap the period covered by the chronology. Dates prior to A.D. 300 obtained in this study are thus subject to an error due to the uncertainty in the number of locally absent rings in the control specimens. Experience in dating younger samples shows that 5–10 percent of the rings may be missing from growth records of highly sensitive trees. The older specimens can be more precisely dated when an extended chronology becomes available.

Through the use of cross dating and the building of a local chronology, the tree-ring dating method can be made very precise in terms of the reproducibility of the results obtained by independent study. But the validity of the calendar dates assigned to individual rings depends on the assumption that the growth increments represented in the chronology are annual rings. At least one line of evidence suggests that they are. Only one ring has been formed each year by most of the bristlecone pines in the 10-year period since the first samples were collected by Schulman, as shown by comparison of samples collected in 1963 with the published chronology (Schulman, 1956, p. 52). In the Reed Flat area the outermost rings in some of the bark-covered stumps of cut trees have been dated in the mid-1860's by cross dating with living trees in the vicinity; this date is corroborated by the fact that bristlecone timbers were used in a nearby mine first located in 1862 (Norman and Stewart, 1951). Because the rings formed during this period are annual rings and do not differ qualitatively from those of earlier periods, it is felt that accurate dates can be assigned to growth rings in the wood of bristlecone pines.

Although the potential accuracy of the ring-dating method is great, definite limitations are inherent in it. Some trees, during long periods of extremely slow growth, have added only one-half an inch of new wood in 100 years. Such intervals are difficult to date because the component rings are only a few cells in width. Resolution of individual rings is poor, and cross dating is almost impossible. It is also difficult to cross date samples in which numerous rings are locally absent. These problems can be partly overcome by sampling sectors of relatively rapid growth within a specimen and by cross dating the samples in intervals of maximum growth rate.

The dating procedure did not include the actual measurement of ring width in wood samples. The razor-cut surface of the mounted sample core, daubed with turpentine, was first scanned under low magnification for distinctive ring patterns of known age. Because the main objective was the dating of the specimen itself rather than the study of its growth record, the older part of a sample or the oldest sample from a given speci-

Digitized by Google

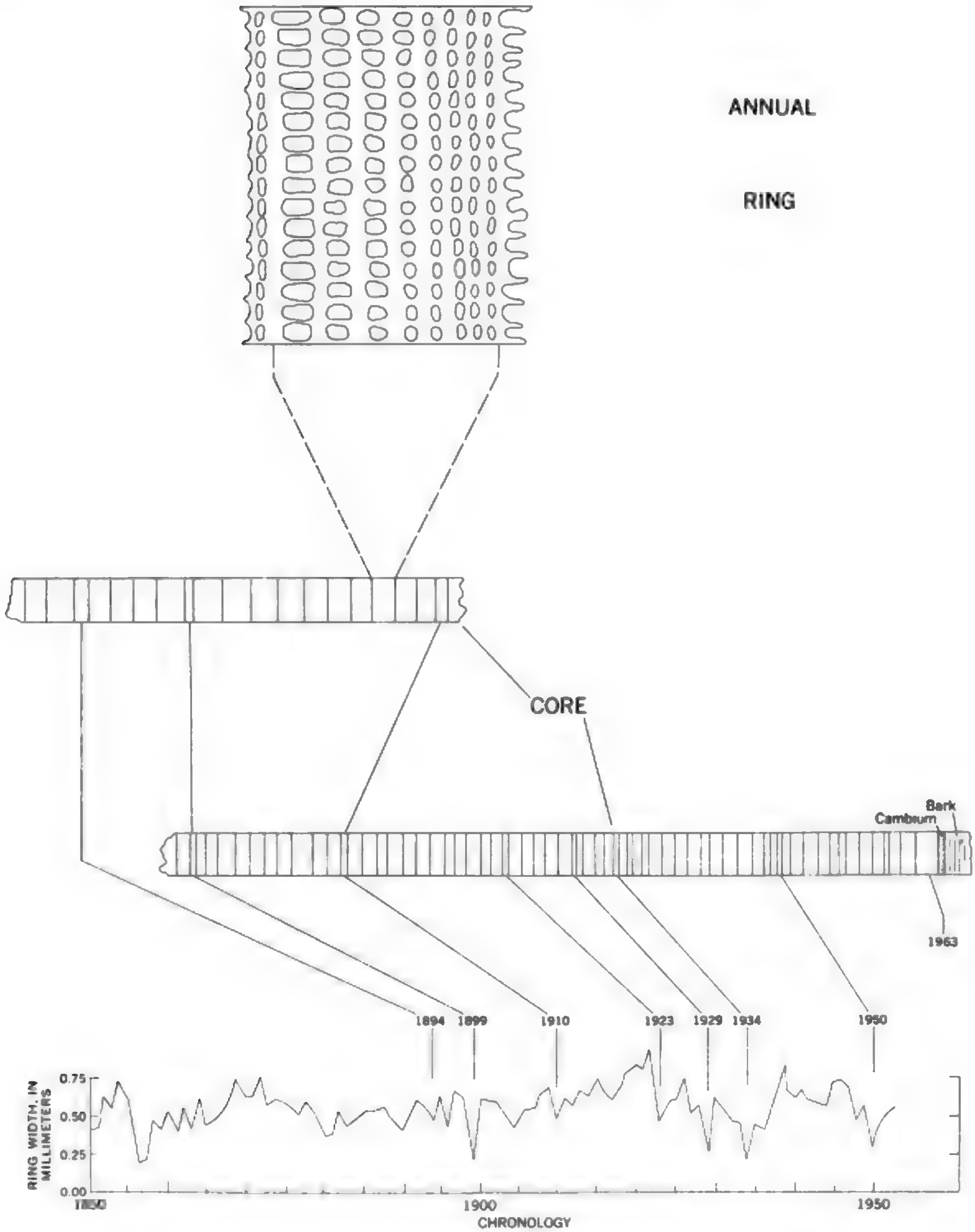

FIGURE 239.—Cross dating between portions of two cores, and chronology with diagrammatic enlargement of transverse section through annual ring. Chronology for White Mountains after Schulman (1956, p. 52).

Digitized by Google

men, was studied first. If no obvious correlation was possible and if the sample included the outermost ring of a living tree, the sample was approximately dated by ring count. Frequently this led to the recognition of cross-dating sequences in which one or more rings are microscopic or locally absent. If not such outer control were present, as with samples from dead trees or logs, a skeleton plot was made showing the relative spacing of narrow rings (Glock, 1937, p. 17). By comparing the skeleton plot with similar plots made from dated samples, or with the chronology, cross dates were often obtained. Wood samples from nearly 200 specimens with an average age of over 1,000 years were dated by these methods.

AGE ESTIMATE

Weathering, erosion, and decay have destroyed the older wood of the stems and roots of many of the bristlecone pines. Therefore, determination of specimen age requires an estimate of the timespan represented by the missing wood as well as the dating of that wood which is still sound. This estimate is based on the probable amount of radial growth missing and on the inferred average growth rate during the period.

The original center of secondary growth (stem or root axis) can be approximately located by inspection of the remaining wood. In the old trees with greatly reduced ratio of cambial area to total circumference, the growth layers formed after initial cambial reduction are not continuous and are not concentric about the axis. However, as shown by well-preserved specimens, even these trees grew at a normal rate during an early period of up to several hundred years, forming an inner core 3–12 inches in diameter. Where portions of this early wood are preserved, the stem or root axis can be located at the intersection of projected branches or branch rootlets or at the intersection of the radii of curvature of concentric rings (fig. 240). Thus, the approximate distance from the end of radially directed increment core to the axis can be estimated.

Also, the average growth rate during the period represented by the missing wood is a source of uncertainty in the age estimate. Samples of sound wood show that most of the trees have an early period of relatively rapid diametral growth. For example, along one radius at a height of 4 feet, the main stem of a 3,000-year-old specimen added 3 inches of wood in the first 40 years of growth, but only 9 more inches in the succeeding 800-year period. However, this is an unusually rapid growth-rate decrease. The growth rate shown by the wood in the inner 1 or 2 inches of a sample was generally used to estimate the timespan represented by the missing wood near the axis.

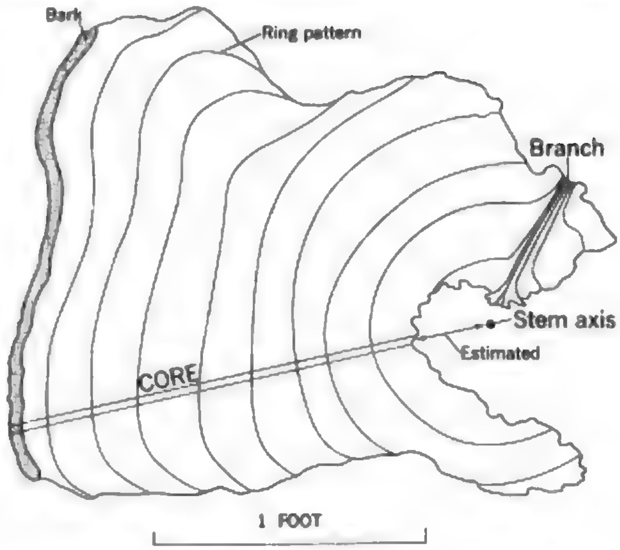

FIGURE 240.—Transverse section of eroded stem showing the geometrical basis for age estimation. The pattern of growth layers results from reduction of the ratio of cambial to total circumference. An early period of concentric diametral growth is indicated by the form of the inner rings. Many exposed roots show the same general features.

The estimated uncertainty in the age assigned to each specimen used in the study is given in tables 2, 3, 4, and 5; it averages about 5 percent of the determined age and is greatest for very old trees with large amounts of wood missing. The uncertainty in the age determinations is comparable in magnitude to the uncertainties in the other measured quantities used in this work.

ROOT EXPOSURE AND SLOPE DEGRADATION

Exposed roots are direct evidence of degradation; unless a tree is overturned, its roots can become exposed only through removal of the enclosing soil. However, this evidence has been little used to investigate degradational rates except where wind erosion is involved. Seybold (1930) described the exposure of pine roots to a depth of 5 feet in 80 years by shifting of dune sand in Holland; Hueck (1951) used the exposure of the root systems of shrubs to estimate rates of aeolian denudation in Patagonia. Deep root exposure is rarely seen on slopes degraded by mass-wasting and through erosion by surface runoff. Degradation proceeds too slowly to cause significant lowering of the ground surface within the relatively short lifetimes of most trees. The uncovering and exposing of root systems, however, affects trees of several species in the White Mountains, including a 1,000-year-old limber pine and a 1,700-year-old juniper (*Juniperus* sp.), as well as the old bristlecone pines. Root exposure is the direct consequence of shallow root development and the great age of these trees.

269-085 O-67-3

Digitized by Google

ROOT SYSTEMS

Bristlecone-pine roots can be seen in excavations and on overturned trees as well as exposed along the ground surface in the White Mountains. The root systems of mature trees are extensive but shallow. Mapping of roots exposed on the wall of a pit showed that more than 75 percent are concentrated in the uppermost foot of soil (Harold C. Fritts, written commun., 1965). Small roots penetrate to depths of several feet, but vertical taproot development is rare. In common with trees in other areas (Stout, 1956), rapid longitudinal growth apparently takes place early in the life of a bristlecone pine. Several major roots extend outward from a center at the base of the stem. Individual roots are largest at the stem junction, and most taper to a diameter of less than an inch within 10 feet; but some sparsely branched roots were seen that extend 20 feet or more with little change in size. The root systems of trees growing in coarse rubble or rooted in bedrock fractures are less regular.

The close relationship of growing roots to the overlying ground surface is also demonstrated by exposed root systems that parallel the profile of the topography that existed at the time of root development. Where individual roots crossed preexisting topographic irregularities, such as those along ridge crests or at the edges of cliffs and steep banks, the exposed roots retain the original irregular form. Conversely, where local relief has developed on a previously smooth slope, as adjacent to trees with asymmetrically exposed root systems (described below), the root system shows the original planar form.

EFFECTS OF EXPOSURE

The roots of woody plants grow in two ways—longitudinal extension by activity of the apical meristem is soon followed by secondary growth around the primary axis through the addition of successive layers of secondary xylem by the cambium (Esau, 1953). Only the terminal parts of the young branch rootlets absorb soil water. The sheaths of secondary wood that make up most of a mature root serve first for conduction of fluid and later as supporting tissue. The structure of mature roots is thus very similar to that of the stems and branches.

Uncovering of a trunk root near the stem of a bristlecone pine apparently has little immediate effect; however the terminal, water-absorbing parts of the root system function only within the soil: they die when exposed, as can be seen along roadcuts and in excavations. Many of the naturally exposed roots dealt with in this study are also dead. The roots on the downhill side of a tree are uncovered more rapidly and more completely than those projecting uphill or to one side. Many of the root systems in this downhill sector have not survived exposure.

BUTTRESS ROOTS

The development of a buttress form by individual lateral roots is a direct result of exposure (LaMarche, 1963). These roots are high but relatively narrow in transverse section. A buttress root is bark covered only on the bottom and owes its asymmetrical form to secondary growth radially downward from the root axis. Only the narrow strip of bark along the base, with its underlying cambium and conductive tissue, connects vertical or inclined branch roots with the stem. Initial reduction of the cambial area follows the uncovering of the upper surface of the root. Continuous concentric growth rings can be seen around the axis of a well-preserved buttress root, but the growth layers that formed after cambial reduction are limited to the lower side of the root and terminate at the sides. This discontinuity in the form of the growth layers marks the approximate time of the initial root exposure.

All stages of buttress root development are seen. The degree of asymmetry depends on the diameter of the root when it is first exposed and on the period of time since its initial exposure, as well as on the average growth rate. Uncovering of a shallow root normally takes place several hundred years after longitudinal growth. This interval is the time required for the removal of the overlying soil and is related to the original depth of root development and to the local degradational rate. Rapid diametral growth is also a factor in early exposure of the upper surface of a root. The buttress form can be developed only by living roots; the roots of trees that died before exposure do not show this feature (fig. 241).

Uncovering of roots is not a recent phenomenon in the White Mountains, as is shown by the existence of buttress roots of different ages, stages of development, and depths of exposure. Root exposure and buttress root development have been regularly associated with increasing tree age during at least the past 3,000 years, as it will be shown subsequently.

PROBLEMS OF MEASUREMENT

CHOICE OF DATUM

Only the axis, or center of radial growth, of an exposed root can be validly used to estimate the position of the ground surface as it existed at the time of root development. The top of a very shallow root may be uncovered simply as the result of increase in diameter with time. Although most developing roots are buried to a certain depth in soil that must be removed before the roots are uncovered, this depth is not known for exposed roots. For any exposed root, all that is known is

igitized by Googl

FIGURE 241.—Stump of 350-year-old bristlecone pine that died about A.D. 1350. Many such standing snags in the Reed Flat area have been cut for poles. Lack of buttress root development shows that root exposure has occurred since the tree died.

that its axis developed within the soil and that the position of the root axis marks the minimum possible level of the original surface.

The depth of root exposure is the vertical distance from the root axis to the underlying ground surface (fig. 242). Use of an arbitrary figure representing the assumed initial depth of burial might improve the estimate of local slope degradation for a single tree, but this may be unnecessary in an area where a large number of trees are studied. As shown in a subsequent section entitled "Degradational Rates," data based on measurements of the depth of root exposure can be extrapolated to estimate the average depth of root development. In two separate areas this depth is shown to have been about one-half a foot, remarkably similar to observed depths of concentration of rootlets.

The point of inflection of the basal flare of a tree (fig. 242C) is commonly misidentified as representing the original ground level at which root exposure occurred. This impression may be fortified by a pronounced change in the character of the wood or bark at this point. However, this typical feature of mature forest trees bears no relation to degradation. Clearly the inflection point will migrate upward with respect to even a static ground surface as a consequence of increasing stem and root diameter. If the inflection point is mistakenly used as the datum for measuring degradation, the degradational rates will be overestimated (fig. 243).

ASYMMETRICAL EXPOSURE

Asymmetrical root exposure causes large discrepancies between maximum depths of root exposure and actual slope degradation. The root systems of most bristlecone pines on debris-mantled slopes have not been uniformly around each tree. Typically (fig. 244), there

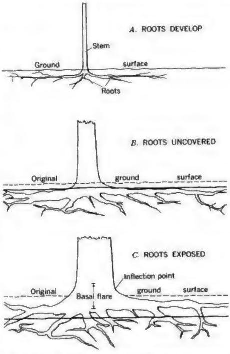

FIGURE 242.—Stages in development and exposure of a root system.

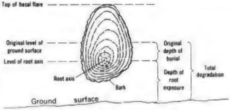

FIGURE 243.—Cross section of exposed root near stem showing relation of root exposure to degradation.

Digitized by Google

exists a gently sloping terrace on the uphill side of an old tree, and a concave hollow on the downhill side. Correspondingly, the roots upslope from the stem may be little exposed or may be buried, whereas those on the downslope side are deeply exposed. The ground surface may drop 6 feet in a horizontal distance of only 3 feet where the surrounding slope is at an angle of 35° or less. As shown by the data in table 4, the maximum depth of root exposure is commonly three to four times greater than the slope degradation.

The prominent topographic discontinuity is caused by the damming effect of the trees and develops where the stem and roots impede the downslope movement of surficial rock debris. Material accumulates above the barrier, forming the terrace. The hollow results from the net removal of surficial debris downslope from the tree, and in many places bedrock is exposed in the hollow. Microrelief features and the orientation of pebbles in the surficial mantle show that the downslope flow lines are divided in the vicinity of such an obstruction and that material moving downslope passes on either side of the tree. Such topographic changes are not associated with deep root exposure in two situations: (1) where the root system extends only upslope or downslope, the exposed roots do not interfere with debris movement (fig. 245), and (2) where the roots of a tree growing on a ridge crest extend down opposite slopes subparallel to the directions of movement and show correspondingly symmetrical exposure (fig. 246).

FIGURE 245.—Root system symmetrically exposed because roots extended directly upslope. Centers of roots are alined parallel to slope but lie about 2 feet above surface—a measure of degradation subsequent to establishment of tree.

FIGURE 244.—Terrace and hollow due to damming effect of old tree. Maximum depth of root exposure is about 4 feet. Note rock fragments spilling over top of root at stem base.

FIGURE 246.—Root system exposed symmetrically because of location on ridge crest. Roots extend down opposite slopes subparallel to directions of movement of rock debris; damming effect is further reduced because volume of debris is small.

Digitized by Google

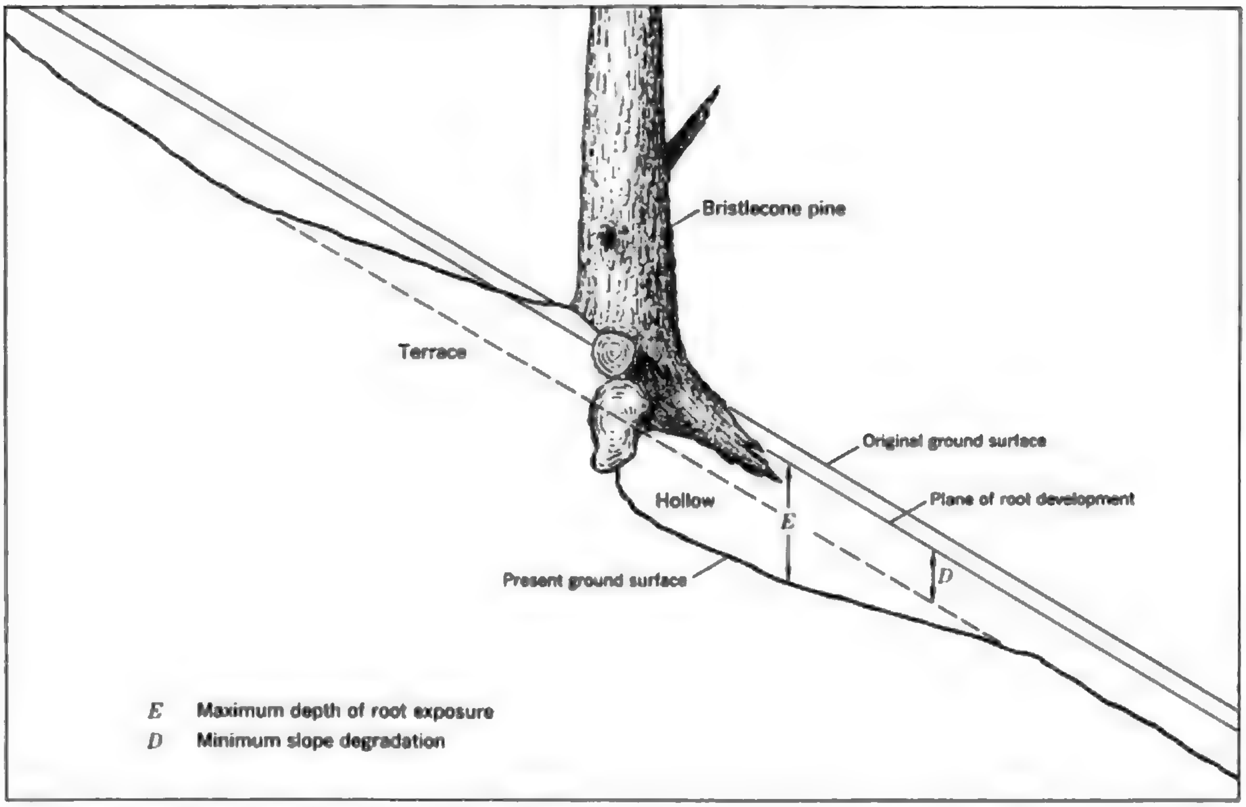

FIGURE 247.—Slope profile in the vicinity of a tree with asymmetrically exposed roots. Shows terrace and hollow, approximate location of original ground surface, and basis for measurement of minimum slope degradation.

Asymmetrically exposed root systems also can be used to estimate slope degradation if the surrounding slope is smooth and regular. In a study of two selected areas, a downslope profile at a scale of 1 inch equals 10 feet was made in the vicinity of each tree having an asymmetrically exposed root system associated with terrace and hollow development. Figure 247 shows that a line passing through the axis of the highest exposed roots lies above, but is parallel to, the line formed by projection of the present surface from points above and below the tree. The vertical distance (D) between the two lines approximates the minimum slope degradation (it does not include the original depth of burial) in the vicinity of the tree since the development of the root system. The vertical distance (E) between the root axis and the underlying ground surface is the maximum depth of root exposure. This depth is always found in the hollow on the downslope side and is always greater than the overall depth of degradation.

CALCULATION OF DEGRADATIONAL RATES

The study of an individual tree and its exposed roots can yield the maximum depth of root exposure and the period of time since the tree's initial root development. A rate of exposure calculated from these data generally will not be equal to the local rate of degradation during the same period. One source of error is the uncertainty as to the original depth of root development, for the vertical distance from the axis of an exposed root to the present ground surface is only a minimum estimate of the total depth of material removed. This error is fairly large for young trees that have only incipient root exposure; the calculated rate of root exposure will be less than the actual rate of degradation. Where the root systems of trees growing on slopes have been asymmetrically exposed, the maximum depth of exposure may be much greater than the actual slope degradation. The increase in degree of asymmetry with size and age of tree introduces a large discrepancy between local degradational rates and the maximum rates of root exposure of many older trees. However, the study of individual old trees will give rates of root exposure that approximate degradational rates if the root exposure has been symmetrical and if the axes of the highest exposed roots are used. An improved estimate of the local degradational rate, as

Digitized by Google

indicated by the depth of root exposure of a single tree, can also be obtained, if the initial depth of root development can be inferred.

DEGRADATIONAL RATES

LOCAL RATES

Evidence of the progressive change in ground-surface altitude provided by the exposed roots of bristlecone pines was used to estimate rates of degradation in areas underlain by the Reed Dolomite. The problems of measurement and interpretation initially met with led to the refinement of methods used during the rest of the investigation. Early work was concentrated in 1-square-mile area near Reed Flat (fig. 235). Attention was focused on trees with deeply exposed roots and on those occupying special topographic sites.

Either a direct determination of root age or an estimate based on stem age was made for each tree. In 1962, 99 trees were sampled in the Reed Flat area and elsewhere in the White Mountains; some of the specimens were not dated, and some are on other substrates and are not included in the results. The age determination, depth of root exposure, and local slope of the ground surface are listed in table 2 for each of the specimens, and the results are graphically summarized in figure 248. The measured depths of root exposure range from 0 to 4.5 feet, and the estimated ages, from about 200 to 2,500 years. A general increase in the maximum depth of exposure with increasing age can be

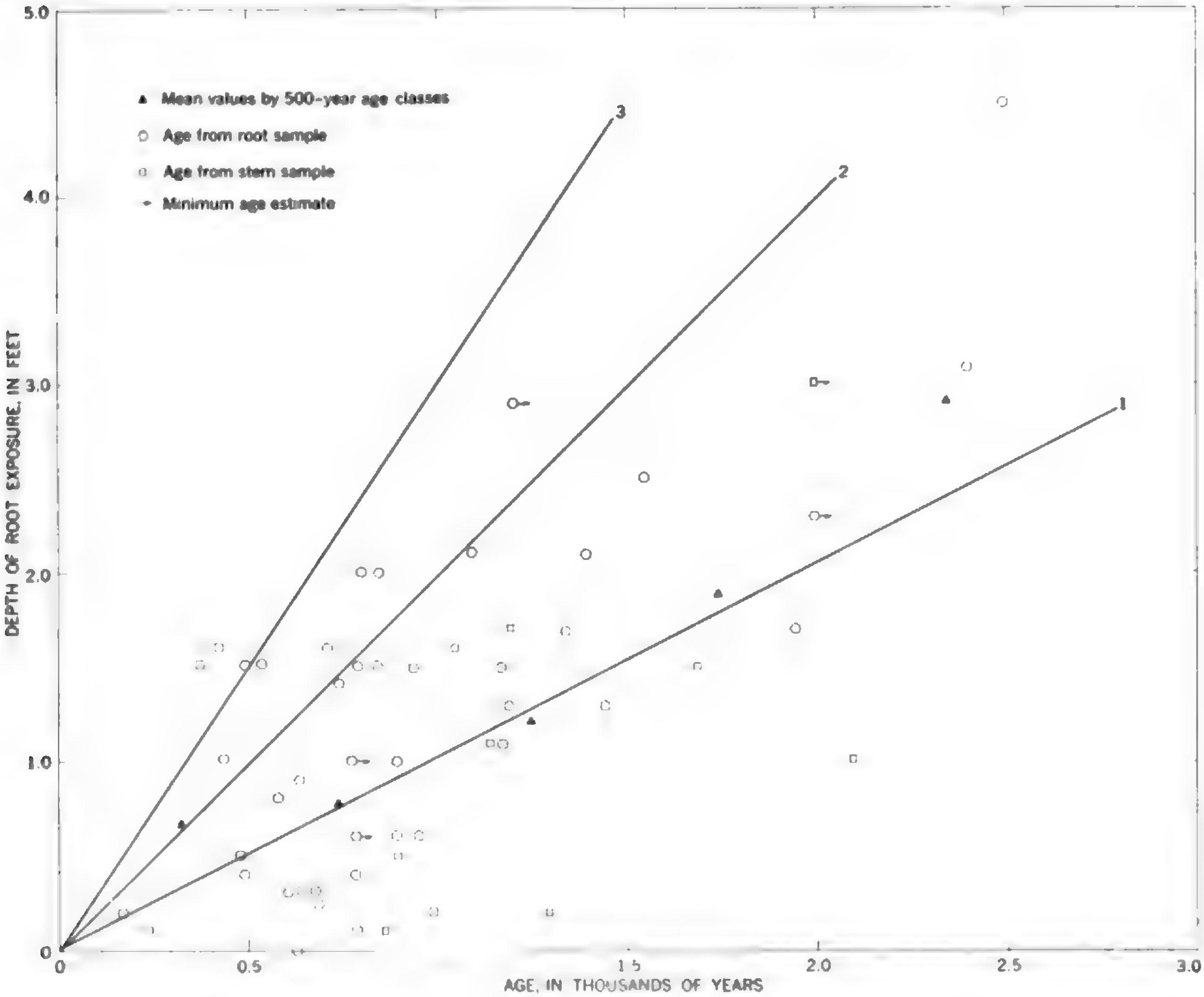

FIGURE 248.—Relation of root exposure to age and probable range of local degradational rates.

seen, but there are great differences in the rates of root exposure indicated by these data. The differences reflect not only different local rates of degradation, but also the effects of differences in the symmetry of exposure and in the original depth of root development.

TABLE 2.—*Age, root exposure, and site data for trees in scattered localities in southern White Mountains*

Specimen	Age estimate (centuries)		Depth of root exposure (feet)	Slope (degrees)
	Age	Uncertainty		
Root age from root sample				
1	9.0	0.6	1.0	33
2	2.8	.1	1.5	28
3	11.7	.1	1.5	12
	12.1	.3	1.7	12
	14.0	.3	2.1	[illegible]
	14.5	.2	1.3	12
	15.5	.6	2.5	12
5	7.5	.5	1.4	26
6	[1] 12.1+	...	2.9	32
7	6.2	.1	.3	26
	6.2	.1	.3	28
9	25.0	2.0	4.5	36
11	10.0	1.5	.2	2
12	8.5	.3	2.0	24
	4.4	.1	1.6	24
13	5.3	.1	1.5	17
14	2.5	.2	.1	8
15	[1] 8.0+	...	1.0	40
17	8.1	[illegible]	2.0	[illegible]
19	8.5	.4	1.5	26
20	13.5	1.0	1.7	20
22	[illegible]	.2	.5	14
23	12.0	2.0	1.3	25
24	2.0	.1	.2	32
57	9.5	1.0	1.5	26
58	[1] 8.0+	...	.5	10
61	6.5	.5	.3	8
62	[illegible]	.2	.4	9
63	6.4	0	.9	16
64	11.9	.1	1.1	30
67	9.0	.5	.6	15
68	[2] 7.1	.1	1.6	28
	[2] 7.8	0	1.5	26
69	4.5	1.0	1.0	19
71	[3] 9.5	1.0	.6	30
73	6.0	.2	.8	21
74	7.0	.1	.3	30
75	[illegible]	.3	0	6
	8.0	.5	.1	6
78	5.0	.2	.4	9
79	7.0	.4	.2	9
80	19.5	1.0	1.7	31
81	[3] 20.0+	...	2.3	24
84	5.0	.3	1.5	16
91	[illegible]	2.0	3.1	23
97	[1] 11.0	...	2.1	36
Tree age from stem sample				
21	1.8	0	...	17
51	8.8	0	0.1	5
59	13.0	.5	.2	8
60	6.5	1.0	...	10
65	11.5	.1	1.1	22
70	21.0	1.0	1.0	20
76	17.0	1.0	1.5	16
95	[3] 20.0+	...	3.0	30
96	9.2	0	1.5	23
98	12.0	.2	1.7	30
99	[2] 10.5	.3	1.6	25

[1] Sample incomplete.
[2] Dead tree. Age based on cross dating.
[3] Dead tree. Minimum-age estimate equals total number of rings counted.

SLOPE TRANSECT

The possible effects of topographic position on root exposure were studied in trees along a line that extends directly up a north-facing slope from the base of the knoll east of Reed Flat to the crest of the adjacent ridge. Each standing tree within 5 feet of the line was sampled for an age determination, and the depth of root exposure was observed; the results are listed in table 3. The slope profile, tree ages, and root exposure are shown graphically in figure 249.

TABLE 3.—*Age, root exposure, and site data for trees on slope transect, listed in order of increasing distance from base of slope*

[Ages based on stem samples]

Specimen	Age estimate (centuries)		Depth of root exposure (feet)	Slope (degrees)
	Age	Uncertainty		
28	4.0	...	([1])	7
29	1.9	...	...	11
30	.8	...	...	3
31	6.2	...	...	10
32	1.5	...	...	15
33	1.9	...	...	18
34	.5	...	...	25
35	2.0	...	...	28
36	10.2	0.1	0.3	28
37	5.5	.3	...	30
38	7.5	.5	...	22
39	6.5	.4	.3	29
40	1.9	...	...	31
41	6.5	1.5	.1	32
42	5.5	.2	...	26
43	6.0	.5	.6	24
44	7.0	.1	.4	26
45	[2] 15.0+	...	...	26
46	12.5	.5	...	34
47	10.5	.4	.9	33
48	6.1	.2	.8	30
50	14.0	2.0	...	28
52	9.0	.2	.2	26
53	10.0	.5	1.4	25
54	17.0	1.0	...	29
55	7.0	.4	.1	18
56	[illegible]	.3	.1	16

[1] Indicates no roots exposed.
[2] Dead tree. Minimum age equals total number of rings counted.

The lower part of the slope, extending about 500 feet to the base of the main slope, is gently rolling; the average slope is about 10°. The line of profile crosses two depressions marking incised channels. The trees in this area are widely spaced, and the ground cover is relatively dense. The main slope, rising 300 feet in a horizontal distance of 500 feet, has a nearly linear profile with a slope of 30°. The surface of the ground is smooth, but the coarse soil is loose and readily dislodged. Litter, including the stems of fallen trees, is abundant. The upper slope is distinctively convex in profile. Its ground surface is much rougher than that of the main slope below. Numerous outcrops and small cliffs protrude through the thin patchy veneer of surficial debris.

A striking relationship between tree age and location is shown in figure 249. The 6 trees on the lower slope have a mean age of 220 years; the 10 trees on the main slope, 520 years; and the 11 trees on the rocky upper slope, near the ridge crest, more than 1,000 years.

Comparison of tree age with depth of exposure shows that the roots of trees less than 500 years old have not yet been exposed, owing to either slow degradation or to

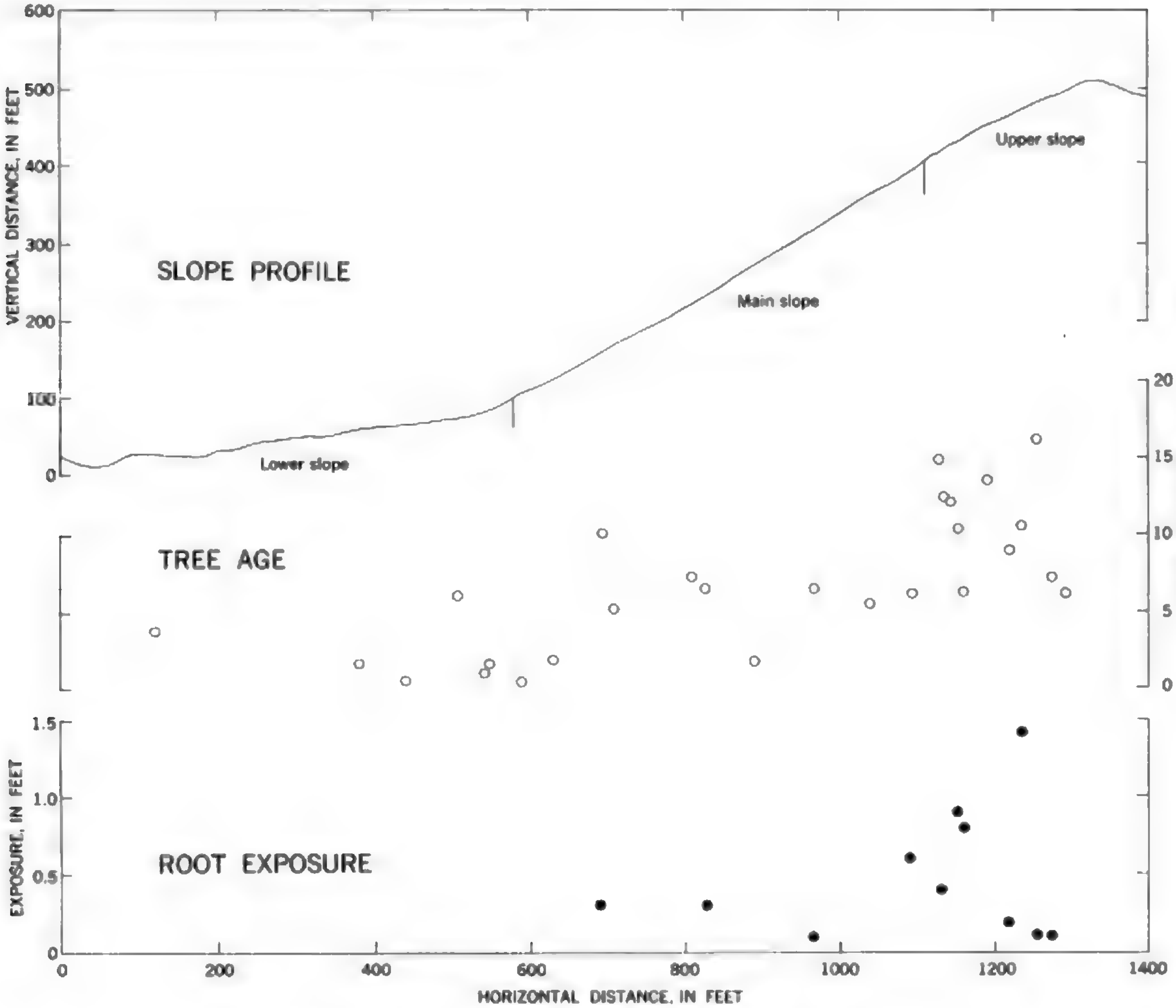

FIGURE 249.—Slope profile, tree age, and depth of root exposure along slope transect.

great depth of development. Incipient exposure, where the roots on the downhill side are partly uncovered, is characteristic of trees in the 500- to 1,000-year age range. Only the fairly old trees have deeply exposed roots; however, the oldest trees do not show the greatest exposure. Roots of two of the oldest trees, 1,400 and 1,700 years old, respectively, are not now exposed. These specimens, which are in the area of irregular topography immediately below the ridge crest, have been partly buried by lobate rock streams.

Although local rates of degradation, suggested by the depth and symmetry of root exposure, are apparently greatest on the upper slope, the conclusions that can be drawn from observation of an individual specimen are valid only for the limited area around that tree. Further, the restricted distribution of trees old enough to show significant root exposure precludes strict comparison of degradational rates at different points along the transect. The average rate of degradation on this slope is probably less than half a foot per 1,000 years.

SELECTED AREAS

The initial reconnaissance study of individual bristlecone pines showed that deep root exposure is generally associated with great age. It suggested that the rate of exposure is proportional to the local degradational rate but also depends on the depth of root development and the degree of symmetry of exposure. The great range in rates of exposure seems to be related to differences in degradational rates in different parts of the landscape.

Digitized by Google

Inconsistencies in the results of study of nearby trees showed, however, that bias in specimen choice could lead to results that are not representative of an area much larger than that included within the root system of a single tree.

The purposes of the second phase of the study were to convert measurements of root exposure to estimates of slope degradation, to characterize local topographic environment closely, and to obtain unbiased samples of the trees in selected areas as a basis for generalization of the results. The approach used included the large-scale planetable mapping of two areas that represent contrasting slope types. The maps (plates 10 and 11) show the general outlines of exposed roots and of fallen trees, in addition to the topography. All the standing trees in one area and a large random sample in the other were studied. Each of the areas was selected because it has old bristlecone pines; the average age of 71 trees in the two areas is 1,100 years.

A third area, significant because it is incised by closely spaced drainage channels, was mapped at a smaller scale. The exposed root systems of six trees on low steeply sloping interfluvial ridges were mapped in great detail. These specimens were selected because they have deeply exposed roots; the trees have a mean age of 1,450 years.

AREA 1

This area of about 2 acres is one-half a mile northwest of Blanco Mountain (fig. 235) and lies at an altitude of 10,500 feet. It is the west end of a hill of Reed Dolomite that rises abruptly from a gentle sagebrush-covered slope (fig. 250). A broad swale at the base of the hill slopes to the south, where it deepens and contains a first-order drainage channel. The center of this topographic depression is also marked by a strong contrast in both vegetation and soils: on one side of the depression is the dolomite slope with its sparse ground cover and scattered bristlecone pines, whereas on the other side is an unforested flat whose soil is composed of sandstone and shale from the slopes of County Line Hill, to the west.

FIGURE 250.—Area 1, as viewed from the west. Blanco Mountain is in background. Note abrupt change in type of soil and vegetation at base of triangular slope.

The mapped area (pl. 10) includes the western slope of the hill and a broad north-sloping shoulder. The linear rocky crest is 100 feet above the base of the slope. Below the irregular cliffs along the crestline, the slope has a fairly smooth concave profile and an average slope of 20°. The ground surface of the hillcrest and of the subsidiary spurs is dolomite bedrock that has local accumulations of coarse rubble. Rock outcrops are numerous, and the mantle is thin over large areas of the shoulder and the upper slopes. The mantle is thicker and more continuous on the lower slopes.

The mantle is fairly coarse textured and contains pebble- to cobble-sized angular dolomite fragments. The average surface-particle size, measured along each of four downslope transects, ranges from 14 mm, on a 10° slope on the shoulder in the northern part of the area, to 33 mm, on a 22° slope extending down from the main hillcrest (fig. 251). There is an irregular decrease of grain size in the swale at the base of the slope, where the soil is a dolomitic sandy loam with few pebbles.

The surface of the debris mantle on the slopes is uneven. The steeper part of the west-facing slope has poorly sorted stone-banked terraces, presumably related to frost action, but there are no miniature patterned-ground features. Terrace and hollow development is locally prominent adjacent to standing trees and to some of the large wood fragments that litter the slopes.

Three main groups of bristlecone pines can be distinguished. One group grows on the north-facing slope on the shoulder of the hill; the second group grows on the west-facing slope; and the third group, which includes the oldest trees in the area, grows on or immediately below the cliffs west of the hillcrest. There are 49 standing trees in the area mapped. Stem core samples were taken from all specimens, and dating provided at least a minimum age estimate for all but four trees. The trees range in age from about 10 to 2,700 years and average nearly 1,000 years.

The root systems of most of the trees are uncovered or are at least partly exposed. The deep symmetrical exposure of the roots of trees along the hillcrest (fig. 252) is especially striking. The minimum local slope deg-

Digitized by Google

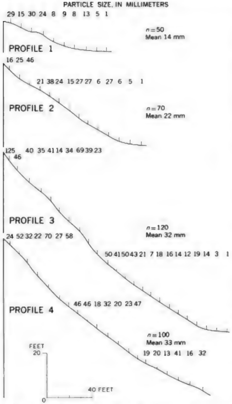

FIGURE 251.—Slope profiles and results of particle-size measurements. Each number represents mean of five measurements of intermediate dimension of rock fragments made at 2-foot intervals along line.

radation represented by the root exposure was measured directly where root systems were symmetrically exposed. It was obtained from the individually constructed downslope profiles for those specimens showing asymmetrical exposure. These data, together with age determinations, are listed in table 4.

The minimum local slope degradation is plotted against specimen age in figure 253. The points are scattered around a straight line representing a slope of 1.2 feet per thousand years, the average degradational rate. The extrapolated average depth of exposure at zero age, based on a least-squares analysis of data from 33 specimens, is one-half foot and represents the average initial depth of development of the roots. The

FIGURE 252.—Exposed root of specimen 110. Depth of root exposure shown by comparison with 18-inch hammer. Exposed bedrock is broken up. Note symmetrical exposure of root of this 2,500-year-old tree.

analysis did not include data from 10 younger trees with no root exposure nor data from 6 specimens which were not reliably dated. Even though the trees are not distributed uniformly over the entire area, the results are thought to be representative of at least the crest and the upper slope areas.

TABLE 4.—*Data for trees in two selected areas*

[Ages from stem samples]

Specimen	Age data (centuries)		*E* Maximum depth of root exposure (feet)	*D* Minimum local slope degradation (feet)
	Age	Uncertainty		
		Area 1		
101	[1] 13.0+	....	1.6	1.4
102	8.5	0.2	1.2	.7
103	4.8	.1	.4	.1
104	7.4	.1	1.2	.4
105	(2)	....	1.8	1.8
106	18.7	.5	2.0	1.5
107	8.1	.2	.8	.4
108	3.7	.1	.8	0
109	6.5	.2	.1	0
110	25.0	2.0	3.2	3.0
111	27.0	2.0	3.2	3.2
112	7.6	.1	.8	.6
113	7.6	.1	.6	.3
114	9.5	1.0	.8	.7
115	7.5	.3	.4	−.1
116	7.0	.2	.5	0
117	4.5	.4	(3)	....
118	4.5	.3	(3)	....
119	7.5	.1	.8	0
120	4.8	.2	.9	.5

See footnotes at end of table.

TABLE 4.—*Data for trees in two selected areas*—Continued

[Ages from stem samples]

Specimen	Age data (centuries)		*E* Maximum depth of root exposure (feet)	*D* Minimum local slope degradation (feet)
	Age	Uncertainty		
Area 1—Continued				
121	1.0	.0	[3]	
122	20.0	1.0	1.7	1.7
123	21.0	1.0	.6	.6
124	[illegible]	2.0	.6	.5
125	18.0	2.0	1.0	1.0
126	[1] 9.0+		1.0	1.0
127	20.0	3.0	2.6	[illegible]
128	16.5	2.0	1.7	1.7
129	.1	0	[3]	
130	6.5	.6	.7	.7
131	7.0	.5	1.5	1.3
132	7.1	.1	.2	.2
133	[1] 22.5+		2.2	1.5
134	6.0	1.0	.8	.4
135	[2]		1.3	1.3
136	5.0	.5	.5	0
137	4.5	.3	.4	−.1
138	13.0	2.0	1.3	.9
139	.1	0	[3]	
140	9.0	3.0	2.2	1.3
141	.4	0	[3]	
142	5.0	.1	.6	.3
143	[2]		.5	.3
144	13.5	1.0	1.2	1.1
145	17.0	1.0	2.5	1.8
146	.6	0	[3]	
147	[2]		[3]	
148	.1	0	[3]	
149	.2	.1	[3]	
Area 2				
150	5.5	0.5	[3]	
151	5.0	.4	[3]	
152	5.5	.2	[3]	
153	2.5	.1	[3]	
154	17.0	2.0	3.6	0.7
155	4.0	.3	[3]	
156	[4] 20.0+		5.4	1.2
157	6.0	.3	.5	0
158	.8	0	[3]	
159	11.0	2.0	1.6	1.1
160	[1] 22.0+		[3]	
161	[illegible]	.5	1.8	.2
162	[illegible]	2.0	3.2	.4
163	31.0	1.0	[3]	
164	[4] 10.0+		4.0	1.3
165	30.0	3.0	5.4	1.7
166	3.1	.1	1.2	0
167	[1] 30.0	3.0	4.2	2.0
168	20.0	2.0	4.6	1.3
169	17.0	2.0	4.0	1.2
170	8.5	1.5	[3]	
171	18.0	2.0	4.6	1.2
172	10.6	.5	.8	.4
173	19.0	1.0	1.0	.5
174	7.5	.5	1.2	.1
175	[illegible]	2.0	2.0	1.1
176	[2]		.5	.2
177	1.4	0	[3]	

[1] Dead tree. Age based on cross dating.
[2] Age not determined.
[3] No exposed roots.
[4] Dead tree. Minimum age equals total ring count.

Systematic deviations from the average degradational rate might be expected owing to the topographic inhomogeneity of the area. Figure 254 shows the estimated rates of degradation, in feet per 1,000 years, at each sampling point. These values were obtained graphically from the scatter plot of tree age and minimum slope degradation (fig. 254). Through the point representing a given specimen, a line was drawn to the −0.5-foot mark on the ordinate (the approximate initial depth of root development). This line intersects the vertical line representing 1,000 years of elapsed time at some value, D, of minimum slope degradation. The vertical distance between this point and the −0.5-foot point represents the degradation taking place in 1,000 years at each point. Most of the values are within the range from 1.0 to 1.4 feet, regardless of specimen location. The highest values are at points along the rocky crest and upper slope; there is some suggestion of a downslope decrease in degradational rate on the west-facing slope. However, because the estimated degradational rates vary widely from point to point and because these variations are not clearly related to topographic position, the author has concluded that no significant trends in slope development can be inferred from these data.

AREA 2

Area 2 is a strip extending from a stream channel in a narrow alluvial flat to the crest of the adjacent ridge. This 1-acre area is representative of the steep side slopes of major canyons incised into the Reed Dolomite. It is 1 mile east of Reed Flat in a canyon tributary to the South Fork of Birch Creek (fig. 255). The narrow alluvial flat is at an altitude of about 9,700 feet. The crest, 350 feet above the base of the slope, is the end of a long dolomite ridge. There are no shrubs and only a few herbaceous ground cover plants on the slope. The only other vegetation is an open stand of old stunted bristlecone pines (fig. 256 and pl. 11). The canyon has a "V-in-V" cross profile in this area, and the lower slopes are about 5° steeper than those above. The slopes are nearly linear in cross profile except at the narrow rounded crest.

Coarse soil forms a continuous mantle over the lower two-thirds of the slope. Bedrock is locally exposed on the upper slope and almost continuously along the crest. The surface consists mainly of large angular dolomite fragments (fig. 257) which have been sorted into rock streams or less regular elongate patches of contrasting textures. No measurements of particle size were made, but the surface material is noticeably coarser than in area 1 and is very unstable.

The slope surface has moderate local relief. On the lower part of the slope, microrelief features apparently reflect differences in the thickness of the mantle rather than bedrock irregularities. Upslope terraces and downslope hollows have developed adjacent to many of the older bristlecone pines (fig. 244). The large maximum depths of root exposure (table 4) are related to this extreme asymmetry.

Digitized by Google

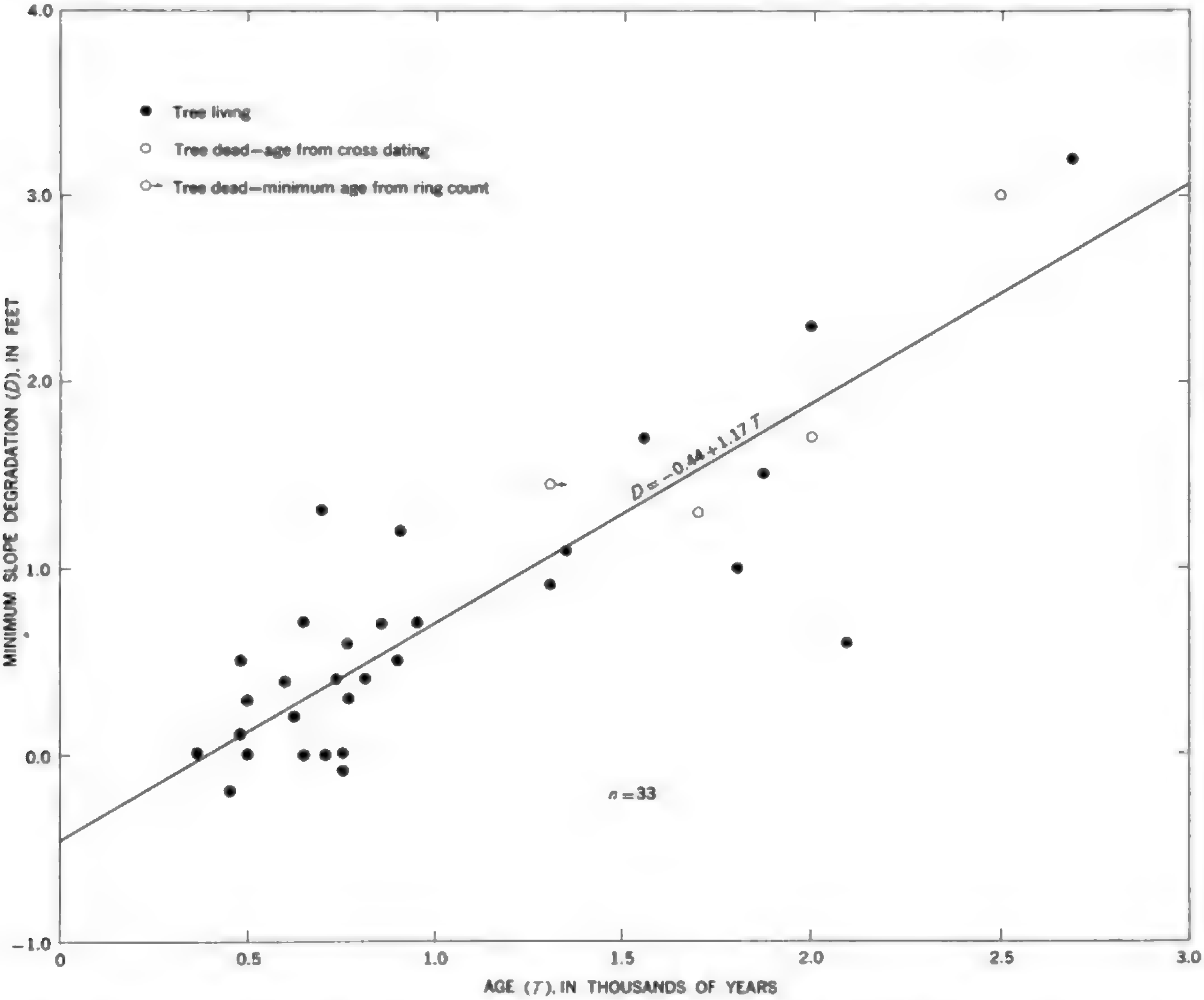

FIGURE 258.—Age and minimum slope degradation for area 1. Average age of 10 trees with no exposed roots is about 125 years. Line fitted by least squares gives average degradational rate of about 1.2 feet per 1,000 years; intercept with vertical axis at $T=0$ gives average depth of root development of about one-half foot.

All trees on the slope and the alluvial flat were included in the mapping. From a total of 80 standing trees, 28 (including 2 on the flat) were selected for detailed study by means of an overlay of randomly plotted points. A minimum-age estimate was obtained for 26 trees; they range from 80 to 3,100 years in age. Measurements of the maximum depth of root exposure, estimated local degradation, and estimated tree age are given in table 3.

The relation of local slope degradation to tree age is shown in figure 258; six trees with a mean age of only 380 years show no root exposure, and two are incompletely dated. A straight line fitted to the rest of the plotted points indicates an average degradational rate on the slope of about 0.8 foot per 1,000 years and an average depth of root development of one-half a foot.

The distribution of estimated values of local degradational rates was plotted and mapped for areas 2 and 3, which lie on opposite slopes of the same canyon (fig. 259). Most of the values for the local degradational rate at points in area 2 ranged from 0.5 to 1.0 foot per 1,000 years. Neither the crest nor the lower part of the slope are well represented by points, partly reflecting the actual distribution of old trees and partly owing to the random sampling method used. (Compare with fig. 256.) A stratified sampling procedure would have been a more effective method of study. Little evidence was found to suggest a systematic downslope change

Digitized by Google

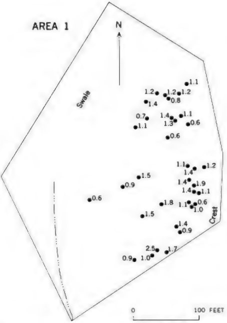

FIGURE 254.—Distribution of values of estimated local degradational rates, in feet per 1,000 years, in area 1.

FIGURE 255.—Valley tributary to the South Fork of Birch Creek. View is toward the south. Area 2 extends from channel in center of photograph up the light-colored slope to the ridge crest at left; area 3 is on lower part of opposite slope.

FIGURE 256.—Upper part of area 2. View is toward the southeast. Low density of trees and absence of ground cover are typical of stands of old bristlecone pines.

FIGURE 257.—Surficial mantle in area 2. Scale shown by 6-inch rule. Beneath surface, angular dolomitic rubble has matrix of finer soil.

Digitized by Google

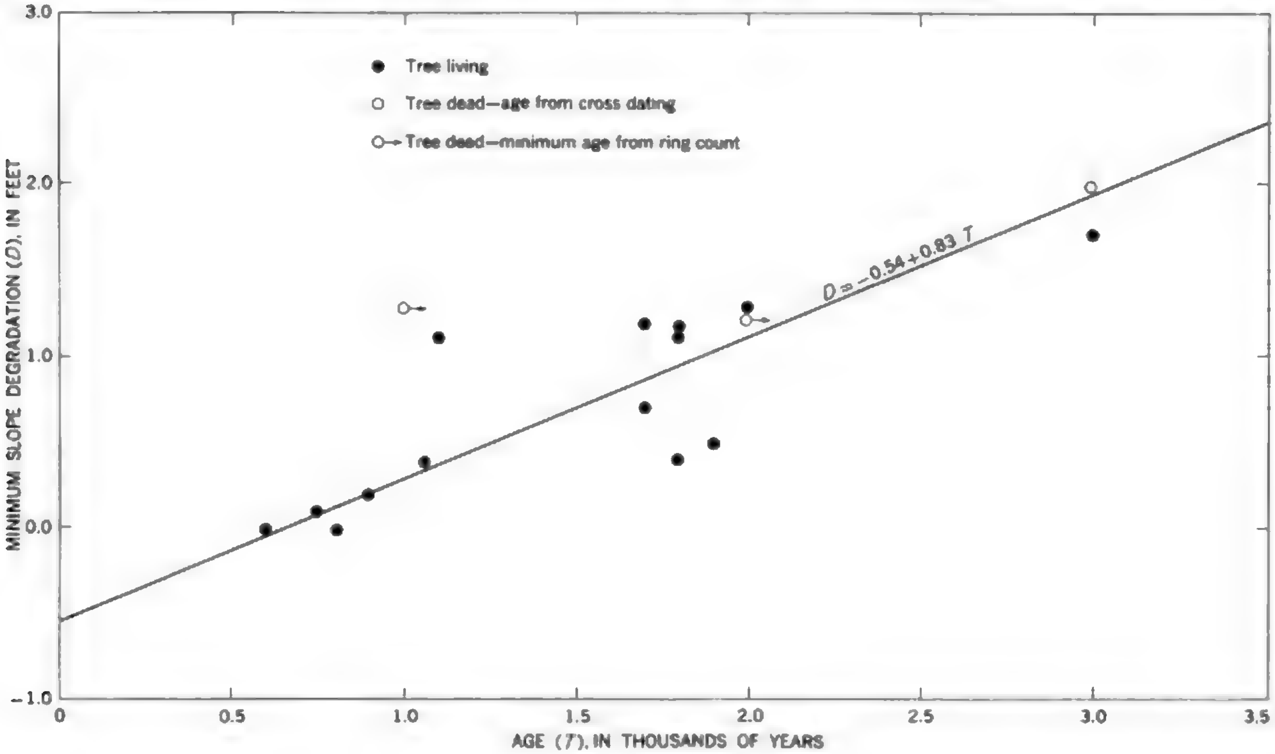

FIGURE 258.—Age and minimum slope degradation for area 2. Average age of six trees with no exposed roots is about 375 years; data for two trees on alluvial flat at base of slope are not included. Line fitted by least squares gives average degradational rate of about 0.8 foot per 1,000 years; intercept with vertical axis at $T=0$ gives average depth of root development of about one-half a foot.

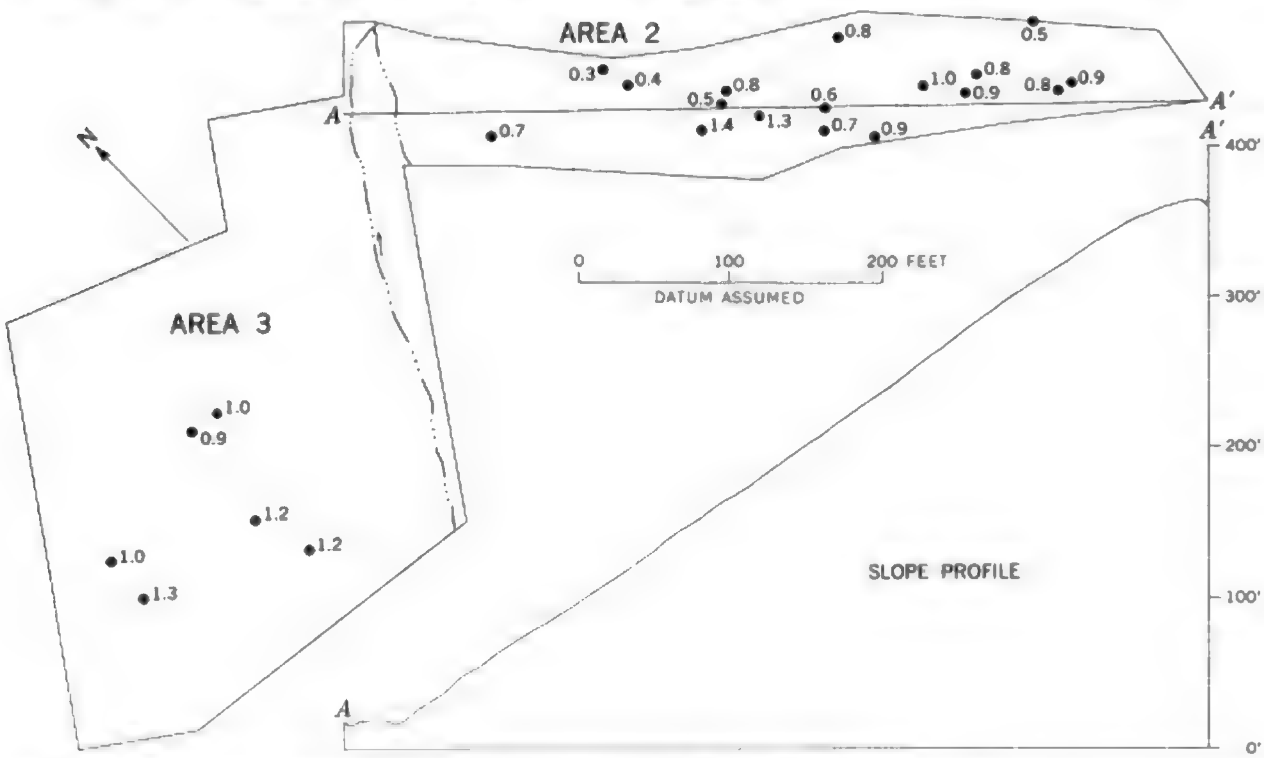

FIGURE 259.—Distribution of values of estimated local degradational rates, in feet per 1,000 years, in areas 2 and 3, and slope profile of area 2.

Digitized by Google

in degradational rate in the upper two-thirds of the area. Three specimens in the lower third give relatively low values of local degradational rates, perhaps indicating that the rates have been lowest in the lower part of the area, above the slightly oversteepened slope at the base.

AREA 3

Area 3 is distinctly different from those previously discussed. Although it is nearly opposite area 2, on the southeast-facing slope of the same canyon, area 3 does not have the same smooth to irregularly hummocked appearance. Instead, it appears to be corrugated because it is incised by steep straight drainage channels (fig. 260) in smoothly rounded miniature valleys. The channels head higher up on the slope, about 200 feet from the ridge crest. A map of a 2-acre area on the lower slope, with an average slope of 28°, is shown in figure 261.

Bristlecone pines and a sparse cover of shrubs and smaller plants grow on the slope. Some of the older trees growing on low, rounded interfluvial ridges show deep and extensive root exposure (fig. 262). The root systems of six of these trees, which range from 1,100 to 1,900 years in age (table 5), were mapped in detail (fig. 263), and the depth of root exposure was measured at many points on each. The average and maximum depths of exposure and the estimated ages are given in table 5.

FIGURE 260.—Part of area 3, viewed upslope. Shallow swales and rounded interfluvial ridges give slope a corrugated appearance. Trail in foreground.

TABLE 5.—*Age and root-exposure data for trees in area 3*

Specimen	Age data (centuries)		Root exposure		
	Age	Uncertainty	Number of measurements	Mean (ft)	Maximum (ft)
183	13.5	0.5	14	0.9	1.9
184	19.3	.3	14	1.3	2.5
185	11.0	2.0	9	.8	1.7
186	13.3	.5	16	1.1	2.3
187	13.0	1.0	17	1.2	2.4
188	17.5	.5	15	1.2	2.4

The exposed root systems generally parallel the present ground surface; thus, the valley-and-ridge topography must have existed as much as 1,900 years ago, when the root system of specimen 184 was developing. The symmetry of exposure, however, is different from that shown by trees on unchanneled slopes. The depth of exposure here varies radially from the base of the stem, reflecting the bilateral symmetry in the directions of movement of material away from the sloping miniature crest. The depth of exposure is least immediately upslope from the stem, where a narrow terrace exists; it is greatest on the downslope side. The results are summarized graphically in figure 264. For each specimen, the maximum depth of exposure is about twice the average depth of exposure, reflecting the asymmetry discussed above. The average depth of root exposure is a fair measure of the local degradation of the crest in the vicinity of each tree. As shown in figure 264, a trend line through paried values of age and average depth of exposure for these trees is flatter than one originating at zero time and zero exposure. This trend suggests that the degradation of this slope has not proceeded uniformly with time.

COMPARISON

Measurements of root exposure, minimum slope degradation, and elapsed time obtained by the same methods and based on comparable samples can be directly compared for areas 1 and 2. The results have previously been reduced to estimates of local degradational rates for each area (figs. 254, 259). The frequency distribution of this measure of degradational rate in the two areas is shown in figure 265. The modal value for area 1 is clearly greater than that for area 2, corresponding to the average degradational rates (obtained by least-squares analysis) of 1.2 and 0.8 feet per 1,000 years, respectively.

The rocky crestal areas and relatively short gentle slopes of area 1 are being degraded at a significantly greater rate than the long steep valley side slope represented by area 2. Confidence intervals can be computed (Wallis and Roberts, 1956) for the regression lines fitted to data from each area. In figure 266, the 95-percent confidence bands for the lines do not overlap

Digitized by Google

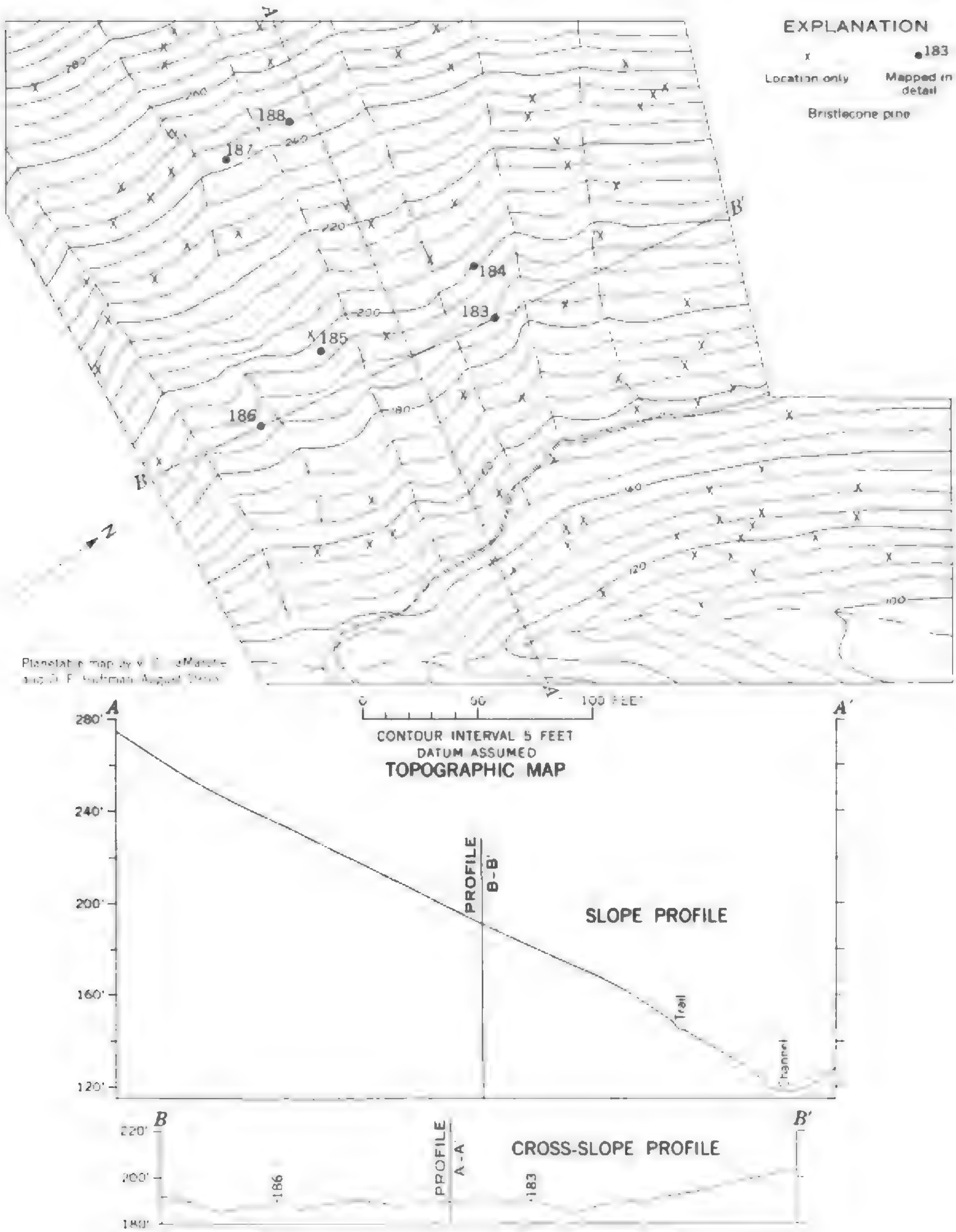

FIGURE 261 — Location of trees studied in area 3, and profiles of area 3.

FIGURE 262.—Specimen 184 in area 3. Depth of exposure of root in foreground is about 2.5 feet, shown by comparison with stadia rod. Tree, which is 1,900 years old, is on crest of low ridge that extends down the main slope.

except near their point of convergence, at low values of the variables.

RELATION TO TOPOGRAPHY

Differences in the long-term degradational rate from place to place within an area underlain by a homogeneous formation are clearly related to differences in topography and reflect variations in the intensity of degradational processes. The local rate of degration is not solely dependent on the slope of the ground surface but is also related to the geomorphic setting of the point of observation. Comparison of data obtained in two areas showed that a gently sloping knoll may be degraded more rapidly than a long steep slope (table 6). Grouping of many local estimates of degrational rates by slope and site classes (table 7) substantiates these results. In general, rocky ridge crests, upper slopes, and steeply inclined spurs are being degraded more rapidly than the long valley side slopes. Furthermore, where degradational rates in crestal areas apparently increase with increase in slope angle, the main slopes are degraded at fairly constant rates that do not vary systematically with slope angle.

TABLE 6.—*Summary of degradational rates and topographic characteristics in three selected areas*

Area	Number of specimens dated	Sampling method	Average[1] slope (degrees)	Degradational rate (ft per 1,000 yr)	Topographic character
1	43	Total	20	[2] 1.2	Rocky knoll.
2	26	Random	35	[3] .8	Long smooth slope.
3	6	Selective	28	[4] 1.1	Gullied slope.

[1] Mean of measurements, vicinity each specimen.
[2] From least-squares analysis of data from 33 trees.
[3] From least-squares analysis of data from 15 trees.
[4] Estimated from mean 1,000-year degradation.

TABLE 7.—*Degradational rates for slope classes in crestal areas and on main slopes*

[Rates estimated from mean values of age and root exposure for specimens listed in tables 1 and 2]

Slope	Number of observations	Age (thousands of years)	Exposure (ft)	Estimated degradational rate (ft per 1,000 yr)
Crestal Areas				
Gentle	9	0.65	0.2	0.3
Moderate	16	1.00	1.0	1.0
Steep	13	1.13	1.5	1.3
Very steep	2	1.70	2.8	1.6
Main slopes				
Steep	13	0.87	0.7	0.8
Very steep	6	.86	.4	.5

The dolomite areas being degraded most slowly, if at all, are the gentle, lower slopes of high ridges, illustrated in figure 249. Direct evidence of degradational rates in this topographic setting cannot be cited, because the maximum ages of trees at these sites are low. The trees apparently do not survive long enough to show significant root exposure, although several bristlecone pines on gently slopes (<10°) have attained ages of about 1,000 years. Low rates of slope degradation can also be inferred from the development of a soil profile in the surficial mantle of these areas.

Of special geomorphic interest is the evidence of the breakdown of bedrock in progressive and relatively rapid degradation of the ridge-crest areas. The crests of high ridges on Reed Dolomite range in character from angular and irregular to gently rounded and fairly smooth. Bedrock outcrops are abundant, and the soil is coarse and patchy. Small cliffs—steep bedrock faces as much as 10 feet high and 50 feet long—have formed on the upper slopes of most ridges and along the crests of steeply inclined spurs. The shape and the appearance of such cliffs are controlled by the spacing and orientation of joints. Overturning of trees has accompanied

Digitized by Google

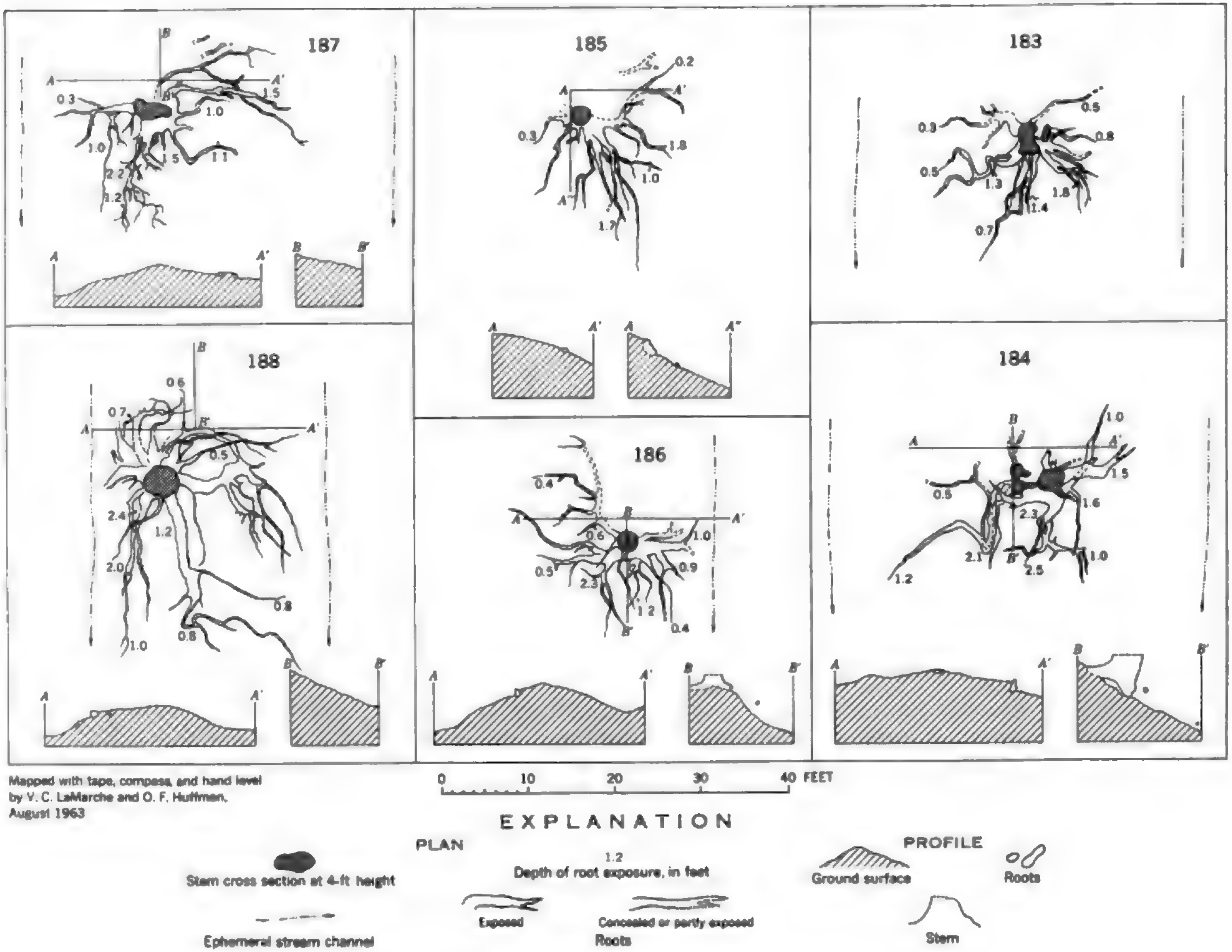

FIGURE 203.—Exposed roots of six trees in area 3, and profiles in vicinity of five of the trees.

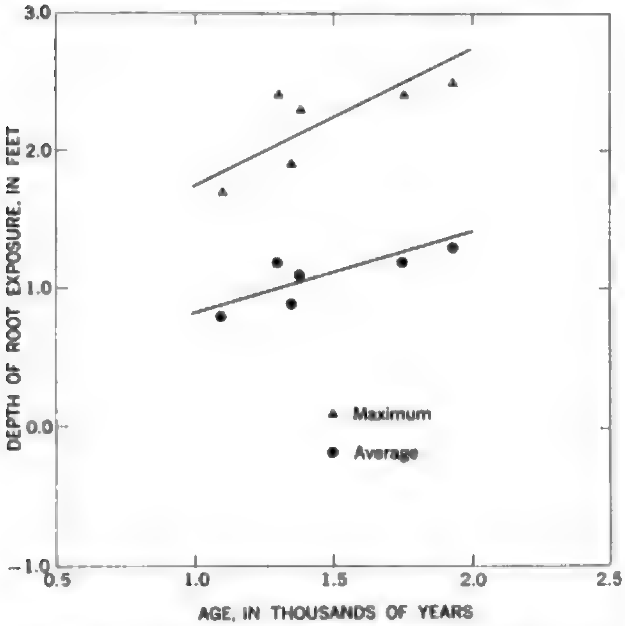

FIGURE 264.—Comparison of average and maximum depths of root exposure of trees in area 3. Average values approximate slope degradation.

the dislodgement of bedrock masses, showing that large-scale mass movement is occurring locally. Less catastrophic cliff retreat also takes place at a rate similar to that of debris-mantled slopes. The roots of a tree near upper tree line, 12 miles north of Reed Flat, extend 20 feet down a 45° cliff. These roots, which apparently followed fractures, have well-developed buttress forms and are exposed to a depth of 1.5 feet. A talus slope with fragments as much as a foot in diameter mantles the foot of this low bedrock face. The buttress root of another tree, about 800 years old, is exposed to a depth of 1 foot along a 40° bedrock surface above a high talus slope. Root exposure is seen above steeply inclined but thinly mantled bedrock surfaces and gently sloping outcrops, as well as along cliffs. The trees are firmly rooted and cannot have been elevated relative to the underlying rock. The surfaces are too steep, in many places, to have had a thick veneer of soil or rubble at the time of root development. Thus, root exposure must be due to the breakdown and removal of bedrock.

The steep embankments bordering the channels incised into the alluvial and colluvial valley fill are retreating more rapidly than valley side slopes of comparable steepness. The roots of two trees (specimens 2, 17) growing along the edges of embankments in the

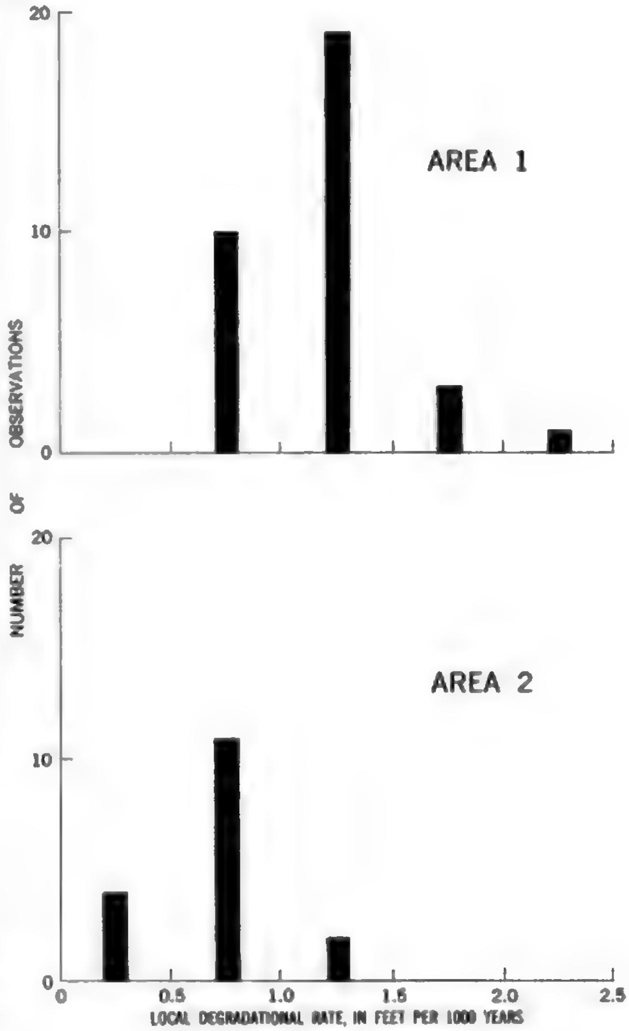

FIGURE 265.—Comparison of degradational rates in areas 1 and 2, as indicated by frequency distributions of local values of degradational rates.

Reed Flat area were studied in detail. The root systems have been differentially exposed—the roots projecting down the steep bank have been deeply exposed, but those projecting upslope have not yet been uncovered. Although youthful in appearance, these steep-walled inner valleys (which locally form a ramifying gully network) are not recent features of the landscape. Not only do 800-year-old roots parallel the banks, but trees 1,000 years old or more grow within the local areas of erosional topography. On the basis of present rates of development, however, channel cutting in the headwater areas of the White Mountains probably began less than 10,000 years ago.

Digitized by Google

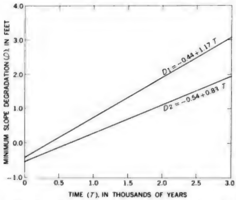

FIGURE 266.—Comparison of degradational rates in areas 1 and 2. Heavy lines represent least squares fit to scattered data. Shaded areas represent 95-percent confidence bands for lines.

DEGRADATIONAL PROCESSES AND EVIDENCE OF MOVEMENT

The land surface at some places in areas underlain by the Reed Dolomite has been lowered a few inches to several feet in the past 3,000 years; consequently, a large volume of rock debris must have been removed from these areas to account for the calculated slope degradation. The significance of mechanical weathering in the breakdown of bedrock can be inferred from the texture and mineralogy of the surficial mantle. Textural and microrelief features of the mantle suggest that downslope movement was rapid. Also, evidence indicates that large volumes of sediment are moved in stream channels during rare floods. In most of the area the movement of rock particles must take place at or near the surface of the mantle of surficial debris that overlies the dolomite bedrock. The massive, competent character of the rock and the absence of a mechanically weak, chemically weathered upper bedrock zone preclude bedrock creep and large-scale slumping. Neither chemical solution, whose action is minimal under the cool dry conditions, nor wind erosion seem to be significant mechanisms. The shallow mass-wasting and rapid erosion that occur during infrequent cloudbursts apparently cause most of the degradation.

Evidence of movement of weathering products on the dolomite slopes is abundant, but the effects of erosion and mass-wasting are difficult to distinguish. Movement of rock debris by flowing water concentrated in channels may be more significant in the long-term degradation of the Reed Dolomite slopes than is indicated by the low drainage density of about 6 miles per square mile. In a few local areas there are numerous closely spaced drainage lines. Runoff from infrequent intense storms possibly causes the headward extension of existing streams and the development of gullies on previously smooth slopes. Because the recurrence interval of flood-producing rainfall at any given point in the White Mountains seems to be about 50–100 years, according to historical evidence, such gullies would be healed by mass movement and slope wash in the intervening periods.

DEBRIS DAMMING

The terraces and hollows adjacent to old bristlecone pines are evidence that differential downslope movement of material has taken place. Similar features are the terraces that extend upslope from the trunks of fallen trees that lie across the slope and act as debris dams (fig. 267). The terrace surface is nearly horizontal, even where the surrounding area slopes steeply; and at many places, soil seems to be spilling over the top of the obstruction. An attempt was made to date such logs in order to estimate rates of accumulation; however, this was found to be impractical because the trees commonly remain standing several hundred years after they die. The date of the outermost ring in a log is a poor guide to the length of time that the log has been on the ground. The fact that such ephemeral features as logs do act as temporary barriers to downslope movement shows that the movement is frequent or continuous

FIGURE 267.—Log that forms debris dam on slope; longitudinal view. Ground surface drops about 1 foot across this barrier to downslope movement of rock debris

Digitized by Google

and that it is shallow; there is no evidence that debris is moving beneath these logs, and only on the steepest slopes do the fallen trunks appear to be moving downslope. The material composing the terraces could thus have been transported by shallow mass-wasting or by surface runoff or both.

ASYMMETRICAL ROOT EXPOSURE

The maximum depth of root exposure in the hollow below an old bristlecone pine is a measure of the rate of movement of rock debris on the slope. The results of measurements of the maximum depth of exposure for trees with asymmetrically exposed roots are given in table 3. The rate of root exposure was calculated for each area by least-squares analysis of these data. Although the degradational rate is greater in area 1 than in area 2, the maximum rates of root exposure are about 1.0 and 1.7 feet per 1,000 years, respectively; these rates reflect the extreme asymmetry of root exposure in area 2. Although the significance of the results is not immediately clear, the differences must be related to the differences in the slope gradient in the two areas; the average slope angle, measured in the vicinity of each of the specimens on which the results are based, is only 20° in area 1 but is 38° in area 2. Another notable difference is the distance downslope from the ridge crest to the points at which the measurements were made; this averages 200 feet in area 2 but only about 100 feet in area 1. However, within each area, there is no discernible tendency for the rate of root exposure to increase either with increasing slope of the local ground surface or with distance downslope.

A possible interpretation is that different processes are dominant in the two areas. Thus, it may be that the terrace and hollow can result only from mass movement and that the effect of the transport of sediment by water flowing over the ground surface would be to erase this topographic inhomogeneity. The degree of asymmetry of root exposure would then depend on the balance between the opposing processes. This is an attractive alternative because of the surface characteristics of the surficial mantle in the two areas. Although there are large rock fragments on the slopes of area 1, there is no continuous veneer of very coarse debris; large areas of the ground surface are silty in texture. Further, the presence of silty dolomitic sediment in the swale at the base of the slope shows that selective transport of debris is taking place on the slope, probably by surface runoff carrying only the smaller particles. In contrast, the upper 2–10 inches of the mantle in area 2 is composed exclusively of relatively large fragments that are very loosely packed and have a large interstitial volume. A rainfall intense enough to produce runoff on the surface of the compacted, relatively fine grained soil of area 1 could be expected to flow downslope within the veneer of rubble mantling the slope in area 2 without attaining great velocity or significant above-surface depth. Such interstitial water could, however, be expected to cause downslope movement of saturated debris masses. The slope material is at the angle of repose (35°–40°) when dry; the lubricating and buoyant effects of water might cause the material to move.

DEBRIS LOBES AND FANS

Evidence for recent movement of rock debris in ephemeral stream channels is widespread in the White Mountains. Much of the sediment produced by drainage basins in the range reaches the alluvial fans along the margins of the range in the form of dense mudflows (Kesseli and Beaty, 1959; Lustig, 1965). Smaller alluvial fans extend from the mouths of tributaries into the channels of streams within the range. The lobate form, the unsorted nature of the sediment, and the large size of some fragments suggest that these alluvial fans are formed by similar flows. Direct evidence for the occurrence of mudflows was found in area 3, where a debris lobe has completely filled one of the steep miniature valleys for a distance of 40 feet (between specimens 186 and 187, fig. 263). About 30 feet in maximum width and 4 feet deep, this deposit is composed of an unstratified mixture of silt, pebbles, and cobbles. A tangle of wood debris bounds the steep lower margin. This is clearly a mudflow that stopped before reaching the main canyon bottom. Although the channel slope at this locality is about 25°, it is even greater (30°) immediately upslope; the change in gradient may explain the loss of mobility.

Much larger piles of rock and wood debris choke the channelway in a narrow canyon west of Blanco Mountain. One of the largest of these (fig. 268) is a deposit of cobbles and boulders, up to 3 feet in diameter, behind a tangle of large logs; it fills the 50-foot-wide canyon floor to a depth of 10 feet.

Several other debris jams of similar size are located downstream, and all were probably produced at the same time by a flood of catastrophic proportions. There is evidence that this flood occurred within the past 300 years. Tree-ring dating of a standing tree deeply buried by the debris shows that it died in A.D. 1640; it was probably already dead at the time of burial. One of the best preserved logs in another pile represents a tree that died about A.D. 1600, establishing the earliest possible date of the event.

FIGURE 268.—Large debris pile in canyon tributary to Wyman Creek, as viewed upstream. This tangle of logs and large boulders was apparently produced by a single flood.

SUMMARY AND CONCLUSIONS

Degradation is the decrease in altitude of the land surface that results from gradual removal of surficial rock debris. Slope degradation in dolomite areas of the White Mountains, Calif., has resulted in the uncovering and progressive exposure of the initially shallow root systems of many bristlecone pines. Root exposure has occurred in a variety of topographic sites—from cliffs and steep talus slopes to rounded ridge crests and gently sloping valley bottoms. The extensively exposed root systems of certain individual trees, as well as the deeply exposed roots of large numbers of old trees in large tracts, show that material has been uniformly removed from large areas. At many sites, the roots of young trees have not yet been uncovered, whereas older trees show depths of root exposure proportional to their ages. Thus, root exposure is the result of degradational processes operating uniformly over large areas for long periods of time.

The Precambrian Reed Dolomite is a massive homogeneous unit that underlies a fluvially eroded terrain of moderate to high relief. The dolomite bedrock is covered by a mantle of surficial rock debris except along ridge crests, spurs, and rocky knolls. Ranging in texture from pebbly silt loam to coarse rubble, the debris is produced by the mechanical breakdown of the closely jointed dolomite. Frost shattering appears to be the dominant weathering process. Miniature patterned-ground features suggest that the approximately 220 diurnal freeze-thaw cycles per year, indicated by weather records, are also effective in sorting and causing downslope creep of the surficial debris.

Bristlecone pines dominate the subalpine coniferous forest that is almost entirely limited to dolomite terrane in the White Mountains. Although noted for their great age, few bristlecone pines have attained an age of more than 4,000 years. Only trees less than about 3,000 years old are relatively abundant. Typically, the oldest trees in a given area are restricted to the crests of high ridges and to rocky subsidiary spurs. Although the older trees might reliably indicate long-term degradational rates, selective study of trees of great age necessarily introduces a bias toward a particular kind of topographic situation. Because degradational rates appear to be a function of topography, such results may not be representative. Total or random samples of bristlecone pines in two areas, even though the stands were chosen because of the great apparent ages of many individual trees, give average ages of about 1,000 years and maximum ages of about 3,000 years.

Counting and correlation of annual growth rings form the basis for reliable age determinations of bristlecone pines. The most significant source of uncertainty in estimates of the time of establishment of a tree and its root system is the frequent loss of the oldest wood through weathering and decay. The absence of certain growth rings from a sample results in age estimates that are systematically too young if dating is based on a simple ring count. Cross dating of distinctive ring patterns in such a sample and in the complete growth record of another tree will increase the accuracy of the age estimate. The cross-dating techniques may also be used to estimate the age of a log or stump, but large error can be introduced by erroneous correlations in the absence of the approximate dating control provided by a ring count based on the outermost ring of a living tree.

The basis for relating root exposure to slope degradation is the shallow depth of initial root development that characterizes certain conifers. Root systems of many bristlecone pines and of a few old trees of other species in the White Mountains have been uncovered and exposed as a consequence of increasing age on sites subject to degradation. The axis of a root, which must have been within the soil at the time of longitudinal growth, is the only unequivocal datum for the measurement of root exposure. The top of a shallow root may become exposed through diametral increase alone. The sharp inflection of the basal flare, low on the stem of a tree, bears no relation to degradation, but is a normal feature of mature forest trees.

Digitized by Google

Local degradational rates can be calculated by combining a measure of root exposure with an estimate of tree age for each of a number of individual trees. However, the depth of root exposure, measured vertically from the root axis to the underlying ground surface, will be less than the actual degradation by an amount equal to the original depth of root burial. This factor would thus lead to underestimation of individually calculated degradational rates; it would affect the results from study of younger trees with little root exposure much more than those from older trees with roots exposed to depths of several feet.

A much more significant source of error is related to the asymmetrical exposure of root systems. The maximum depth of root exposure may be several times the actual slope degradation, and the disparity will tend to increase with time. An upslope terrace and downslope hollow are microrelief features associated with old trees on sloping terrain. These features reflect the damming effect of the tree itself—the stem and roots impede the direct downslope movement of surficial debris. The result is deep exposure of roots that extend downslope but little exposure or actual burial of roots directed upslope. The depth of root exposure can be averaged over the affected area to give a more reliable estimate of local degradation. When this procedure was followed on a steep (38°) slope (area 2), a sample of 14 trees showed that the maximum depth of exposure increased about twice as rapidly as the degradation of the surrounding area. These problems of measurement, combined with the possibility of bias in selective sampling, cast doubt on the significance of degradational rates calculated only from observations of age and maximum root exposure of individual trees.

Even casual observation of deeply exposed roots can indicate the order of magnitude of degradational rates. More accurate estimates must be based on careful measurements related to a valid index of both present and preexisting ground levels. The inferences that can be drawn from examination of exposed roots depend on observations of the relationships of developing root systems to the contemporary land surface. Furthermore, study of the response of the roots to uncovering and exposure may provide additional information on the local topographic history. Finally, the trees themselves are static features in a changing landscape, and they can induce pronounced local topographic changes that must be considered in quantitatively relating exposed roots to degradation.

Despite the problems of measurement, the grouping of the scattered observations of tree or root age and uncorrected depth of root exposure by topographic character of the individual sites gives at least a rough comparative estimate of degradational rates. The numbers obtained are probably significant only in their relative magnitudes. Degradational rates are greatest, perhaps 3–4 feet per 1,000 years, where the landscape is changing most rapidly—on the steep banks adjacent to channels now being incised into alluvium and colluvium that fills the valleys. The undissected surface of this fill represents the gentle ($< 10°$) lower slopes of the flanking ridges. Here, degradational rates are too low to be directly measured but must be less than about 0.5 foot per 1,000 years. In contrast, there is much evidence for rapid degradation of rocky ridge crests and upper slopes. Furthermore, the degradational rate seems to increase with increasing slope, from about 0.3 foot per 1,000 years (slope $< 10°$) to about 1.6 feet per 1,000 years (slope $> 30°$). Because root exposure tends to be symmetrical in crestal areas, this result probably reflects real differences in degradational rates rather than the effect of slope angle in increasing the asymmetry of exposure. The long comparatively steep (30°–40°) slopes that extend from the valley floors to the crests of the main ridges are apparently being degraded more slowly (0.4–0.8 ft. per 1,000 yr.) than the crestal areas (1.2 ft. per 1,000 yr.). Because such slopes make up a major part of the terrain underlain by the Reed Dolomite, the average degradational rate for the entire area must also be less than 1 foot per 1,000 years.

The most accurate estimate of the long-term rate of slope degradation based on study of exposed roots is obtained through unbiased (total or random) sampling of a fairly large number of specimens within a small area. Measurements of root exposure are reduced to estimates of minimum slope degradation by correcting for the local topographic changes induced by the presence of the tree itself. Results of study of two contrasting areas, using this approach, reinforce conclusions based on analysis of data from individual trees scattered over a large area. A rocky knoll, representative of crestal and upper slope areas, has been degraded at the average rate of 1.2 feet per 1,000 years during the past 2,500 years. Study of trees in a long narrow strip extending from a canyon bottom to the adjacent ridge crest showed that it has been degraded at a rate of only 0.8 foot per 1,000 years in the same period.

The extent of slope degradation indicated by the widespread exposure of root systems of trees in the White Mountains requires the movement of large volumes of rock debris from the slopes to the stream channels. The accumulation of material behind logs and the pro-

Digitized by Google

nounced damming effect of standing trees show that such movement does take place. Relatively rapid movement is suggested by the fact that the appearance of an obstruction is reflected in the microtopography within a few hundred years.

Removal of the debris produced from individual slopes, and perhaps a significant amount of slope erosion, may take place at infrequent intervals. Historical evidence shows that cloudbursts in White Mountain watersheds have generated floods that appeared as mudflows on alluvial fans flanking the range. Small debris lobes and alluvial fans and large bouldery deposits in channels within the study area illustrate that large volumes of coarse dolomitic debris can be transported in single flood events. However, from the straight-line variation of degradation with time in each of two areas and from evidence from scattered observations of gradual and progressive root exposure provided by many buttress roots, it appears that degradational rates have not fluctuated greatly within the past 3,000 years. The landscape seems to be roughly adjusted to the nearly steady transportation of the products of rock weathering on this scale in time, even though major erosional events may recur only infrequently. A summary of the kind and scope of processes that are inferred to be significant in the degradation of the Reed Dolomite terrane in the White Mountains is given in table 8.

TABLE 8.—*Qualitative summary of major transport mechanisms*

Process	Frequency	Scope	Rate of movement	Associated features	Associated events
Creep	Continuous.	Ridge-crests and slopes.	Slow	Rock stream.	Diurnal temperature change and freeze-thaw cycles.
Solifluction	Seasonal			Patterned ground.	
Erosion	Occasional	Slopes and channels.	Rapid	Debris piles.	Snowmelt and cloudburst runoff.

The magnitude of degradational rates in the White Mountains generally corresponds to the results of calculations based on indirect evidence of degradational rates in comparable areas. From data on sediment and dissolved loads of 17 streams draining mountain basins in semiarid and subalpine regions, Corbel (1959) calculated an average denudational rate of 0.3 mm per year, or about 1 foot per 1,000 years. Schumm (1963), in a recent review of rates of denudation of small drainage basins, suggested a maximum long-term denudational rate of 3 feet per 1,000 years in the early stages of the erosion cycle in semiarid areas underlain mostly by sedimentary rocks.

REFERENCES

Anderson, H. W., 1957, Relating sediment yield to watershed variables: Am. Geophys. Union Trans., v. 38, p. 921–924.

Billings, W. D., and Thompson, J. H., 1957, Composition of a stand of old bristlecone pine in the White Mountains of California: Ecology, v. 38, p. 158–160.

Corbel, J., 1959, Vitesse de l'erosion: Zeitschr. Geomorphologie, v. 3, p. 1–28.

Currey, D. R., 1965, An ancient bristlecone pine stand in eastern Nevada: Ecology, v. 46, p. 564–566.

D'Ooge, C. L., 1955, Five years of weather observations on the White Mountain Range, California: American Meteorol. Soc. Bull., v. 36, p. 172–175.

Douglass, A. E., 1914, A method of estimating rainfall by the growth of trees, *in* Huntington, Ellsworth, The climatic factor as illustrated in arid America: Carnegie Inst. Washington Pub. 192, p. 101–138.

Esau, Katherine, 1953, Plant anatomy: New York, John Wiley & Sons, 733 p.

Fritts, H. C., 1966, Growth-rings of trees; their correlation with climate: Science, v. 154, p. 973–979.

Garrels, R. M., Thompson, M. E., and Siever, R., 1960, Stability of some carbonates at 25°C and one atmosphere total pressure: Am. Jour. Sci., v. 258, p. 402–418.

Glock, W. S., 1937, Principles and methods of tree-ring analysis: Carnegie Inst. Washington Pub. 486, 100 p.

Glymph, L. M., Jr., 1954, Studies of sediment yield from watersheds: Internat. Assoc. Sci. Hydrol., Gen. Assembly, Rome 1954, v. 1, p. 178–191.

Hueck, K., 1951, Eine biologische Methode zum messen der erodieren Tatigkeit des Windes und des Wassers: Deutsche Bot. Gesell. Ber., v. 64, p. 53–56.

Judson, Sheldon, and Ritter, D. F., 1964, Rates of regional denudation in the United States: Jour. Geophys. Research, v. 69, p. 3395–3401.

Kesseli, J. E., and Beaty, C. B., 1959, Desert flood conditions in the White Mountains of California and Nevada: U.S. Army Quartermaster Research and Eng. Tech. Rept. EP–108, 107 p.

Knopf, Adolf, 1918, A geologic reconnaissance of the Inyo Range and the eastern slope of the southern Sierra Nevada, California; U.S. Geol. Survey Prof. Paper 110, 130 p.

LaMarche, V. C., Jr., 1963, Origin and geologic significance of buttress roots of bristlecone pines, White Mountains, California, *in* Geological Survey Research 1963: U.S. Geol. Survey Prof. Paper 475–C, p. C149–C150.

Leopold, L. B., 1956, Land use and sediment yield, *in* Thomas, W. L., ed., The role of Man in changing the face of the Earth: Univ. Chicago Press, p. 639–647.

Lustig, L. K., 1965, Clastic sedimentation in Deep Springs Valley, California: U.S. Geol. Survey Prof. Paper 352–F., p. 131–192.

Merriam, C. H., 1890, Results of a biological survey of the San Francisco Mountain Region and the desert of the Little Colorado, Arizona: N. Am. Fauna, v. 3, p. 1–113.

Mooney, H. A., St. Andre, G., and Wright, R. D., 1962, Alpine and subalpine vegetation patterns in the White Mountains of California: Am. Midland Naturalist, v. 68, p. 257–273.

Munns, E. N., 1938, The distribution of important forest trees of the United States: U.S. Dept. Agriculture Misc. Pub. 27, 176 p.

Nelson, C. A., 1962, Lower Cambrian-Precambrian succession, White-Inyo Mountains, California: Geol. Soc. America Bull., v. 73, p. 139–144.

Nelson, C. A., 1963, Preliminary geologic map of the Blanco Mountain quadrangle, Inyo and Mono Counties, California: U.S. Geol. Survey Mineral Inv. Field Studies Map MF-256.

Norman, L. A., Jr., and Stewart, R. M., 1951, Mines and mineral resources of Inyo County: California Jour. Mines and Geology, v. 47, p. 17-223.

Pace, Nello, 1963, Climatological data summary for the decade 1 Jan. 1953 to 31 Dec. 1962 from the Crooked Creek Laboratory and the Barcroft Laboratory: Berkeley, California Univ. White Mountain Research Station, duplicated report, 52 p.

Rice, C. M., 1940, Dictionary of Geological Terms: Ann Arbor, Mich., Edwards Bros., 364 p.

Ruhe, R. V., and Daniels, R. B., 1965, Landscape erosion—geologic and historic: Jour. Soil and Water Conserv., v. 20, p. 52-57.

Schulman, Edmund, 1954, Longevity under adversity in conifers: Science, v. 119, p. 396-399.

——— 1956, Dendroclimatic changes in semiarid America: Tucson, Univ. Ariz. Press, 142 p.

——— 1958, Bristlecone pine, oldest known living thing: Natl. Geog. Mag., v. 113, p. 355-372.

Schulman, Edmund, and Ferguson, C. W., 1956, Millenia old pine trees sampled in 1954 and 1955, *in* Schulman, Edmund, Dendroclimatic changes in semiarid America, Tucson, Univ. Ariz. Press, p. 136-138.

Schumm, S. A., 1963, Disparity between present rates of orogeny and denudation: U.S. Geol. Survey Prof. Paper 454-H, 13 p.

——— 1964, Seasonal variation of erosion rates and processes on hillslopes in western Colorado: Zeitschr. Geomorphologie, v. 5, p. 215-238.

Seybold, A., 1930, Uber die Blosslegung des Wurzelsystems durch aolische und fluviatile erosion: Deutsche Bot. Gesell. Ber., v. 48, p. 335-341.

Stewart, John H., 1966, Precambrian and Lower Cambrian formations in the Last Chance Range area, Inyo County, California, *in* Cohee, G. V., and West, W. S., Changes in stratigraphic nomenclature by the U.S. Geological Survey, 1964: U.S. Geol. Survey Bull. 1224-A, p. A60-A70.

Stout, B. B., 1956, Studies of the root systems of deciduous trees: Black Rock Forest Bull. 15, Harvard Black Rock Forest, Cornwall on the Hudson, N.Y., and Cambridge, Mass., 45 p.

Troll, Karl, 1958, Structure soils, solifluction, and frost climates of the Earth: U.S. Army Snow, Ice, and Permafrost Research Establishment, Hanover, N.H., Translation 43, 121 p.

Washburn, A. L., 1956, Classification of patterned ground and review of suggested origins: Geol. Soc. America Bull., v. 67, p. 823-866.

Wallis, W. A., and Roberts, H. V., 1956, Statistics—a new approach: Glencoe, Ill., Free Press, 646 p.

U.S. GOVERNMENT PRINTING OFFICE : 1967 O—[illegible]

Digitized by Google

QE75
f.A25
no.352-J.

Geo.

Chemical Weathering, Soil Development, and Geochemical Fractionation in a Part of the White Mountains, Mono and Inyo Counties, California

GEOLOGICAL SURVEY PROFESSIONAL PAPER 352-J

THE UNIVERSITY OF CHICAGO LIBRARY
OCT 2

THE UNIVERSITY OF CHICAGO LIBRARY
SEP 30 1974
DEPOSITORY DOCUMENT

Marchand—CHEMICAL WEATHERING, SOIL DEVELOPMENT, WHITE MOUNTAINS, CALIFORNIA—Geological Survey Professional Paper 352-J

Chemical Weathering, Soil Development, and Geochemical Fractionation in a Part of the White Mountains, Mono and Inyo Counties, California

By DENIS E. MARCHAND

EROSION AND SEDIMENTATION IN A SEMIARID ENVIRONMENT

GEOLOGICAL SURVEY PROFESSIONAL PAPER 352-J

UNITED STATES GOVERNMENT PRINTING OFFICE, WASHINGTON 1974

Digitized by Google

UNITED STATES DEPARTMENT OF THE INTERIOR

ROGERS C. B. MORTON, *Secretary*

GEOLOGICAL SURVEY

V. E. McKelvey, *Director*

Library of Congress catalog–card No. 73-600361

For sale by the Superintendent of Documents, U.S. Government Printing Office
Washington, D.C. 20402 – Price $1.35 (paper cover)
Stock Number 2401-02484

Digitized by Google

CONTENTS

	Page
Abstract	379
Introduction	379
Study area	381
Location and description	381
Previous work in the region	382
Climate	382
Vegetation	384
Geology	385
Chemical weathering and soil development	388
Method of approach	388
Field methods	388
Laboratory methods	388
Description of soils	389
Clarification of terms	389
Reed Dolomite soils	390
Adamellite soils of Sage Hen Flat	390
Basalt soils	391
Andrews Mountain sandstone soils	391
Soil contamination	392
Physical weathering	392
Reed Dolomite	392
Adamellite of Sage Hen Flat	393
Mechanisms of disintegration	394
Chemical weathering	395
Changes in the solid phases	395
Mineralogical changes	395
Reed Dolomite	395
Adamellite of Sage Hen Flat	396
Electron microprobe studies of adamellite mineral weathering	398
Biotites	398
Feldspars	400
Other minerals	400
Chemical weathering and soil development—Continued	
Chemical weathering—Continued	
Changes in the solid phases—Continued	
Chemical changes from bedrock to soil	400
Reed Dolomite	401
Adamellite of Sage Hen Flat	403
Changes in the liquid phase	405
Chemical composition of precipitation	405
Chemical composition of soil water	406
Soil pH	406
Exchangeable cations	406
Chemical composition of spring waters	407
Waters related in part to the Reed Dolomite	407
Waters related largely to the adamellite of Sage Hen Flat	408
Analysis of chemical changes	408
Relative mobilities	408
Stability with respect to solid and gas phases	409
Relation of soil water to precipitation and spring waters	411
Chemical fractionation in the bedrock-soil-water-plant system	413
Summary and discussion	416
Weathering of Reed Dolomite	417
Weathering of adamellite of Sage Hen Flat	417
General weathering relations	418
References cited	418
Supplemental information—Methods, reproducibility, and accuracy	422

ILLUSTRATIONS

	Page
Figure 269. Diagram showing reversible, irreversible, and cyclical processes associated with weathering and erosion	380
270. Map of east-central California and adjacent part of Nevada, indicating location of the study area	381
271. Photograph showing part of the upland surface in the White Mountains	381
272. Map of generalized topography of a part of the southern White Mountains	381
273. Photograph showing North Sage Hen Flat auxiliary weather station and dust trap	383
274. Graph showing maximum and minimum temperature and relative evaporation rates at Crooked Creek Laboratory and five auxiliary weather stations	384
275. Graph showing precipitation recorded at Crooked Creek Laboratory and at five auxiliary weather stations	384
276. Photograph showing vegetational contrast between dolomite outcrops and colluvium and sandstone colluvium	385
277. Generalized geologic map of the study area	386
278. Photograph showing view north across Sage Hen Flat, showing degraded White Mountain erosion surface and outcrop areas of adamellite of Sage Hen Flat, Reed Dolomite, and Andrews Mountain sandstone	387
279. Photograph showing view east from Sage Hen Flat, showing resistant basalt capping less resistant metasediments and granitic intrusive rock	387

Digitized by Google

Page

FIGURE 280. Photograph showing exposures of reworked rhyolitic ash interbedded with terrace alluvium along Crooked Creek 387
281-284. Maps showing:
281. Depth of soil and colluvium at planetable map site R-1, Reed Dolomite, 10,600 feet 389
282. Depth of soil and colluvium at planetable map site R-2, Reed Dolomite, 11,200 feet 390
283. Depth of soil and colluvium at planetable map site S-1, adamellite of Sage Hen Flat 390
284. Depth of soil and colluvium at planetable map site B-1. on basalt 391
285. Photograph showing Reed Dolomite soil pit 391
286. Photograph showing soil pit in adamellite of Sage Hen Flat 391
287. Graph showing cumulative grain size frequency curves for dolomite soils and comparison with ranges in bedrock grain size 392
288. Diagram showing gravel-sand-silt and clay distribution for soil above the C horizon 392
289. Diagram showing sand-silt-clay distribution for soil above the C horizon 393
290. Photograph of weathered adamellite outcrop on Sage Hen Flat 393
291. Graph showing cumulative grain size frequency curves for adamellite soils and comparison with ranges of bedrock grain size 394
292. Photomicrographs showing fresh, crushed bedrock dolomite and etched, embayed, altered soil dolomite grain 395
293. Photomicrographs showing fresh, crushed bedrock talc and soil talc grains 396
294. Diagram showing mineral weathering sequence in Reed Dolomite soils, in order of decreasing resistance 396
295. Photomicrograph of weathered grains in adamellite soil thin section 397
296. Photomicrograph of soil biotite grains 397
297. Diagram showing mineral weathering sequence in adamellite soils of Sage Hen Flat in order of decreasing resistance 398
298-301. Graphs showing:
298. Electron microprobe traverses normal to (001) cleavage of two soil biotite grains 399
299. Electron microprobe traverses parallel to (001) cleavage of two soil biotite grains 399
300. Electron microprobe analyses of 10 parts of a single plagioclase grain 400
301. Percentage chemical losses for the indicated Reed Dolomite and adamellite soils of Sage Hen Flat with respect to bedrock 402
302. Photograph of rock saw chips showing weathering rind on spheroidally weathered dolomite analyzed by electron microprobe 403
303-308. Graphs showing:
303. Electron microprobe transect showing Ca, Mg, and Fe variation across an alteration rind in spheroidally weathered Reed Dolomite 403
304. Electron microprobe transect for Ca, Mg, and Mn across same dolomite weathering rind 403
305. Mineral percentage changes with respect to bedrock in two size fractions of a relatively uncontaminated adamellite soil 404
306. Relative mobilities for eight elements in spring waters related to adamellite 409
307. Stability diagram for Na silicates 411
308. Stability diagram for K silicates 411
309. Compositional diagram showing progressive cation changes from precipitation water to soil and spring waters related to Reed Dolomite 412
310. Compositional diagram showing progressive cation changes from precipitation water to soil and spring waters related to adamellite 412
311-314. Graphs showing:
311. Mg/Fe and Ca/Fe ratio comparisons of waters related to adamellite 413
312. Silica-cation ratio comparisons of adamellite-related waters 413
313. Comparison of elemental and total concentrations in soil, soil water, colloidal exchange, and plants 415
314. Fractionation of nine elements in the adamellite bedrock-soil-water-plant system 416
315. Diagram of flowsheet for laboratory treatment of bedrock samples 422
316. Diagram of flowsheet for laboratory treatment of soil samples 422

TABLES

Page

TABLE 1. Summary of climatic means and extremes from Crooked Creek and Mount Barcroft Laboratories 383
2. Types of information obtained at Crooked Creek Laboratory and five auxiliary weather stations during the period June 1966 to August 1967 383
3. Estimated precision of measurement for some analytical quantities discussed in this paper 389
4. Mineral weight percentages in five Reed Dolomite bedrock samples 395
5. Mineral weight percentages in five adamellite bedrock samples from Sage Hen Flat 396
6. Chemical compositions of 10 major minerals in the adamellite of Sage Hen Flat 397
7. Layer silicates in silt and clay fractions of some adamellite soils 398
8. Averaged electron microprobe analyses of fresh and weathered biotites 399

Digitized by Google

Page

TABLE 9. Individual electron microprobe analyses of altered and relatively fresh parts of soil biotites 399
10. Averaged electron microprobe analyses of feldspars from fresh adamellite bedrock, grus, and soils 400
11. Electron microprobe analyses of four minerals from fresh adamellite of Sage Hen Flat and from derived soil 400
12. Chemical analyses of Reed Dolomite bedrock and soils 401
13. Chemical compositions of minerals and glass in soils used to correct chemical analyses 402
14. Absolute losses of chemical constituents from bedrock to soil, assuming constant Zr percentage 402
15. Averaged values for X-ray fluorescence chemical analyses of adamellite bedrock and soils from Sage Hen Flat 404
16. Adamellite sample 94—bedrock chemical analysis and adjustment of <2-mm-soil analysis for ash and local contamination by biotite and hornblende 405
17. Chemical analyses of precipitation collected near Crooked Creek Station and comparison with analyses of snow from the east slope of the Sierra Nevada 406
18. Chemical constituents in water saturation extracts of two groups of White Mountains soils 406
19. Mean values for total exchangeable cations, percentage exchangeable cations, and pH in Reed Dolomite and adamellite soils of Sage Hen Flat 407
20. Field and laboratory analytical data for two natural waters associated in part with the Reed Dolomite 407
21. Field and laboratory analytical data for two natural waters associated with the adamellite of Sage Hen Flat 408
22. Relative mobilities for four elements in Cottonwood Spring waters 409
23. Degree of saturation with respect to calcite and dolomite for four spring waters 410
24. Partial pressures of carbon dioxide in four spring waters and a comparison with atmospheric PCO_2 410
25. Chemical composition of some major plant species on Reed Dolomite and adamellite of Sage Hen Flat 414
26. Fractionation by plants with respect to soil water for seven elements in adamellite and dolomite terranes 416
27. Reproducibility of X-ray fluorescence analyses 423
28. Comparison of analytical results for some adamellite and Reed Dolomite samples, as analyzed by X-ray fluorescence, wet chemistry, and flame photometry 423
29. Variation in measured parameters of four White Mountains soil types 424

Digitized by Google

CHEMICAL WEATHERING, SOIL DEVELOPMENT, AND GEOCHEMICAL FRACTIONATION IN A PART OF THE WHITE MOUNTAINS, MONO AND INYO COUNTIES, CALIFORNIA

By DENIS E. MARCHAND

ABSTRACT

The White Mountain erosion surface truncates a variety of late Precambrian and Cambrian metasedimentary units and several Mesozoic plutonic bodies; it is overlain by Tertiary basalts. Present climatic gradients in the 30-square-mile study area are not pronounced, and thus weathering of diverse lithologies under a reasonably uniform semiarid subalpine environment may be studied here. The local vegetation, consisting primarily of sagebrush, bristlecone and limber pine, and associated perennial herbs, is relatively sparse and shows marked discontinuities across geologic contacts. Soils in the region are immature lithosols, usually less than 1 foot deep, but better developed soils may have formed prior to or during late Tertiary uplift, only to be stripped by subsequent erosion. A reworked rhyolitic late Pleistocene ash and local windblown fragments are abundant soil contaminants and complicate efforts to decipher mineralogical and chemical changes due to weathering.

Rock weathering in this region appears to be primarily a function of mineral composition and of the density and degree of physical rock flaws which serve as avenues for penetrating fluids. Physical breakdown, which tends to precede chemical weathering, seems as closely related to lithologic features as to climate. Since erosion is aided by rapid weathering, easily disintegrated rock types such as course-grained carbonate and adamellite and fissile shale have eroded to topographic lows while slow-weathering fine-grained carbonate, quartzose sandstone, basalt, aplitic dikes, and mafic inclusions have resisted erosion.

Reed Dolomite, a Precambrian unit, weathers by frost riving to polycrystalline, cleavage-bounded grains, except where the presence of thermally recrystallized rock has led to production of single-crystal fragments. Mineral weathering occurs in the sequence dolomite ≫ tremolite, epidote > talc, K-feldspar, biotite ≥ apatite > quartz and ilmenite. Percentage chemical losses from bedrock to soil are Mg > Ca > Sr > Mn ≈ Fe, for carbonate-constituent elements. Authigenic calcite is apparently precipitated in the soil during dry seasons and partially dissolved during wet periods. Spring waters related in part to the dolomite show relative mobilities of Mg > Ca > Fe > Mn. Ion-activity product computations indicate that these waters are undersaturated with respect to both calcite and dolomite. P_{CO_2} exceeds atmospheric values by over an order of magnitude and those of adamellite-derived waters by several times. Dolomite soil water extracts appear closer in pH to the spring waters than to rain or snow, although the soil water composition is obviously quite different from either of these fluids. Chemical changes in both solid and liquid phases related to the dolomite appear to begin along with physical breakdown in the early stages of rock weathering.

Adamellite of Sage Hen Flat weathers by frost riving along intergranular weaknesses, causing boulder exfoliation and accumulation of grus. This coarse material, largely unaltered except for minor Fe oxidation, later undergoes important chemical breakdown during its transformation to finer sized particles. Primary minerals weather in the sequence plagioclase (An_{25-30}) > hornblende > biotite, epidote > microcline, plagioclase (An_{10-15}), allanite > apatite, chlorite, magnetite > ilmenite, muscovite, quartz, sphene > zircon, resulting in percentage chemical losses from fresh rock to soil in the sequence Rb $\overset{?}{>}$ Na ≈ K ≈ Mg > Sr > Mn ≈ Ca > Ba > Si > Al ≫ Fe > Ti.[1] Kaolinite, and possibly some vermiculite, is forming from feldspar, biotite, and other silicates. Microprobe analyses of biotite indicate losses in the sequence Ba $\overset{?}{>}$ K > Mg > Fe > Si > Al; cations having eightfold to twelvefold coordination are most readily lost, then cations in octahedral coordination, and finally ions in sixfold and fourfold coordination. Microclines reveal losses of Na and K, and plagioclases show changes implying removal of Na > Ca > Si > Al. Water saturation extracts from adamellite soils are distinct in composition from rain and snow water and from spring water in adamellite terrane. Relative mobilities of dissolved constituents in adamellite ground waters indicate changes with regard to bedrock of Ca > Mg ≈ Na ≫ Si ≈ K ≥ Mn ≈ Fe > Al. Owing to plant extraction, K and Al mobilities may be lower than bedrock-to-soil losses would suggest. High Ca and Mg mobilities could result from solution of carbonate grains blown into the soils.

Chemical equilibrium does not exist in the natural waters studied, but steady-state conditions are closely approximated in spring waters. Contact with weathering rock over a considerable space-time interval is apparently necessary for the achievement of a steady state, but this interval may decrease for mobile constituents in readily weathered minerals. The chemistry of spring waters related to all lithologies studied appears very sensitive to differences in source material.

Nine elements released by weathering appear to apportion themselves between vegetation, colloidal exchange, and solution as follows: Na, soln ≫ exch > veg; Si, soln ≫ veg; Ca, exch > soln > veg; Mg, exch > soln = veg; K, veg ≫ soln > exch; Fe, Mn, P, veg ≫ soln; Al, veg ⋙ soln.

INTRODUCTION

Bedrock, soil, vegetation, natural waters, and the atmosphere are interrelated by a highly complex system of reactions and processes, some of which are shown in figure 269. To adequately understand such a system, a broad investigation is necessary, including study of the many related and potentially significant aspects. It

1 A question mark is used in conjunction with greater than or less than symbols in this paper to indicate uncertain position in the sequence.

Digitized by Google

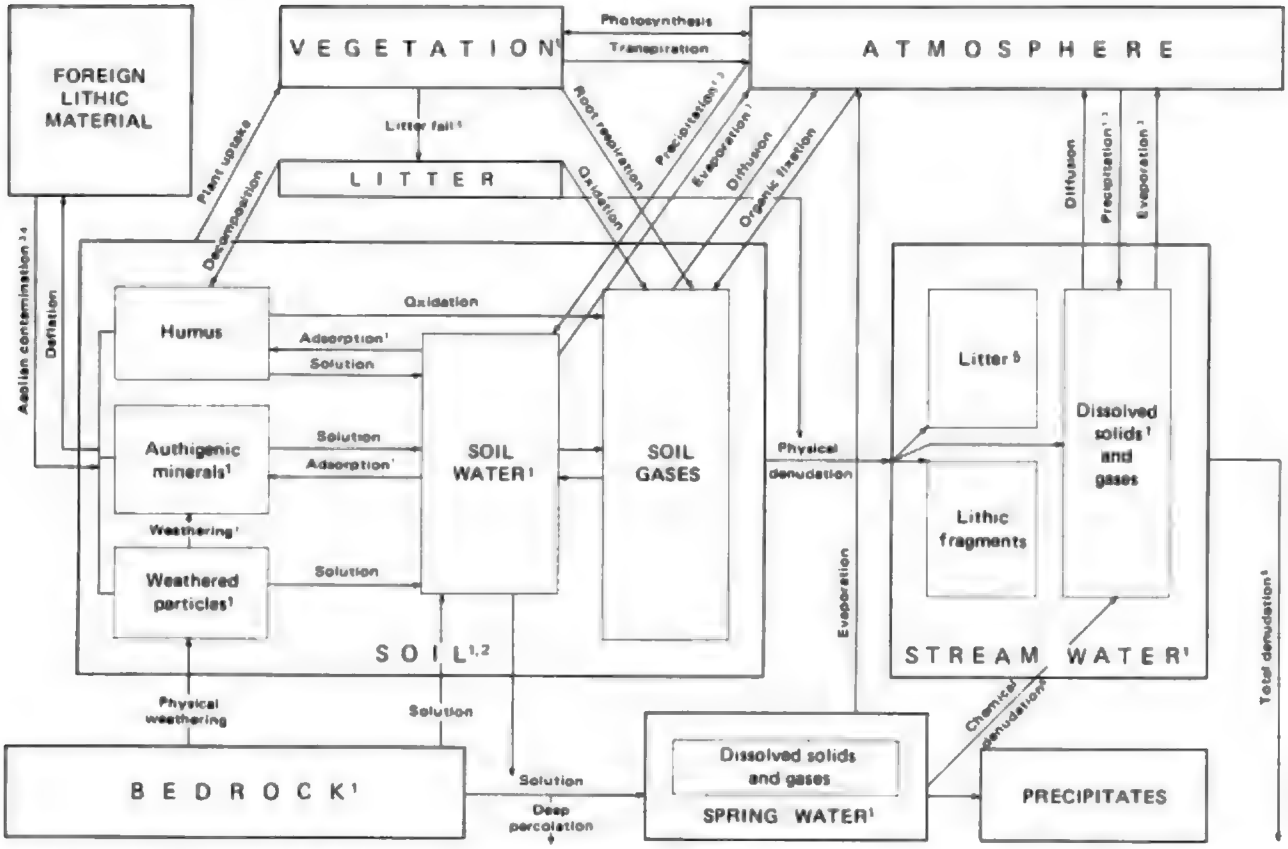

FIGURE 269.—Some reversible, irreversible, and cyclical processes associated with weathering and erosion. Footnotes refer to data given in this and other papers. [1]Total or partial chemical analysis. [2]Physical analysis. [3]Rate evaluation. [4]Physical analysis and rate evaluation (data in Marchand, 1970). [5]Rate evaluation (data in Marchand, 1971).

is impossible, for example, to clearly comprehend the transformation of bedrock into soil by studying changes in the mineral phases alone, for weathering involves important alteration of liquid and gas phases in contact with the minerals as well. This paper constitutes the fourth in a series of vegetational, erosional, and weathering studies in the southern White Mountains of eastern California (Marchand, 1970, 1971, 1973). The focus here is primarily on the chemical weathering of two widely distributed rock types, dolomite and adamellite, utilizing chemical and physical data from all of the five system components mentioned. Chemical analyses of bedrock, soils, plants, and natural waters permit estimates of the direction and magnitude of chemical fractionation in parts of the geochemical system described in figure 269.

The upland surface of the White Mountains, truncating a diversity of sedimentary and plutonic bodies and overlain locally by basalt, provides an excellent area in which to study the extent, sequence, and processes of weathering and soil development applied to many lithologies in a semiarid, subalpine environment. Quantitative chemical weathering studies have previously been largely confined to tropical or humid temperate regions, for example, Mead (1915), Goldich (1938), Cady (1951), Sherman and Uehera (1956), Hay (1959), and Wolfenden (1965). In such areas weathering has proceeded to such an extent that initial trends are difficult or impossible to recognize. Soils in the White Mountains are immature and clearly illustrate some of the early stages of the weathering process.

Gerald Osborn and Francis H. Brown assisted with sample collection and planetable mapping during the summer of 1966. J. Ross Wagner aided in preparing X-ray fluorescence pellets of bedrock and soil samples, conducting mineral separations, and in determining many physical and chemical soil parameters. Electron microprobe studies were conducted by Lary K. Burns. Joaquim Hampel determined Na and K in eight bedrock and soil samples by flame photometer. Barbara Lewis and James Clayton analyzed plant materials for inorganic constituents.

This paper represents a major portion of a Ph. D. dissertation carried out at the University of California, Berkeley, and financially supported by the U.S. Geological Survey. Many members of the Survey, especially

Ivan Barnes, John Hem, and Edward J. Helley, rendered indispensable aid and advice. The manuscript in its various stages of preparation was aided by the critical reading of F. J. Kleinhampl, John D. Hem, Richard L. Hay, Clyde Wahrhaftig, Peter W. Birkeland, and R. R. Tidball.

STUDY AREA

LOCATION AND DESCRIPTION

The White Mountains, often termed the northern Inyo Range in older publications, extend from Westgard Pass in eastern California north to Montgomery Peak (north of map shown in fig. 270) in western Nevada. White Mountain Peak (14,246 ft.) is the highest point in the range.

The area investigated encompasses approximately 30 square miles along the crest of the southern White Mountains, east of Bishop, Calif., in Mono and Inyo Counties (fig. 270). It is characterized by a gently undulating summit upland (fig. 271) sloping southward from 11,500 feet near Sheep Mountain to about 10,000 feet east of Bucks Peak (fig. 272). Summits such as

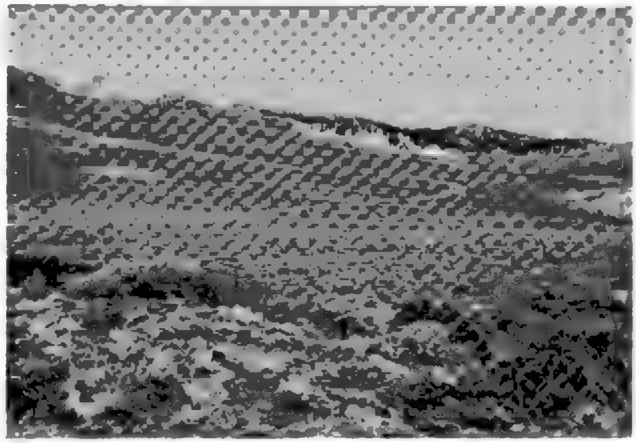

FIGURE 271.—Part of the upland surface in the White Mountains. View north across Big Prospector Meadow. Outcrops of Andrews Mountain Member of Campito Formation in foreground, white tree-covered exposures in middle and far distance are Reed Dolomite.

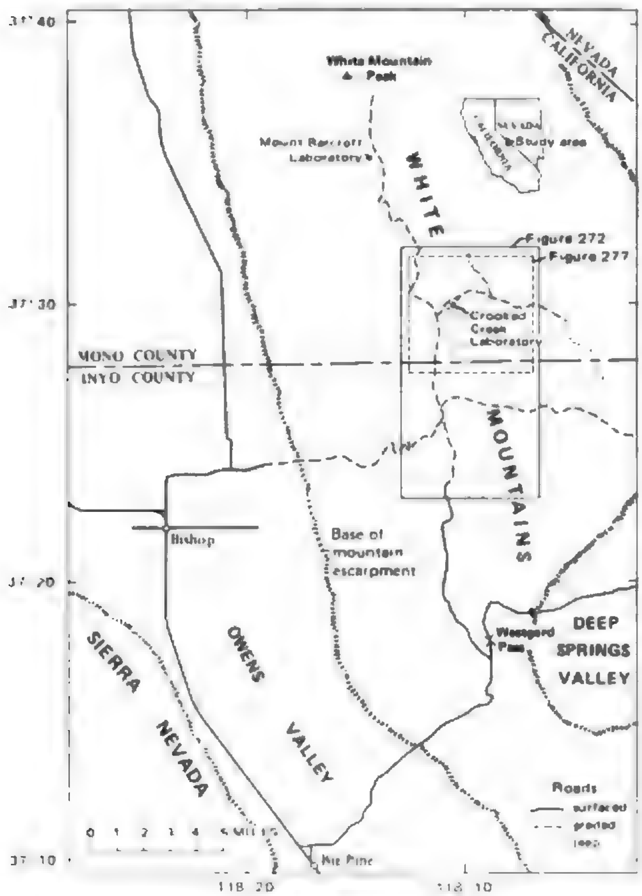

FIGURE 270.—East-central California and adjacent part of Nevada [illegible] study area and of the maps shown in figures 272 and 2[illegible]

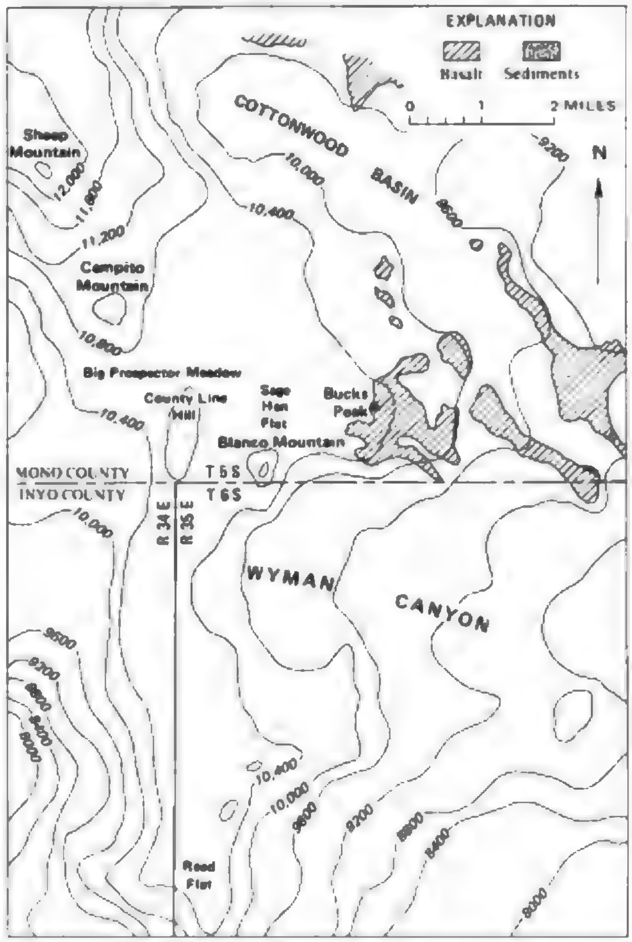

FIGURE 272.—Generalized topography (contours in feet above mean sea level) of a part of the southern White Mountains. [illegible] surface deposits shown locally.

Blanco Mountain, County Line Hill, and Campito Mountain stand 500 feet or more above this rolling surface. The steep western escarpment of the range, not included within the study area, descends 6,000–7,000 feet in 6 or 7 miles to the floor of the Owens Valley. The eastern flank slopes much more gradually, but is incised by a series of canyons as much as 1,000 feet deep, which drain southwestward to Deep Springs Valley and eastward to Fish Lake Valley.

PREVIOUS WORK IN THE REGION

The brief description of Spurr's (1903, p. 206–212) and Knopf's (1918) reconnaissance of the northern Inyo Range and eastern Sierra Nevada, which included a section on the stratigraphy of the Inyo Range by Edwin Kirk, marked the first geological studies of the White Mountains. Anderson and Maxson (1935) and Maxson (1935) described the physiography and Precambrian stratigraphy, respectively, of the northern Inyo Range. Recent work in the White Mountains led to publications on Precambrian and Cambrian stratigraphy, paleontology, and boundary problems by Nelson and Perry (1955), Nelson (1962), Taylor (1966), and Cloud and Nelson (1966). Anderson's (1937) arguments for the granitization in the formation of the Inyo batholith were challenged by Hall (1964) and Emerson (1966). McKee and Nash (1967) dated most of the plutonic bodies and several metamorphic units in the area by K/Ar methods, and Krauskopf (1968) discussed the complex intrusive history of the region. Cenozoic volcanism and tectonics were considered by Taylor (1965), and Dalrymple (1963) dated Tertiary volcanic rocks on the northwest edge of Deep Springs Valley. The Blanco Mountain 15-minute quadrangle (Nelson, 1963, 1966) and the Mount Barcroft (Krauskopf, 1971) 15-minute quadrangles were mapped. Hall (1964), Pittman (1958), and Gallick (1964) mapped parts of the White Mountain Peak, Mount Barcroft, and Blanco Mountain quadrangles. A general summary of the area's geologic history was provided by Nicholls (1965).

Geomorphic processes in the White Mountains were investigated by Powell (1963) and Kesseli and Beaty (1959), who studied desert flood conditions, and by Beaty (1959, 1960), who discussed slope evolution and gullying. LaMarche (1967, 1968) estimated erosion rates on the Reed Dolomite from tree-ring data and described spheroidal weathering in the carbonate rocks of the area.

Several members of the U.S. Geological Survey discussed dissolved constituents in snow (Feth, Rogers, and Roberson, 1964) and ground water (Feth, Roberson, and Polzer, 1964) in the eastern California region. Barnes (1965) studied the geochemistry of Birch Creek, which drains the southernmost part of the area and is similar in some respects to spring waters discussed here.

Pace (1963) and Nicholls (1965) summarized climatic data collected at the Mount Barcroft and Crooked Creek Laboratories of the White Mountain Research Station for the decade 1953–62.

CLIMATE

The White Mountains lie in the rain shadow of the Sierra Nevada and are generally characterized by a cold, dry climate (BWk to BSk of Köppen notation) with precipitation occurring largely in the form of snow and in sudden summer storms. Mean annual precipitation is about 13 inches at Crooked Creek and mean annual temperature is approximately 35°F.

Climatic data from the Crooked Creek and Mount Barcroft Laboratories (fig. 270) of the White Mountain Research Station are summarized in table 1. The Crooked Creek Station (10,150 ft.) is located in a valley at the approximate center of the study area; the Mt. Barcroft Station (12,470 ft.) lies on the upland surface about 5–6 miles to the northwest. Both stations are situated about 1 mile east of the range crest. Therefore climatic data from the two laboratories indicate differences due to elevation and exposure. Precipitation, relative humidity, and wind velocity are higher at Barcroft. Temperature and diurnal temperature change are greater at Crooked Creek, and a greater proportion of the total precipitation occurs as rainfall there. Both stations show principal wind directional maximums from the west and southwest and a lesser maximum from the north or northeast throughout the year. Major (1967, p. 119–122) evaluated climatic data at the two stations in terms of evapotranspiration and water balance.

Because pronounced geographical climatic gradients might produce similar trends in weathering intensities or soil development, it was desired to determine whether significant east-west or north-south climatic gradients exist today in the study area. For this reason five auxiliary weather stations (AWS) on the upland surface were maintained from June 1966 to August 1967 (fig. 273). The stations chosen were the Patriarch AWS, just south of the Patriarch picnic area; the Campito AWS, on the south flank of Campito Mountain; North Sage Hen AWS, on the north edge of Sage Hen Flat, above Crooked Creek Station; the Basalt AWS, on basalt cappings south of Crooked Creek Canyon; and the South Sage Hen AWS, on the southeast flank of County Line Hill. (See fig. 277 for locations.) Wind measurements recorded at Crooked Creek Laboratory were obtained from anemometers near the North Sage Hen AWS. All AWS sites were situated on relatively level topographic highs at spacings of 1½–3 miles.

Digitized by Google

TABLE 1.—*Summary of climatic means and extremes from Crooked Creek (10,150 ft) and Mount Barcroft Laboratories (12,470 ft) for the indicated periods*

	Crooked Creek Laboratory (1949–1965)												Crooked Creek Laboratory	Mount Barcroft Laboratory
	Jan.	Feb.	Mar.	Apr.	May	June	July	Aug.	Sept.	Oct.	Nov.	Dec.	1949-65	1953-65
Highest maximum temperature °F	52	51	52	62	69	76	78	74	72	76	61	57	76	72
Mean maximum temperature °F	30.1	31.7	32.7	40.7	46.9	58.3	65.2	63.9	58.4	50.3	40.6	34.3	46.1	35.5
Mean temperature °F	19.6	21.4	22.5	30.3	36.2	46.0	52.6	51.4	45.7	38.4	29.3	23.5	34.8	27.4
Mean minimum temperature °F	9.1	11.0	12.2	19.9	25.6	33.8	40.1	38.9	33.1	26.5	18.1	12.7	23.4	19.7
Lowest minimum temperature °F	-21	-21	-16	-10	2	12	22	17	10	-7	-13	-19	-21	-35
Mean diurnal differeno °F	21.0	20.7	20.5	20.8	21.2	24.5	25.1	25.0	25.3	23.8	22.5	21.6	22.7	16.1
Largest diurnal difference °F	41	46	47	42	45	38	42	41	49	58	49	40	58	44
Smallest diurnal difference °F	1	4	5	3	2	9	10	6	6	6	2	3	1	2
Mean days 33°F or above	13.8	13.8	17.1	24.0	28.4	29.9	30.9	31.0	30.0	29.4	23.9	19.4	291.6 per yr	204.5 per yr
Mean 8 a.m. relative humidity (percent)	57.5	61.2	59.1	55.4	51.5	40.1	40.6	41.4	44.8	45.5	52.5	55.1	50.7	55.1
Mean 8 a.m. barometer mm Hg	517.6	517.7	516.4	518.1	519.2	522.5	526.1	525.6	524.3	523.1	521.3	520.1	[1]523.8	[1]481.3
Mean snowfall in	15.0	18.1	17.0	16.8	12.9	3.5	.4	.2	1.2	5.1	11.1	13.3	114.4 per yr	164.4 per yr
Mean snow depth in	10.2	15.5	16.5	11.0	2.4	.1	.0	0	.0	.3	3.4	5.7	[1]4.7	[1]7.2
Highest snow depth in	72	74	84	62	47	12	1	3	1	12	30	50	94	73
Mean snow water in	1.51	1.62	1.38	1.63	1.11	.34	.04	.02	.12	.48	.92	.96	10.14 per yr	14.87 per yr
Mean rainfall in	.00	.00	.00	.00	.10	.06	1.30	.74	.48	.04	.00	.04	2.73 per yr	2.11 per yr
Mean total precipitation in	1.51	1.62	1.38	1.63	1.21	.40	1.34	.76	.60	.52	.92	1.00	12.87 per yr	16.98 per yr
Mean maximum wind (knots)	19.8	19.0	18.8	16.8	15.3	13.5	12.3	12.2	13.0	13.8	15.8	17.9	15.8	22.5
Maximum wind direction (percent):														
North	8.3	7.7	4.9	7.6	7.3	3.0	3.4	1.7	4.1	5.0	7.8	6.6	5.8	12.7
Northeast	10.3	16.8	11.4	10.3	14.2	10.3	8.0	7.2	5.8	11.8	13.6	12.3	11.0	5.6
East	2.3	3.6	2.2	2.7	1.4	4.8	4.1	6.1	5.4	3.8	3.0	2.4	3.5	5.4
Southeast	3.5	1.7	3.5	4.9	5.4	9.8	15.2	13.7	9.8	10.9	5.6	5.1	7.5	5.0
South	2.9	2.9	1.9	1.7	4.2	5.0	14.5	11.1	13.3	9.1	6.5	7.4	6.5	7.9
Southwest	26.1	15.7	23.5	29.9	25.1	32.7	25.1	33.9	29.1	27.3	24.2	23.4	26.2	17.0
West	32.4	36.0	33.8	33.1	31.5	27.7	26.1	22.3	26.9	25.8	29.4	27.1	29.6	39.9
Northwest	14.5	16.0	18.8	9.9	11.1	6.5	3.4	4.4	5.8	6.6	9.8	15.7	10.3	9.8

[1] 1953–62.

FIGURE 273.—North Sage Hen Flat auxiliary weather station and dust trap. Evaporimeter to left of pole, thermometer in white container to right of pole, dust trap on top. Rain gage to left and rear of stand. View west, showing parts of the upland surface, with the Sierra Nevada in distance.

Four-inch-diameter sections of stovepipe, 2½ feet long and sealed at the bottom, were used as rain gages. Lightweight oil was added to minimize surface evaporation. Taylor maximum-minimum window thermometers, suspended inside white ½-gallon ice cream containers, were used for temperature readings. Relative evaporation rates were obtained with modified Piche evaporimeters (Waring and Hermann, 1966). Temperature and precipitation readings were taken at bimonthly intervals from June 20 through September 1966, at the end of October 1966, and at monthly intervals from June to August 1967. Evaporation readings were obtained only during the summer of 1966. Table 2 summarizes types of data collected at each weather station.

TABLE 2.—*Types of information obtained at Crooked Creek Laboratory and five auxiliary weather stations during the period June 1966 to August 1967*

Name	Abbreviation	Position relative to center of area	Elevation (ft)	Maximum-minimum temperature	Precipitation	Evaporation rate
Crooked Creek	CC	Center	10,150	Yes	Yes	No.
Basalt	B	East	10,200	Yes	Yes	Yes.
Campito	C	West	10,440	Yes	Yes	No.
North Sage Hen	NSH	Center	10,660	Yes	Yes	Yes.
South Sage Hen	SSH	South	10,740	No	Yes	Yes.
Patriarch	P	North	11,250	No	Yes	Yes.

A plot of temperature and evaporation rates for the auxiliary weather stations and Crooked Creek is shown in figure 274. The Campito and North Sage Hen AWS sites show nearly the same maximum and minimum temperatures; the Basalt commonly has lower maximums and higher minimums. All Crooked Creek temperatures fall below those obtained on the upland surface, often by as much as 10–15°F. Evaporation data are quite spotty owing to malfunctioning at several sites, but the Basalt AWS values tend to be highest, followed by North Sage Hen, South Sage Hen, and the Patriarch. The comparison suggests a slight trend toward increasing evaporation rates from west to east, possibly owing to decreasing elevation. Since temperatures do not appear to increase eastward, the increased evaporation may be the result of a lower relative humidity. A comparison of precipitation at the five AWS sites and Crooked Creek (fig. 275) indicates highest values at

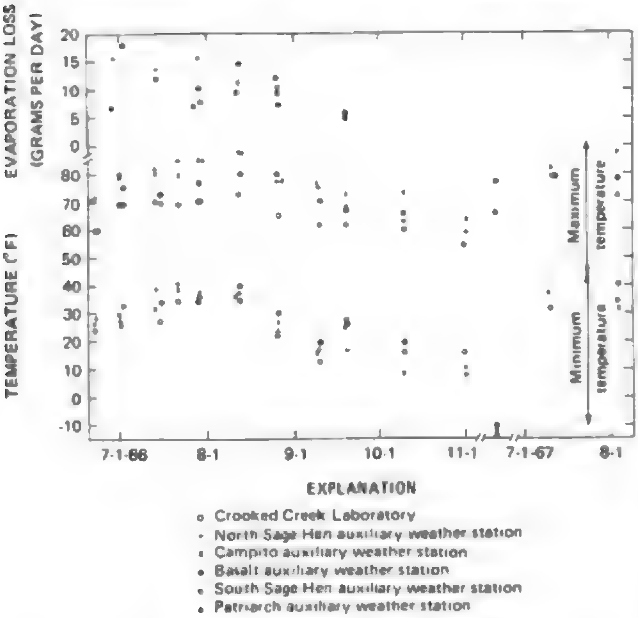

FIGURE 274.—Maximum and minimum temperature and relative evaporation rates at Crooked Creek Laboratory and five auxiliary weather stations in the study area

Crooked Creek, closely followed by the Patriarch AWS. All the other sites received much less precipitation and tend to follow the order North Sage Hen > Basalt > Campito > South Sage Hen. There is a general trend of increasing precipitation toward the north, and higher values were recorded in the valley of Crooked Creek than on the surrounding upland surface, probably because the AWS sites were exposed to high winds which would tend to decrease catchment of precipitation and to deflate snow accumulations.

Crooked Creek data for wind velocity and direction, barometric pressure, and to some extent, relative humidity, approximate present-day climatic conditions for most of the study area. Absolute precipitation values at Crooked Creek are probably much more reliable than those obtained at the auxiliary stations, but the fact that the latter are much lower should not be dismissed altogether, for they suggest that Crooked Creek values may be high owing to drifted snow blown from adjacent slopes. To obtain representative temperature estimates for nearby upland surface areas, Crooked Creek maximum temperatures should be increased by about 10°F and minimum temperatures by about 5°F. In the northern part of the study area, precipitation and relative humidity are probably somewhat higher and temperatures slightly lower than further south owing primarily to differences in elevation. With this exception, present climatic gradients in the study area are not marked.

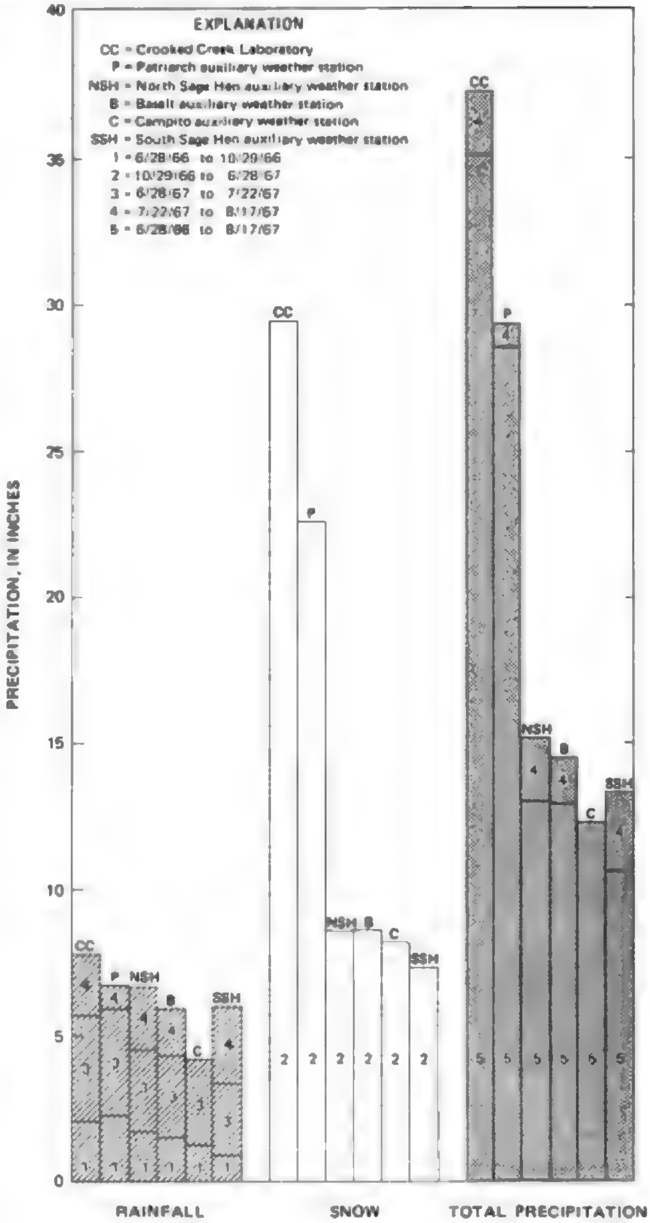

FIGURE 275.—Precipitation recorded at Crooked Creek Laboratory and at five auxiliary weather stations for the indicated periods

VEGETATION

The flora of the study area includes the Bristlecone Pine Forest and Sagebrush Scrub plant community types of Munz and Keck (1959, p. 11–18). Toward lower elevations the vegetation passes into Pinyon Juniper Woodland, and at higher elevations into Alpine Fell Fields. Stands of bristlecone pine (*Pinus aristata*), limber pine (*Pinus flexilis*), and aspen (*Populus tremuloides*) make up a discontinuous tree canopy along the

Digitized by Google

crest of the range below about 11,500 feet. A continuous shrub understory on noncarbonate soils is dominated by sagebrush (*Artemisia tridentata* and *A. arbuscula*) and to a lesser extent by rabbitbrush (*Chrysothamnus viscidiflorus*), mountain mahogany (*Cercocarpus ledifolius* and *C. intricatus*), creambush (*Holodiscus microphyllus*), mountain misery (*Chamaebatiaria millefolium*), and currant (*Ribes velutinum*). Beneath this two-story canopy of trees and sagebrush scrub is a nearly ubiquitous but sparse cover of grasses and herbaceous perennials, mostly low to the ground and often inconspicuous.

Most areas are dry, but moister conditions occur locally along streams and near seeps and springs. Such sites are characterized by annual grasses as well as *Carex spp.* (sedges), *Cirsium drummondii* (thistle), *Artemisia ludoviciana* (sagebrush), *Castilleja miniata* (paintbrush), and several species of *Penstemon* (beardtongue), *Mimulus* (monkey flower), and *Oenothera* (evening primrose).

Many plant species in the White Mountains are partly controlled by substrate in their distribution (Marchand, 1973). Edaphic restriction is evident in all vegetational strata, from bristlecone and limber pine to the smallest perennials. The principal botanical discontinuities occur across carbonate-noncarbonate boundaries (fig. 276): dolomites and limestones support similar vegetation as do, with a few notable exceptions, noncarbonate lithologies. Vegetation on sandstone and shale, granitic bodies, and basalt shows subtle differences which are sufficiently consistent to permit identification of three noncarbonate plant communities, each characteristic of a given bedrock type.

FIGURE 276.—Vegetational contrast between dolomite outcrops and colluvium (foreground and right rear) and sandstone colluvium (darker colored). Sandstone is covered by sagebrush and numerous other perennials, dolomite by certain [illegible] perennial herbs and bristlecone pine.

GEOLOGY

A complex mixture of sedimentary, igneous, and metamorphic rocks constitute the bedrock of the southern White Mountains (fig. 277). The oldest strata in the region are a slightly metamorphosed Precambrian to Early Cambrian succession of sandstones, shales, limestones, and dolomites. The Precambrian Wyman Formation, consisting primarily of sandstone and shale with minor but conspicuous lenses of white limestone, is the oldest of this group. Overlying the Wyman is the Reed Dolomite, a massive and very pure carbonate rock. The Deep Spring Formation, composed of alternating members of carbonate rocks (both limestone and dolomite) and clastic sediments (quartzitic sandstone and shale) overlies the Reed. The next youngest formation is the Campito, consisting of a lower quartzose sandstone member, the Andrews Mountain, and an upper shale member, the Montenegro. The Precambrian-Cambrian boundary, coinciding with the base of the *Fallotaspis* Olenellid biozone (Taylor, 1966), occurs within the upper part of the Andrews Mountain Member. The youngest stratigraphic unit of the group is the Poleta Formation, a somewhat shaly carbonate.

This succession was tilted toward the west and then intruded by the adamellites of Sage Hen Flat (130–138 m.y. (million years)) and Cottonwood area (151-170 m.y.) during the late Mesozoic (McKee and Nash, 1967, p. 672). Early to middle Tertiary erosion resulted in the beveling of a surface of low relief across the region (fig. 278), although monadnocks of Reed Dolomite and Andrews Mountain sandstone stood well above the erosion surface during its development. Parts of this surface were subsequently covered by thin local sediment and extensive basaltic flows (figs. 272, 279), K/Ar dated by Dalrymple (1963) at 10.8 m.y.

In terms of late Cenozoic structure, the White Mountains are an eastward-tilted horst which exhibits relatively greater uplift on the west, where a steeply dipping fault zone bounding the range has undergone as much as 10,000 feet of normal displacement. The east margin is also faulted along the northwest side of Deep Springs Valley, but individual displacements here are about 1,000 feet or less. The basalts and underlying erosion surface are tilted and faulted up from 6,000 feet at the northeast end of Deep Springs Valley to 10,800 feet at Bucks Peak, showing that tectonic activity occurred later than 10.8 m.y. ago. Bateman and Wahrhaftig (1966) presented convincing evidence for regional uplift of east-central California and western Nevada between about 9 and 3.5 m.y. before present and formation of Owens Valley and other collapse structures along the axis of uplift during a period of downfaulting beginning about 2.5 m.y. ago. The "Waucoba Lake

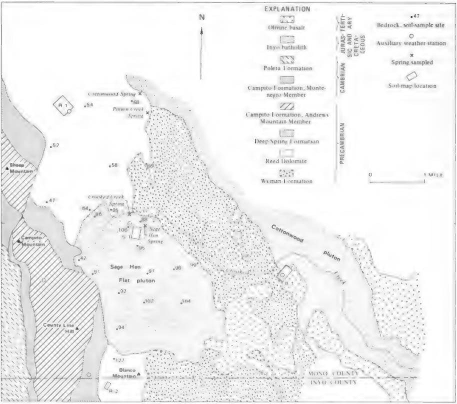

FIGURE 277.—General geology and sample locations in the study area.

Beds," exposed on the upthrown side of the frontal fault east of Big Pine, possess a predominantly Sierran mineralogy and apparently represent deposition in an early Pleistocene pluvial lake prior to the downfaulting of Owens Valley. The uppermost of several rhyolitic tuffs in the lakebeds has given a K/Ar age of 2.3 m.y. (Hay, 1966, p. 20). Coarse clastic debris from the White Mountains overlies and intertongues with the upper part of the lakebeds, which now dip westward at 5–7°, indicating some uplift of the range or downwarping of Owens Valley during the latter part of lakebed deposition, about 2.3 m.y. ago. The range-front faulting may have begun at this time, but cannot have preceded the lakebed deposition. Regional arching therefore appears to have preceded faulting by at least 1 million years in this area, although some uplift in the White Mountains may have occurred as recently as 2.3 m.y. before present.

Pleistocene glaciation along the eastern slope of the White Mountains north of the study area has incised cirques and U-shaped valleys into the upland surface and has left morainal and outwash deposits along the valley walls and floors. According to D. R. Powell (1967, oral commun.), recognizable glacial advances in the White Mountains appear to correlate with those of the eastern Sierra Nevada. Quaternary alluvium and terrace deposits are present along most of the major streams draining the range, especially on the east flank where gradients are gentler. Interbedded with terrace alluvium along Crooked Creek and its tributaries is a

Digitized by Google

FIGURE 278.—View north across Sage Hen Flat, showing degraded White Mountain erosion surface and outcrop areas of adamellite of Sage Hen Flat (light colored, foreground and middle distance), Reed Dolomite (white, tree covered), and Andrews Mountain sandstone (dark, left distance).

FIGURE 279.—View east from Sage Hen Flat, showing resistant basalt capping less resistant metasedimentary and granitic intrusive rock.

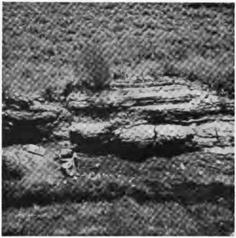

FIGURE 280.—Exposures of reworked rhyolitic ash interbedded with terrace alluvium along Crooked Creek. White layers are largely composed of pumiceous material.

white, reworked pumiceous ash (fig. 280), rhyolitic in composition and as much as 0.6 feet thick. Although glass shards and rhyolitic mineral fragments occur in soils throughout the area, no primary deposits have been seen. On the basis of major elements, trace elements, refractive indices, mineralogy, and physical appearance, the ash has been correlated with a source at Mono Craters (probable) or Mono Glass Mountain (possible), both located on the eastern Sierra Nevada slope south of Mono Lake (Marchand, 1968, 1970).

Those parts of the White Mountain erosion surface which have not been totally destroyed have been lowered several hundred feet to the level of Sage Hen Flat (fig. 278), Reed Flat (fig. 272), or similar areas of subdued, rolling topography by late Tertiary or Quaternary erosion. Frost heaving, solifluction (including altiplanation), nivation, and other periglacial phenomena continue to affect the range, becoming increasingly important toward higher elevations. Rillwash channels as much as 2 inches deep and debris accumulations behind trees, fallen limbs, bushes, and large boulders testify to the effectiveness of slope runoff processes, particularly on the relatively bare surfaces beneath bristlecone pine forest. Talus cones and stone stripes are frequent, particularly in the Campito Formation and other sandstones or shales. Although eastward draining canyons are gradually eroding headward into degraded remnants of the erosion surface, fairly extensive parts of the lowered surface are still relatively undissected and

Digitized by Google

often serve as a local or temporary base level for periglacial processes and slopewash. The effect of these circumstances is the accumulation of colluvium (consisting of weathered and unweathered rock, mineral, and organic material) on gentle slopes and in topographic lows on these surfaces.

To put present climatic data into perspective, it is necessary to consider the regional climatic and tectonic changes that have occurred in the area during the late Cenozoic. Any attempt at backward extrapolation of climatic conditions is extremely hazardous, especially in areas such as this where faulting and uplift have complicated an already complex series of fluctuations, but a few conclusions appear to be valid: (1) Cold, dry, climatic conditions such as those which currently characterize the area, and the more severe climates of glacial periods, are not conducive to rapid soil formation (for example, cf. Morrison, 1964, p. 114); (2) the White Mountains area was at a lower and presumably warmer elevation and probably did not lie in the Sierran rain shadow prior to regional uparching, between 9 and 3.5 m.y. ago; (3) considering the total duration of warm, wet, or warm and wet intervals which promote rapid weathering, it would appear likely that most of the total amount of soil formed on the White Mountain surface occurred prior to or during the regional uplift, perhaps augmented during extended interglacial periods. The immaturity of present soils indicates that most of the weathered debris has been stripped by erosion, but the extreme weathering of some soil grains may date from an earlier period of soil formation.

CHEMICAL WEATHERING AND SOIL DEVELOPMENT

Chemical weathering is so closely interrelated with physical weathering that it is sometimes difficult to distinguish their separate effects. Taken together these two processes are responsible, along with various organic effects, for the development of soil. Because of the close ties between physical and chemical processes in the evolution of soils, both aspects are considered here, although primary emphasis is placed on chemical weathering.

METHOD OF APPROACH

The immature soils in this area formed on four widespread parent materials. Because spring waters closely related to sandstone and basalt were not available and because changes in the liquid phase are important considerations in this study, detailed discussion is restricted to the Reed Dolomite and adamellite of Sage Hen Flat, two commonly recurring lithologies for which closely related spring waters could be obtained. For the dolomite and adamellite the sequence and degree of physical weathering is evaluated, and problems of soil contamination are discussed. Chemical weathering is approached from the perspectives of chemical and mineralogical changes in dolomite and adamellite and of chemical changes in liquid phases associated with each lithology.

FIELD METHODS

After the geologic and soil mapping of the area (figs. 277, 281–284), 84 sample sites, about 20 to each lithology, were chosen at relatively even spacings on Reed Dolomite, adamellite of Sage Hen Flat, basalt, and sandstone of the Andrews Mountain Member of the Campito Formation. (See fig. 277 for site locations.) Topographic highs were selected for sample locations to minimize contamination by slopewash, mass wasting, and aeolian processes. Soil samples encompassing the entire profile above the C horizon were collected at every site and fresh bedrock samples were also obtained on dolomite and adamellite sites. Eight surface soil pH measurements (determined using pHydrion paper and a Truog indicator kit) were made at each site within a 7-foot radius of the soil pit. The dimensions of the pit were measured as closely as possible, its volume was calculated, and the soil samples were weighed (air dry) after collection to obtain bulk density figures for the whole soil. Representative profiles were described, and field impregnations were made at several sites for dolomite, adamellite, and basalt soils. Over a 14-month period from June 1966 to August 1967, samples of rain, snow, and of spring waters related to the adamellite and dolomite were collected.

LABORATORY METHODS

Samples of both dolomite and adamellite were randomly selected for detailed chemical and mineralogical study in the laboratory. Minerals were identified primarily by petrographic microscope, aided by reflecting microscope for opaque minerals. Compositions of glass fragments were determined by immersion oils, universal stage, and electron microprobe. The microprobe was also used to assess chemical alteration within weathered minerals. Estimates of major mineral percentages in fresh adamellite were determined from point counts of stained thin sections. Percentages of minor mineral phases in adamellite, all dolomite constituents, and all minerals in sand fractions of soils were obtained from line counts of grain mounts, after two heavy-liquid separations. Silt- and clay-sized fractions were analyzed qualitatively and quantitatively by X-ray diffraction. Layer silicates were identified following the methods of Warshaw and Roy (1961). Contaminative rhyolitic glass in the silt range of soils was estimated visually in oil immersion mounts. X-ray fluorescence was employed in the chemical analysis of bedrock and soil samples. Standard sieve and pipette techniques were utilized in size analyses of 26 dolomite

igitized by Google

and adamellite soils. Other analytical methods used are discussed at appropriate places in the report. For a more detailed account of procedures, precision, reproducibility, and comparisons of methods, the reader is referred to the section "Supplemental Information."

Table 3 summarizes the estimated precision of measurement for some of the analyzed quantities discussed in the text. All percentages in the text, tables, and figures are weight percent, unless otherwise noted.

TABLE 3.—*Estimated precision of measurement for some analytical quantities discussed in this paper*

[See also "Supplemental Information"]

Analytical method	Estimated range of precision (percent of given value)
X-ray fluorescence	±6
Grain counting:	
Major minerals	±5
Minor minerals	±10–15
X-ray diffraction (silts)	±15
Size distribution:	
Sieve range	±2
Pipette range (silt and clay)	±10
Plant ash analyses	±20 (usually < 10)
Analyses of water-saturation extracts	±25
NH_4Ac extract analyses	±20

DESCRIPTION OF SOILS

CLARIFICATION OF TERMS

In the White Mountains, as in other areas of high relief, absolute distinctions between residual soil and weathered colluvium are essentially arbitrary. Periglacial processes, as well as mass wasting, slopewash, and aeolian transport, are actively moving loose material into topographic lows. Many definitions of soil imply formation by in situ weathering alone (for example, cf. Brewer, 1964, p. 7–8), apart from the effects of erosion and deposition. For purposes of this discussion, the term "soil" will be expanded from this usage to include some colluvial and windblown material. In the present context, "soil" encompasses all weathered or slightly weathered surficial debris other than talus, stone stripe boulders, slopewash fans, alluvium, and sand dunes and necessarily includes debris that has undergone some slope transport, albeit of relatively short distance in many cases.

The White Mountains soils are almost exclusively poorly developed lithosols having general $A_{11}/A_{12}/C/R$ profiles less than 13 inches deep. Color, structural, or textural B horizons are faintly visible in a few profiles, but such occurrences are rare. Calcium carbonate crusts can be found on all lithologies, but are abundant only on dolomite soils. An irregular surface layer of relatively large fragments (A_{11} horizon), brought to the surface by frost heaving, is a common feature of most profiles, independent of parent material. Beneath this stratum is a layer of finer grained weathered material (A_{12} horizon), usually overlying large partly weathered fragments in a matrix of silt and sand (C). Fresh bedrock (R) is generally encountered within 1 or 2 feet of the top of the C.

Planetable maps of topography and maximum soil depth for representative areas within dolomite, adamellite, and basalt terranes are shown in figures 281–284. Maximum soil depth was taken as the greatest penetration of a 1-inch-diameter soil auger in repeated borings at a given location. These depths correspond to the approximate top of fresh bedrock, except in deep profiles where lateral friction on the auger made further penetration impossible. The map isochores indicate a general thinning over topographic highs and steep slopes and thickening in local depressions, especially on Sage Hen Flat. Soil thickness appears to be somewhat erratic on the basalt and dolomite. Two dolomite areas at different elevations show no appreciable differences in soil depth. In the Patriarch area, the thickest soils occur in minor interfluves, and the thinnest are found in the intermittent stream channels, suggesting that the latter are presently sites of erosion or slow weathering. This relation contrasts with that of Sage Hen Flat, where surficial material is thickest along topographic lows.

The application of lithologic names to soil units (that is, Reed Dolomite soil) represent informal usage only;

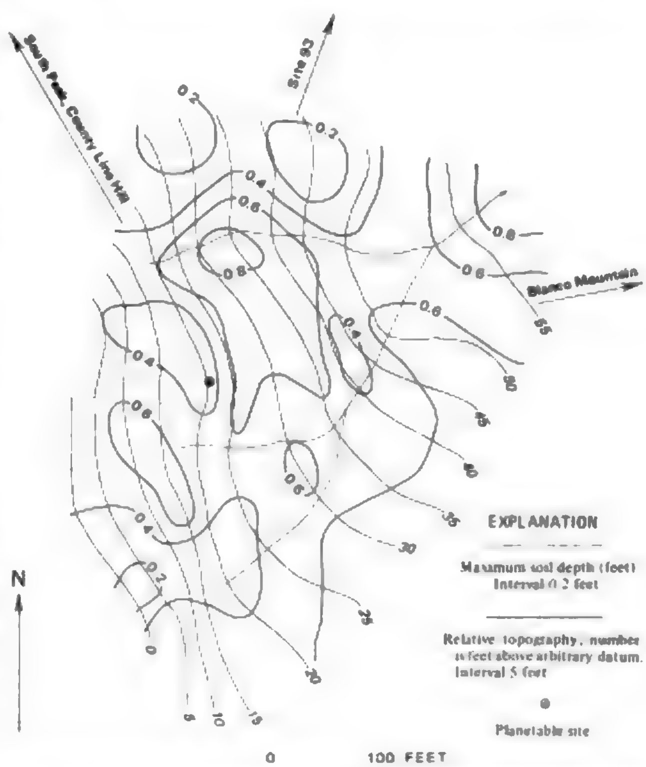

FIGURE 281.—Depth of soil and colluvium at planetable map site R-1, Reed Dolomite, 10,600 feet.

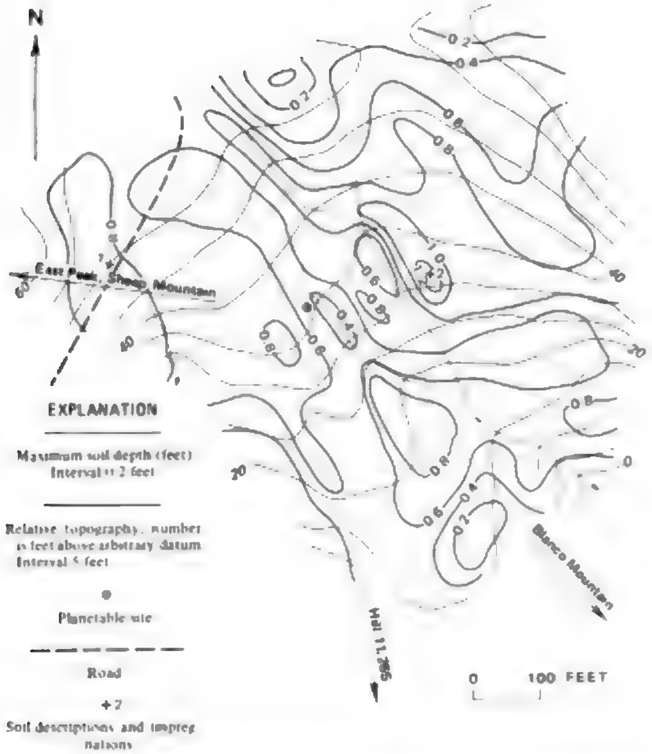

FIGURE 282.—Depth of soil and colluvium at planetable map site R-2, Reed Dolomite, 11,200 feet.

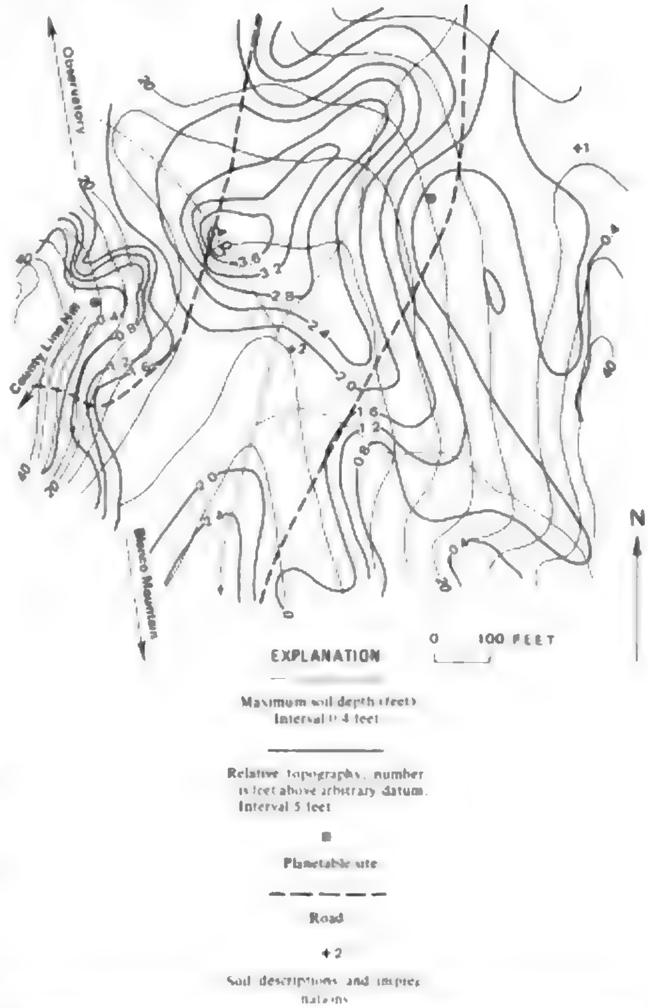

FIGURE 283.—Depth of soil and colluvium at planetable map site S-1, adamellite of Sage Hen Flat.

no attempt has been made to formally designate or map soil series in this area.

REED DOLOMITE SOILS

Average soil profile thickness to Reed Dolomite bedrock, about 7 inches at sampled sites, is slightly greater than for other soil groups. White calcium carbonate surface crusts, usually discontinuous and less than one-half inch thick, are one of the most conspicuous features of the Reed profiles. Calcium carbonate is absent in lower parts of the A horizon, but occurs at the A–C interface and on nearly all rock fragments within the profile. Local O horizons, consisting of undecomposed and partially humified plant litter together with a few mineral grains occur sporadically beneath trees. Where O horizons are present, carbonate crusts are absent. Rock fragments concentrated near the surface in A_{11} horizons (fig. 285) usually appear quite fresh, except for minor solution pitting. Rock in the C horizon, however, is often so thoroughly decomposed that it is easily broken with a trowel. A_{12} horizons are occasionally quite red owing to oxidation of Fe-bearing minerals. Subangular blocky peds are common here, but structure in other horizons is generally single grained or massive. The pH may be below 7.0 in or near O horizons, but the normal range is between 7.5 and 8.2, appreciably higher than in noncarbonate soils. The pH tends to be high at the surface, lower in the A horizon, and high again near and within the C horizon, causing precipitation of calcium carbonate in localized areas of high pH within the soils.

ADAMELLITE SOILS OF SAGE HEN FLAT

The soils on adamellite of Sage Hen Flat are characterized by a general lack of large rock fragments above the C horizon. The surface horizon is commonly a grus, consisting of granules and coarse sand, and is usually less than 1 inch thick (fig. 286). Calcium carbonate crusts, although occasionally present, are not common and may result from solution of inblown carbonate grains. O horizons occur in forested areas. Sandy loam A_{12} horizons are infrequently underlain by weak color, structural, or textural B horizons, in which iron oxidation, subangular blocky structure, and very weak clay

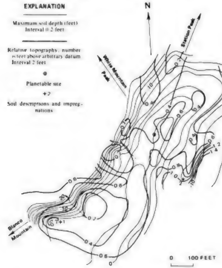

FIGURE 284.—Depth of soil and colluvium at planetable map site B-1, on basalt.

FIGURE 285.—Reed Dolomite soil pit showing accumulation of large fragments (A_{11} horizon) overlying finer grained A_{12} horizon.

films may be visible. The transition to the C horizon is often abrupt on topographic highs, but gradual in areas where the parent material is largely colluvial. Fragments in the C horizon may bear only thin weathering

FIGURE 286.—Soil pit in adamellite of Sage Hen Flat. Thin grus layer (A_{11} horizon) overlies A_{12} horizon, which tends toward a color and textural B at some sites. Lighter colored C horizon is transitional downward into unweathered colluvium (not shown).

rinds or may be quite thoroughly decomposed. Depth to bedrock averages about 6 inches on topographic highs.

BASALT SOILS

Basalt soil profiles average about 6 inches in depth and are characterized by good crumb structure in most A horizons and by a sharp A–C contact. Calcium carbonate crusts are rare, the surface layer generally consisting of coarse fragments or basaltic grus. Beneath this pavement is a vesicular gravelly loam to clay loam A_{12} horizon, as much as 4 inches thick, with subangular blocky peds. The lower part of the A horizon is often oxidized, but rarely is there other evidence of an incipient B horizon. Surface cracking and the degree of aggregation suggest higher clay contents than in other soils. Roots are uncommon, and O horizons are never present. The pH does not vary consistently with depth in the profiles.

ANDREWS MOUNTAIN SANDSTONE SOILS

Soils formed on the Andrews Mountain sandstones

Digitized by Google

and shales show a striking bimodal size distribution: Large rock fragments are concentrated at the surface near and within the C horizon, while sand, silt, and minor clay occur primarily in the A_{12} horizon. Calcium carbonate crusts are present locally but are not common. The A_{12} horizon is usually single grained or massive, although aggregation into crumbs may occur. The C horizon consists of colluvium or slightly weathered bedrock. As in other noncarbonate soils, the pH is generally 7.0 or slightly below and does not change systematically within the profile.

SOIL CONTAMINATION

Mineralogical analyses of five soils derived from the Reed Dolomite reveal from 3 to 73 percent of material, primarily volcanic glass, quartz, feldspars, biotite, and hornblende, that cannot be accounted for by weathering changes. The principal sources of this contamination are the pumiceous ash from the Mono Craters or Mono Glass Mountain (as much as 30 percent) and local windblown fragments (as much as 50 percent). The extent, nature, and implications of the soil contaminants were discussed elsewhere (Marchand, 1970). Their abundance necessitates considerable correction of soil data at most sites, as explained under "Chemical Weathering," and renders many soil samples uninterpretable in terms of weathering.

PHYSICAL WEATHERING

REED DOLOMITE

The Reed Dolomite is strongly jointed in one direction. Cross jointing is common, breaking the crystalline rock into angular fragments of about 3 feet to less than one-half inch in maximum dimension.

Bedrock grain size varies considerably depending on degree of recrystallization due to thermal metamorphism. Micrometer eyepiece examination of 16 bedrock samples indicate a mean diameter range of from 0.002 to 2 mm. Dolomite displaying spheroidal weathering has a bedrock grain size range from 0.125 to 2 mm, but angular dolomite is much finer grained, ranging from 0.002 to 0.125 mm.

Cumulative grain size frequency curves for 10 dolomite soil samples (fig. 287) show strong bimodal distributions indicative of immature weathering. The two modes are in fragments above 8 mm (jointed blocks) and in finer materials derived from the large blocks. For comparison, the range of bedrock grain size has been superimposed on the diagram. Triangular plots of dolomite, adamellite, and Andrews Mountain sandstone soils in terms of gravel, sand, and silt and clay, and of sand, silt, and clay are shown in figures 288 and 289, respectively. Gravel percentages vary greatly owing to extremely large fragments whose presence or

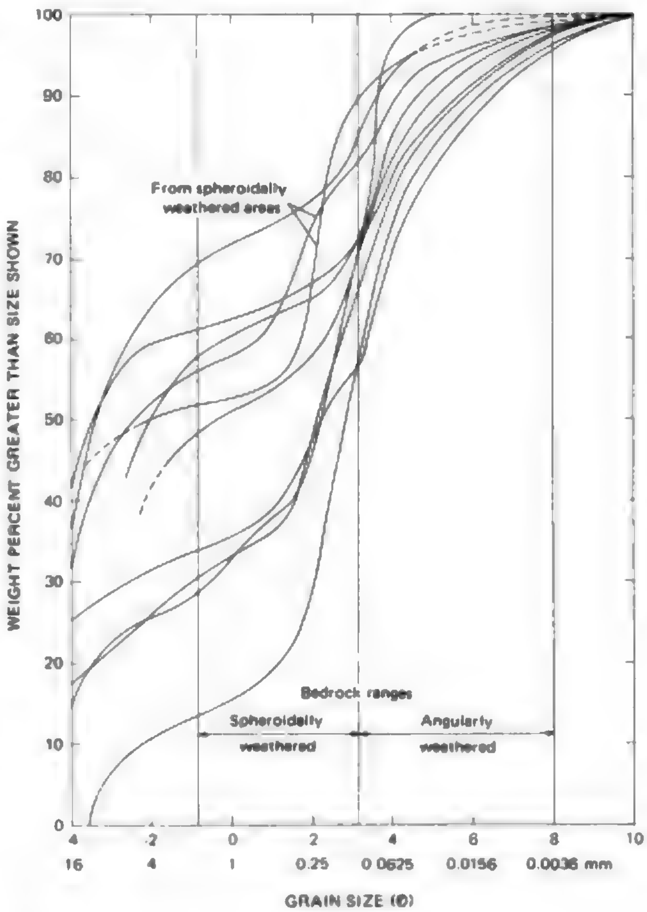

FIGURE 287.—Cumulative grain size frequency curves for dolomite soils and comparison with ranges in bedrock grain size based on samples from both spheroidally and angularly weathered sites.

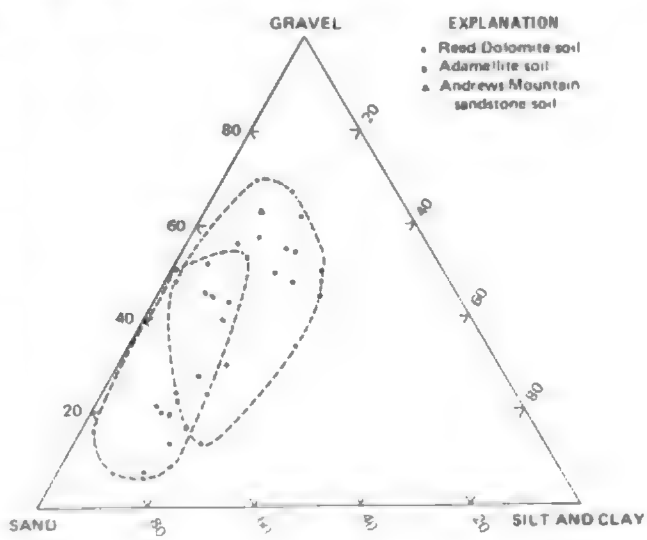

FIGURE 288.—Gravel, sand, silt, and clay distribution for soil above the C horizon.

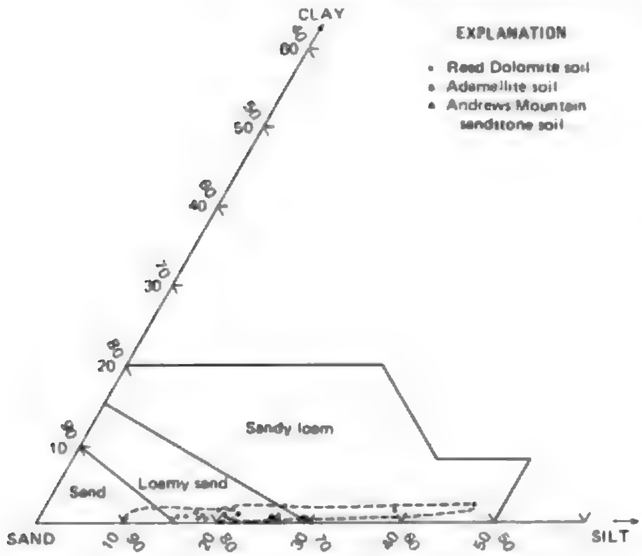

FIGURE 289.—Sand-silt-clay distribution for soil above the C horizon.

absence strongly influences the results. Relative amounts of sand, silt, and clay are more consistent.

The pattern of physical rock weathering after jointing and surface exposure appears to be a function of the earlier thermal history of the rock. Carbonates (both limestones and dolomites) adjacent to the Sage Hen and Cottonwood plutons tend to weather relatively rapidly to produce spheroidal boulders, whereas slower weathering of angular blocks characterizes carbonate terrane away from plutonic contacts. Most dolomite soils show maximums in the 2–4 phi interval, but several samples derived from thermally metamorphosed and spheroidally weathered dolomite have modes in the 1–2 phi range. Dolomite joint blocks have thus undergone two types of breakdown: (1) Fine-grained dolomite blocks have remained angular, and slow physical disintegration has produced smaller polycrystalline aggregates; (2) intergranular stresses within coarse-grained recrystallized dolomite developed during cooling from metamorphic conditions to subaerial temperatures have caused breakdown to single-crystal grains. This second weathering pattern was first noted and explained by LaMarche (1967), who contended that spheroidal forms are created by preferential attack at corners and edges of the more susceptible rock and are maintained by the greater porosity of the weathering block exterior. The author's observations corroborate those of LaMarche except that unrecrystallized dolomite commonly weathers to polycrystalline rather than monocrystalline grains as suggested by LaMarche, at least in the initial phase of physical weathering. Cleavages apparently afford an easier avenue of parting than the tightly held grain boundaries, except where contraction has created intergranular weaknesses.

ADAMELLITE OF SAGE HEN FLAT

Joints spaced as closely as 2–6 inches, but more commonly several feet apart, occur throughout the Sage Hen Flat pluton and tend to fall into two categories: A principal group trending north-northeast and dipping steeply to the southeast and a secondary group striking northwest and inclined to both northeast and southwest. Joint blocks are larger than in the dolomites and consequently have a lesser effect on weathering processes. Some joint openings and adjacent wallrocks have been silicified, sericitized, and tightly cemented with iron oxides. Such alteration is almost certainly deuteric or hydrothermal, as large crystals of mica have grown within feldspars adjacent to joint planes, in contrast with the fine-grained feldspar weathering products observed in soil thin sections. The altered joint planes and adjacent rock weather in positive relief with respect to adjacent adamellite (fig. 290), as do fine-grained mafic inclusions and aplitic dikes.

The medium-grained hypidiomorphic-granular texture of the adamellite locally tends toward porphyritic, but microscopic examination of 17 thin sections indicates that mean grain size never exceeds 4 mm. Average grain diameters commonly range from −0.5 to 3.5 phi.

In figure 291, cumulative grain size frequency curves for 10 adamellite soil samples and two grus samples are shown, along with the superimposed average and extreme ranges of bedrock grain size. With few exceptions, the adamellite soils are unimodal, the maximum frequency occurring between 2 and 9 phi in most samples. This mode falls within the mean bedrock range, sug-

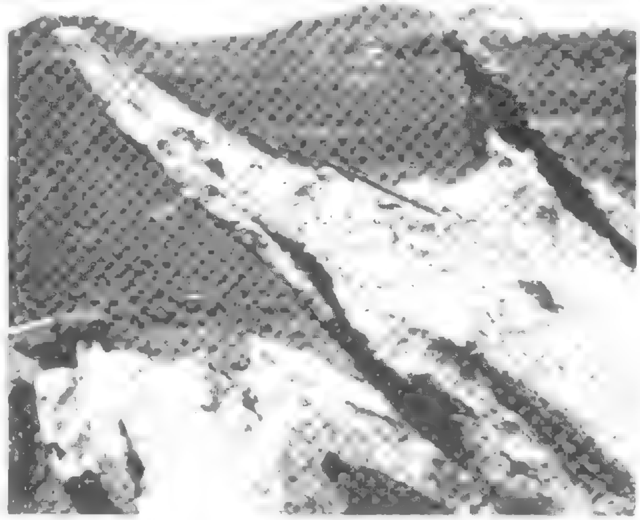

FIGURE 290.—Weathered adamellite outcrop on Sage Hen Flat. Note relative resistance of altered joint planes. Pencil gives scale.

Digitized by Google

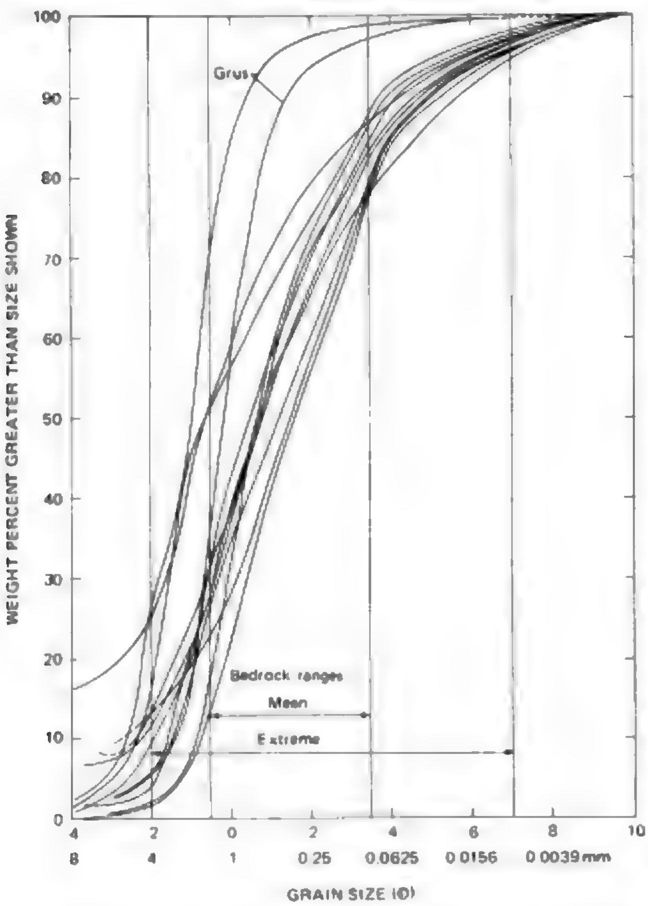

FIGURE 291.—Cumulative grain size frequency curves for adamellite soils and comparison with ranges of bedrock grain size.

gesting a tendency toward production of single-crystal grains by physical weathering. Two grus samples, however, collected beneath exfoliating boulders, show modes of -1–0 phi. This material is commonly composed of polycrystalline aggregates and occasional large grains.

On textural triangular diagrams (figs. 288, 289), adamellite soils of Sage Hen Flat plot closer to the sand component and farther from the gravel and silt components than do the Reed soils. Large joint blocks are rare in the adamellite soils, unlike the dolomite soils. Silt-sized grains are not common in fresh adamellite and have not been produced to any notable degree by weathering.

A two-stage process of physical weathering is suggested by the data. An initial breakdown into polycrystalline grus, occurring at the weathering surface of rock masses, is followed by a size reduction to monomineralic grains within the soil profile.

MECHANISMS OF DISINTEGRATION

Of the many mechanisms suggested for physical weathering and exfoliation, repetitive freezing of interstitial water seems the most applicable to relatively cold regions such as the White Mountains. At Crooked Creek Laboratory, temperatures descend below freezing on an average of about 220 days per year, and most of the precipitation occurs during the winter.

A striking feature of physical disintegration in the study area is that the same process applied to several lithologies has resulted in differing soil grain size distributions. This observation and the similarity of grus development from granitic rock here with that in much wetter and warmer areas suggest that rates and products of physical weathering may be as much a function of inherent lithologic properties as of climatic conditions. For frost riving to be effective, water must be able to penetrate the rock. The fact that coarse-grained lithologies weather more rapidly than fine-grained rocks of the same composition lends credence to LaMarche's (1967) hypothesis that contraction of large mineral grains during cooling from elevated temperatures may result in weakened intergranular bonds, affording access to water during weathering. Grain size may thus be one factor causing plutonic rocks to weather more rapidly than basalt: A larger grain will contract more than will a smaller grain having cooled the same amount, creating wider intergranular spaces or, if no separation occurs, greater intergranular tensional stresses. Fissility, grain adhesion and cohesion, and jointing may also be important factors in determining degree of water penetration.

It is not the author's intent to imply that the contraction mechanism is the only likely cause of grus formation. Wahrhaftig (1965, p. 1178–1179) suggested that alteration of biotite to swelling clays may aid in splitting apart intrusive rock into granular fragments. Evidence presented in the following pages indicates that expandable clays are not an important biotite weathering product in this area, but Helley (1966) showed that biotite can swell without being chemically altered. The absence of biotite or similar alterable minerals in the dolomite, however, necessitates an explanation other than presence of expandable minerals in this case.

An interesting aspect of erosion in the White Mountains is the striking correlation between erosional resistances and the manner of physical weathering in various lithologies. Fine-grained carbonate, quartzose sandstone, basalt, and aplitic dikes and mafic inclusions within the plutons are relatively resistant to erosion. These lithologies tend to produce immature soils having bimodal size distributions, large fragments representing one of the modes. Physical breakdown of such mat-

erial into fine particles is obviously very slow and the larger blocks are not easily eroded. Recrystallized carbonates, plutonic rock, and shales are much less resistant to physical weathering. These lithologies tend to yield submature soils lacking strong bimodal size distributions and containing sand-, silt-, and clay-sized particles which can be removed by rillwash and sheetwash. Thus erosion is faster in areas underlain by coarse-grained or fissile rock types (Marchand, 1971).

CHEMICAL WEATHERING

CHANGES IN THE SOLID PHASES

MINERALOGICAL CHANGES

Reed Dolomite

The Reed Dolomite is close to a pure carbonate, containing less than 0.5 percent of minerals other than dolomite (table 4). Talc comprises as much as 0.46 percent, but is generally less than 0.1 percent. Ilmenite, quartz, K-feldspar, plagioclase, apatite, epidote, and garnet are often present in trace amounts, and tremolite occurs in two of the five samples studied quantitatively. Although never observed in thin sections or oil immersion mounts, a few grains of biotite, hornblende, and magnetite were found in several grain mounts, possibly as a result of sieve contamination. Traces of chlorite and sericite were identified by X-ray diffraction of dolomite residues.

Table 4.—*Mineral weight percentages in five Reed Dolomite bedrock samples, based on line counts of grain mounts*

	54	68	47	65	127
Dolomite	99.51	99.68	99.97	99.96	99.93
Talc	.46	.090	.0336	.0067	.065
Tremolite	......	......	.0005	.0010	......
Ilmenite	.0496	.0214	.0143	.0117	.006
Magnetite	.01	Trace	......	......	......
Quartz	.0012	.0001	.0119	.0008	.001
K-feldspar	.0002	......	.001	.0013	.00003
Plagioclase	.0004	.20	.004	......	.001
Biotite	.0007	.006	.0003	.0013	......
Hornblende	......	.0003	.0005	.0004	.00012
Apatite	......	.0068	.0002	.0004	.00012
Epidote	......	......	.0001	.0004	......
Garnet	......	.0001	.0001	.0009	......
Chlorite	......	......	......	.0014	......
Zircon	.0003	.0002	......	......	......

Oil immersion and grain mounts of 3–8 phi (125–4 μm) size fractions of five dolomite soils were examined for degree of etching or alteration of primary noncontaminative grains. Dolomite is strongly etched in all samples and in all size fractions (fig. 292), although effects are increasingly evident in finer particles. Tremolite is consistently etched, especially at the grain terminations, its degree of weathering being generally comparable to or slightly less than that of hornblende in adamellite soils. The weathering of talc is variable: In some samples it appears to be quite fresh, but in others has produced extremely irregular grain boundaries (fig. 293). K-feldspar, plagioclase, and biotite show minor weathering alteration. Apatite grains are often rounded, showing effects of some solution. Quartz and ilmenite show little or no alteration, with the exception of very minor oxidation around the edges of a few ilmenite fragments. A general four-category weathering sequence, based on the preceding observations, is shown in figure 294. Attempts to quantify the sequence through grain counts proved unsuccessful owing to the abundance of contaminants.

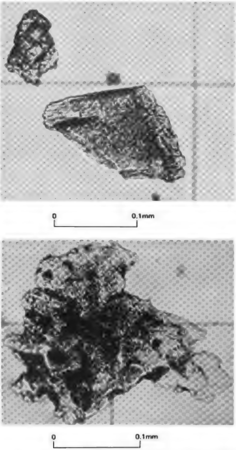

Figure 292.—Dolomite. *A*, Fresh, crushed bedrock (#47). Plane light. *B*, Etched, embayed, altered soil grain (#68 soil, fine sand). Plane light. Note tendency of etching to follow cleavage directions.

Digitized by Google

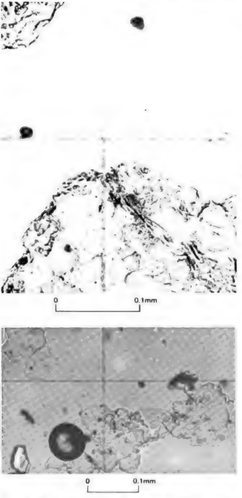

FIGURE 293.—Talc. A, Fresh crushed bedrock talc (#47). Plane light. B, Soil talc grains (#47 soil, crushed 50–230 mesh). Grains to upper left are not strongly etched but lower right grain shows large embayment. Plane light.

The only mineral that is definitely authigenic in Reed soils is calcite, which appears in both silt and clay fractions of about half of the analyzed samples. Several soil samples contain 7 A, 10 A, and 14 A layer silicates in both silt and clay fractions. These clay minerals are not believed to be authigenic; they possibly represent the chlorite and sericite originally present in the dolomite, plus aeolian additions from the surrounding terrain.

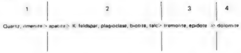

FIGURE 294.—Mineral weathering sequence in Reed Dolomite soils, in order of decreasing resistance. Based on visual comparison of bedrock and noncontaminative soil grains. Vertical lines separate major divisions of resistance.

ADAMELLITE OF SAGE HEN FLAT

The mineralogy of the Sage Hen Flat pluton is typical of an adamellite. Quartz, microcline, and plagioclase make up more than 90 percent of the rock; biotite ranges from 3 to 7 percent; hornblende, muscovite, chlorite, epidote, sphene, ilmenite, and magnetite account for as much as 4 percent of the total; and allanite, zircon, apatite, and tourmaline are commonly present in trace amounts. A few pyrite grains were noted under the reflecting microscope.[2] Mineral percentages in five adamellite bedrock samples are given in table 5, and chemical compositions of principal minerals in the pluton are given in table 6.

Minerals in the silt and fine-sand fractions of Sage Hen soils and in soil thin sections were examined for size reduction and weathering modifications of margins, as compared with fresh bedrock grains. Plagioclase of composition An_{25-30} in the cores of zoned crystals is generally the most strongly weathered mineral in adamellite soils (fig. 295); fine-grained alteration products, chiefly kaolinite, sometimes make up much of the original plagioclase. Hornblende grains frequently possess no unmodified boundaries, the terminations

TABLE 5.—*Mineral weight percentages in five adamellite bedrock samples from Sage Hen Flat based on point counts of stained thin sections*

	86	101	94	97	105
Quartz	29.2	30.2	23.9	30.8	39.7
K-feldspar	25.8	19.1	25.4	25.7	23.4
Plagioclase	37.9	41.0	38.8	33.5	26.9
Biotite	6.7	5.4	5.5	3.2	7.1
Chlorite	.022	.24	.42	.102	.32
Muscovite	.05	.3	2.1	1.2	1.62
Hornblende	.13		.61	.008	
Epidote	.037	.75	.76	2.8	.39
Allanite	.0004	.088	.18	Trace(?)	.018
Sphene	.0081	1.10	.32	.0003	.0854
Zircon	.0064	.008	.0005		.0037
Ilmenite	.0016	.60	.0045	.105	.42
Magnetite	.0016	1.27	1.98	2.65	Trace
Apatite	.015	.025	.03	.003	.025
Tourmaline			.03		

---

[2] Sulfides are localized along joints and near the margins of the pluton and are consequently not common in the samples examined. All nonmagnetic opaque minerals are therefore contained under the term "ilmenite" for the purposes of this discussion. The weathering of [illegible] concentrations, however, could definitely [illegible] as evidenced by significant [illegible] among the pluton.

TABLE 6.—*Chemical compositions of 10 major minerals in the adamellite of Sage Hen Flat*

[Methods of determination as indicated. All Fe assumed to be in ferric state]

	Electron microprobe (percent)											U Stage	Oil immersion		
													Indices of refraction		
	An	Ab	Or	Annite (Fe biotite)	Phlogopite	K	Ca	Mg	Fe	Al	Ti	An	Nx'	Ny	Nz'
Plagioclase:															
Maximum	30.5	88.2	2.1						.3			29			
Minimum	10.5	66.9	.4						.1			15			
Mean	20.9	77.2	1.1	(Ba=0.0)					.3						
Microcline:															
Maximum	.2	12.7	95.8						.3						
Minimum	.0	2.4	85.4						.1						
Mean	.0	7.1	93.7	(Ba=0.0)					.2					1.522	1.525
Biotite:															
Maximum				48.8	44.4	7.7									
Minimum				40.6	31.5	7.0									
Mean				43.4	38.1	7.5	(Ba=0.79)							1.633	
Chlorite:															
Maximum							Trace	10.0	19.8						
Minimum							.0	8.9	18.2						
Mean							.0	9.5	18.6					1.624	
Hornblende:															
Maximum							7.6	8.5	10.4						
Minimum							7.0	7.3	9.2						
Mean							7.3	7.7	9.9						
Epidote:															
Maximum							17.2	.0	9.9						
Minimum							16.0	.0	8.5						
Mean							16.5	.0	9.2					1.756	1.773
Allanite:															
Maximum							9.4		12.7	9.3					
Minimum							7.1		10.9	7.0					
Mean							8.0		11.5	8.2			< 1.775	1.772	>1.775
Sphene:															
Maximum							24.5	.0	1.5	0.8	19.8				
Minimum							21.7	.0	1.1	0.6	18.7				
Mean							23.3	.0	1.2	0.7	19.1		1.898	1.941	>2.00
Magnetite:															
Maximum								.08	71.7		.19			No	Ne'
Minimum								.00	70.4		.10		Apatite	1.630	
Mean								.01	70.8		.13		Tremolite	1.624	1.610
Ilmenite:															
Maximum								.15	33.0		27.9				
Minimum								.01	31.0		24.9				
Mean								.06	32.2		27.2				

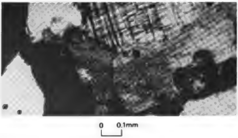

FIGURE 295.—Weathered grains in adamellite soil thin section. Core of plagioclase (lower center to right center) is considerably altered. Microcline (upper center and upper right) has parted along cleavages and shows slight alteration. Quartz (left) is fresh. Crossed nicols.

often displaying considerable etching. Many grains show no such effects, however, suggesting that the more severely etched fragments, and perhaps the dolomite soil talc grains as well, may owe their modifications to an earlier and more intense period of weathering. Along edges and cleavages biotite (fig. 296) is altering to secondary products, which are discussed in the section

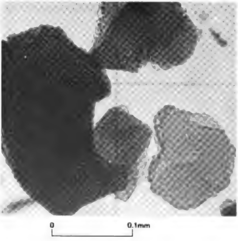

FIGURE 296.—Soil biotite grains (#86 soil, fine sand), showing both altered (upper left and upper center) and relatively unaltered margins (lower center). Plane light.

Digitized by Google

"Biotites." Biotites and epidotes have lost appreciable portions of their original margins, but irregular grain boundaries are only occasionally found on soil allanites. Microcline (fig. 295) and An_{10-15} plagioclase in the rims of normally zoned fragments commonly show some alteration to clay. Chlorite and apatite grains are frequently rounded, but are never deeply etched. Ilmenite and magnetite, especially the latter, may show minor external oxidation, but such changes are not common. Sphene, quartz (fig. 295), and muscovite display very little evidence of etching or alterations, but irregular boundaries not seen in bedrock grains are occasionally present. Soil zircons show perfectly euhedral margins. A seven-category weathering sequence for minerals in adamellite soils, based on the preceding evidence, is given in figure 297. In any given sample, a mineral may deviate from the sequence by one category, either above or below, but in general the order is consistent in all the samples studied. As in the case of the dolomite soils, quantitative mineral weathering studies were complicated by contaminants and yielded no substantial information not given by figure 297. In figure 305, mineral percentage changes with respect to bedrock are shown for the sand and silt fractions of #94 soil, a relatively uncontaminated site.

Qualitative data for phyllosilicates in the silt and clay fractions of some adamellite soils are summarized in table 7. Sericite, normal chlorite, and septechlorite are present in the silt fraction as well as in the clay and may be metamorphic or hydrothermal. Kaolinite and vermiculite are confined to clay fractions. As kaolinite occurs only in the adamellite soils, it is believed to be authigenic, but the vermiculite occurs widely and may have been partially or entirely added by aeolian processes. A small amount of montmorillonite is present in the clay fraction of one sample. The presence of several coexisting authigenic clay minerals, perhaps forming from different primary phases, is not inconsistent with the immature nature of the White Mountains soils.

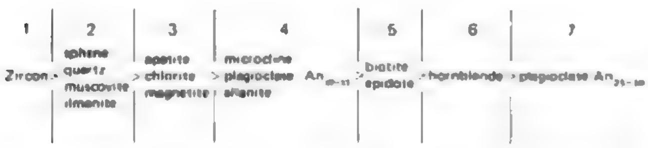

FIGURE 297.—Mineral weathering sequence in adamellite soils of Sage Hen Flat, in order of decreasing resistance. Based on visual comparison of bedrock and noncontaminative soil grains. Vertical lines separate major divisions of resistance.

ELECTRON MICROPROBE STUDIES OF ADAMELLITE MINERAL WEATHERING

Seven minerals from adamellite bedrock, grus, and soil on Sage Hen Flat were chemically analyzed by electron microprobe. Biotite showed major weathering alteration; microcline, plagioclase, allanite, and some magnetite gave detectable changes; ilmenite and sphene yielded no measurable variations because of weathering.

BIOTITES

Biotite analyses reveal progressively lowered contents of K, Ba, Mg, and Si and increases in Fe and Al, from bedrock to grus to soil (table 8). Biotite in grus is chemically similar to fresh bedrock biotite, but both of these differ markedly from soil biotite grains (1–3 phi), suggesting that little chemical weathering of biotites occurs prior to or during grus formation. Decreases in grus Mg with respect to bedrock is apparently due to primary solid solution substitution of Fe for Mg rather than weathering losses. Some grus biotites, however, are obviously breaking apart along cleavages prior to chemical alteration.

In terms of lattice sites, the biotite cations in 8–12-fold coordination appear to be the most vulnerable to weathering attack, followed by cations in octahedral coordination. (The values of table 8 assume no ferric iron is present and that all ferrous iron is in octahedral coordination.) Ions in sixfold and fourfold coordination taken together show little evidence of change. Within the 8–12-fold coordination sites, Ba appears to be more

TABLE 7.—*Layer silicates in silt and clay fractions of some adamellite soils*

[+ = present; 0 = absent; n.d. = not determined. Clay is < 2 μm soil fragments]

Sample number	42	86	88	91	92	94	95	97	98	99	101	102	106
Kaolinite													
Silt	n.d.	0	n.d.	n.d.	n.d.	0	n.d.	0	0	0	0	0	0
Clay	+	0	+	+	+	n.d.	+	+	+	n.d.	n.d.	n.d.	n.d.
Chlorite and (or) septechlorite													
Silt	n.d.	+	n.d.	n.d.	n.d.	+	n.d.	+	0	+	(?)	+	+
Clay	+	+	0	0	0	n.d.	0	0	0	n.d.	n.d.	n.d.	n.d.
Vermiculite													
Silt	n.d.	0	n.d.	n.d.	n.d.	0	n.d.	0	0	0	0	0	0
Clay	0	+	0	+	0	n.d.	+	+	0	n.d.	n.d.	n.d.	n.d.
Montmorillonite													
Silt	n.d.	0	n.d.	n.d.	n.d.	0	n.d.	0	0	0	0	0	0
Clay	0	0	0	0	0	0	0	0	0	0	n.d.	0	+(?)
Sericite													
Silt	n.d.	+	n.d.	n.d.	n.d.	+	n.d.	+	n.d.	+	+	+	+
Clay	+	+	+	+	+	+	+	+	+	+	n.d.	+	(?)
Biotite													
Silt	n.d.	+	+	+	+	+	+	+	+	+	+	+	+
Clay	+	+	+	+	+	+	+	+	+	0	n.d.	+	(?)

Digitized by Google

TABLE 8.—*Averaged electron microprobe analyses of fresh and weathered biotites*

[CN=coordination number with respect to oxygen]

Source of analyzed grains	Elemental percentages						Total of analyzed elements as oxides[1] (percent)	Total: Annite + phlogopite[1] molecules	CN=8 to 12	CN=8	CN=4 to 6	CN=8 to 12	CN=8	CN=4 to 6
	K	Ba	Mg	Fe	Al	Si			K+Ba	Mg+Fe	Si+Al	K/Ba	Mg/Fe	Si/Al
Fresh bedrock	7.5	0.79	6.9	14.9	7.5	16.7	90.4	81.6	8.3	21.8	24.2	9.5	0.46	2.22
Grus	7.3	.51	5.8	15.8	6.7	16.5	87.3	81.6	7.8	21.6	23.2	14	.37	2.46
Soil (1–3ϕ)	5.8	10	4.4	15.7	13.7	10.5	82.9	73.3	5.9	20.1	24.2	58	.28	.77

[1]Assuming all Fe in ferrous state

easily mobilized than K, but the extremely low Ba counting rate precludes any definite conclusions. Mg in the octahedral site is obviously more mobile than Fe, and Si, largely located in the sixfold to fourfold site, is much more readily removed than Al, which occurs in both octahedral and tetrahedral positions.

Microprobe analyses are usually grouped and averaged to compare changes in more than three elements, because only three elements may be analyzed simultaneously and because it is virtually impossible to return to the same location on the same grain in a subsequent analysis. Soil grains may often contain appreciable unaltered parts, however, and primary compositional differences between grains may obscure changes due to weathering. Comparisons were made between weathered and fresh parts of the same soil grain to eliminate those problems. Ratios of K/Fe and Mg/Fe along five typical transects across soil biotites, both parallel and perpendicular to the (001) cleavage, are reproduced in figures 298 and 299. Several conclusions seem apparent from the data: (1) Lower K/Fe and Mg/Fe ratios invariably occur either along edges or cleavages, but every edge and cleavage does not show changed ratios, (2) traverses perpendicular to the basal cleavage are more variable than transects parallel to cleavages, and (3) K losses with respect to Fe are generally more frequent and larger than those of Mg. Examination of the original data (not shown) reveals a relatively constant Fe percentage across the grains, indicating that Fe losses are comparatively minor. Decreased K/Fe and Mg/Fe ratios therefore reflect absolute losses, an observation consistent with the data of table 8. Some red-brown to yellow-brown Fe oxidation, though, was observed in soil biotites examined under the petrographic microscope, especially along grain margins.

To gain further information concerning the end product of biotite weathering, analyses of fresh and altered portions of soil biotites for Si, Al, and Ba were also conducted (table 9), using a finely focused electron beam. The Si/Al ratio drops from above 2 in fresh portions to less than 1, and even approaches 0 in the fine-grained alteration products that commonly occur adjacent to edges and cleavages. Ba also shows somewhat lower values in the alteration products. The Mg losses

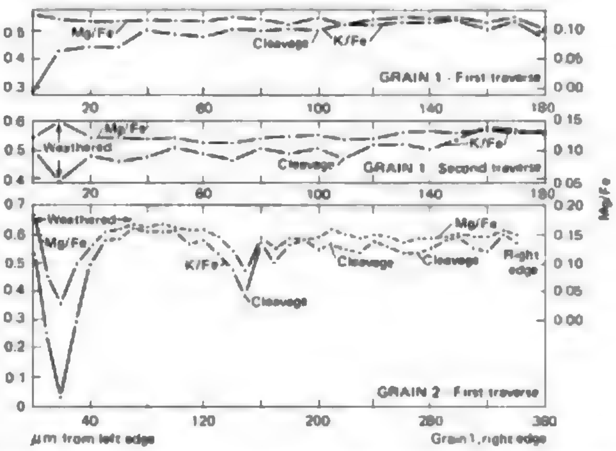

FIGURE 298.—Electron microprobe traverses normal to (001) cleavage of two soil biotite grains.

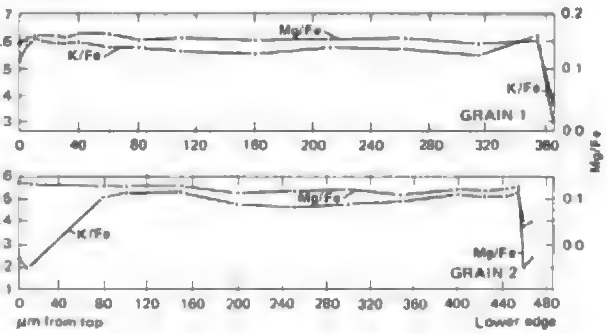

FIGURE 299.—Electron microprobe traverses parallel to (001) cleavage of two soil biotite grains.

TABLE 9.—*Individual electron microprobe analyses, in weight percent, of altered and relatively fresh parts of soil biotites*

Ba	Si	Al	Si/Al	Description	Number of analyses
0.10	16.70	7.38	2.26	Fresh	1
.30	16.57	7.55	2.19	do	4
.00	7.44	9.17	.81	Alteration product	1
.16	11.54	14.80	.78	do	1
.04	10.33	15.10	.68	do	1
.36	9.91	18.57	.53	do	1
.00	1.88	16.90	.11	do	1
.00	.86	22.43	.04	do	1
.00	.67	29.91	.01	do	1

Digitized by Google

and Si/Al ratios rule out vermiculite and montmorillonite as possible weathering products. The Si/Al ratios suggest that complete alteration to gibbsite may have occurred, but microprobe analyses of porous and probably hydrous materials such as these must be regarded with some caution. Four Si/Al values fall between 0.5 and 1.0, and 1:1 clays (but not gibbsite) were detected in X-ray diffraction patterns of soil and clay fractions; so, the formation of kaolinite from biotite, if only as a temporary weathering product, seems a more likely possibility. Presence of colloidal, noncrystalline aluminum hydroxide may account for the low Si/Al ratios.

Feldspars

Microscopic evidence indicates that plagioclase, especially the more calcic zones, and microcline are altering to clays. The soil feldspars analyzed by the microprobe are much less severely altered than feldspars observed in some soil thin sections and grain mounts; so, chemical differences between averaged microprobe analyses of fresh bedrock grains and soil fragments (table 10) are not striking.

Table 10.—*Averaged electron microprobe analyses, in weight percent, of feldspars from fresh adamellite bedrock, grus, and soils*

	K	Ba	Na	Ca	Fe	Total An+Ab+Or	Number of grains analyzed
Microcline:							
Fresh	13.2	0.0	0.53	0.01	0.2	99.6	1
Grus	13.0	.0	57	.01	.2	99.2	4
Soil	13.0	0	31	00	2	96.4	2
Plagioclase:							
Fresh	1	.0	6.9	2.9	.3	99.4	4
Grus	.2	0	6.4	3.3	0	98.0	2
Soil	.1	0	6.5	3.4	1	98.4	8

The analyzed microclines appear to have undergone some chemical losses during weathering, as evidenced by the 3.4 percent decrease in molecular totals (An+Ab+Or), from bedrock to soil. Microcline grains from grus samples, like biotites (table 8), do not appear to be appreciably weathered. Microprobe transverses across K-feldspars from seven grus and soil samples (data not shown) suggest that lattice deficiencies, indicated by low molecular totals, most commonly occur near grain edges and that low Na and K values tend to be associated with these deficiencies. Primary crystal zonation, however, often obscures weathering losses.

Zoning is so prominent in the plagioclases that weathering changes are largely masked, but the molecular totals of table 10 indicate that losses due to weathering have occurred and that sodium may be the most mobile constituent. Plagioclases from both grus and soil appear to show detectable deficiencies of molecular totals. A very small electron beam was used to analyze fine-grained plagioclase alteration products within soil grains for Si and Al (fig. 300). The marked

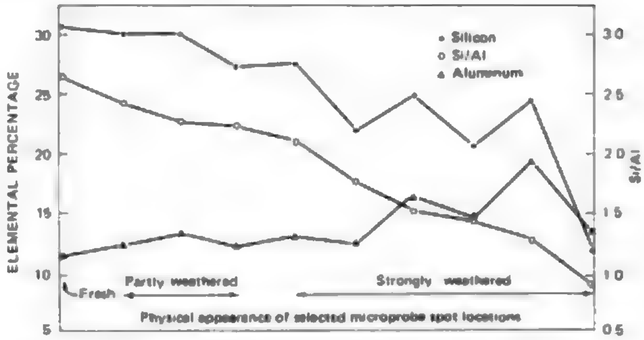

Figure 300.—Electron microprobe analyses of 10 parts of a single plagioclase grain.

decrease in Si/Al ratios from 2.7 in fresh portions to about 1–1.5 in altered areas suggests that kaolinite may be the principal weathering product. As weathering proceeds, Si percentages appear to decrease more rapidly than Al percentages increase, such that Si + Al steadily decreases.

Other Minerals

Analyses of fresh and weathered allanite, magnetite, ilmenite, and sphene are compiled in table 11. The one soil allanite examined is lower in Ca and Al and higher in Fe percentage than fresh grains. Analytical results from 35 magnetite and ilmenite grains in both bedrock and soil gave little indication of weathering changes, but a few magnetite grains showed some visible alteration and less Fe (apparently due to oxidation) near their margins. Soil and bedrock sphenes gave virtually identical chemical analyses, and traverses across soil grains showed no significant variations.

Table 11.—*Electron microprobe analyses, in weight percent, of four minerals from fresh adamellite of Sage Hen Flat and from derived soil*

	Ca	Mg	Fe	Al	Ti	Number of analyses
Allanite:						
Fresh	8.0		11.5	8.2		12
Soil	6.5		12.9	6.7		1
Magnetite:						
Fresh		0.00	70.8		0.13	13
Soil		.03	72.6		.25	10
Ilmenite:						
Fresh	—	05	32.2	—	27.2	11
Soil	—	26	30.0	—	29.4	1
Sphene:						
Fresh	23.3	0	1.2	7	19.1	11
Soil	23.8	—	—	.9	19.0	2

Chemical Changes from Bedrock to Soil

Chemical analyses of bedrock and soil samples were conducted by X-ray fluorescence techniques to assess the degree and sequence of bulk chemical changes due to weathering. For the adamellite and its derived soils, the U.S. Geological Survey samples G–1, G–2, GSP–1, AGV–1, BCR–1, and W–1 were used as standards. The U.S. Bureau of Standards' Dolomite #88 and five Reed

bedrock and soil samples analyzed by Ken-ichiro Aoki, Tohoku University, Japan, were used as standards for the dolomite group.

Reed Dolomite

Arithmetic means and standard deviations for analyses of dolomite bedrock, soil greater than 2 mm, soil less than 2 mm, and soil less than 62 μm are given in table 12. Standard deviations refer to differences between samples collected at different locations rather than to analytical precision (replicate analysis).

The principal reason for collection of numerous and widely distributed bedrock and soil samples was to obtain an indication of chemical and mineralogical variability within each parent material and soil, such that changes due to weathering could be clearly differentiated from apparent changes caused by sampling deficiencies. Unfortunately, careful study of soil mineralogy shows most of the Reed soil samples to be contaminated by both rhyolitic ash and local materials to the extent that corrections for contamination would be meaningless. The effects of external aeolian addition are also indicated by the large increases in Na and K in the finer size fractions of the soils. Only one sample for which the mineralogy was determined, #65 soil less than 2 mm, appears to be little affected by contamination. Corrections for the minor chemical effects of the tuff and local contaminants in this sample were made using weighted averages of glass and contaminative mineral percentages[3] in the sand and silt fractions (percentage clay was less than 1 percent and was therefore neglected in the calculations). Chemical composition of minerals and glass used to correct the original soil analysis are given, together with sources of information, in table 13. Local contaminants in this sample are assumed to be derived from the nearby Sage Hen Flat pluton. Soil analytical values from which corrections had been subtracted were recalculated to the previous oxide percentage total and converted back to elemental percentages. Total estimated contamination in #65 soil less than 2 mm is only 3.9 percent, and thus any errors due to inaccurate amounts of correction are relatively small.

Absolute losses (weight percent in bedrock minus weight percent in soil) are shown for the five carbonate-component elements in mean soil greater than 2 mm (hereafter termed "soil gravel") and #65 soil less than 2 mm (corrected for both ash and local contaminants) on the left side of table 14. To eliminate differential effects of heavy and light elements, the absolute losses are divided by atomic weight in the adjacent columns. Percentage losses with respect to bedrock, determined as

$$\text{percentage loss} = \frac{\text{weight percent in bedrock-weight percent in soil}}{\text{weight percent in bedrock}}$$

are shown in bar graph form in the left side of figure 301. Both calculations were made holding constant the percentage of Zr, the most stable element during the weathering process for the samples studied here. Undoubtedly Zr percentage does change between bedrock and soil, but this assumption permits relative comparison of all elements investigated, the principal concern of this study. The soil gravel fraction is assumed to be little affected by contamination, and #65 soil less than 2 mm has been corrected for all external additions; so, these two soil analyses should be chemically representative of Reed terrane. Elemental absolute losses from dolomite bedrock to soil follow the sequence Ca > Mg >>> Fe >> Mn >> Sr, a trend strongly controlled by bedrock composition. When atomic weight is taken into account, the position of Ca and Mg in the sequence converge or trade places, but other relations remain

[3]The methods by which percentages of ash and aeolian contaminants were determined has been discussed elsewhere (Marchand, 1970) in some detail.

Table 12.—*Chemical analyses, in weight percent except as noted, of Reed Dolomite bedrock and soils*

[Data are from X-ray fluorescence techniques except as noted. n.d.=not determined; S.D.=standard deviation. Soil analyses are not corrected for contamination]

		Bedrock			Soil > 2 mm			Soil < 2 mm			Soil < 62 μm		
		Mean	S.D.	Number of samples	Mean	S.D.	Number of samples	Mean	S.D.	Number of samples	Mean	S.D.	Number of samples
Si		0.11	0.07	7	0.80	0.10	2	13.24	5.84	6	22.01	1.00	5
Ti		.0069	.0050	6	.022	.002	2	.20	.11	6	.40	.02	5
Zr	ppm	6.5	5.3	4	13	3	2	104	51	5	246	31	5
Al		.092	.059	6	.38	.06	2	4.15	1.70	6	7.16	.28	5
Fe		.26	.09	12	.36	.005	2	1.83	.62	11	3.13	.06	5
Mn		.055	.020	12	.08	.01	2	.11	.031	11	.12	.02	5
Mg		12.46	.43	7	11.01	.16	2	5.67	1.57	6	2.21	.38	5
Ca		21.52	.93	12	22.54	.43	2	12.93	4.16	11	8.38	.88	5
Ba		.00	.00	6	.00	.00	2	.028	.012	5	.06	.004	5
Sr	ppm	56	7	6	62	3	2	124	27	5	222	17	5
Na[1]		.027	.001	2	.0550	.003	2	.755	.395	2	n.d.	n.d.	0
K[1]		.011	.006	2	.0545	.0055	2	1.281	.335	3	n.d.	n.d.	0
Rb	ppm	.81	2.00	8	1.10	.50	2	25.8	11.7	11	51.0	4.0	5
P[2]		.0175	.0085	2	n.d.	n.d.		.0545	.....	2	n.d.	n.d.	0
Oxide total[3]				[2]98.63			[4]97.69	......		[5]101.39			[6]94.63

[1]Flame photometer analyses by Joaquin Hampel.
[2]Wet chemical analyses by Ken-ichiro Aoki.
[3]CO_2 taken as stoichiometric. Iron computed as Fe_2O_3.
[4]Includes H_2O+ and H_2O- analyzed by Ken-ichiro Aoki for three samples.
[5]Includes H_2O+ and H_2O- analyzed by Ken-ichiro Aoki for two samples.
[6]Does not include H_2O+ and H_2O-.

Digitized by Google

TABLE 13.—*Chemical compositions, in weight percent except as noted, of minerals and glass in soils used to correct chemical analyses*

[Probe analyses supplemented by data from Deer, Howie, and Zussman (1952a, b, 1963a, b), as indicated, except analyses for volcanic glass and biotite, which are supplemented by data from Carmichael (1967, p. 50 and 52, respectively)]

	Volcanic					Plutonic (local)					
	Glass	Sanidine	Plagioclase	Biotite	Quartz	Microcline	Plagioclase	Biotite	Hornblende	Epidote	Chlorite
		Sample 10 sanidine (1963b, p. 41)	Sample 7 albite (1963b, p. 108)			Sample 13 microcline (1963b, p. 39)	Sample 8 oligoclase (1963b, p. 113)	Sample 5 igneous biotite (1963a, p. 58)	Sample 17 hornblende (1962b, p. 277)	Sample 8 epidote (1962a, p. 198)	Sample 18 chlorite (1962a, p. 141)
Si	35.31	30.7	30.2	16.8	46.75	30.1	29.6	16.3	22.5	17.4	12.0
Ti	.04	......	......	3.2	......	......	.01	2.4	.6	.05	.53
Zr ppm	106	......	......	......	......	......	......	......	......	......	......
Al	6.58	10.0	10.6	6.7	......	10.1	12.1	8.1	3.1	12.8	11.2
Fe	.97	0	.64	16.4	......	.2	.06	[1]14.8	[1]9.9	[1]9.2	[1]18.6
Mn	.04	......	......	.3	......	.01	......	.3	.3	[1].03	.27
Mg	.02	.1	.19	6.4	......	.02	......	[1]6.4	[1]7.7	......	[1]9.5
Ca	.43	.1	[1]1.9	.01	......	......	[1]3.0	.8	[1]7.3	16.5	.11
Sr ppm	5	......	......	......	......	......	......	......	......	......	......
Ba	None	.4	......	.4	......	......	......	......	......	......	......
Na	3.00	3.0	[1]6.9	.5	......	.6	[1]6.8	.3	1.1	......	......
K	3.89	[1]10.9	[1]1.2	7.4	......	[1]12.8	[1].1	[1]7.4	.6	......	......
Rb ppm	190	......	......	......	......	......	......	......	......	......	......

[1] Analyzed by electron microprobe

TABLE 14.—*Absolute losses, in weight percent, of chemical constituents from bedrock to soil, assuming constant Zr percentage*

[Figures in parentheses under mean dolomite column are losses expressed as percentages of #65 bedrock-to-soil losses for the given elements]

Element	Dolomite				Adamellite	
	Mean dolomite bedrock minus mean dolomite soil > 2 mm		#65 bedrock minus #65 soil < 2 mm[1]		#94 bedrock minus #94 soil < 2 mm[1]	
	Absolute loss	Loss atomic weight	Absolute loss	Loss atomic weight	Absolute loss	Loss atomic weight
Si	......	......	......	......	-16.67	-0.5934
Al	......	......	......	......	-4.33	.160
K	......	......	......	......	-2.12	-.0542
Na	......	......	......	......	-1.77	.0770
Fe	-0.08(67)	-0.001	-0.12	-0.0022	-.98	-.017
Ca	-10.25(57)	.256	17.99	.449	.92	.023
Mg	-6.96(65)	-.286	-10.72	-.441	-.43	-.01
Ti	......	......	......	......	.09	.002
Ba	......	......	......	......	-.07	-.0005
Mn	-.015(54)	-.00027	-.028	.00051	.05	.0009
Sr	-.0025(65)	-.000028	-.0038	-.000043	-.0368	-.000420
Rb	......	......	......	......	.0041	.000047

[1] Corrected for both ash and local contaminants

essentially unchanged. Percentage losses, a more significant indication of weathering mobility, occur in the sequence $\mathrm{Mg} > \mathrm{Ca} > \mathrm{Sr} > \mathrm{Mn} \overset{?}{\approx} \mathrm{Fe}$. In the percentage loss calculation, the atomic weight factor is automatically taken into account. Loss of Mg relative to Ca, as indicated by the percentage losses, is in agreement with the presence of secondary calcium carbonate in dolomite soils. Comparisons of both absolute and percentage losses indicate that, of the five elements shown (with the possible exception of Mn), well over half of the total elemental losses in bedrock to soil less than 2 mm occur during the transformation of bedrock into soil gravel.

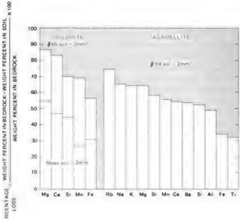

FIGURE 301.—Percentage chemical losses for the indicated Reed Dolomite and adamellite soils of Sage Hen Flat with respect to bedrock, assuming constant Zr percentage. [1]Corrected for both ash and local contamination.

Obviously chemical breakdown of the dolomite begins almost simultaneously with physical disintegration in the early stages of the carbonate weathering process.

Sections cut through spheroidally weathered dolomite fragments occurring at the surface or within the soil profile commonly show an abrupt change from fresh light cream to pink crystalline dolomite outward into a

porous gray or white concentrically layered weathering rind (fig. 302). Under the petrographic microscope, alternating layers of fresh dolomite and a fine-grained alteration product are evident within the rind. Electron microprobe analyses of one of the rinds for Ca, Mg, Mn, and Fe and microprobe transects from unaltered dolomite into the rind (figs. 303, 304) indicate that the weathering product is a very pure calcite, as shown in the following table.

	CaO	MgO	MnO	FeO
Fresh dolomite .... percent....	30.2	20.6	0.3	0.2
Alteration product .... percent....	54.1	.3	.2	.1

Leaching of Mg and deposition of calcite are undoubtedly responsible for the development of carbonate horizons and other calcium carbonate accumulations in dolomite soils. Fe and Mn are more variable within the rind, but appear to occur in approximately equal concentrations in both dolomite and calcite.

ADAMELLITE OF SAGE HEN FLAT

Mean analytical values for bedrock, grus, soil less than 2 mm, and soil less than 2 μm are given in table 15. The grus values are generally comparable to those of the bedrock, and where they differ, the direction of change suggests primary variability rather than weathering. Therefore, in the third column of table 15, means weighted on the basis of number of samples have been calculated for both bedrock and grus and were used as the bedrock values in all further computations.

As in the case of the Reed, almost all adamellite soils are greatly contaminated by both rhyolitic ash and local debris. The first step in preparing the soil analyses for interpretation was to correct for the contaminating ash. After ash correction, only #94 < 2 mm gave a reasonable sequence of bedrock-to-soil mineralogical changes, on the basis of grain counts (fig. 305), suggesting ab-

FIGURE 302.—Rock saw chips showing weathering rind on spheroidally weathered dolomite (#68) analyzed by electron microprobe. Rind is about 0.2 inch thick.

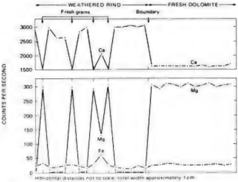

FIGURE 303.—Electron microprobe transect showing Ca, Mg, and Fe variation across an alteration rind in spheroidally weathered Reed Dolomite (#68).

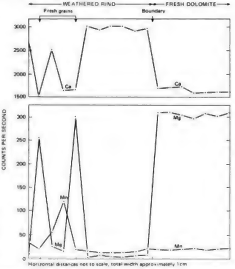

FIGURE 304.—Electron microprobe transect for Ca, Mg, and Mn across dolomite weathering rind (#68).

Digitized by Google

TABLE 15.—*Averaged values for X-ray fluorescence chemical analyses, in weight percent except as noted, of adamellite bedrock and soils of Sage Hen Flat*

[S.D.=standard deviation, n.d.=not determined. Soil analyses are uncorrected for contamination]

		Bedrock		Grus		"Bedrock" (=weighted average of bedrock and grus; see text)		Soil < 2 mm		Soil < 62 μm	
		Mean	S.D.	Mean	S.D.	Mean	S.D.	Mean	S.D.	Mean	S.D.
Si		32.39	0.98	31.16	1.67	31.79	1.08	31.51	0.61	28.21	0.85
Ti		.24	.04	.23	.04	.24	.04	.32	.05	.51	.03
Zr	ppm	164	32	123	16	152	27	217	[illegible]	517	65
Al		8.36	.41	8.94	.50	8.53	.44	8.03	.55	8.38	.22
Fe		2.16	.56	1.55	.04	1.99	.41	2.77	.62	4.53	.50
Mn		.06	.02	.06	.04	.06	.03	[illegible]	.02	.12	.01
Mg		.46	.18	.31	.03	.42	.14	.56	.12	1.32	.22
Ca		1.44	.29	1.45	.09	1.44	.23	1.32	.17	2.24	.12
Ba		.12	.02	.15	.05	.13	.03	.10	.01	.08	.01
Sr	ppm	600	111	533	129	581	116	455	91	321	21
Na		2.70	.24	2.53	.23	2.65	.24	2.19	.14	1.57	.10
K		3.20	.45	4.41	.84	3.55	.56	3.00	.24	2.97	.06
Rb	ppm	53.9	12.9	65.3	12.8	57.1	12.9	59.8	8.0	67.3	1.9
P		[1].048	......	n.d.	......	[1].048	......	[2].0455	......	n.d.	
C		[1]none	...	n.d.	......	[1]none	......	[2].001	......	n.d.	......
H		[1].053	......	n.d.	......	[1].053	......	[2]2.04	......	n.d.	
Oxide total[3]		100.20	......	97.73	......	99.32	......	100.47	......	94.89	
Number of total analyses		10	......	4	......	14	......	6	......	5	...
Number of partial analyses		8	......	0	......	8	......	5	......	2	......

[1]Based on one wet chemical analysis by Ken-ichiro Aoki.
[2]Based on two wet chemical analyses by Ken-ichiro Aoki.
[3]Fe calculated as Fe_2O_3; H_2O+, H_2O-, P_2O_5, CO_2 not analyzed in grus and < 62 μm soil samples.

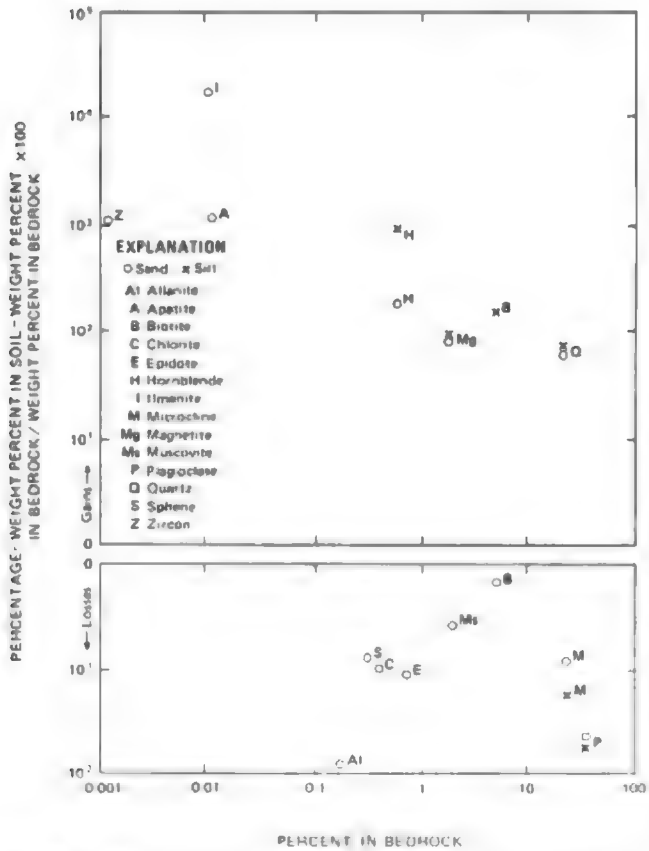

FIGURE 305.—Mineral percentage changes with respect to bedrock in two size fractions of a relatively uncontaminated adamellite soil, #94, after ash corrections.

sence of significant local contamination. All major minerals except biotite and hornblende appear in place in the #94 sand and #94 silt mineral sequences, based on the observed weathering sequence (cf. fig. 297). By using percentage changes consistent with those of quartz, microcline, and plagioclase and with the observed weathering sequence, corrections were computed for biotite and hornblende in the less-than-2-mm fraction of #94 soil, as shown in the left part of table 16. Chemical corrections using the values of table 13 assume that the biotite and hornblende came from the Sage Hen Flat pluton or do not differ greatly from that of the pluton. The adjustments, including those from the ash, were subtracted from the original analysis of #94 soil, followed by correction to the previous oxide total and reconversion to elemental values, as shown in the right part of table 16.

Chemical changes due to weathering at site 94 may now be assessed from bedrock and corrected soil analyses. Absolute losses and losses divided by atomic weight from #94 bedrock to less-than-2-mm soil are given on the right side of table 14. Percentage losses with respect to bedrock, computed from concentrations in weight percent and assuming constant Zr percentage, are presented graphically in figure 301 (right side). Bedrock-to-soil absolute losses occur in the sequence Si >> Al > K > Na > Fe > Ca > Mg >> Ti > Ba > Mn > Sr >> Rb, in close accordance with bedrock abundances. Absolute losses adjusted for atomic weight yield a slightly different sequence, Si >> Al > Na > K > Ca > Mg >

TABLE 16.—*Adamellite sample 94–bedrock chemical analysis and adjustment of < 2-mm-soil analysis for ash and local contamination by biotite and hornblende*

[All analytical data in weight percent, except as noted]

	Calculated percent change (fig. 305)	Assumed percent change	Percent in bedrock	Percent in soil	New soil value	Difference	Weighted average	Local component	Ash component	Original analysis	Corrections for ash	Corrections for local contaminants	Analysis corrections	Oxides	Recalculated to previous 13 element total	Corrected element values	Bedrock analysis
94 sand.																	
Biotite	1 8	−30	6 7	8 2	4 7	−3 5											
Hornblende	+200	−40	.13	.42	.08	−.34											
94 silt																	
Biotite	+170	−35	6.7	15	4.4	−10.6											
Hornblende	+1,050	45	13	7	07	6.93											
94 soil < 2 mm.																	
Biotite							4.7	4 4	0.27								
Hornblende							−.97	−.97									
Si										31 13	6.59	0 94	21 60	46.21	65 66	30.70	31 72
Ti										.40	−.02	−.11	.27	.45	64	.38	28
Zr ppm										306	−24		284	364	546	404	198
Al										8.35	−1.62	39	6.34	11 98	17 02	9.01	8 75
Fe										3.75	26	75	2.74	3 92	5.57	3.90	2.89
Mn										.09	−.01	−.02	.06	08	.12	.09	09
Mg										.71	.02	−.36	.33	.55	.78	.47	66
Ca										1.29	−.10	−.11	1 08	1 51	2 15	1.54	1 67
Ba										.09	.005		[illegible]	.096	.135	.12	13
Sr ppm										368	−1		367	434	617	522	624
Na										2.07	−.73	02	1.32	1.78	2.53	1.88	2.69
K										2.95	.99	.34	1.62	1.96	2.77	2.30	3 25
Rb ppm										52.3	−43		19 3	42 2	60.0	27.4	54.0

Fe ≫ Ti > Mn > Ba > Sr ≫ Rb. Percentage losses, the most significant indicator of chemical behavior during weathering, follow the sequence Rb $\overset{?}{>}$ Na ≈ K ≈ Mg > Sr > Mn ≈ Ca > Ba > Si > Al ≫ Fe > Ti. The placement of Rb within the latter sequence is somewhat uncertain owing to its low concentration in both bedrock and soil and to its susceptibility to contamination from biotite, feldspars, and glass.

Examination of figure 301 shows that percentage chemical losses generally follow the sequence alkali metals > alkaline earths > Si > Al > metals. Some notable differences in element mobility between the dolomite and adamellite are also evident. Greater absolute amounts of Sr, Fe, and Mn are lost from adamellite than from dolomite, whereas Ca, Mg, Sr, Mn, and Fe all undergo greater percentage losses from dolomite bedrock to less-than-2-mm soil than from adamellite bedrock to less-than-2-mm soil. The soluble dolomite obviously releases all its constituent elements more readily than they can be weathered from silicate and oxide phases in the plutonic rock.

The preceding interpretations are based on bedrock-to-soil changes recorded at only two sites, although mean dolomite soil gravel values and microprobe analyses of both dolomite and adamellite minerals give additional confidence to the patterns of chemical weathering. The extensive soil contamination rendered study of all other samples virtually meaningless. For confirmation of the chemical weathering sequences suggested by the limited data provided by bulk changes in the solid phases, it was necessary to examine the chemical composition of natural waters related to both dolomite and adamellite.

CHANGES IN THE LIQUID PHASE

Chemical weathering usually occurs only in the presence of a liquid phase which is undersaturated with respect to the altering phases. A considerable amount of information concerning processes and sequences of decomposition can be obtained from observations of progressive chemical changes in water as it passes from the form of precipitation into soil water and finally into ground water and springs. The following discussion considers the chemical nature of rain and snow water, soil water extracts, and spring waters related to both dolomite and adamellite, the saturation pH and exchangeable cations of the soils, and finally the significance of geochemical differences between the various fluids in terms of chemical weathering.

CHEMICAL COMPOSITION OF PRECIPITATION

Four rain samples and four snow samples, obtained during the period July 30, 1966, to June 29, 1967, were collected in plastic-lined pans and filtered through 0.45-μm filter membranes into airtight polyethylene containers. The analytical data[4] for these samples, together with mean values for Sierra Nevada snow, are given in table 17. The White Mountains samples tend to

[4] The procedures of Barnes (1964) were followed for field determination of pH and alkalinity for all water samples. All other chemical analyses of water were performed by the U.S. Geological Survey.

TABLE 17.—*Chemical analyses, in milligrams per liter except as noted, of precipitation collected near Crooked Creek Station and comparison with analyses of snow from the east slope of the Sierra Nevada*

[Mean for snow from Feth, Rogers, and Robinson (1964, p. 18-26)]

	Crooked Creek Station			Mean for snow, east slope of Sierra Nevada
	Mean[1] ± standard deviation	Maximum	Minimum	
Specific conductance .... μmhos	7 ± 3	11	4	
K	14 ± 10	31	.06	41
Na	34 ± 25	90	.16	43
Ca	36 ± 12	57	.23	84
Mg	9 ± 07	22	034	19
Ba	< 5	------	------	------
Mn	003 ± 002	006	000	[2] 00
Fe	014 ± 010	024	000	[2] 01
Al	012 ± 011	032	001	[2] 03
B	01	02	00	[2] 05
SiO_2	11 ± 06	2	035	[2] 17
HCO_3	2 7 ± 1 3	4 3	1 2	3 59
NO_3	2 ± 0	2	2	[2] .07
SO_4	06 ± 09	2	0	1 14
PO_4	00 ± 00	00	00	[2] .03
Cl	4 ± 2	7	2	.47

[1]Mean for four rain and three snow samples.
[2]Value for entire Sierra Nevada

TABLE 18.—*Chemical constituents in water saturation extracts of two groups of White Mountains soils*

[All analytical values other than pH are in milligrams per liter]

	Mean	Standard deviation	High	Low	Number of analyses
Reed Dolomite					
K	13	±8	43	5.5	23
Na	13	±4	24	7.1	23
Ca	100	±29	150	42	23
Mg	21	±6	33	7 0	23
PO_4	0082	0052	0210	0021	11
Na K	1 00				
Ca Mg	4 8				
Field pH	8 0 } saturation paste				
Laboratory pH	7 5 } saturation paste				
Adamellite of Sage Hen Flat					
K	22	±9	94	9.8	23
Na	14	±4	28	7.4	23
Ca	61	±22	110	28	23
Mg	10	±3	17	5 6	22
Fe	.24	±.10	.56	.12	20
Si	10 1	±1 3	14	8.0	21
PO_4	0150	.0040	.0190	0110	2
Na K	64				
Ca·Mg	6.1				
Field pH	6.8 } saturation paste				
Laboratory pH	7.0 } saturation paste				

have lower mean concentrations of most constituents, especially sulfate, than do the Sierra samples. Mn, Fe, Cl, and nitrate are comparable or slightly higher in the White Mountains.

CHEMICAL COMPOSITION OF SOIL WATER

Obtaining representative soil water samples is a considerable problem that has been approached from several angles. Lysimeters and other elaborate devices probably collect the most typical fluids, but they are often difficult to install and maintain and give no indication of geographical variation unless employed in large numbers. In the White Mountains, soils are either dry or frozen except for brief periods during spring snowmelt and after very heavy summer storms, making field collections difficult to obtain. For this study, water saturation pastes of 46 Reed Dolomite soils and adamellite soils of Sage Hen Flat were prepared, and after 1 hour water samples were vacuum-extracted by Buchner funnel in the laboratory. (See section "Supplemental Information" for methods). Saturation, rather than excess water mixtures, was chosen for initial soil moisture content in the belief that this would more closely reflect actual soil water conditions. Distilled water was used in all extractions, the assumption being that any differences between precipitation and distilled water, with regard to the analyzed species, would not be significant in comparison to the soil water concentrations.

Analyses of these extracts, summarized in table 18, indicate that standard deviations within a given soil type are often nearly as large as or larger than differences between soil types. Comparison between some chemical species of the two soil water groups, however, is still possible. The adamellite extracts are lower in Ca and Mg and apparently higher in K and phosphate than the Reed samples. Na is surprisingly low in the adamellite soil water extracts.

The large deviations in soil water composition, which exceed the standard deviations in total soil composition (compare table 19 with tables 12 and 15), imply considerable departures from equilibrium and steady state (rate of ion gains = rate of ion losses) conditions, perhaps accentuated by the relatively short duration of the extraction process. For this reason, soil water extractions may differ to some extent, primarily in degree of variability between sites but probably in ionic proportions as well, from meteoric water that has been in contact with the soil for several days or weeks during snowmelt or after heavy rains.

SOIL pH

Table 19 gives a compilation of field and laboratory pH data for Reed Dolomite soils and adamellite soils of Sage Hen Flat. These data, together with similar information from basalt and sandstone soils in the area, indicate that instrumental laboratory pH values and indicator-determined field pH values are comparable to pH's about 8.0, where the field methods begin to give consistently higher readings. A comparison of the figures for the two soil types shows the Reed soils to have values 0.5–1.5 pH units higher than the adamellite soils.

EXCHANGEABLE CATIONS

Amounts of total extractable soil cations (in milliequivalents per 100 grams of ovendry soil) were ob-

TABLE 19.—*Mean values for total exchangeable cations, percentage exchangeable cations, and pH in Reed Dolomite and adamellite soils of Sage Hen Flat*

	Mean	Standard deviation	Standard deviation (% of mean)	Number of samples
Reed Dolomite soils				
pH				
Average mean field	8.0	0.1	1	25
Average maximum field	8.2	.1	1	25
Average minimum field	7.9	.01	5	25
Laboratory	7.5	.2	3	25
Exchangeable cations (me/100 g ovendry soil):				
K	.58	.30	52	25
Na	.27	.09	33	25
Ca	32.4	13.3	41	25
Mg	6.1	2.5	41	25
Percent of exchangeable cations:				
K	1.6	.9	56	21
Na	.73	.27	37	21
Ca	80.7	7.6	9	21
Mg	16.9	6.7	40	21
Adamellite soils				
pH				
Average mean field	6.8	0.5	8	22
Average maximum field	7.6	.6	8	22
Average minimum field	6.2	.5	7	22
Laboratory	7.0	.4	5	22
Exchangeable cations (me/100 g ovendry soil):				
K	.33	.13	40	22
Na	.07	.05	69	22
Ca	7.7	2.5	31	22
Mg	1.09	.34	31	22
Percent of exchangeable cations:				
K	3.8	1.8	47	21
Na	.70	.25	33	21
Ca	83.2	4.2	5	21
Mg	12.2	3.3	27	21

tained by repetitive leaching with 1.0 N NH_4Ac at pH=7.0. (See "Supplemental Information" for details.) Values for exchangeable cations (table 19) were calculated from the total extractable and water-soluble cations as follows:

Exchangeable cations=total (NH_4Ac) extractable cations—cations in water saturation extracts (all values in milliequivalents per 100 grams of dry soil).

The exchangeable cations were then recalculated to 100 percent (table 19). The adamellite soils are much lower than Reed soils in amounts of all exchangeable cations; they are higher in percentage exchangeable K, slightly higher in percentage Ca, comparable in Na percentage, and somewhat lower in percentage Mg.

CHEMICAL COMPOSITION OF SPRING WATERS

Water samples from four springs related to Reed Dolomite and adamellite of Sage Hen Flat were collected during the summer and fall of 1966 and during the summer of 1967. Water samples were filtered through 0.45-μm filters into airtight polyethylene containers. The samples were usually collected near sunrise or sunset to minimize air-water temperature differences, which would affect pH measurements. A part of each sample collected during the summer of 1967 was acidified to pH 2 to prevent precipitation of metals and was used for analysis of Al, Fe, and Mn. Al values are markedly higher for the 1967 samples, reflecting either precipitation of Al in previously collected samples or solution of particles less than 0.45 μm in the acidified parts. There was relatively good agreement of Fe and Al values in the 1967 samples with those reported for granitic waters in the Sierra Nevada by Feth, Roberson, and Polzer (1964). Changes caused by orifice location, diurnal variation, and seasonal fluctuation at a given spring were found to be negligible compared with differences between springs.

WATERS RELATED IN PART TO THE REED DOLOMITE

Poison Creek Spring emerges from the east side of a canyon wall about 400 feet east of the Wyman-Reed contact, which dips about 60° westward at this location. The spring water would appear to be chemically controlled in large part by the dolomite, which crops out continuously for several miles west of the Wyman contact, but the water is also influenced to a lesser degree by the sandstones, shales, and limestones near the orifice. Waters emerge from three orifices (herein designated A, B, and C, from south to north) about 15 feet apart. Discharge from orifice C, the major outlet, averages about 0.1 cfs (cubic feet per second), as measured with a Pygmy current meter.

Cottonwood Spring, the principal source of the south fork of Cottonwood Creek, is in a valley that partially separates the Reed Dolomite from the Cottonwood pluton. The orifice lies within the Reed, though, and the apparent catchment basin is dominated by dolomite. Discharge is quite constant at about 1.8–2.0 cfs.

Analytical data for these two sampling locations are summarized in table 20. The predominant ions are Ca,

TABLE 20.—*Field and laboratory analytical data for two natural waters associated in part with the Reed Dolomite*

[All concentrations in milligram per liter]

	Poison Creek Spring		Cottonwood Spring	
	Mean	Standard deviation	Mean	Standard deviation
Field pH	7.71	0.14	7.72	0.27
Specific conductance K	[1]286	------	[1]252	------
K^+	.99	.03	.81	.01
Na^+	3.35	.09	1.54	.07
Ca^{++}	29	2	24	1
Mg^{++}	14.9	.3	15.9	1
Ba^{++}	[1]<.5	------	[1]<.5	------
Mn	[1].002	------	[1].004	------
Fe	[1].001	------	[1].043	------
Al	[1].019	------	[1].013	------
SiO_2	13	.5	9.0	.2
B	[1].02	------	[1].01	------
Cl^-	[1].8	------	[1].6	------
Field HCO_3^-	178	7	162	4
NO_3^-	[1].3	------	[1].3	------
SO_4^{-2}	7.8	.7	3.1	.1
PO_4^{-3}	[1].00	------	[1].12	------
Water temperature (°C)	5.8	.3	6.9	1.0
Cation epm	2.84	------	2.59	------
Anion epm	3.06	------	2.75	------
Number of analyses	7	------	6	------

[1]Based on one analysis.

Digitized by Google

Mg, and bicarbonate; Na and sulfate are quite low. Poison Creek Spring shows the influence of the Wyman beds in its increased Na, K, Si, and sulfate with respect to the Cottonwood samples, and its higher Ca/Mg ratio reflects the presence of limestones near the orifice. The pH of Poison Creek is the same as that of Cottonwood Spring, however, and in most respects the waters of the two springs are similar.

Waters Related Largely to the Adamellite of Sage Hen Flat

Sage Hen Spring and Crooked Creek Spring appear to be almost entirely related to the Sage Hen Flat pluton. Formations adjacent to the adamellites, such as the Wyman Formation, Reed Dolomite, Deep Spring Formation, or Campito Formation could have some slight effect on the chemical composition of these waters. Discharge at Sage Hen Spring is about 0.1 cfs, but fluctuates appreciably. Discharge at Crooked Creek Spring is even smaller, its mean about 0.05 cfs or less.

Analytical data for the two sampling sites related to the adamellite are given in table 21. Crooked Creek Spring has a higher pH than Sage Hen Spring and contains less Mg and slightly less Na. The fact that the two waters, draining the same plutonic body, can be consistently distinguished chemically is an indication of the sensitivity of natural water to variation in bedrock composition and weathering conditions. The adamellite-derived spring waters, however, are virtually identical in most other respects and contrast sharply with those related to dolomite. Waters draining the adamellite are much higher in Na, sulfate, and chloride than are the dolomite waters and much lower in Ca, Mg, and bicarbonate. The pH values of the four spring waters are almost the same except for Crooked Creek Spring, which is more alkaline than either of the springs related to the dolomite.

Table 21.—*Field and laboratory analytical data for two natural waters associated with the adamellite of Sage Hen Flat*

[All concentrations in milligrams per liter]

	Crooked Creek Spring		Sage Hen Spring	
	Mean	Standard deviation	Mean	Standard deviation
Field pH	7.96	0.15	7.72	0.11
Specific conductance K	[1]129		[1]127	
K^+	.79	.05	.64	.02
Na^+	6.23	.19	6.56	.16
Ca^{++}	17	1	16	.5
Mg^{++}	.93	.06	1.55	.08
Ba^{++}	[2]< .5		[2]< .5	
Mn	[1].014		[1].000	
Fe	[1].02		[1].019	
Al	[1].014		[1].033	
SiO_2	15.4	.8	16.4	.5
B	[1].015		[2].01	
Cl^-	[1].9		[1].85	
Field HCO_3^-	61	3	60	1
NO_3^-	[1]3.3		[1].8	
$SO_4^{=}$	9.8	.5	9.4	1.1
$PO_4^{≡}$	[1].145		[1].11	
Water temperature (°C)	5.6	1	6.5	1
Cation epm	1.22		1.24	
Anion epm	1.29		1.22	
Number of analyses	13		7	

[1]Based on two analyses
[2]Based on one analysis

Analysis of Chemical Changes

For purposes of analysis and interpretation, the chemical data for natural waters related to both dolomite and adamellite are viewed in the following discussion from three perspectives: (1) Relative mobilities, showing the degree to which the various chemical species are mobilized from bedrock by weathering and released into solution, (2) stability with respect to some important solid and gas phases, including a discussion of water chemistry in relation to several equilibrium reactions, and (3) a chemical comparison of soil water with precipitation and spring waters.

Relative Mobilities

A common means of evaluating the ease with which various chemical constituents are released by weathering from bedrock to ground water is through the calculation of relative mobility:

$$\begin{matrix}\text{Relative mobility}\\ \text{(element X)}\end{matrix} = \frac{\text{Percent X of N-element total in water}}{\text{Percent X of N-element total in bedrock}}$$

where N is the number of elements considered. This computation assumes that a given water can be definitely correlated with a given lithology, that the mean analytical values for that lithology are representative, and that the composition of the water with regard to the investigated constituents is entirely a function of contact with the bedrock material. It is likely that the waters sampled in the White Mountains have been affected to some extent by windblown contaminants and the rhyolitic ash, but evidence presented here (see "Relationship of Soil Water to Precipitation and Spring Waters") suggests that major influences on ground-water composition occur after percolation through the soil.

Relative mobilities calculated for Cottonwood Spring with respect to dolomite bedrock (table 22) fall into the sequence $Mg > Ca \gg Fe > Mn$. Mobilities of other elements, for example, Si, Al, Ti, Na, and K, are more susceptible to influence by weathering of contaminants than of the bedrock, which contains only trace amounts of these constituents. Interpretation is therefore confined to the carbonate-component elements. The relative mobility sequence of table 22 agrees well with the order of percentage losses from dolomite bedrock to soil (cf. fig. 301), except that the mobility of Fe in dolomite is clearly greater than that of Mn, a relation not evident from solid-phase considerations.

In figure 306, ranges of relative mobilities for eight elements, based on analytical means and standard de-

Digitized by Google

TABLE 22.—*Relative mobilities for four elements in Cottonwood Spring waters*

	Mg	Ca	Fe	Mn
Concentration in bedrock................percent..	12.46	21.52	0.26	0.066
Concentration in Cottonwood Spring water..........mg/l..	15.9	24	.043	.004
Percent of four-element total (bedrock)...........	36.33	62.75	.76	.16
Percent of four-element total (spring)...........	39.79	60.08	.108	.010
Relative mobility..........................	1.095	.957	.142	.063

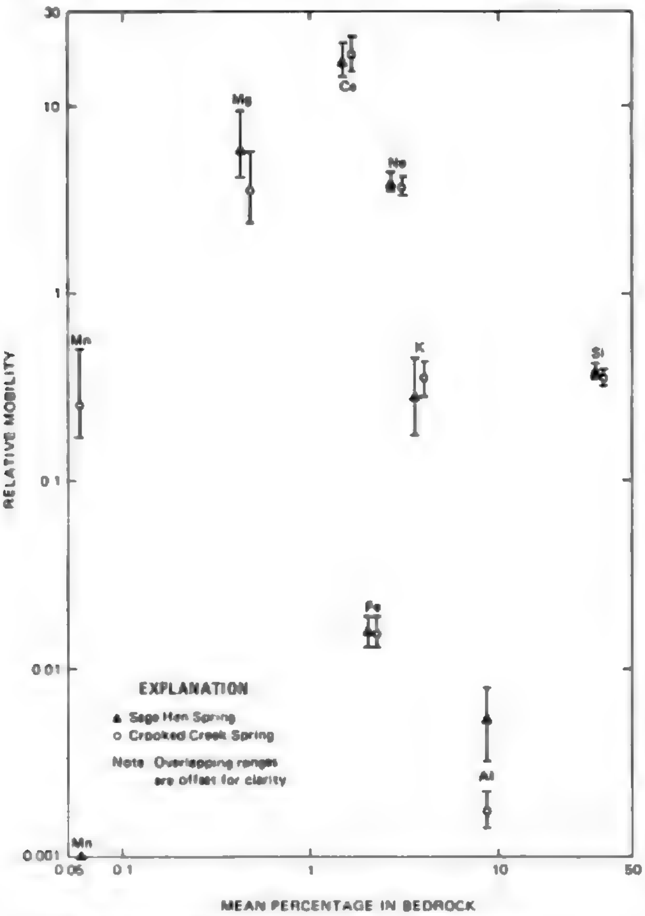

FIGURE 306.—Relative mobilities for eight elements in spring waters related to adamellite. Vertical bars indicate ranges of values.

viations at Crooked Creek Spring and Sage Hen Spring, are plotted against mean bedrock percentage on a log-log scale. The horizontal scale serves to emphasize the importance of the various constituents with regard to bedrock weathering and to their net contribution to the ground water. Elements plotting in the upper right of the diagram (Ca, Na, and Si in this case) are mobile constituents present in appreciable quantities in the bedrock and will be liberated in relatively large total amounts to the ground water. Elements that plot toward the lower left (such as Mn) are comparatively immobile, are not abundant in the adamellite, and are therefore released to the ground water in trace amounts.

The apparent sequence of mobilities for the adamellite-draining springs is Ca > Mg ≈ Na >> Si ≈ K ≥ Mn ≈ Fe > Al. Values for Mn, and to some extent for Mg, vary considerably between the two springs, making the placement of these elements within the order somewhat uncertain. The results as a whole are in good agreement with those of Feth, Roberson, and Polzer (1964) for quartz monzonite (adamellite) terrane in the Sierra Nevada and are generally similar to losses from bedrock to soil (table 14; fig. 301). The relative positions of Ca, Mg, and Na in the weathering sequence differ, however, between the solid phase and liquid phase perspectives. Considering the problems of soil contamination, one possibility is that carbonate grains may be continually blown into adamellite soils and quickly dissolved, resulting in increased Ca and Mg concentrations in waters draining the pluton. Only a few carbonate fragments were observed in adamellite soils; however, soluble grains (especially those reactive fragments of silt or clay size) would not be expected to persist in nonsoluble soils, and both dolomite and calcite were found in dust trap residues collected within the area (Marchand, 1970). Ruhe (1967, p. 57–59) suggested solution of windblown contaminants to explain the formation of thick caliche horizons in soils formed on low-Ca parent materials in New Mexico.

STABILITY WITH RESPECT TO SOLID AND GAS PHASES[5]

By using means and standard deviations for ion concentrations, pH, and temperature from Cottonwood Spring and Poison Creek Spring, maximum, minimum, and most probable values of ion-activity products (IAP) were calculated for both calcite and dolomite as follows:

$$IAP_c = \left[{}^{a}Ca^{++}\right]\left[{}^{a}CO_3^{-2}\right]$$

and

$$IAP_d = \left[{}^{a}Ca^{++}\right]\left[{}^{a}Mg^{++}\right]\left[{}^{a}CO_3^{-2}\right]^2,$$

where [a] is the ionic activity of the solutions (approximately equal to concentration). A comparison of the spring waters with regard to carbonate equilibria is presented in table 23. All waters are undersaturated with regard to both calcite and dolomite, yet minor amounts of calcium carbonate have precipitated on exposed rocks near all the springs sampled. Calcite lacks saturation by a factor of about 2.5–10 in the dolomite-

[5]Sources for physical constants used in calculations.
K_1 first carbonic acid dissociation, Harned and Davis (1943, p. 2030).
K_2 second carbonic acid dissociation, Harned and Scholes (1941, p. 1706).
KCO_2 graphical solution, using data of Markham and Kobe (1941, p. 449).
A first constant, Debye-Huckel equation, Manov, Bates, Hamer, and Acree (1943, p. 1765).
Kc calcite equilibrium constant, Larson and Buswell (1942, p. 1667).
Kd dolomite equilibrium constant, (Hsu, 1964).

TABLE 23.—*Degree of saturation with respect to calcite and dolomite for four spring waters*

[Ranges of values reflect temperature and compositional extremes. M.P. = most probable value; IAP = ion-activity product]

	Cottonwood Spring	Poison Creek Spring	Crooked Creek Spring	Sage Hen Spring
IAPc				
Maximum	2.83×10^{-9}	2.51×10^{-9}	....	....
M.P.	1.37×10^{-9}	1.67×10^{-9}	0.746×10^{-9}	0.401×10^{-9}
Minimum	$.682\times10^{-9}$	$.672\times10^{-9}$	....	....
Kc[1]				
Maximum	7.44×10^{-9}	7.92×10^{-9}	....	....
M.P.	7.69×10^{-9}	7.98×10^{-9}	8.02×10^{-9}	7.79×10^{-9}
Minimum	7.92×10^{-9}	8.02×10^{-9}	....	....
IAPc/Kc				
Maximum	.381	.317	....	....
M.P.	.178	.209	.093	.062
Minimum	.086	.083	....	....
IAPd				
Maximum	8.38×10^{-18}	5.09×10^{-18}	....	....
M.P.	2.03×10^{-18}	2.34×10^{-18}	4.99×10^{-20}	2.56×10^{-20}
Minimum	$.528\times10^{-18}$	$.401\times10^{-18}$	....	....
Kd[2]	2.0×10^{-17}	2.0×10^{-17}	2.0×10^{-17}	2.0×10^{-17}
IAPd/Kd				
Maximum	.419	.254	....	....
M.P.	.103	.117	2.5×10^{-3}	1.28×10^{-3}
Minimum	.026	.020	....	....

[1] From Larson and Buswell (1942, p. 1667).
[2] From Hsu (1964).

TABLE 24.—*Partial pressures of carbon dioxide in four spring waters and a comparison with atmospheric PCO_2*

[M.P. = most probable value]

	Cottonwood Spring	Poison Creek Spring	Crooked Creek Spring	Sage Hen Spring
PCO_2 of water (atm)				
Maximum	5.05×10^{-3}	4.10×10^{-3}	....	....
M.P.	2.66×10^{-3}	2.86×10^{-3}	5.70×10^{-4}	9.79×10^{-4}
Minimum	1.44×10^{-3}	1.98×10^{-3}	....	....
PCO_2 of atmosphere (atm)	2.3×10^{-4}	2.3×10^{-4}	2.3×10^{-4}	2.3×10^{-4}
$PCO_2(w)/PCO_2(a)$:				
Maximum	22	18	....	....
M.P.	12	12	2.5	4.2
Minimum	6.3	8.6	....	....

draining waters and by more than 10 in adamellite-derived waters. Cottonwood Spring and Poison Creek Spring are also much closer to dolomite saturation than are their counterparts in the pluton, but all waters are even more undersaturated with respect to dolomite than to calcite.

The undersaturation of calcium carbonate in the Crooked Creek and Cottonwood drainage basins contrasts with the fourfold supersaturation reported by Barnes (1965, p. 92) in the headwater springs of Birch Creek, just south of the study area. The latter drains a mixed terrane in which solution of Wyman limestones, as well as the Reed Dolomite, may have a profound influence on the state of the ground-water calcite reaction.

Partial pressures of carbon dioxide in the four spring waters (table 24) were computed from the following relation:

$$PCO_2(aq) = \frac{(H+)(HCO_3-)}{K_1 KCO_2}$$

where

$$K_1 = \frac{(H+)(HCO_3-)}{(H_2CO_3)}$$

and

$$KCO_2 = \frac{(H_2CO_3)}{PCO_2}.$$

All calculated values for the waters are at least twice that of the atmosphere, and Cottonwood Spring shows CO_2 partial pressures as much as 22 times greater than the air. The two springs related to the dolomite terrain have partial pressures much greater than the springs in the adamellite, yet the pH of all springs is similar. Solution of dolomite would tend to increase PCO_2 but would also increase pH, the net effect being to decrease free CO_2. The explanation for the striking contrast between the two groups of springs must partly lie in the marked vegetational differences between the two lithologies: The adamellites are dominated by relatively dense growth of sagebrush, limber pine, grasses, and perennials, whereas bristlecone pine and sparse low perennials cover most of the Reed terrane. Perhaps photosynthetic rates, and hence root respiration, differ greatly between the two plant communities. In any event, it is apparent that local vegetational changes may play an important role in controlling the pH of ground water and hence in regulating rates of chemical degradation.

For the adamellite-draining springs and adamellite soil water, means and standard deviations were used to compute molalities and activities for Na+, K+, H+, and H_4SiO_4 and to plot the range of each fluid on low-temperature stability diagrams for Na silicates (fig. 307) and K silicates (fig. 308). Plots based on activities did not differ significantly from those based on molality and are not reproduced on the diagrams. Sage Hen Flat pluton water plots within the kaolinite field in both figures, as do most stream and spring waters. The position of the water plots, toward the silica-rich side of the kaolinite field and away from the gibbsite field, tends to support the X-ray diffraction and microprobe evidence that kaolinite is forming as a stable authigenic phase in the adamellite soils. The waters are well above quartz saturation, probably owing to the weathering of Si from feldspars, biotite, and other silicates, in addition to quartz, but are significantly below saturation with amorphous silica.

Major departures from equilibrium are evidenced in adamellite-related waters by oversaturation with respect to quartz and undersaturation with respect to colloidal silica and in waters draining the Reed by undersaturation with regard to dolomite. Such departures, however, do not preclude the existence of steady-state conditions in the spring waters.

Digitized by Google

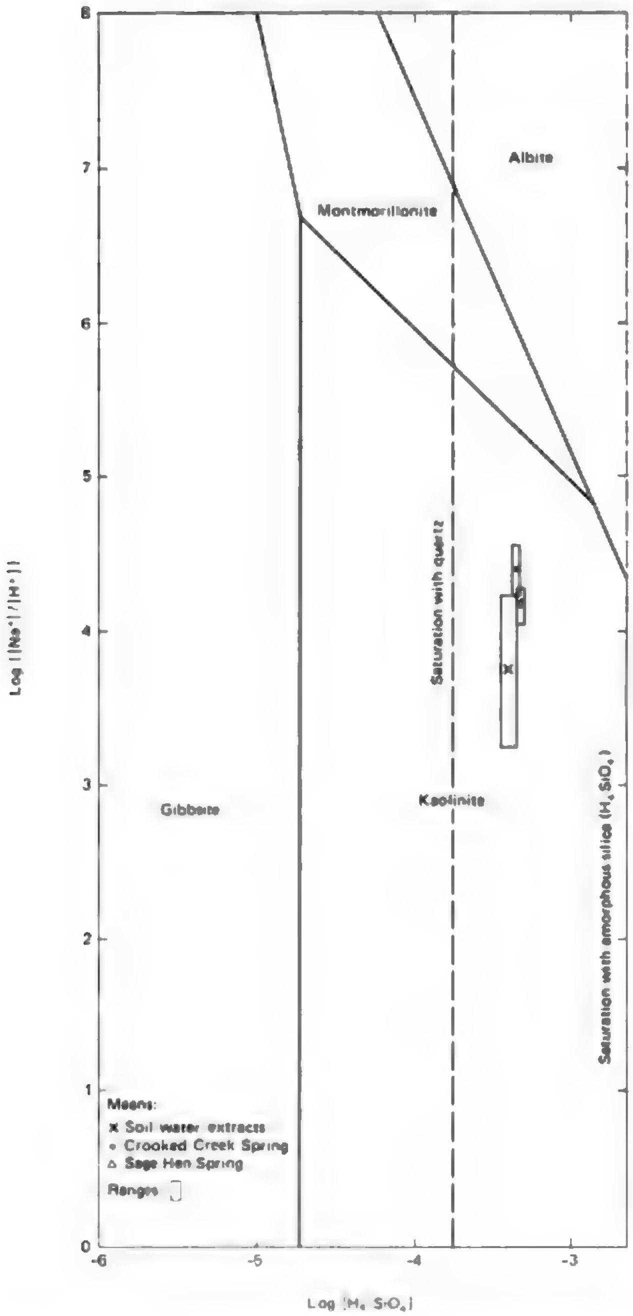

FIGURE 307.—Stability relations of phases in the system Na_2O-Al_2O_3-SiO_2-H_2O at 25°C and 1 atmosphere total pressure as functions of (Na^+)/(H^+) and (H_4SiO_4). After Feth, Roberson, and Polzer (1964, p. 63).

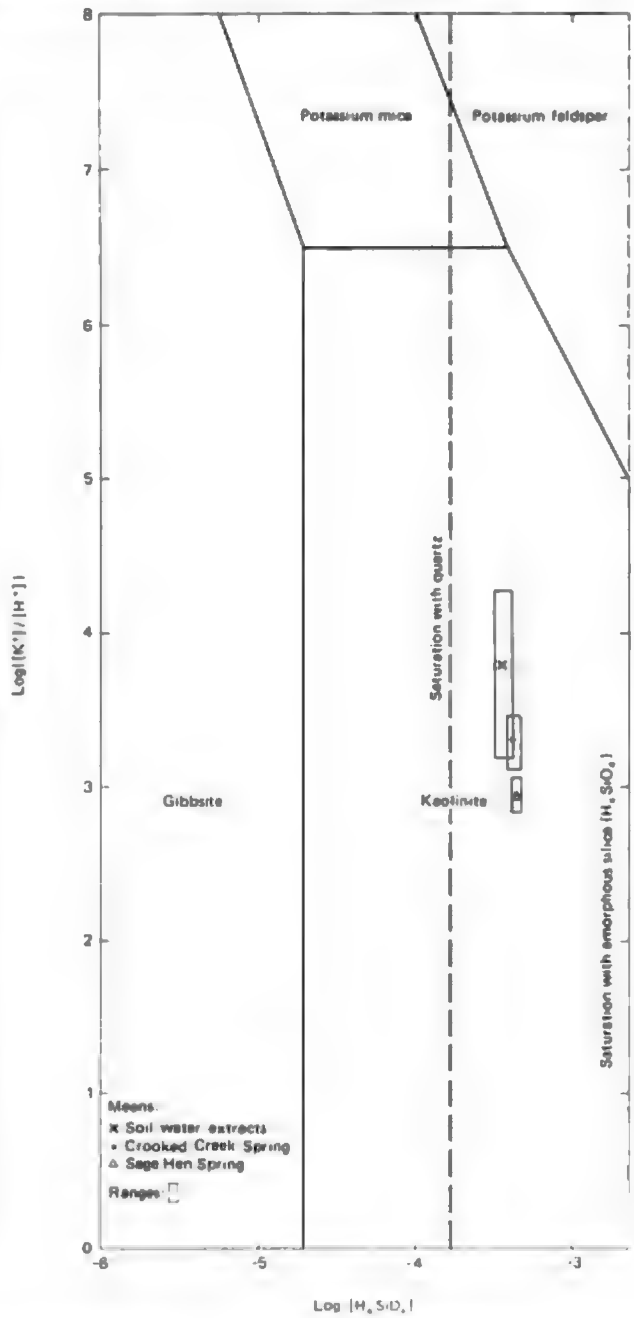

FIGURE 308.—Stability relations of phases in the system K_2O-Al_2O_3-SiO_2-H_2O at 25°C and 1 atmosphere total pressure as functions of (K^+)/(H^+) and (H_4SiO_4). After Garrels and Christ (1965, p. 361).

Relation of Soil Water to Precipitation and Spring Waters

An important question in the chemistry of natural waters is the space-time dimension of chemical weathering changes. Do most of the chemical additions to rain and snow water occur quickly within the soil, or does the composition of percolating ground waters continue to change, even if the lithology remains the same? Although absolute concentrations of chemical species in the soil water extracts are much higher than those in precipitation and spring water, comparisons are possible through ratios of dissolved constituents.

Digitized by Google

Figure 309 compares the composition of waters related to the Reed Dolomite in the ternary system Na + K − Ca− Mg.[6] The dolomite soil water extracts are more or less intermediate in composition between precipitation and spring water values, but somewhat higher in percentage Ca than either of the other fluids. A progressive increase in the divalent/monovalent cation ratio occurs from precipitation to soil water to springs. The Ca/Mg ratio increases slightly from about 1.8 in precipitation to a value of nearly 5 (the ratio in bedrock is about 1.6) in soil water, but then decreases substantially from soil water to spring water. This decrease may be in response not only to bedrock composition, but to selective adsorption and removal of Ca by the soil exchange complex. The fact that the spring waters do not plot closer to the bedrock is probably attributable to the weathering of ash and local soil contaminants and to differing relative mobilities of the plotted cations.

Waters related to the adamellite are compared for the same ternary system in figure 310 (bottom). Soil water plots over a wide range and shows a definite increase in Ca/Na + K and Ca/Mg with respect to both precipitation and bedrock. It appears to be closer in composition to spring water than precipitation in terms of Ca concentration. The hydrolysis of plagioclase, solution of secondary calcium carbonate in the soil, and the high mobility of Ca is probably responsible for this trend, which proceeds away from bedrock composition. Also in figure 310 (top), it appears that the Na/K ratio in the soil water extracts has decreased relative to precipitation in response to bedrock and perhaps ash composition. The large increase in Na/K from soil water to

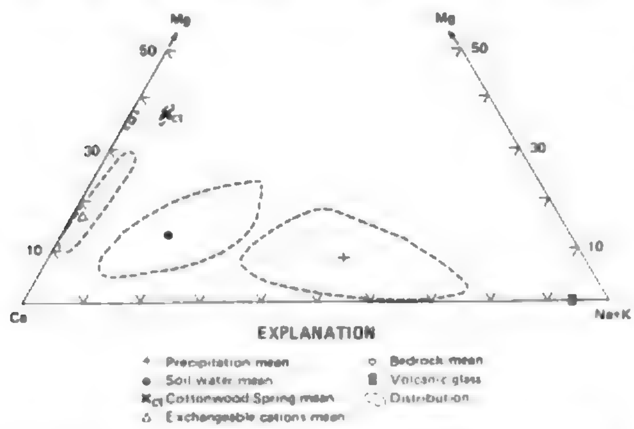

FIGURE 309.—Progressive cation changes from precipitation water to soil and spring waters related to Reed Dolomite. Plots of bedrock, volcanic glass, and exchangeable cations suggest relative influence of these factors.

[6]Values plotted on compositional diagrams in this paper were calculated on a parts per million (milligrams per liter) rather than an equivalents per million basis because the oxidation states of Fe and Mn were not known and a uniform basis between diagrams was desired.

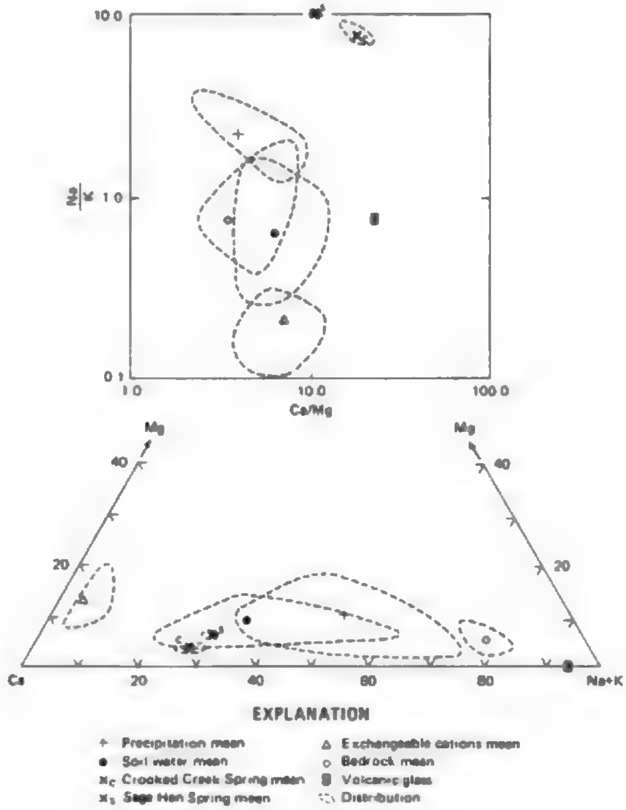

FIGURE 310.—Progressive cation changes from precipitation water to soil and spring waters related to adamellite.

ground water is interpreted as the result of K fixation by colloidal adsorption and selective plant uptake, and of high Na mobility. Soil water has a Na/K ratio much closer to precipitation than to spring water, but is quite distinct from both.

Figure 311 shows regular increases in both Mg/Fe and Ca/Fe from precipitation to soil water to spring water, with soil water plotting approximately intermediate in position between the other two fluids. Both trends are away from bedrock composition and apparently result from low Fe mobility due to precipitation of Fe oxides within the soil.

From precipitation water to soil water to ground water, increases are evident in Si relative to Na+K and Mg+Fe (fig. 312), presumably in response to bedrock composition and possibly also to the rhyolitic ash. Soil water extracts on this diagram plot much closer to precipitation than to spring waters.

The pH value is probably the best single indicator of water chemistry. The median pH of snow samples from the Sierra Nevada is reported as 5.8, close to the value for pure water in equilibrium with atmospheric carbon dioxide (Feth, Rogers, Roberson, 1964, p. 24-25). All soil and ground waters in the White Mountains have much

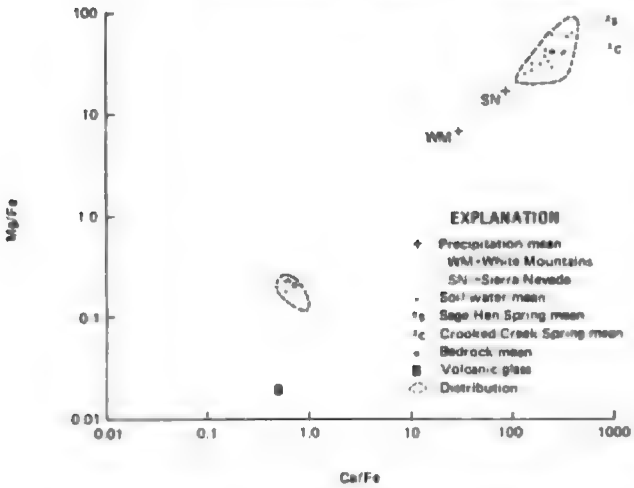

FIGURE 311.—Mg/Fe and Ca/Fe ratio comparisons of waters related to adamellite.

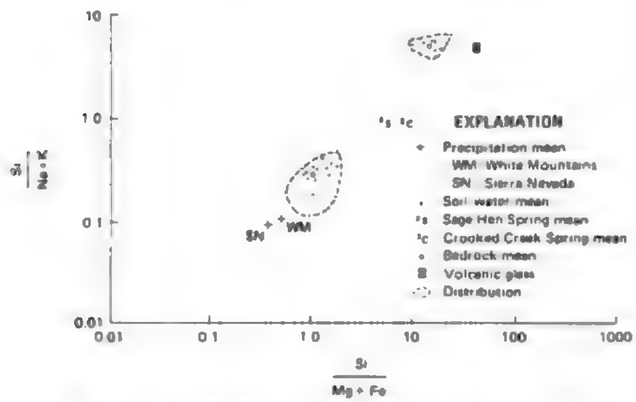

FIGURE 312.—Silica-cation ratio comparisons of adamellite-related waters.

higher pH's (tables 18, 20, 21) than this figure, owing principally to solution and hydrolysis reactions. For the dolomites, soil saturation pH is comparable to spring water pH, but for the adamellite, soil saturation values are intermediate between the pH of precipitation and that of the springs.

Most of the chemical trends just described appear to be controlled by bedrock composition or relative mobility, but the ground waters plot in tight groups distinct from the bedrock, suggesting that a steady-state condition, rather than chemical equilibrium, exists in spring waters that have passed through both lithologies. In the soils, absence of both equilibrium and steady state is manifested by the scatter of soil water points on the compositional diagrams.

Soil water extracts from both dolomite and adamellite terrain are notably distinct in composition from precipitation and spring waters draining the respective lithologies. Total concentrations are much greater in soil saturation extracts than in spring waters owing to the diluting effects of percolating precipitation water on the latter. The contrasting ionic composition of these two groups of fluids imply the existence of weathering reactions at considerable depth and preferential channeling of ground-water flow from certain localized areas of high recharge and possibly of different lithology. Most of the soil water extracts plot in an intermediate position between precipitation and ground water, but some (Na/K for adamellite-related water, for example) soil water plots do not fall in a position between the other two fluids. The pH of dolomite soil water extracts is much closer to spring water than to precipitation, however, suggesting that chemical adjustments in systems having soluble phases occur more rapidly than in those involving silicate or oxide phases.

Precipitation of calcium carbonate, probably sporadic in response to wet and dry seasons, and the contaminating influence of the rhyolitic ash, local aeolian debris, and foreign waters complicate the interpretation of soil water compositions. Also, the preceding conclusions assume that saturation extracts approximate actual soil water, an assumption which may not be entirely valid. A longer period of water contact with the soil might be expected to shift soil water composition closer to that of spring waters and to decrease the variability of extract compositions. A need exists for methods of soil water extraction which will produce fluids clearly representative of the actual soil solution under field conditions.

CHEMICAL FRACTIONATION IN THE BEDROCK-SOIL-WATER-PLANT SYSTEM

Elements released by solution or hydrolysis of mineral grains follow a variety of courses. They may dissolve in the soil water and be flushed out of the system, precipitate as a solid soil phase, become adsorbed on colloidal soil particles, or be utilized by organisms, especially vegetation. Chemical analyses of representative plants from the area, together with data already presented, make possible the location and apportionment of a number of chemical species within the bedrock-soil-water-plant systems of the Reed Dolomite and the adamellite of Sage Hen Flat.

Soil water and exchangeable cation concentrations were converted from milliequivalents per 100 g of soil to grams per cubic centimeter of soil, using milliequivalent weights and mean bulk densities of the total soil. Since the laboratory data apply to only the less-than-2-mm fraction, two sets of figures were calculated for the soil water, one assuming no contributions from the soil gravel fraction (minimum) and a second assuming a contribution from the coarse material proportional to its weight percentage of the whole soil (maximum).

For practical reasons, only a few of the hundreds of

White Mountains plant species could be analyzed. Aboveground parts of sagebrush (*Artemisia arbuscula*), junegrass (*Koeleria cristata*), and sandwort (*Arenaria kingii*), and twigs, needles, and cones of bristlecone pine (*Pinus aristata*) and limber pine (*P. flexilis*) were collected on both dolomite and adamellite. Aboveground parts of flax (*Linum perenne*) were obtained from dolomite terrain. These six species were chosen to represent vegetational groups as follows: *Pinus aristata* and *P. flexilis*—trees; *Artemisia arbuscula*—sagebrush and shrubs; *Koeleria cristata*—grasses; *Arenaria kingii*—noncarbonate-associated herbs; and *Linum perenne*— carbonate-associated herbs. Plant samples were washed with distilled water and ovendried at 104°C prior to ash analysis (table 25; see section "Supplemental Information" for analytical procedures.)

Percentage cover for the preceding groups, estimated at about 20 randomly selected sites on each lithology and then averaged for dolomite and for adamellite, is given in column 12 of table 25. These figures are recalculated to 100 percent in the last column. The percentages of total vegetation (in terms of cover) were then used to obtain weighted averages for each element in plants on each substrate, as follows:

Weighted average Si = (percent Si in species $\times$) (percent $\times$ in total vegetation) + (percent Si in species y) (percent y in total vegetation) + . . . + (percent Si in species N) (percent N in total vegetation),

where N is the total number of species considered. Vegetational concentrations from table 25 were adjusted to a grams per cubic centimeter basis using the weight and percent cover of each plant sampled (giving grams per square centimeter) and dividing by the mean depth of each soil type (giving grams per cubic centimeter of soil). Calculations were made for the individual species and for the weighted averages applicable to each soil type. Since these averages assume continuous vegetative cover, a second pair of weighted averages were computed, adjusting for the actual plant cover. Plots of total soil (uncorrected for contamination), exchangeable cation, soil water, and plant concentrations for adamellite and dolomite terrane are shown in figure 313. The adamellite comparisons, expressed on a percentage basis, are extended to precipitation, bedrock, and spring waters in figure 314. Vegetational concentrations are computed as percentage of soil water plus plant concentration in table 26.

An examination of element totals in figure 313 indicates that constituents released by weathering are concentrated primarily in exchangeable positions (cations only) and secondarily in soil water and plants. Exchangeable cations are adsorbed in the sequence Ca > Mg > K > Na. Cation exchange in soils therefore tends to decrease the Ca/Mg and K/Na ratios with respect to ratios of cations initially made available by weathering. Cation exchange is less important as a fractionation mechanism than these illustrations would imply, because after the exchange complex becomes saturated, no further removal by exchange can occur unless the exchange capacity increases.

Although trends vary to some extent between species, the overall tendency of the White Mountains flora, with respect to soil water (table 26), is to withdraw elements in the sequence P > Fe ≫ K > Ca ≅ Mg > Si ≫ Na. The ratio of plant concentration to soil water concentration is less for the dolomite, but the sequence is the same regardless of lithology. As the result of plant uptake, the soil K/Na ratio is further decreased, and Fe and P are extracted in relatively large quantities. Si is sufficiently soluble at the moderate to high pH's of the adamellite and dolomite soils to become concentrated in the liquid phase, although plant concentrations consti-

TABLE 25.—*Chemical composition (dry weight percentage basis) of some major plant species on Reed Dolomite and adamellite of Sage Hen Flat and weighted averages used for geochemical comparisons*

	Si	Al	Fe	Mn	Mg	Ca	Na	K	P	Number of plants	Number of duplicate analyses	Mean percent cover (see text)	Percent of total vegetation (see text)
Dolomite													
Pinus aristata	0.0080	0.073	0.015	0.0016	0.17	0.58	0.0063	0.20	0.0480	2	1	17.60	64.9
Pinus flexilis	.0140	.071	.013	.0061	.09	.57	.0133	.23	.0630	1	1	.77	2.8
Artemisia arbuscula	.0300	.60	.062	.0063	.23	.71	.0081	.77	.0874	3	3	1.45	5.4
Koeleria cristata	.0600	.82	.10	.0165	.26	.81	.0068	.27	.0560	3	1	2.74	10.1
Arenaria kingii	.0760	1.1	.108	.0100	.47	3.39	.0219	.69	.0530	4	1	2.43	9.0
Linum perenne	.0549	.42	.040	.0102	.26	.85	.0034	.82	.0745	6	1	2.11	7.8
Weighted average	.0292	.29	.036	.0049	.21	.88	.0072	.33	.0539			(27.10)	(100.0)
Adamellite													
Pinus aristata	.0120	.051	.010	.0049	.06	.55	.0078	.31	.0690	1	1	.05	.2
Pinus flexilis	.0120	.034	.0068	.0044	.06	.44	.0063	.45	.1100	1	1	2.61	9.6
Artemisia arbuscula	.0600	1.07	.147	.0131	.13	.57	.0118	.90	.1029	4	4	9.85	36.0
Koeleria cristata	.0300	.47	.064	.0064	.09	.34	.0058	.27	.1085	2	1	6.17	23.7
Arenaria kingii	.1200	5.5	.43	.0267	.33	2.52	.0153	.92	.1055	2	1	8.32	30.8
Weighted average	.0665	2.18	.20	.0148	.18	1.10	.0172	.68	[illegible]			(27.30)	(100.0)

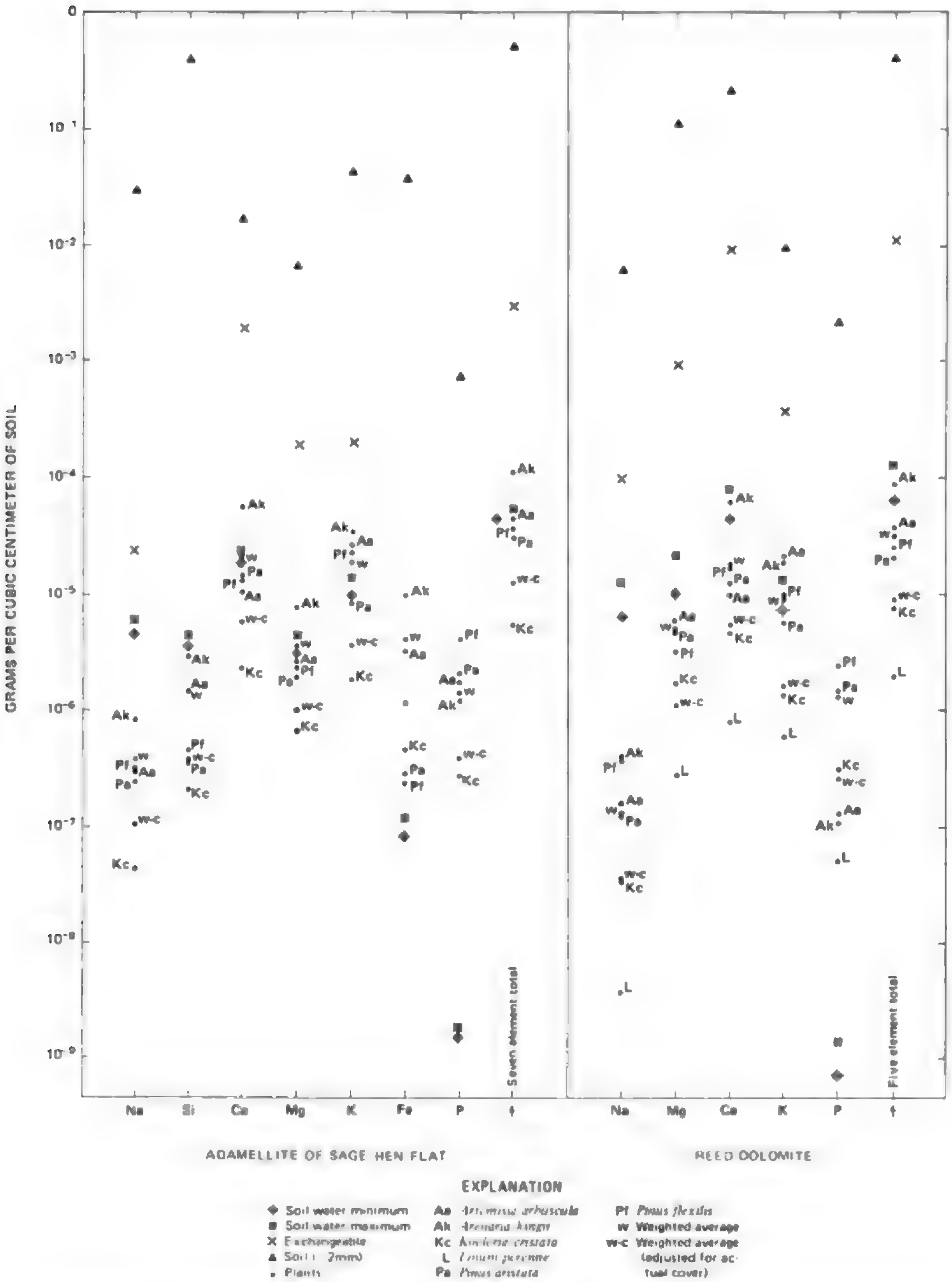

FIGURE 313.—Comparison of elemental and total concentrations in soil, soil water, colloidal exchange, and plants, expressed in terms of grams per cubic centimeter of soil.

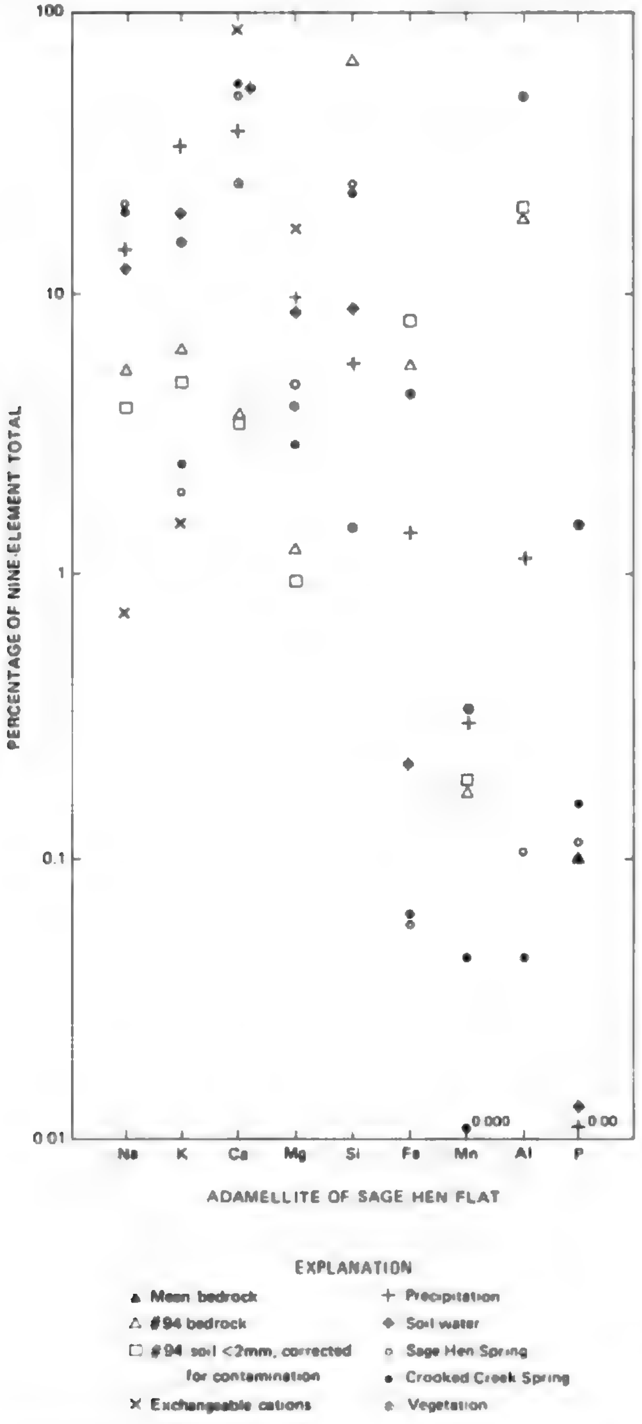

FIGURE 314.—Fractionation of nine elements in the adamellite bedrock-soil-water-plant system based on percentage concentrations.

tute as much as 30 percent of the nonexchangeable total for areas of continuous vegetative cover. Fe and P tend to be quite insoluble under these oxidizing and alkaline soil conditions.

TABLE 26.—*Fractionation by plants with respect to soil water for seven elements in adamellite and dolomite terranes*

$$\left[\text{Elemental percentage} = \frac{\text{Plant concentration (g/cc soil)}}{\text{Plant concentration + soil water concentration (g/cc soil)}} \times 100\right]$$

	Si	Ca	Mg	Na
Adamellite:				
Continuous cover	25–30	46–53	47–54	5.9 –7.4
Actual cover	8.3–11	19–23	19–24	1.7 –2.1
Dolomite:				
Continuous cover	......	17–30	17–30	1.1 –2.3
Actual cover	......	5.1–10.0	5.2–10.2	0.31–0.65
	K	**Fe**	**P**	**Total**
Adamellite:				
Continuous cover	51–58	98	~100	47–54
Actual cover	22–27	92	99	20–24
Dolomite:				
Continuous cover	34–51	--	100	18–32
Actual cover	12–22	--	99–~100	5.7–11

The actual extent to which vegetational fractionation occurs is of course dependent on the rate of plant uptake with respect to the rate of leaching. It has been demonstrated (Marchand, 1971) that chemical denudation by plant uptake and litter erosion in this area, although of much less significance than leaching in terms of total chemical removal, may be of considerable importance in the extraction of certain elements, especially metals such as Al, Fe, and Mn. It should also be remembered that elemental concentrations in vegetation represent large static quantities which are unavailable to leaching and which are potentially removable by sporadic accelerated erosion owing to fires or flooding, as well as by normal seasonal denudation.

SUMMARY AND DISCUSSION

The influences of erosion, deposition, vegetation, and microbial activity combine to further complicate an already complex series of chemical and physical alterations (fig. 269) in the weathering processes by which unstable minerals are converted to stable forms under the prevailing surficial conditions, which may themselves change with time. A complete analysis of all aspects of the weathering process is beyond the scope of this paper (the influences of microorganisms, for example, is not evaluated), but the data of the preceding pages suggest the direction and approximate magnitude of some physical, mineralogical, and chemical changes resulting from the weathering of dolomite and biotite adamellite in a present-day semiarid, subalpine climate. These changes involve alterations not only in the solid phases, but in the associated liquid and gas phases as well. Elements released by weathering are fractionated through the effects of plants, colloidal exchange, and leaching.

Digitized by Google

WEATHERING OF REED DOLOMITE

Field observations and size analyses of soils and bedrock indicate that the initial step of dolomite weathering in the White Mountains involves both physical and chemical breakdown of angular blocks produced by jointing. Polycrystalline soil grains, commonly bounded by cleavages, slowly accumulate from freeze-and-thaw disintegration of these blocks, except in areas of recrystallization near plutonic bodies; here postthermal contraction may have created intergranular stresses, leading to accelerated weathering and spheroidal forms. Chemical weathering is evident throughout the process of grain diminution, but appears to exert a greater effect in the interval between bedrock and soil gravel than between soil gravel and less-than-2-mm soil. Mineralogical decomposition, occurring in the sequence dolomite $\gg$ tremolite, epidote $>$ talc, K-feldspar, plagioclase, biotite $\geq$ apatite $>$ quartz and ilmenite (fig. 294), resulted in percentage chemical losses, from bedrock to soil, of Mg $>$ Ca $>$ Sr $>$ Mn $\overset{?}{\approx}$ Fe (fig. 301). Pure calcite, apparently precipitated during periods of desiccation and partially dissolved during seasonal influx of meteoric waters, occurs as the single verifiably authigenic soil phase, in rinds on spheroidally weathering boulders, on surfaces of soil fragments, and as a discontinuous calcium carbonate soil crust.

Relative mobilities of spring waters with respect to the dolomite bedrock yield the sequence Mg $>$ Ca $\gg$ Fe $>$ Mn (table 22). These findings agree with losses from bedrock to soil, except that they show Fe to be more easily mobilized from dolomite than Mn. Dolomite soil water extracts differ notably in composition from both spring and precipitation waters, probably owing in part to secondary calcite, ash fragments, and local contaminants in the soils. The soil water extracts have pH's much closer to the spring waters than to rain or snow, suggesting a fairly rapid adjustment to soil composition in these soluble soils. Comparisons of ion-activity products with solubility constants indicate that waters draining the terrane are undersaturated with respect to both calcite and dolomite.

Calculated carbon dioxide partial pressures for dolomite-derived waters exceed atmospheric values by more than an order of magnitude and those of waters from the adamellites by several times. The excesses above atmospheric PCO_2 are presumably created by a combination of root respiration, humus oxidation, and other organic processes; the greater PCO_2 values in the dolomite waters must primarily reflect the change in vegetation with substrate, not solution of carbonate.

WEATHERING OF ADAMELLITE OF SAGE HEN FLAT

Weathering in the Sage Hen pluton occurs in several stages. Physical disintegration proceeds by frost riving along intergranular weaknesses caused by cooling and contraction of the rock or possibly by swelling of biotite during initial weathering. Boulders exfoliate and grus accumulates in the A_{11} soil horizon. This coarse material is largely unaltered chemically or mineralogically except for minor Fe oxidation; the principal chemical attack occurs during the transformation of grus to finer sized particles. Primary minerals weather in the sequence plagioclase (An_{25-30}) $>$ hornblende $>$ biotite, epidote $>$ microcline, plagioclase (An_{10-15}), allanite $>$ apatite, chlorite, magnetite $>$ sphene, quartz, muscovite, ilmenite $>$ zircon (fig. 297), resulting in percentage chemical losses, from fresh rock to soil, in the sequence Rb $\overset{?}{>}$ Na $\approx$ K $\approx$ Mg $>$ Sr $>$ Mn $\approx$ Ca $>$ Ba $>$ Si $>$ Al $\gg$ Fe $>$ Ti (fig. 301). X-ray diffractometer and electron microprobe results suggest that kaolinite, and possibly small amounts of vermiculite and montmorillonite, are forming as authigenic alteration products of feldspars, biotite, and other silicates. Microprobe analyses of biotite indicate losses in the sequence Ba $\overset{?}{>}$ K $>$ Mg $>$ Fe $>$ Si $>$ Al (table 8); cations in eightfold to twelvefold coordination appear to be lost most readily, followed by octahedral cations, and finally elements in sixfold and fourfold coordination. Microcline shows some losses of both Na and K, and plagioclase (An_{10-30}) shows changes that imply removal in the sequence Na $>$ Ca $>$ Si $>$ Al (table 10; fig. 300).

Relative mobilities of chemical species in adamellite spring waters indicate that changes with regard to bedrock occur in the sequence Ca $>$ Mg $\approx$ Na $\gg$ Si $\approx$ K $\geq$ Mn $\approx$ Fe $>$ Al (fig. 306). Although this order shows some agreement with bedrock-to-soil losses, it is not entirely consistent with conclusions based on the solid phases alone. The low K mobility is probably the result of plant extraction and fixation within the soil. Plant uptake and litter erosion may explain the low Al content of spring waters. It is suggested that Mg and especially Ca are augmented in waters draining the pluton owing to the solution of fine-grained carbonate particles continually blown into the adamellite terrane. If this latter hypothesis is correct, the chemistry of ground waters is extremely sensitive to the presence of small quantities of soluble materials, including those foreign to the area. The fact that waters from two springs draining the adamellite can be chemically distinguished is another indication of such sensitivity. Both soil and spring waters associated with the pluton plot within the kaolinite stability field (figs. 307, 308) and are supersaturated with quartz but undersaturated with respect to colloidal silica. Proportions of solutes in adamellite soil water extracts appear to be roughly intermediate between precipitation and spring water in the adamellite terrane.

Digitized by Google

GENERAL WEATHERING RELATIONSHIPS

Observations in the White Mountains, as well as in warmer and wetter regions, suggest that physical weathering of a given lithology may be chiefly a function of the nature and spacing of initial physical weaknesses, particularly intergranular openings, cleavages, fissility, and planar weaknesses, especially joints, which may serve as avenues for fluids. The process of physical breakdown, which tends to precede chemical weathering, may be as closely related to lithologic features as to external conditions. Thermal history or inherent properties such as grain size, grain adhesion or cohesion, crystallographic properties of mineral constituents, bedding characteristics, or jointing may be more critical in affecting rates of physical weathering than climate.

Chemical weathering of any mineral is a function of the chemical composition and crystalline structure of the mineral and of the chemical environment in which weathering occurs. Ca, Mg, Fe, Mn, and Sr, for example, are all lost more readily from dolomite than from silicates and oxides in the adamellite. Dolomite-to-soil percentage losses of Fe are about the same as for Mn, but adamellite Mn losses are much greater than those of Fe. In nonsoluble lithologies such as the adamellite of Sage Hen Flat, chemical losses tend to adhere to the general pattern of alkali metals > alkaline earth metals > nonmetals > metals.

Precipitation water undergoes major chemical changes upon entering the soil, but significant additional modifications occur during percolation to springs. The state of both soil and spring waters with respect to calcite, dolomite, and silica saturation preclude chemical equilibrium in the natural waters studied. This result is not surprising since chemical weathering, which supplies most of the constituents to the waters, is itself an open-system disequilibrium process. It is noteworthy, however, that although steady-state conditions are definitely not attained in soil waters, spring waters closely approximate constant composition. Contact with weathering materials over a considerable space-time interval is apparently necessary for the achievement of a steady state, but this interval may be decreased somewhat in the case of mobile constituents in readily weatherable minerals. The existence of steady-state spring water compositions indicates another area of applicability of the "dynamic equilibrium" concept suggested by Hack (1960) and others in regard to surficial processes.

Elements removed from lattice sites in primary minerals undergo fractionation by (1) formation of secondary phases—primarily clay minerals, calcium carbonate, and various insoluble precipitates, (2) adsorption on colloidal mineral or organic particles, (3) plant uptake, and (4) solution. Quantitative information concerning fractionation of elements into secondary phases is not available for the two lithologies studied here (Al, Si, Fe, Mn, P, and Ca probably undergo fixation to some extent, in this form), but nine principal elements appear to apportion themselves between vegetation, colloidal exchange, and solution as follows (figs. 313, 314; table 25):

Na,	soln ≫ exch > veg
Si,	soln ≫ veg
Ca,	exch > soln > veg
Mg,	exch > soln $\stackrel{?}{=}$ veg
K,	veg ≫ soln > exch
Fe, Mn, P,	veg ≫ soln
Al,	veg ⋙ soln

Constituents entering authigenic phases or exchangeable positions are retained within the soil and are removed only through soil erosion or change in chemical environment. Elements taken up by plants are recycled through the soil to the extent that decomposition takes precedence over litter erosion. Evidence presented elsewhere (Marchand, 1971) suggests that, in this area at least, most elements are eventually dissolved and carried out of the soil by deep percolation. Results from the preceding study indicate that removal by plant uptake and litter erosion, although probably not significant in terms of total chemical denudation, may play some part in the total extraction of P and K from the bedrock and soil and undoubtedly accounts for appreciable parts of the chemical denudation of Al, Fe, and Mn. Another effect of vegetation in the weathering process may lie in the conversion of relatively insoluble constituents to more soluble chemical forms in which they could be carried out of the system. Plant uptake, litter fall, and decomposition may thus facilitate leaching, but data are lacking to evaluate the quantitative importance of this aspect of the geochemical cycle.

REFERENCES CITED

Anderson, G. H., 1937, Granitization, albitization, and related phenomena in the northern Inyo Range of California-Nevada: Geol. Soc. America Bull., v. 48, no. 1, p. 1–74.

Anderson, G. H., and Maxson, J. H., 1935, Physiography of the northern Inyo Range [abs.]: Geol. Soc. America Proc., 33d, Berkeley 1934, Cordilleran Sec., p. 318.

Barnes, Ivan, 1964, Field measurement of alkalinity and pH: U.S. Geol. Survey Water-Supply Paper 1535–H, 17 p.

———1965, Geochemistry of Birch Creek, Inyo County, California, a travertine depositing creek in an arid climate: Geochim. et Cosmochim. Acta, v. 29, no. 2, p. 85–112.

Bateman, P. C., and Wahrhaftig, Clyde, 1966, Geology of the Sierra Nevada, *in* Geology of northern California: California Div. Mines and Geol. Bull. 190, p. 107–172.

Beaty, C. B., 1959, Slope retreat by gullying [California-Nevada]: Geol. Soc. America Bull., v. 70, p. 1479–1482.

———1960, Gradational processes in the White Mountains of California and Nevada: Ph.D. thesis, Univ. California, Berkeley, 260 p.

Bower, C. A., Reitemeier, R. F., and Fireman, M., 1952, Exchangeable cation analysis of saline and alkali soils: Soil Sci., v. 73, no. 4, p. 251–261.

Bower, C. A., and Wilcox, L. V., 1965, Soluble salts, *in* Methods of soil analysis; Part 2, Chemical and microbiological properties: Madison, Wis., Am. Soc. Agronomy (Agronomy, no. 9), p. 933–951.

Brewer, Roy, 1964, Fabric and mineral analysis of soils: New York, John Wiley and Sons, Inc., 470 p.

Cady, J. G., 1951, Rock weathering and soil formation in the North Carolina Piedmont region: Soil Sci. Soc. America Proc., v. 15, p. 337–342.

Carmichael, I. S. E., 1967, The iron-titanium oxides of salic volcanic rocks and their associated ferromagnesian silicates: Contr. Mineralogy and Petrology, v. 14, no. 1, p. 36–64.

Cloud, P. E., Jr., and Nelson, C. A., 1966, Phanerozoic-cryptozoic and related transitions—new evidence: Science, v. 154, no. 3750, p. 766–770.

Dalrymple, G. B., 1963, Potassium-argon dates of some Cenozoic volcanic rocks of the Sierra Nevada, California: Geol. Soc. America Bull., v. 74, no. 4, p. 379–390.

Deer, W. A., Howie, R. A., and Zussman, J., 1962a, Rock-forming minerals; Volume 3, Sheet silicates: New York, John Wiley and Sons, Inc., 270 p.

———1962b, Rock-forming minerals; Volume 1, Ortho- and ring-silicates: New York, John Wiley and Sons, Inc., 333 p.

———1963a, Rock-forming minerals; Volume 2, Chain silicates: New York, John Wiley and Sons, Inc., 379 p.

———1963b, Rock-forming minerals; Volume 4, Framework silicates: New York, John Wiley and Sons, Inc., 435 p.

Emerson, D. O., 1966, Granitic rocks of the Mt. Barcroft quadrangle, Inyo batholith, California-Nevada: Geol. Soc. America Bull., v. 77, no. 2, p. 127–152.

Feth, J. H., Roberson, C. E., and Polzer, W. L., 1964, Sources of mineral constituents in water from granitic rocks, Sierra Nevada, California and Nevada: U.S. Geol. Survey Water-Supply Paper 1535–I, 70. p.

Feth, J. H., Rogers, S. M., and Roberson, C. E., 1964, Chemical composition of snow in the northern Sierra Nevada and other areas: U.S. Geol. Survey Water-Supply Paper 1535–J, 39. p.

Folk, R. L., 1965, Petrology of sedimentary rocks: Austin, Texas, Hemphill's, 159 p.

Gallick, C. M., 1964, Geology of a part of the Blanco Mountain quadrangle, Inyo County, California: M. A. thesis (unpub.), Univ. California, Los Angeles.

Garrels, R. M., and Christ, C. L., 1965, Solutions, minerals, and equilibria: New York, Harper and Row, 450 p.

Goldich, S. S., 1938, A study in rock-weathering: Jour. Geology, v. 46, p. 17–58.

Hack, J. T., 1960, Interpretation of erosional topography in humid temperate regions (Bradley volume): Am. Jour. Sci., v. 258–A, p. 80–97.

Hall, M. L., 1964, Intrusive truncation of the Precambrian-Cambrian succession in the White Mountains, California: M. A. thesis, Univ. California, Berkeley, 90 p.

Harned, H. S., and Davis, Raymond, Jr., 1943, The ionization constant of carbonic acid in water and the solubility of carbon dioxide in water and aqueous salt solutions from 0° to 50° C.: Am. Chem. Soc. Jour., v. 65, p. 2030–2037.

Harned, H. S., and Scholes, S. R., Jr., 1941, The ionization constant of HCO_3 from 0° to 50° C.: Am. Chem. Soc. Jour., v. 63, p. 1706–1709.

Hay, R. L., 1959, Origin and weathering of late Pleistocene ash deposits on St. Vincent, B. W. I.: Jour. Geology, v. 67, no. 1, p. 65–87.

———1966, Zeolites and zeolitic reactions in sedimentary rocks: Geol. Soc. America Spec. Paper 85, 130 p.

Helley, E. J., 1966, Sediment transport in the Chowchilla River basin: Mariposa, Madera, and Merced Counties, California: Ph. D. thesis (unpub.), Univ. California, Berkeley, 153 p.

Hsu, K. J., 1964, Solubility of dolomite estimated on the basis of the chemical composition of Florida ground waters [abs]: Geol. Soc. America Spec. Paper 76, p. 84–85; Ground Water, v. 2, no. 1, p. 56.

Johnson, C. M., and Ulrich, Albert, 1959, Analytical methods for use in plant analyses: California Agr. Expt. Sta. Bull. 766, Part 2, p. 26–77.

Jones, L. H., and Thurman, D. A., 1957, The determination of aluminum in soil, ash, and plant materials using Eriochrome Cyanine R. A.: Plant and Soil, v. 9, p. 131–142.

Kesseli, J. E., and Beaty, C. B., 1959, Desert flood conditions in the White Mountains of California and Nevada: U.S. Army Quartermaster Research and Eng. Center, Tech. Rept. EP–108, 107 p.

Kilmer, V. J., 1965, Silicon, *in* Methods of soil analysis; Part 2, Chemical and microbiological properties: Madison, Wis., Am. Soc. Agronomy (Agronomy, no. 9), p. 959–962.

Knopf, Adolf, 1918, A geologic reconnaissance of the Inyo Range and the eastern slope of the southern Sierra Nevada, California: U.S. Geol. Survey Prof. Paper 110, 130 p.

Krauskopf, K. B., 1968, A tale of ten plutons: Geol. Soc. America Bull., v. 79, no. 1, p. 1–18.

———1971, Geologic map of the Mount Barcroft quadrangle, California-Nevada: U.S. Geol. Survey Geol. Quad. Map GQ–960.

LaMarche, V. C., Jr., 1967, Spheroidal weathering of thermally metamorphosed limestone and dolomite, White Mountains, California, *in* Geological Survey research, 1967: U.S. Geol. Survey Prof. Paper 575–C, p. C32–C37.

———1968, Rates of slope degradation as determined from botanical evidence, White Mountains, California: U.S. Geol. Survey Prof. Paper 352–I, p. 341–377.

Larson, T. E., and Buswell, A. M., 1942, Calcium carbonate saturation index and alkalinity interpretations: Am. Water Works Assoc. Jour., v. 34, no. 11, p. 1667–1684.

McKee, E. H., and Nash, D. B., 1967, Potassium-argon ages of granitic rocks in the Inyo batholith, east-central California: Geol. Soc. America Bull., v. 78, no. 5, p. 669–680.

Major, Jack, 1967, Potential evapotranspiration and plant distribution in Western States with emphasis on California, *in* Shaw, R. H., ed., Symposium on ground level climatology, 1965, Berkeley, Calif.: Am. Assoc. Adv. Sci. Pub. 86, p. 93–126.

Manov, G. G., Bates, R. G., Hamer, W. J., and Acree, S. F., 1943, Values of the constants in the Debye-Huckel equation for activity coefficients: Am. Chem. Soc. Jour., v. 65, p. 1765.

Marchand, D. E., 1968, Chemical weathering, soil formation, and geobotanical correlations in a portion of the White Mountains, Mono and Inyo Counties, California: Ph. D. thesis, Univ. California, Berkeley, 376 p.

———1970, Soil contamination in the White Mountains, eastern California: Geol. Soc. America Bull., v. 81, no. 8, p. 2497–2505.

———1971, Rates and modes of denudation, White Mountains, eastern California: Am. Jour. Sci., v. 270, p. 109–135.

———1973, Edaphic control of plant distribution in the White Mountains, eastern California: Ecology, v. 54, no. 2, p. 233–250.

Markam, A. A., and Kobe, K. A., 1941, The solubility of carbon dioxide and nitrous oxide in aqueous salt solutions: Am. Chem. Soc. Jour., v. 63, p. 449.

Maxson, J. H., 1935, Pre-Cambrian stratigraphy of the Inyo Range [abs.]: Geol. Soc. America Proc., 33d, Berkeley 1934, Cordilleran Sec., p. 314.

Mead, W. J., 1915, Occurrence and origin of the bauxite deposits of Arkansas: Econ. Geology, v. 10, p. 28–54.

Digitized by Google

Morrison, R. B., 1964, Lake Lahontan: Geology of southern Carson Desert, Nevada: U.S. Geol. Survey Prof. Paper 401, 156 p.

Munz, P. A., and Keck, D. D., 1959, A California flora: Berkeley, Univ. California Press, 1681 p.

Nelson, C. A., 1962, Lower Cambrian-Precambrian succession, White-Inyo Mountains, California: Geol. Soc. America Bull., v. 73, p. 139–144.

———1963, Preliminary geologic map of the Blanco Mountain quadrangle, Inyo and Mono Counties, California: U.S. Geol. Survey Mineral Inv. Field Studies Map MF-256.

———1966, Geologic map of the Blanco Mountain quadrangle, Inyo and Mono Counties, California: U.S. Geol. Survey Geol. Quad. Map GQ-529.

Nelson, C. A., and Perry, L. J., 1955, Late Precambrian-early Cambrian strata, White-Inyo Mountains, California [abs]: Geol. Soc. America Bull., v. 66, no. 12, Part 2, p. 1657–1658.

Nicholls, J. W., 1965, Summary of the climatic conditions and geologic history of the White Mountains region, California: Space Sci. Lab. Pub., Univ. California, Berkeley.

Olsen, S. R., and Dean, L. A., 1965, Phosphorus, *in* Methods of soil analysis; Part 2, Chemical and microbiological properties: Madison, Wis., Am. Soc. Agronomy (Agronomy, no. 9), p. 1035–1049.

Pace, Nello, 1963, Climatological data summary for the decade 1 January 1953 through 31 December 1962 from the Crooked Creek Laboratory (10,150 ft) and the Barcroft Laboratory (12,470 ft): Berkeley, Univ. California, White Mountain Research Sta. rept., 52 p.

Pittman, E. D., 1958, Geology of the northwestern portion of the Blanco Mountain quadrangle, California: M. S. thesis (unpub.), Univ. California, Los Angeles, 103 p.

Powell, D. R., 1963, The physical geography of the White Mountains, California-Nevada: M. A. thesis (unpub.), Univ. California, Berkeley.

Rosenblum, Samuel, 1956, Improved techniques for staining potash feldspars: Am. Mineralogist, v. 41, nos. 7–8, p. 662–664.

Ruhe, R. V., 1967, Geomorphic surfaces and surficial deposits in southern New Mexico: New Mexico Bur. Mines and Mineral Resources Mem. 18, 65 p.

Sherman, G. D., and Uehara, Goro, 1956, The weathering of olivine basalt in Hawaii and its pedogenic significance: Soil Sci. Soc. America Proc., v. 20, p. 337–340.

Spurr, J. E., 1903, Descriptive geology of Nevada south of the fortieth parallel and adjacent portions of California: U.S. Geol. Survey Bull. 208, p. 206–212.

Taylor, M. E., 1966, Precambrian mollusc-like fossils from Inyo County, California: Science, v. 153, no. 3732, p. 198–201.

Taylor, R. L., 1965, Cenozoic volcanism, block faulting, and erosion in the northern White Mountains, Nevada: M. A. thesis (unpub.), Univ. California, Berkeley, 95 p.

Wahrhaftig, Clyde, 1965, Stepped topography of the southern Sierra Nevada, California: Geol. Soc. America Bull., v. 76, no. 10, p. 1165–1190.

Waring, R. H., and Hermann, R. K., 1966, A modified Piche evaporimeter: Ecology, v. 47, no. 2, p. 308–310.

Warshaw, C. M., and Roy, Rustum, 1961, Classification and a scheme for the identification of layer silicates: Geol. Soc. America Bull., v. 72, p. 1455–1492.

Wolfenden, E. B., 1965, Geochemical behavior of trace elements during bauxite formation in Sarawak, Malaysia: Geochim. et Cosmochim. Acta, v. 29, p. 1051–1062.

Wooley, J. T., and Johnson, C. M., 1957, Silicon determination in ashed plant material: Agr. and Food Chemistry, v. 5, no. 11, 872. p.

SUPPLEMENTAL INFORMATION

Digitized by Google

METHODS, REPRODUCIBILITY, AND ACCURACY

Field procedures for the collection of data and samples have been discussed in the text. Several temporary field impregnations were obtained from soil pits with Quickmont (available from E. V. Roberts and Associates, Culver City, Calif.) and later fully impregnated under vacuum with leucite. The advantage of the field impregnation is that natural orientation and textures are maintained. Bedrock and soil samples were treated in the laboratory as outlined in figures 315 and 316.[7]

Fresh bedrock chips and soil samples (soil gravel, less than 2 mm) were crushed with a tungsten carbide mortar and pestle and ground to −50 mesh in a tungsten carbide ball mill. Each fraction was then split and made into an X-ray fluorescence pellet. The values of table 27 (top), representing chips of the same sample, ground in different mortars and separately prepared, indicate no significant source of error in the grinding, splitting, or pellet-making operations. The replicate analyses of the table suggest precision of about ± 0–6 percent of the analyzed value and generally below 2 percent for values above 2.0 percent. Table 28 compares X-ray fluorescence results with those of wet chemistry (unpub. data of Ken-ichiro Aoki) and those for Na and K by flame photometer (by Joaquin Hampel; see "Introduction"). Agreement is good in some cases and very poor in others. Lighter elements such as Na, Mg, Al, and Si are not as easily excited by X-rays as heavier elements and are most susceptible to error. Where samples approximate the composition of well-analyzed standards, however, X-ray results appear to be both precise and accurate. The values of Hampel were used for Na and K, but all other figures were taken from X-ray determinations (except values of Aoki used as X-ray standards).

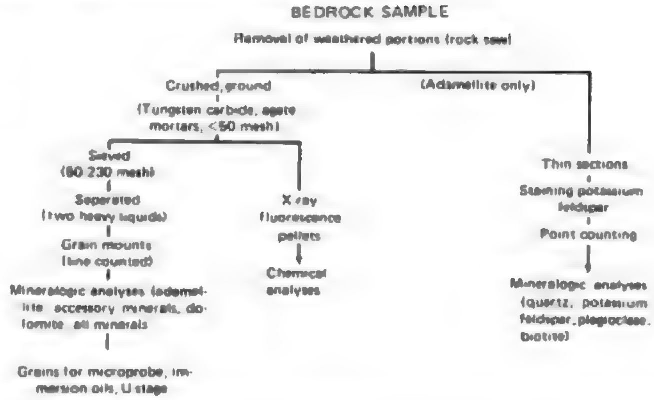

FIGURE 315.—Flowsheet for laboratory treatment of bedrock samples.

Thin sections of five adamellite bedrock samples were stained for K-feldspar (Rosenblum, 1956) and point counted to determine quartz, K-feldspar, plagioclase, and biotite percentages. Mineralogical analyses of crushed bedrock (50–230 mesh) and less-than-2-mm-sand (greater than 62 μm, crushed to -50 mesh), fine sand and very fine sand fractions of soils were obtained from line counts of grain mounts after removal of organic matter with 2 percent hydrogen peroxide (soils only) and two successive heavy liquid separations. For the dolomite samples, liquids of specific gravity 2.69 (bromoform plus alcohol) and 2.95 (tetrabromoethane) were used; liquids having densities of 2.88 (bromoform) and 3.3 (methylene iodide) were used for adamellite samples. A minimum of 900 grains, and usually more than

[7]The following parameters were determined for the less-than-2-mm fraction of many soil samples for purposes outside the scope of this paper. Phosphorus in 10:1 water extracts, permanent wilting point (soil moisture at 15-atm tension), moisture equivalent (soil moisture at 1/3-atm tension), available water (moisture equivalent minus permanent wilting point), percentage carbonate, and total carbon.

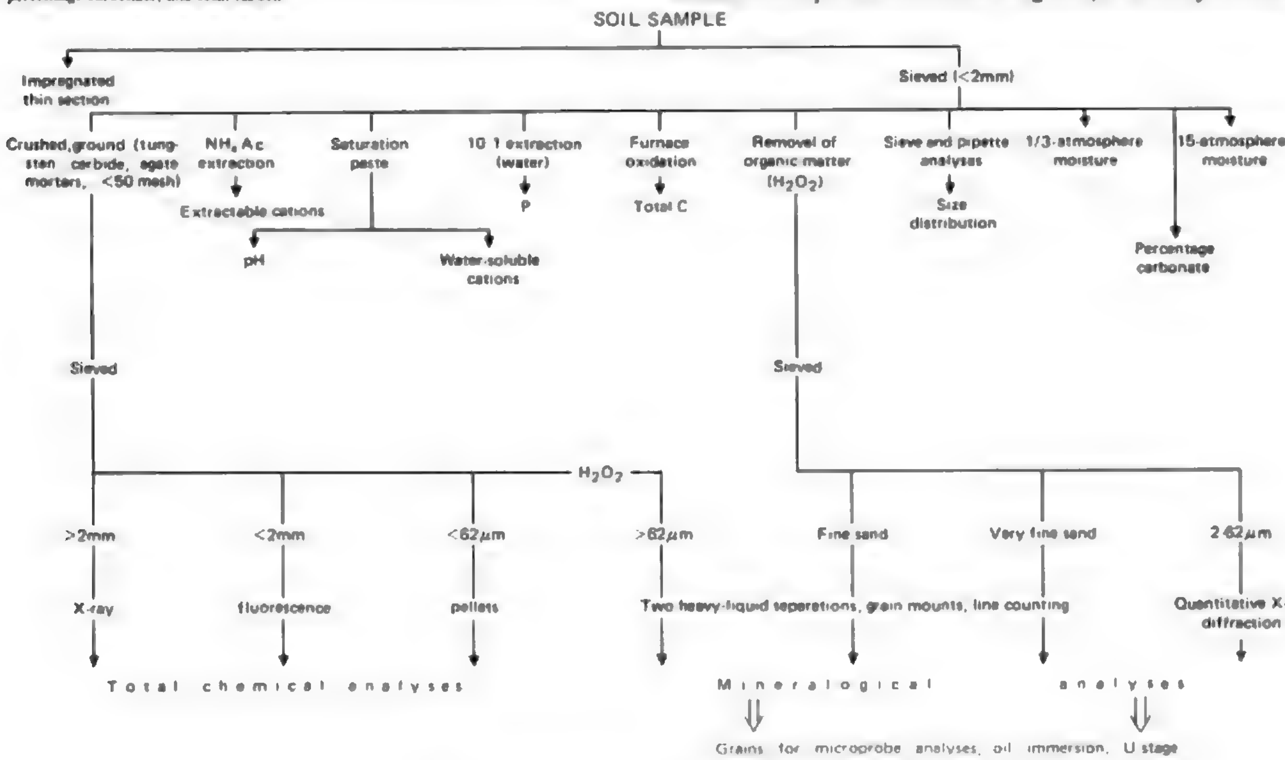

FIGURE 316.—Flowsheet for laboratory treatment of soil samples.

Digitized by Google

TABLE 27.—*Reproducibility of X-ray fluorescence analyses*

[Values yielded by opposite sides of the same pellet, except sample 58]

	Fe	Mn	Ca	Sr	Rb
	(weight percent)			(ppm)	
58 (agate)	0.22	0.06	21.86	59.3	0.0
58 (tungsten carbide)	.22	.06	21.99	59.5	.0
47 soil	3.26	------	------	------	------
47 soil	3.26	------	------	------	------
52 soil	------	------	------	------	43.1
52 soil	------	------	------	------	44.1
64 soil	------	------	22.98	------	------
64 soil	------	------	23.31	------	------
66 soil	------	------	22.76	------	------
66 soil	------	------	23.00	------	------
68 soil	------	------	------	166	------
68 soil	------	------	------	167	------
97	1.32	------	------	------	------
97	1.32	------	------	------	------
98	------	.042	------	------	------
98	------	.045	------	------	------

1,500 grains, per sample was counted. The statistical analysis of Brewer (1964, p. 46–50) indicates that counts of 1,500 grains yield results within about 5 percent probable error for major constituents and less than 15 percent for minor minerals. Mineral densities used to compute weight percentages from grain mounts were obtained by direct measurement or from chemical composition information.

Line-counted samples were used as standards for quantitative X-ray diffraction analyses of silt fractions. Both standards and samples were finely ground in a mortar, mounted on glass slides with the aid of acetone, and X-rayed under identical conditions on the same day. Abundances were based on peak heights above background. Glass was assumed to make up the difference between totals and 100 percent, an assumption verified by many visual estimations of silt-glass percentage under the polarizing microscope. Probable error is estimated at less than 15 percent of the given value.

Laboratory soil pH measurements were made with a Beckman Zeromatic pH meter on water-saturation pastes. Replicate analyses of samples yielded results within 0.1 pH unit. Similar pastes were extracted by the Buchner funnel method of Bower and Wilcox (1965, p. 935). Replicate analyses of 19 saturation extract samples indicate reproducibility at the level of ±25 percent of the stated value. Soil samples were extracted with NH_4Ac solutions at pH 7.0, using the centrifuging method of Bower, Reitemeier, and Fireman (1952, p. 253), and analyzed for total extractable Na, K, Ca, and Mg. Results are reproducible to within 20 percent of the stated values. Na and K in water and NH_4Ac extracts were analyzed by flame photometry. Ca, Mg, and Fe in soil extracts were determined by atomic absorption spectrophotometry. Si was analyzed using colorimetric procedures described by Kilmer (1965, p. 959–962). P in water-saturation extracts was determined by the methods of Olsen and Dean (1965, p. 104–107).

Plant samples from the field and greenhouse were washed with distilled water and ovendried at 104°C. Into 30-milliliter digestion flasks, 0.2000–0.5000 grams of each dry sample was weighed. Five milliliters of concentrated HNO_3 and $HClO_4$ were added, and the samples were digested overnight in a sand bath. The samples were then heated on Kjeldahl burners until they appeared colorless and $HClO_4$ fumes were evident. The solutions were cooled and diluted to 100 milliliters in volumetric flasks with 10 milliequivalents per liter $SrCl_2$ (to mask interferences). Aliquots were taken for subsequent analysis. K, Na, Ca, Mg, Fe, and Mn were analyzed by atomic absorption spectrophotometry. P was determined colorimetrically by the molybdenum blue method described by Johnson and Ulrich (1959), using stannous chloride as a reducing agent. Al was determined by the Eriochrome Cyanine R. A. method of Jones and Thurman (1957). The methods of Wooley and Johnson (1957, p. 872) were employed in the dry ashing and Si analysis of plants. Absolute limits of precision are ±20 percent of the given value, but analytical results are within ±10 percent in all but a few cases.

The preceding discussion has been confined to methods and precision of measurements for any given sample. Statistical computer data (table 29) permit a comparison of various physical and chemical soil parameters with regard to variation within a given soil type. Geographic patterns of variation within and between soil types were not assessed. The figures of table 29, based on samplings of from 12 to 25 sites per soil type, indicate seven general groups of soil parameter variation for this area, decreasing in reliability as follows:

TABLE 28.—*Comparison of analytical results for some adamellite of Sage Hen Flat (samples 92, 98) and Reed Dolomite samples, as analyzed by X-ray fluorescence (XRF), wet chemistry (Ken-ichior Aoki), and flame photometry (Joaquim Hampel)*

	52 bedrock			52 soil, < 2 mm			54 bedrock			54 soil, < 2 mm			54 soil, > 2 mm	
	XRF	Aoki	Hampel	XRF	Aoki	Hampel	XRF	Aoki	Hampel	XRF	Aoki	Hampel	XRF	Hampel
SiO_2	0.17	0.16	------	41.19	23.01	------	0.55	0.81	------	[1]35.74	35.74	------	1.95	------
TiO_2	------	Trace	------	------	.44	------	.03	.03	------	.47	.50	------	.01	------
Al_2O_3	.13	.16	------	11.48	7.87	------	.40	.47	------	[1]9.89	9.89	------	.08	------
Total Fe as Fe_2O_3	.23	.23	------	3.78	3.56	------	.39	.39	------	[1]3.14	3.14	------	.53	------
MnO	.05	.04	------	.21	.17	------	.07	.05	------	[1].16	.16	------	.09	------
MgO	20.47	21.29	------	6.96	8.86	------	20.75	21.76	------	[1]8.44	8.44	------	18.54	------
CaO	30.79	31.24	------	9.16	22.09	------	29.74	30.29	------	[1]14.14	14.14	------	30.92	------
Na_2O	.04	.03	0.04	1.00	.46	0.48	<.01	.08	0.04	.72	.16	1.55	<.01	0.07
K_2O	.00	.02	.02	1.81	.82	.98	.01	.07	.03	------	1.63	1.88	.07	.06

	68 bedrock		68 soil, > 2 mm		64 bedrock		92 bedrock		92 soil, < 2 mm		98 soil, < 2 mm		
	XRF	Hampel	XRF	Hampel	XRF	Aoki	XRF	Aoki	XRF	Aoki	XRF	Aoki	Hampel
SiO_2	0.09	------	1.49	------	0.75	0.59	65.83	67.20	65.93	65.40	66.93	69.65	------
TiO_2	.01	------	.04	------	------	0.03	------	.53	------	.63	.50	.43	------
Al_2O_3	.12	------	.61	------	.19	.12	------	16.33	------	15.77	------	14.57	------
Total Fe as Fe_2O_3	.39	------	.51	------	.33	.46	3.96	3.12	4.73	3.54	2.67	2.50	------
MnO	.12	------	.12	------	.03	.03	.10	.06	.11	.05	.04	.04	------
MgO	19.83	------	19.83	------	7.20	7.42	1.06	.77	[1]1.15	1.15	.79	.65	------
CaO	30.41	------	30.41	------	39.69	46.87	2.37	2.86	2.14	2.32	1.60	1.63	------
Na_2O	<.01	.03	<.01	.08	<.01	.07	3.44	3.73	3.31	3.35	2.84	3.24	3.39
K_2O	.00	.01	.08	.07	.05	.06	3.88	.11	3.77	3.82	3.69	3.53	3.63

[1]Valve of Aoki used for standard.

Digitized by Google

TABLE 29.—*Variation in measured parameters of four White Mountains soil types*

	Reed Dolomite		Basalt		Adamellite of Sage Hen Flat		Andrews Mountain Sandstone		Range of percent standard deviation
	Number of samples	Percent standard deviation from mean	Number of samples	Percent standard deviation from mean	Number of samples	Percent standard deviation from mean	Number of samples	Percent standard deviation from mean	
Total extractable K	25	51	18	20	22	37	19	26	20-51
Total extractable Na	25	31	18	20	22	62	19	23	20-62
Total extractable Ca	25	41	18	16	22	32	19	22	16-14
Total extractable Mg	25	40	18	23	22	31	19	18	18-40
K in water-saturation extracts	21	78	17	42	21	83	12	55	42-83
Na in water-saturation extracts	21	35	17	53	21	28	12	59	28-59
Ca in water-saturation extracts	21	39	17	49	21	40	12	51	39-51
Mg in water-saturation extracts	21	36	17	42	21	36	12	37	36-42
Percent exchangeable K	21	56	17	19	21	47	12	31	19-56
Percent exchangeable Na	21	37	17	19	21	33	12	17	17-37
Percent exchangeable Ca	21	9	17	2	21	5	12	3	2- 9
Percent exchangeable Mg	21	40	17	12	21	27	12	13	12-40
Sum of exchangeable cations	21	32	17	15	21	29	12	14	14-32
P in 10:1 water extracts	18	73	17	67	21	59	15	111	59-111
High field pH	25	1	18	8	22	8	19	8	1- 8
Low field pH	25	5	18	5	22	7	19	8	5- 8
Mean field pH	25	1	18	7	22	8	19	8	1- 8
Laboratory pH	25	3	18	4	22	5	17	7	3- 7
Soil moisture at ⅓-atm tension	17	28	16	9	22	16	16	14	9-28
Soil moisture at 15-atm tension	23	45	17	24	22	25	17	30	24-45
Available water	17	28	16	21	22	12	15	18	12-28
Soil depth on topographic highs	24	27	17	22	21	22	17	14	14-27
Bulk density	24	34	17	20	21	17	----	----	17-34
Percent fragments greater than 2 mm	14	20	----	----	14	61	19	16	16-61

1. Laboratory and field pH
2. Available water, ⅓-atmosphere moisture, soil depth on topographic highs
3. Exchangeable cations, bulk density
4. Total extractable cations, 15-atmosphere moisture
5. Percentage of soil gravel fragments
6. Cations in water-saturation extracts
7. 10:1 available phosphorus

Many soil surveys and soil descriptions include only one or two analyses of these soil properties for each soil series. Information presented here would suggest that although a few pH and ⅓-atmosphere moisture determinations may suffice to characterize properties of a soil series as a whole, most other parameters range widely within a given soil type and cannot be accurately evaluated by a few analyses. The White Mountains soils are, of course, lithosols and therefore may show more variation than finer textured soils formed on alluvium or strongly developed soils on almost any parent material. Nonetheless it is unlikely that analyses at one type locality are sufficient to describe accurately properties of a soil series having any appreciable lateral extent.

* U.S. GOVERNMENT PRINTING OFFICE: 1974—543-583/ 93

Digitized by Google

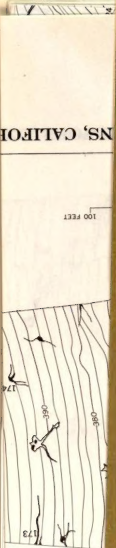

UNIVERSITY OF CHICAGO
18 981 765

TITLE NUMBER
SHIPMENT NO.
NEW
THIR
FOU

f
QE 75
.A26
no. 352
United States.
Geological Survey.
Professional
papers.
03 OCT 24 '79

f
QE 75
.A26
no. 352
United States.
Geological Survey.
Professional
papers.
THE UNIVERSITY OF CHICAGO LIBRARY

U of Chicago
18981765

Digitized by Google